

UNVEILING INCIPIENT REACTIVITY VIA TANDEM  
HYDROSILYLATION REACTION CASCADES AND  
THE PROGRESS TOWARD THE TOTAL SYNTHESIS  
OF (-)-CYLINDROCYCLOPHANE A

Thesis by  
Tyler Daniel Casselman

In Partial Fulfillment of the Requirements for  
the degree of  
Doctor of Philosophy

CALIFORNIA INSTITUTE OF TECHNOLOGY  
Pasadena, California

2023  
(Defended May 10, 2023)

© 2023

Tyler Daniel Casselman  
ORCID: 0000-0002-1691-3969

*For Dad, Mom and Janel*

*“There are always two choices. Two paths to take. One is easy, and its only reward is that it’s easy”*

*–Unknown*

## ACKNOWLEDGEMENTS

The hardest decisions in life result in the most rewarding of outcomes for those brave enough to make them. This sentiment was expressed to me during one of the most challenging moments of my life by a mentor of mine at Columbia university. I was given two-months to either “play it safe” and transfer to another group at Columbia to finish the remaining three years of my PhD, or “risk it all” and potentially start over from scratch with a different PhD program at a different university. My choices boiled down to either becoming Dr. Casselman at 27-years old, or 30-years old. Given how tumultuous those first two years ended up being, could I knowingly sign myself up for another six? This choice was a lot harder to make than I care to admit. The defining moment happened during a meeting with the professor I wanted to transfer to within Columbia university. His chemistry interests were not aligned with mine, but his lab was located a floor above my old lab. Additionally, I had a bunch of friends already in his group. It was the safe option. Luckily for me, he challenged me to not take the safe option. During the most challenging moment of my life, the hardest decision in my life ended up having the most rewarding outcome of my life.

As cliché as it sounds, I knew I wanted to work for Brian as soon as I gathered the courage to uproot my life and potentially start my PhD program from the beginning. There is some irony reflecting on this because I had a choice in 2017 to avoid this whole ordeal and choose Caltech instead of Columbia to begin my graduate school career. I often imagine “what could have been” if I had made the choice to start (and finish) my PhD at Caltech. However, my conclusion is always the same. If I could turn back time and have a chance to

change how I began graduate school, I wouldn't make the change. I believe that the summation of these experiences, both the good and the bad, made me into the scientist (and person) I am today. I really love who I have become throughout my PhD career.

First of all, I have to thank Brian for everything he has done for me. I genuinely believe that your influence has far surpassed the job description as a PhD research advisor, and I cannot thank him enough for what he has provided me throughout his mentorship. Brian is an incredible advisor as his intellect, compassion, empathy, and understanding are all out-of-this-world. I embarked on the PhD adventure with one main mission in mind that Brian has helped me accomplish, which is to be a sound scientist. I have always had the ability to design and carry out thoughtful experiments or solve reaction mechanisms. However, I often felt like my creativity was not grounded in a sense of reality and would often find myself going down chemical rabbit holes of my own design. For example, in my undergrad research I began my sophomore year synthesizing 3,6-disubstituted tetrazines and ended up embedding them in nylon polymers to make materials that would chelate ions dissolved in water. The creativity was there as a young scientist, but being left to my own devices would often lead me astray. I knew Brian was exceptional in one of our first one-on-one meetings together. There was a misunderstanding between us during one of my early subgroup presentations and I needed to speak to him to clear the air. During that time, he told me that he knew from the beginning that his role as my advisor was not to push me, but rather to ground me. I felt confident that I could accomplish what I set out to accomplish throughout my PhD because I had an advisor that not only trusts me to pursue my own ideas, but rather encourages me to reach for the stars because he was there to pull me down if I got too close to the sun. While

I am still learning, I believe that I have succeeded in becoming a sound scientist because of Brian.

I must also thank Sarah Reisman for acting as chair of my committee as well as being like a second advisor to our group. I have enjoyed the discussions we have had during my committee meetings and exams and have especially appreciated Sarah's skill in chairing these meetings. Throughout the years it has been a privilege to benefit from her feedback and suggestions on my chemistry and proposals. Having the perspectives from both Sarah and Brian on my research during group meetings or practice job talks was truly a gift to my professional development that I will cherish. I also need to thank the rest of my committee, Profs. Theo Agapie and Greg Fu for their great input during the last few years of my graduate studies.

I have to thank Dr. Scott Virgil for all of his help throughout the years. It is incredible to have a wonderful person to talk to with such an incredible wealth of knowledge on a daily basis. Seemingly every chemistry problem or intellectual curiosity I have is answerable by Scott with a passion and wisdom that I feel is one-of-a-kind. I also appreciate how Scott and Silva are some of the most welcoming people I know and will greatly miss their annual holiday parties. He is invaluable not only to me, but to everyone on the 3<sup>rd</sup> floor of Schlinger.

I also must thank Dr. Dave Vander Velde for maintaining the incredible NMR facility that we have at Caltech, and for his helpful suggestions with difficult NMR problems. Also, thanks to Dr. Mike Takase and Larry Henling for assistance with X-ray diffraction. I only wish I was able to provide Mike with more usable crystals as, more often than not, I would come down to his facility all excited and present him with terrible crystals. Many thanks to Dr. Mona Shahgholi for maintaining the mass spec. facility and for help getting HRMS data

for publications, especially during the pandemic and when the 3<sup>rd</sup> floor TOF was down for a period of time during my PhD. Finally, thanks to Joe Drew, as well as Greg Rolette and Armando Villasenor for working so hard to keep everything running smoothly regarding the facilities and behind-the-scenes.

During my time at Columbia, I had the privilege to be mentored by a fantastic chemist, Makeda Tekle-Smith. Makeda is one of the most competent chemists in both knowledge and technical skills I have met to date, and it was an incredible experience learning under her tutelage in my first year to serve as my first introduction into total synthesis. Jimistatin<sup>TM</sup> was a beast of a molecule, and I was grateful to take part in its synthesis (however stressful it may be for a first-year student during crunch time). I was lucky to overlap with Makeda, Isaac Hughes, Noushad Mohd, Hunter Imlay, Mario Rivera and Roshan Bhaskar during my time in the Leighton group. Looking back, that experience is priceless to my early development as a scientist, and really helped me hit the metaphorical ground running when I joined the Stoltz group.

The last group of people I wish to think is the informal Columbia Scotch Club (dubbed as Columbia PAHS). The founding members consisted of Erik Phipps, Sean Treacy, Ben Ravetz and Neil Foegen when we began sometime in Spring 2018. Apart from providing me a pathway to try dozens of various single malt scotch bottles over the years, this club served as my support group to emotionally get me through the hardships that occurred during my final months at Columbia. These are truly remarkable people and will serve as lifelong friends that I cherish deeply.

Joining the lab in the middle of the summer term, I was extremely lucky to be accepted by most of the Stoltz group on day one of my arrival. I will never forget the early



days (when I actually would eat lunch during the work day) of travelling to Ernie's taco truck or Daisy Mint with the lunch crew. In particular, Nick Hafeman, Fa Ngamnithiporn and Chris Reimann served as my mentors in some capacity throughout my first few years at Caltech. Chris was a remarkable bay mate whose dedication to research motivated me to push myself and adapt to the high-octane experimental research style present at Caltech. Nick assumed a critical role as mentor throughout the pandemic as he was a helping hand that got me through the lockdowns in Spring 2020 as well as the Church 130 crew. I will never forget the scramble during candidacy when I would pull consecutive all-nighters creating my proposals and frantically sending Nick my edits, which he provided me within 24 hours. Fa was one of the most influential people in my life during the Church 130 days. Only permitted to physically see four of my lab members due to COVID restrictions, it was a challenging time for me to achieve gainful research. Fa was there to guide me during a particularly important part of my project, and I give her credit for being such an incredible coworker.

I need to thank my fellow class, Alexia Kim, Alex Cusumano and Zack Sercel for providing excellent conversations and insights. It was challenging to relate to my entire class in the beginning since I did not take any classes during my time at Caltech, so we weren't able to bond through shared misery of doing Ch242 problem sets together. However, I have been grateful to get to know these wonderful people overtime and I am excited to see the remarkable things they will accomplish.

I must also thank the class in the Stoltz group that joined in the Fall of 2019, Melinda Chan, Ally Stanko, and Joel Monroy for being good friends and colleagues throughout my time at Caltech. I joined Caltech three months prior so I was able to relate to them as we all were just figuring out the PhD process at Caltech. To this day, I see them as good friends as

we have overlapped heavily during my time on the 3<sup>rd</sup> floor of Schlinger and I wish them the best. I am confident they will excel in whatever they set their minds to after grad school.

In addition to terrific graduate students, the Stoltz group also has had its fair share of incredible Postdocs that have had memorable relationships with during my time here. I felt like I could relate to the postdocs more than the graduate students since the circumstances in which I joined the group were more comparable to the postdocs than the graduate students. The only (albeit major) difference I felt between me and the postdocs when I joined was the degree. This has caused me to dub my time at Columbia as my “Predoc.” In particular, I must thank Trevor Lohrey for being a remarkable desk neighbor, gym buddy and friend. He joined a few months after I did and our relationship really blossomed with our shared interest in getting swole. In addition to being a great gym partner, he is also one of the smartest people I know and I learned so many things through our great conversations. My only regret was waiting until after the lockdowns to really begin to hangout outside of the gym or work. Other influential postdocs during my time at Caltech include Veronica Hubble, Stephen Sardini, Trevor Butcher, Steffen Griesses, and Lars Suesse. We shared pleasant conversations daily that would help me get through the work day and I will look fondly back on those memories.

I want to thank Chris Cooze, Samir Rezgui, Elliot Hicks, Simon Cooper, Jordan Thompson and Enric Adillion as the Caltech golf crew. During my last year, I was able to get my hands on 28-year-old clubs and would go hit 18 holes on a Saturday with whoever could fill the tee time that Chris scheduled. Even though my game took a real tailspin as I was working out too much for my golf swing, it was the missing piece to decompress during the heavy writing period at the second half of my last year. I want to thank Chris for the

motivation to sink two eagle putts on drivable par 4's during my 2023 golf outings, much to his chagrin.

The entire third-year class in the Stoltz group is jam packed with absolute scientific studs. It was incredible being able to socialize via game nights and chemistry happy hours during their first year, and I am proud of what the entire class has been able to accomplish thus far. I look forward to our future encounters at conferences or wherever we may meet as they are all fantastic human beings. Finally, I'd like to thank all of the second and first years for making the lab such a fun place to be. It has been hard to socialize and get to know them as my final few years have been the most strenuous. However, attending the group meetings for the second-years and hearing about the projects that the first year students are on has been a wonderful experience and I am excited to see them excel in the best lab in the world!

I'd like to thank members of the Reisman group for being so kind as our labmates from across the hall. Interactions at the LC/MS, joint group meetings, happy hours, or whenever I decide to barge into the lab offices have always been pleasant and fruitful. It was nice to have an informal "lab away from lab" filled with people both intelligent and inviting. The members include, but are not limited to, Ray Turro, Cedric Lozano, Simon Cooper, Jordan Thompson, Philip Boehm, and Stanna Dorn. It has been a pleasure getting to know all of you during my time here and I hope our paths cross sometime in the future. Finally, I must thank Liam Hunt, with whom I had the pleasure of collaborating with on the cylindrocyclophane project for the past few months. I wish we had been able to overlap longer, but I am happy for the time we have spent together smashing away at cylindrocyclophane.

None of this would have been possible without the incredible mentorship I received during my undergraduate years. Starting at Boston University, Professor John Snyder and Professor Binyomin Abrams really inspired me to pursue my passion in organic chemistry. Binyomin convinced me to leave the Pre-Med track and finish my undergraduate studies as a chemistry major, so none of this would have happened without his guidance as my academic advisor. My research advisor at BU, Prof. John Snyder, was instrumental in teaching me the fundamentals of the craft of organic chemistry. Sitting in his Organic chemistry class and observing how passionate he was about all things synthetic organic chemistry piqued my interest and made the decision to join his lab very easy. I was lucky enough to have incredible freedom in John's lab, as I only briefly overlapped with the last few full graduate students he had. Before I knew it, I was the most senior member in the lab teaching fellow undergraduates how to synthesize tetrazines from ethyl diazoacetate. This freedom allowed me to reach my full potential as an undergraduate chemist, and I believe this was crucial to making me into the scientist I am today. I also have to thank Gerald and Jerry, who were fellow chemistry majors I became extremely close with during our last few years at BU. I am excited to join both of you in Boston working as colleagues once again.

I have been blessed with incredible family members who have been supportive of me my entire time throughout graduate school. My father has been the most important factor keeping me afloat all of these years. Whether it is moving me across the country, coordinating much needed family vacations, or providing sage advice after I call him to "beard" him, he has been there for me every step of the way. My mother has provided the emotional support needed. During my lowest times mentally, I have been able to reach out to her and she always answers my call with the love I need. My siblings, although incredibly difficult to handle,

motivate me to be the best Tyler I can be. Otherwise, they'll remind me of my failures for the next decade. My aunts and uncles in the California and Arizona have been incredibly helpful over the years, providing family safe havens for when I need a dose of familial bonding over the holidays but can't make it across the country to see my immediate family. Finally, I owe so much to my grandparents for being my #1 cheerleaders. It doesn't matter what I am doing, they make me feel like I am the best there ever was and I am so happy that they are able to witness me crossing this finish line.

Last, but certainly not least, I dedicate the last acknowledgement to my girlfriend, Janel. I am sure under normal circumstances, I am not easy to love. However, she has provided me the world's supply of love over the past few years during one of the most emotionally, mentally and physically demanding times of my life. I am grateful to have met her during my time here and I am excited to see what the next chapter in life has in store for us in Boston. It fits the theme that the easiest decision is often not the most rewarding, because if I had not picked up my entire life and moved, I would not have met her.

## ABSTRACT

The two pillars of synthetic organic chemistry, reaction methodology development and total synthesis of complex natural products, has remained the focus of chemical research for synthetic chemists since their fundamental inception. In particular, harnessing the reactivity of unstable, but useful, chemical intermediates through telescoping reaction conditions is emerging as an attractive approach to rapidly access complex molecular architecture from readily available building blocks. Herein is described two unique reaction methodologies relying on tandem hydrosilylation reaction cascades to synthesis saturated *N*-heterocyclic products in a stereoselective manner. We have developed a diastereoselective Mannich reaction combining  $\alpha$ -substituted- $\gamma$ -lactam pronucleophiles with *N*-silyl imine electrophiles generated *in situ* via catalytic hydrosilylation of aryl nitriles. Additionally, we have developed a tandem hydrosilylation, enantioselective allylic alkylation reaction of substituted pyridines to yield chiral tetrahydropyridine products. This serves as the first example of using hydrosilylation of pyridines to generate enamine nucleophiles that can undergo an asymmetric allylic alkylation reaction. The final portion of this thesis describes the progress toward a total synthesis of (–)-cylindrocyclophane using C–H functionalization logic. We were able to access the necessary [7.7]-paracyclophane core in 8 steps from a feedstock aryl diazoacetate compound and *n*-hexene. Through functional group manipulations, we were able to advance this paracyclophane core to an intermediate possessing the exact stereocenters and carbon framework in (–)-cylindrocyclophane A. We are currently modeling the necessary deoxygenation needed to advance this intermediate and complete the total synthesis.

## PUBLISHED CONTENT AND CONTRIBUTIONS

1. Greßies, S.; Süße, L.; Casselman, T.; Stoltz, B. M. Tandem Dearomatization/Enantioselective Allylic Alkylation of Pyridines. *J. Am. Chem. Soc.* **2023**. <https://doi.org/10.1021/jacs.3c02470>.

T.D.C. participated in project design, experimental work (synthesis), data acquisition and analysis, and manuscript preparation.

## TABLE OF CONTENTS

Dedication .....	iii
Acknowledgements.....	v
Abstract.....	xiv
Published Content and Contributions.....	xv
Table of Contents .....	xvi
List of Figures .....	xix
List of Schemes .....	xli
List of Tables .....	xlix
List of Abbreviations.....	lvi
 <b>CHAPTER 1</b>	 <b>1</b>
<i>Diastereoselective Direct Mannich Reaction of <math>\alpha</math>-Substituted-<math>\gamma</math>-Lactams</i>	
1.1 Introduction .....	1
1.2 Initial Investigation Into the Mannich Reaction .....	13
1.3 Probing the Potassium <i>tert</i> -Butoxide Promoted Reaction .....	19
1.4 Alternative Synthesis of <i>N</i> -Silyl Imine Electrophiles.....	22
1.5 Telescoped Hydrosilylation/Direct Mannich Reaction .....	25
1.6 <i>KOt</i> -Bu Catalyzed Diastereoselective Mannich Reaction.....	34
1.7 Identification of the <i>KOt</i> -Bu Catalyzed Mannich Reaction .....	39
1.8 Product Derivatization of $\beta$ -Amino Lactams .....	41



1.9	Conclusion.....	47
1.10	Experimental Section.....	48
1.10.1	Materials and Methods.....	48
1.10.2	Experimental Procedures.....	49
1.11	Notes and References .....	112
	<b>APPENDIX 1</b>	<b>128</b>
	<i>Spectra Relevant for Chapter 1</i>	
	<b>APPENDIX 2</b>	<b>261</b>
	<i>Computational Reports to Chapter 1</i>	
	<b>APPENDIX 3</b>	<b>292</b>
	<i>X-Ray Crystallography Reports Relevant to Chapter 1</i>	
	<b>CHAPTER 2</b>	<b>347</b>
	<i>Enantioselective Dearomative Allylic Alkylation of Pyridines</i>	
2.1	Introduction .....	347
2.2	Initial Investigation .....	353
2.3	Scope of the Dearomative Asymmetric Allylic Alkylation .....	360
2.4	Product Derivatizations.....	367
2.5	Proposed Mechanism.....	369
2.6	Synthesis of Bisalkylated Tetrahydropyridine Product .....	370
2.7	Conclusion.....	372
2.8	Experimental Section .....	373
2.8.1	Materials and Methods .....	373
2.8.2	Experimental Procedures .....	374
2.9	Notes and References.....	447

<b>APPENDIX 4</b>	<b>457</b>
<i>Spectra Relevant to Chapter 2</i>	
<b>APPENDIX 5</b>	<b>565</b>
<i>X-Ray Crystallography Reports Relevant to Chapter 2</i>	
<b>APPENDIX 6</b>	<b>586</b>
<i>Progress Toward the Total Synthesis of (-)-Cylindrocyclophane A</i>	
A6.1	Introduction .....586
A6.2	Prior Collaborative Work Within the CCHF .....594
A6.3	Development of Model to Elaborate Key Macrocyclic Intermediate to (-)- Cylindrocyclophane A .....602
A6.4	Modeling the Necessary Deoxygenation .....607
A6.5	Failed Attempt to Deoxygenate Key Macrocyclic Intermediate .....611
A6.6	Second Generation Model Deoxygenation Strategies .....614
A6.7	Second Generation Model Design.....620
A6.8	Conclusion .....623
A6.9	Experimental Section .....624
A6.9.1	Materials and Methods.....624
A6.9.2	Synthetic Procedures.....626
A6.10	Notes and References .....687
<b>APPENDIX 7</b>	<b>697</b>
<i>Spectra Relevant to Appendix 6</i>	
<b>APPENDIX 8</b>	<b>802</b>
<i>X-Ray Crystallography Reports Relevant to Appendix 6</i>	

## LIST OF FIGURES

### CHAPTER 1

#### *Diastereoselective Direct Mannich Reaction of $\alpha$ -Substituted- $\gamma$ -Lactams*

<b>Figure 1.5.1</b>	Description of the numbering system for Mannich products <b>69</b> .....	26
---------------------	--	----

### APPENDIX 1

#### *Spectra Relevant to Chapter 1*

<b>Figure A1.1</b>	$^1\text{H}$ NMR (400 MHz, $\text{CDCl}_3$ ) of compound <b>61c</b> .....	129
<b>Figure A1.2</b>	Infrared spectrum (thin film, NaCl) of compound <b>61c</b> .....	130
<b>Figure A1.3</b>	$^{13}\text{C}$ NMR (100 MHz, $\text{CDCl}_3$ ) of compound <b>61c</b> .....	130
<b>Figure A1.4</b>	$^1\text{H}$ NMR (400 MHz, $\text{CDCl}_3$ ) of compound <b>68a</b> .....	131
<b>Figure A1.5</b>	Infrared spectrum (thin film, NaCl) of compound <b>68a</b> .....	132
<b>Figure A1.6</b>	$^{13}\text{C}$ NMR (100 MHz, $\text{CDCl}_3$ ) of compound <b>68a</b> .....	132
<b>Figure A1.7</b>	$^1\text{H}$ NMR (400 MHz, $\text{CDCl}_3$ ) of compound <b>61a</b> .....	133
<b>Figure A1.8</b>	$^1\text{H}$ NMR (400 MHz, $\text{CDCl}_3$ ) of compound <b>61b</b> .....	134
<b>Figure A1.9</b>	$^1\text{H}$ NMR (400 MHz, $\text{CDCl}_3$ ) of compound <b>56a</b> .....	135
<b>Figure A1.10</b>	$^1\text{H}$ NMR (400 MHz, $\text{CDCl}_3$ ) of compound <b>68b</b> .....	136
<b>Figure A1.11</b>	Infrared spectrum (thin film, NaCl) of compound <b>68b</b> .....	137
<b>Figure A1.12</b>	$^{13}\text{C}$ NMR (100 MHz, $\text{CDCl}_3$ ) of compound <b>68b</b> .....	137
<b>Figure A1.13</b>	$^1\text{H}$ NMR (400 MHz, $\text{CDCl}_3$ ) of compound <b>68c</b> .....	138
<b>Figure A1.14</b>	Infrared spectrum (thin film, NaCl) of compound <b>68c</b> .....	139
<b>Figure A1.15</b>	$^{13}\text{C}$ NMR (100 MHz, $\text{CDCl}_3$ ) of compound <b>68c</b> .....	139
<b>Figure A1.16</b>	$^1\text{H}$ NMR (400 MHz, $\text{CDCl}_3$ ) of compound <b>68d</b> .....	140

<b>Figure A1.17</b>	Infrared spectrum (thin film, NaCl) of compound <b>68d</b> .....	141
<b>Figure A1.18</b>	<sup>13</sup> C NMR (100 MHz, CDCl <sub>3</sub> ) of compound <b>68d</b> .....	141
<b>Figure A1.19</b>	<sup>1</sup> H NMR (400 MHz, CDCl <sub>3</sub> ) of compound <b>68e</b> .....	142
<b>Figure A1.20</b>	Infrared spectrum (thin film, NaCl) of compound <b>68e</b> .....	143
<b>Figure A1.21</b>	<sup>13</sup> C NMR (100 MHz, CDCl <sub>3</sub> ) of compound <b>68e</b> .....	143
<b>Figure A1.22</b>	<sup>1</sup> H NMR (400 MHz, CDCl <sub>3</sub> ) of compound <b>68f</b> .....	144
<b>Figure A1.23</b>	Infrared spectrum (thin film, NaCl) of compound <b>68f</b> .....	145
<b>Figure A1.24</b>	<sup>13</sup> C NMR (100 MHz, CDCl <sub>3</sub> ) of compound <b>68f</b> .....	145
<b>Figure A1.25</b>	<sup>1</sup> H NMR (400 MHz, CDCl <sub>3</sub> ) of compound <b>68g</b> .....	146
<b>Figure A1.26</b>	Infrared spectrum (thin film, NaCl) of compound <b>68g</b> .....	147
<b>Figure A1.27</b>	<sup>13</sup> C NMR (100 MHz, CDCl <sub>3</sub> ) of compound <b>68g</b> .....	147
<b>Figure A1.28</b>	<sup>1</sup> H NMR (400 MHz, CDCl <sub>3</sub> ) of compound <b>68h</b> .....	148
<b>Figure A1.29</b>	Infrared spectrum (thin film, NaCl) of compound <b>68h</b> .....	149
<b>Figure A1.30</b>	<sup>13</sup> C NMR (100 MHz, CDCl <sub>3</sub> ) of compound <b>68h</b> .....	149
<b>Figure A1.31</b>	<sup>1</sup> H NMR (400 MHz, CDCl <sub>3</sub> ) of compound <b>68i</b> .....	150
<b>Figure A1.32</b>	Infrared spectrum (thin film, NaCl) of compound <b>68i</b> .....	151
<b>Figure A1.33</b>	<sup>13</sup> C NMR (100 MHz, CDCl <sub>3</sub> ) of compound <b>68i</b> .....	151
<b>Figure A1.34</b>	<sup>1</sup> H NMR (400 MHz, CDCl <sub>3</sub> ) of compound <b>68j</b> .....	152
<b>Figure A1.35</b>	Infrared spectrum (thin film, NaCl) of compound <b>68j</b> .....	153
<b>Figure A1.36</b>	<sup>13</sup> C NMR (100 MHz, CDCl <sub>3</sub> ) of compound <b>68j</b> .....	153
<b>Figure A1.37</b>	<sup>1</sup> H NMR (400 MHz, CDCl <sub>3</sub> ) of compound <b>64</b> .....	154
<b>Figure A1.38</b>	Infrared spectrum (thin film, NaCl) of compound <b>64</b> .....	155
<b>Figure A1.39</b>	<sup>13</sup> C NMR (100 MHz, CDCl <sub>3</sub> ) of compound <b>64</b> .....	155

<b>Figure A1.40</b>	$^1\text{H}$ NMR (400 MHz, $\text{CDCl}_3$ ) of compound <b>69aa</b> .....	156
<b>Figure A1.41</b>	Infrared spectrum (thin film, NaCl) of compound <b>69aa</b> .....	157
<b>Figure A1.42</b>	$^{13}\text{C}$ NMR (100 MHz, $\text{CDCl}_3$ ) of compound <b>69aa</b> .....	157
<b>Figure A1.43</b>	$^1\text{H}$ NMR (400 MHz, $\text{CDCl}_3$ ) of compound <b>70</b> .....	158
<b>Figure A1.44</b>	Infrared spectrum (thin film, NaCl) of compound <b>70</b> .....	159
<b>Figure A1.45</b>	$^{13}\text{C}$ NMR (100 MHz, $\text{CDCl}_3$ ) of compound <b>70</b> .....	159
<b>Figure A1.46</b>	$^1\text{H}$ NMR (400 MHz, $\text{CDCl}_3$ ) of compound <b>69ba</b> .....	160
<b>Figure A1.47</b>	Infrared spectrum (thin film, NaCl) of compound <b>69ba</b> .....	161
<b>Figure A1.48</b>	$^{13}\text{C}$ NMR (100 MHz, $\text{CDCl}_3$ ) of compound <b>69ba</b> .....	161
<b>Figure A1.49</b>	$^1\text{H}$ NMR (400 MHz, $\text{CDCl}_3$ ) of compound <b>69ca</b> .....	162
<b>Figure A1.50</b>	Infrared spectrum (thin film, NaCl) of compound <b>69ca</b> .....	163
<b>Figure A1.51</b>	$^{13}\text{C}$ NMR (100 MHz, $\text{CDCl}_3$ ) of compound <b>69ca</b> .....	163
<b>Figure A1.52</b>	$^1\text{H}$ NMR (400 MHz, $\text{CDCl}_3$ ) of compound <b>69da</b> .....	164
<b>Figure A1.53</b>	Infrared spectrum (thin film, NaCl) of compound <b>69da</b> .....	165
<b>Figure A1.54</b>	$^{13}\text{C}$ NMR (100 MHz, $\text{CDCl}_3$ ) of compound <b>69da</b> .....	165
<b>Figure A1.55</b>	$^1\text{H}$ NMR (400 MHz, $\text{C}_6\text{D}_6$ ) of compound <b>69ea</b> .....	166
<b>Figure A1.56</b>	Infrared spectrum (thin film, NaCl) of compound <b>69ea</b> .....	167
<b>Figure A1.57</b>	$^{13}\text{C}$ NMR (100 MHz, $\text{C}_6\text{D}_6$ ) of compound <b>69ea</b> .....	167
<b>Figure A1.58</b>	$^1\text{H}$ NMR (400 MHz, $\text{CDCl}_3$ ) of compound <b>69fa</b> .....	168
<b>Figure A1.59</b>	Infrared spectrum (thin film, NaCl) of compound <b>69fa</b> .....	169
<b>Figure A1.60</b>	$^{13}\text{C}$ NMR (100 MHz, $\text{CDCl}_3$ ) of compound <b>69fa</b> .....	169
<b>Figure A1.61</b>	$^1\text{H}$ NMR (400 MHz, $\text{CDCl}_3$ ) of compound <b>69ga</b> .....	170
<b>Figure A1.62</b>	Infrared spectrum (thin film, NaCl) of compound <b>69ga</b> .....	171

<b>Figure A1.63</b>	$^{13}\text{C}$ NMR (100 MHz, $\text{CDCl}_3$ ) of compound <b>69ga</b> .....	171
<b>Figure A1.64</b>	$^1\text{H}$ NMR (400 MHz, $\text{CDCl}_3$ ) of compound <b>69ha</b> .....	172
<b>Figure A1.65</b>	Infrared spectrum (thin film, NaCl) of compound <b>69ha</b> .....	173
<b>Figure A1.66</b>	$^{13}\text{C}$ NMR (100 MHz, $\text{CDCl}_3$ ) of compound <b>69ha</b> .....	173
<b>Figure A1.67</b>	$^1\text{H}$ NMR (400 MHz, $\text{CDCl}_3$ ) of compound <b>69ia</b> .....	174
<b>Figure A1.68</b>	Infrared spectrum (thin film, NaCl) of compound <b>69ia</b> .....	175
<b>Figure A1.69</b>	$^{13}\text{C}$ NMR (100 MHz, $\text{CDCl}_3$ ) of compound <b>69ia</b> .....	175
<b>Figure A1.70</b>	$^1\text{H}$ NMR (400 MHz, $\text{CDCl}_3$ ) of compound <b>69ja</b> .....	176
<b>Figure A1.71</b>	Infrared spectrum (thin film, NaCl) of compound <b>69ja</b> .....	177
<b>Figure A1.72</b>	$^{13}\text{C}$ NMR (100 MHz, $\text{CDCl}_3$ ) of compound <b>69ja</b> .....	177
<b>Figure A1.73</b>	$^1\text{H}$ NMR (400 MHz, $\text{CDCl}_3$ ) of compound <b>69bb</b> .....	178
<b>Figure A1.74</b>	Infrared spectrum (thin film, NaCl) of compound <b>69bb</b> .....	179
<b>Figure A1.75</b>	$^{13}\text{C}$ NMR (100 MHz, $\text{CDCl}_3$ ) of compound <b>69bb</b> .....	179
<b>Figure A1.76</b>	$^1\text{H}$ NMR (400 MHz, $\text{CDCl}_3$ ) of compound <b>69cb</b> .....	180
<b>Figure A1.77</b>	Infrared spectrum (thin film, NaCl) of compound <b>69cb</b> .....	181
<b>Figure A1.78</b>	$^{13}\text{C}$ NMR (100 MHz, $\text{CDCl}_3$ ) of compound <b>69cb</b> .....	181
<b>Figure A1.79</b>	$^1\text{H}$ NMR (400 MHz, $\text{CDCl}_3$ ) of compound <b>69db</b> .....	182
<b>Figure A1.80</b>	Infrared spectrum (thin film, NaCl) of compound <b>69db</b> .....	183
<b>Figure A1.81</b>	$^{13}\text{C}$ NMR (100 MHz, $\text{CDCl}_3$ ) of compound <b>69db</b> .....	183
<b>Figure A1.82</b>	$^1\text{H}$ NMR (400 MHz, $\text{CDCl}_3$ ) of compound <b>69eb</b> .....	184
<b>Figure A1.83</b>	Infrared spectrum (thin film, NaCl) of compound <b>69eb</b> .....	185
<b>Figure A1.84</b>	$^{13}\text{C}$ NMR (100 MHz, $\text{CDCl}_3$ ) of compound <b>69eb</b> .....	185
<b>Figure A1.85</b>	$^1\text{H}$ NMR (400 MHz, $\text{CDCl}_3$ ) of compound <b>69dc</b> .....	186

<b>Figure A1.86</b>	Infrared spectrum (thin film, NaCl) of compound <b>69dc</b> .....	187
<b>Figure A1.87</b>	$^{13}\text{C}$ NMR (100 MHz, $\text{CDCl}_3$ ) of compound <b>69dc</b> .....	187
<b>Figure A1.88</b>	$^{19}\text{F}$ NMR (282 MHz, $\text{CDCl}_3$ ) of compound <b>69dc</b> .....	188
<b>Figure A1.89</b>	$^1\text{H}$ NMR (400 MHz, $\text{CDCl}_3$ ) of compound <b>69dd</b> .....	189
<b>Figure A1.90</b>	Infrared spectrum (thin film, NaCl) of compound <b>69dd</b> .....	190
<b>Figure A1.91</b>	$^{13}\text{C}$ NMR (100 MHz, $\text{CDCl}_3$ ) of compound <b>69dd</b> .....	190
<b>Figure A1.92</b>	$^{19}\text{F}$ NMR (282 MHz, $\text{CDCl}_3$ ) of compound <b>69dd</b> .....	191
<b>Figure A1.93</b>	$^1\text{H}$ NMR (400 MHz, $\text{CDCl}_3$ ) of compound <b>69de</b> .....	192
<b>Figure A1.94</b>	Infrared spectrum (thin film, NaCl) of compound <b>69de</b> .....	193
<b>Figure A1.95</b>	$^{13}\text{C}$ NMR (100 MHz, $\text{CDCl}_3$ ) of compound <b>69de</b> .....	193
<b>Figure A1.96</b>	$^{19}\text{F}$ NMR (282 MHz, $\text{CDCl}_3$ ) of compound <b>69de</b> .....	194
<b>Figure A1.97</b>	$^1\text{H}$ NMR (400 MHz, $\text{CDCl}_3$ ) of compound <b>69df</b> .....	195
<b>Figure A1.98</b>	Infrared spectrum (thin film, NaCl) of compound <b>69df</b> .....	196
<b>Figure A1.99</b>	$^{13}\text{C}$ NMR (100 MHz, $\text{CDCl}_3$ ) of compound <b>69df</b> .....	196
<b>Figure A1.100</b>	$^{19}\text{F}$ NMR (282 MHz, $\text{CDCl}_3$ ) of compound <b>69df</b> .....	197
<b>Figure A1.101</b>	$^1\text{H}$ NMR (400 MHz, $\text{CDCl}_3$ ) of compound <b>69dg</b> .....	198
<b>Figure A1.102</b>	Infrared spectrum (thin film, NaCl) of compound <b>69dg</b> .....	199
<b>Figure A1.103</b>	$^{13}\text{C}$ NMR (100 MHz, $\text{CDCl}_3$ ) of compound <b>69dg</b> .....	199
<b>Figure A1.104</b>	$^{19}\text{F}$ NMR (282 MHz, $\text{CDCl}_3$ ) of compound <b>69dg</b> .....	200
<b>Figure A1.105</b>	$^1\text{H}$ NMR (400 MHz, $\text{CDCl}_3$ ) of compound <b>69dh</b> .....	201
<b>Figure A1.106</b>	Infrared spectrum (thin film, NaCl) of compound <b>69dh</b> .....	202
<b>Figure A1.107</b>	$^{13}\text{C}$ NMR (100 MHz, $\text{CDCl}_3$ ) of compound <b>69dh</b> .....	202
<b>Figure A1.108</b>	$^{19}\text{F}$ NMR (282 MHz, $\text{CDCl}_3$ ) of compound <b>69dh</b> .....	203

<b>Figure A1.109</b>	$^1\text{H}$ NMR (400 MHz, $\text{CDCl}_3$ ) of compound <b>69dj</b> .....	204
<b>Figure A1.110</b>	Infrared spectrum (thin film, NaCl) of compound <b>69dj</b> .....	205
<b>Figure A1.111</b>	$^{13}\text{C}$ NMR (100 MHz, $\text{CDCl}_3$ ) of compound <b>69dj</b> .....	205
<b>Figure A1.112</b>	$^1\text{H}$ NMR (400 MHz, $\text{CDCl}_3$ ) of compound <b>69dk</b> .....	206
<b>Figure A1.113</b>	Infrared spectrum (thin film, NaCl) of compound <b>69dk</b> .....	207
<b>Figure A1.114</b>	$^{13}\text{C}$ NMR (100 MHz, $\text{CDCl}_3$ ) of compound <b>69dk</b> .....	207
<b>Figure A1.115</b>	$^1\text{H}$ NMR (400 MHz, $\text{CDCl}_3$ ) of compound <b>69dl</b> .....	208
<b>Figure A1.116</b>	Infrared spectrum (thin film, NaCl) of compound <b>69dl</b> .....	209
<b>Figure A1.117</b>	$^{13}\text{C}$ NMR (100 MHz, $\text{CDCl}_3$ ) of compound <b>69dl</b> .....	209
<b>Figure A1.118</b>	$^1\text{H}$ NMR (400 MHz, $\text{CDCl}_3$ ) of compound <b>69dm</b> .....	210
<b>Figure A1.119</b>	Infrared spectrum (thin film, NaCl) of compound <b>69dm</b> .....	211
<b>Figure A1.120</b>	$^{13}\text{C}$ NMR (100 MHz, $\text{CDCl}_3$ ) of compound <b>69dm</b> .....	211
<b>Figure A1.121</b>	$^1\text{H}$ NMR (400 MHz, $\text{CDCl}_3$ ) of compound <b>69dn</b> .....	212
<b>Figure A1.122</b>	Infrared spectrum (thin film, NaCl) of compound <b>69dn</b> .....	213
<b>Figure A1.123</b>	$^{13}\text{C}$ NMR (100 MHz, $\text{CDCl}_3$ ) of compound <b>69dn</b> .....	213
<b>Figure A1.124</b>	$^1\text{H}$ NMR (400 MHz, $\text{CDCl}_3$ ) of compound <b>69dp</b> .....	214
<b>Figure A1.125</b>	Infrared spectrum (thin film, NaCl) of compound <b>69dp</b> .....	215
<b>Figure A1.126</b>	$^{13}\text{C}$ NMR (100 MHz, $\text{CDCl}_3$ ) of compound <b>69dp</b> .....	215
<b>Figure A1.127</b>	$^1\text{H}$ NMR (400 MHz, $\text{CDCl}_3$ ) of compound <b>69dq</b> .....	216
<b>Figure A1.128</b>	Infrared spectrum (thin film, NaCl) of compound <b>69dq</b> .....	217
<b>Figure A1.129</b>	$^{13}\text{C}$ NMR (100 MHz, $\text{CDCl}_3$ ) of compound <b>69dq</b> .....	217
<b>Figure A1.130</b>	$^1\text{H}$ NMR (400 MHz, $\text{CDCl}_3$ ) of compound <b>86a</b> .....	218
<b>Figure A1.131</b>	Infrared spectrum (thin film, NaCl) of compound <b>86a</b> .....	219



<b>Figure A1.132</b>	$^{13}\text{C}$ NMR (100 MHz, $\text{CDCl}_3$ ) of compound <b>86a</b> .....	219
<b>Figure A1.133</b>	$^1\text{H}$ NMR (400 MHz, $\text{CDCl}_3$ ) of compound <b>87</b> .....	220
<b>Figure A1.134</b>	Infrared spectrum (thin film, NaCl) of compound <b>87</b> .....	221
<b>Figure A1.135</b>	$^{13}\text{C}$ NMR (100 MHz, $\text{CDCl}_3$ ) of compound <b>87</b> .....	221
<b>Figure A1.136</b>	$^1\text{H}$ NMR (400 MHz, $\text{CDCl}_3$ ) of compound <b>88</b> .....	222
<b>Figure A1.137</b>	Infrared spectrum (thin film, NaCl) of compound <b>88</b> .....	223
<b>Figure A1.138</b>	$^{13}\text{C}$ NMR (100 MHz, $\text{CDCl}_3$ ) of compound <b>88</b> .....	223
<b>Figure A1.139</b>	$^1\text{H}$ NMR (400 MHz, $\text{CDCl}_3$ ) of compound <b>89</b> .....	224
<b>Figure A1.140</b>	Infrared spectrum (thin film, NaCl) of compound <b>89</b> .....	225
<b>Figure A1.141</b>	$^{13}\text{C}$ NMR (100 MHz, $\text{CDCl}_3$ ) of compound <b>89</b> .....	225
<b>Figure A1.142</b>	$^1\text{H}$ NMR (400 MHz, $\text{CDCl}_3$ ) of compound <b>91</b> .....	226
<b>Figure A1.143</b>	Infrared spectrum (thin film, NaCl) of compound <b>91</b> .....	227
<b>Figure A1.144</b>	$^{13}\text{C}$ NMR (100 MHz, $\text{CDCl}_3$ ) of compound <b>91</b> .....	227
<b>Figure A1.145</b>	$^1\text{H}$ NMR (400 MHz, $\text{CDCl}_3$ ) of compound <b>92</b> .....	228
<b>Figure A1.146</b>	Infrared spectrum (thin film, NaCl) of compound <b>92</b> .....	229
<b>Figure A1.147</b>	$^{13}\text{C}$ NMR (100 MHz, $\text{CDCl}_3$ ) of compound <b>92</b> .....	229
<b>Figure A1.148</b>	$^1\text{H}$ NMR (400 MHz, $\text{CDCl}_3$ ) of compound <b>94a</b> .....	230
<b>Figure A1.149</b>	Infrared spectrum (thin film, NaCl) of compound <b>94a</b> .....	231
<b>Figure A1.150</b>	$^{13}\text{C}$ NMR (100 MHz, $\text{CDCl}_3$ ) of compound <b>94a</b> .....	231
<b>Figure A1.151</b>	$^1\text{H}$ NMR (400 MHz, $\text{CDCl}_3$ ) of compound <b>94b</b> .....	232
<b>Figure A1.152</b>	Infrared spectrum (thin film, NaCl) of compound <b>94b</b> .....	233
<b>Figure A1.153</b>	$^{13}\text{C}$ NMR (100 MHz, $\text{CDCl}_3$ ) of compound <b>94b</b> .....	233
<b>Figure A1.154</b>	$^1\text{H}$ NMR (400 MHz, $\text{CDCl}_3$ ) of compound <b>94c</b> .....	234

<b>Figure A1.155</b>	Infrared spectrum (thin film, NaCl) of compound <b>94c</b> .....	235
<b>Figure A1.156</b>	<sup>13</sup> C NMR (100 MHz, CDCl <sub>3</sub> ) of compound <b>94c</b> .....	235
<b>Figure A1.157</b>	<sup>1</sup> H NMR (400 MHz, CDCl <sub>3</sub> ) of compound <b>95a</b> .....	236
<b>Figure A1.158</b>	Infrared spectrum (thin film, NaCl) of compound <b>95a</b> .....	237
<b>Figure A1.159</b>	<sup>13</sup> C NMR (100 MHz, CDCl <sub>3</sub> ) of compound <b>95a</b> .....	237
<b>Figure A1.160</b>	<sup>1</sup> H NMR (400 MHz, CDCl <sub>3</sub> ) of compound <b>95b</b> .....	238
<b>Figure A1.161</b>	Infrared spectrum (thin film, NaCl) of compound <b>95b</b> .....	239
<b>Figure A1.162</b>	<sup>13</sup> C NMR (100 MHz, CDCl <sub>3</sub> ) of compound <b>95b</b> .....	239
<b>Figure A1.163</b>	<sup>1</sup> H NMR (400 MHz, CDCl <sub>3</sub> ) of compound <b>syn-96</b> .....	240
<b>Figure A1.164</b>	Infrared spectrum (thin film, NaCl) of compound <b>syn-96</b> .....	241
<b>Figure A1.165</b>	<sup>13</sup> C NMR (100 MHz, CDCl <sub>3</sub> ) of compound <b>syn-96</b> .....	241
<b>Figure A1.166</b>	<sup>1</sup> H NMR (400 MHz, CDCl <sub>3</sub> ) of compound <b>anti-96</b> .....	242
<b>Figure A1.167</b>	Infrared spectrum (thin film, NaCl) of compound <b>anti-96</b> .....	243
<b>Figure A1.168</b>	<sup>13</sup> C NMR (100 MHz, CDCl <sub>3</sub> ) of compound <b>anti-96</b> .....	243
<b>Figure A1.169</b>	<sup>1</sup> H NMR (400 MHz, CDCl <sub>3</sub> ) of compound <b>104</b> .....	244
<b>Figure A1.170</b>	Infrared spectrum (thin film, NaCl) of compound <b>104</b> .....	245
<b>Figure A1.171</b>	<sup>13</sup> C NMR (100 MHz, CDCl <sub>3</sub> ) of compound <b>104</b> .....	245
<b>Figure A1.172</b>	<sup>1</sup> H NMR (400 MHz, CDCl <sub>3</sub> ) of compound <b>80</b> .....	246
<b>Figure A1.173</b>	Infrared spectrum (thin film, NaCl) of compound <b>80</b> .....	247
<b>Figure A1.174</b>	<sup>13</sup> C NMR (100 MHz, CDCl <sub>3</sub> ) of compound <b>80</b> .....	247
<b>Figure A1.175</b>	<sup>1</sup> H NMR (400 MHz, CDCl <sub>3</sub> ) of compound <b>SI17</b> .....	248
<b>Figure A1.176</b>	Infrared spectrum (thin film, NaCl) of compound <b>SI17</b> .....	249
<b>Figure A1.177</b>	<sup>13</sup> C NMR (100 MHz, CDCl <sub>3</sub> ) of compound <b>SI17</b> .....	249

<b>Figure A1.178</b>	$^1\text{H}$ NMR (400 MHz, $\text{CDCl}_3$ ) of compound <b>SI16</b> .....	250
<b>Figure A1.179</b>	Infrared spectrum (thin film, NaCl) of compound <b>SI16</b> .....	251
<b>Figure A1.180</b>	$^{13}\text{C}$ NMR (100 MHz, $\text{CDCl}_3$ ) of compound <b>SI16</b> .....	251
<b>Figure A1.181</b>	$^1\text{H}$ NMR (400 MHz, $\text{CDCl}_3$ ) of compound <b>SI16a</b> .....	252
<b>Figure A1.182</b>	Infrared spectrum (thin film, NaCl) of compound <b>SI16a</b> .....	253
<b>Figure A1.183</b>	$^{13}\text{C}$ NMR (100 MHz, $\text{CDCl}_3$ ) of compound <b>SI16a</b> .....	253
<b>Figure A1.184</b>	$^1\text{H}$ NMR (400 MHz, $\text{CDCl}_3$ ) of compound <b>SI18</b> .....	254
<b>Figure A1.185</b>	Infrared spectrum (thin film, NaCl) of compound <b>SI18</b> .....	255
<b>Figure A1.186</b>	$^{13}\text{C}$ NMR (100 MHz, $\text{CDCl}_3$ ) of compound <b>SI18</b> .....	255
<b>Figure A1.187</b>	$^1\text{H}$ NMR (400 MHz, $\text{CDCl}_3$ ) of compound <b>102b</b> .....	256
<b>Figure A1.188</b>	$^{13}\text{C}$ NMR (100 MHz, $\text{CDCl}_3$ ) of compound <b>102b</b> .....	257
<b>Figure A1.189</b>	$^{19}\text{F}$ NMR (282 MHz, $\text{CDCl}_3$ ) of compound <b>102b</b> .....	258
<b>Figure A1.190</b>	$^1\text{H}$ NMR (400 MHz, $\text{CDCl}_3$ ) of compound <b>69jc</b> .....	259
<b>Figure A1.191</b>	Infrared spectrum (thin film, NaCl) of compound <b>69jc</b> .....	260

## **APPENDIX 2**

**261**

### *Computational Reports to Chapter 1*

<b>Figure A2.1.1</b>	Optimized structure of representative low-energy conformers of <b>TS1</b> , <b>TS1-b</b> , <b>TS1-c</b> , <b>TS1-rotamer</b> and <b>TS1-rotamer2</b> .....	263
<b>Figure A2.1.2</b>	Optimized structures of representative low-energy conformers of <b>TS2</b> , <b>TS2-b</b> , <b>TS2-c</b> , <b>TS2-rotamer1</b> and <b>TS2-rotamer2</b> .....	263
<b>Figure A2.1.3</b>	Computed Gibbs free energy of lactam <b>68</b> and enolate <b>68a'</b> .....	264
<b>Figure A2.1.4</b>	Computed NPA charges for <b>TS1</b> , <b>65</b> and <b>TS2</b> .....	264
<b>Figure A2.1.5</b>	Calculated reaction energy profile .....	265

**APPENDIX 3***X-Ray Crystallography Reports Relevant to Chapter 1*

<b>Figure A3.1.1</b>	X-ray Crystal Structure of Amine <b>69dn</b> .....	293
<b>Figure A3.2.1</b>	X-ray Crystal Structure of Imine <b>80</b> .....	307
<b>Figure A3.3.1</b>	X-ray Crystal Structure of Imine <b>70</b> .....	332

**APPENDIX 4***Spectra Relevant to Appendix 5*

<b>Figure A4.1</b>	<sup>1</sup> H NMR (400 MHz, CDCl <sub>3</sub> ) of compound <b>L23</b> .....	458
<b>Figure A4.2</b>	Infrared spectrum (thin film, NaCl) of compound <b>L23</b> .....	459
<b>Figure A4.3</b>	<sup>13</sup> C NMR (100 MHz, CDCl <sub>3</sub> ) of compound <b>L23</b> .....	459
<b>Figure A4.4</b>	<sup>31</sup> P NMR (121 MHz, CDCl <sub>3</sub> ) of compound <b>L23</b> .....	460
<b>Figure A4.5</b>	<sup>1</sup> H NMR (400 MHz, CDCl <sub>3</sub> ) of compound <b>142l</b> .....	461
<b>Figure A4.6</b>	Infrared spectrum (thin film, NaCl) of compound <b>142l</b> .....	462
<b>Figure A4.7</b>	<sup>13</sup> C NMR (100 MHz, CDCl <sub>3</sub> ) of compound <b>142l</b> .....	462
<b>Figure A4.8</b>	<sup>1</sup> H NMR (400 MHz, CDCl <sub>3</sub> ) of compound <b>142m</b> .....	463
<b>Figure A4.9</b>	Infrared spectrum (thin film, NaCl) of compound <b>142m</b> .....	464
<b>Figure A4.10</b>	<sup>13</sup> C NMR (100 MHz, CDCl <sub>3</sub> ) of compound <b>142m</b> .....	464
<b>Figure A4.11</b>	<sup>19</sup> F NMR (282 MHz, CDCl <sub>3</sub> ) of compound <b>142m</b> .....	465
<b>Figure A4.12</b>	<sup>1</sup> H NMR (400 MHz, CDCl <sub>3</sub> ) of compound <b>149a</b> .....	466
<b>Figure A4.13</b>	Infrared spectrum (thin film, NaCl) of compound <b>149a</b> .....	467
<b>Figure A4.14</b>	<sup>13</sup> C NMR (100 MHz, CDCl <sub>3</sub> ) of compound <b>149a</b> .....	467
<b>Figure A4.15</b>	<sup>19</sup> F NMR (282 MHz, CDCl <sub>3</sub> ) of compound <b>149a</b> .....	468
<b>Figure A4.16</b>	<sup>1</sup> H NMR (400 MHz, CDCl <sub>3</sub> ) of compound <b>149b</b> .....	469

<b>Figure A4.17</b>	Infrared spectrum (thin film, NaCl) of compound <b>149b</b> .....	470
<b>Figure A4.18</b>	$^{13}\text{C}$ NMR (100 MHz, $\text{CDCl}_3$ ) of compound <b>149b</b> .....	470
<b>Figure A4.19</b>	$^1\text{H}$ NMR (400 MHz, $\text{CDCl}_3$ ) of compound <b>149c</b> .....	471
<b>Figure A4.20</b>	Infrared spectrum (thin film, NaCl) of compound <b>149c</b> .....	472
<b>Figure A4.21</b>	$^{13}\text{C}$ NMR (100 MHz, $\text{CDCl}_3$ ) of compound <b>149c</b> .....	472
<b>Figure A4.22</b>	$^1\text{H}$ NMR (400 MHz, $\text{CDCl}_3$ ) of compound <b>149d</b> .....	473
<b>Figure A4.23</b>	Infrared spectrum (thin film, NaCl) of compound <b>149d</b> .....	474
<b>Figure A4.24</b>	$^{13}\text{C}$ NMR (100 MHz, $\text{CDCl}_3$ ) of compound <b>149d</b> .....	474
<b>Figure A4.25</b>	$^1\text{H}$ NMR (400 MHz, $\text{CDCl}_3$ ) of compound <b>149e</b> .....	475
<b>Figure A4.26</b>	Infrared spectrum (thin film, NaCl) of compound <b>149e</b> .....	476
<b>Figure A4.27</b>	$^{13}\text{C}$ NMR (100 MHz, $\text{CDCl}_3$ ) of compound <b>149e</b> .....	476
<b>Figure A4.28</b>	$^1\text{H}$ NMR (400 MHz, $\text{CDCl}_3$ ) of compound <b>149f</b> .....	477
<b>Figure A4.29</b>	Infrared spectrum (thin film, NaCl) of compound <b>149f</b> .....	478
<b>Figure A4.30</b>	$^{13}\text{C}$ NMR (100 MHz, $\text{CDCl}_3$ ) of compound <b>149f</b> .....	478
<b>Figure A4.31</b>	$^{19}\text{F}$ NMR (282 MHz, $\text{CDCl}_3$ ) of compound <b>149f</b> .....	479
<b>Figure A4.32</b>	$^1\text{H}$ NMR (400 MHz, $\text{CDCl}_3$ ) of compound <b>150a</b> .....	480
<b>Figure A4.33</b>	Infrared spectrum (thin film, NaCl) of compound <b>150a</b> .....	481
<b>Figure A4.34</b>	$^{13}\text{C}$ NMR (100 MHz, $\text{CDCl}_3$ ) of compound <b>150a</b> .....	481
<b>Figure A4.35</b>	$^{19}\text{F}$ NMR (282 MHz, $\text{CDCl}_3$ ) of compound <b>150a</b> .....	482
<b>Figure A4.36</b>	$^1\text{H}$ NMR (400 MHz, $\text{CDCl}_3$ ) of compound <b>150b</b> .....	483
<b>Figure A4.37</b>	Infrared spectrum (thin film, NaCl) of compound <b>150b</b> .....	484
<b>Figure A4.38</b>	$^{13}\text{C}$ NMR (100 MHz, $\text{CDCl}_3$ ) of compound <b>150b</b> .....	484
<b>Figure A4.39</b>	$^1\text{H}$ NMR (400 MHz, $\text{CDCl}_3$ ) of compound <b>150c</b> .....	485

<b>Figure A4.40</b>	Infrared spectrum (thin film, NaCl) of compound <b>150c</b> .....	486
<b>Figure A4.41</b>	$^{13}\text{C}$ NMR (100 MHz, $\text{CDCl}_3$ ) of compound <b>150c</b> .....	486
<b>Figure A4.42</b>	$^1\text{H}$ NMR (400 MHz, $\text{CDCl}_3$ ) of compound <b>150d</b> .....	487
<b>Figure A4.43</b>	Infrared spectrum (thin film, NaCl) of compound <b>150d</b> .....	488
<b>Figure A4.44</b>	$^{13}\text{C}$ NMR (100 MHz, $\text{CDCl}_3$ ) of compound <b>150d</b> .....	488
<b>Figure A4.45</b>	$^{19}\text{F}$ NMR (282 MHz, $\text{CDCl}_3$ ) of compound <b>150d</b> .....	489
<b>Figure A4.46</b>	$^1\text{H}$ NMR (400 MHz, $\text{CDCl}_3$ ) of compound <b>150e</b> .....	490
<b>Figure A4.47</b>	Infrared spectrum (thin film, NaCl) of compound <b>150e</b> .....	491
<b>Figure A4.48</b>	$^{13}\text{C}$ NMR (100 MHz, $\text{CDCl}_3$ ) of compound <b>150e</b> .....	491
<b>Figure A4.49</b>	$^1\text{H}$ NMR (400 MHz, $\text{CDCl}_3$ ) of compound <b>150f</b> .....	492
<b>Figure A4.50</b>	Infrared spectrum (thin film, NaCl) of compound <b>150f</b> .....	493
<b>Figure A4.51</b>	$^{13}\text{C}$ NMR (100 MHz, $\text{CDCl}_3$ ) of compound <b>150f</b> .....	493
<b>Figure A4.52</b>	$^1\text{H}$ NMR (400 MHz, $\text{CDCl}_3$ ) of compound <b>150g</b> .....	494
<b>Figure A4.53</b>	Infrared spectrum (thin film, NaCl) of compound <b>150g</b> .....	495
<b>Figure A4.54</b>	$^{13}\text{C}$ NMR (100 MHz, $\text{CDCl}_3$ ) of compound <b>150g</b> .....	495
<b>Figure A4.55</b>	$^{19}\text{F}$ NMR (282 MHz, $\text{CDCl}_3$ ) of compound <b>150g</b> .....	496
<b>Figure A4.56</b>	$^1\text{H}$ NMR (400 MHz, $\text{CDCl}_3$ ) of compound <b>150h</b> .....	497
<b>Figure A4.57</b>	Infrared spectrum (thin film, NaCl) of compound <b>150h</b> .....	498
<b>Figure A4.58</b>	$^{13}\text{C}$ NMR (100 MHz, $\text{CDCl}_3$ ) of compound <b>150h</b> .....	498
<b>Figure A4.59</b>	$^{19}\text{F}$ NMR (282 MHz, $\text{CDCl}_3$ ) of compound <b>150h</b> .....	499
<b>Figure A4.60</b>	$^1\text{H}$ NMR (400 MHz, $\text{CDCl}_3$ ) of compound <b>150i</b> .....	500
<b>Figure A4.61</b>	Infrared spectrum (thin film, NaCl) of compound <b>150i</b> .....	501
<b>Figure A4.62</b>	$^{13}\text{C}$ NMR (100 MHz, $\text{CDCl}_3$ ) of compound <b>150i</b> .....	501

<b>Figure A4.63</b>	$^{19}\text{F}$ NMR (282 MHz, $\text{CDCl}_3$ ) of compound <b>150i</b> .....	502
<b>Figure A4.64</b>	$^1\text{H}$ NMR (400 MHz, $\text{CDCl}_3$ ) of compound <b>150j</b> .....	503
<b>Figure A4.65</b>	Infrared spectrum (thin film, NaCl) of compound <b>150j</b> .....	504
<b>Figure A4.66</b>	$^{13}\text{C}$ NMR (100 MHz, $\text{CDCl}_3$ ) of compound <b>150j</b> .....	504
<b>Figure A4.67</b>	$^1\text{H}$ NMR (400 MHz, $\text{CDCl}_3$ ) of compound <b>150k</b> .....	505
<b>Figure A4.68</b>	Infrared spectrum (thin film, NaCl) of compound <b>150k</b> .....	506
<b>Figure A4.69</b>	$^{13}\text{C}$ NMR (100 MHz, $\text{CDCl}_3$ ) of compound <b>150k</b> .....	506
<b>Figure A4.70</b>	$^{19}\text{F}$ NMR (282 MHz, $\text{CDCl}_3$ ) of compound <b>150k</b> .....	507
<b>Figure A4.71</b>	$^1\text{H}$ NMR (400 MHz, $\text{CDCl}_3$ ) of compound <b>150l</b> .....	508
<b>Figure A4.72</b>	Infrared spectrum (thin film, NaCl) of compound <b>150l</b> .....	509
<b>Figure A4.73</b>	$^{13}\text{C}$ NMR (100 MHz, $\text{CDCl}_3$ ) of compound <b>150l</b> .....	509
<b>Figure A4.74</b>	$^1\text{H}$ NMR (400 MHz, $\text{CDCl}_3$ ) of compound <b>150m</b> .....	510
<b>Figure A4.75</b>	Infrared spectrum (thin film, NaCl) of compound <b>150m</b> .....	511
<b>Figure A4.76</b>	$^{13}\text{C}$ NMR (100 MHz, $\text{CDCl}_3$ ) of compound <b>150m</b> .....	511
<b>Figure A4.77</b>	$^{19}\text{F}$ NMR (282 MHz, $\text{CDCl}_3$ ) of compound <b>150m</b> .....	512
<b>Figure A4.78</b>	$^1\text{H}$ NMR (400 MHz, $\text{CDCl}_3$ ) of compound <b>150n</b> .....	513
<b>Figure A4.79</b>	Infrared spectrum (thin film, NaCl) of compound <b>150n</b> .....	514
<b>Figure A4.80</b>	$^{13}\text{C}$ NMR (100 MHz, $\text{CDCl}_3$ ) of compound <b>150n</b> .....	514
<b>Figure A4.81</b>	$^{19}\text{F}$ NMR (282 MHz, $\text{CDCl}_3$ ) of compound <b>150n</b> .....	515
<b>Figure A4.82</b>	$^1\text{H}$ NMR (400 MHz, $\text{CDCl}_3$ ) of compound <b>150o</b> .....	516
<b>Figure A4.83</b>	Infrared spectrum (thin film, NaCl) of compound <b>150o</b> .....	517
<b>Figure A4.84</b>	$^{13}\text{C}$ NMR (100 MHz, $\text{CDCl}_3$ ) of compound <b>150o</b> .....	517
<b>Figure A4.85</b>	$^{19}\text{F}$ NMR (282 MHz, $\text{CDCl}_3$ ) of compound <b>150o</b> .....	518

<b>Figure A4.86</b>	$^1\text{H}$ NMR (400 MHz, $\text{CDCl}_3$ ) of compound <b>150p</b> .....	519
<b>Figure A4.87</b>	Infrared spectrum (thin film, NaCl) of compound <b>150p</b> .....	520
<b>Figure A4.88</b>	$^{13}\text{C}$ NMR (100 MHz, $\text{CDCl}_3$ ) of compound <b>150p</b> .....	520
<b>Figure A4.89</b>	$^{19}\text{F}$ NMR (282 MHz, $\text{CDCl}_3$ ) of compound <b>150p</b> .....	521
<b>Figure A4.90</b>	$^1\text{H}$ NMR (400 MHz, $\text{CDCl}_3$ ) of compound <b>150q</b> .....	522
<b>Figure A4.91</b>	Infrared spectrum (thin film, NaCl) of compound <b>150q</b> .....	523
<b>Figure A4.92</b>	$^{13}\text{C}$ NMR (100 MHz, $\text{CDCl}_3$ ) of compound <b>150q</b> .....	523
<b>Figure A4.93</b>	$^{19}\text{F}$ NMR (282 MHz, $\text{CDCl}_3$ ) of compound <b>150q</b> .....	524
<b>Figure A4.94</b>	$^1\text{H}$ NMR (400 MHz, $\text{CDCl}_3$ ) of compound <b>150r</b> .....	525
<b>Figure A4.95</b>	Infrared spectrum (thin film, NaCl) of compound <b>150r</b> .....	526
<b>Figure A4.96</b>	$^{13}\text{C}$ NMR (100 MHz, $\text{CDCl}_3$ ) of compound <b>150r</b> .....	526
<b>Figure A4.97</b>	$^{19}\text{F}$ NMR (282 MHz, $\text{CDCl}_3$ ) of compound <b>150r</b> .....	527
<b>Figure A4.98</b>	$^1\text{H}$ NMR (400 MHz, $\text{CDCl}_3$ ) of compound <b>150s</b> .....	528
<b>Figure A4.99</b>	Infrared spectrum (thin film, NaCl) of compound <b>150s</b> .....	529
<b>Figure A4.100</b>	$^{13}\text{C}$ NMR (100 MHz, $\text{CDCl}_3$ ) of compound <b>150s</b> .....	529
<b>Figure A4.101</b>	$^{19}\text{F}$ NMR (282 MHz, $\text{CDCl}_3$ ) of compound <b>150s</b> .....	530
<b>Figure A4.102</b>	$^1\text{H}$ NMR (400 MHz, $\text{CDCl}_3$ ) of compound <b>150t</b> .....	531
<b>Figure A4.103</b>	Infrared spectrum (thin film, NaCl) of compound <b>150t</b> .....	532
<b>Figure A4.104</b>	$^{13}\text{C}$ NMR (100 MHz, $\text{CDCl}_3$ ) of compound <b>150t</b> .....	532
<b>Figure A4.105</b>	$^{19}\text{F}$ NMR (282 MHz, $\text{CDCl}_3$ ) of compound <b>150t</b> .....	533
<b>Figure A4.106</b>	$^1\text{H}$ NMR (400 MHz, $\text{CDCl}_3$ ) of compound <b>150u</b> .....	534
<b>Figure A4.107</b>	Infrared spectrum (thin film, NaCl) of compound <b>150u</b> .....	535
<b>Figure A4.108</b>	$^{13}\text{C}$ NMR (100 MHz, $\text{CDCl}_3$ ) of compound <b>150u</b> .....	535



<b>Figure A4.109</b>	$^{19}\text{F}$ NMR (282 MHz, $\text{CDCl}_3$ ) of compound <b>150u</b> .....	536
<b>Figure A4.110</b>	$^1\text{H}$ NMR (400 MHz, $\text{CDCl}_3$ ) of compound <b>150v</b> .....	537
<b>Figure A4.111</b>	Infrared spectrum (thin film, NaCl) of compound <b>150v</b> .....	538
<b>Figure A4.112</b>	$^{13}\text{C}$ NMR (100 MHz, $\text{CDCl}_3$ ) of compound <b>150v</b> .....	538
<b>Figure A4.113</b>	$^{19}\text{F}$ NMR (282 MHz, $\text{CDCl}_3$ ) of compound <b>150v</b> .....	539
<b>Figure A4.114</b>	$^1\text{H}$ NMR (400 MHz, $\text{CDCl}_3$ ) of compound <b>150w</b> .....	540
<b>Figure A4.115</b>	Infrared spectrum (thin film, NaCl) of compound <b>150w</b> .....	541
<b>Figure A4.116</b>	$^{13}\text{C}$ NMR (100 MHz, $\text{CDCl}_3$ ) of compound <b>150w</b> .....	541
<b>Figure A4.117</b>	$^{19}\text{F}$ NMR (282 MHz, $\text{CDCl}_3$ ) of compound <b>150w</b> .....	542
<b>Figure A4.118</b>	$^1\text{H}$ NMR (400 MHz, $\text{CDCl}_3$ ) of compound <b>150x</b> .....	543
<b>Figure A4.119</b>	Infrared spectrum (thin film, NaCl) of compound <b>150x</b> .....	544
<b>Figure A4.120</b>	$^{13}\text{C}$ NMR (100 MHz, $\text{CDCl}_3$ ) of compound <b>150x</b> .....	544
<b>Figure A4.121</b>	$^{19}\text{F}$ NMR (282 MHz, $\text{CDCl}_3$ ) of compound <b>150x</b> .....	545
<b>Figure A4.122</b>	$^1\text{H}$ NMR (400 MHz, $\text{CDCl}_3$ ) of compound <b>148a</b> .....	546
<b>Figure A4.123</b>	Infrared spectrum (thin film, NaCl) of compound <b>148a</b> .....	547
<b>Figure A4.124</b>	$^{13}\text{C}$ NMR (100 MHz, $\text{CDCl}_3$ ) of compound <b>148a</b> .....	547
<b>Figure A4.125</b>	$^{19}\text{F}$ NMR (282 MHz, $\text{CDCl}_3$ ) of compound <b>148a</b> .....	548
<b>Figure A4.126</b>	$^1\text{H}$ NMR (400 MHz, $\text{CDCl}_3$ ) of compound <b>147a</b> .....	549
<b>Figure A4.127</b>	Infrared spectrum (thin film, NaCl) of compound <b>147a</b> .....	550
<b>Figure A4.128</b>	$^{13}\text{C}$ NMR (100 MHz, $\text{CDCl}_3$ ) of compound <b>147a</b> .....	550
<b>Figure A4.129</b>	$^{19}\text{F}$ NMR (282 MHz, $\text{CDCl}_3$ ) of compound <b>147a</b> .....	551
<b>Figure A4.130</b>	$^1\text{H}$ NMR (400 MHz, $\text{CDCl}_3$ ) of compound <b>147b</b> .....	552
<b>Figure A4.131</b>	Infrared spectrum (thin film, NaCl) of compound <b>147b</b> .....	553

<b>Figure A4.132</b>	$^{13}\text{C}$ NMR (100 MHz, $\text{CDCl}_3$ ) of compound <b>147b</b> .....	553
<b>Figure A4.133</b>	$^1\text{H}$ NMR (400 MHz, $\text{CDCl}_3$ ) of compound <b>152</b> .....	554
<b>Figure A4.134</b>	Infrared spectrum (thin film, NaCl) of compound <b>152</b> .....	555
<b>Figure A4.135</b>	$^{13}\text{C}$ NMR (100 MHz, $\text{CDCl}_3$ ) of compound <b>152</b> .....	555
<b>Figure A4.136</b>	$^1\text{H}$ NMR (400 MHz, $\text{CDCl}_3$ ) of compound <b>153</b> .....	556
<b>Figure A4.137</b>	Infrared spectrum (thin film, NaCl) of compound <b>153</b> .....	557
<b>Figure A4.138</b>	$^{13}\text{C}$ NMR (100 MHz, $\text{CDCl}_3$ ) of compound <b>153</b> .....	557
<b>Figure A4.139</b>	$^1\text{H}$ NMR (400 MHz, $\text{CDCl}_3$ ) of compound <b>158</b> .....	558
<b>Figure A4.140</b>	Infrared spectrum (thin film, NaCl) of compound <b>158</b> .....	559
<b>Figure A4.141</b>	$^{13}\text{C}$ NMR (100 MHz, $\text{CDCl}_3$ ) of compound <b>158</b> .....	559
<b>Figure A4.142</b>	$^1\text{H}$ NMR (400 MHz, $\text{CDCl}_3$ ) of compound <b>159/159'</b> .....	560
<b>Figure A4.143</b>	Infrared spectrum (thin film, NaCl) of compound <b>159/159'</b> .....	561
<b>Figure A4.144</b>	$^{13}\text{C}$ NMR (100 MHz, $\text{CDCl}_3$ ) of compound <b>159/159'</b> .....	561
<b>Figure A4.145</b>	$^1\text{H}$ NMR (400 MHz, $\text{CDCl}_3$ ) of compound <b>151</b> .....	562
<b>Figure A4.146</b>	Infrared spectrum (thin film, NaCl) of compound <b>151</b> .....	563
<b>Figure A4.147</b>	$^{13}\text{C}$ NMR (100 MHz, $\text{CDCl}_3$ ) of compound <b>151</b> .....	563
<b>Figure A4.148</b>	$^{19}\text{F}$ NMR (282 MHz, $\text{CDCl}_3$ ) of compound <b>151</b> .....	564

## **APPENDIX 5**

### *X-Ray Crystallography Reports Relevant to Chapter 2*

<b>Figure A5.1.1</b>	X-ray Coordinate of compound <b>151</b> .....	566
----------------------	---	-----

**APPENDIX 6***Progress Toward the Total Synthesis of (-)-Cylindrocyclophane A*

<b>Figure A6.1.1</b>	Representative examples of [7.7]paracyclophane natural products .....	587
<b>Figure A6.1.2</b>	Biological activity of select cylindrocyclophanes .....	588

**APPENDIX 7***Spectra Relevant to Appendix 6*

<b>Figure A7.1</b>	<sup>1</sup> H NMR (400 MHz, CDCl <sub>3</sub> ) of compound <b>SI27</b> .....	698
<b>Figure A7.2</b>	<sup>1</sup> H NMR (400 MHz, CDCl <sub>3</sub> ) of compound <b>202</b> .....	699
<b>Figure A7.3</b>	<sup>1</sup> H NMR (400 MHz, CDCl <sub>3</sub> ) of compound <b>SI29</b> .....	700
<b>Figure A7.4</b>	Infrared spectrum (thin film, NaCl) of compound <b>SI29</b> .....	701
<b>Figure A7.5</b>	<sup>13</sup> C NMR (100 MHz, CDCl <sub>3</sub> ) of compound <b>SI29</b> .....	701
<b>Figure A7.6</b>	<sup>1</sup> H NMR (400 MHz, CDCl <sub>3</sub> ) of compound <b>204</b> .....	702
<b>Figure A7.7</b>	Infrared spectrum (thin film, NaCl) of compound <b>204</b> .....	703
<b>Figure A7.8</b>	<sup>13</sup> C NMR (100 MHz, CDCl <sub>3</sub> ) of compound <b>204</b> .....	703
<b>Figure A7.9</b>	<sup>1</sup> H NMR (400 MHz, CDCl <sub>3</sub> ) of compound <b>199</b> .....	704
<b>Figure A7.10</b>	<sup>13</sup> C NMR (100 MHz, CDCl <sub>3</sub> ) of compound <b>199</b> .....	705
<b>Figure A7.11</b>	<sup>1</sup> H NMR (400 MHz, CDCl <sub>3</sub> ) of compound <b>201</b> .....	706
<b>Figure A7.12</b>	<sup>13</sup> C NMR (100 MHz, CDCl <sub>3</sub> ) of compound <b>201</b> .....	707
<b>Figure A7.13</b>	<sup>19</sup> F NMR (282 MHz, CDCl <sub>3</sub> ) of compound <b>201</b> .....	708
<b>Figure A7.14</b>	<sup>1</sup> H NMR (400 MHz, CDCl <sub>3</sub> ) of compound <b>205</b> .....	709
<b>Figure A7.15</b>	Infrared spectrum (thin film, NaCl) of compound <b>205</b> .....	710
<b>Figure A7.16</b>	<sup>13</sup> C NMR (100 MHz, CDCl <sub>3</sub> ) of compound <b>205</b> .....	710

<b>Figure A7.17</b>	$^{19}\text{F}$ NMR (282 MHz, $\text{CDCl}_3$ ) of compound <b>205</b> .....	711
<b>Figure A7.18</b>	$^1\text{H}$ NMR (400 MHz, $\text{CDCl}_3$ ) of compound <b>206</b> .....	712
<b>Figure A7.19</b>	Infrared spectrum (thin film, NaCl) of compound <b>206</b> .....	713
<b>Figure A7.20</b>	$^{13}\text{C}$ NMR (100 MHz, $\text{CDCl}_3$ ) of compound <b>206</b> .....	713
<b>Figure A7.21</b>	$^{19}\text{F}$ NMR (282 MHz, $\text{CDCl}_3$ ) of compound <b>206</b> .....	714
<b>Figure A7.22</b>	$^1\text{H}$ NMR (400 MHz, $\text{CDCl}_3$ ) of compound <b>SI30</b> .....	715
<b>Figure A7.23</b>	$^1\text{H}$ NMR (400 MHz, $\text{CDCl}_3$ ) of compound <b>207</b> .....	716
<b>Figure A7.24</b>	Infrared spectrum (thin film, NaCl) of compound <b>207</b> .....	717
<b>Figure A7.25</b>	$^{13}\text{C}$ NMR (100 MHz, $\text{CDCl}_3$ ) of compound <b>207</b> .....	717
<b>Figure A7.26</b>	$^{19}\text{F}$ NMR (282 MHz, $\text{CDCl}_3$ ) of compound <b>207</b> .....	718
<b>Figure A7.27</b>	$^1\text{H}$ NMR (400 MHz, $\text{CDCl}_3$ ) of compound <b>208</b> .....	719
<b>Figure A7.28</b>	Infrared spectrum (thin film, NaCl) of compound <b>208</b> .....	720
<b>Figure A7.29</b>	$^{13}\text{C}$ NMR (100 MHz, $\text{CDCl}_3$ ) of compound <b>208</b> .....	720
<b>Figure A7.30</b>	$^{19}\text{F}$ NMR (282 MHz, $\text{CDCl}_3$ ) of compound <b>208</b> .....	721
<b>Figure A7.31</b>	$^1\text{H}$ NMR (400 MHz, $\text{CDCl}_3$ ) of compound <b>209</b> .....	722
<b>Figure A7.32</b>	Infrared spectrum (thin film, NaCl) of compound <b>209</b> .....	723
<b>Figure A7.33</b>	$^{13}\text{C}$ NMR (100 MHz, $\text{CDCl}_3$ ) of compound <b>209</b> .....	723
<b>Figure A7.34</b>	$^{19}\text{F}$ NMR (282 MHz, $\text{CDCl}_3$ ) of compound <b>209</b> .....	724
<b>Figure A7.35</b>	$^1\text{H}$ NMR (400 MHz, $\text{CDCl}_3$ ) of compound <b>211</b> .....	725
<b>Figure A7.36</b>	Infrared spectrum (thin film, NaCl) of compound <b>211</b> .....	726
<b>Figure A7.37</b>	$^{13}\text{C}$ NMR (100 MHz, $\text{CDCl}_3$ ) of compound <b>211</b> .....	726
<b>Figure A7.38</b>	$^{19}\text{F}$ NMR (282 MHz, $\text{CDCl}_3$ ) of compound <b>211</b> .....	727
<b>Figure A7.39</b>	$^1\text{H}$ NMR (400 MHz, $\text{CDCl}_3$ ) of compound <b>SI32</b> .....	728

<b>Figure A7.40</b>	Infrared spectrum (thin film, NaCl) of compound <b>SI32</b> .....	729
<b>Figure A7.41</b>	$^{13}\text{C}$ NMR (100 MHz, $\text{CDCl}_3$ ) of compound <b>SI32</b> .....	729
<b>Figure A7.42</b>	$^{19}\text{F}$ NMR (282 MHz, $\text{CDCl}_3$ ) of compound <b>SI32</b> .....	730
<b>Figure A7.43</b>	$^1\text{H}$ NMR (400 MHz, $\text{CDCl}_3$ ) of compound <b>212</b> .....	731
<b>Figure A7.44</b>	Infrared spectrum (thin film, NaCl) of compound <b>212</b> .....	732
<b>Figure A7.45</b>	$^{13}\text{C}$ NMR (100 MHz, $\text{CDCl}_3$ ) of compound <b>212</b> .....	732
<b>Figure A7.46</b>	$^1\text{H}$ NMR (400 MHz, $\text{CDCl}_3$ ) of compound <b>214</b> .....	733
<b>Figure A7.47</b>	Infrared spectrum (thin film, NaCl) of compound <b>214</b> .....	734
<b>Figure A7.48</b>	$^{13}\text{C}$ NMR (100 MHz, $\text{CDCl}_3$ ) of compound <b>214</b> .....	734
<b>Figure A7.49</b>	$^1\text{H}$ NMR (400 MHz, $\text{CDCl}_3$ ) of compound <b>216</b> .....	735
<b>Figure A7.50</b>	Infrared spectrum (thin film, NaCl) of compound <b>216</b> .....	736
<b>Figure A7.51</b>	$^{13}\text{C}$ NMR (100 MHz, $\text{CDCl}_3$ ) of compound <b>216</b> .....	736
<b>Figure A7.52</b>	$^1\text{H}$ NMR (400 MHz, $\text{CDCl}_3$ ) of compound <b>254</b> .....	737
<b>Figure A7.53</b>	$^1\text{H}$ NMR (400 MHz, $\text{CDCl}_3$ ) of compound <b>218</b> .....	738
<b>Figure A7.54</b>	Infrared spectrum (thin film, NaCl) of compound <b>218</b> .....	739
<b>Figure A7.55</b>	$^{13}\text{C}$ NMR (100 MHz, $\text{CDCl}_3$ ) of compound <b>218</b> .....	739
<b>Figure A7.56</b>	$^1\text{H}$ NMR (400 MHz, $\text{CDCl}_3$ ) of compound <b>219</b> .....	740
<b>Figure A7.57</b>	Infrared spectrum (thin film, NaCl) of compound <b>219</b> .....	741
<b>Figure A7.58</b>	$^{13}\text{C}$ NMR (100 MHz, $\text{CDCl}_3$ ) of compound <b>219</b> .....	741
<b>Figure A7.59</b>	$^1\text{H}$ NMR (400 MHz, $\text{CDCl}_3$ ) of compound <b>220</b> .....	742
<b>Figure A7.60</b>	Infrared spectrum (thin film, NaCl) of compound <b>220</b> .....	743
<b>Figure A7.61</b>	$^{13}\text{C}$ NMR (100 MHz, $\text{CDCl}_3$ ) of compound <b>220</b> .....	743
<b>Figure A7.62</b>	$^1\text{H}$ NMR (400 MHz, $\text{CDCl}_3$ ) of compound <b>SI33</b> .....	744

<b>Figure A7.63</b>	$^{13}\text{C}$ NMR (100 MHz, $\text{CDCl}_3$ ) of compound <b>SI33</b> .....	745
<b>Figure A7.64</b>	$^1\text{H}$ NMR (400 MHz, $\text{CDCl}_3$ ) of compound <b>SI34</b> .....	746
<b>Figure A7.65</b>	$^1\text{H}$ NMR (400 MHz, $\text{CDCl}_3$ ) of compound <b>221</b> .....	747
<b>Figure A7.66</b>	$^{13}\text{C}$ NMR (100 MHz, $\text{CDCl}_3$ ) of compound <b>221</b> .....	748
<b>Figure A7.67</b>	$^1\text{H}$ NMR (400 MHz, $\text{CDCl}_3$ ) of compound <b>223</b> .....	749
<b>Figure A7.68</b>	$^{13}\text{C}$ NMR (100 MHz, $\text{CDCl}_3$ ) of compound <b>223</b> .....	750
<b>Figure A7.69</b>	$^1\text{H}$ NMR (400 MHz, $\text{CDCl}_3$ ) of compound <b>224</b> .....	751
<b>Figure A7.70</b>	$^1\text{H}$ NMR (400 MHz, $\text{CDCl}_3$ ) of compound <b>225</b> .....	752
<b>Figure A7.71</b>	$^1\text{H}$ NMR (400 MHz, $\text{CDCl}_3$ ) of compound <b>227</b> .....	753
<b>Figure A7.72</b>	$^{13}\text{C}$ NMR (100 MHz, $\text{CDCl}_3$ ) of compound <b>227</b> .....	754
<b>Figure A7.73</b>	$^1\text{H}$ NMR (400 MHz, $\text{CDCl}_3$ ) of compound <b>231</b> .....	755
<b>Figure A7.74</b>	$^{13}\text{C}$ NMR (100 MHz, $\text{CDCl}_3$ ) of compound <b>231</b> .....	756
<b>Figure A7.75</b>	$^1\text{H}$ NMR (400 MHz, $\text{CDCl}_3$ ) of compound <b>SI32</b> .....	757
<b>Figure A7.76</b>	$^1\text{H}$ NMR (400 MHz, $\text{CDCl}_3$ ) of compound <b>235</b> .....	758
<b>Figure A7.77</b>	$^{13}\text{C}$ NMR (100 MHz, $\text{CDCl}_3$ ) of compound <b>235</b> .....	759
<b>Figure A7.78</b>	$^1\text{H}$ NMR (400 MHz, $\text{CDCl}_3$ ) of compound <b>236</b> .....	760
<b>Figure A7.79</b>	$^1\text{H}$ NMR (400 MHz, $\text{CDCl}_3$ ) of compound <b>239</b> .....	761
<b>Figure A7.80</b>	$^{13}\text{C}$ NMR (100 MHz, $\text{CDCl}_3$ ) of compound <b>239</b> .....	762
<b>Figure A7.81</b>	$^1\text{H}$ NMR (400 MHz, $\text{CDCl}_3$ ) of compound <b>238</b> .....	763
<b>Figure A7.82</b>	$^{13}\text{C}$ NMR (100 MHz, $\text{CDCl}_3$ ) of compound <b>238</b> .....	764
<b>Figure A7.83</b>	$^1\text{H}$ NMR (400 MHz, $\text{CDCl}_3$ ) of compound <b>283</b> .....	765
<b>Figure A7.84</b>	$^1\text{H}$ NMR (400 MHz, $\text{CDCl}_3$ ) of compound <b>SI35</b> .....	766
<b>Figure A7.85</b>	$^1\text{H}$ NMR (400 MHz, $\text{CDCl}_3$ ) of compound <b>261</b> .....	767

<b>Figure A7.86</b>	$^{13}\text{C}$ NMR (100 MHz, $\text{CDCl}_3$ ) of compound <b>261</b> .....	768
<b>Figure A7.87</b>	$^1\text{H}$ NMR (400 MHz, $\text{CDCl}_3$ ) of compound <b>241</b> .....	769
<b>Figure A7.88</b>	$^{13}\text{C}$ NMR (100 MHz, $\text{CDCl}_3$ ) of compound <b>241</b> .....	770
<b>Figure A7.89</b>	$^1\text{H}$ NMR (400 MHz, $\text{CDCl}_3$ ) of compound <b>248</b> .....	771
<b>Figure A7.90</b>	$^1\text{H}$ NMR (400 MHz, $\text{CDCl}_3$ ) of compound <b>245</b> .....	772
<b>Figure A7.91</b>	$^1\text{H}$ NMR (400 MHz, $\text{CDCl}_3$ ) of compound <b>249</b> .....	773
<b>Figure A7.92</b>	$^1\text{H}$ NMR (400 MHz, $\text{CDCl}_3$ ) of compound <b>250 (major)</b> .....	774
<b>Figure A7.93</b>	$^1\text{H}$ NMR (400 MHz, $\text{CDCl}_3$ ) of compound <b>250 (minor)</b> .....	775
<b>Figure A7.94</b>	$^1\text{H}$ NMR (400 MHz, $\text{CDCl}_3$ ) of compound <b>252 (major)</b> .....	776
<b>Figure A7.95</b>	$^1\text{H}$ NMR (400 MHz, $\text{CDCl}_3$ ) of compound <b>252 (minor)</b> .....	777
<b>Figure A7.96</b>	$^1\text{H}$ NMR (400 MHz, $\text{CDCl}_3$ ) of compound <b>245/253</b> .....	778
<b>Figure A7.97</b>	$^1\text{H}$ NMR (400 MHz, $\text{CDCl}_3$ ) of compound <b>255</b> .....	779
<b>Figure A7.98</b>	$^1\text{H}$ NMR (400 MHz, $\text{CDCl}_3$ ) of compound <b>256</b> .....	780
<b>Figure A7.99</b>	$^1\text{H}$ NMR (400 MHz, $\text{CDCl}_3$ ) of compound <b>257</b> .....	781
<b>Figure A7.100</b>	$^1\text{H}$ NMR (400 MHz, $\text{CDCl}_3$ ) of compound <b>261</b> .....	782
<b>Figure A7.101</b>	$^1\text{H}$ NMR (400 MHz, $\text{CDCl}_3$ ) of compound <b>262</b> .....	783
<b>Figure A7.102</b>	$^1\text{H}$ NMR (400 MHz, $\text{CDCl}_3$ ) of compound <b>263</b> .....	784
<b>Figure A7.103</b>	$^1\text{H}$ NMR (400 MHz, $\text{CDCl}_3$ ) of compound <b>264</b> .....	785
<b>Figure A7.104</b>	$^1\text{H}$ NMR (400 MHz, $\text{CDCl}_3$ ) of compound <b>265</b> .....	786
<b>Figure A7.105</b>	$^1\text{H}$ NMR (400 MHz, $\text{CDCl}_3$ ) of compound <b>267</b> .....	787
<b>Figure A7.106</b>	$^1\text{H}$ NMR (400 MHz, $\text{CDCl}_3$ ) of compound <b>272</b> .....	788
<b>Figure A7.107</b>	$^{13}\text{C}$ NMR (100 MHz, $\text{CDCl}_3$ ) of compound <b>272</b> .....	789
<b>Figure A7.108</b>	$^1\text{H}$ NMR (400 MHz, $\text{CDCl}_3$ ) of compound <b>290</b> .....	790

<b>Figure A7.109</b>	$^{13}\text{C}$ NMR (100 MHz, $\text{CDCl}_3$ ) of compound <b>290</b> .....	791
<b>Figure A7.110</b>	$^1\text{H}$ NMR (400 MHz, $\text{CDCl}_3$ ) of compound <b>291</b> .....	792
<b>Figure A7.111</b>	$^{13}\text{C}$ NMR (100 MHz, $\text{CDCl}_3$ ) of compound <b>291</b> .....	793
<b>Figure A7.112</b>	$^1\text{H}$ NMR (400 MHz, $\text{CDCl}_3$ ) of compound <b>281</b> .....	794
<b>Figure A7.113</b>	$^1\text{H}$ NMR (400 MHz, $\text{CDCl}_3$ ) of compound <b>295</b> .....	795
<b>Figure A7.114</b>	$^{13}\text{C}$ NMR (100 MHz, $\text{CDCl}_3$ ) of compound <b>295</b> .....	796
<b>Figure A7.115</b>	$^1\text{H}$ NMR (400 MHz, $\text{CDCl}_3$ ) of compound <b>297</b> .....	797
<b>Figure A7.116</b>	$^1\text{H}$ NMR (400 MHz, $\text{CDCl}_3$ ) of compound <b>286/287</b> .....	798
<b>Figure A7.117</b>	$^{13}\text{C}$ NMR (100 MHz, $\text{CDCl}_3$ ) of compound <b>286/287</b> .....	799
<b>Figure A7.118</b>	$^1\text{H}$ NMR (400 MHz, $\text{CDCl}_3$ ) of compound <b>234</b> .....	800
<b>Figure A7.119</b>	$^{13}\text{C}$ NMR (100 MHz, $\text{CDCl}_3$ ) of compound <b>234</b> .....	801

## **APPENDIX 8**

### *X-Ray Crystallography Reports Relevant to Appendix 6*

<b>Figure A8.1.1</b>	X-Ray Crystal Structure of Macrocycle <b>S131</b> .....	804
<b>Figure A8.1.2</b>	The asymmetric unit of compound <b>S131</b> .....	809
<b>Figure A8.2.1</b>	X-Ray Crystal Structure of Macrocycle <b>208</b> .....	826
<b>Figure A8.2.2</b>	The asymmetric unit of Macrocycle <b>208</b> .....	831
<b>Figure A8.2.3</b>	The disorder model of Macrocycle <b>208</b> .....	831
<b>Figure A8.3.1</b>	X-Ray Crystal structure of Macrocycle <b>212</b> .....	858
<b>Figure A8.3.2</b>	The asymmetric unit of Macrocycle <b>212</b> .....	863



## LIST OF SCHEMES

### CHAPTER 1

#### *Diastereoselective Direct Mannich Reaction of $\alpha$ -Substituted- $\gamma$ -Lactams*

- Scheme 1.1.1** First reports of the asymmetric Mannich reaction ..... 3
- Scheme 1.1.2** First catalytic asymmetric Mannich reaction and select examples of Kobayashi's bisbinaphthol Zr(IV) catalyst system..... 4
- Scheme 1.1.3** Proline catalyzed asymmetric direct Mannich reaction using ketone and aldehyde pronucleophiles..... 6
- Scheme 1.1.4** Summary of pro-nucleophiles reported in asymmetric, catalytic Mannich reactions that form all-carbon quaternary centers..... 7
- Scheme 1.1.5** Catalytic asymmetric Mannich reactions of  $\alpha$ -substituted ketones and  $\alpha$ -substituted aldehydes catalyzed by Trost's Zn-prophenol catalyst ..... 8
- Scheme 1.1.6** Catalytic stereoselective Mannich reactions of  $\alpha$ -substituted carbonyl pro-nucleophiles in the carboxylic acid oxidation state ..... 9
- Scheme 1.1.7** Summary of stereoselective Mannich reactions of amide pro-nucleophiles..... 11
- Scheme 1.2.1** Stoltz Ni-catalyzed asymmetric acylation of  $\alpha$ -substituted- $\gamma$ -lactam nucleophiles with aryl nitriles ..... 13

<b>Scheme 1.2.2</b>	Initial investigation into the stereoselective Mannich reaction .....	15
<b>Scheme 1.2.3</b>	Investigating the Ni-catalyzed Mannich reaction using an $\alpha$ - methyl- $\gamma$ -substituted lactam nucleophiles .....	16
<b>Scheme 1.2.4</b>	Influence of temperature on the desired Mannich reaction .....	17
<b>Scheme 1.2.5</b>	Mannich reaction using <i>N</i> -TMS imine electrophile <b>65</b> .....	17
<b>Scheme 1.2.6</b>	Influence of base and Lewis acid additives on the Mannich reaction .....	18
<b>Scheme 1.2.7</b>	Discovery of the <i>KOt</i> -Bu promoted diastereoselective Mannich reaction .....	19
<b>Scheme 1.3.1</b>	Screen of Mannich product stability with Lewis Acid Additives .....	20
<b>Scheme 1.3.2</b>	Representative temperature screen of the diastereoselective Mannich reaction and scale-up result.....	21
<b>Scheme 1.3.3</b>	Preliminary scope of $\alpha$ -substitution of the $\gamma$ -lactam pro-nucleophile.....	22
<b>Scheme 1.4.1</b>	Aza-Peterson olefination of benzaldehyde to access imine <b>65</b> .....	23
<b>Scheme 1.4.2</b>	Catalytic hydrosilylation of aryl nitriles to access <i>N</i> -silyl imines <b>76</b> .....	24

<b>Scheme 1.5.1</b>	Comparison of telescoped diastereoselective Mannich reaction to the first-generation approach.....	27
<b>Scheme 1.5.2</b>	Scope of tandem reaction using imine <b>76ab</b> as the electrophile .....	28
<b>Scheme 1.5.3</b>	Substrate scope of $\alpha$ -substituted- $\gamma$ -lactam pro-nucleophiles <b>68</b> .....	29
<b>Scheme 1.5.4</b>	Diastereoselective synthesis of Mannich bases bearing stereotriads .....	30
<b>Scheme 1.5.5</b>	Substrate Scope of aryl nitrile pro-electrophiles <b>74</b> .....	32
<b>Scheme 1.6.1</b>	Computational analysis of transition states leading to major and minor diastereomers of the Mannich reaction .....	35
<b>Scheme 1.6.2</b>	Extension of the computed major transition state .....	38
<b>Scheme 1.6.3</b>	Determination of the relative configuration of Mannich product <b>69ja</b> .....	39
<b>Scheme 1.7.1</b>	Discovery of the KO $t$ -Bu catalyzed diastereoselective Mannich reaction .....	40
<b>Scheme 1.7.2</b>	Proposed catalytic cycle of the diastereoselective Mannich reaction .....	41
<b>Scheme 1.8.1</b>	Protecting group manipulation of the Mannich products.....	42
<b>Scheme 1.8.2</b>	Ring-Closing-Metathesis approach to form spirocycle <b>92</b> .....	42
<b>Scheme 1.8.3</b>	Intramolecular Pd-catalyzed carboamination to form	

	spirocycles <b>94</b> and <b>95</b> .....	43
<b>Scheme 1.8.4</b>	Intramolecular Pd-catalyzed Buchwald-Hartwig amination to form spirocycle <b>96</b> .....	44
<b>Scheme 1.8.5</b>	Failed attempts at intramolecular halo-amination of product <b>69da</b> .....	45
<b>Scheme 1.8.6</b>	Failed attempts at intramolecular cyclization following olefin oxidation of $\beta$ -amino lactam <b>69da</b> .....	46
<b>Scheme 1.8.7</b>	Intermolecular Pd-catalyzed cross-coupling reactions of aryl bromide substituted $\beta$ -amino lactam products .....	47

## **CHAPTER 2**

### *Enantioselective Dearomative Allylic Alkylation of Pyridines*

<b>Scheme 2.1.1</b>	Approaches toward the dearomative functionalization of pyridines.....	348
<b>Scheme 2.1.2</b>	Proposed transformation featuring a telescoped dearomative hydrosilylation, asymmetric allylic alkylation of pyridines .....	349
<b>Scheme 2.1.3</b>	Dearomative asymmetric allylic alkylation of electron-rich arenes.....	350
<b>Scheme 2.1.4</b>	Dearomative asymmetric allylic alkylation using inherent nucleophilicity of arenes .....	351
<b>Scheme 2.1.5</b>	Asymmetric allylic alkylation reaction of enamine nucleophiles.....	352

<b>Scheme 2.1.6</b>	Proposed transformation to deliver chiral tetrahydropyridine products .....	353
<b>Scheme 2.2.1</b>	Chang et al. Ir-catalyzed 1,2-hydrosilylation of pyridines <b>142</b> .....	354
<b>Scheme 2.3.1</b>	Pyridine pro-nucleophile scope of the enantioselective allylic alkylation.....	361
<b>Scheme 2.3.2</b>	Outcome of the pyridine asymmetric allylic alkylation using electron-poor pyridine substrates.....	362
<b>Scheme 2.3.3</b>	Outcome of the pyridine asymmetric allylic alkylation using electron-rich pyridine substrates.....	363
<b>Scheme 2.3.4</b>	Outcome of the pyridine asymmetric allylic alkylation using electron-rich pyridine substrates using higher catalyst loadings.....	364
<b>Scheme 2.3.5</b>	Carbonate electrophile scope of the enantioselective allylic alkylation .....	365
<b>Scheme 2.3.6</b>	Mixed pyridine control experiment .....	366
<b>Scheme 2.4.1</b>	X-ray crystallization of derivatized tetrahydropyridine product <b>151</b> .....	367
<b>Scheme 2.4.2</b>	Divergent cross-coupling methods of vinyl halide product.....	368
<b>Scheme 2.4.3</b>	Synthesis of chiral N–H tetrahydropyridine products .....	368

<b>Scheme 2.5.1</b>	Proposed mechanism for the formation of the observed products .....	369
---------------------	---	-----

<b>Scheme 2.6.1</b>	Scope of bisalkylated products and RCM derivatization .....	372
---------------------	---	-----

## **APPENDIX 6**

### *Progress Toward the Total Synthesis of (-)-Cylindrocyclophane A*

<b>Scheme A6.1.1</b>	Proposed biosynthesis toward (-)-cylindrocyclophane F (165).....	589
----------------------	--	-----

<b>Scheme A6.1.2</b>	Hoye's total synthesis of (-)-cylindrocyclophane A (175) .....	591
----------------------	--	-----

<b>Scheme A6.1.3</b>	Smith's total synthesis of (-)-cylindrocyclophane A (175).....	592
----------------------	--	-----

<b>Scheme A6.1.4</b>	Nicolaou's total synthesis of (-)-cylindrocyclophane A (175) ...	593
----------------------	--	-----

<b>Scheme A6.2.1</b>	Summary of strategies and our generalized C–H functionalization macrocyclization sequence.....	594
----------------------	--	-----

<b>Scheme A6.2.2</b>	Validation of Rh-catalyzed selective C–H insertion as a macrocyclization strategy using a model system .....	597
----------------------	--	-----

<b>Scheme A6.2.3</b>	Forward synthesis to elaborate phenyl acetic acid derivative <b>202</b> to chiral macrocycle <b>208</b> using various C–H functionalization reactions.....	598
----------------------	--	-----

<b>Scheme A6.2.4</b>	Elaboration of macrocycle to key hexa-acetylated intermediate <b>216</b> .....	600
----------------------	--	-----

<b>Scheme A6.3.1</b>	Elaboration of key intermediate <b>216</b> toward (-)-cylindrocyclophane A (175) and synthesis of truncated model	
----------------------	---	--

	Weinreb amide <b>220</b> .....	602
<b>Scheme A6.3.2</b>	Outcome of hydrolysis of model Weinreb amide <b>220</b> .....	603
<b>Scheme A6.3.3</b>	Unexpected Lewis acid promoted deacetylation/lactone formation of model Weinreb amide <b>220</b> and macrocycle <b>216</b> .....	604
<b>Scheme A6.3.4</b>	Undesired transformations of Weinreb amide <b>220</b> utilizing Ir-catalyzed or $\text{BF}_3 \cdot \text{OEt}_2$ promoted hydrosilylation strategies .	604
<b>Scheme A6.3.5</b>	Treatment of model Weinreb amide <b>220</b> with <i>n</i> -PrMgCl .....	605
<b>Scheme A6.4.1</b>	Phenol selective methylation followed by attempted diazo decomposition strategy from model ketone <b>234/235</b> .....	607
<b>Scheme A6.4.2</b>	Summary of desulfurization strategies to convert ketone <b>239</b> to desired alkane <b>245</b> .....	609
<b>Scheme A6.4.3</b>	Summary of alcohol deoxygenation strategies to elaborate model ketone <b>239</b> to desired alkane <b>245</b> .....	610
<b>Scheme A6.5.1</b>	Failed Appel reaction of diol <b>257</b> synthesized from key macrocyclic intermediate <b>216</b> .....	612
<b>Scheme A6.5.2</b>	Detrimental benzylic silyl ether elimination of <b>262</b> promoted via Appel reaction conditions .....	613
<b>Scheme A6.5.3</b>	Formation of styrene <b>264</b> from Appel reaction of model diol <b>266</b> .....	614
<b>Scheme A6.6.1</b>	Proposed radical deoxygenation sequence to deliver alkane <b>270</b> or (-)-cylindrocyclophane F ( <b>165</b> ) from synthesized macrocyclic	

	intermediates .....	615
<b>Scheme A6.6.2</b>	Barton-McCombie type deoxygenation of model alcohol <b>250</b> to alkane <b>245</b> .....	616
<b>Scheme A6.6.3</b>	Proposed strategy to synthesize alkane <b>245</b> through an exhaustive reduction of enol triflate <b>276</b> to <b>278</b> .....	617
<b>Scheme A6.6.4</b>	Synthesis of alkane <b>245</b> through an AlH <sub>3</sub> promoted propargylic alcohol deoxygenation/allene reduction sequence .....	619
<b>Scheme A6.7.1</b>	Proposed model substrate for endgame deoxygenation .....	621
<b>Scheme A6.7.2</b>	Modeling the endgame deoxygenation from both allene reduction and Barton-McCombie type deoxygenation .....	622



## LIST OF TABLES

### **APPENDIX 2**

#### *Computational Reports for Chapter 1*

<b>Table A2.1.1</b>	Computational details for the diastereoselective Mannich reaction .....	262
<b>Table A2.1.2</b>	Cartesian coordinates and energies of all optimized structures and imaginary frequencies of transition states .....	265
<b>Table A2.1.3</b>	Computed cartesian coordinates of compounds .....	266

### **APPENDIX 3**

#### *X-Ray Crystallography Reports for Chapter 1*

<b>Table A3.1.1</b>	Experimental Details for X-Ray Structure Determination of Amine <b>69dn</b> .....	294
<b>Table A3.1.2</b>	Crystal Data and Structure Refinement for Amine <b>69dn</b> .....	295
<b>Table A3.1.3</b>	Atomic Coordinates ( $\times 10^4$ ) and Equivalent Isotropic Displacement Parameters ( $\text{\AA}^2 \times 10^3$ ) for Amine <b>69dn</b> U(eq) is Defined as One Third of the Orthogonalized $U^{ij}$ Tensor .....	296
<b>Table A3.1.4</b>	Bond Lengths [ $\text{\AA}$ ] and angles [ $^\circ$ ] for Amine <b>69dn</b> .....	297
<b>Table A3.1.5</b>	Anisotropic Displacement Parameters ( $\text{\AA}^2 \times 10^3$ ) for Amine <b>69dn</b> . The Anisotropic Displacement Factor Exponent Takes the Form: $-2p^2[h^2a^*2U^{11} + \dots + 2hka^*b^*U^{12}]$ .....	302

<b>Table A3.1.6</b>	Hydrogen Coordinates ( $\times 10^4$ ) and Isotropic Displacement Parameters ( $\text{\AA}^2 \times 10^3$ ) for Amine <b>69dn</b> .....	303
<b>Table A3.1.7</b>	Torsion Angles [ $^\circ$ ] for Amine <b>69dn</b> .....	304
<b>Table A3.1.8</b>	Hydrogen Bonds for Amine <b>69dn</b> [ $\text{\AA}$ and $^\circ$ ].....	306
<b>Table A3.2.1</b>	Experimental Details for X-Ray Structure Determination of Imine <b>80</b> .....	308
<b>Table A3.2.2</b>	Crystal Data and Structure Refinement for Imine <b>80</b> .....	309
<b>Table A3.2.3</b>	Atomic Coordinates ( $\times 10^4$ ) and Equivalent Isotropic Displacement Parameters ( $\text{\AA}^2 \times 10^3$ ) for Imine <b>80</b> . $U(\text{eq})$ is Defined as One Third of the Orthogonalized $U^{ij}$ Tensor.....	310
<b>Table A3.2.4</b>	Bond Lengths [ $\text{\AA}$ ] and angles [ $^\circ$ ] for Imine <b>80</b> .....	313
<b>Table A3.2.5</b>	Anisotropic Displacement Parameters ( $\text{\AA}^2 \times 10^3$ ) for Imine <b>80</b> . The Anisotropic Displacement Factor Exponent Takes the Form: $-2p^2[h^2a^2U^{11} + \dots + 2hka^*b^*U^{12}]$ .....	323
<b>Table A3.2.6</b>	Hydrogen Coordinates ( $\times 10^4$ ) and Isotropic Displacement Parameters ( $\text{\AA}^2 \times 10^3$ ) for Imine <b>80</b> .....	326
<b>Table A3.2.7</b>	Torsion Angles [ $^\circ$ ] for Imine <b>80</b> .....	328
<b>Table A3.3.1</b>	Experimental Details for X-Ray Structure Determination of Imine <b>70</b> .....	333
<b>Table A3.3.2</b>	Crystal Data and Structure Refinement for Imine <b>70</b> .....	334

<b>Table A3.3.3</b>	Atomic Coordinates ( $\times 10^4$ ) and Equivalent Isotropic Displacement Parameters ( $\text{\AA}^2 \times 10^3$ ) for Imine <b>70</b> . $U(\text{eq})$ is Defined as One Third of the Orthogonalized $U^{ij}$ Tensor.....	335
<b>Table A3.3.4</b>	Bond Lengths [ $\text{\AA}$ ] and angles [ $^\circ$ ] for Imine <b>70</b> .....	337
<b>Table A3.3.5</b>	Anisotropic Displacement Parameters ( $\text{\AA}^2 \times 10^3$ ) for Imine <b>70</b> . The Anisotropic Displacement Factor Exponent Takes the Form: $-2p^2[h^2a^*2U^{11} + \dots + 2hka^*b^*U^{12}]$ .....	342
<b>Table A3.3.6</b>	Hydrogen Coordinates ( $\times 10^4$ ) and Isotropic Displacement Parameters ( $\text{\AA}^2 \times 10^3$ ) for Imine <b>70</b> .....	344
<b>Table A3.3.7</b>	Torsion Angles [ $^\circ$ ] for Imine <b>70</b> .....	345

## CHAPTER 2

### *Enantioselective Dearomative Allylic Alkylation of Pyridines*

<b>Table 2.2.1</b>	Ligand optimization screen of the dearomatization/asymmetric allylic alkylation of 3-fluoropyridine <b>142a</b> .....	355
<b>Table 2.2.2</b>	Solvent optimization screen of the dearomatization/asymmetric allylic alkylation of 3-fluoropyridine <b>142a</b> .....	357
<b>Table 2.2.3</b>	Pd-catalyst screen of the dearomatization/asymmetric allylic alkylation of 3-fluoropyridine <b>142a</b> .....	358
<b>Table 2.2.4</b>	Additive screen of the dearomatization/asymmetric allylic alkylation of 3-fluoropyridine <b>142a</b> .....	359

<b>Table 2.2.5</b>	Catalyst loading screen of the dearomatization/asymmetric allylic alkylation of 3-fluoropyridine <b>142a</b> .....	360
<b>Table 2.6.1</b>	Alkylating reagents screen of the dearomative allylic alkylation ....	360

## **APPENDIX 5**

### *X-Ray Crystallography Reports for Chapter 2*

<b>Table A5.1.1</b>	Experimental Details for X-Ray Structure Determination of Amide <b>151</b> .....	567
<b>Table A5.1.2</b>	Crystal Data and Structure Refinement for compound <b>151</b> .....	568
<b>Table A5.1.3</b>	Atomic coordinates ( $\times 10^4$ ) and equivalent isotropic displacement parameters ( $\text{\AA}^2 10^3$ ) for compound <b>151</b> . $U(\text{eq})$ is defined as one third of the trace of the orthogonalized $U^{ij}$ tensor.....	569
<b>Table A5.1.4</b>	Bond Lengths [ $\text{\AA}$ ] and angles [ $^\circ$ ] for compound <b>151</b> .....	571
<b>Table A5.1.5</b>	Anisotropic displacement parameters ( $\text{\AA}^2 \times 10^3$ ) for compound <b>151</b> . The anisotropic displacement factor exponent takes the form: $-2\pi^2 [ h^2 a^{*2} U^{11} + \dots + 2 h k a^* b^* U^{12} ]$ .....	579
<b>Table A5.1.6</b>	Hydrogen Coordinates ( $\times 10^4$ ) and Isotropic Displacement Parameters ( $\text{\AA}^2 \times 10^3$ ) for compound <b>151</b> .....	581
<b>Table A5.1.7</b>	Torsion Angles [ $^\circ$ ] for compound <b>151</b> .....	583

**APPENDIX 8***X-Ray Crystallography Reports for Appendix 6*

<b>Table A8.1.1</b>	Experimental Details for X-Ray Structure Determination of Macrocycle <b>SI31</b> .....	805
<b>Table A8.1.2</b>	Crystal Data and Structure Refinement for Macrocycle <b>SI31</b> .....	806
<b>Table A8.1.3</b>	Reflection Statistics .....	810
<b>Table A8.1.4</b>	Fractional Atomic Coordinates ( $\times 10^4$ ) and Equivalent Isotropic Displacement Parameters ( $\text{\AA}^2 \times 10^3$ ) for Macrocycle <b>SI31</b> . $U_{eq}$ is defined as 1/3 of the trace of the orthogonalized $U_{ij}$ .....	811
<b>Table A8.1.5</b>	Bond Lengths [ $\text{\AA}$ ] and Angles [ $^\circ$ ] for Macrocycle <b>SI31</b> .....	813
<b>Table A8.1.6</b>	Anisotropic Displacement Parameters ( $\text{\AA}^2 \times 10^3$ ) for Macrocycle <b>SI31</b> . The Anisotropic Displacement Factor Exponent Takes the Form: $-2p^2[h^2a^*2U^{11} + \dots + 2hka^*b^*U^{12}]$ . .....	815
<b>Table A8.1.7</b>	Hydrogen Coordinates ( $\times 10^4$ ) and Isotropic Displacement Parameters ( $\text{\AA}^2 \times 10^3$ ) for Macrocycle <b>SI31</b> .....	817
<b>Table A8.1.8</b>	Bonds Angles [ $^\circ$ ] for Macrocycle <b>SI31</b> .....	819
<b>Table A8.1.9</b>	Torsion Angles [ $^\circ$ ] for Macrocycle <b>SI31</b> .....	822
<b>Table A8.2.1</b>	Experimental Details for X-Ray Structure Determination of Macrocycle <b>208</b> .....	827
<b>Table A8.2.2</b>	Crystal Data and Structure Refinement for Macrocycle <b>208</b> .....	828
<b>Table A8.2.3</b>	Reflection Statistics .....	832

<b>Table A8.2.4</b>	Fractional Atomic Coordinates ( $\times 10^4$ ) and Equivalent Isotropic Displacement Parameters ( $\text{\AA}^2 \times 10^3$ ) for Macrocycle <b>208</b> . $U_{eq}$ is defined as 1/3 of the trace of the orthogonalized $U_{ij}$ .....	833
<b>Table A8.2.5</b>	Bond Lengths [ $\text{\AA}$ ] and Angles [ $^\circ$ ] for Macrocycle <b>208</b> .....	836
<b>Table A8.2.6</b>	Anisotropic Displacement Parameters ( $\text{\AA}^2 \times 10^3$ ) for Macrocycle <b>208</b> . The Anisotropic Displacement Factor Exponent Takes the Form: $-2p^2[h^2a^*2U^{11} + \dots + 2hka^*b^*U^{12}]$ . .....	839
<b>Table A8.2.7</b>	Hydrogen Coordinates ( $\times 10^4$ ) and Isotropic Displacement Parameters ( $\text{\AA}^2 \times 10^3$ ) for Macrocycle <b>208</b> .....	842
<b>Table A8.2.8</b>	Bonds Angles [ $^\circ$ ] for Macrocycle <b>208</b> .....	844
<b>Table A8.2.9</b>	Torsion Angles [ $^\circ$ ] for Macrocycle <b>208</b> .....	849
<b>Table A8.2.10</b>	Atomic Occupancies for all atoms that are not fully occupied in Macrocycle <b>208</b> .....	854
<b>Table A8.3.1</b>	Experimental Details for X-Ray Structure Determination of Macrocycle <b>212</b> .....	859
<b>Table A8.3.2</b>	Crystal Data and Structure Refinement for Macrocycle <b>212</b> .....	860
<b>Table A8.3.3</b>	Reflection Statistics .....	864
<b>Table A8.3.4</b>	Fractional Atomic Coordinates ( $\times 10^4$ ) and Equivalent Isotropic Displacement Parameters ( $\text{\AA}^2 \times 10^3$ ) for Macrocycle <b>212</b> . $U_{eq}$ is defined as 1/3 of the trace of the orthogonalized $U_{ij}$ .....	865
<b>Table A8.3.5</b>	Bond Lengths [ $\text{\AA}$ ] and Angles [ $^\circ$ ] for Macrocycle <b>212</b> .....	867

<b>Table A8.3.6</b>	Anisotropic Displacement Parameters ( $\text{\AA}^2 \times 10^3$ ) for Macrocycle <b>212</b> . The Anisotropic Displacement Factor Exponent Takes the Form: $-2p^2[h^2a^*2U^{11} + \dots + 2hka^*b^*U^{12}]$ . .....	869
<b>Table A8.3.7</b>	Hydrogen Coordinates ( $\times 10^4$ ) and Isotropic Displacement Parameters ( $\text{\AA}^2 \times 10^3$ ) for Macrocycle <b>212</b> .....	871
<b>Table A8.3.8</b>	Bonds Angles [ $^\circ$ ] for Macrocycle <b>212</b> .....	873
<b>Table A8.3.9</b>	Torsion Angles [ $^\circ$ ] for Macrocycle <b>212</b> .....	875
<b>Table A8.3.10</b>	Hydrogen Bond Information for Macrocycle <b>212</b> .....	877
<b>Table A8.3.11</b>	Atomic Occupancies for all atoms that are not fully occupied in Macrocycle <b>212</b> .....	878

**LIST OF ABBREVIATIONS**

$[\alpha]_D$	specific rotation at wavelength of sodium D line
$^{\circ}\text{C}$	degrees Celcius
Å	Ångstrom
app	apparent
aq	aqueous
Ar	aryl
atm	atmosphere
Bn	benzyl
bp	boiling point
br	broad
<i>c</i>	concentration for specific rotation measurements
calc'd	calculated
$\text{cm}^{-1}$	wavenumber(s)
d	doublet
D	deuterium
DIC	N,N'-diisopropylcarbodiimide



DDQ	2,3-dichloro-5,6-dicyano- <i>p</i> -benzoquinone
DMAP	4-dimethylaminopyridine
DMF	dimethylformamide
DMS	dimethylsulfide
dr	diastereomeric ratio
EDC	<i>N</i> -(3-dimethylaminopropyl)- <i>N</i> '-ethylcarbodiimide
ee	enantiomeric excess
EI+	electron impact
equiv	equivalent(s)
ESI	electrospray ionization
Et	ethyl
EtOAc	ethyl acetate
FAB	fast atom bombardment
g	gram(s)
h	hour(s)
HG-II	Hoveyda–Grubbs catalyst 2 <sup>nd</sup> generation
HPLC	high-performance liquid chromatography

HRMS	high-resolution mass spectrometry
Hz	hertz
<i>i</i> -Bu	<i>iso</i> -butyl
IR	infrared (spectroscopy)
<i>J</i>	coupling constant
K	Kelvin (absolute temperature)
kcal	kilocalorie
KHMDS	potassium hexamethyldisilazide
L	liter; ligand
LDA	lithium diisopropylamide
m	multiplet, milli
<i>m</i>	meta
<i>m/z</i>	mass to charge ratio
Me	methyl
mg	milligram(s)
MHz	megahertz
min	minute(s)

mol	mole(s)
mp	melting point
n	nano
<i>n</i> -Bu	<i>n</i> -butyl
NBS	<i>N</i> -bromosuccimide
NMR	nuclear magnetic resonance
NPhth	phthalimide
Nu	nucleophile
<i>o</i>	ortho
<i>p</i>	para
Pd/C	palladium on carbon
Ph	phenyl
pH	hydrogen ion concentration in aqueous solution
PHOX	phosphinooxazoline
ppm	parts per million
Pr	propyl

q	quartet
R	generic for any atom or functional group
Ref.	reference
$R_f$	retention factor
s	singlet
sat.	saturated
t	triplet
<i>t</i> -Bu	<i>tert</i> -butyl
TBAF	tetrabutylammonium fluoride
TBS	<i>tert</i> -butyldimethylsilyl
TES	triethylsilyl
THF	tetrahydrofuran
TLC	thin-layer chromatography
TMS	trimethylsilyl
$t_R$	retention time
UV	ultraviolet
$v/v$	volume to volume

w/v weight to volume

$\lambda$  wavelength

$\mu$  micro

## **CHAPTER 1**

### *Diastereoselective Direct Mannich Reaction of $\alpha$ -Substituted- $\gamma$ -lactams and aryl N-silyl imines<sup>†</sup>*

#### **1.1 INTRODUCTION**

The Mannich reaction was first reported in 1912 and has since become an important method for C–C bond formation in synthetic organic chemistry.<sup>1</sup> It was originally disclosed as a three-component reaction between an enolizable ketone, an aldehyde and an amine. However, synthetic chemists have since broadened the definition of a Mannich reaction to encompass all reactions that involve the addition of an enolizable carbonyl into an imine. The resulting characteristic  $\beta$ -amino carbonyl product, known as a Mannich base, has immense synthetic utility that can be leveraged for the construction of many nitrogen-containing natural products<sup>2</sup> and biologically relevant molecules.<sup>3</sup> Consequently, the Mannich reaction has received significant attention since the early 1990's, particularly toward the development of a stereoselective Mannich reaction, to expand the chemical space of accessible stereogenic Mannich base products for the construction of stereochemically enriched nitrogen-containing molecules.<sup>4</sup>

<sup>†</sup> This research was performed in collaboration with Mithun C. Madhusudhanan, Binh Khanh Mai, Peng Liu.

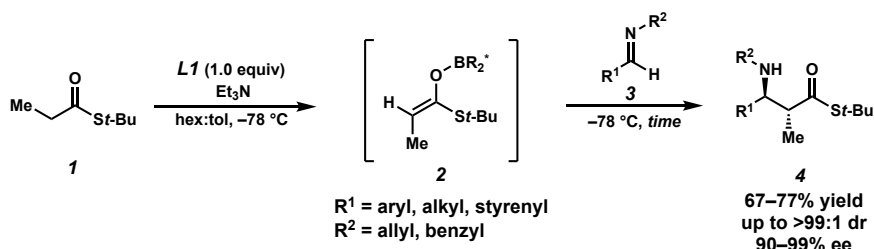
There are two fundamental variants of the Mannich reaction that have emerged throughout its rich, 110-year history: the *direct* and *indirect* Mannich reaction.<sup>5</sup> The *direct* variant involves a multi-component reaction with an unmodified carbonyl donor (e.g. involving *in situ* enolization) and the *indirect* variant utilizes preformed enolate equivalents to furnish the desired bond between the carbonyl donor and imine acceptor. While the original Mannich reaction generates the active imine electrophile *in situ*, there is no nomenclature to distinguish between a protocol that forms the imine electrophile *in situ* to one that uses isolated imine electrophiles. The original, three-component *direct* Mannich reaction invokes the reversible formation of the  $\beta$ -amino carbonyl product from the *in situ* generated enolate nucleophile and imine electrophile. This inherent reversibility involved in both the formation of the product and the active species in the *direct* Mannich reaction proved to be a challenge at the outset of developing an asymmetric Mannich reaction.

As a result, the first reports of an asymmetric Mannich-type reaction were disclosed as *indirect* variants in the early 1990's. In 1991, the Corey group in 1991 synthesized discrete, chiral boron enolates from thioesters, which were then treated with various *N*-alkyl imines **3** to perform desired asymmetric transformation (Scheme 1.1.1).<sup>6</sup> The preformation of the transoid boron enolate **2** in this *indirect* variant of the Mannich reaction proved critical for the reaction to afford Mannich product **4** in good yield and outstanding diastereoselectivity (up to >99:1 dr) and enantioselectivity between 90–99% ee. In 1994, Ishihara and coworkers developed an *indirect* asymmetric Mannich using preformed silyl ketene acetal nucleophiles **6** and a stoichiometric chiral boron Lewis acid **L2** to isolate the corresponding chiral  $\beta$ -amino ester products **7** in moderate yield and excellent enantioselectivity (between 95–98% ee).<sup>7</sup> The use of chiral boron activating groups such

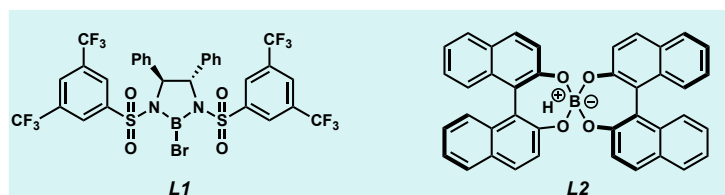
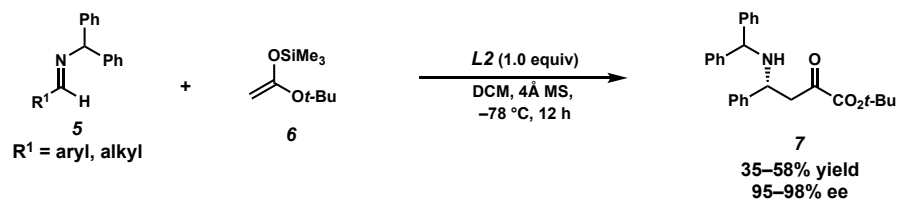
as **L1** and **L2** was excellent at furnishing the desired C–C bond between the preformed nucleophile and imine; however, rendered catalysis challenging due to the strong interaction between the product and the boron activator. Additionally, imine-chiral Lewis acid complexes have several stable conformers partially due to the *E/Z*-configurations of imines, which can render asymmetric catalysis challenging using chiral Lewis acid catalysts.<sup>4a,8</sup>

**Scheme 1.1.1** First Reports of the Asymmetric Mannich Reaction.

Corey et al. 1991



Ishihara et al. 1994



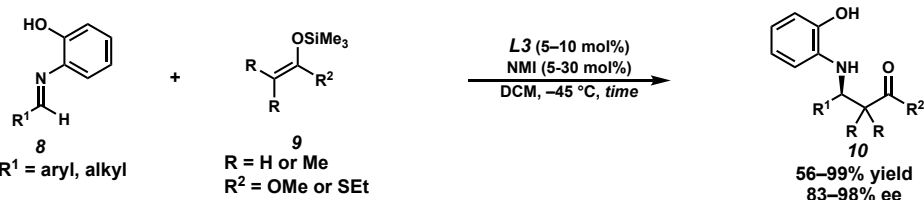
The first asymmetric catalytic Mannich reaction was reported in 1997 by Kobayashi and coworkers altering the metal from boron to zirconium in a bisbinaphthol system (Scheme 1.1.2).<sup>9</sup> Many Lewis acid salts were investigated, and it was discovered that zirconium(IV) possessed a unique ability to promote the reaction between imines and silylated enolate nucleophiles. *N*-Me imidazole was necessary as an additive to increase



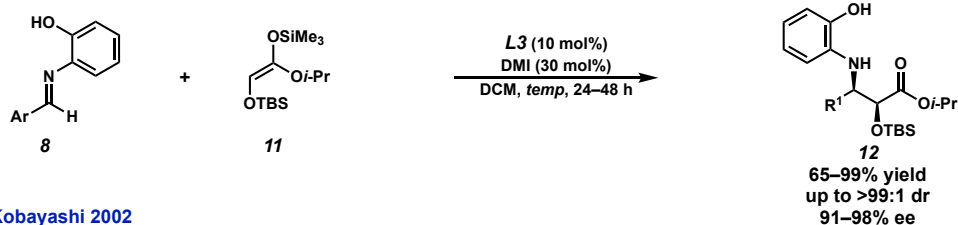
enantioselectivity, potentially to assist in the dissociation of the catalyst as well as limit the non-selective imine-chiral Lewis acid complexes that can be adopted. Through their optimization, they discovered the *ortho*-phenol *N*-aryl protecting group for the imine electrophile **8** was critical to achieve the observed reactivity and enantioselectivity, presumably to promote the catalyst association to the imine electrophile. The silyl ketene acetal or thioacetal nucleophiles could even be tetra-substituted, resulting in congested chiral  $\beta$ -amino ester products in good yield and enantioselectivity up to 98% ee.

**Scheme 1.1.2** First Catalytic Asymmetric Mannich Reaction and Select Examples of Kobayashi's bisbinaphthol Zr(IV) Catalyst System

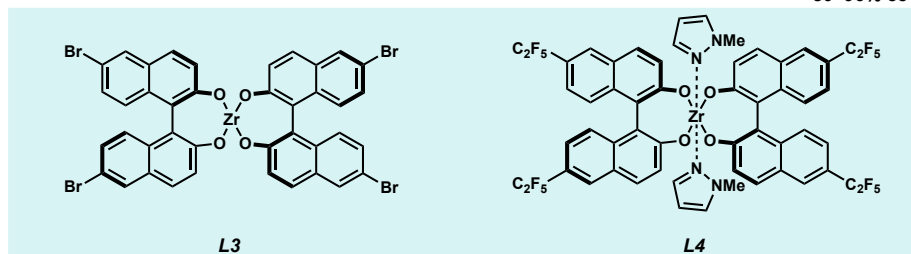
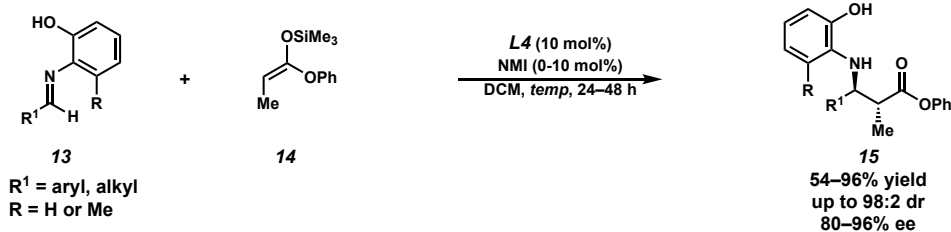
**Kobayashi 1997**



**Kobayashi 1998**



**Kobayashi 2002**



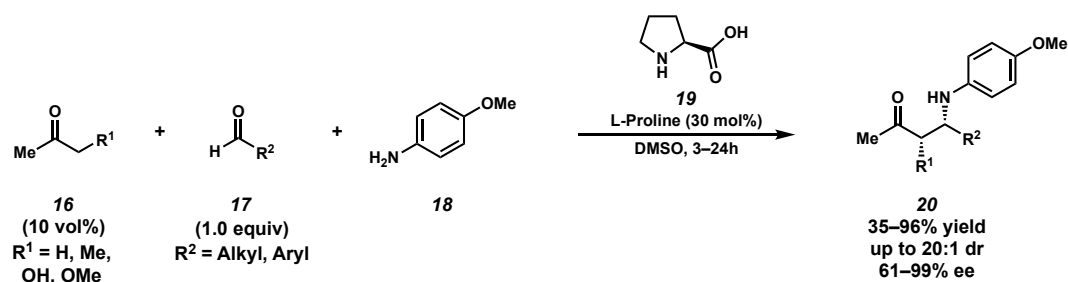
This technology using a chiral bisbinaphthol zirconium catalyst has been elaborated to accommodate more functionalized classes of silyl ketene acetal nucleophiles to obtain various  $\beta$ -amino ester products with  $\alpha$ -stereocenters in great yield and selectivity.<sup>10</sup> The early work reported by Kobayashi and coworkers established a foundation that organometallic and transition metal catalysts containing axial chirality are excellent at performing both *direct* and *indirect* Mannich reaction variants.<sup>11</sup>

Shortly after the first asymmetric catalytic *indirect* Mannich reaction reported by Kobayashi and coworkers, the List group in 2000 disclosed the first asymmetric, catalytic three-component *direct* Mannich reaction promoted by proline (Scheme 1.1.3).<sup>5</sup> The key to this reaction is the generation of the nucleophilic chiral enamine between proline **19** and the  $\alpha$ -enolizable ketone **16**, which reacts with the *N*-Ar imine generated *in situ* via the condensation of *p*-anisidine and aldehyde **17**. The  $\beta$ -amino ketone products **20** were isolated with diastereoselectivity up to 20:1 dr and enantioselectivities between 61–99% ee; however, solvent quantities of the ketone pro-nucleophile **16** were needed to obtain the product in up to 96% yield.<sup>12</sup> A similar catalytic system was employed by Barbas and coworkers that uses aldehyde pronucleophiles and privileged *N*-PMP-protected  $\alpha$ -imino ethyl glyoxylate (PMP = *p*-methoxyphenyl) electrophiles **22** to synthesize various chiral  $\alpha$ - and  $\beta$ - amino acid derivatives in good yield and excellent enantioselectivities between 93–99% ee.<sup>13</sup> In this system, the amount of aldehyde pro-nucleophile **21** could be reduced to 1.5 equivalents, which is dramatically lower compared to the solvent quantities of ketone pro-nucleophile used in the reports from List.<sup>5,12</sup> Shortly after, the Barbas group reported the first *direct* asymmetric catalytic Mannich reaction using  $\alpha$ -branched aldehyde pro-nucleophiles **24** to afford  $\alpha$ - and  $\beta$ -amino acid derivatives bearing an all-carbon quaternary

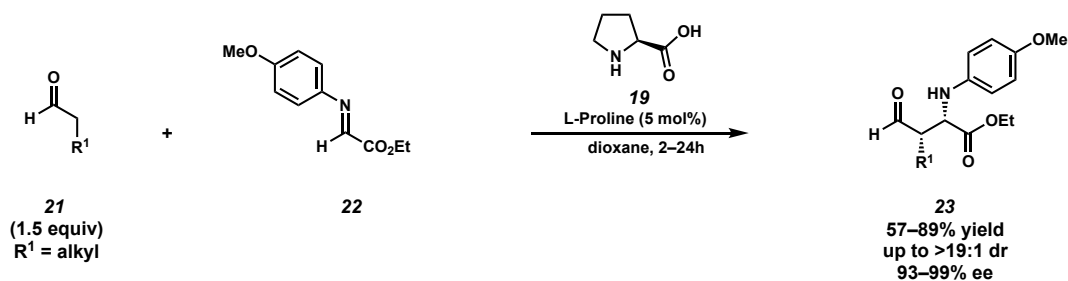
center.<sup>14</sup> Using this strategy,  $\alpha$ -alkyl and  $\alpha$ -aryl branched aliphatic aldehydes are competent pro-nucleophiles to undergo the proline catalyzed reaction to form the corresponding quaternary center containing  $\alpha$ -amino ester products in high diastereoselectivity up to 96:4 dr and enantioselectivities between 86–99% ee.

**Scheme 1.1.3** Proline catalyzed asymmetric direct Mannich reaction using ketone and aldehyde pronucleophiles

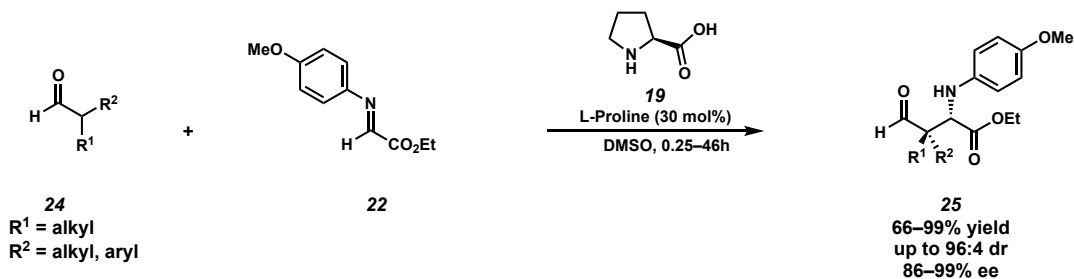
List et al. 2002



Barbas et al. 2002



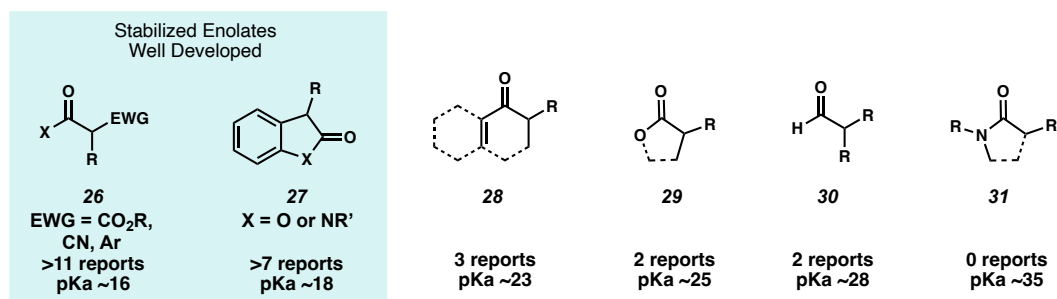
Barbas et al. 2004



The stereoselective synthesis of all-carbon quaternary centers using asymmetric catalysis is highly sought after and an ongoing challenge pursued by the synthetic community.<sup>15</sup> Throughout the rich history of the Mannich reaction, there are very few

reports of stereoselective Mannich reactions that form quaternary centers using non-stabilized enolates as the nucleophilic donor. A significant number of these reports rely on enolate stabilization, categorized as an  $\alpha$ -proton with a  $pK_a < 30$  in DMSO,<sup>16</sup> provided by an  $\alpha$ -carbonyl<sup>17</sup>, or an  $\alpha$ -aryl<sup>18</sup> to achieve *in situ* enolization and the desired reactivity (Scheme 1.1.4). The lower  $pK_a$  of this  $\alpha$ -proton corresponds to more stable metal enolates and a more facile generation of the active nucleophile, which allows for a greater accessible range of chemical space to promote the asymmetric, catalytic Mannich reaction. As a result, the desired asymmetric transformation using these nucleophiles have been performed using proline catalysis, organocatalysis and transition metal catalyzed processes.<sup>18,17</sup>

**Scheme 1.1.4** Summary of Pro-nucleophiles Reported in Asymmetric, Catalytic Mannich Reactions that Form All-Carbon Quaternary Centers

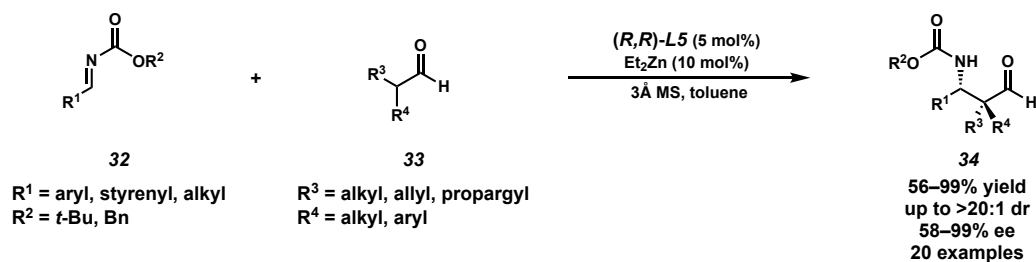


The synthetic community has been interested in the development of stereoselective reaction conditions using non-stabilized enolates to form quaternary centers to expand the chemical toolbox available to synthesize a variety of stereogenic  $\beta$ -amino carbonyl compounds. The first notable example is the report from the Barbas group in 2004 using  $\alpha$ -substituted aldehydes as the pro-nucleophile in an asymmetric Mannich reaction (Scheme 1.1.3).<sup>14</sup> The investigation into  $\alpha$ -substituted aldehyde enolate donors was

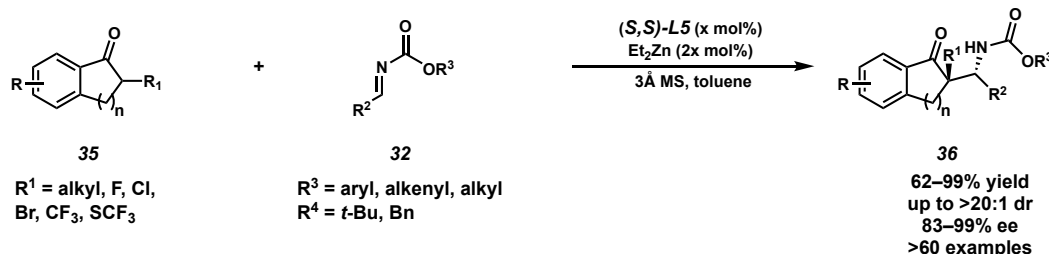
elaborated on by the Trost group in 2018 that expands the electrophile scope beyond highly reactive glyoxal-derived *N*-aryl imines using a transient chiral Zn enolate system (Scheme 1.1.5).<sup>19</sup> The stereodefined metal enolates derived from their reported Zn-ProPhenol catalyzed system allowed for control over enolate geometry as well as activation of the *N*-carbamate protected imines **32**.<sup>20</sup>

**Scheme 1.1.5** Catalytic Asymmetric Mannich Reactions of  $\alpha$ -Substituted Ketones and  $\alpha$ -Substituted Aldehydes Catalyzed by Trost's Zn-ProPhenol Catalyst

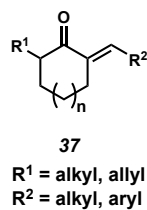
Trost et al. 2018



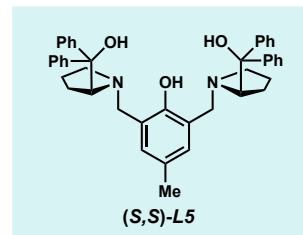
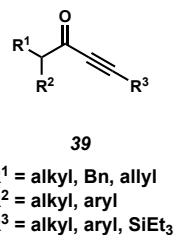
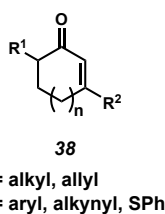
Trost et al. 2015–2020



Trost et al. 2019



Other successful pro-nucleophiles

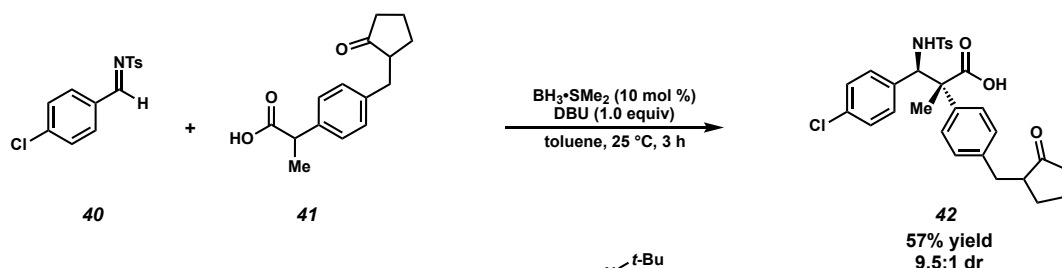


The use of  $\alpha$ -substituted ketone pro-nucleophiles in an asymmetric Mannich reaction was first reported by the Toste group as a sole example in 2015,<sup>21</sup> but was later elaborated into a more general and robust reaction by the Trost group using their Zn-

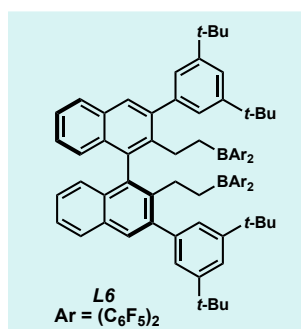
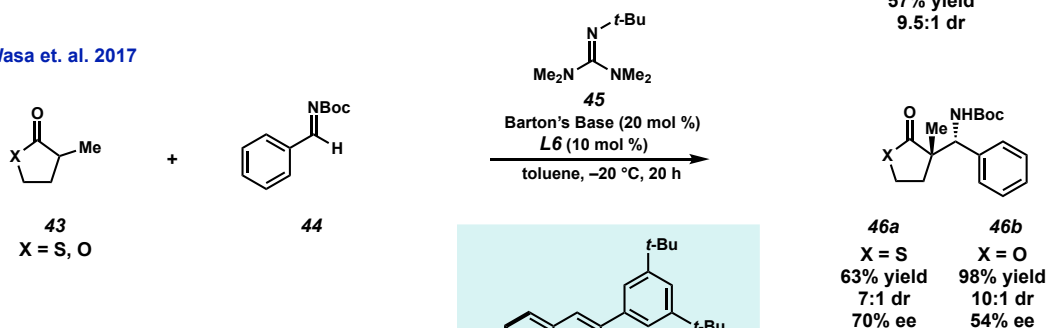
ProPhenol catalyst technology.<sup>22</sup> The Trost group has expanded the scope of amenable pro-nucleophiles to include both cyclic and acyclic  $\alpha$ -substituted ketones **37–39** bearing a degree of unsaturation at the  $\alpha'$  position of the ketone.<sup>22a–c</sup> This unsaturation present in the  $\alpha$ -substituted ketone pro-nucleophiles is presumably to assist in the regioselectivity of *in situ* enolate formation; however, the unsaturation could also favorably increase the reactivity of the enolate and stereoselectivity of the quaternary center formed after the asymmetric, catalytic *direct* Mannich reaction.

**Scheme 1.1.6** Catalytic Stereoselective Mannich Reactions of  $\alpha$ -Substituted Carbonyl Pro-nucleophiles in the Carboxylic Acid Oxidation State

Kanai et. al. 2015



Wasa et. al. 2017



Examples of an enantioselective Mannich reaction using less acidic carbonyl pro-nucleophiles, such as those in the carboxylic acid oxidation state with no  $\alpha$ -carbonyl or  $\alpha$ -

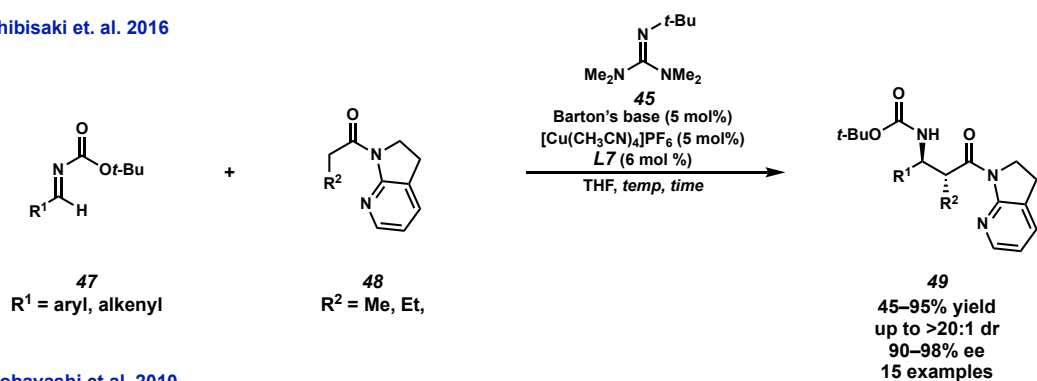
aryl stabilization of the *in situ* generated enolate, are sparse in the literature compared to the more acidic pro-nucleophiles.<sup>23</sup> This includes asymmetric Mannich reactions to set quaternary centers<sup>23a,b</sup> as well as tertiary centers,<sup>23c-e</sup> as the increase in pKa of the pro-nucleophiles in the carboxylic acid oxidation state significantly decrease the range of chemical space available to promote asymmetric catalysis. For carboxylic acid nucleophiles, the first chemoselective, enantioselective Mannich reaction was reported by the Kanai group that shows excellent enantioselectivity for  $\alpha$ -tertiary centers, but only one example of synthesizing an  $\alpha$ -quaternary center diastereoselectively (Scheme 1.1.6).<sup>23b</sup> To render the transformation asymmetric, the Kanai group synthesizes an asymmetric boron catalyst from 3,3'-I<sub>2</sub>-BINOL and BH<sub>3</sub>•SMe<sub>2</sub>, which can synthesize the desired chiral  $\beta$ -amino acid in enantioselectivities of up to 97% ee. An example of an  $\alpha$ -substituted lactone and a cyclic,  $\alpha$ -substituted thioester each have been reported by the Wasa group in 2017 using a chiral boron Lewis acid using axial chirality to establish the stereocenter.<sup>23a</sup> However, these isolated examples report modest enantioselectivities of 54% ee and 70% ee for the lactone and thioester nucleophiles respectively. To date, the research from Wasa and coworkers serves as the sole precedent of using  $\alpha$ -substituted esters or thioesters as nucleophiles in an asymmetric Mannich reaction to form a quaternary center.

Using amide as the pro-nucleophile has been a significant challenge in developing stereoselective Mannich reactions due to their low acidity<sup>24</sup> and instability of the corresponding metal enolates.<sup>25</sup> To overcome these challenges, amide auxiliaries such as 7-azaindolines<sup>26</sup> or pyrazoleamides<sup>27</sup> have been critical to promote the desired stereoselective transformation. The additional Lewis basic nitrogen in these N-acyl heterocycles assist in the chelation of chiral organometallic catalysts to assist in both the

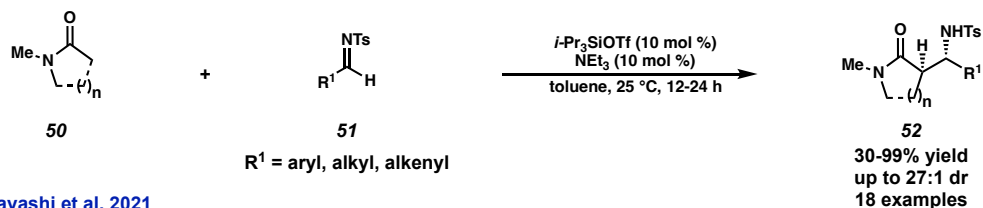
reactivity as well as the stereoselectivity of the *in situ* generation of the active enolate nucleophile. These auxiliaries have proven to be effective; however, they require an additional step to remove and are incompatible to synthesize simple  $\beta$ -amino amides.

**Scheme 1.1.7** Summary of Stereoselective Mannich Reactions of Amide Pro-Nucleophiles

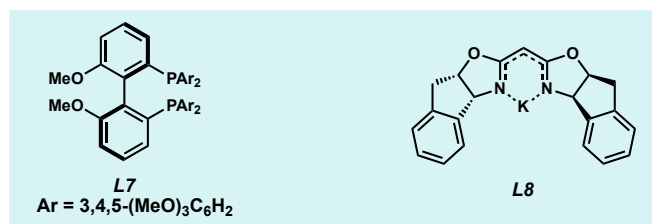
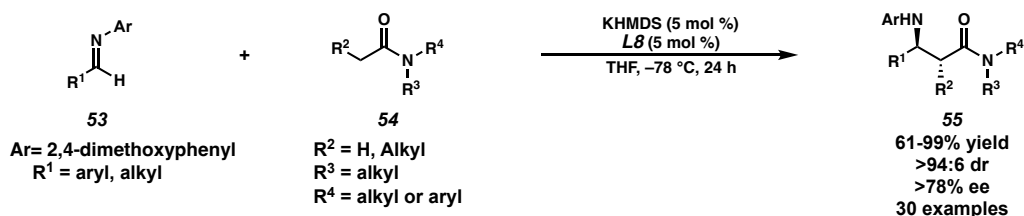
Shibasaki et. al. 2016



Kobayashi et al. 2010



Kobayashi et al. 2021



The first general, stereoselective Mannich reaction with simple amide pro-nucleophiles was reported by the Kobayashi group in 2010 using a catalytic silicon enolate system (Scheme 1.1.7).<sup>28</sup> The catalytic generation of silicon amide enolates avoided the



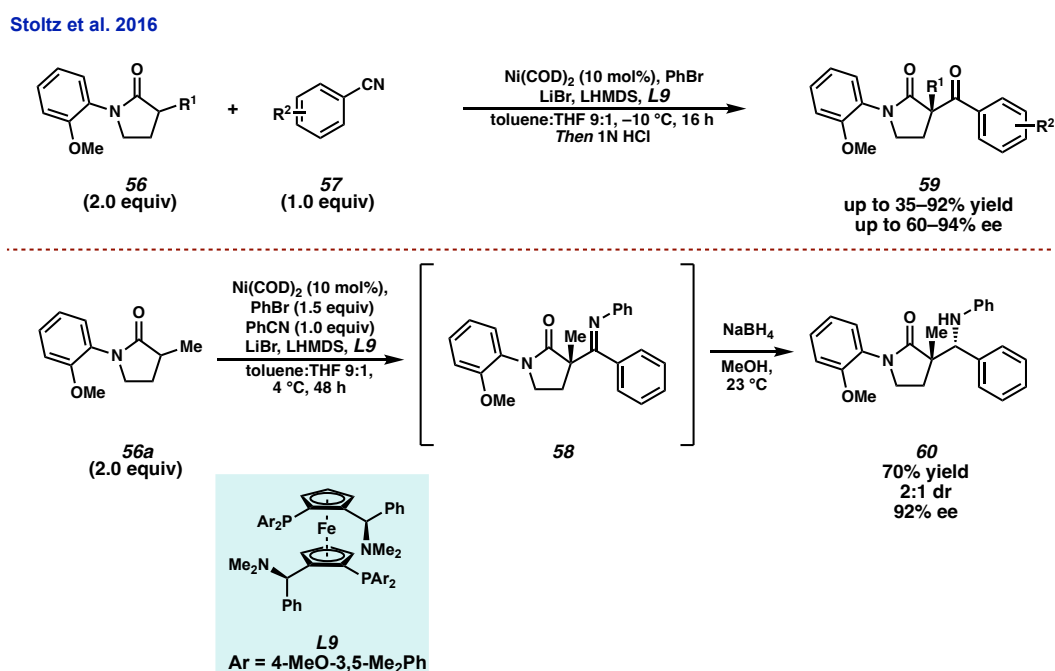
preparation and isolation of the unstable silyl ketene aminal, which allowed for the synthesis of various simple, unactivated  $\beta$ -amino amides in great yields and diastereoselectivity of up to 27:1 dr. The first catalytic, asymmetric Mannich reaction of simple, unactivated amide pro-nucleophiles was reported by the Kobayashi group in 2021 which worked to address enolate stability by designing a chiral potassium salt catalyst **L8** to afford enantioenriched amines with simple, acyclic amides in excellent enantioselectivity.<sup>29</sup> However, despite the ability of both methods to stereoselectively functionalize simple amides catalytically, these systems have not proven accommodating to  $\alpha$ -substituted unactivated amides.

Given our laboratory's interest in the stereoselective synthesis of all-carbon quaternary centers, we sought to develop a catalytic, stereoselective Mannich reaction using a simple,  $\alpha$ -substituted amide as the pro-nucleophile. Our laboratory has a rich history of synthesizing a variety of saturated *N*-heterocycles bearing an all-carbon quaternary center, and we have continued our pursuit of developing general methods to synthesize such motifs.<sup>30</sup> Considering our interest in saturated *N*-heterocycles, in conjunction with the prevalence of pyrrolidines and other saturated *N*-heterocycles in natural products and pharmaceutically relevant molecules,<sup>31</sup> we sought to design a system wherein an unactivated  $\alpha$ -substituted- $\gamma$ -lactam may function as the enolate donor in a stereoselective Mannich reaction. Our efforts resulted in the first stereoselective *direct* Mannich reaction using unactivated  $\alpha$ -substituted- $\gamma$ -lactam pro-nucleophiles to synthesize an all-carbon quaternary center. This chapter contains a complete account of this research toward the development of a diastereoselective and asymmetric Mannich reaction, which should serve as a prelude to the development of a catalytic, enantioselective variant.

## 1.2 INITIAL INVESTIGATION INTO THE MANNICH REACTION

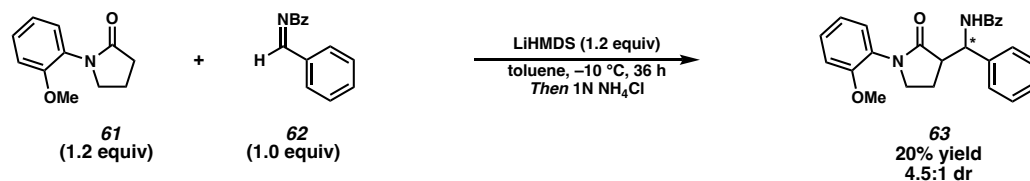
At the outset, we gained inspiration from our previous research toward the Ni catalyzed asymmetric acylation of  $\alpha$ -substituted- $\gamma$ -lactam nucleophiles using aryl nitriles (Scheme 1.2.1).<sup>30a</sup> Formally, this involves the generation of a lactam enolate that adds into the aryl nitrile **57**, and the resulting imine undergoes a C–N cross coupling event mediated by an aryl Ni(II) species to turn over the catalyst. For this research, the intermediate *N*-aryl imine **58** could be hydrolyzed to the corresponding ketone and result in the acylated  $\gamma$ -lactam products **59** bearing an all-carbon quaternary center in up to 92% yield and 94% ee. We were interested in expanding this catalytic system to include alternative classes of electrophiles to not only investigate the limits of this synthetic technology, but also to access more saturated *N*-heterocyclic motifs containing quaternary centers.

**Scheme 1.2.1** Stoltz Ni-Catalyzed Asymmetric Acylation of  $\alpha$ -Substituted- $\gamma$ -Lactam Nucleophiles with Aryl Nitriles

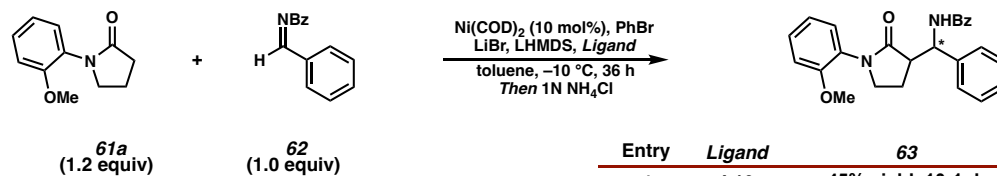


In the 2016 report,<sup>30a</sup> we showed that this *N*-aryl imine product formed after C–N bond formation **58** can be reduced via NaBH<sub>4</sub> to afford the  $\beta$ -amino lactam **60** bearing a quaternary center in a 70% yield, 92% ee and 2:1 dr favoring the *anti*-diastereomer. This modest diastereoselectivity observed in the Mannich-type product arises from the non-selective imine reduction from NaBH<sub>4</sub>. We hypothesized that altering the electrophile from an aryl nitrile to an imine would allow us to have greater control over the diastereoselectivity due to the chiral Ni species mediating the desired bond formation.

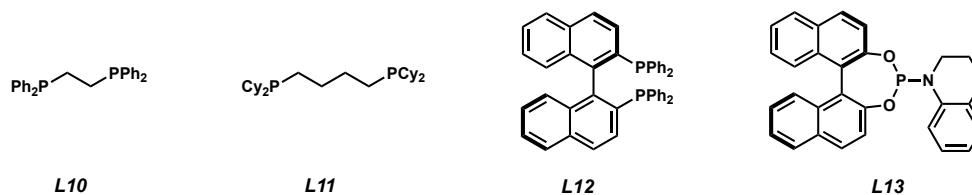
Our investigation into the Ni-catalyzed stereoselective Mannich reaction began using the *N*-Bz protected imine<sup>32</sup> of benzaldehyde **62** as the electrophile and the *N*-*ortho*-methoxyphenyl (OMP) protected  $\gamma$ -lactam **61** as the pro-nucleophile (Scheme 1.2.2). As a proof of concept for the transformation, we explored using a pro-nucleophile bearing no  $\alpha$ -substitution since it was unclear how the more electrophilic *N*-Bz imine **62** would react in a system designed for aryl nitrile electrophiles. Treatment of *N*-OMP lactam **61** with LiHMDS in the presence of *N*-Bz imine **62** led to the isolation of the desired Mannich product **63** in a 20% yield with a 4.5:1 dr. With the establishment of a competing, base promoted background reaction, we wanted to observe the effect of a Ni-catalyst on the Mannich reaction. A small screen of phosphine ligands was performed adopting conditions identical to the Ni-catalyzed asymmetric acylation, and we observed that the Ni-catalyst complexed with diphenylphosphinoethane **L10** delivered the desired Mannich product **63** in a greater yield of 45% and improved the diastereoselectivity to 10:1 dr compared to the background reaction. However, these Ni-catalyzed conditions promoted an undesired dimerization of the unsubstituted lactam nucleophile, which discouraged further investigation into this system bearing no  $\alpha$ -substitution on the lactam.

**Scheme 1.2.2** Initial Investigation into the Stereoselective Mannich Reaction

## Ligand Screen for Mannich Reaction



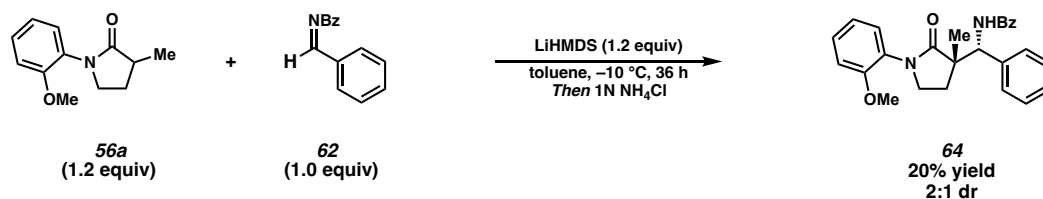
Entry	Ligand	$\text{63}$
1	L10	45% yield, 10:1 dr
2	L11	35% yield, 4:1 dr
3	L12	0% yield, n.d. dr
4	L13	15% yield, 4.5:1 dr, n.d. ee



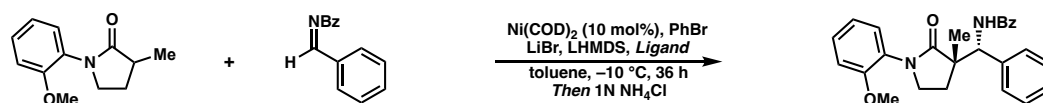
In our new reaction design, we chose  $\alpha$ -methyl substituted  $\gamma$ -lactam **56a** as the pro-nucleophile as we hypothesized this substitution on the lactam would prevent the base promoted dimerization (Scheme 1.2.3). Treatment of lactam **56a** with LiHMDS in the presence of the *N*-Bz imine electrophile **62** led to the desired  $\beta$ -amino lactam product **64** in a 20% yield and a modest 2:1 dr. This was promising as the additional substitution of our nucleophile did not completely inhibit the desired C–C bond formation; however, the results of a preliminary ligand screen of our proposed Ni-catalyzed Mannich reaction were discouraging. Our best result was obtained using phosphoramidite **L13** as the ligand for our Ni-catalyzed conditions, delivering the  $\beta$ -amino lactam product **64** in an increased 40% yield with a slightly increased diastereoselectivity of 3:1 dr. With these preliminary results,

we believed the presence of the Ni-catalyst only had a minor influence on the desired Mannich reaction relative to the base promoted, background reaction.

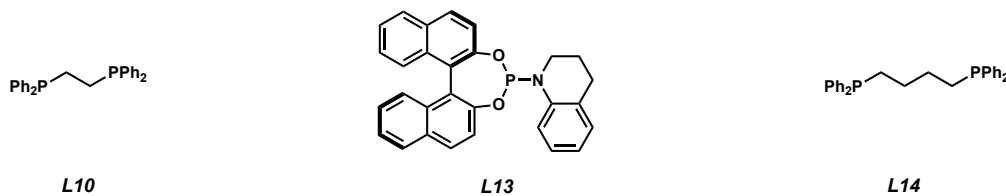
**Scheme 1.2.3** Investigating the Ni-Catalyzed Mannich Reaction Using an  $\alpha$ -Methyl- $\gamma$ -Substituted Lactam Nucleophile



**Ligand Screen for Mannich Reaction**



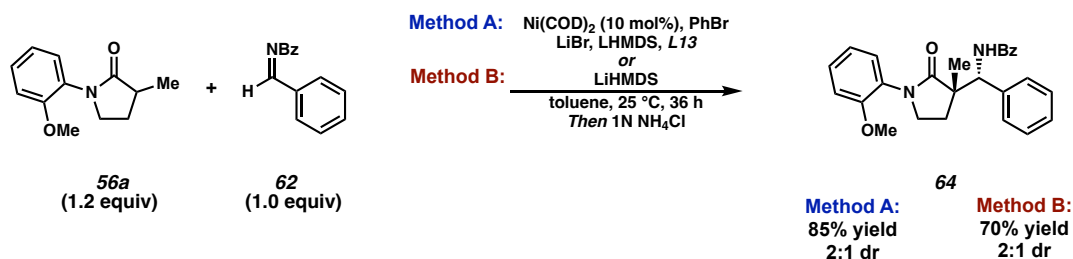
Entry	Ligand	<b>64</b>
1	L10	10% yield, 5:1 dr
2	L13	40% yield, 3:1 dr, 9% ee
3	L14	20% yield, 4:1 dr



To confirm this hypothesis, we wanted to compare the Ni-catalyzed reaction conditions to the uncatalyzed background reaction at elevated temperatures (Scheme 1.2.4). Using phosphoramidite **L13** as the ligand, the Ni-catalyzed Mannich reaction afforded the desired  $\beta$ -amino lactam **64** in an increased yield of 85%, with a reduction of diastereoselectivity to 2:1 dr. Comparatively, the base promoted background reaction afforded the desired  $\beta$ -amino lactam **64** in a 70% yield with a 2:1 dr. The prevalent background reaction at ambient temperatures in combination with the low conversion of the Ni-catalyzed Mannich reaction at reduced temperatures motivated us to redesign our

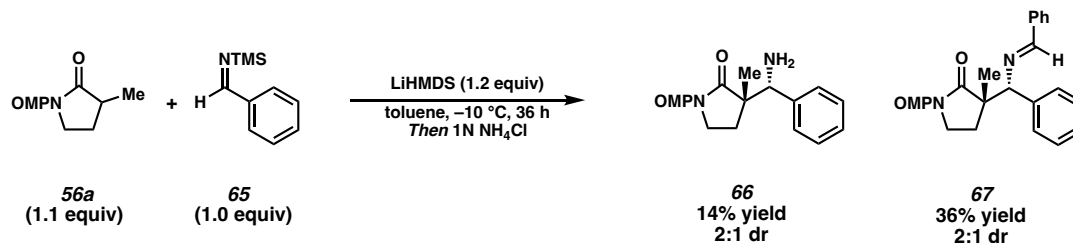
system away from the *N*-Bz imine electrophile **62** toward a less electrophilic species. With the hopes to tune the electrophilicity of the imine in our favor, we opted to investigate the stereoselective Mannich reaction using the *N*-TMS imine of benzaldehyde **65**.

**Scheme 1.2.4** Influence of Temperature on the Desired Mannich Reaction



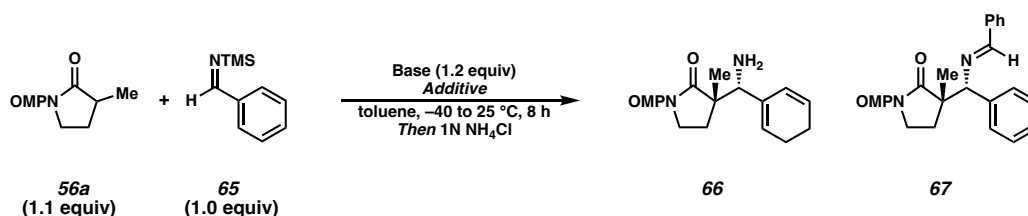
Treatment of  $\alpha$ -methyl lactam **56a** with LiHMDS in the presence of the *N*-TMS imine electrophile **65** afforded the desired  $\beta$ -amino lactam product **66** in 14% yield as well as an unexpected imine **67** in 36% yield (Scheme 1.2.5). The imine product **67** is believed to form from the nucleophilic addition of amine **66** into the *N*-TMS imine **65** followed by elimination of TMSN<sub>2</sub>H to afford the imine transfer product **67**. With the *N*-TMS imine being the limiting reagent, this competing imine transfer side reaction was deleterious to the conversion; however, we were encouraged by the formation of the desired C–C bond in a combined yield of 50% between the two products and a modest selectivity of 2:1 dr. Our efforts were focused on altering the base used in combination with various activating additives to probe the reaction profile for this desired diastereoselective transformation

**Scheme 1.2.5** Mannich Reaction Using *N*-TMS Imine Electrophile **65**



(Scheme 1.2.6). Allowing the reaction of lactam **56a** and imine **65** with LiHMDS to warm up to ambient temperatures corresponded with an increase in yield of both amine **66** and imine **67** to 25% and 40% respectively with no change to the diastereoselectivity. Performing the same reaction in the presence of stoichiometric amounts of  $\text{Al}(\text{O}t\text{-Bu})_3$  resulted in the exclusive formation of the imine transfer product **67** in 50% yield and 2:1 dr with complete consumption of the starting material imine **65**.

**Scheme 1.2.6** Influence of Base and Lewis Acid Additives on the Mannich Reaction

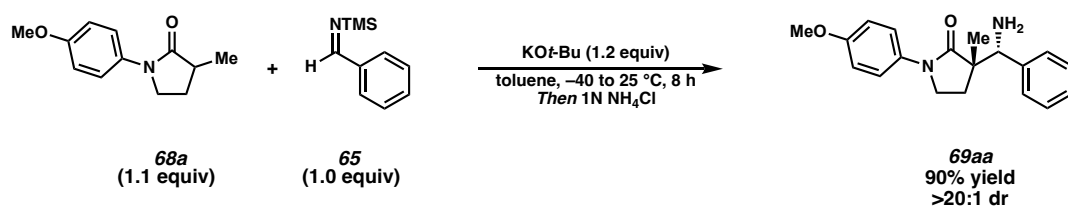


Entry	Base	Additive	Yield <b>66</b>	Yield <b>67</b>	dr
1	LiHMDS	None	25%	40%	2:1
2	LiHMDS	$\text{Al}(\text{O}t\text{-Bu})_3$	0%	50%	2:1
3	LiHMDS	TMSI	0%	50%	1:2
4	KHMDS	None	0%	0%	n.d.
5	KHMDS	18-crown-6	0%	0%	n.d.
6	$\text{LiO}t\text{-Bu}$	None	0%	0%	n.d.
7	NaOMe	None	0%	0%	n.d.
8	$\text{KO}t\text{-Bu}$	None	85%	5%	9:1

Alteration of the additive to TMSI afforded the imine transfer product **67** in a 50% yield; however, the diastereoselectivity of the isolated product was inverted to 1:2 dr favoring the *syn* product. The use of KHMDS as the base for the Mannich reaction resulted in decomposition of the starting material, with or without the addition of 18-crown-6 as a stoichiometric additive. These unfavorable results shifted our focus away from disilazane derived bases toward alkoxide bases. Both  $\text{LiO}t\text{-Bu}$  and NaOMe were unable to promote the desired reaction, resulting in complete recovery of the starting material lactam **56a**. To our delight, the use of  $\text{KO}t\text{-Bu}$  as the base in our designed Mannich reaction resulted in an 85% yield of the desired amine product **66** in a 9:1 dr as the major product. In addition,

alteration of the *N*-Ar protecting group from *ortho*-methoxyphenyl (OMP) to *para*-methoxyphenyl (PMP) afforded the desired amine **69aa** in comparably high yields of 90% with an increased diastereoselectivity to 20:1 (Scheme 1.2.7).

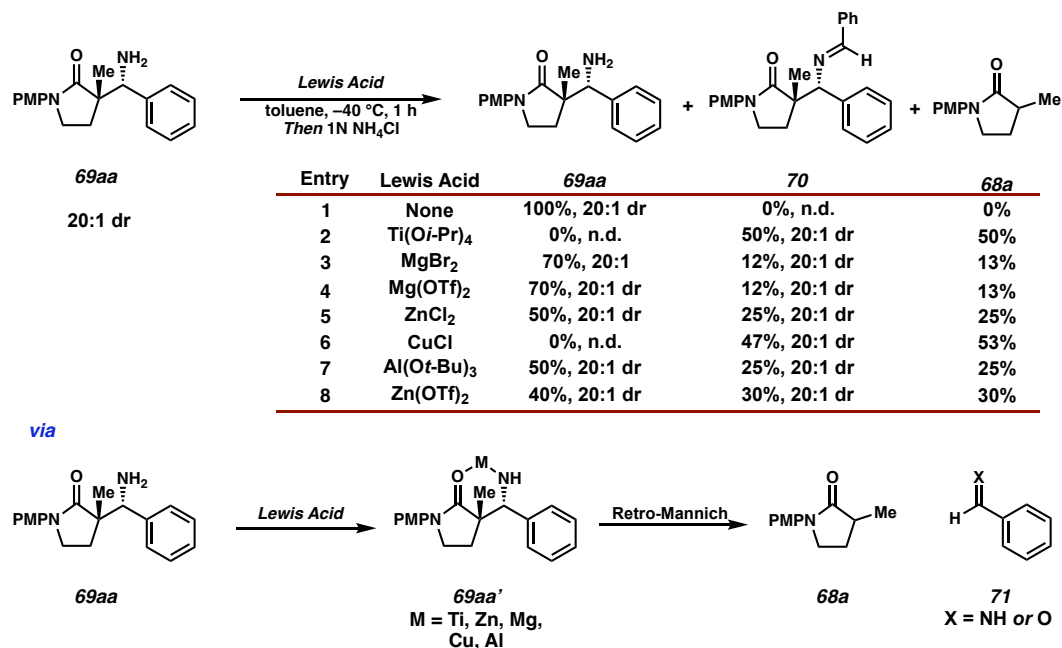
**Scheme 1.2.7** Discovery of the *KOt*-Bu Promoted Diastereoselective Mannich Reaction



### 1.3 PROBING THE POTASSIUM *TERT*-BUTOXIDE PROMOTED MANNICH REACTION

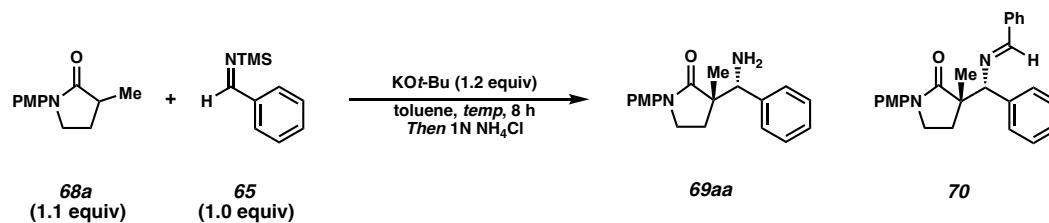
We wanted to probe the stability of the  $\beta$ -amino carbonyl product with Lewis acid additives to identify the presence of an undesired retro-Mannich process, which could erode any enantioselectivity established at the desired quaternary center (Scheme 1.3.1). We treated our  $\beta$ -amino lactam **69aa** with various Lewis acid additives and monitored the formation of benzaldehyde **71** or imine transfer product **70** that could only be formed from the liberation of a unit of electrophile due to a retro-Mannich process. Every transition metal Lewis acid additive investigated, which includes:  $\text{Ti}(\text{O}i\text{-Pr})_4$ ,  $\text{MgBr}_2$ ,  $\text{Mg}(\text{OTf})_2$ ,  $\text{ZnCl}_2$ ,  $\text{CuCl}$ ,  $\text{Al}(\text{O}t\text{-Bu})_3$  and  $\text{Zn}(\text{OTf})_2$ , showed significant formation of the imine transfer adduct **70**. This suggests that Lewis acids have detrimental effects on the overall transformation since they promote the undesired retro-Mannich reaction.



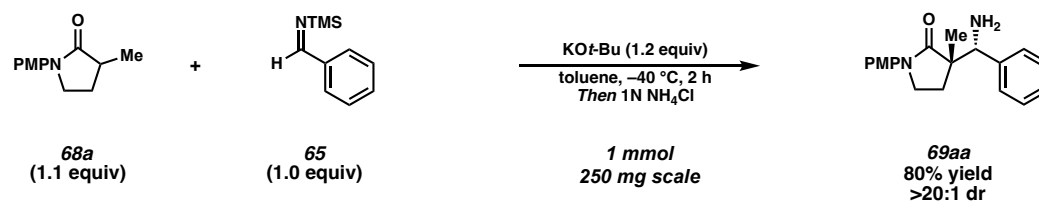
**Scheme 1.3.1** Screen of Mannich Product Stability with Lewis Acid Additives

At this stage, we were interested in investigating the effect of temperature on the KO*t*-Bu promoted diastereoselective Mannich reaction (Scheme 1.3.2). The yield of the isolated product amine **69aa** was at least 85% at all temperatures investigated. Performing the reaction at constant temperatures below  $-10\text{ }^{\circ}\text{C}$  was critical to form the desired Mannich product **69aa** in excellent diastereoselectivity of 20:1 dr. The diastereoselectivity of the reaction decreased to 8:1 dr of the desired  $\beta$ -amino lactam **69aa** when the reaction was performed at ambient temperature. In conjunction with the results from the Lewis acid stability screen, the results from the temperature screen suggest that this diastereoselective Mannich reaction would be difficult to render asymmetric with the addition of a transition metal or chiral boron catalyst due to the significant background reaction that occurs at temperatures as low as  $-40\text{ }^{\circ}\text{C}$ . Scaling up this reaction to 1 mmol affords the desired amine product **69aa** in 80% yield and diastereoselectivity of >20:1 dr, suggesting that this reaction performs consistently well at modest scales.

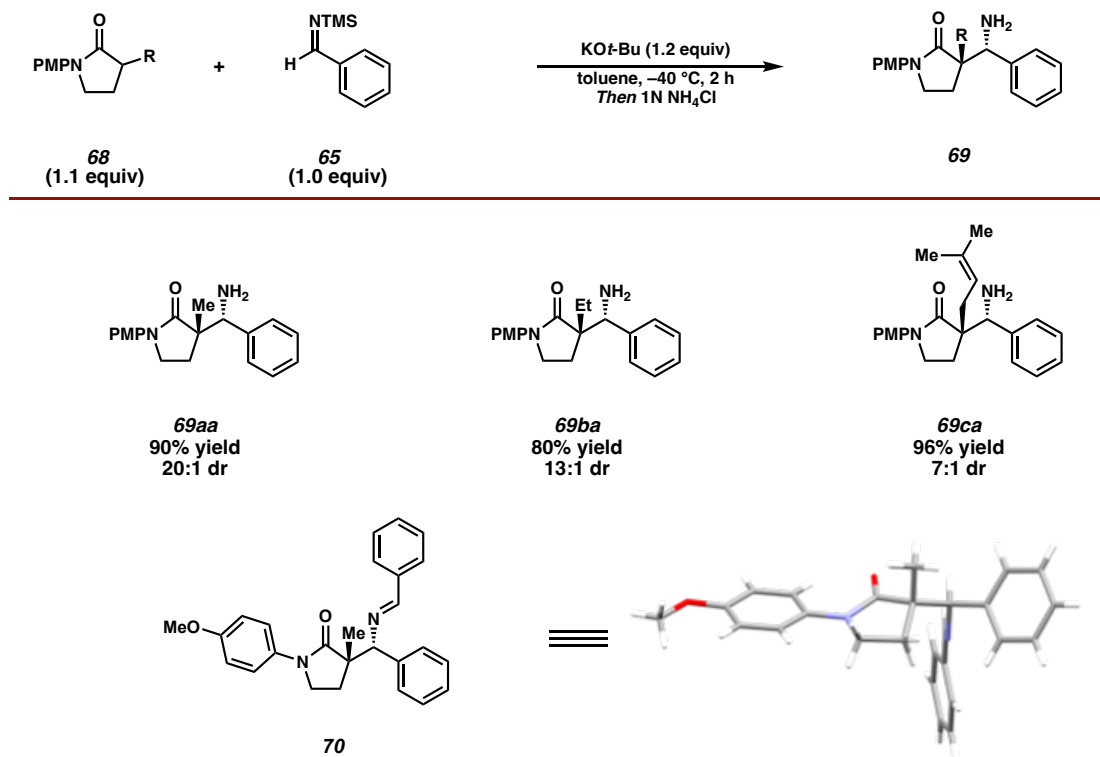
**Scheme 1.3.2** Representative Temperature Screen of the Diastereoselective Mannich Reaction and Scale-up Result



Entry	temp	Yield $69aa$	Yield $70$	dr
1	-40 °C	85%	0%	20:1
2	-10 °C	90%	0%	20:1
3	25 °C	90%	0%	8:1



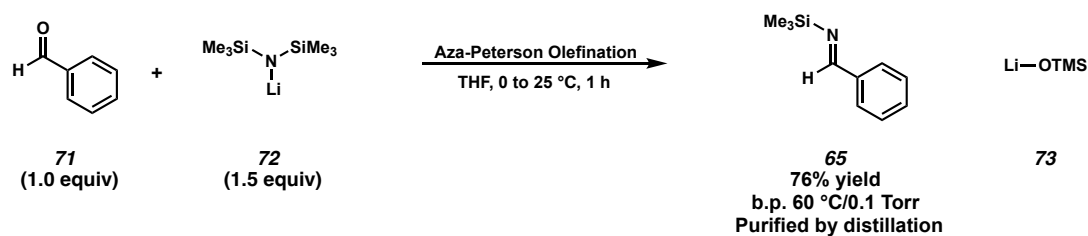
With optimal reaction conditions in hand, we looked to explore the generality of the overall transformation with respect to the  $\alpha$ -substituent on the  $\gamma$ -lactam pro-nucleophile (Scheme 1.3.3). Simple alkyl substituents such as  $\alpha$ -Me and  $\alpha$ -Et are well tolerated, delivering the corresponding  $\beta$ -amino lactam product in 90% yield, 20:1 dr and 80% yield, 13:1 dr for amines **69aa** and **69ba** respectively. Large alkyl substituents at the  $\alpha$ -position such as the prenyl group are also tolerated, as the corresponding Mannich product **69ca** was isolated in a 96% yield; however, the diastereoselectivity of the transformation decreased to 7:1 dr. We obtained an X-ray crystal structure of the imine transfer adduct **70** to confirm the relative stereochemistry for the developed diastereoselective Mannich reaction to be *anti* with respect to the  $\alpha$ -substituent and the amine functional group.

**Scheme 1.3.3** Preliminary Scope of  $\alpha$ -Substitution of the  $\gamma$ -Lactam Pro-Nucleophile**1.4 ALTERNATIVE SYNTHESIS OF  $N$ -SILYL IMINE ELECTROPHILES**

The establishment of a preliminary scope with respect to the  $\alpha$ -substitution on the  $\gamma$ -lactam pro-nucleophile directed our attention to redesign our reaction system. Our early results suggested this transformation was somewhat general with respect to the pro-nucleophile; however, our reaction setup was inherently limiting in scope with respect to the electrophile. At the outset of reaction discovery, we were synthesizing the  $N$ -TMS imine **65** via an aza-Peterson olefination of benzaldehyde **71** (Scheme 1.4.1).<sup>33</sup> This protocol involves the treatment of benzaldehyde **71** with excess LiHMDS, which results in the elimination of an equivalent of LiOTMS to generate the desired  $N$ -silyl imine **65**. Isolation of the  $N$ -silyl imine **65** is critical as we have observed the identity of the base

greatly influences the outcome of our diastereoselective Mannich reaction. Furthermore, these purified *N*-silyl imines have been reported as extremely moisture-sensitive and are often reacted immediately after purification.<sup>34</sup>

**Scheme 1.4.1** Aza-Peterson Olefination of Benzaldehyde to Access Imine **65**

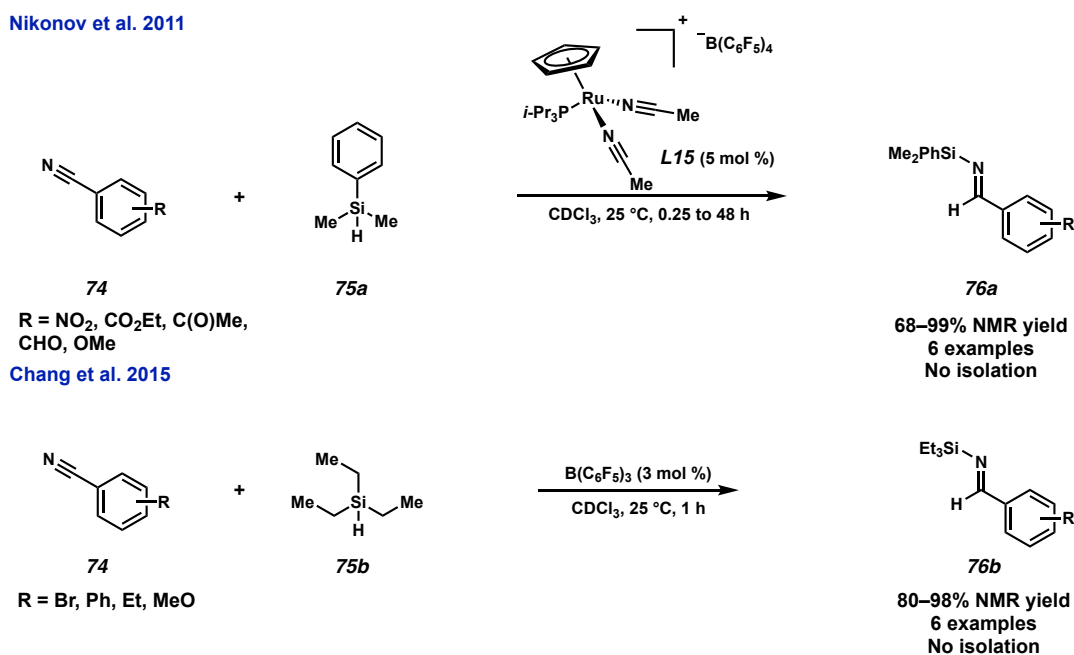


For the distillation of *N*-silyl imine electrophile **65**, the observed boiling point was 60  $^\circ\text{C}$  at 0.1 Torr, which is synthetically accessible. However, adding substitution to the arene could prohibitively increase the boiling point and render the purification process unfeasible, thus limiting the scope of electrophile aryl imines that may be investigated.<sup>33,34</sup> In addition, accessing alternative lithium disilazane bases to alter the *N*-silyl protecting group is challenging as there are limited methods in the literature to synthesize a library of disilazane derivatives.

Inspired by research from both the Chang group<sup>35</sup> and Nikonov group,<sup>36</sup> we focused our synthetic efforts toward investigating the synthesis of *N*-silyl imines via catalytic hydrosilylation of aryl nitriles (Scheme 1.4.2). We were encouraged by this alternative approach because this procedure does not generate any basic side products, and thus the generation of our desired *N*-silyl imine could be telescoped with our desired diastereoselective Mannich reaction. Furthermore, this reaction appears robust with respect to the aryl nitrile used and can be used to synthesize a library of *N*-silyl protected imine electrophiles since both aryl nitriles and silanes are highly accessible via commercial or

synthetic means. The report from Chang and coworkers<sup>35</sup> suggests that their reported  $B(C_6F_5)_3$  catalyzed hydrosilylation of *p*-substituted aryl nitriles requires the use bulky, trialkyl silanes for efficient reduction to the imine. This is because less substituted mono- or bis-alkyl silanes promote the exhaustive reduction of the aryl nitrile to the benzylic amine. The cationic Ru-catalyst **L15** reported by Nikonov and coworkers efficiently promoted the hydrosilylation of both aryl and alkyl nitriles to the corresponding *N*- $SiMe_2Ph$  protected imines.<sup>36</sup> The catalyst selectively reduced the desired aryl nitrile in the presence of C=C, C=O and even N=O bonds and delivered the desired imine with both electron-rich and electron-poor arenes. However, the reaction times of more electron deficient aryl nitriles could be up to 48 h, which was undesirable to initially investigate the tandem hydrosilylation, direct Mannich reaction approach.

**Scheme 1.4.2** Catalytic Hydrosilylation of Aryl Nitriles to Access *N*-Silyl Imines **76**

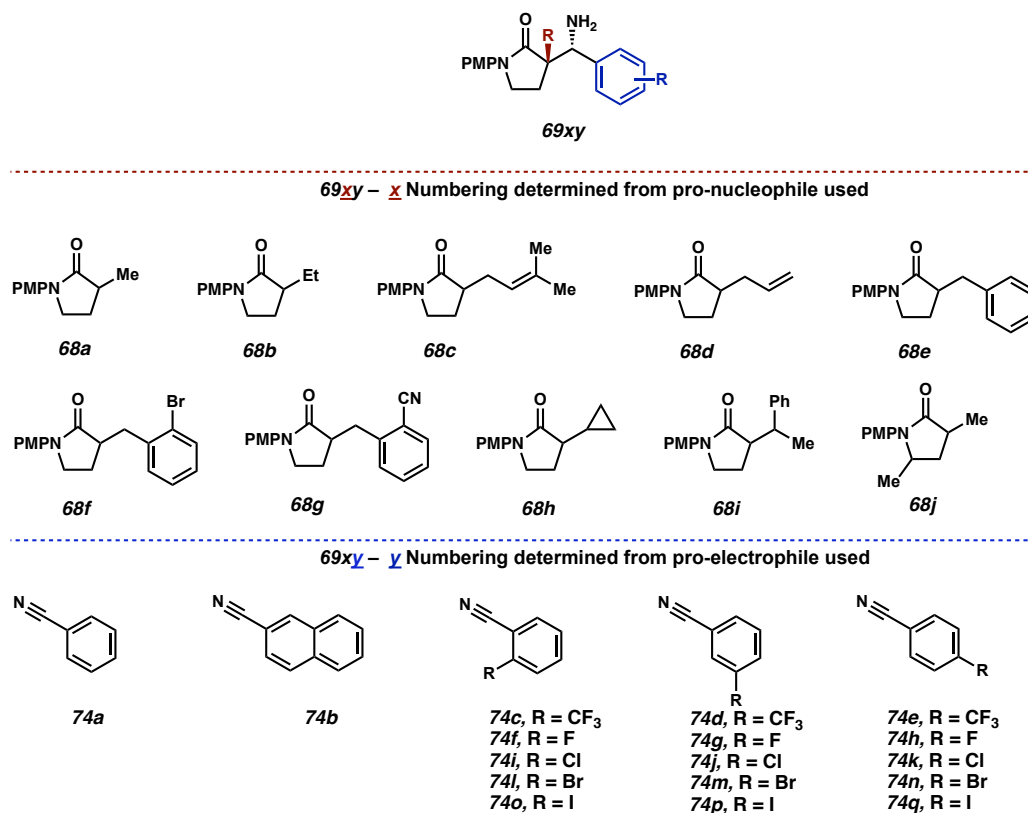


For our initial studies, we wanted to explore a silane that would deliver an *N*-silyl imine product that most closely resembles our original *N*-TMS imine electrophile. We

hypothesized that the *N*-SiMe<sub>2</sub>Ph protected imines would be sterically similar to the original *N*-SiMe<sub>3</sub> imine electrophiles since the more sterically bulky phenyl group could reside in a conformation away from the C=N  $\pi^*$  orbital. As a result, we developed a hybrid protocol using PhMe<sub>2</sub>SiH as our silane source and B(C<sub>6</sub>F<sub>5</sub>)<sub>3</sub> as the catalyst to synthesize a library of *N*-SiMe<sub>2</sub>Ph protected aryl imine derivatives to be used as electrophiles in our second generation, telescoped approach.

## 1.5 TELESCOPED HYDROSILYLATION/DIRECT MANNICH REACTION

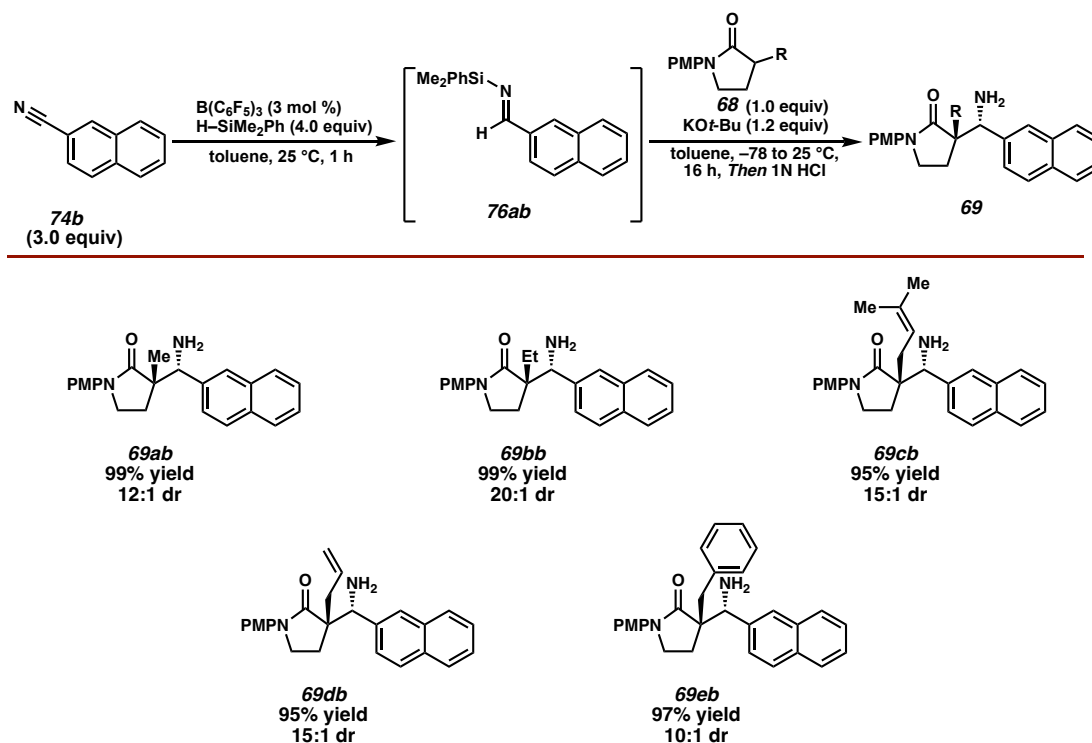
There are a few key considerations that needed to be addressed as we focused on developing a tandem catalytic hydrosilylation/direct Mannich reaction from aryl nitrile pro-electrophiles. The main concern is the potential for overreduction of the aryl *N*-silyl imine electrophile to the undesired benzylic amine and the challenge to introduce precise equivalents of electrophile to the reaction mixture. This overreduction in combination with the imine transfer adduct that can form from the reaction between the *N*-Si imine and the Mannich product amine suggests that excess imine must be generated to ensure complete consumption of the lactam pro-nucleophile. With the imine no longer serving as the limiting reagent, there will be reagents and byproducts in excess for our telescoped approach that were not present in the original discovery of the diastereoselective Mannich reaction. Before investigating the substrate scope (Figure 1.5.1), we sought to directly compare this proposed telescoped approach to the First-generation, aza-Peterson mediated diastereoselective Mannich reaction.

**Figure 1.5.1** Description of the numbering system for the Mannich products **69**

The telescoped sequence involves the catalytic hydrosilylation of benzonitrile **74a** with Me<sub>2</sub>PhSi–H as the silane source with B(C<sub>6</sub>F<sub>5</sub>)<sub>3</sub> as the catalyst for 1 h (Scheme 1.5.1). Upon completion of the hydrosilylation, determined via TLC or LC/MS, the solution of *N*-SiMe<sub>2</sub>Ph imine **76aa** was added to a mixture of lactam pro-nucleophile **68** and KO*t*-Bu in toluene at –78 °C. The reaction was slowly allowed to warm to ambient temperature over 16 h and was quenched with 1N HCl to facilitate the hydrolysis of any imine transfer product **70** to the desired  $\beta$ -amino lactam **69**. This Second-generation approach proved superior to the First-generation approach for all three substrates investigated, as the major diastereomer of **69aa–ca** was isolated in higher yield using the telescoped approach. This series of experiments served as a good proof of concept to show altering the silane *N*-

substituent and the addition of excess silane and imine were not detrimental to the reactivity or selectivity of the desired transformation.

**Scheme 1.5.1** Comparison of Telescoped Diastereoselective Mannich Reaction to the First-Generation Approach.

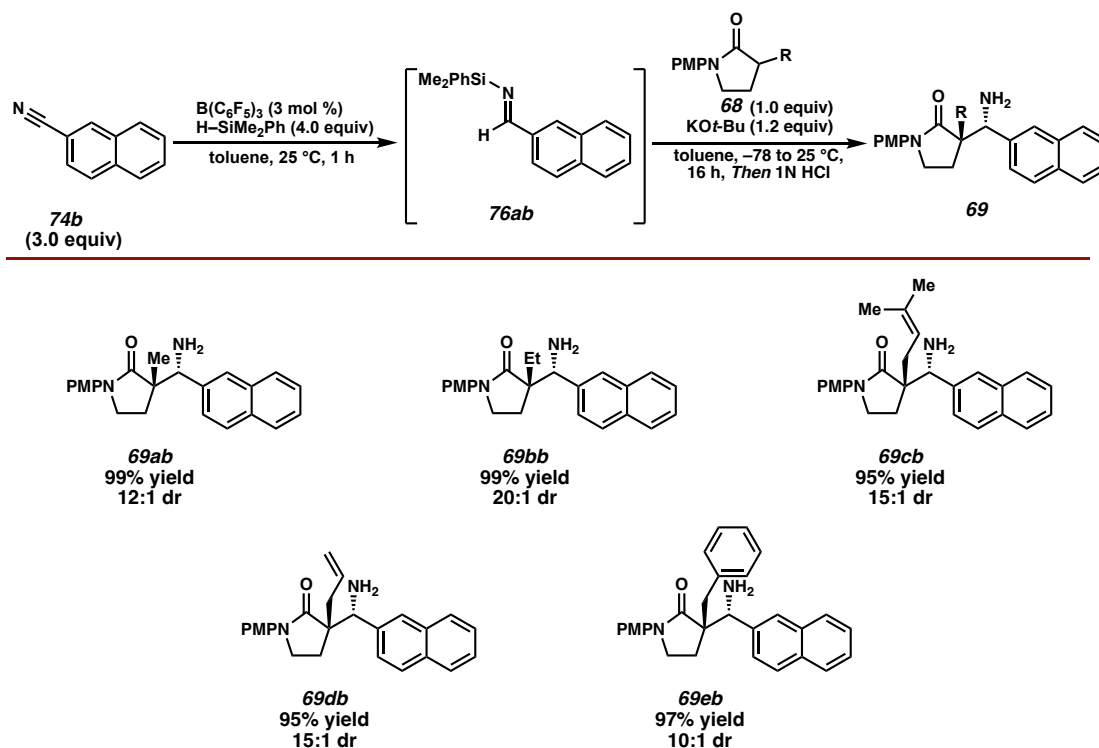


To show the potential of this telescoped approach, we targeted *N*- $SiMe_2Ph$  imine **76ab** derived from 2-naphthonitrile **74b** to be used as the electrophile in our telescoped, diastereoselective *direct* Mannich reaction (Scheme 1.5.2). We chose *N*- $SiMe_2Ph$  imine **76ab** to evaluate the synthetic potential for our developed, second-generation Mannich reaction since the boiling point of *N*- $Si$  imine **76ab** is predicted to be very high, and thus synthesis and isolation of this imine would be unfeasible via the aza-Peterson olefination and the corresponding distillation protocol required for purification. To our delight, the reaction sequence was shown to be highly tolerant to simple alkyl substitution at the  $\alpha$ -



position of the lactam pro-nucleophile **68**, with the corresponding  $\alpha$ -Me **69ab** and  $\alpha$ -Et **69bb** Mannich product being isolated in 99% yield and 12:1 dr, and 99% yield and 20:1 dr respectively. Allylic substitution was also well tolerated at the  $\alpha$ -position of the lactam pro-nucleophile **68**, as both the  $\alpha$ -prenyl,  $\beta$ -amino lactam **69cb** and  $\alpha$ -allyl,  $\beta$ -amino lactam **69db** were isolated in an excellent yield and diastereoselectivity. We also isolated Mannich product **69eb** bearing an  $\alpha$ -benzyl group in 97% yield, but with a slightly decreased 10:1 dr.

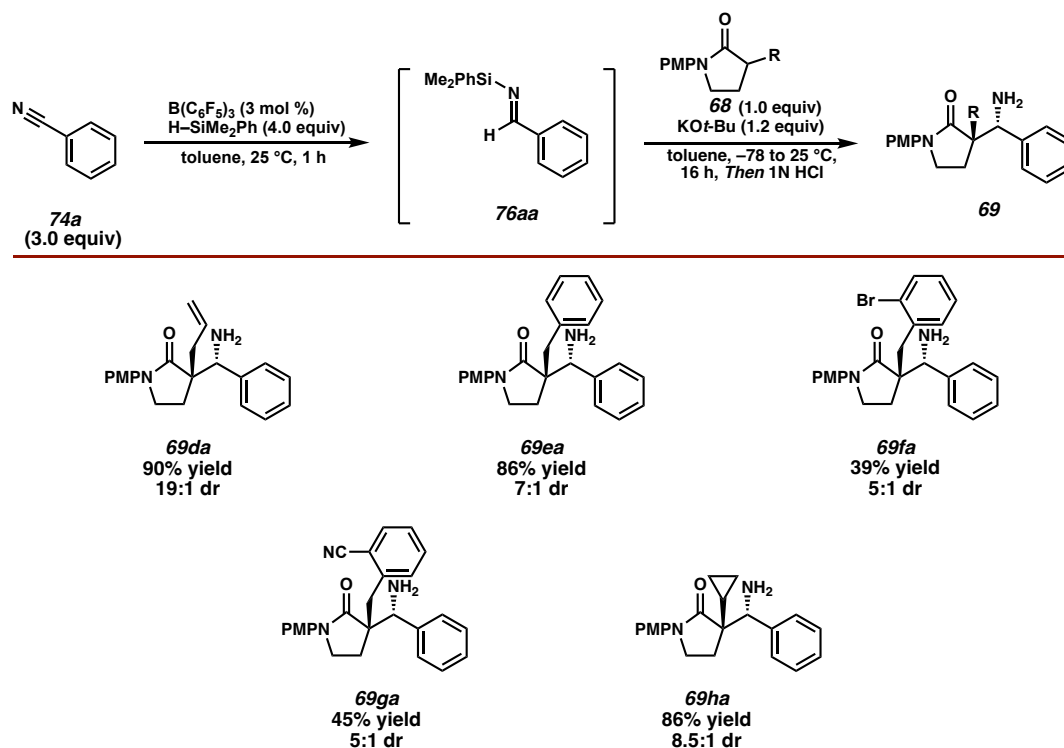
**Scheme 1.5.2** Scope of Tandem Reaction Using Imine **76ab** as the Electrophile



With optimized reaction conditions in hand, we moved our efforts toward establishing the substrate scope with respect to the lactam pro-nucleophile using *N*- $\text{SiMe}_2\text{Ph}$  imine **76aa** as the electrophile (Scheme 1.5.3). Lactam **68d** containing an  $\alpha$ -allyl

group was a competent pro-nucleophile in the telescoped process affording the corresponding  $\alpha$ -allyl,  $\beta$ -amino lactam product **69da** in a 90% yield and 19:1 dr.

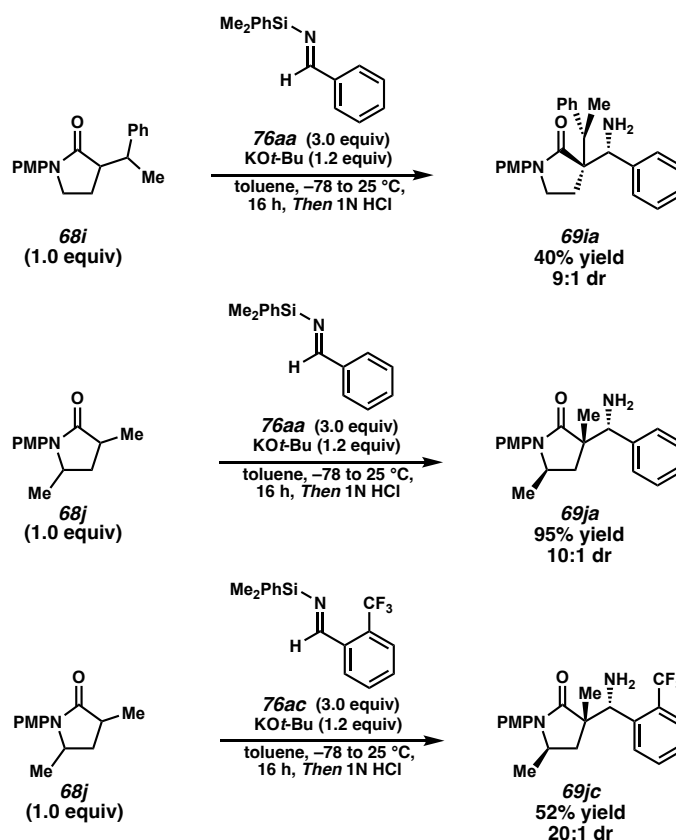
**Scheme 1.5.3** Substrate Scope of  $\alpha$ -Substituted- $\gamma$ -Lactam Pro-Nucleophiles **68**



Benzylic substitution at the  $\alpha$ -position was also well tolerated as the desired  $\alpha$ -benzyl Mannich product **69ea** in an 86% yield, albeit slightly diminished diastereoselectivity of 7:1 dr. An even more sterically demanding *ortho*-Br benzyl group substituted at the  $\alpha$ -position of the lactam **69f** was also tolerated; however, the isolated amine **69fa** was obtained at a lower 39% yield with a moderate diastereoselectivity of 5:1 dr. Similarly, *ortho*-cyano benzyl substituted lactam **68g** was also a competent pro-nucleophile with the desired aryl nitrile containing product **69ga** being isolated in a 45% yield and 5:1 dr. The lower yields of the bulkier, more sterically demanding  $\alpha$ -substituted lactams could be attributed to their notably slower reaction rates and their lower solubility

in the reaction conditions. The addition of ethereal solvents proved beneficial to increase the conversion as well as made the reaction outcomes more reproducible with minimal changes to the diastereoselectivity of the isolated products. The use of lactam **68h** bearing an  $\alpha$ -cyclopropyl group as the pro- nucleophile resulted in the isolation of the  $\beta$ -amino lactam **69ha** in a good yield of 86% and diastereoselectivity of 8.5:1 dr.

**Scheme 1.5.4** Diastereoselective Synthesis of Mannich Bases Bearing Stereotriads



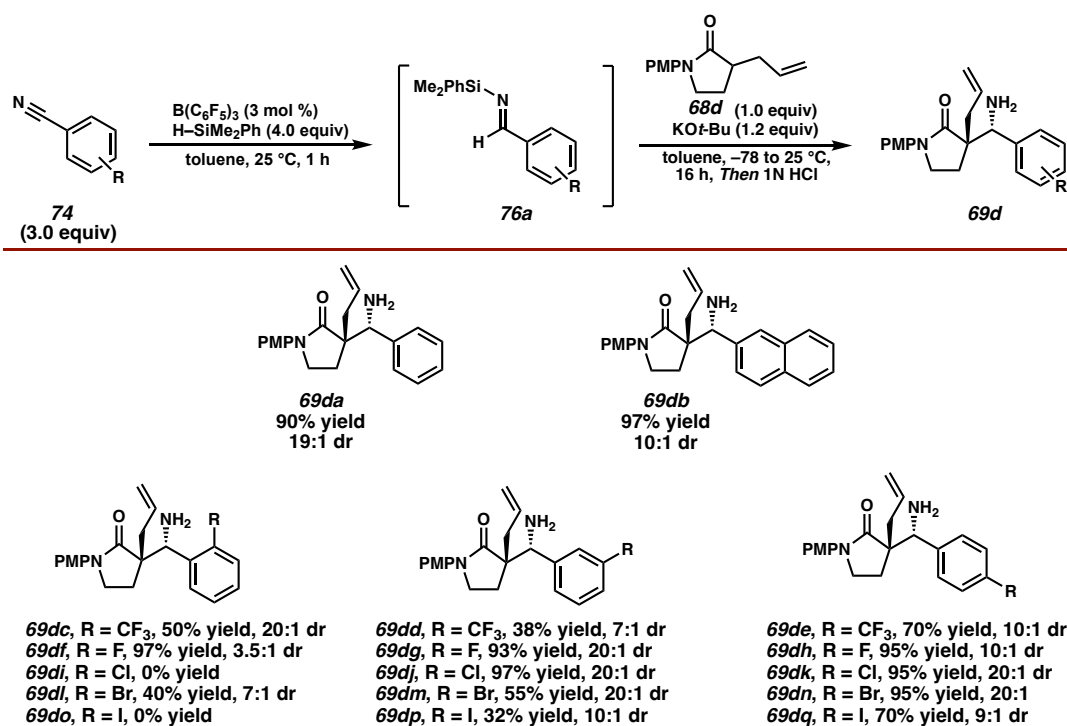
This was an exciting result because we hypothesized if the reaction tolerates lactam pro-nucleophiles bearing an  $\alpha$ -tertiary carbon, then perhaps we can stereoselectively synthesize Mannich bases containing three contiguous stereocenters using our telescoped reaction sequence. To our delight, lactam **68i** bearing an  $\alpha$ -phenethyl substituent afforded the corresponding  $\beta$ -amino lactam **69ia** possessing three contiguous stereocenters in a 9:1

dr as a ratio of the major diastereomer relative to all other observable diastereomers (Scheme 1.5.4). The diminished 40% yield of amine **69ia** can be explained by the poor solubility of lactam **68i**, even with diethyl ether used as a cosolvent. A similar effect was observed with substitution at the  $\gamma$ -position, as  $\alpha,\gamma$ -dimethyl lactam **68j** afforded the corresponding amine **69ja** in a 95% yield and 10:1 dr as a ratio of the major diastereomer relative to all other observable diastereomers. Additionally, the use of  $\alpha,\gamma$ -dimethyl lactam **68j** and *ortho*-CF<sub>3</sub> substituted imine **76ac** delivers the Mannich product **69jc** in a modest 52% yield and high diastereoselectivity of 20:1 dr.

After establishing the substrate scope with respect to the  $\alpha$ -substituted- $\gamma$ -lactam pro-nucleophiles, we then focused our efforts on determining the substrate scope with respect to the aryl nitrile pro-electrophile (Scheme 1.5.5). Unsubstituted benzonitrile **74a** and naphthonitrile **74b** were well tolerated in the reaction, affording the corresponding Mannich products **69da** and **69db** in excellent yield and diastereoselectivity. The introduction of substitution on the aryl nitrile corresponded to an observable change in the reaction profile of the hydrosilylation stage. The rate of hydrosilylation as well as the susceptibility of the imines to undergo a second hydrosilylation event were observed to be significantly dependent on the substitution of the aryl nitrile.<sup>35</sup> Generally, the use of electron-deficient aryl nitriles as pro-electrophiles was shown to be highly effective in our telescoped process. Trifluorobenzonitriles **74c-e** were shown to be tolerated at the *ortho*-, *meta*-, and *para*-positions in our telescoped diastereoselective Mannich reaction. Of note, the sterically congested *N*-SiMe<sub>2</sub>Ph imine **76ac** derived from bulky *ortho*-trifluoromethyl benzonitrile **74c** afforded the corresponding  $\beta$ -amino lactam **69dc** in a 50% yield with an excellent diastereoselectivity of 20:1 dr. This result is particularly exciting because the

reaction was successful despite the associated steric profile<sup>37</sup> and electron withdrawing nature<sup>38</sup> of the *ortho*-CF<sub>3</sub> group. The use of *meta*-trifluoromethyl benzonitrile **74d** resulted in a decrease in isolated yield of the corresponding Mannich base **69dd** to 38% yield as well as a diminished 7:1 dr.

**Scheme 1.5.5** Substrate Scope of Aryl Nitrile Pro-Electrophiles **74**



The observed difference in yield and selectivity between the *ortho*- and *meta*-CF<sub>3</sub> substitution suggests that electronics of the arene have a more profound influence on the reactivity profile than the steric influence of the substituent.<sup>37,38</sup> This notion is further supported by the increase in yield and selectivity observed in the synthesis of Mannich base **69de**, where the trifluoromethyl group is substituted at the *para*-position of the arene with the electronics more comparable to the *ortho*-CF<sub>3</sub> substrate **69dc** than to the *meta*-CF<sub>3</sub> substrate **69dd**.<sup>38</sup> We sought to probe the extent of the reactivity trends observed in the trifluoromethyl series by examining the series of halogen substituted benzonitriles as

various electron deficient pro-electrophiles. Generally, the fluorobenzonitrile pro-electrophiles **74f–h** were shown to be well tolerated as products fluorobenzene Mannich products **69df–69dh** in excellent yields. The  $\beta$ -amino lactam products **69dg** and **69dh** bearing fluorine substituted at the *meta*- and *para*-position of the arene were isolated in great diastereoselectivity of 20:1 dr and 10:1 dr respectively. To our surprise, *N*-SiMe<sub>2</sub>Ph imine electrophile **76af** derived from *ortho*-fluorobenzonitrile **74f** resulted in the isolation of amine **69df** in an excellent 97% yield, with a significantly diminished 3.5:1 dr. The decrease in diastereoselectivity observed with the *ortho*-fluorobenzene *N*-SiMe<sub>2</sub>Ph imine electrophile **76af** serves as a stark contrast to the high diastereoselectivity observed using *ortho*-trifluoromethyl *N*-SiMe<sub>2</sub>Ph imine electrophile **76ac** as the more sterically encumbered imine resulted in higher diastereoselectivity.<sup>37</sup> The positioning of the aryl fluoride allows for an interaction between the sp<sup>2</sup> C–F bond<sup>39</sup> and the silyl iminium to promote the formation of the disfavored *syn* Mannich product.<sup>40</sup> The observed decrease in selectivity suggests that the silicon species is crucial for the formation of the Mannich base with high diastereoselectivity.

We observed no productive reactivity using *ortho*-chlorobenzonitrile **74i** as the pro-electrophile, and an unknown side product was exclusively formed after the tandem reaction sequence. To our delight, *meta*- and *para*-chlorobenzonitriles **74j** and **74k** were shown to be excellent substrates as the corresponding  $\beta$ -amino lactams **69dj** and **69dk** were both isolated in greater than 95% yield and 20:1 dr. Generally, bromobenzonitriles were shown to be tolerated as substrates for the telescoped reaction sequence. The imine derived from the *ortho*-bromobenzonitrile **74l** resulted in the formation of Mannich product **69dl** in a modest 40% yield and 7:1 dr. The *meta*- and *para*-bromobenzonitriles **74m** and **74n**

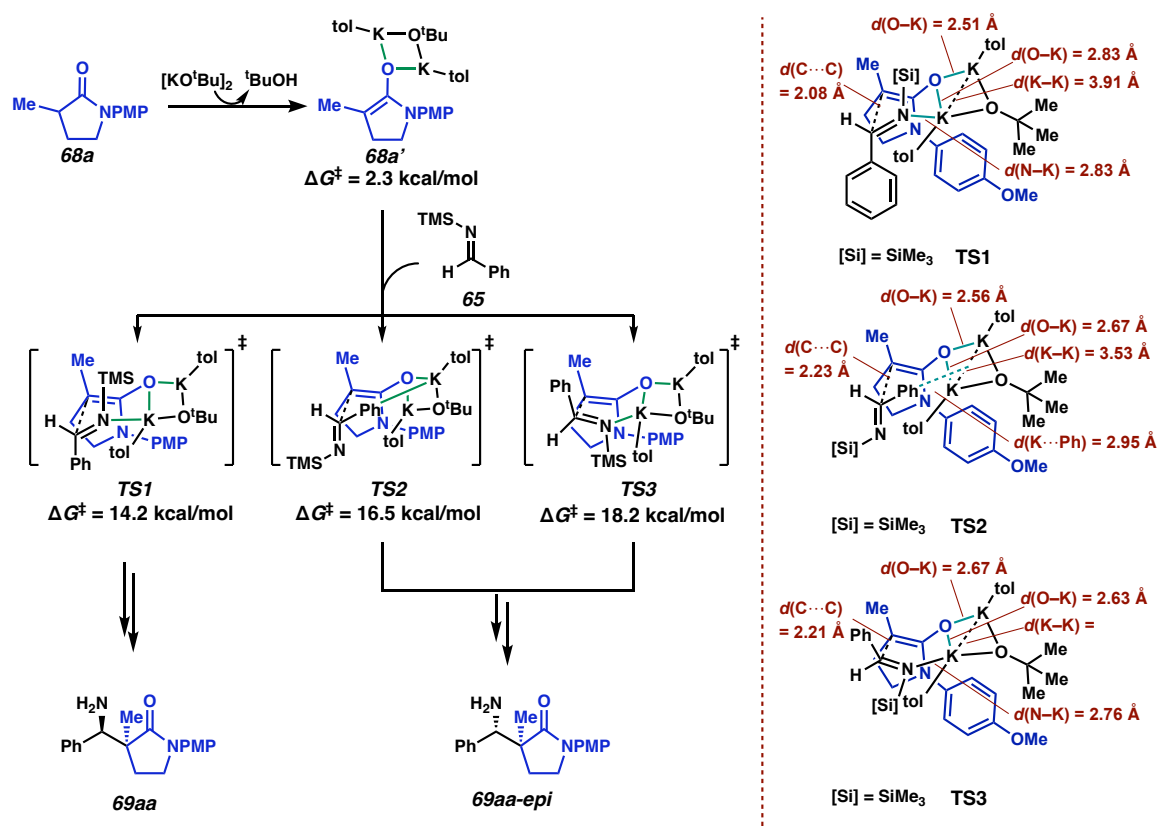
were shown to be good substrates as the corresponding  $\beta$ -amino lactams **69dj** and **69dk** were both isolated in excellent diastereoselectivity of 20:1 dr. The use of *ortho*-iodobenzonitrile **74o** was not amenable to our reaction conditions since no hydrosilylation of the aryl nitrile to the *N*-SiMe<sub>2</sub>Ph imine was observed due to poor solubility of the aryl nitrile **74o** in toluene. Gratifyingly, *meta*- and *para*-iodobenzonitrile **74p** and **74q** did undergo the hydrosilylation, and the reaction of the corresponding *N*-SiMe<sub>2</sub>Ph imine delivered the  $\beta$ -amino lactam products **69do** and **69dq** in moderate yield and good diastereoselectivity. Electron-rich arenes were not viable pro-electrophiles for the transformation due to their inability to engage in the B(C<sub>6</sub>F<sub>5</sub>)<sub>3</sub>-catalyzed hydrosilylation under our optimized reaction conditions. Cheng and co-workers reported diminished reactivity with substrates containing Lewis basic heteroatoms,<sup>35</sup> which combined with solubility issues in toluene led to these substrates being incompetent precursors to the *N*-silyl imines.

## 1.6 COMPUTATIONAL INVESTIGATION INTO THE MANNICH REACTION

With the scope of our diastereoselective Mannich reaction established, we were then interested in determining a model to explain the observed diastereoselectivity for this transformation. In collaboration with the Liu group at the University of Pittsburgh, the mechanism that controls the diastereoselectivity of the Mannich reaction and the potential role of KO*t*-Bu<sup>17,41</sup> were investigated using density functional theory (DFT) calculations.<sup>42</sup> Considering potassium *tert*-butoxide tetramer can easily dissociate to a dimer,<sup>41a</sup> and binuclear potassium complexes<sup>41,43</sup> have been described in previous reports as the active species in the potassium-catalyzed  $\alpha$ -alkylation of benzyl sulfides,<sup>44</sup> dimeric potassium

*tert*-butoxide was used as the base in the calculations, in which one toluene solvent molecule was added to bind to each K to account for explicit solvent effects.

**Scheme 1.6.1** Computational Analysis of Transition States Leading to Major and Minor Diastereomers of the Mannich Reaction



Our DFT calculations indicate that deprotonation of lactam **68a** with potassium *tert*-butoxide dimer to form potassium enolate **68a'** is endergonic by 2.3 kcal/mol (see Figure A2.1.3). The nucleophile used was  $\alpha$ -Me lactam **68a** and the electrophile was the  $N$ -TMS imine **65** in the calculations. An exhaustive conformational search was performed using CREST/GFN2-xTB and the most stable 20 conformers were then fully optimized using DFT at the M06-2X/6-31G(d) level of theory. As a result of the conformation search, we located the lowest-energy TS conformers, **TS1** and **TS2**, leading to the *anti*- and *syn*-



products **69aa** and **69aa-epi** respectively (Scheme 1.6.1). The computed activation free energy for **TS1** ( $\Delta G^\ddagger = 14.2$  kcal/mol with respect to **68a**) is 2.3 kcal/mol lower than that for **TS2** ( $\Delta G^\ddagger = 16.5$  kcal/mol), which is in agreement with the experimentally observed diastereoselectivity of 20:1. In **TS1** and **TS2**, both potassium atoms bind to the *tert*-butoxide oxygen and the lactam enolate oxygen, forming a rhombus-shaped geometry that resembles the  $M_2X_2$  core of the  $KOt$ -Bu dimer. Although this four-atom  $K_2O_2$  structure remains similar in **TS1** and **TS2**, when the different prochiral  $\pi$ -faces of the imine are involved in bond formation, different interactions between the imine and  $K_2O_2$  core are observed.

In the transition state leading to the favored *anti*-product (**TS1**), the imine C=N bond is *syn*-clinal with the enolate oxygen, enabling a stabilizing interaction (2.69 Å) between the electron-rich imine nitrogen and one of the potassium atoms. The relatively late transition state, evidenced by the shorter forming C–C bond (2.08 Å compared to 2.23 Å in **TS2**), increases the negative charge on the imine N (see Figure A2.1.4 for computed NPA charges) and thus further promotes the N–K interaction in **TS1**. In **TS2**, the Ph group on the imine, rather than the imine C=N bond, points toward the enolate oxygen and the K atoms. As a result, a cation- $\pi$  interaction<sup>45</sup> (2.95 Å) between a K and the Ph group in **TS2** is observed in place of the N–K interaction in **TS1**. Because the Ph group is less negatively charged and is a worse electron donor than the imine N, this cation- $\pi$  is expected to be weaker than the N–K interactions in **TS1**.

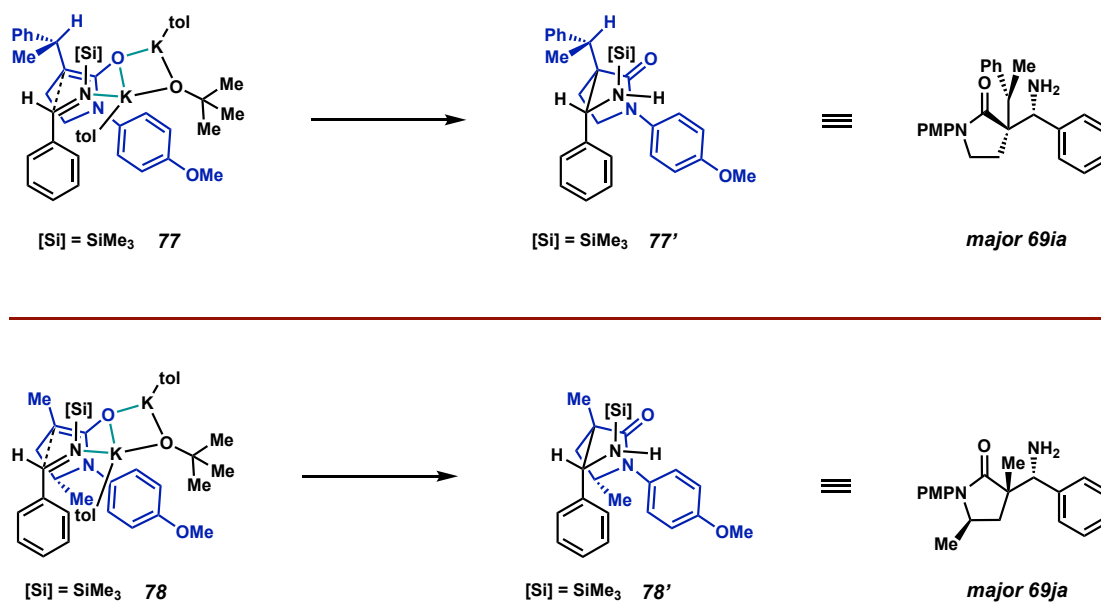
This electron donation difference is observed in the difference between the K–K bond distance the  $K_2O_2$  core between **TS1** and **TS2**. The stronger electron donation from the imine nitrogen in **TS1** causes an elongation of the K–K bond distance to 3.91 Å

compared to 3.71 Å in enolate **68a'**. The weaker cation- $\pi$  interaction observed in **TS2** results in a shortening of the K–K bond distance in the K<sub>2</sub>O<sub>2</sub> core to 3.53 Å, which suggests the nitrogen lone pair is a stronger electron donor in **TS1**. The imine N–K interaction was also observed in a less stable TS conformer (**TS3**) leading to the minor product **4a-epi**. However, **TS3** is computed to be less stable than both **TS1** and **TS2** because this stereoisomeric transition state has a boat geometry rather than the chair geometry in **TS1** and **TS2**. Taken together, the DFT calculations indicate that the stabilizing N–K interaction in the chair-like imine addition transition state (**TS1**) controls the diastereoselectivity of the Mannich reaction. Furthermore, the electropositive silicon atom increases the electron-density of the imine nitrogen responsible for the exquisite diastereoselectivity observed in the transformation. This suggests that the *N*-silyl imine electrophiles are more favorable compared to the conventional *N*-carbonyl or *N*-Ts imine electrophiles due to the more electron rich *N*-center in the *N*-silyl imines. Additionally, the generally high diastereoselectivity observed for electron deficient arenes in the imine electrophile could potentially be due to the diminished cation- $\pi$  interaction between the imine and the K<sub>2</sub>O<sub>2</sub> core in **TS2** leading to the undesired *syn*-diastereomer (See Figure A2.1.5 for a reaction coordinate energy diagram).

We could also extend this model to explain the observed diastereoselectivity achieved in products **69ia** and **69ja** containing three stereocenters (Scheme 1.6.2). In both cases, we believe the substitution present on the lactam pro-nucleophile imparts a bias to the facial approach of the imine electrophile, resulting in the diastereoselective synthesis of the stereotriad. In the case of product **69ia**, we believe the enolate derived from lactam **68i** exists locked in a conformation that minimizes A<sub>1,3</sub> strain. This rigid enolate geometry

biases the imine electrophile to approach from the face away from the bulky phenyl group in **77**, resulting in the synthesis of major **69ia** containing three contiguous stereocenters in good diastereoselectivity. A similar argument regarding biasing facial approach of the electrophile can be extended to the enolate derived from  $\alpha,\gamma$ -dimethyl lactam **68j**. In **78**, we believe the imine electrophile approaches from the less hindered face away from the protruding  $\gamma$ -methyl group on the enolate derived from lactam **68j**, resulting in the synthesis of major **69ja** containing three stereocenters in a 10:1 dr.

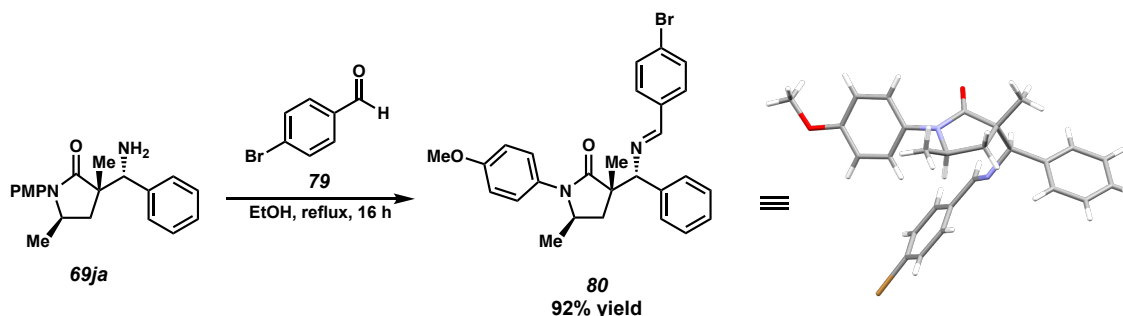
**Scheme 1.6.2** Extension of the Computed Major Transition State



To further confirm this model, we sought to obtain a crystal structure of  $\beta$ -amino lactam product **69ja** to observe the relative stereochemistry of the three stereocenters (Scheme 1.6.3). Treating amine **69ja** with *para*-bromo benzaldehyde **79** and refluxing the reaction mixture in ethanol overnight promoted formation of the desired Schiff base **80**. A

crystal structure of this imine was obtained to confirm the relative stereochemistry as the *syn*,*anti*-product, which is consistent with the extension of our computational model.

**Scheme 1.6.3** Determination of the Relative Configuration of Mannich Product **69ja**

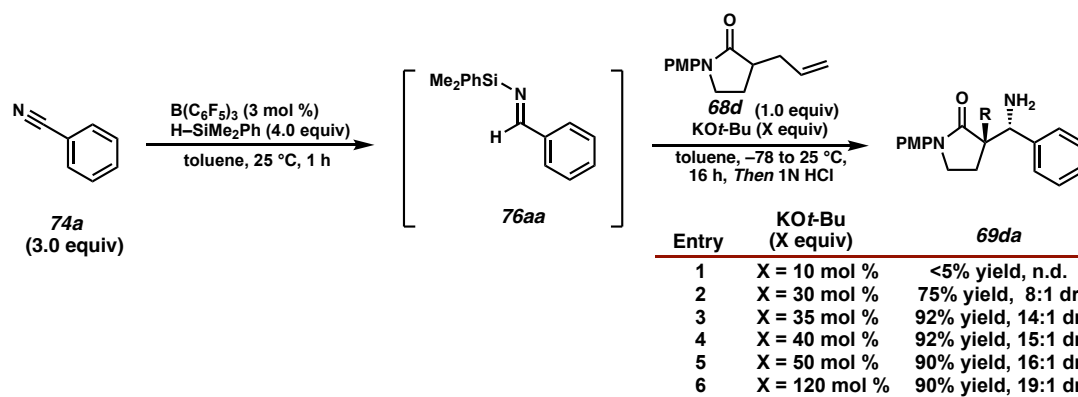


## 1.7 IDENTIFICATION OF THE KO $t$ -BU CATALYZED DIASTEREOSELECTIVE MANNICH REACTION

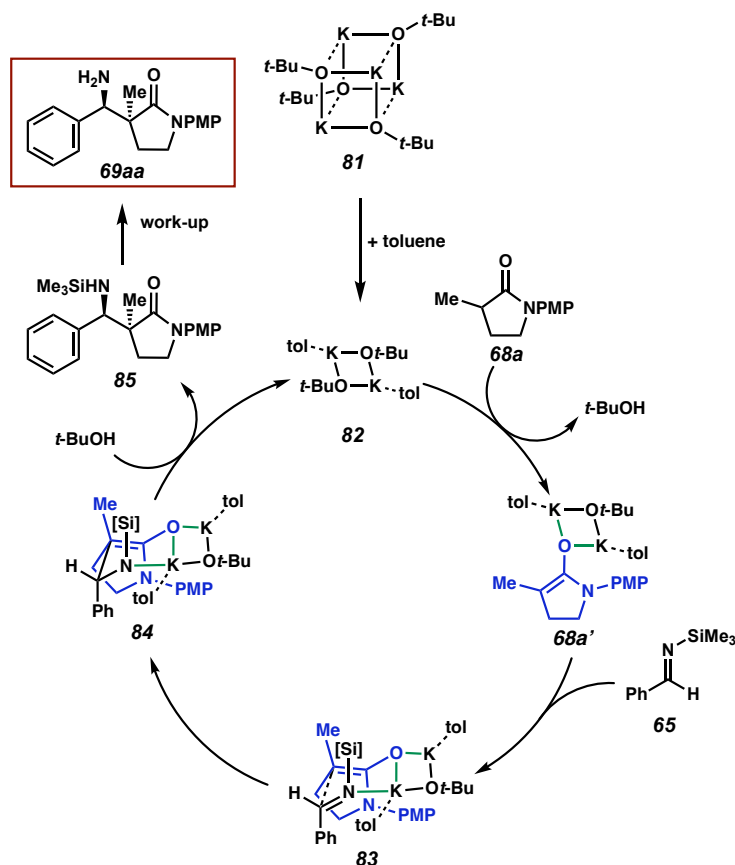
Mechanistically, we were interested in how potassium *tert*-butoxide was a competent base for this diastereoselective Mannich reaction since the pK<sub>a</sub> of an  $\alpha$ -substituted amide is approximated to be 17 pK<sub>a</sub> units higher than potassium *tert*-butoxide. As a result, the active enolate nucleophile is orders of magnitude less concentrated than the solvated *tert*-butoxide M<sub>2</sub>X<sub>2</sub> cluster. The product potassium amide delivered after C–C bond formation is a highly basic intermediate that can serve to either regenerate our potassium *tert*-butoxide base or our active enolate nucleophile directly, thus rendering this reaction catalytic in base. To test this hypothesis, we performed a reaction screen that varied the equivalents of potassium *tert*-butoxide to probe whether desired reactivity was observed at substoichiometric amounts of base (Scheme 1.7.1). Gratifyingly, we obtained the desired  $\beta$ -amino lactam product **69da** in 92% yield and 15:1 dr using 35 mol% of

potassium *tert*-butoxide, which suggests that there exists a catalytic cycle to regenerate our active enolate nucleophile.

**Scheme 1.7.1** Discovery of the KO*t*-Bu Catalyzed Diastereoselective Mannich Reaction

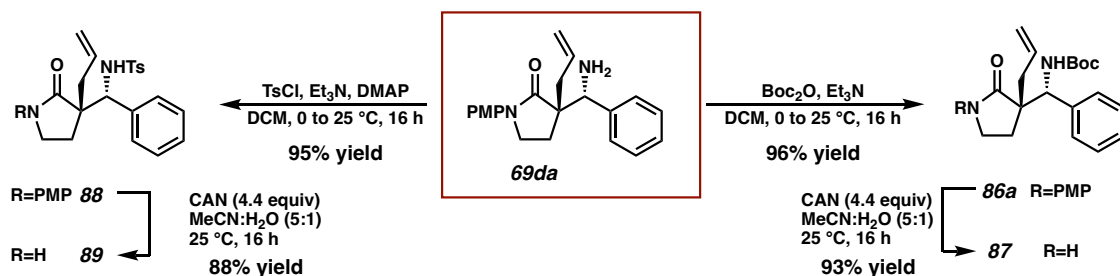


We propose the following mechanism summarizing our computational and experimental results during our investigation into the diastereoselective Mannich reaction of  $\alpha$ -substituted- $\gamma$ -lactam pro-nucleophiles (Scheme 1.7.2). To enter the cycle, we propose *tert*-butoxide dimer<sup>46</sup> **82** initially deprotonates lactam **68a** to generate our active  $M_2X_2$  bound enolate **68a'** as well as generates *tert*-butanol. This complex associates with the imine electrophile **65** to form the intermediate **83** which is primed to undergo the *anti*-selective Mannich reaction to form potassium amide **84**. This intermediate can deprotonate the *tert*-butanol generated from the deprotonation of lactam **68a** to form the  $K_2O_2$  *tert*-butoxide dimer **82** to continue the catalytic cycle. The *N*-silyl amine Mannich product **85** persists upon protonation *via* aqueous work-up to yield the desired *anti*-selective Mannich base **69aa**.

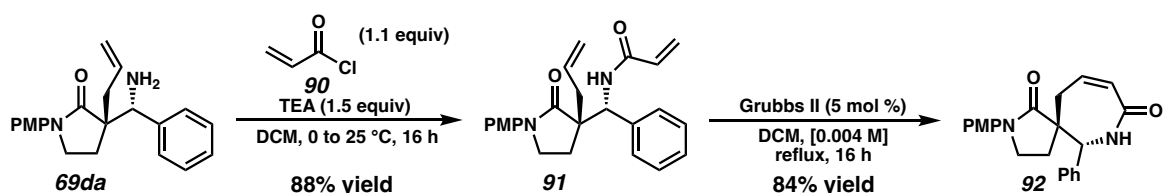
**Scheme 1.7.2** Proposed Catalytic Cycle of the Diastereoselective Mannich Reaction

## 1.8 PRODUCT DERIVATIZATION OF $\beta$ -AMINO LACTAMS

With the scope and mechanism of the diastereoselective Mannich reaction established, we sought to further elaborate  $\beta$ -amino lactam products to demonstrate the synthetic utility of the amines delivered by our reaction. The primary amine **69da** underwent a facile *N*-Ts and *N*-Boc protection to afford the corresponding protected amines **86a** and **88** in 96% and 95% yields, respectively (Scheme 1.8.1). These two protected amines smoothly undergo CAN-promoted *N*-PMP cleavage to afford the secondary amides **87** and **89** in 88% and 93% yields, respectively. Unfortunately, amide reduction of Mannich products **69da**, **86a** or **88** with LAH was unsuccessful, presumably due to the steric bulk of the adjacent quaternary center.

**Scheme 1.8.1** Protecting Group Manipulation of the Mannich Products.

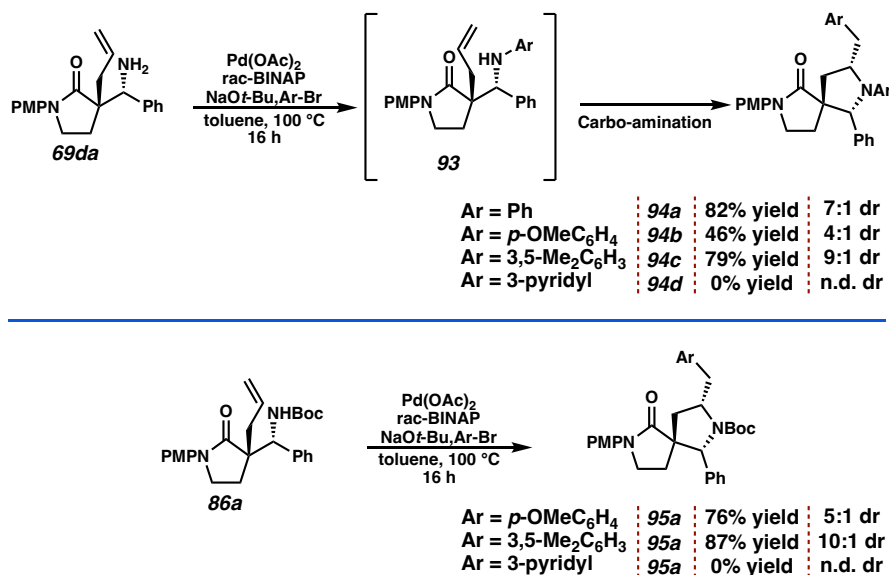
After demonstrating that the primary amine in our Mannich base products can be easily functionalized, we sought to leverage this reactive functional group handle to access various, novel bis-*N*-heterocyclic spiro lactam motifs. The allyl group present in  $\beta$ -amino lactam **69da** appeared primed to undergo a ring closing metathesis (RCM) reaction with an appropriately functionalized amine handle (Scheme 1.8.2). Concerned about selectivity issues between mono- and bis-alkylation of the primary amine, we treated the  $\beta$ -amino lactam **69da** with acryloyl chloride **90** to deliver acrylamide **91** in 88% yield. Subjecting acrylamide **91** to Grubbs' 2<sup>nd</sup> generation catalyst led to the isolation of the desired spirocyclic  $\epsilon$ -lactam **92** in 84% yield.<sup>47</sup>

**Scheme 1.8.2** Ring Closing Metathesis Approach to Form Spirocycle **92**

We identified  $\beta$ -amino lactam **69da** as a suitable substrate to investigate a Pd-catalyzed spiro-cyclization involving intramolecular C–N bond formation (Scheme 1.8.3). Inspired by Wolfe's two-step, one-pot intramolecular carboamination, we subjected Mannich product **69da** to the disclosed Pd-catalyzed conditions.<sup>48</sup> This reaction initiates

via an intermolecular amino arylation between the primary amine and bromobenzene. The newly formed aniline **93** is now a competent reaction partner to undergo the Pd-catalyzed intramolecular carboamination to deliver the desired bis-arylated spirocyclic pyrrolidine **94** in an 82% yield and modest 7:1 dr. We showed that electron-rich aryl bromides were tolerated in the one-pot *N*-arylation, carboamination; however, the resulting spirocycle was obtained in lower yield and diastereoselectivity (46% yield and 4:1 dr for spirocycle **94b**). Electron-neutral aryl bromides were well tolerated, as 3,5-dimethylbromobenzene delivered the corresponding spirocycle **94c** in good yield and diastereoselectivity. Electron-deficient aryl bromides such as 3-bromopyridine were not tolerated in the one-pot spirocyclization. Additionally, the *N*-Boc allyl Mannich product **86a** was a sufficient substrate in the intramolecular carboamination to deliver spirocycles **95** in good yield and modest to good diastereoselectivity.

**Scheme 1.8.3** Intramolecular Pd-catalyzed Carboamination to Form Spirocycles

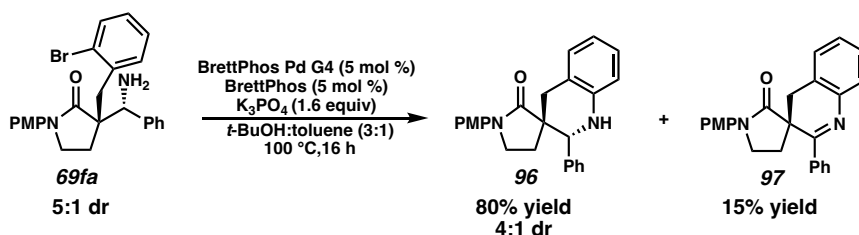


With the successful spirocyclization inspired by the Pd-catalyzed carboamination reported by Wolfe and coworkers to yield pyrrolidine **94**, we wished to extend our library



of spirocycles to include a spirocyclic tetrahydroquinoline motif (Scheme 1.8.4). To achieve this, we identified Mannich base **69fa** as a suitable candidate for a Pd-catalyzed spirocyclization, as a facile Buchwald-Hartwig type coupling would yield the desired spirocycle.<sup>49</sup> To our delight, treatment of the  $\beta$ -amino lactam **69fa** with BrettPhos Pd G4 and BrettPhos in a 3:1 mixture of *t*-BuOH:toluene led to the desired spirocyclic tetrahydroquinoline **96** in a 80% yield. However, an unexpected dihydroquinoline product **97** was observed after column chromatography, presumably due to the acid promoted oxidation of the major *anti*-diastereomer of the desired tetrahydroquinoline **96**.

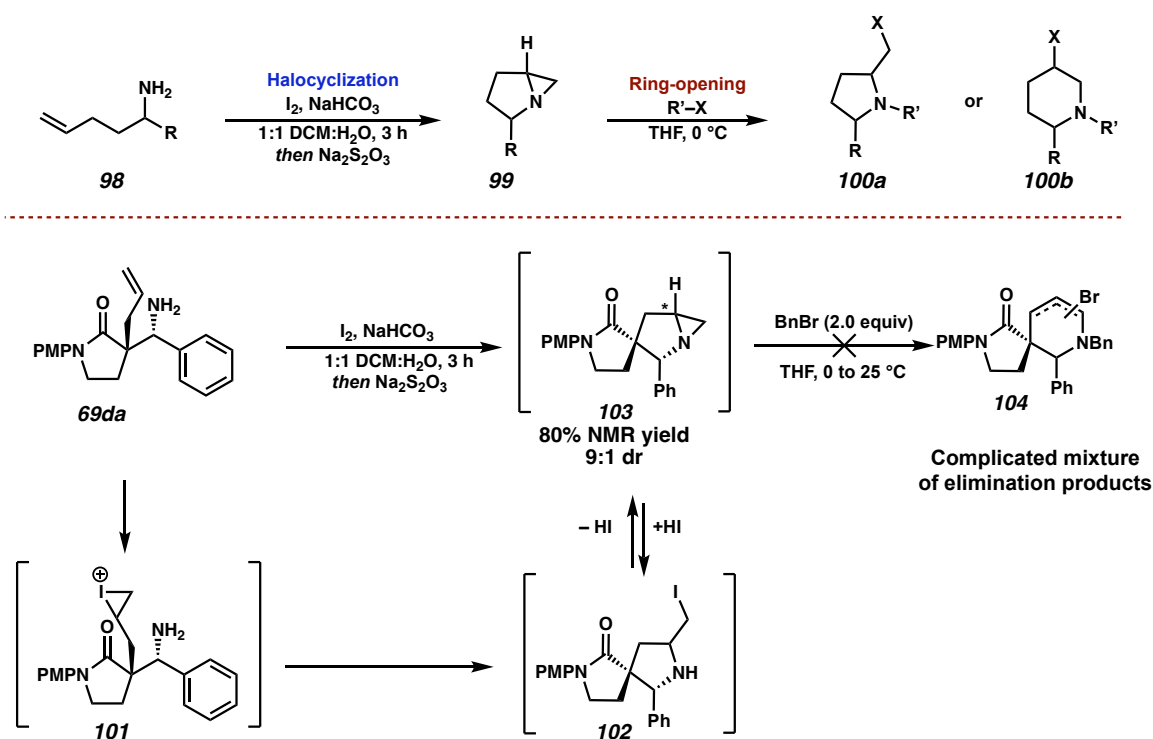
**Scheme 1.8.4** Intramolecular Pd-catalyzed Buchwald-Hartwig Amination to Form Spirocycle **96**



Motivated by our successful spirocyclization attempts leveraging transition metal catalysis, we dedicated our efforts toward chemoselective olefin functionalization of the pendant allyl group to facilitate spirocyclization. We envisioned that activation of the olefin with an electrophilic halide source would deliver a halonium species, which could be trapped by the pendant amine to afford the desired spirocyclized product. In similar systems, treatment of a similar olefin with  $I_2$  and  $NaHCO_3$  led to complete conversion to the corresponding azabicyclo[3.1.0]hexane (Scheme 1.8.5).<sup>50</sup> In addition to being structurally unique, these azabicycles have been shown to undergo a facile ring expansion reaction to the corresponding 3-halopiperidine when treated with an alkyl halide.<sup>51</sup> We

found that reacting  $\beta$ -amino lactam **69da** with  $I_2$  in a biphasic mixture of DCM:water buffered with  $NaHCO_3$  resulted in the formation of the desired azabicyclic intermediate **103** in an 80% NMR yield. It was critical to quench any remaining iodine with copious washings of  $Na_2S_2O_3$ , as any residual iodine in the crude reaction mixture was able to open the azabicyclic intermediate **103** *in vacuo* to the undesired pyrrolidine **102**. The azabicyclic intermediate **103** was found to be highly sensitive toward any nucleophilic ring-opening, so purification or isolation of this compound using silica gel chromatography proved to be challenging. Unfortunately, all efforts to perform the desired ring expansion to the corresponding 3-Br-piperidine led to a complicated mixture of halogenated and unsaturated piperidine products **104**.

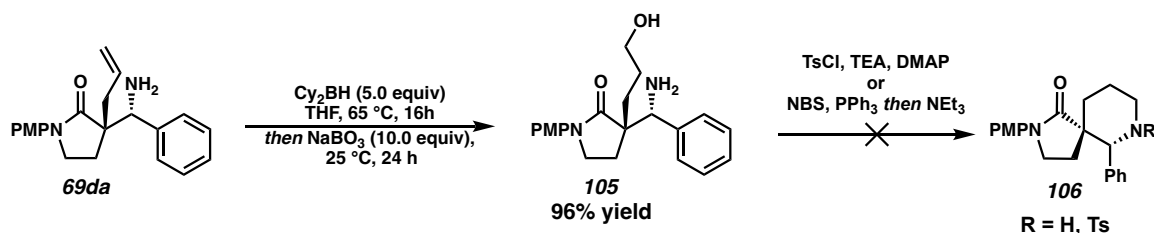
**Scheme 1.8.5** Failed Attempts at Intramolecular Halo-amination of Product **69da**



Even though the desired ring formation ultimately failed, we were excited to observe chemoselective olefin functionalization in this system and focused our efforts

toward investigating a chemoselective oxidation of the pendent olefin in the presence of the unprotected amine. Oxidation of the olefin in  $\beta$ -amino lactam **69da** under ozonolysis or Lemieux-Johnson conditions led to a complex mixture of products. To our delight, hydroboration of lactam **69da** using 5.0 equivalents of  $\text{Cy}_2\text{BH}$  and reflux in THF led to the desired amino alcohol **105** in a 96% yield after an oxidative workup with  $\text{NaBO}_3$  (Scheme 1.8.6).<sup>52</sup> Unfortunately, attempts to convert the alcohol into a sufficient leaving group via tosylation or an Appel reaction to promote the intramolecular annulation to the corresponding spirocyclic piperidine **106** failed in our hands.

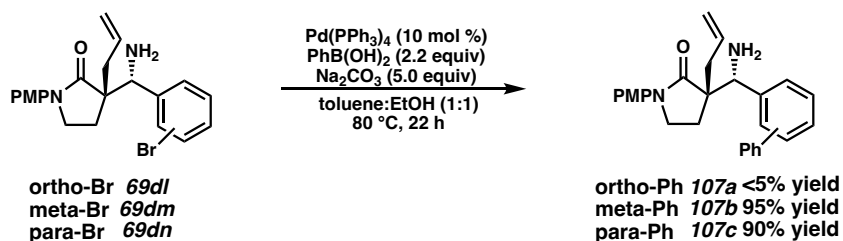
**Scheme 1.8.6** Failed Attempts at Intramolecular Cyclization Following Olefin Oxidation of  $\beta$ -Amino Lactam **69da**



Our final product derivatizations centered on developing a Pd-catalyzed cross-coupling protocol using the aryl halide in our  $\beta$ -amino lactam products **69d** as a coupling partner directly to form C–C bonds without protection of the Lewis basic primary amine (Scheme 1.8.7). There are not many reports of Pd-catalyzed C–C bond formation reactions in the presence of an unprotected amine on the coupling partner,<sup>53</sup> and we wished to investigate the compatibility of our  $\beta$ -amino lactam products directly as the aryl halide electrophile. Under standard Suzuki-Miyura arylation conditions, *meta*- and *para*-bromo substituted  $\beta$ -amino lactams **69dm** and **69dn** were excellent electrophiles, delivering the corresponding biaryl products **107b** and **107c** in 95% yield and 90% yield respectively.

Unfortunately, *ortho*-bromo substituted Mannich base **69dl** was not a suitable coupling partner in the Pd-catalyzed arylation, as the reaction resulted in a complex mixture of products.

**Scheme 1.8.7** Intermolecular Pd-catalyzed Cross-Coupling Reactions of Aryl Bromide Substituted  $\beta$ -Amino-Lactam Products



## 1.9 CONCLUSION

Disclosed herein is the full account of our development of a diastereoselective Mannich reaction between  $\alpha$ -substituted- $\gamma$ -lactam pro-nucleophiles and aryl *N*-silyl imines. Initially, we synthesized the moisture sensitive *N*-TMS imine electrophile via an Aza-Peterson olefination and isolated the electrophile via vacuum distillation. However, we revealed that our imine electrophiles can be made *in situ* via a catalytic hydrosilylation from a readily available aryl nitriles and used directly without purification to afford a variety of  $\beta$ -amino lactam Mannich products in good yield and diastereoselectivity. After computational investigation into the transition state of the diastereoselective C–C bond formation, we identified that the *direct* Mannich reaction can be performed with catalytic amounts of *KOt*-Bu successfully while maintaining the high diastereoselectivity and yield observed using stoichiometric amounts of base. The  $\beta$ -amino lactam products were shown to be highly versatile intermediates toward the synthesis of various saturated, nitrogen containing spirocycles. Our telescoped hydrosilylation, *direct* Mannich reaction serves as

the first stereoselective Mannich reaction using simple,  $\alpha$ -substituted amide pronucleophiles to deliver  $\beta$ -amino lactam Mannich products bearing an all-carbon quaternary center.

## 1.10 EXPERIMENTAL SECTION

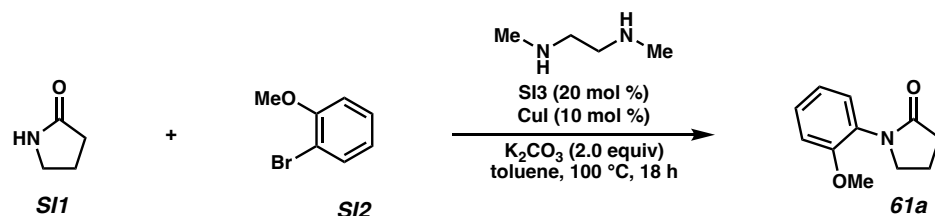
### 1.10.1 MATERIALS AND METHODS

Unless otherwise stated, reactions were performed in flame-dried glassware under a nitrogen atmosphere using dry, deoxygenated solvents. Solvents were dried by passage through an activated alumina column under argon.<sup>54</sup> Reaction progress was monitored by thin-layer chromatography (TLC). TLC was performed using E. Merck silica gel 60 F254 precoated glass plates (0.25 mm) and visualized by UV fluorescence quenching, *p*-anisaldehyde, or KMnO<sub>4</sub> staining. Silicycle SiliaFlash® P60 Academic Silica gel (particle size 40–63  $\mu$ m) was used for flash chromatography. <sup>1</sup>H NMR spectra were recorded on Varian Inova 500 MHz and 600 MHz and Bruker 400 MHz spectrometers and are reported relative to residual CHCl<sub>3</sub> ( $\delta$  7.26 ppm), C<sub>6</sub>D<sub>6</sub> ( $\delta$  7.16 ppm) or CD<sub>3</sub>OD ( $\delta$  3.31 ppm). <sup>13</sup>C NMR spectra were recorded on a Varian Inova 500 MHz spectrometer (125 MHz) and Bruker 400 MHz spectrometers (100 MHz) and are reported relative to CHCl<sub>3</sub> ( $\delta$  77.16 ppm), C<sub>6</sub>D<sub>6</sub> ( $\delta$  128.06 ppm) or CD<sub>3</sub>OD ( $\delta$  49.01 ppm). Data for <sup>1</sup>H NMR are reported as follows: chemical shift ( $\delta$  ppm) (multiplicity, coupling constant (Hz), integration). Multiplicities are reported as follows: s = singlet, d = doublet, t = triplet, q = quartet, p = pentet, sept = septuplet, m = multiplet, br s = broad singlet, br d = broad doublet. Data for <sup>13</sup>C NMR are reported in terms of chemical shifts ( $\delta$  ppm). IR spectra were obtained by use of a Perkin Elmer Spectrum BXII spectrometer or Nicolet 6700 FTIR spectrometer using thin films deposited on NaCl plates and reported in frequency of absorption (cm<sup>-1</sup>).

Optical rotations were measured with a Jasco P-2000 polarimeter operating on the sodium D-line (589 nm), using a 100 mm path-length cell. High resolution mass spectra (HRMS) were obtained from the Caltech Mass Spectral Facility using a JEOL JMS-600H High Resolution Mass Spectrometer in fast atom bombardment (FAB+) or electron ionization (EI+) mode or using an Agilent 6200 Series TOF with an Agilent G1978A Multimode source in electrospray ionization (ESI+), atmospheric pressure chemical ionization (APCI+), or mixed ionization mode (MM: ESI-APCI+).

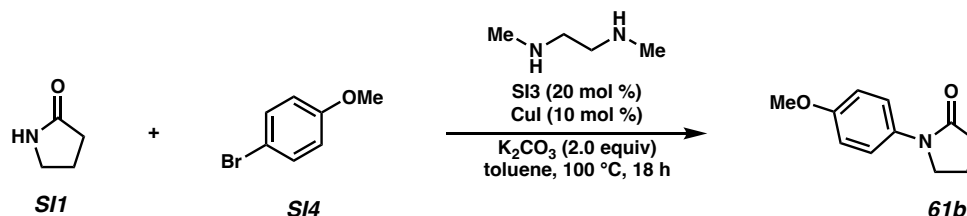
### 1.10.2 EXPERIMENTAL PROCEDURES

#### General Procedure 1: Synthesis of *N*-Substituted- $\gamma$ -Lactam Starting Materials

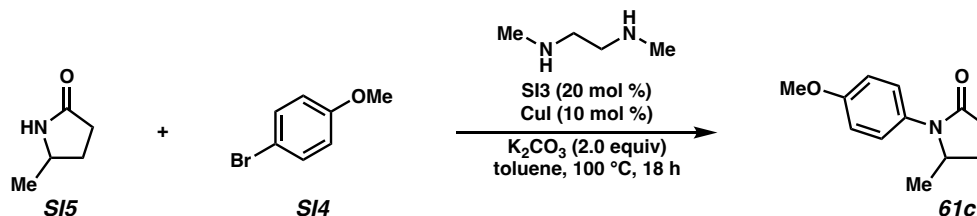


**1-(2-methoxyphenyl)pyrrolidin-2-one (61a):**<sup>30a</sup> To a solution of CuI (1.52 g, 8 mmol, 0.1 equiv) in toluene (80 mL 1.0 M) was added dimethylethylene diamine **SI3** (1.68 mL, 16 mmol, 0.2 equiv), 2-pyrrolidinone **SI1** (8.2 g, 96 mmol, 1.2 equiv), 2-bromoanisole **SI2** (10.84 mL, 80 mmol, 1.0 equiv), and K<sub>2</sub>CO<sub>3</sub> (22.1 g, 160 mmol, 2.0 equiv). The resultant suspension was heated to 100 °C and allowed to stir for 18 hours. The reaction was cooled to ambient temperature, diluted with EtOAc (100 mL) and filtered through a plug of silica. The filter was concentrated via rotary evaporation. The crude product was purified by flash column chromatography (70% EtOAc in hexanes) to afford the desired *N*-arylated product **61a** as a pale-yellow oil (13.6 g, 70.4 mmol, 88% yield); <sup>1</sup>H NMR (400 MHz, CDCl<sub>3</sub>)  $\delta$  7.32 – 7.23 (m, 2H), 7.02 – 6.93 (m, 2H), 3.84 (s, 3H), 3.76 (dd, *J* = 7.3, 6.7 Hz,

2H), 2.56 (dd,  $J = 8.6, 7.6$  Hz, 2H), 2.30 – 2.12 (m, 2H). All characterization data match those reported.<sup>30a</sup>



**1-(4-methoxyphenyl)pyrrolidin-2-one (61b)**: To a solution of **CuI** (1.52 g, 8 mmol, 0.1 equiv) in toluene (80 mL 1.0 M) was added dimethylethylenediamine **SI3** (1.68 mL, 16 mmol, 0.2 equiv), 2-pyrrolidinone **SI1** (8.2 g, 96 mmol, 1.2 equiv), 4-bromoanisole **SI4** (10.84 mL, 80 mmol, 1.0 equiv), and  $\text{K}_2\text{CO}_3$  (22.1 g, 160 mmol, 2.0 equiv). The resultant suspension was heated to 100 °C and allowed to stir for 18 hours. The reaction was cooled to ambient temperature, diluted with EtOAc (100 mL) and filtered through a plug of silica. The filter was concentrated by rotary evaporation. The crude product was purified by flash column chromatography (80% EtOAc in hexanes) to afford the desired *N*-arylated product **61b** as a colorless solid (13.1 g, 69 mmol, 86% yield);  $^1\text{H NMR}$  (400 MHz,  $\text{CDCl}_3$ )  $\delta$  7.57 – 7.43 (m, 2H), 6.96 – 6.86 (m, 2H), 3.85 – 3.81 (m, 2H), 3.80 (s, 3H), 2.60 (dd,  $J = 8.5, 7.7$  Hz, 2H), 2.22 – 2.10 (m, 2H). All characterization data match those reported.<sup>30a</sup>

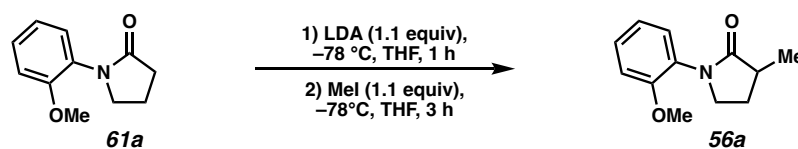


**1-(4-methoxyphenyl)-5-methylpyrrolidin-2-one (61c)**: To a solution of **CuI** (1.52 g, 8 mmol, 0.1 equiv) in toluene (80 mL 1.0 M) was added dimethylethylenediamine **SI3** (1.68 mL, 16 mmol, 0.2 equiv), 4-bromoanisole **SI4** (10.84 mL, 80 mmol, 1.0 equiv), 5-

methylpyrrolidin-2-one **SI5** (9.6 g, 96 mmol, 1.2 equiv), and  $K_2CO_3$  (22.1 g, 160 mmol, 2.0 equiv). The resultant suspension was heated to 100 °C and allowed to stir for 18 hours. The reaction was cooled to ambient temperature, diluted with EtOAc (100 mL) and filtered through a plug of silica. The filter was concentrated via rotary evaporation. The crude product was purified by flash column chromatography (90% EtOAc in hexanes) to afford the desired *N*-arylated product **61c** as a pale-yellow oil (14.1 g, 68.8 mmol, 86% yield);  $^1H$  NMR (400 MHz,  $CDCl_3$ )  $\delta$  7.32 – 7.27 (m, 0.4H)\*, 7.26 – 7.21 (m, 1.6H), 7.02 – 6.95 (m, 0.4H)\*, 6.96 – 6.88 (m, 1.6H)\*, 4.25 – 4.13 (m, 1H), 3.83 (s, 0.6H)\*, 3.81 (s, 2.4H)\*, 2.67 – 2.49 (m, 2H), 2.37 (dddd,  $J = 13.2, 9.3, 7.4, 6.0$  Hz, 1H), 1.75 (dddd,  $J = 12.5, 9.5, 7.4, 5.9$  Hz, 1H), 1.18 (d,  $J = 6.3$  Hz, 2.4H), 1.08 (d,  $J = 6.3$  Hz, 0.4H);  $^{13}C$  NMR (101 MHz,  $CDCl_3$ )  $\delta$  175.11,\* 174.35, 157.69, 155.30,\* 132.23,\* 130.38, 130.19,\* 128.88,\* 126.12, 120.81,\* 114.35, 111.95,\* 56.14, 55.86,\* 55.64,\* 55.46, 31.17, 30.93,\* 27.74,\* 26.86, 20.36,\* 20.30; IR (Neat Film, NaCl) 2968, 2836, 1693, 1513, 1462, 1392, 1286, 1248, 1180, 1033, 831  $cm^{-1}$ ; (MM:ESI<sup>+</sup>)  $m/z$  calc'd for  $C_{12}H_{16}NO_2$  [M+H]<sup>+</sup>: 206.1181, found 206.1166. Rotomeric peaks (approx. 4:1) denoted with\*

### Synthesis of Mannich Donors: Experimental Procedures and Spectroscopic Data

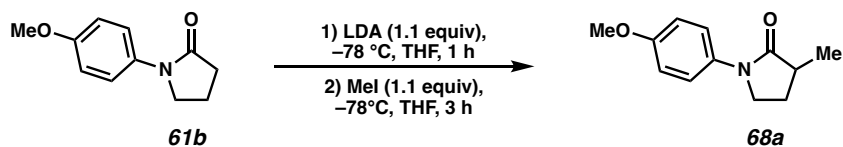
**General Procedure 2:**  $\alpha$ -alkylation of *N*-substituted lactams with alkyl halides.



**1-(2-methoxyphenyl)-3-methylpyrrolidin-2-one (56a):** To a solution of *i*-Pr<sub>2</sub>NH (710  $\mu$ L, 5.5 mmol, 1.1 equiv) in THF (15 mL) was added *n*-BuLi (2.50 M in hexanes, 2 mL, 5.5 mmol, 1.1 equiv) dropwise at  $-78$  °C. The resulting mixture was stirred at  $-78$  °C for 20 min. A solution of 1-(4-methoxyphenyl)-3-methylpyrrolidin-2-one **61a** (950 mg, 5

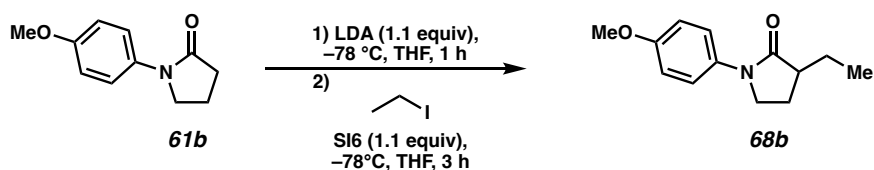


mmol, 1.0 equiv) in THF (10 mL) was added dropwise to the reaction mixture at  $-78\text{ }^{\circ}\text{C}$ . The resulting mixture was stirred for 30 min at  $-78\text{ }^{\circ}\text{C}$ , then MeI (345  $\mu\text{L}$ , 5.5 mmol, 1.1 equiv) was added dropwise. The resulting mixture was stirred for 3 hours at  $-78\text{ }^{\circ}\text{C}$ . The reaction mixture was allowed to warm to ambient temperature overnight, diluted with EtOAc and then quenched with a saturated aqueous  $\text{NH}_4\text{Cl}$  solution. The aqueous layer was extracted three times with EtOAc, and the resulting organic layers were dried over  $\text{Na}_2\text{SO}_4$  and concentrated by rotary evaporation. The resulting crude oil was purified from column chromatography (55% EtOAc in hexanes) to afford **56a** as an off-yellow solid. (965 mg, 4.7 mmol, 94% yield);  $^1\text{H NMR}$  (400 MHz,  $\text{CDCl}_3$ )  $\delta$  7.33 – 7.24 (m, 2H), 7.03 – 6.94 (m, 2H), 3.83 (s, 3H), 3.78 – 3.62 (m, 2H), 2.66 (tq,  $J = 8.6, 7.1$  Hz, 1H), 2.39 (dddd,  $J = 12.2, 8.4, 7.2, 3.6$  Hz, 1H), 1.81 (dq,  $J = 12.4, 8.5$  Hz, 1H), 1.31 (d,  $J = 7.1$  Hz, 3H). All characterization data match those reported.<sup>30a</sup>

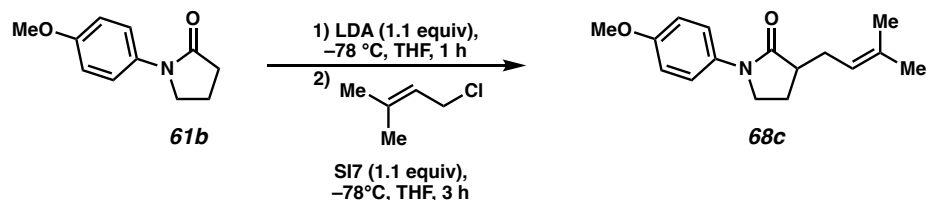


**1-(4-methoxyphenyl)-3-methylpyrrolidin-2-one (68a):** To a solution of  $i\text{-Pr}_2\text{NH}$  (710  $\mu\text{L}$ , 5.5 mmol, 1.1 equiv) in THF (15 mL) was added  $n\text{-BuLi}$  (2.50 M in hexanes, 2 mL, 5.5 mmol, 1.1 equiv) dropwise at  $-78\text{ }^{\circ}\text{C}$ . The resulting mixture was stirred at  $-78\text{ }^{\circ}\text{C}$  for 20 min. A solution of 1-(4-methoxyphenyl)-3-methylpyrrolidin-2-one **61b** (950 mg, 5 mmol, 1.0 equiv) in THF (10 mL) was added dropwise to the reaction mixture at  $-78\text{ }^{\circ}\text{C}$ . The resulting mixture was stirred for 30 min at  $-78\text{ }^{\circ}\text{C}$ , then MeI (345  $\mu\text{L}$ , 5.5 mmol, 1.1 equiv) was added dropwise. The resulting mixture was stirred for 3 hours at  $-78\text{ }^{\circ}\text{C}$ . The

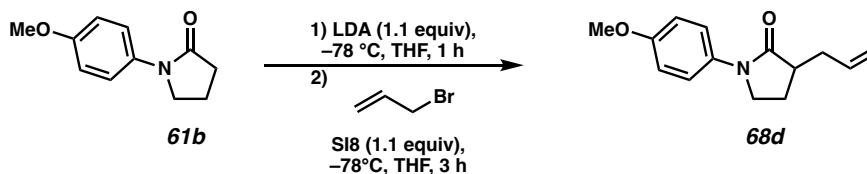
reaction mixture was allowed to warm to ambient temperature overnight, diluted with EtOAc and then quenched with a saturated aqueous  $\text{NH}_4\text{Cl}$  solution. The aqueous layer was extracted three times with EtOAc, and the resulting organic layers were dried over  $\text{Na}_2\text{SO}_4$  and concentrated by rotary evaporation. The crude oil was purified by column chromatography (50% EtOAc in hexanes) to afford **68a** as a colorless solid (970 mg, 4.73 mmol, 95% yield);  $^1\text{H}$  NMR (400 MHz,  $\text{CDCl}_3$ )  $\delta$  7.53 (d,  $J = 9.1$  Hz, 2H), 6.90 (d,  $J = 9.1$  Hz, 2H), 3.80 (s, 3H), 3.78 – 3.68 (m, 1H), 2.74 – 2.57 (m, 1H), 2.36 (dddd,  $J = 12.3, 8.5, 6.7, 3.6$  Hz, 1H), 1.76 (ddt,  $J = 12.5, 9.4, 8.6$  Hz, 1H) 1.30 (d,  $J = 7.1$  Hz, 3H);  $^{13}\text{C}$  NMR (101 MHz,  $\text{CDCl}_3$ )  $\delta$  176.43, 156.51, 133.08, 121.57, 114.11, 55.59, 47.06, 38.17, 27.21, 16.42; all characterization data match those reported.<sup>30a</sup>



**3-ethyl-1-(4-methoxyphenyl)pyrrolidin-2-one (68b)**: Compound **68b** was prepared from iodoethane **SI6** using General Procedure 2. The resulting crude oil was purified by column chromatography (50% EtOAc in hexanes) to afford **68b** as a colorless solid (710 mg, 3.3 mmol, 92% yield);  $^1\text{H}$  NMR (400 MHz,  $\text{CDCl}_3$ )  $\delta$  7.72 – 7.41 (m, 2H), 7.08 – 6.74 (m, 2H), 3.81 (s, 3H), 3.78 – 3.69 (m, 2H), 2.54 (qd,  $J = 9.0, 4.3$  Hz, 1H), 2.32 (dddd,  $J = 12.6, 8.7, 6.9, 3.9$  Hz, 1H), 1.98 (dq,  $J = 13.7, 7.5, 4.2$  Hz, 1H), 1.81 (dq,  $J = 12.6, 8.7$  Hz, 1H), 1.51 (ddt,  $J = 13.7, 9.0, 7.3$  Hz, 1H), 1.02 (t,  $J = 7.4$  Hz, 3H);  $^{13}\text{C}$  NMR (101 MHz,  $\text{CDCl}_3$ )  $\delta$  175.80, 156.54, 133.07, 121.66, 114.14, 55.63, 47.31, 44.75, 24.42, 24.38, 11.63. All characterization data match those reported.<sup>30b</sup>

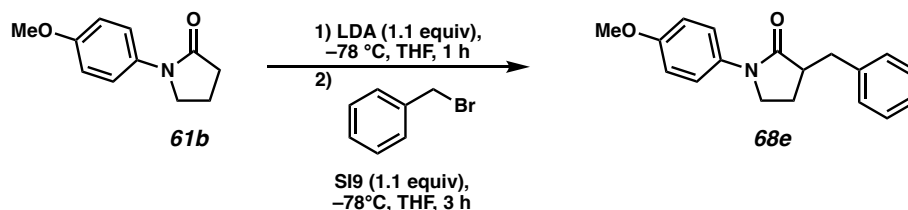


**1-(4-methoxyphenyl)-3-(3-methylbut-2-en-1-yl)pyrrolidin-2-one (68c):** Compound **68c** was prepared from prenyl chloride **SI7** using General Procedure 2. The resulting crude oil was purified by column chromatography (50% EtOAc in hexanes) to afford **68c** as an off-brown solid. (1.15 g, 4.5 mmol, 45% yield);  $^1\text{H}$  NMR (400 MHz,  $\text{CDCl}_3$ )  $\delta$  7.68 – 7.43 (m, 2H), 7.04 – 6.80 (m, 2H), 5.16 (tp,  $J = 7.2, 1.4$  Hz, 1H), 3.80 (s, 3H), 3.73 (ddd,  $J = 8.5, 5.5, 2.7$  Hz, 2H), 2.66 (td,  $J = 8.8, 4.3$  Hz, 1H), 2.63 – 2.53 (m, 1H), 2.32 – 2.21 (m, 2H), 1.82 (dq,  $J = 12.7, 8.5$  Hz, 1H), 1.73 (d,  $J = 1.5$  Hz, 3H), 1.66 (d,  $J = 1.4$  Hz, 3H);  $^{13}\text{C}$  NMR (101 MHz,  $\text{CDCl}_3$ )  $\delta$  175.51, 156.53, 134.09, 133.06, 121.61, 121.09, 114.11, 55.60, 47.31, 43.66, 29.61, 26.00, 24.23, 18.09.; IR (Neat Film, NaCl) 2954, 1680, 1519, 1253, 1225, 1031, 916, 825, 715  $\text{cm}^{-1}$ ; (MM:ESI $^+$ )  $m/z$  calc'd for  $\text{C}_{16}\text{H}_{22}\text{NO}_2$   $[\text{M}+\text{H}]^+$ : 260.1651, found 260.1660.

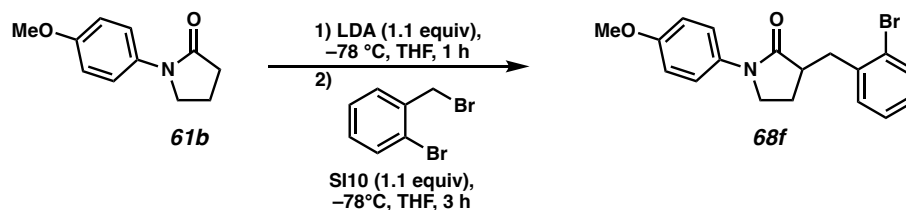


**3-allyl-1-(4-methoxyphenyl)pyrrolidin-2-one (68d):** Compound **68d** was prepared from allyl bromide **SI8** using General Procedure 2. The resulting crude oil was purified by column chromatography (50% EtOAc in hexanes) to afford **68d** as an off-yellow solid. (1.18 g, 4.75 mmol, 95% yield);  $^1\text{H}$  NMR (400 MHz,  $\text{CDCl}_3$ )  $\delta$  7.58 – 7.47 (m, 2H), 7.00

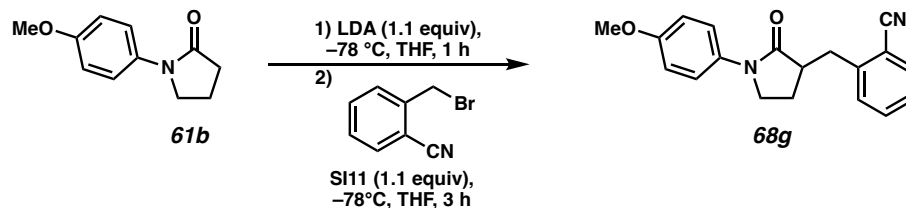
– 6.84 (m, 2H), 5.91 – 5.79 (m, 1H), 5.18 – 5.12 (m, 1H), 5.09 (ddt,  $J = 10.1, 2.0, 1.1$  Hz, 1H), 3.81 (s, 3H), 3.80 – 3.62 (m, 2H), 2.77 – 2.63 (m, 2H), 2.35 – 2.22 (m, 2H), 1.87 (dq,  $J = 12.8, 8.6$  Hz, 1H);  $^{13}\text{C}$  NMR (101 MHz,  $\text{CDCl}_3$ )  $\delta$  175.1, 156.6, 135.6, 132.9, 121.7, 117.2, 114.2, 55.6, 47.3, 42.9, 35.6, 24.1; IR (Neat Film, NaCl) 2954, 1680, 1519, 1253, 1225, 1031, 916, 825, 715  $\text{cm}^{-1}$ ; (MM:ESI $^+$ )  $m/z$  calc'd for  $\text{C}_{14}\text{H}_{18}\text{NO}_2$   $[\text{M}+\text{H}]^+$ : 232.1338, found 232.1358.



**3-benzyl-1-(4-methoxyphenyl)pyrrolidin-2-one (68e):** Compound **68e** was prepared from benzyl bromide **SI9** using General Procedure 2. The resulting crude oil was purified by column chromatography (50% EtOAc in hexanes) to afford **68e** as a colorless solid (1.32 g, 4.75 mmol, 95 % yield);  $^1\text{H}$  NMR (400 MHz,  $\text{CDCl}_3$ )  $\delta$  7.61 – 7.40 (m, 2H), 7.42 – 7.28 (m, 2H), 7.26 – 7.18 (m, 3H), 7.04 – 6.70 (m, 2H), 3.81 (s, 3H), 3.68 (dt,  $J = 9.5, 7.7$  Hz, 1H), 3.56 (ddd,  $J = 9.5, 8.6, 3.5$  Hz, 1H), 3.31 (dd,  $J = 13.6, 4.0$  Hz, 1H), 2.92 (dtd,  $J = 9.4, 8.6, 4.0$  Hz, 1H), 2.80 (dd,  $J = 13.6, 9.4$  Hz, 1H), 2.17 (dddd,  $J = 12.7, 8.6, 7.7, 3.5$  Hz, 1H), 1.86 (dtd,  $J = 12.7, 8.6, 7.9$  Hz, 1H).  $^{13}\text{C}$  NMR (101 MHz,  $\text{CDCl}_3$ )  $\delta$  174.94, 156.68, 139.46, 132.88, 129.23, 128.64, 126.53, 121.80, 114.16, 55.62, 47.26, 45.06, 37.24, 24.31. All characterization data match those reported.<sup>30b</sup>

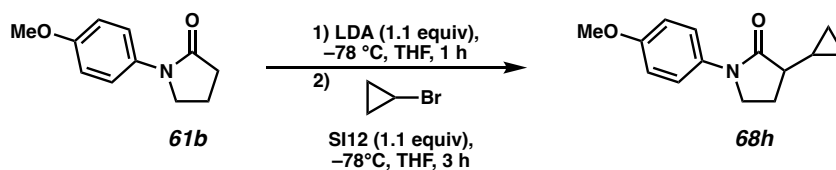


**3-(2-bromobenzyl)-1-(4-methoxyphenyl)pyrrolidin-2-one (68f)**: Compound **68f** was prepared from 1-bromo-2-(bromomethyl)benzene **SI10** using General Procedure 2. The resulting crude oil was purified by column chromatography (55% EtOAc in hexanes) to afford **68f** as a yellow crystalline solid. (1.36 g, 3.73 mmol, 98% yield);  $^1\text{H}$  NMR (400 MHz,  $\text{CDCl}_3$ )  $\delta$  7.57 (dd,  $J = 8.0, 1.3$  Hz, 1H), 7.56 – 7.51 (m, 2H), 7.35 – 7.30 (m, 1H), 7.30 – 7.22 (m, 1H), 7.13 – 7.07 (m, 1H), 6.98 – 6.87 (m, 2H), 3.81 (s, 3H), 3.75 – 3.63 (m, 2H), 3.50 (dd,  $J = 13.7, 4.4$  Hz, 1H), 3.04 (tdd,  $J = 9.3, 8.3, 4.3$  Hz, 1H), 2.93 (dd,  $J = 13.7, 9.5$  Hz, 1H), 2.16 (dddd,  $J = 12.7, 8.4, 6.8, 3.6$  Hz, 1H), 1.92 (ddt,  $J = 12.7, 9.5, 8.5$  Hz, 1H);  $^{13}\text{C}$  NMR (101 MHz,  $\text{CDCl}_3$ )  $\delta$  174.64, 156.65, 139.13, 133.09, 132.91, 131.27, 128.25, 127.68, 125.03, 121.64, 114.16, 55.62, 47.21, 44.00, 36.82, 24.45; IR (Neat Film, NaCl) 2952, 1692, 1512, 1469, 1441, 1397, 1248, 1181, 1025, 830, 751  $\text{cm}^{-1}$ ; (MM:ESI $^+$ )  $m/z$  calc'd for  $\text{C}_{18}\text{H}_{19}\text{BrNO}_2$   $[\text{M}+\text{H}]^+$ : 360.0599, found 360.0613.

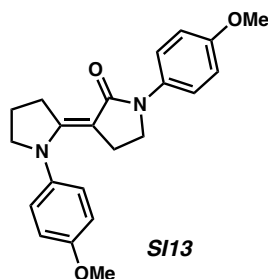


**2-((1-(4-methoxyphenyl)-2-oxopyrrolidin-3-yl)methyl)benzonitrile (68g)**: Compound **68g** was prepared from 2-(bromomethyl)benzonitrile **SI11** using General Procedure 2. The resulting crude oil was purified by column chromatography (50% EtOAc in hexanes) to

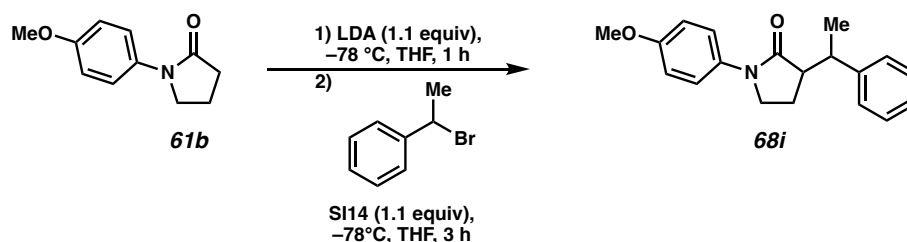
afford **68g** as an off-brown solid. (660 mg, 2.13 mmol, 97% yield);  $^1\text{H}$  NMR (400 MHz,  $\text{CDCl}_3$ )  $\delta$  7.66 (ddd,  $J = 7.7, 1.4, 0.6$  Hz, 1H), 7.59 – 7.52 (m, 1H), 7.52 – 7.46 (m, 3H), 7.35 (td,  $J = 7.5, 1.4$  Hz, 1H), 6.95 – 6.85 (m, 2H), 3.81 (s, 3H), 3.78 – 3.61 (m, 2H), 3.47 (dd,  $J = 14.0, 5.0$  Hz, 1H), 3.14 (dd,  $J = 14.0, 8.6$  Hz, 1H), 3.00 (dtd,  $J = 9.4, 8.5, 5.0$  Hz, 1H), 2.23 (dddd,  $J = 12.7, 8.4, 7.1, 3.3$  Hz, 1H), 1.93 (ddt,  $J = 12.7, 9.4, 8.5$  Hz, 1H);  $^{13}\text{C}$  NMR (101 MHz,  $\text{CDCl}_3$ )  $\delta$  173.93, 156.80, 143.65, 133.18, 132.93, 132.65, 130.51, 127.22, 121.81, 118.44, 114.20, 113.25, 55.62, 47.17, 44.96, 35.16, 24.28.; IR (Neat Film, NaCl) 2942, 2223, 1692, 1513, 1486, 1397, 1285, 1248, 1181, 1034, 831, 762  $\text{cm}^{-1}$ ; (MM:ESI $^+$ )  $m/z$  calc'd for  $\text{C}_{19}\text{H}_{19}\text{N}_2\text{O}_2$   $[\text{M}+\text{H}]^+$ : 307.1447, found 307.1453.



**3-cyclopropyl-1-(4-methoxyphenyl)pyrrolidin-2-one (68h):** Compound **68h** was prepared from bromocyclopropane **SI12** using General Procedure 2. The resulting crude oil was purified by column chromatography (50% EtOAc in hexanes) to afford **68h** as a yellow crystalline solid. (150 mg, 0.65 mmol, 30% yield);  $^1\text{H}$  NMR (400 MHz,  $\text{CDCl}_3$ )  $\delta$  7.58 – 7.53 (m, 2H), 6.94 – 6.88 (m, 2H), 3.80 (s, 3H), 3.78 – 3.71 (m, 2H), 2.32 – 2.15 (m, 2H), 1.95 – 1.82 (m, 1H), 1.08 – 0.98 (m, 1H), 0.71 – 0.63 (m, 1H), 0.55 – 0.42 (m, 2H), 0.32 – 0.23 (m, 1H);  $^{13}\text{C}$  NMR (101 MHz,  $\text{CDCl}_3$ )  $\delta$  175.12, 156.47, 133.06, 121.48, 114.07, 55.59, 47.09, 46.82, 24.54, 12.48, 3.52, 1.89; IR (Neat Film, NaCl) 3077, 3003, 2954, 2838, 1681, 1512, 1384, 1286, 1245, 1180, 1032, 824, 704  $\text{cm}^{-1}$ ; (MM:ESI $^+$ )  $m/z$  calc'd for  $\text{C}_{14}\text{H}_{18}\text{NO}_2$   $[\text{M}+\text{H}]^+$ : 232.1338, found 232.1349.

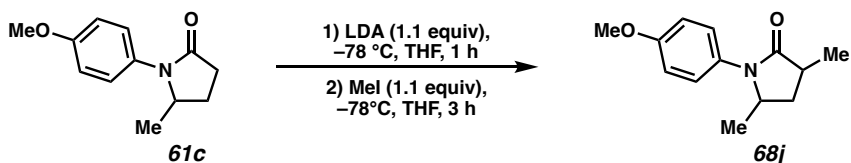


Inseparable from lactam dimerization impurity **SI13** (20 %);  $^1\text{H}$  NMR (400 MHz,  $\text{CDCl}_3$ )  $\delta$  7.29 – 7.24 (m, 2H), 7.21 – 7.15 (m, 2H), 7.11 – 7.03 (m, 2H), 6.92 – 6.86 (m, 2H), 3.83 (s, 3H), 3.78 (s, 3H), 3.70 – 3.64 (m, 2H), 3.53 (dd,  $J = 7.8, 6.8$  Hz, 2H), 3.36 (tt,  $J = 7.6, 1.8$  Hz, 2H), 2.13 – 1.99 (m, 4H);  $^{13}\text{C}$  NMR (101 MHz,  $\text{CDCl}_3$ )  $\delta$  171.26, 157.15, 155.40, 153.40, 137.99, 136.65, 134.63, 129.15, 128.34, 127.03, 125.41, 120.55, 113.91, 94.96, 56.86, 46.00, 31.65, 24.26, 22.69, 21.58. (tentative assignment)



**1-(4-methoxyphenyl)-3-(1-phenylethyl)pyrrolidin-2-one (68i)**: Compound **68i** was prepared from (1-bromoethyl)benzene **SI14** using General Procedure 2. The resulting crude oil was purified by column chromatography (45% EtOAc in hexanes) to afford **68i** as an off-yellow amorphous solid. (570 mg, 1.93 mmol, 88% yield, 9:1 dr);  $^1\text{H}$  NMR (400 MHz,  $\text{CDCl}_3$ )  $\delta$  7.35 (d,  $J = 9.2$  Hz, 2H), 7.33 – 7.27 (m, 4H), 7.25 – 7.15 (m, 1H), 6.87 (d,  $J = 9.2$  Hz, 2H), 3.79 (s, 3H), 3.53 – 3.42 (m, 2H), 3.09 (ddd,  $J = 9.4, 8.4, 5.4$  Hz, 1H), 2.82 (ddd,  $J = 9.2, 6.7, 5.5$  Hz, 1H), 2.08 (dddd,  $J = 12.8, 9.1, 8.4, 5.5$  Hz, 1H), 1.80 (dddd,  $J = 12.8, 8.4, 6.7, 5.8$  Hz, 1H), 1.50 (d,  $J = 7.2$  Hz, 3H);  $^{13}\text{C}$  NMR (101 MHz,  $\text{CDCl}_3$ )  $\delta$

174.98, 156.71, 143.15, 132.71, 128.38, 128.15, 126.74, 122.16, 114.09, 55.60, 49.75, 47.39, 39.89, 21.16, 19.53; IR (Neat Film, NaCl) 2959, 1681, 1512, 1452, 1396, 1294, 1247, 1034, 831, 701  $\text{cm}^{-1}$ ; (MM:ESI<sup>+</sup>)  $m/z$  calc'd for  $\text{C}_{19}\text{H}_{22}\text{NO}_2$  [M+H]<sup>+</sup>: 296.1651, found 296.1667.

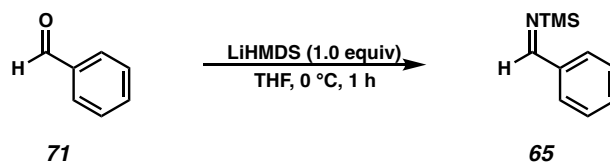


**1-(4-methoxyphenyl)-3,5-dimethylpyrrolidin-2-one (68j):** Compound **68j** was prepared from lactam **61c** and methyl iodide using General Procedure 2. The resulting crude oil was purified by column chromatography (70% EtOAc in hexanes) to afford **68j** as an off-brown crystalline solid. (1.035 g, 4.7 mmol, 94% yield, 5:1 dr); <sup>1</sup>H NMR (400 MHz, CDCl<sub>3</sub>)  $\delta$  7.36 – 7.28 (m, 2H), 6.96 – 6.87 (m, 2H), 4.17 (pd,  $J = 6.4, 4.5$  Hz, 1H), 3.80 (s, 3H), 2.74 (ddt,  $J = 15.7, 8.6, 7.1$  Hz, 1H), 2.05 – 1.94 (m, 2H), 1.27 (d,  $J = 7.2$  Hz, 3H), 1.18 (d,  $J = 6.3$  Hz, 3H); <sup>13</sup>C NMR (101 MHz, CDCl<sub>3</sub>)  $\delta$  176.55, 157.38, 131.00, 125.31, 114.36, 55.55, 54.06, 36.27, 35.32, 19.70, 16.41.; IR (Neat Film, NaCl) 2966, 1693, 1513, 1461, 1392, 1295, 1247, 1181, 1034, 830  $\text{cm}^{-1}$ ; (MM:ESI<sup>+</sup>)  $m/z$  calc'd for  $\text{C}_{13}\text{H}_{18}\text{NO}_2$  [M+H]<sup>+</sup>: 220.1338, found 220.1330.



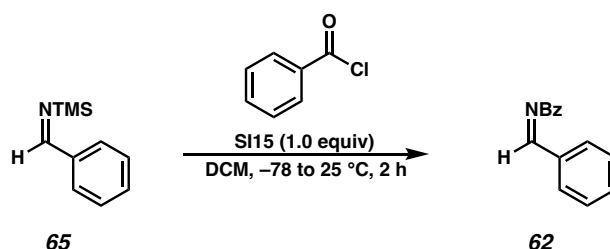
## Synthesis of Isolated Mannich Acceptors: Experimental Procedures and Spectroscopic Data

### Procedure 3: Synthesis of *N*-trimethylsilyl

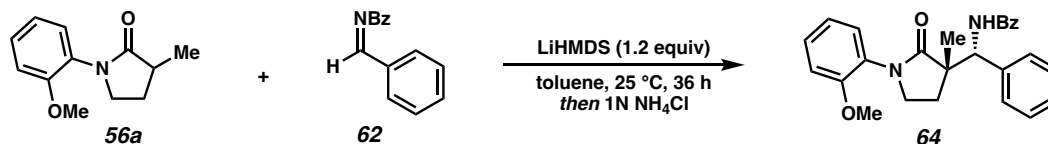


**1-phenyl-*N*-(trimethylsilyl)methanimine (65):** *N*-TMS imine **65** was prepared from a previously reported procedure.<sup>27</sup> To a solution of benzaldehyde **71** (5.2 mL, 50 mmol, 1.0 equiv) in THF (50 mL) was added LiHMDS (8.35 g, 50 mmol, 1.0 equiv) at 0 °C under a positive stream of N<sub>2</sub>. The reaction mixture was stirred at 0 °C for 1 hour. The solvent was removed by rotary evaporation and the crude oil was purified by vacuum distillation (77 °C, 0.8 torr. Boiling point Lit = 45 °C at 0.15 torr) to afford imine **65** as a pale-yellow oil (5.5 g, 31.0 mmol, 62% yield), which was stored under argon at –20 °C. All characterization data match those reported.<sup>27</sup>

### Procedure 4: Synthesis of *N*-Bz benzaldimine



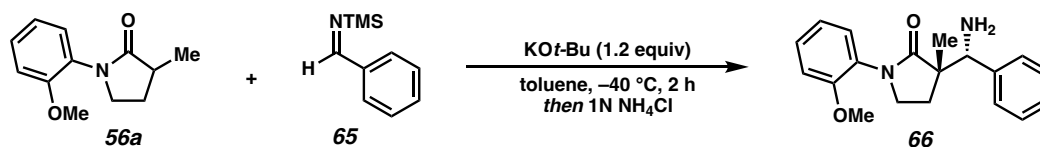
***N*-benzylidenebenzamide (62):** *N*-Bz imine **62** was prepared from a previously reported procedure.<sup>27</sup> To a solution of *N*-TMS imine **65** (177.3 mg, 1.0 mmol, 1.0 equiv) in DCM (2 mL) was added benzoyl chloride **SI15** in one portion at –78 °C. Let warm up to ambient temperature and stir for 2 hours. The solvent and TMSCl were removed *in vacuo* to afford the *N*-Bz imine **62**. The crude product was used directly without further purification.

**Diastereoselective Mannich Reaction: Experimental Procedures and Spectroscopic****Data*****N*-((*R*<sup>\*</sup>)-((*S*<sup>\*</sup>)-1-(2-methoxyphenyl)-3-methyl-2-oxopyrrolidin-3-**

**yl)(phenyl)methyl)benzamide (**64**):** To a solution of *N*-OMP lactam **56a** (42 mg, 0.2 mmol, 1.0 equiv) in toluene (2 mL) was added LiHMDS (40.2 mg, 0.24 mmol, 1.2 equiv) at 25 °C. A solution of *N*-benzoyl imine **62** (42.4 mg, 0.2 mmol, 1.0 equiv) in toluene (1 mL) was added to the reaction mixture, and the reaction was stirred at 25 °C for 36 hours. The reaction was quenched with saturated NH<sub>4</sub>Cl (10 mL) and the aqueous layer was extracted with ethyl acetate (3 x 15 mL). The combined organic layers were dried over Na<sub>2</sub>SO<sub>4</sub>, and the solvent was removed via rotary evaporator. The crude mixture was purified directly from column chromatography (80% EtOAc in hexanes) to afford Mannich product **64** as a pale-yellow oil. (56 mg, 0.14 mmol, 70% yield, 2:1 dr). Major diastereomer: <sup>1</sup>H NMR (400 MHz, CDCl<sub>3</sub>)  $\delta$  7.90 (d, *J* = 5.8 Hz, 1H), 7.88 – 7.79 (m, 2H), 7.56 – 7.49 (m, 2H), 7.49 – 7.44 (m, 1H), 7.43 – 7.38 (m, 2H), 7.38 – 7.33 (m, 2H), 7.33 – 7.28 (m, 2H), 7.20 (dd, *J* = 7.7, 1.7 Hz, 1H), 6.99 (td, *J* = 7.6, 1.2 Hz, 1H), 6.94 (d, *J* = 1.2 Hz, 1H), 5.22 (d, *J* = 5.8 Hz, 1H), 3.79 – 3.72 (m, 1H), 3.70 (s, 3H), 3.69 – 3.62 (m, 1H), 2.49 (ddd, *J* = 13.0, 7.8, 5.2 Hz, 1H), 1.94 (ddd, *J* = 13.0, 8.1, 6.3 Hz, 1H), 1.25 (s, 3H). <sup>13</sup>C NMR (101 MHz, CDCl<sub>3</sub>)  $\delta$  177.75, 167.35, 154.82, 138.75, 134.54, 131.43, 129.26, 128.69, 128.59, 128.53, 128.39, 128.13, 127.52, 127.17, 120.96, 111.99, 58.73, 55.58, 47.15, 46.94, 32.08, 19.94; IR (Neat Film, NaCl) 3325, 2930, 1667, 1504, 1416, 1303,

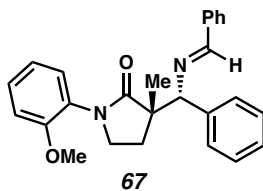
1122, 1046, 1026, 914, 782, 728  $\text{cm}^{-1}$ ; (MM:ESI<sup>+</sup>)  $m/z$  calc'd for  $\text{C}_{26}\text{H}_{27}\text{N}_2\text{O}_3$  [M+H]<sup>+</sup>: 415.2016, found 415.2023.

### General Procedure 5: Indirect Mannich Reaction with *N*-TMS benzaldimine Mannich Acceptor



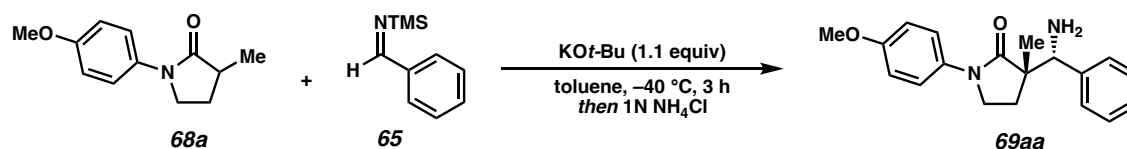
#### (*S*<sup>\*</sup>)-3-((*R*<sup>\*</sup>)-amino(phenyl)methyl)-1-(2-methoxyphenyl)-3-methylpyrrolidin-2-one

**(66)**: To a solution of *N*-OMP lactam **56a** (42 mg, 0.2 mmol, 1.0 equiv) in toluene (3 mL) was added potassium *tert*-butoxide (27 mg, 0.22 mmol, 1.1 equiv) at -40 °C. The reaction mixture was stirred at -40 °C for 2 hours. The reaction was allowed to warm to ambient temperature and loaded directly onto a silica gel column. The crude mixture was purified directly from column chromatography (80% EtOAc in hexanes, 1% TEA) to afford Mannich product **66** as a pale-yellow oil. (56 mg, 0.16 mmol, 80% yield, 8:1 dr). <sup>1</sup>H NMR (400 MHz, CDCl<sub>3</sub>)  $\delta$  7.57 – 7.47 (m, 2H), 7.42 – 7.28 (m, 5H), 6.94 – 6.88 (m, 2H), 4.29 (s, 1H), 3.81 (s, 3H), 3.63 (dt,  $J = 9.4, 7.9$  Hz, 1H), 3.47 (td,  $J = 9.2, 3.1$  Hz, 1H), 2.71 (ddd,  $J = 12.5, 9.1, 8.1$  Hz, 1H), 2.11 – 1.85 (br, 2H, NH<sub>2</sub>), 1.50 (ddd,  $J = 12.5, 7.7, 3.1$  Hz, 1H), 1.17 (s, 3H); <sup>13</sup>C NMR (101 MHz, CDCl<sub>3</sub>)  $\delta$  177.4, 156.7, 142.1, 132.8, 128.3, 128.0, 127.7, 121.9, 114.1, 60.6, 55.6, 50.9, 45.9, 26.2, 22.2 (toluene present 137.8); IR (Neat Film, NaCl) 3367, 2955, 1681, 1513, 1455, 1402, 1296, 1249, 1088, 833, 707  $\text{cm}^{-1}$ ; (MM:ESI<sup>+</sup>)  $m/z$  calc'd for  $\text{C}_{19}\text{H}_{23}\text{N}_2\text{O}_2$  [M+H]<sup>+</sup>: 311.1760, found 311.1747.



**(*S*<sup>\*</sup>)-3-((*R*<sup>\*</sup>)-(((*E*)-benzylidene)amino)(phenyl)methyl)-1-(2-methoxyphenyl)-3-methylpyrrolidin-2-one (67):** An isolable imine transfer product **67** was also observed

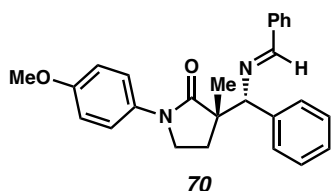
and purified from via column (35% EtOAc in hexanes) <sup>1</sup>H NMR (400 MHz, CDCl<sub>3</sub>)  $\delta$  8.37 (s, 1H), 7.77 – 7.66 (m, 2H), 7.55 (dt,  $J$  = 6.7, 1.6 Hz, 2H), 7.40 – 7.33 (m, 5H), 7.33 – 7.28 (m, 3H), 6.81 – 6.72 (m, 2H), 4.71 (s, 1H), 3.88 – 3.80 (m, 1H), 3.75 (s, 3H), 3.74 – 3.65 (m, 1H), 3.12 (ddd,  $J$  = 12.7, 8.8, 6.0 Hz, 1H), 1.75 – 1.66 (m, 1H), 1.18 (s, 3H).<sup>x</sup> (tentative assignment)



**(*S*<sup>\*</sup>)-3-((*R*<sup>\*</sup>)-amino(phenyl)methyl)-1-(2-methoxyphenyl)-3-methylpyrrolidin-2-one**

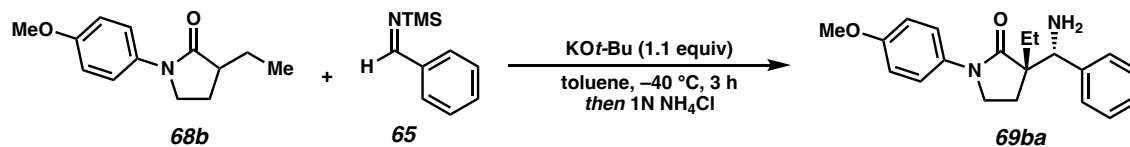
**(69aa):** To a solution of *N*-OMP lactam **68a** (42 mg, 0.2 mmol, 1.0 equiv) in toluene (3 mL) was added potassium *tert*-butoxide (27 mg, 0.22 mmol, 1.1 equiv) at  $-40$  °C. The reaction mixture was stirred at  $-40$  °C for 3 hours. The reaction was allowed to warm to ambient temperature and loaded directly onto a silica gel column. The crude mixture was purified directly from column chromatography (80% EtOAc in hexanes, 1% TEA) to afford Mannich product **69aa** as a pale-yellow oil. (56 mg, 0.18 mmol, 90% yield, >20:1 dr). <sup>1</sup>H NMR (400 MHz, CDCl<sub>3</sub>)  $\delta$  7.57 – 7.47 (m, 2H), 7.42 – 7.28 (m, 5H), 6.94 – 6.88 (m, 2H), 4.29 (s, 1H), 3.81 (s, 3H), 3.63 (dt,  $J$  = 9.4, 7.9 Hz, 1H), 3.47 (td,  $J$  = 9.2, 3.1 Hz, 1H), 2.71 (ddd,  $J$  = 12.5, 9.1, 8.1 Hz, 1H), 2.11 – 1.85 (br, 2H, NH<sub>2</sub>), 1.50 (ddd,  $J$  = 12.5, 7.7, 3.1 Hz,

1H), 1.17 (s, 3H);  $^{13}\text{C}$  NMR (101 MHz,  $\text{CDCl}_3$ )  $\delta$  177.40, 156.72, 142.11, 132.84, 128.25, 128.01, 127.65, 121.91, 114.12, 60.64, 55.60, 50.89, 45.91, 26.19, 22.24; IR (Neat Film, NaCl) 3367, 2955, 1681, 1513, 1455, 1402, 1296, 1249, 1088, 833, 707  $\text{cm}^{-1}$ ; (MM:ESI $^+$ )  $m/z$  calc'd for  $\text{C}_{19}\text{H}_{23}\text{N}_2\text{O}_2$   $[\text{M}+\text{H}]^+$ : 311.1760, found 311.1747.



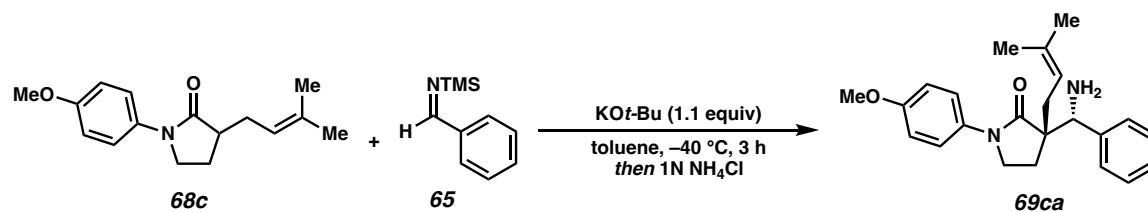
**(*S* $^*$ )-3-((*R* $^*$ )-(((*E*)-benzylidene)amino)(phenyl)methyl)-1-(2-methoxyphenyl)-3-**

**methylpyrrolidin-2-one (70):** An isolable imine transfer product **70** was also observed and purified from via column (40% EtOAc in hexanes):  $^1\text{H}$  NMR (400 MHz,  $\text{CDCl}_3$ )  $\delta$  8.37 (s, 1H), 7.77 – 7.66 (m, 2H), 7.55 (dt,  $J = 6.7, 1.6$  Hz, 2H), 7.40 – 7.33 (m, 5H), 7.33 – 7.28 (m, 3H), 6.81 – 6.72 (m, 2H), 4.71 (s, 1H), 3.88 – 3.80 (m, 1H), 3.75 (s, 3H), 3.74 – 3.65 (m, 1H), 3.12 (ddd,  $J = 12.7, 8.8, 6.0$  Hz, 1H), 1.75 – 1.66 (m, 1H), 1.18 (s, 3H);  $^{13}\text{C}$  NMR (101 MHz,  $\text{CDCl}_3$ )  $\delta$  176.95, 161.84, 156.70, 140.85, 136.52, 132.85, 130.70, 128.80, 128.52, 128.49, 128.18, 127.49, 122.42, 114.01, 78.79, 55.58, 51.71, 46.78, 26.37, 22.53; IR (Neat Film, NaCl) 2958, 1682, 1512, 1453, 1402, 1289, 1249, 1180, 1089, 1030, 829, 755, 702, 637  $\text{cm}^{-1}$ ; (MM:ESI $^+$ )  $m/z$  calc'd for  $\text{C}_{26}\text{H}_{27}\text{N}_2\text{O}_2$   $[\text{M}+\text{H}]^+$ : 399.2067, found 399.2074. Structure and relative configuration was confirmed via X-ray crystallography. Crystals were obtained from slow evaporation of a solution of **70** in  $\text{CDCl}_3$ . CCDC 2253012



**(*S*\*)-3-((*R*\*)-amino(phenyl)methyl)-3-ethyl-1-(4-methoxyphenyl)pyrrolidin-2-one**

**(69ba):** Compound **69ba** was prepared from *N*-PMP lactam **68b** using General procedure 5. The crude reaction mixture was purified directly from column chromatography (80% EtOAc in hexanes, 1% TEA) to afford Mannich product **69ba** as a pale-yellow oil (52 mg, 0.16 mmol, 80% yield, 13:1 dr);  $^1\text{H NMR}$  (400 MHz,  $\text{CDCl}_3$ )  $\delta$  7.49 – 7.43 (m, 2H), 7.40 – 7.34 (m, 2H), 7.34 – 7.28 (m, 3H), 6.95 – 6.86 (m, 2H), 4.26 (s, 1H), 3.81 (s, 3H), 3.51 (td,  $J = 9.1, 6.1$  Hz, 1H), 3.24 (td,  $J = 9.4, 4.7$  Hz, 1H), 2.55 (ddd,  $J = 13.0, 9.5, 6.1$  Hz, 1H), 1.89 – 1.74 (m, 3H, overlap  $\text{NH}_2$ ), 1.71 (ddd,  $J = 13.4, 8.9, 4.7$  Hz, 1H), 1.54 (dq,  $J = 13.6, 7.5$  Hz, 1H), 0.95 (t,  $J = 7.5$  Hz, 3H);  $^{13}\text{C NMR}$  (101 MHz,  $\text{CDCl}_3$ )  $\delta$  176.58, 156.84, 142.61, 132.63, 128.30, 127.99, 127.67, 122.22, 114.14, 60.19, 55.62, 54.63, 46.75, 29.73, 24.10, 8.92; IR (Neat Film, NaCl) 3314, 2965, 1681, 1513, 1455, 1404, 1296, 1249, 1034, 833, 721  $\text{cm}^{-1}$ ; (MM:ESI $^+$ )  $\text{C}_{20}\text{H}_{25}\text{N}_2\text{O}_2$   $m/z$  calc'd for  $[\text{M}+\text{H}]^+$ : 325.1916, found 325.1931.

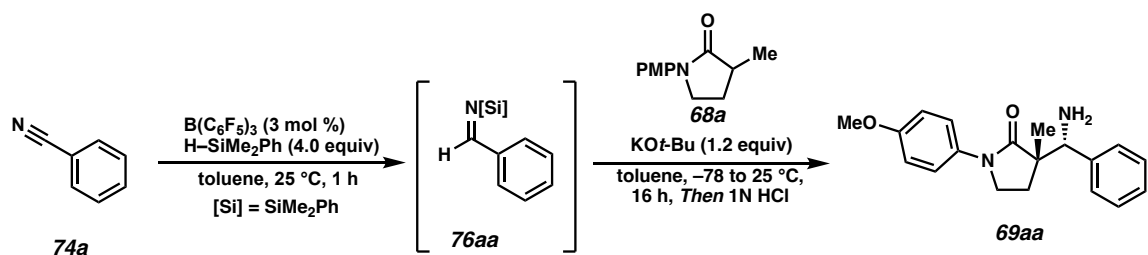


**(*S*\*)-3-((*R*\*)-amino(phenyl)methyl)-1-(4-methoxyphenyl)-3-(3-methylbut-2-en-1-**

**yl)pyrrolidin-2-one (69ca):** Compound **69ca** was prepared from *N*-PMP lactam **68c** using General Procedure 5. The crude reaction mixture was purified directly from column chromatography (65% EtOAc in hexanes, 1% TEA) to afford Mannich product **69ca** as a

pale-yellow oil (70 mg, 0.192 mmol, 96% yield, 7:1 dr)  $^1\text{H}$  NMR (400 MHz,  $\text{CDCl}_3$ )  $\delta$  7.43 – 7.39 (m, 2H), 7.38 – 7.27 (m, 5H), 6.94 – 6.86 (m, 2H), 5.17 (dddd,  $J = 6.9, 5.4, 2.8, 1.4$  Hz, 1H), 4.24 (s, 1H), 3.81 (s, 3H), 3.43 (td,  $J = 8.9, 6.2$  Hz, 1H), 3.14 (td,  $J = 9.2, 4.6$  Hz, 1H), 2.54 – 2.41 (m, 2H), 2.25 (dd,  $J = 14.2, 8.3$  Hz, 1H), 2.08 – 1.79 (br, 2H,  $\text{NH}_2$ ), 1.77 – 1.68 (m, 1H)\*, 1.68 (s, 3H), 1.57 – 1.56 (m, 3H);  $^{13}\text{C}$  NMR (101 MHz,  $\text{CDCl}_3$ )  $\delta$  176.45, 156.80, 142.57, 135.13, 132.68, 128.29, 127.98, 127.64, 122.28, 119.07, 114.11, 60.48, 55.59, 54.46, 46.71, 35.26, 26.21, 24.50, 18.17; IR (Neat Film, NaCl) 3234, 2930, 1681, 1513, 1453, 1402, 1293, 1250, 1033, 827, 703  $\text{cm}^{-1}$ ; (MM:ESI $^+$ )  $\text{C}_{23}\text{H}_{29}\text{N}_2\text{O}_2$   $m/z$  calc'd for  $[\text{M}+\text{H}]^+$ : 365.2229, found 365.2240.

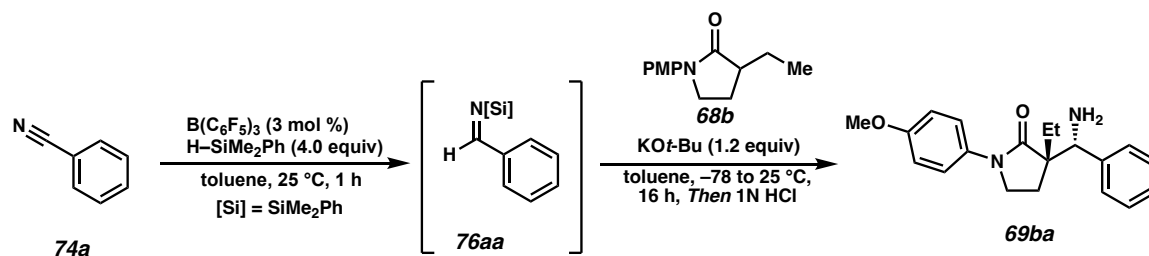
### General Procedure 6: Direct Mannich Reaction Using *In-Situ* Generated *N*-SiMe $_2$ Ph Benzaldimine Mannich Acceptor



#### (*S* $^*$ )-3-((*R* $^*$ )-amino(phenyl)methyl)-1-(4-methoxyphenyl)-3-methylpyrrolidin-2-one

**(69aa)**:  $\text{B}(\text{C}_6\text{F}_5)_3$  (4 mg, 0.009 mmol, 0.06 equiv) was added to a solution of  $\text{H-SiMe}_2\text{Ph}$  (92  $\mu\text{L}$ , 0.6 mmol, 3.0 equiv) in toluene (1 mL). Benzonitrile **74a** (55  $\mu\text{L}$ , 0.6 mmol, 3.0 equiv) was added to the reaction mixture and stirred at ambient temperature for 45 minutes. Meanwhile, *N*-PMP lactam **68a** (42 mg, 0.2 mmol, 1.0 equiv) was added to a solution of potassium *tert*-butoxide (24 mg, 0.2 mmol, 1.0 equiv) in toluene (2 mL) and cooled to  $-78\text{ }^\circ\text{C}$ . After 45 minutes, the yellow imine mixture of *N*-SiMe $_2$ Ph imine **76aa** was added to the cooled reaction mixture at  $-78\text{ }^\circ\text{C}$  dropwise. The reaction mixture was stirred at  $-78\text{ }^\circ\text{C}$

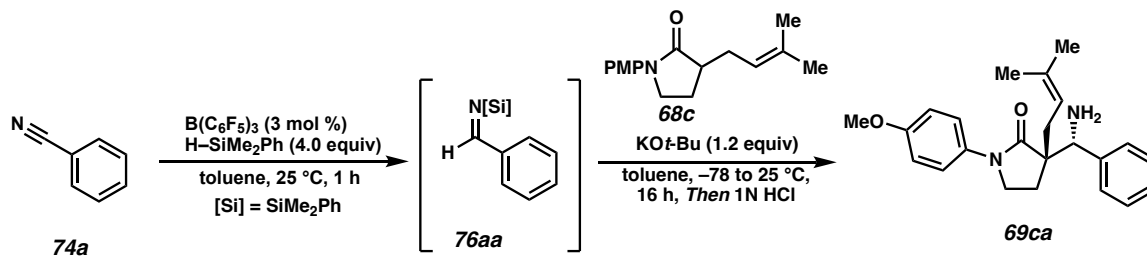
for 2 hours and allowed to warm to ambient temperature overnight. The reaction was quenched with 1 N HCl (4 mL) and diluted with EtOAc (10 mL) and stirred vigorously for 1 hour at ambient temperature. The aqueous layer was separated and extracted with EtOAc (2 x 8 mL). The combined organic layer can be purified to recover any unreacted lactam or aryl nitrile. The aqueous layer was basified with a saturated solution of NaHCO<sub>3</sub> (10 mL) and diluted with EtOAc (10 mL). The biphasic mixture was stirred vigorously for 1 hour at ambient temperature. The layers were separated, and the aqueous layer was extracted with EtOAc (3 x 10 mL). The organic layers were combined, dried over Na<sub>2</sub>SO<sub>4</sub> and concentrated by rotary evaporation. The crude oil was purified by column chromatography (3% MeOH in EtOAc, 1% TEA) to afford Mannich product **69aa** as a pale-yellow oil (60 mg, 0.194 mmol, 97% yield, 20:1 dr); the characterization data matches the data acquired from the product obtained using General Procedure 5.



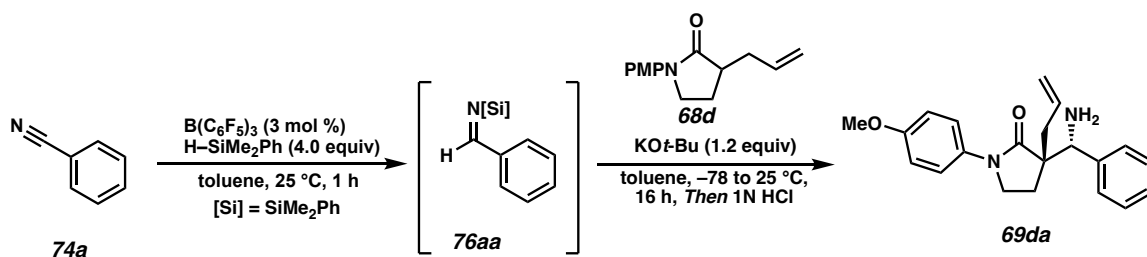
**(*S*<sup>\*</sup>)-3-((*R*<sup>\*</sup>)-amino(phenyl)methyl)-3-ethyl-1-(4-methoxyphenyl)pyrrolidin-2-one**

**(69ba):** Compound **69ba** was prepared from *N*-PMP lactam **68b** using General procedure 6. The crude oil was purified from column chromatography (3% MeOH in EtOAc, 1% TEA) to afford Mannich product **69ba** as a pale-yellow oil (55 mg, 0.17 mmol, 85% yield, 14:1 dr); the characterization data matches the data acquired from the product obtained using General Procedure 5.



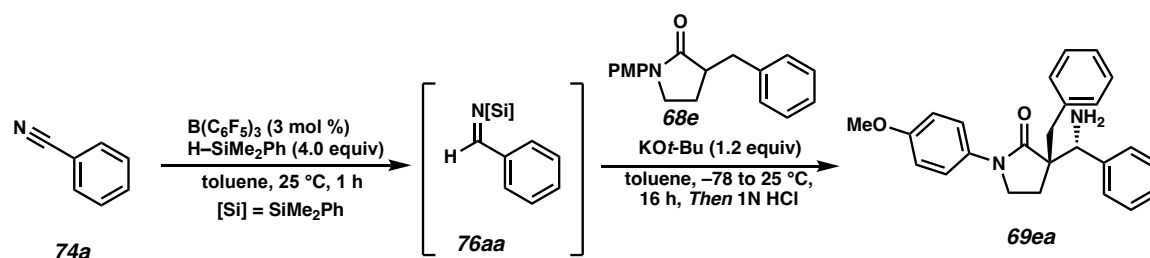


**(*S*<sup>\*</sup>)-3-((*R*<sup>\*</sup>)-amino(phenyl)methyl)-1-(4-methoxyphenyl)-3-(3-methylbut-2-en-1-yl)pyrrolidin-2-one (69ca):** Compound **69ca** was prepared from *N*-PMP lactam **69c** using General Procedure 6. The crude oil was purified from column chromatography (3% MeOH in EtOAc, 1% TEA) to afford Mannich product **69ca** as a pale-yellow oil (66 mg, 0.18 mmol, 90% yield, 10:1 dr); the characterization data matches the data acquired from the product obtained using General Procedure 5.



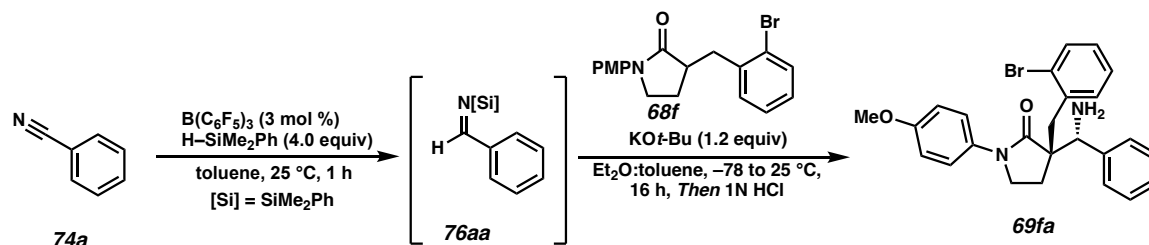
**(*S*<sup>\*</sup>)-3-allyl-3-((*R*<sup>\*</sup>)-amino(phenyl)methyl)-1-(4-methoxyphenyl)pyrrolidin-2-one (69da):** Compound **69da** was prepared from *N*-PMP lactam **68d** using General Procedure 6. The crude oil was purified from column chromatography (3% MeOH in EtOAc, 1% TEA) to afford Mannich product **69da** as a pale-yellow oil (60 mg, 0.18 mmol, 90% yield, 19:1 dr); <sup>1</sup>H NMR (400 MHz, CDCl<sub>3</sub>)  $\delta$  7.46 – 7.40 (m, 2H), 7.39 – 7.34 (m, 2H), 7.34 – 7.29 (m, 3H), 6.96 – 6.87 (m, 2H), 5.79 (dddd,  $J$  = 16.7, 10.1, 8.4, 6.5 Hz, 1H), 5.17 – 5.05 (m, 2H), 4.25 (s, 1H), 3.81 (s, 3H), 3.47 (td,  $J$  = 9.0, 6.2 Hz, 1H), 3.21 (td,  $J$  = 9.4, 4.6 Hz, 1H), 2.63 – 2.47 (m, 2H), 2.19 (ddt,  $J$  = 13.5, 8.3, 0.9 Hz, 1H), 2.05-1.80 (br, 2H, NH<sub>2</sub>)

1.77 (ddd,  $J = 13.2, 8.8, 4.6$  Hz, 1H);  $^{13}\text{C}$  NMR (101 MHz,  $\text{CDCl}_3$ )  $\delta$  176.06, 156.89, 142.34, 133.77, 132.54, 128.37, 128.01, 127.77, 122.31, 118.96, 114.14, 60.53, 55.62, 54.21, 46.68, 41.47, 24.04; IR (Neat Film, NaCl) 3054, 2917, 1681, 1512, 1454, 1401, 1295, 1248, 1036, 827, 703  $\text{cm}^{-1}$ ; (MM:ESI $^+$ )  $\text{C}_{21}\text{H}_{25}\text{N}_2\text{O}_2$   $m/z$  calc'd for  $[\text{M}+\text{H}]^+$ : 337.1916, found 337.1930.



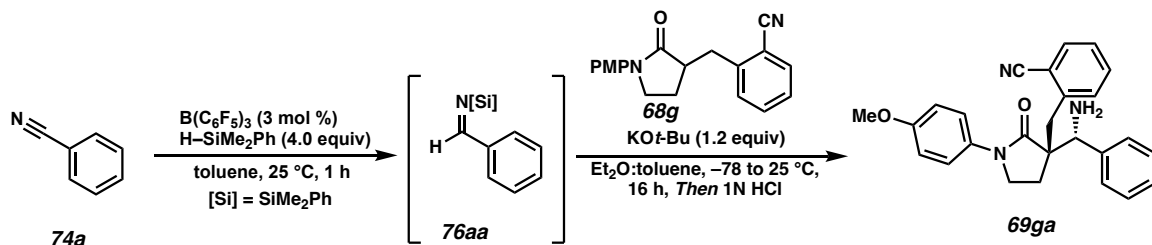
**(*S* $^*$ )-3-((*R* $^*$ )-amino(phenyl)methyl)-3-benzyl-1-(4-methoxyphenyl)pyrrolidin-2-one**

**(69ea):** Compound **69ea** was prepared from *N*-PMP lactam **68e** using General Procedure 6. The crude oil was purified from column chromatography (3% MeOH in EtOAc, 1% TEA) to afford Mannich product **69ea** as a yellow oil (65 mg, 0.172 mmol, 86% yield, 7:1 dr);  $^1\text{H}$  NMR (400 MHz,  $\text{C}_6\text{D}_6$ )  $\delta$  7.48 – 7.41 (m, 2H), 7.31 – 7.25 (m, 2H), 7.16 – 7.11 (m, 3H), 7.10 – 7.05 (m, 2H), 6.98 – 6.94 (m, 3H), 6.80 – 6.73 (m, 2H), 4.38 (s, 1H), 3.28 (s, 3H), 3.27 – 3.23 (m, 1H), 2.71 – 2.59 (m, 1H), 2.57 – 2.47 (m, 2H), 2.12 (td,  $J = 8.4, 7.3$  Hz, 1H), 1.43 (ddd,  $J = 12.5, 8.3, 2.8$  Hz, 1H);  $^{13}\text{C}$  NMR (101 MHz,  $\text{CDCl}_3$ )  $\delta$  175.90, 156.82, 142.08, 137.28, 132.18, 129.98, 128.33, 128.15, 128.09, 127.75, 126.73, 122.55, 113.90, 60.74, 55.81, 55.45, 46.35, 42.84, 22.90; IR (Neat Film, NaCl) 3254, 2923, 1676, 1513, 1405, 1295, 1248, 1035, 823, 702  $\text{cm}^{-1}$ ; (MM:ESI $^+$ )  $\text{C}_{25}\text{H}_{27}\text{N}_2\text{O}_2$   $m/z$  calc'd for  $[\text{M}+\text{H}]^+$ : 387.2073, found 387.2064.



**(*S*<sup>\*</sup>)-3-((*R*<sup>\*</sup>)-amino(phenyl)methyl)-3-(2-bromobenzyl)-1-(4-**

**methoxyphenyl)pyrrolidin-2-one (69fa):** Compound **69fa** was prepared from *N*-PMP lactam **68f** using a slightly modified General Procedure 6 that involves adding 0.5 mL of  $Et_2O$  to the reaction mixture to ensure solubility of *N*-PMP lactam **68f**. The crude oil was purified from column chromatography (3% MeOH in EtOAc, 1% TEA) to afford Mannich product **69fa** as a yellow oil (36 mg, 0.077 mmol, 39% yield, 8.5:1 dr);  $^1H$  NMR (400 MHz,  $CDCl_3$ )  $\delta$  7.49 (dd,  $J = 7.7, 1.6$  Hz, 1H), 7.46 – 7.41 (m, 2H), 7.39 – 7.32 (m, 3H), 7.30 – 7.21 (m, 3H), 7.13 – 6.99 (m, 2H), 6.91 – 6.83 (m, 2H), 4.39 (s, 1H), 3.80 (s, 3H), 3.29 (d,  $J = 13.4$  Hz, 1H), 3.18 (d,  $J = 13.4$  Hz, 1H), 3.03 – 2.88 (m, 1H), 2.57 – 2.45 (m, 2H), 2.41 – 2.08 (br,  $NH_2$ , 2H), 2.08 – 1.87 (m, 1H);  $^{13}C$  NMR (101 MHz,  $CDCl_3$ )  $\delta$  175.99, 156.95, 141.99, 137.66, 132.95, 132.25, 131.93, 128.48, 128.20, 127.98, 127.53, 125.93, 122.39, 114.06, 61.57, 56.30, 55.59, 46.69, 40.57, 22.45; IR (Neat Film, NaCl) 3216, 2923, 1681, 1512, 1295, 1249, 1036, 823, 744  $cm^{-1}$ ; (MM:ESI<sup>+</sup>)  $C_{25}H_{26}BrN_2O_2$   $m/z$  calc'd for  $[M+H]^+$ : 465.1178, found 465.1179.



**2-(((*S*\*)-3-(((*R*\*)-amino(phenyl)methyl)-1-(4-methoxyphenyl)-2-oxopyrrolidin-3-**

**yl)methyl)benzonitrile (69ga):** Compound **69ga** was prepared from *N*-PMP lactam **68g**

using a slightly modified General Procedure 6 that involves adding 0.5 mL of Et<sub>2</sub>O to the

reaction mixture to ensure solubility of *N*-PMP lactam **68g**. The crude oil was purified from

column chromatography (3% MeOH in EtOAc, 1% TEA) to afford Mannich product as a

yellow oil (40 mg, 0.1 mmol, 50% yield, 5:1); <sup>1</sup>H NMR (400 MHz, CDCl<sub>3</sub>)  $\delta$  7.64 – 7.57

(m, 1H), 7.51 (dd, *J* = 8.0, 1.4 Hz, 2H), 7.47 – 7.29 (m, 6H), 7.24 – 7.15 (m, 2H), 6.90 –

6.83 (m, 2H), 4.32 (s, 1H), 3.80 (s, 3H), 3.46 (d, *J* = 13.4 Hz, 1H), 3.11 (d, *J* = 13.5 Hz,

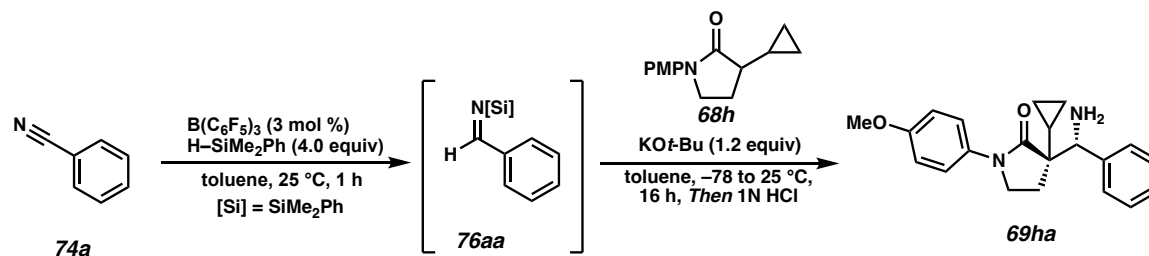
1H), 2.92 – 2.82 (m, 1H), 2.63 – 2.48 (m, 2H), 2.02 – 1.86 (m, 1H); <sup>13</sup>C NMR (101 MHz,

CDCl<sub>3</sub>)  $\delta$  175.20, 157.03, 142.11, 141.98, 132.84, 132.79, 132.04, 131.41, 128.66, 128.18,

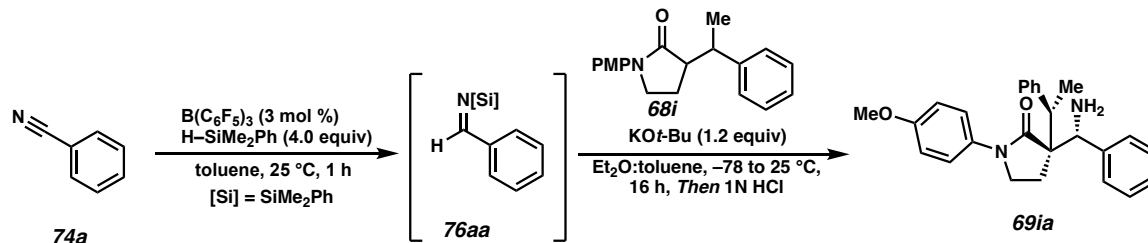
127.96, 127.49, 122.31, 118.36, 114.10, 61.81, 56.06, 55.59, 46.36, 40.07, 23.40; IR (Neat

Film, NaCl) 3254, 2923, 2250, 1681, 1512, 1295, 1249, 1034, 823, 701 cm<sup>-1</sup>; (MM:ESI<sup>+</sup>)

C<sub>26</sub>H<sub>26</sub>N<sub>3</sub>O<sub>2</sub> *m/z* calc'd for [M+H]<sup>+</sup>: 412.2025, found 412.2012.

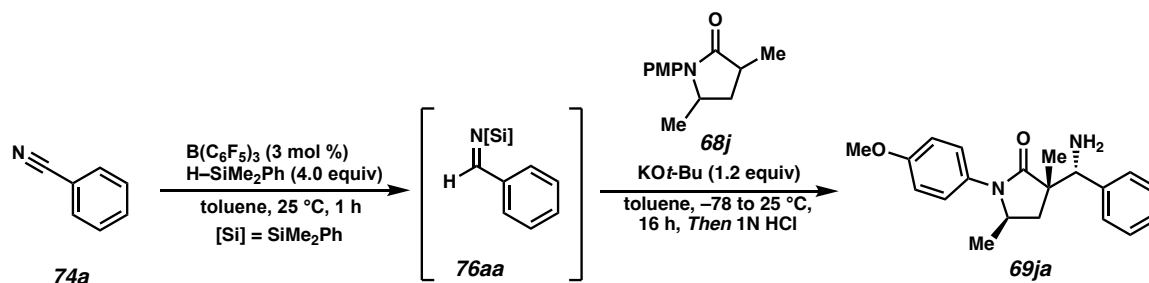


**(*S*<sup>\*</sup>)-3-((*R*<sup>\*</sup>)-amino(phenyl)methyl)-3-cyclopropyl-1-(4-methoxyphenyl)pyrrolidin-2-one (**69ha**):** Compound **69ha** was prepared from *N*-PMP lactam **68h** using General Procedure 6. The crude oil was purified from column chromatography (3% MeOH in EtOAc, 1% TEA) to afford Mannich product **69ha** as a pale-yellow oil (58 mg, 0.172 mmol, 86% yield, 8.5:1 dr);  $^1\text{H}$  NMR (400 MHz,  $\text{CDCl}_3$ )  $\delta$  7.56 – 7.43 (m, 4H), 7.40 – 7.28 (m, 3H), 6.98 – 6.87 (m, 2H), 4.51 (s, 1H), 3.81 (s, 3H), 3.76 – 3.62 (m, 1H), 3.53 (td,  $J = 9.2, 2.1$  Hz, 1H), 2.77 (dt,  $J = 12.4, 9.2$  Hz, 1H), 2.09 – 1.84 (br, 2H,  $\text{NH}_2$ ), 1.51 (ddd,  $J = 12.4, 7.4, 2.1$  Hz, 1H), 0.68 (tdd,  $J = 6.9, 5.2, 2.4$  Hz, 2H), 0.49 – 0.38 (m, 2H), 0.05 – -0.03 (m, 1H);  $^{13}\text{C}$  NMR (101 MHz,  $\text{CDCl}_3$ )  $\delta$  174.67, 156.79, 142.22, 132.58, 128.13, 128.07, 127.54, 122.04, 114.17, 59.81, 55.63, 54.46, 46.38, 24.85, 16.53, 2.26, 0.30; IR (Neat Film, NaCl) 3254, 2930, 1681, 1512, 1452, 1401, 1297, 1248, 1180, 1034, 833, 702, 680  $\text{cm}^{-1}$ ; (MM:ESI<sup>+</sup>)  $\text{C}_{21}\text{H}_{25}\text{N}_2\text{O}_2$   $m/z$  calc'd for  $[\text{M}+\text{H}]^+$ : 337.1916, found 337.1913.



**(3*S*\*)-3-((*R*\*)-amino(phenyl)methyl)-1-(4-methoxyphenyl)-3-(1-**

**phenylethyl)pyrrolidin-2-one (69ia):** Compound **69ia** was prepared from *N*-PMP lactam **68i** using a slightly modified General Procedure 6 that involves adding 0.5 mL of  $\text{Et}_2\text{O}$  to the reaction mixture to ensure solubility of *N*-PMP lactam **68i**. The crude oil was purified from column chromatography (3% MeOH in EtOAc, 1% TEA) to afford Mannich product **69ia** as a yellow oil (30 mg, 0.075 mmol, 37% yield, 9:1);  $^1\text{H}$  NMR (400 MHz,  $\text{CDCl}_3$ )  $\delta$  7.44 – 7.40 (m, 2H), 7.39 – 7.34 (m, 3H), 7.30 – 7.22 (m, 4H), 7.22 – 7.15 (m, 1H), 6.83 (d,  $J = 9.3$  Hz, 2H), 6.80 – 6.74 (m, 2H), 4.13 (q,  $J = 7.1$  Hz, 1H), 4.04 (s, 1H), 3.76 (s, 3H), 3.01 – 2.57 (br,  $\text{NH}_2$ , 2H), 2.47 – 2.37 (m, 1H), 2.29 – 2.19 (m, 1H), 2.18 – 2.09 (m, 1H), 1.79 (ddd,  $J = 13.5, 9.1, 4.5$  Hz, 1H), 1.54 (d,  $J = 7.1$  Hz, 3H);  $^{13}\text{C}$  NMR (101 MHz,  $\text{CDCl}_3$ )  $\delta$  175.45, 157.08, 144.21, 142.93, 131.83, 129.56, 128.44, 128.34, 128.00, 127.61, 126.69, 123.25, 113.95, 61.54, 56.59, 55.55, 46.16, 40.41, 22.19, 14.53; IR (Neat Film, NaCl) 2964, 1673, 1512, 1295, 1248, 1034, 703  $\text{cm}^{-1}$ ; (MM:ESI<sup>+</sup>)  $\text{C}_{26}\text{H}_{29}\text{N}_2\text{O}_2$   $m/z$  calc'd for  $[\text{M}+\text{H}]^+$ : 401.2229, found 401.2209.



**(3*S*\*,5*R*\*)-3-((*R*\*)-amino(phenyl)methyl)-1-(4-methoxyphenyl)-3,5-**

**dimethylpyrrolidin-2-one (**69ja**):** Compound **69ja** was prepared from *N*-PMP lactam **68j**

using General Procedure 6. The crude oil was purified from column chromatography (3%

MeOH in EtOAc, 1% TEA) to afford Mannich product **69ja** as a yellow oil (70 mg, 0.195

mmol, 95% yield, 10:1);  $^1\text{H}$  NMR (400 MHz,  $\text{CDCl}_3$ )  $\delta$  7.40 – 7.30 (m, 5H), 7.13 – 7.05

(m, 2H), 7.00 – 6.87 (m, 2H), 4.09 (s, 1H), 3.82 (s, 3H), 3.40 (dp,  $J = 8.2, 6.3$  Hz, 1H),

2.69 (dd,  $J = 13.2, 8.2$  Hz, 1H), 1.84 (br, 4H\*,  $\text{NH}_2$ ), 1.40 (s, 3H), 1.33 (dd,  $J = 13.2, 6.2$

Hz, 1H), 1.01 (d,  $J = 6.3$  Hz, 3H);  $^{13}\text{C}$  NMR (101 MHz,  $\text{CDCl}_3$ )  $\delta$  177.31, 157.78, 142.61,

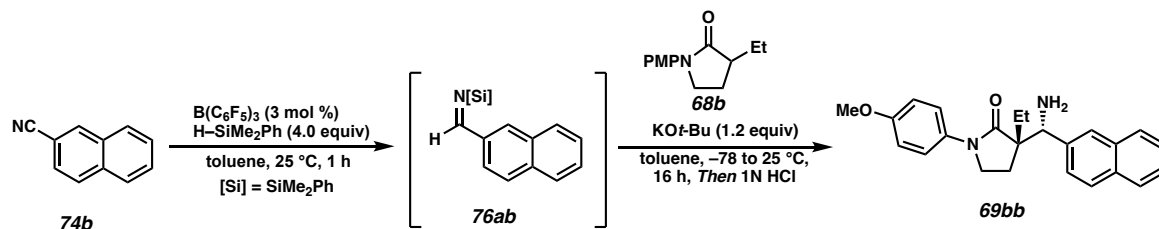
130.30, 128.39, 127.94, 127.76, 126.03, 114.36, 62.63, 55.61, 52.99, 49.59, 37.26, 25.63,

21.36; IR (Neat Film, NaCl) 3374, 2967, 2932, 1682, 1514, 1455, 1394, 1296, 1248, 1181,

1134, 1032, 829, 800, 763, 706  $\text{cm}^{-1}$ ; (MM:ESI $^+$ )  $\text{C}_{20}\text{H}_{25}\text{N}_2\text{O}_2$   $m/z$  calc'd for  $[\text{M}+\text{H}]^+$ :

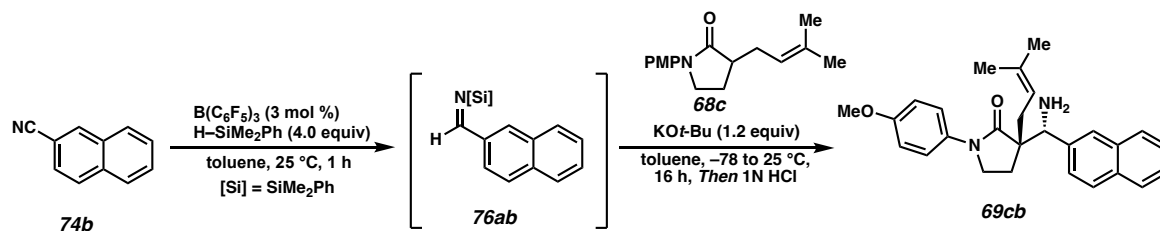
325.1916, found 325.1909.

**General Procedure 7: Direct Mannich Reaction Using *In-Situ* Generated *N*-SiMe<sub>2</sub>Ph Aryl Imine Mannich Acceptor.**

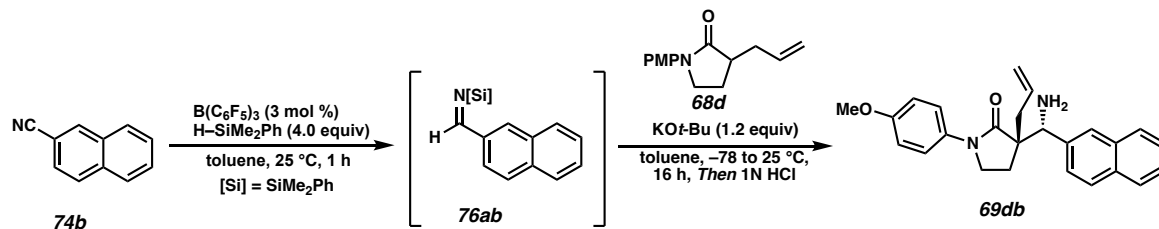


**(*S*<sup>\*</sup>)-3-((*R*<sup>\*</sup>)-amino(naphthalen-2-yl)methyl)-3-ethyl-1-(4-methoxyphenyl)pyrrolidin-2-one (**69bb**):** Compound **69bb** was prepared from 2-naphthonitrile **74b** and *N*-PMP lactam **68b** using General Procedure 7. The crude oil was purified from column chromatography (3% MeOH in EtOAc, 1% TEA) to afford Mannich product **69bb** as a yellow powder (75 mg, 0.194 mmol, 97% yield, 10:1 dr); <sup>1</sup>H NMR (400 MHz, CDCl<sub>3</sub>)  $\delta$  7.95 – 7.72 (m, 4H), 7.52 – 7.42 (m, 5H), 6.95 – 6.87 (m, 2H), 4.44 (s, 1H), 3.81 (s, 3H), 3.51 (td,  $J = 9.1, 6.2$  Hz, 1H), 3.27 (td,  $J = 9.4, 4.5$  Hz, 1H), 2.66 (ddd,  $J = 13.0, 9.5, 6.2$  Hz, 1H), 1.96 – 1.80 (m, 1H), 1.95–1.65 (br, NH<sub>2</sub>, 2H), 1.72 (ddd,  $J = 13.2, 8.9, 4.6$  Hz, 1H), 1.66 – 1.51 (m, 1H), 1.07 – 0.82 (m, 3H); <sup>13</sup>C NMR (101 MHz, CDCl<sub>3</sub>)  $\delta$  176.64, 156.87, 140.20, 133.25, 133.03, 132.61, 128.06, 127.85, 127.73, 126.82, 126.27, 126.15, 125.99, 122.28, 114.15, 60.35, 55.62, 54.78, 46.85, 29.85, 24.12, 8.93; IR (Neat Film, NaCl) 3368, 3052, 2967, 1681, 1513, 1504, 1455, 1403, 1297, 1249, 1181, 1122, 1096, 1035, 859, 832, 8200, 743 cm<sup>-1</sup>; (MM:ESI<sup>+</sup>) C<sub>24</sub>H<sub>27</sub>N<sub>2</sub>O<sub>2</sub>  $m/z$  calc'd for [M+H]<sup>+</sup>: 375.2067, found 375.2072.

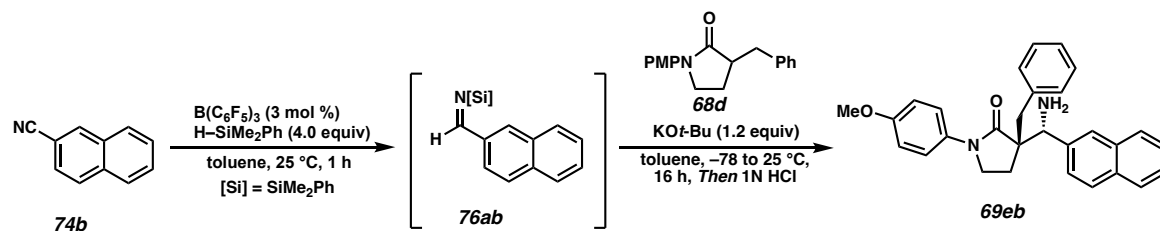




**(*S*<sup>\*</sup>)-3-((*R*<sup>\*</sup>)-amino(naphthalen-2-yl)methyl)-1-(4-methoxyphenyl)-3-(3-methylbut-2-en-1-yl)pyrrolidin-2-one (69cb):** Compound **69cb** was prepared from 2-naphthonitrile **74b** and *N*-PMP lactam **68c** using General Procedure 7. The crude oil was purified from column chromatography (3% MeOH in EtOAc, 1% TEA) to afford Mannich product **69cb** as a yellow powder (78 mg, 0.194 mmol, 95% yield, 10:1 dr); <sup>1</sup>H NMR (400 MHz, CDCl<sub>3</sub>)  $\delta$  7.89 – 7.74 (m, 4H), 7.59 – 7.44 (m, 3H), 7.44 – 7.33 (m, 2H), 6.96 – 6.83 (m, 2H), 5.20 (ddp, *J* = 8.3, 6.8, 1.4 Hz, 1H), 4.43 (s, 1H), 3.81 (s, 3H), 3.43 (td, *J* = 8.9, 6.4 Hz, 1H), 3.16 (td, *J* = 9.3, 4.4 Hz, 1H), 2.69 – 2.48 (m, 2H), 2.30 (dd, *J* = 14.3, 8.1 Hz, 1H), 1.96 – 1.77 (br, NH<sub>2</sub>, 2H), 1.69 (m, overlap, 4H), 1.58 – 1.55 (m, overlap, 3H); <sup>13</sup>C NMR (101 MHz, CDCl<sub>3</sub>)  $\delta$  176.40, 156.73, 140.05, 135.10, 133.16, 132.92, 132.55, 127.95, 127.76, 127.61, 126.75, 126.12, 126.01, 125.84, 122.23, 118.94, 114.01, 60.46, 55.49, 54.47, 46.68, 35.22, 26.11, 24.49, 18.12; (EtOAc present in <sup>1</sup>H NMR and <sup>13</sup>C NMR) IR (Neat Film, NaCl) 3390, 3050, 2929, 1681, 1512, 1442, 1402, 1293, 1248, 1180, 1120, 1103, 1034 855, 826, 745 cm<sup>-1</sup>; (MM:ESI<sup>+</sup>) C<sub>27</sub>H<sub>31</sub>N<sub>2</sub>O<sub>2</sub> *m/z* calc'd for [M+H]<sup>+</sup>: 415.2380, found 415.2386.

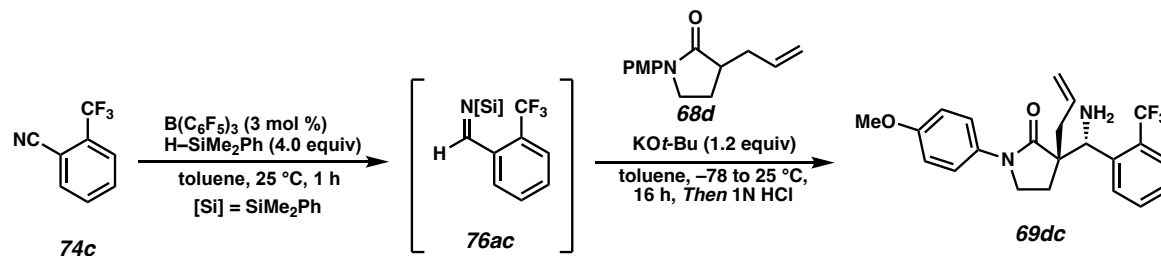


**(*S*\*)-3-allyl-3-((*R*\*)-amino(naphthalen-2-yl)methyl)-1-(4-methoxyphenyl)pyrrolidin-2-one (**69db**):** Compound **69db** was prepared from 2-naphthonitrile **74b** and *N*-PMP lactam **68d** using General Procedure 7. The crude oil was purified from column chromatography (3% MeOH in EtOAc, 1% TEA) to afford Mannich product **69db** as a yellow powder (75 mg, 0.194 mmol, 97% yield, 10:1 dr);  $^1\text{H}$  NMR (400 MHz,  $\text{CDCl}_3$ )  $\delta$  7.90 – 7.76 (m, 4H), 7.62 – 7.49 (m, 3H), 7.47 – 7.39 (m, 2H), 6.96 – 6.85 (m, 2H), 5.81 (dddd,  $J = 16.7, 10.1, 8.4, 6.4$  Hz, 1H), 5.16 – 5.05 (m, 2H), 4.43 (s, 1H), 3.82 (s, 3H), 3.48 (td,  $J = 9.0, 6.4$  Hz, 1H), 3.25 (qd,  $J = 9.4, 4.1$  Hz, 1H), 2.75 – 2.58 (m, 2H), 2.22 (dd,  $J = 13.5, 8.4$  Hz, 1H), 1.78 (ddd,  $J = 13.1, 8.8, 4.4$  Hz, 1H) ( $\text{C}_6\text{H}_6$  present);  $^{13}\text{C}$  NMR (101 MHz,  $\text{CDCl}_3$ )  $\delta$  176.14, 156.93, 139.90, 133.74, 133.27, 133.09, 128.48, 128.10, 127.97, 127.75, 126.92, 126.32, 126.10, 126.06, 122.38, 119.04, 114.16, 60.66, 55.64, 54.38, 46.78, 41.58, 24.05; IR (Neat Film, NaCl) 3054, 2923, 1681, 1512, 1455, 1296, 1249, 1035, 922, 826, 753  $\text{cm}^{-1}$ ; (MM:ESI $^+$ )  $\text{C}_{25}\text{H}_{27}\text{N}_2\text{O}_2$   $m/z$  calc'd for  $[\text{M}+\text{H}]^+$ : 387.2073, found 387.2070.



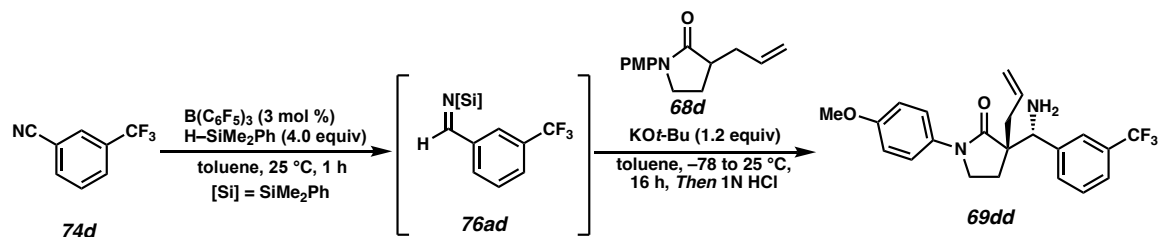
**(*S*<sup>\*</sup>)-3-((*R*<sup>\*</sup>)-amino(naphthalen-2-yl)methyl)-3-benzyl-1-(4-**

**methoxyphenyl)pyrrolidin-2-one (69eb):** Compound **69eb** was prepared from 2-naphthonitrile **74b** and *N*-PMP lactam **68e** using General Procedure 7. The crude oil was purified from column chromatography (3% MeOH in EtOAc, 1% TEA) to afford Mannich product **69eb** as a yellow amorphous solid (83 mg, 0.191 mmol, 95% yield, 10:1 dr);  $^1H$  NMR (400 MHz,  $CDCl_3$ )  $\delta$  7.96 – 7.77 (m, 4H), 7.61 – 7.54 (m, 1H), 7.51 (ddt,  $J = 8.0, 5.6, 3.6$  Hz, 3H), 7.21 – 7.12 (m, 6H), 6.85 (d,  $J = 9.0$  Hz, 2H), 4.59 (s, 1H), 3.80 (s, 3H), 3.29 (d,  $J = 12.9$  Hz, 1H), 3.03 (td,  $J = 9.4, 2.7$  Hz, 1H), 2.77 (ddd,  $J = 12.7, 9.6, 7.8$  Hz, 1H), 2.55 (d,  $J = 13.0$  Hz, 1H), 2.39 (dt,  $J = 9.0, 8.1$  Hz, 1H), 1.75 (ddd,  $J = 12.8, 8.2, 2.7$  Hz, 1H);  $^{13}C$  NMR (101 MHz,  $CDCl_3$ )  $\delta$  176.07, 156.96, 139.90, 137.38, 133.32, 133.15, 132.32, 130.10, 128.27, 128.20, 128.14, 128.03, 127.77, 127.14, 126.87, 126.35, 126.31, 126.10, 122.71, 114.03, 60.98, 56.17, 55.58, 46.53, 43.06, 23.09; IR (Neat Film, NaCl) 3342, 3058, 2950, 1680, 1602, 1512, 1453, 1404, 1294, 1249, 1181, 1119, 1032, 860, 830, 741, 702  $cm^{-1}$ ; (MM:ESI<sup>+</sup>)  $C_{29}H_{29}N_2O_2$   $m/z$  calc'd for  $[M+H]^+$ : 437.2224, found 437.2223.



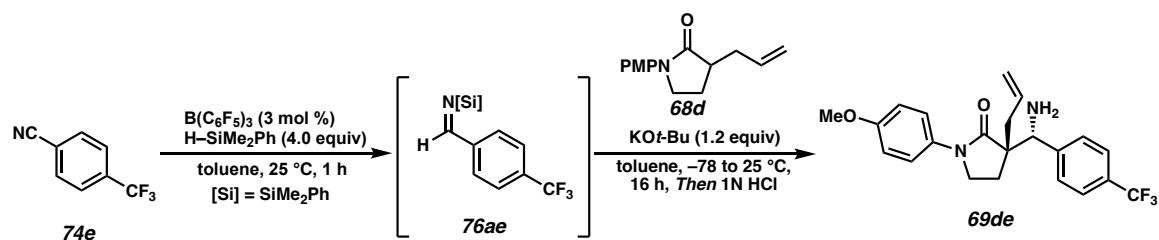
**(*S*<sup>\*</sup>)-3-allyl-3-((*R*<sup>\*</sup>)-amino(2-(trifluoromethyl)phenyl)methyl)-1-(4-**

**methoxyphenyl)pyrrolidin-2-one (69dc):** Compound **69dc** was prepared from 2-(trifluoromethyl)benzonitrile **74c** and *N*-PMP lactam **68d** using General Procedure 7. The crude oil was purified by column chromatography (3% MeOH in EtOAc, 1% TEA) to afford Mannich product **69dc** as a pale-yellow oil (40 mg, 0.10 mmol, 50% yield, 20:1 dr);  $^1\text{H}$  NMR (400 MHz,  $\text{CDCl}_3$ )  $\delta$  7.70 – 7.62 (m, 2H), 7.63 – 7.45 (m, 1H), 7.48 – 7.41 (m, 2H), 7.41 – 7.32 (m, 1H), 6.96 – 6.86 (m, 2H), 5.81 (dddd,  $J = 17.0, 10.1, 8.5, 6.3$  Hz, 1H), 5.25 – 5.16 (m, 1H), 5.14 (dddd,  $J = 10.1, 2.0, 1.2, 0.6$  Hz, 1H), 4.67 – 4.54 (m, 1H), 3.82 (s, 3H), 3.50 – 3.44 (m, 1H), 3.03 (td,  $J = 9.3, 4.8$  Hz, 1H), 2.71 (ddt,  $J = 13.6, 6.3, 1.4$  Hz, 1H), 2.42 (dd,  $J = 13.6, 8.6$  Hz, 1H), 2.22 (ddd,  $J = 13.2, 9.2, 6.1$  Hz, 1H), 2.04 (ddd,  $J = 13.4, 8.8, 4.8$  Hz, 1H);  $^{13}\text{C}$  NMR (101 MHz,  $\text{CDCl}_3$ )  $\delta$  176.33, 156.99, 143.34, 133.32, 132.43 (d,  $J = 2.2$  Hz), 132.38, 128.57, 128.53 (q,  $J = 29.3$  Hz), 127.46, 126.01 (q,  $J = 6.0$  Hz), 125.87 (q,  $J = 274.0$  Hz), 122.17, 119.40, 114.20, 55.64, 55.26 (d,  $J = 2.5$  Hz), 53.22, 46.39, 41.14, 25.08.;  $^{19}\text{F}$  NMR (282 MHz,  $\text{CDCl}_3$ )  $\delta$  -56.68; IR (Neat Film, NaCl) 2924, 1684, 1511, 1405, 1308, 1249, 1158, 1121, 1036, 772  $\text{cm}^{-1}$ ; (MM:ESI<sup>+</sup>)  $\text{C}_{22}\text{H}_{24}\text{F}_3\text{N}_2\text{O}_2$   $m/z$  calc'd for  $[\text{M}+\text{H}]^+$ : 405.1790, found 405.1789.



**(*S*<sup>\*</sup>)-3-allyl-3-((*S*<sup>\*</sup>)-amino(3-(trifluoromethyl)phenyl)methyl)-1-(4-**

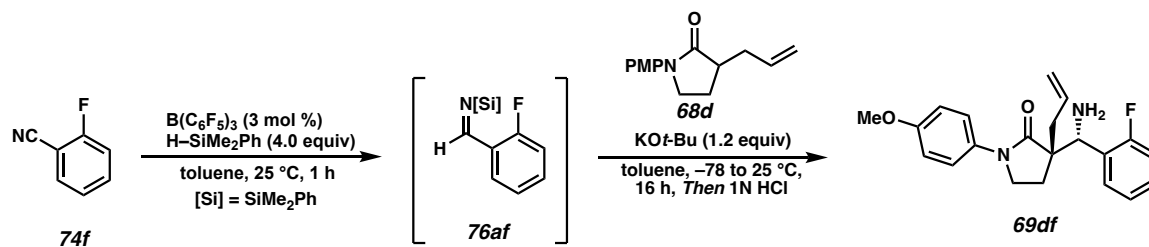
**methoxyphenyl)pyrrolidin-2-one (69dd):** Compound **69dd** was prepared from 3-(trifluoromethyl)benzonitrile **74d** using General Procedure 7. The crude oil was purified from column chromatography (3% MeOH in EtOAc, 1% TEA) to afford Mannich product **69dd** as a pale-yellow oil (30 mg, 0.75 mmol, 38% yield, 7:1 dr); <sup>1</sup>H NMR (400 MHz, CDCl<sub>3</sub>)  $\delta$  7.67 (s, 1H), 7.63 – 7.50 (m, 3H), 7.46 (d,  $J$  = 9.1 Hz, 2H), 6.97 – 6.87 (m, 2H), 5.93 – 5.71 (m, 1H), 5.22 – 5.06 (m, 2H), 4.36 (s, 1H), 3.82 (s, 3H), 3.55 (ddd,  $J$  = 9.4, 8.7, 6.7 Hz, 1H), 3.32 (td,  $J$  = 9.5, 4.0 Hz, 1H), 2.62 – 2.49 (m, 2H), 2.13 (dd,  $J$  = 13.6, 8.2 Hz, 1H), 1.79 – 1.55 (br, NH<sub>2</sub>, 2H), 1.73 (ddd,  $J$  = 12.8, 8.7, 4.0 Hz, 1H); <sup>13</sup>C NMR (101 MHz, CDCl<sub>3</sub>)  $\delta$  175.63, 157.04, 143.17, 133.30, 132.34, 131.58, 130.97 (q,  $J$  = 32.8 Hz), 128.84, 124.73 (m), 122.30, 119.34, 114.21, 59.96, 55.64, 54.15, 46.66, 41.31, 23.68 (not identified,  $J^1_{C-F}$  carbon); <sup>19</sup>F NMR (282 MHz, CDCl<sub>3</sub>) –62.54; IR (Neat Film, NaCl) 2923, 1681, 1512, 1422, 1328, 1249, 1163, 1122, 1073, 833 cm<sup>-1</sup>; (MM:ESI<sup>+</sup>) C<sub>22</sub>H<sub>24</sub>F<sub>3</sub>N<sub>2</sub>O<sub>2</sub>  $m/z$  calc'd for [M+H]<sup>+</sup>: 405.1790, found 405.1773.



**(*S*<sup>\*</sup>)-3-allyl-3-((*R*<sup>\*</sup>)-amino(4-(trifluoromethyl)phenyl)methyl)-1-(4-**

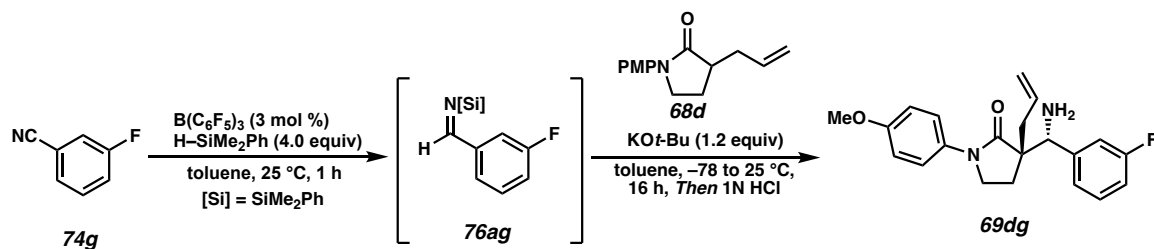
**methoxyphenyl)pyrrolidin-2-one (69de):** Compound **69de** was prepared from 4-

(trifluoromethyl)benzotrile **74e** using General Procedure 7. The crude oil was purified from column chromatography (3% MeOH in EtOAc, 1% TEA) to afford Mannich product **69de** as a pale-yellow oil (57 mg, 0.14 mmol, 70% yield, 17:1 dr);  $^1\text{H}$  NMR (400 MHz,  $\text{CDCl}_3$ )  $\delta$  7.62 – 7.56 (m, 2H), 7.51 (d,  $J = 8.0$  Hz, 2H), 7.47 – 7.39 (m, 2H), 6.95 – 6.87 (m, 2H), 5.79 (dddd,  $J = 16.8, 10.1, 8.3, 6.6$  Hz, 1H), 5.19 – 5.07 (m, 2H), 4.35 (s, 1H), 3.82 (s, 3H), 3.58 – 3.47 (m, 1H), 3.40 – 3.27 (m, 1H), 2.63 – 2.48 (m, 2H), 2.12 (ddt,  $J = 13.5, 8.3, 1.0$  Hz, 1H), 1.95 – 1.68 (br,  $\text{NH}_2$ , 2H\*), 1.73 (ddd,  $J = 12.8, 8.6, 4.0$  Hz, 1H);  $^{13}\text{C}$  NMR (101 MHz,  $\text{CDCl}_3$ )  $\delta$  175.66, 157.03, 146.36, 136.18 (d,  $J = 30.9$  Hz), 133.32, 132.36, 130.43–125.2 (m), 128.46, 125.30 (q,  $J = 3.9$  Hz), 122.28, 119.30, 114.23, 60.02, 55.64, 54.22, 46.67, 41.38, 23.63;  $^{19}\text{F}$  NMR (282 MHz,  $\text{CDCl}_3$ )  $\delta$  –62.48; IR (Neat Film, NaCl) 2923, 1681, 1512, 1405, 1325, 1250, 1165, 1122, 1068, 833  $\text{cm}^{-1}$ ; (MM:ESI $^+$ )  $\text{C}_{22}\text{H}_{24}\text{F}_3\text{N}_2\text{O}_2$   $m/z$  calc'd for  $[\text{M}+\text{H}]^+$ : 405.1790, found 405.1790.



**( $S^*$ )-3-allyl-3-(( $S^*$ )-amino(2-fluorophenyl)methyl)-1-(4-methoxyphenyl)pyrrolidin-2-one (**69df**):** Compound **69df** was prepared from 2-fluorobenzonitrile **74f** using General Procedure 7. The crude oil was purified from column chromatography (3% MeOH in EtOAc, 1% TEA) to afford Mannich product **69df** as a pale-yellow oil (68 mg, 0.194 mmol, 97% yield, 3.5:1 dr);  $^1\text{H}$  NMR (400 MHz,  $\text{CDCl}_3$ )  $\delta$  7.48 – 7.38 (m, 2.7H), 7.30 – 7.22 (m, 1.3H), 7.18 – 6.98 (m, 2H), 6.92 – 6.86 (m, 2H), 5.87 – 5.73 (m, 1H), 5.16 (dtd,  $J = 16.9, 1.8, 1.0$  Hz, 1H), 5.12 – 5.06 (m, 1H), 4.66 (s, 0.78H), 4.62 (s, 0.22H), 3.81 (s, 2.34H),

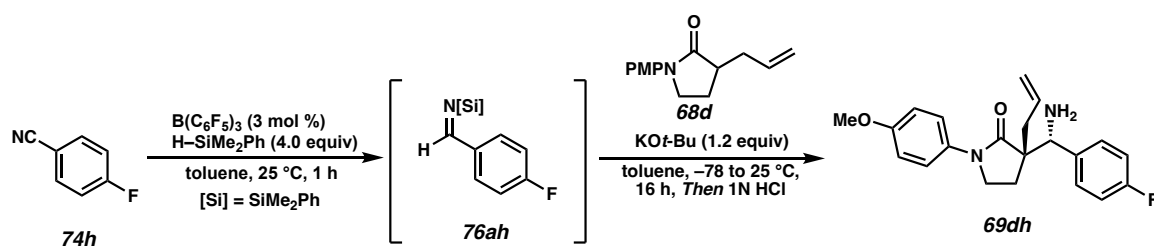
3.80 (s, 0.66H), 3.55 (dd,  $J = 7.9, 6.4$  Hz, 0.44H), 3.47 (td,  $J = 9.1, 5.6$  Hz, 0.78H), 3.13 (td,  $J = 9.3, 5.1$  Hz, 0.78H), 2.95 (ddt,  $J = 13.6, 5.8, 1.5$  Hz, 0.22H), 2.69 (ddq,  $J = 13.5, 6.3, 1.3$  Hz, 0.78H), 2.43 (ddd,  $J = 13.1, 9.2, 5.7$  Hz, 0.78H), 2.31 – 2.15 (m, 1.22H), 2.03 – 1.93 (m, 0.22H), 1.93 – 1.84 (m, 1H), 1.83 – 1.72 (br, NH<sub>2</sub>, 2H); <sup>13</sup>C NMR (101 MHz, CDCl<sub>3</sub>)  $\delta$  175.80,\* 175.75, 160.70 (d,  $J = 244.1$  Hz),\* 160.30 (d,  $J = 244.9$  Hz), 156.92, 156.89,\* 134.36,\* 133.57, 132.54,\* 132.39, 130.54 (d,  $J = 4.0$  Hz),\* 129.74 (d,  $J = 13.5$  Hz), 129.08 (d,  $J = 8.9$  Hz),\* 129.04 (d,  $J = 8.5$  Hz), 128.90 (d,  $J = 4.0$  Hz), 128.47,\* 124.48 (d,  $J = 3.5$  Hz), 124.20 (d,  $J = 3.4$  Hz),\* 122.32,\* 122.29, 119.12,\*\* 115.44 (d,  $J = 23.5$  Hz),\*\* 114.14,\*\* 55.61,\*\* 54.23, 53.86,\* 53.47,\* 52.49, 46.63, 46.55,\* 41.01, 37.11,\* 25.57 (d,  $J = 2.1$  Hz),\* 24.09 (d,  $J = 2.2$  Hz) minor diastereomer denoted with\*, overlap\*\*  
<sup>19</sup>F NMR (282 MHz, CDCl<sub>3</sub>)  $\delta$  -115.83 (m)\*\*; IR (Neat Film, NaCl) 2923, 1681, 1512, 1487, 1455, 1403, 1296, 1249, 1182, 1100, 1035, 923, 826, 761 cm<sup>-1</sup>; (MM:ESI<sup>+</sup>) C<sub>21</sub>H<sub>24</sub>FN<sub>2</sub>O<sub>2</sub>  $m/z$  calc'd for [M+H]<sup>+</sup>: 355.1822, found 355.1812.



**(*S*<sup>\*</sup>)-3-allyl-3-((*R*<sup>\*</sup>)-amino(3-fluorophenyl)methyl)-1-(4-methoxyphenyl)pyrrolidin-**

**2-one (69dg):** Compound **69dg** was prepared from 3-fluorobenzonitrile **74g** using General Procedure 7. The crude oil was purified from column chromatography (3% MeOH in EtOAc, 1% TEA) to afford Mannich product **69dg** as a pale-yellow oil (65 mg, 0.186 mmol, 93% yield, 20:1 dr); <sup>1</sup>H NMR (400 MHz, CDCl<sub>3</sub>)  $\delta$  7.48 – 7.40 (m, 2H), 7.33 – 7.23 (m, 1H), 7.16 – 7.10 (m, 2H), 6.99 (tdd,  $J = 8.4, 2.6, 1.0$  Hz, 1H), 6.95 – 6.87 (m, 2H), 5.78

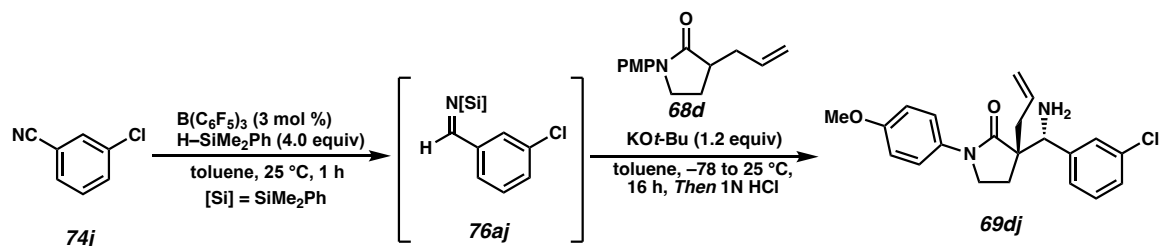
(dddd,  $J = 16.8, 10.1, 8.3, 6.5$  Hz, 1H), 5.18 – 5.06 (m, 2H), 4.28 (s, 1H), 3.81 (s, 3H), 3.53 (ddd,  $J = 9.3, 8.7, 6.6$  Hz, 1H), 3.34 (td,  $J = 9.4, 4.1$  Hz, 1H), 2.62 – 2.50 (m, 1H), 2.14 (ddt,  $J = 13.6, 8.3, 1.0$  Hz, 2H), 1.86 – 1.77 (br, NH<sub>2</sub>, 2H), 1.77 – 1.69 (m, 1H); <sup>13</sup>C NMR (101 MHz, CDCl<sub>3</sub>)  $\delta$  175.82, 162.85 (d,  $J = 246.1$  Hz), 156.99, 144.90 (d,  $J = 6.6$  Hz), 133.47, 132.41, 129.77 (d,  $J = 8.2$  Hz), 123.87 (d,  $J = 2.8$  Hz), 122.35, 119.17, 114.88 (d,  $J = 20.92$  Hz), 114.67 (d,  $J = 20.46$  Hz), 114.19, 59.96 (d,  $J = 1.7$  Hz), 55.62, 54.20, 46.73, 41.42, 23.72; <sup>19</sup>F NMR (282 MHz, CDCl<sub>3</sub>)  $\delta$  -112.81 – -112.94 (m); IR (Neat Film, NaCl) 2909, 1681, 1613, 1588, 1513, 1487, 1404, 1296, 1249, 1181, 1101, 1036, 922, 834, 793 cm<sup>-1</sup>; (MM:ESI<sup>+</sup>) C<sub>21</sub>H<sub>24</sub>FN<sub>2</sub>O<sub>2</sub>  $m/z$  calc'd for [M+H]<sup>+</sup>: 355.1822, found 355.1819.



**(S<sup>\*</sup>)-3-allyl-3-((R<sup>\*</sup>)-amino(4-fluorophenyl)methyl)-1-(4-methoxyphenyl)pyrrolidin-2-one (69dh):** Compound **69dh** was prepared from 4-fluorobenzonitrile **74h** using General Procedure 7. The crude oil was purified from column chromatography (3% MeOH in EtOAc, 1% TEA) to afford Mannich product **69dh** as a pale-yellow oil (67 mg, 0.190 mmol, 95% yield, 10:1 dr); <sup>1</sup>H NMR (400 MHz, CDCl<sub>3</sub>)  $\delta$  7.47 – 7.42 (m, 2H), 7.37 – 7.31 (m, 2H), 7.06 – 6.97 (m, 2H), 6.94 – 6.87 (m, 2H), 5.78 (dddd,  $J = 16.7, 10.1, 8.3, 6.5$  Hz, 1H), 5.17 – 5.06 (m, 2H), 4.25 (s, 1H), 3.81 (s, 3H), 3.50 (td,  $J = 8.9, 6.4$  Hz, 1H), 3.26 (td,  $J = 9.4, 4.4$  Hz, 1H), 2.58 – 2.45 (m, 2H), 2.21 – 2.10 (m, 1H), 2.11 – 1.94 (br, NH<sub>2</sub>, 2H), 1.74 (ddd,  $J = 13.0, 8.8, 4.4$  Hz, 1H); <sup>13</sup>C NMR (101 MHz, CDCl<sub>3</sub>)  $\delta$  175.91, 162.39 (d,  $J = 245.9$  Hz), 156.95, 137.99 (d,  $J = 3.2$  Hz), 133.56, 132.43, 129.49 (d,  $J = 7.9$  Hz), 122.27,

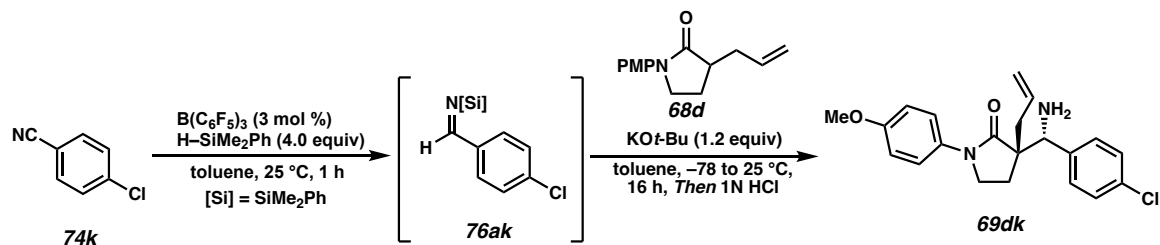


119.09, 115.20 (d,  $J = 21.1$  Hz), 114.18, 59.75, 55.62, 54.19, 46.65, 41.43, 23.85;  $^{19}\text{F}$  NMR (282 MHz,  $\text{CDCl}_3$ )  $\delta -114.82$  (tt,  $J = 8.5, 5.3$  Hz); IR (Neat Film, NaCl) 2909, 1681, 1603, 1512, 1403, 1295, 1249, 1181, 1035, 833  $\text{cm}^{-1}$ ; (MM:ESI $^+$ )  $\text{C}_{21}\text{H}_{24}\text{FN}_2\text{O}_2$   $m/z$  calc'd for  $[\text{M}+\text{H}]^+$ : 355.1822, found 355.1829.

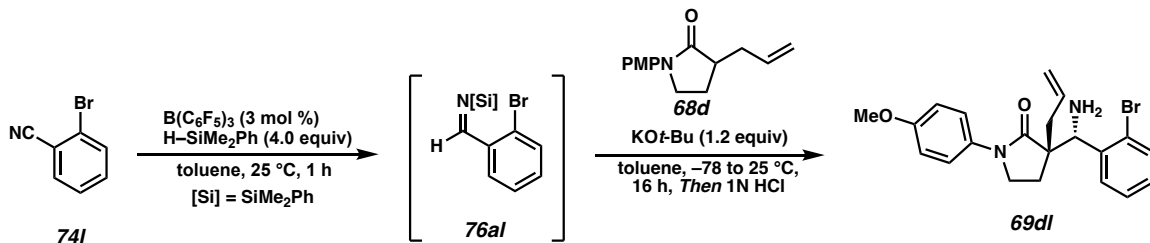


**(*S* $^*$ )-3-allyl-3-((*R* $^*$ )-amino(3-chlorophenyl)methyl)-1-(4-methoxyphenyl)pyrrolidin-**

**2-one (69dj):** Compound **69dj** was prepared from 3-chlorobenzonitrile **74j** using General Procedure 7. The crude oil was purified from column chromatography (3% MeOH in EtOAc, 1% TEA) to afford Mannich product **69dj** as a pale-yellow oil (72 mg, 0.195 mmol, 97% yield, 20:1 dr);  $^1\text{H}$  NMR (400 MHz,  $\text{CDCl}_3$ )  $\delta$  7.46 – 7.41 (m, 2H), 7.39 (ddd,  $J = 2.2, 1.5, 0.9$  Hz, 1H), 7.28 – 7.22 (m, 3H), 6.92 – 6.87 (m, 2H), 5.77 (dddd,  $J = 16.8, 10.1, 8.3, 6.5$  Hz, 1H), 5.18 – 5.05 (m, 2H), 4.23 (s, 1H), 3.80 (s, 3H), 3.56 – 3.47 (m, 1H), 3.29 (td,  $J = 9.4, 4.2$  Hz, 1H), 2.52 (ddd,  $J = 13.0, 9.4, 6.6$  Hz, 2H), 2.14 (ddt,  $J = 13.5, 8.3, 1.0$  Hz, 1H), 1.75 (ddd,  $J = 13.0, 8.7, 4.2$  Hz, 1H);  $^{13}\text{C}$  NMR (101 MHz,  $\text{CDCl}_3$ )  $\delta$  175.75, 156.99, 144.45, 134.33, 133.44, 132.36, 129.60, 128.06, 127.95, 126.36, 122.39, 119.19, 114.18, 60.03, 55.61, 54.13, 46.71, 41.37, 23.79; IR (Neat Film, NaCl) 2891, 1681, 1512, 1486, 1430, 1404, 1296, 1249, 1180, 1100, 1035, 826, 790  $\text{cm}^{-1}$ ; (MM:ESI $^+$ )  $\text{C}_{21}\text{H}_{24}\text{ClN}_2\text{O}_2$   $m/z$  calc'd for  $[\text{M}+\text{H}]^+$ : 371.1526, found 371.1547.

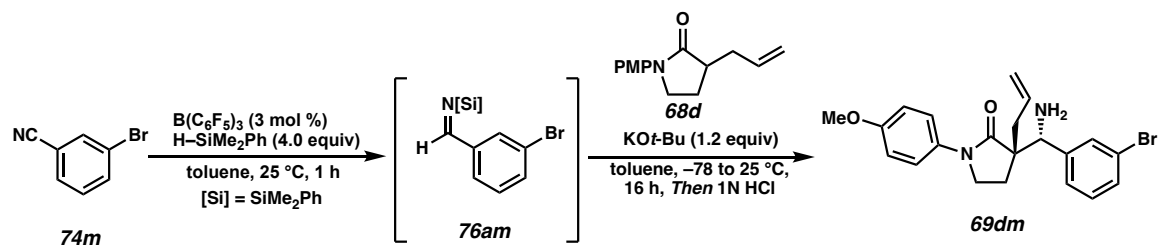


**(*S*<sup>\*</sup>)-3-allyl-3-((*R*<sup>\*</sup>)-amino(4-chlorophenyl)methyl)-1-(4-methoxyphenyl)pyrrolidin-2-one (69dk):** Compound **69dk** was prepared from 4-chlorobenzonitrile **74k** using General Procedure 7. The crude oil was purified from column chromatography (3% MeOH in EtOAc, 1% TEA) to afford Mannich product **69dk** as a pale-yellow oil (70 mg, 0.190 mmol, 95% yield, 20:1 dr); <sup>1</sup>H NMR (400 MHz, CDCl<sub>3</sub>)  $\delta$  7.48 – 7.43 (m, 2H), 7.35 – 7.31 (m, 2H), 7.31 – 7.28 (m, 2H), 6.95 – 6.88 (m, 2H), 5.78 (dddd,  $J$  = 16.8, 10.1, 8.3, 6.5 Hz, 1H), 5.16 – 5.06 (m, 2H), 4.25 (s, 1H), 3.82 (s, 3H), 3.57 – 3.48 (m, 1H), 3.32 (td,  $J$  = 9.4, 4.2 Hz, 1H), 2.52 (ddd,  $J$  = 12.9, 9.6, 6.6 Hz, 2H), 2.18 – 2.08 (m, 1H), 1.72 (ddd,  $J$  = 12.9, 8.7, 4.2 Hz, 1H), 1.61 (br, NH<sub>2</sub>, 2H); <sup>13</sup>C NMR (101 MHz, CDCl<sub>3</sub>)  $\delta$  175.85, 156.98, 140.80, 133.53, 133.50, 132.44, 129.39, 128.52, 122.28, 119.15, 114.21, 59.80, 55.64, 54.21, 46.69, 41.43, 23.71; IR (Neat Film, NaCl) 2908, 1681, 1512, 1403, 1295, 1249, 1179, 1090, 1035, 922, 833 cm<sup>-1</sup>; (MM:ESI<sup>+</sup>) C<sub>21</sub>H<sub>24</sub>ClN<sub>2</sub>O<sub>2</sub>  $m/z$  calc'd for [M+H]<sup>+</sup>: 371.1526, found 371.1523.

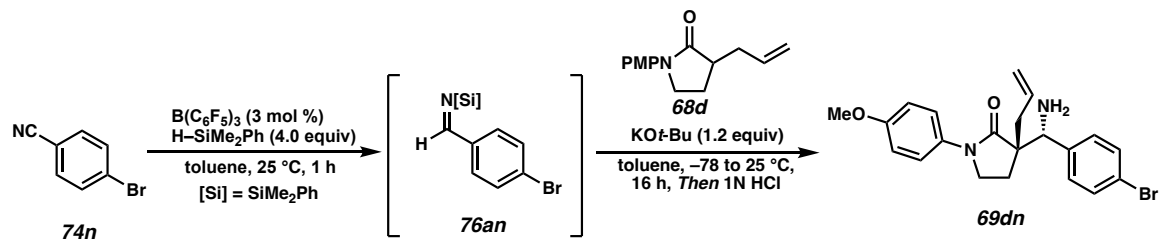


**(*S*<sup>\*</sup>)-3-allyl-3-((*S*<sup>\*</sup>)-amino(2-bromophenyl)methyl)-1-(4-methoxyphenyl)pyrrolidin-**

**2-one (69dl):** Compound **69dl** was prepared from 2-bromobenzonitrile **74l** using General Procedure 7. The crude oil was purified from column chromatography (3% MeOH in EtOAc, 1% TEA) to afford Mannich product **69dl** as a pale-yellow oil (29 mg, 0.07 mmol, 35% yield, 7:1 dr);  $^1\text{H}$  NMR (400 MHz,  $\text{CDCl}_3$ )  $\delta$  7.59 – 7.53 (m, 1H), 7.43 (dd,  $J = 7.8, 1.8$  Hz, 1H), 7.39 – 7.35 (m, 1H), 7.21 (td,  $J = 7.5, 1.5$  Hz, 1H), 7.14 – 7.10 (m, 1H), 6.92 – 6.87 (m, 2H), 5.92 – 5.78 (m, 1H), 5.25 – 5.18 (m, 1H), 5.18 – 5.13 (m, 1H), 4.79 (s, 1H), 3.81 (s, 3H), 3.40 (td,  $J = 9.2, 4.9$  Hz, 1H), 2.87 (td,  $J = 9.1, 6.0$  Hz, 1H), 2.77 (ddt,  $J = 13.7, 6.2, 1.5$  Hz, 1H), 2.52 – 2.38 (m, 1H), 2.04 – 1.95 (m, 1H);  $^{13}\text{C}$  NMR (101 MHz,  $\text{CDCl}_3$ )  $\delta$  175.78, 156.92, 142.69, 133.62, 133.05, 132.32, 129.02, 128.96, 127.95, 122.30, 122.18, 119.23, 114.14, 58.11, 55.62, 53.98, 46.53, 40.88, 24.72; IR (Neat Film, NaCl) 2923, 1683, 1511, 1296, 1248, 1024, 822, 760  $\text{cm}^{-1}$ ; (MM:ESI<sup>+</sup>)  $\text{C}_{21}\text{H}_{24}\text{BrN}_2\text{O}_2$   $m/z$  calc'd for  $[\text{M}+\text{H}]^+$ : 415.1021, found 415.1027.

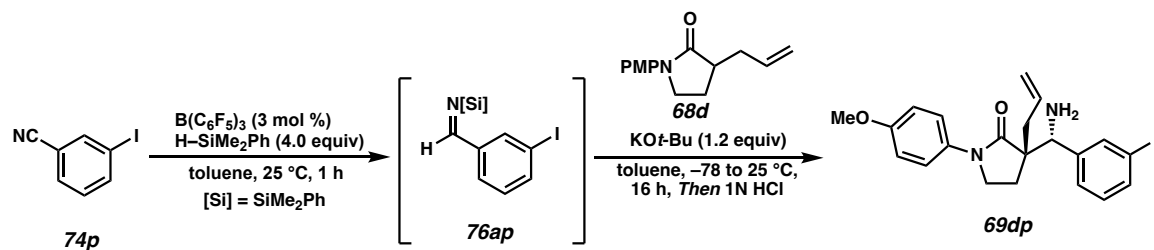


**(*S*<sup>\*</sup>)-3-allyl-3-((*R*<sup>\*</sup>)-amino(3-bromophenyl)methyl)-1-(4-methoxyphenyl)pyrrolidin-2-one (69dm):** Compound **69dm** was prepared from 3-bromobenzonitrile **74m** using General Procedure 7. The crude oil was purified from column chromatography (3% MeOH in EtOAc, 1% TEA) to afford Mannich product **69dm** as a pale-yellow oil (45 mg, 0.108 mmol, 55% yield, 20:1 dr); <sup>1</sup>H NMR (400 MHz, CDCl<sub>3</sub>)  $\delta$  7.55 (t,  $J$  = 1.9 Hz, 1H), 7.50 – 7.40 (m, 3H), 7.29 (dt,  $J$  = 7.8, 1.5 Hz, 1H), 7.18 (t,  $J$  = 7.8 Hz, 1H), 6.96 – 6.87 (m, 2H), 5.79 (dddd,  $J$  = 16.8, 10.1, 8.3, 6.5 Hz, 1H), 5.19 – 5.06 (m, 2H), 4.22 (s, 1H), 3.81 (s, 3H), 3.56 – 3.49 (m, 1H), 3.29 (td,  $J$  = 9.4, 4.3 Hz, 1H), 2.60 – 2.45 (m, 2H), 2.16 (ddt,  $J$  = 13.5, 8.3, 1.0 Hz, 1H), 1.76 (ddd,  $J$  = 13.0, 8.7, 4.3 Hz, 1H); <sup>13</sup>C NMR (101 MHz, CDCl<sub>3</sub>)  $\delta$  175.60, 156.88, 144.63, 133.33, 132.25, 130.84, 130.79, 129.79, 126.71, 122.48, 122.27, 119.09, 114.07, 59.92, 55.51, 54.00, 46.58, 41.24, 23.71; IR (Neat Film, NaCl) 2950, 1681, 1512, 1429, 1403, 1295, 1249, 1180, 1101, 1035, 923, 833, 792 cm<sup>-1</sup>; (MM:ESI<sup>+</sup>) C<sub>21</sub>H<sub>24</sub>BrN<sub>2</sub>O<sub>2</sub>  $m/z$  calc'd for [M+H]<sup>+</sup>: 415.1021, found 415.1036.

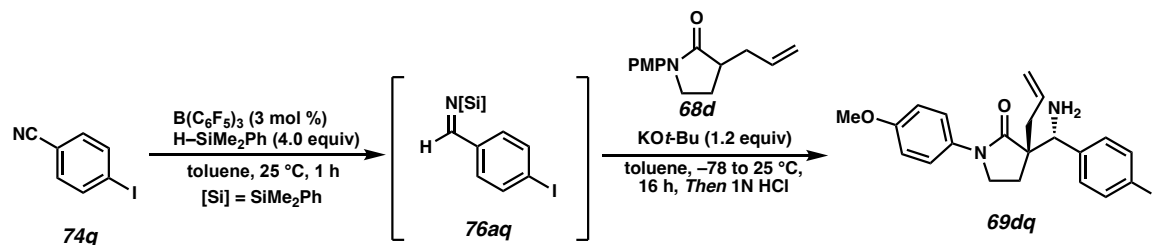


**(*S*<sup>\*</sup>)-3-allyl-3-((*R*<sup>\*</sup>)-amino(4-bromophenyl)methyl)-1-(4-methoxyphenyl)pyrrolidin-**

**2-one (69dn):** Compound **69dn** was prepared from 4-bromobenzonitrile **74n** using General Procedure 7. The crude oil was purified from column chromatography (3% MeOH in EtOAc, 1% TEA) to afford Mannich product **69dn** as a pale-yellow oil (79 mg, 0.190 mmol, 95% yield, 20:1 dr<sup>1</sup>H NMR (400 MHz, CDCl<sub>3</sub>)  $\delta$  7.50 – 7.43 (m, 4H), 7.36 – 7.23 (m, 2H), 6.99 – 6.87 (m, 2H), 5.79 (dddd,  $J = 16.7, 10.1, 8.3, 6.5$  Hz, 1H), 5.20 – 5.07 (m, 2H), 4.26 (s, 1H), 3.83 (s, 3H), 3.54 (ddd,  $J = 9.3, 8.7, 6.6$  Hz, 1H), 3.35 (td,  $J = 9.4, 4.1$  Hz, 1H), 2.61 – 2.49 (m, 2H), 2.14 (ddt,  $J = 13.5, 8.3, 1.0$  Hz, 1H), 1.74 (td,  $J = 8.8, 4.4$  Hz, 1H), 1.69 (br, NH<sub>2</sub>, 2H); <sup>13</sup>C NMR (101 MHz, CDCl<sub>3</sub>)  $\delta$  175.81, 156.97, 141.30, 133.47, 132.42, 131.46, 129.75, 122.27, 121.63, 119.16, 114.20, 59.84, 55.63, 54.16, 46.68, 41.41, 23.66; IR (Neat Film, NaCl) 2923, 1681, 1512, 1486, 1404, 1295, 1249, 1178, 1073, 1010, 825 cm<sup>-1</sup>; (MM:ESI<sup>+</sup>) C<sub>21</sub>H<sub>24</sub>BrN<sub>2</sub>O<sub>2</sub>  $m/z$  calc'd for [M+H]<sup>+</sup>: 415.1021, found 415.1015. Structure and relative configuration was confirmed via X-ray crystallography. Crystals were obtained from slow evaporation of a solution of **69dn** in toluene. CCDC 2253010

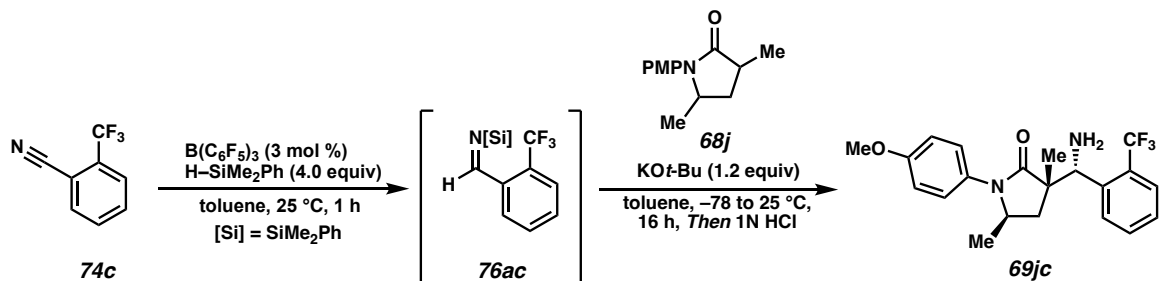


**(*S*<sup>\*</sup>)-3-allyl-3-((*R*<sup>\*</sup>)-amino(3-iodophenyl)methyl)-1-(4-methoxyphenyl)pyrrolidin-2-one (69dp):** Compound **69dp** was prepared from 3-iodobenzonitrile **74p** using General Procedure 7. The crude oil was purified from column chromatography (3% MeOH in EtOAc, 1% TEA) to afford Mannich product **69dp** as a pale-yellow oil (30 mg, 0.065 mmol, 32% yield, 10:1 dr); <sup>1</sup>H NMR (400 MHz, CDCl<sub>3</sub>)  $\delta$  7.75 (t,  $J$  = 1.8 Hz, 1H), 7.63 (ddd,  $J$  = 7.9, 1.8, 1.0 Hz, 1H), 7.56 – 7.38 (m, 2H), 7.32 (d,  $J$  = 1.5 Hz, 1H), 7.05 (t,  $J$  = 7.8 Hz, 1H), 7.01 – 6.78 (m, 2H), 5.79 (dddd,  $J$  = 16.8, 10.1, 8.2, 6.5 Hz, 1H), 5.24 – 5.03 (m, 2H), 4.18 (s, 1H), 3.81 (s, 3H), 3.57 – 3.46 (m, 1H), 3.32 – 3.21 (m, 1H), 2.61 – 2.43 (m, 2H), 2.17 (ddt,  $J$  = 13.5, 8.3, 1.0 Hz, 1H), 1.77 (td,  $J$  = 8.7, 4.4 Hz, 1H); <sup>13</sup>C NMR (101 MHz, CDCl<sub>3</sub>)  $\delta$  175.72, 157.01, 144.81, 136.88, 133.46, 132.36, 130.10, 127.44, 122.40, 119.22, 114.21, 94.47, 59.99, 55.64, 54.07, 46.69, 41.33, 23.91; IR (Neat Film, NaCl) 2932, 1681, 1563, 1512, 1429, 1403, 1296, 1248, 1180, 1100, 1035, 922, 832, 791, 701 cm<sup>-1</sup>; (MM:ESI<sup>+</sup>) C<sub>21</sub>H<sub>24</sub>IN<sub>2</sub>O<sub>2</sub>  $m/z$  calc'd for [M+H]<sup>+</sup>: 463.0883, found 463.0892.



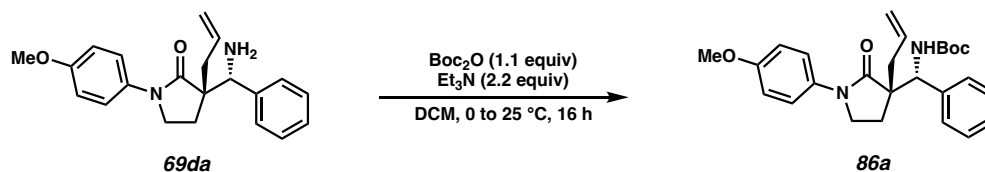
**(*S*<sup>\*</sup>)-3-allyl-3-((*R*<sup>\*</sup>)-amino(4-iodophenyl)methyl)-1-(4-methoxyphenyl)pyrrolidin-2-**

**one (69dq):** Compound **69dq** was prepared from 4-iodobenzonitrile **74q** using General Procedure 7. The crude oil was purified from column chromatography (3% MeOH in EtOAc, 1% TEA) to afford Mannich product **69dq** as a pale-yellow oil (65 mg, 0.14 mmol, 70% yield, 9:1 dr);  $^1\text{H}$  NMR (400 MHz,  $\text{CDCl}_3$ )  $\delta$  7.72 – 7.54 (m, 2H), 7.53 – 7.39 (m, 2H), 7.16 – 7.07 (m, 2H), 6.97 – 6.85 (m, 2H), 5.77 (dddd,  $J = 16.7, 10.1, 8.3, 6.5$  Hz, 1H), 5.17 – 5.06 (m, 2H), 4.24 (s, 1H), 3.81 (s, 3H), 3.52 (ddd,  $J = 9.4, 8.7, 6.7$  Hz, 1H), 3.32 (dt,  $J = 9.5, 4.7$  Hz, 1H), 2.57 – 2.46 (m, 2H), 2.43 – 2.17 (br,  $\text{NH}_2$ , 2H), 2.13 (ddt,  $J = 13.5, 8.3, 0.9$  Hz, 1H), 1.73 (ddd,  $J = 12.9, 8.7, 4.1$  Hz, 1H);  $^{13}\text{C}$  NMR (101 MHz,  $\text{CDCl}_3$ )  $\delta$  175.77, 157.01, 141.68, 137.47, 133.39, 132.37, 130.05, 122.32, 119.25, 114.21, 93.30, 59.90, 55.64, 54.06, 46.71, 41.38, 23.68; IR (Neat Film, NaCl) 2923, 1681, 1511, 1484, 1403, 1295, 1249, 1180, 1035, 1005, 921, 823  $\text{cm}^{-1}$ ; (MM:ESI<sup>+</sup>)  $\text{C}_{21}\text{H}_{24}\text{IN}_2\text{O}_2$   $m/z$  calc'd for  $[\text{M}+\text{H}]^+$ : 463.0883, found 463.0876.

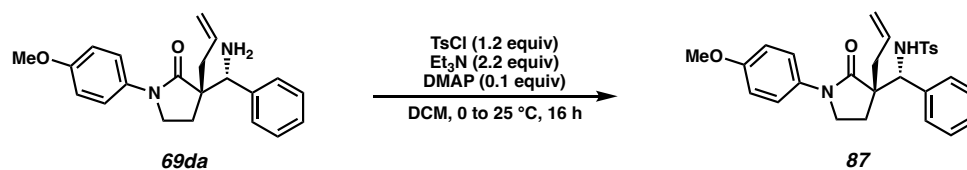


**(*S*\*)-3-allyl-3-((*R*\*)-amino(4-iodophenyl)methyl)-1-(4-methoxyphenyl)pyrrolidin-2-one (**69jc**):** Compound **69jc** was prepared from 2-trifluoromethylbenzonitrile **74c** using General Procedure 7. The crude oil was purified from column chromatography (3% MeOH in EtOAc, 1% TEA) to afford Mannich product **69jc** as a pale-yellow oil (39 mg, 0.10 mmol, 52% yield, 20:1 dr);  $^1\text{H NMR}$  (300 MHz,  $\text{CDCl}_3$ )  $\delta$  7.73 – 7.65 (m, 1H), 7.58 – 7.51 (m, 1H), 7.48 (dd,  $J = 7.7, 1.6$  Hz, 1H), 7.41 (q,  $J = 7.2$  Hz, 1H), 7.15 – 7.06 (m, 2H), 7.00 – 6.89 (m, 2H), 4.43 (s, 1H), 3.83 (d,  $J = 0.4$  Hz, 3H), 3.17 (dt,  $J = 8.0, 6.3$  Hz, 1H), 2.58 (dd,  $J = 13.5, 8.1$  Hz, 1H), 1.97 (br,  $\text{NH}_2$ , 2H), 1.52 – 1.46 (m, 4H), 1.01 (d,  $J = 6.3$  Hz, 3H); IR (Neat Film, NaCl) 2968, 1681, 1607, 1513, 1462, 1453, 1394, 1310, 1249, 1158  $\text{cm}^{-1}$ ; (MM:ESI $^+$ )  $\text{C}_{21}\text{H}_{25}\text{F}_3\text{N}_2\text{O}_2$   $m/z$  calc'd for  $[\text{M}+\text{H}]^+$ : 393.1795, found 393.1791.



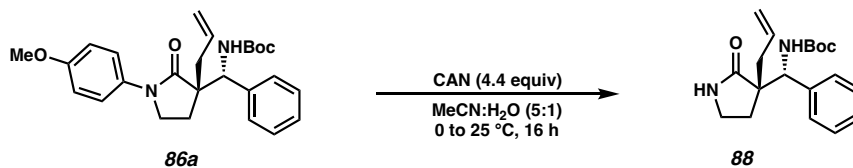
**Product Derivatizations: N-Protection Followed by Lactam N-PMP Deprotection.****tert-butyl-((*R*\*)-((*S*\*)-3-allyl-1-(4-methoxyphenyl)-2-oxopyrrolidin-3-**

**yl)(phenyl)methyl)carbamate (86a):** Allyl Mannich product **69da** (23 mg, 0.067 mmol, 1.0 equiv) was dissolved in DCM (2 mL) and cooled to 0 °C. Boc<sub>2</sub>O (15 mg, 0.074 mmol, 1.1 equiv) was added to the reaction mixture followed by TEA (21 μL, 0.147 mmol, 2.2 equiv) and stirred at 0 °C for 1 h. The reaction mixture was allowed to warm to 25 °C over the next 15 h. The reaction mixture was diluted with DCM (10 mL) and washed with NH<sub>4</sub>Cl (10 mL). The organic layer was separated, and the aqueous layer was extracted with DCM (3 x 10 mL). The organic layers were combined, washed with NaHCO<sub>3</sub> (10 mL), dried over Na<sub>2</sub>SO<sub>4</sub> and concentrated by rotary evaporation. The crude oil was purified by column chromatography (50% EtOAc in Hexanes, 1% TEA) to afford carbamate product **86a** as a pale-yellow oil (28 mg, 0.64 mmol, 96% yield); <sup>1</sup>H NMR (400 MHz, CDCl<sub>3</sub>) δ 7.31 – 7.17 (m, 7H), 6.97 – 6.83 (m, 2H), 6.81 (d, *J* = 8.7 Hz, 1H), 5.91 – 5.79 (m, 1H), 5.32 – 5.18 (m, 2H), 4.65 (d, *J* = 8.9 Hz, 1H), 3.80 (s, 3H), 3.20 (td, *J* = 9.3, 2.9 Hz, 1H), 2.66 (dd, *J* = 7.6, 3.5 Hz, 2H), 2.25 (q, *J* = 8.5 Hz, 1H), 2.13 (ddd, *J* = 13.5, 9.4, 7.9 Hz, 1H), 1.91 (ddd, *J* = 13.4, 8.3, 2.9 Hz, 1H), 1.38 (s, 9H); <sup>13</sup>C NMR (101 MHz, CDCl<sub>3</sub>) δ 175.58, 157.15, 155.40, 140.03, 133.15, 131.82, 128.45, 127.96, 127.88, 122.42, 119.92, 114.12, 79.29, 59.63, 55.61, 51.34, 46.22, 40.61, 28.53, 26.25; IR (Neat Film, NaCl) 3392, 2978, 1712, 1670, 1512, 1456, 1366, 1295, 1249, 1169, 1036, 831, 702 cm<sup>-1</sup>; (MM:ESI<sup>+</sup>) : C<sub>26</sub>H<sub>33</sub>N<sub>2</sub>O<sub>4</sub> *m/z* calc'd for [M+H]<sup>+</sup>: 437.2440, found 437.2453.



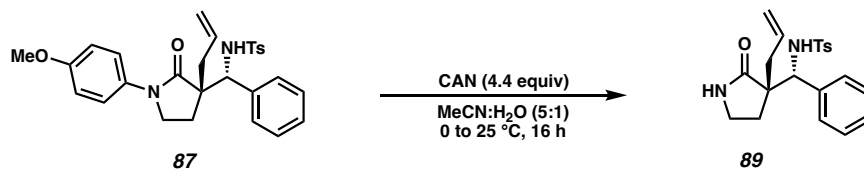
***N*-((*R*<sup>\*</sup>)-((*S*<sup>\*</sup>)-3-allyl-1-(4-methoxyphenyl)-2-oxopyrrolidin-3-yl)(phenyl)methyl)-4-methylbenzenesulfonamide (**87**):** Allyl Mannich product **69da** (23 mg, 0.067 mmol, 1.0 equiv) was dissolved in DCM (2 mL) and cooled to 0 °C. TEA (21  $\mu$ L, 0.147 mmol, 2.2 equiv) was added to the reaction mixture followed by DMAP (0.7 mg, 0.006 mmol, 0.1 equiv) and TsCl (15 mg, 0.08 mmol, 1.2 equivs) and then stirred at 0 °C for 1 h. The reaction mixture was allowed to warm to 25 °C over the next 15 h. The reaction mixture was diluted with DCM (10 mL) and washed with NH<sub>4</sub>Cl (10 mL). The organic layer was separated, and the aqueous layer was extracted with DCM (3 x 10 mL). The organic layers were combined, washed with NaHCO<sub>3</sub> (10 mL), dried over Na<sub>2</sub>SO<sub>4</sub> and concentrated by rotary evaporation. The crude oil was purified by column chromatography (60% EtOAc in Hexanes, 1% TEA) to afford *N*-tosylated product **87** as a pale-yellow oil (32 mg, 0.63 mmol, 95% yield); <sup>1</sup>H NMR (400 MHz, CDCl<sub>3</sub>)  $\delta$  7.30 – 7.24 (m, 2H), 7.18 – 7.13 (m, 2H), 7.10 (ddt, *J* = 7.7, 6.6, 1.6 Hz, 1H), 7.02 – 6.93 (m, 4H), 6.91 – 6.84 (m, 3H), 6.86 – 6.81 (m, 2H), 5.97 – 5.82 (m, 1H), 5.35 – 5.20 (m, 2H), 4.52 (d, *J* = 8.9 Hz, 1H), 3.78 (s, 3H), 3.23 (td, *J* = 9.4, 3.8 Hz, 1H), 2.74 (ddd, *J* = 6.9, 3.6, 2.4 Hz, 2H), 2.40 – 2.32 (m, 1H), 2.24 (s, 3H), 2.10 (ddd, *J* = 13.5, 9.3, 6.9 Hz, 1H), 1.81 (ddd, *J* = 13.5, 8.7, 3.8 Hz, 1H); <sup>13</sup>C NMR (101 MHz, CDCl<sub>3</sub>)  $\delta$  175.42, 157.31, 142.24, 138.49, 137.10, 132.51, 131.51, 128.93, 128.23, 128.21, 127.79, 126.75, 122.54, 120.40, 114.17, 62.29, 55.61, 51.51, 46.35, 40.28, 25.80, 21.44; IR (Neat Film, NaCl) 3386, 2923, 1667, 1513, 1404,

1323, 1301, 1249, 1160, 1090, 831, 702, 667  $\text{cm}^{-1}$ ; (MM:ESI<sup>+</sup>) : C<sub>28</sub>H<sub>31</sub>N<sub>2</sub>O<sub>4</sub>S  $m/z$  calc'd for [M+H]<sup>+</sup>: 491.2005, found 491.1993.



***tert*-butyl ((*R*<sup>\*</sup>)-((*S*<sup>\*</sup>)-3-allyl-2-oxopyrrolidin-3-yl)(phenyl)methyl)carbamate (**88**):** *N*-

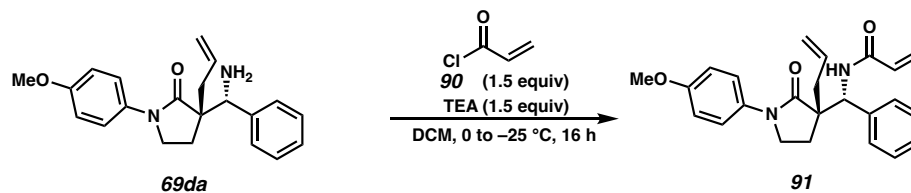
Boc protected allyl Mannich product **86a** (20 mg, 0.04 mmol, 1.0 equiv) was dissolved in a 5:1 mixture of MeCN:H<sub>2</sub>O (3.5 mL) and cooled to 0 °C. CAN (88 mg, 0.18 mmol, 4.5 equiv) was added to the reaction mixture and stirred at 0 °C for 1 h and allowed to warm to 25 °C overnight. The reaction mixture was diluted with EtOAc (10 mL) and washed with sat'd NaHCO<sub>3</sub> (10 mL) and brine (10 mL). The aqueous layers were combined and extracted with EtOAc (3 x 10 mL). The organic layers were combined, dried with Na<sub>2</sub>SO<sub>4</sub>, concentrated by rotary evaporator, and purified via column chromatography (80% EtOAc in hexanes) to afford *N*-H lactam product **88** as an orange-yellow crystal (11 mg, 0.033 mmol, 83% yield); <sup>1</sup>H NMR (400 MHz, CDCl<sub>3</sub>)  $\delta$  7.34 – 7.20 (m, 5H), 6.78 (d, *J* = 9.0 Hz, 1H), 5.93 – 5.72 (m, 1H), 5.50 (s, 1H), 5.25 – 5.16 (m, 2H), 4.62 (d, *J* = 9.0 Hz, 1H), 3.47 – 3.23 (m, 1H), 2.92 (td, *J* = 8.6, 3.5 Hz, 1H), 2.64 – 2.45 (m, 2H), 2.18 – 1.99 (m, 1H), 1.98 – 1.88 (m, 1H), 1.39 (s, 9H); <sup>13</sup>C NMR (101 MHz, CDCl<sub>3</sub>)  $\delta$  180.06, 155.40, 140.00, 133.08, 128.44, 128.11, 127.78, 119.83, 79.35, 59.13, 49.24, 40.03, 39.18, 28.71, 28.55; IR (Neat Film, NaCl) 3264, 2924, 1694, 1494, 1363, 1325, 1248, 1172, 1161, 918, 778, 703  $\text{cm}^{-1}$ ; (MM:ESI<sup>+</sup>) : C<sub>19</sub>H<sub>27</sub>N<sub>2</sub>O<sub>3</sub>  $m/z$  calc'd for [M+H]<sup>+</sup>: 331.2022, found 331.2015.



***N*-((*R*<sup>\*</sup>)-((*S*<sup>\*</sup>)-3-allyl-2-oxopyrrolidin-3-yl)(phenyl)methyl)-4-**

**methylbenzenesulfonamide (89):** *N*-Ts protected allyl Mannich product **87** (20 mg, 0.04 mmol, 1.0 equiv) was dissolved in a 5:1 mixture of MeCN:H<sub>2</sub>O (3.5 mL) and cooled to 0 °C. CAN (88 mg, 0.18 mmol, 4.5 equiv) was added to the reaction mixture and stirred at 0 °C for 1 h and allowed to warm to 25 °C overnight. The reaction mixture was diluted with EtOAc (10 mL) and washed with sat'd NaHCO<sub>3</sub> (10 mL) and brine (10 mL). The aqueous layers were combined and extracted with EtOAc (3 x 10mL). The organic layers were combined, dried with Na<sub>2</sub>SO<sub>4</sub>, concentrated by rotary evaporator, and purified via column chromatography (85% EtOAc in hexanes) to afford *N*-H lactam product **89** as an orange-yellow amorphous solid (13 mg, 0.034 mmol, 84% yield); <sup>1</sup>H NMR (400 MHz, CDCl<sub>3</sub>)  $\delta$  7.34 – 7.27 (m, 5H), 7.05 – 6.98 (m, 4H), 6.90 (d, *J* = 8.0 Hz, 1H), 5.94 – 5.80 (m, 1H), 5.64 (s, 1H), 5.28 – 5.20 (m, 2H), 4.46 (s, 1H), 2.96 (td, *J* = 9.0, 4.9 Hz, 1H), 2.71 – 2.57 (m, 2H), 2.26 (s, 3H), 2.17 (td, *J* = 9.1, 5.6 Hz, 1H), 2.11 – 2.01 (m, H), 1.80 (ddd, *J* = 13.6, 8.8, 4.9 Hz, 1H); <sup>13</sup>C NMR (101 MHz, CDCl<sub>3</sub>)  $\delta$  179.89, 142.26, 138.41, 137.16, 132.50, 128.94, 128.28, 128.24, 127.67, 126.78, 120.29, 61.93, 49.50, 39.65, 39.27, 28.09, 21.45; IR (Neat Film, NaCl) 3265, 2923, 2853, 1682, 1513, 1456, 1326, 1249, 1160, 1089, 924, 801, 723, 703 cm<sup>-1</sup>; (MM:ESI<sup>+</sup>) : C<sub>21</sub>H<sub>25</sub>N<sub>2</sub>O<sub>3</sub>S *m/z* calc'd for [M+H]<sup>+</sup>:385.1586, found 385.1562.

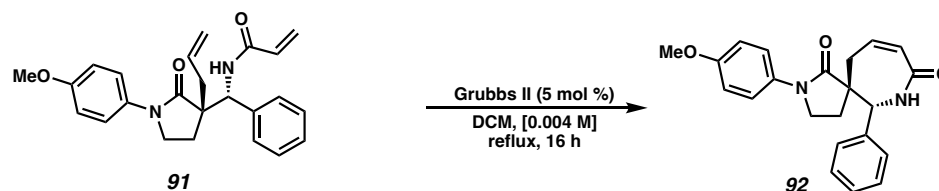
**Product Derivatizations: Acrylamide Formation Followed by Ring Closing Metathesis**



***N*-((*R*<sup>\*</sup>)-((*S*<sup>\*</sup>)-3-allyl-1-(4-methoxyphenyl)-2-oxopyrrolidin-3-**

**yl)(phenyl)methyl)acrylamide (91):** Allyl Mannich product **69da** (27 mg, 0.08 mmol, 1.0 equiv) was dissolved in DCM (5 mL) and cooled to 0 °C. TEA (21  $\mu\text{L}$ , 0.15 mmol, 2.0 equiv) and acryloyl chloride **90** (10  $\mu\text{L}$ , 0.11 mmol, 1.4 equiv) were added sequentially to the reaction mixture and stirred at 0 °C for 1 h and allowed to warm to 25 °C overnight. The reaction was diluted with DCM (10 mL) and washed with sat'd  $\text{NaHCO}_3$  (10 mL). The layers were separated, and the aqueous layer was extracted with EtOAc (3 x 10 mL). The organic layers were combined, dried over  $\text{Na}_2\text{SO}_4$ , concentrated by rotary evaporator and purified via column chromatography (60% EtOAc in hexanes) to afford acrylamide product **91** as a yellow oil (28 mg, 0.072 mmol, 90% yield);  $^1\text{H}$  NMR (400 MHz,  $\text{CDCl}_3$ )  $\delta$  8.01 (d,  $J = 8.5$  Hz, 1H), 7.27 – 7.20 (m, 2H), 7.20 – 7.16 (m, 3H), 7.17 – 7.11 (m, 2H), 6.90 – 6.73 (m, 2H), 6.18 (dd,  $J = 17.1, 1.9$  Hz, 1H), 6.13 – 6.01 (m, 1H), 5.77 (dddd,  $J = 16.2, 10.8, 8.2, 6.6$  Hz, 1H), 5.55 (dd,  $J = 9.8, 1.9$  Hz, 1H), 5.20 – 5.07 (m, 2H), 5.00 (d,  $J = 8.6$  Hz, 1H), 3.73 (s, 3H), 3.18 (td,  $J = 9.5, 3.4$  Hz, 1H), 2.66 – 2.56 (m, 1H), 2.52 (ddt,  $J = 13.8, 8.2, 1.0$  Hz, 1H), 2.33 (ddd,  $J = 9.5, 8.7, 7.4$  Hz, 1H), 2.07 (ddd,  $J = 13.4, 9.4, 7.4$  Hz, 1H), 1.86 (ddd,  $J = 13.5, 8.6, 3.4$  Hz, 1H);  $^{13}\text{C}$  NMR (101 MHz,  $\text{CDCl}_3$ )  $\delta$  176.03, 164.75, 157.42, 139.30, 132.74, 131.55, 131.19, 128.61, 128.13, 126.50, 122.72, 120.24, 114.26, 58.14, 55.63, 51.07, 46.58, 40.73, 29.85, 25.99; IR (Neat Film, NaCl) 3350, 2922, 1674,

1634, 1513, 1404, 1298, 1249, 1182, 1034, 922, 830, 800, 704  $\text{cm}^{-1}$ ; (MM:ESI<sup>+</sup>) :  $\text{C}_{24}\text{H}_{27}\text{N}_2\text{O}_3$   $m/z$  calc'd for  $[\text{M}+\text{H}]^+$  391.2022, found 391.2037.

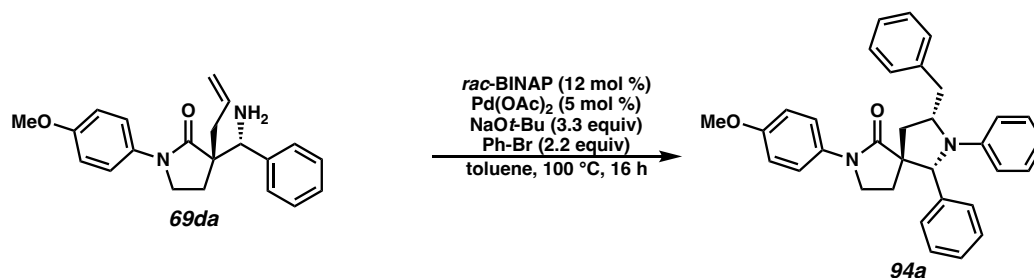


**(5*S*\*,6*R*\*)-2-(4-methoxyphenyl)-6-phenyl-2,7-diazaspiro[4.6]undec-9-ene-1,8-dione**

**(92):** Acrylamide product **91** (15 mg, 0.04 mmol, 1.0 equiv) was dissolved in DCM (8 mL). The resulting solution was sparged with argon for 10 minutes. The Grubbs' second generation catalyst (2 mg, 0.002 mmol, 5 mol %) was added to the reaction mixture under a positive pressure of argon. The reaction was bubbled with argon for 5 minutes and heated to 40 °C for 16 h. The crude reaction mixture was concentrated by rotary evaporation and purified directly via column chromatography (90% EtOAc in hexanes with 1% Et<sub>3</sub>N) in order to afford  $\epsilon$ -lactam **92** as a brown amorphous solid (11 mg, 0.03 mmol, 75% yield); <sup>1</sup>H NMR (400 MHz, CDCl<sub>3</sub>)  $\delta$  7.41 – 7.35 (m, 2H), 7.34 – 7.28 (m, 3H), 7.17 – 7.10 (m, 2H), 6.84 – 6.75 (m, 2H), 6.57 (ddd,  $J$  = 11.0, 8.3, 5.8 Hz, 1H), 6.25 – 6.16 (m, 2H), 4.48 (d,  $J$  = 5.6 Hz, 1H), 3.78 (s, 3H), 3.43 – 3.24 (m, 3H), 2.74 (dt,  $J$  = 9.7, 7.9 Hz, 1H), 2.28 (dd,  $J$  = 14.2, 8.2 Hz, 1H), 2.25 – 2.11 (m, 1H); <sup>13</sup>C NMR (101 MHz, CDCl<sub>3</sub>)  $\delta$  173.52, 170.30, 157.02, 136.78, 136.20, 131.93, 129.16, 129.13, 128.90, 128.29, 122.33, 114.07, 64.64, 58.77, 45.98, 45.36, 36.29, 30.39; IR (Neat Film, NaCl)  $\text{cm}^{-1}$ ; (MM:ESI<sup>+</sup>) :  $\text{C}_{22}\text{H}_{23}\text{N}_2\text{O}_3$   $m/z$  calc'd for  $[\text{M}+\text{H}]^+$  363.1703, found 363.1710.

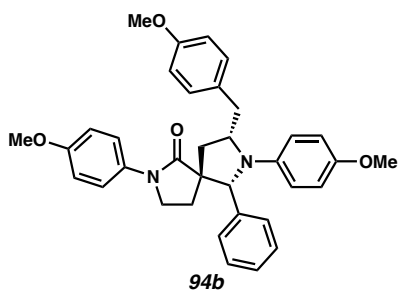
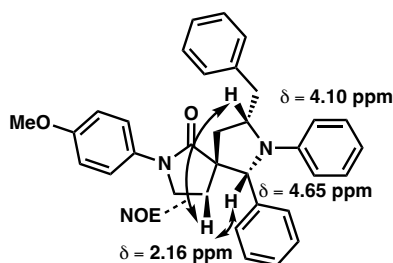
Et<sub>3</sub>N•HCl Present (1:1 ratio)

## Product Derivatizations: C–N Cross-Coupling Reactions



**(5*R*\*,6*R*\*,8*R*\*)-8-benzyl-2-(4-methoxyphenyl)-6,7-diphenyl-2,7-diazaspiro[4.4]nonan-1-one (94a):** Pd(OAc)<sub>2</sub> (0.6 mg, 0.0027 mmol, 5 mol %) and *rac*-BINAP (4 mg, 0.0065 mmol, 12 mol %) were dissolved in toluene (1.0 mL) and stirred for 10 minutes at 25 °C. Meanwhile, allyl Mannich product **69da** (18 mg, 0.054 mmol, 1.0 equiv) was added to a solution of bromobenzene (12  $\mu$ L, 0.12 mmol, 2.2 equiv) and NaO*t*-Bu (17 mg, 0.18 mmol, 3.4 equiv) in toluene (1.0 mL). The metal-ligand complex solution was added to the reaction mixture. The resulting solution was sparged with argon for 5 minutes, then heated to 100 °C for 20 h. The reaction mixture was cooled to 25 °C, diluted with DCM, then filtered through a pad of celite. The celite was washed with copious amounts of toluene, and the resulting filtrate was concentrated via rotary evaporation and purified via column chromatography (50% EtOAc in hexanes) to afford the spirocyclic pyrrolidine product **94a** as a red-orange amorphous solid (24 mg, 0.049 mmol, 82% yield, 7:1 dr); <sup>1</sup>H NMR (400 MHz, CDCl<sub>3</sub>)  $\delta$  7.44 – 7.36 (m, 7H), 7.26 – 7.20 (m, 5H), 7.12 – 7.05 (m, 2H), 7.02 – 6.96 (m, 1H), 6.86 (d, *J* = 9.1 Hz, 2H), 6.75 – 6.70 (m, 2H), 4.66 (s, 1H), 4.12 – 4.05 (m, 1H), 3.96 (td, *J* = 10.2, 6.2 Hz, 1H), 3.80 (s, 3H), 3.79 – 3.77 (m, 1H), 3.75 (qd, *J* = 3.2, 1.7 Hz, 1H), 2.99 (dd, *J* = 13.3, 10.0 Hz, 1H), 2.67 (dd, *J* = 12.9, 9.8 Hz, 1H), 2.17 (dd, *J* = 12.5, 6.1 Hz, 1H), 2.05 – 1.97 (m, 1H), 1.93 (dd, *J* = 13.0, 6.3 Hz, 1H); <sup>13</sup>C NMR (101 MHz, CDCl<sub>3</sub>)  $\delta$  171.87, 156.46, 147.67, 140.78, 138.93, 132.62, 129.32, 129.15, 128.64, 128.50,

127.68, 126.56, 121.45, 117.78, 114.03, 113.85, 75.32, 60.14, 56.43, 55.46, 45.43, 40.52, 39.16, 33.61; IR (Neat Film, NaCl) 2928, 1692, 1602, 1510, 1475, 1445, 1384, 1301, 1249, 1171, 1115, 1033, 909, 827, 741, 730, 701  $\text{cm}^{-1}$ ; (MM:ESI<sup>+</sup>) : C<sub>33</sub>H<sub>33</sub>N<sub>2</sub>O<sub>2</sub>  $m/z$  calc'd for [M+H]<sup>+</sup> 489.2542, found 489.2549.

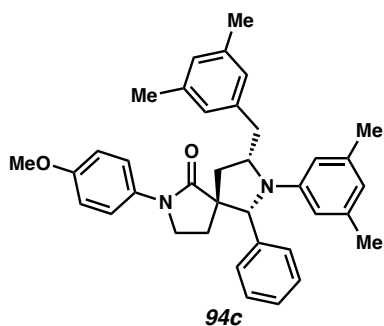


**(5*R*,6*R*,8*S*)-8-(4-methoxybenzyl)-2,7-bis(4-methoxyphenyl)-6-phenyl-2,7-**

**diazaspiro[4.4]nonan-1-one (94b):** Spirocyclic **94b** was synthesized using General Procedure above with 4-bromoanisole (28  $\mu\text{L}$ , 0.22 mmol, 2.2 equiv) and allyl Mannich product **69da** (33.6 mg, 0.1 mmol, 1.0 equiv). The crude oil was isolated via column chromatography (50% EtOAc in hexanes) as a yellow amorphous solid (25 mg, 0.046 mmol, 46% yield, 4:1 dr). Note: the major diastereomer coelutes with the retro-Mannich product **2d** after column chromatography as a 2:1 mixture of **94b**:**68d**: <sup>1</sup>H NMR (400 MHz, CDCl<sub>3</sub>)  $\delta$  7.99 – 7.81 (m, 2H), 7.61 – 7.57 (m, 2H), 7.50 – 7.47 (m, 2H), 7.42 – 7.37 (m, 3H), 7.32 (ddd,  $J = 8.7, 5.7, 2.6$  Hz, 2H), 7.23 (d,  $J = 8.7$  Hz, 2H), 6.94 (d,  $J = 9.2$  Hz, 2H), 6.88 (d,  $J = 6.8$  Hz, 2H), 4.66 (s, 1H)\*, 3.91 – 3.86 (m, 2H), 3.84 (m, 6H), 3.82 (s, 3H),

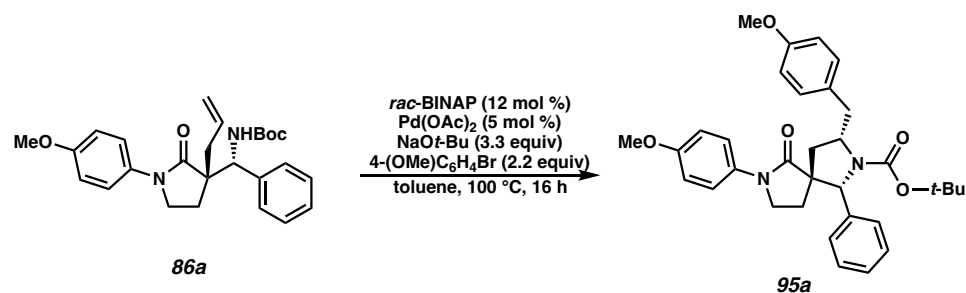


3.80 – 3.75 (m, 2H), 3.44 (d,  $J = 16.2$  Hz, 1H), 2.85 (d,  $J = 16.2$  Hz, 1H), 2.65 – 2.58 (m, 1H), 2.16 (ddd,  $J = 13.3, 6.7, 3.2$  Hz, 1H), 2.05 – 1.93 (m, 1H);  $^{13}\text{C}$  NMR (101 MHz,  $\text{CDCl}_3$ )  $\delta$  **175.10**, 174.58, 173.60, 158.76, **158.73**, 158.47, 157.00, 156.64, 149.66, **135.62**, 134.57, 133.40, **132.92**, 132.84, 132.56, 132.48, 132.34, 131.33, 130.68, 130.39, 129.26, 128.81, 128.65, 128.61, 126.70, **121.72**, 121.63, 121.57, **117.20**, 114.33, **114.15**, 113.79, 113.01, 60.98, 55.67, **55.62**, 55.58, 55.44, 55.40, **47.30**, 46.47, 44.06, **42.85**, **35.63**, 30.38, **24.12**; IR (Neat Film, NaCl) 2928, 1692, 1602, 1510, 1475, 1445, 1384, 1301, 1249, 1171, 1115, 1033, 909, 827, 741, 730, 701  $\text{cm}^{-1}$ ; (MM:ESI $^+$ ):  $\text{C}_{35}\text{H}_{37}\text{N}_2\text{O}_4$   $m/z$  calc'd for  $[\text{M}+\text{H}]^+$  549.2748, found 549.2749. (Bold is compound **68d**)



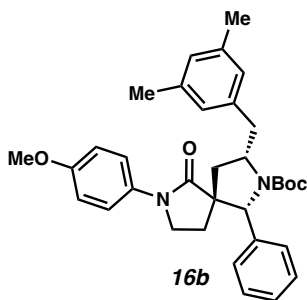
**(5R,6R,8S)-8-(3,5-dimethylbenzyl)-7-(3,5-dimethylphenyl)-2-(4-methoxyphenyl)-6-phenyl-2,7-diazaspiro[4.4]nonan-1-one (94c)**: Spirocycle **94c** was synthesized using General Procedure above with 3,5-dimethyl bromobenzene (30  $\mu\text{L}$ , 0.22 mmol, 2.2 equiv) and allyl Mannich product **69da** (33.6 mg, 0.1 mmol, 1.0 equiv). The crude oil was isolated via column chromatography (50% EtOAc in hexanes) as a yellow amorphous solid (43 mg, 0.079 mmol, 79% yield, 9:1 dr);  $^1\text{H}$  NMR (400 MHz,  $\text{CDCl}_3$ )  $\delta$  7.47 – 7.39 (m, 2H), 7.30 (ddd,  $J = 6.1, 3.2, 1.5$  Hz, 3H), 7.23 (dd,  $J = 7.8, 1.7$  Hz, 2H), 7.02 (s, 2H), 6.93 (s, 1H), 6.87 (d,  $J = 9.2$  Hz, 2H), 6.48 (s, 1H), 6.36 (s, 2H), 4.65 (s, 1H), 4.10 – 4.02 (m, 1H), 3.98

(dt,  $J = 10.1, 5.0$  Hz, 1H), 3.80 (d,  $J = 0.9$  Hz, 3H), 3.79 – 3.74 (m, 1H), 3.67 (dd,  $J = 13.1, 2.6$  Hz, 1H), 2.85 (dd,  $J = 13.1, 10.0$  Hz, 1H), 2.70 – 2.60 (m, 1H), 2.36 (s, 6H), 2.26 (s, 6H), 2.18 – 2.09 (m, 1H), 2.04 – 1.97 (m, 1H), 1.97 – 1.90 (m, 1H);  $^{13}\text{C}$  NMR (101 MHz,  $\text{CDCl}_3$ )  $\delta$  171.96, 156.42, 147.85, 140.95, 139.04, 138.69, 138.12, 132.73, 128.42, 128.14, 127.56, 127.02, 126.58, 121.36, 119.77, 114.03, 111.77, 74.91, 60.11, 56.50, 55.46, 45.42, 40.69, 39.25, 33.46, 21.84, 21.38; IR (Neat Film, NaCl) 2928, 1692, 1602, 1510, 1475, 1445, 1384, 1301, 1249, 1171, 1115, 1033, 909, 827, 741, 730, 701  $\text{cm}^{-1}$ ; (MM:ESI $^+$ ) :  $\text{C}_{37}\text{H}_{41}\text{N}_2\text{O}_2$   $m/z$  calc'd for  $[\text{M}+\text{H}]^+$  545.3163, found 545.3173.



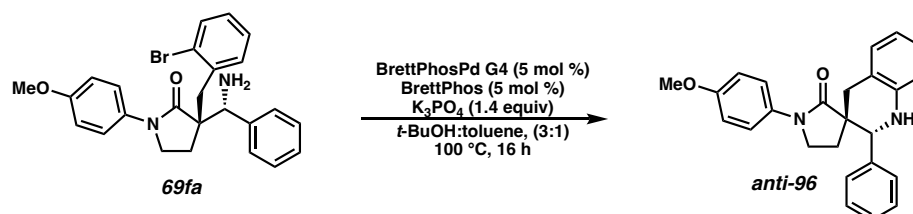
***tert*-butyl (1*R*,3*S*,5*R*)-3-(4-methoxybenzyl)-7-(4-methoxyphenyl)-6-oxo-1-phenyl-2,7-diazaspiro[4.4]nonane-2-carboxylate (95a):**  $\text{Pd(OAc)}_2$  (0.6 mg, 0.0027 mmol, 5 mol %) and *rac*-BINAP (4 mg, 0.0065 mmol, 12 mol %) were dissolved in toluene (1.0 mL) and stirred for 10 minutes at 25 °C. Meanwhile, allyl Mannich product **86a** (23.5 mg, 0.054 mmol, 1.0 equiv) was added to a solution of bromobenzene (12  $\mu\text{L}$ , 0.12 mmol, 2.2 equiv) and  $\text{NaOt-Bu}$  (17 mg, 0.18 mmol, 3.4 equiv) in toluene (1.0 mL). The metal-ligand complex solution was added to the reaction mixture. The resulting solution was sparged with argon for 5 minutes, then heated to 100 °C for 20 h. The reaction mixture was cooled to 25 °C, diluted with DCM, then filtered through a pad of celite. The celite was washed

with copious amounts of toluene, and the resulting filtrate was concentrated via rotary evaporation and purified via column chromatography (50% EtOAc in hexanes) to afford the spirocyclic pyrrolidine product **95a** as a yellow amorphous solid (24.1 mg, 0.044 mmol, 76% yield, 5:1 dr);  $^1\text{H}$  NMR (400 MHz,  $\text{CDCl}_3$ )  $\delta$  7.30 – 7.27 (m, 2H), 7.25 – 7.20 (m, 5H), 7.09 (d,  $J = 7.2$  Hz, 2H), 6.88 – 6.84 (m, 2H), 6.84 – 6.79 (m, 2H), 4.96 (br, 1H), 4.23 – 3.98 (m, 1H), 3.84 (dd,  $J = 6.1, 5.1$  Hz, 1H), 3.81 (s, 3H), 3.78 (s, 3H), 3.75 – 3.69 (m, 2H), 3.11 (br, 1H), 2.49 (dd,  $J = 13.3, 9.1$  Hz, 1H), 2.29 (dd,  $J = 12.5, 6.1$  Hz, 1H), 2.15 – 1.98 (m, 1H), 1.76 (dd,  $J = 13.3, 7.0$  Hz, 1H), 1.55 – 1.13 (br, 9H);  $^{13}\text{C}$  NMR (101 MHz,  $\text{CDCl}_3$ )  $\delta$  171.96, 158.23, 156.62, 155.18, 139.85, 132.37, 130.99, 130.60, 128.04, 127.41, 126.44, 121.92, 114.00, 113.88, 80.20, 70.83, 60.24, 55.61, 55.44, 55.27, 45.65, 38.45, 34.00, 29.72, 28.38; IR (Neat Film, NaCl) 2935, 1693, 1611, 1512, 1454, 1384, 1298, 1248, 1177, 1144, 1111, 1032, 910, 828, 730, 700  $\text{cm}^{-1}$ ; (MM:ESI $^+$ ) :  $\text{C}_{33}\text{H}_{39}\text{N}_2\text{O}_5$   $m/z$  calc'd for  $[\text{M}+\text{H}]^+$  543.2853, found 543.2866.



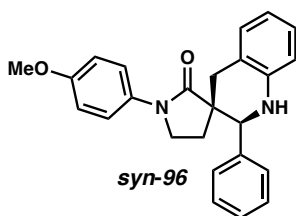
*tert*-butyl (1*R*,3*S*,5*R*)-3-(3,5-dimethylbenzyl)-7-(4-methoxyphenyl)-6-oxo-1-phenyl-2,7-diazaspiro[4.4]nonane-2-carboxylate (**95b**): Spirocyclic **95b** was synthesized using General Procedure above with 3,5-dimethyl bromobenzene (30  $\mu\text{L}$ , 0.22 mmol, 2.2 equiv) and allyl Mannich product **86a** (23.5 mg, 0.054 mmol, 1.0 equiv). The crude oil was

isolated via column chromatography (50% EtOAc in hexanes) as a yellow amorphous solid (25.4 mg, 0.047 mmol, 87% yield, 10:1 dr);  $^1\text{H}$  NMR (400 MHz,  $\text{CDCl}_3$ )  $\delta$  7.27 – 7.19 (m, 5H), 7.11 (d,  $J = 7.2$  Hz, 2H), 6.98 (s, 2H), 6.89 – 6.87 (m, 1H), 6.85 – 6.80 (m, 2H), 4.95 (s, 1H), 4.08 (d,  $J = 13.2$  Hz, 1H), 4.02 – 3.88 (m, 1H), 3.84 – 3.79 (m, 1H), 3.78 (s, 3H), 3.76 – 3.70 (m, 2H), 3.04 (s, 1H), 2.51 (dd,  $J = 13.3, 9.2$  Hz, 1H), 2.30 (s, 6H), 2.11 – 2.01 (m, 1H), 1.78 (dd,  $J = 13.3, 7.0$  Hz, 1H), 1.52 – 1.18 (m, 9H);  $^{13}\text{C}$  NMR (101 MHz,  $\text{CDCl}_3$ )  $\delta$  177.01, 172.04, 156.73, 155.33, 138.93, 138.06, 132.53, 129.85, 128.18, 128.11, 127.54, 126.58, 122.00, 114.13, 80.34, 71.08, 60.26, 55.76, 55.57, 45.76, 38.59, 34.09, 29.71, 28.51, 21.40; IR (Neat Film, NaCl) 2927, 1691, 1604, 1511, 1455, 1381, 1248, 1172, 1142, 1115, 1033, 909, 828, 730, 697  $\text{cm}^{-1}$ ; (MM:ESI $^+$ ) :  $\text{C}_{34}\text{H}_{41}\text{N}_2\text{O}_4$   $m/z$  calc'd for  $[\text{M}+\text{H}]^+$  541.3061, found 541.3072.



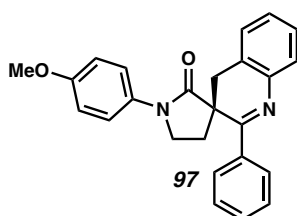
**(2' $R^*$ ,3 $S^*$ )-1-(4-methoxyphenyl)-2'-phenyl-1',4'-dihydro-2' $H$ -spiro[pyrrolidine-3,3'-quinolin]-2-one (96):** BrettPhos Pd G4 (2.5 mg, 0.0025 mmol, 5 mol %) was added to a flame dried vial charged with BrettPhos (1.5 mg, 0.0025 mmol, 5 mol %) and  $\text{K}_3\text{PO}_4$  (15 mg, 0.07 mmol, 1.4 equiv). The *ortho*-Br benzyl Mannich product **69fa** (23 mg, 0.05 mmol, 1.0 equiv, 5:1 dr) was dissolved in a mixture of *t*-BuOH:toluene (0.6 mL:0.2 mL) and added to the reaction mixture. The reaction was then heated to 100  $^\circ\text{C}$  for 16 h. After the stirring period, the reaction was then cooled to 25  $^\circ\text{C}$ , diluted with DCM and filtered through a pad

of celite. The celite pad was washed with copious amounts of DCM. The filtrate was concentrated via rotary evaporation and purified via column chromatography (50% EtOAc in hexanes) to afford spirocyclic tetrahydroquinoline **96** as a pale-yellow solid (15.5 mg, 0.04 mmol, 80% yield, 4:1 dr); Note: The major diastereomer was observed to be unstable to silica gel chromatography or when dissolved in  $\text{CDCl}_3$ , as there was an identified product **97** assigned as the dihydroquinoline observed arising from the NMR sample of the *trans* diastereomer;  $^1\text{H}$  NMR (400 MHz,  $\text{CDCl}_3$ )  $\delta$  7.40 – 7.35 (m, 2H), 7.35 – 7.30 (m, 3H), 7.28 – 7.23 (m, 2H), 7.11 – 7.06 (m, 2H), 6.85 – 6.81 (m, 2H), 6.74 (td,  $J = 7.4, 1.2$  Hz, 1H), 6.66 – 6.62 (m, 1H), 4.36 (s, 1H), 3.84 (s, 1H), 3.79 (s, 3H), 3.39 (td,  $J = 9.4, 1.7$  Hz, 1H), 3.18 (d,  $J = 16.7$  Hz, 1H), 2.92 (d,  $J = 16.6$  Hz, 1H), 2.73 (td,  $J = 9.5, 7.4$  Hz, 1H), 2.22 (ddd,  $J = 13.3, 7.3, 1.8$  Hz, 1H), 2.11 – 1.99 (m, 1H);  $^{13}\text{C}$  NMR (101 MHz,  $\text{CDCl}_3$ )  $\delta$  173.56, 156.38, 143.70, 140.25, 132.82, 129.39, 128.60, 128.51, 128.08, 127.10, 121.35, 117.94, 113.89, 62.61, 55.56, 46.43, 45.00, 36.43, 30.94.



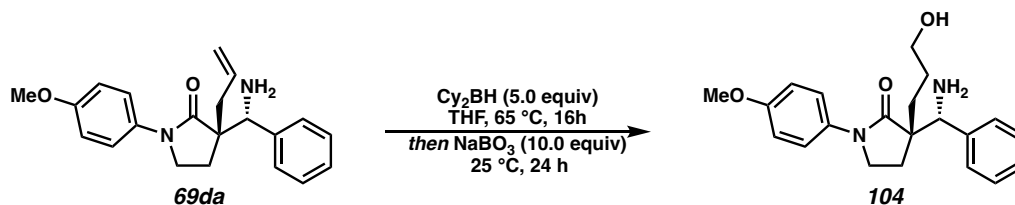
**(2'*S*,3*S*)-1-(4-methoxyphenyl)-2'-phenyl-1',4'-dihydro-2'*H*-spiro[pyrrolidine-3,3'-quinolin]-2-one (syn-96)**:  $^1\text{H}$  NMR (400 MHz,  $\text{CDCl}_3$ )  $\delta$  7.60 – 7.53 (m, 2H), 7.35 – 7.27 (m, 3H), 7.20 – 7.12 (m, 2H), 7.08 (dd,  $J = 7.4, 0.9$  Hz, 2H), 6.85 – 6.79 (m, 2H), 6.72 (td,  $J = 7.4, 1.2$  Hz, 1H), 6.65 (d,  $J = 1.2$  Hz, 1H), 4.77 (s, 1H), 4.18 (s, 1H), 3.78 (s, 3H), 3.66 (dd,  $J = 16.6, 8.5$  Hz, 1H), 3.35 (td,  $J = 9.6, 3.0$  Hz, 1H), 2.66 (d,  $J = 16.1$  Hz, 1H), 2.63 – 2.57 (m, 1H), 2.43 (ddd,  $J = 13.5, 8.6, 3.0$  Hz, 1H), 1.79 (ddd,  $J = 13.6, 9.7, 7.7$  Hz, 1H);

$^{13}\text{C}$  NMR (101 MHz,  $\text{CDCl}_3$ )  $\delta$  175.10, 156.90, 143.71, 139.32, 132.30, 129.94, 128.55, 128.49, 127.51, 127.32, 122.57, 117.88, 114.04, 114.01, 59.43, 55.57, 48.29, 46.35, 38.73, 24.70. IR (Neat Film, NaCl) 2931, 1690, 1587, 1559, 1512, 1454, 1427, 1399, 1297, 1250, 1181, 1120, 1084, 1033, 909, 829, 768, 730, 692  $\text{cm}^{-1}$ ; (MM:ESI $^+$ ) :  $\text{C}_{25}\text{H}_{25}\text{N}_2\text{O}_2$   $m/z$  calc'd for  $[\text{M}+\text{H}]^+$  385.1911, found 385.1906.



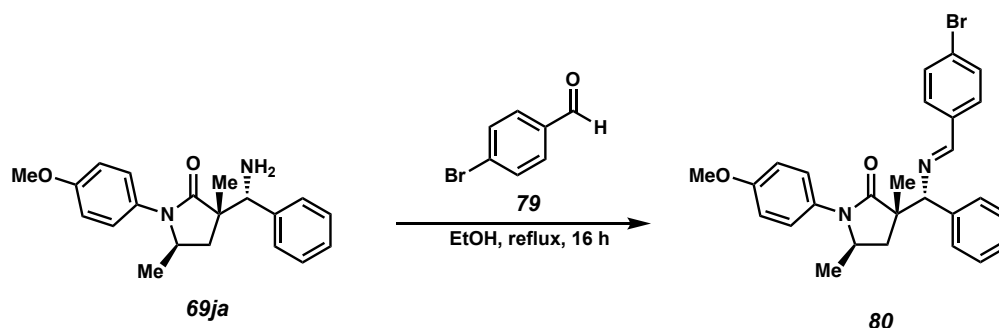
**(S)-1-(4-methoxyphenyl)-2'-phenyl-4'H-spiro[pyrrolidine-3,3'-quinolin]-2-one (18):**

$^{13}\text{C}$  NMR (101 MHz,  $\text{CDCl}_3$ )  $\delta$  174.96, 157.21, 153.58, 146.38, 145.78, 132.17, 128.63, 128.52, 128.27, 128.08, 127.81, 122.11, 119.84, 114.33, 113.95, 55.65, 45.83, 34.53, 30.95, 28.41; (MM:ESI $^+$ ) :  $\text{C}_{25}\text{H}_{23}\text{N}_2\text{O}_2$   $m/z$  calc'd for  $[\text{M}+\text{H}]^+$  383.1754, found 383.1763.



$^1\text{H}$  NMR (400 MHz,  $\text{CD}_3\text{CN}$ )  $\delta$  7.50 – 7.41 (m, 1H), 7.41 – 7.13 (m, 8H), 6.97 – 6.87 (m, 1H), 4.18 (s, 1H), 3.78 (s, 2H), 3.73 – 3.64 (m, 0H), 3.53 (td,  $J = 9.2, 5.8$  Hz, 0H), 3.47 – 3.37 (m, 1H), 3.10 (td,  $J = 9.5, 5.0$  Hz, 0H), 2.48 – 2.39 (m, 0H), 1.77 (tdd,  $J = 13.0, 6.4, 3.2$  Hz, 1H), 1.27 – 1.11 (m, 1H);  $^{13}\text{C}$  NMR (101 MHz,  $\text{CDCl}_3$ )  $\delta$  181.58, 162.05, 137.99,

133.38, 133.25, 132.79, 127.62, 119.11, 67.10, 60.37, 51.56, 40.68, 38.19, 32.56, 30.73, 29.58; IR (Neat Film, NaCl) 3350, 2922, 1674, 1634, 1513, 1404, 1298, 1249, 1182, 1034, 922, 830, 800, 704  $\text{cm}^{-1}$ ; (MM:ESI<sup>+</sup>) :  $\text{C}_{21}\text{H}_{27}\text{N}_2\text{O}_3$   $m/z$  calc'd for  $[\text{M}+\text{H}]^+$  355.2017, found 355.2027.

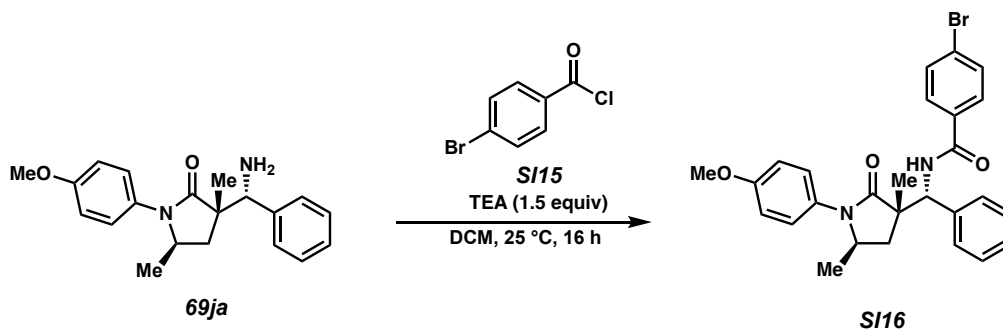


**(3*S*,5*R*)-3-((*R*)-((*E*)-4-bromobenzylidene)amino)(phenyl)methyl)-1-(4-**

**methoxyphenyl)-3,5-dimethylpyrrolidin-2-one (80):** Dimethyl Mannich product **69ja**

(35 mg, 0.108 mmol, 1.0 equiv) was dissolved in ethanol. *Para*-bromo benzaldehyde **79** (20 mg, 0.108 mmol, 1.0 equiv) was added to the reaction mixture and the solution was heated to reflux for 16 hours. The reaction was cooled to ambient temperatures and concentrated via rotary evaporator. The crude reaction mixture was then purified via column chromatography (40% EtOAc in hexanes) to afford the *p*-Br imine product **80** (48.7 mg, 0.99 mmol, 92% yield) as a yellow crystalline solid. The diastereomeric mixture could not be separated. Crystals suitable for X-ray diffraction were obtained via a vapor diffusion of DCM/hexanes to afford clear crystals. CCDC 2253013. <sup>1</sup>H NMR (400 MHz,  $\text{CDCl}_3$ )  $\delta$  8.39 (s, 0.29H), 8.20 (s, 0.71H), 7.70 – 7.65 (m, 0.58H), 7.65 – 7.59 (m, 1.52H), 7.58 – 7.49 (m, 4H)\*, 7.42 – 7.34 (m, 2H), 7.34 (s, 1H), 7.01 – 6.94 (m, 0.58H), 6.86 – 6.80 (m, 2H), 6.76 – 6.69 (m, 1.52H), 4.71 (s, 0.29H), 4.62 (s, 0.71H), 4.25 – 4.15 (m, 0.71H), 4.15 – 4.05 (m, 0.29H), 3.77 (s, 0.87H), 3.75 (s, 2.12H), 3.20 (dd,  $J = 13.3, 7.6$  Hz, 0.71H), 2.81

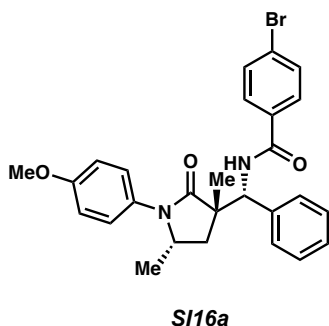
(dd,  $J = 12.6, 8.2$  Hz, 0.29H), 1.88 (dd,  $J = 12.6, 7.3$  Hz, 0.29H), 1.32 – 1.25 (m, 0.71H)\*, 1.24 (s, 2.21H), 1.19 (d,  $J = 6.1$  Hz, 0.88H), 1.16 (s, 0.88H), 1.09 (d,  $J = 6.3$  Hz, 2.21H). (2.5:1 dr);  $^{13}\text{C}$  NMR (101 MHz,  $\text{CDCl}_3$ )  $\delta$  177.63, 177.09,\* 160.72,\* 160.34, **157.80,\*** 140.64,\* 140.41, 135.57,\* 135.35, 131.91, 131.87,\* 130.37,\* 130.34, 129.92, 129.85,\* 128.84, 128.64,\* 128.25,\* 128.17, 127.63, 127.52,\* 126.62, 126.46,\* 125.25, 125.11,\* 114.29, 114.21,\* 79.77, 77.36,\* 55.56,\* 55.53, 54.02, 52.25,\* 51.43, 51.25,\* 36.36, 34.98,\* 24.43, 22.38,\* 21.59, 21.08.\* Carbon signals of the minor diastereomer are denoted with an asterisk (\*), overlap of both diastereomers are bolded; IR (Neat Film, NaCl) 3264, 2922, 2853, 1691, 1494, 1454, 1377, 1319, 1242, 1150, 910, 768, 702  $\text{cm}^{-1}$ ; (MM:ESI $^+$ ) :  $\text{C}_{27}\text{H}_{28}\text{BrN}_2\text{O}_2$   $m/z$  calc'd for  $[\text{M}+\text{H}]^+$ : 491.1329, found 491.1329. Crystals suitable for X-ray diffraction were obtained via a vapor diffusion of DCM/hexanes to afford clear crystals. CCDC 2253013.



**4-bromo-N-((R)-((3S,5R)-1-(4-methoxyphenyl)-3,5-dimethyl-2-oxopyrrolidin-3-yl)(phenyl)methyl)benzamide (SI16):** Dimethyl Mannich product **69ja** (25 mg, 0.077 mmol, 1.0 equiv) was dissolved in DCM (5 mL) and cooled to 0 °C. TEA (21  $\mu\text{L}$ , 0.15 mmol, 2.0 equiv) and *para*-bromo-benzoyl chloride **SI15** (18.5 mg, 0.11 mmol, 1.1 equiv) were added sequentially to the reaction mixture and stirred at 0 °C for 1 h and allowed to warm to 25 °C overnight. The reaction was diluted with DCM (10 mL) and washed with

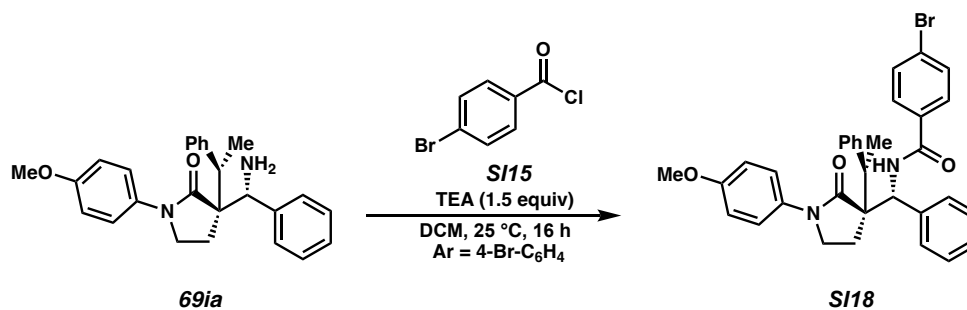


sat'd NaHCO<sub>3</sub> (10 mL). The layers were separated, and the aqueous layer was extracted with EtOAc (3 x 10 mL). The organic layers were combined, dried over Na<sub>2</sub>SO<sub>4</sub>, concentrated by rotary evaporator and purified via column chromatography (60% EtOAc in hexanes) to afford benzoyl product **SI16** as a colorless amorphous solid (37 mg, 0.073 mmol, 95% yield, 5:1 dr) separable diastereomers. Major diastereomer **SI16**: <sup>1</sup>H NMR (400 MHz, CDCl<sub>3</sub>)  $\delta$  8.75 (d,  $J$  = 8.1 Hz, 1H), 7.77 – 7.71 (m, 2H), 7.57 – 7.49 (m, 2H), 7.41 – 7.29 (m, 5H), 6.96 – 6.87 (m, 4H), 5.05 (d,  $J$  = 8.1 Hz, 1H), 3.82 (s, 3H), 2.57 (ddt,  $J$  = 14.0, 7.8, 6.2 Hz, 1H), 2.45 (dd,  $J$  = 13.5, 7.6 Hz, 1H), 1.67 – 1.58 (m, 4H), 0.90 (d,  $J$  = 6.2 Hz, 3H). <sup>13</sup>C NMR (101 MHz, CDCl<sub>3</sub>)  $\delta$  177.50, 165.22, 158.36, 139.60, 132.95, 131.82, 129.20, 128.89, 128.71, 128.33, 127.96, 126.34, 126.20, 114.61, 60.94, 55.63, 53.08, 47.44, 39.82, 25.95, 20.96; IR (Neat Film, NaCl) 3362, 2931, 1666, 1588, 1510, 1479, 1455, 1327, 1291, 1248, 1180, 1133, 1028, 1010, 828, 751, 705 cm<sup>-1</sup>; (MM:ESI<sup>+</sup>) : C<sub>27</sub>H<sub>28</sub>BrN<sub>2</sub>O<sub>3</sub>  $m/z$  calc'd for [M+H]<sup>+</sup>: 507.1278, found 507.1291.



Minor diastereomer **SI16a**: <sup>1</sup>H NMR (400 MHz, CDCl<sub>3</sub>)  $\delta$  9.50 (d,  $J$  = 8.5 Hz, 1H), 7.82 – 7.76 (m, 2H), 7.57 – 7.50 (m, 2H), 7.50 – 7.43 (m, 2H), 7.43 – 7.33 (m, 2H), 7.33 – 7.28 (m, 1H), 7.15 – 7.04 (m, 2H), 7.01 – 6.93 (m, 2H), 5.14 (d,  $J$  = 8.5 Hz, 1H), 4.08 – 3.99 (m, 1H), 3.82 (s, 3H), 2.17 – 2.06 (m, 1H), 1.67 – 1.55 (m, 4H), 0.63 (d,  $J$  = 6.2 Hz, 3H). <sup>13</sup>C NMR (101 MHz, CDCl<sub>3</sub>)  $\delta$  178.68, 165.33, 158.69, 140.02, 133.14, 131.81, 129.28,

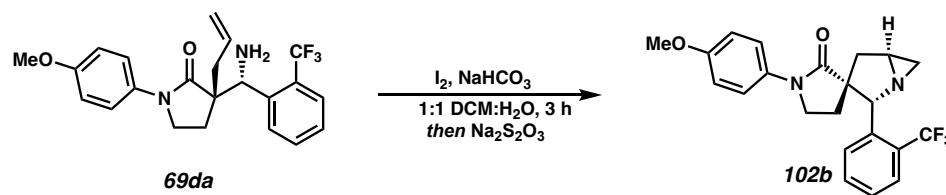
128.95, 128.75, 128.55, 128.13, 126.99, 126.25, 114.74, 60.59, 55.67, 53.32, 47.33, 37.76, 23.96, 20.20; IR (Neat Film, NaCl) 3362, 2931, 1666, 1588, 1510, 1479, 1455, 1327, 1291, 1248, 1180, 1133, 1028, 1010, 828, 751, 705  $\text{cm}^{-1}$ ; (MM:ESI<sup>+</sup>) : C<sub>27</sub>H<sub>28</sub>BrN<sub>2</sub>O<sub>3</sub> *m/z* calc'd for [M+H]<sup>+</sup>: 507.1278, found 507.1291.



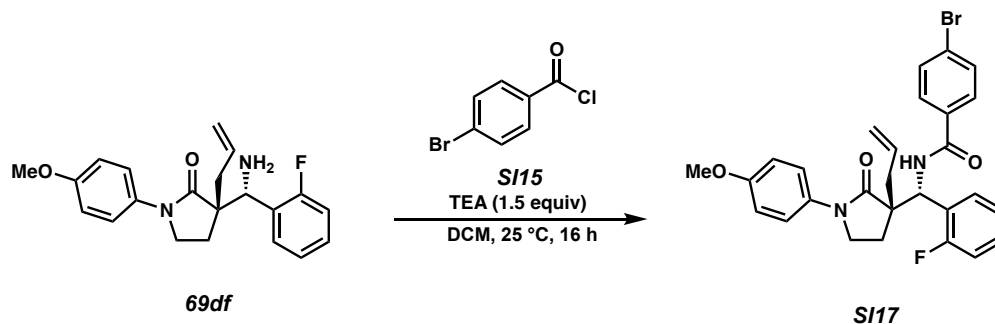
**4-bromo-*N*-((1*R*)-((3*S*)-1-(4-methoxyphenyl)-2-oxo-3-(1-phenylethyl)pyrrolidin-3-**

**yl)(phenyl)methyl)benzamide (SI18):** Benzyl Mannich product **69ia** (8 mg, 0.02 mmol, 1.0 equiv) was dissolved in DCM (2 mL) and cooled to 0 °C. TEA (3.2  $\mu\text{L}$ , 0.04 mmol, 2.0 equiv) and *para*-bromo-benzoyl chloride **SI15** (4.8 mg, 0.022 mmol, 1.1 equiv) were added sequentially to the reaction mixture and stirred at 0 °C for 1 h and allowed to warm to 25 °C overnight. The reaction was diluted with DCM (4 mL) and washed with sat'd NaHCO<sub>3</sub> (4 mL). The layers were separated, and the aqueous layer was extracted with EtOAc (3 x 5 mL). The organic layers were combined, dried over Na<sub>2</sub>SO<sub>4</sub>, concentrated by rotary evaporator and purified via column chromatography (60% EtOAc in hexanes) to afford benzoyl product **SI18** as a colorless amorphous solid (10.7 mg, 0.0184 mmol, 92% yield single diastereomer); <sup>1</sup>H NMR (400 MHz, CDCl<sub>3</sub>)  $\delta$  9.43 (d, *J* = 8.6 Hz, 1H), 7.89 – 7.78 (m, 2H), 7.61 – 7.56 (m, 2H), 7.47 – 7.43 (m, 2H), 7.41 – 7.38 (m, 2H), 7.34 – 7.27 (m, 5H), 7.26 – 7.21 (m, 1H), 6.82 (s, 4H), 5.42 (d, *J* = 8.6 Hz, 1H), 3.87 – 3.79 (m, 1H), 3.78

(s, 3H), 2.43 (ddd,  $J = 7.9, 6.0, 1.6$  Hz, 2H), 2.21 (ddd,  $J = 13.5, 8.1, 6.5$  Hz, 1H), 1.91 (ddd,  $J = 13.6, 8.6, 6.3$  Hz, 1H), 1.51 (d,  $J = 7.1$  Hz, 3H).  $^{13}\text{C}$  NMR (101 MHz,  $\text{CDCl}_3$ )  $\delta$  176.57, 164.92, 157.80, 141.84, 139.55, 133.04, 131.92, 130.98, 129.16, 129.00, 128.71, 128.69, 128.27, 128.19, 127.19, 126.42, 123.87, 114.29, 57.55, 55.85, 55.60, 47.07, 41.55, 21.42, 14.73; IR (Neat Film, NaCl) 3362, 2958, 1731, 1666, 1589, 1512, 1478, 1409, 1329, 1292, 1250, 1180, 1151, 1032, 1009, 828, 753, 735, 702  $\text{cm}^{-1}$ ; (MM:ESI $^+$ ):  $\text{C}_{33}\text{H}_{32}\text{BrN}_2\text{O}_3$   $m/z$  calc'd for  $[\text{M}+\text{H}]^+$ : 583.1591, found 583.1617.



$^1\text{H}$  NMR (400 MHz,  $\text{CDCl}_3$ )  $\delta$  7.72 (t,  $J = 6.6$  Hz, 1H), 7.61 – 7.48 (m, 2H), 7.32 (tdd,  $J = 7.2, 6.1, 2.4$  Hz, 1H), 7.23 – 7.13 (m, 2H), 6.83 – 6.74 (m, 2H), 4.56 (q,  $J = 1.6$  Hz, 1H), 3.75 (s, 2H), 3.70 (td,  $J = 7.9, 2.3$  Hz, 1H), 3.64 – 3.55 (m, 1H), 3.04 (ddd,  $J = 13.8, 5.5, 1.4$  Hz, 1H), 2.93 (ddt,  $J = 6.4, 4.6, 2.4$  Hz, 1H), 2.39 (ddd,  $J = 13.0, 7.9, 3.3$  Hz, 1H), 2.28 – 2.19 (m, 2H), 2.05 (dt,  $J = 5.4, 1.4$  Hz, 1H), 1.74 (dd,  $J = 3.5, 1.3$  Hz, 1H).  $^{13}\text{C}$  NMR (101 MHz,  $\text{CDCl}_3$ )  $\delta$  172.86, 156.76, 139.99, 132.49, 131.50, 131.01, 127.31, 126.36 (q,  $J = 283.3$  Hz), 125.07 (d,  $J = 6.0$  Hz), 122.39, 122.10 (q,  $J = 21.5$  Hz), 114.25, 74.29 (d,  $J = 2.4$  Hz), 56.53, 55.53, 45.67, 42.11, 40.39, 37.68, 32.67, **29.85**. bold is impurity (Tentative assignment)



***N*-((*S*)-((*S*)-3-allyl-1-(4-methoxyphenyl)-2-oxopyrrolidin-3-yl)(2-**

**fluorophenyl)methyl)-4-bromobenzamide (SI17): *Ortho*-fluoro-Mannich product **69df****

(14 mg, 0.04 mmol, 1.0 equiv) was dissolved in DCM (2 mL) and cooled to 0 °C. TEA (6.5  $\mu$ L, 0.08 mmol, 2.0 equiv) and *para*-bromo-benzoyl chloride **SI15** (9.6 mg, 0.044 mmol, 1.1 equiv) were added sequentially to the reaction mixture and stirred at 0 °C for 1 h and allowed to warm to 25 °C overnight. The reaction was diluted with DCM (8 mL) and washed with sat'd NaHCO<sub>3</sub> (8 mL). The layers were separated, and the aqueous layer was extracted with EtOAc (3 x 10 mL). The organic layers were combined, dried over Na<sub>2</sub>SO<sub>4</sub>, concentrated by rotary evaporator and purified via column chromatography (60% EtOAc in hexanes) to afford benzoyl product **SI17** as a colorless amorphous solid (14.4 mg, 0.0367 mmol, 67% yield, single diastereomer); <sup>1</sup>H NMR (400 MHz, CDCl<sub>3</sub>)  $\delta$  8.90 (d,  $J$  = 8.1 Hz, 1H), 7.75 – 7.66 (m, 2H), 7.51 – 7.43 (m, 2H), 7.26 – 7.12 (m, 1H), 7.06 – 6.98 (m, 4H), 6.94 (td,  $J$  = 7.6, 1.2 Hz, 1H), 6.89 – 6.79 (m, 2H), 5.80 (dddd,  $J$  = 16.8, 10.4, 8.3, 6.5 Hz, 1H), 5.60 (d,  $J$  = 8.1 Hz, 1H), 5.22 – 5.12 (m, 2H), 3.74 (s, 3H), 3.33 (td,  $J$  = 9.4, 4.0 Hz, 1H), 2.73 – 2.64 (m, 1H), 2.64 – 2.50 (m, 2H), 2.15 (ddd,  $J$  = 13.8, 9.3, 6.9 Hz, 1H), 1.97 – 1.87 (m, 1H); <sup>13</sup>C NMR (101 MHz, CDCl<sub>3</sub>)  $\delta$  176.13, 164.94, 160.55 (d,  $J$  = 244.1 Hz), 157.52, 132.67, 132.23, 131.80, 131.79 (d,  $J$  = 23.0 Hz), 131.18, 129.67 (d,  $J$  = 8.2 Hz), 128.78, 128.40, 126.76 (d,  $J$  = 13.6 Hz), 126.37, 124.52 (d,  $J$  = 3.4 Hz), 122.91, 120.43,

115.58 (d,  $J = 22.6$  Hz), 114.27, 55.52, 51.11, 46.95, 40.69, 25.12; IR (Neat Film, NaCl) 3361, 2922, 1681, 1666, 1512, 1481, 1329, 1292, 1251, 753, 702  $\text{cm}^{-1}$ ; (MM:ESI<sup>+</sup>) :  $\text{C}_{28}\text{H}_{27}\text{BrFN}_2\text{O}_3$   $m/z$  calc'd for  $[\text{M}+\text{H}]^+$ : 537.1184, found 537.1200.

## 1.11 NOTES AND REFERENCES

<sup>1</sup> Mannich, C.; Krösche, W. Ueber Ein Kondensationsprodukt Aus Formaldehyd, Ammoniak Und Antipyrin. *Archiv der Pharmazie* **1912**, 250 (1), 647–667.

<sup>2</sup> (a) Shi, Y.; Wang, Q.; Gao, S. Recent Advances in the Intramolecular Mannich Reaction in Natural Products Total Synthesis. *Org. Chem. Front.* **2018**, 5 (6), 1049–1066. (b) Numajiri, Y.; Pritchett, B. P.; Chiyoda, K.; Stoltz, B. M. Enantioselective Synthesis of  $\alpha$ -Quaternary Mannich Adducts by Palladium-Catalyzed Allylic Alkylation: Total Synthesis of (+)-Sibirinine. *J. Am. Chem. Soc.* **2015**, 137 (3), 1040–1043. (c) Cushman, M.; Chen, J. K. Utilization of the 1-Ferrocenyl-2-Methylpropyl Substituent as a Chiral Auxiliary in the Asymmetric Syntheses of the Benzophenanthridine Alkaloids (+)- and (-)-Corynoline. *J. Org. Chem.* **1987**, 52 (8), 1517–1521. (d) Trost, B. M.; Hung, C.-I. J.; Jiao, Z. Enantioselective Divergent Syntheses of (+)-Bulleyaniline and Related Isoquinoline Alkaloids from the Genus *Corydalis*. *J. Am. Chem. Soc.* **2019**, 141 (40), 16085–16092. (e) Cholewczynski, A. E.; Williams, P. C.; Pierce, J. G. Stereocontrolled Synthesis of ( $\pm$ )-Melokhanine E via an Intramolecular Formal [3 + 2] Cycloaddition. *Org. Lett.* **2020**, 22 (2), 714–717.

<sup>3</sup> Roman, G. Mannich Bases in Medicinal Chemistry and Drug Design. *European Journal of Medicinal Chemistry* **2015**, 89, 743–816.

<sup>4</sup> (a) Kobayashi, S.; Ishitani, H. Catalytic Enantioselective Addition to Imines. *Chem. Rev.* **1999**, 99 (5), 1069–1094. (b) Kobayashi, S.; Mori, Y.; Fossey, J. S.; Salter, M. M. Catalytic

Enantioselective Formation of C–C Bonds by Addition to Imines and Hydrazones: A Ten-Year Update. *Chem. Rev.* **2011**, *111* (4), 2626–2704. (c) Karimi, B. E., Dieter; Jafari, Ehsan. Recent Advances in Metal-Catalyzed Asymmetric Mannich Reactions. *Synthesis* **2013**, *45* (20), 2769–2812. (d) Shibasaki, M.; Kanai, M.; Matsunaga, S.; Kumagai, N. Recent Progress in Asymmetric Bifunctional Catalysis Using Multimetallic Systems. *Acc. Chem. Res.* **2009**, *42* (8), 1117–1127. (e) Ting, A.; Schaus, S. E. Organocatalytic Asymmetric Mannich Reactions: New Methodology, Catalyst Design, and Synthetic Applications. *European Journal of Organic Chemistry* **2007**, *2007* (35), 5797–5815. (f) Córdova, A. The Direct Catalytic Asymmetric Mannich Reaction. *Acc. Chem. Res.* **2004**, *37* (2), 102–112.

<sup>5</sup> Distinguishing the *Direct* and *Indirect* Mannich reaction appears as early as 2000 in List, B. The Direct Catalytic Asymmetric Three-Component Mannich Reaction. *J. Am. Chem. Soc.* **2000**, *122* (38), 9336–9337.

<sup>6</sup> Corey, E. J.; Decicco, C. P.; Newbold, R. C. Highly Enantioselective and Diastereoselective Synthesis of  $\beta$ -Amino Acid Esters and  $\beta$ -Lactams from Achiral Esters and Imines. *Tetrahedron Letters* **1991**, *32* (39), 5287–5290.

<sup>7</sup> Ishihara, K.; Miyata, M.; Hattori, K.; Tada, T.; Yamamoto, H. A New Chiral BLA Promoter for Asymmetric Aza Diels-Alder and Aldol-Type Reactions of Imines. *J. Am. Chem. Soc.* **1994**, *116* (23), 10520–10524.

<sup>8</sup>(a) McCarty, C. G. In *The Chemistry of the Carbon-Nitrogen Double Bond*; Patai, S., Ed.; John Wiley & Sons: New York, **1970**; Chapter 9. (b) Bjørgero, J.; Boyd, D. R.; Watson, C. G.; Jennings, W. B. Equilibrium Distribution of E–Z-Ketimine Isomers. *J. Chem. Soc., Perkin Trans. 2* **1974**, No. 7, 757–762.

<sup>9</sup> Ishitani, H.; Ueno, M.; Kobayashi, S. Catalytic Enantioselective Mannich-Type Reactions Using a Novel Chiral Zirconium Catalyst. *J. Am. Chem. Soc.* **1997**, *119* (30), 7153–7154.

<sup>10</sup> (a) Kobayashi, S.; Ishitani, H.; Ueno, M. Catalytic Asymmetric Synthesis of Both Syn- and Anti- $\beta$ -Amino Alcohols. *J. Am. Chem. Soc.* **1998**, *120* (2), 431–432. (b) Kobayashi, S.; Kobayashi, J.; Ishitani, H.; Ueno, M. Catalytic Enantioselective Addition of Propionate Units to Imines: An Efficient Synthesis of Anti- $\alpha$ -Methyl- $\beta$ -Amino Acid Derivatives. *Chemistry – A European Journal* **2002**, *8* (18), 4185–4190. (c) Kobayashi, S.; Ueno, M.; Saito, S.; Mizuki, Y.; Ishitani, H.; Yamashita, Y. Air-Stable, Storable, and Highly Efficient Chiral Zirconium Catalysts for Enantioselective Mannich-Type, Aza Diels–Alder, Aldol, and Hetero Diels–Alder Reactions. *Proceedings of the National Academy of Sciences* **2004**, *101* (15), 5476–5481.

<sup>11</sup> (a) Yamasaki, S.; Iida, T.; Shibasaki, M. Direct Catalytic Asymmetric Mannich Reaction of Unmodified Ketones: Cooperative Catalysis of an Al<sub>2</sub>Li<sub>2</sub>(Binaphthoxide) Complex and La(OTf)<sub>3</sub>·nH<sub>2</sub>O. *Tetrahedron* **1999**, *55* (29), 8857–8867. (b) Fujii, A.; Hagiwara, E.; Sodeoka, M. Mechanism of Palladium Complex-Catalyzed Enantioselective Mannich-Type Reaction: Characterization of A Novel Binuclear Palladium Enolate Complex. *J. Am. Chem. Soc.* **1999**, *121* (23), 5450–5458. (c) Matsunaga, S.; Kumagai, N.; Harada, S.; Shibasaki, M. Anti-Selective Direct Catalytic Asymmetric Mannich-Type Reaction of Hydroxyketone Providing  $\beta$ -Amino Alcohols. *J. Am. Chem. Soc.* **2003**, *125* (16), 4712–4713. (d) Trost, B. M.; Terrell, L. R. A Direct Catalytic Asymmetric Mannich-Type Reaction to Syn-Amino Alcohols. *J. Am. Chem. Soc.* **2003**, *125* (2), 338–339.

<sup>12</sup> List, B.; Pojarliev, P.; Biller, W. T.; Martin, H. J. The Proline-Catalyzed Direct Asymmetric Three-Component Mannich Reaction: Scope, Optimization, and Application

to the Highly Enantioselective Synthesis of 1,2-Amino Alcohols. *J. Am. Chem. Soc.* **2002**, *124* (5), 827–833.

<sup>13</sup> Córdova, A.; Watanabe, S.; Tanaka, F.; Notz, W.; Barbas, C. F. A Highly Enantioselective Route to Either Enantiomer of Both  $\alpha$ - and  $\beta$ -Amino Acid Derivatives. *J. Am. Chem. Soc.* **2002**, *124* (9), 1866–1867.

<sup>14</sup> Chowdari, N. S.; Suri, J. T.; Barbas, C. F. Asymmetric Synthesis of Quaternary  $\alpha$ - and  $\beta$ -Amino Acids and  $\beta$ -Lactams via Proline-Catalyzed Mannich Reactions with Branched Aldehyde Donors. *Org. Lett.* **2004**, *6* (15), 2507–2510.

<sup>15</sup> (a) Christoffers, J.; Mann, A. Enantioselective Construction of Quaternary Stereocenters. *Angewandte Chemie International Edition* **2001**, *40* (24), 4591–4597. (b) Douglas, C. J.; Overman, L. E. Catalytic Asymmetric Synthesis of All-Carbon Quaternary Stereocenters. *Proceedings of the National Academy of Sciences* **2004**, *101* (15), 5363–5367. (c) Ling, T.; Rivas, F. All-Carbon Quaternary Centers in Natural Products and Medicinal Chemistry: Recent Advances. *Tetrahedron* **2016**, *72* (43), 6729–6777. (d) Xin, Z.; Wang, H.; He, H.; Gao, S. Recent Advances in the Total Synthesis of Natural Products Bearing the Contiguous All-Carbon Quaternary Stereocenters. *Tetrahedron Letters* **2021**, *71*, 153029. (e) Prusov, E. V. Construction of Quaternary Stereogenic Centers in the Total Synthesis of Natural Products. *Angewandte Chemie International Edition* **2017**, *56* (46), 14356–14358. (f) Li, C.; Ragab, S. S.; Liu, G.; Tang, W. Enantioselective Formation of Quaternary Carbon Stereocenters in Natural Product Synthesis: A Recent Update. *Natural Product Reports* **2020**, *37* (2), 276–292.

<sup>16</sup> Bordwell, F. G. Equilibrium Acidities in Dimethyl Sulfoxide Solution. *Acc. Chem. Res.* **1988**, *21* (12), 456–463.



<sup>17</sup> (a) Hatano, M.; Horibe, T.; Ishihara, K. Chiral Lithium(I) Binaphtholate Salts for the Enantioselective Direct Mannich-Type Reaction with a Change of Syn/Anti and Absolute Stereochemistry. *J. Am. Chem. Soc.* **2010**, *132* (1), 56–57. (b) Poisson, T.; Tsubogo, T.; Yamashita, Y.; Kobayashi, S. Asymmetric Mannich Reaction of Malonates with Imines Catalyzed by a Chiral Calcium Complex. *J. Org. Chem.* **2010**, *75* (3), 963–965. (c) Kang, Y. K.; Kim, D. Y. Organocatalytic Highly Enantio- and Diastereoselective Mannich Reaction of  $\beta$ -Ketoesters with N-Boc-Aldimines. *J. Org. Chem.* **2009**, *74* (15), 5734–5737. (d) Kano, T.; Homma, C.; Maruoka, K. In Situ Generation of Less Accessible Boc-Imines from Aldehydes: Construction of a Quaternary Carbon by the Mannich Reaction or Unprecedented Aldol Reaction. *Org. Biomol. Chem.* **2017**, *15* (21), 4527–4530. (e) Kano, T.; Yurino, T.; Maruoka, K. Organocatalytic Asymmetric Synthesis of Propargylamines with Two Adjacent Stereocenters: Mannich-Type Reactions of In Situ Generated C-Alkynyl Imines with  $\beta$ -Keto Esters. *Angewandte Chemie International Edition* **2013**, *52* (44), 11509–11512. (f) Lou, S.; Dai, P.; Schaus, S. E. Asymmetric Mannich Reaction of Dicarboxyl Compounds with  $\alpha$ -Amido Sulfones Catalyzed by Cinchona Alkaloids and Synthesis of Chiral Dihydropyrimidones. *J. Org. Chem.* **2007**, *72* (26), 9998–10008. (g) Lou, Y.-P.; Zheng, C.-W.; Pan, R.-M.; Jin, Q.-W.; Zhao, G.; Li, Z. Enantioselective Direct Mannich Reactions of Cyclic  $\beta$ -Ketoesters Catalyzed by Chiral Phosphine via a Novel Dual-Reagent Catalysis. *Org. Lett.* **2015**, *17* (3), 688–691. (h) Lee, J. H.; Kim, D. Y. Enantio- and Diastereoselective Mannich-Type Reactions of  $\alpha$ -Cyano Ketones with N-Boc Aldimines Catalyzed by Chiral Bifunctional Urea. *Advanced Synthesis & Catalysis* **2009**, *351* (11–12), 1779–1782. (i) Pan, R.; Zhang, J.; Zheng, C.; Wang, H.; Cao, D.; Cao, W.; Zhao, G. Enantioselective Direct Mannich Reaction of Functionalized Acetonitrile to N-

Boc Imines Catalyzed by Quaternary Phosphonium Catalysis. *Tetrahedron* **2017**, *73* (17), 2349–2358. (j) Guo, Q.; Zhao, J. C.-G. Highly Enantioselective Three-Component Direct Mannich Reactions of Unfunctionalized Ketones Catalyzed by Bifunctional Organocatalysts. *Org. Lett.* **2013**, *15* (3), 508–511. (k) Jiang, X.; Fu, D.; Zhang, G.; Cao, Y.; Liu, L.; Song, J.; Wang, R. Highly Diastereo- and Enantioselective Mannich Reaction of Lactones with N-Boc-Aldimines Catalyzed by Bifunctional Rosin-Derived Amine Thiourea Catalysts. *Chem. Commun.* **2010**, *46* (24), 4294–4296.

<sup>18</sup> (a) Shimizu, S.; Tsubogo, T.; Xu, P.; Kobayashi, S. Calcium-Catalyzed Asymmetric Synthesis of 3-Tetrasubstituted Oxindoles: Efficient Construction of Adjacent Quaternary and Tertiary Chiral Centers. *Org. Lett.* **2015**, *17* (8), 2006–2009. (b) He, R.; Ding, C.; Maruoka, K. Phosphonium Salts as Chiral Phase-Transfer Catalysts: Asymmetric Michael and Mannich Reactions of 3-Aryloxindoles. *Angewandte Chemie International Edition* **2009**, *48* (25), 4559–4561. (c) Tian, X.; Jiang, K.; Peng, J.; Du, W.; Chen, Y.-C. Organocatalytic Stereoselective Mannich Reaction of 3-Substituted Oxindoles. *Org. Lett.* **2008**, *10* (16), 3583–3586. (d) Cheng, L.; Liu, L.; Jia, H.; Wang, D.; Chen, Y.-J. Enantioselective Organocatalytic Anti-Mannich-Type Reaction of N-Unprotected 3-Substituted 2-Oxindoles with Aromatic N-Ts-Aldimines. *J. Org. Chem.* **2009**, *74* (12), 4650–4653. (e) Jin, Q.; Zheng, C.; Zhao, G.; Zou, G. Enantioselective Direct Mannich Reactions of 3-Substituted Oxindoles Catalyzed by Chiral Phosphine via Dual-Reagent Catalysis. *Tetrahedron* **2018**, *74* (30), 4134–4144. (f) Torii, M.; Kato, K.; Uruguchi, D.; Ooi, T. Chiral Ammonium Betaine-Catalyzed Asymmetric Mannich-Type Reaction of Oxindoles. *Beilstein Journal of Organic Chemistry* **2016**, *12*, 2099–2103.

<sup>19</sup> Trost, B. M.; Hung, C.-I. (Joey); Saget, T.; Gnanamani, E. Branched Aldehydes as Linchpins for the Enantioselective and Stereodivergent Synthesis of 1,3-Aminoalcohols Featuring a Quaternary Stereocentre. *Nature Catalysis* **2018**, *1* (7), 523–530.

<sup>20</sup> Trost, B. M.; Hung, C.-I. (Joey); Mata, G. Dinuclear Metal-ProPhenol Catalysts: Development and Synthetic Applications. *Angewandte Chemie International Edition* **2020**, *59* (11), 4240–4261.

<sup>21</sup> Yang, X.; Toste, F. D. Direct Asymmetric Amination of  $\alpha$ -Branched Cyclic Ketones Catalyzed by a Chiral Phosphoric Acid. *J. Am. Chem. Soc.* **2015**, *137* (9), 3205–3208.

<sup>22</sup> (a) Trost, B. M.; Saget, T.; Hung, C.-I. (Joey). Direct Catalytic Asymmetric Mannich Reactions for the Construction of Quaternary Carbon Stereocenters. *J. Am. Chem. Soc.* **2016**, *138* (11), 3659–3662. (b) Trost, B. M.; Hung, C.-I. J.; Gnanamani, E. Tuning the Reactivity of Ketones through Unsaturation: Construction of Cyclic and Acyclic Quaternary Stereocenters via Zn-ProPhenol Catalyzed Mannich Reactions. *ACS Catal.* **2019**, *9* (2), 1549–1557. (c) Trost, B. M.; Hung, C.-I. (Joey). Broad Spectrum Enolate Equivalent for Catalytic Chemo-, Diastereo-, and Enantioselective Addition to N-Boc Imines. *J. Am. Chem. Soc.* **2015**, *137* (50), 15940–15946. (d) Trost, B. M.; Hung, C.-I. J.; Mata, G.; Liu, Y.; Lu, Y.; Gnanamani, E. Direct Enantio- and Diastereoselective Zn-ProPhenol-Catalyzed Mannich Reactions of CF<sub>3</sub>- and SCF<sub>3</sub>-Substituted Ketones. *Org. Lett.* **2020**, *22* (6), 2437–2441. (e) Trost, B. M.; Saget, T.; Lerchen, A.; Hung, C.-I. (Joey). Catalytic Asymmetric Mannich Reactions with Fluorinated Aromatic Ketones: Efficient Access to Chiral  $\beta$ -Fluoroamines. *Angewandte Chemie International Edition* **2016**, *55* (2), 781–784. (f) Trost, B. M.; Saget, T.; Hung, C.-I. (Joey). Efficient Access to Chiral

Trisubstituted Aziridines via Catalytic Enantioselective Aza-Darzens Reactions. *Angewandte Chemie International Edition* **2017**, 56 (9), 2440–2444.

<sup>23</sup> (a) Shang, M.; Cao, M.; Wang, Q.; Wasa, M. Enantioselective Direct Mannich-Type Reactions Catalyzed by Frustrated Lewis Acid/Brønsted Base Complexes. *Angewandte Chemie International Edition* **2017**, 56 (43), 13338–13341. (b) Morita, Y.; Yamamoto, T.; Nagai, H.; Shimizu, Y.; Kanai, M. Chemoselective Boron-Catalyzed Nucleophilic Activation of Carboxylic Acids for Mannich-Type Reactions. *J. Am. Chem. Soc.* **2015**, 137 (22), 7075–7078. (c) Suzuki, Y.; Yazaki, R.; Kumagai, N.; Shibasaki, M. Direct Catalytic Asymmetric Mannich-Type Reaction of Thioamides. *Angewandte Chemie International Edition* **2009**, 48 (27), 5026–5029. (d) Kumagai, N.; Shibasaki, M. Nucleophilic and Electrophilic Activation of Non-Heteroaromatic Amides in Atom-Economical Asymmetric Catalysis. *Chemistry – A European Journal* **2016**, 22 (43), 15192–15200. (e) Saito, S.; Tsubogo, T.; Kobayashi, S. Direct-Type Catalytic Mannich Reactions of Amides with Imines. *Chem. Commun.* **2007**, No. 12, 1236–1237.

<sup>24</sup> (a) Frick, U.; Simchen, G. Reaktionen Der Trialkylsilyl-trifluormethansulfonate, VIII. Synthese von O-(Trimethylsilyl) Keten-O, N-acetalen, 2, 5-Bis (Trimethylsiloxy) Pyrrolen,-furanen Und-thiophenen. *Liebigs Annalen der Chemie* **1987**, 1987 (10), 839–845. (b) Woodbury, R. P.; Rathke, M. W. Reaction of Lithium N, N-Dialkylamide Enolates with Trialkylchlorosilanes. *The Journal of Organic Chemistry* **1978**, 43 (5), 881–884. (c) Nagao, Y.; Miyamoto, S.; Miyamoto, M.; Takeshige, H.; Hayashi, K.; Sano, S.; Shiro, M.; Yamaguchi, K.; Sei, Y. Highly Stereoselective Asymmetric Pummerer Reactions That Incorporate Intermolecular and Intramolecular Nonbonded S $\cdots$ O Interactions. *J. Am. Chem. Soc.* **2006**, 128 (30), 9722–9729. (d) Djuric, S. W. A Mild and Convenient

Procedure for the N-Formylation of Secondary Amines Using Organosilicon Chemistry. *The Journal of Organic Chemistry* **1984**, *49* (7), 1311–1312.

<sup>25</sup> (a) Richard, J. P.; Williams, G.; O'Donoghue, A. C.; Amyes, T. L. Formation and Stability of Enolates of Acetamide and Acetate Anion: An Eigen Plot for Proton Transfer at  $\alpha$ -Carbonyl Carbon. *Journal of the American Chemical Society* **2002**, *124* (12), 2957–2968.

(b) Rablen, P. R.; Bentrup, K. H. Are the Enolates of Amides and Esters Stabilized by Electrostatics? *J. Am. Chem. Soc.* **2003**, *125* (8), 2142–2147.

<sup>26</sup> (a) Arteaga, F. A.; Liu, Z.; Brewitz, L.; Chen, J.; Sun, B.; Kumagai, N.; Shibasaki, M. Direct Catalytic Asymmetric Mannich-Type Reaction of Alkylamides. *Org. Lett.* **2016**, *18* (10), 2391–2394 (b) Brewitz, L.; Arteaga, F. A.; Yin, L.; Alagiri, K.; Kumagai, N.; Shibasaki, M. Direct Catalytic Asymmetric Mannich-Type Reaction of  $\alpha$ - and  $\beta$ -Fluorinated Amides. *J. Am. Chem. Soc.* **2015**, *137* (50), 15929–15939. (c) Sun, B.; Balaji, P. V.; Kumagai, N.; Shibasaki, M.  $\alpha$ -Halo Amides as Competent Latent Enolates: Direct Catalytic Asymmetric Mannich-Type Reaction. *J. Am. Chem. Soc.* **2017**, *139* (24), 8295–8301. (d) Yin, L.; Brewitz, L.; Kumagai, N.; Shibasaki, M. Catalytic Generation of  $\alpha$ -CF<sub>3</sub> Enolate: Direct Catalytic Asymmetric Mannich-Type Reaction of  $\alpha$ -CF<sub>3</sub> Amide. *J. Am. Chem. Soc.* **2014**, *136* (52), 17958–17961.

<sup>27</sup> Lu, J.; Fan, Y.; Sha, F.; Li, Q.; Wu, X.-Y. Copper-Catalyzed Enantioselective Mannich Reaction between N-Acylpyrazoles and Isatin-Derived Ketimines. *Org. Chem. Front.* **2019**, *6* (15), 2687–2691.

<sup>28</sup> Kobayashi, S.; Kiyohara, H.; Yamaguchi, M. Catalytic Silicon-Mediated Carbon–Carbon Bond-Forming Reactions of Unactivated Amides. *J. Am. Chem. Soc.* **2011**, *133* (4), 708–711.

<sup>29</sup> Yamashita, Y.; Noguchi, A.; Fushimi, S.; Hatanaka, M.; Kobayashi, S. Chiral Metal Salts as Ligands for Catalytic Asymmetric Mannich Reactions with Simple Amides. *J. Am. Chem. Soc.* **2021**, *143* (15), 5598–5604.

<sup>30</sup> (a) Hayashi, M.; Bachman, S.; Hashimoto, S.; Eichman, C. C.; Stoltz, B. M. Ni-Catalyzed Enantioselective C-Acylation of  $\alpha$ -Substituted Lactams. *J. Am. Chem. Soc.* **2016**, *138* (29), 8997–9000. (b) Jette, C. I.; Geibel, I.; Bachman, S.; Hayashi, M.; Sakurai, S.; Shimizu, H.; Morgan, J. B.; Stoltz, B. M. Palladium-Catalyzed Construction of Quaternary Stereocenters by Enantioselective Arylation of  $\gamma$ -Lactams with Aryl Chlorides and Bromides. *Angewandte Chemie International Edition* **2019**, *58* (13), 4297–4301. (c) Sercel, Z. P.; Sun, A. W.; Stoltz, B. M. Palladium-Catalyzed Decarboxylative Asymmetric Allylic Alkylation of 1,4-Diazepan-5-Ones. *Org. Lett.* **2019**, *21* (22), 9158–9161. (d) Sun, A. W.; Hess, S. N.; Stoltz, B. M. Enantioselective Synthesis of Gem-Disubstituted N-Boc Diazaheterocycles via Decarboxylative Asymmetric Allylic Alkylation. *Chem. Sci.* **2019**, *10* (3), 788–792. (e) Behenna, D. C.; Liu, Y.; Yurino, T.; Kim, J.; White, D. E.; Virgil, S. C.; Stoltz, B. M. Enantioselective Construction of Quaternary N-Heterocycles by Palladium-Catalysed Decarboxylative Allylic Alkylation of Lactams. *Nature Chemistry* **2012**, *4* (2), 130–133. (f) Numajiri, Y.; Jiménez-Osés, G.; Wang, B.; Houk, K. N.; Stoltz, B. M. Enantioselective Synthesis of Dialkylated N-Heterocycles by Palladium-Catalyzed Allylic Alkylation. *Org. Lett.* **2015**, *17* (5), 1082–1085.

<sup>31</sup> (a) Michael, J. P. Indolizidine and Quinolizidine Alkaloids. *Nat. Prod. Rep.* **2005**, *22* (5), 603–626. (b) O'Hagan, D. Pyrrole, Pyrrolidine, Pyridine, Piperidine and Tropane Alkaloids. *Natural product reports* **2000**, *17* (5), 435–446. (c) Bhat, C.; Tilve, S. G. Recent Advances in the Synthesis of Naturally Occurring Pyrrolidines, Pyrrolizidines and

Indolizidine Alkaloids Using Proline as a Unique Chiral Synthone. *RSC Advances* **2014**, *4* (11), 5405–5452.

<sup>32</sup> For the synthesis of N-Bz imines, see: Lou, S.; Moquist, P. N.; Schaus, S. E. Asymmetric Allylboration of Acyl Imines Catalyzed by Chiral Diols. *J. Am. Chem. Soc.* **2007**, *129* (49), 15398–15404.

<sup>33</sup> (a) Cainelli, G.; Giacomini, D.; Panunzio, M.; Martelli, G.; Spunta, G.  $\beta$ -Lactams from Esters and Silylimines: A Reevaluation. Synthesis of N-Unsubstituted 4-Alkyl- $\beta$ -Lactams. *Tetrahedron Letters* **1987**, *28* (44), 5369–5372. (b) Hart, D. J.; Kanai, K.; Thomas, D. G.; Yang, T. K. Preparation of Primary Amines and 2-Azetidinones via N-(Trimethylsilyl) Imines. *The Journal of Organic Chemistry* **1983**, *48* (3), 289–294.

<sup>34</sup> (a) Fernández-García, J. M.; Fernández-Rodríguez, M. Á.; Aguilar, E. Catalytic Intermolecular Hetero-Dehydro-Diels–Alder Cycloadditions: Regio- and Diastereoselective Synthesis of 5,6-Dihydropyridin-2-Ones. *Org. Lett.* **2011**, *13* (19), 5172–5175. (b) Kikuchi, J.; Ye, H.; Terada, M. Chiral Phosphoric Acid Catalyzed Enantioselective [4 + 2] Cycloaddition Reaction of  $\alpha$ -Fluorostyrenes with Imines. *Org. Lett.* **2020**, *22* (22), 8957–8961. (c) Ramachandran, P. V.; Burghardt, T. E. Highly Diastereoselective and Enantioselective Preparation of Homoallylic Amines: Application for the Synthesis of  $\beta$ -Amino Acids and  $\gamma$ -Lactams. *Chemistry – A European Journal* **2005**, *11* (15), 4387–4395. (d) Candito, D. A.; Lautens, M. Palladium-Catalyzed Domino Direct Arylation/N-Arylation: Convenient Synthesis of Phenanthridines. *Angewandte Chemie International Edition* **2009**, *48* (36), 6713–6716. (e) Vidal, J.; Damestoy, S.; Guy, L.; Hannachi, J.-C.; Aubry, A.; Collet, A.; Aubry, A. N-Alkyloxycarbonyl-3-Aryloxaziridines: Their Preparation, Structure, and Utilization As Electrophilic Amination Reagents. *Chemistry –*

*A European Journal* **1997**, 3 (10), 1691–1709. (f) Denmark, S. E.; Su, X.; Nishigaichi, Y.; Coe, D. M.; Wong, K.-T.; Winter, S. B. D.; Choi, J. Y. Synthesis of Phosphoramides for the Lewis Base-Catalyzed Allylation and Aldol Addition Reactions. *J. Org. Chem.* **1999**, 64 (6), 1958–1967.

<sup>35</sup> Gandhamsetty, N.; Jeong, J.; Park, J.; Park, S.; Chang, S. Boron-Catalyzed Silylative Reduction of Nitriles in Accessing Primary Amines and Imines. *J. Org. Chem.* **2015**, 80 (14), 7281–7287.

<sup>36</sup> Gutsulyak, D. V.; Nikonov, G. I. Chemoselective Catalytic Hydrosilylation of Nitriles. *Angewandte Chemie International Edition* **2010**, 49 (41), 7553–7556.

<sup>37</sup> Belot, V.; Farran, D.; Jean, M.; Albalat, M.; Vanthuynne, N.; Roussel, C. Steric Scale of Common Substituents from Rotational Barriers of N-(o-Substituted Aryl)Thiazoline-2-Thione Atropisomers. *J. Org. Chem.* **2017**, 82 (19), 10188–10200.

<sup>38</sup> Hansch, Corwin.; Leo, A.; Taft, R. W. A Survey of Hammett Substituent Constants and Resonance and Field Parameters. *Chem. Rev.* **1991**, 91 (2), 165–195.

<sup>39</sup> (a) Romanato, P.; Duttwyler, S.; Linden, A.; Baldrige, K. K.; Siegel, J. S. Intramolecular Halogen Stabilization of Silylium Ions Directs Gearing Dynamics. *J Am Chem Soc* **2010**, 132 (23), 7828–7829. (b) Reed, C. A.; Xie, Z.; Bau, R.; Benesi, A. Closely Approaching the Silylium Ion ( $R_3Si^+$ ). *Science* **1993**, 262 (5132), 402–404.

<sup>40</sup> (a) Parks, D. J.; Blackwell, J. M.; Piers, W. E. Studies on the Mechanism of  $B(C_6F_5)_3$ -Catalyzed Hydrosilation of Carbonyl Functions. *J. Org. Chem.* **2000**, 65 (10), 3090–3098.

(b) Parks, D. J.; Piers, W. E. Tris(Pentafluorophenyl)Boron-Catalyzed Hydrosilation of Aromatic Aldehydes, Ketones, and Esters. *J. Am. Chem. Soc.* **1996**, 118 (39), 9440–9441.

(c) Hermeke, J.; Mewald, M.; Oestreich, M. Experimental Analysis of the Catalytic Cycle



of the Borane-Promoted Imine Reduction with Hydrosilanes: Spectroscopic Detection of Unexpected Intermediates and a Refined Mechanism. *J. Am. Chem. Soc.* **2013**, *135* (46), 17537–17546. (d) Blackwell, J. M.; Sonmor, E. R.; Scoccitti, T.; Piers, W. E. B(C<sub>6</sub>F<sub>5</sub>)<sub>3</sub>-Catalyzed Hydrosilation of Imines via Silyliminium Intermediates. *Org. Lett.* **2000**, *2* (24), 3921–3923.

<sup>41</sup> For computational studies of KO<sup>t</sup>-Bu tetramer-mediated reactions, see (a) Liu, W.-B.; Schuman, D. P.; Yang, Y.-F.; Toutov, A. A.; Liang, Y.; Klare, H. F. T.; Nesnas, N.; Oestreich, M.; Blackmond, D. G.; Virgil, S. C.; Banerjee, S.; Zare, R. N.; Grubbs, R. H.; Houk, K. N.; Stoltz, B. M. Potassium Tert-Butoxide-Catalyzed Dehydrogenative C–H Silylation of Heteroaromatics: A Combined Experimental and Computational Mechanistic Study. *J. Am. Chem. Soc.* **2017**, *139*, 6867–6879. (b) Lu, Y.; Zhao, R.; Guo, J.; Liu, Z.; Menberu, W.; Wang, Z.-X. A Unified Mechanism to Account for Manganese- or Ruthenium-Catalyzed Nitrile  $\alpha$ -Olefinations by Primary or Secondary Alcohols: A DFT Mechanistic Study. *Chem. – Eur. J.* **2019**, *25*, 3939–3949. (c) Jenkins, I. D.; Krenske, E. H. Mechanistic Aspects of Hydrosilane/Potassium Tert-Butoxide (HSiR<sub>3</sub>/KO<sup>t</sup>Bu)-Mediated Reactions. *ACS Omega* **2020**, *5*, 7053–7058.

<sup>42</sup> For a recent computational study of stereoselective Mannich reactions, see: Feng, M.; Mosiagin, I.; Kaiser, D.; Maryasin, B.; Maulide, N. Deployment of Sulfinimines in Charge-Accelerated Sulfonium Rearrangement Enables a Surrogate Asymmetric Mannich Reaction. *J. Am. Chem. Soc.* **2022**, *144*, 13044–13049.

<sup>43</sup> Gentner, T. X.; Mulvey, R. E. Alkali-Metal Mediation: Diversity of Applications in Main-Group Organometallic Chemistry. *Angew. Chem. Int. Ed.* **2021**, *60*, 9247–9262.

<sup>44</sup> Liu, Y.-F.; Zheng, L.; Zhai, D.-D.; Zhang, X.-Y.; Guan, B.-T. Dimeric Potassium Amide-Catalyzed  $\alpha$ -Alkylation of Benzyl Sulfides and 1,3-Dithianes. *Org. Lett.* **2019**, *21*, 5351–5356.

<sup>45</sup> Dougherty, D. A. The Cation– $\pi$  Interaction. *Acc. Chem. Res.* **2013**, *46*, 885–893. (b) Qu, Z.-W.; Zhu, H.; Streubel, R.; Grimme, S. Organo-Group 2 Metal-Mediated Nucleophilic Alkylation of Benzene: Crucial Role of Strong Cation– $\pi$  Interaction. *ACS Catal.* **2023**, *13*, 1686–1692.

<sup>46</sup> Liu, W.-B.; Schuman, D. P.; Yang, Y.-F.; Toutov, A. A.; Liang, Y.; Klare, H. F. T.; Nesnas, N.; Oestreich, M.; Blackmond, D. G.; Virgil, S. C.; Banerjee, S.; Zare, R. N.; Grubbs, R. H.; Houk, K. N.; Stoltz, B. M. Potassium Tert-Butoxide-Catalyzed Dehydrogenative C–H Silylation of Heteroaromatics: A Combined Experimental and Computational Mechanistic Study. *J. Am. Chem. Soc.* **2017**, *139* (20), 6867–6879.

<sup>47</sup> (a) Fustero, S.; Mojarrad, F.; Carrión, M. D. P.; Sanz-Cervera, J. F.; Aceña, J. L. Organocatalytic Anti-Selective Mannich Reactions with Fluorinated Aldimines: Synthesis of Anti- $\gamma$ -Fluoroalkyl- $\gamma$ -Amino Alcohols. *European Journal of Organic Chemistry* **2009**, *2009* (30), 5208–5214. (b) Sundararaju, B.; Sridhar, T.; Achard, M.; Sharma, G. V. M.; Bruneau, C. Preparation of Sugar  $\beta$ -Amino Acid Derivatives with Cyclic Structures by Ring-Closing Metathesis. *European Journal of Organic Chemistry* **2010**, *2010* (31), 6092–6096.

<sup>48</sup> (a) Yang, Q.; Ney, J. E.; Wolfe, J. P. Palladium-Catalyzed Tandem N-Arylation/Carboamination Reactions for the Stereoselective Synthesis of N-Aryl-2-Benzyl Pyrrolidines. *Org. Lett.* **2005**, *7* (13), 2575–2578. (b) Ney, J. E.; Wolfe, J. P. Selective Synthesis of 5- or 6-Aryl Octahydrocyclopenta[b]Pyrroles from a Common Precursor through Control of Competing Pathways in a Pd-Catalyzed Reaction. *J. Am. Chem. Soc.* **2005**, *127* (24), 8644–8651. (c) Lemen, G. S.; Wolfe, J. P. Cascade Intramolecular N-Arylation/Intermolecular Carboamination Reactions for the Construction of Tricyclic Heterocycles. *Org. Lett.* **2011**, *13* (12), 3218–3221. (d) Bertrand, M. B.; Leathen, M. L.; Wolfe, J. P. Mild Conditions for the Synthesis of Functionalized Pyrrolidines via Pd-Catalyzed Carboamination Reactions. *Org. Lett.* **2007**, *9* (3), 457–460.

<sup>49</sup> (a) Sirvent, J. A.; Foubelo, F.; Yus, M. Stereoselective Synthesis of Indoline, Tetrahydroquinoline, and Tetrahydrobenzazepine Derivatives from o-Bromophenyl N-Tert-Butylsulfinyl Aldimines. *J. Org. Chem.* **2014**, *79* (3), 1356–1367. (b) Ding, L.; Chen, J.; Hu, Y.; Xu, J.; Gong, X.; Xu, D.; Zhao, B.; Li, H. Aminative Umpolung of Aldehydes to  $\alpha$ -Amino Anion Equivalents for Pd-Catalyzed Allylation: An Efficient Synthesis of Homoallylic Amines. *Org. Lett.* **2014**, *16* (3), 720–723. (c) Notte, G. T.; Leighton, J. L. A New Silicon Lewis Acid for Highly Enantioselective Mannich Reactions of Aliphatic Ketone-Derived Hydrazones. *J. Am. Chem. Soc.* **2008**, *130* (21), 6676–6677.

<sup>50</sup> For the synthesis of and ring opening of a 1-Azabicyclo[3.1.0]Hexane tag, see the SI of: Breton, N. L.; Martinho, M.; Kabytaev, K.; Topin, J.; Mileo, E.; Blocquel, D.; Habchi, J.; Longhi, S.; Rockenbauer, A.; Golebiowski, J.; Guigliarelli, B.; Marque, S. R. A.; Belle, V. Diversification of EPR Signatures in Site Directed Spin Labeling Using a  $\beta$ -Phosphorylated Nitroxide. *Phys. Chem. Chem. Phys.* **2014**, *16* (9), 4202–4209.

<sup>51</sup> Hayashi, K.; Kujime, E.; Katayama, H.; Sano, S.; Shiro, M.; Nagao, Y. Synthesis and Reaction of 1-Azabicyclo[3.1.0]Hexane. *Chemical and Pharmaceutical Bulletin* **2009**, *57* (10), 1142–1146.

<sup>52</sup> Alexy, E. J.; Zhang, H.; Stoltz, B. M. Catalytic Enantioselective Synthesis of Acyclic Quaternary Centers: Palladium-Catalyzed Decarboxylative Allylic Alkylation of Fully Substituted Acyclic Enol Carbonates. *J. Am. Chem. Soc.* **2018**, *140* (32), 10109–10112.

<sup>53</sup> (a) Wilckens, K.; Lentz, D.; Czekelius, C. Synthesis of Gold Complexes Bearing Sterically Highly Encumbered, Chiral Carbene Ligands. *Organometallics* **2011**, *30* (6), 1287–1290. (b) Vinh, N. B.; Drinkwater, N.; Malcolm, T. R.; Kassiou, M.; Lucantoni, L.; Grin, P. M.; Butler, G. S.; Duffy, S.; Overall, C. M.; Avery, V. M.; Scammells, P. J.; McGowan, S. Hydroxamic Acid Inhibitors Provide Cross-Species Inhibition of Plasmodium M1 and M17 Aminopeptidases. *J. Med. Chem.* **2019**, *62* (2), 622–640.

<sup>54</sup> Safe and Convenient Procedure for Solvent Purification. A. M. Pangborn, M. A. Giardello, R. H. Grubbs, R. K. Rosen, F. J. Timmers, *Organometallics* **1996**, *15*, 1518–1520.

## **APPENDIX 1**

*Spectra Relevant to Chapter 1:  
Diastereoselective Mannich Reaction*

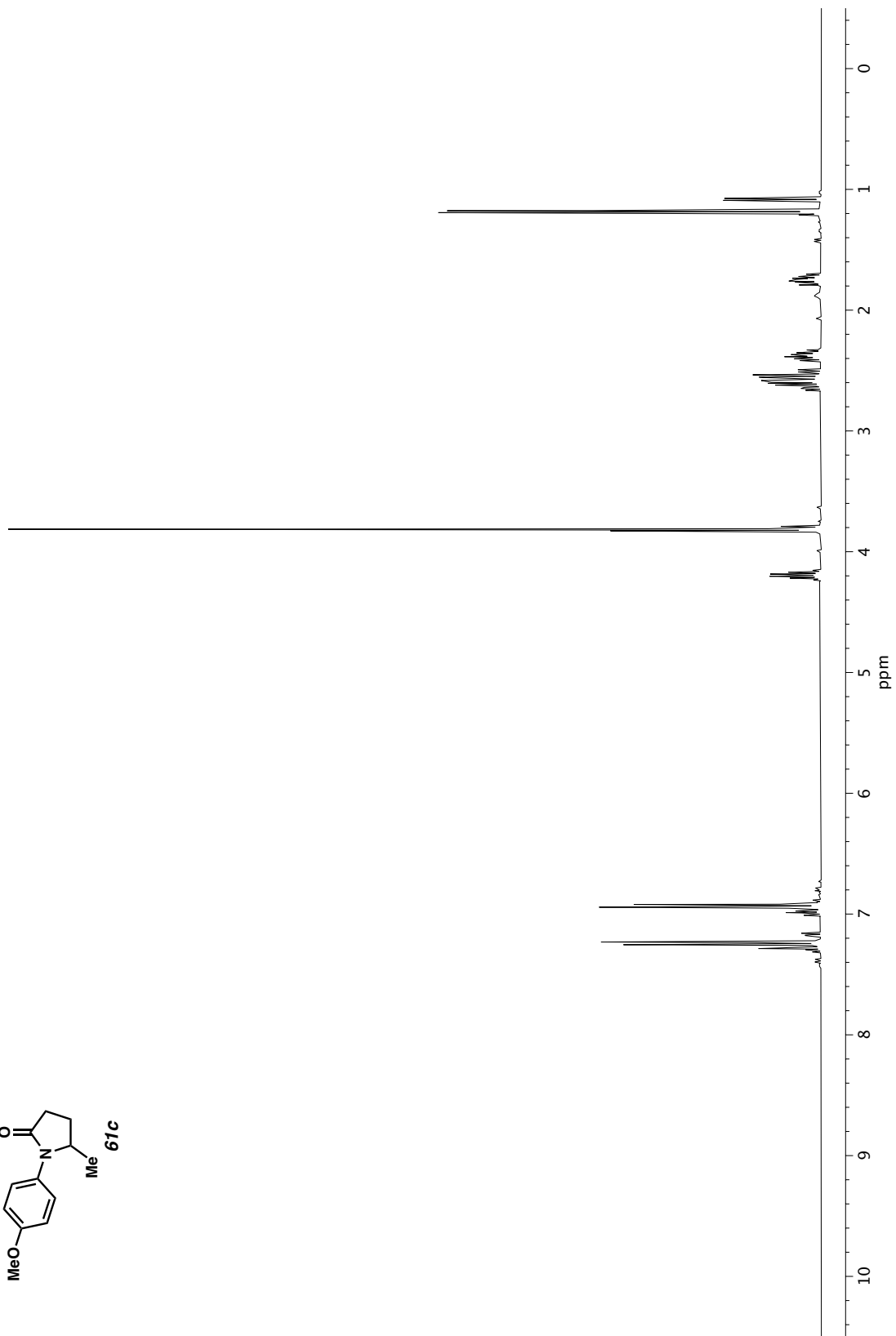
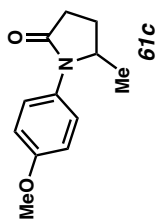


**Figure A1.1** <sup>1</sup>H NMR (400 MHz, CDCl<sub>3</sub>) of compound **61c**.

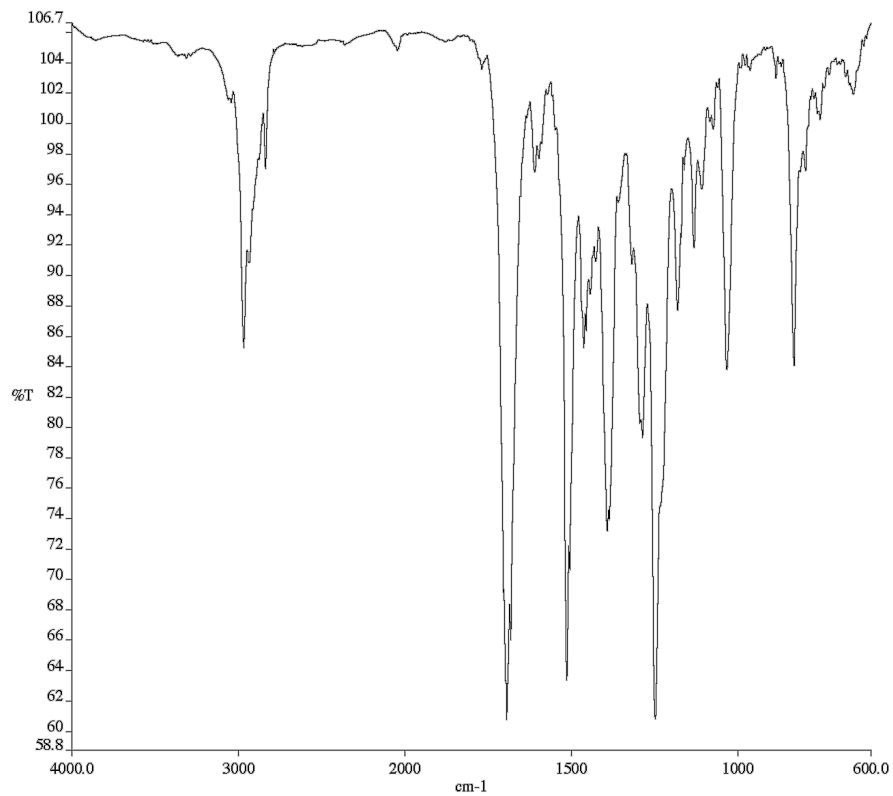


**Figure A1.2** Infrared spectrum (Thin Film, NaCl) of compound **61c**.

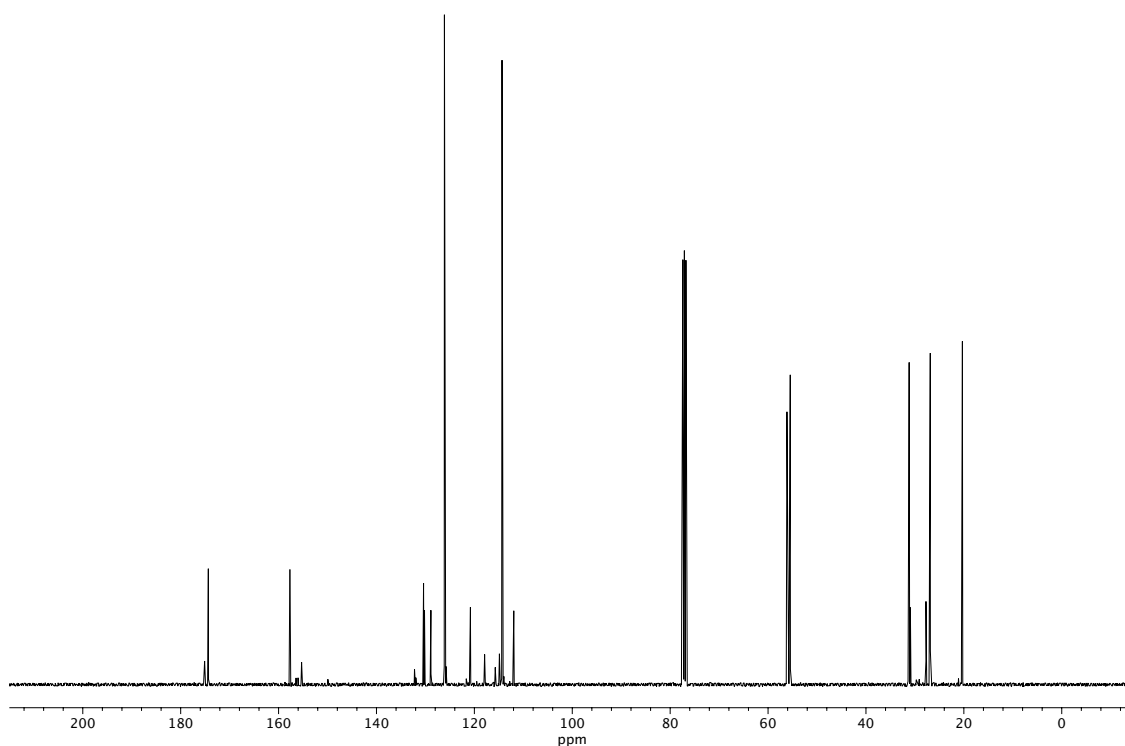


**Figure A1.3** <sup>13</sup>C NMR (100 MHz, CDCl<sub>3</sub>) of compound **61c**.

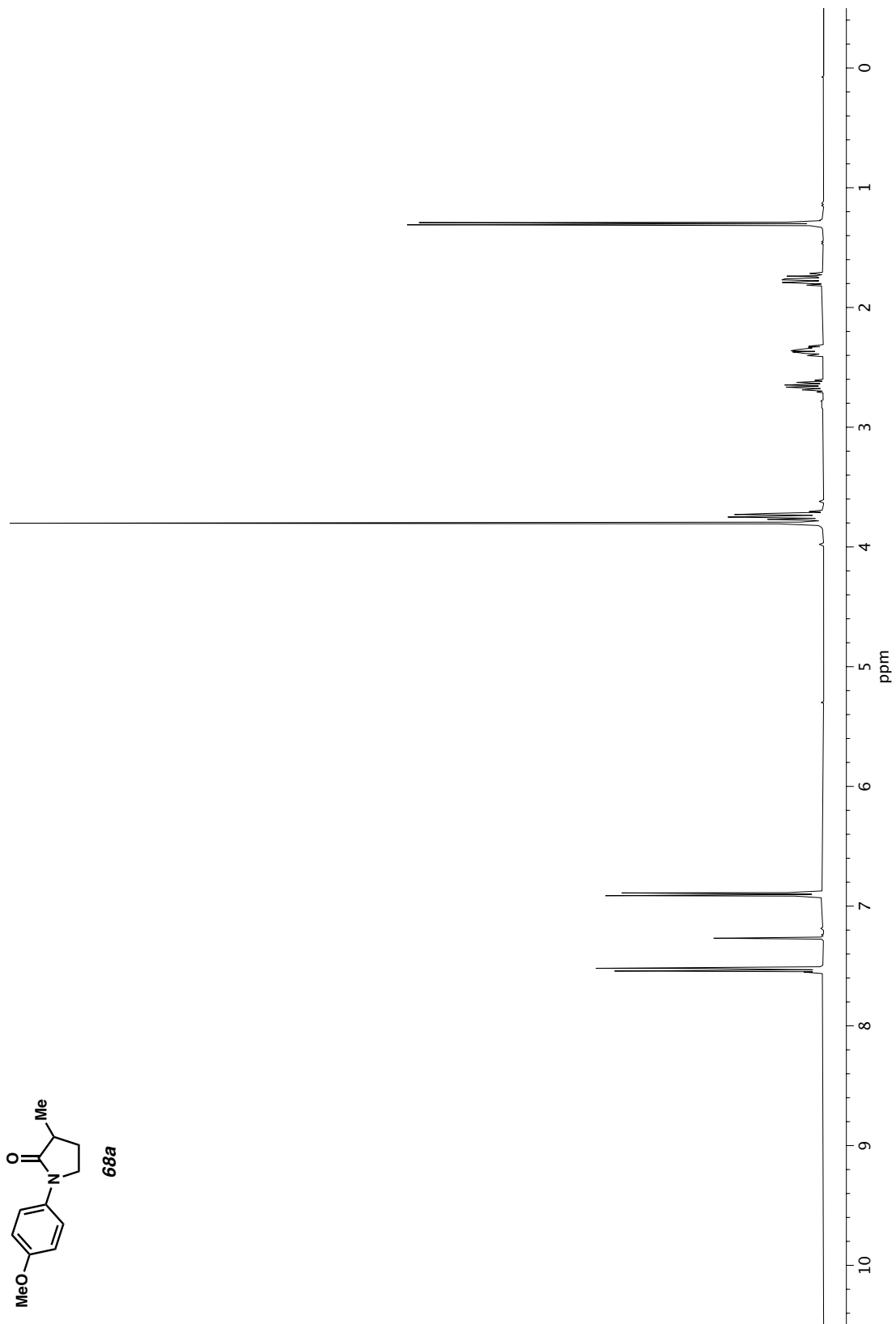
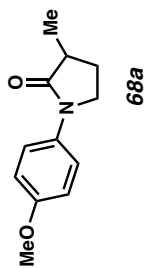


**Figure A1.4**  $^1\text{H}$  NMR (400 MHz,  $\text{CDCl}_3$ ) of compound **68a**.



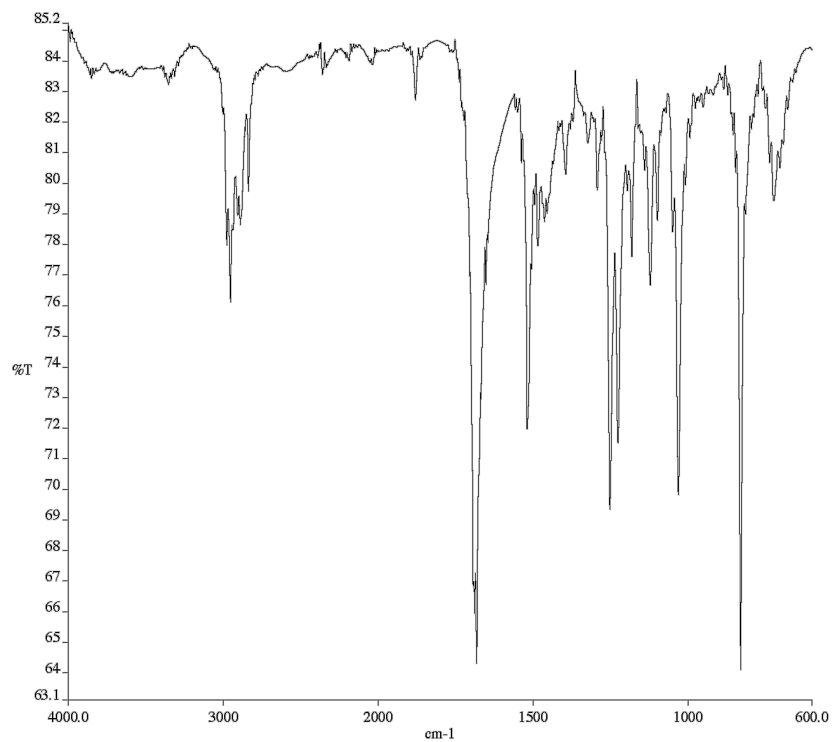


**Figure A1.5** Infrared spectrum (Thin Film, NaCl) of compound **68a**.

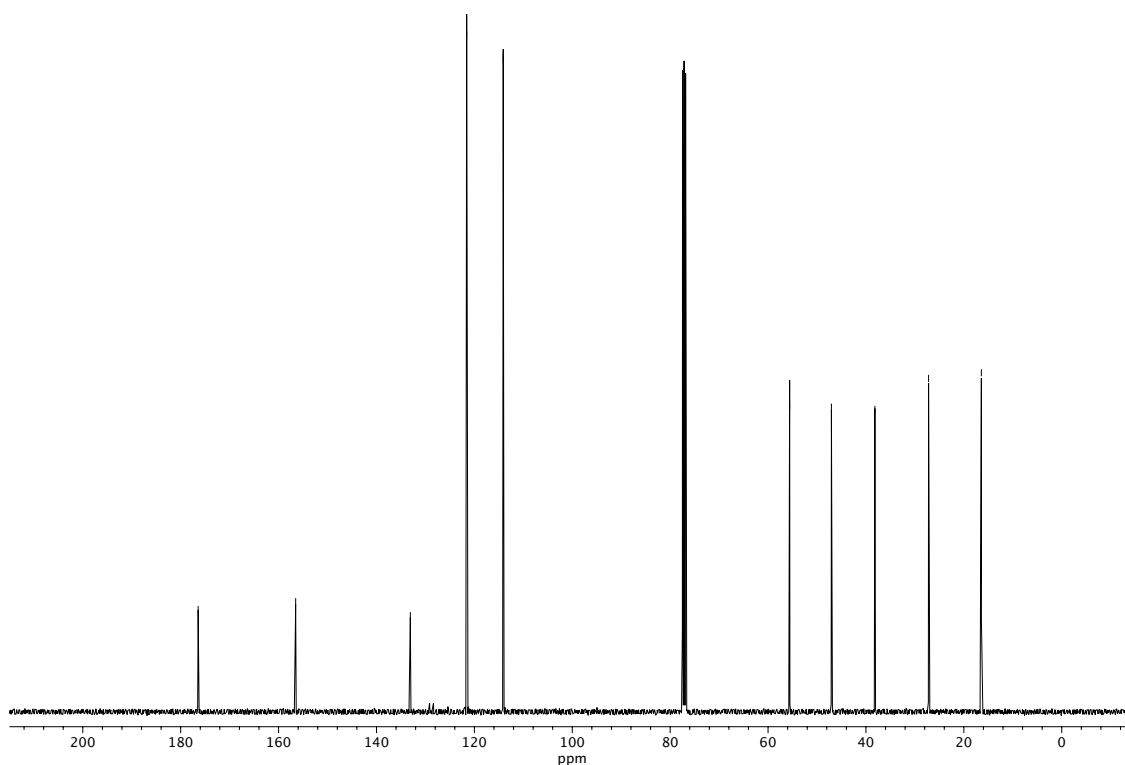


**Figure A1.6** <sup>13</sup>C NMR (125 MHz, CDCl<sub>3</sub>) of compound **68a**.

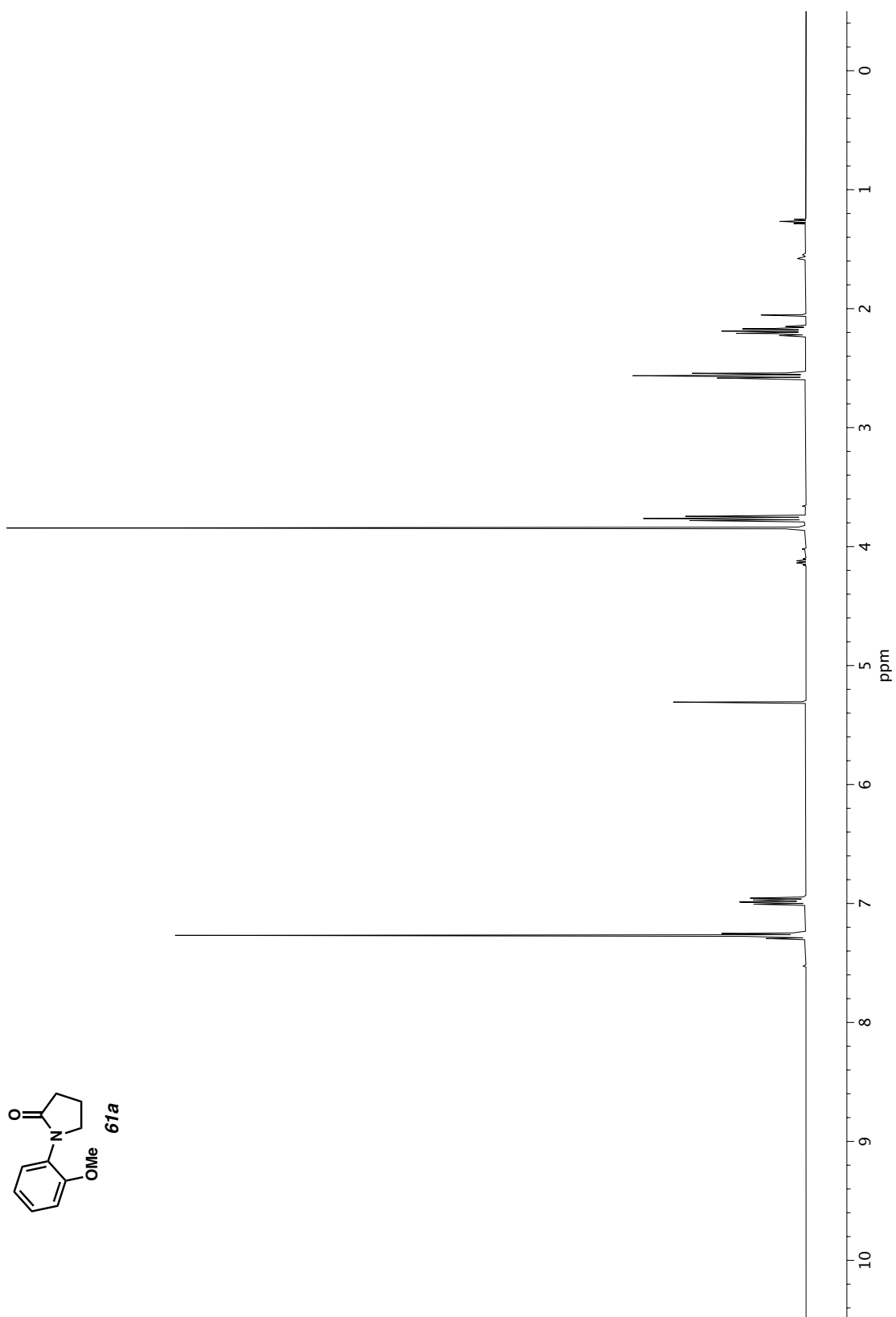


**Figure A1.7** <sup>1</sup>H NMR (400 MHz, CDCl<sub>3</sub>) of compound **61a**.

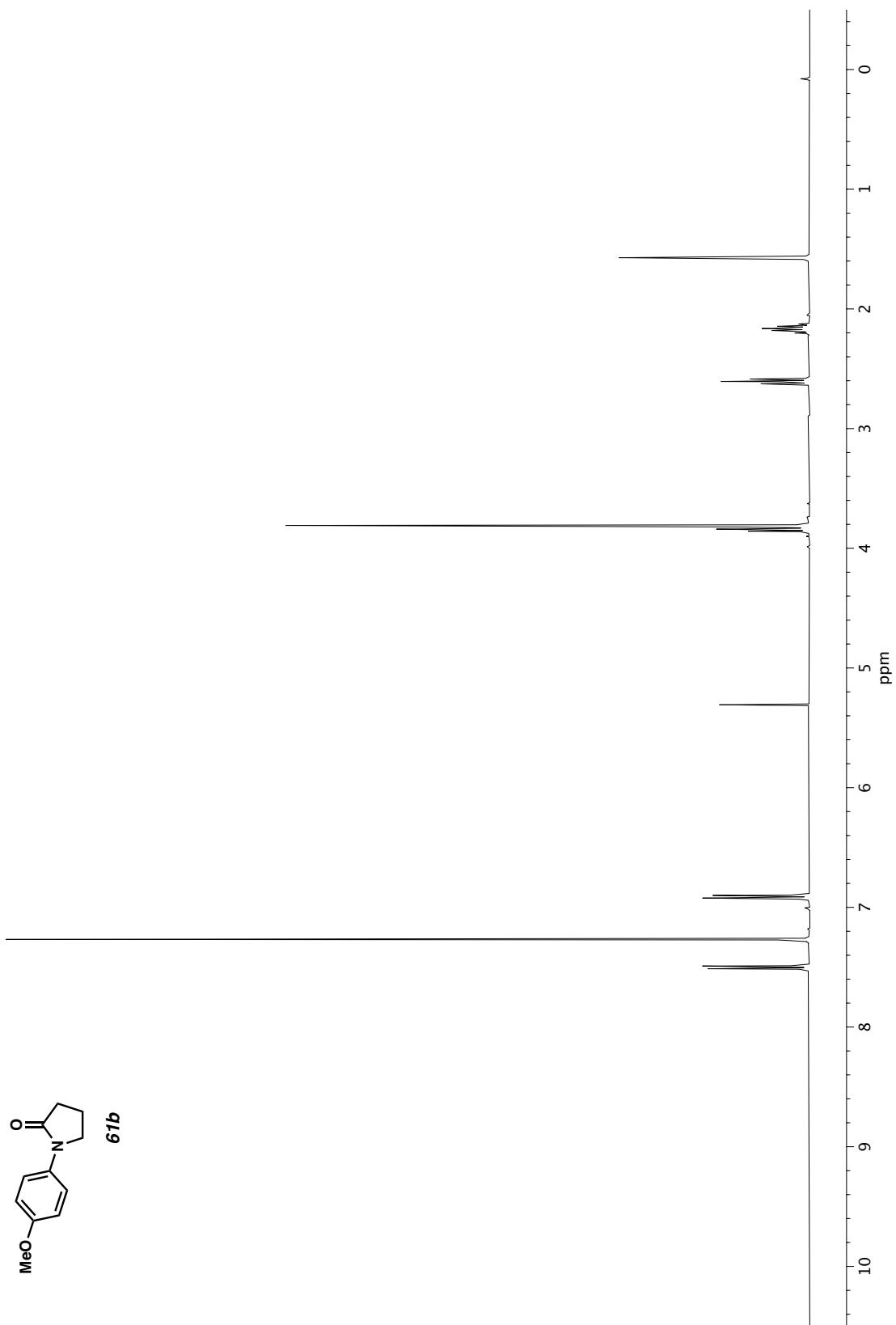


**Figure A1.8** <sup>1</sup>H NMR (400 MHz, CDCl<sub>3</sub>) of compound **61b**.

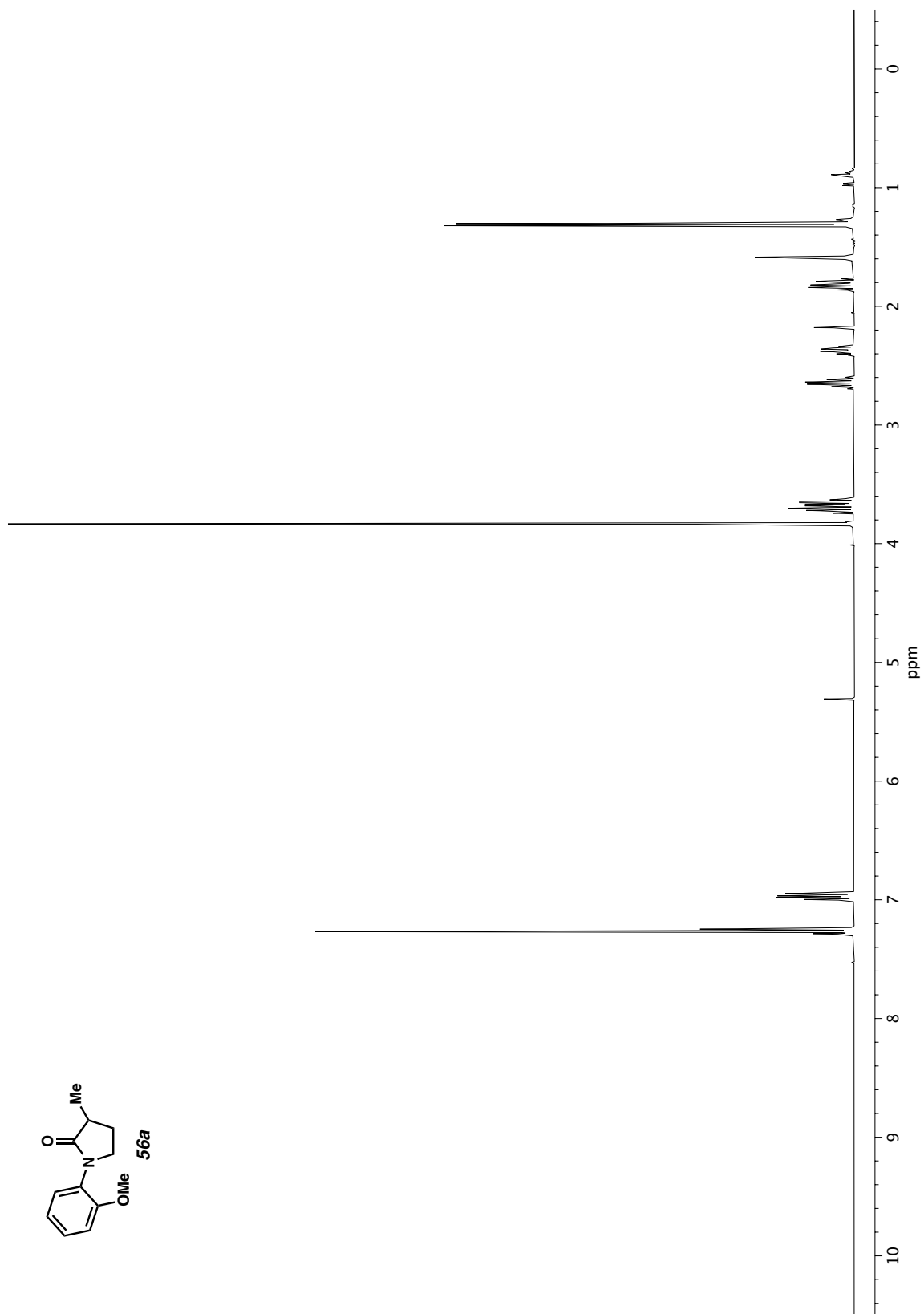
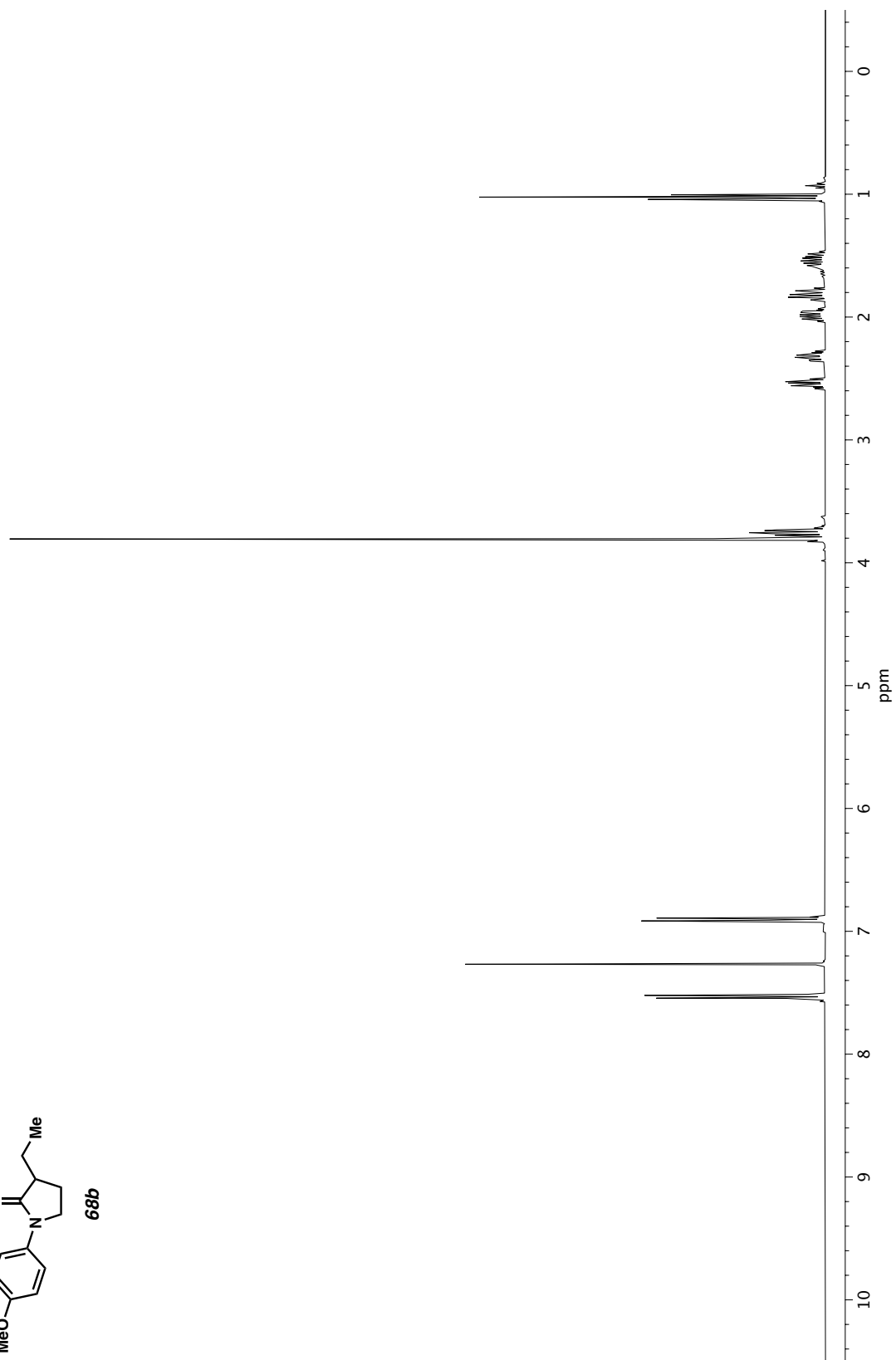
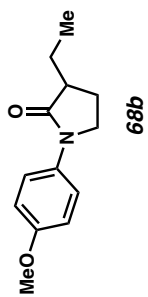
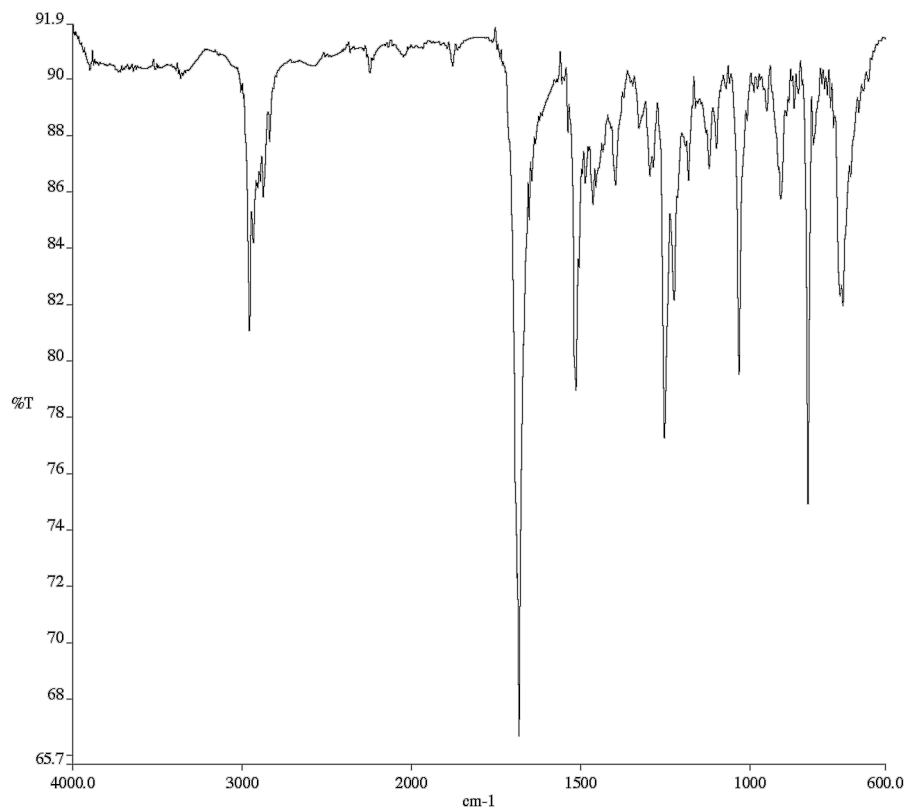


Figure A1.9  $^1\text{H}$  NMR (400 MHz,  $\text{CDCl}_3$ ) of compound 56a.



**Figure A1.10** <sup>1</sup>H NMR (400 MHz, CDCl<sub>3</sub>) of compound **68b**.



**Figure A1.11** Infrared spectrum (Thin Film, NaCl) of compound **68b**.

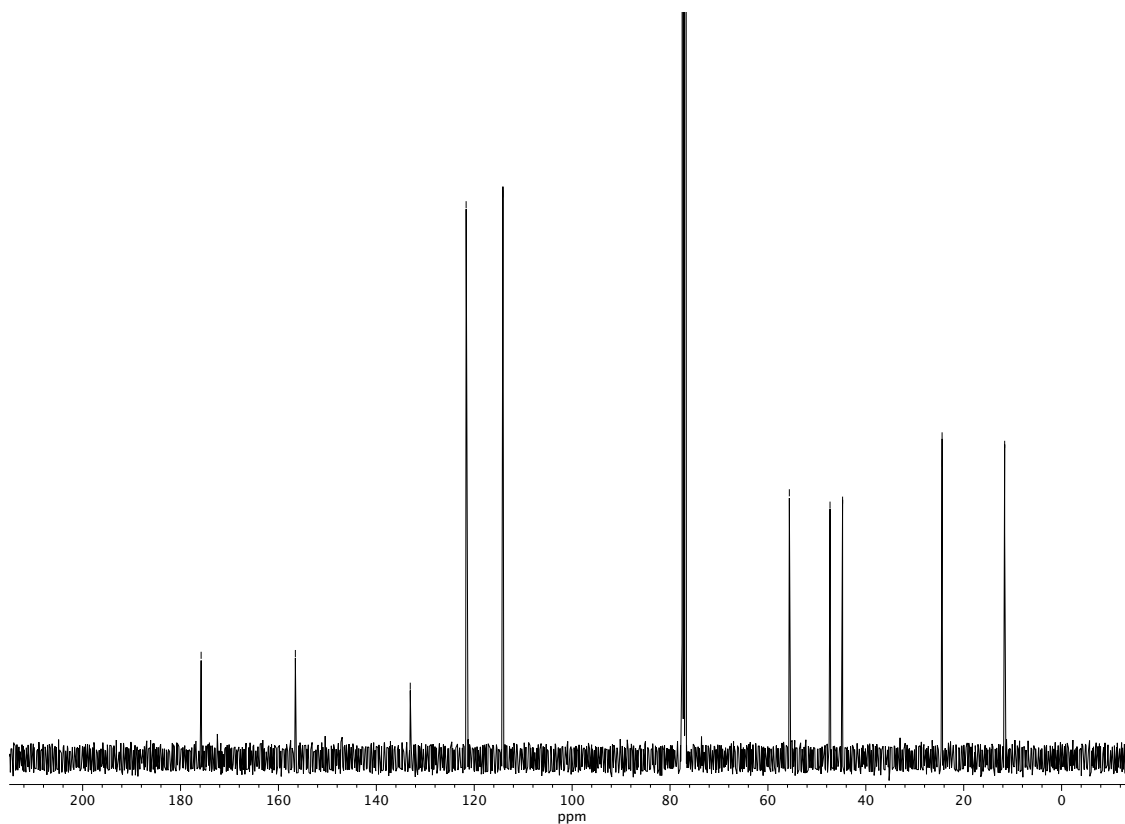


**Figure A1.12** <sup>13</sup>C NMR (100 MHz, CDCl<sub>3</sub>) of compound **68b**.

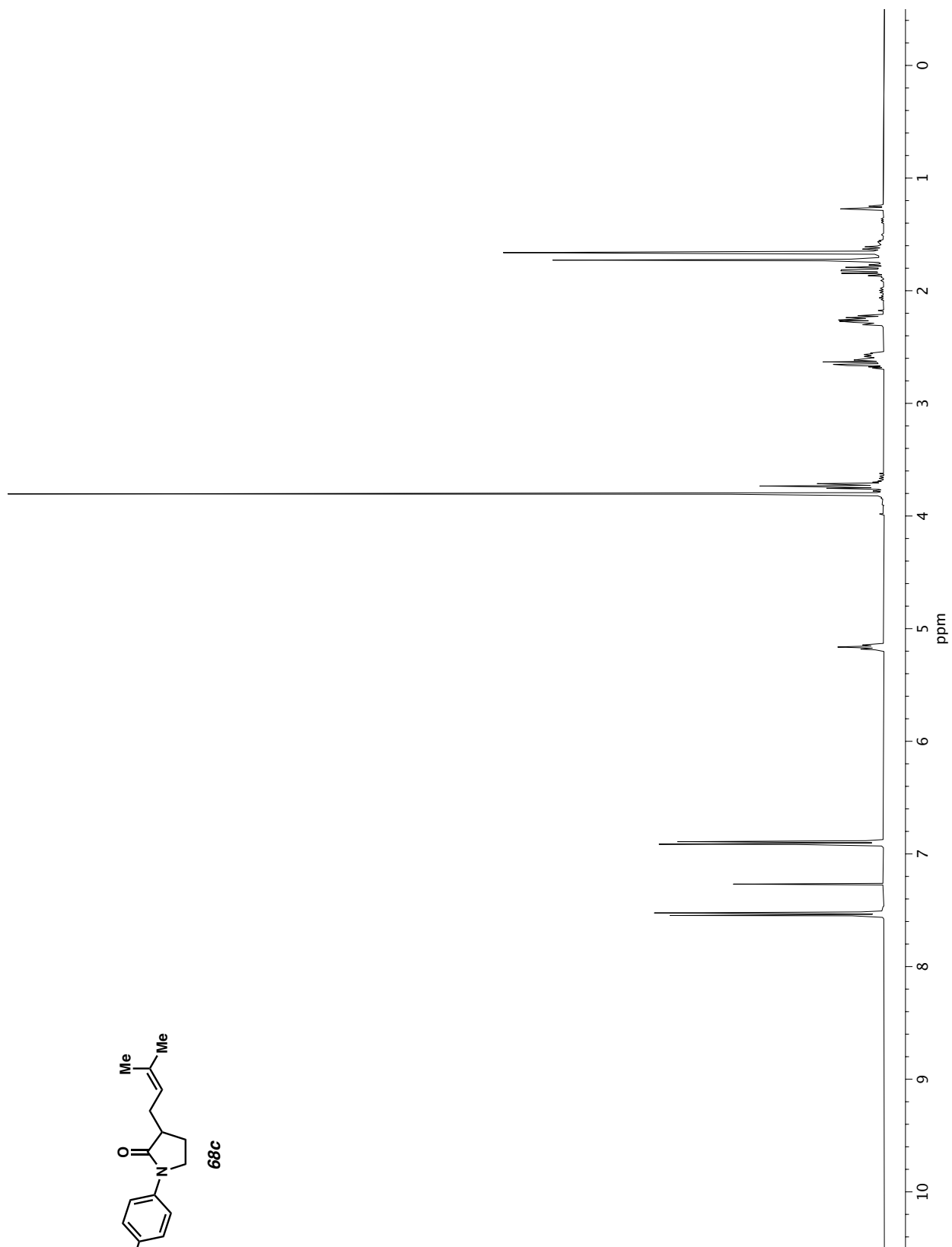
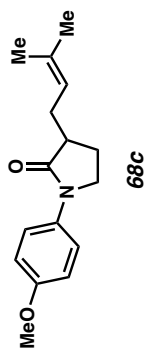


**Figure A1.13** <sup>1</sup>H NMR (400 MHz, CDCl<sub>3</sub>) of compound **68c**.

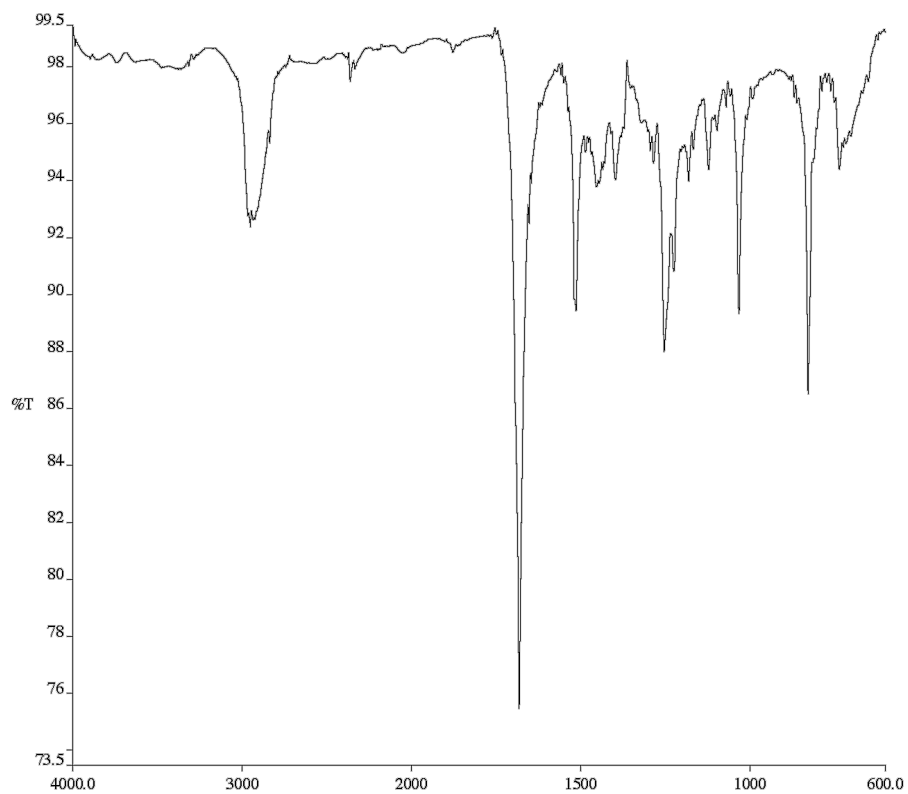


**Figure A1.14** Infrared spectrum (Thin Film, NaCl) of compound **68c**.

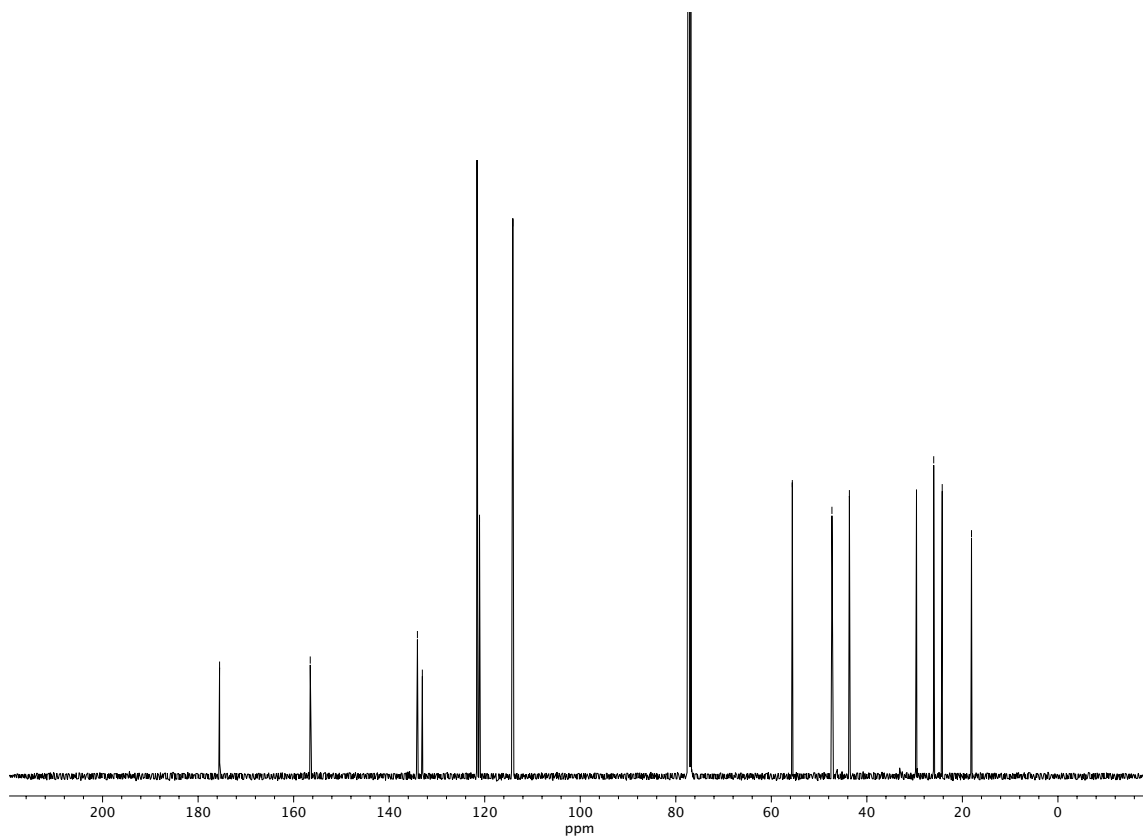


**Figure A1.15** <sup>13</sup>C NMR (100 MHz, CDCl<sub>3</sub>) of compound **68c**.



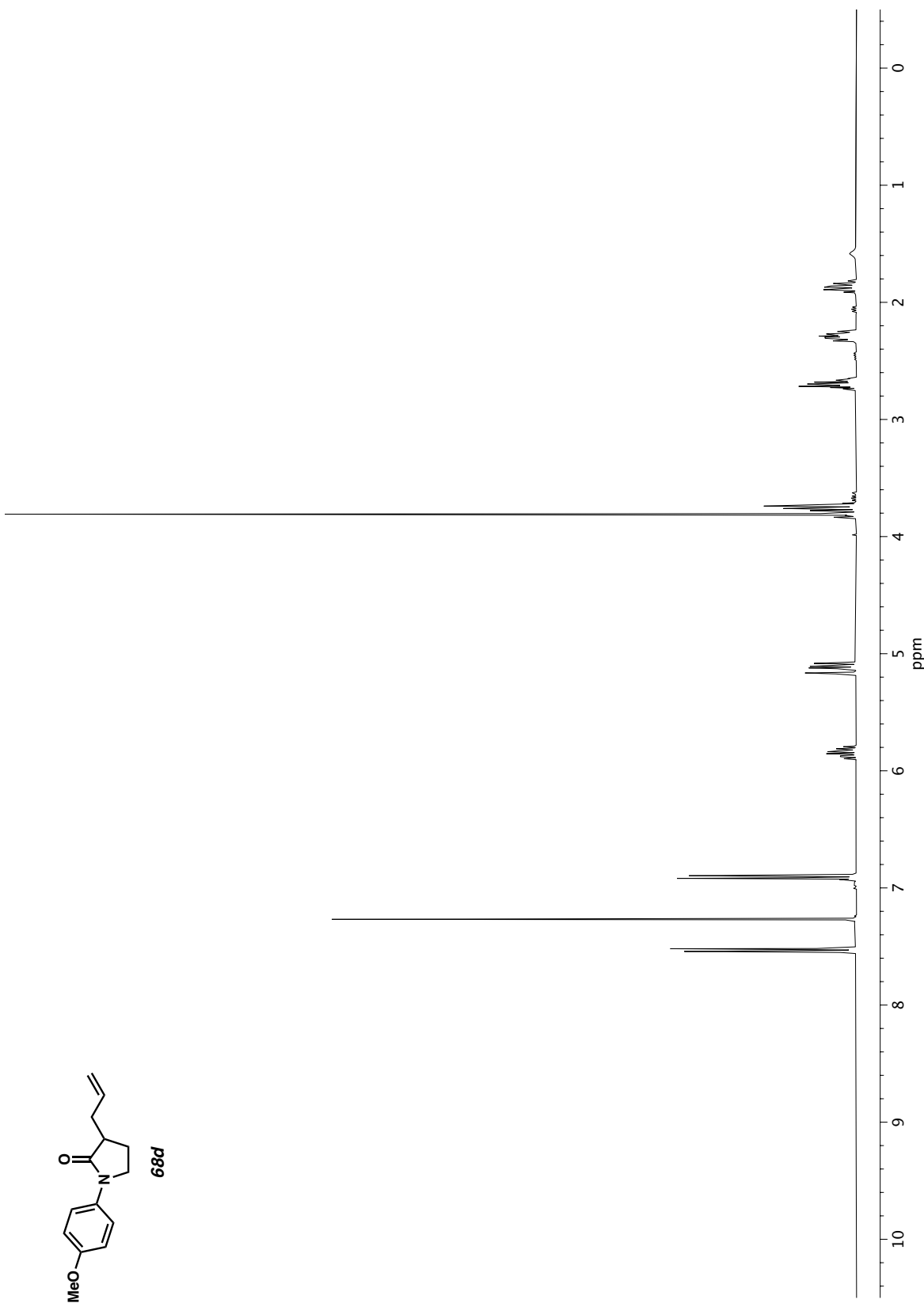
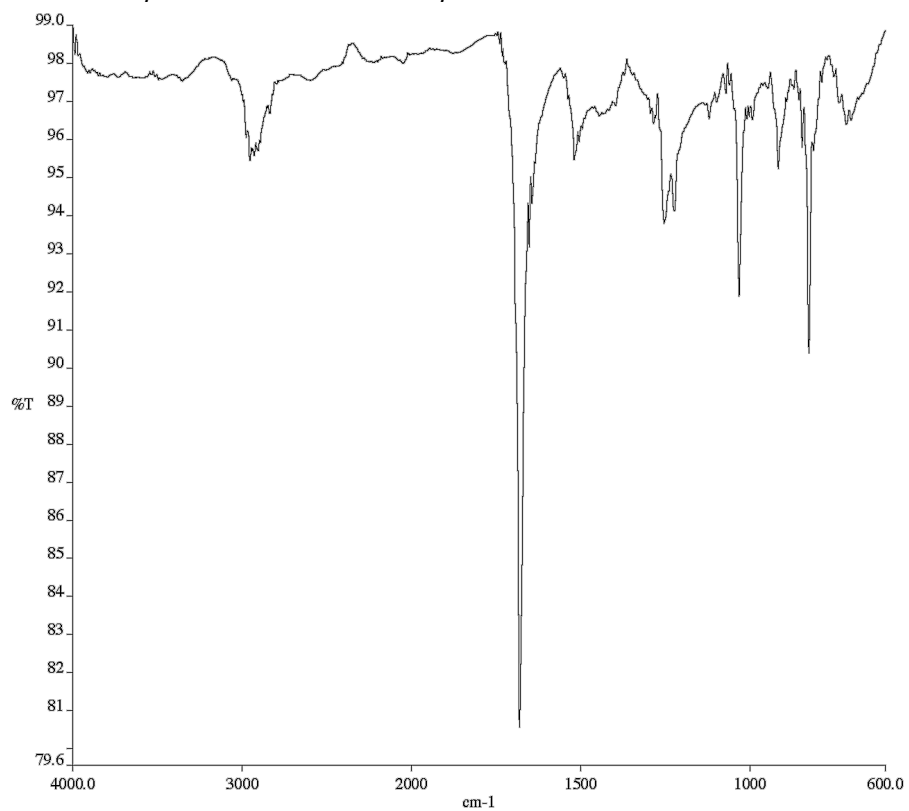
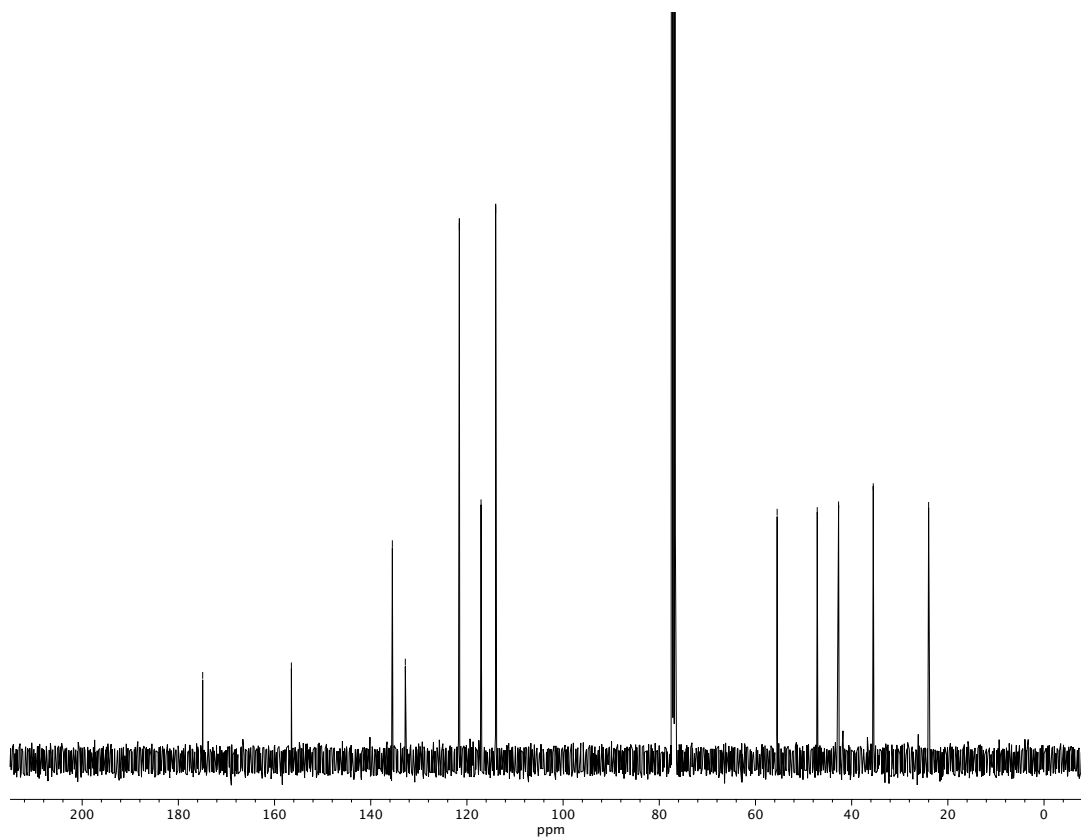


Figure A1.16 <sup>1</sup>H NMR (400 MHz, CDCl<sub>3</sub>) of compound **68d**.



**Figure A1.17** Infrared spectrum (Thin Film, NaCl) of compound **68d**.



**Figure A1.18** <sup>13</sup>C NMR (100 MHz, CDCl<sub>3</sub>) of compound **68d**.

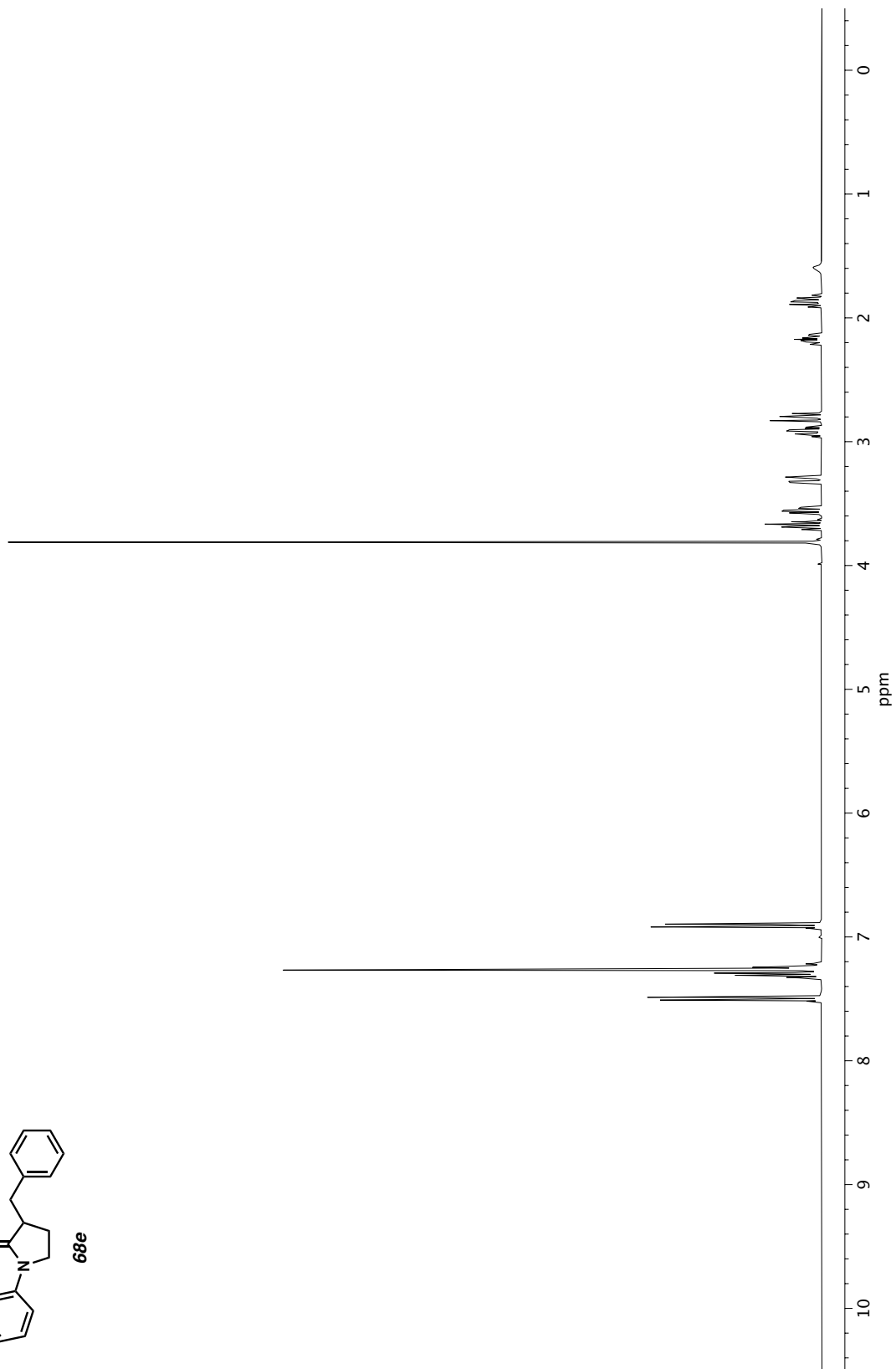
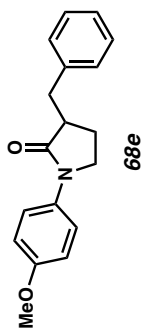
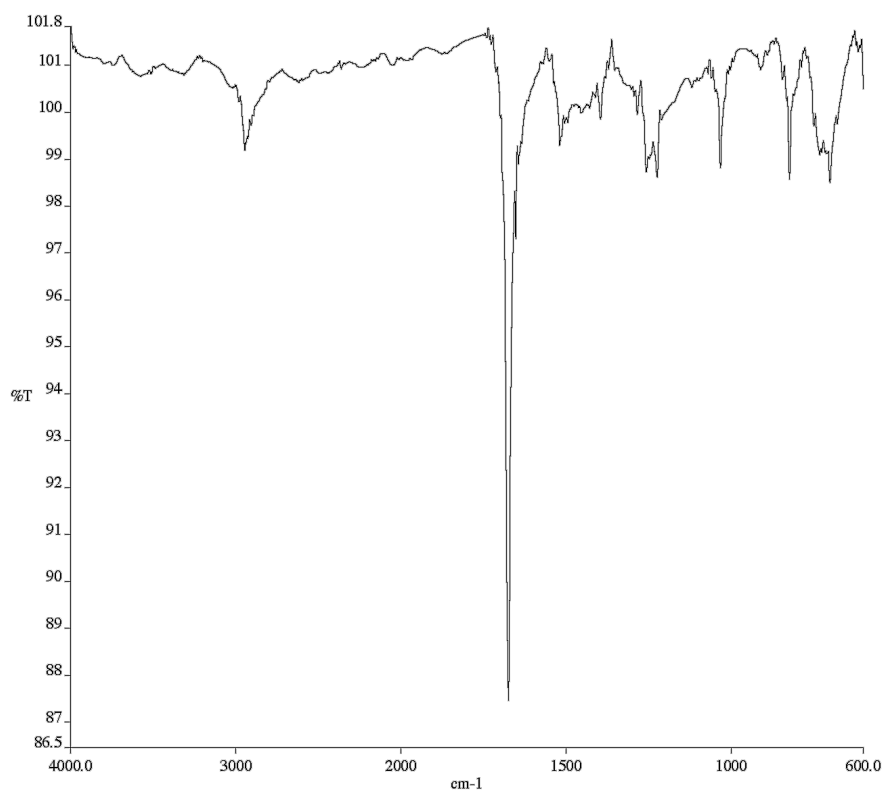
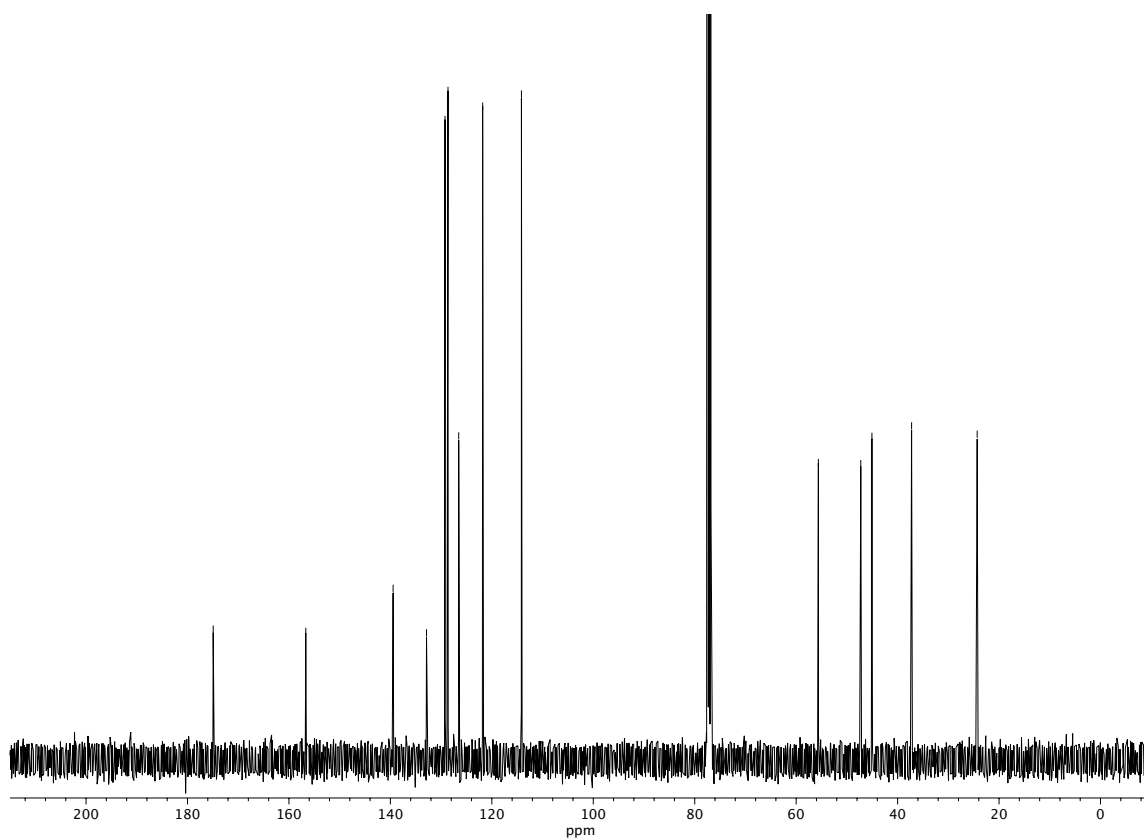


Figure A1.19 <sup>1</sup>H NMR (400 MHz, CDCl<sub>3</sub>) of compound 68e.



**Figure A1.20** Infrared spectrum (Thin Film, NaCl) of compound **68e**.



**Figure A1.21** <sup>13</sup>C NMR (100 MHz, CDCl<sub>3</sub>) of compound **68e**.

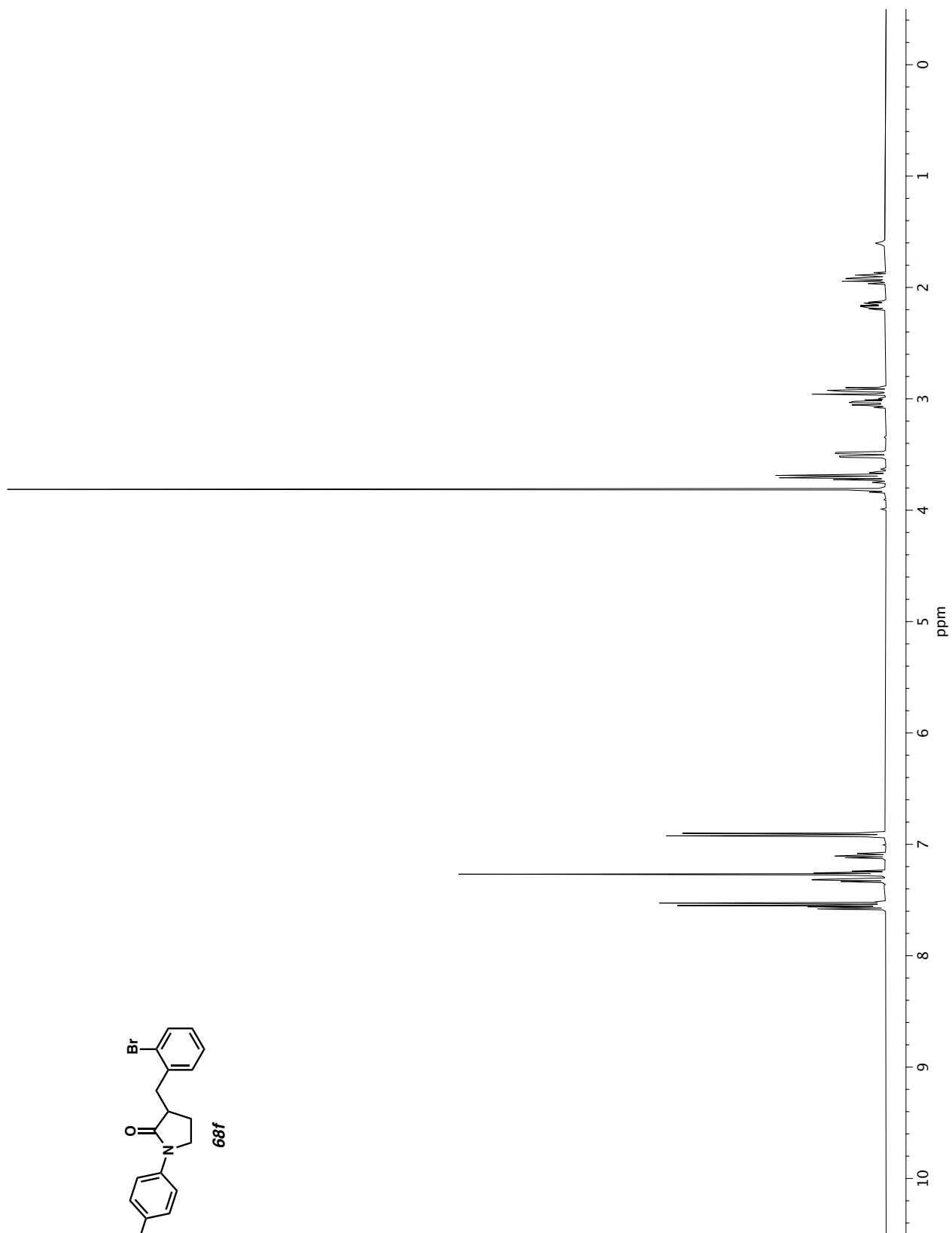
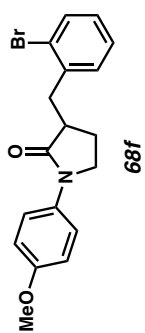
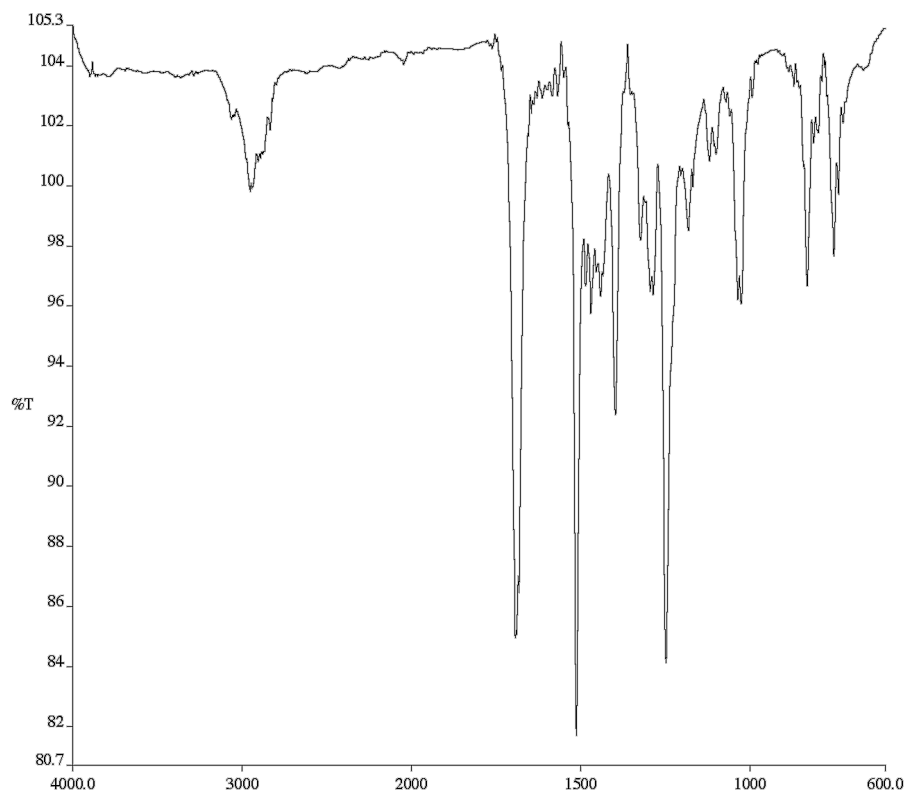
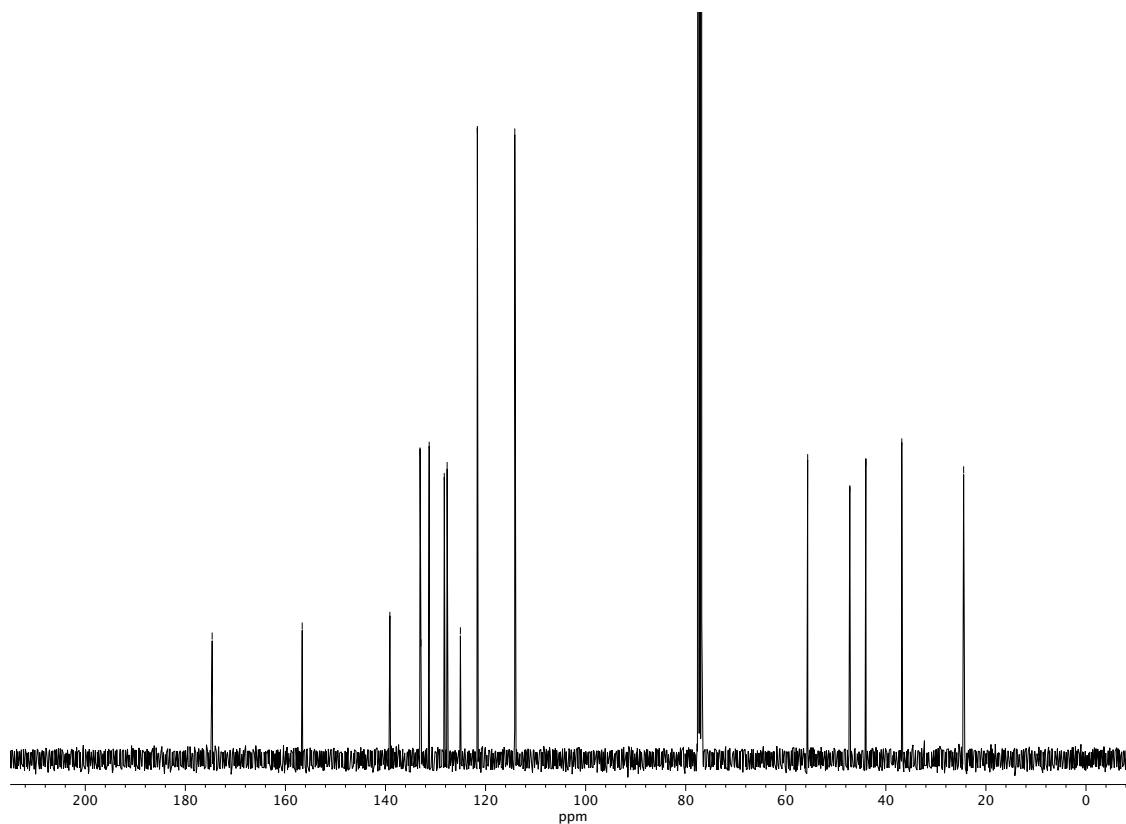


Figure A1.22 <sup>1</sup>H NMR (400 MHz, CDCl<sub>3</sub>) of compound 68f.



**Figure A1.23** Infrared spectrum (Thin Film, NaCl) of compound **68f**.



**Figure A1.24** <sup>13</sup>C NMR (100 MHz, CDCl<sub>3</sub>) of compound **68f**.

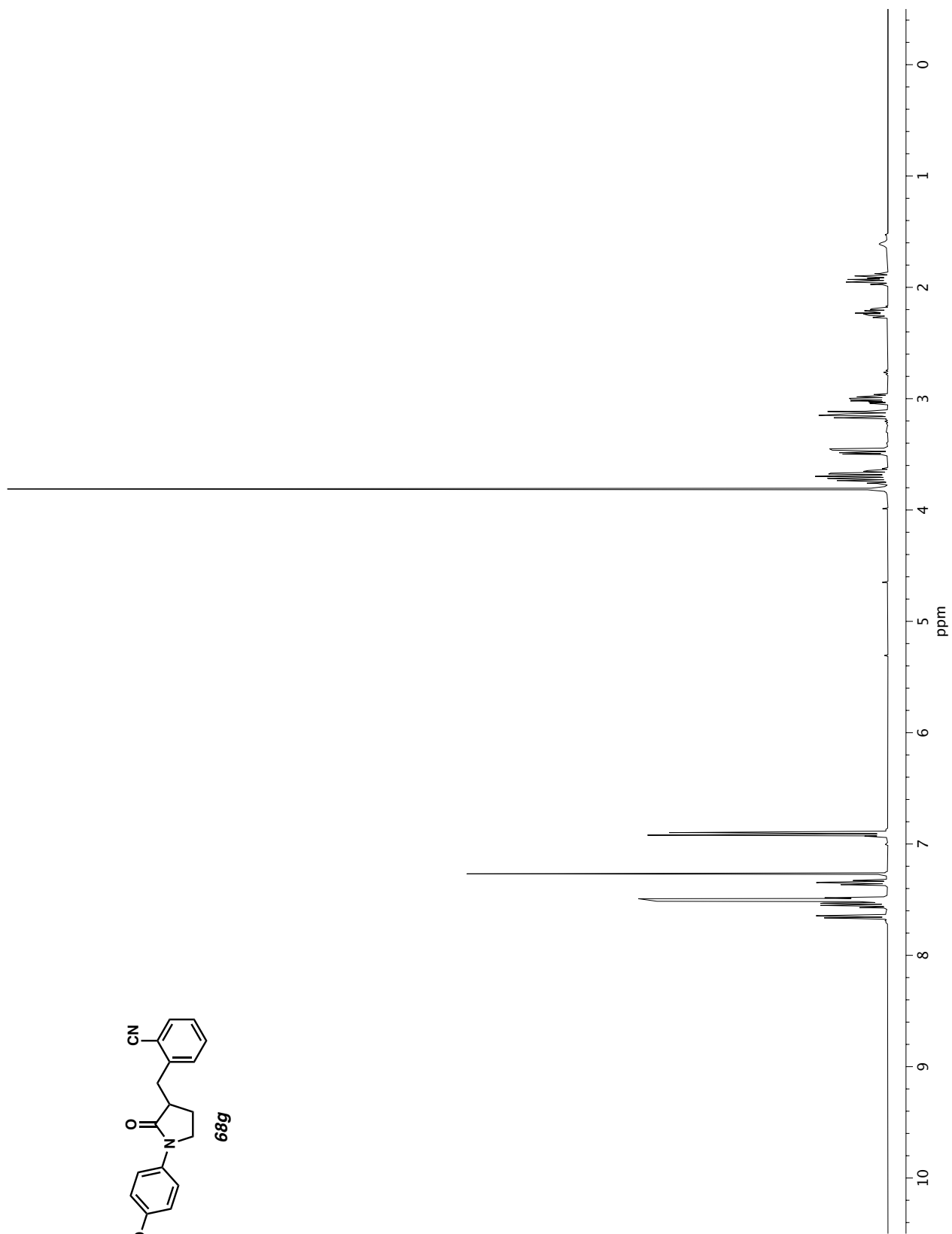
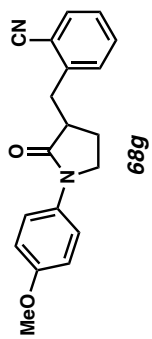


**Figure A1.25**  $^1\text{H}$  NMR (400 MHz,  $\text{CDCl}_3$ ) of compound **68g**.

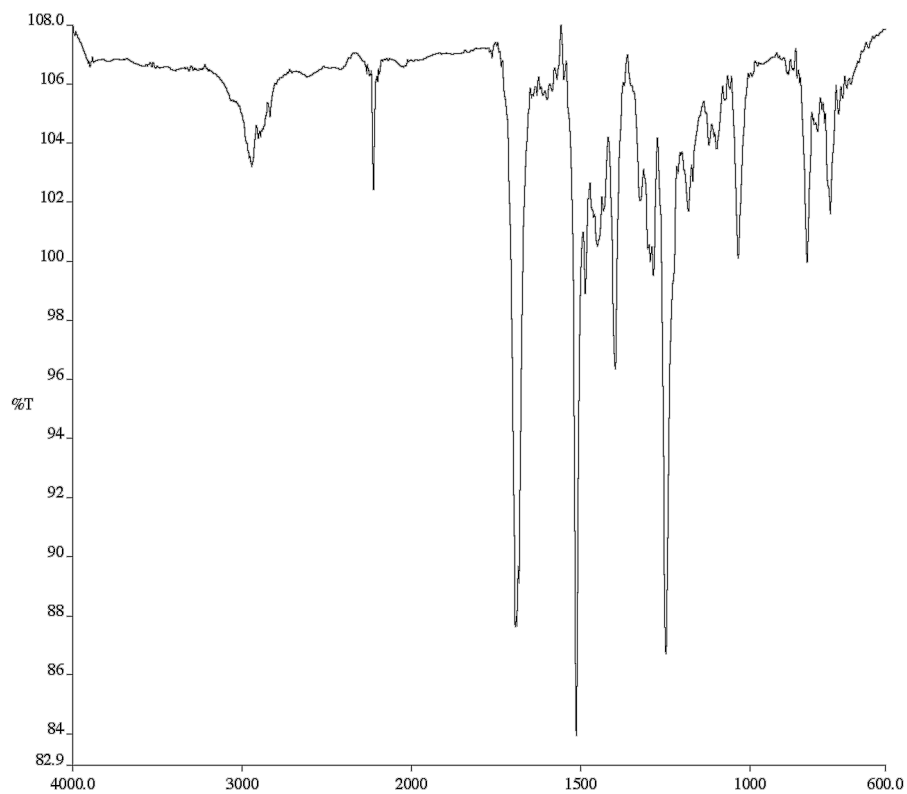


**Figure A1.26** Infrared spectrum (Thin Film, NaCl) of compound **68g**.

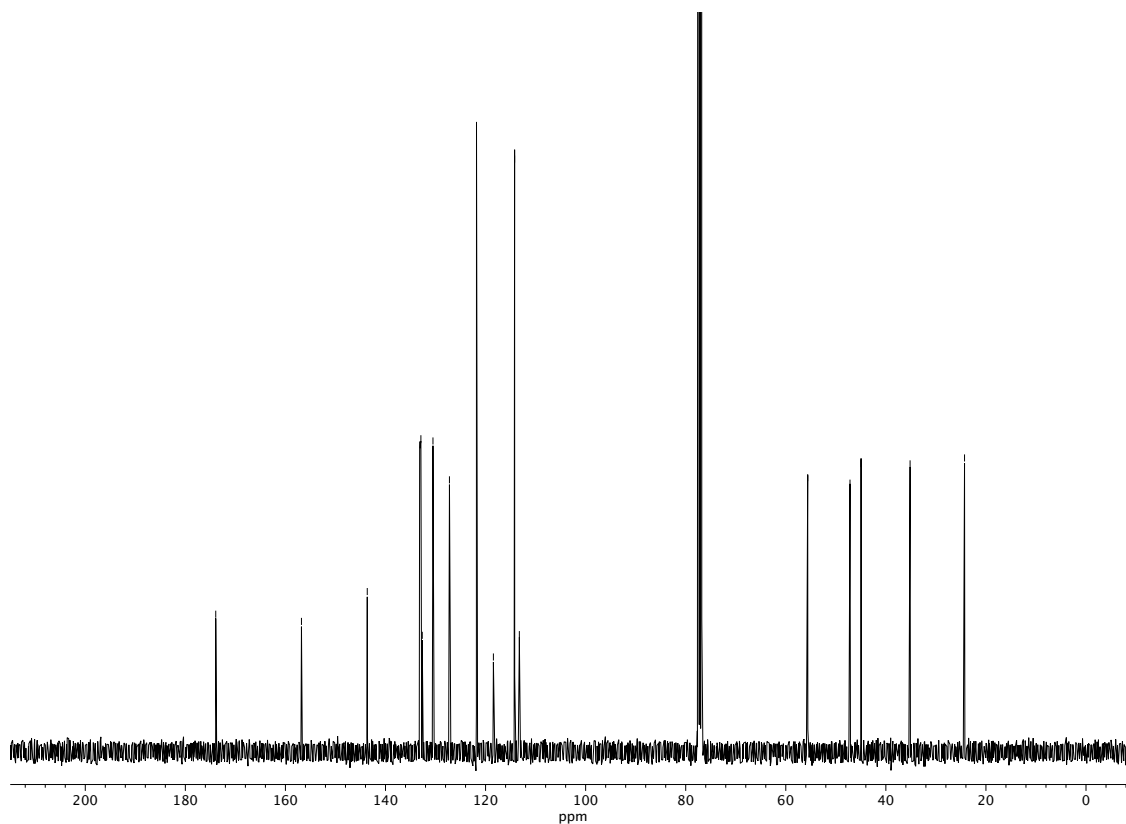


**Figure A1.27** <sup>13</sup>C NMR (100 MHz, CDCl<sub>3</sub>) of compound **68g**.



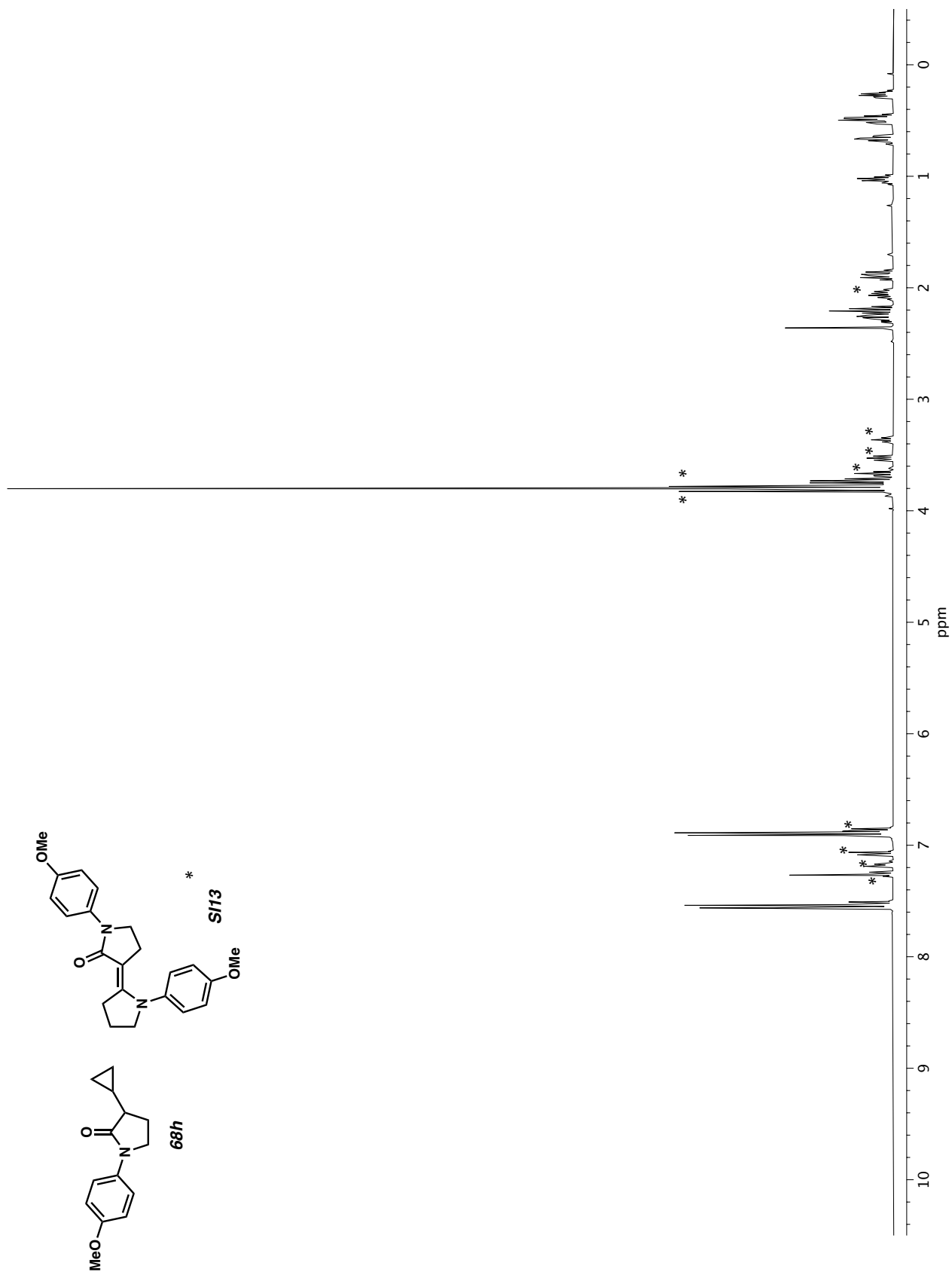
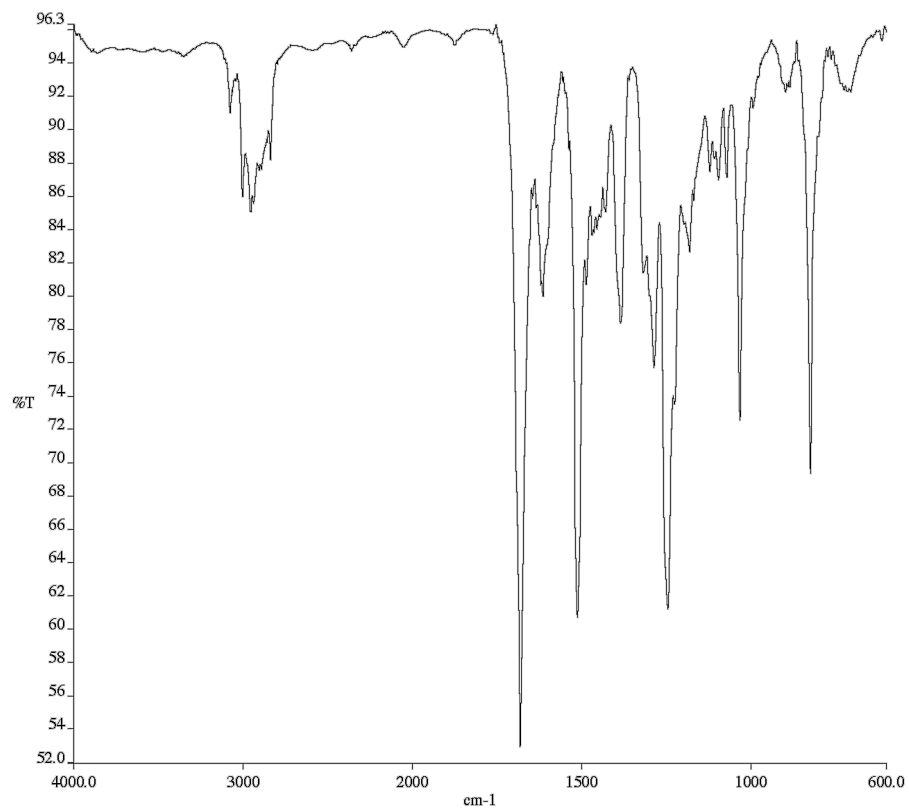
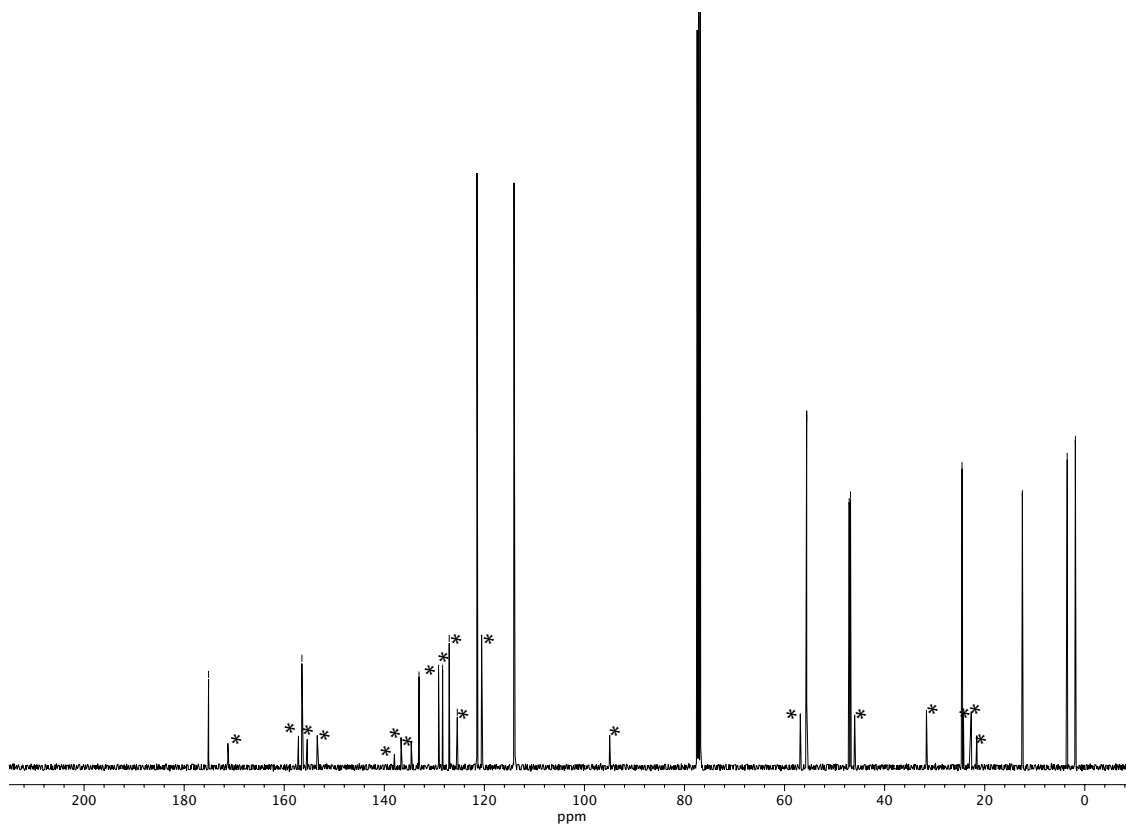


Figure A1.28  $^1\text{H}$  NMR (400 MHz,  $\text{CDCl}_3$ ) of compound **68h** + **S113** (4:1).



**Figure A1.29** Infrared spectrum (Thin Film, NaCl) of compound **68h** + **SI13** (4:1).



**Figure A1.30** <sup>13</sup>C NMR (100 MHz, CDCl<sub>3</sub>) of compound **68h** + **SI13** (4:1)

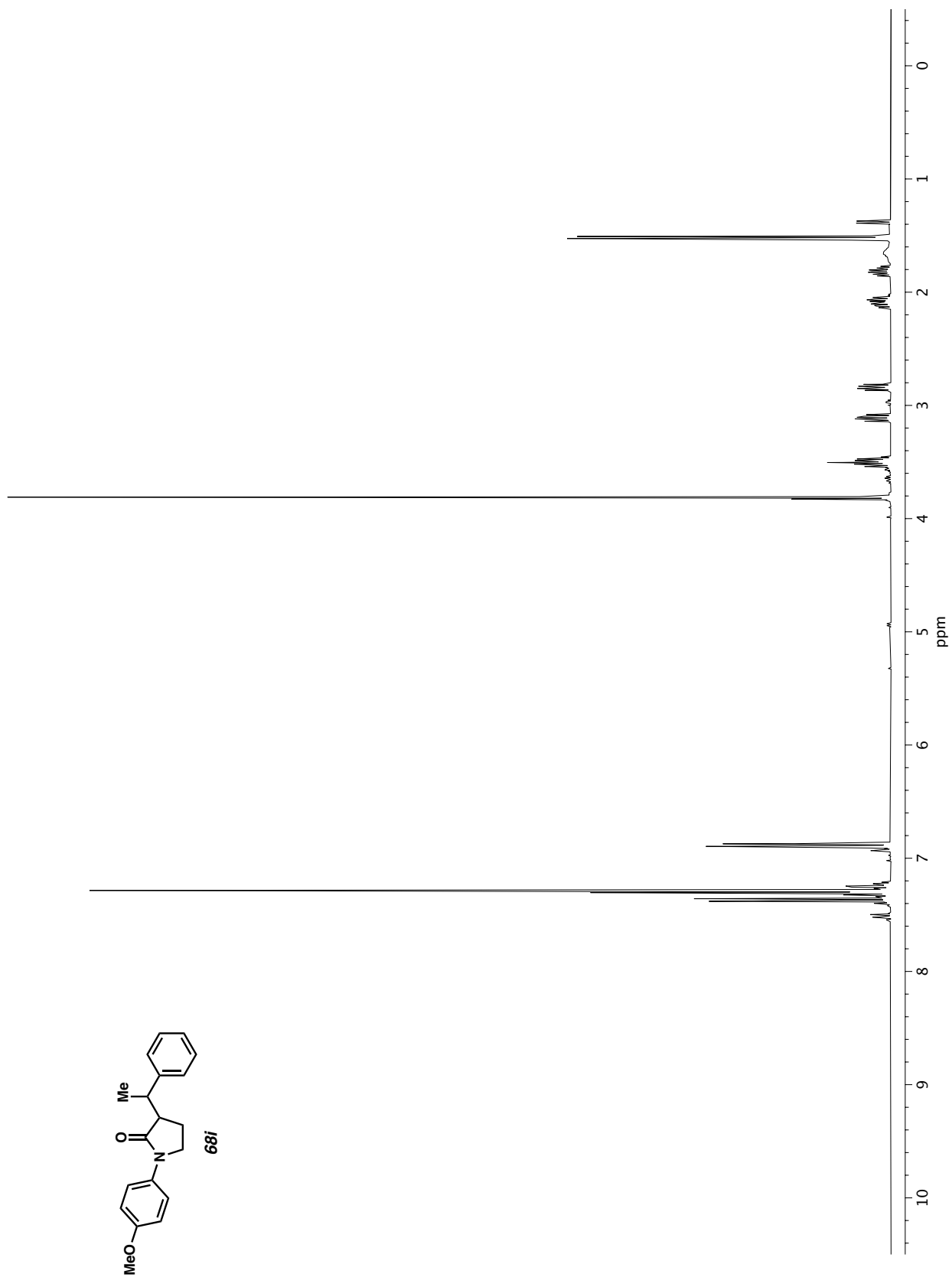


**Figure A1.31** <sup>1</sup>H NMR (400 MHz, CDCl<sub>3</sub>) of compound **68i**.

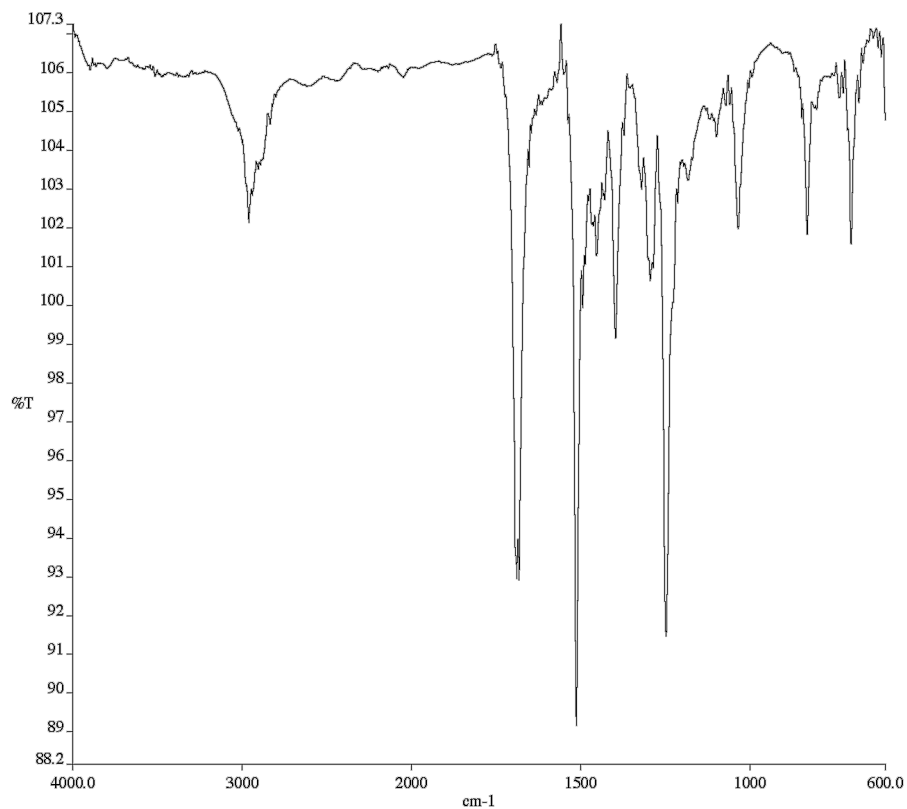


**Figure A1.32** Infrared spectrum (Thin Film, NaCl) of compound **68i**.

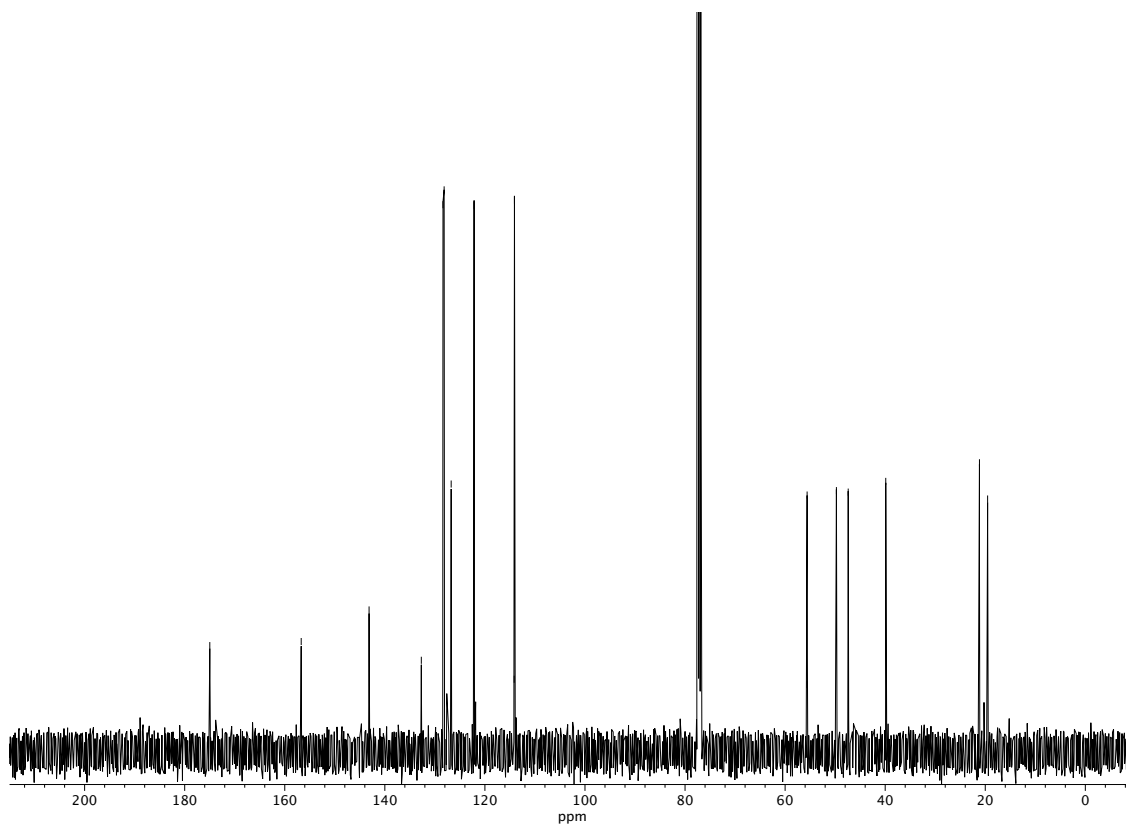


**Figure A1.33** <sup>13</sup>C NMR (100 MHz, CDCl<sub>3</sub>) of compound **68i**.

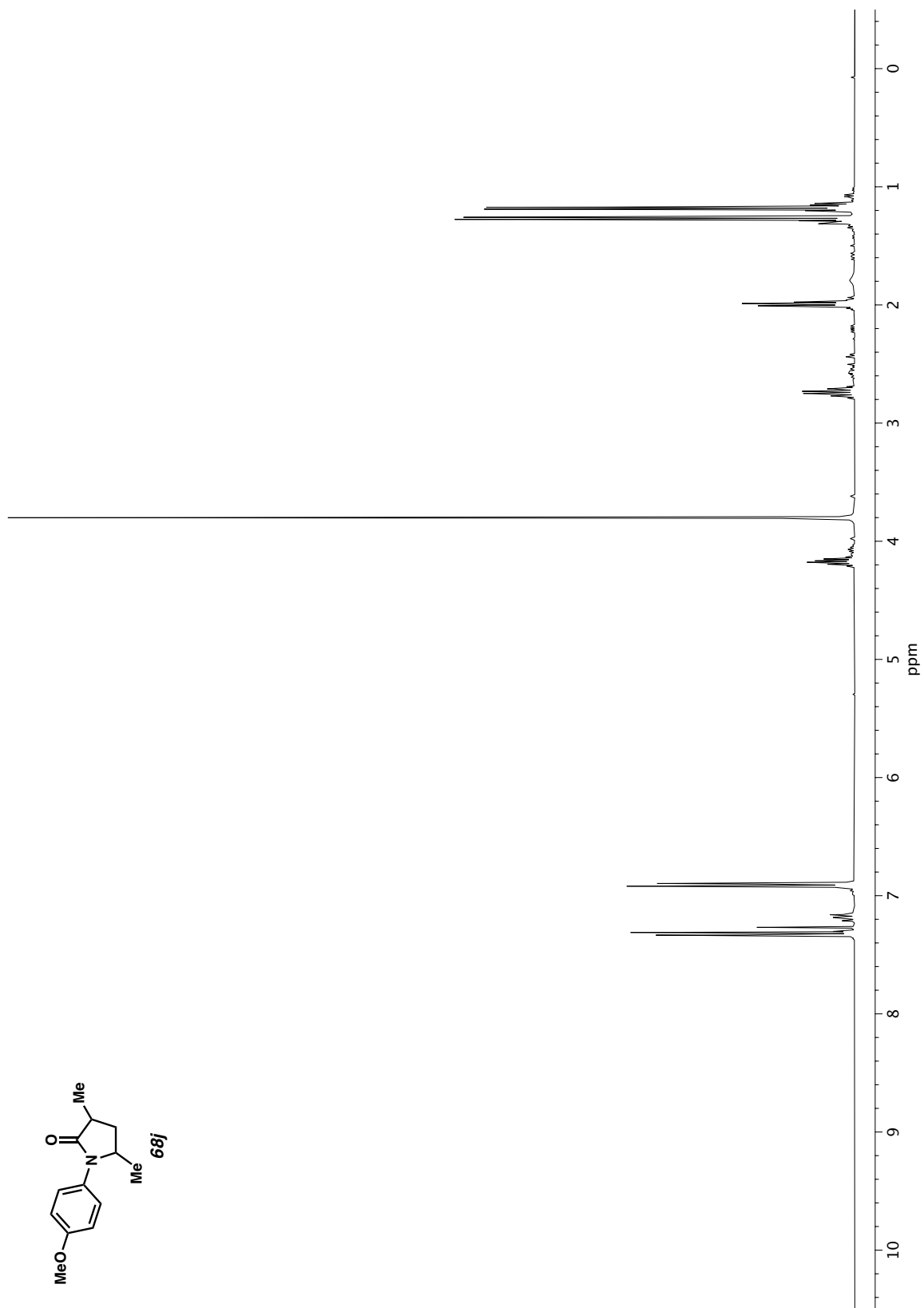
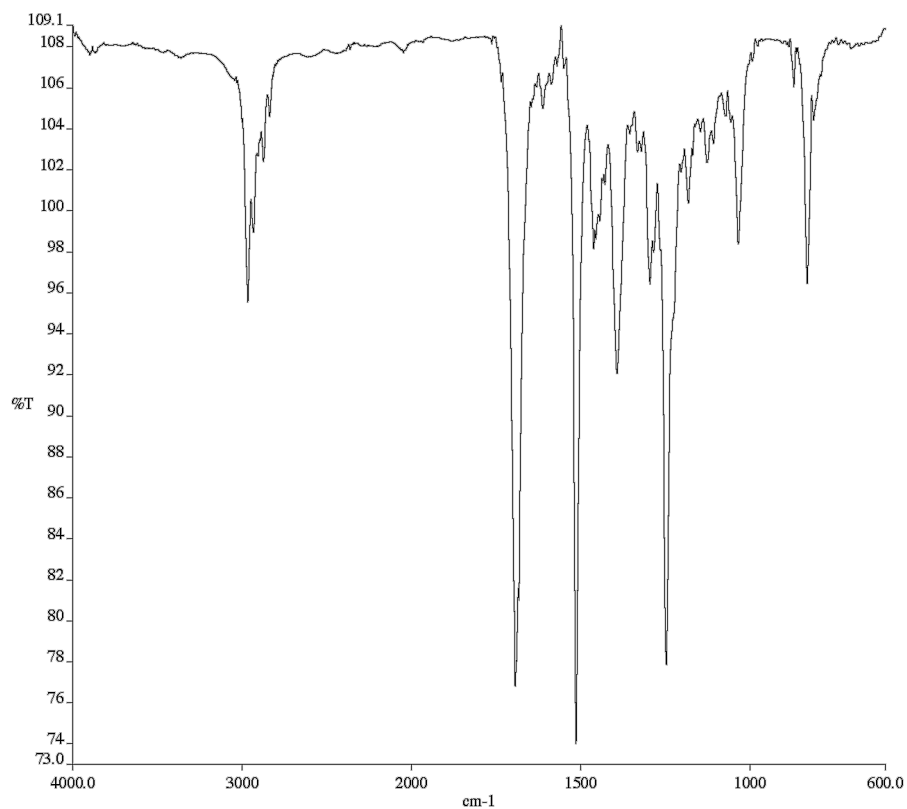
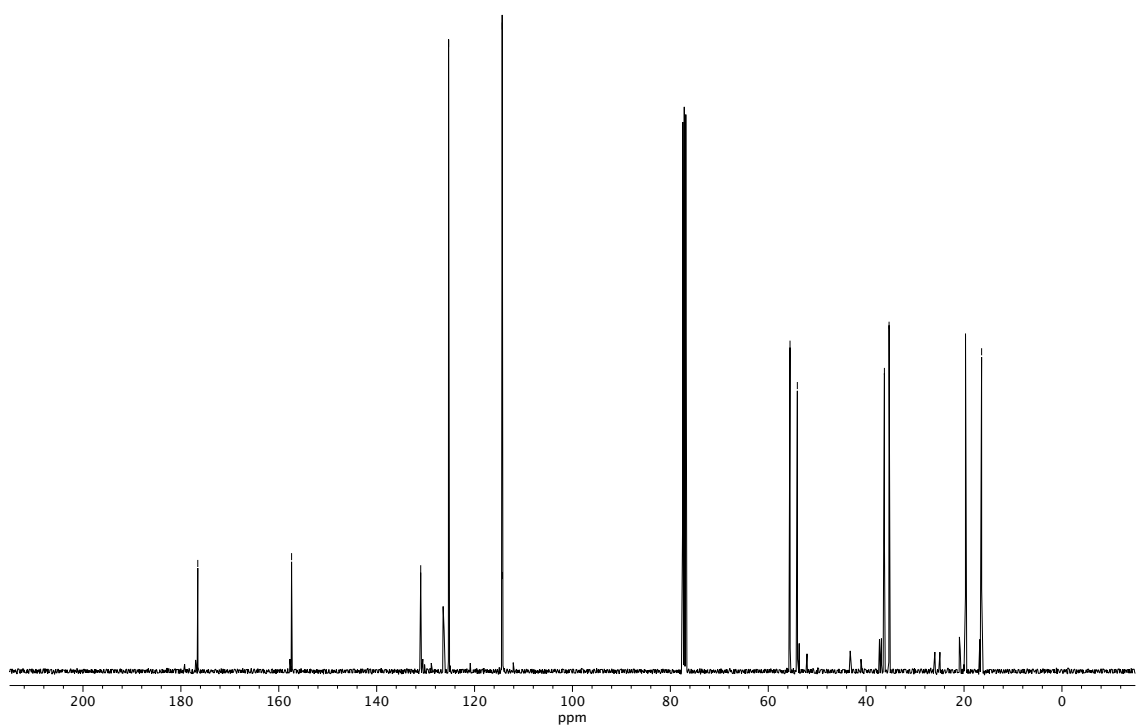


Figure A1.34  $^1\text{H}$  NMR (400 MHz,  $\text{CDCl}_3$ ) of compound **68j**.



**Figure A1.35** Infrared spectrum (Thin Film, NaCl) of compound **68j**.



**Figure A1.36** <sup>13</sup>C NMR (100 MHz, CDCl<sub>3</sub>) of compound **68j**.

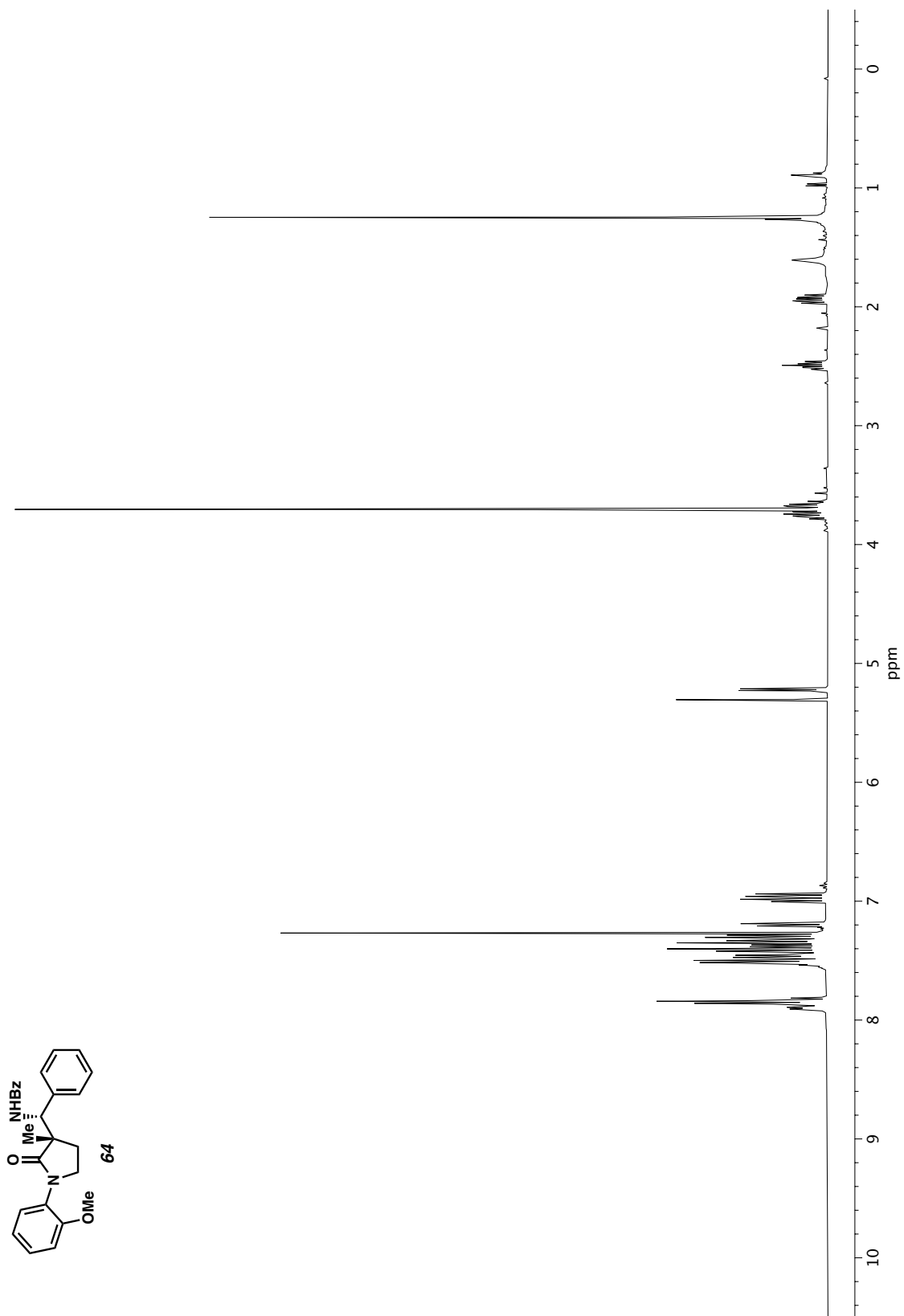
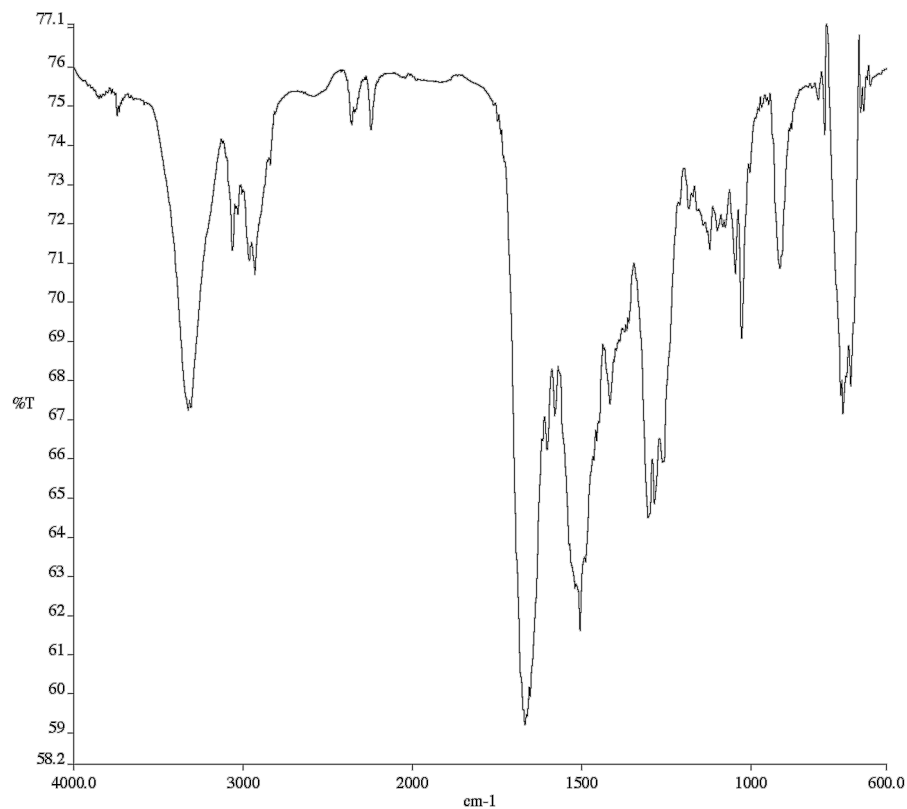
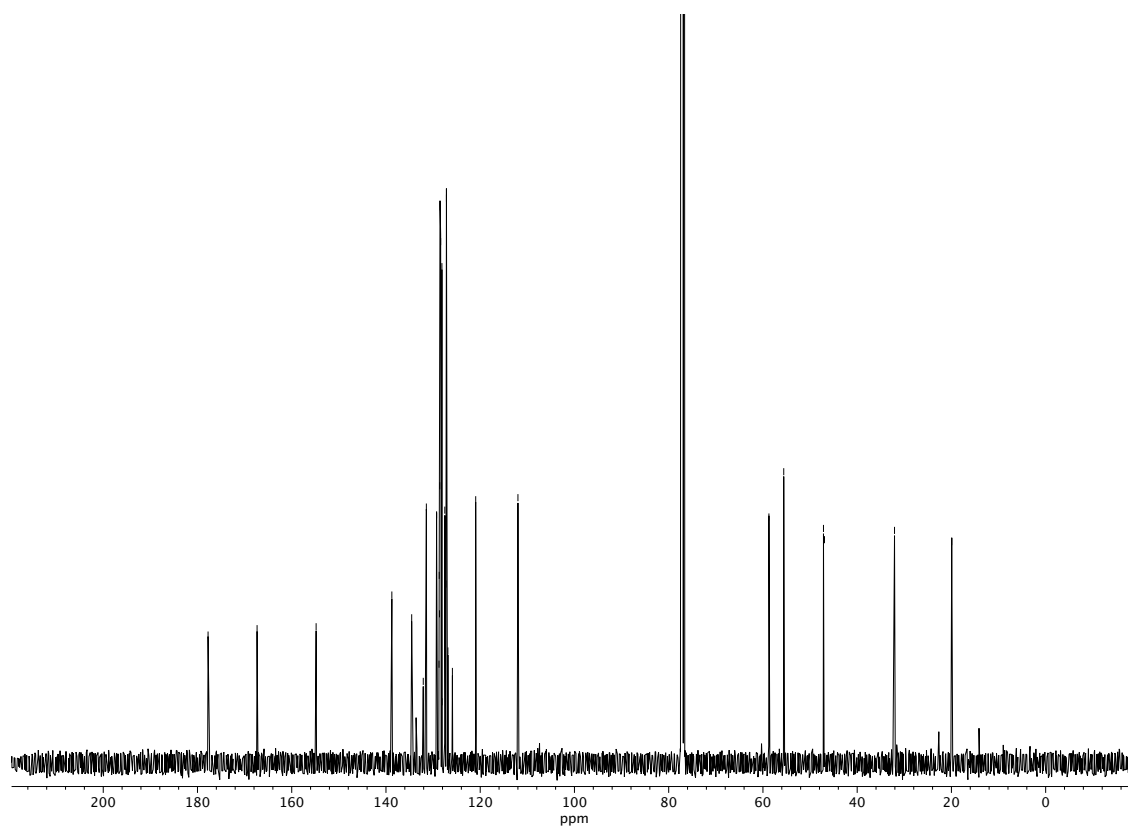


Figure A1.37 <sup>1</sup>H NMR (400 MHz, CDCl<sub>3</sub>) of compound **64**.

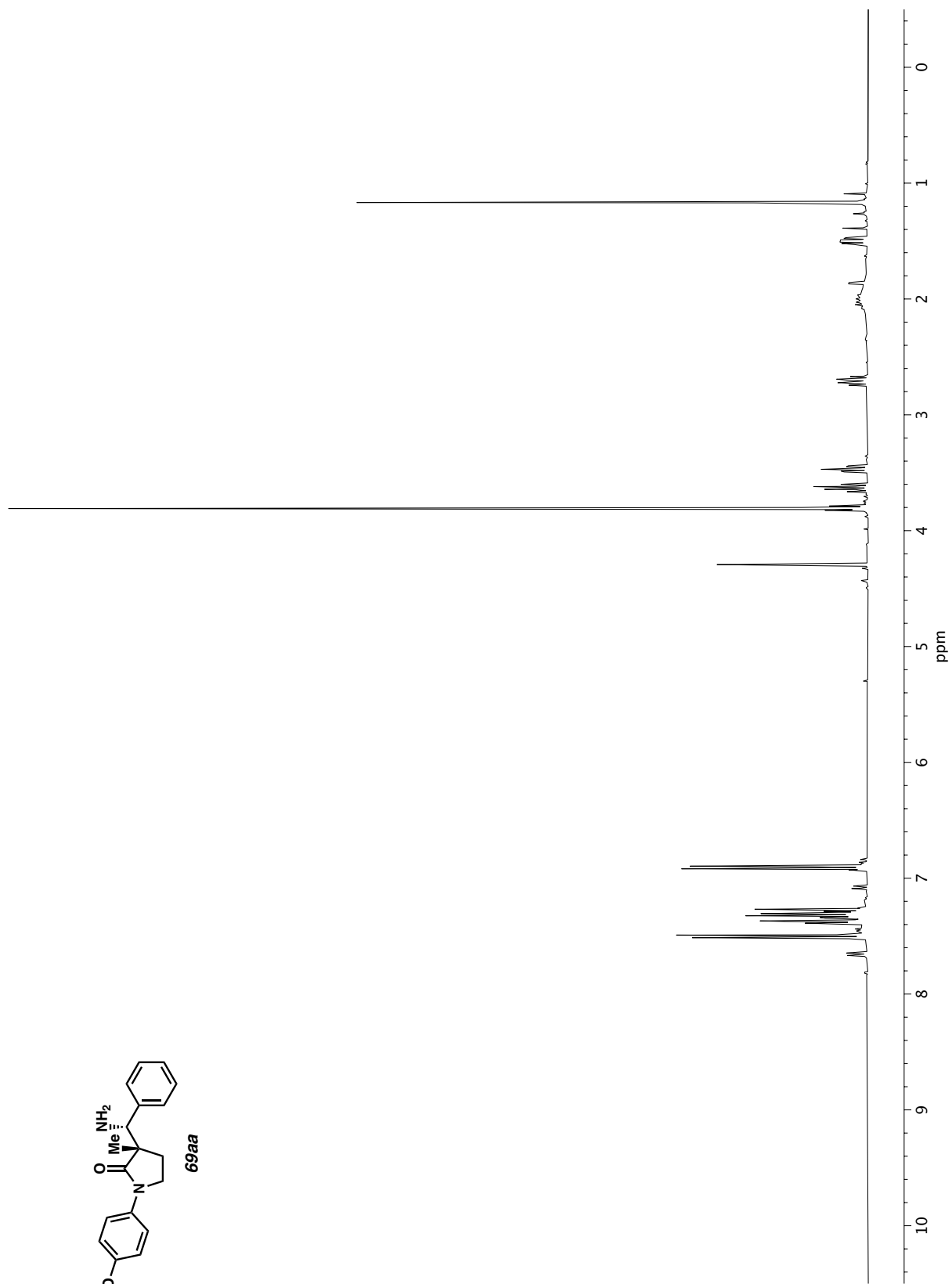
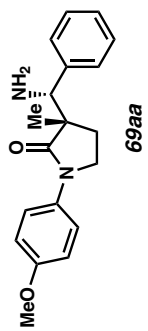


**Figure A1.38** Infrared spectrum (Thin Film, NaCl) of compound **64**.

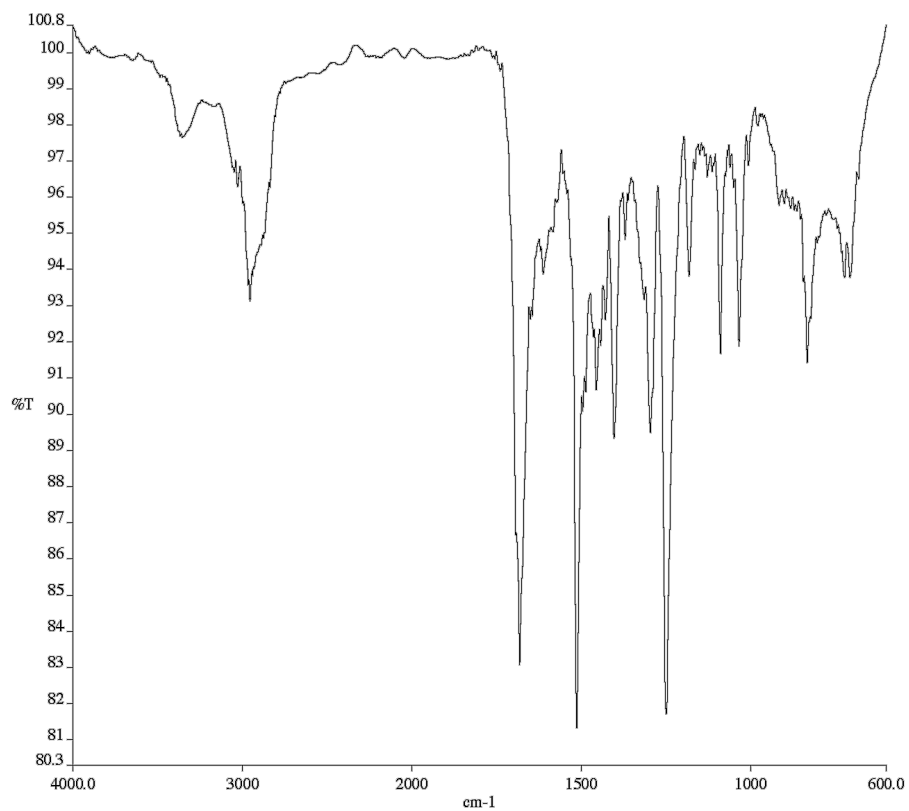


**Figure A1.39** <sup>13</sup>C NMR (100 MHz, CDCl<sub>3</sub>) of compound **64**.

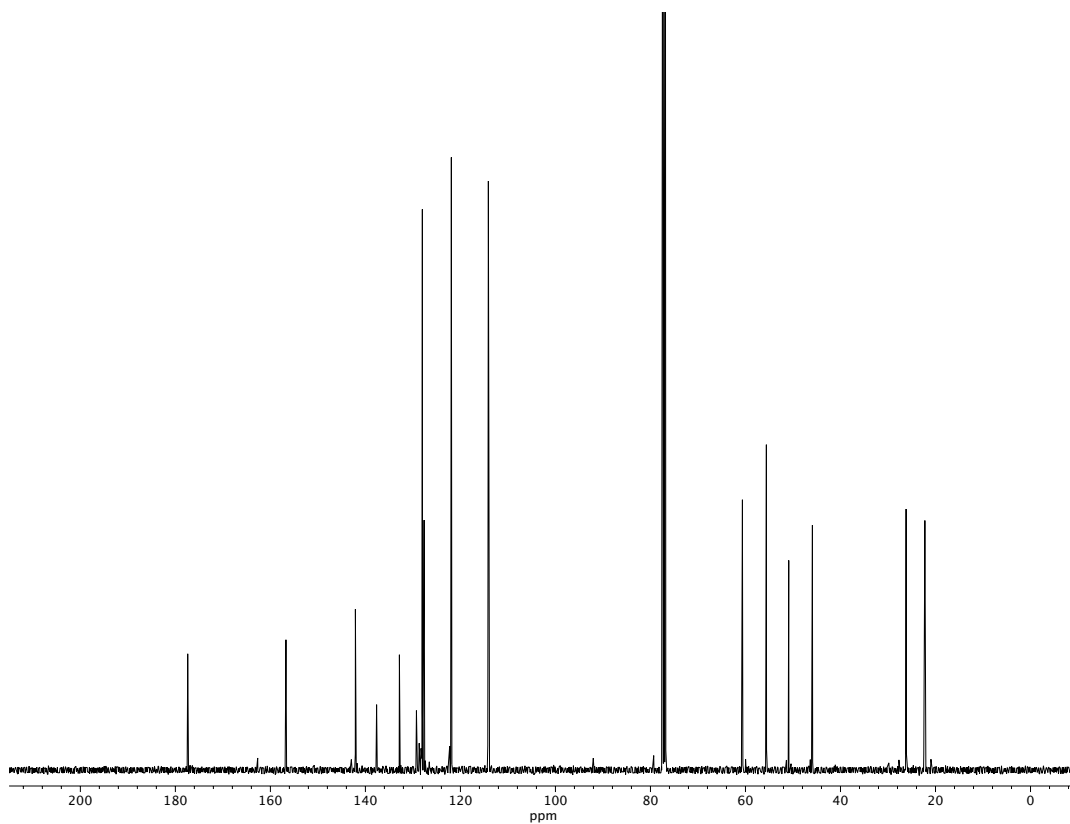




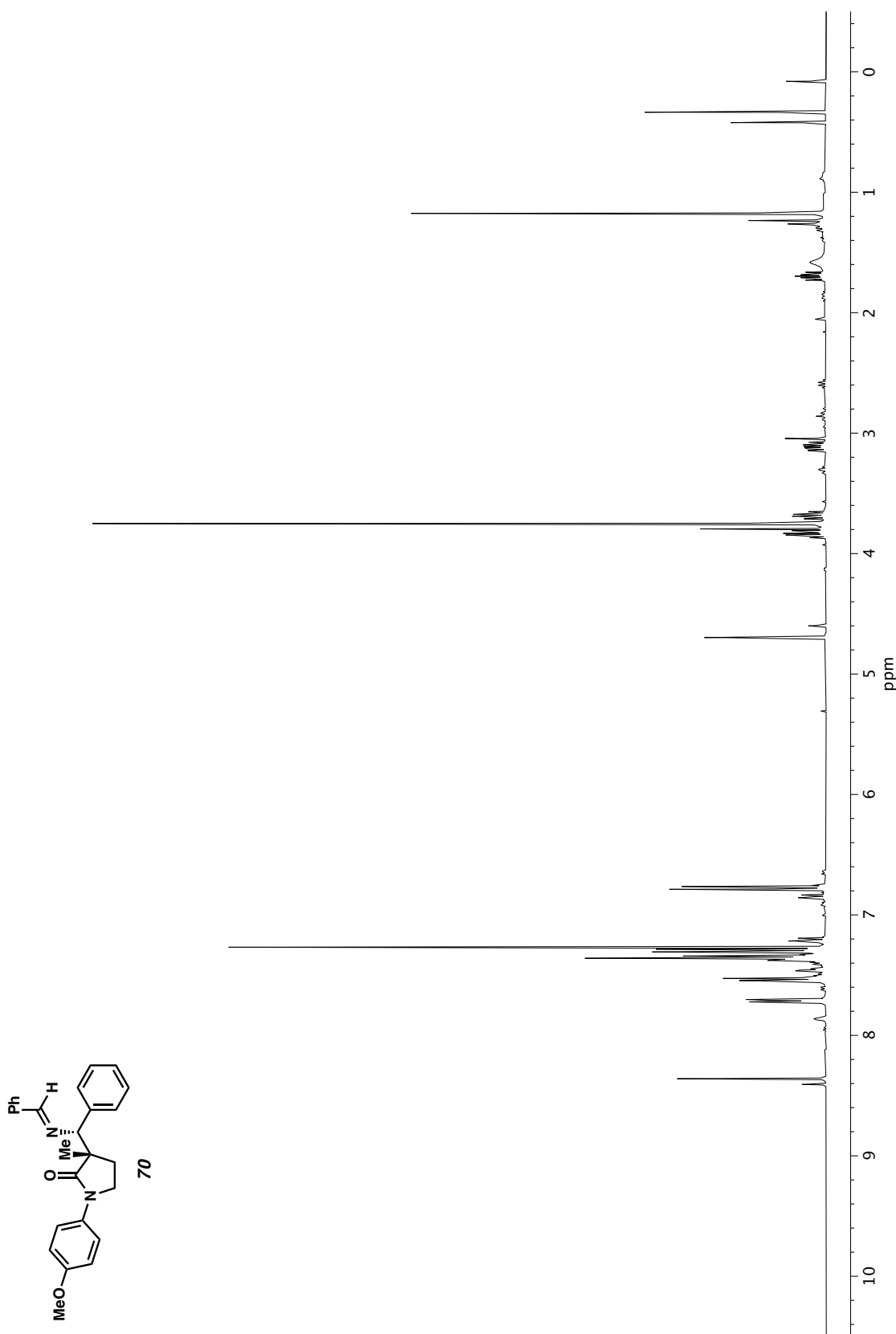
**Figure A1.40** <sup>1</sup>H NMR (400 MHz, CDCl<sub>3</sub>) of compound **69aa**.



**Figure A1.41** Infrared spectrum (Thin Film, NaCl) of compound **69aa**.



**Figure A1.42** <sup>13</sup>C NMR (100 MHz, CDCl<sub>3</sub>) of compound **69aa**.



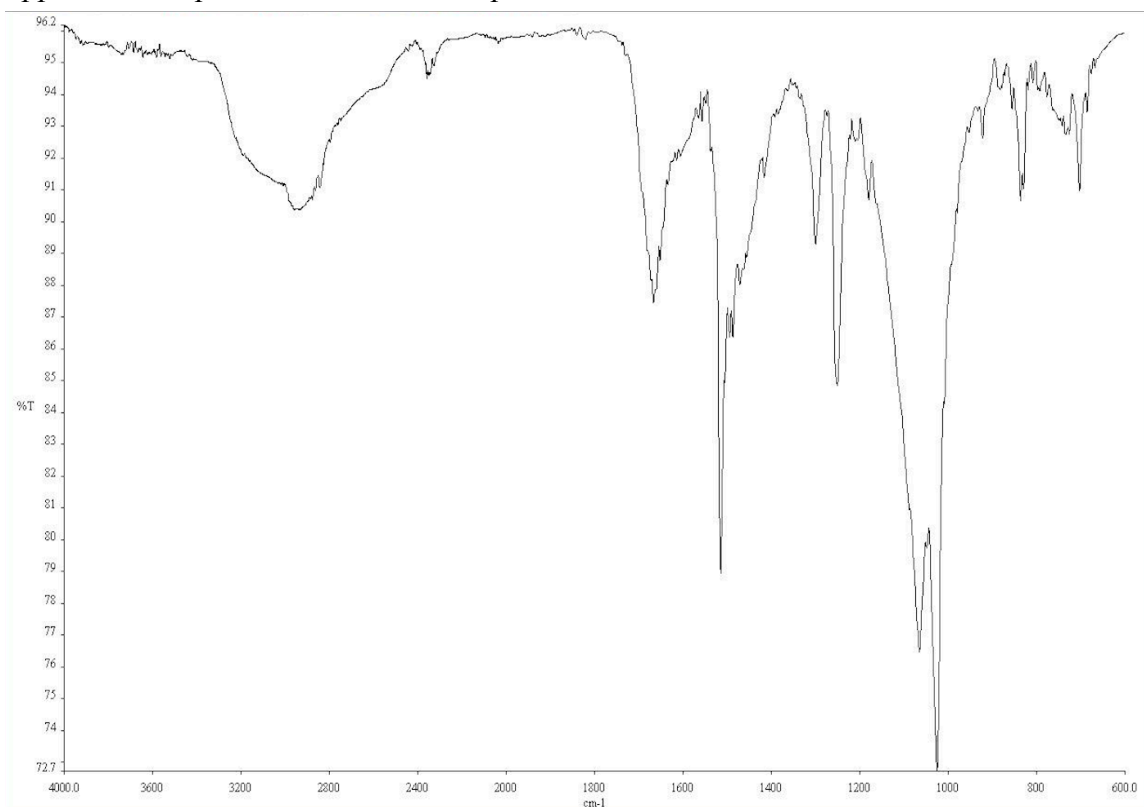


**Figure A1.44** Infrared spectrum (Thin Film, NaCl) of compound **70**.

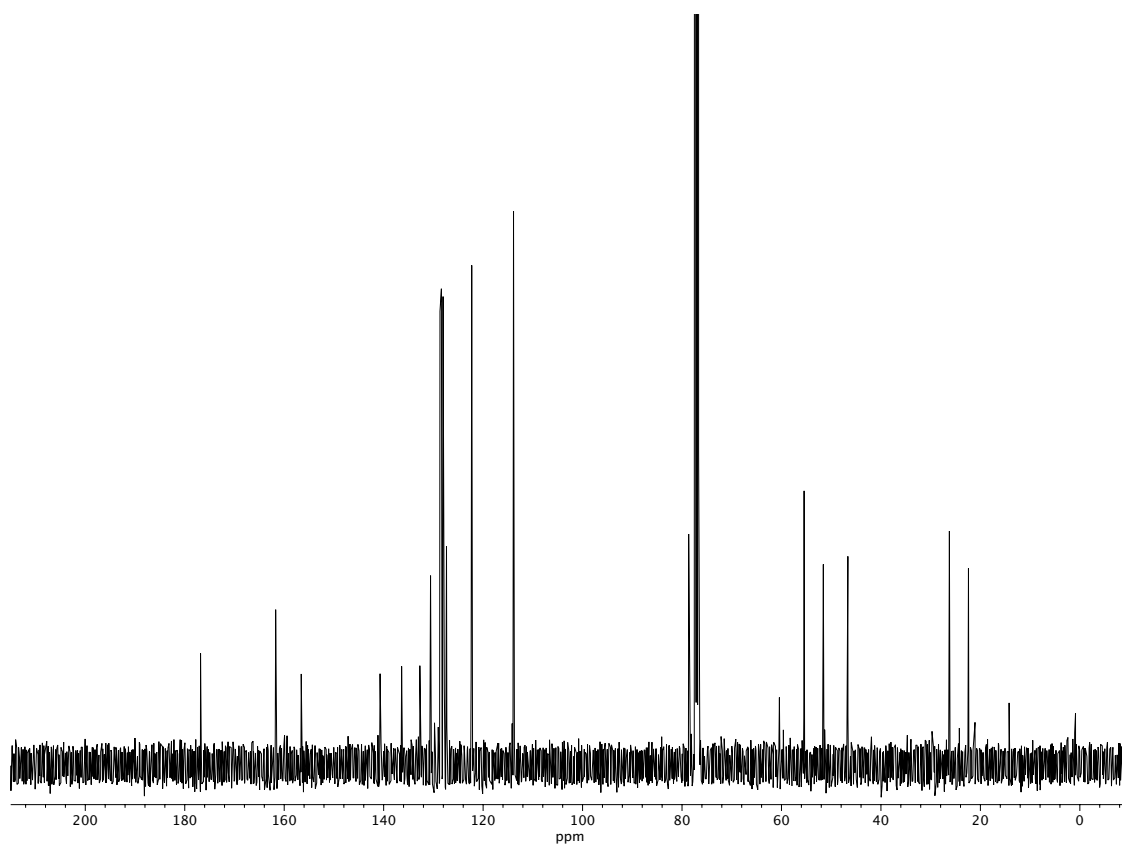


**Figure A1.45** <sup>13</sup>C NMR (100 MHz, CDCl<sub>3</sub>) of compound **70**.

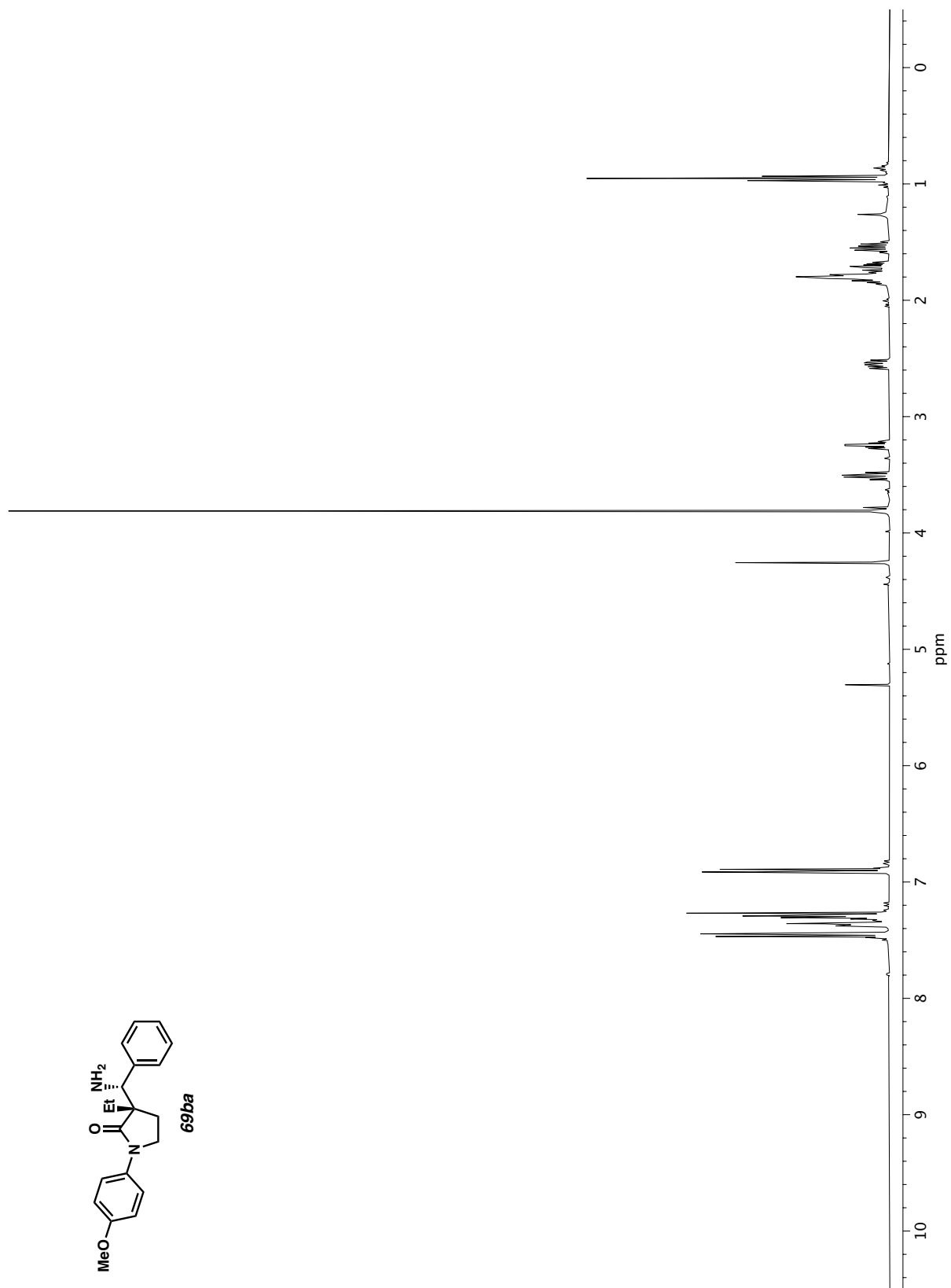


**Figure A1.46** <sup>1</sup>H NMR (400 MHz, CDCl<sub>3</sub>) of compound **69ba**.

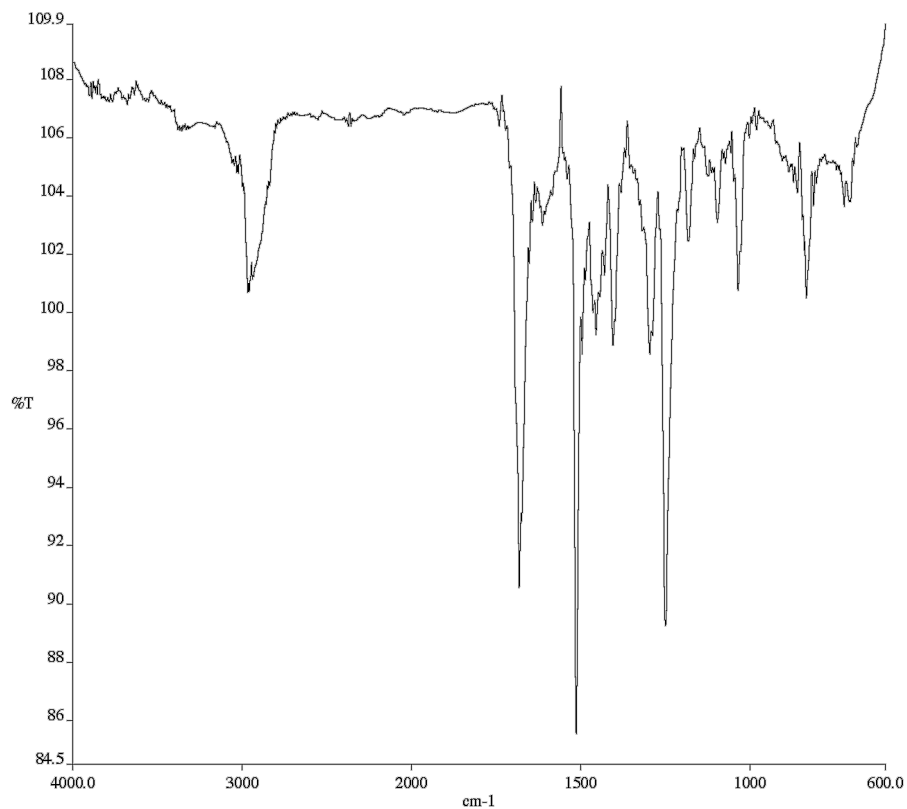


**Figure A1.47** Infrared spectrum (Thin Film, NaCl) of compound **69ba**.

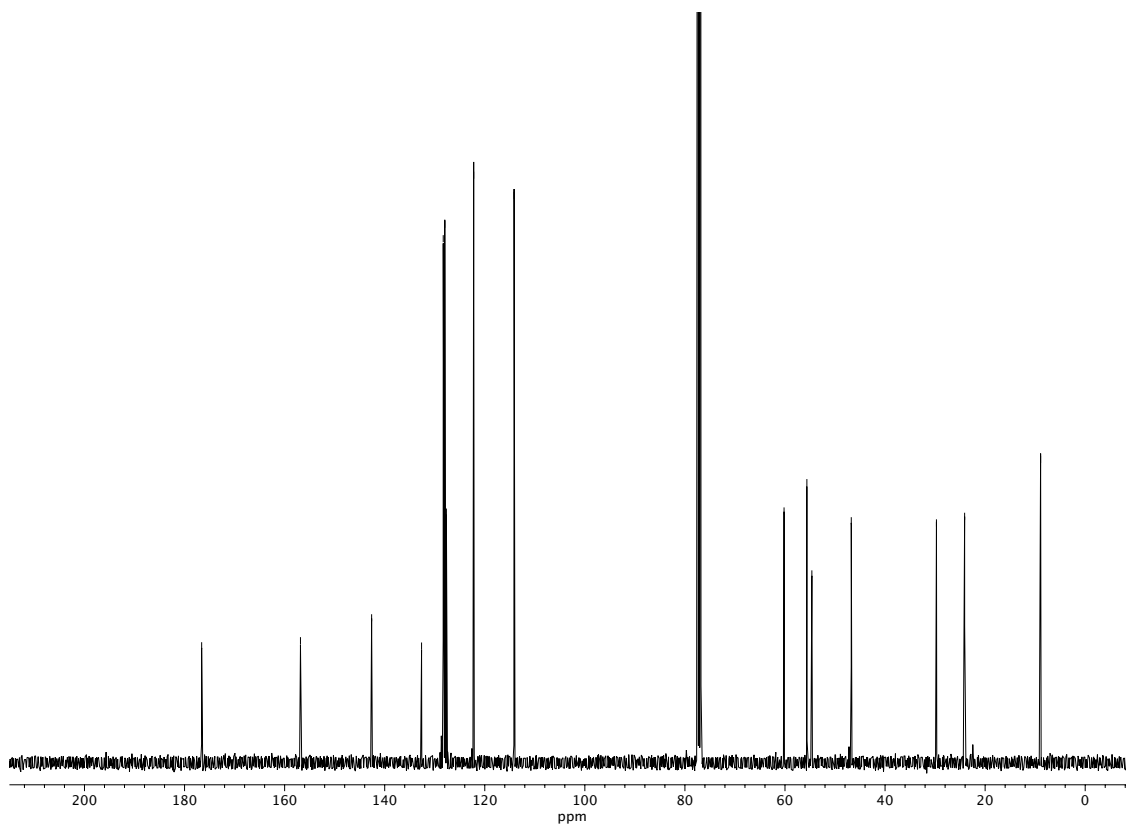


**Figure A1.48** <sup>13</sup>C NMR (100 MHz, CDCl<sub>3</sub>) of compound **69ba**.

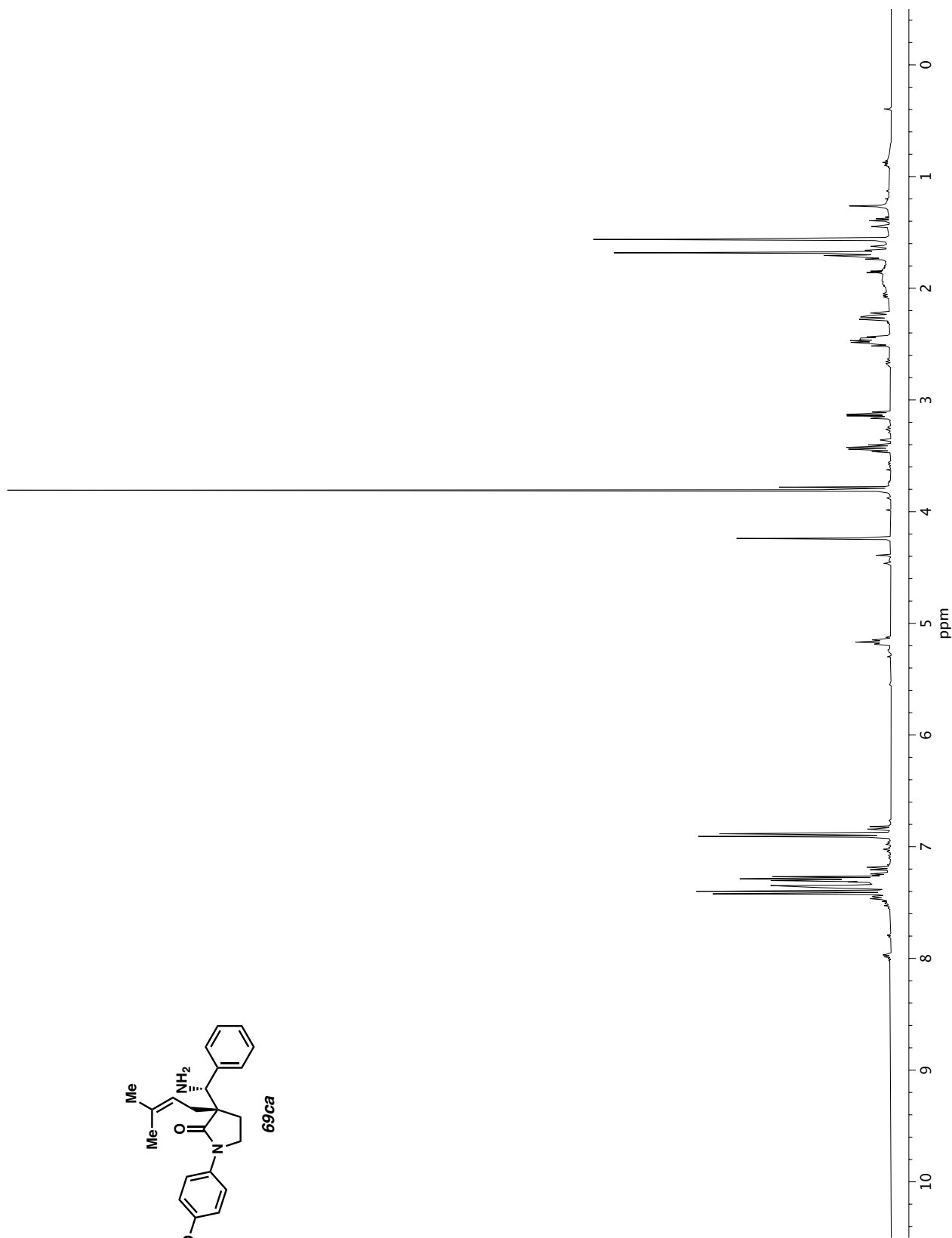
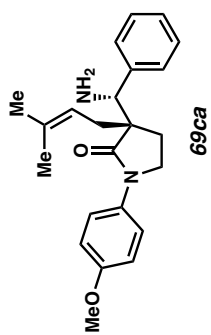
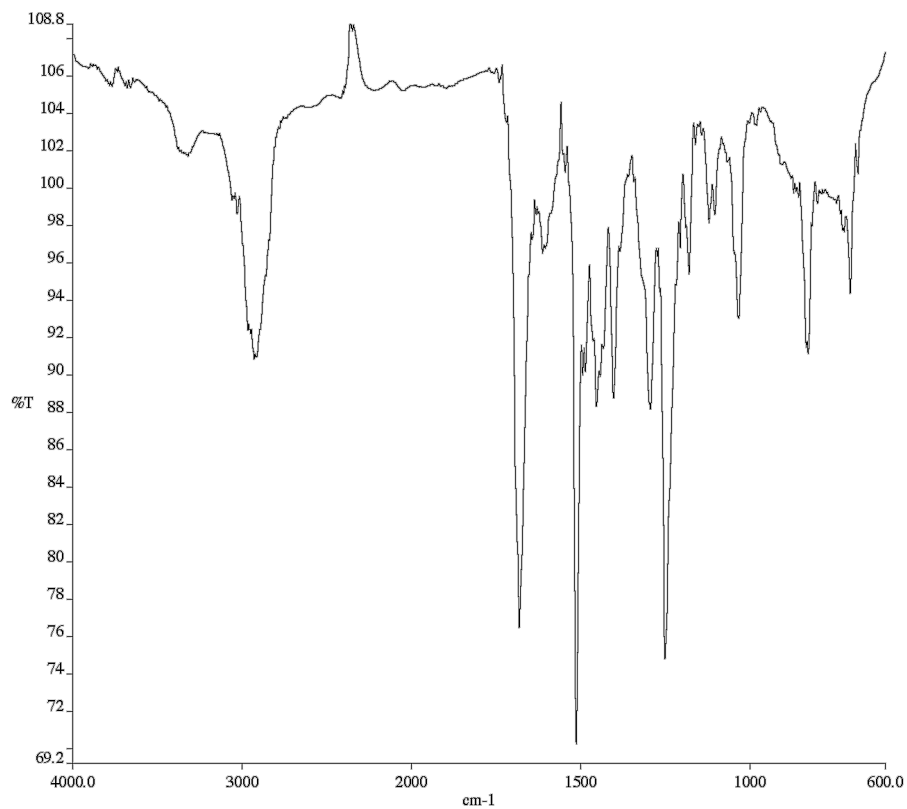
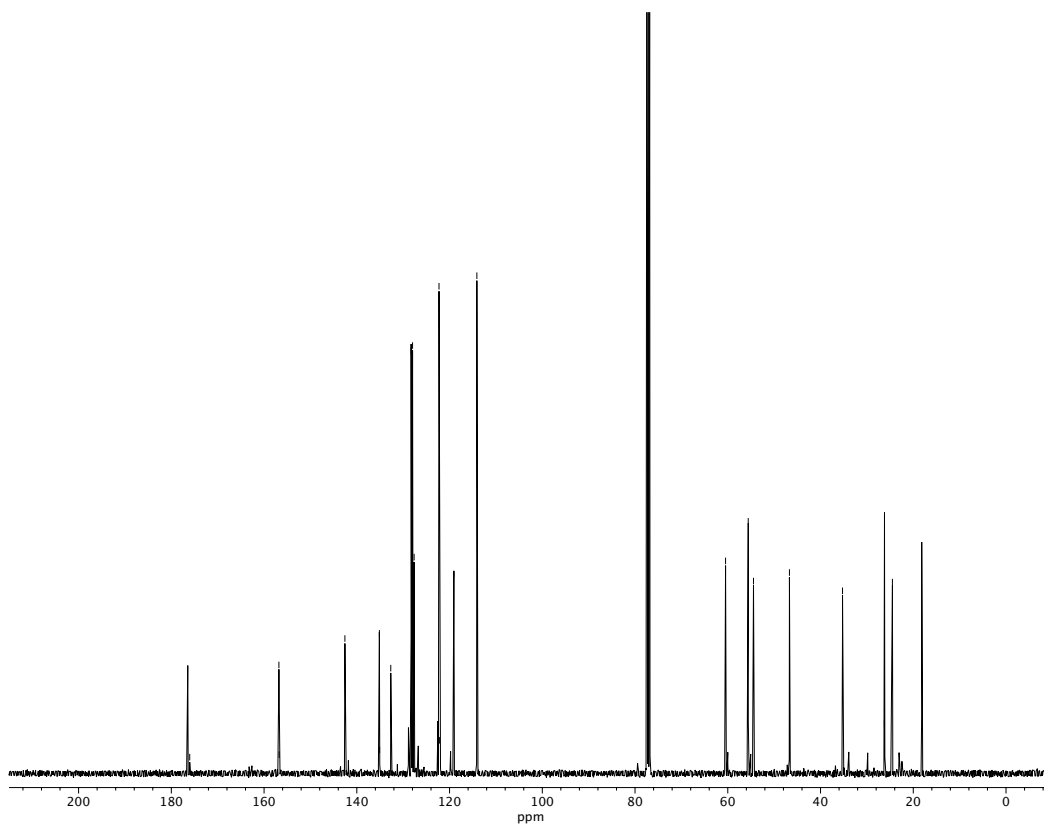


Figure A1.49 <sup>1</sup>H NMR (400 MHz, CDCl<sub>3</sub>) of compound **69ca**.



**Figure A1.50** Infrared spectrum (Thin Film, NaCl) of compound **69ca**.



**Figure A1.51** <sup>13</sup>C NMR (100 MHz, CDCl<sub>3</sub>) of compound **69ca**.



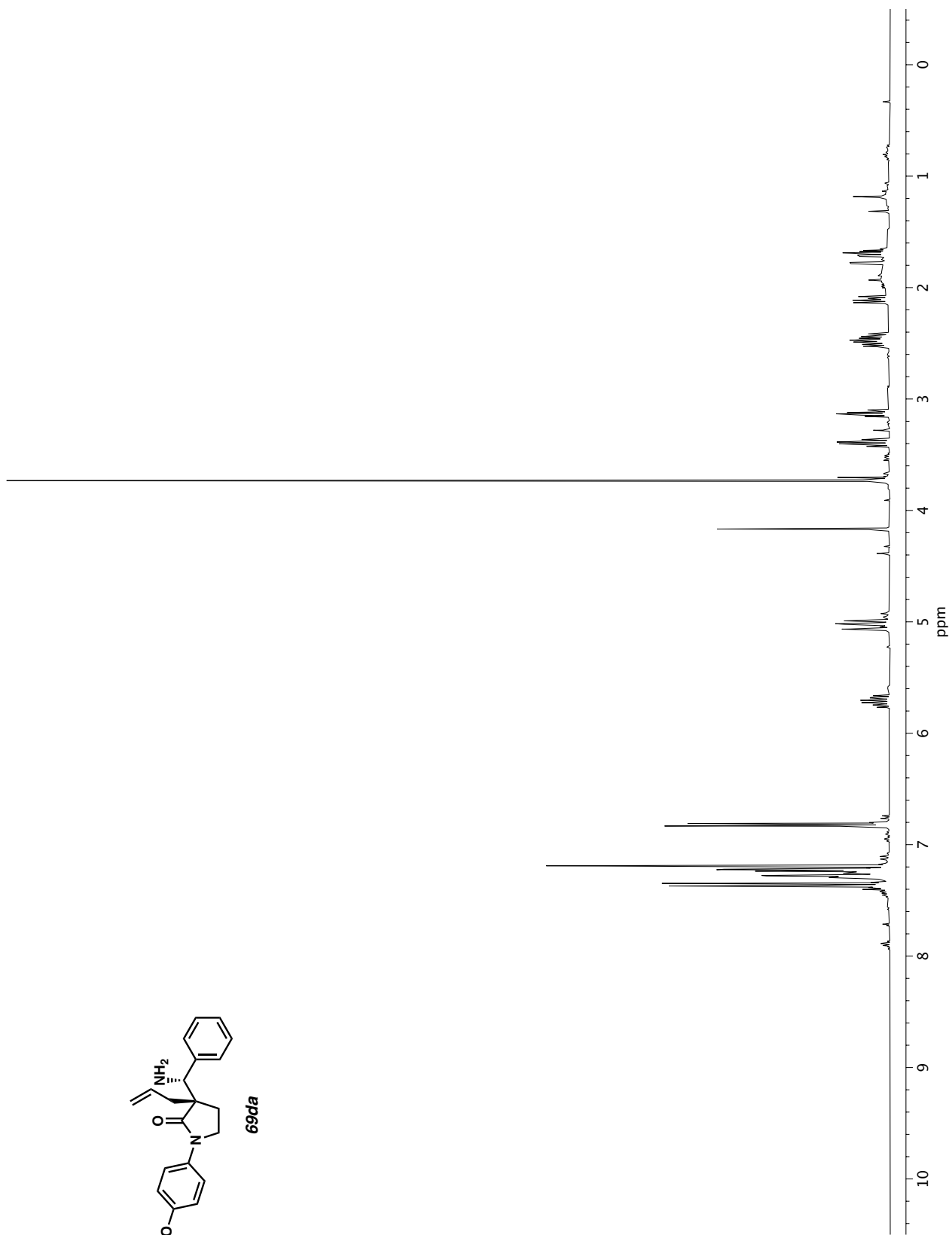
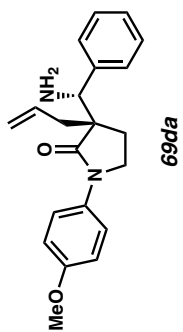
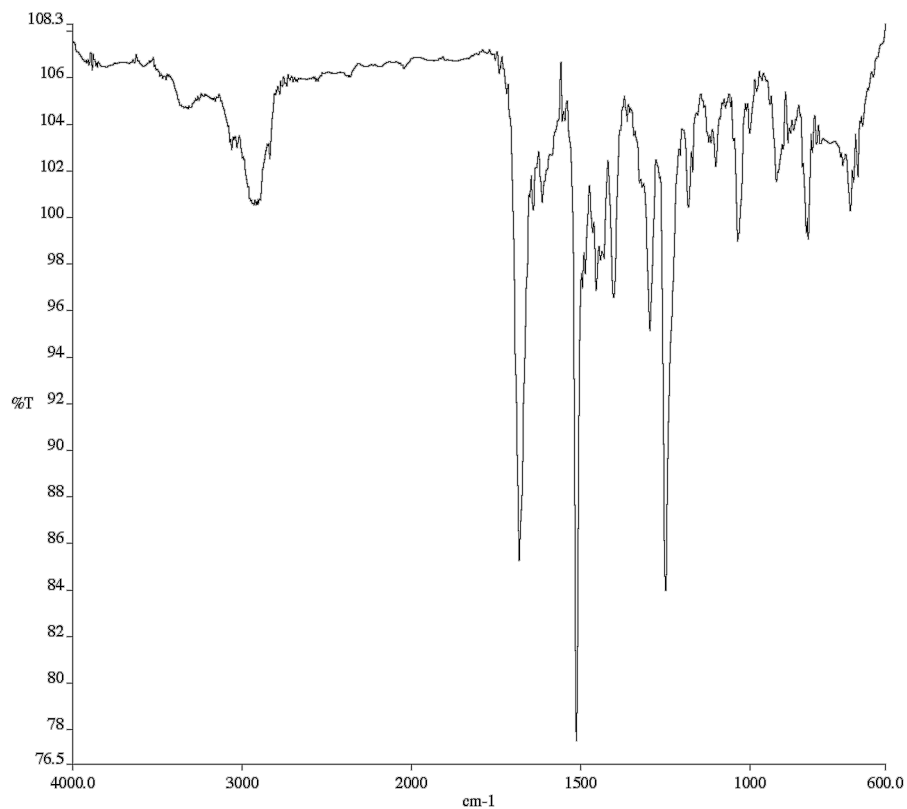
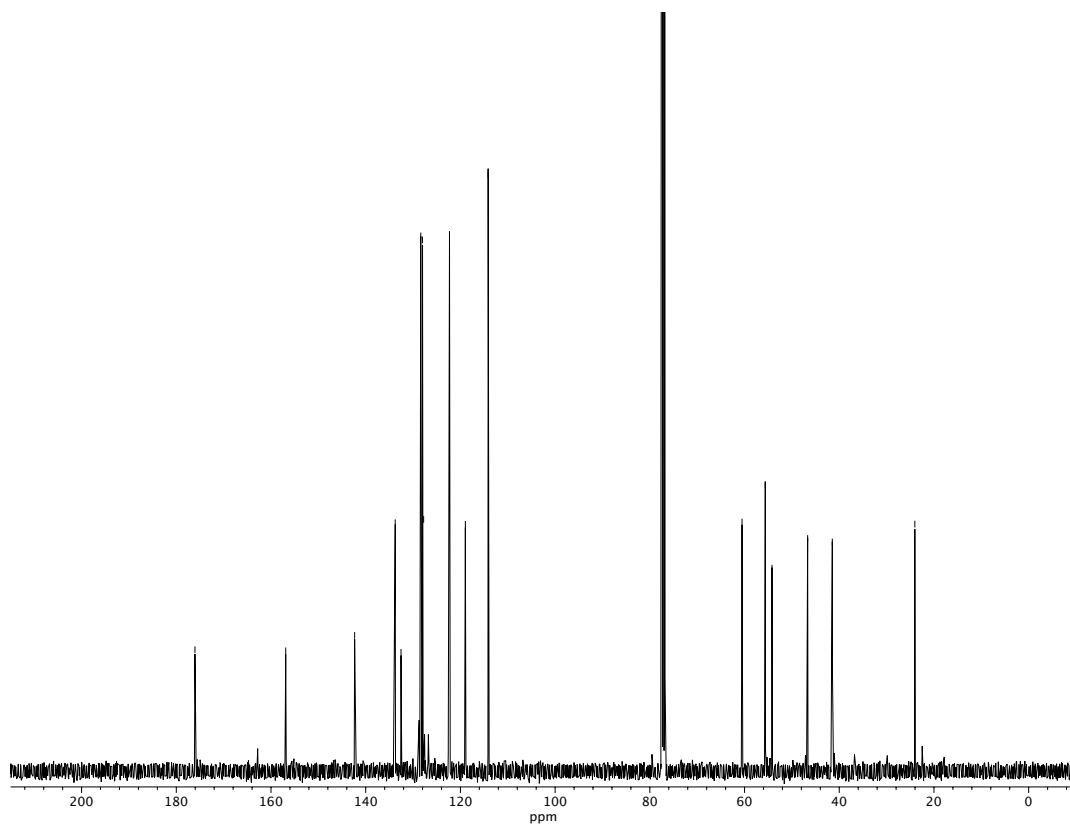


Figure A1.52 <sup>1</sup>H NMR (400 MHz, CDCl<sub>3</sub>) of compound **69da**.



**Figure A1.53** Infrared spectrum (Thin Film, NaCl) of compound **69da**.



**Figure A1.54** <sup>13</sup>C NMR (100 MHz, CDCl<sub>3</sub>) of compound **69da**.

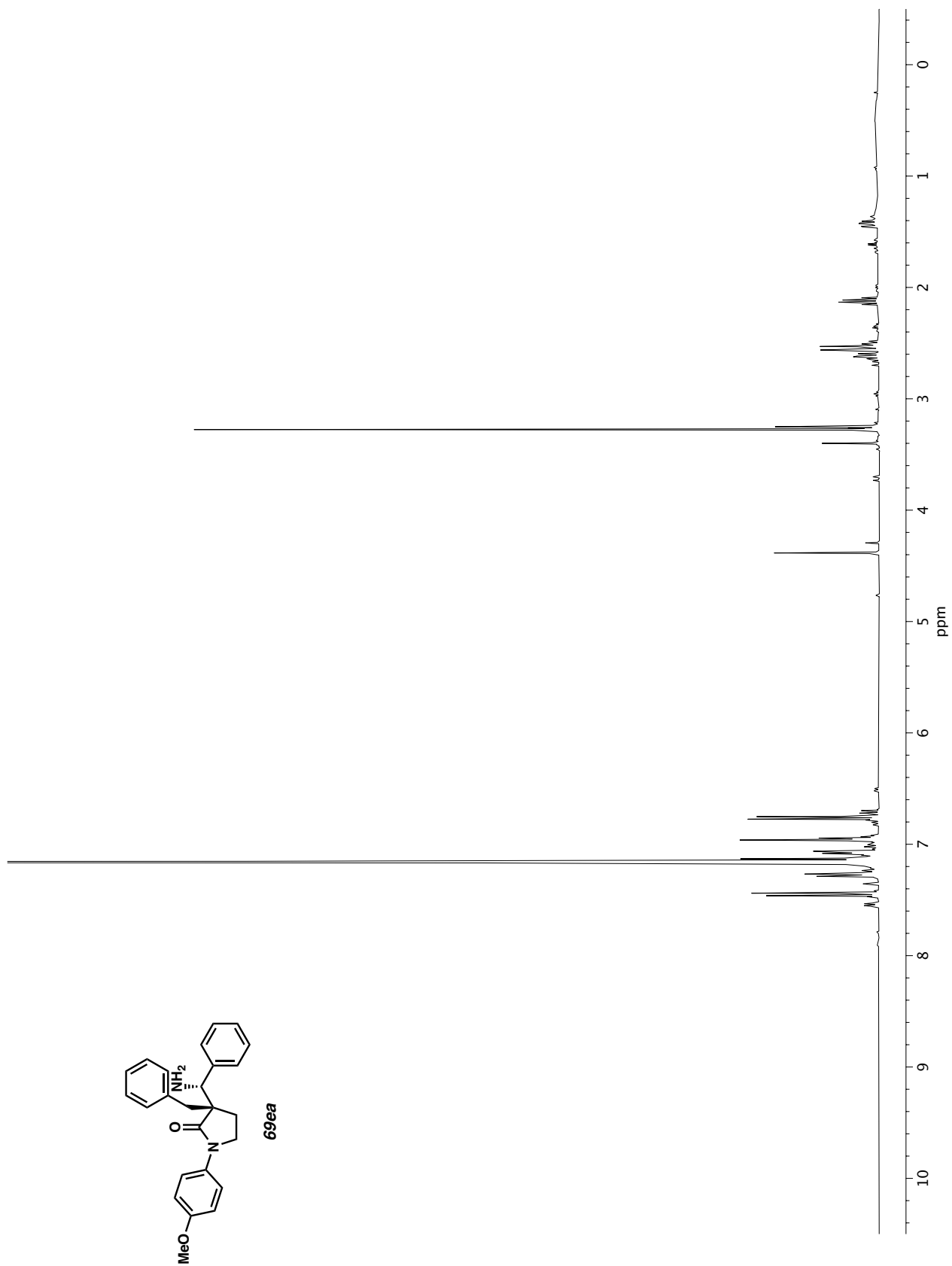
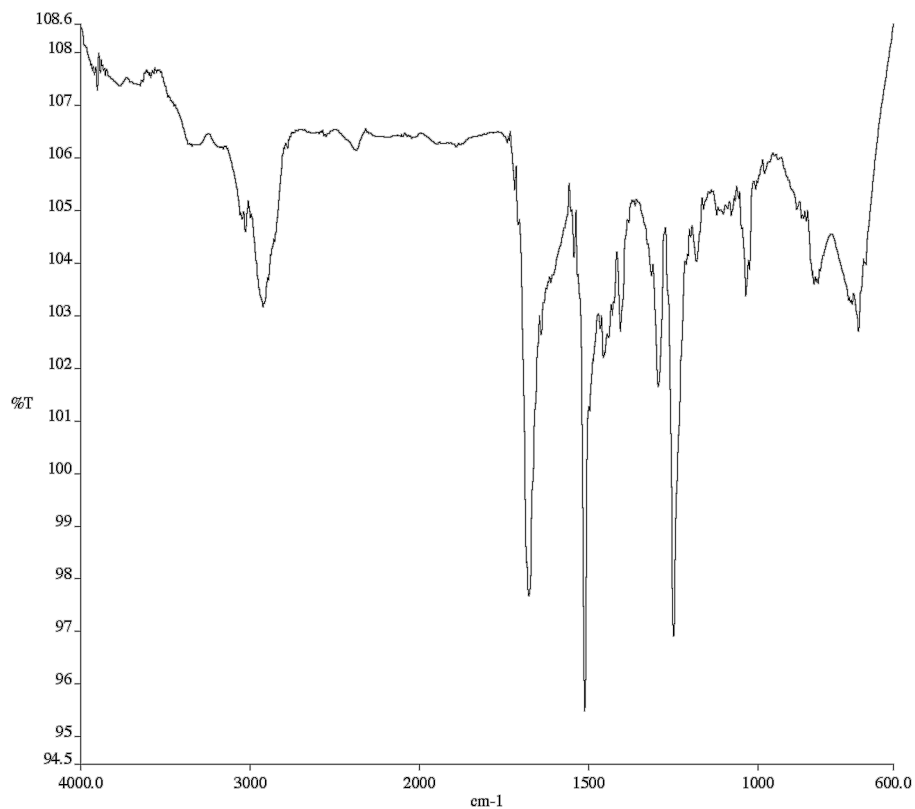
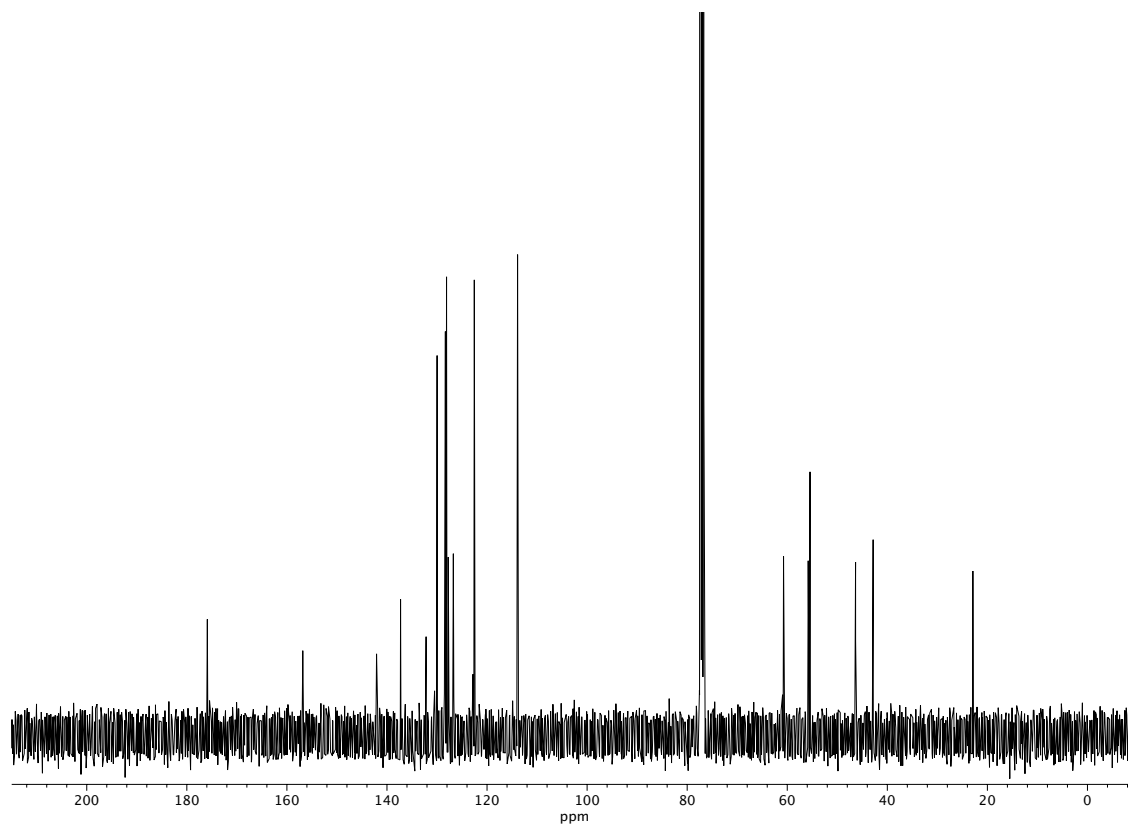


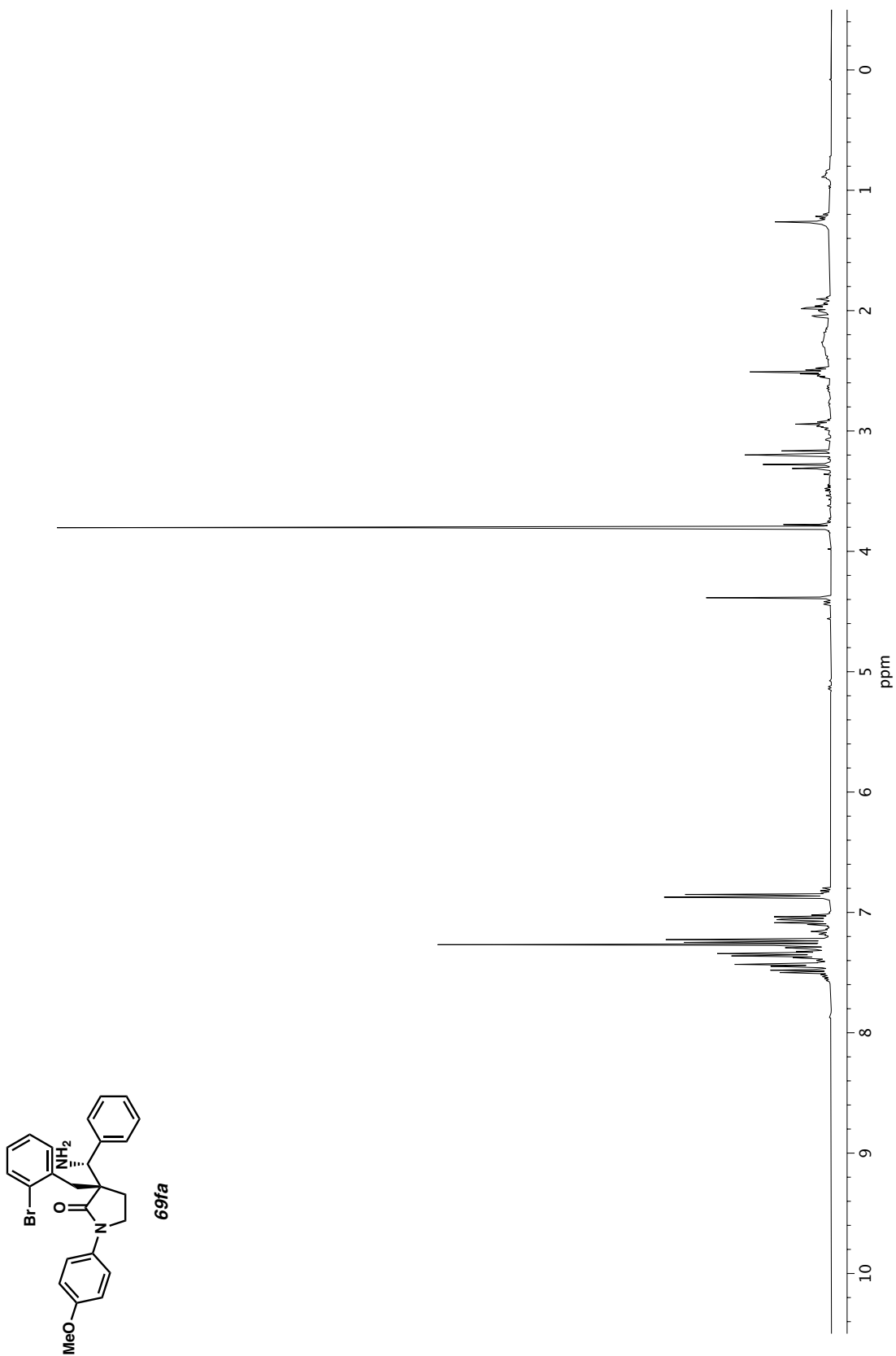
Figure A1.55 <sup>1</sup>H NMR (400 MHz, C<sub>6</sub>D<sub>6</sub>) of compound **69ea**.



**Figure A1.56** Infrared spectrum (Thin Film, NaCl) of compound **69ea**.



**Figure A1.57** <sup>13</sup>C NMR (100 MHz, CDCl<sub>3</sub>) of compound **69ea**.

Figure A1.58 <sup>1</sup>H NMR (400 MHz, CDCl<sub>3</sub>) of compound **69fa**.

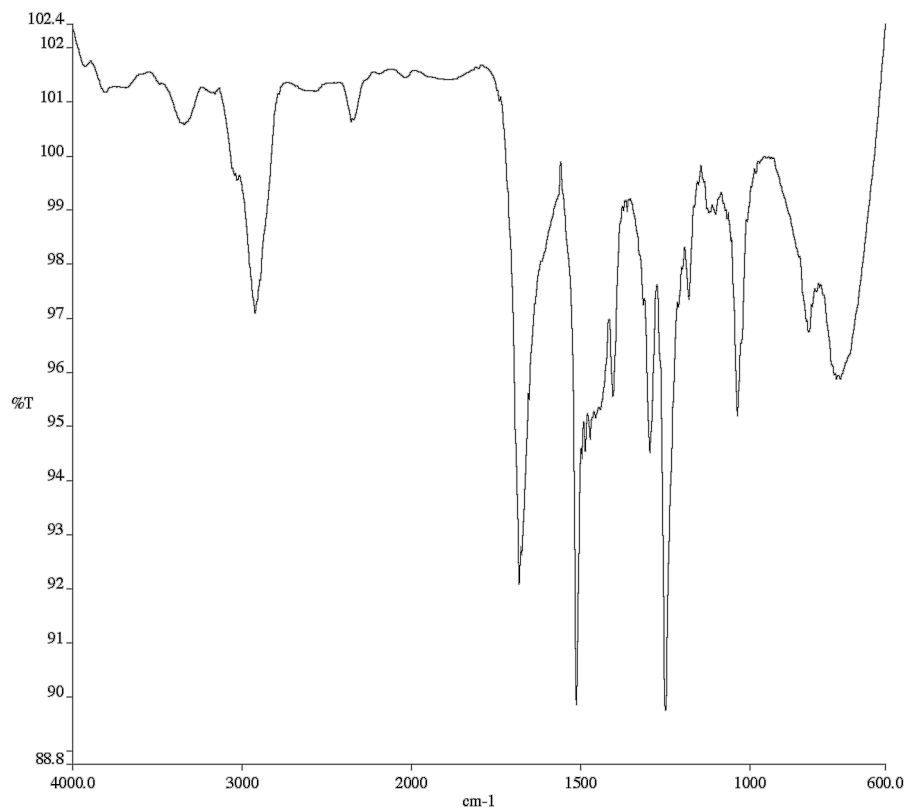


**Figure A1.59** Infrared spectrum (Thin Film, NaCl) of compound **69fa**.

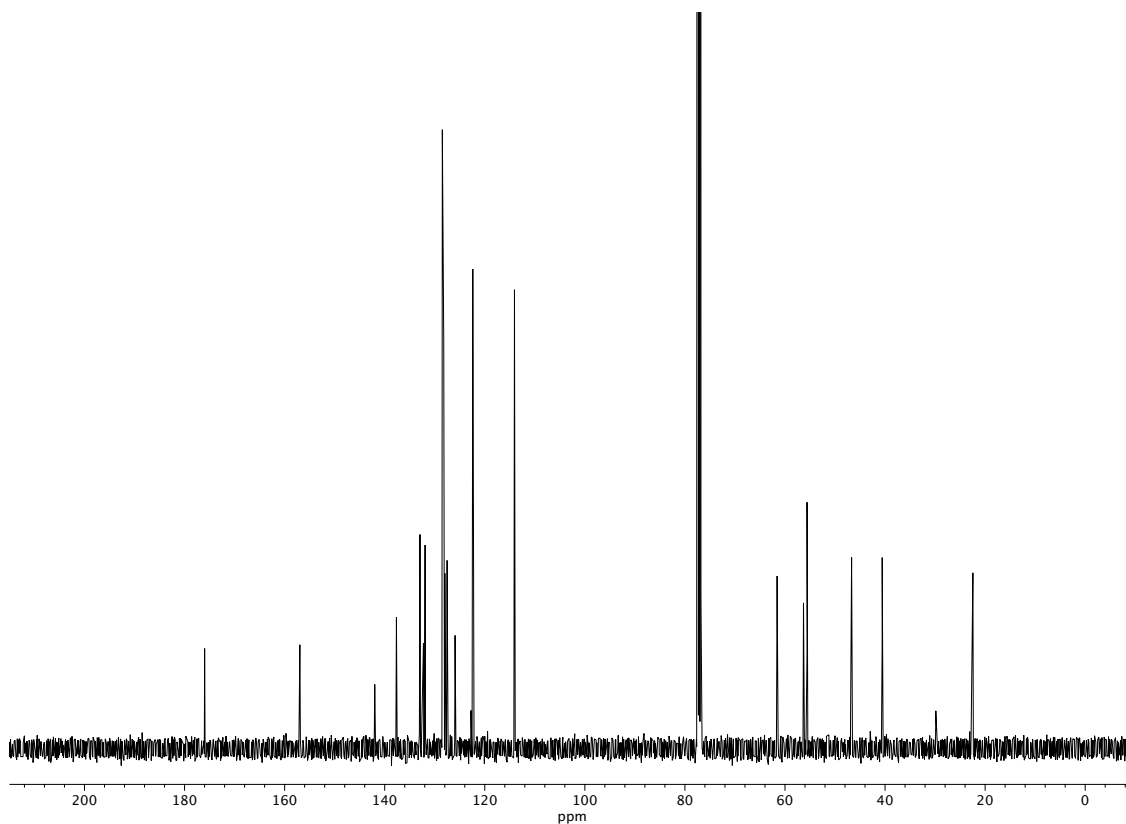


**Figure A1.60** <sup>13</sup>C NMR (100 MHz, CDCl<sub>3</sub>) of compound **69fa**.



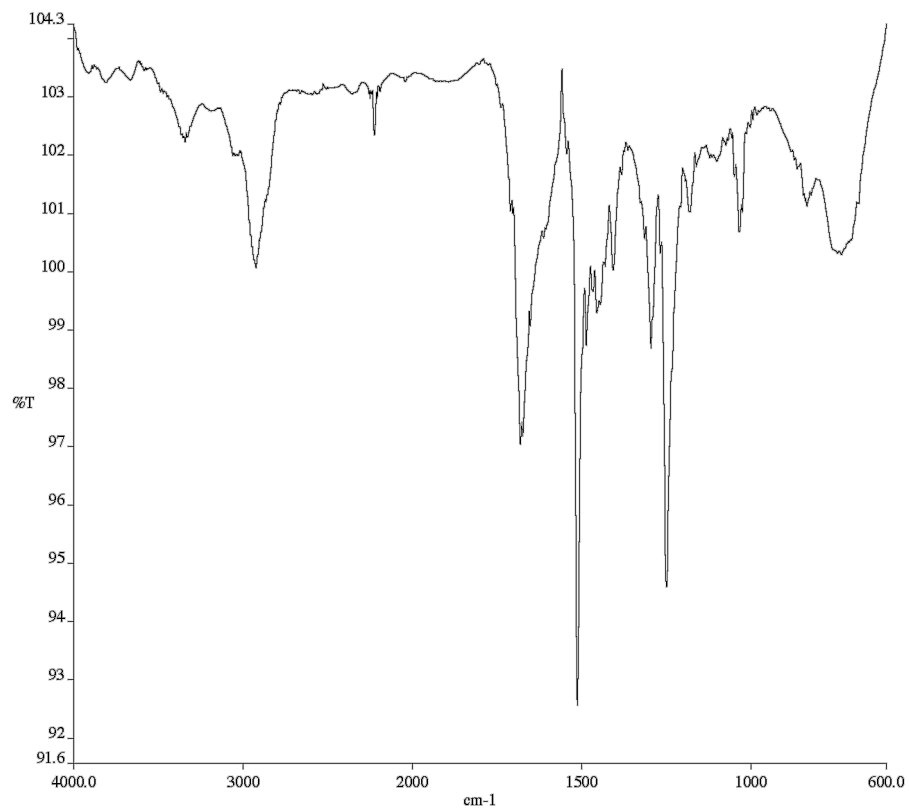


**Figure A1.62** Infrared spectrum (Thin Film, NaCl) of compound **69ga**.

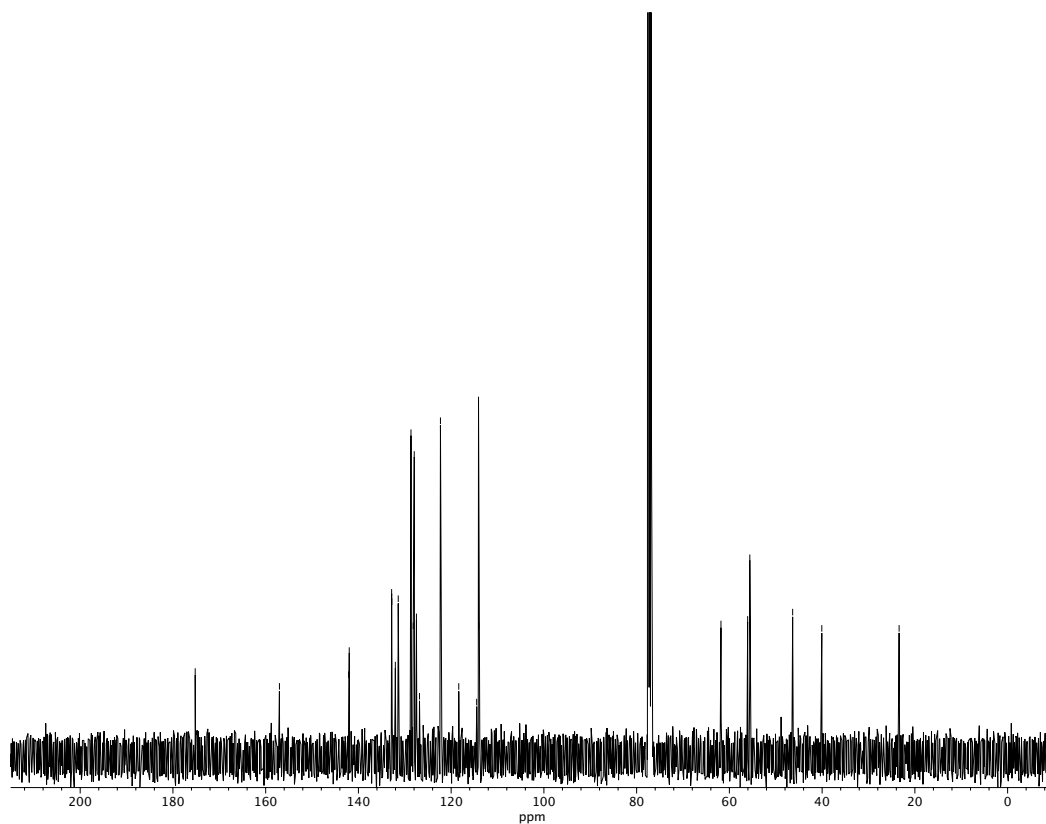


**Figure A1.63** <sup>13</sup>C NMR (100 MHz, CDCl<sub>3</sub>) of compound **69ga**.



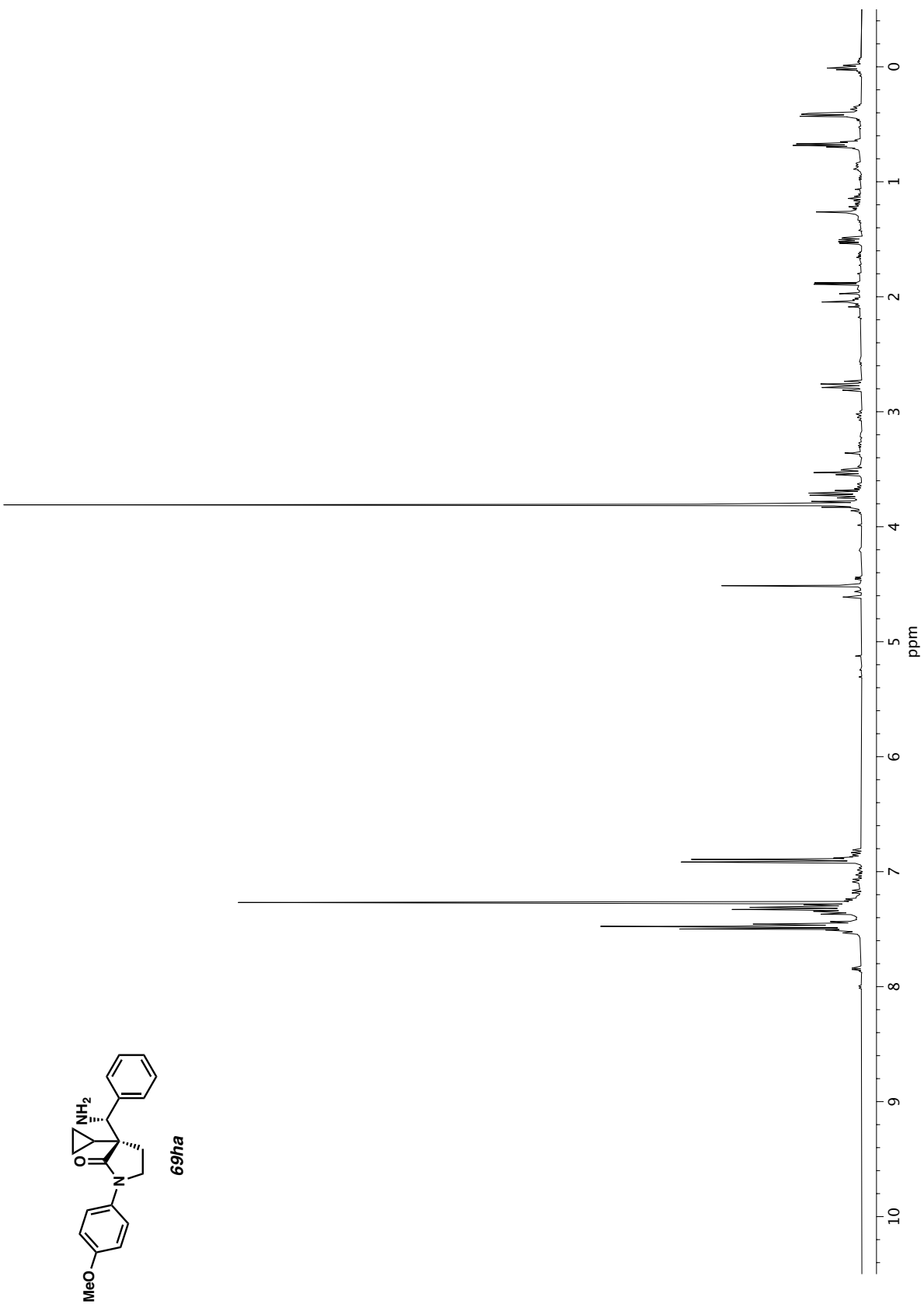
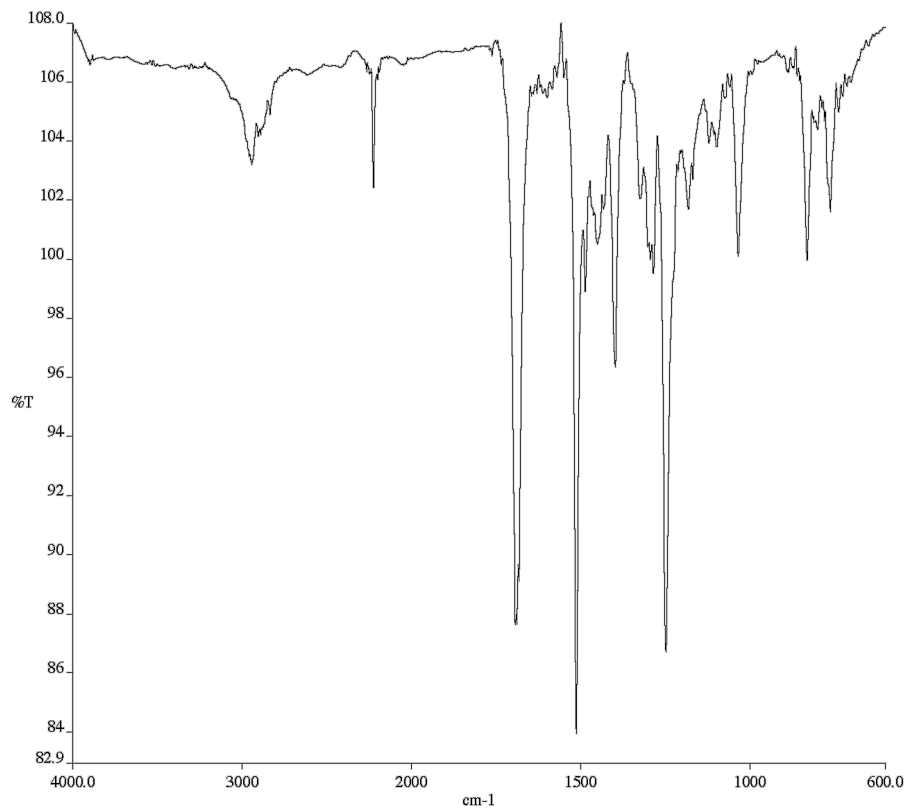
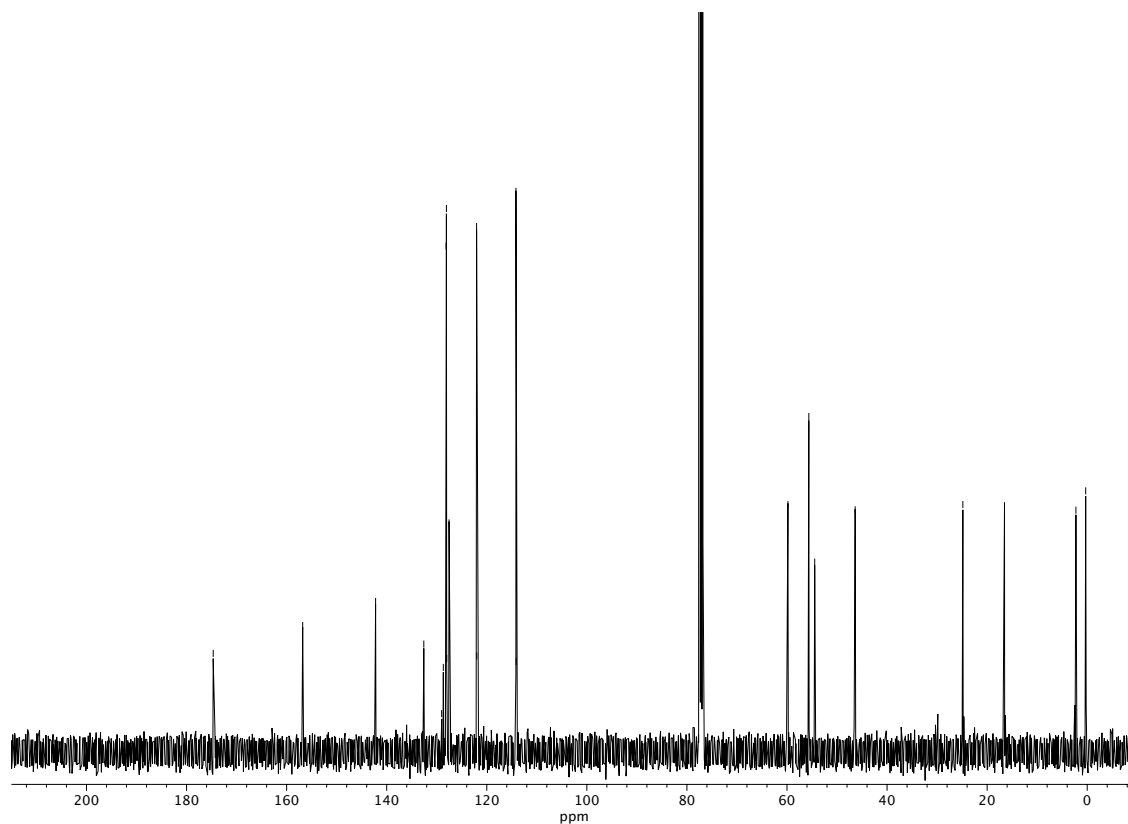


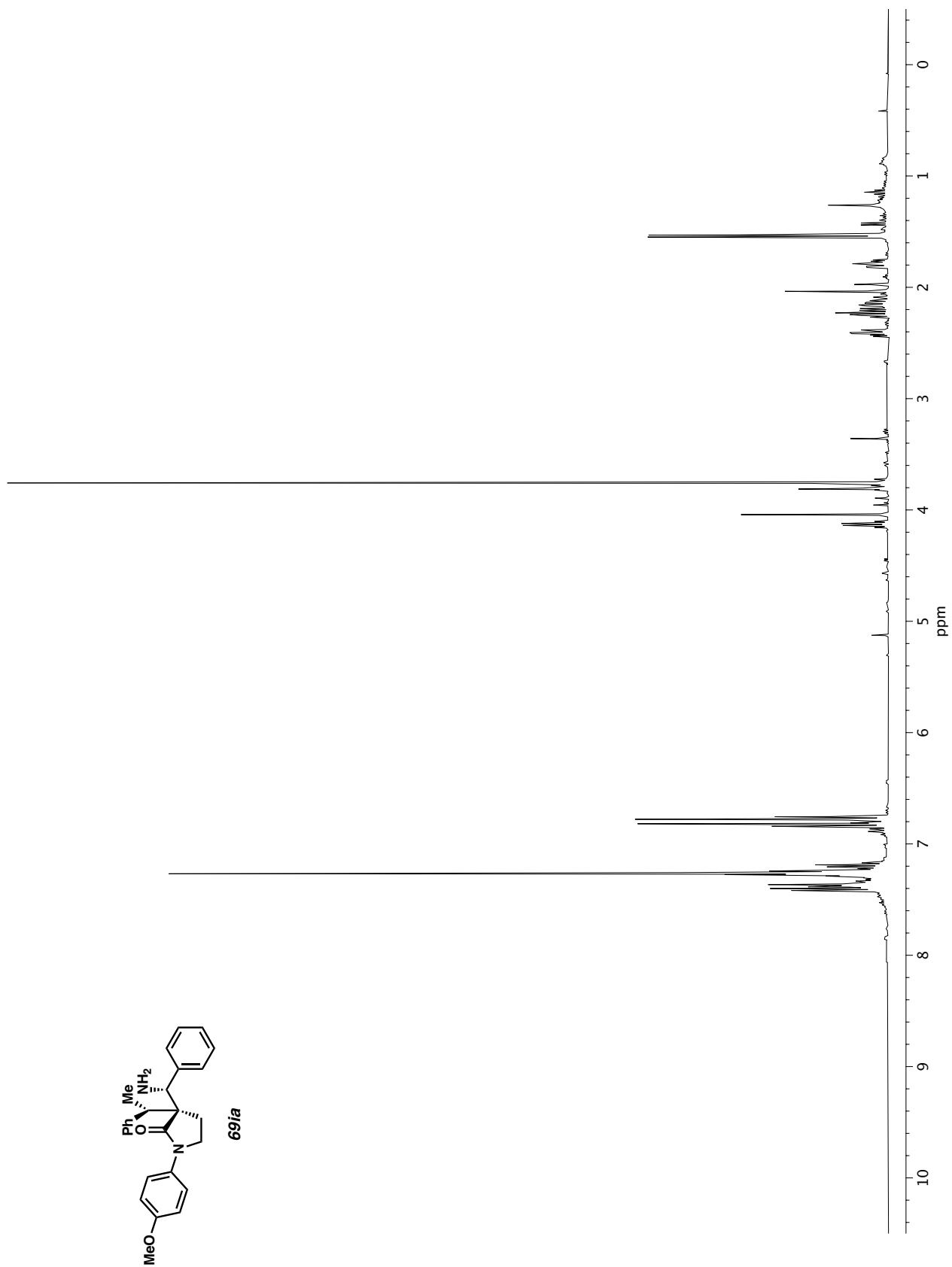
Figure A1.64 <sup>1</sup>H NMR (400 MHz, CDCl<sub>3</sub>) of compound **69ha**.



**Figure A1.65** Infrared spectrum (Thin Film, NaCl) of compound **69ha**.



**Figure A1.66** <sup>13</sup>C NMR (100 MHz, CDCl<sub>3</sub>) of compound **69ha**.

Figure A1.67  $^1\text{H}$  NMR (400 MHz,  $\text{CDCl}_3$ ) of compound **69ia**.

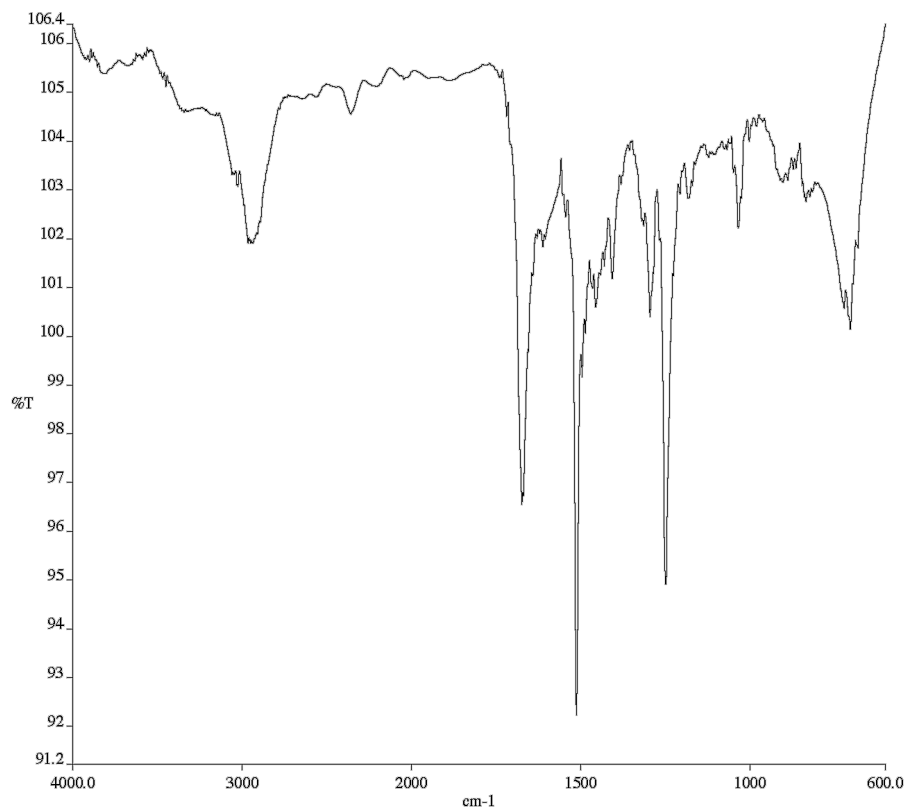


**Figure A1.68** Infrared spectrum (Thin Film, NaCl) of compound **69ia**.

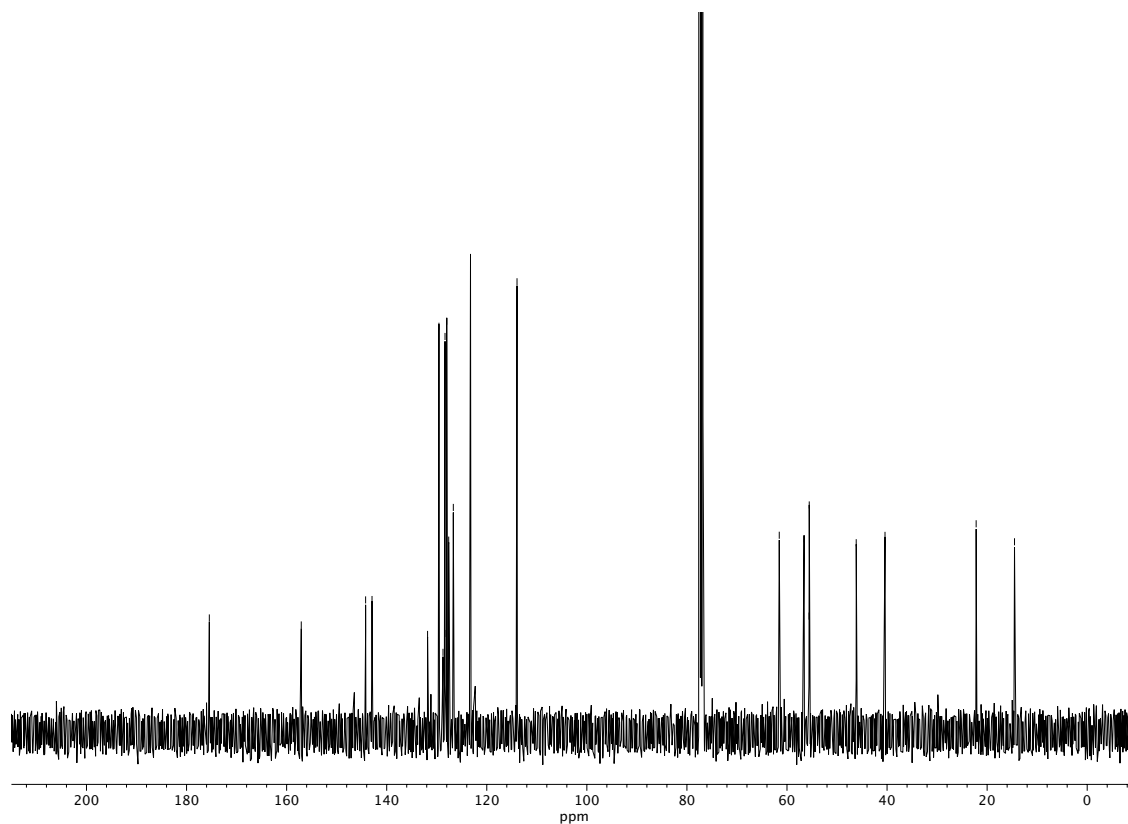


**Figure A1.69** <sup>13</sup>C NMR (100 MHz, CDCl<sub>3</sub>) of compound **69ia**.

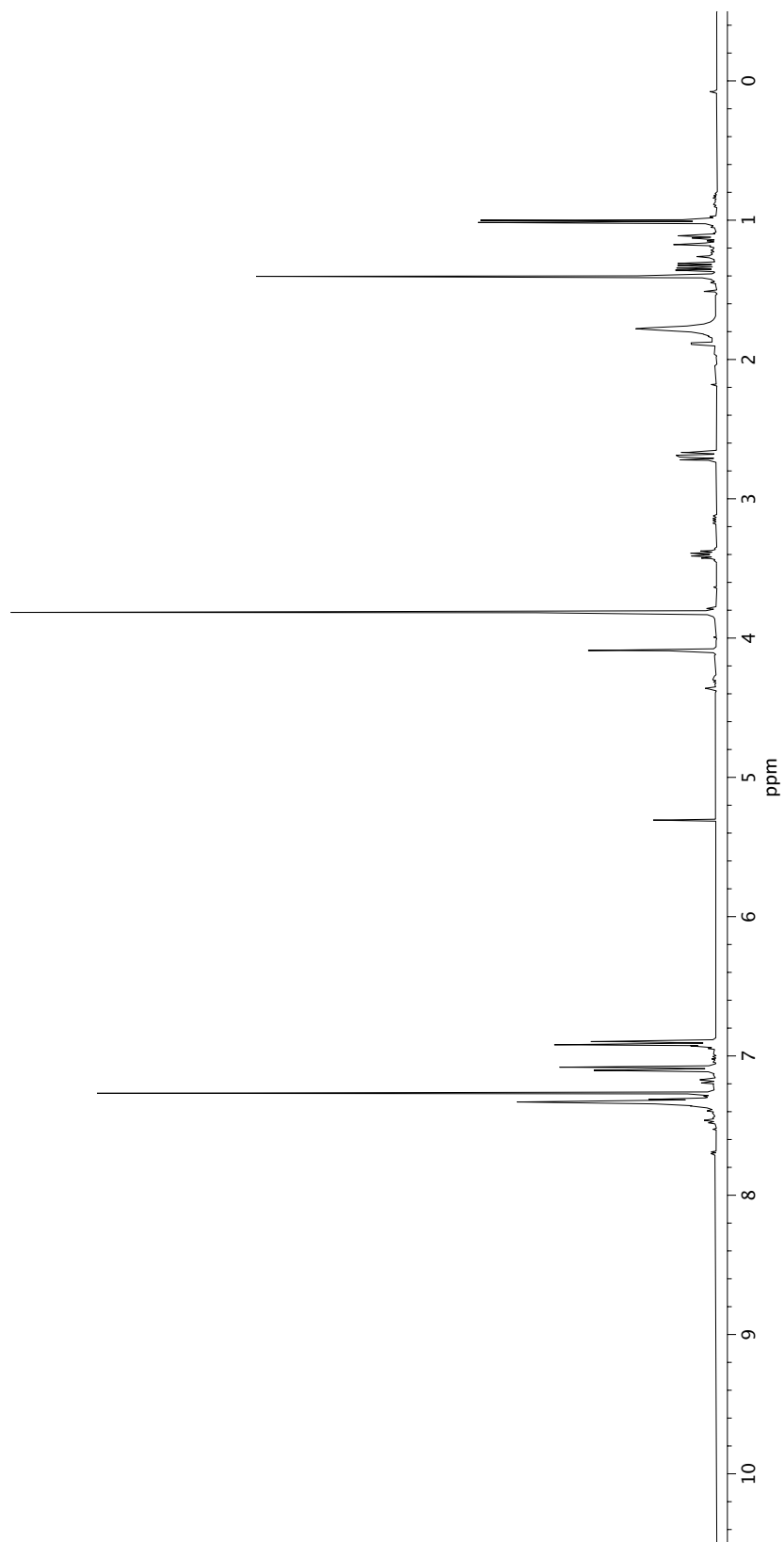
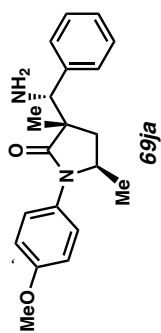


**Figure A1.70** <sup>1</sup>H NMR (400 MHz, CDCl<sub>3</sub>) of compound **69ja**.

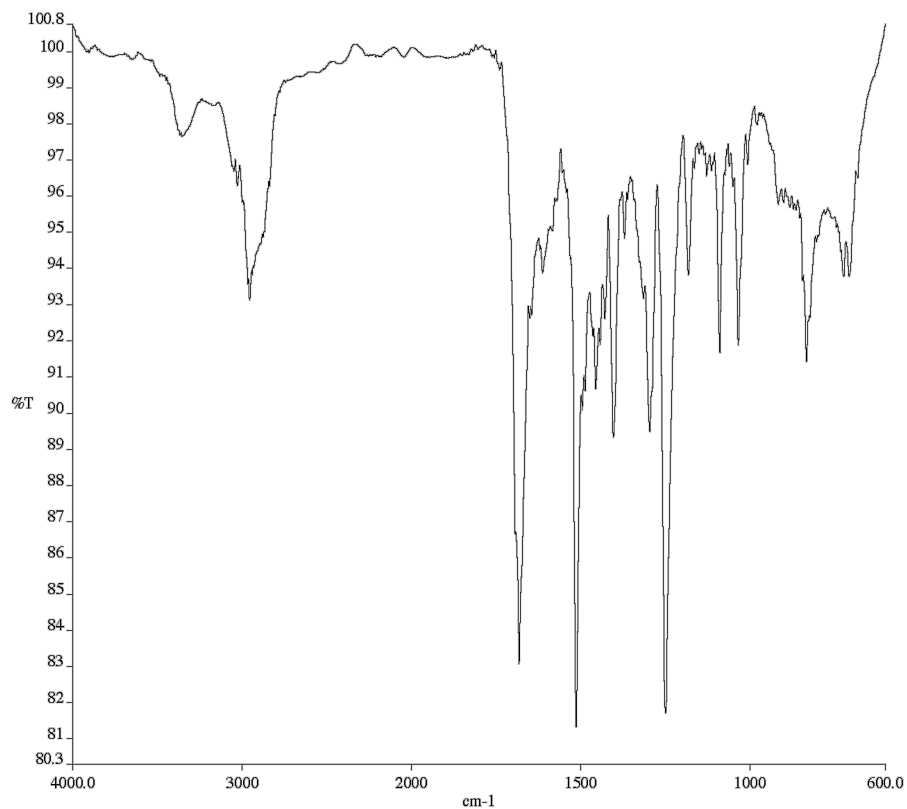


**Figure A1.71** Infrared spectrum (Thin Film, NaCl) of compound **69ja**.

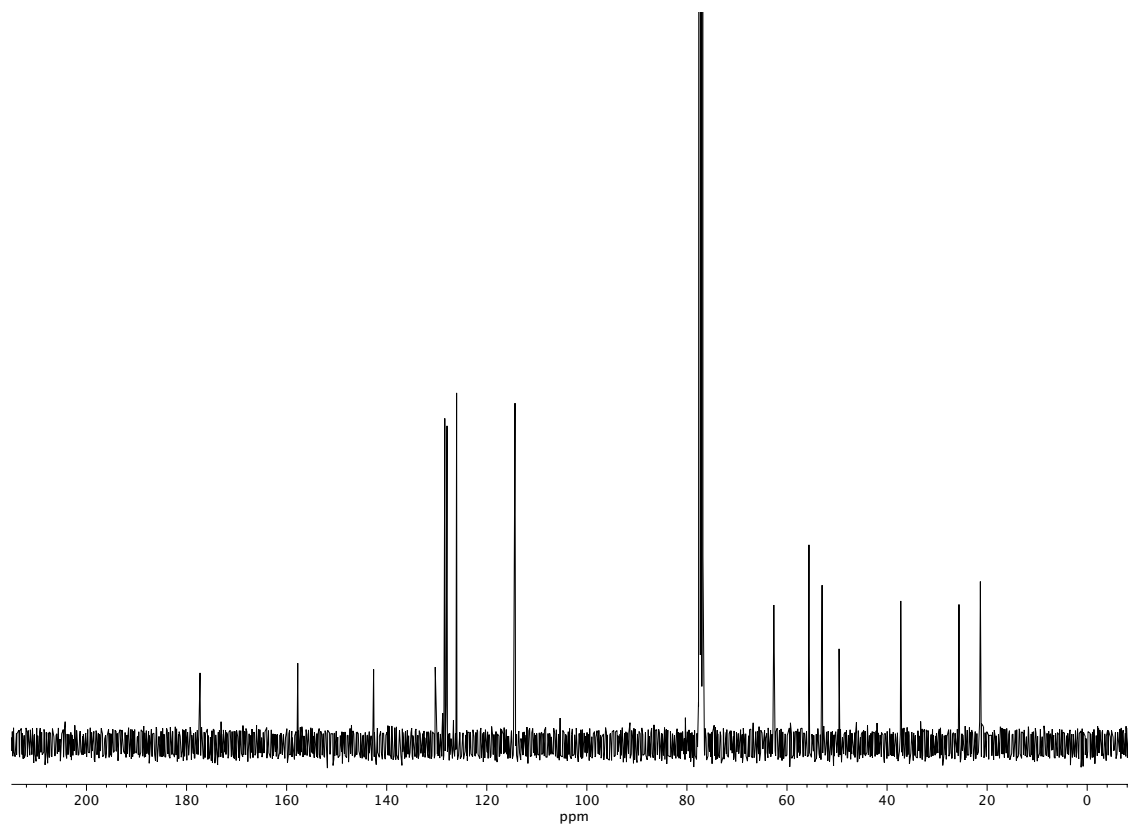


**Figure A1.72**  $^{13}\text{C}$  NMR (100 MHz,  $\text{CDCl}_3$ ) of compound **69ja**.

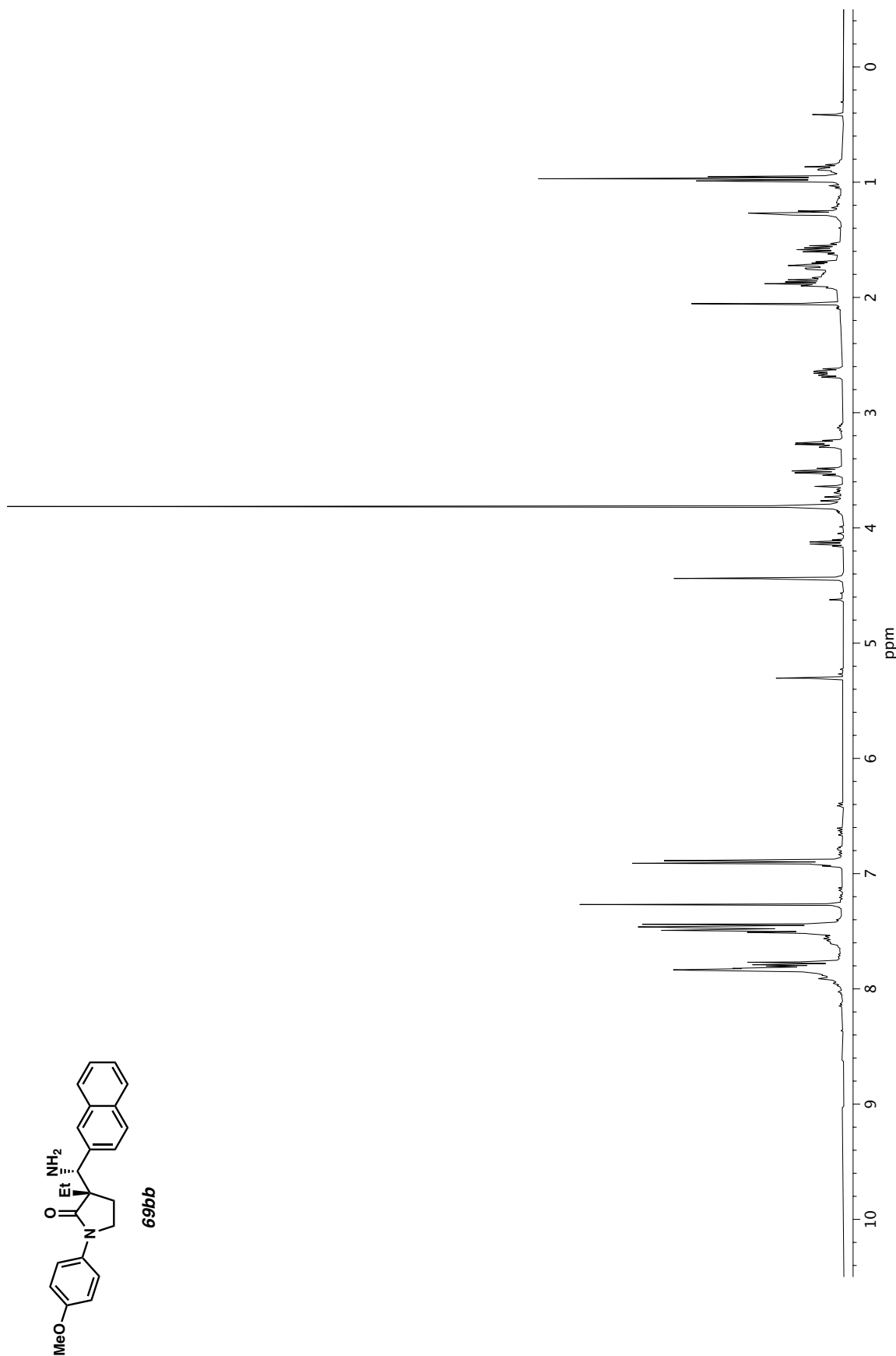
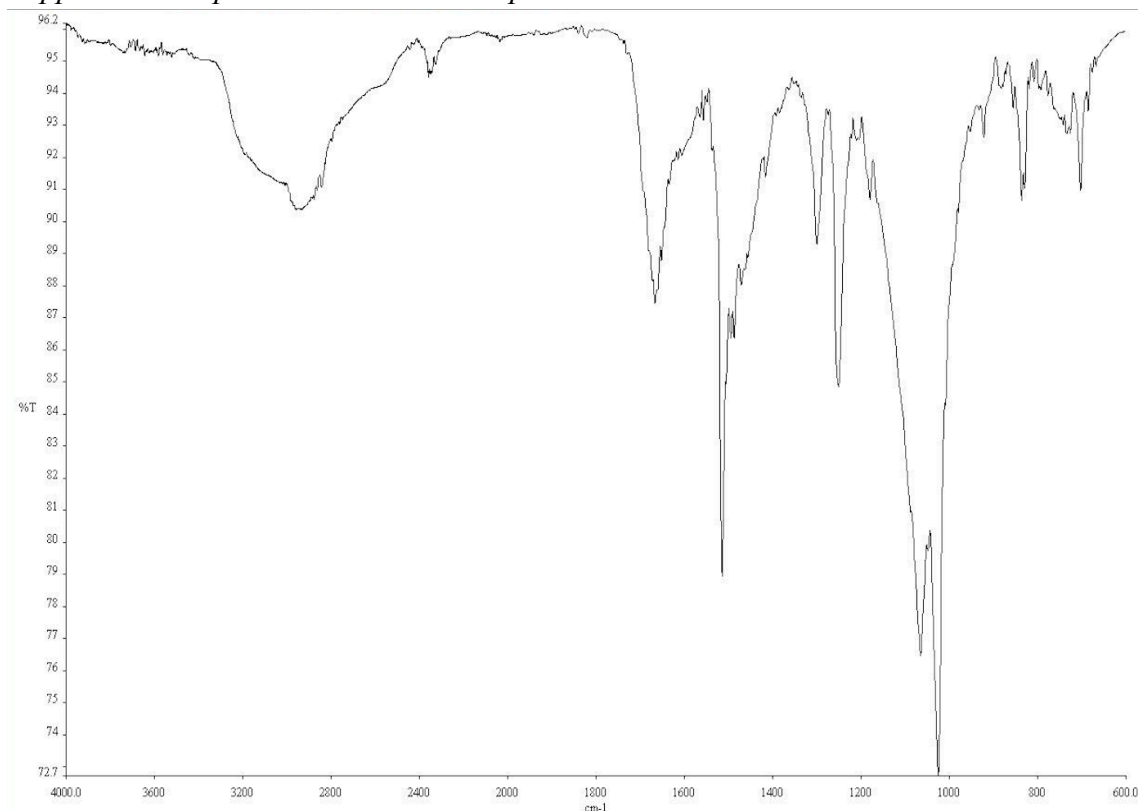
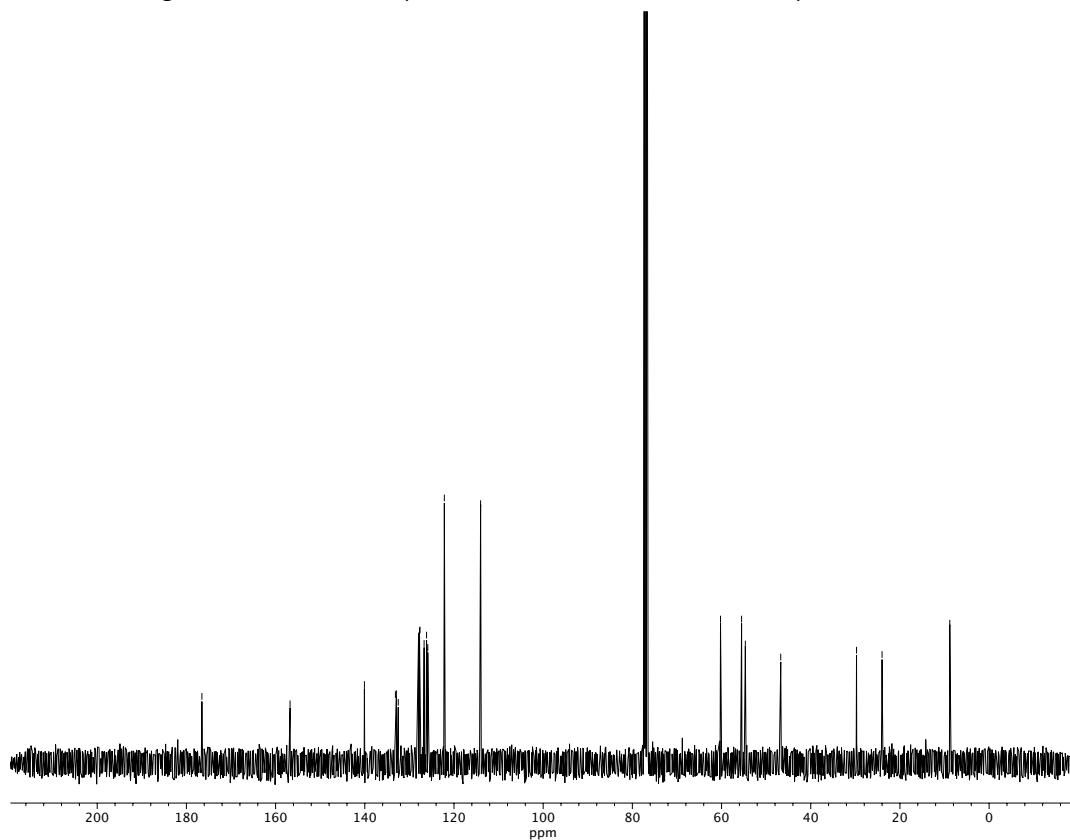


Figure A1.73  $^1\text{H}$  NMR (400 MHz,  $\text{CDCl}_3$ ) of compound **69bb**.



**Figure A1.74** Infrared spectrum (Thin Film, NaCl) of compound **69bb**.



**Figure A1.75** <sup>13</sup>C NMR (100 MHz, CDCl<sub>3</sub>) of compound **69bb**.



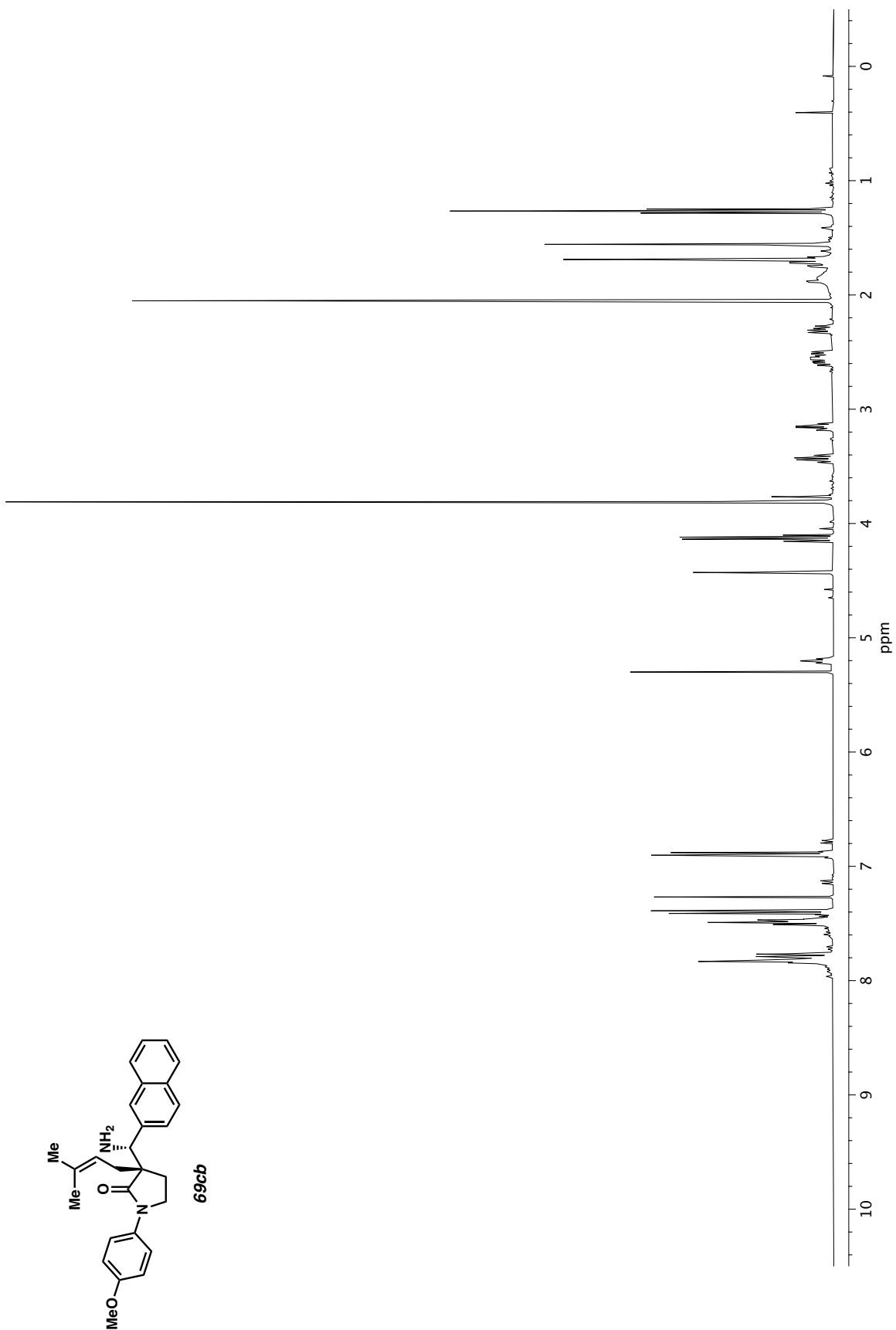
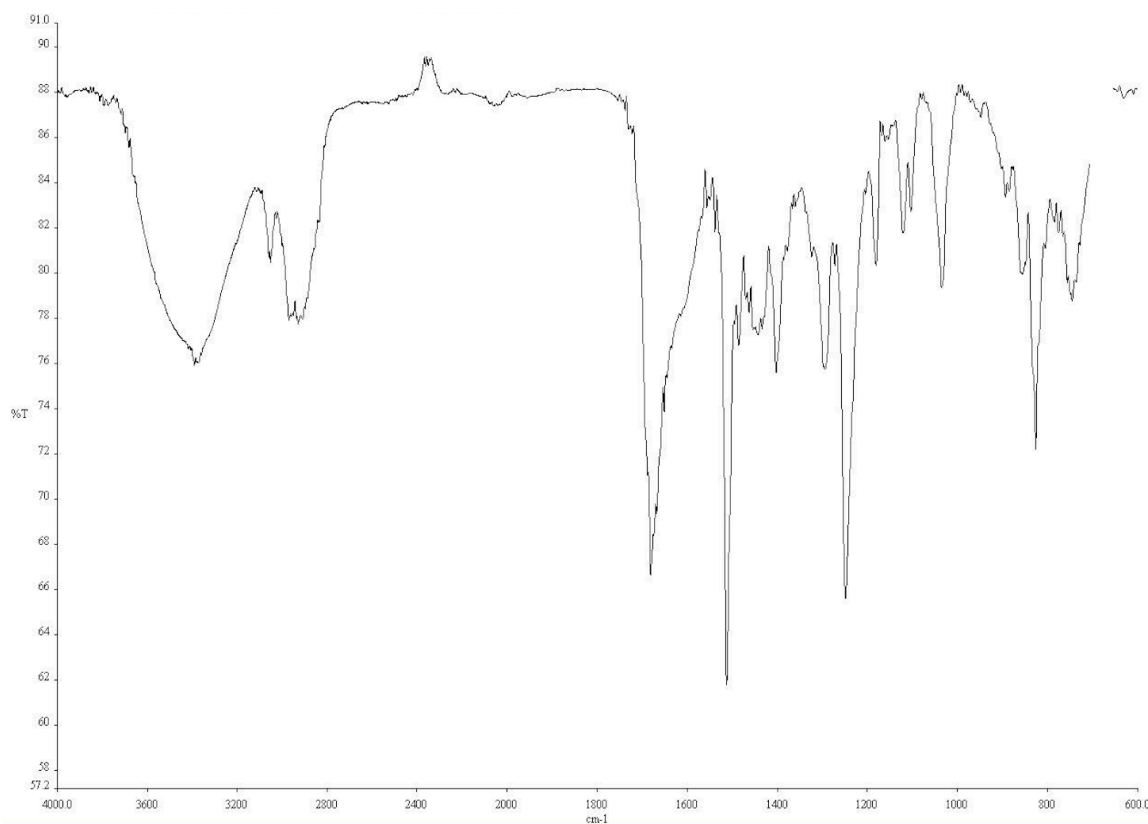
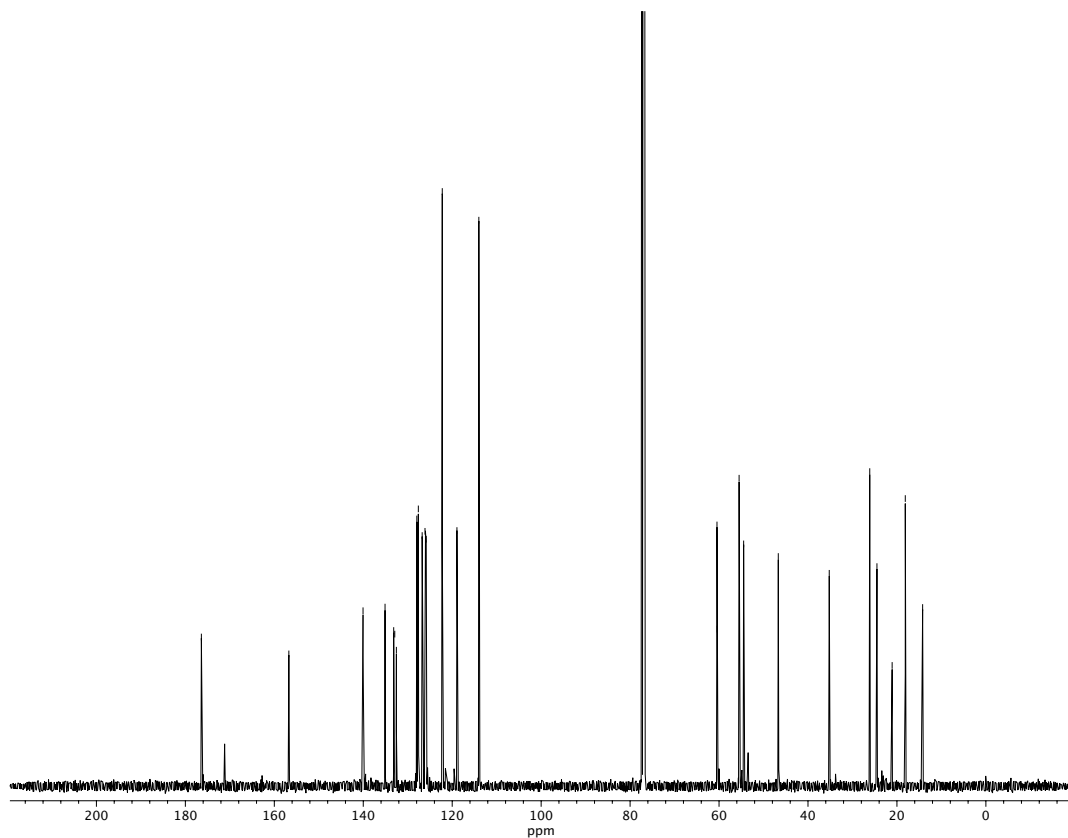


Figure A1.76  $^1\text{H}$  NMR (400 MHz,  $\text{CDCl}_3$ ) of compound **69cb**.



**Figure A1.77** Infrared spectrum (Thin Film, NaCl) of compound **69cb**.



**Figure A1.78** <sup>13</sup>C NMR (100 MHz, CDCl<sub>3</sub>) of compound **69cb**.

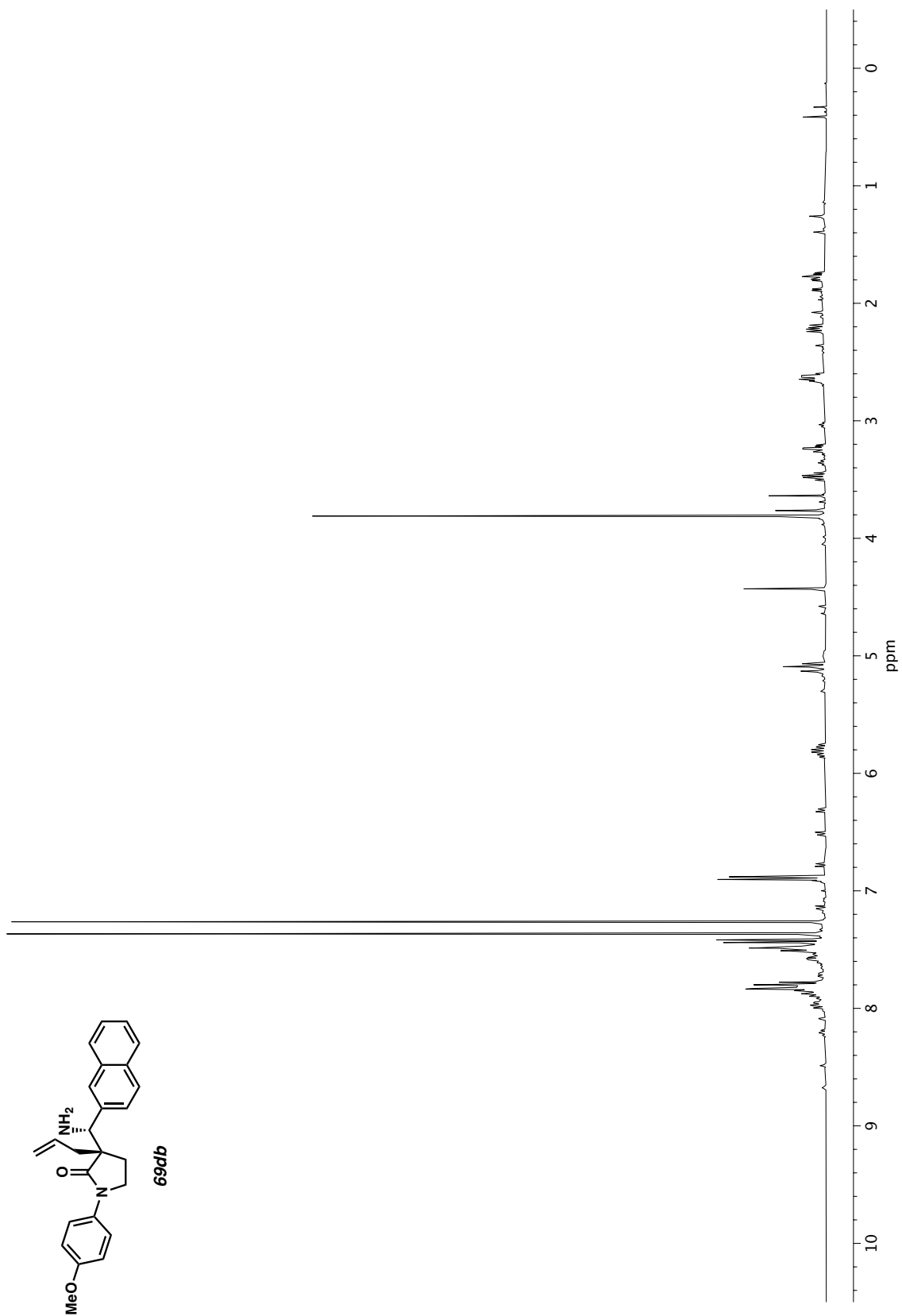
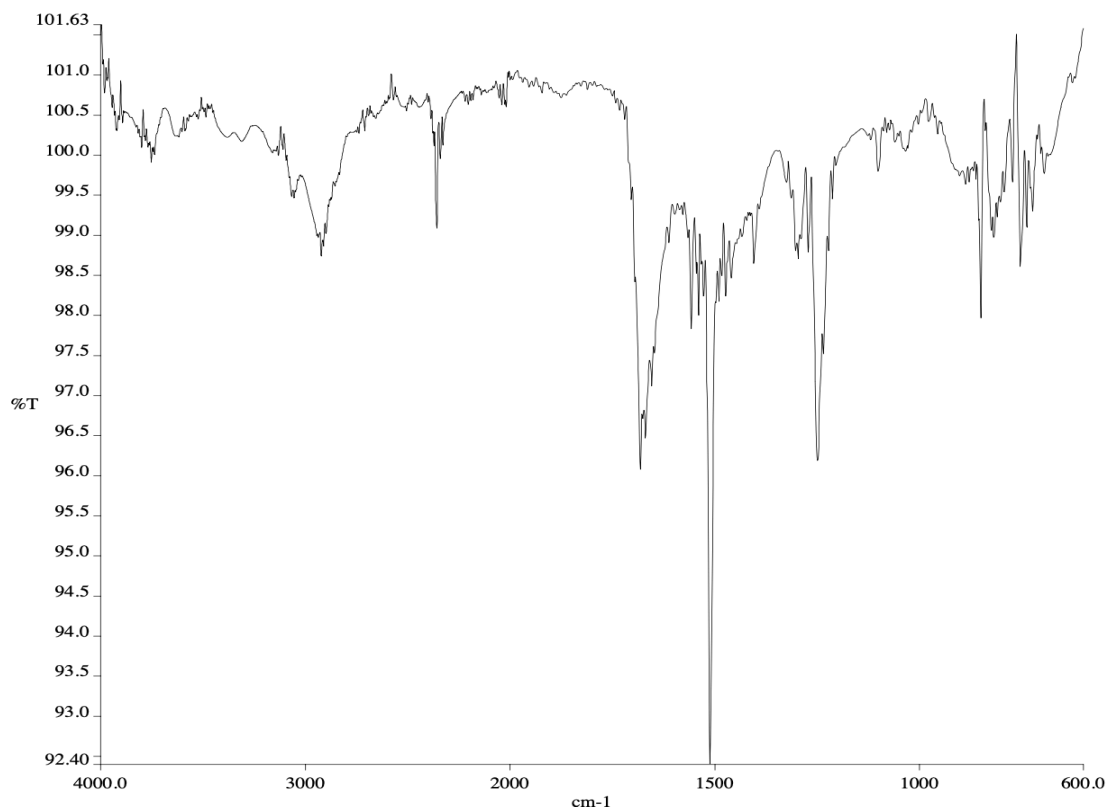
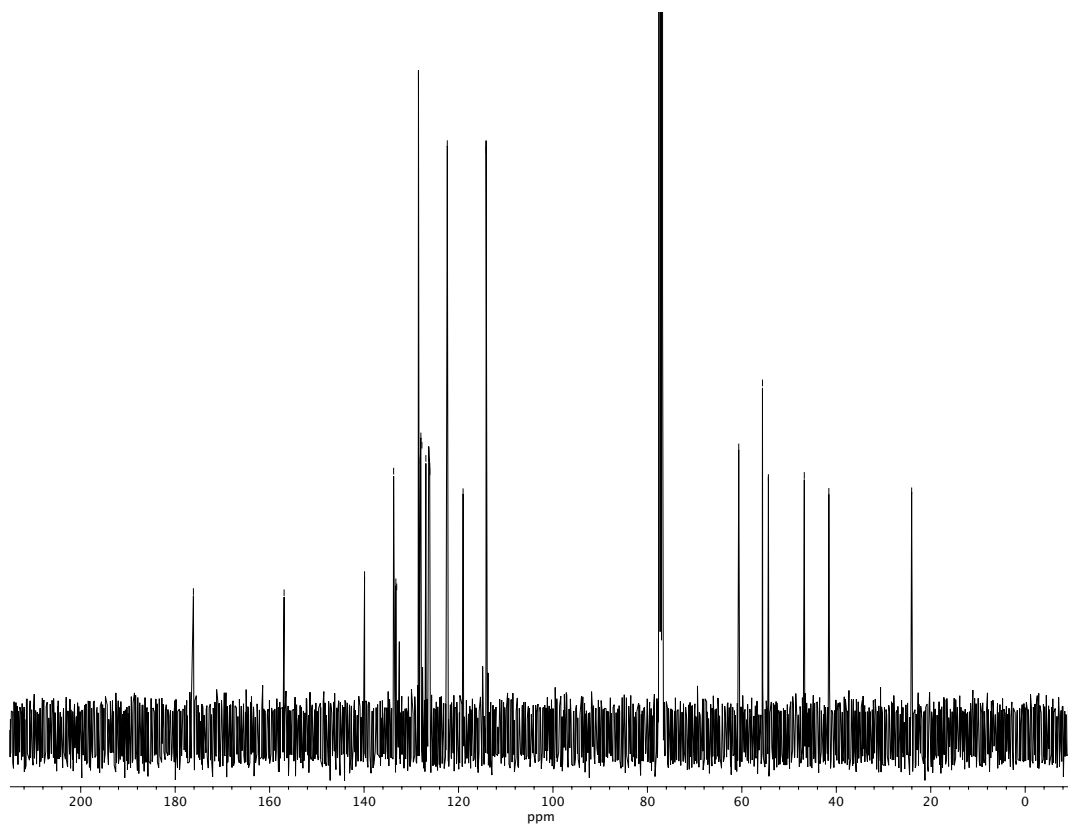


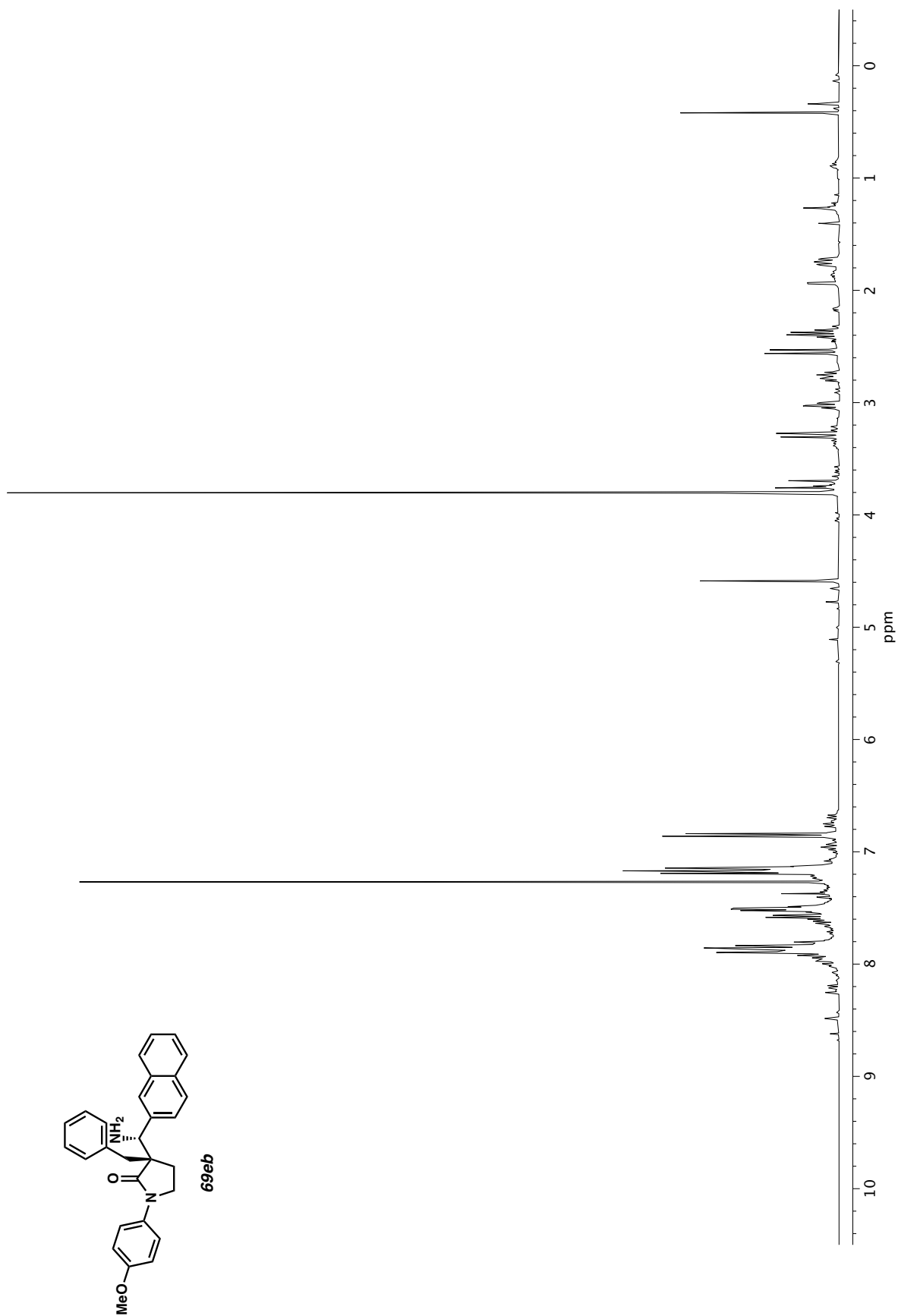
Figure A1.79  $^1\text{H}$  NMR (400 MHz,  $\text{CDCl}_3$ ) of compound **69db**.



**Figure A1.80** Infrared spectrum (Thin Film, NaCl) of compound **69db**.



**Figure A1.81** <sup>13</sup>C NMR (100 MHz, CDCl<sub>3</sub>) of compound **69db**.



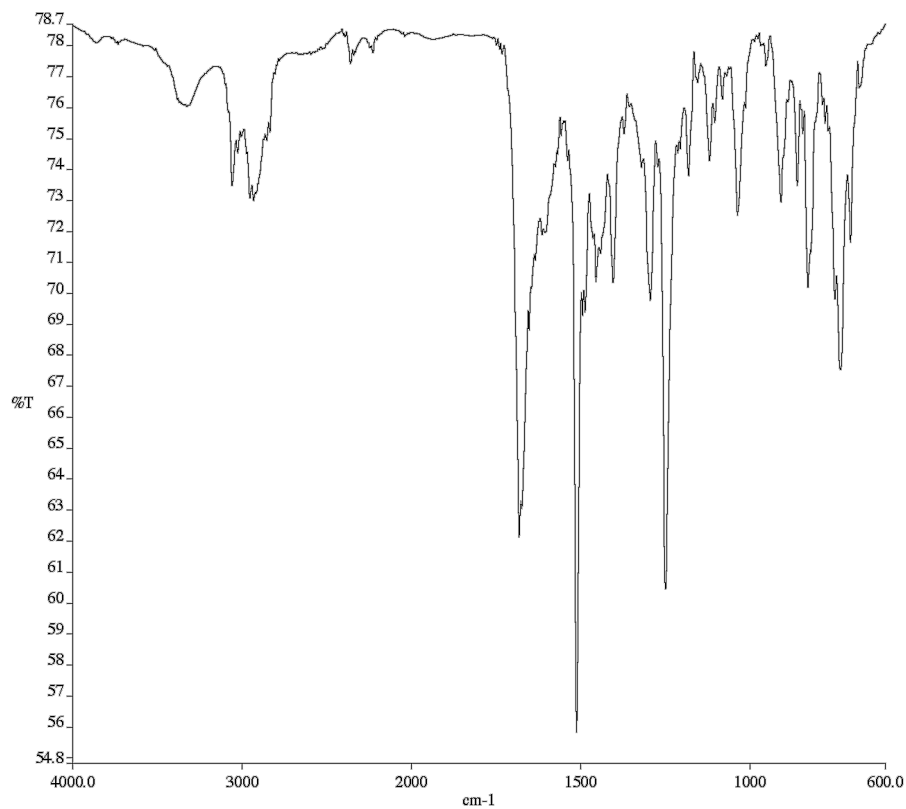


**Figure A1.83** Infrared spectrum (Thin Film, NaCl) of compound **69eb**

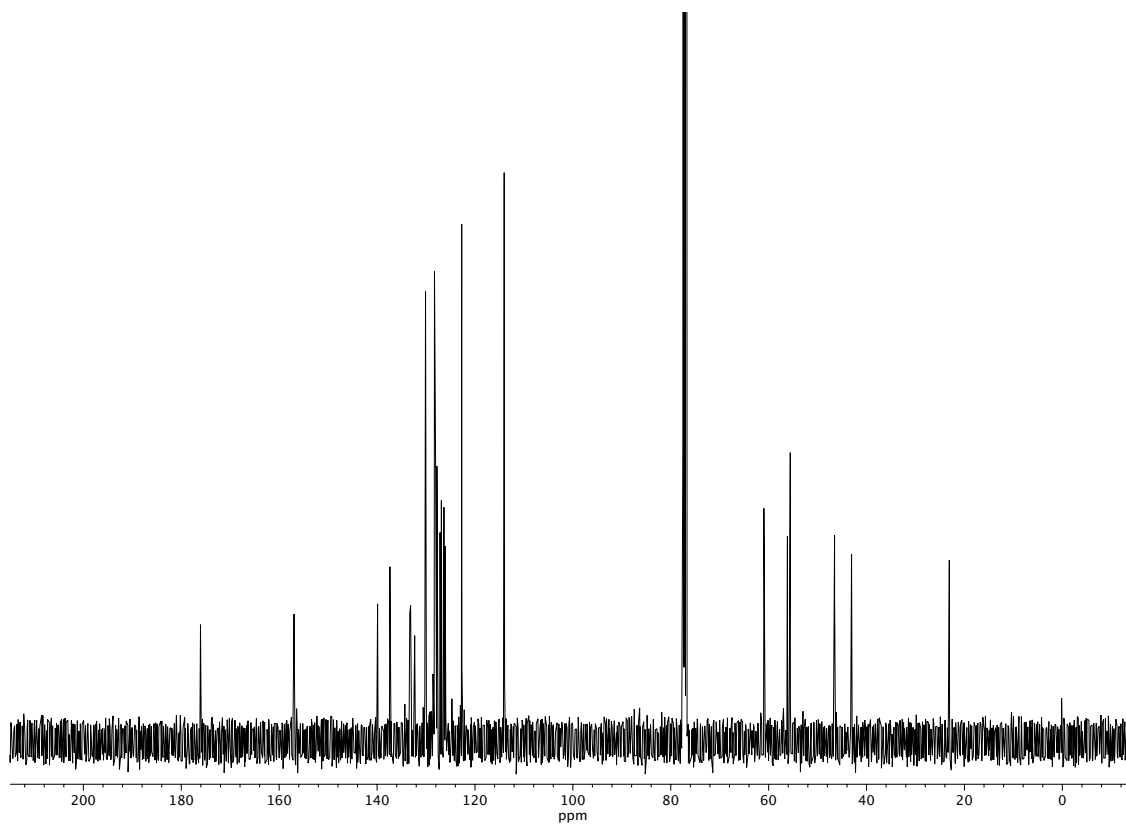


**Figure A1.84** <sup>13</sup>C NMR (100 MHz, CDCl<sub>3</sub>) of compound **69eb**.

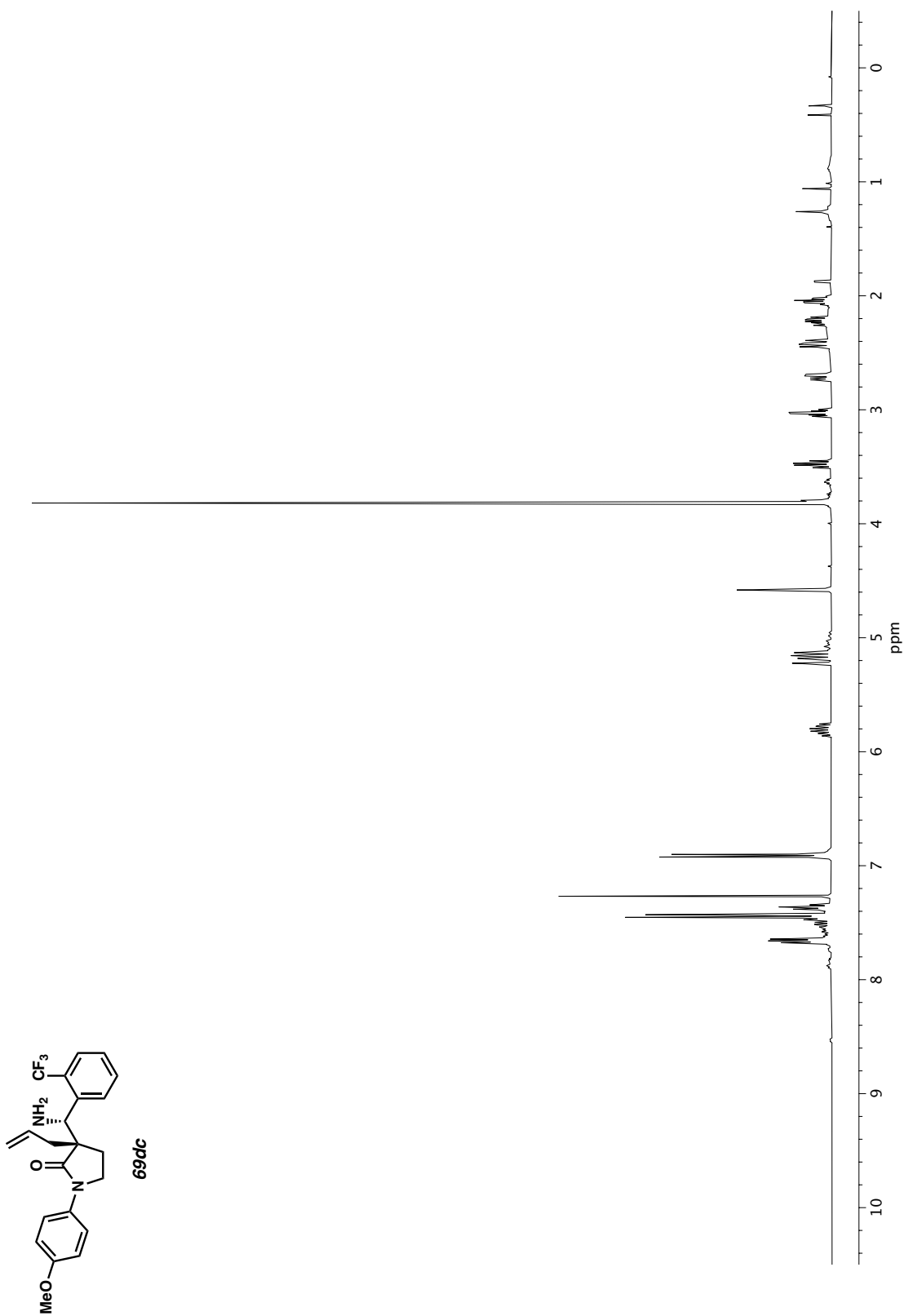
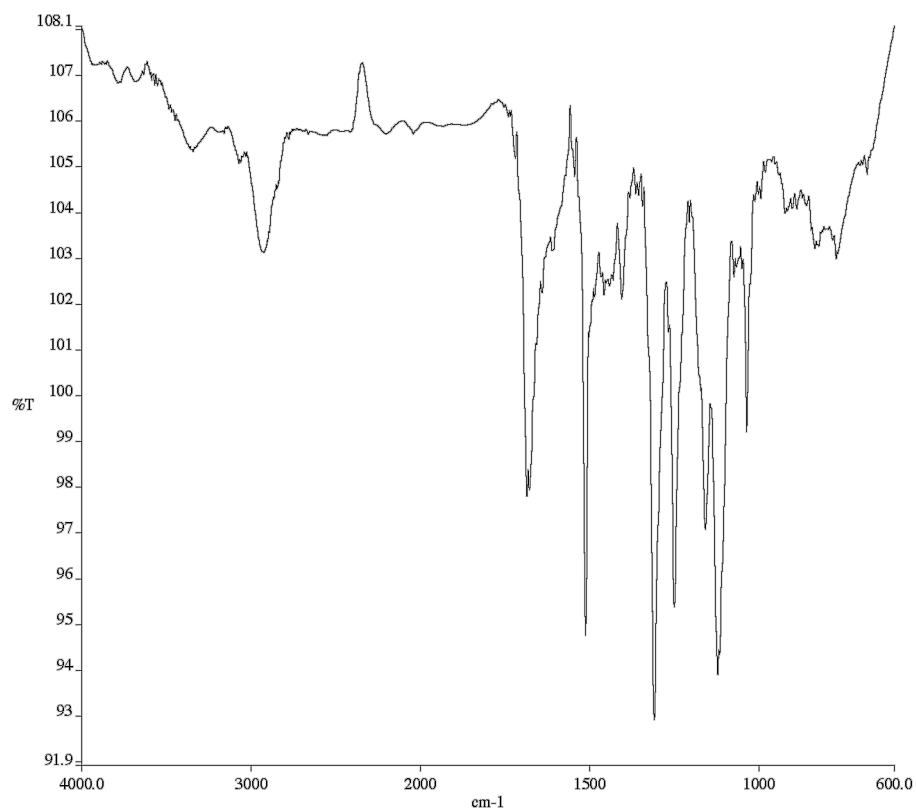
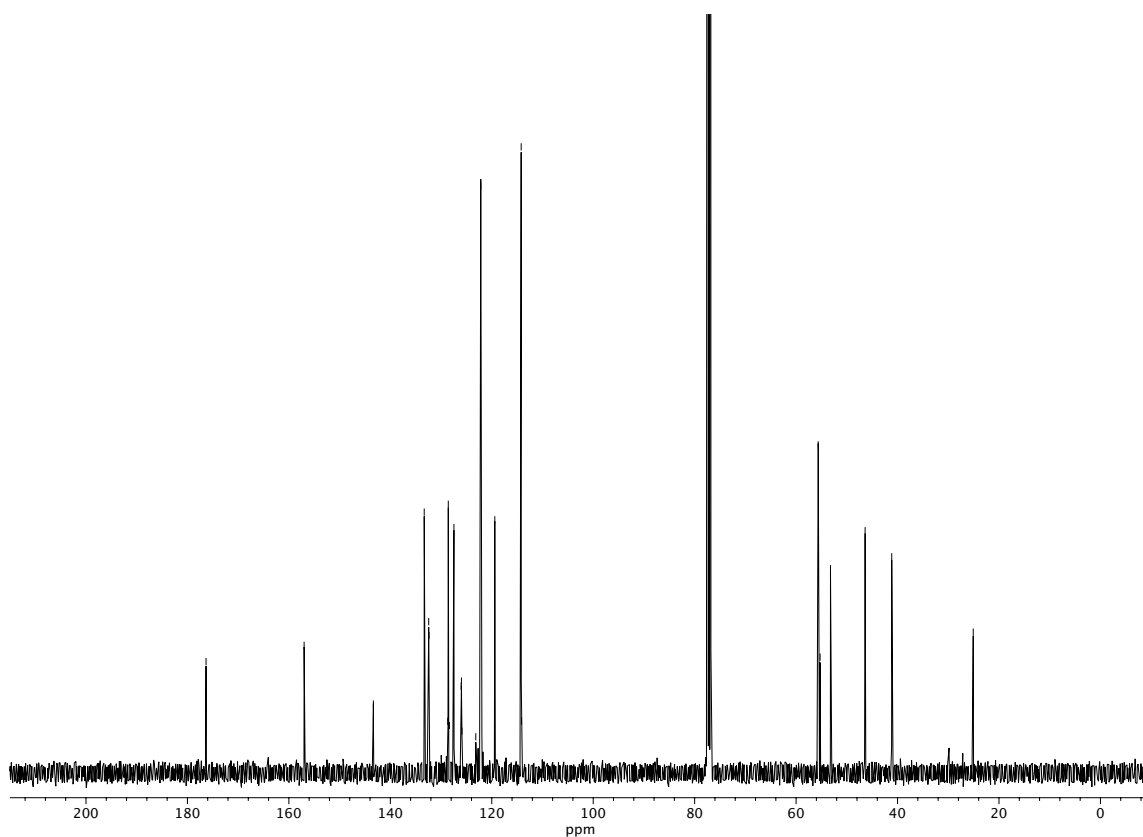


Figure A1.85 <sup>1</sup>H NMR (400 MHz, CDCl<sub>3</sub>) of compound **69dc**.



**Figure A1.86** Infrared spectrum (Thin Film, NaCl) of compound **69dc**.



**Figure A1.87** <sup>13</sup>C NMR (100 MHz, CDCl<sub>3</sub>) of compound **69dc**.



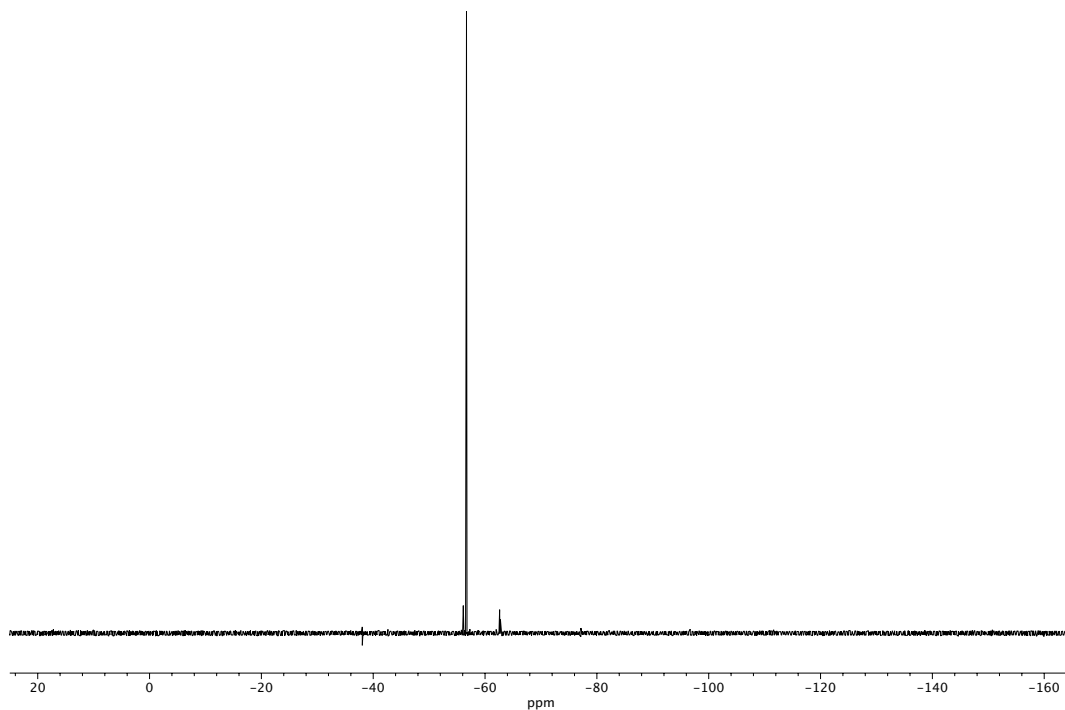


**Figure A1.88**  $^{19}\text{F}$  NMR (282 MHz,  $\text{CDCl}_3$ ) of compound **69dc**.

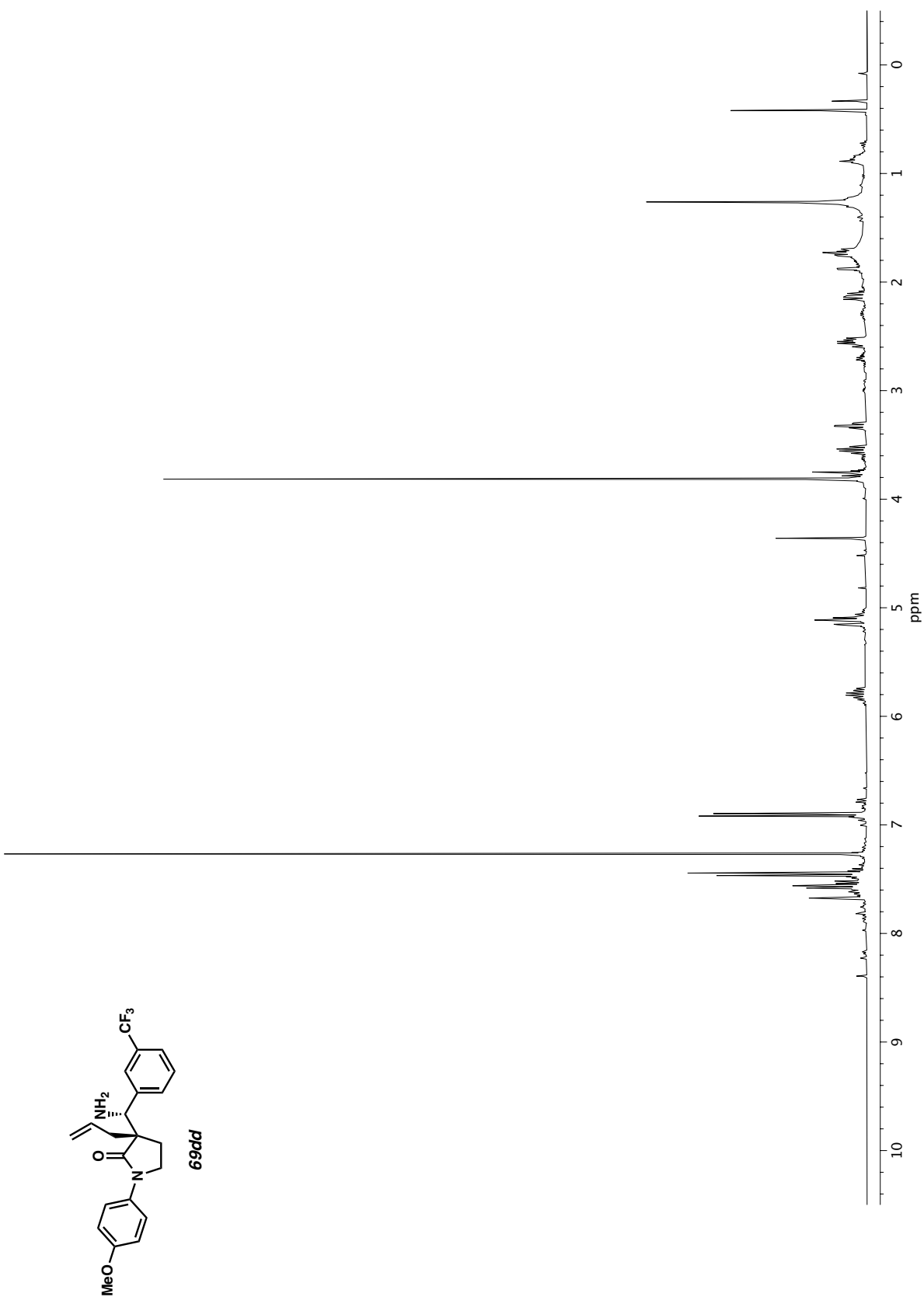


**Figure A1.89** <sup>1</sup>H NMR (400 MHz, CDCl<sub>3</sub>) of compound **69dd**.

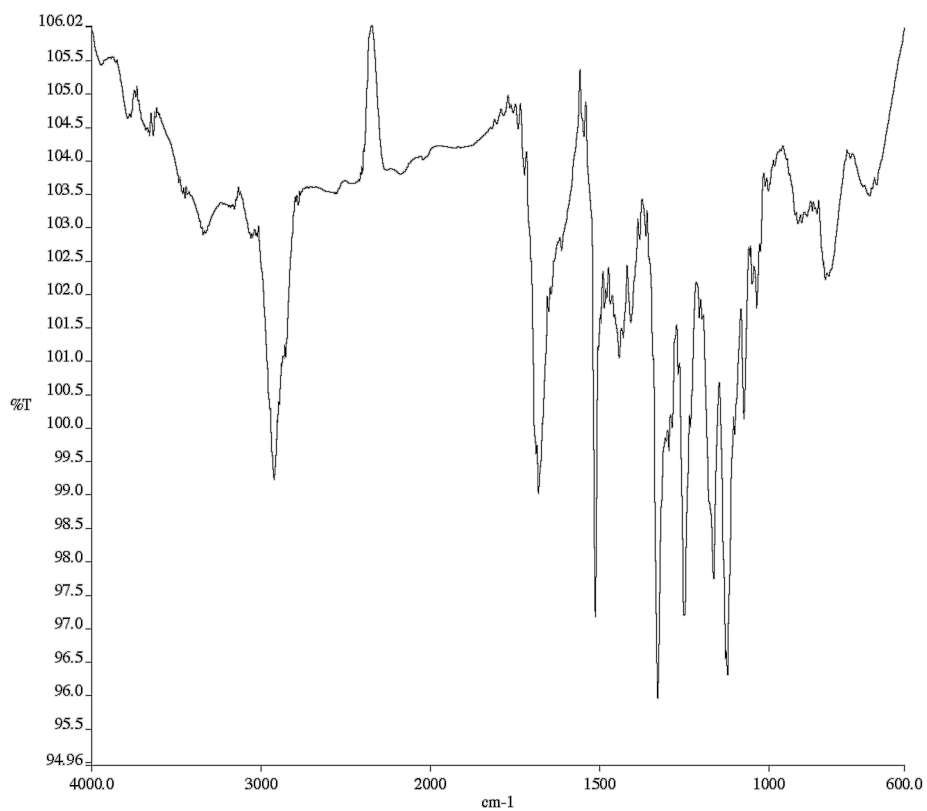


**Figure A1.90** Infrared spectrum (Thin Film, NaCl) of compound **69dd**.

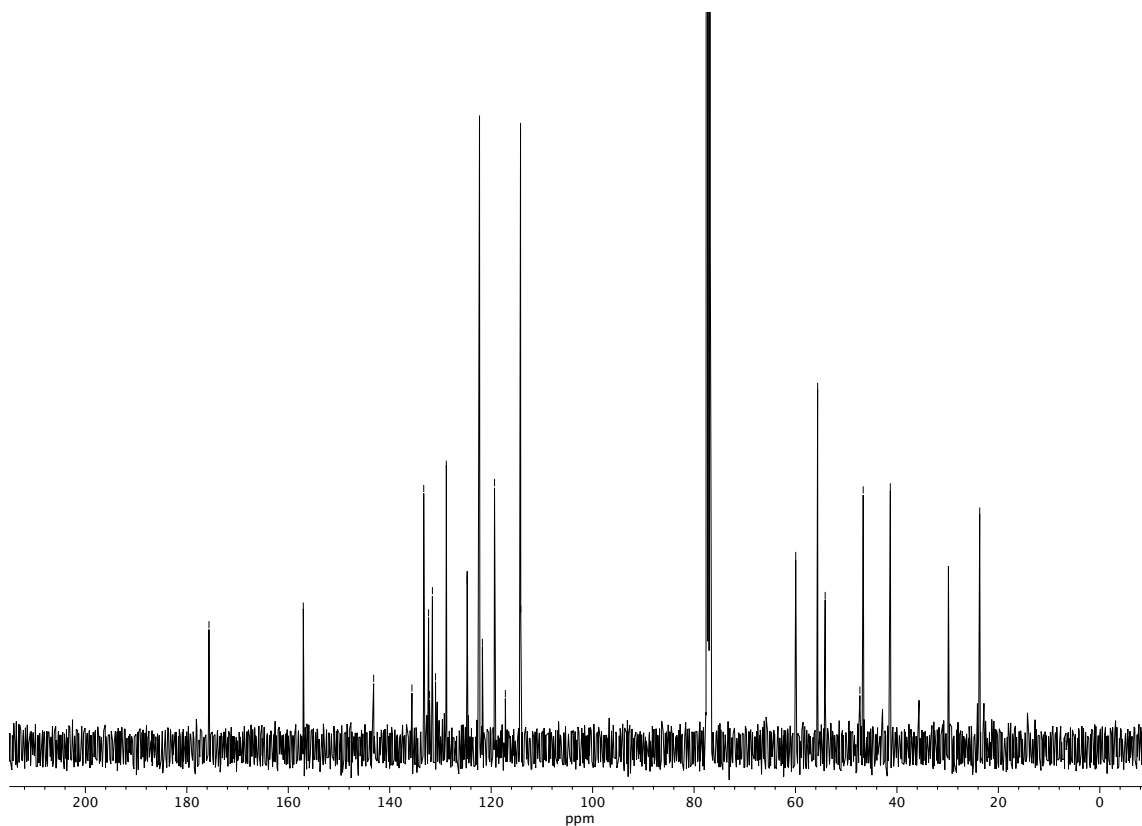


**Figure A1.91**  $^{13}\text{C}$  NMR (100 MHz,  $\text{CDCl}_3$ ) of compound **69dd**.

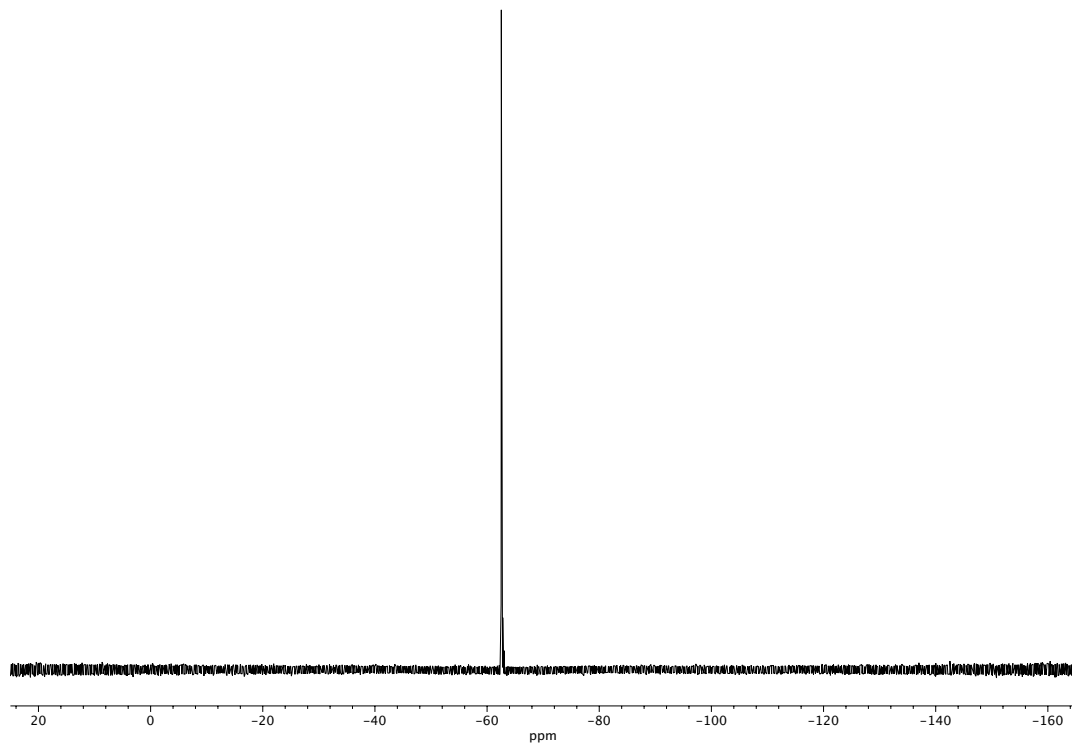


**Figure A1.92**  $^{19}\text{F}$  NMR (282 MHz,  $\text{CDCl}_3$ ) of compound **69dd**.

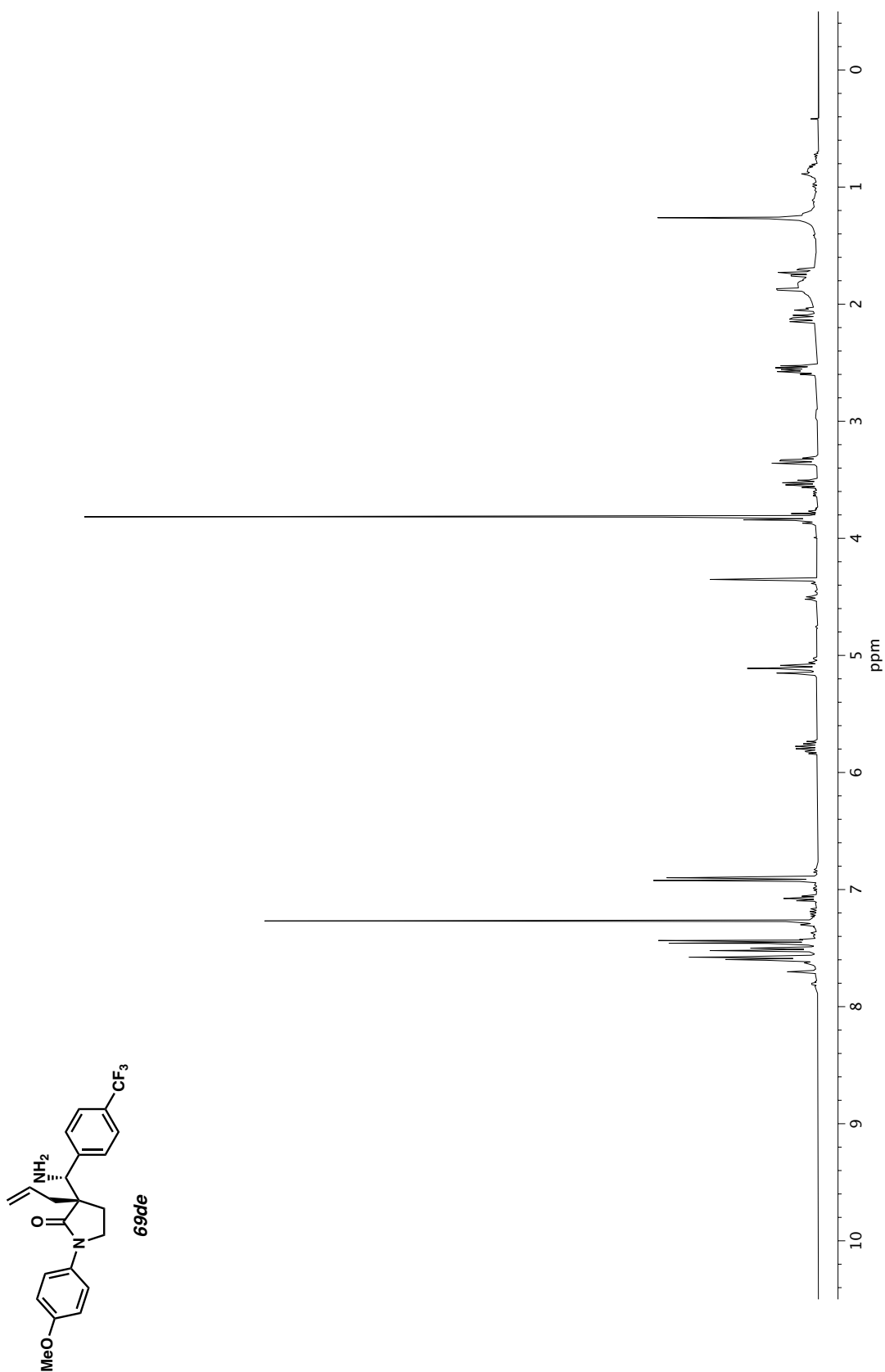
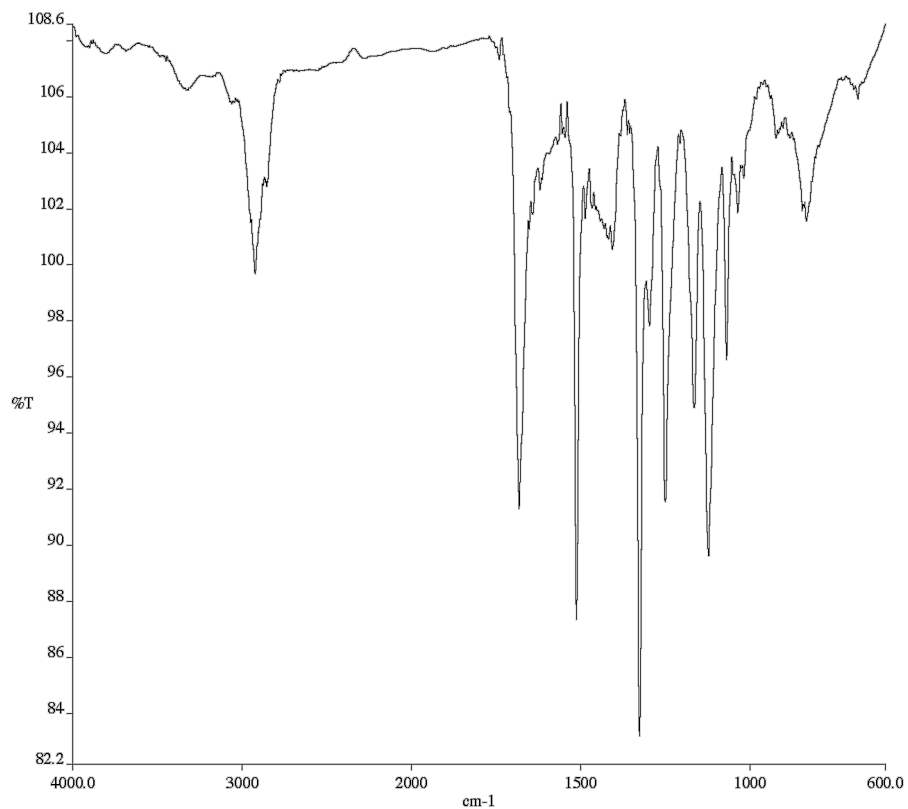
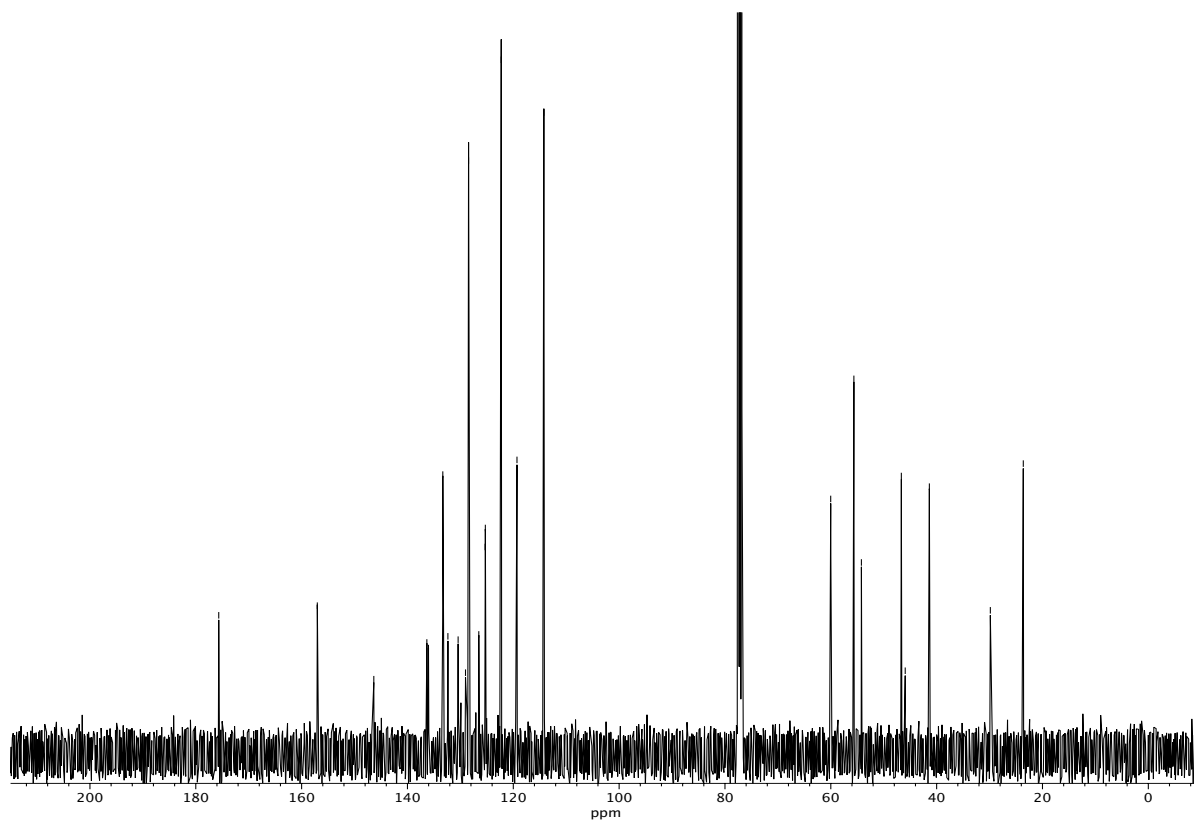


Figure A1.93 <sup>1</sup>H NMR (400 MHz, CDCl<sub>3</sub>) of compound **69de**.



**Figure A1.94** Infrared spectrum (Thin Film, NaCl) of compound **69de**.



**Figure A1.95** <sup>13</sup>C NMR (100 MHz, CDCl<sub>3</sub>) of compound **69de**.

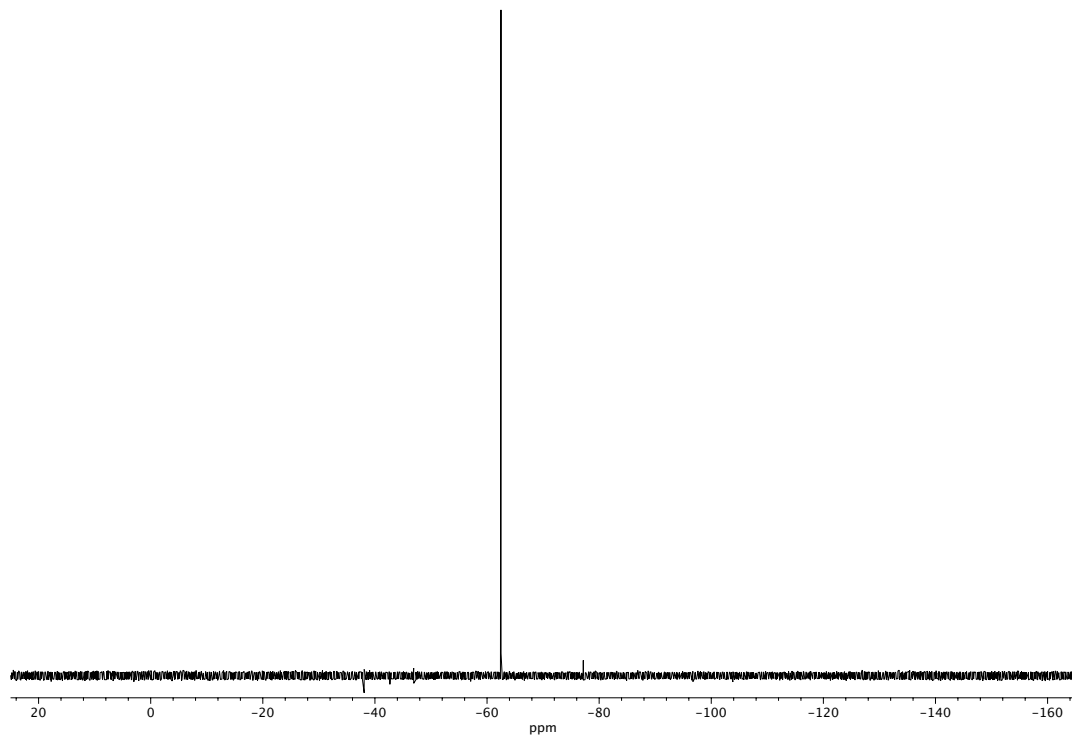


**Figure A1.96**  $^{19}\text{F}$  NMR (282 MHz,  $\text{CDCl}_3$ ) of compound **69de**.

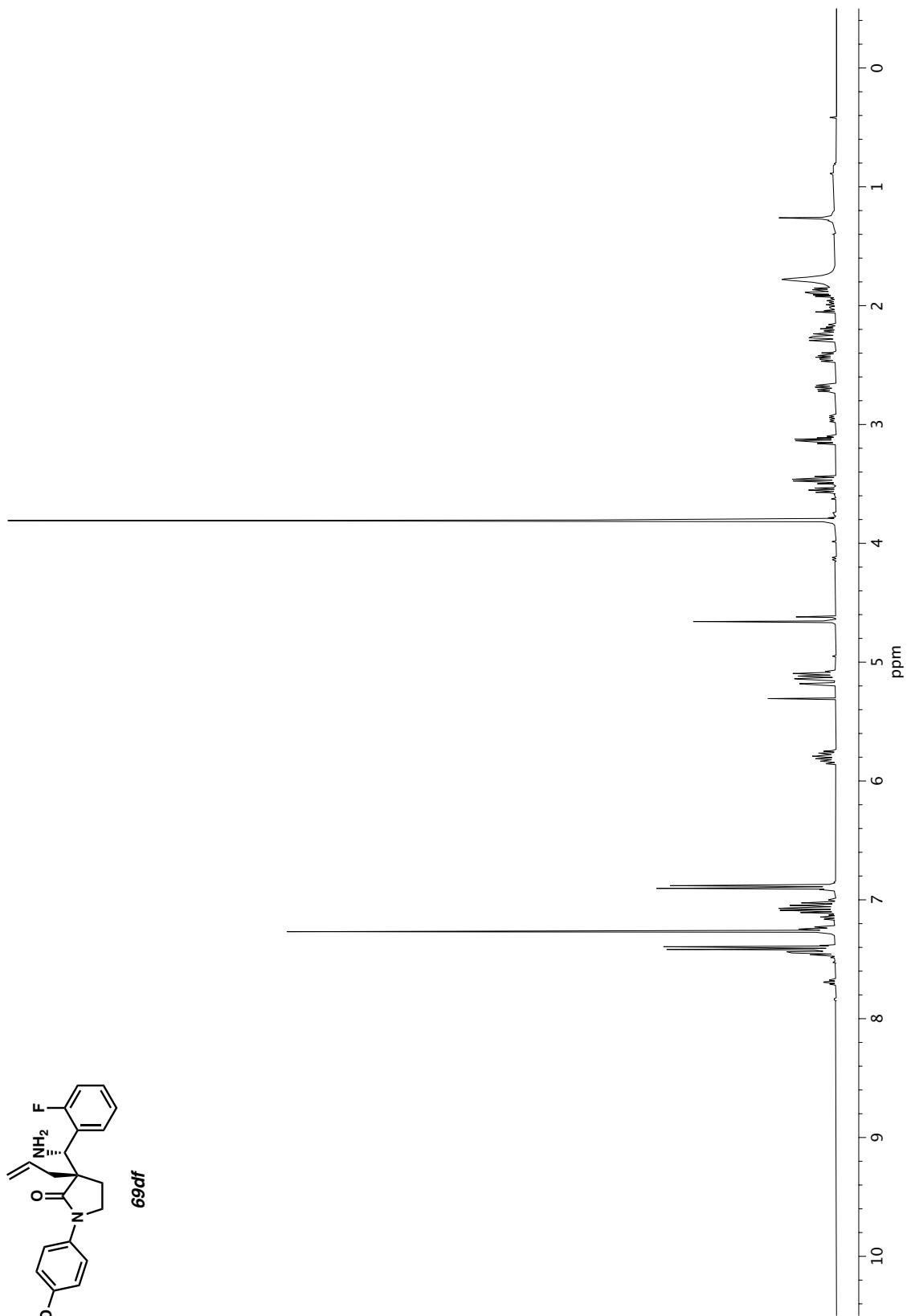
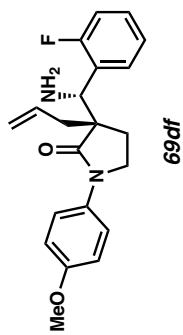
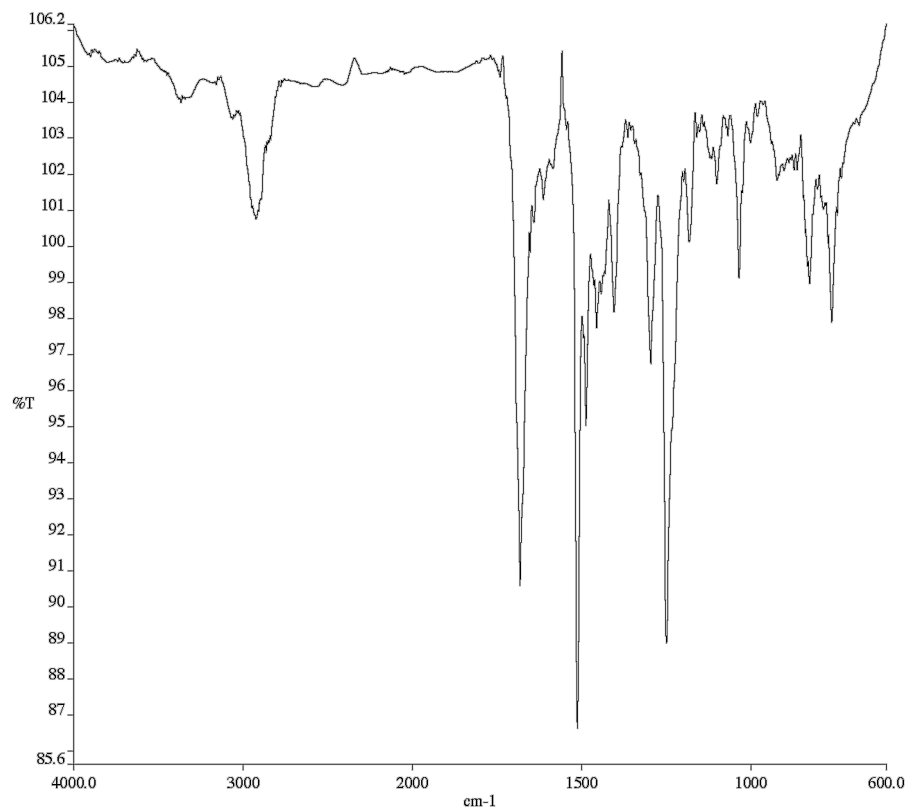
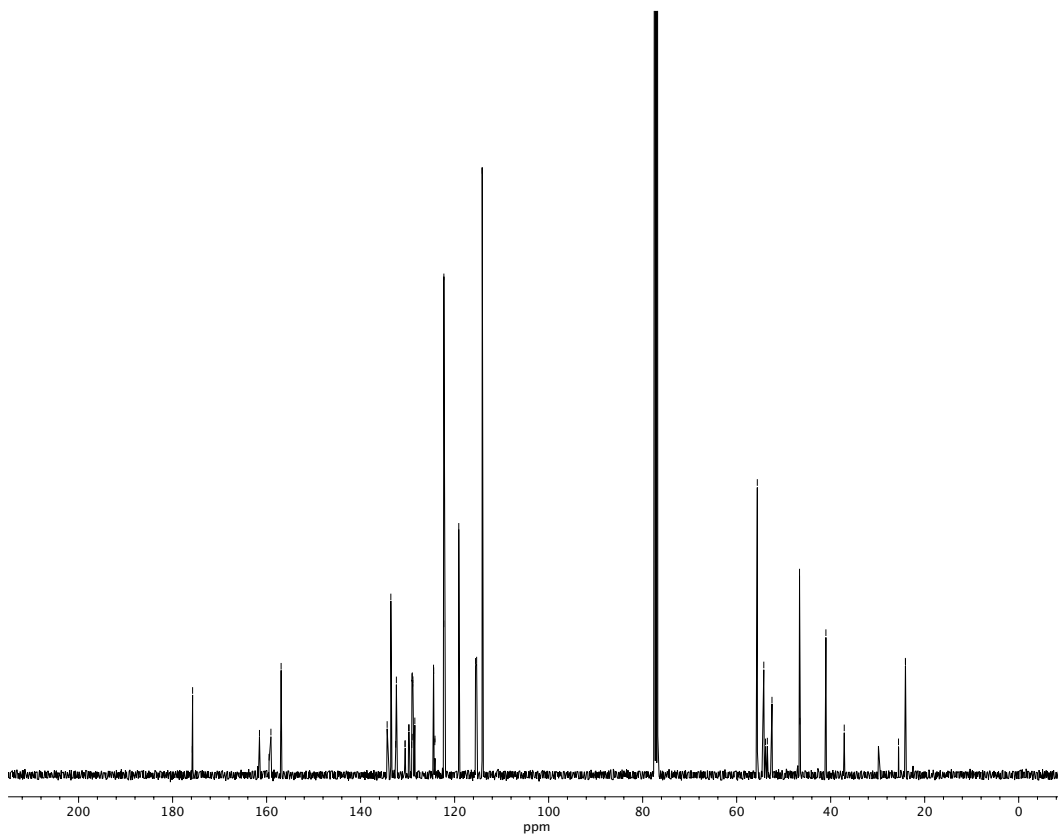


Figure A1.97 <sup>1</sup>H NMR (400 MHz, CDCl<sub>3</sub>) of compound **69df**.

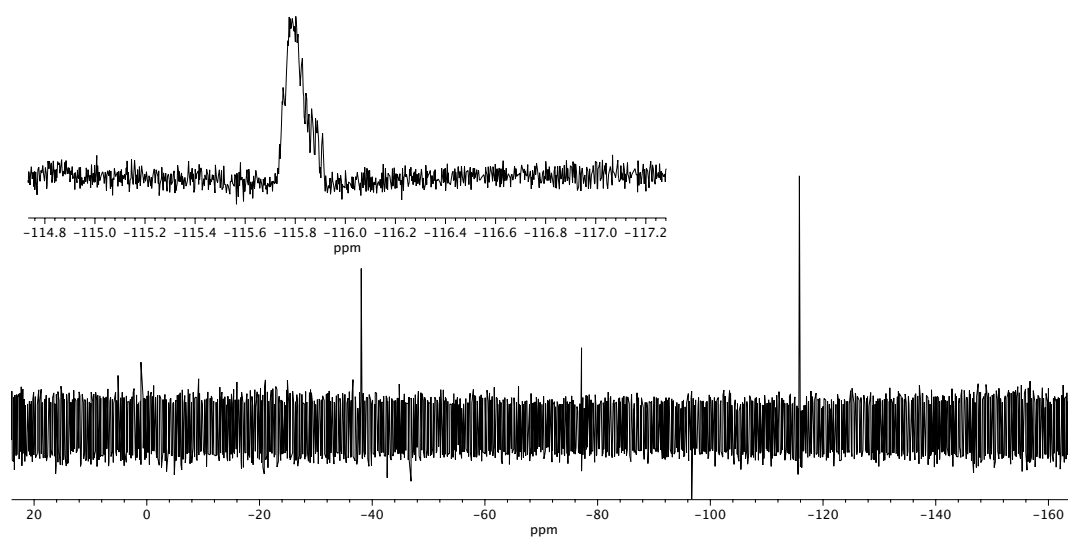




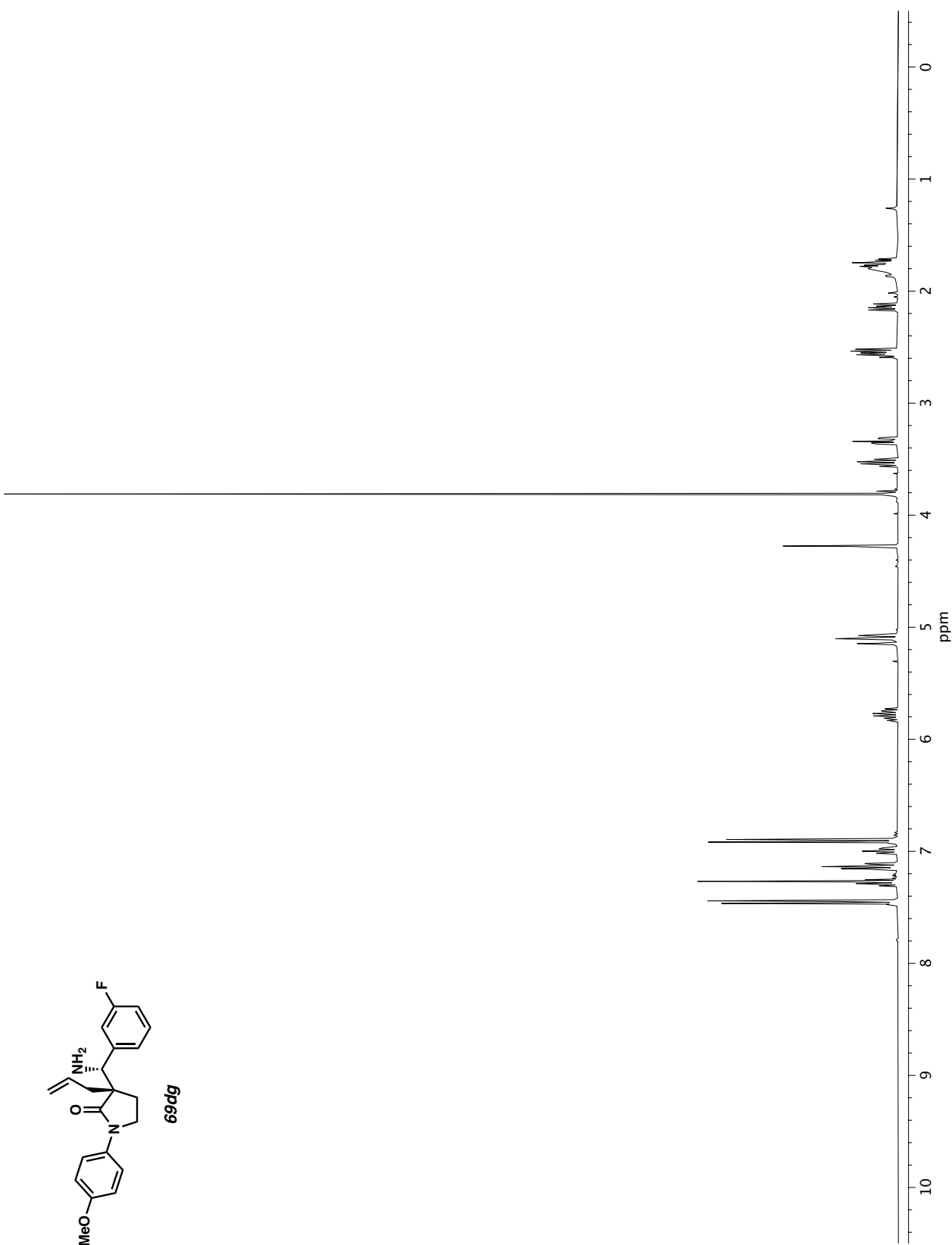
**Figure A1.98** Infrared spectrum (Thin Film, NaCl) of compound **69df**.

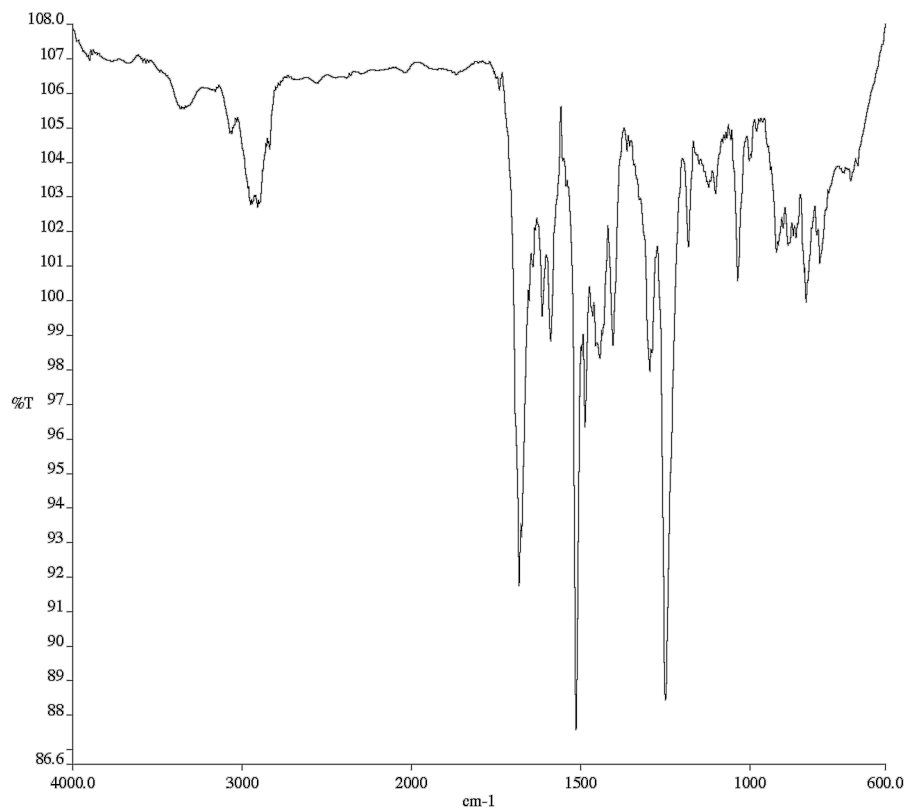


**Figure A1.99** <sup>13</sup>C NMR (100 MHz, CDCl<sub>3</sub>) of compound **69df**.

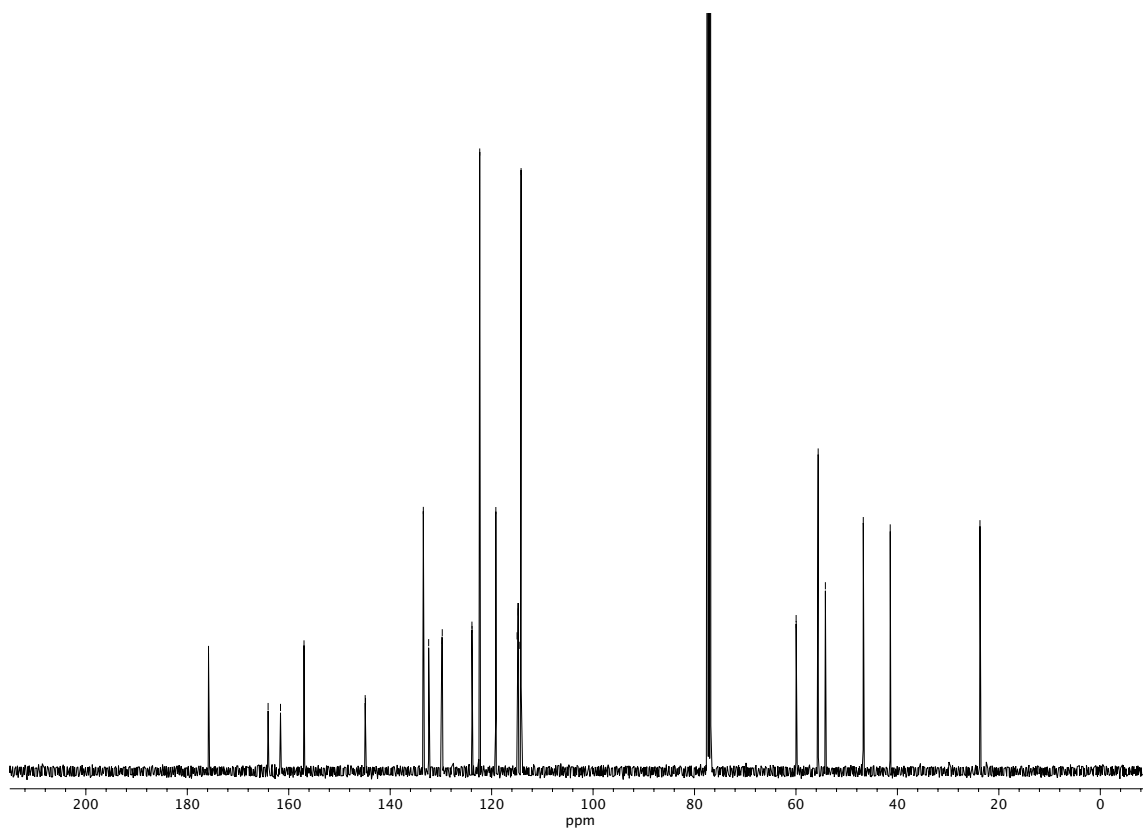


**Figure A1.100**  $^{19}\text{F}$  NMR (282 MHz,  $\text{CDCl}_3$ ) of compound **69df**

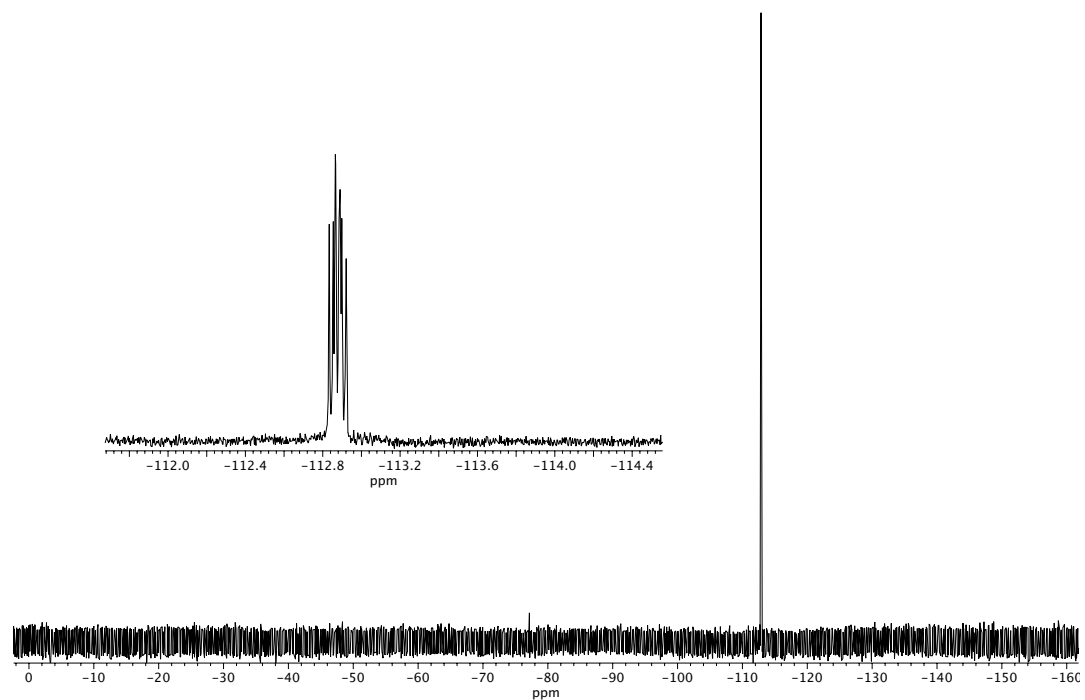
Figure A1.101  $^1\text{H}$  NMR (400 MHz,  $\text{CDCl}_3$ ) of compound **69dg**.



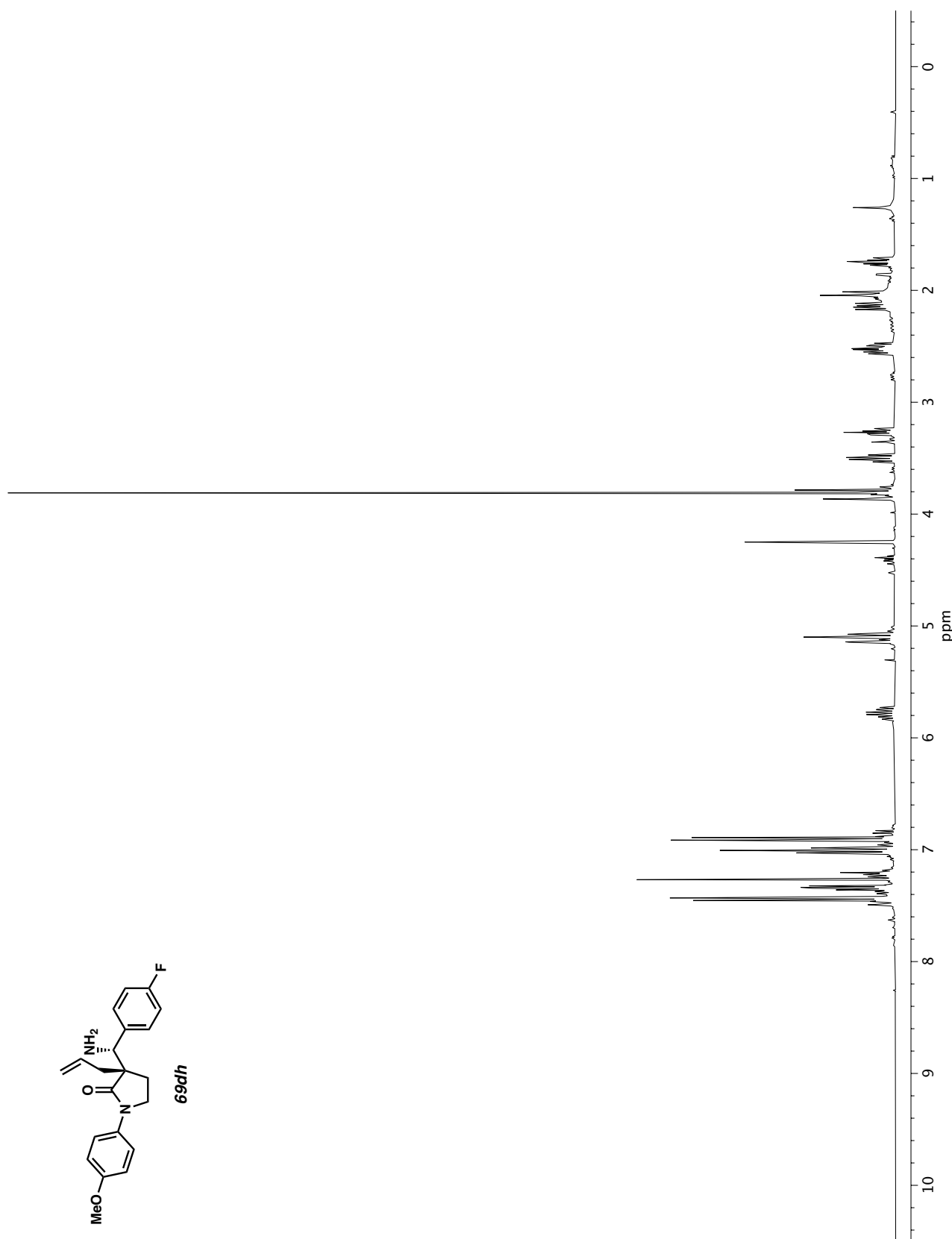
**Figure A1.102** Infrared spectrum (Thin Film, NaCl) of compound **69dg**.



**Figure A1.103** <sup>13</sup>C NMR (100 MHz, CDCl<sub>3</sub>) of compound **69dg**.



**Figure A1.104**  $^{19}\text{F}$  NMR (282 MHz,  $\text{CDCl}_3$ ) of compound **69dg**



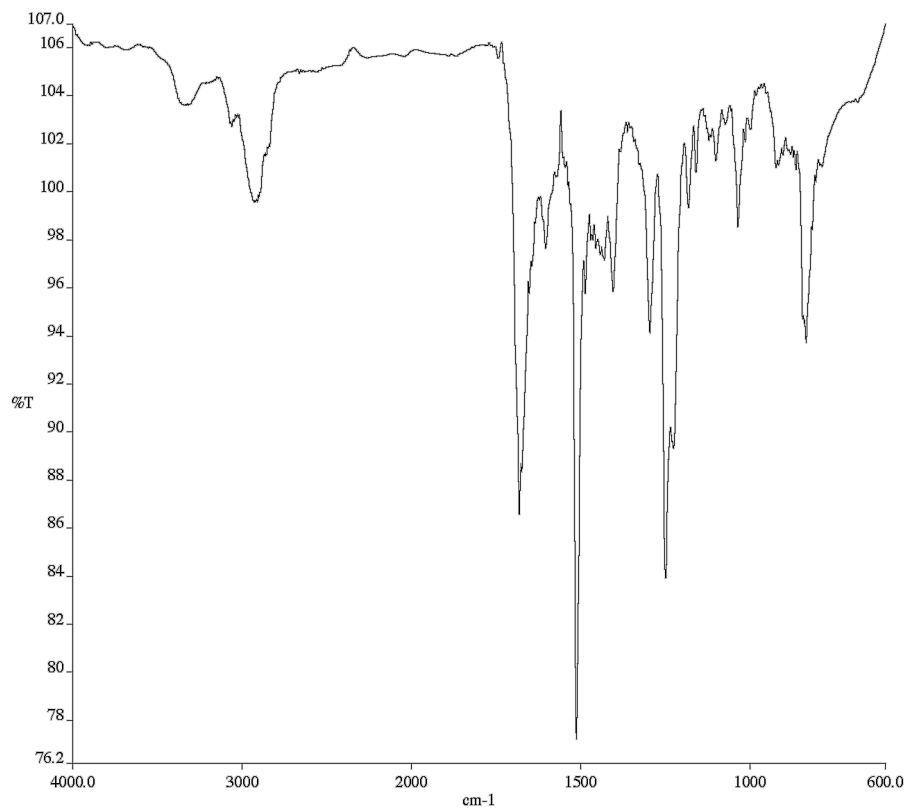


**Figure A1.106** Infrared spectrum (Thin Film, NaCl) of compound **69dh**.

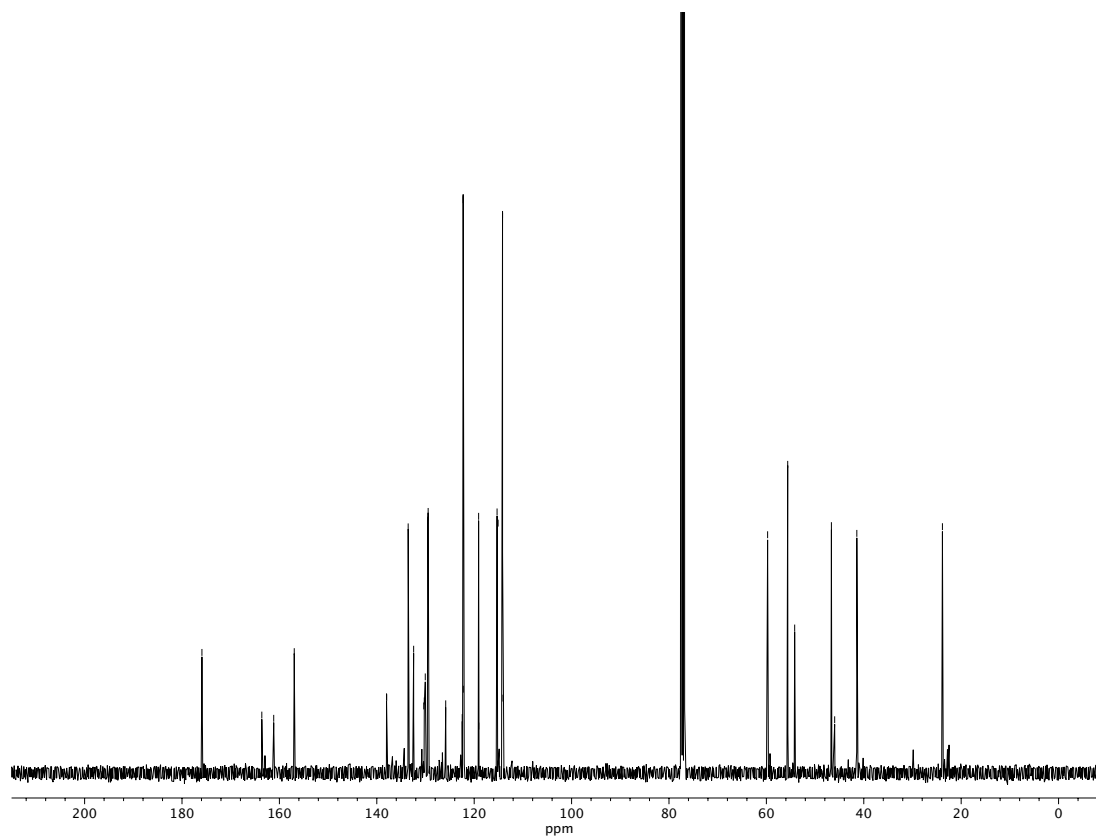


**Figure A1.107** <sup>13</sup>C NMR (100 MHz, CDCl<sub>3</sub>) of compound **69dh**.

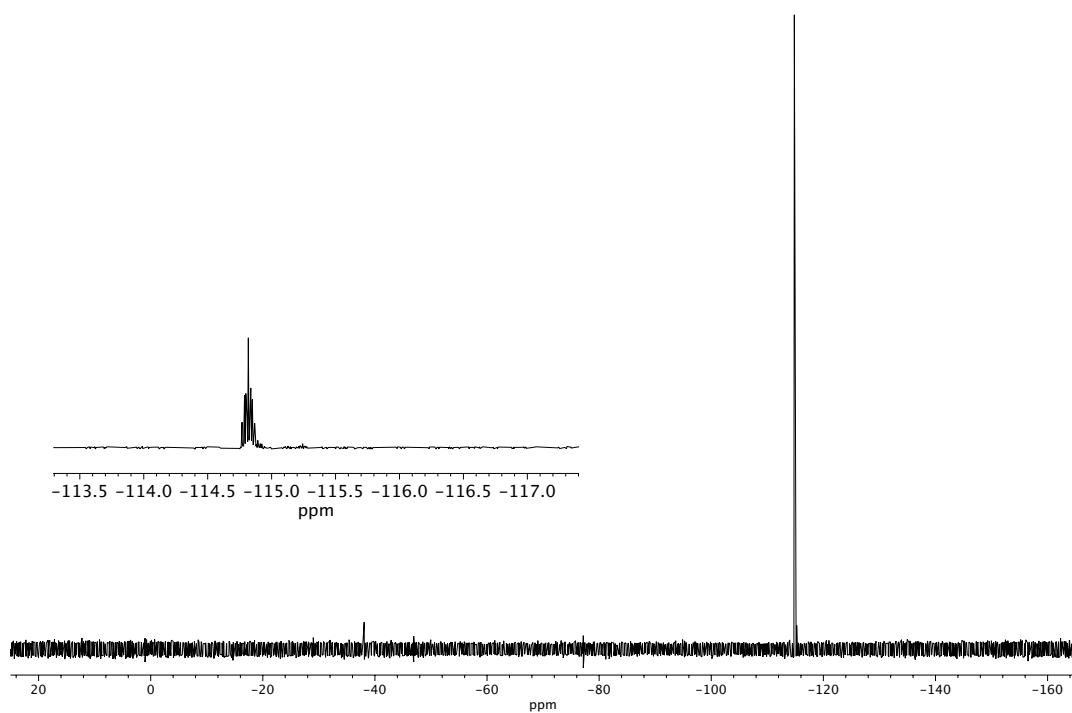


**Figure A1.108**  $^{19}\text{F}$  NMR (282 MHz,  $\text{CDCl}_3$ ) of compound **69dh**.



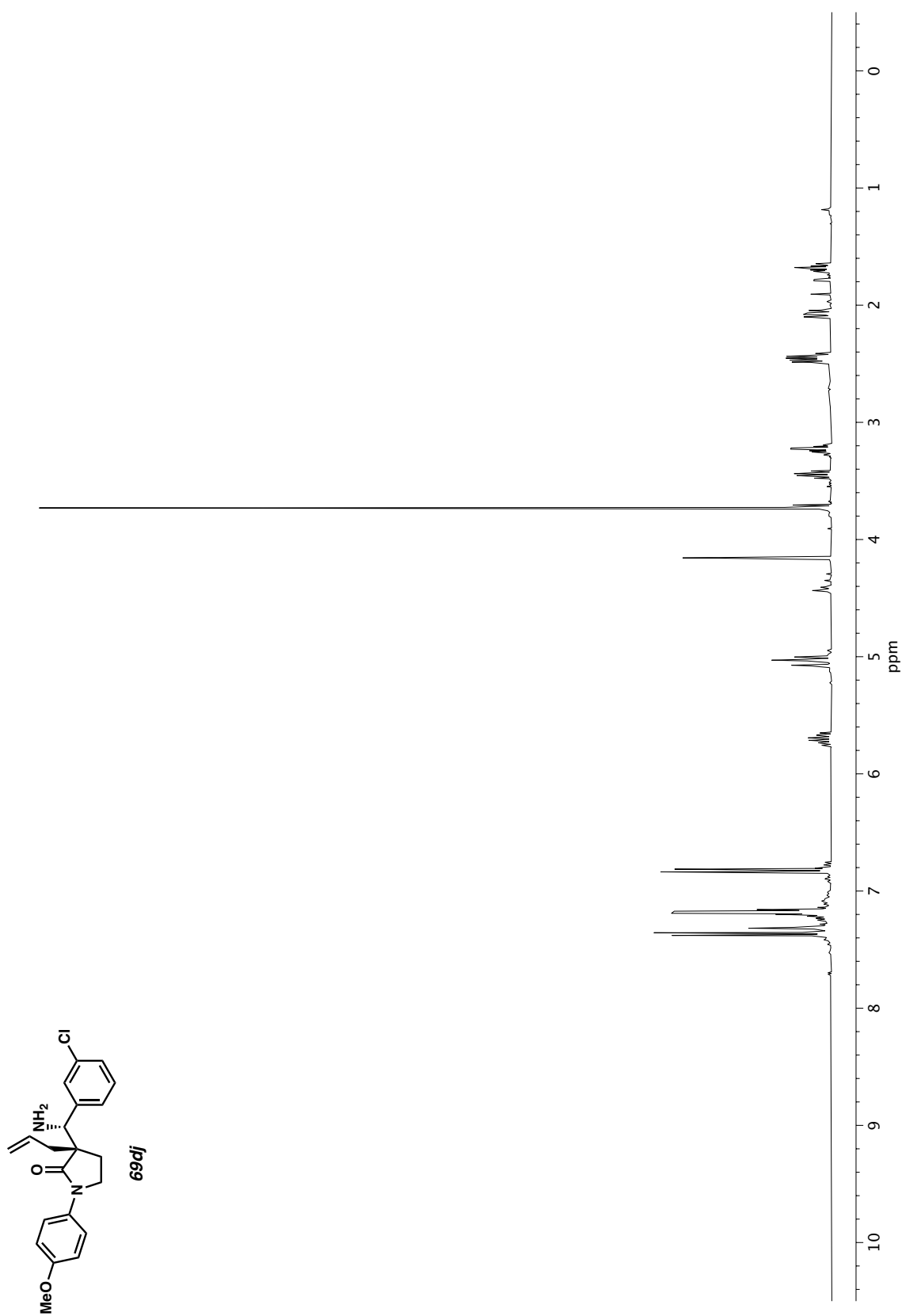


**Figure A1.109**  $^1\text{H}$  NMR (400 MHz,  $\text{CDCl}_3$ ) of compound **69dj**.

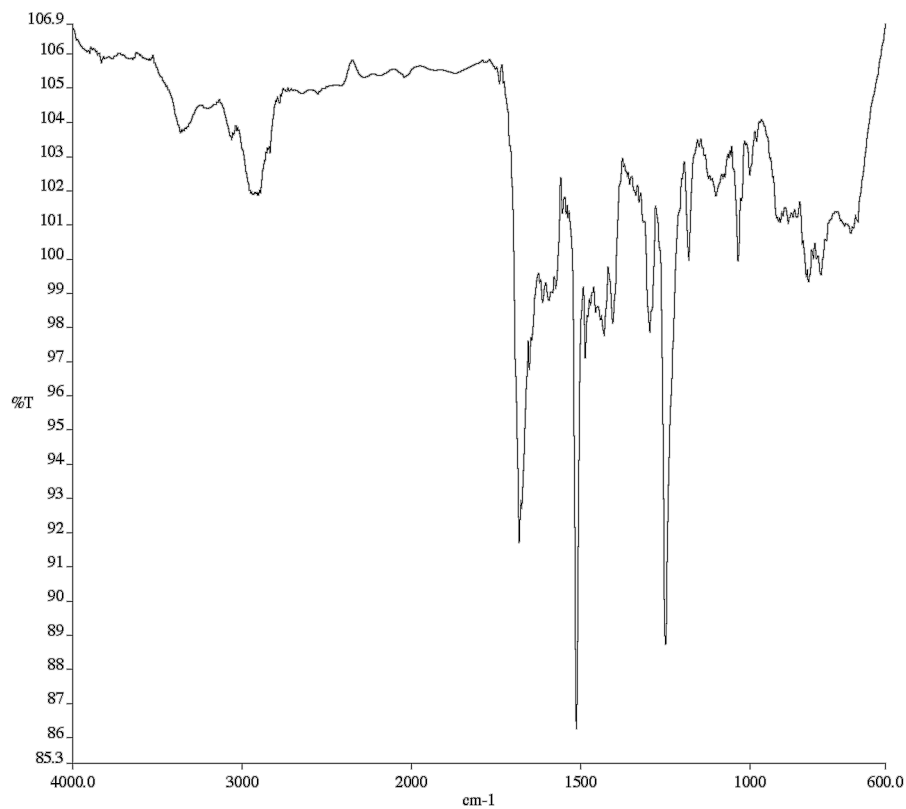


**Figure A1.110** Infrared spectrum (Thin Film, NaCl) of compound **69dj**

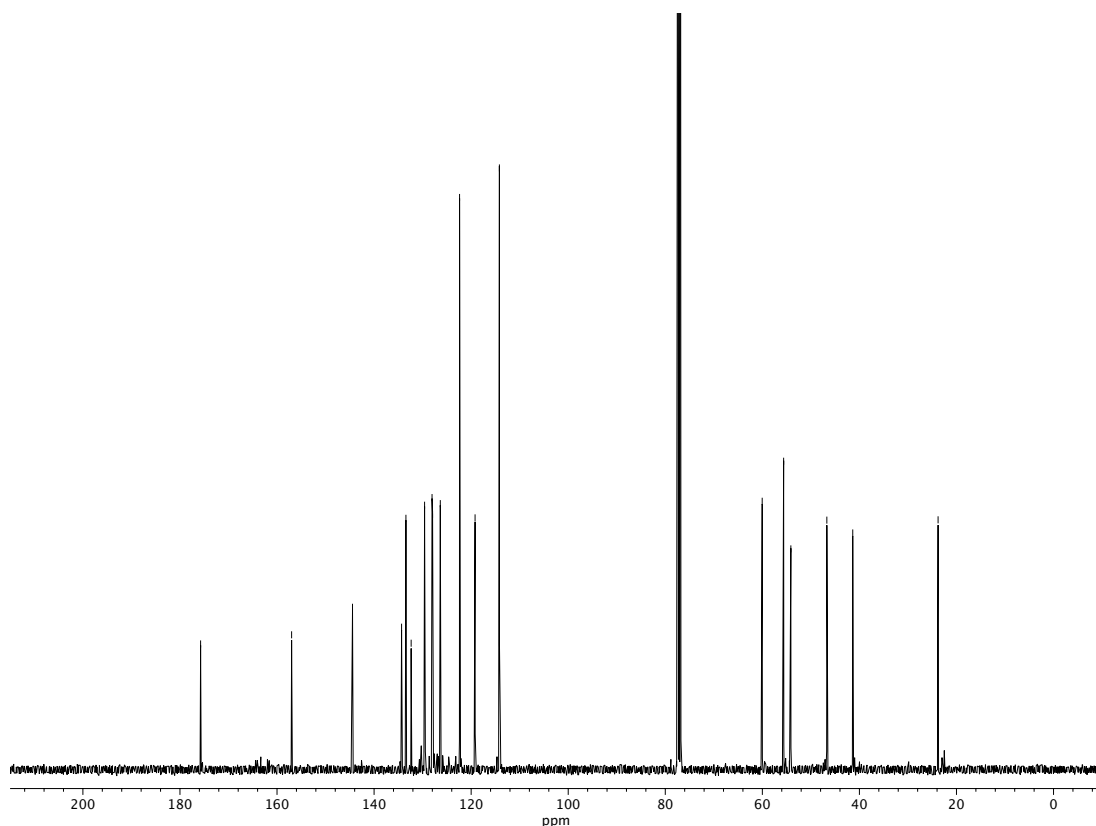


**Figure A1.111** <sup>13</sup>C NMR (100 MHz, CDCl<sub>3</sub>) of compound **69dj**



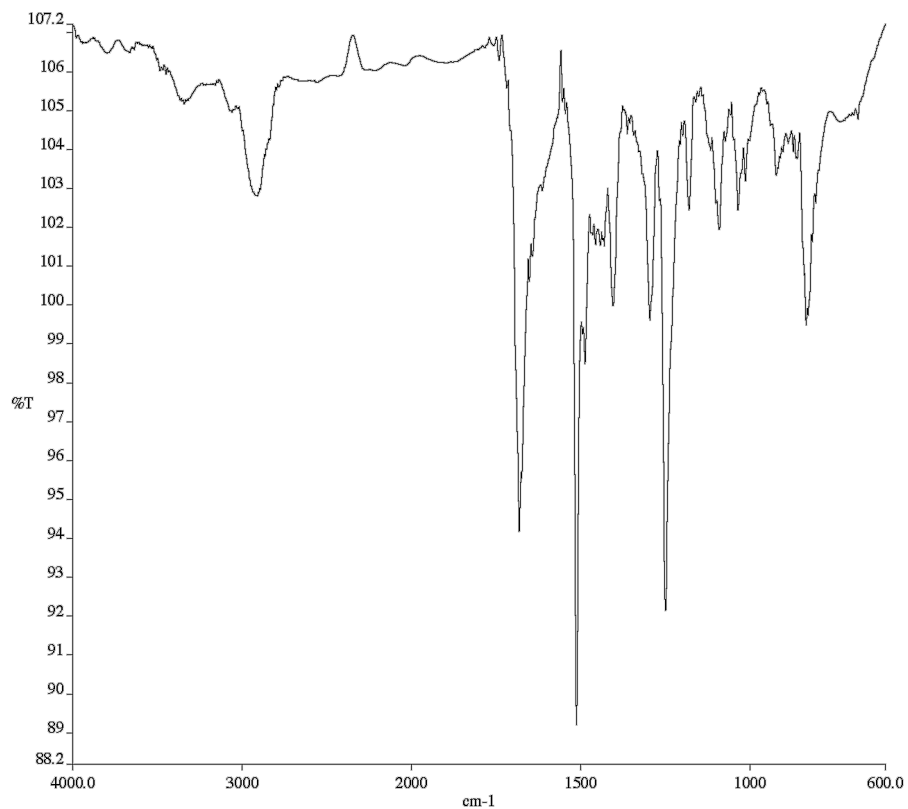


**Figure A1.113** Infrared spectrum (Thin Film, NaCl) of compound **69dk**.

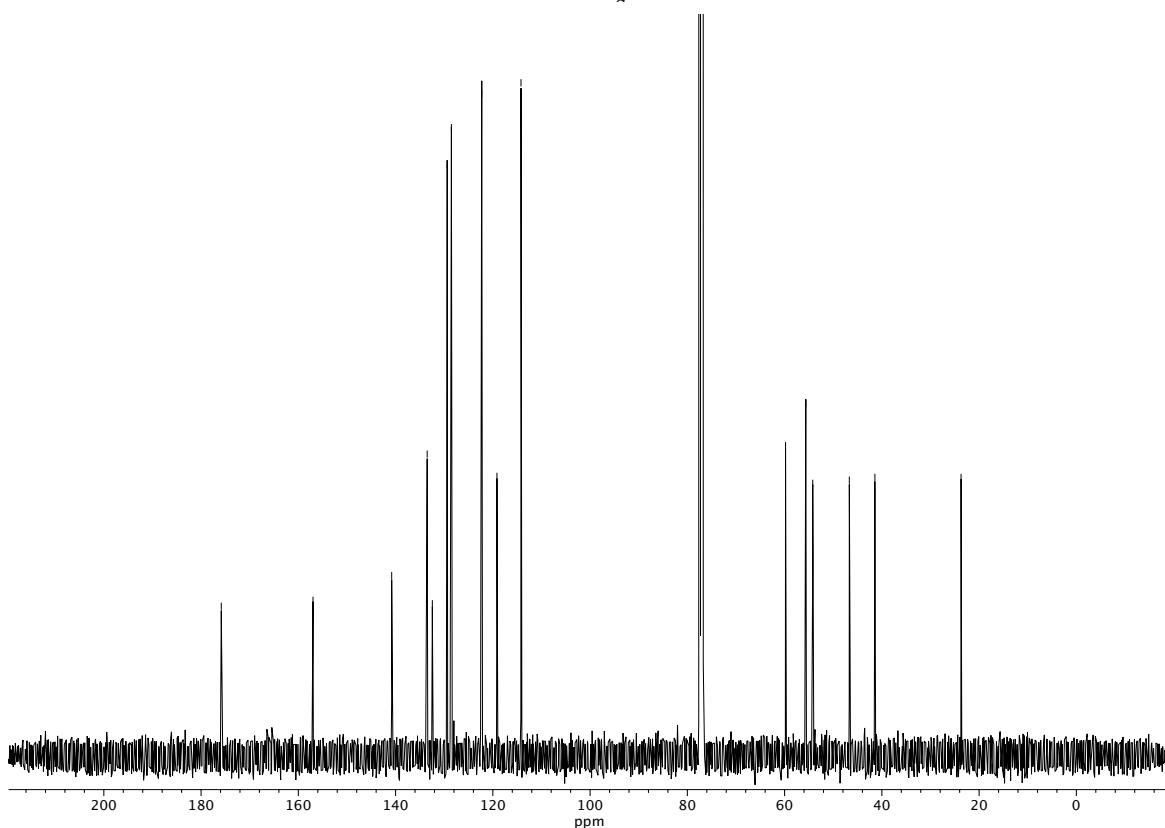


**Figure A1.114** <sup>13</sup>C NMR (100 MHz, CDCl<sub>3</sub>) of compound **69dk**

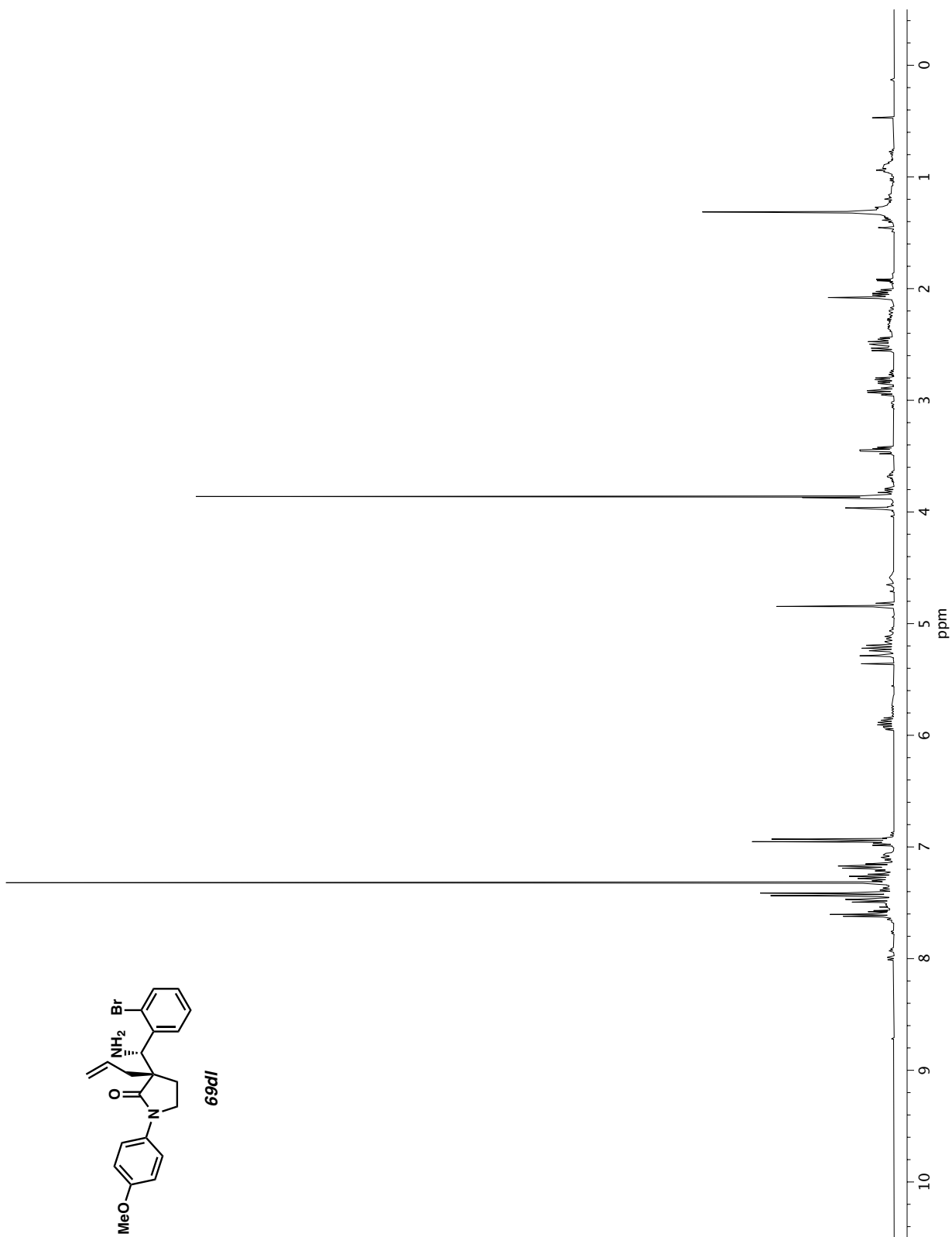


**Figure A1.115**  $^1\text{H}$  NMR (400 MHz, CDCl<sub>3</sub>) of compound **69dl**.

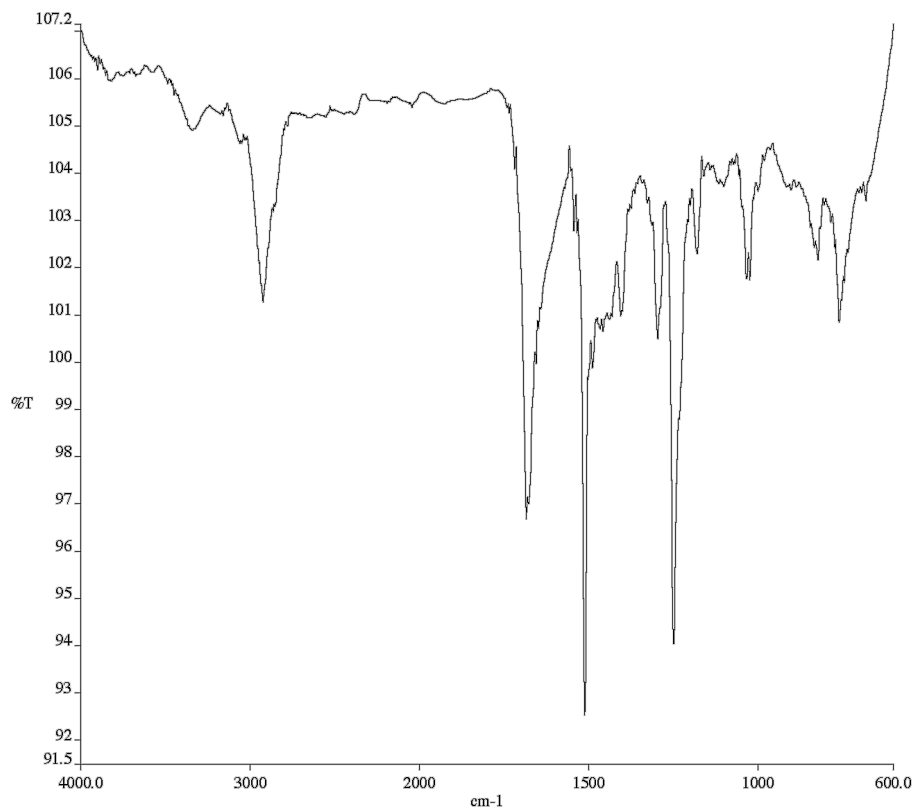


**Figure A1.116** Infrared spectrum (Thin Film, NaCl) of compound **69dl**

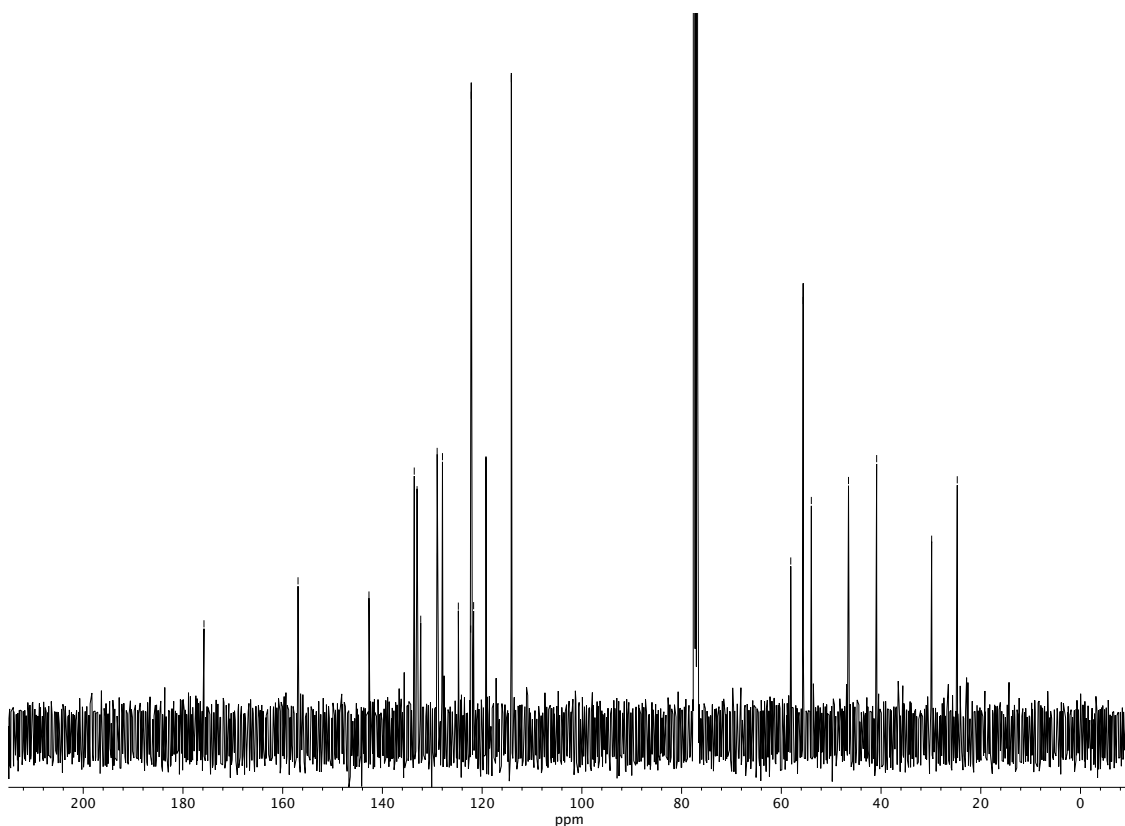


**Figure A1.117** <sup>13</sup>C NMR (100 MHz, CDCl<sub>3</sub>) of compound **69dl**

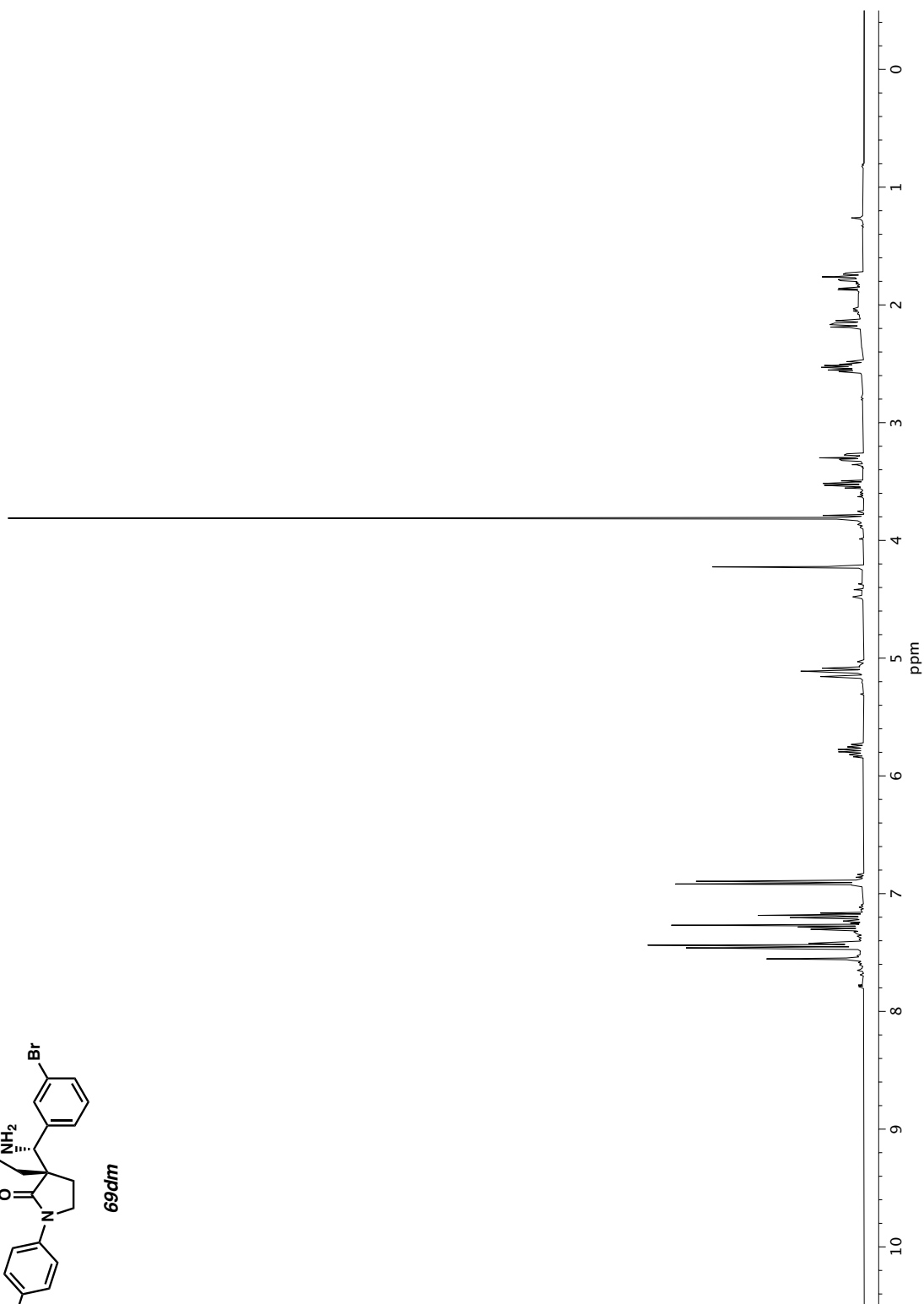
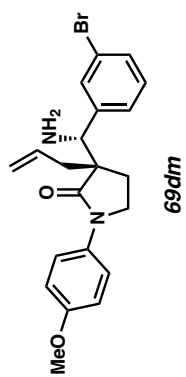
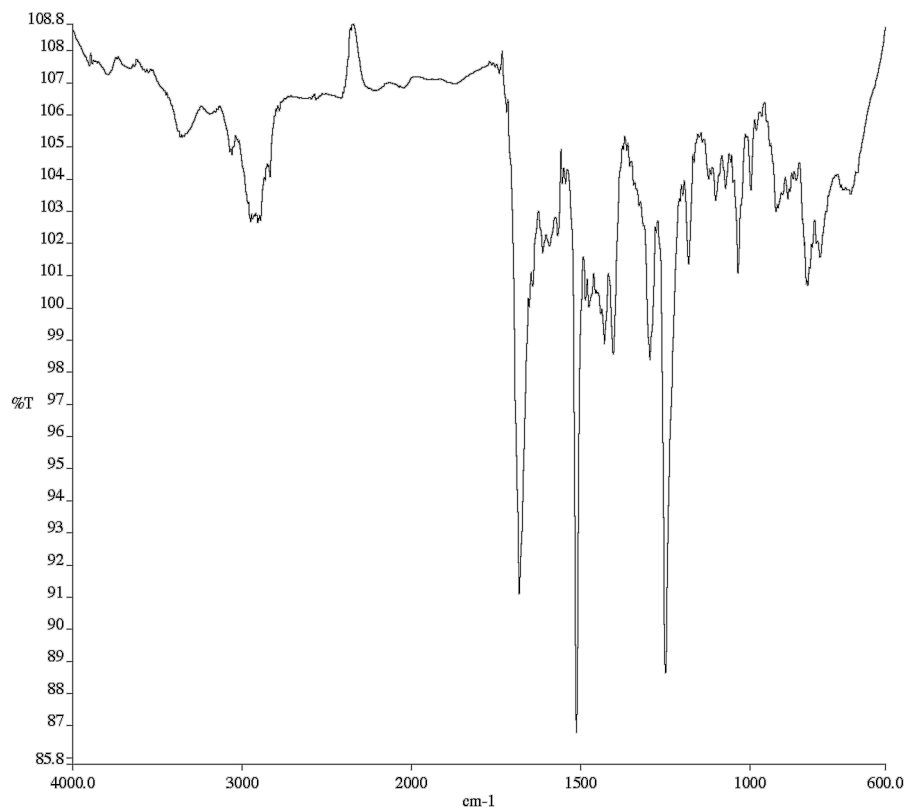
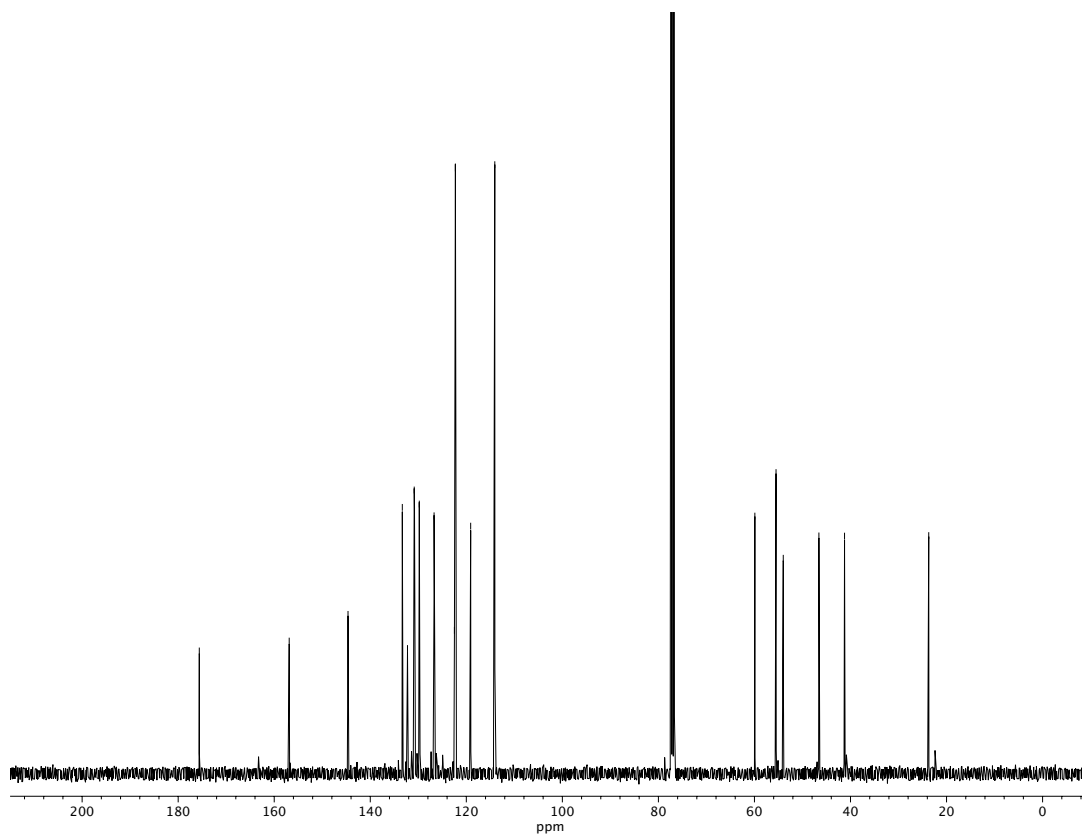


Figure A1.118  $^1\text{H}$  NMR (400 MHz,  $\text{CDCl}_3$ ) of compound 69dm.

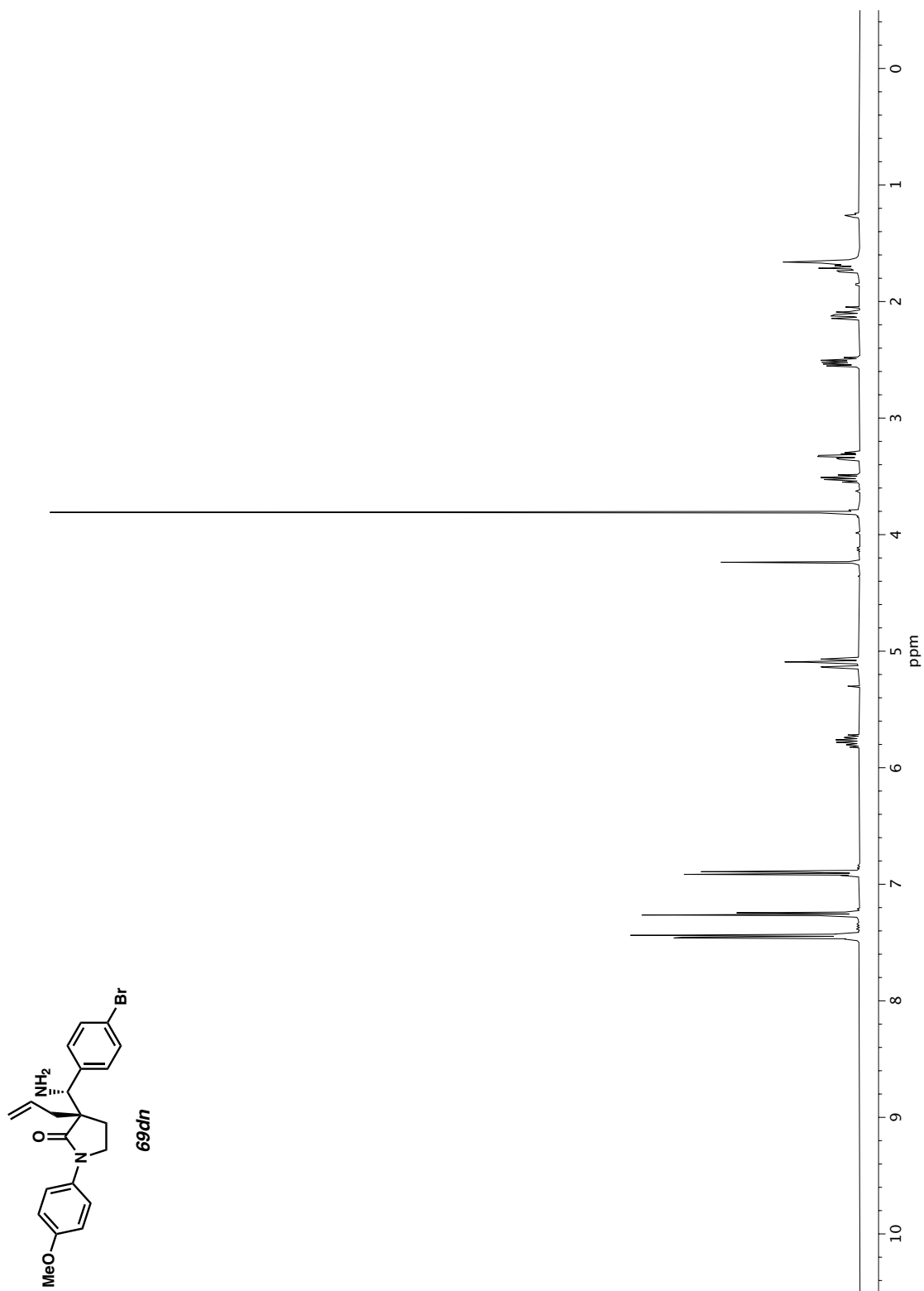


**Figure A1.119** Infrared spectrum (Thin Film, NaCl) of compound **69dm**.

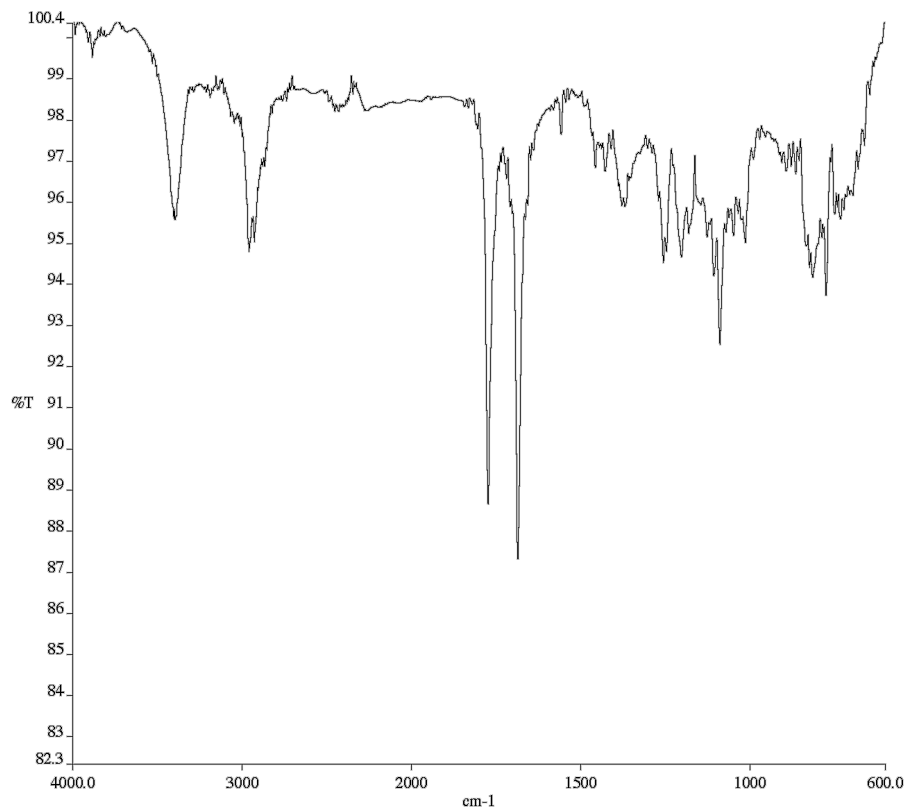


**Figure A1.120** <sup>13</sup>C NMR (100 MHz, CDCl<sub>3</sub>) of compound **69dm**

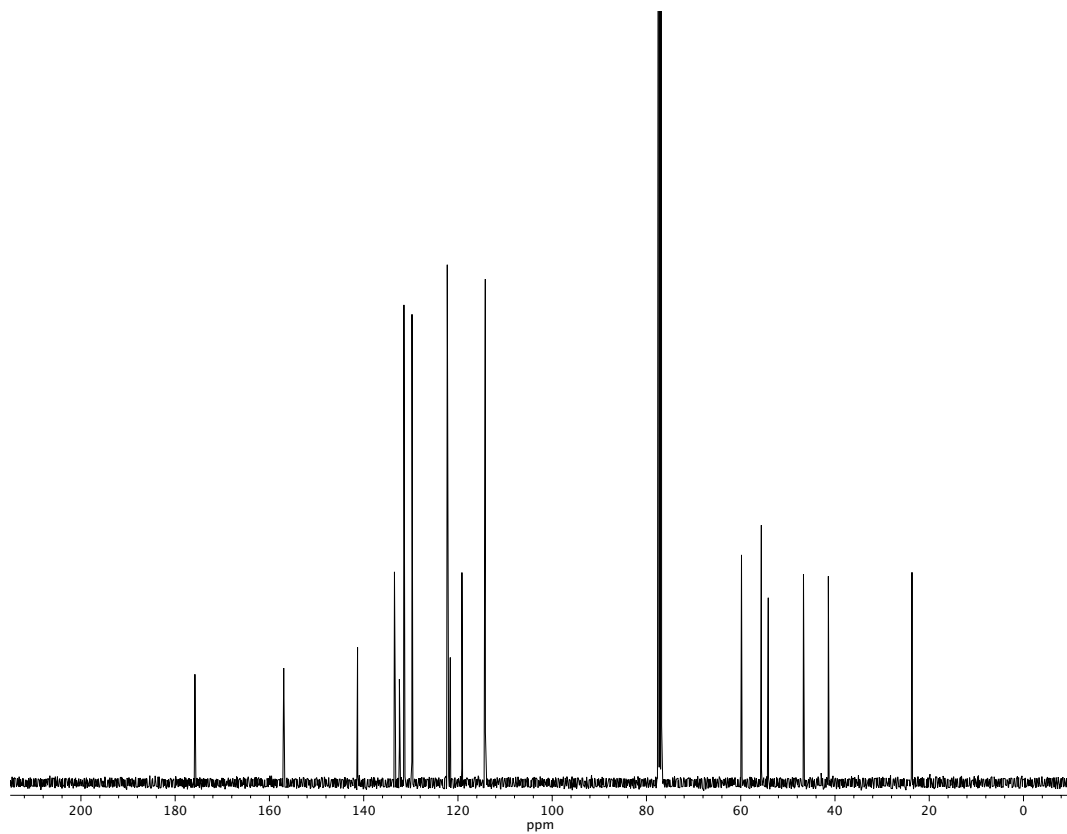




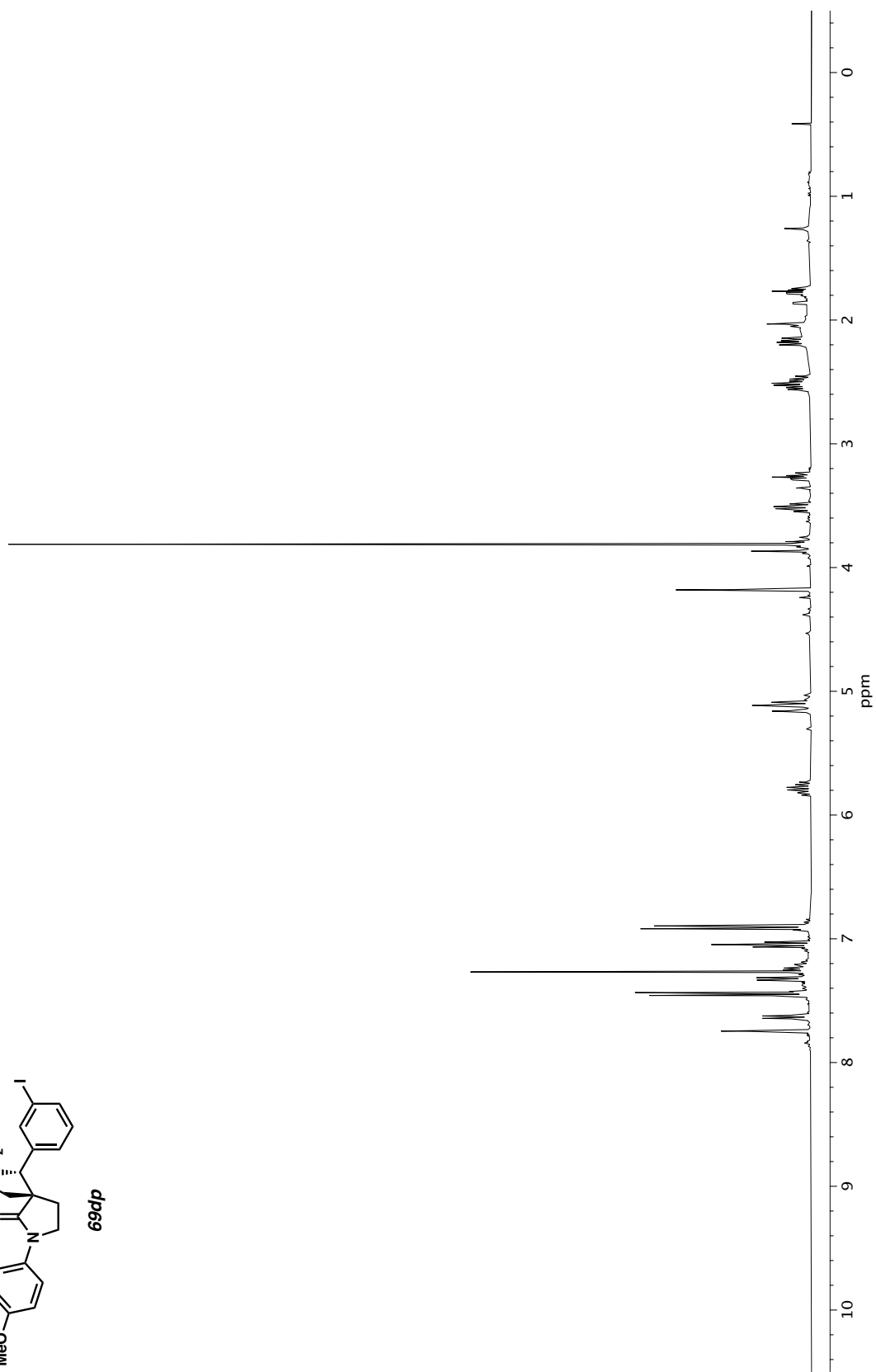
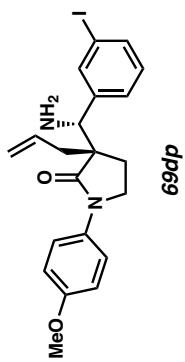
**Figure A1.121** <sup>1</sup>H NMR (400 MHz, CDCl<sub>3</sub>) of compound **69dn**



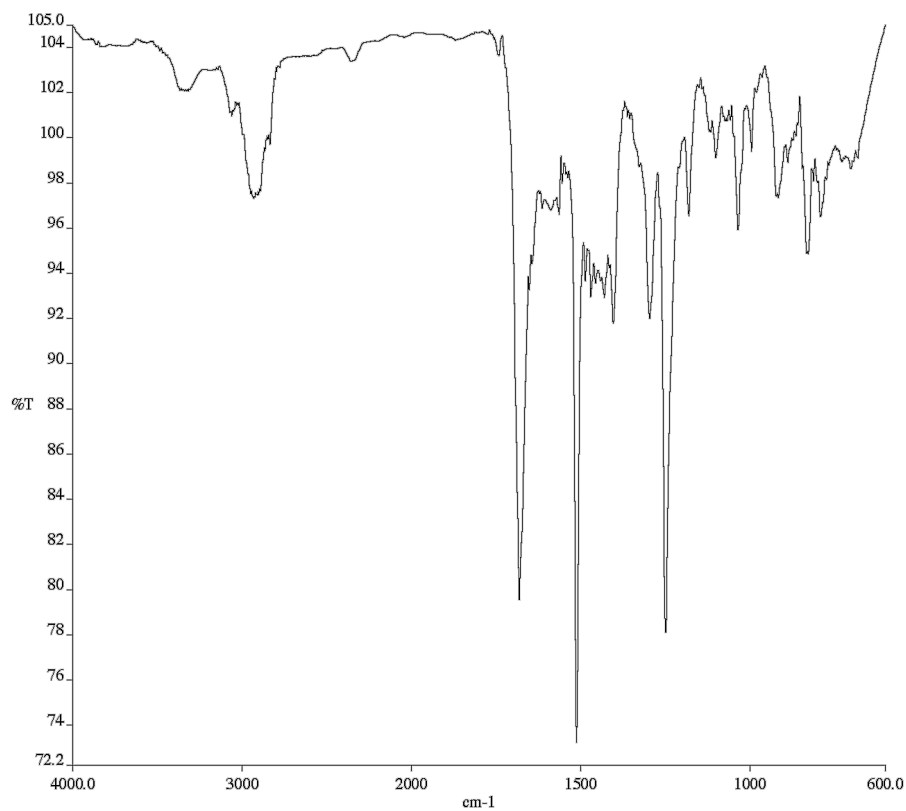
**Figure A1.122** Infrared spectrum (Thin Film, NaCl) of compound **69dn**



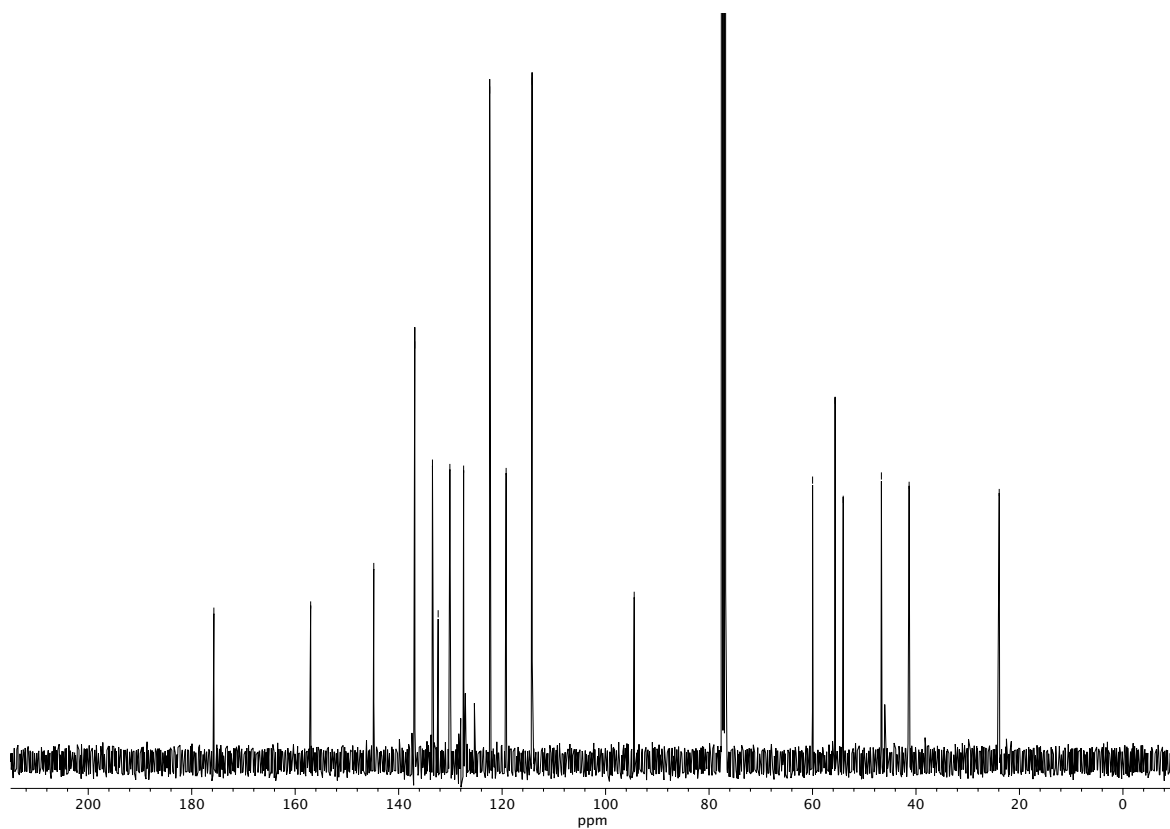
**Figure A1.123** <sup>13</sup>C NMR (100 MHz, CDCl<sub>3</sub>) of compound **69dn**



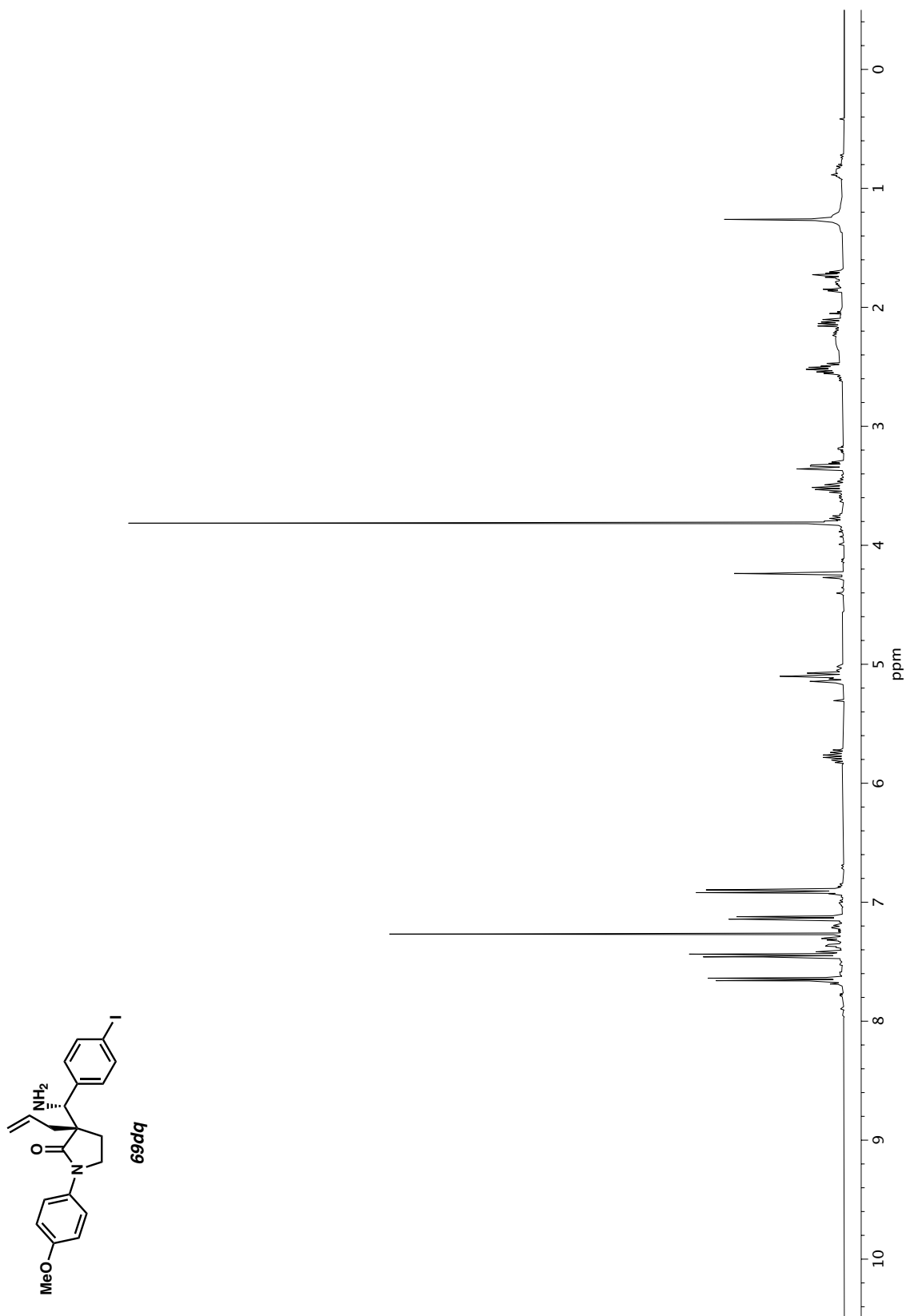
**Figure A1.124**  $^1\text{H}$  NMR (400 MHz,  $\text{CDCl}_3$ ) of compound **69dp**

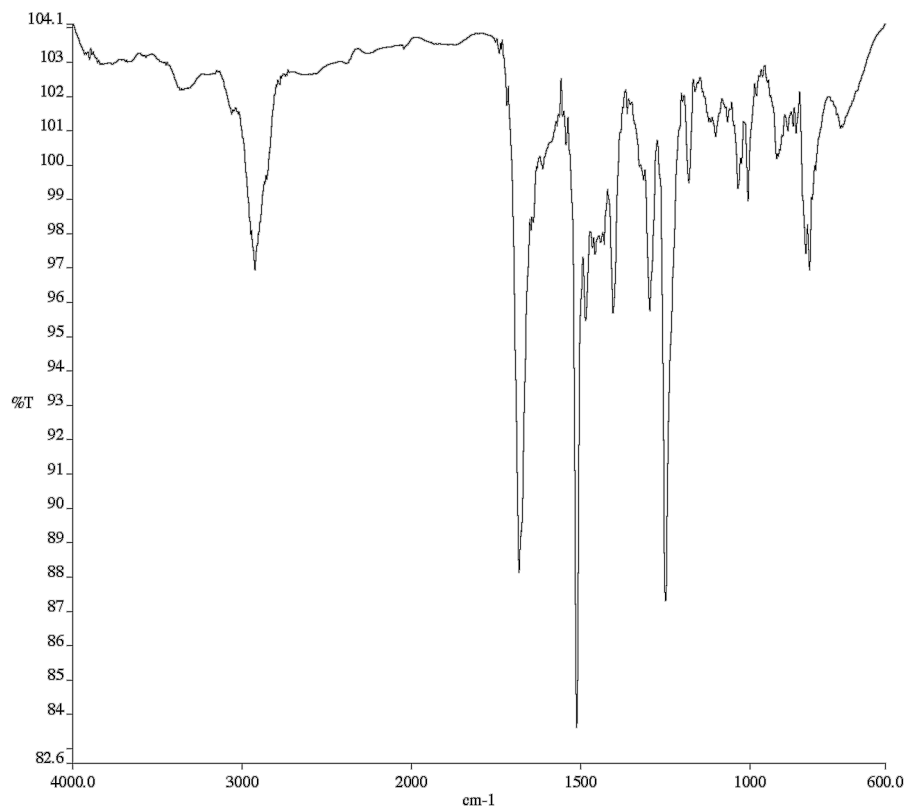


**Figure A1.125** Infrared spectrum (Thin Film, NaCl) of compound **69dp**

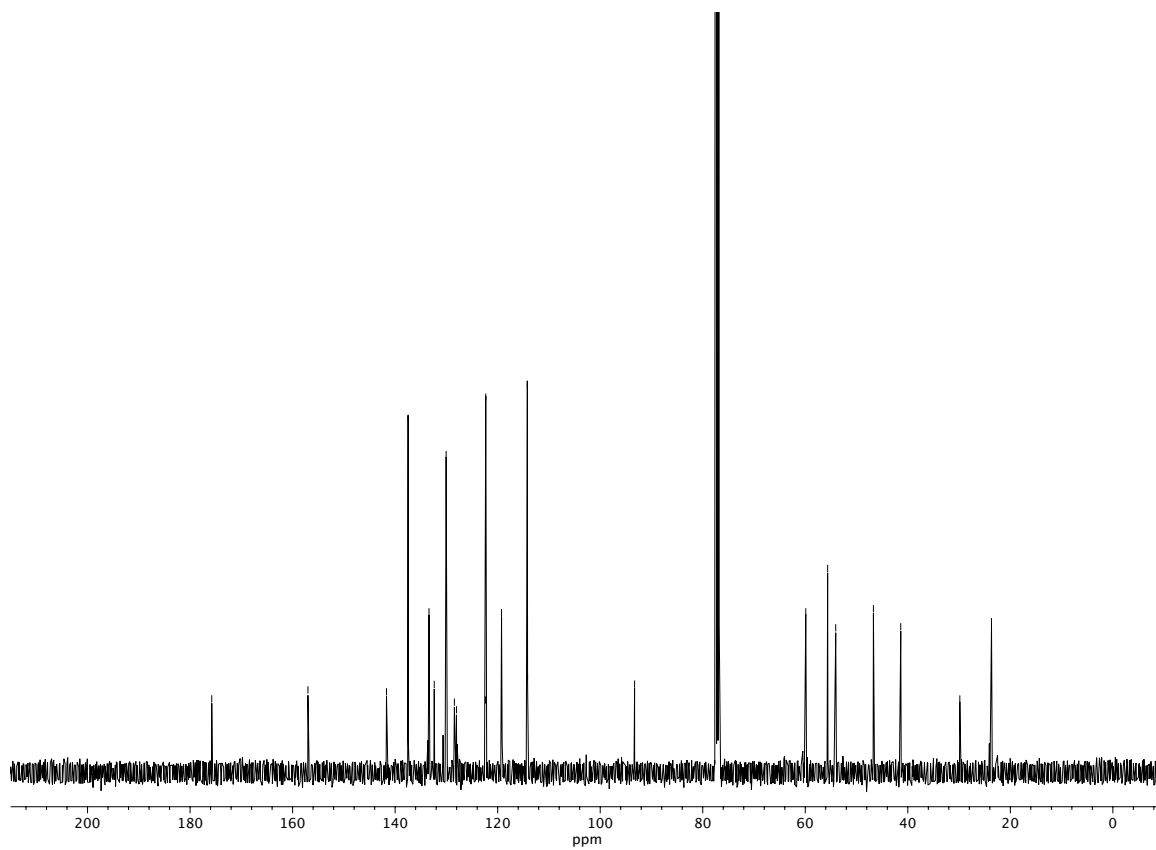


**Figure A1.126** <sup>13</sup>C NMR (100 MHz, CDCl<sub>3</sub>) of compound **69dp**

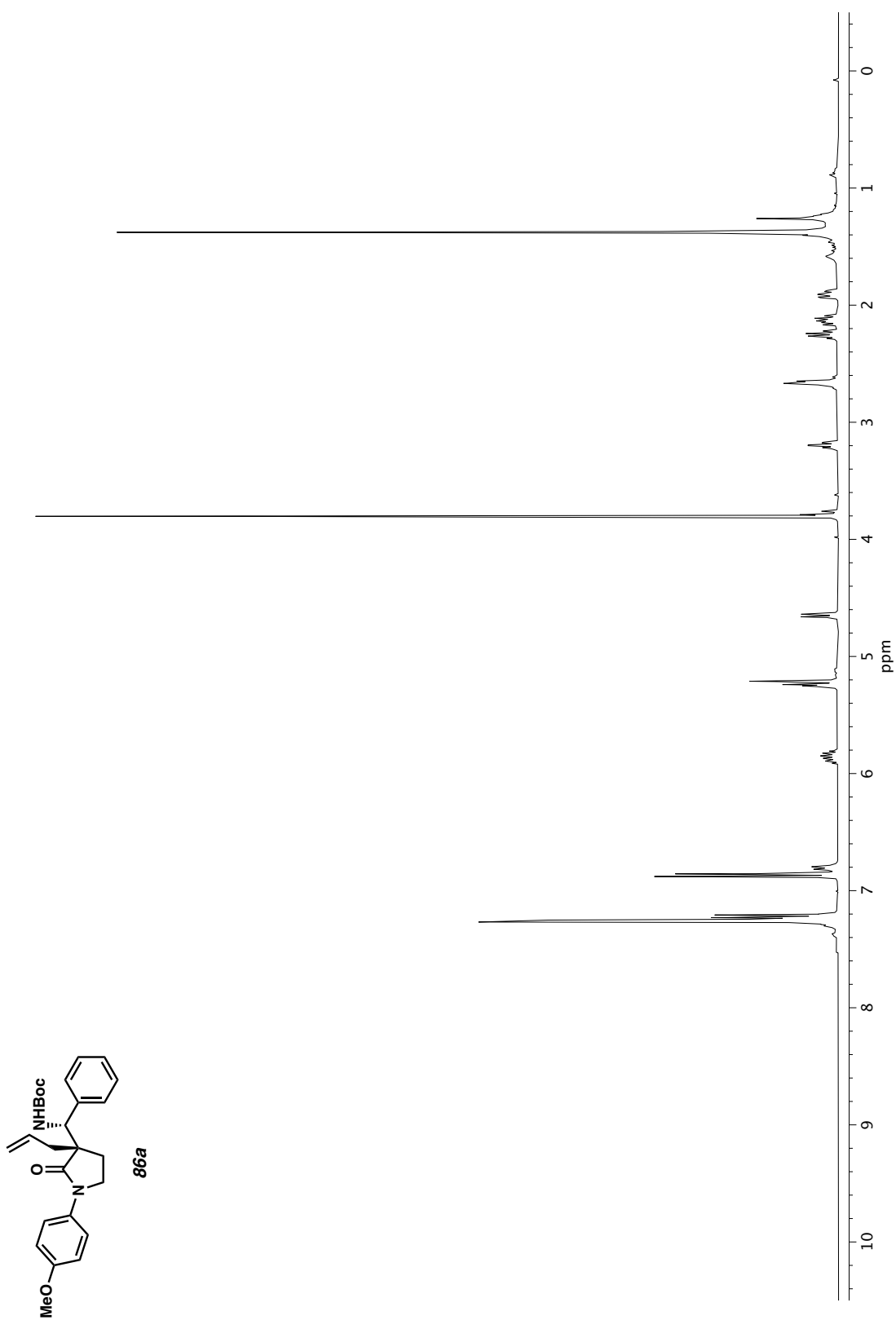
Figure A1.127 <sup>1</sup>H NMR (400 MHz, CDCl<sub>3</sub>) of compound **69dq**



**Figure A1.128** Infrared spectrum (Thin Film, NaCl) of compound **69dq**



**Figure A1.129** <sup>13</sup>C NMR (100 MHz, CDCl<sub>3</sub>) of compound **69dq**.



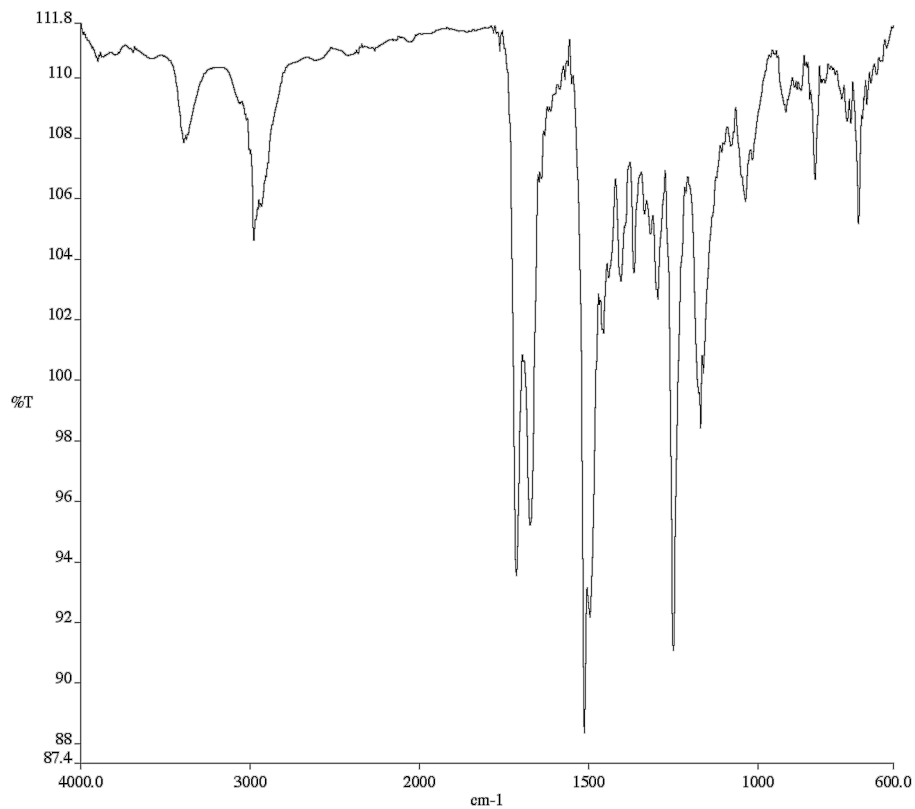


**Figure A1.131** Infrared spectrum (Thin Film, NaCl) of compound **86a**.

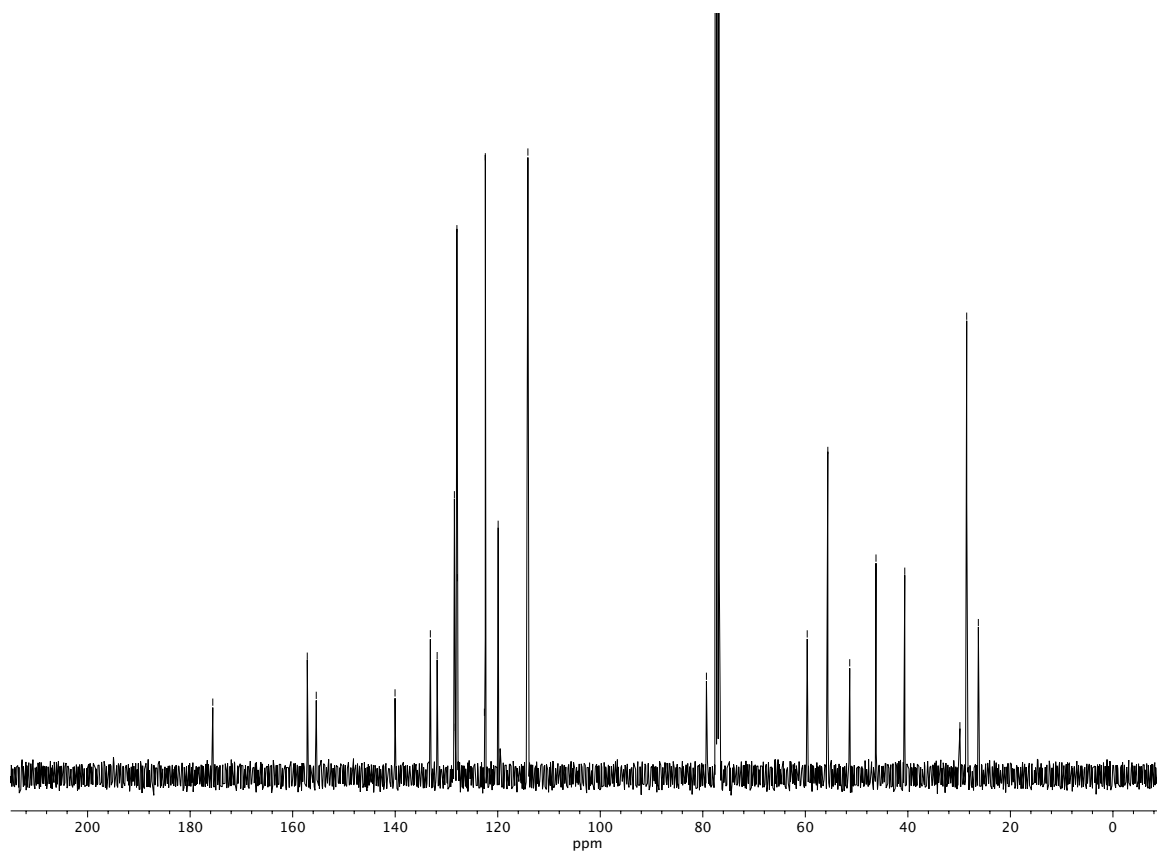


**Figure A1.132** <sup>13</sup>C NMR (100 MHz, CDCl<sub>3</sub>) of compound **86a**.



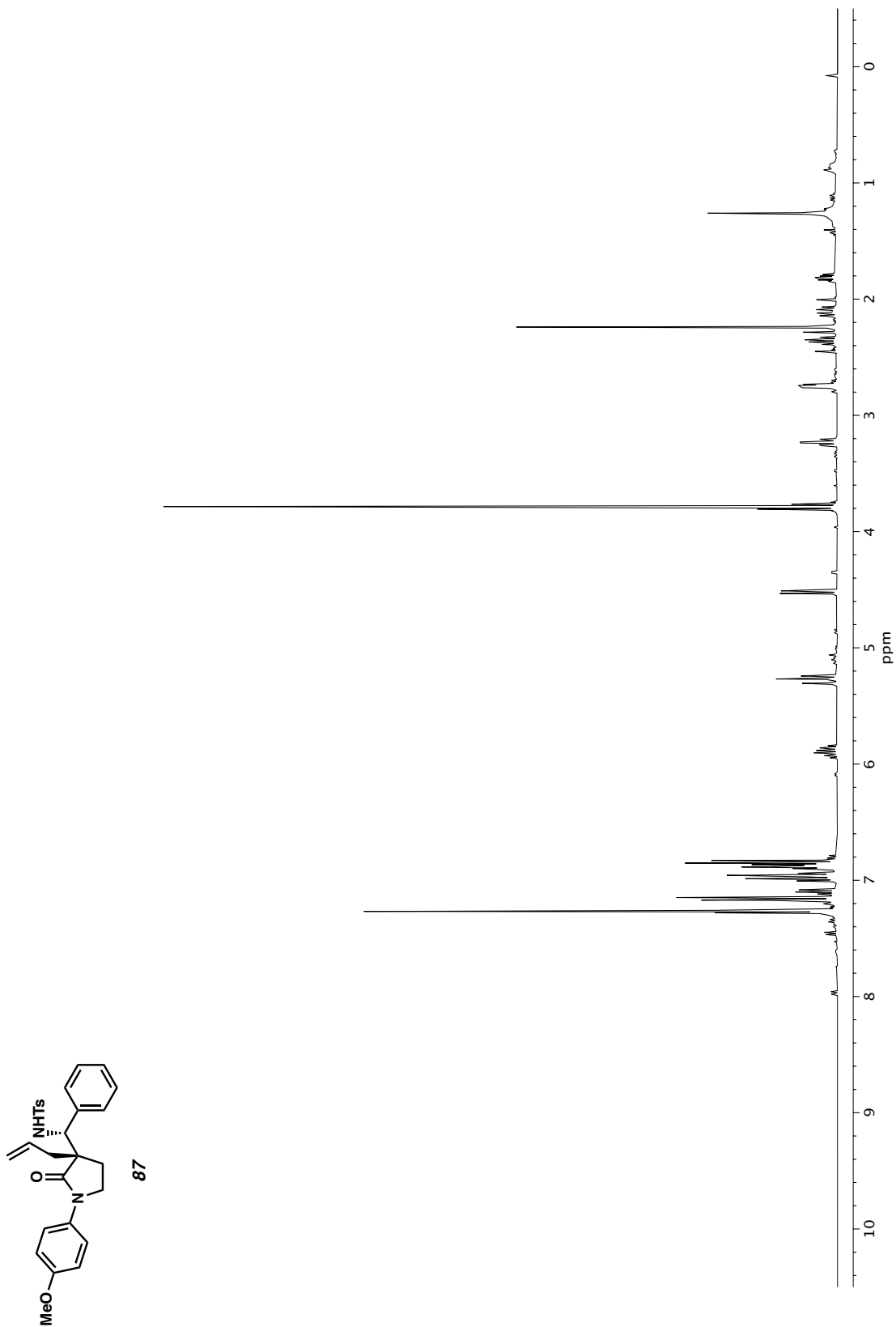
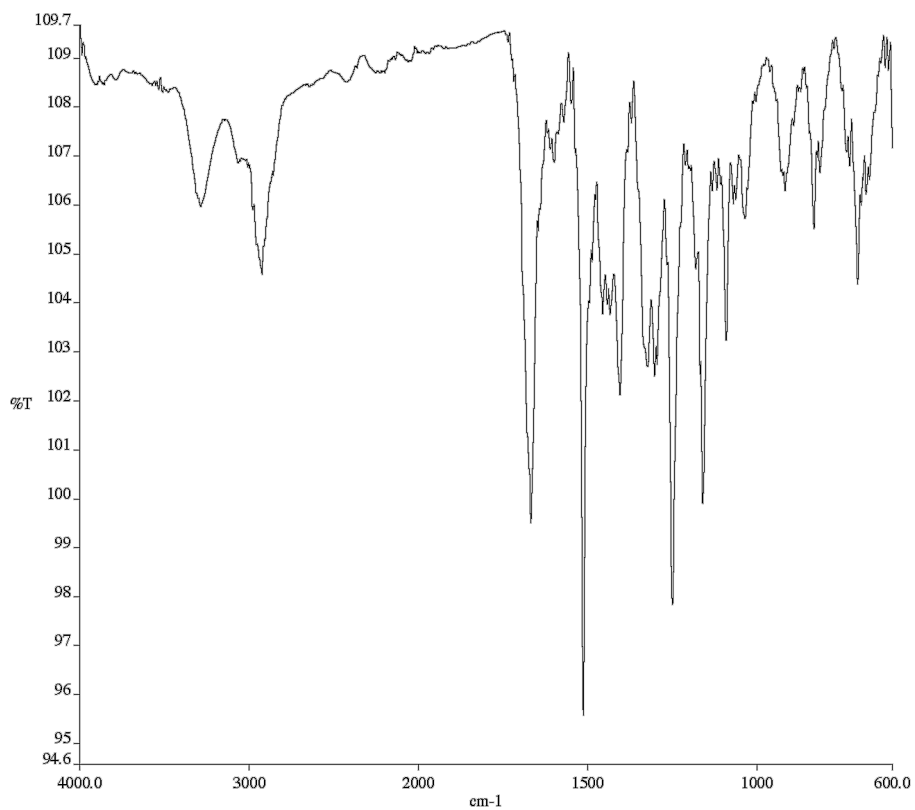
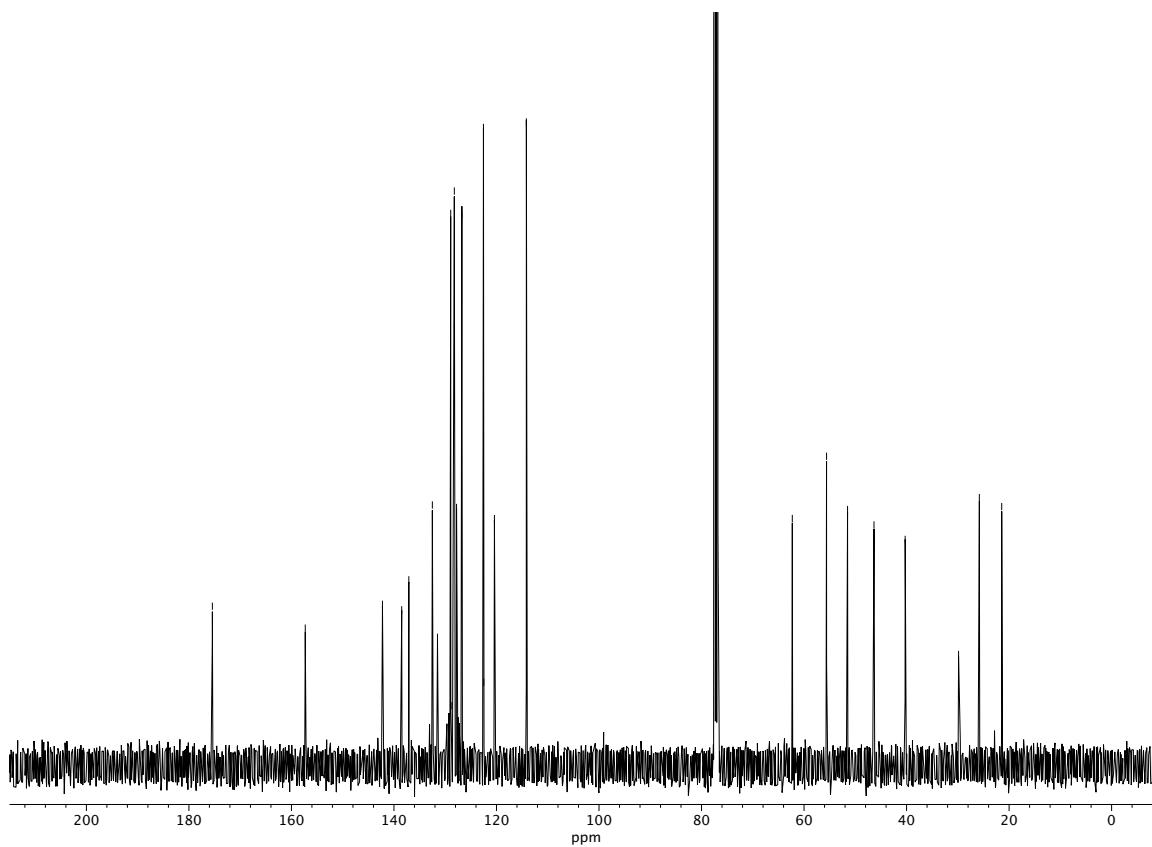


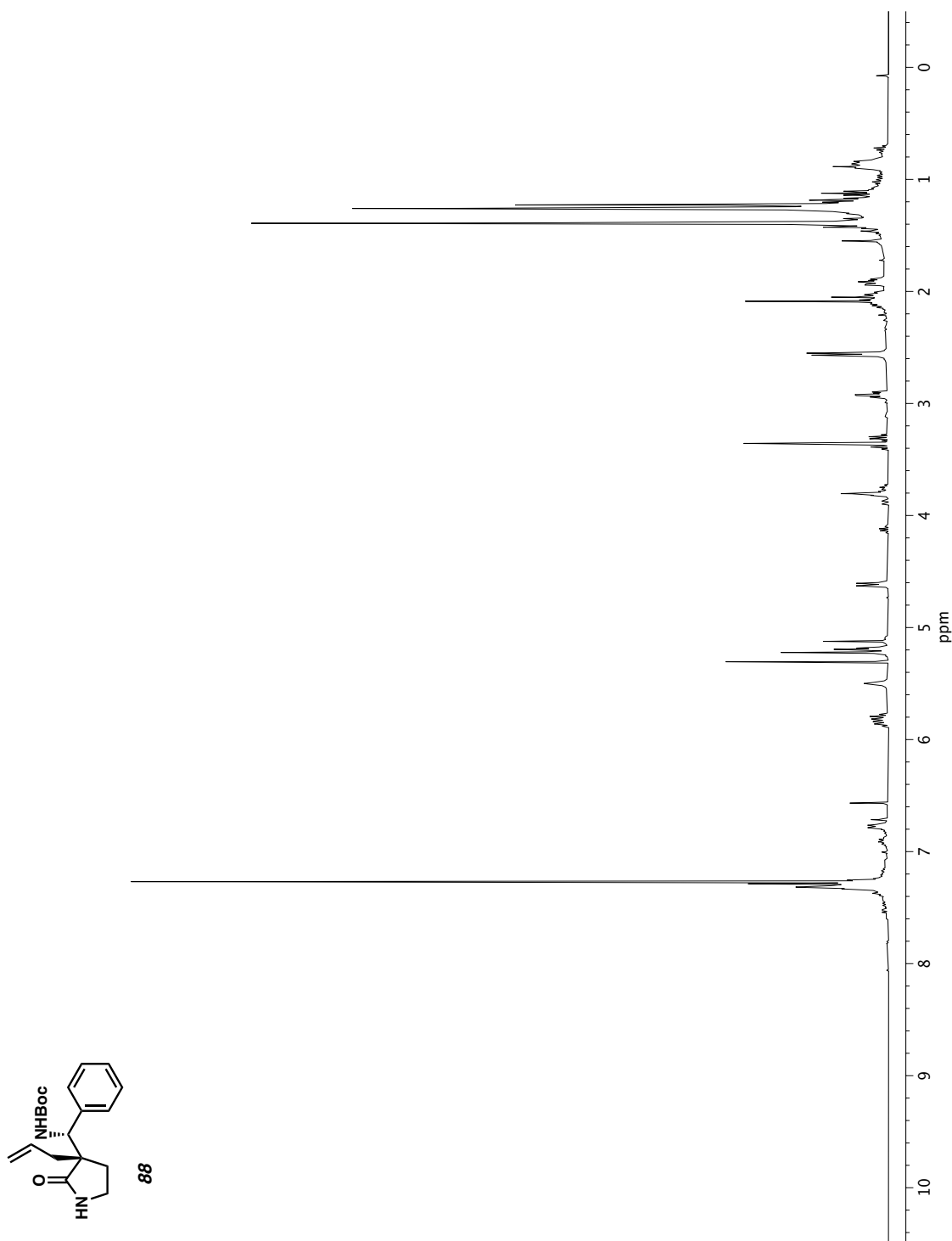
Figure A1.133  $^1\text{H}$  NMR (400 MHz,  $\text{CDCl}_3$ ) of compound **87**.



**Figure A1.134** Infrared spectrum (Thin Film, NaCl) of compound **87**.



**Figure A1.135** <sup>13</sup>C NMR (100 MHz, CDCl<sub>3</sub>) of compound **87**.



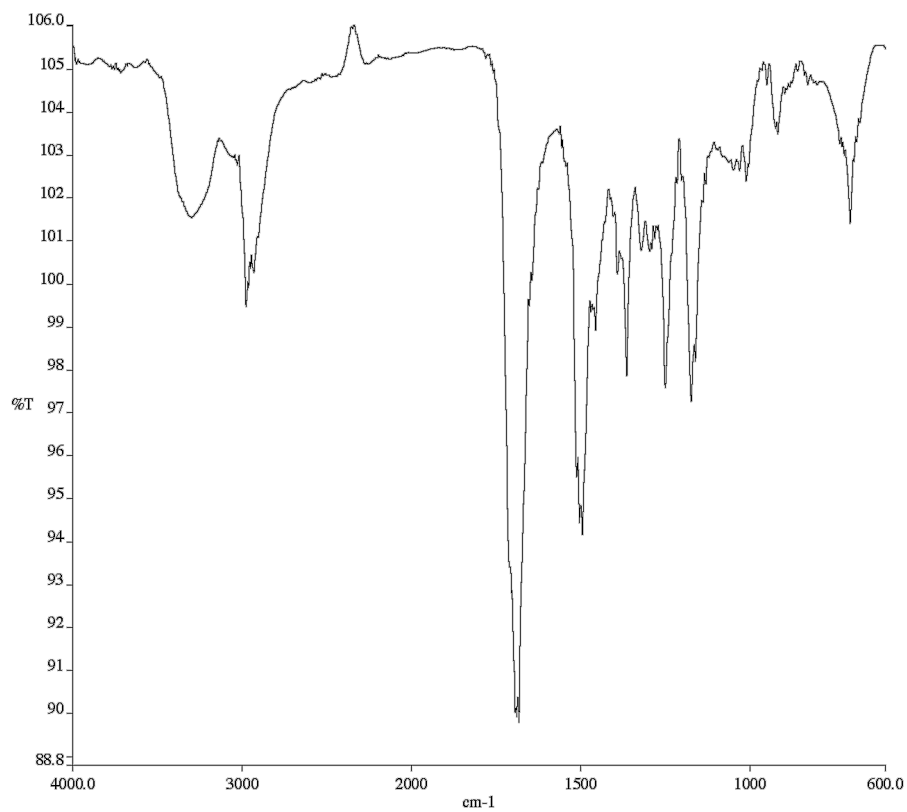


**Figure A1.137** Infrared spectrum (Thin Film, NaCl) of compound **88**.

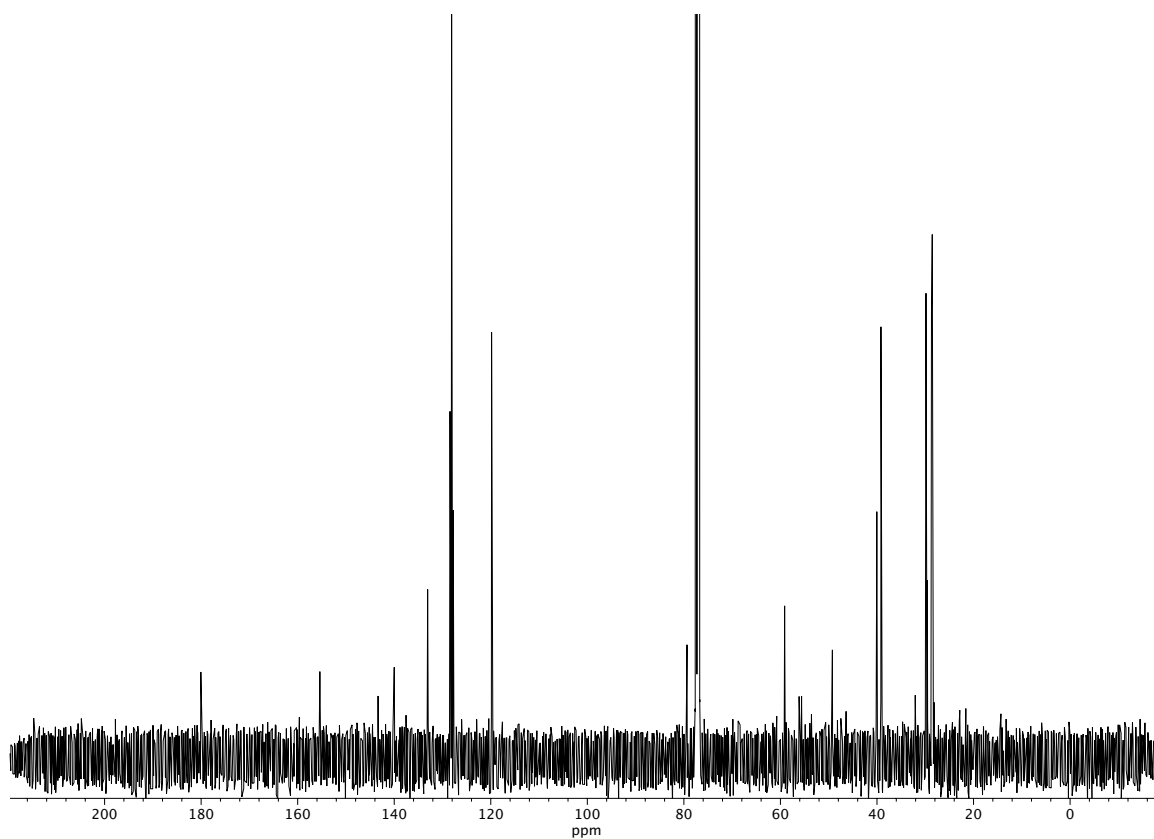


**Figure A1.138** <sup>13</sup>C NMR (100 MHz, CDCl<sub>3</sub>) of compound **88**.

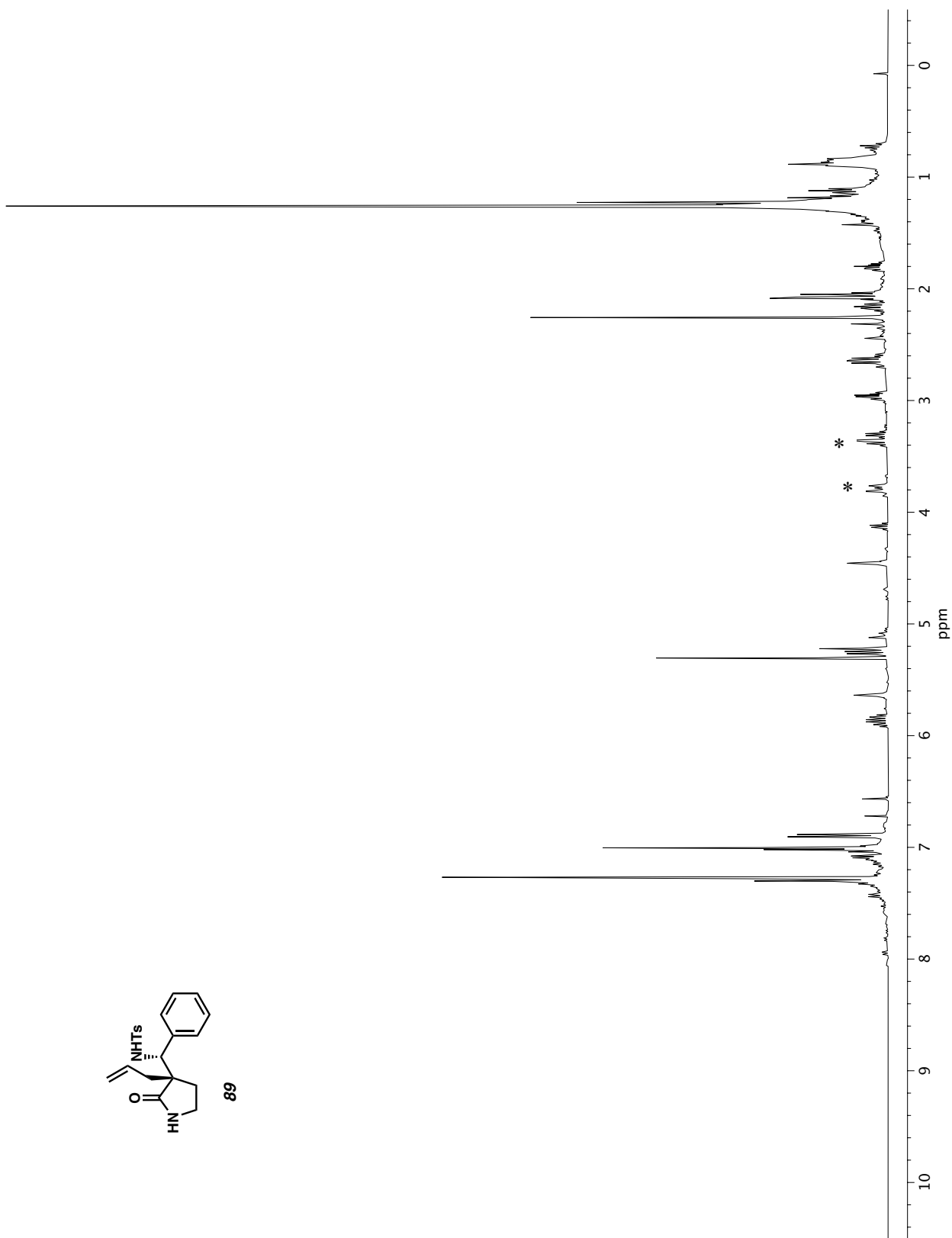
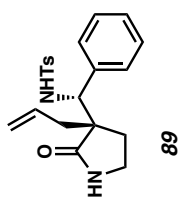
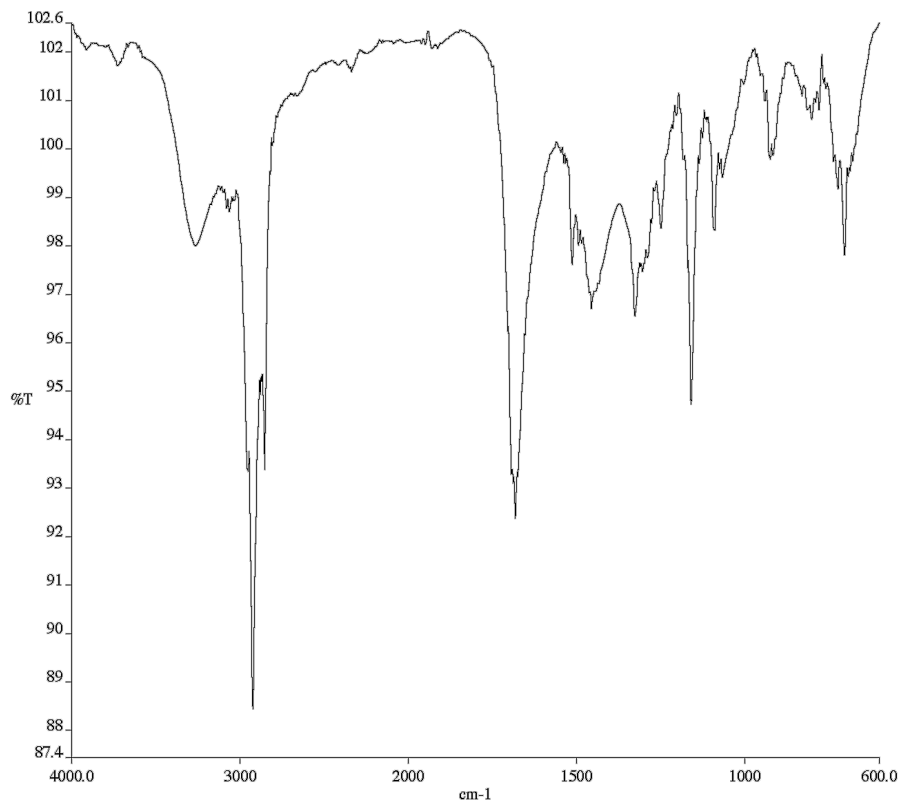
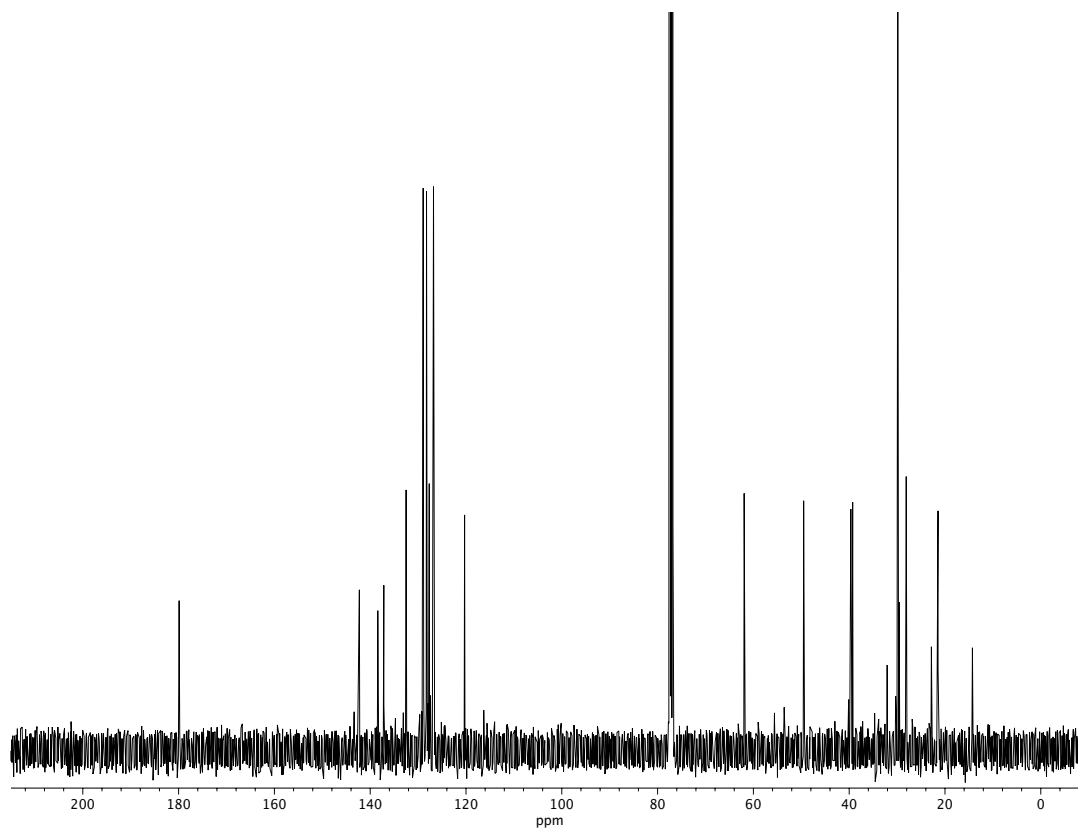


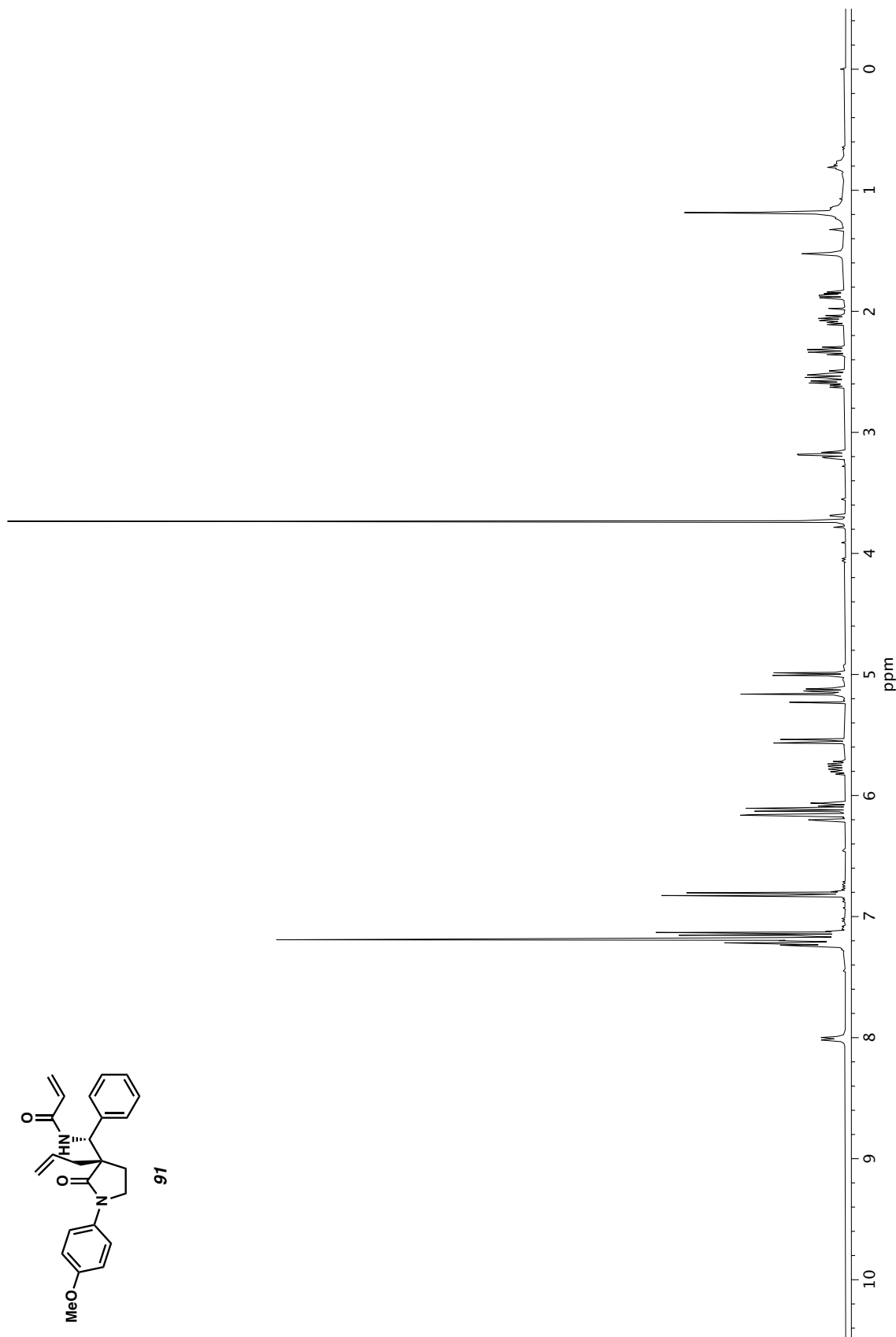
Figure A1.139 <sup>1</sup>H NMR (400 MHz, CDCl<sub>3</sub>) of compound **89**.



**Figure A1.140** Infrared spectrum (Thin Film, NaCl) of compound **89**.



**Figure A1.141** <sup>13</sup>C NMR (100 MHz, CDCl<sub>3</sub>) of compound **89**.



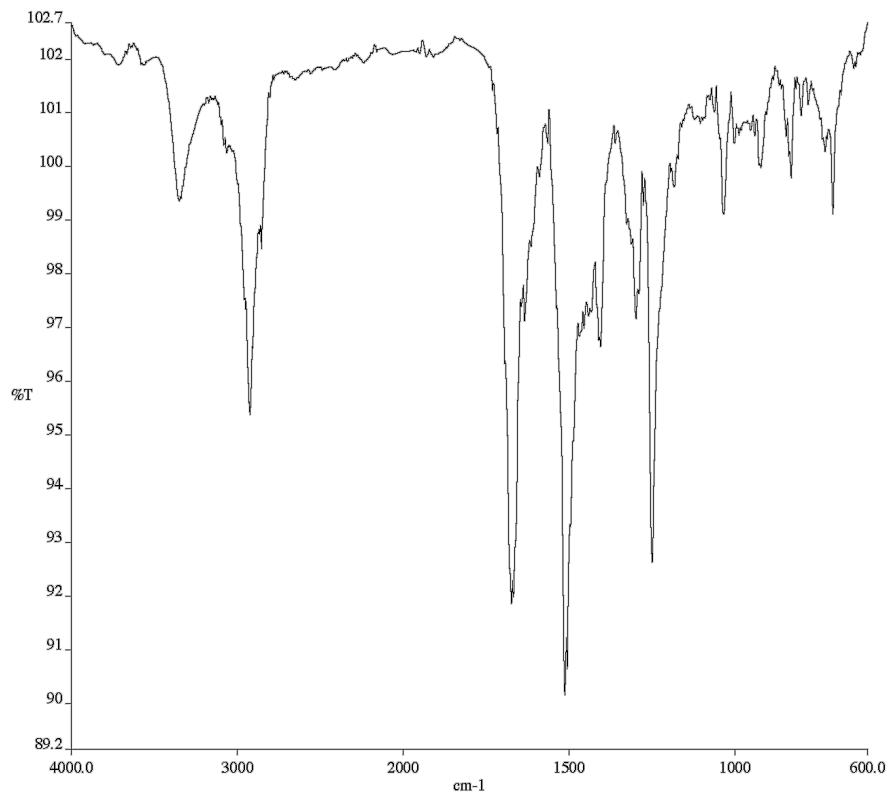


**Figure A1.143** Infrared spectrum (Thin Film, NaCl) of compound **91**.

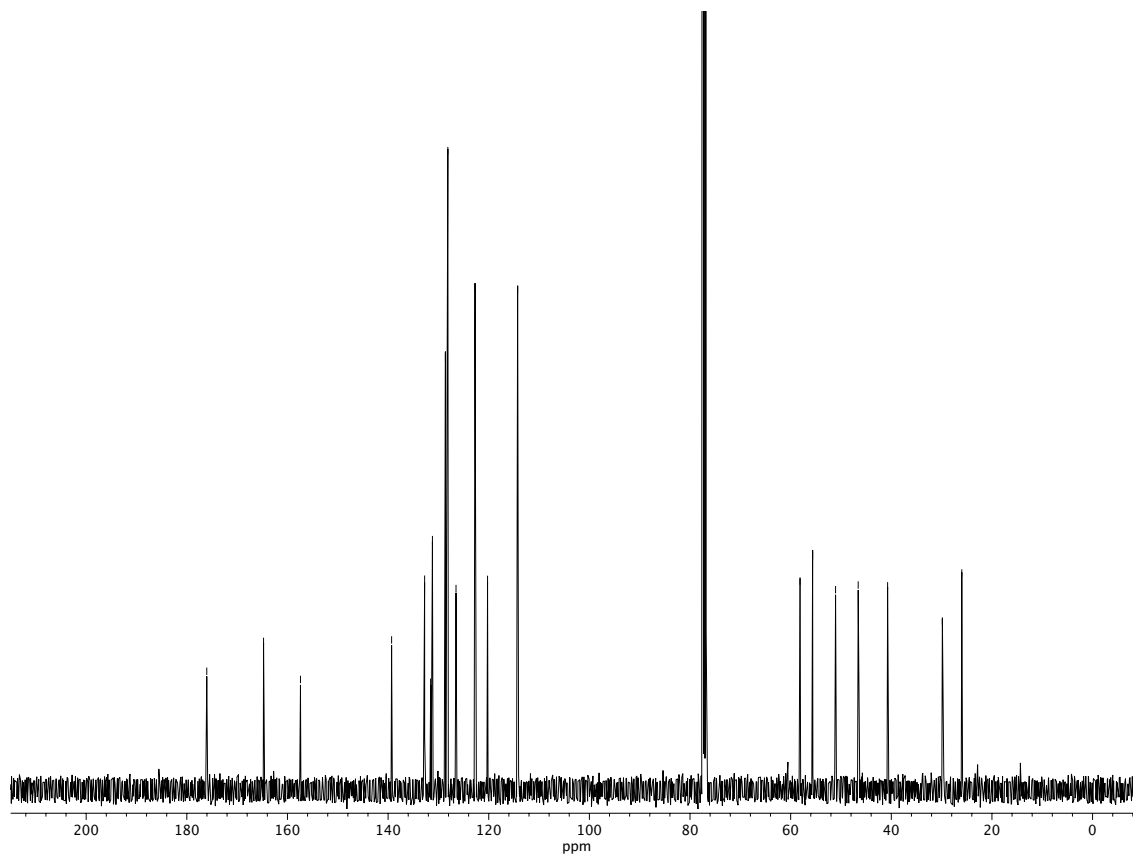


**Figure A1.144** <sup>13</sup>C NMR (100 MHz, CDCl<sub>3</sub>) of compound **91**.



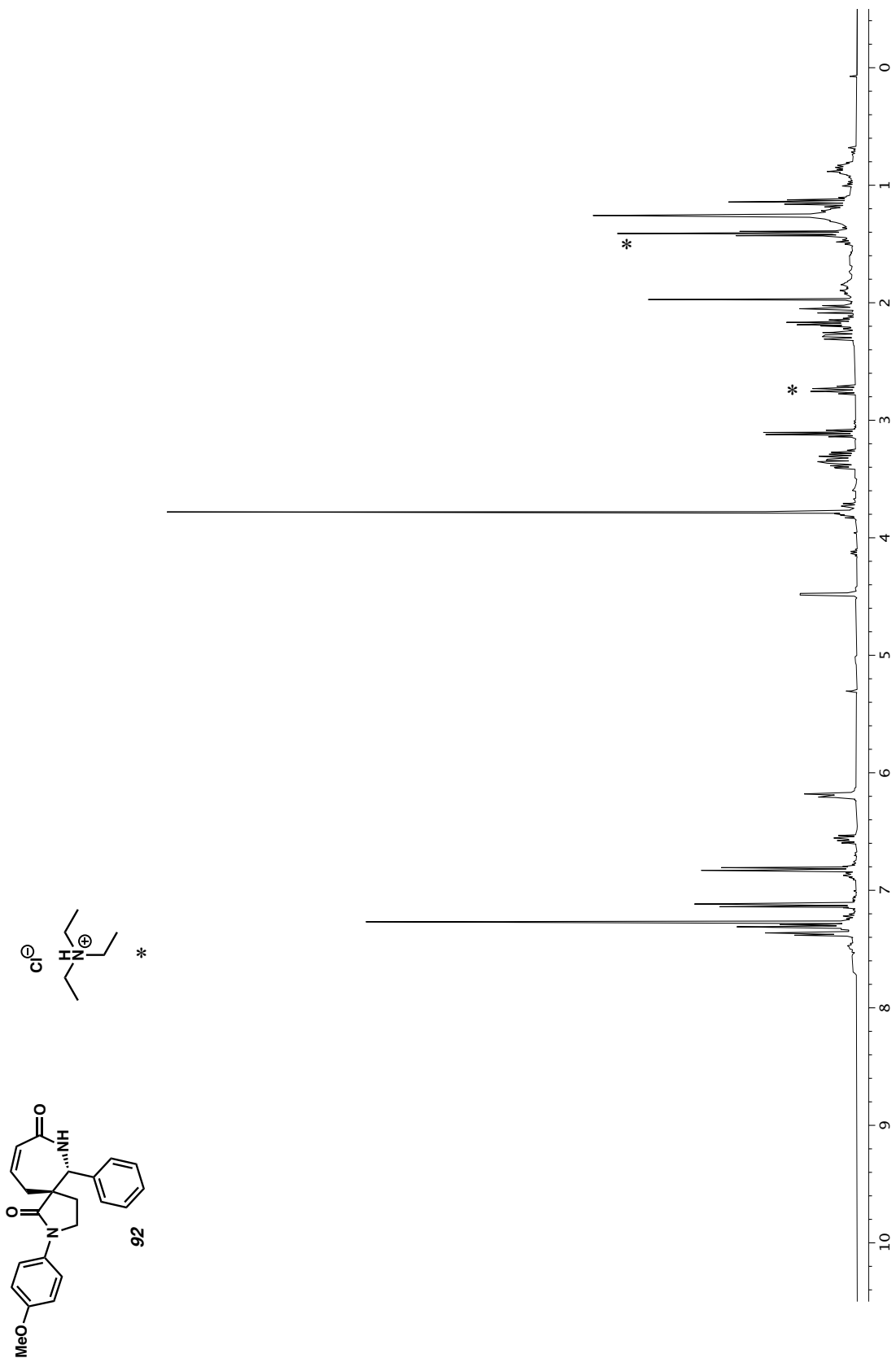
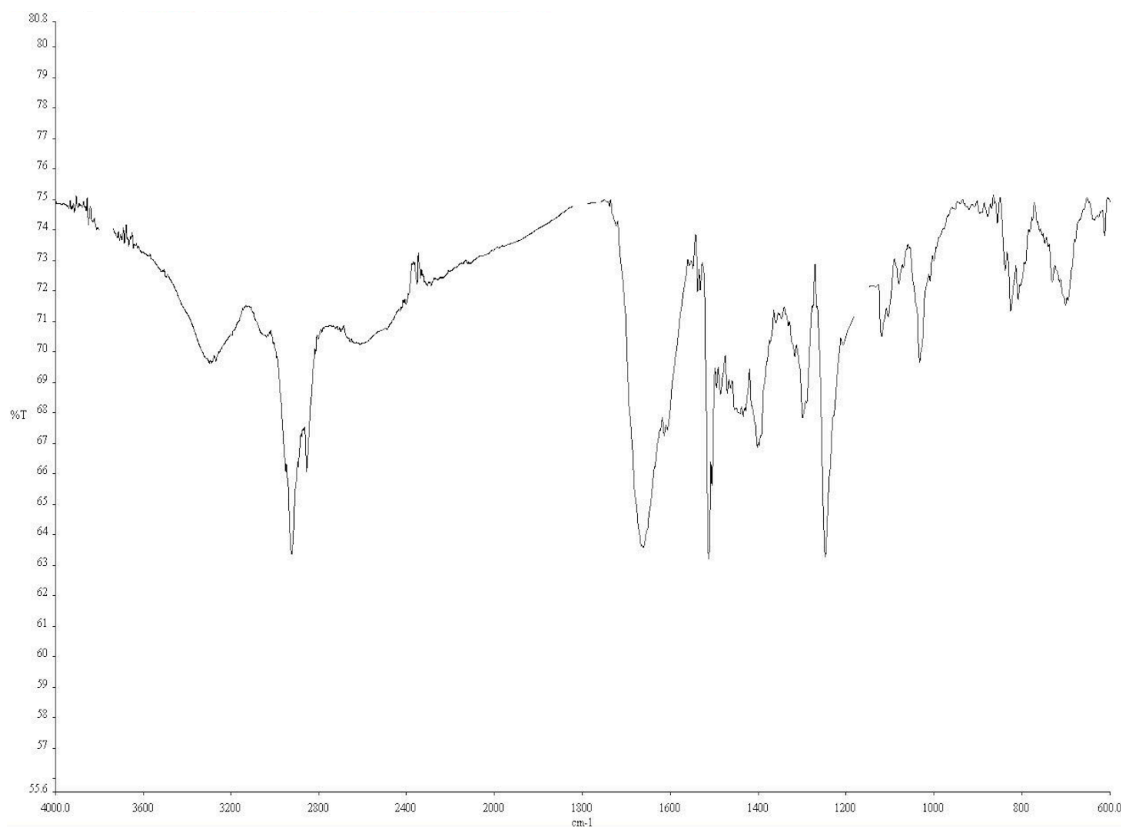
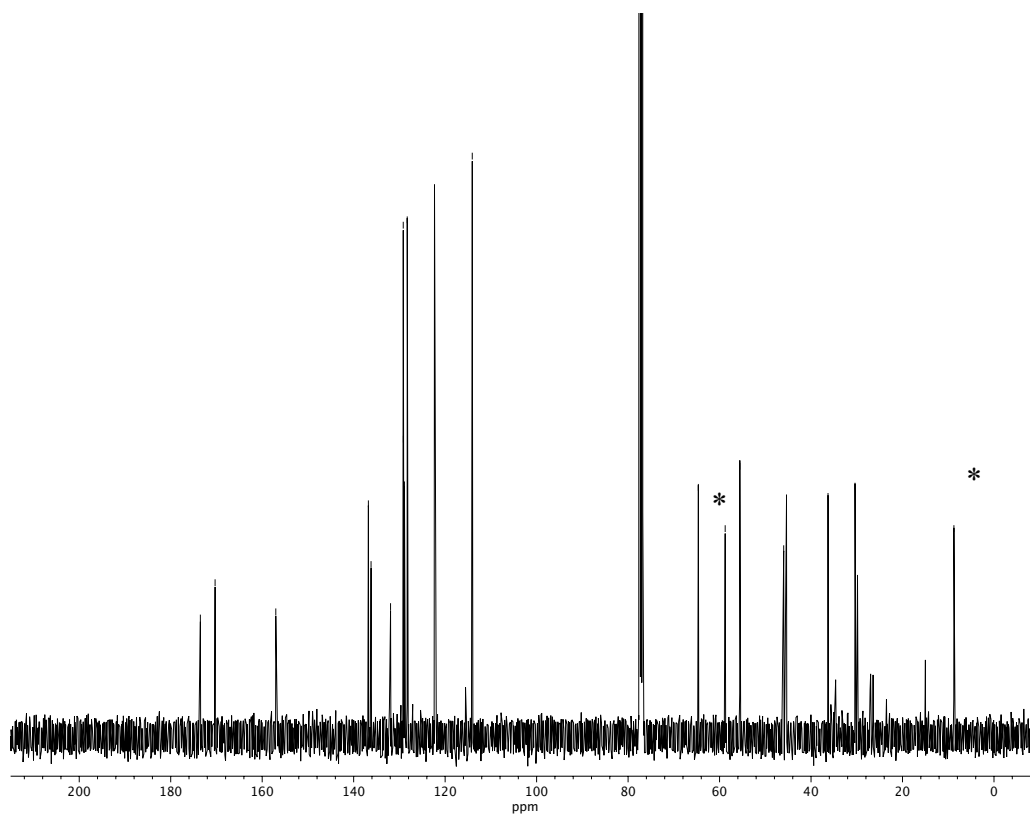


Figure A1.145  $^1\text{H}$  NMR (400 MHz,  $\text{CDCl}_3$ ) of compound **92**.



**Figure A1.146** Infrared spectrum (Thin Film, NaCl) of compound **92**.



**Figure A1.147** <sup>13</sup>C NMR (100 MHz, CDCl<sub>3</sub>) of compound **92**.

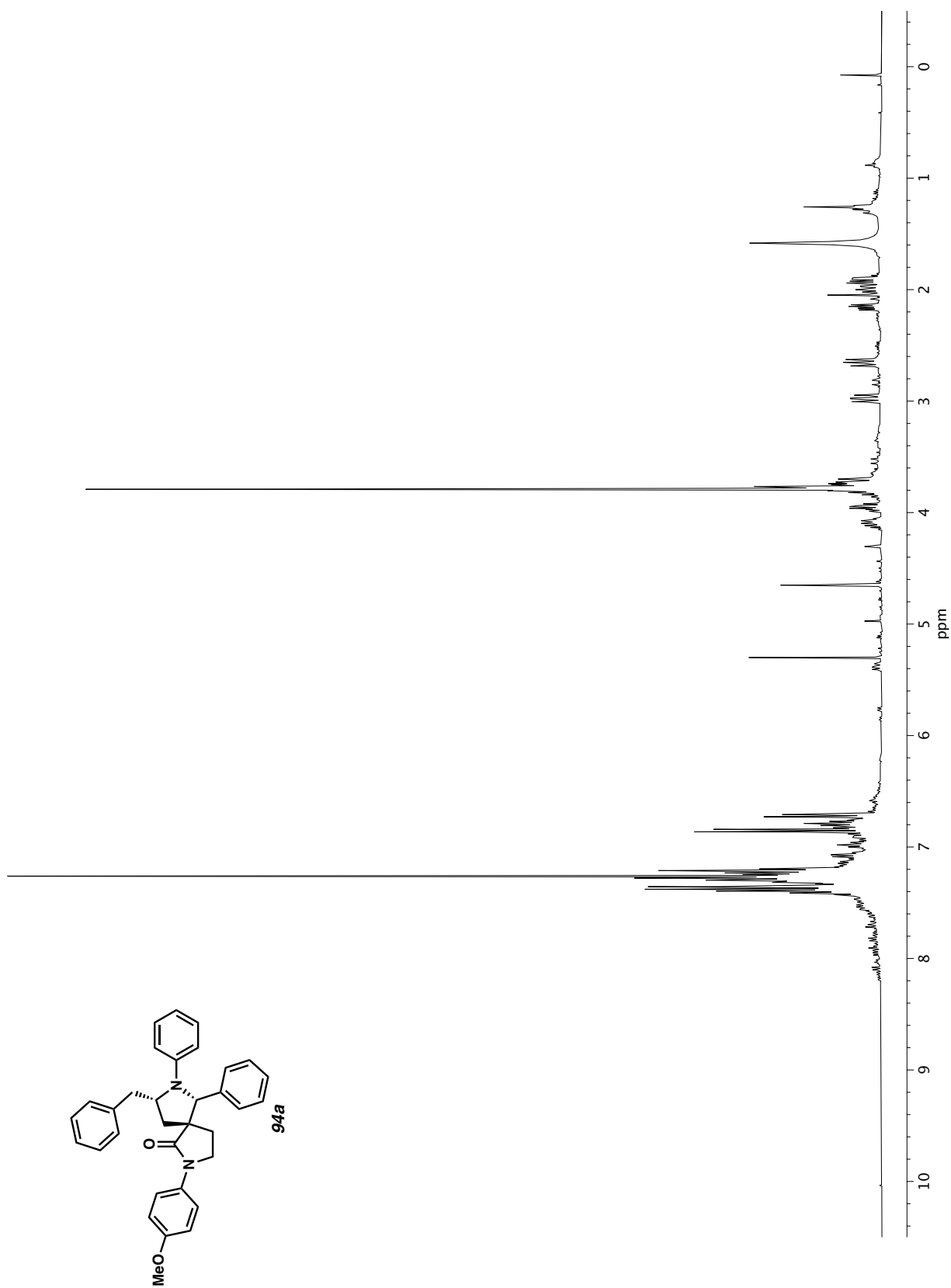


**Figure A1.148**  $^1\text{H}$  NMR (400 MHz,  $\text{CDCl}_3$ ) of compound **94a**.

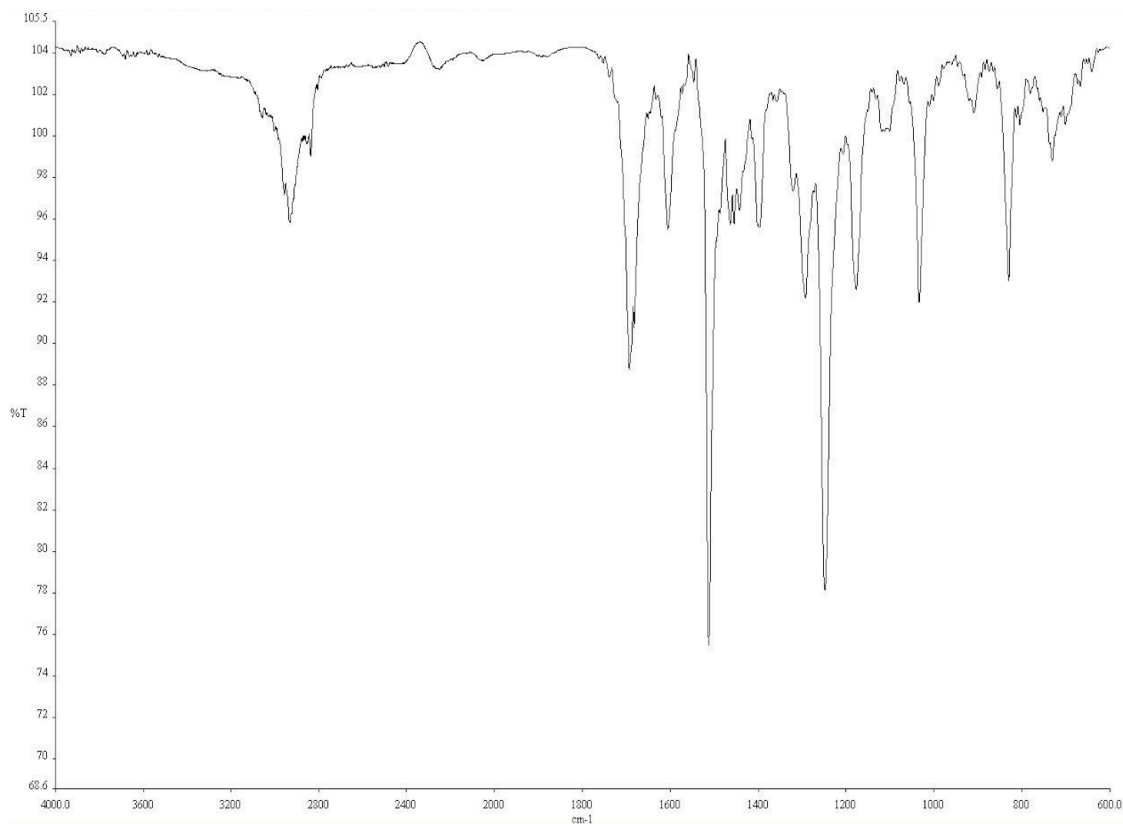


**Figure A1.149** Infrared spectrum (Thin Film, NaCl) of compound **94a**.

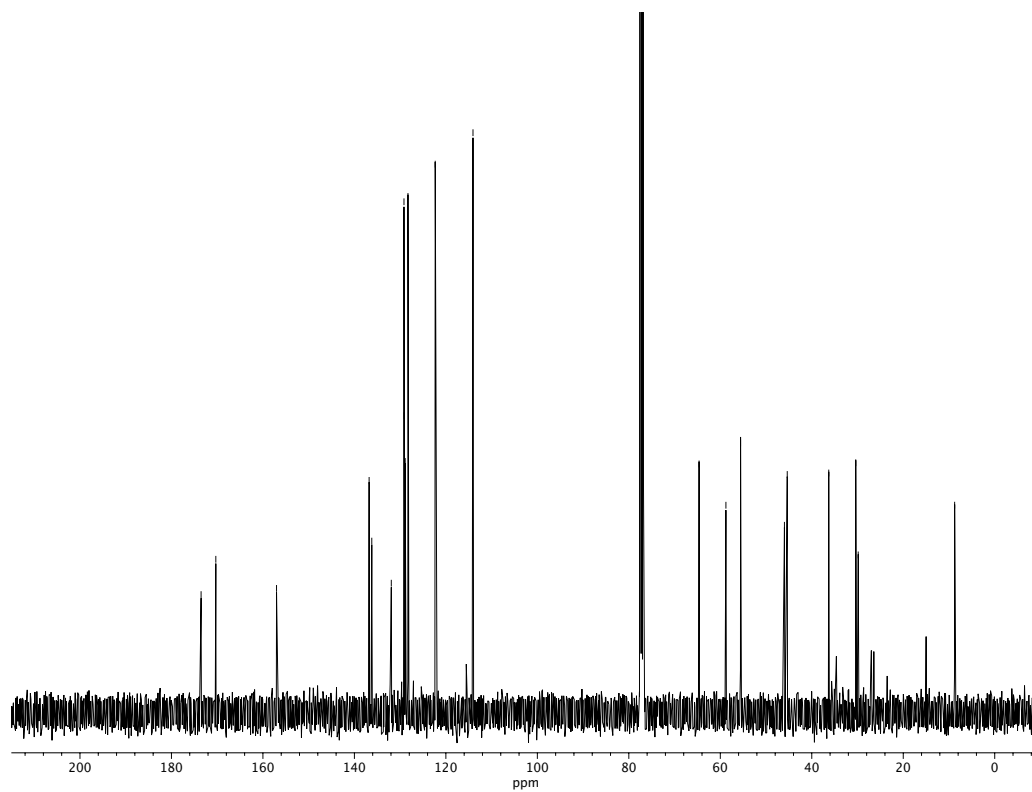


**Figure A1.150**  $^{13}\text{C}$  NMR (100 MHz,  $\text{CDCl}_3$ ) of compound **94a**.

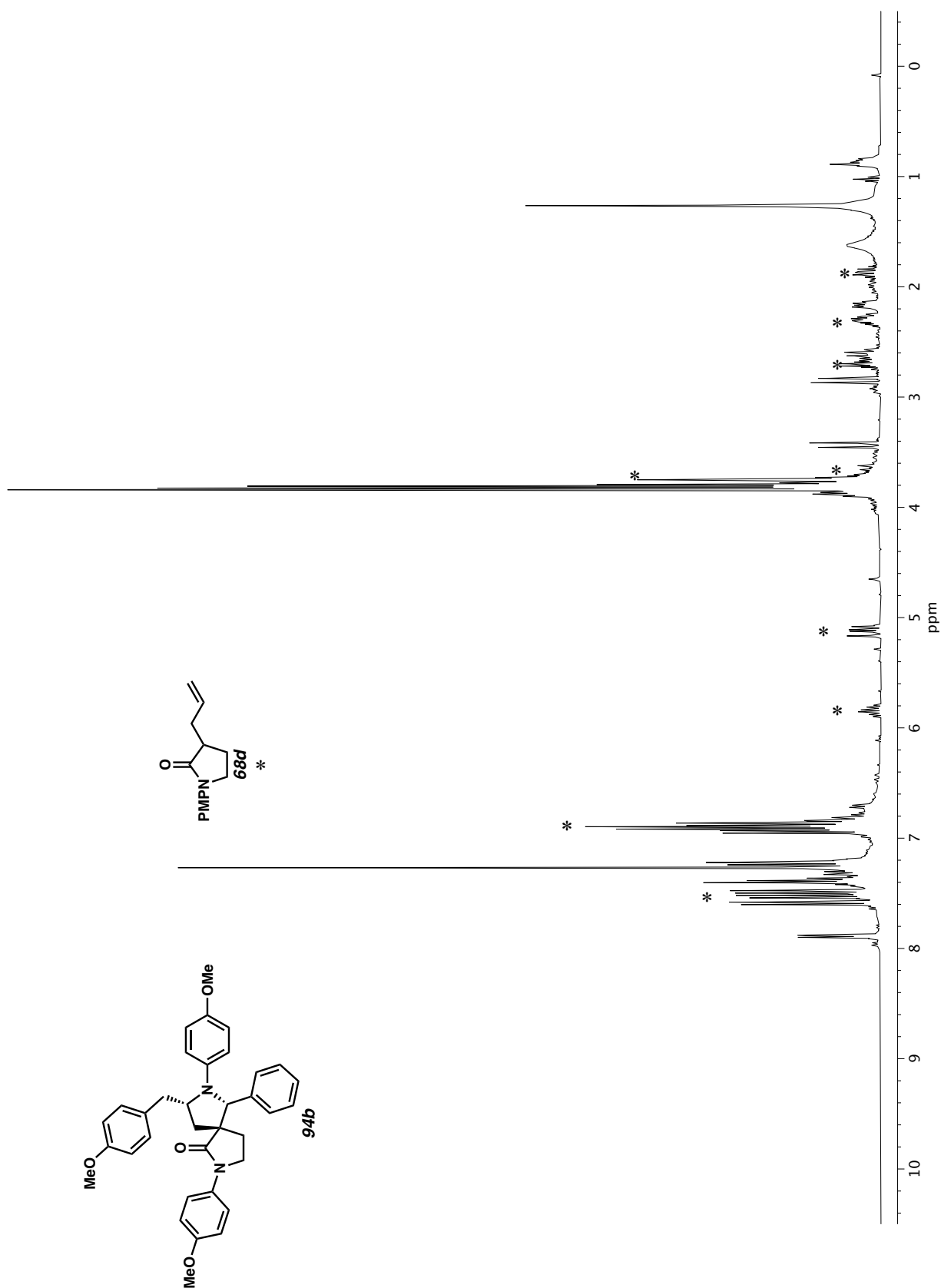
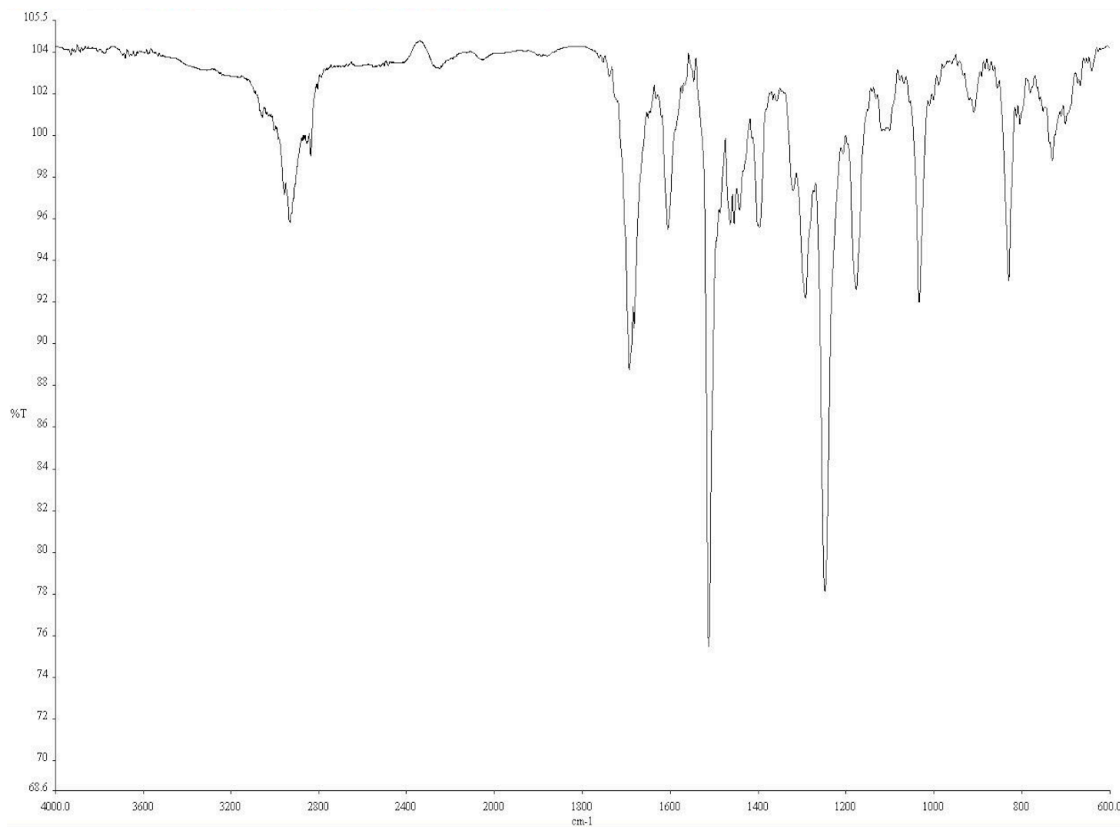
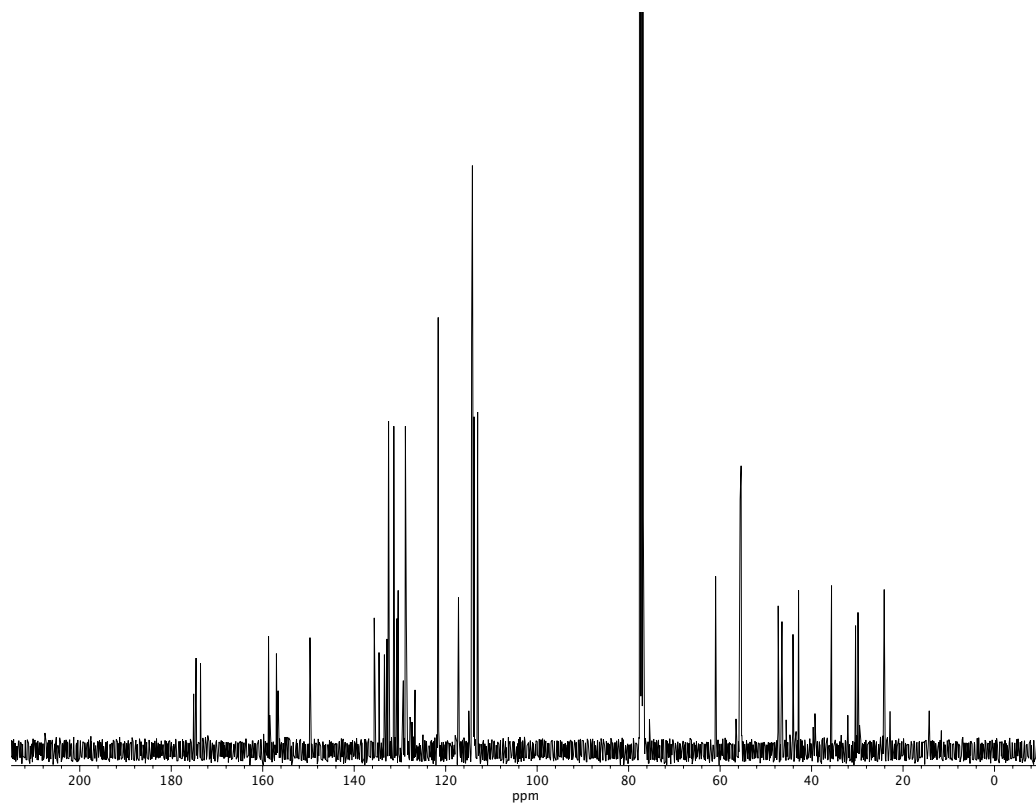


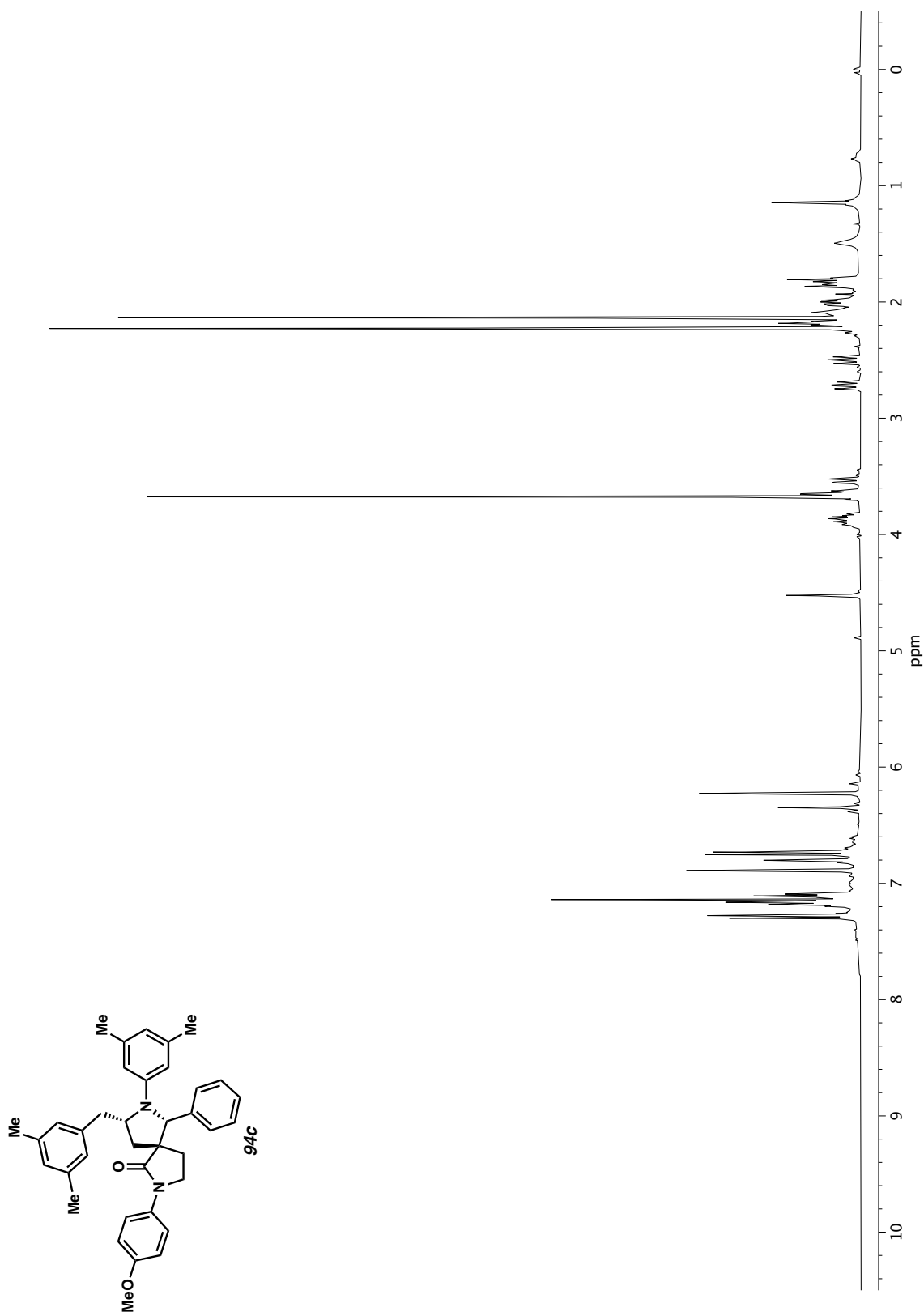
Figure A1.151  $^1\text{H}$  NMR (400 MHz,  $\text{CDCl}_3$ ) of compound **94b**.



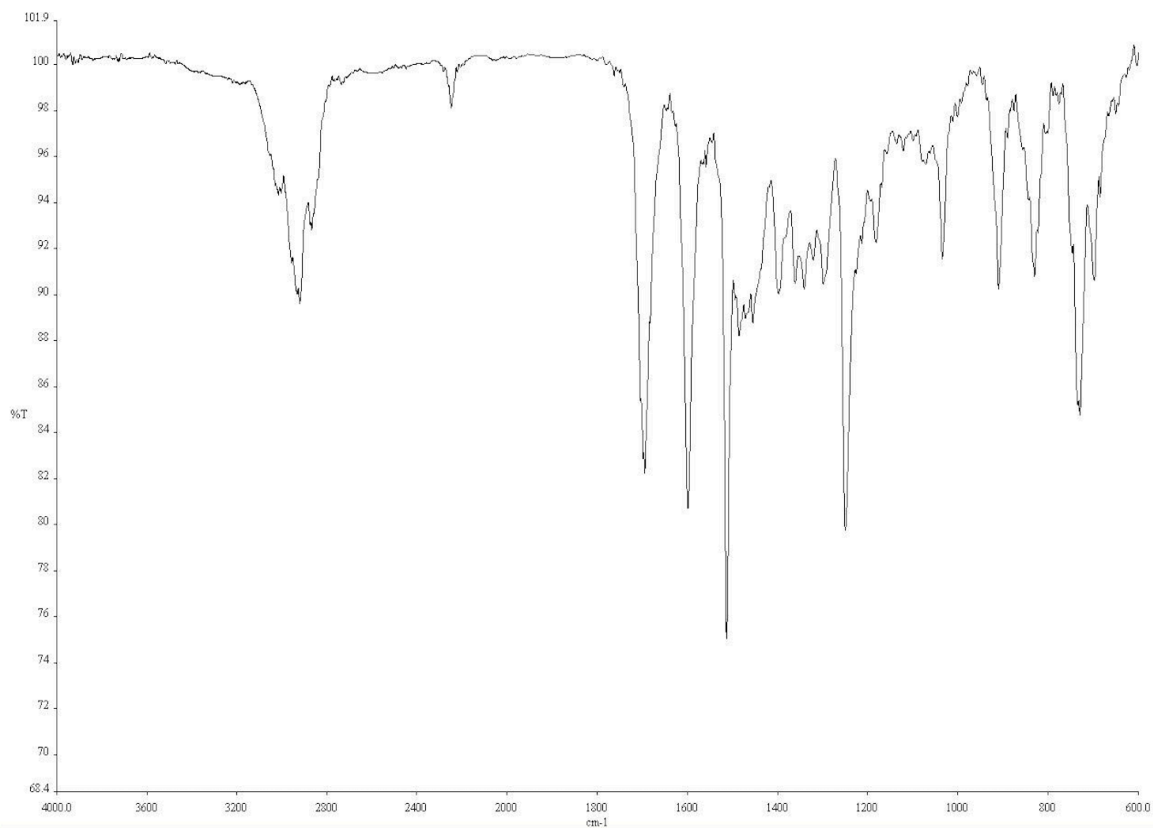
**Figure A1.152** Infrared spectrum (Thin Film, NaCl) of compound **94b**.



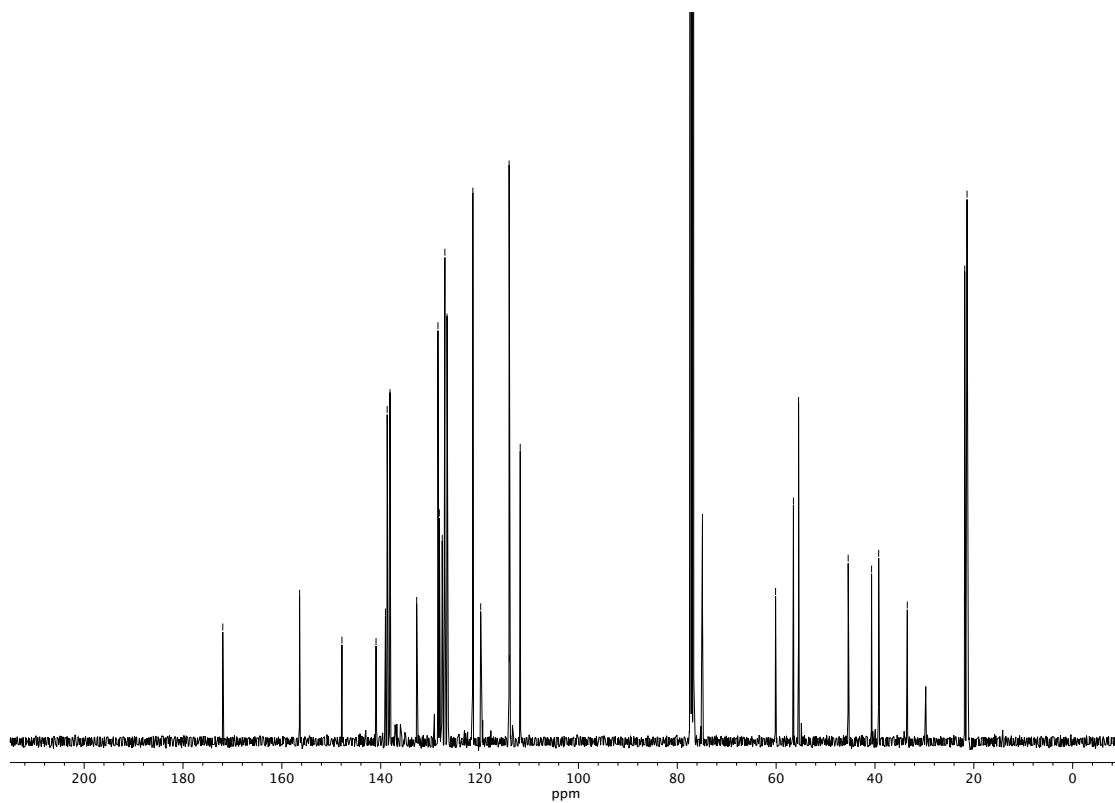
**Figure A1.153** <sup>13</sup>C NMR (100 MHz, CDCl<sub>3</sub>) of compound **94b**.



**Figure A1.154**  $^1\text{H}$  NMR (400 MHz,  $\text{CDCl}_3$ ) of compound **94c**.



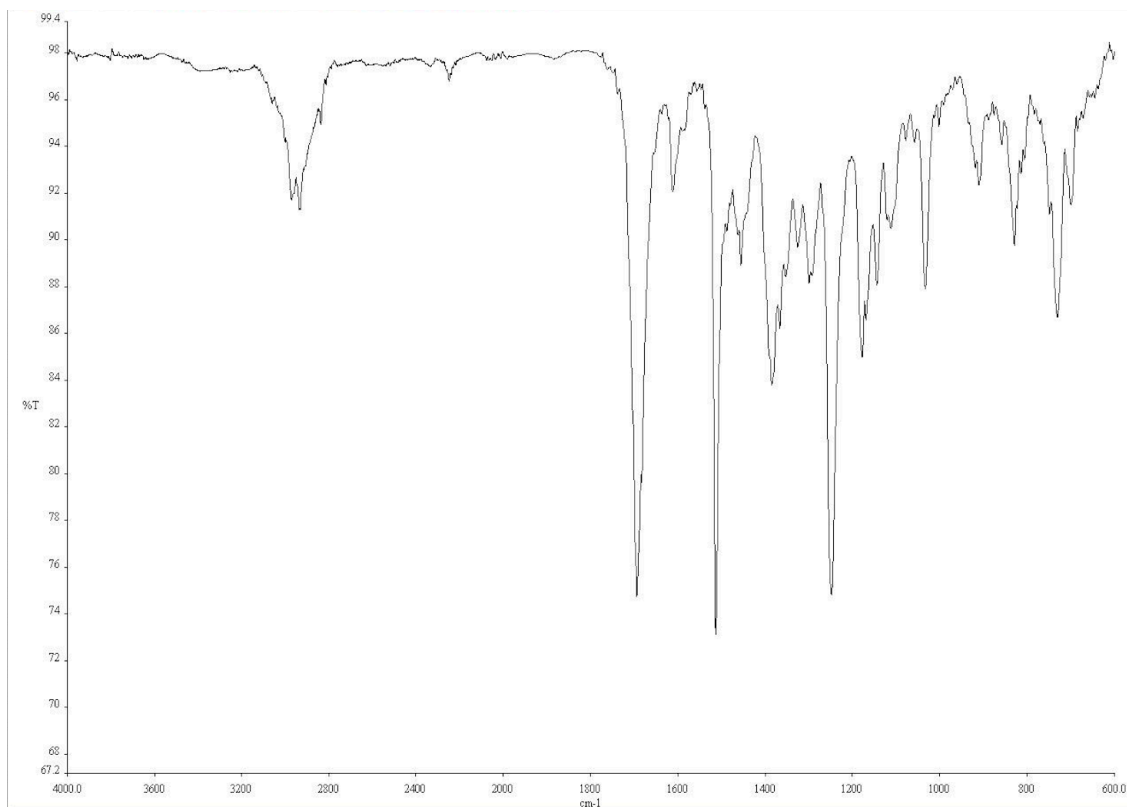
**Figure A1.155** Infrared spectrum (Thin Film, NaCl) of compound **94c**.



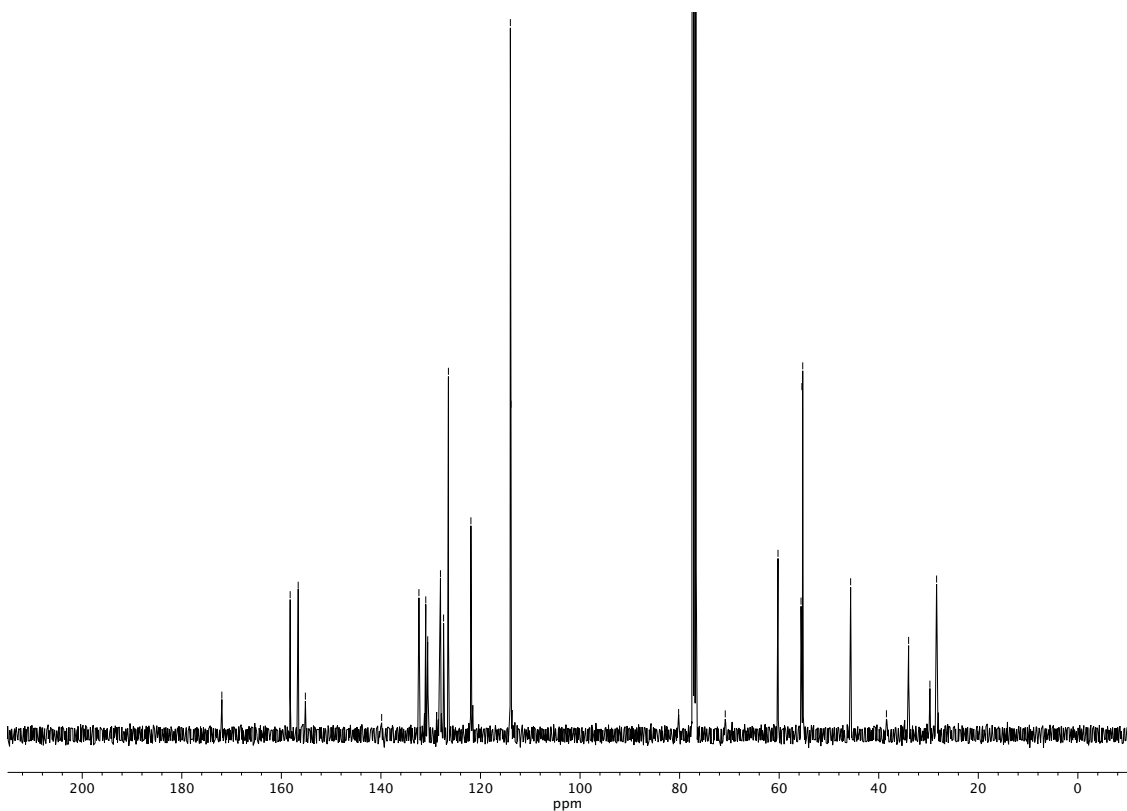
**Figure A1.156** <sup>13</sup>C NMR (100 MHz, CDCl<sub>3</sub>) of compound **94c**.





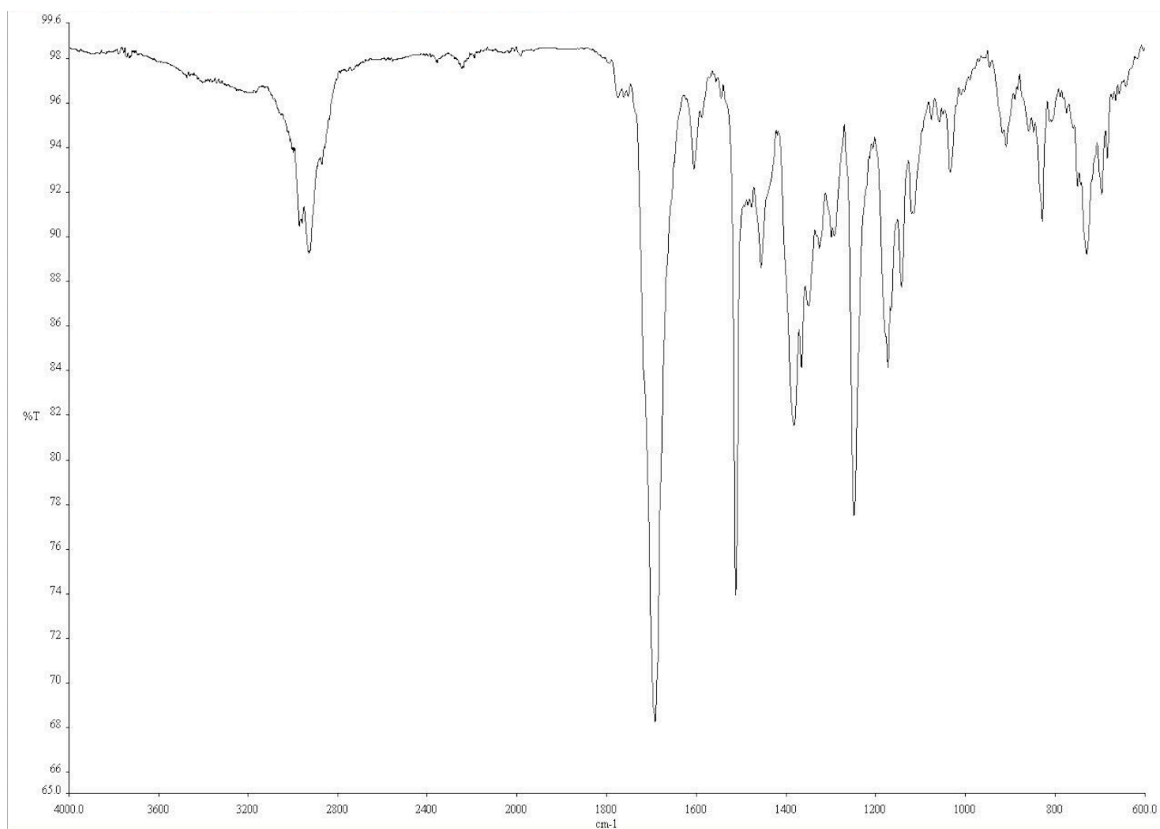


**Figure A1.158** Infrared spectrum (Thin Film, NaCl) of compound **95a**.

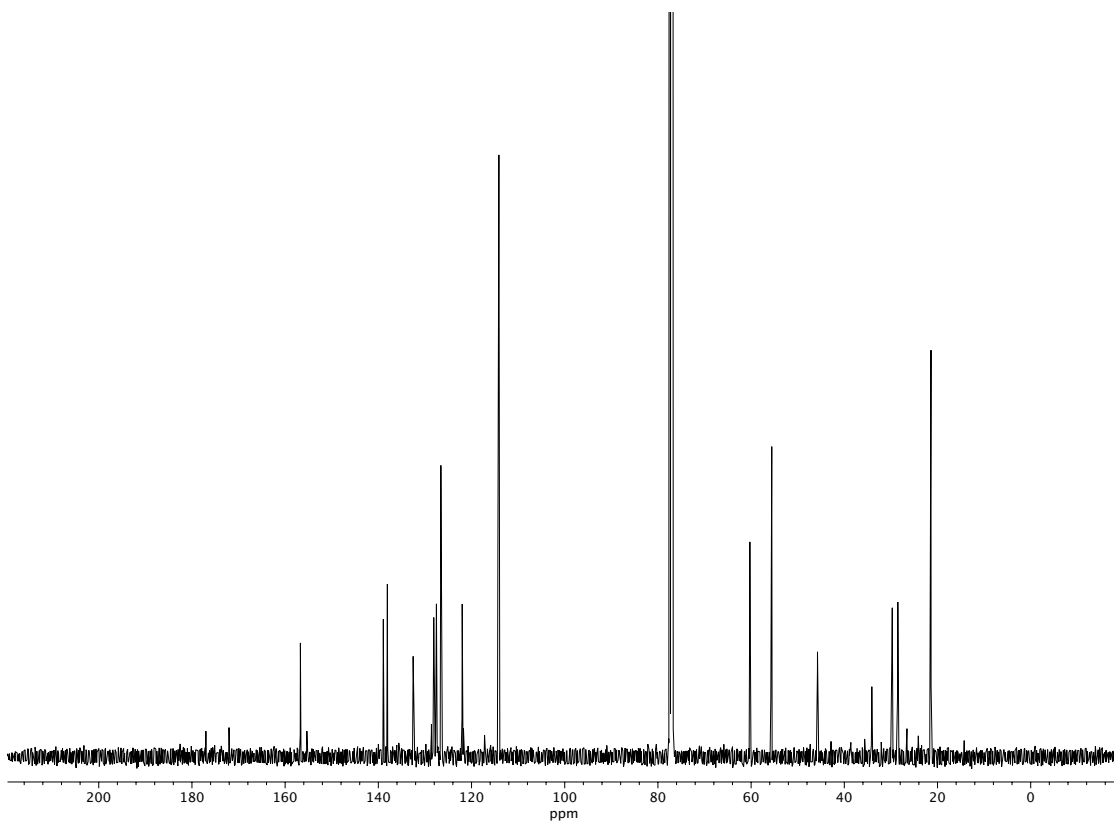


**Figure A1.159** <sup>13</sup>C NMR (100 MHz, CDCl<sub>3</sub>) of compound **95a**.



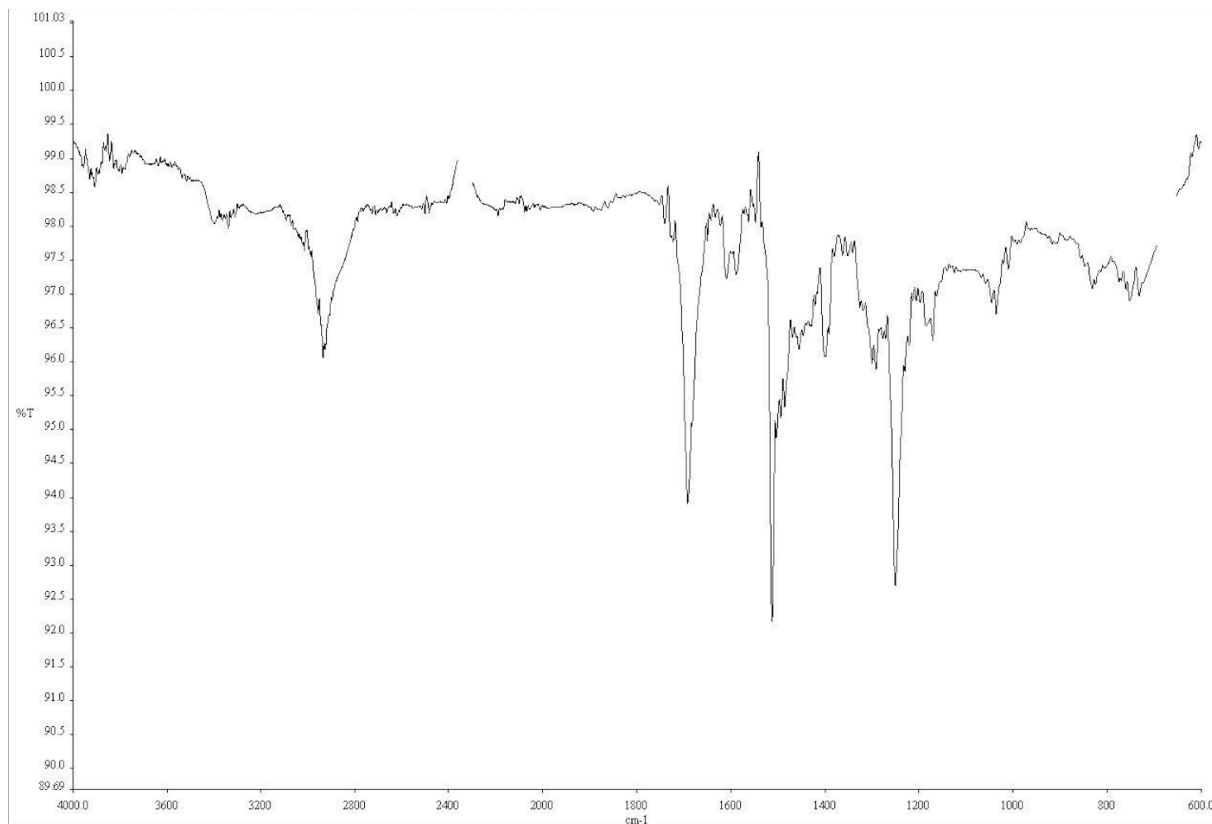


**Figure A1.161** Infrared spectrum (Thin Film, NaCl) of compound **95b**.

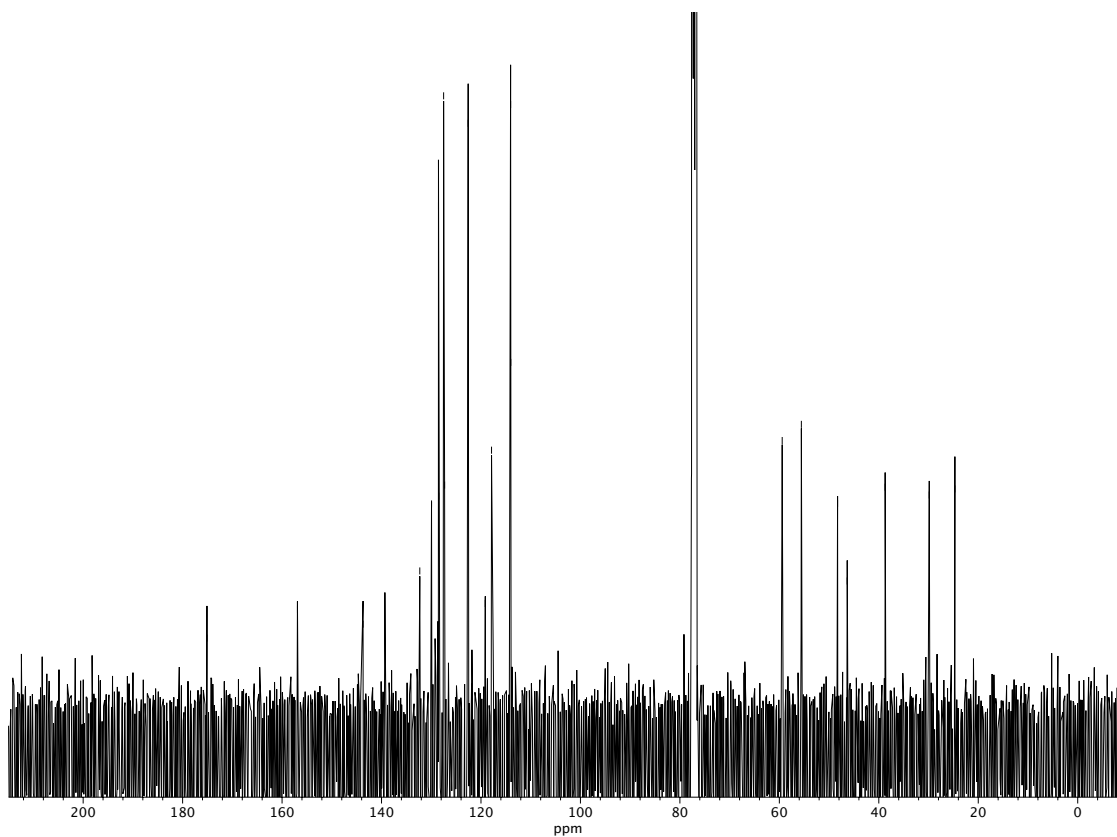


**Figure A1.162**  $^{13}\text{C}$  NMR (100 MHz,  $\text{CDCl}_3$ ) of compound **95b**.

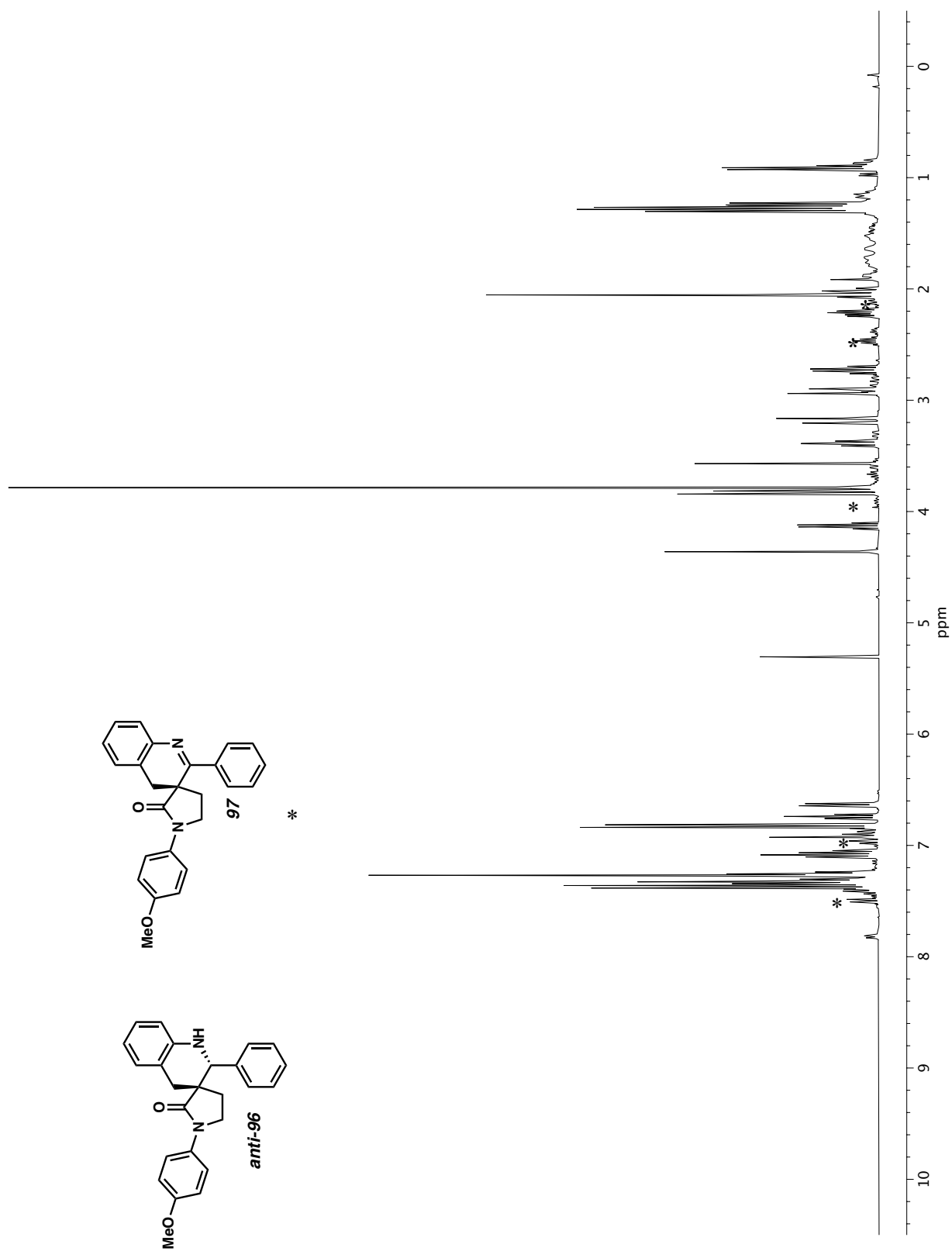


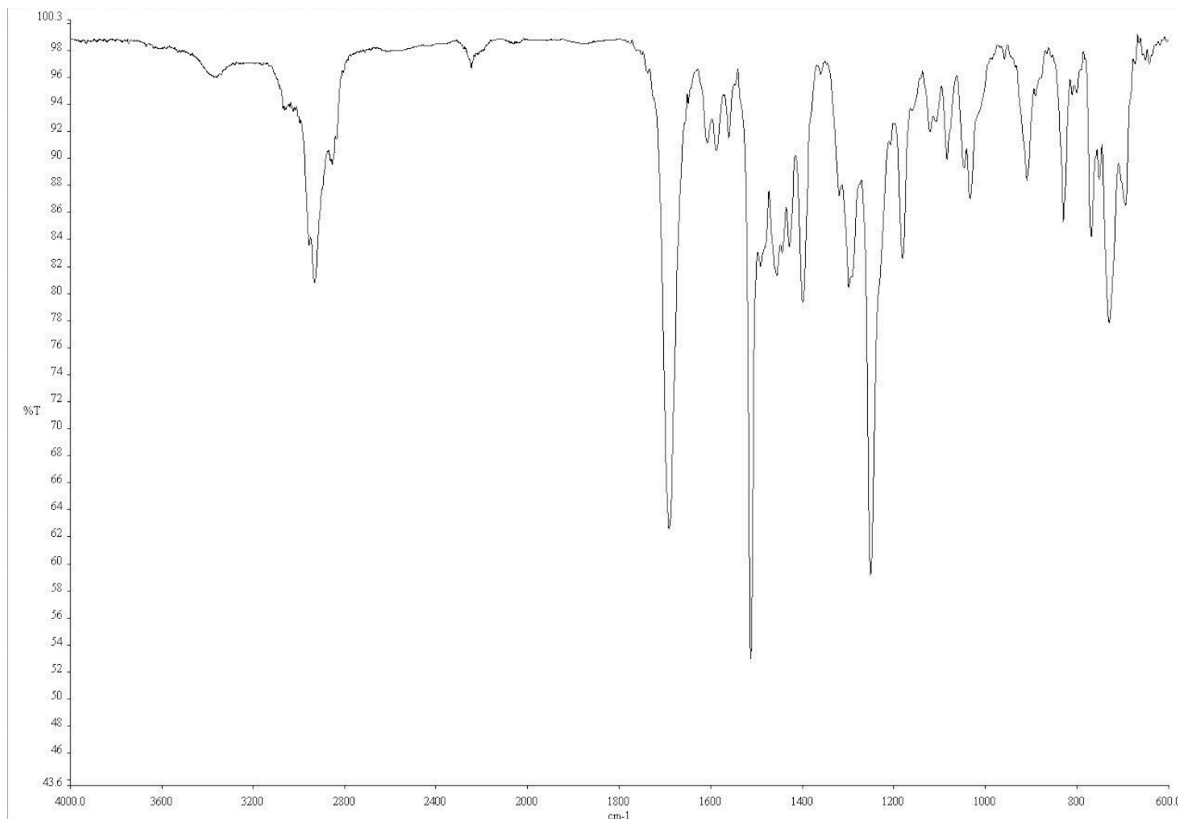


**Figure A1.164** Infrared spectrum (Thin Film, NaCl) of compound **syn-96**.

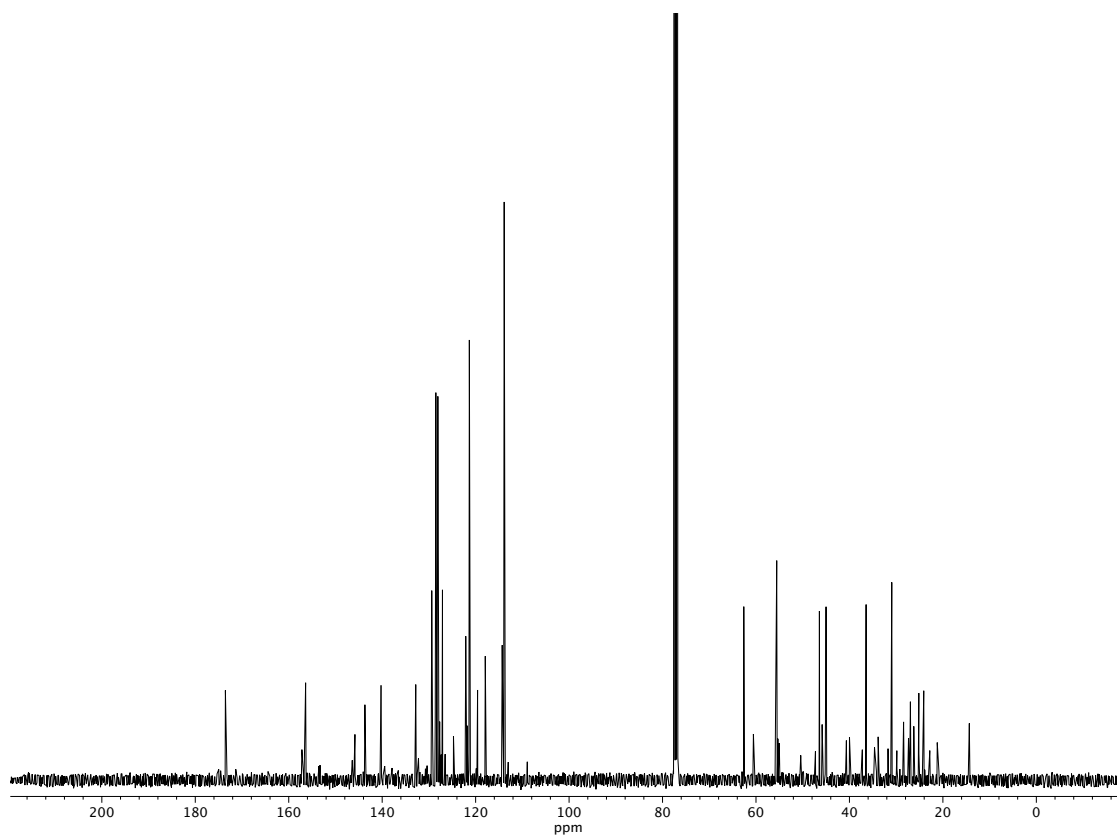


**Figure A1.165**  $^{13}\text{C}$  NMR (100 MHz,  $\text{CDCl}_3$ ) of compound **syn-96**.

Figure A1.166  $^1\text{H}$  NMR (400 MHz  $\text{CD}_3\text{CN}$ ) of compound **anti-96**.

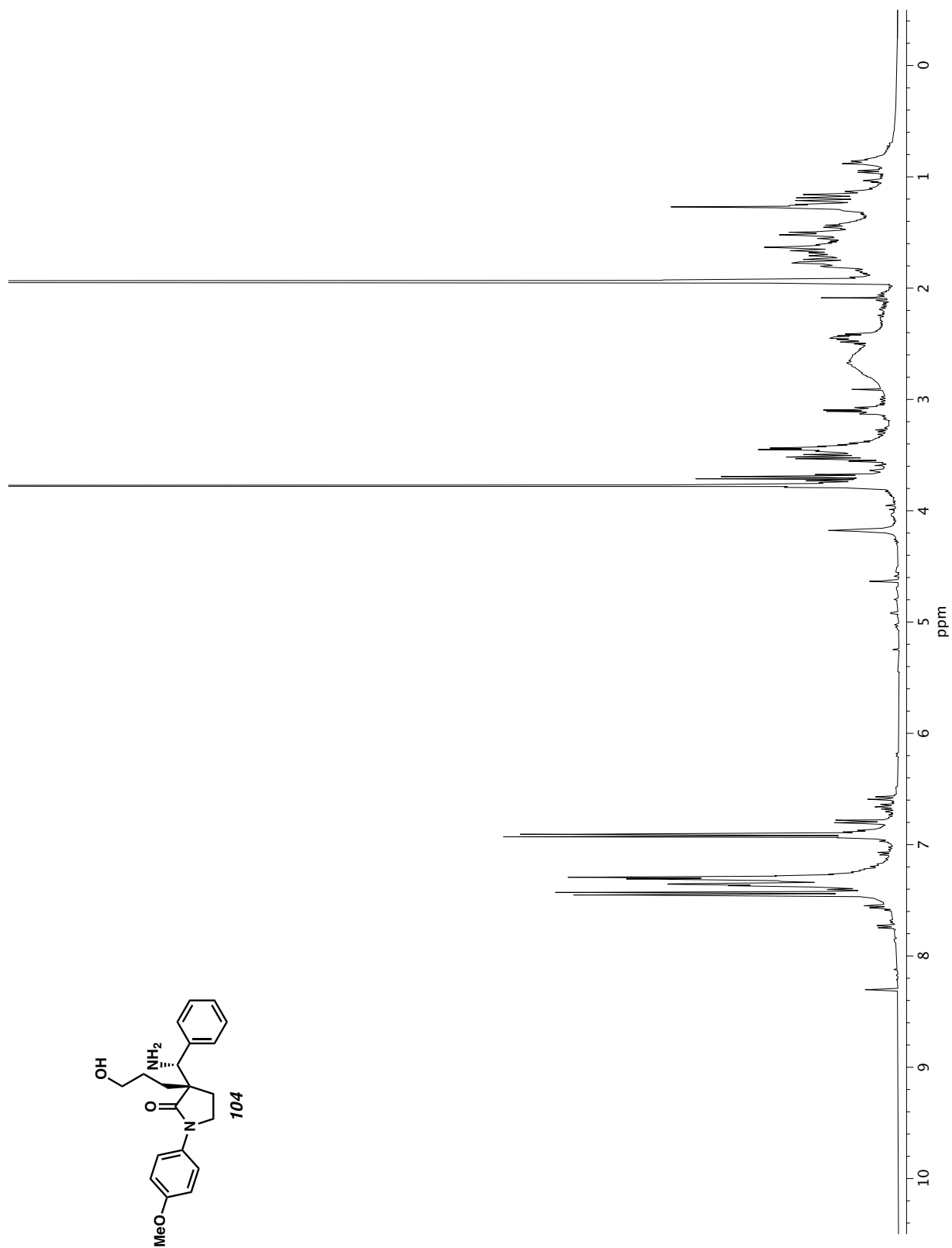


**Figure A1.167** Infrared spectrum (Thin Film, NaCl) of compound **anti-96**.

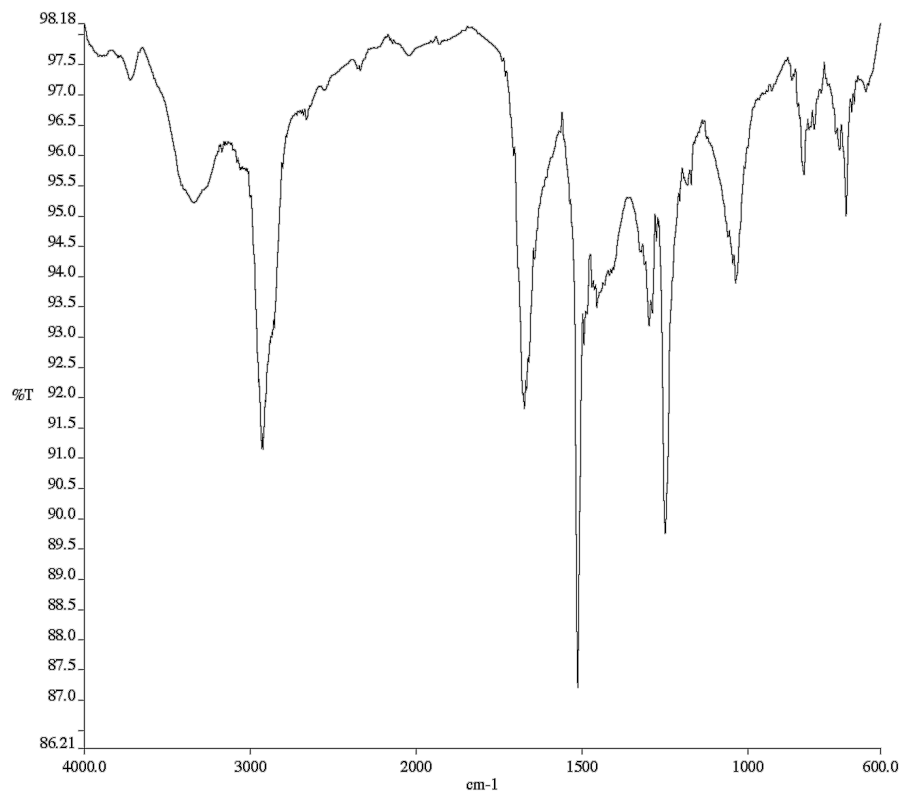


**Figure A1.168** <sup>13</sup>C NMR (100 MHz, CD<sub>3</sub>CN) of compound **anti-96**.

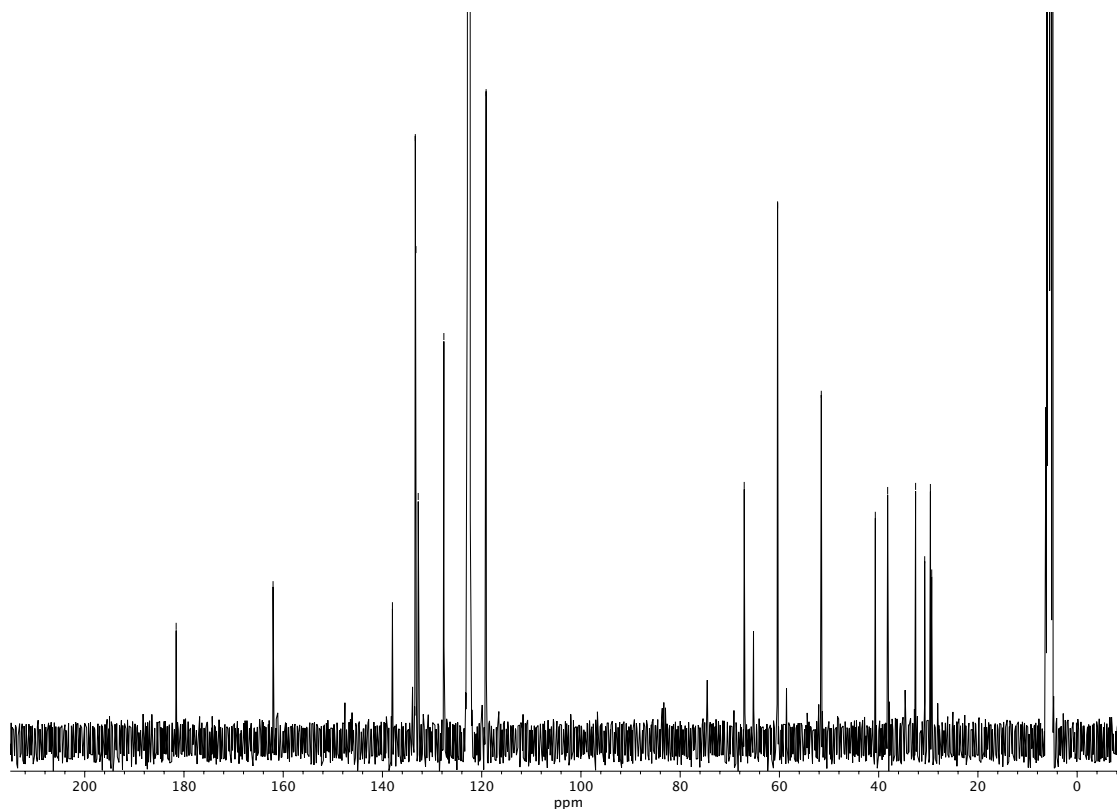




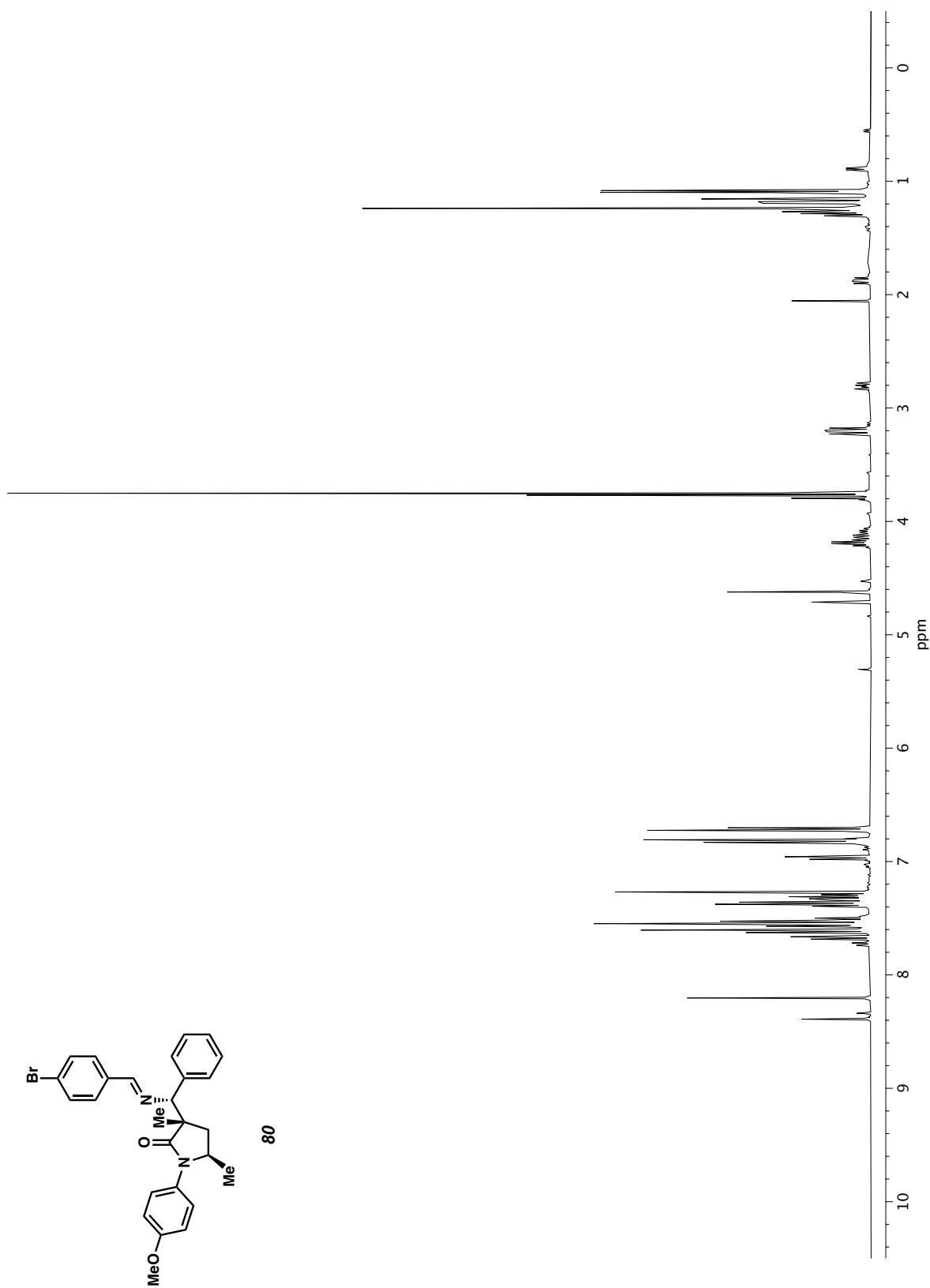
**Figure A1.169**  $^1\text{H}$  NMR (400 MHz  $\text{CD}_3\text{CN}$ ) of compound **104**.

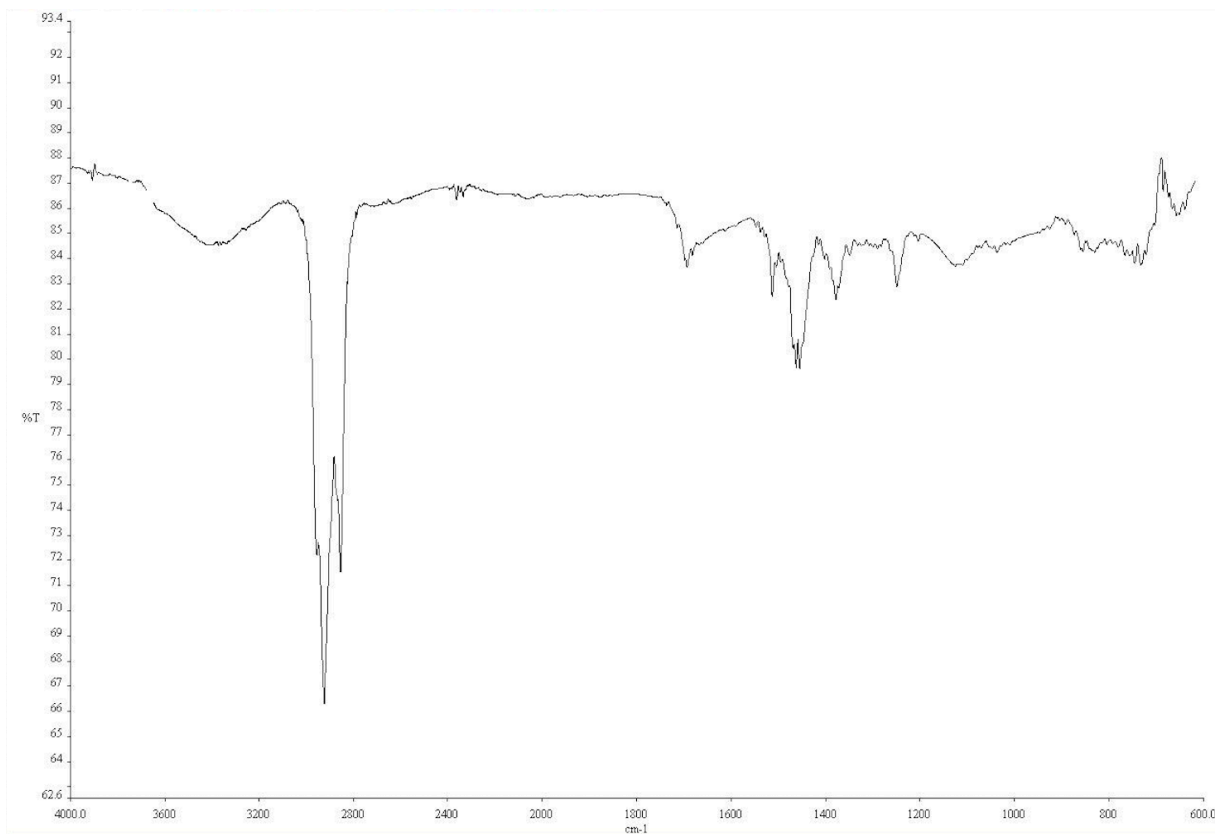


**Figure A1.170** Infrared spectrum (Thin Film, NaCl) of compound **104**.

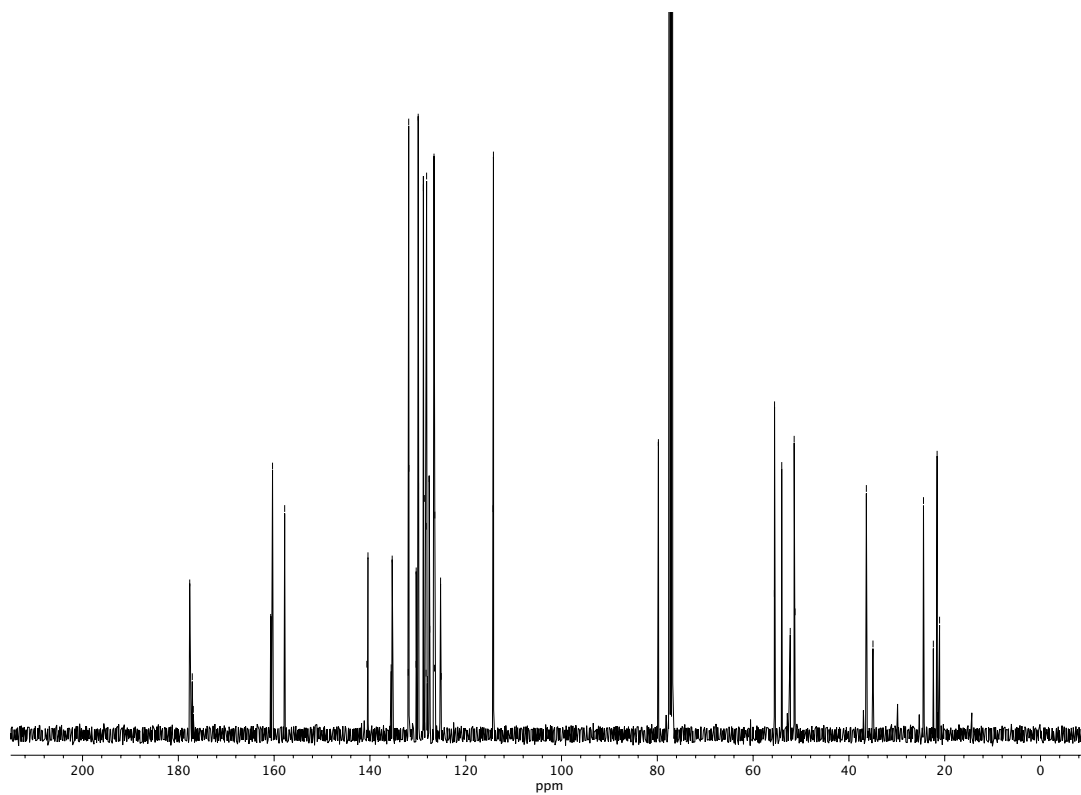


**Figure A1.171** <sup>13</sup>C NMR (100 MHz, CD<sub>3</sub>CN) of compound **104**.

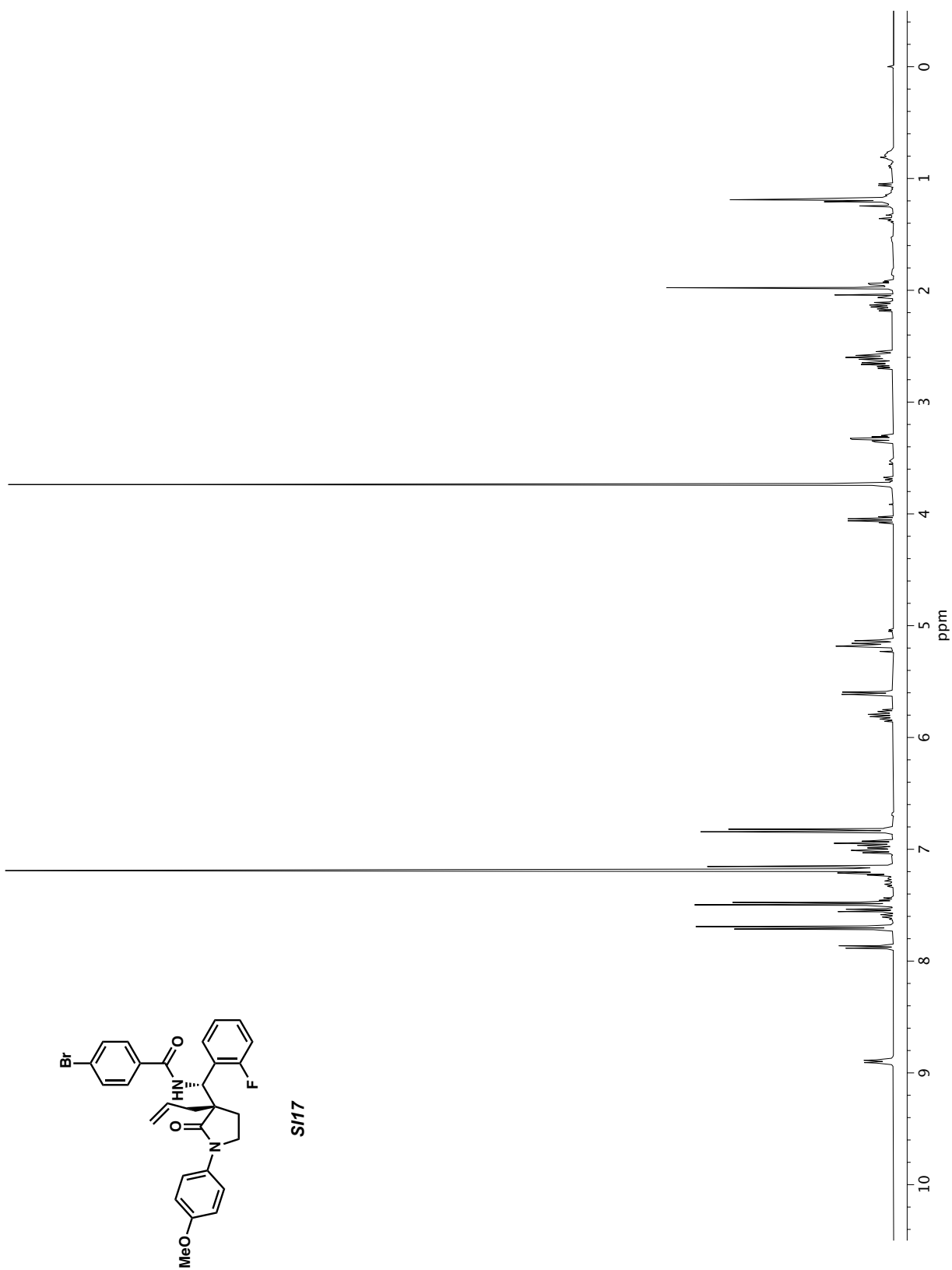


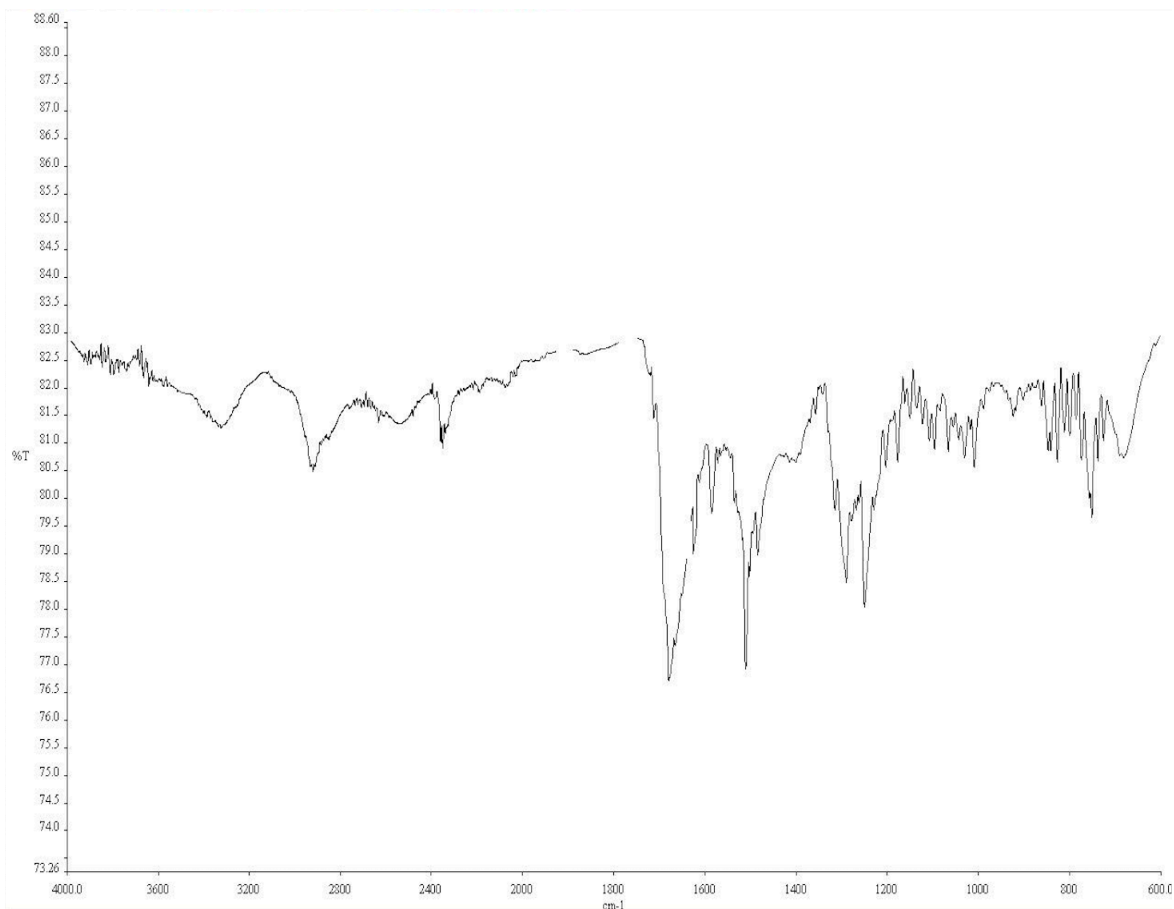


**Figure A1.173** Infrared spectrum (Thin Film, NaCl) of compound **80**.

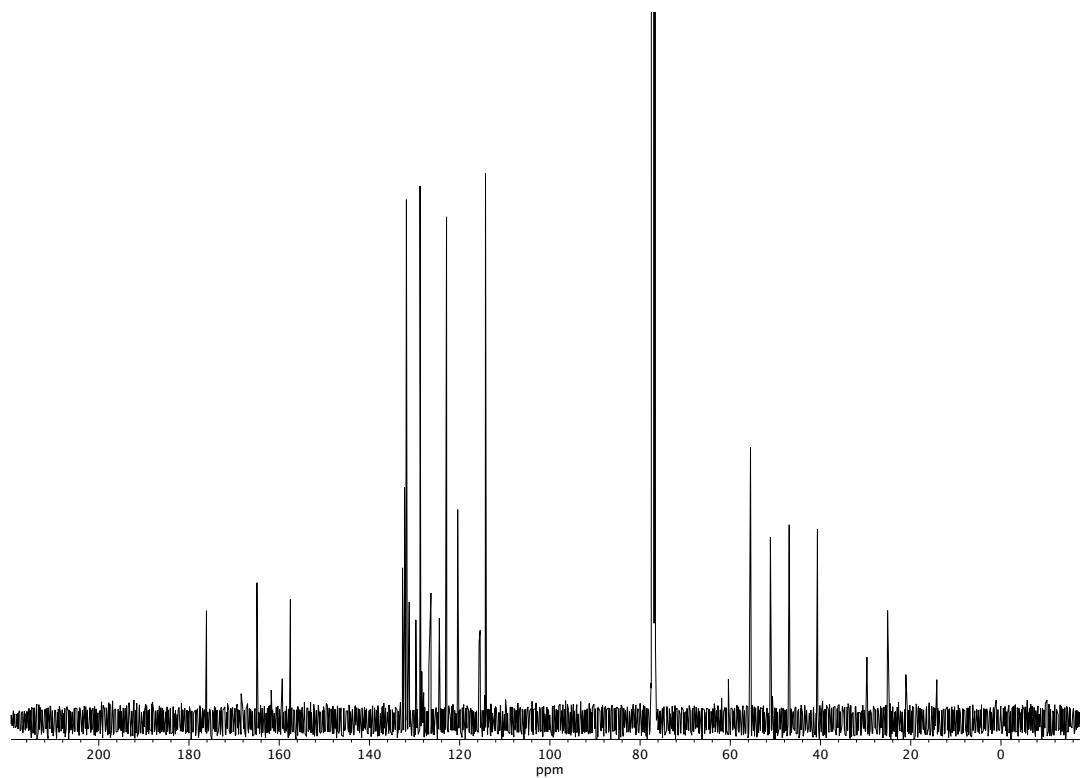


**Figure A1.174** <sup>13</sup>C NMR (100 MHz, CDCl<sub>3</sub>) of compound **80**.

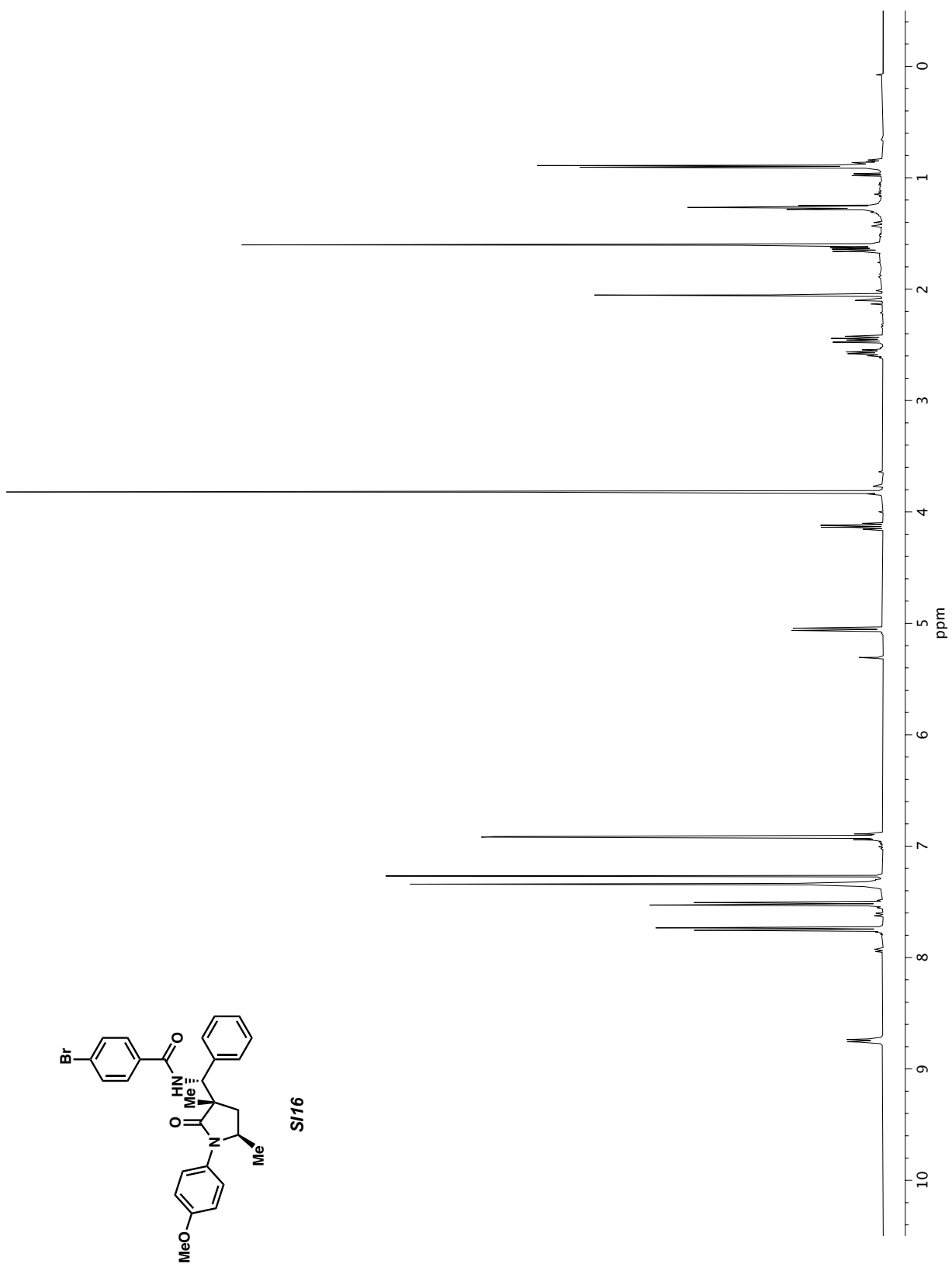


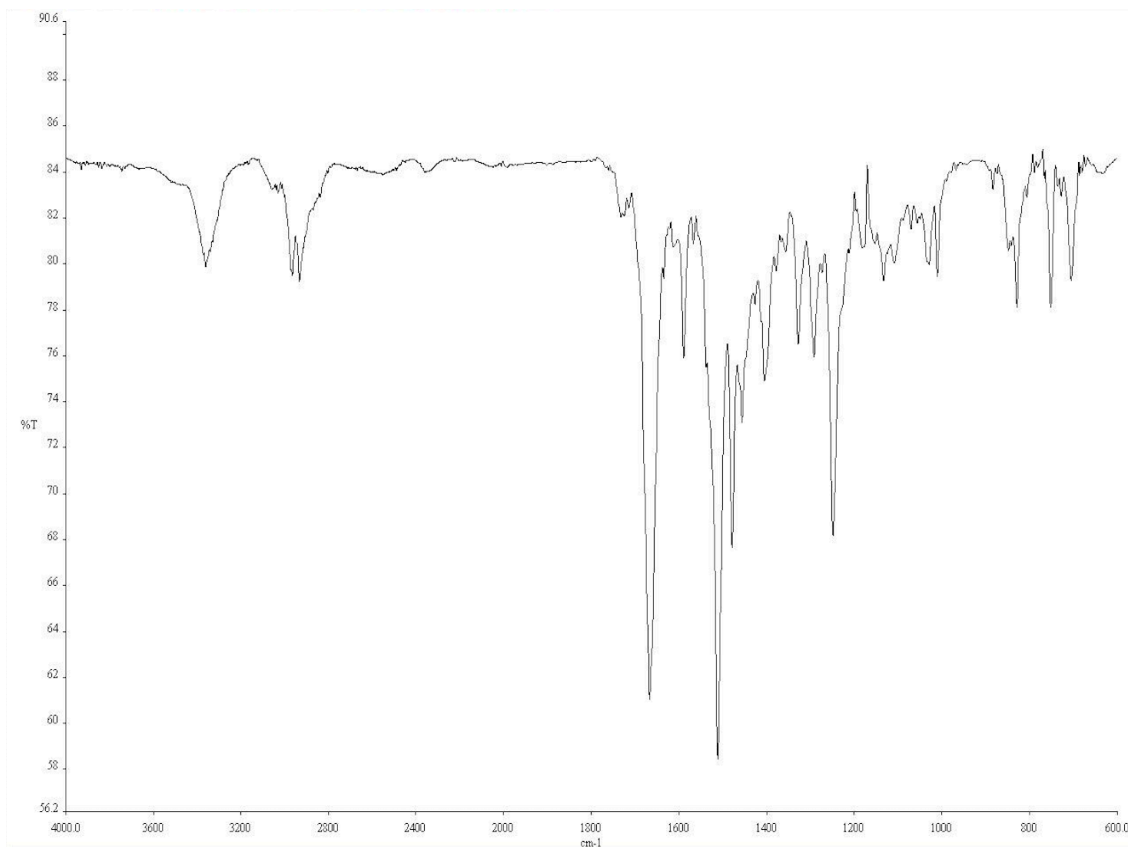


**Figure A1.176** Infrared spectrum (Thin Film, NaCl) of compound **SI17**.

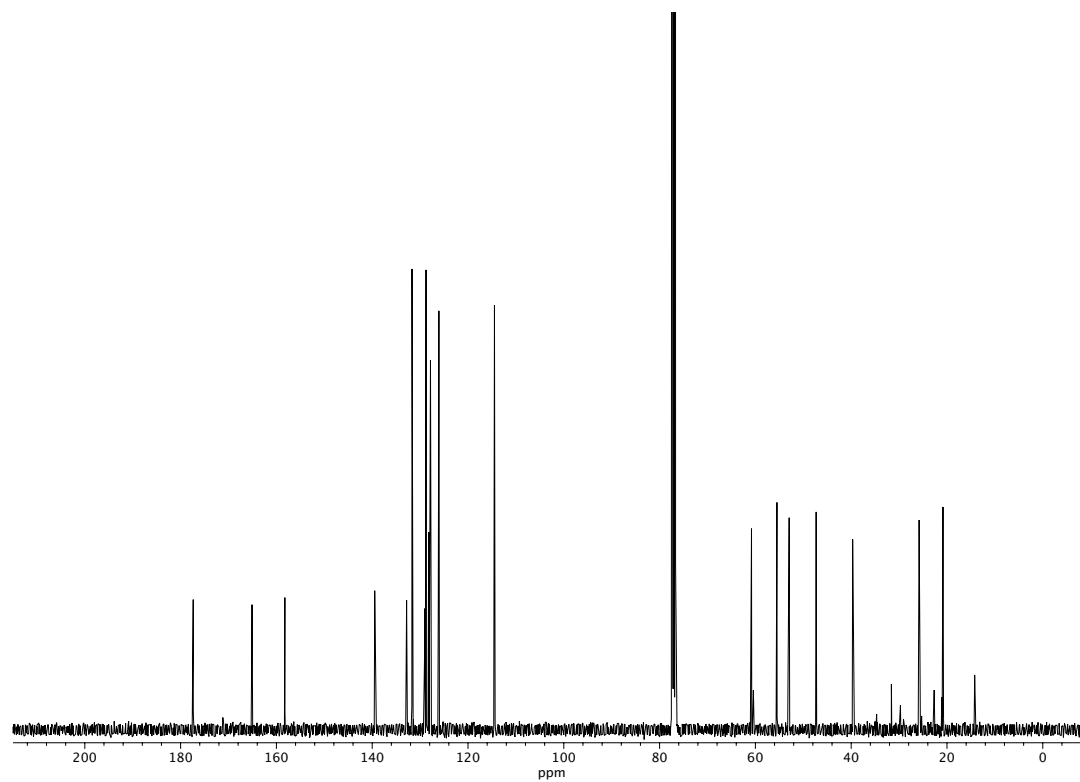


**Figure A1.177** <sup>13</sup>C NMR (100 MHz, CDCl<sub>3</sub>) of compound **SI17**.



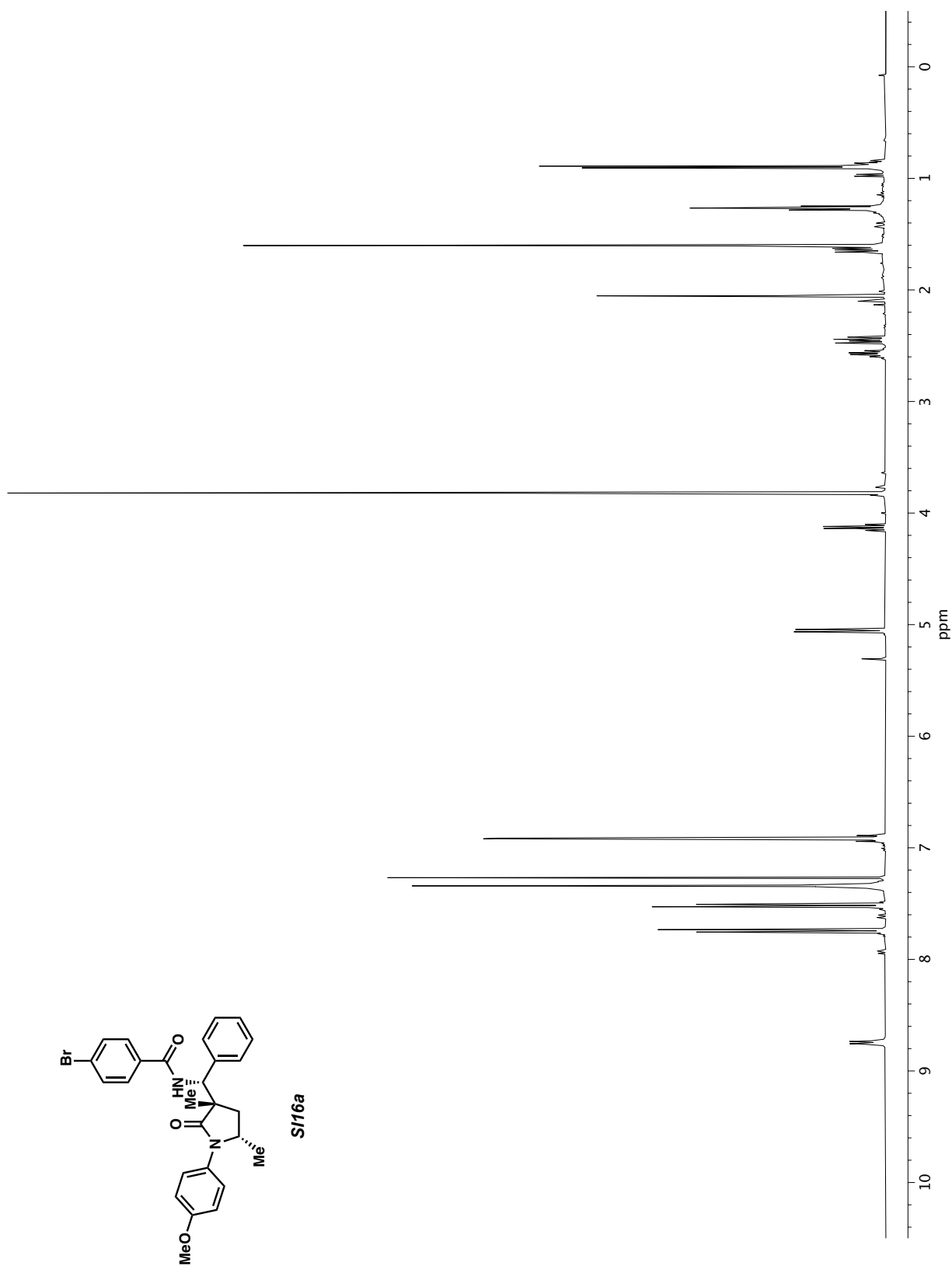


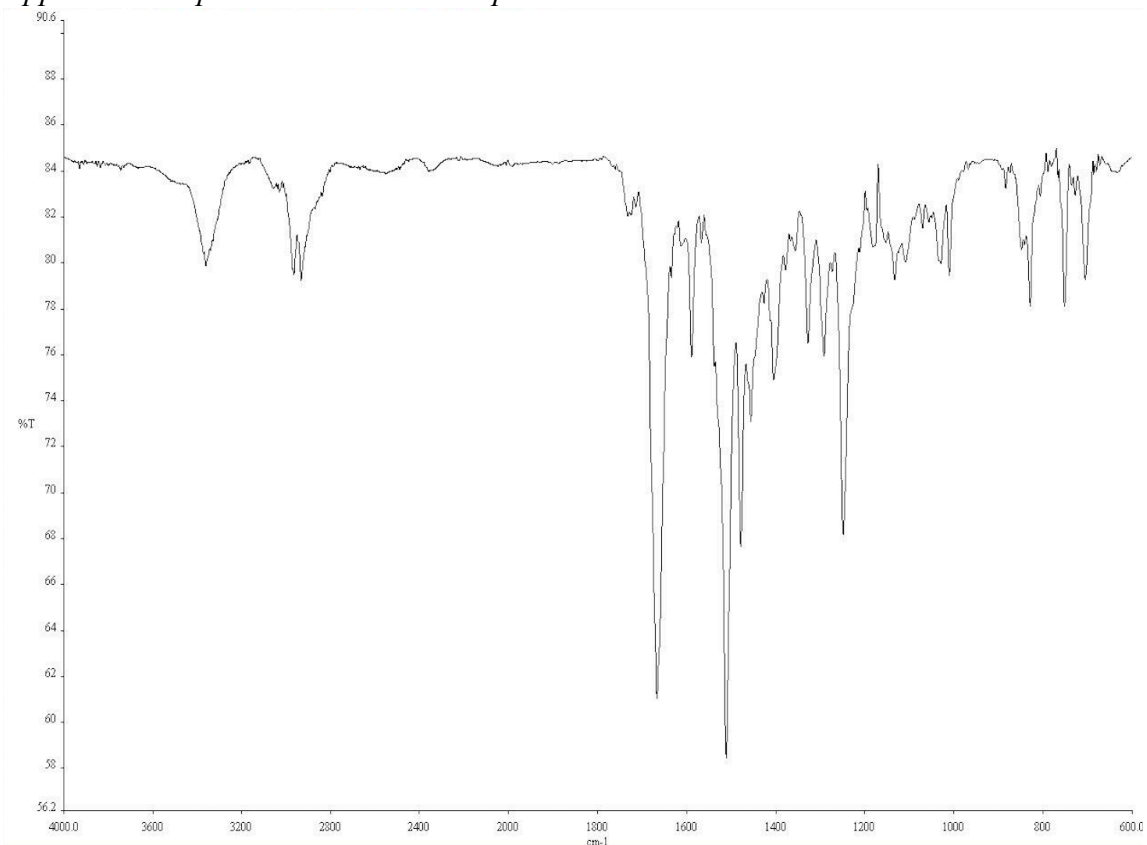
**Figure A1.179** Infrared spectrum (Thin Film, NaCl) of compound **SI16**.



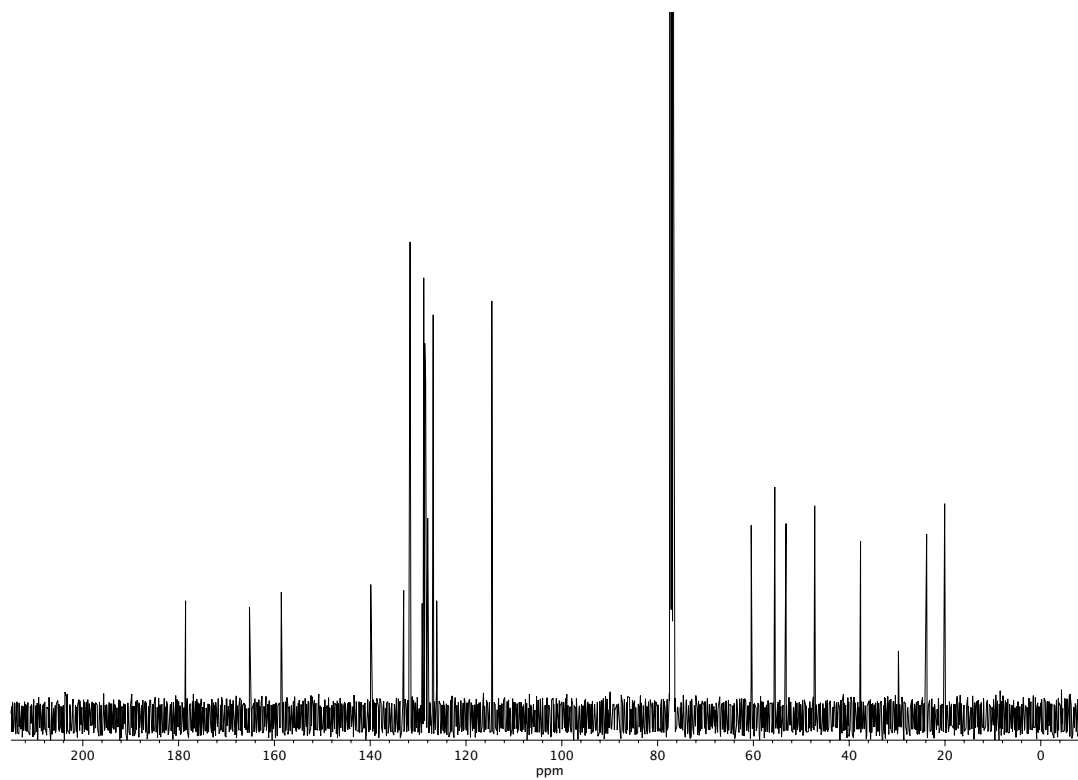
**Figure A1.180** <sup>13</sup>C NMR (100 MHz, CDCl<sub>3</sub>) of compound **SI16**.



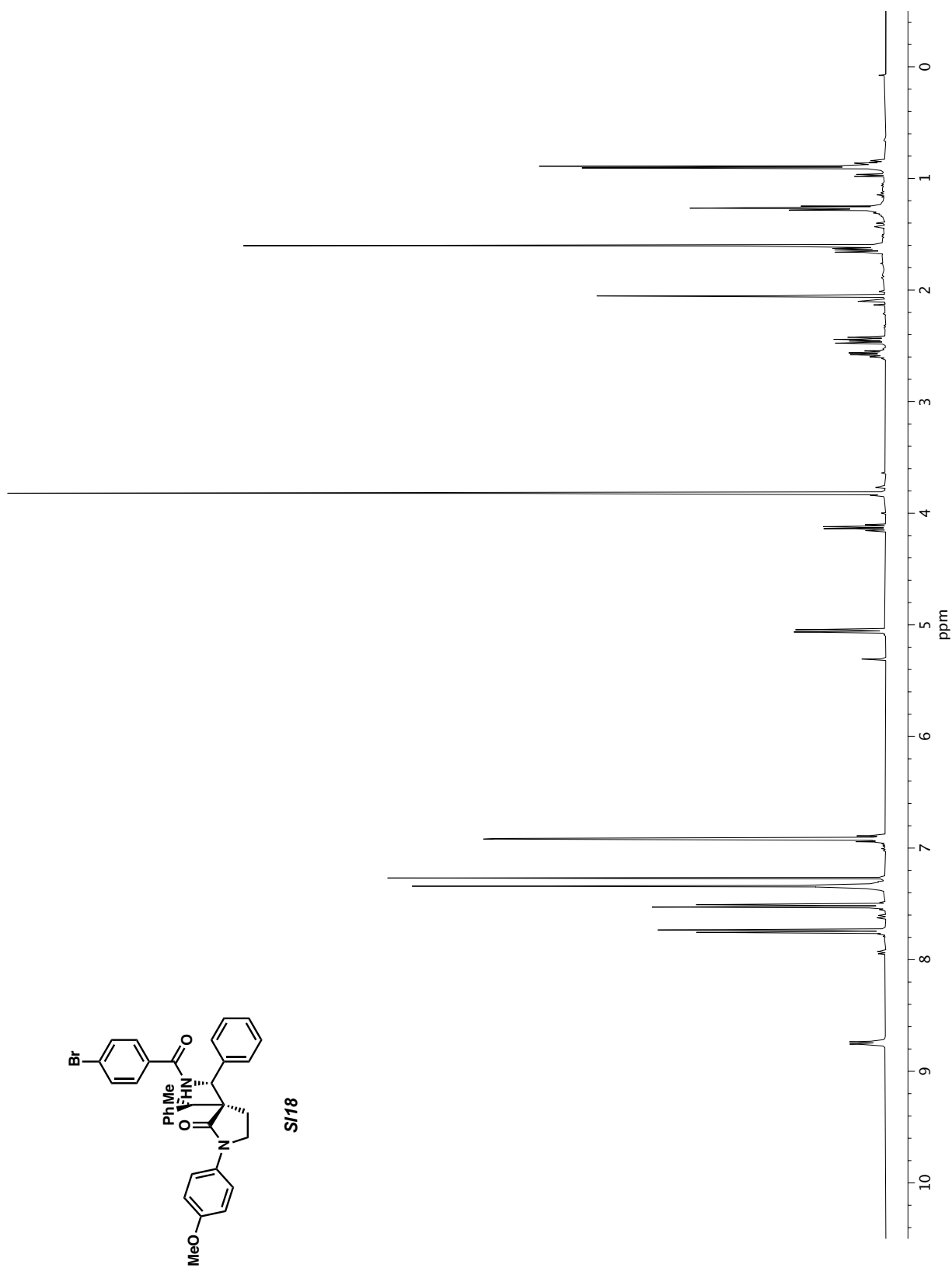


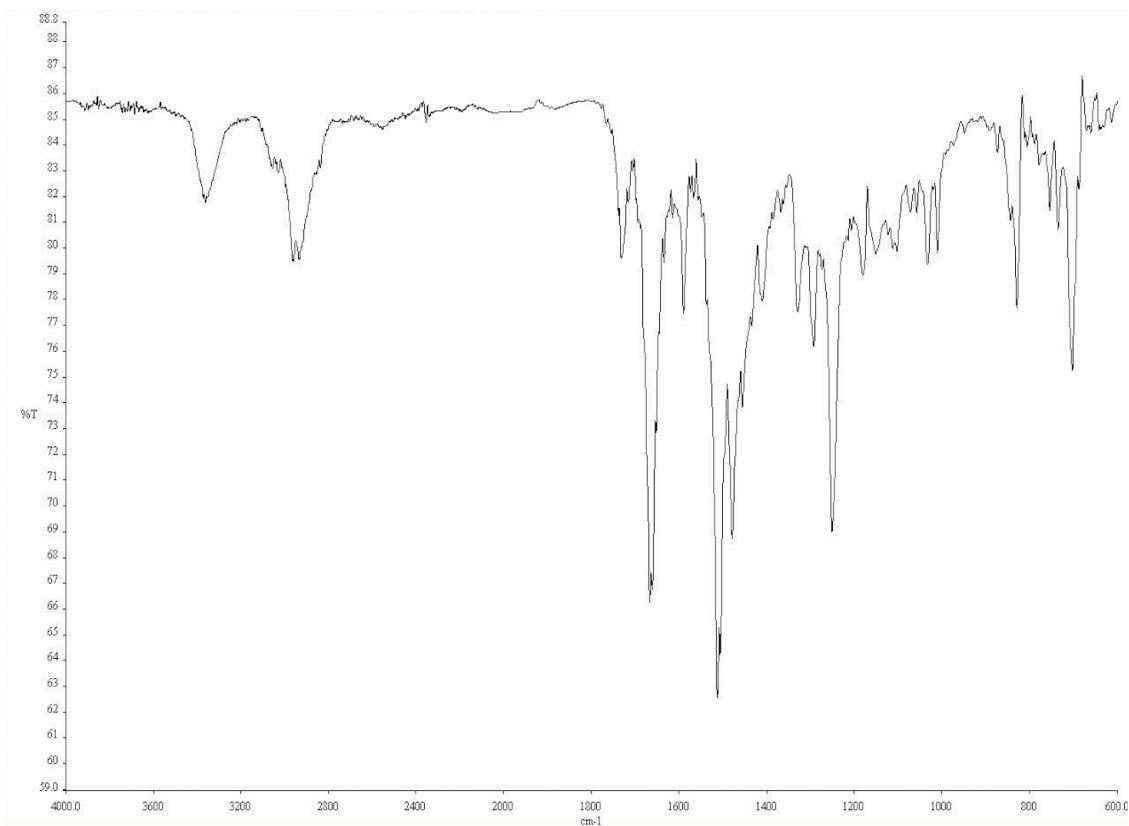


**Figure A1.182** Infrared spectrum (Thin Film, NaCl) of compound **S116a**.

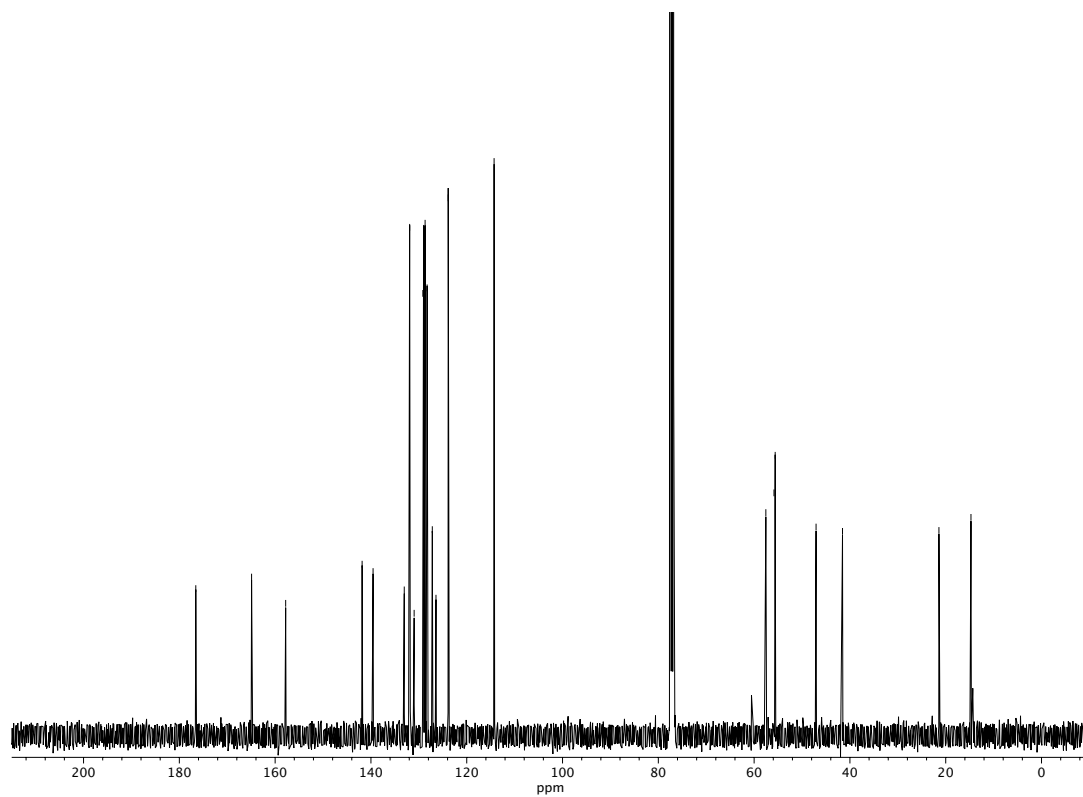


**Figure A1.183** <sup>13</sup>C NMR (100 MHz, CDCl<sub>3</sub>) of compound **S116a**.

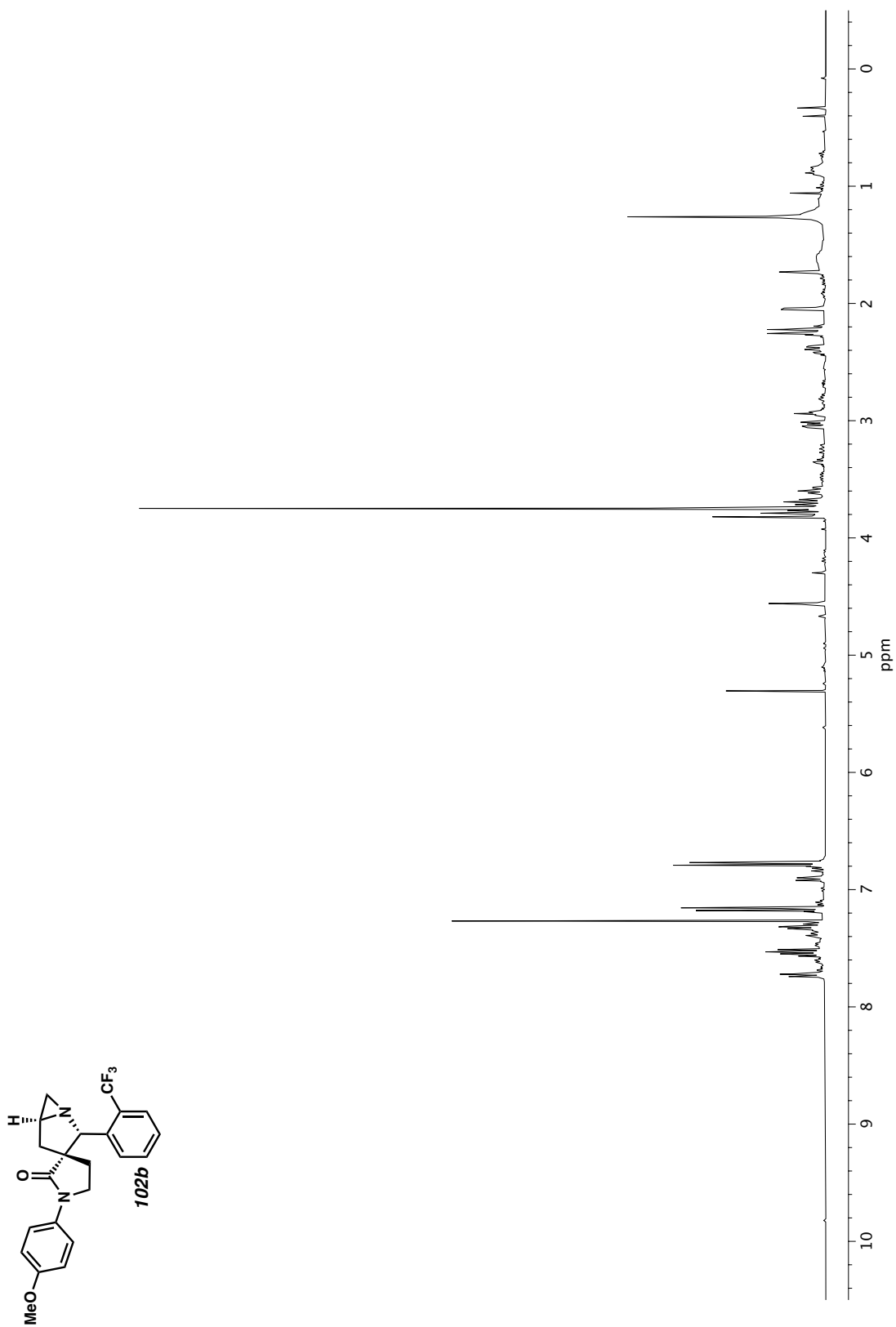
Figure A1.184  $^1\text{H}$  NMR (400 MHz,  $\text{CDCl}_3$ ) of compound **SI18**.



**Figure A1.185** Infrared spectrum (Thin Film, NaCl) of compound **SI18**.



**Figure A1.186**  $^{13}\text{C}$  NMR (100 MHz,  $\text{CDCl}_3$ ) of compound **SI18**.



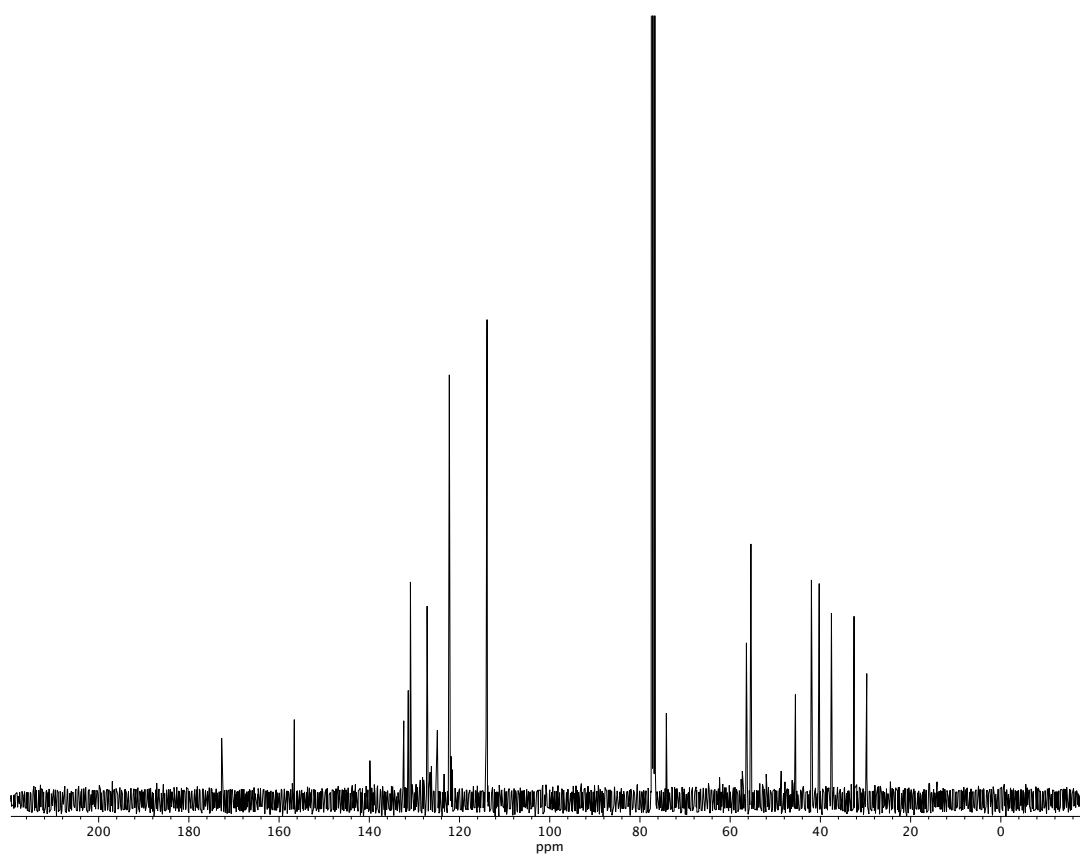


**Figure A1.188**  $^{13}\text{C}$  NMR (100 MHz,  $\text{CDCl}_3$ ) of compound **102b**.

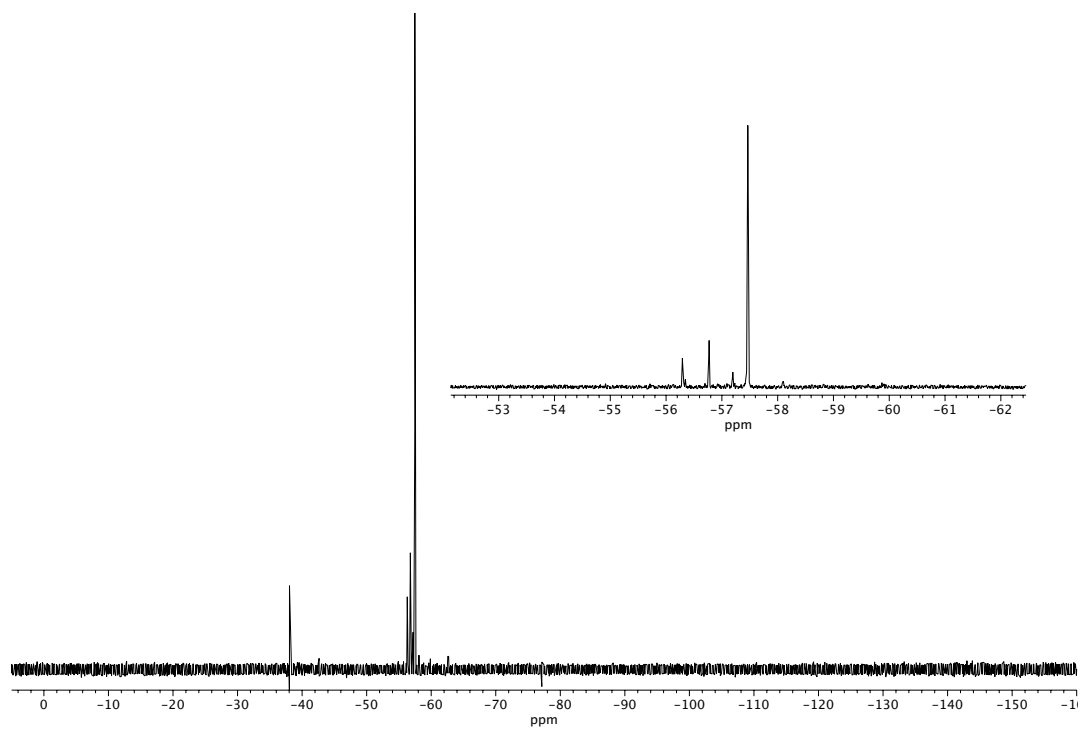


**Figure A1.189**  $^{19}\text{F}$  NMR (282 MHz,  $\text{CDCl}_3$ ) of compound **102b**

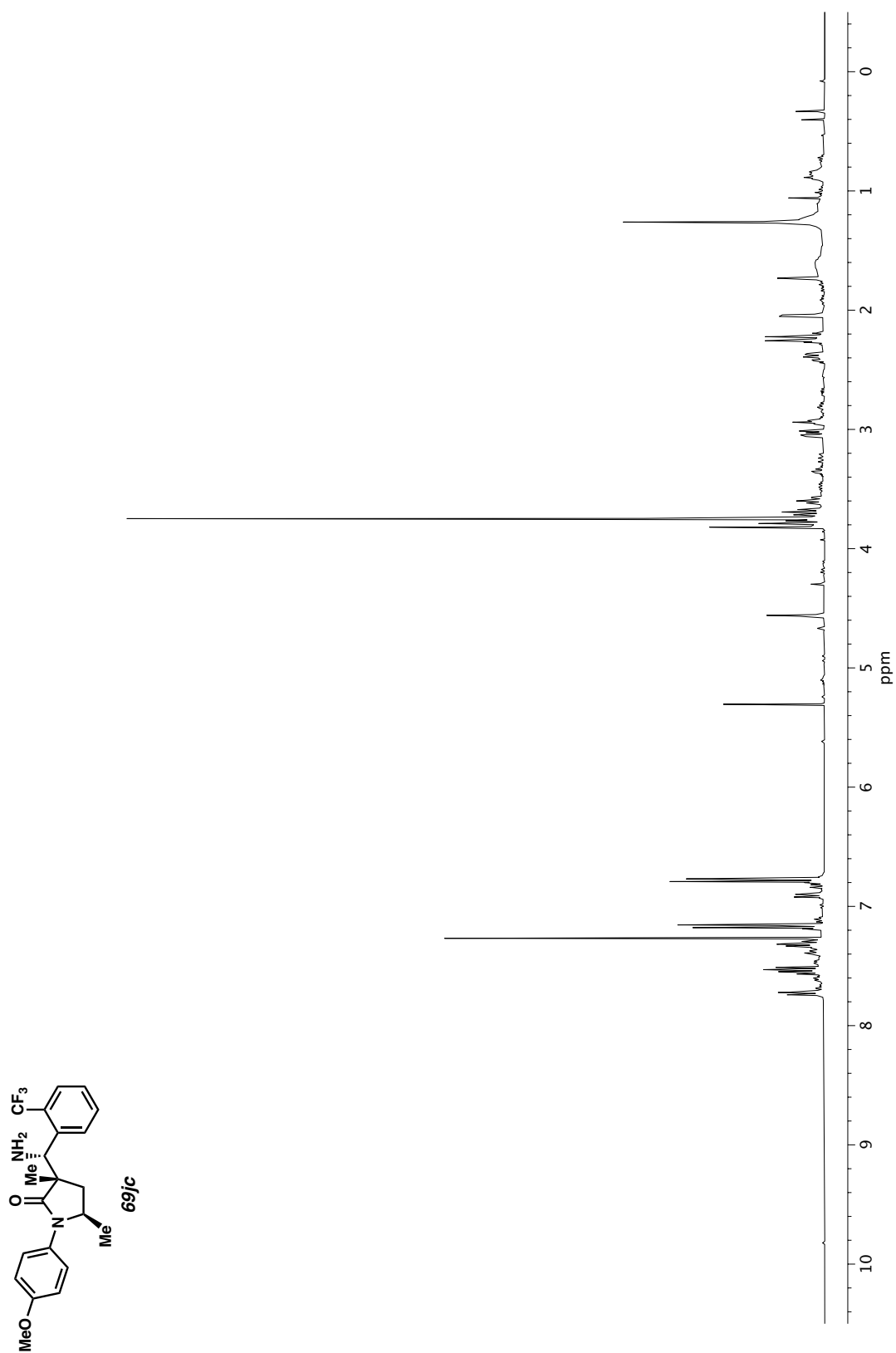


**Figure A1.190**  $^1\text{H}$  NMR (400 MHz,  $\text{CDCl}_3$ ) of compound **69jc**.



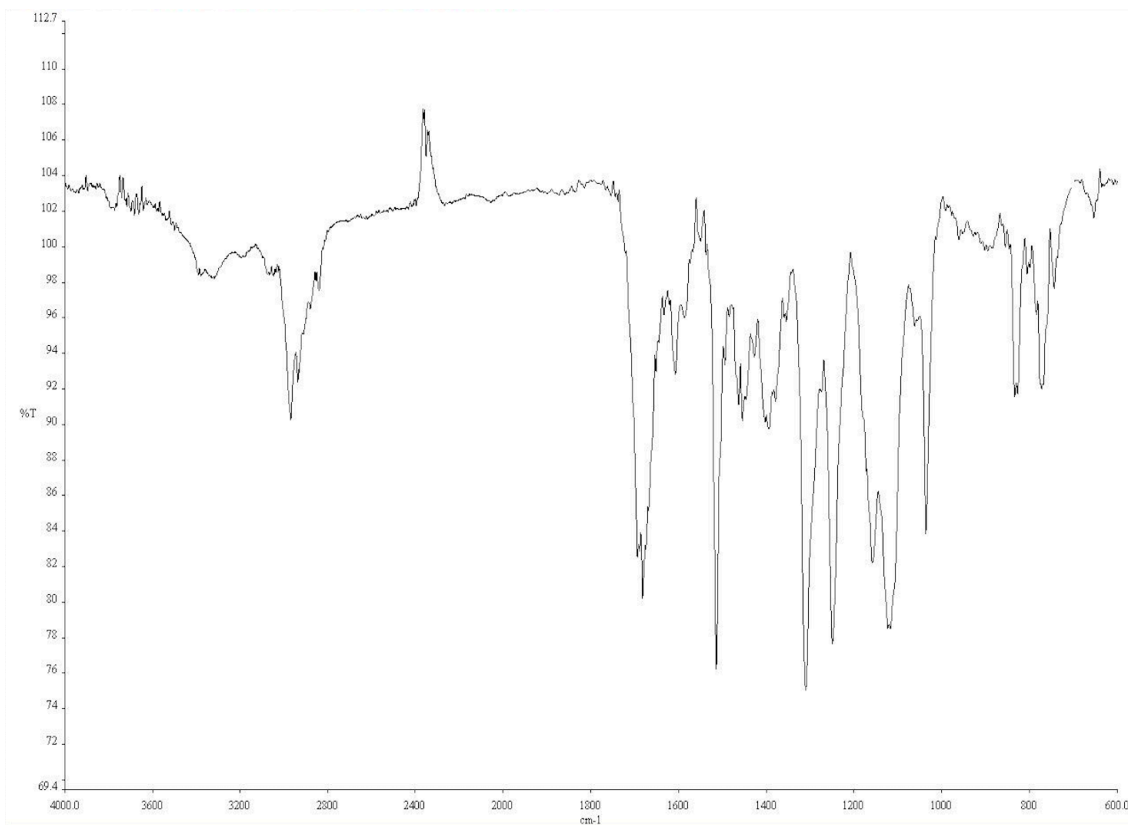


**Figure A1.191** Infrared spectrum (Thin Film, NaCl) of compound **69jc**.

## **APPENDIX 2**

*Computational Reports for Chapter 1:*

*Diastereoselective Direct Mannich Reaction of  $\alpha$ -Substituted- $\gamma$ -lactams  
and aryl N-silyl imines*

## A2.1 COMPUTATIONAL ANALYSIS OF POTASSIUM *TERT*-BUTOXIDE PROMOTED DIASTEREOSELECTIVE MANNICH REACTION

### Contents

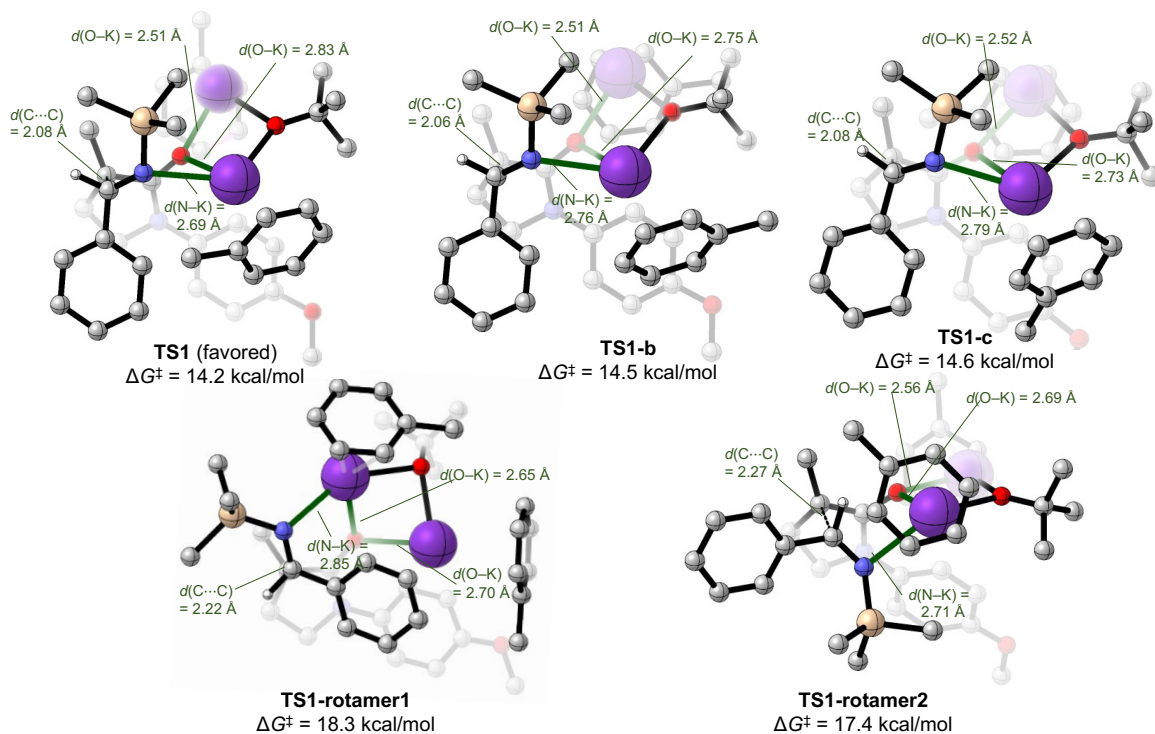
Table A2.1.1. Computational Details

Table A2.1.2. Cartesian Coordinates and Energies

Table A2.1.3. Computed Cartesian Coordinates

### **Table A2.1.1.** Computational Details for the Diastereoselective Mannich Reaction

All density functional theory (DFT) calculations were carried out using *Gaussian 16*<sup>1</sup> software on Pitt CRC and the Expanse and Bridges-2 supercomputers through allocation from the Advanced Cyberinfrastructure Coordination Ecosystem: Services & Support (ACCESS) program. A thorough conformational analysis was carried out for transition states **TS1** and **TS2** using the CREST/xTB<sup>2</sup> package. During the TS conformational sampling, forming C–C bond distances and distances between oxygen atom of the enolate and potassium atoms were constrained. Low-energy conformers from CREST conformational search were then fully optimized at the M06-2X/6-31G(d)<sup>3</sup> level of theory. Vibrational frequency calculations were performed at the M06-2X/6-31G(d) level of theory to confirm whether the optimized structure is a local minimum or a transition state. Single point energies and natural population analysis (NPA) charges were calculated at the M06-2X/6-311G++(d,p) level of theory using SMD<sup>4</sup> solvation model and toluene as solvent.



**Figure A2.1.1.** Optimized structures of representative low-energy conformers of TS1 that lead to the major diastereomeric product **69aa**. Gibbs free energies are with respect to lactam **68a**,  $[\text{KO}^t\text{Bu}]_2$ , and imine **65**. The three lowest-energy conformers (TS1, TS1-b, and TS1-c) and two other representative rotamers about the forming C–C bonds (TS1-rotamer1 and TS1-rotamer2) are shown.

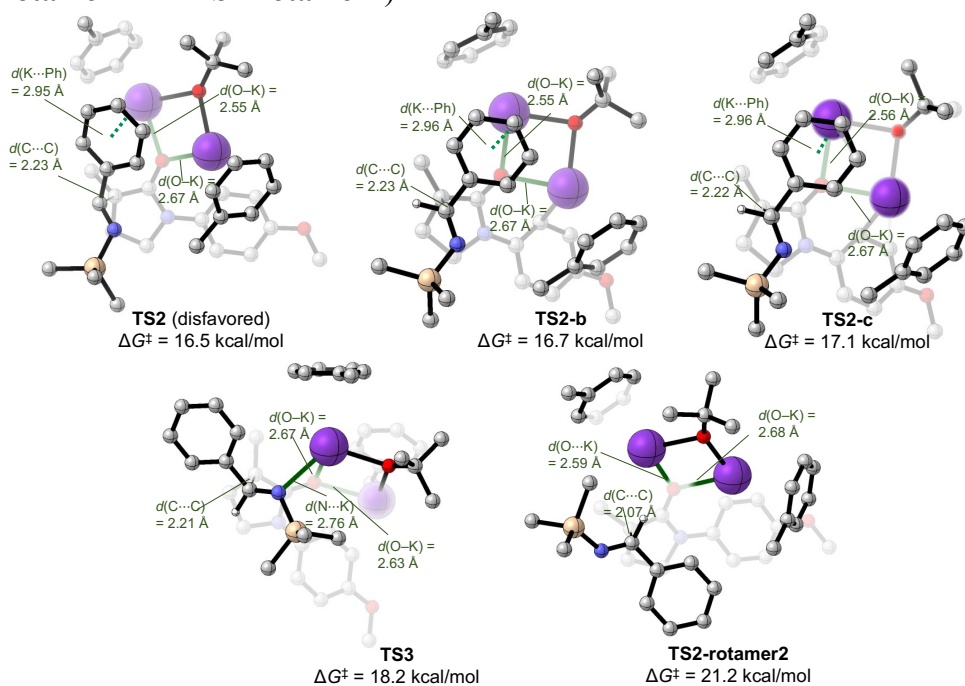


**Figure A2.1.2.** Optimized structures of representative low-energy conformers of TS2 that lead to the minor diastereomeric product **69aa-ent**. Gibbs free energies are with

respect to lactam **68a**, [KO<sup>t</sup>Bu]<sub>2</sub>, and imine **65**. The three lowest-energy conformers (TS2, TS2-b, and TS2-c) and two other representative rotamers about the forming C–C bonds (TS2-rotamer1 and TS2-rotamer2) are shown.

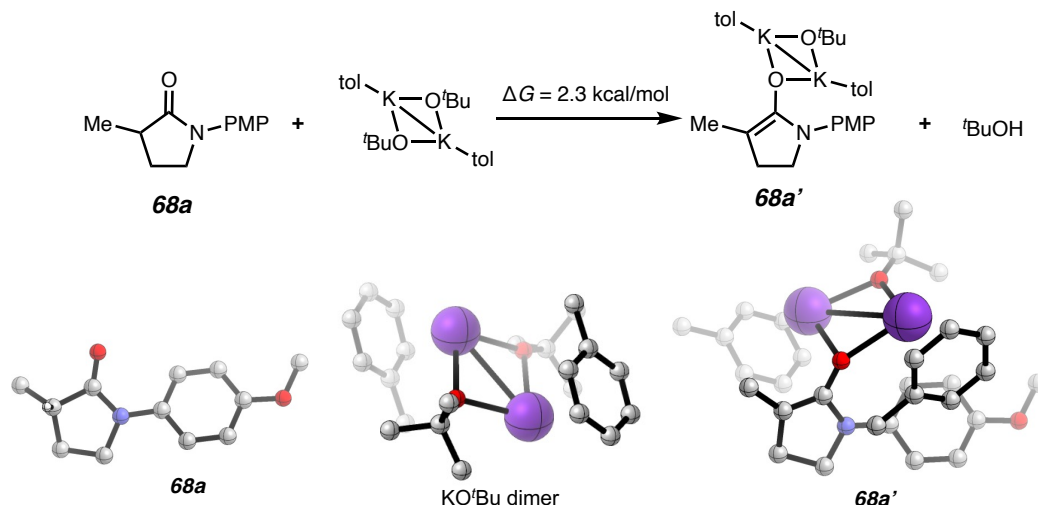


**Figure A2.1.3.** Computed Gibbs free energy of the deprotonation of lactam **68a** with [KO<sup>t</sup>Bu]<sub>2</sub> to give potassium enolate **68a'**.

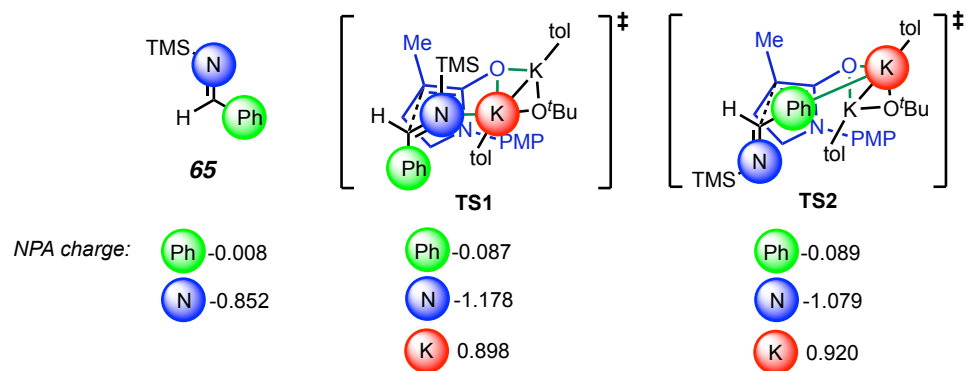


**Figure A2.1.4.** Computed NPA charges for **TS1**, **65**, and **TS2**. The imine N becomes more negatively charged in the TS, promoting the N–K interaction in **TS1**, whereas a much smaller increase of negative charge was observed for the Ph group on the imine.

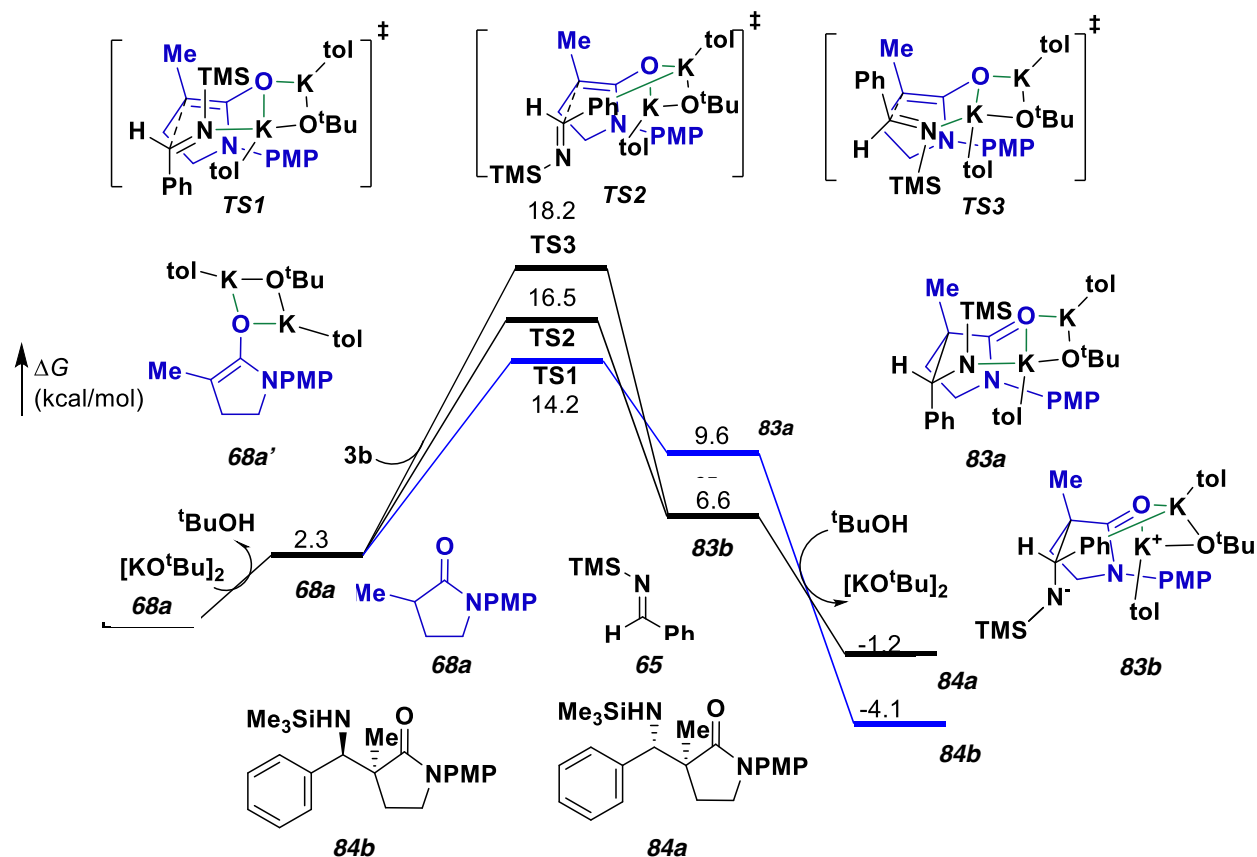


**Figure A2.1.5.** Calculated reaction energy profile of the imine addition pathways involving **68a** and **65**.

**Table A2.1.2.** Cartesian Coordinates and Energies of All Optimized Structures and Imaginary Frequencies of Transition States

Compound	M06-2X/6-31G(d) (gas)			M06-2X/6-311++G(d,p)/SMD(toluene)//M06-2X/6-31G(d)			Imaginary frequency (cm <sup>-1</sup> )
	E (a.u.)	H (a.u.)	G (a.u.)	E (a.u.)	H (a.u.)	G (a.u.)	
<b>68a</b>	-671.23376	-670.9625	-671.0177	-671.4360	-671.1648	-671.2200	
<b>KOt-Bu dimer</b>	-2208.6855	-2208.1371	-2208.2373	-2209.0839	-2208.5356	-2208.6357	
<b>68a'</b>	-2646.3614	-2645.6881	-2645.8074	-2646.8772	-2646.2038	-2646.3231	
<i>t</i> -BuOH	-233.5506	-233.4054	-233.4418	-233.6377	-233.4925	-233.5289	
<b>65</b>	-734.1366	-733.8949	-733.9516	-734.2983	-734.0566	-734.1133	
<b>TS1</b>	-3380.5195	-3379.6031	-3379.7511	-3381.1859	-3380.2695	-3380.4175	-258
<b>TS1-b</b>	-3380.5211	-3379.6046	-3379.7503	-3381.1879	-3380.2714	-3380.4170	-265
<b>TS1-c</b>	-3380.5191	-3379.6028	-3379.7503	-3381.1856	-3380.2693	-3380.4168	-260
<b>TS1-rotamer1</b>	-3380.5186	-3379.6028	-3379.7478	-3381.1818	-3380.2660	-3380.4110	-178

TS1-rotamer2	-3380.5069	-3379.5910	-3379.7435	-3381.1758	-3380.2599	-3380.4124	-167
TS2	-3380.5093	-3379.5937	-3379.7452	-3381.1780	-3380.2624	-3380.4138	-194
TS2-b	-3380.5093	-3379.5936	-3379.7449	-3381.1779	-3380.2623	-3380.4135	-191
TS2-c	-3380.5090	-3379.5933	-3379.7439	-3381.1780	-3380.2622	-3380.4128	-196
TS2-rotamer1	-3380.5099	-3379.5942	-3379.7430	-3381.1780	-3380.2623	-3380.4112	-221
TS2-rotamer2	-3380.5001	-3379.5841	-3379.7349	-3381.1715	-3380.2555	-3380.4063	-257

**Table A2.1.3.** Computed Cartesian Coordinates of Compounds**Compound 68a**

C -1.0651 0.9094 -0.0929  
 C -0.5310 0.2657 1.1852  
 O -1.7034 1.9415 -0.1440  
 C 0.5519 -0.6795 0.6651  
 H 1.4970 -0.1330 0.5715  
 H 0.7208 -1.5482 1.3048  
 C 0.0459 -1.0703 -0.7272  
 H 0.8568 -1.2766 -1.4316  
 H -0.6070 -1.9536 -0.6880  
 N -0.7047 0.1071 -1.1556  
 C -0.0922 1.3062 2.2032  
 H -0.9114 2.0009 2.4025  
 H 0.2116 0.8348 3.1420  
 H 0.7537 1.8849 1.8181  
 C -1.1322 0.2632 -2.4938  
 C -1.0584 -0.8275 -3.3723  
 C -1.6141 1.4821 -2.9785  
 C -1.4533 -0.7015 -4.6939  
 H -0.6985 -1.7898 -3.0251  
 C -2.0163 1.6054 -4.3065  
 H -1.6840 2.3312 -2.3137  
 C -1.9374 0.5165 -5.1741  
 H -1.3986 -1.5430 -5.3763  
 H -2.3864 2.5651 -4.6476  
 O -2.3015 0.5402 -6.4856  
 C -2.7957 1.7574 -6.9953  
 H -2.0456 2.5548 -6.9240  
 H -3.0305 1.5748 -8.0439  
 H -3.7048 2.0720 -6.4681  
 H -1.3644 -0.3228 1.5962

**KOt-Bu dimer**

K 0.3226 3.3884 0.5853  
 K -0.6717 0.3096 -0.8138  
 O -1.7717 2.0664 0.6342  
 O 1.3808 1.7738 -0.9721

**Table A2.1.3. Cont.**

C	-3.0017	1.7968	1.1859
C	-3.7383	0.7027	0.3764
H	-3.1759	-0.2422	0.4213
H	-4.7496	0.4963	0.7473
H	-3.8165	1.0154	-0.6736
C	-2.8616	1.2996	2.6389
H	-2.3249	2.0513	3.2299
H	-3.8286	1.1054	3.1198
H	-2.2760	0.3735	2.6576
C	-3.8915	3.0561	1.2007
H	-4.0253	3.4314	0.1791
H	-4.8829	2.8725	1.6331
H	-3.3976	3.8370	1.7917
C	2.2489	1.6155	-2.0256
C	3.6670	1.2721	-1.5276
H	4.3946	1.1776	-2.3431
H	4.0103	2.0566	-0.8426
H	3.6488	0.3270	-0.9717
C	2.3286	2.9039	-2.8682
H	3.0310	2.8281	-3.7077
H	1.3337	3.1337	-3.2687
H	2.6398	3.7384	-2.2271
C	1.7836	0.4744	-2.9623
H	1.7139	-0.4661	-2.3981
H	0.7919	0.7126	-3.3738
H	2.4609	0.3080	-3.8088
C	0.0848	-1.0463	1.9399
C	1.3137	-0.9372	1.2827
C	1.5523	-1.7747	0.1847
C	0.5863	-2.6783	-0.2538
C	-0.6432	-2.7665	0.4042
C	-0.8872	-1.9505	1.5083
H	-0.1212	-0.4013	2.7897
H	2.5036	-1.7047	-0.3371
H	0.7936	-3.3166	-1.1081
H	-1.3958	-3.4731	0.0677
H	-1.8369	-2.0102	2.0326
C	0.8639	6.2940	-0.9635
C	0.4463	6.8015	0.2656
C	-0.8457	6.5228	0.7187
C	-1.6987	5.7269	-0.0421
C	-1.2812	5.1880	-1.2668
C	0.0028	5.4996	-1.7230
H	1.8614	6.5107	-1.3344
H	1.1131	7.4203	0.8586
H	-1.1879	6.9254	1.6678
H	-2.6931	5.4917	0.3252
H	0.3456	5.0922	-2.6691
C	2.3193	0.1108	1.6743
H	2.2783	0.9101	0.9192



**Table A2.1.3. Cont.**

H	2.0993	0.5203	2.6649
H	3.3366	-0.2930	1.6847
C	-2.1583	4.2045	-1.9956
H	-3.1753	4.5901	-2.1202
H	-1.7525	3.9642	-2.9823
H	-2.2164	3.2882	-1.3887

**Compound 68a'**

K	-0.6232	3.6995	-1.2400
K	0.9879	0.5343	0.0379
O	0.3071	1.5704	-2.1180
C	0.3084	0.9650	-3.3503
C	1.3650	1.6016	-4.2736
H	1.4102	1.1317	-5.2639
H	1.1400	2.6671	-4.4076
H	2.3526	1.5250	-3.8046
C	-1.0758	1.0964	-4.0204
H	-1.1185	0.6454	-5.0198
H	-1.8311	0.6136	-3.3885
H	-1.3363	2.1603	-4.1167
C	0.6201	-0.5420	-3.2148
H	1.6134	-0.6777	-2.7629
H	-0.1260	-1.0027	-2.5541
H	0.6106	-1.0775	-4.1722
C	-0.9390	1.9015	1.9529
C	-0.4327	1.6019	3.1860
O	-0.4063	2.4755	0.9396
C	-1.4816	0.9323	4.0317
H	-1.3469	-0.1617	4.1261
H	-1.5350	1.3212	5.0560
C	-2.7724	1.2523	3.2566
H	-3.5334	0.4663	3.3138
H	-3.2116	2.1863	3.6480
N	-2.3141	1.4334	1.8858
C	0.9641	1.8934	3.6199
H	1.4734	2.4799	2.8455
H	1.0066	2.4740	4.5525
H	1.5675	0.9857	3.8016
C	-3.1953	1.7945	0.8707
C	-4.5241	2.1677	1.1469
C	-2.8102	1.7290	-0.4806
C	-5.4020	2.5209	0.1285
H	-4.8791	2.1878	2.1720
C	-3.6803	2.1144	-1.4981
H	-1.8185	1.3773	-0.7574
C	-4.9815	2.5276	-1.2009
H	-6.4249	2.8088	0.3505
H	-3.3332	2.0518	-2.5242

**Table A2.1.3. Cont.**

O	-5.8976	2.9325	-2.1313
C	-5.5114	2.8510	-3.4828
H	-5.2572	1.8221	-3.7671
H	-6.3680	3.1881	-4.0667
H	-4.6501	3.4988	-3.6961
C	-0.6665	-1.5683	1.5935
C	0.4991	-1.5557	2.3612
C	1.6889	-2.1085	1.8759
C	1.6879	-2.6666	0.5904
C	0.5265	-2.6872	-0.1804
C	-0.6562	-2.1377	0.3202
H	-1.5688	-1.0962	1.9735
H	0.4854	-1.0930	3.3448
H	2.6060	-3.0944	0.1941
H	0.5471	-3.1191	-1.1764
H	-1.5578	-2.1362	-0.2852
C	2.9335	-2.1286	2.7282
H	2.9693	-3.0405	3.3343
H	3.8391	-2.1059	2.1152
H	2.9585	-1.2768	3.4136
C	-3.0391	5.7940	-1.2717
C	-3.0251	5.2696	0.0218
C	-1.9748	5.5468	0.9030
C	-0.9339	6.3707	0.4522
C	-0.9419	6.8995	-0.8380
C	-1.9963	6.6106	-1.7093
H	-3.8694	5.5559	-1.9316
H	-3.8329	4.6186	0.3449
H	-0.1074	6.5950	1.1227
H	-0.1283	7.5413	-1.1642
H	-2.0059	7.0262	-2.7126
C	-1.9571	4.9685	2.2929
H	-0.9993	4.4855	2.5071
H	-2.1307	5.7499	3.0413
H	-2.7366	4.2085	2.4011

***t*-BuOH**

O	1.0016	1.9025	-1.3929
C	2.0915	2.0588	-2.2994
C	3.2821	2.6831	-1.5709
H	4.1195	2.8573	-2.2541
H	2.9882	3.6368	-1.1234
H	3.6346	2.0209	-0.7707
C	1.5721	2.9938	-3.3843
H	2.3429	3.1795	-4.1381
H	0.6993	2.5509	-3.8722
H	1.2722	3.9481	-2.9422
C	2.4690	0.7002	-2.8906

**Table A2.1.3. Cont.**

H	2.8142	0.0196	-2.1027
H	1.5991	0.2497	-3.3770
H	3.2740	0.7963	-3.6261
H	1.2953	1.3123	-0.6833

**Compound 65**

C	-3.3042	-0.9405	0.6638
H	-3.0568	-1.2307	1.7025
Si	-4.7203	1.1377	1.5926
N	-4.0212	0.0668	0.3818
C	-2.7211	-1.8360	-0.3607
C	-2.9412	-1.6014	-1.7217
C	-1.9443	-2.9255	0.0358
C	-2.3882	-2.4502	-2.6705
H	-3.5489	-0.7474	-2.0044
C	-1.3894	-3.7772	-0.9153
H	-1.7758	-3.1040	1.0956
C	-1.6117	-3.5391	-2.2687
H	-2.5591	-2.2678	-3.7270
H	-0.7860	-4.6235	-0.6021
H	-1.1804	-4.2013	-3.0133
C	-4.2756	0.6134	3.3476
H	-4.6434	-0.3917	3.5801
H	-3.1933	0.6237	3.5160
H	-4.7267	1.3031	4.0693
C	-6.5808	1.0887	1.3589
H	-6.8472	1.3670	0.3348
H	-6.9768	0.0859	1.5477
H	-7.0816	1.7832	2.0419
C	-4.0599	2.8594	1.2491
H	-4.5057	3.5942	1.9279
H	-2.9735	2.8989	1.3759
H	-4.2889	3.1614	0.2227

**TS1**

C	0.8293	1.1922	1.1914
C	0.4804	2.1196	2.2225
C	-1.5561	2.1840	1.7838
H	-1.7376	2.6247	2.7800
O	0.5957	-0.0283	1.1839
Si	-2.7543	-0.0902	2.6198
N	-2.0657	0.9886	1.4830
C	1.2524	3.3881	1.9252
H	0.7086	4.3102	2.1582
H	2.1877	3.4128	2.5070

**Table A2.1.3. Cont.**

C	1.5533	3.2975	0.4173
H	0.8417	3.9021	-0.1543
H	2.5668	3.6248	0.1591
N	1.3948	1.8731	0.1049
C	0.4525	1.6156	3.6371
H	-0.0924	0.6681	3.6872
H	1.4626	1.4453	4.0431
H	-0.0478	2.3286	4.3042
K	-1.3302	-0.9391	-0.4595
K	1.3925	-2.2538	2.0216
C	-1.5595	3.2390	0.7204
C	-1.5253	2.8973	-0.6342
C	-1.5976	4.5944	1.0625
C	-1.4817	3.8791	-1.6177
H	-1.5198	1.8459	-0.9063
C	-1.5592	5.5831	0.0820
H	-1.6576	4.8728	2.1126
C	-1.4907	5.2288	-1.2638
H	-1.4256	3.5930	-2.6654
H	-1.5879	6.6305	0.3681
H	-1.4575	5.9969	-2.0306
C	1.4150	1.4037	-1.2213
C	1.4610	2.3166	-2.2806
C	1.3891	0.0276	-1.5426
C	1.4069	1.8983	-3.6111
H	1.5048	3.3808	-2.0808
C	1.3251	-0.3833	-2.8647
H	1.3813	-0.7336	-0.7702
C	1.3156	0.5426	-3.9109
H	1.4282	2.6483	-4.3936
H	1.2790	-1.4428	-3.1000
C	-4.3256	-0.8127	1.8520
H	-5.0204	-0.0189	1.5565
H	-4.0901	-1.3973	0.9528
H	-4.8435	-1.4833	2.5474
C	-3.2061	0.7025	4.2772
H	-3.8998	1.5386	4.1348
H	-3.6945	-0.0278	4.9320
H	-2.3272	1.0870	4.8060
C	-1.6892	-1.6253	3.0056
H	-2.2740	-2.3381	3.6005
H	-1.3628	-2.1493	2.0961
H	-0.8055	-1.3502	3.5946
O	0.1607	-2.9033	-0.0105
C	0.2514	-4.1644	-0.5434
C	1.1632	-5.0648	0.3248
H	1.2634	-6.0859	-0.0625
H	2.1712	-4.6268	0.3778
H	0.7528	-5.1324	1.3426
C	-1.1411	-4.8222	-0.6197

**Table A2.1.3. Cont.**

H	-1.1197	-5.8417	-1.0253
H	-1.5852	-4.8511	0.3824
H	-1.7906	-4.2103	-1.2591
C	0.8474	-4.1073	-1.9633
H	0.1926	-3.5004	-2.6018
H	1.8288	-3.6177	-1.9247
H	0.9650	-5.0950	-2.4269
O	1.2005	0.0262	-5.1703
C	1.1791	0.9440	-6.2393
H	0.3281	1.6325	-6.1567
H	2.1079	1.5260	-6.2846
H	1.0785	0.3518	-7.1486
C	3.8041	-0.4378	0.9475
C	3.7289	-0.0062	2.2719
C	4.0684	-0.8705	3.3121
C	4.4964	-2.1792	3.0504
C	4.5559	-2.6038	1.7178
C	4.2139	-1.7418	0.6734
H	3.5204	0.2319	0.1418
H	3.3843	1.0018	2.4892
H	4.0068	-0.5262	4.3422
H	4.8757	-3.6194	1.4957
H	4.2527	-2.0933	-0.3536
C	4.9156	-3.0951	4.1737
H	5.9869	-2.9893	4.3762
H	4.3824	-2.8618	5.0996
H	4.7310	-4.1438	3.9241
C	-2.4928	-1.9765	-3.3976
C	-3.5835	-2.1769	-2.5495
C	-4.2016	-1.0895	-1.9349
C	-3.7419	0.2181	-2.1423
C	-2.6561	0.4039	-3.0078
C	-2.0362	-0.6800	-3.6342
H	-2.0080	-2.8233	-3.8735
H	-3.9524	-3.1820	-2.3670
H	-5.0529	-1.2513	-1.2781
H	-2.2879	1.4110	-3.1922
H	-1.1931	-0.5144	-4.2997
C	-4.3716	1.3707	-1.4039
H	-5.4499	1.2212	-1.2946
H	-3.9328	1.4552	-0.3995
H	-4.1979	2.3192	-1.9193

**TS1-b**

C	-0.8778	-0.8109	-1.5205
C	-0.9867	-0.6827	-2.9431
C	0.0624	1.0851	-3.1236
H	0.1727	0.8972	-4.2069

**Table A2.1.3. Cont.**

O	0.1310	-1.1564	-0.8805
Si	2.7133	0.6306	-2.8143
N	1.1446	1.1272	-2.3464
C	-2.4679	-0.5830	-3.2443
H	-2.7130	0.1026	-4.0621
H	-2.8701	-1.5692	-3.5242
C	-3.0911	-0.0999	-1.9203
H	-3.3094	0.9734	-1.9522
H	-4.0162	-0.6316	-1.6684
N	-2.0644	-0.3839	-0.9123
C	-0.1495	-1.5972	-3.7918
H	0.8837	-1.6012	-3.4323
H	-0.5175	-2.6345	-3.7788
H	-0.1418	-1.2680	-4.8383
K	1.4542	0.8944	0.3893
K	1.5840	-3.0250	-0.0198
C	-1.0384	2.0717	-2.8694
C	-1.2639	2.6102	-1.5981
C	-1.8728	2.4757	-3.9161
C	-2.3247	3.4807	-1.3705
H	-0.6028	2.3265	-0.7840
C	-2.9336	3.3513	-3.6962
H	-1.6837	2.0941	-4.9174
C	-3.1710	3.8487	-2.4176
H	-2.4986	3.8748	-0.3733
H	-3.5704	3.6491	-4.5241
H	-3.9975	4.5298	-2.2392
C	-2.2274	-0.0021	0.4276
C	-3.3946	0.6700	0.8145
C	-1.2749	-0.2856	1.4355
C	-3.6084	1.0698	2.1350
H	-4.1556	0.9047	0.0797
C	-1.4826	0.1337	2.7406
H	-0.3733	-0.8459	1.2155
C	-2.6437	0.8199	3.1061
H	-4.5263	1.5937	2.3760
H	-0.7336	-0.0767	3.4996
C	3.9485	1.9230	-2.1899
H	4.9741	1.6760	-2.4882
H	3.7035	2.9147	-2.5850
H	3.9383	1.9924	-1.0935
C	2.9502	0.4402	-4.6821
H	2.3148	-0.3468	-5.1025
H	2.7111	1.3740	-5.2030
H	3.9906	0.1864	-4.9138
C	3.2968	-0.9913	-1.9972
H	2.7366	-1.8503	-2.3875
H	4.3581	-1.1582	-2.2205
H	3.1915	-0.9636	-0.9029
O	2.2239	-1.2084	1.5072

**Table A2.1.3. Cont.**

C	3.0262	-1.3975	2.6045
C	2.2767	-0.9925	3.8892
H	1.3654	-1.5973	3.9795
H	2.8728	-1.1185	4.8021
H	1.9733	0.0597	3.8119
C	3.4405	-2.8821	2.7361
H	4.0805	-3.0801	3.6046
H	2.5421	-3.5082	2.8293
H	3.9931	-3.1908	1.8371
C	4.3142	-0.5571	2.4855
H	4.8529	-0.8462	1.5752
H	4.0496	0.5036	2.3929
H	4.9889	-0.6712	3.3436
O	-2.7223	1.2228	4.4075
C	-3.8883	1.9131	4.7939
H	-4.0037	2.8481	4.2302
H	-4.7839	1.2959	4.6508
H	-3.7714	2.1415	5.8531
C	-0.0196	-4.8987	2.0345
C	-0.8443	-3.7849	1.8619
C	-1.4810	-3.5703	0.6413
C	-1.3081	-4.4570	-0.4285
C	-0.4677	-5.5611	-0.2489
C	0.1697	-5.7852	0.9740
H	0.4754	-5.0693	2.9855
H	-0.9803	-3.0710	2.6693
H	-2.1105	-2.6942	0.5071
H	-0.3204	-6.2587	-1.0703
H	0.8094	-6.6542	1.0983
C	-2.0331	-4.2217	-1.7282
H	-3.0597	-4.6002	-1.6707
H	-2.0863	-3.1514	-1.9527
H	-1.5382	-4.7266	-2.5626
C	3.1560	3.3600	1.6921
C	2.3902	3.9685	0.6956
C	1.0049	4.0494	0.8298
C	0.3595	3.5197	1.9549
C	1.1370	2.9087	2.9442
C	2.5247	2.8339	2.8193
H	4.2350	3.2933	1.5890
H	2.8695	4.3706	-0.1918
H	0.4136	4.5167	0.0453
H	0.6467	2.4865	3.8186
H	3.1102	2.3558	3.5988
C	-1.1403	3.5744	2.0763
H	-1.6095	2.8283	1.4225
H	-1.4613	3.3559	3.0988
H	-1.5217	4.5601	1.7907

**TS1-c**

C	-0.8452	-1.5780	1.2830
C	-0.5127	-2.7425	2.0412
C	1.4498	-2.9105	1.3612
H	1.6731	-3.5755	2.2145
O	-0.4818	-0.4108	1.5117
Si	3.0215	-1.0078	2.4727
N	2.0618	-1.7327	1.2568
C	-1.4563	-3.8310	1.5739
H	-1.0085	-4.8303	1.5436
H	-2.3314	-3.8897	2.2395
C	-1.8796	-3.3789	0.1629
H	-1.3069	-3.9116	-0.6032
H	-2.9462	-3.5329	-0.0368
N	-1.5726	-1.9449	0.1412
C	-0.2844	-2.5728	3.5159
H	-1.2184	-2.3766	4.0651
H	0.1676	-3.4713	3.9540
H	0.3947	-1.7333	3.6953
K	1.4119	0.5581	-0.210
K	-0.7911	1.6974	2.8620
C	1.2213	-3.7013	0.1091
C	1.0952	-3.0640	-1.1280
C	1.1343	-5.0958	0.1478
C	0.8476	-3.7899	-2.2871
H	1.1743	-1.9835	-1.1638
C	0.8877	-5.8309	-1.0101
H	1.2623	-5.6078	1.0993
C	0.7348	-5.1801	-2.2324
H	0.7329	-3.2713	-3.2365
H	0.8216	-6.9139	-0.9591
H	0.5432	-5.7510	-3.1359
C	-1.7001	-1.1785	-1.0280
C	-1.9890	-1.8069	-2.2454
C	-1.5606	0.2279	-1.0356
C	-2.0935	-1.0850	-3.4362
H	-2.1137	-2.8829	-2.2848
C	-1.6600	0.9400	-2.2201
H	-1.3437	0.7715	-0.1237
C	-1.9146	0.2958	-3.4332
H	-2.3079	-1.6226	-4.3531
H	-1.5304	2.0189	-2.2154
C	4.5735	-0.3084	1.6442
H	5.1209	-1.0988	1.1198
H	4.3187	0.4623	0.9036
H	5.2487	0.1551	2.3728
C	3.5556	-2.1904	3.8498
H	2.6990	-2.5842	4.4081
H	4.1066	-3.0447	3.4413
H	4.2117	-1.6808	4.5642



**Table A2.1.3. Cont.**

C	2.2167	0.5049	3.3065
H	1.8793	1.2481	2.5696
H	1.3639	0.1966	3.9246
H	2.9427	0.9985	3.9647
O	0.3976	2.5688	0.9168
C	0.6654	3.8589	0.5385
C	0.1955	4.8539	1.6225
H	-0.8848	4.7314	1.7847
H	0.7146	4.6342	2.5650
H	0.3830	5.9039	1.3659
C	2.1824	4.0565	0.3297
H	2.5388	3.3655	-0.4474
H	2.4526	5.0769	0.0273
H	2.7116	3.8150	1.2592
C	-0.0647	4.1836	-0.7795
H	0.1174	5.2017	-1.1482
H	0.2591	3.4705	-1.5494
H	-1.1448	4.0484	-0.6352
O	-1.9506	1.0930	-4.5418
C	-2.1245	0.4523	-5.7849
H	-1.3192	-0.2691	-5.9756
H	-3.0902	-0.0653	-5.8367
H	-2.0947	1.2373	-6.5403
C	-3.6361	0.2721	3.1144
C	-3.7811	1.3096	4.0357
C	-3.8272	2.6349	3.5969
C	-3.7370	2.9456	2.2347
C	-3.5821	1.8936	1.3228
C	-3.5347	0.5691	1.7543
H	-3.5916	-0.7598	3.4497
H	-3.8619	1.0898	5.0966
H	-3.9465	3.4391	4.3193
H	-3.4849	2.1144	0.2622
H	-3.3954	-0.2304	1.0319
C	-3.8356	4.3707	1.7531
H	-3.5251	5.0772	2.5278
H	-3.2099	4.5338	0.8711
H	-4.8685	4.6107	1.4777
C	2.8382	-0.5782	-2.7831
C	1.6379	-0.1093	-3.3165
C	1.4462	1.2598	-3.5203
C	2.4435	2.1816	-3.1870
C	3.6280	1.7006	-2.6118
C	3.8300	0.3358	-2.4183
H	2.9925	-1.6413	-2.6253
H	0.8357	-0.8022	-3.5648
H	0.5110	1.6121	-3.9507
H	4.4042	2.4074	-2.3263
H	4.7570	-0.0187	-1.9774
C	2.2759	3.6530	-3.4705

**Table A2.1.3. Cont.**

H	2.4987	4.2581	-2.5859
H	2.9573	3.9670	-4.2687
H	1.2551	3.8817	-3.7868

**TS1-rotamer1**

C	1.3014	1.2550	0.0192
C	1.1234	2.4096	0.8333
C	-0.6491	1.8717	2.0683
H	-0.9925	2.8978	1.8555
O	1.6308	0.1034	0.3812
Si	-0.1336	2.6065	4.6012
N	-0.2714	1.5068	3.2758
C	0.8238	3.5786	-0.0855
H	-0.0488	4.1663	0.2353
H	1.6693	4.2790	-0.1264
C	0.5870	2.9493	-1.4787
H	-0.4604	3.0424	-1.7887
H	1.1978	3.4060	-2.2658
N	0.9643	1.5516	-1.3080
C	2.0990	2.6413	1.9470
H	2.1030	1.8161	2.6654
H	3.1264	2.7747	1.5782
H	1.8329	3.5418	2.5125
K	0.4831	-2.1923	-0.2996
K	1.4046	-0.7790	2.9271
C	-1.3296	0.8520	1.2024
C	-1.5776	-0.4366	1.6906
C	-1.8068	1.1758	-0.0709
C	-2.2366	-1.3873	0.9109
H	-1.2988	-0.6562	2.7170
C	-2.4537	0.2309	-0.8604
H	-1.6792	2.1923	-0.4335
C	-2.6626	-1.0626	-0.3776
H	-2.4254	-2.3809	1.3142
H	-2.8093	0.5023	-1.8504
H	-3.1813	-1.7945	-0.9896
C	0.8642	0.6108	-2.3393
C	-0.1069	0.7296	-3.3362
C	1.7662	-0.4670	-2.4220
C	-0.2286	-0.2228	-4.3494
H	-0.7926	1.5706	-3.3267
C	1.6280	-1.4342	-3.4052
H	2.5689	-0.5356	-1.6978
C	0.6178	-1.3295	-4.3690
H	-0.9978	-0.0927	-5.1022
H	2.3202	-2.2699	-3.4609
C	-1.3995	2.1668	5.9350

**Table A2.1.3. Cont.**

H	-2.4041	2.0885	5.5053
H	-1.1728	1.2165	6.4293
H	-1.4255	2.9408	6.7111
C	-0.4891	4.4044	4.1238
H	-1.5345	4.5243	3.8165
H	-0.3243	5.0626	4.9843
H	0.1394	4.7674	3.3037
C	1.5721	2.4896	5.4115
H	1.5474	2.8941	6.4302
H	1.8948	1.4428	5.4816
H	2.3372	3.0354	4.8507
O	1.8839	-2.9433	1.6380
C	3.2186	-3.2289	1.4807
C	4.1010	-2.3336	2.3854
H	5.1667	-2.5867	2.3280
H	3.9997	-1.2801	2.0876
H	3.7846	-2.4422	3.4324
C	3.5132	-4.6983	1.8402
H	4.5714	-4.9651	1.7265
H	3.2155	-4.8886	2.8784
H	2.9193	-5.3575	1.1955
C	3.6653	-2.9789	0.0215
H	3.0771	-3.6132	-0.6571
H	3.4788	-1.9261	-0.2271
H	4.7275	-3.1911	-0.1542
O	0.5429	-2.3453	-5.2775
C	-0.3321	-2.1679	-6.3707
H	-1.3775	-2.1059	-6.0434
H	-0.0780	-1.2627	-6.9349
H	-0.2050	-3.0433	-7.0074
C	0.4759	-1.1864	6.0305
C	-0.7008	-1.4552	5.3332
C	-0.8031	-2.6110	4.5571
C	0.2604	-3.5123	4.4491
C	1.4377	-3.2257	5.1520
C	1.5461	-2.0797	5.9375
H	0.5597	-0.2917	6.6404
H	-1.5336	-0.7594	5.3799
H	-1.7281	-2.8166	4.0214
H	2.2789	-3.9099	5.0727
H	2.4675	-1.8820	6.4786
C	0.1819	-4.7078	3.5420
H	-0.8585	-4.9804	3.3371
H	0.6992	-4.4361	2.6079
H	0.6860	-5.5746	3.9811
C	0.2528	-5.3942	-0.4096
C	-1.0679	-5.0519	-0.1259
C	-1.8423	-4.3953	-1.0830
C	-1.3118	-4.0594	-2.3329
C	0.0129	-4.4195	-2.6126

**Table A2.1.3. Cont.**

C	0.7866	-5.0852	-1.6618
H	0.8602	-5.8876	0.3413
H	-1.4944	-5.2957	0.8425
H	-2.8773	-4.1469	-0.8581
H	0.4302	-4.1726	-3.5867
H	1.8115	-5.3590	-1.8950
C	-2.1298	-3.3107	-3.3538
H	-1.9292	-3.6864	-4.3615
H	-3.2011	-3.4099	-3.1561
H	-1.8802	-2.2411	-3.3439

**TS1-rotamer2**

C	0.6643	0.7051	1.5107
C	0.3573	1.6434	2.5217
C	-1.8131	1.5684	1.8619
H	-1.8461	0.7469	2.6030
O	0.5269	-0.5451	1.5430
Si	-2.6565	1.8929	-0.8195
N	-1.9611	1.2504	0.6039
C	0.9599	2.9655	2.1360
H	0.3203	3.8279	2.3604
H	1.9135	3.1368	2.6607
C	1.1951	2.8227	0.6207
H	0.4478	3.3619	0.0259
H	2.1855	3.1929	0.3341
N	1.0731	1.3879	0.3605
C	0.2915	1.2140	3.9516
H	-0.0132	0.1631	4.0158
H	1.2652	1.3067	4.4572
H	-0.4211	1.8201	4.5270
K	-1.9356	-1.4467	0.9110
K	1.7556	-2.6039	0.6206
C	-2.2160	2.8650	2.4776
C	-2.1310	4.0731	1.7755
C	-2.7204	2.8893	3.7828
C	-2.5395	5.2666	2.3593
H	-1.7286	4.0691	0.7658
C	-3.1343	4.0824	4.3699
H	-2.7983	1.9552	4.3353
C	-3.0456	5.2758	3.6591
H	-2.4622	6.1945	1.8002
H	-3.5305	4.0787	5.3811
H	-3.3680	6.2079	4.1128
C	1.2667	0.8591	-0.9199
C	2.0057	1.5838	-1.8639
C	0.7456	-0.3869	-1.3308
C	2.2444	1.0942	-3.1513
H	2.4026	2.5603	-1.6124

**Table A2.1.3. Cont.**

C	0.9996	-0.8814	-2.5990
H	0.1348	-0.9904	-0.6736
C	1.7539	-0.1533	-3.5258
H	2.8134	1.7056	-3.8423
H	0.5847	-1.8398	-2.8979
C	-4.2776	2.8275	-0.5008
H	-4.8215	2.4033	0.3512
H	-4.1024	3.8834	-0.2712
H	-4.9319	2.7791	-1.3793
C	-3.0257	0.3978	-1.9162
H	-3.6937	-0.3214	-1.4250
H	-3.4932	0.6881	-2.8644
H	-2.0896	-0.1233	-2.1557
C	-1.5589	3.0100	-1.8821
H	-2.0812	3.2273	-2.8221
H	-1.3195	3.9724	-1.4164
H	-0.6179	2.5087	-2.1358
O	-0.4998	-3.2900	-0.0247
C	-1.0242	-4.2527	-0.8520
C	0.0820	-4.8753	-1.7315
H	-0.2897	-5.6429	-2.4213
H	0.5692	-4.0895	-2.3221
H	0.8411	-5.3385	-1.0864
C	-1.6770	-5.3810	-0.0287
H	-2.1150	-6.1710	-0.6518
H	-0.9286	-5.8319	0.6331
H	-2.4681	-4.9573	0.6032
C	-2.0975	-3.6438	-1.7805
H	-2.9363	-3.2594	-1.1808
H	-1.6674	-2.8013	-2.3357
H	-2.5085	-4.3629	-2.5001
O	1.9363	-0.7315	-4.7462
C	2.6545	0.0090	-5.7045
H	2.1577	0.9615	-5.9279
H	3.6801	0.2105	-5.3688
H	2.6836	-0.6039	-6.6052
C	4.1621	-0.9990	-0.6385
C	3.9925	-0.3683	0.5956
C	4.3213	-1.0346	1.7751
C	4.8322	-2.3386	1.7492
C	4.9945	-2.9623	0.5066
C	4.6658	-2.2993	-0.6780
H	3.8823	-0.4861	-1.5548
H	3.5741	0.6331	0.6390
H	4.1703	-0.5390	2.7314
H	5.3887	-3.9753	0.4668
H	4.7963	-2.8024	-1.6318
C	5.2250	-3.0374	3.0271
H	6.2349	-2.7424	3.3320
H	4.5475	-2.7797	3.8462

**Table A2.1.3. Cont.**

H	5.2210	-4.1240	2.9057
C	-5.1374	-1.9720	0.7146
C	-4.7189	-2.9603	1.6054
C	-4.2424	-2.6054	2.8683
C	-4.1755	-1.2640	3.2628
C	-4.5988	-0.2817	2.3589
C	-5.0765	-0.6311	1.0968
H	-5.5047	-2.2440	-0.2706
H	-4.7606	-4.0064	1.3176
H	-3.9194	-3.3810	3.5586
H	-4.5410	0.7685	2.6401
H	-5.3908	0.1461	0.4064
C	-3.6352	-0.8808	4.6184
H	-3.6779	-1.7228	5.3144
H	-2.5885	-0.5579	4.5496
H	-4.2056	-0.0519	5.0475

**TS2**

C	-0.4120	-1.1921	1.6241
C	-0.0238	-2.5543	1.6135
C	-0.1427	-3.0419	-0.5600
H	0.3133	-4.0017	-0.2538
O	0.2939	-0.1667	1.4303
Si	-2.3401	-4.3566	-1.3734
N	-1.3650	-2.9815	-1.0166
C	-1.1957	-3.3783	2.0846
H	-1.3581	-4.2790	1.4747
H	-1.0643	-3.7129	3.1241
C	-2.3985	-2.4237	1.9617
H	-3.0013	-2.6588	1.0836
H	-3.0475	-2.4322	2.8459
N	-1.7954	-1.1003	1.8091
C	1.3662	-2.9481	2.0095
H	2.0993	-2.2010	1.6859
H	1.4700	-3.0606	3.1003
H	1.6620	-3.9080	1.5622
K	-0.4534	1.8440	-0.1644
K	2.6751	0.3488	0.6575
C	0.8788	-2.0754	-1.0682
C	0.4763	-0.8726	-1.6635
C	2.2347	-2.4162	-1.1079
C	1.3983	-0.0313	-2.2769
H	-0.5901	-0.6579	-1.6745
C	3.1619	-1.5881	-1.7465
H	2.5582	-3.3613	-0.6779
C	2.7490	-0.3923	-2.3322
H	1.0739	0.9035	-2.7294
H	4.2050	-1.8889	-1.8044

**Table A2.1.3. Cont.**

H	3.4636	0.2527	-2.8348
C	-2.5574	0.0576	1.9555
C	-3.9467	0.0020	1.7858
C	-2.0003	1.2890	2.3665
C	-4.7543	1.1244	1.9788
H	-4.4151	-0.9331	1.4974
C	-2.7971	2.4125	2.5183
H	-0.9400	1.3409	2.5836
C	-4.1813	2.3469	2.3208
H	-5.8254	1.0256	1.8417
H	-2.3654	3.3588	2.8315
C	-4.0074	-4.3641	-0.4785
H	-4.5077	-3.3908	-0.5506
H	-4.6664	-5.1065	-0.9435
H	-3.9161	-4.6231	0.5820
C	-1.4811	-6.0051	-1.0093
H	-2.1315	-6.8360	-1.3052
H	-0.5474	-6.1014	-1.5747
H	-1.2422	-6.1373	0.0516
C	-2.7355	-4.3178	-3.2177
H	-1.8164	-4.3426	-3.8122
H	-3.3584	-5.1685	-3.5169
H	-3.2724	-3.3993	-3.4783
O	1.8953	2.5629	-0.1411
C	2.5923	3.6297	-0.6448
C	3.3117	4.3917	0.4860
H	4.0064	3.7106	0.9950
H	3.8771	5.2623	0.1304
H	2.5744	4.7276	1.2235
C	3.6505	3.1533	-1.6638
H	3.1515	2.6337	-2.4909
H	4.2544	3.9700	-2.0793
H	4.3288	2.4383	-1.1751
C	1.6411	4.6074	-1.3684
H	2.1506	5.4851	-1.7857
H	1.1369	4.0786	-2.1887
H	0.8740	4.9556	-0.6640
O	-4.8679	3.5125	2.4893
C	-6.2632	3.4673	2.2990
H	-6.5168	3.1603	1.2758
H	-6.7417	2.7805	3.0081
H	-6.6282	4.4793	2.4735
C	4.7811	-0.0481	3.0660
C	4.8930	-1.2504	2.3678
C	5.4175	-1.2625	1.0739
C	5.8412	-0.0802	0.4571
C	5.7259	1.1196	1.1711
C	5.2006	1.1388	2.4623
H	4.3721	-0.0360	4.0714
H	4.5701	-2.1795	2.8279

**Table A2.1.3. Cont.**

H	5.5012	-2.2044	0.5368
H	6.0458	2.0493	0.7064
H	5.1139	2.0819	2.9934
C	6.3851	-0.0810	-0.9489
H	5.6456	0.3216	-1.6517
H	7.2793	0.5442	-1.0249
H	6.6456	-1.0918	-1.2739
C	-1.9544	3.6255	-2.3127
C	-1.4970	2.5681	-3.1031
C	-2.0112	1.2835	-2.9265
C	-2.9903	1.0227	-1.9559
C	-3.4397	2.0930	-1.1742
C	-2.9311	3.3818	-1.3475
H	-1.5490	4.6234	-2.4479
H	-0.7393	2.7473	-3.8610
H	-1.6519	0.4675	-3.5504
H	-4.1934	1.9107	-0.4139
H	-3.2991	4.1902	-0.7212
C	-3.5271	-0.3703	-1.7467
H	-3.7270	-0.8580	-2.7062
H	-2.8084	-1.0107	-1.2137
H	-4.4565	-0.3422	-1.1710

**TS2-b**

C	-0.4262	-1.1684	1.6274
C	-0.0764	-2.5407	1.6168
C	-0.2349	-3.0325	-0.5571
H	0.1980	-4.0029	-0.2507
O	0.3050	-0.1637	1.4196
Si	-2.4769	-4.2914	-1.3361
N	-1.4600	-2.9409	-0.9999
C	-1.2650	-3.3304	2.1040
H	-1.4597	-4.2281	1.4991
H	-1.1310	-3.6656	3.1431
C	-2.4420	-2.3429	1.9918
H	-3.0591	-2.5612	1.1192
H	-3.0831	-2.3333	2.8818
N	-1.8036	-1.0373	1.8328
C	1.3071	-2.9715	1.9965
H	2.0556	-2.2431	1.6654
H	1.4200	-3.0877	3.0861
H	1.5729	-3.9385	1.5456
K	-0.4173	1.8495	-0.1849
K	2.6860	0.2918	0.6114
C	0.8069	-2.0962	-1.0797
C	0.4312	-0.8861	-1.6778
C	2.1527	-2.4736	-1.1309
C	1.3693	-0.0733	-2.3052



**Table A2.1.3. Cont.**

H	-0.6288	-0.6418	-1.6793
C	3.0954	-1.6745	-1.7834
H	2.4549	-3.4248	-0.6989
C	2.7091	-0.4712	-2.3720
H	1.0656	0.8678	-2.7588
H	4.1294	-2.0038	-1.8499
H	3.4358	0.1513	-2.8854
C	-2.5327	0.1419	1.9752
C	-3.9245	0.1233	1.8184
C	-1.9381	1.3612	2.3695
C	-4.6988	1.2698	2.0062
H	-4.4215	-0.8013	1.5440
C	-2.7019	2.5080	2.5162
H	-0.8748	1.3858	2.5767
C	-4.0890	2.4793	2.3305
H	-5.7733	1.1996	1.8790
H	-2.2412	3.4450	2.8160
C	-4.1294	-4.2534	-0.4150
H	-4.6064	-3.2682	-0.4831
H	-4.8140	-4.9807	-0.8667
H	-4.0277	-4.5108	0.6449
C	-1.6546	-5.9600	-0.9800
H	-2.3307	-6.7751	-1.2620
H	-0.7331	-6.0819	-1.5603
H	-1.4016	-6.0946	0.0773
C	-2.8994	-4.2457	-3.1741
H	-1.9905	-4.2977	-3.7824
H	-3.5507	-5.0789	-3.4617
H	-3.4138	-3.3126	-3.4285
O	1.9451	2.5179	-0.1965
C	2.6710	3.5613	-0.7083
C	3.4181	4.3068	0.4156
H	4.0948	3.6078	0.9248
H	4.0074	5.1585	0.0532
H	2.6946	4.6679	1.1549
C	3.7098	3.0492	-1.7299
H	3.1917	2.5396	-2.5514
H	4.3348	3.8459	-2.1531
H	4.3702	2.3178	-1.2408
C	1.7457	4.5634	-1.4319
H	2.2789	5.4242	-1.8549
H	1.2228	4.0462	-2.2478
H	0.9921	4.9363	-0.7257
O	-4.7415	3.6654	2.4918
C	-6.1390	3.6571	2.3133
H	-6.6304	2.9910	3.0333
H	-6.4744	4.6805	2.4800
H	-6.4096	3.3467	1.2954
C	4.8013	-0.1509	3.0059
C	4.8732	-1.3599	2.3141

**Table A2.1.3. Cont.**

C	5.3858	-1.3943	1.0159
C	5.8373	-0.2281	0.3883
C	5.7621	0.9787	1.0960
C	5.2489	1.0202	2.3915
H	4.4014	-0.1215	4.0146
H	4.5281	-2.2769	2.7825
H	5.4384	-2.3413	0.4837
H	6.1041	1.8963	0.6230
H	5.1933	1.9683	2.9177
C	6.3687	-0.2522	-1.0222
H	7.2822	0.3430	-1.1084
H	6.5933	-1.2723	-1.3451
H	5.6369	0.1716	-1.7205
C	-1.8809	3.6627	-2.3282
C	-1.4631	2.5892	-3.1190
C	-2.0158	1.3219	-2.9347
C	-2.9957	1.0949	-1.9562
C	-3.4040	2.1804	-1.1733
C	-2.8565	3.4522	-1.3542
H	-1.4452	4.6468	-2.4694
H	-0.7058	2.7424	-3.8830
H	-1.6869	0.4932	-3.5585
H	-4.1562	2.0237	-0.4057
H	-3.1933	4.2732	-0.7267
C	-3.5784	-0.2792	-1.7444
H	-2.8578	-0.9620	-1.2695
H	-4.4697	-0.2257	-1.1131
H	-3.8584	-0.7325	-2.7009

**TS2-c**

C	0.4527	1.0688	1.6733
C	0.1605	2.4555	1.6732
C	0.3368	2.9683	-0.4860
H	-0.0691	3.9475	-0.1714
O	-0.3207	0.0977	1.4589
Si	2.6195	4.1715	-1.2375
N	1.5607	2.8479	-0.9287
C	1.3791	3.1892	2.1737
H	1.6096	4.0883	1.5837
H	1.2579	3.5116	3.2184
C	2.5150	2.1571	2.0450
H	3.1346	2.3592	1.1704
H	3.1604	2.1127	2.9308
N	1.8233	0.8798	1.8773
C	-1.2063	2.9305	2.0584
H	-1.9768	2.2396	1.7000
H	-1.3230	3.0189	3.1505
H	-1.4310	3.9196	1.6338

**Table A2.1.3. Cont.**

K	0.4173	-1.8587	-0.2165
K	-2.7103	-0.3434	0.6486
C	-0.7290	2.0674	-1.0234
C	-0.3793	0.8657	-1.6521
C	-2.0689	2.4666	-1.0530
C	-1.3358	0.0765	-2.2806
H	0.6776	0.6094	-1.6735
C	-3.0309	1.6928	-1.7081
H	-2.3522	3.4142	-0.6007
C	-2.6710	0.4927	-2.3200
H	-1.0516	-0.8606	-2.7533
H	-4.0594	2.0410	-1.7577
H	-3.4143	-0.1112	-2.8337
C	2.5076	-0.3290	1.9948
C	3.8966	-0.3631	1.8176
C	1.8699	-1.5296	2.3787
C	4.6264	-1.5430	1.9739
H	4.4263	0.5454	1.5512
C	2.5885	-2.7089	2.4935
H	0.8083	-1.5159	2.5956
C	3.9728	-2.7325	2.2865
H	5.7010	-1.5140	1.8317
H	2.0943	-3.6320	2.7823
C	4.2619	4.0727	-0.3022
H	4.1559	4.3071	0.7626
H	4.7170	3.0787	-0.3894
H	4.9675	4.7944	-0.7301
C	1.8443	5.8589	-0.8644
H	2.5472	6.6576	-1.1270
H	0.9328	6.0170	-1.4517
H	1.5844	5.9849	0.1924
C	3.0584	4.1386	-3.0721
H	3.5438	3.1924	-3.3350
H	2.1576	4.2294	-3.6877
H	3.7399	4.9535	-3.3418
O	-1.9355	-2.5125	-0.3196
C	-2.7329	-3.4749	-0.8812
C	-4.2239	-3.1664	-0.6151
H	-4.4723	-2.1802	-1.0368
H	-4.9095	-3.9035	-1.0519
H	-4.3986	-3.1312	0.4685
C	-2.5225	-3.5349	-2.4087
H	-1.4634	-3.7352	-2.6178
H	-3.1251	-4.3093	-2.9000
H	-2.7771	-2.5650	-2.8541
C	-2.4124	-4.8619	-0.2891
H	-3.0420	-5.6629	-0.6967
H	-1.3629	-5.1085	-0.4954
H	-2.5423	-4.8303	0.7984
O	4.5791	-3.9462	2.4176

**Table A2.1.3. Cont.**

C	5.9730	-3.9914	2.2172
H	6.5020	-3.3590	2.9408
H	6.2686	-5.0305	2.3608
H	6.2408	-3.6742	1.2007
C	-4.7208	0.4225	3.1235
C	-4.6658	1.6224	2.4150
C	-5.2147	1.7054	1.1342
C	-5.8341	0.5987	0.5433
C	-5.8901	-0.5976	1.2693
C	-5.3369	-0.6890	2.5454
H	-4.2922	0.3557	4.1185
H	-4.1937	2.4944	2.8572
H	-5.1656	2.6450	0.5887
H	-6.3666	-1.4675	0.8245
H	-5.3882	-1.6282	3.0883
C	-6.4107	0.6709	-0.8480
H	-7.3872	0.1808	-0.8947
H	-6.5322	1.7069	-1.1754
H	-5.7567	0.1637	-1.5680
C	1.7441	-3.6931	-2.4364
C	1.3809	-2.5772	-3.1948
C	2.0003	-1.3469	-2.9769
C	2.9937	-1.1995	-1.9969
C	3.3507	-2.3280	-1.2503
C	2.7358	-3.5636	-1.4644
H	1.2564	-4.6488	-2.6026
H	0.6115	-2.6675	-3.9565
H	1.7109	-0.4838	-3.5731
H	4.1133	-2.2335	-0.4826
H	3.0314	-4.4194	-0.8633
C	3.6396	0.1393	-1.7450
H	2.9399	0.8476	-1.2758
H	4.5106	0.0306	-1.0928
H	3.9671	0.5937	-2.6858

**TS2-rotamer1**

C	-0.4738	-1.3733	1.7620
C	-0.2956	-2.7840	1.6837
C	-0.2561	-2.9151	-0.5237
H	-1.3515	-3.0427	-0.5321
O	0.3948	-0.4754	1.6923
Si	-0.6240	-0.6482	-1.8897
N	0.3049	-1.8670	-1.0989
C	-1.6013	-3.4006	2.1407
H	-1.8497	-4.3400	1.6361
H	-1.5843	-3.6159	3.2218
C	-2.6403	-2.3045	1.8368
H	-3.1036	-2.4598	0.8528

**Table A2.1.3. Cont.**

H	-3.4397	-2.2394	2.5818
N	-1.8396	-1.0828	1.8520
C	0.9988	-3.3469	2.1996
H	1.8618	-2.9053	1.6865
H	1.1305	-3.1623	3.2785
H	1.0566	-4.4287	2.0351
K	0.7839	2.1324	1.6104
K	2.5205	-0.7141	0.0826
C	0.4455	-4.2347	-0.5322
C	1.8126	-4.3153	-0.8091
C	-0.2534	-5.4229	-0.2947
C	2.4758	-5.5378	-0.7841
H	2.3368	-3.4006	-1.0693
C	0.4053	-6.6488	-0.2696
H	-1.3291	-5.3857	-0.1434
C	1.7779	-6.7107	-0.5004
H	3.5412	-5.5835	-1.0000
H	-0.1559	-7.5594	-0.0817
H	2.2938	-7.6658	-0.4839
C	-2.3838	0.1943	2.0264
C	-3.5726	0.5720	1.4022
C	-1.7669	1.1173	2.8879
C	-4.1110	1.8470	1.5827
H	-4.0832	-0.1315	0.7515
C	-2.2805	2.3936	3.0529
H	-0.8767	0.8097	3.4281
C	-3.4561	2.7741	2.3925
H	-5.0342	2.1025	1.0762
H	-1.8085	3.1071	3.7244
C	-0.4409	1.0623	-1.1033
H	0.6140	1.3130	-0.9220
H	-0.8625	1.8322	-1.7617
H	-0.9968	1.0781	-0.1569
C	-2.4752	-1.0395	-1.9096
H	-3.0322	-0.2340	-2.4010
H	-2.7001	-1.9742	-2.4345
H	-2.8543	-1.1271	-0.8850
C	-0.0115	-0.4941	-3.6673
H	-0.1265	-1.4431	-4.2012
H	-0.5566	0.2801	-4.2191
H	1.0527	-0.2317	-3.6845
O	2.7631	1.7896	0.1760
C	3.4439	2.6200	-0.6796
C	4.6999	3.1943	0.0055
H	5.3437	2.3698	0.3362
H	5.2859	3.8535	-0.6472
H	4.4018	3.7644	0.8946
C	3.8829	1.8477	-1.9417
H	2.9982	1.4256	-2.4365
H	4.4235	2.4659	-2.6695

**Table A2.1.3. Cont.**

H	4.5394	1.0183	-1.6447
C	2.5521	3.8015	-1.1189
H	3.0553	4.4907	-1.8085
H	1.6483	3.4209	-1.6095
H	2.2470	4.3770	-0.2332
O	-3.8827	4.0453	2.6211
C	-5.0656	4.4563	1.9720
H	-4.9594	4.4054	0.8815
H	-5.9221	3.8444	2.2803
H	-5.2330	5.4903	2.2721
C	4.7440	-2.2135	1.9902
C	4.5657	-3.1385	0.9588
C	5.0152	-2.8426	-0.3262
C	5.6493	-1.6258	-0.6100
C	5.8173	-0.7084	0.4313
C	5.3712	-0.9977	1.7222
H	4.3949	-2.4437	2.9929
H	4.0617	-4.0819	1.1499
H	4.8723	-3.5652	-1.1274
H	6.3005	0.2434	0.2280
H	5.5148	-0.2714	2.5174
C	6.1290	-1.3234	-2.0074
H	6.6607	-0.3696	-2.0456
H	6.8037	-2.1073	-2.3655
H	5.2894	-1.2654	-2.7089
C	3.3700	1.8559	3.2649
C	2.6727	0.7150	3.6613
C	1.5770	0.8206	4.5165
C	1.1539	2.0659	4.9970
C	1.8565	3.2056	4.5862
C	2.9561	3.1035	3.7327
H	4.1763	1.7838	2.5433
H	2.9569	-0.2617	3.2783
H	1.0331	-0.0777	4.8012
H	1.5420	4.1822	4.9473
H	3.4818	4.0005	3.4183
C	-0.0033	2.1690	5.9596
H	-0.8444	1.5397	5.6507
H	0.2983	1.8421	6.9605
H	-0.3612	3.1992	6.0422

**TS2-rotamer2**

C	-0.6077	-1.1404	1.5287
C	-0.2066	-2.4837	1.2500
C	-0.1056	-2.5539	-0.8244
H	0.4277	-1.5783	-0.8675
O	0.0557	-0.0810	1.3724
Si	2.0872	-3.8894	-1.7256

**Table A2.1.3. Cont.**

N	0.4875	-3.6702	-1.1907
C	-1.3243	-3.3887	1.7202
H	-1.5111	-4.2072	1.0129
H	-1.0812	-3.8433	2.6916
C	-2.5424	-2.4565	1.8487
H	-3.1986	-2.5409	0.9750
H	-3.1383	-2.6349	2.7500
N	-1.9441	-1.1207	1.9143
C	1.1835	-2.9401	1.5667
H	1.9553	-2.2863	1.1416
H	1.3635	-3.0120	2.6493
H	1.3321	-3.9307	1.1217
K	-0.6169	2.2487	0.2132
K	2.4031	0.1479	0.2805
C	-1.5622	-2.3849	-1.1393
C	-2.3411	-3.5017	-1.4577
C	-2.1701	-1.1266	-1.1177
C	-3.7071	-3.3686	-1.6862
H	-1.8365	-4.4611	-1.5214
C	-3.5356	-0.9888	-1.3491
H	-1.5577	-0.2532	-0.8951
C	-4.3139	-2.1137	-1.6202
H	-4.3038	-4.2452	-1.9222
H	-3.9945	-0.0042	-1.3046
H	-5.3801	-2.0103	-1.7999
C	-2.7106	0.0304	2.1212
C	-4.0696	0.0501	1.7985
C	-2.1570	1.1721	2.7351
C	-4.8577	1.1761	2.0451
H	-4.5239	-0.8204	1.3373
C	-2.9327	2.2968	2.9639
H	-1.1175	1.1504	3.0424
C	-4.2901	2.3087	2.6217
H	-5.9090	1.1470	1.7824
H	-2.5139	3.1777	3.4422
C	3.0462	-5.1744	-0.7231
H	2.4531	-6.0861	-0.5950
H	3.9769	-5.4501	-1.2328
H	3.3065	-4.8050	0.2754
C	3.1523	-2.3007	-1.6923
H	4.0357	-2.4237	-2.3299
H	2.6027	-1.4292	-2.0728
H	3.5198	-2.0916	-0.6785
C	2.0797	-4.4879	-3.5149
H	1.6216	-3.7416	-4.1727
H	3.0915	-4.6929	-3.8832
H	1.4929	-5.4080	-3.6040
O	1.6569	2.3292	-0.6761
C	2.5620	2.9315	-1.5179
C	3.3572	4.0172	-0.7665

**Table A2.1.3. Cont.**

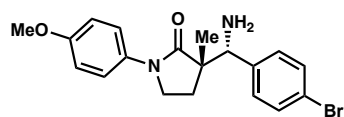
H	3.8939	3.5601	0.0749
H	4.0848	4.5360	-1.4033
H	2.6611	4.7577	-0.3557
C	3.5733	1.9071	-2.0893
H	3.0343	1.0946	-2.5940
H	4.2689	2.3528	-2.8106
H	4.1837	1.4757	-1.2815
C	1.8443	3.5884	-2.7131
H	2.5348	4.0558	-3.4260
H	1.2531	2.8304	-3.2413
H	1.1596	4.3587	-2.3404
O	-4.9593	3.4703	2.8797
C	-6.3224	3.5210	2.5183
H	-6.4516	3.3748	1.4377
H	-6.9053	2.7647	3.0570
H	-6.6737	4.5148	2.7943
C	3.9659	0.4178	3.1059
C	4.0680	-0.9422	2.8182
C	4.8179	-1.3727	1.7214
C	5.4804	-0.4565	0.8973
C	5.3738	0.9078	1.2024
C	4.6239	1.3436	2.2931
H	3.3773	0.7545	3.9534
H	3.5556	-1.6710	3.4386
H	4.8835	-2.4354	1.4980
H	5.8777	1.6359	0.5706
H	4.5459	2.4061	2.5026
C	6.2704	-0.9105	-0.3039
H	5.8418	-0.5066	-1.2285
H	7.3073	-0.5656	-0.2422
H	6.2740	-2.0003	-0.3860
C	-2.2381	5.0709	-0.1813
C	-1.4687	4.9908	-1.3422
C	-1.7374	4.0071	-2.2927
C	-2.7718	3.0823	-2.1037
C	-3.5262	3.1637	-0.9257
C	-3.2696	4.1542	0.0254
H	-2.0425	5.8466	0.5529
H	-0.6602	5.6957	-1.5110
H	-1.1327	3.9526	-3.1938
H	-4.3323	2.4532	-0.7521
H	-3.8754	4.2157	0.9245
C	-3.0462	2.0255	-3.1445
H	-2.8334	2.4049	-4.1475
H	-2.4234	1.1368	-2.9893
H	-4.0896	1.7006	-3.1153



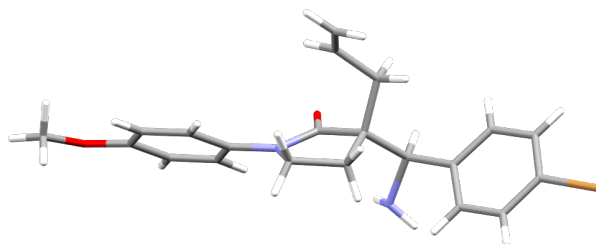
## **APPENDIX 3**

*X-Ray Crystallography Reports Relevant to Chapter 1:*

*Diastereoselective Direct Mannich Reaction of  $\alpha$ -Substituted- $\gamma$ -lactams  
and aryl N-silyl imines*

**A3.1 X-RAY CRYSTAL STRUCTURE ANALYSIS OF AMINE 69dn**

70

Contents*Table A3.1.1. Experimental Details**Table A3.1.2. Crystal Data**Table A3.1.3. Atomic Coordinates**Table A3.1.4. Full Bond Distances and Angles**Table A3.1.5. Anisotropic Displacement Parameters**Table A3.1.6. Hydrogen Atomic Coordinates**Table A3.1.7. Torsion Angles**Table A3.1.8. Hydrogen Bond Distances and Angles***Figure A3.1.1 X-Ray Crystal Structure of Amine 69dn.**

**Table A3.1.1** Experimental Details for X-Ray Structure Determination of Amine **69dn**.

Low-temperature diffraction data ( $\phi$ - and  $\omega$ -scans) were collected on a Bruker AXS KAPPA APEX II diffractometer coupled to an PHOTON 100 CMOS detector with graphite monochromated Mo  $K_{\alpha}$  radiation ( $\lambda = 0.71073 \text{ \AA}$ ) for the structure of compound D21009. The structure was solved by direct methods using SHELXS and refined against  $F^2$  on all data by full-matrix least squares with SHELXL-2017 using established refinement techniques. All non-hydrogen atoms were refined anisotropically. Unless otherwise noted, all hydrogen atoms were included into the model at geometrically calculated positions and refined using a riding model. The isotropic displacement parameters of all hydrogen atoms were fixed to 1.2 times the  $U$  value of the atoms they are linked to (1.5 times for methyl groups).

Compound **69dn** crystallizes in the monoclinic space group  $P2_1/n$  with one molecule in the asymmetric unit. The coordinates for the hydrogen atoms bound to N2 were located in the difference Fourier synthesis and refined semi-freely with the help of a restraint on the N-H distance (0.91(4)  $\text{\AA}$ ).

**Table A3.1.2** Crystal Data and Structure Refinement for Amine **69dn**

Identification code	D21009	
Empirical formula	C <sub>21</sub> H <sub>23</sub> Br N <sub>2</sub> O <sub>2</sub>	
Formula weight	415.32	
Temperature	100(2) K	
Wavelength	0.71073 Å	
Crystal system	Monoclinic	
Space group	P2 <sub>1</sub> /n	
Unit cell dimensions	a = 9.430(3) Å	a = 90°.
	b = 9.489(2) Å	b = 93.651(18)°.
	c = 21.189(5) Å	g = 90°.
Volume	1892.2(9) Å <sup>3</sup>	
Z	4	
Density (calculated)	1.458 Mg/m <sup>3</sup>	
Absorption coefficient	2.190 mm <sup>-1</sup>	
F(000)	856	
Crystal size	0.500 x 0.300 x 0.300 mm <sup>3</sup>	
Theta range for data collection	1.926 to 36.430°.	
Index ranges	-15 ≤ h ≤ 15, -15 ≤ k ≤ 15, -35 ≤ l ≤ 35	
Reflections collected	53031	
Independent reflections	9140 [R(int) = 0.0291]	
Completeness to theta = 25.242°	100.0 %	
Absorption correction	Semi-empirical from equivalents	
Max. and min. transmission	0.7471 and 0.5241	
Refinement method	Full-matrix least-squares on F <sup>2</sup>	
Data / restraints / parameters	9140 / 2 / 242	
Goodness-of-fit on F <sup>2</sup>	1.019	
Final R indices [I > 2σ(I)]	R1 = 0.0267, wR2 = 0.0680	
R indices (all data)	R1 = 0.0342, wR2 = 0.0710	
Extinction coefficient	n/a	
Largest diff. peak and hole	0.656 and -0.498 e.Å <sup>-3</sup>	

**Table A3.1.3** Atomic Coordinates ( $\times 10^4$ ) and Equivalent Isotropic Displacement Parameters ( $\text{\AA}^2 \times 10^3$ ) for Amine **69dn**.  $U(\text{eq})$  is Defined as One Third of the Orthogonalized  $U^{ij}$  Tensor.

	x	y	z	U(eq)
N(1)	8230(1)	6655(1)	5441(1)	14(1)
C(1)	8442(1)	7918(1)	5154(1)	13(1)
O(1)	8819(1)	9011(1)	5422(1)	17(1)
C(2)	8070(1)	7776(1)	4446(1)	12(1)
C(5)	6679(1)	8602(1)	4295(1)	16(1)
C(6)	5492(1)	8192(1)	4695(1)	18(1)
C(7)	4282(1)	7615(1)	4474(1)	22(1)
C(8)	9294(1)	8437(1)	4089(1)	12(1)
N(2)	10651(1)	7820(1)	4338(1)	17(1)
C(3)	7908(1)	6181(1)	4351(1)	16(1)
C(4)	7639(1)	5576(1)	5003(1)	16(1)
C(11)	8328(1)	6449(1)	6104(1)	13(1)
C(12)	7326(1)	5631(1)	6388(1)	16(1)
C(13)	7406(1)	5413(1)	7040(1)	17(1)
C(14)	8500(1)	6034(1)	7412(1)	15(1)
O(2)	8695(1)	5880(1)	8053(1)	19(1)
C(17)	7799(1)	4889(1)	8345(1)	21(1)
C(15)	9514(1)	6853(1)	7129(1)	16(1)
C(16)	9437(1)	7054(1)	6480(1)	16(1)
C(21)	9093(1)	8247(1)	3379(1)	12(1)
C(22)	9536(1)	7023(1)	3080(1)	15(1)
C(23)	9351(1)	6867(1)	2427(1)	15(1)
C(24)	8731(1)	7954(1)	2070(1)	14(1)
Br(1)	8522(1)	7739(1)	1178(1)	19(1)
C(25)	8286(1)	9187(1)	2350(1)	16(1)
C(26)	8473(1)	9320(1)	3003(1)	15(1)

**Table A3.1.4** Bond Lengths [ $\text{\AA}$ ] and angles [ $^\circ$ ] for Amine **69dn**

---

N(1)-C(1)	1.3643(11)
N(1)-C(11)	1.4161(12)
N(1)-C(4)	1.4671(12)
C(1)-O(1)	1.2236(10)
C(1)-C(2)	1.5262(13)
C(2)-C(3)	1.5333(12)
C(2)-C(5)	1.5441(13)
C(2)-C(8)	1.5522(12)
C(5)-C(6)	1.4984(13)
C(5)-H(5A)	0.9900
C(5)-H(5B)	0.9900
C(6)-C(7)	1.3239(14)
C(6)-H(6)	0.9500
C(7)-H(7A)	0.9500
C(7)-H(7B)	0.9500
C(8)-N(2)	1.4736(12)
C(8)-C(21)	1.5133(12)
C(8)-H(8)	1.0000
N(2)-H(2N1)	0.892(13)
N(2)-H(2N2)	0.909(14)
C(3)-C(4)	1.5319(13)
C(3)-H(3A)	0.9900
C(3)-H(3B)	0.9900
C(4)-H(4A)	0.9900
C(4)-H(4B)	0.9900
C(11)-C(12)	1.3890(12)
C(11)-C(16)	1.3969(13)
C(12)-C(13)	1.3948(13)
C(12)-H(12)	0.9500
C(13)-C(14)	1.3896(14)
C(13)-H(13)	0.9500
C(14)-O(2)	1.3658(11)
C(14)-C(15)	1.3956(13)

**Table A3.1.4 Cont.**

O(2)-C(17)	1.4311(13)
C(17)-H(17A)	0.9800
C(17)-H(17B)	0.9800
C(17)-H(17C)	0.9800
C(15)-C(16)	1.3860(13)
C(15)-H(15)	0.9500
C(16)-H(16)	0.9500
C(21)-C(26)	1.3978(12)
C(21)-C(22)	1.4005(12)
C(22)-C(23)	1.3903(13)
C(22)-H(22)	0.9500
C(23)-C(24)	1.3864(13)
C(23)-H(23)	0.9500
C(24)-C(25)	1.3891(12)
C(24)-Br(1)	1.8983(10)
C(25)-C(26)	1.3912(13)
C(25)-H(25)	0.9500
C(26)-H(26)	0.9500
C(1)-N(1)-C(11)	124.10(7)
C(1)-N(1)-C(4)	113.08(7)
C(11)-N(1)-C(4)	121.98(7)
O(1)-C(1)-N(1)	125.77(8)
O(1)-C(1)-C(2)	124.93(8)
N(1)-C(1)-C(2)	109.24(7)
C(1)-C(2)-C(3)	103.31(7)
C(1)-C(2)-C(5)	107.31(7)
C(3)-C(2)-C(5)	113.44(7)
C(1)-C(2)-C(8)	108.23(7)
C(3)-C(2)-C(8)	114.00(7)
C(5)-C(2)-C(8)	110.02(7)
C(6)-C(5)-C(2)	113.98(8)
C(6)-C(5)-H(5A)	108.8
C(2)-C(5)-H(5A)	108.8
C(6)-C(5)-H(5B)	108.8

**Table A3.1.4 Cont.**

C(2)-C(5)-H(5B)	108.8
H(5A)-C(5)-H(5B)	107.7
C(7)-C(6)-C(5)	124.43(9)
C(7)-C(6)-H(6)	117.8
C(5)-C(6)-H(6)	117.8
C(6)-C(7)-H(7A)	120.0
C(6)-C(7)-H(7B)	120.0
H(7A)-C(7)-H(7B)	120.0
N(2)-C(8)-C(21)	111.07(7)
N(2)-C(8)-C(2)	108.67(7)
C(21)-C(8)-C(2)	112.68(7)
N(2)-C(8)-H(8)	108.1
C(21)-C(8)-H(8)	108.1
C(2)-C(8)-H(8)	108.1
C(8)-N(2)-H(2N1)	110.0(10)
C(8)-N(2)-H(2N2)	112.8(11)
H(2N1)-N(2)-H(2N2)	100.0(14)
C(4)-C(3)-C(2)	105.86(7)
C(4)-C(3)-H(3A)	110.6
C(2)-C(3)-H(3A)	110.6
C(4)-C(3)-H(3B)	110.6
C(2)-C(3)-H(3B)	110.6
H(3A)-C(3)-H(3B)	108.7
N(1)-C(4)-C(3)	103.35(7)
N(1)-C(4)-H(4A)	111.1
C(3)-C(4)-H(4A)	111.1
N(1)-C(4)-H(4B)	111.1
C(3)-C(4)-H(4B)	111.1
H(4A)-C(4)-H(4B)	109.1
C(12)-C(11)-C(16)	119.25(8)
C(12)-C(11)-N(1)	120.15(8)
C(16)-C(11)-N(1)	120.60(8)
C(11)-C(12)-C(13)	121.04(8)
C(11)-C(12)-H(12)	119.5
C(13)-C(12)-H(12)	119.5



**Table A3.1.4 Cont.**

C(14)-C(13)-C(12)	119.40(8)
C(14)-C(13)-H(13)	120.3
C(12)-C(13)-H(13)	120.3
O(2)-C(14)-C(13)	124.54(8)
O(2)-C(14)-C(15)	115.67(8)
C(13)-C(14)-C(15)	119.77(8)
C(14)-O(2)-C(17)	117.01(8)
O(2)-C(17)-H(17A)	109.5
O(2)-C(17)-H(17B)	109.5
H(17A)-C(17)-H(17B)	109.5
O(2)-C(17)-H(17C)	109.5
H(17A)-C(17)-H(17C)	109.5
H(17B)-C(17)-H(17C)	109.5
C(16)-C(15)-C(14)	120.58(8)
C(16)-C(15)-H(15)	119.7
C(14)-C(15)-H(15)	119.7
C(15)-C(16)-C(11)	119.95(8)
C(15)-C(16)-H(16)	120.0
C(11)-C(16)-H(16)	120.0
C(26)-C(21)-C(22)	118.13(8)
C(26)-C(21)-C(8)	120.03(7)
C(22)-C(21)-C(8)	121.83(8)
C(23)-C(22)-C(21)	121.14(8)
C(23)-C(22)-H(22)	119.4
C(21)-C(22)-H(22)	119.4
C(24)-C(23)-C(22)	119.08(8)
C(24)-C(23)-H(23)	120.5
C(22)-C(23)-H(23)	120.5
C(23)-C(24)-C(25)	121.45(8)
C(23)-C(24)-Br(1)	118.52(6)
C(25)-C(24)-Br(1)	120.03(7)
C(24)-C(25)-C(26)	118.61(8)
C(24)-C(25)-H(25)	120.7
C(26)-C(25)-H(25)	120.7
C(25)-C(26)-C(21)	121.58(8)

**Table A3.1.4 Cont.**

C(25)-C(26)-H(26)	119.2
C(21)-C(26)-H(26)	119.2

---

Symmetry transformations used to generate equivalent atoms:

**Table A3.1.5** Anisotropic Displacement Parameters ( $\text{\AA}^2 \times 10^3$ ) for Amine **69dn**. The

Anisotropic Displacement Factor Exponent Takes the Form:  $-2p^2[h^2a^*2U^{11} + \dots + 2hka^*b^*U^{12}]$ .

	U <sup>11</sup>	U <sup>22</sup>	U <sup>33</sup>	U <sup>23</sup>	U <sup>13</sup>	U <sup>12</sup>
N(1)	19(1)	12(1)	11(1)	0(1)	-1(1)	-4(1)
C(1)	14(1)	12(1)	12(1)	0(1)	1(1)	-3(1)
O(1)	23(1)	13(1)	15(1)	-3(1)	2(1)	-6(1)
C(2)	14(1)	11(1)	12(1)	0(1)	1(1)	-3(1)
C(5)	13(1)	19(1)	16(1)	3(1)	2(1)	-2(1)
C(6)	14(1)	23(1)	16(1)	3(1)	2(1)	-2(1)
C(7)	15(1)	27(1)	24(1)	7(1)	0(1)	-4(1)
C(8)	12(1)	12(1)	13(1)	0(1)	1(1)	-2(1)
N(2)	14(1)	20(1)	17(1)	0(1)	-1(1)	0(1)
C(3)	24(1)	13(1)	13(1)	-1(1)	1(1)	-6(1)
C(4)	22(1)	12(1)	14(1)	0(1)	-1(1)	-6(1)
C(11)	15(1)	14(1)	12(1)	1(1)	0(1)	-1(1)
C(12)	16(1)	19(1)	14(1)	1(1)	0(1)	-5(1)
C(13)	17(1)	20(1)	14(1)	1(1)	3(1)	-3(1)
C(14)	16(1)	15(1)	12(1)	1(1)	1(1)	2(1)
O(2)	25(1)	20(1)	11(1)	1(1)	1(1)	-1(1)
C(17)	25(1)	24(1)	15(1)	3(1)	7(1)	1(1)
C(15)	16(1)	18(1)	14(1)	1(1)	-2(1)	-2(1)
C(16)	15(1)	18(1)	14(1)	2(1)	-1(1)	-4(1)
C(21)	12(1)	11(1)	13(1)	0(1)	2(1)	-1(1)
C(22)	17(1)	12(1)	15(1)	1(1)	3(1)	2(1)
C(23)	17(1)	13(1)	15(1)	0(1)	4(1)	3(1)
C(24)	16(1)	14(1)	12(1)	0(1)	3(1)	1(1)
Br(1)	28(1)	18(1)	12(1)	0(1)	3(1)	4(1)
C(25)	22(1)	14(1)	14(1)	2(1)	3(1)	4(1)
C(26)	19(1)	12(1)	14(1)	0(1)	3(1)	2(1)

**Table A3.1.6** Hydrogen Coordinates ( $\times 10^4$ ) and Isotropic Displacement Parameters ( $\text{\AA}^2 \times 10^3$ ) for Amine **69dn**.

	x	y	z	U(eq)
H(5A)	6873	9621	4354	19
H(5B)	6368	8452	3845	19
H(6)	5616	8357	5137	21
H(7A)	4123	7435	4034	26
H(7B)	3573	7380	4755	26
H(8)	9320	9471	4180	15
H(2N1)	11033(16)	8353(16)	4651(7)	25
H(2N2)	11345(16)	7879(17)	4060(8)	25
H(3A)	7099	5970	4045	20
H(3B)	8783	5774	4192	20
H(4A)	6610	5442	5051	19
H(4B)	8132	4663	5073	19
H(12)	6573	5214	6133	20
H(13)	6719	4844	7228	21
H(17A)	6805	5182	8275	32
H(17B)	8056	4852	8800	32
H(17C)	7923	3954	8160	32
H(15)	10262	7275	7384	19
H(16)	10139	7602	6291	19
H(22)	9970	6286	3326	17
H(23)	9646	6028	2229	18
H(25)	7863	9925	2100	19
H(26)	8171	10159	3199	18

**Table A3.1.7** Torsion Angles [°] for Amine **69dn**.

---

C(11)-N(1)-C(1)-O(1)	4.40(14)
C(4)-N(1)-C(1)-O(1)	174.10(9)
C(11)-N(1)-C(1)-C(2)	-173.11(8)
C(4)-N(1)-C(1)-C(2)	-3.42(10)
O(1)-C(1)-C(2)-C(3)	171.34(9)
N(1)-C(1)-C(2)-C(3)	-11.12(9)
O(1)-C(1)-C(2)-C(5)	-68.54(11)
N(1)-C(1)-C(2)-C(5)	109.00(8)
O(1)-C(1)-C(2)-C(8)	50.15(11)
N(1)-C(1)-C(2)-C(8)	-132.31(7)
C(1)-C(2)-C(5)-C(6)	-53.25(10)
C(3)-C(2)-C(5)-C(6)	60.20(10)
C(8)-C(2)-C(5)-C(6)	-170.78(8)
C(2)-C(5)-C(6)-C(7)	-116.39(11)
C(1)-C(2)-C(8)-N(2)	51.73(9)
C(3)-C(2)-C(8)-N(2)	-62.58(9)
C(5)-C(2)-C(8)-N(2)	168.70(7)
C(1)-C(2)-C(8)-C(21)	175.27(7)
C(3)-C(2)-C(8)-C(21)	60.95(10)
C(5)-C(2)-C(8)-C(21)	-67.77(9)
C(1)-C(2)-C(3)-C(4)	20.57(9)
C(5)-C(2)-C(3)-C(4)	-95.27(9)
C(8)-C(2)-C(3)-C(4)	137.77(8)
C(1)-N(1)-C(4)-C(3)	16.44(10)
C(11)-N(1)-C(4)-C(3)	-173.62(8)
C(2)-C(3)-C(4)-N(1)	-22.45(10)
C(1)-N(1)-C(11)-C(12)	137.17(9)
C(4)-N(1)-C(11)-C(12)	-31.65(13)
C(1)-N(1)-C(11)-C(16)	-43.40(13)
C(4)-N(1)-C(11)-C(16)	147.79(9)
C(16)-C(11)-C(12)-C(13)	0.39(14)
N(1)-C(11)-C(12)-C(13)	179.83(9)
C(11)-C(12)-C(13)-C(14)	0.55(15)

**Table A3.1.7 Cont.**

C(12)-C(13)-C(14)-O(2)	-179.15(9)
C(12)-C(13)-C(14)-C(15)	-0.80(14)
C(13)-C(14)-O(2)-C(17)	7.12(13)
C(15)-C(14)-O(2)-C(17)	-171.29(8)
O(2)-C(14)-C(15)-C(16)	178.62(8)
C(13)-C(14)-C(15)-C(16)	0.13(14)
C(14)-C(15)-C(16)-C(11)	0.81(14)
C(12)-C(11)-C(16)-C(15)	-1.06(14)
N(1)-C(11)-C(16)-C(15)	179.49(9)
N(2)-C(8)-C(21)-C(26)	-141.92(8)
C(2)-C(8)-C(21)-C(26)	95.89(9)
N(2)-C(8)-C(21)-C(22)	36.94(11)
C(2)-C(8)-C(21)-C(22)	-85.25(10)
C(26)-C(21)-C(22)-C(23)	-0.73(13)
C(8)-C(21)-C(22)-C(23)	-179.61(8)
C(21)-C(22)-C(23)-C(24)	0.71(13)
C(22)-C(23)-C(24)-C(25)	-0.30(14)
C(22)-C(23)-C(24)-Br(1)	178.74(7)
C(23)-C(24)-C(25)-C(26)	-0.06(14)
Br(1)-C(24)-C(25)-C(26)	-179.09(7)
C(24)-C(25)-C(26)-C(21)	0.03(14)
C(22)-C(21)-C(26)-C(25)	0.35(13)
C(8)-C(21)-C(26)-C(25)	179.25(8)

---

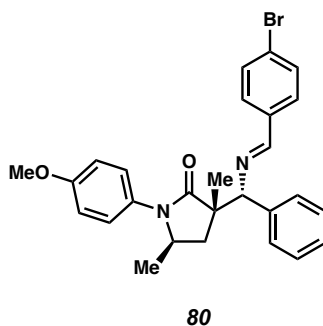
Symmetry transformations used to generate equivalent atoms:

**Table A3.1.8** Hydrogen Bonds for Amine **69dn** [ $\text{\AA}$  and  $^\circ$ ].

D-H...A	d(D-H)	d(H...A)	d(D...A)	<(DHA)
C(8)-H(8)...O(1)#1	1.00	2.38	3.1416(12)	132.1
N(2)-H(2N1)...O(1)#1	0.892(13)	2.511(16)	3.0855(13)	122.6(13)
C(17)-H(17B)...O(1)#2	0.98	2.62	3.2190(14)	119.7
C(23)-H(23)...O(2)#3	0.95	2.49	3.3858(13)	157.1

Symmetry transformations used to generate equivalent atoms:

#1  $-x+2, -y+2, -z+1$  #2  $-x+3/2, y-1/2, -z+3/2$  #3  $-x+2, -y+1, -z+1$

**A3.2 X-RAY CRYSTAL STRUCTURE ANALYSIS OF IMINE 80**Contents

*Table A3.2.1. Experimental Details*

*Table A3.2.2. Crystal Data*

*Table A3.2.3. Atomic Coordinates*

*Table A3.2.4. Full Bond Distances and Angles*

*Table A3.2.5. Anisotropic Displacement Parameters*

*Table A3.2.6. Hydrogen Atomic Coordinates*

*Table A3.2.7. Torsion Angles*

**Figure A3.2.1** X-Ray Crystal Structure of Imine **80**.

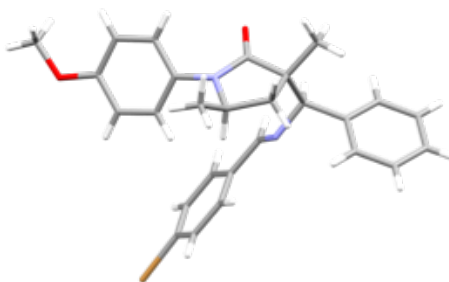




**Table A3.2.1** Experimental Details for X-Ray Structure Determination of Imine **80**.

Low-temperature diffraction data ( $\phi$ - and  $\omega$ -scans) were collected on a Bruker AXS D8 VENTURE KAPPA diffractometer coupled to a PHOTON II CPAD detector with Cu  $K_{\alpha}$  radiation ( $\lambda = 1.54178 \text{ \AA}$ ) from an I $\mu$ S micro-source for the structure of compound **80**. The structure was solved by direct methods using SHELXS and refined against  $F^2$  on all data by full-matrix least squares with SHELXL-2017 using established refinement techniques. All non-hydrogen atoms were refined anisotropically. All hydrogen atoms were included into the model at geometrically calculated positions and refined using a riding model. The isotropic displacement parameters of all hydrogen atoms were fixed to 1.2 times the  $U$  value of the atoms they are linked to (1.5 times for methyl groups).

Compound **80** crystallizes in the monoclinic space group  $P2_1/c$  with two molecules in the asymmetric unit. The crystal is not stable at lower temperatures and the data was collected at 200K.

**Table A3.2.2** Crystal Data and Structure Refinement for Imine **80**.

Identification code	V20240	
Empirical formula	C <sub>27</sub> H <sub>27</sub> Br N <sub>2</sub> O <sub>2</sub>	
Formula weight	491.41	
Temperature	200(2) K	
Wavelength	1.54178 Å	
Crystal system	Monoclinic	
Space group	P2 <sub>1</sub> /c	
Unit cell dimensions	a = 11.8500(11) Å	a = 90°.
	b = 49.858(4) Å	b = 90.083(7)°.
	c = 8.0771(10) Å	g = 90°.
Volume	4772.1(8) Å <sup>3</sup>	
Z	8	
Density (calculated)	1.368 Mg/m <sup>3</sup>	
Absorption coefficient	2.548 mm <sup>-1</sup>	
F(000)	2032	
Crystal size	0.300 x 0.250 x 0.050 mm <sup>3</sup>	
Theta range for data collection	3.546 to 74.545°.	
Index ranges	-14 ≤ h ≤ 14, -62 ≤ k ≤ 62, -9 ≤ l ≤ 10	
Reflections collected	75046	
Independent reflections	9652 [R(int) = 0.0709]	
Completeness to theta = 67.679°	99.5 %	
Absorption correction	Semi-empirical from equivalents	
Max. and min. transmission	0.7538 and 0.4919	
Refinement method	Full-matrix least-squares on F <sup>2</sup>	
Data / restraints / parameters	9652 / 0 / 583	
Goodness-of-fit on F <sup>2</sup>	1.149	
Final R indices [I > 2σ(I)]	R1 = 0.0679, wR2 = 0.1654	
R indices (all data)	R1 = 0.0732, wR2 = 0.1686	
Extinction coefficient	n/a	
Largest diff. peak and hole	1.211 and -0.757 e.Å <sup>-3</sup>	

**Table A3.2.3** Atomic Coordinates ( $\times 10^4$ ) and Equivalent Isotropic Displacement Parameters ( $\text{\AA}^2 \times 10^3$ ) for Imine **80**.  $U(\text{eq})$  is Defined as One Third of the Trace of the Orthogonalized  $U^{ij}$  Tensor.

	x	y	z	U(eq)
N(1)	3314(3)	1358(1)	2404(4)	33(1)
C(11)	3013(3)	1088(1)	1978(5)	31(1)
C(12)	2057(3)	1035(1)	1048(5)	34(1)
C(13)	1748(3)	771(1)	684(5)	34(1)
C(14)	2413(3)	562(1)	1246(5)	33(1)
O(2)	2215(2)	295(1)	957(4)	42(1)
C(17)	1255(5)	225(1)	23(8)	64(2)
C(15)	3362(3)	617(1)	2186(5)	38(1)
C(16)	3664(3)	877(1)	2558(5)	37(1)
C(1)	2622(3)	1522(1)	3282(5)	33(1)
O(1)	1619(2)	1488(1)	3541(4)	40(1)
C(2)	3329(3)	1753(1)	3990(5)	34(1)
C(5)	2701(4)	2018(1)	3839(6)	46(1)
C(6)	3497(3)	1678(1)	5860(5)	31(1)
C(21)	4009(3)	1902(1)	6899(5)	32(1)
C(22)	5144(3)	1968(1)	6879(5)	37(1)
C(23)	5558(4)	2170(1)	7894(6)	44(1)
C(24)	4857(4)	2306(1)	8962(5)	48(1)
C(25)	3728(4)	2240(1)	9013(6)	52(1)
C(26)	3306(4)	2041(1)	7989(6)	43(1)
N(2)	4233(3)	1440(1)	5976(4)	30(1)
C(7)	3812(3)	1236(1)	6687(4)	31(1)
C(31)	4457(3)	986(1)	6876(4)	30(1)
C(32)	5529(3)	955(1)	6229(5)	34(1)
C(33)	6128(3)	719(1)	6433(5)	37(1)
C(34)	5633(3)	511(1)	7316(5)	33(1)
Br(1)	6462(1)	190(1)	7684(1)	47(1)
C(35)	4570(4)	534(1)	7954(5)	39(1)

**Table A3.2.3 Cont.**

C(36)	3973(4)	771(1)	7725(5)	39(1)
C(3)	4401(3)	1742(1)	2950(5)	36(1)
C(4)	4490(3)	1455(1)	2267(5)	34(1)
C(8)	4896(4)	1443(1)	485(5)	44(1)
N(201)	9412(3)	1360(1)	-2554(4)	35(1)
C(211)	9711(3)	1091(1)	-2970(5)	34(1)
C(212)	9050(3)	879(1)	-2431(5)	38(1)
C(213)	9334(3)	618(1)	-2792(5)	38(1)
C(214)	10298(3)	566(1)	-3726(5)	35(1)
O(202)	10490(3)	299(1)	-4048(4)	45(1)
C(217)	11414(5)	233(1)	-5088(7)	62(1)
C(215)	10976(3)	774(1)	-4267(5)	37(1)
C(216)	10669(3)	1039(1)	-3895(5)	36(1)
C(201)	10110(3)	1527(1)	-1683(5)	33(1)
O(201)	11119(2)	1493(1)	-1448(4)	39(1)
C(202)	9405(3)	1757(1)	-978(5)	34(1)
C(205)	10040(4)	2023(1)	-1132(6)	47(1)
C(206)	9246(3)	1683(1)	894(5)	32(1)
C(221)	8727(3)	1907(1)	1943(5)	35(1)
C(222)	7591(3)	1969(1)	1908(5)	39(1)
C(223)	7156(4)	2169(1)	2921(6)	46(1)
C(224)	7863(4)	2308(1)	3990(6)	50(1)
C(225)	8990(4)	2244(1)	4048(6)	53(1)
C(226)	9424(4)	2045(1)	3030(6)	46(1)
N(202)	8528(3)	1444(1)	1018(4)	32(1)
C(207)	8962(3)	1240(1)	1713(4)	32(1)
C(231)	8320(3)	989(1)	1888(4)	31(1)
C(232)	8844(4)	767(1)	2627(5)	42(1)
C(233)	8246(4)	528(1)	2840(6)	46(1)
C(234)	7158(4)	511(1)	2269(5)	38(1)
Br(2)	6311(1)	193(1)	2601(1)	61(1)
C(235)	6628(4)	726(1)	1500(5)	42(1)
C(236)	7225(3)	962(1)	1317(5)	39(1)
C(203)	8322(3)	1744(1)	-2017(5)	38(1)
C(204)	8239(3)	1458(1)	-2693(5)	36(1)

**Table A3.2.3 Cont.**

C(208)	7826(4)	1444(1)	-4468(5)	46(1)
--------	---------	---------	----------	-------

---

**Table A3.2.4** Bond Lengths [ $\text{\AA}$ ] and angles [ $^\circ$ ] for Imine **80**.

---

N(1)-C(1)	1.358(5)
N(1)-C(11)	1.434(5)
N(1)-C(4)	1.479(5)
C(11)-C(12)	1.384(5)
C(11)-C(16)	1.384(5)
C(12)-C(13)	1.397(5)
C(12)-H(12)	0.9500
C(13)-C(14)	1.383(5)
C(13)-H(13)	0.9500
C(14)-O(2)	1.375(4)
C(14)-C(15)	1.382(5)
O(2)-C(17)	1.406(5)
C(17)-H(17A)	0.9800
C(17)-H(17B)	0.9800
C(17)-H(17C)	0.9800
C(15)-C(16)	1.380(5)
C(15)-H(15)	0.9500
C(16)-H(16)	0.9500
C(1)-O(1)	1.219(5)
C(1)-C(2)	1.535(5)
C(2)-C(5)	1.522(5)
C(2)-C(3)	1.525(6)
C(2)-C(6)	1.568(5)
C(5)-H(5A)	0.9800
C(5)-H(5B)	0.9800
C(5)-H(5C)	0.9800
C(6)-N(2)	1.476(4)
C(6)-C(21)	1.523(5)
C(6)-H(6)	1.0000
C(21)-C(22)	1.385(5)
C(21)-C(26)	1.395(6)
C(22)-C(23)	1.388(5)
C(22)-H(22)	0.9500

**Table A3.2.4 Cont.**

C(23)-C(24)	1.378(7)
C(23)-H(23)	0.9500
C(24)-C(25)	1.378(7)
C(24)-H(24)	0.9500
C(25)-C(26)	1.388(6)
C(25)-H(25)	0.9500
C(26)-H(26)	0.9500
N(2)-C(7)	1.272(5)
C(7)-C(31)	1.470(5)
C(7)-H(7)	0.9500
C(31)-C(32)	1.383(5)
C(31)-C(36)	1.394(5)
C(32)-C(33)	1.385(5)
C(32)-H(32)	0.9500
C(33)-C(34)	1.388(5)
C(33)-H(33)	0.9500
C(34)-C(35)	1.367(6)
C(34)-Br(1)	1.901(4)
C(35)-C(36)	1.390(6)
C(35)-H(35)	0.9500
C(36)-H(36)	0.9500
C(3)-C(4)	1.538(5)
C(3)-H(3A)	0.9900
C(3)-H(3B)	0.9900
C(4)-C(8)	1.519(6)
C(4)-H(4)	1.0000
C(8)-H(8A)	0.9800
C(8)-H(8B)	0.9800
C(8)-H(8C)	0.9800
N(201)-C(201)	1.368(5)
N(201)-C(211)	1.425(5)
N(201)-C(204)	1.476(5)
C(211)-C(216)	1.384(5)
C(211)-C(212)	1.387(5)
C(212)-C(213)	1.377(6)

**Table A3.2.4 Cont.**

C(212)-H(212)	0.9500
C(213)-C(214)	1.395(6)
C(213)-H(213)	0.9500
C(214)-O(202)	1.376(5)
C(214)-C(215)	1.385(6)
O(202)-C(217)	1.419(5)
C(217)-H(21A)	0.9800
C(217)-H(21B)	0.9800
C(217)-H(21C)	0.9800
C(215)-C(216)	1.403(5)
C(215)-H(215)	0.9500
C(216)-H(216)	0.9500
C(201)-O(201)	1.222(5)
C(201)-C(202)	1.531(5)
C(202)-C(205)	1.530(5)
C(202)-C(203)	1.534(5)
C(202)-C(206)	1.568(5)
C(205)-H(20A)	0.9800
C(205)-H(20B)	0.9800
C(205)-H(20C)	0.9800
C(206)-N(202)	1.470(5)
C(206)-C(221)	1.528(5)
C(206)-H(206)	1.0000
C(221)-C(222)	1.382(6)
C(221)-C(226)	1.387(6)
C(222)-C(223)	1.389(6)
C(222)-H(222)	0.9500
C(223)-C(224)	1.390(7)
C(223)-H(223)	0.9500
C(224)-C(225)	1.374(7)
C(224)-H(224)	0.9500
C(225)-C(226)	1.389(7)
C(225)-H(225)	0.9500
C(226)-H(226)	0.9500
N(202)-C(207)	1.270(5)



**Table A3.2.4 Cont.**

C(207)-C(231)	1.472(5)
C(207)-H(207)	0.9500
C(231)-C(236)	1.383(5)
C(231)-C(232)	1.400(5)
C(232)-C(233)	1.396(6)
C(232)-H(232)	0.9500
C(233)-C(234)	1.371(6)
C(233)-H(233)	0.9500
C(234)-C(235)	1.385(6)
C(234)-Br(2)	1.897(4)
C(235)-C(236)	1.385(6)
C(235)-H(235)	0.9500
C(236)-H(236)	0.9500
C(203)-C(204)	1.533(5)
C(203)-H(20D)	0.9900
C(203)-H(20E)	0.9900
C(204)-C(208)	1.516(6)
C(204)-H(204)	1.0000
C(208)-H(20F)	0.9800
C(208)-H(20G)	0.9800
C(208)-H(20H)	0.9800
C(1)-N(1)-C(11)	122.7(3)
C(1)-N(1)-C(4)	114.4(3)
C(11)-N(1)-C(4)	121.4(3)
C(12)-C(11)-C(16)	119.6(3)
C(12)-C(11)-N(1)	120.7(3)
C(16)-C(11)-N(1)	119.6(3)
C(11)-C(12)-C(13)	120.5(3)
C(11)-C(12)-H(12)	119.8
C(13)-C(12)-H(12)	119.8
C(14)-C(13)-C(12)	119.5(3)
C(14)-C(13)-H(13)	120.3
C(12)-C(13)-H(13)	120.3
O(2)-C(14)-C(15)	115.0(3)

**Table A3.2.4 Cont.**

O(2)-C(14)-C(13)	125.3(3)
C(15)-C(14)-C(13)	119.6(3)
C(14)-O(2)-C(17)	117.9(3)
O(2)-C(17)-H(17A)	109.5
O(2)-C(17)-H(17B)	109.5
H(17A)-C(17)-H(17B)	109.5
O(2)-C(17)-H(17C)	109.5
H(17A)-C(17)-H(17C)	109.5
H(17B)-C(17)-H(17C)	109.5
C(16)-C(15)-C(14)	121.0(3)
C(16)-C(15)-H(15)	119.5
C(14)-C(15)-H(15)	119.5
C(15)-C(16)-C(11)	119.7(3)
C(15)-C(16)-H(16)	120.1
C(11)-C(16)-H(16)	120.1
O(1)-C(1)-N(1)	126.5(3)
O(1)-C(1)-C(2)	125.0(4)
N(1)-C(1)-C(2)	108.5(3)
C(5)-C(2)-C(3)	113.3(3)
C(5)-C(2)-C(1)	110.8(3)
C(3)-C(2)-C(1)	102.8(3)
C(5)-C(2)-C(6)	110.2(3)
C(3)-C(2)-C(6)	114.7(3)
C(1)-C(2)-C(6)	104.4(3)
C(2)-C(5)-H(5A)	109.5
C(2)-C(5)-H(5B)	109.5
H(5A)-C(5)-H(5B)	109.5
C(2)-C(5)-H(5C)	109.5
H(5A)-C(5)-H(5C)	109.5
H(5B)-C(5)-H(5C)	109.5
N(2)-C(6)-C(21)	108.6(3)
N(2)-C(6)-C(2)	109.1(3)
C(21)-C(6)-C(2)	114.0(3)
N(2)-C(6)-H(6)	108.3
C(21)-C(6)-H(6)	108.3

**Table A3.2.4 Cont.**

C(2)-C(6)-H(6)	108.3
C(22)-C(21)-C(26)	118.2(4)
C(22)-C(21)-C(6)	123.6(3)
C(26)-C(21)-C(6)	118.2(3)
C(21)-C(22)-C(23)	120.5(4)
C(21)-C(22)-H(22)	119.8
C(23)-C(22)-H(22)	119.8
C(24)-C(23)-C(22)	121.0(4)
C(24)-C(23)-H(23)	119.5
C(22)-C(23)-H(23)	119.5
C(23)-C(24)-C(25)	119.2(4)
C(23)-C(24)-H(24)	120.4
C(25)-C(24)-H(24)	120.4
C(24)-C(25)-C(26)	120.1(4)
C(24)-C(25)-H(25)	119.9
C(26)-C(25)-H(25)	119.9
C(25)-C(26)-C(21)	121.0(4)
C(25)-C(26)-H(26)	119.5
C(21)-C(26)-H(26)	119.5
C(7)-N(2)-C(6)	116.2(3)
N(2)-C(7)-C(31)	121.5(3)
N(2)-C(7)-H(7)	119.2
C(31)-C(7)-H(7)	119.2
C(32)-C(31)-C(36)	118.6(3)
C(32)-C(31)-C(7)	122.1(3)
C(36)-C(31)-C(7)	119.2(3)
C(31)-C(32)-C(33)	121.4(3)
C(31)-C(32)-H(32)	119.3
C(33)-C(32)-H(32)	119.3
C(32)-C(33)-C(34)	118.6(4)
C(32)-C(33)-H(33)	120.7
C(34)-C(33)-H(33)	120.7
C(35)-C(34)-C(33)	121.4(3)
C(35)-C(34)-Br(1)	119.2(3)
C(33)-C(34)-Br(1)	119.3(3)

**Table A3.2.4 Cont.**

C(34)-C(35)-C(36)	119.4(3)
C(34)-C(35)-H(35)	120.3
C(36)-C(35)-H(35)	120.3
C(35)-C(36)-C(31)	120.6(4)
C(35)-C(36)-H(36)	119.7
C(31)-C(36)-H(36)	119.7
C(2)-C(3)-C(4)	106.8(3)
C(2)-C(3)-H(3A)	110.4
C(4)-C(3)-H(3A)	110.4
C(2)-C(3)-H(3B)	110.4
C(4)-C(3)-H(3B)	110.4
H(3A)-C(3)-H(3B)	108.6
N(1)-C(4)-C(8)	111.0(3)
N(1)-C(4)-C(3)	102.2(3)
C(8)-C(4)-C(3)	113.5(3)
N(1)-C(4)-H(4)	110.0
C(8)-C(4)-H(4)	110.0
C(3)-C(4)-H(4)	110.0
C(4)-C(8)-H(8A)	109.5
C(4)-C(8)-H(8B)	109.5
H(8A)-C(8)-H(8B)	109.5
C(4)-C(8)-H(8C)	109.5
H(8A)-C(8)-H(8C)	109.5
H(8B)-C(8)-H(8C)	109.5
C(201)-N(201)-C(211)	122.8(3)
C(201)-N(201)-C(204)	114.0(3)
C(211)-N(201)-C(204)	121.8(3)
C(216)-C(211)-C(212)	119.3(4)
C(216)-C(211)-N(201)	120.6(3)
C(212)-C(211)-N(201)	120.1(3)
C(213)-C(212)-C(211)	121.2(4)
C(213)-C(212)-H(212)	119.4
C(211)-C(212)-H(212)	119.4
C(212)-C(213)-C(214)	119.4(4)
C(212)-C(213)-H(213)	120.3

**Table A3.2.4 Cont.**

C(214)-C(213)-H(213)	120.3
O(202)-C(214)-C(215)	124.8(4)
O(202)-C(214)-C(213)	114.8(3)
C(215)-C(214)-C(213)	120.5(4)
C(214)-O(202)-C(217)	117.6(3)
O(202)-C(217)-H(21A)	109.5
O(202)-C(217)-H(21B)	109.5
H(21A)-C(217)-H(21B)	109.5
O(202)-C(217)-H(21C)	109.5
H(21A)-C(217)-H(21C)	109.5
H(21B)-C(217)-H(21C)	109.5
C(214)-C(215)-C(216)	119.2(4)
C(214)-C(215)-H(215)	120.4
C(216)-C(215)-H(215)	120.4
C(211)-C(216)-C(215)	120.4(4)
C(211)-C(216)-H(216)	119.8
C(215)-C(216)-H(216)	119.8
O(201)-C(201)-N(201)	126.0(3)
O(201)-C(201)-C(202)	125.5(3)
N(201)-C(201)-C(202)	108.5(3)
C(205)-C(202)-C(201)	110.6(3)
C(205)-C(202)-C(203)	113.8(3)
C(201)-C(202)-C(203)	102.8(3)
C(205)-C(202)-C(206)	110.0(3)
C(201)-C(202)-C(206)	104.4(3)
C(203)-C(202)-C(206)	114.5(3)
C(202)-C(205)-H(20A)	109.5
C(202)-C(205)-H(20B)	109.5
H(20A)-C(205)-H(20B)	109.5
C(202)-C(205)-H(20C)	109.5
H(20A)-C(205)-H(20C)	109.5
H(20B)-C(205)-H(20C)	109.5
N(202)-C(206)-C(221)	108.7(3)
N(202)-C(206)-C(202)	109.0(3)
C(221)-C(206)-C(202)	114.4(3)

**Table A3.2.4 Cont.**

N(202)-C(206)-H(206)	108.2
C(221)-C(206)-H(206)	108.2
C(202)-C(206)-H(206)	108.2
C(222)-C(221)-C(226)	118.7(4)
C(222)-C(221)-C(206)	123.0(3)
C(226)-C(221)-C(206)	118.2(4)
C(221)-C(222)-C(223)	120.8(4)
C(221)-C(222)-H(222)	119.6
C(223)-C(222)-H(222)	119.6
C(222)-C(223)-C(224)	120.1(4)
C(222)-C(223)-H(223)	120.0
C(224)-C(223)-H(223)	120.0
C(225)-C(224)-C(223)	119.3(4)
C(225)-C(224)-H(224)	120.3
C(223)-C(224)-H(224)	120.3
C(224)-C(225)-C(226)	120.5(4)
C(224)-C(225)-H(225)	119.7
C(226)-C(225)-H(225)	119.7
C(221)-C(226)-C(225)	120.6(4)
C(221)-C(226)-H(226)	119.7
C(225)-C(226)-H(226)	119.7
C(207)-N(202)-C(206)	116.6(3)
N(202)-C(207)-C(231)	121.0(3)
N(202)-C(207)-H(207)	119.5
C(231)-C(207)-H(207)	119.5
C(236)-C(231)-C(232)	118.9(3)
C(236)-C(231)-C(207)	122.2(3)
C(232)-C(231)-C(207)	118.9(3)
C(233)-C(232)-C(231)	120.0(4)
C(233)-C(232)-H(232)	120.0
C(231)-C(232)-H(232)	120.0
C(234)-C(233)-C(232)	119.2(4)
C(234)-C(233)-H(233)	120.4
C(232)-C(233)-H(233)	120.4
C(233)-C(234)-C(235)	122.0(4)

**Table A3.2.4 Cont.**

C(233)-C(234)-Br(2)	120.1(3)
C(235)-C(234)-Br(2)	117.9(3)
C(234)-C(235)-C(236)	118.2(4)
C(234)-C(235)-H(235)	120.9
C(236)-C(235)-H(235)	120.9
C(231)-C(236)-C(235)	121.7(4)
C(231)-C(236)-H(236)	119.2
C(235)-C(236)-H(236)	119.2
C(204)-C(203)-C(202)	106.7(3)
C(204)-C(203)-H(20D)	110.4
C(202)-C(203)-H(20D)	110.4
C(204)-C(203)-H(20E)	110.4
C(202)-C(203)-H(20E)	110.4
H(20D)-C(203)-H(20E)	108.6
N(201)-C(204)-C(208)	111.1(3)
N(201)-C(204)-C(203)	102.8(3)
C(208)-C(204)-C(203)	113.6(3)
N(201)-C(204)-H(204)	109.7
C(208)-C(204)-H(204)	109.7
C(203)-C(204)-H(204)	109.7
C(204)-C(208)-H(20F)	109.5
C(204)-C(208)-H(20G)	109.5
H(20F)-C(208)-H(20G)	109.5
C(204)-C(208)-H(20H)	109.5
H(20F)-C(208)-H(20H)	109.5
H(20G)-C(208)-H(20H)	109.5

---

Symmetry transformations used to generate equivalent atoms:

**Table A3.2.5** Anisotropic Displacement Parameters ( $\text{\AA}^2 \times 10^3$ ) for Imine **80**. The

Anisotropic Displacement Factor Exponent Takes the Form:  $-2p^2[h^2a^{*2}U^{11} + \dots + 2hka^*b^*U^{12}]$ .

	U <sup>11</sup>	U <sup>22</sup>	U <sup>33</sup>	U <sup>23</sup>	U <sup>13</sup>	U <sup>12</sup>
N(1)	28(2)	30(2)	41(2)	1(1)	-4(1)	-3(1)
C(11)	28(2)	32(2)	34(2)	2(1)	-2(1)	-2(1)
C(12)	31(2)	32(2)	39(2)	0(2)	-6(2)	3(1)
C(13)	28(2)	38(2)	37(2)	-1(2)	-7(2)	-5(2)
C(14)	35(2)	28(2)	36(2)	0(1)	0(2)	-4(1)
O(2)	48(2)	29(1)	50(2)	-3(1)	-13(1)	-4(1)
C(17)	65(3)	40(2)	87(4)	-14(2)	-34(3)	-7(2)
C(15)	39(2)	31(2)	45(2)	6(2)	-11(2)	5(2)
C(16)	30(2)	38(2)	42(2)	0(2)	-13(2)	-2(2)
C(1)	28(2)	31(2)	40(2)	6(2)	-7(2)	-1(1)
O(1)	28(1)	38(1)	53(2)	-1(1)	-5(1)	-1(1)
C(2)	30(2)	27(2)	45(2)	5(2)	-8(2)	-2(1)
C(5)	48(2)	32(2)	60(3)	6(2)	-15(2)	3(2)
C(6)	24(2)	28(2)	41(2)	1(1)	-2(1)	-2(1)
C(21)	31(2)	27(2)	37(2)	2(1)	0(2)	0(1)
C(22)	33(2)	34(2)	44(2)	-4(2)	-4(2)	1(2)
C(23)	39(2)	40(2)	51(2)	-4(2)	-10(2)	-7(2)
C(24)	64(3)	36(2)	44(2)	-4(2)	-7(2)	-6(2)
C(25)	65(3)	39(2)	53(3)	-9(2)	10(2)	5(2)
C(26)	41(2)	38(2)	51(2)	-3(2)	7(2)	2(2)
N(2)	29(2)	29(1)	33(2)	1(1)	-5(1)	0(1)
C(7)	31(2)	30(2)	31(2)	0(1)	-3(1)	-2(1)
C(31)	31(2)	30(2)	28(2)	2(1)	-2(1)	-1(1)
C(32)	32(2)	34(2)	38(2)	6(2)	1(2)	-2(1)
C(33)	30(2)	40(2)	40(2)	3(2)	5(2)	2(2)
C(34)	39(2)	28(2)	32(2)	0(1)	-6(2)	3(1)
Br(1)	49(1)	31(1)	61(1)	4(1)	-1(1)	7(1)
C(35)	47(2)	28(2)	42(2)	6(2)	10(2)	-4(2)



**Table A3.2.5 Cont.**

C(36)	40(2)	32(2)	47(2)	5(2)	12(2)	-1(2)
C(3)	39(2)	33(2)	36(2)	4(2)	-2(2)	-8(2)
C(4)	28(2)	36(2)	37(2)	6(2)	-5(2)	-4(1)
C(8)	44(2)	49(2)	39(2)	2(2)	-4(2)	-4(2)
N(201)	28(2)	34(2)	42(2)	-1(1)	3(1)	4(1)
C(211)	31(2)	33(2)	37(2)	2(2)	-2(2)	2(1)
C(212)	32(2)	42(2)	41(2)	-2(2)	9(2)	1(2)
C(213)	36(2)	39(2)	40(2)	0(2)	2(2)	-5(2)
C(214)	35(2)	35(2)	35(2)	-1(2)	-2(2)	3(2)
O(202)	54(2)	33(1)	49(2)	-2(1)	10(1)	1(1)
C(217)	80(4)	40(2)	65(3)	-4(2)	24(3)	11(2)
C(215)	31(2)	39(2)	40(2)	-2(2)	3(2)	5(2)
C(216)	30(2)	36(2)	44(2)	2(2)	2(2)	-1(2)
C(201)	32(2)	32(2)	35(2)	6(1)	4(2)	2(1)
O(201)	27(1)	40(1)	51(2)	0(1)	3(1)	4(1)
C(202)	31(2)	28(2)	43(2)	3(2)	1(2)	3(1)
C(205)	47(3)	32(2)	63(3)	5(2)	11(2)	-1(2)
C(206)	24(2)	31(2)	41(2)	-1(1)	-2(1)	2(1)
C(221)	38(2)	29(2)	38(2)	1(1)	0(2)	-1(2)
C(222)	34(2)	36(2)	48(2)	-4(2)	2(2)	-1(2)
C(223)	46(2)	39(2)	52(2)	-2(2)	8(2)	8(2)
C(224)	71(3)	32(2)	47(2)	-5(2)	2(2)	5(2)
C(225)	69(3)	37(2)	54(3)	-8(2)	-15(2)	-5(2)
C(226)	45(2)	40(2)	54(3)	-2(2)	-9(2)	-4(2)
N(202)	30(2)	30(2)	36(2)	2(1)	-1(1)	0(1)
C(207)	31(2)	33(2)	31(2)	1(1)	0(1)	1(1)
C(231)	33(2)	32(2)	30(2)	2(1)	-2(1)	0(1)
C(232)	39(2)	42(2)	45(2)	10(2)	-13(2)	-3(2)
C(233)	53(3)	34(2)	51(2)	10(2)	-11(2)	-1(2)
C(234)	43(2)	36(2)	35(2)	-1(2)	2(2)	-11(2)
Br(2)	68(1)	43(1)	70(1)	5(1)	-3(1)	-21(1)
C(235)	35(2)	46(2)	45(2)	1(2)	-3(2)	-7(2)
C(236)	31(2)	39(2)	47(2)	7(2)	-2(2)	4(2)
C(203)	36(2)	37(2)	40(2)	5(2)	2(2)	8(2)
C(204)	29(2)	40(2)	38(2)	4(2)	3(2)	5(2)

**Table A3.2.5 Cont.**

C(208)	43(2)	54(3)	41(2)	1(2)	-4(2)	2(2)
--------	-------	-------	-------	------	-------	------

---

**Table A3.2.6** Hydrogen Coordinates ( $\times 10^4$ ) and Isotropic Displacement Parameters ( $\text{\AA}^2 \times 10^3$ ) for Imine **80**.

	x	y	z	U(eq)
H(12)	1608	1180	654	41
H(13)	1086	736	56	41
H(17A)	576	289	588	96
H(17B)	1218	30	-93	96
H(17C)	1304	308	-1075	96
H(15)	3812	473	2581	46
H(16)	4316	912	3210	44
H(5A)	2499	2049	2677	69
H(5B)	3186	2164	4231	69
H(5C)	2014	2012	4510	69
H(6)	2744	1631	6336	37
H(22)	5643	1874	6164	44
H(23)	6337	2215	7853	52
H(24)	5148	2444	9656	57
H(25)	3238	2332	9751	63
H(26)	2525	1998	8029	52
H(7)	3064	1245	7104	37
H(32)	5861	1099	5632	41
H(33)	6862	699	5978	44
H(35)	4241	389	8549	47
H(36)	3229	787	8150	47
H(3A)	5069	1785	3638	43
H(3B)	4359	1873	2030	43
H(4)	4995	1345	2991	41
H(8A)	4855	1257	86	66
H(8B)	5678	1506	428	66
H(8C)	4416	1557	-207	66
H(212)	8390	915	-1801	46

H(213)	8876	474	-2408	46
H(21A)	11324	323	-6158	92
H(21B)	11438	38	-5258	92
H(21C)	12118	292	-4566	92
H(215)	11641	738	-4882	45
H(216)	11120	1183	-4281	44
H(20A)	10261	2051	-2288	71
H(20B)	10717	2018	-433	71
H(20C)	9550	2170	-774	71
H(206)	10003	1639	1367	38
H(222)	7102	1874	1182	47
H(223)	6373	2210	2883	55
H(224)	7570	2447	4675	60
H(225)	9475	2337	4790	64
H(226)	10206	2003	3078	55
H(207)	9711	1250	2127	38
H(232)	9607	779	2983	51
H(233)	8589	379	3374	56
H(235)	5874	710	1107	50
H(236)	6874	1111	786	47
H(20D)	7656	1786	-1323	45
H(20E)	8355	1875	-2938	45
H(204)	7736	1348	-1966	43
H(20F)	8316	1553	-5174	69
H(20G)	7051	1512	-4530	69
H(20H)	7842	1257	-4848	69

---

**Table A3.2.7** Torsion Angles [°] for Imine **80**.

---

C(1)-N(1)-C(11)-C(12)	59.0(5)
C(4)-N(1)-C(11)-C(12)	-135.8(4)
C(1)-N(1)-C(11)-C(16)	-118.5(4)
C(4)-N(1)-C(11)-C(16)	46.7(5)
C(16)-C(11)-C(12)-C(13)	-0.3(6)
N(1)-C(11)-C(12)-C(13)	-177.8(4)
C(11)-C(12)-C(13)-C(14)	-0.7(6)
C(12)-C(13)-C(14)-O(2)	-179.0(4)
C(12)-C(13)-C(14)-C(15)	1.2(6)
C(15)-C(14)-O(2)-C(17)	179.3(4)
C(13)-C(14)-O(2)-C(17)	-0.4(6)
O(2)-C(14)-C(15)-C(16)	179.5(4)
C(13)-C(14)-C(15)-C(16)	-0.7(6)
C(14)-C(15)-C(16)-C(11)	-0.3(7)
C(12)-C(11)-C(16)-C(15)	0.8(6)
N(1)-C(11)-C(16)-C(15)	178.4(4)
C(11)-N(1)-C(1)-O(1)	-15.1(6)
C(4)-N(1)-C(1)-O(1)	178.7(4)
C(11)-N(1)-C(1)-C(2)	161.8(3)
C(4)-N(1)-C(1)-C(2)	-4.4(4)
O(1)-C(1)-C(2)-C(5)	-44.6(5)
N(1)-C(1)-C(2)-C(5)	138.5(4)
O(1)-C(1)-C(2)-C(3)	-166.0(4)
N(1)-C(1)-C(2)-C(3)	17.1(4)
O(1)-C(1)-C(2)-C(6)	74.0(4)
N(1)-C(1)-C(2)-C(6)	-102.9(3)
C(5)-C(2)-C(6)-N(2)	-172.7(3)
C(3)-C(2)-C(6)-N(2)	-43.4(4)
C(1)-C(2)-C(6)-N(2)	68.3(3)
C(5)-C(2)-C(6)-C(21)	-51.1(4)
C(3)-C(2)-C(6)-C(21)	78.2(4)
C(1)-C(2)-C(6)-C(21)	-170.1(3)
N(2)-C(6)-C(21)-C(22)	44.8(5)

**Table A3.2.7 Cont.**

C(2)-C(6)-C(21)-C(22)	-77.0(4)
N(2)-C(6)-C(21)-C(26)	-132.1(4)
C(2)-C(6)-C(21)-C(26)	106.0(4)
C(26)-C(21)-C(22)-C(23)	-1.3(6)
C(6)-C(21)-C(22)-C(23)	-178.2(4)
C(21)-C(22)-C(23)-C(24)	1.1(6)
C(22)-C(23)-C(24)-C(25)	-0.2(7)
C(23)-C(24)-C(25)-C(26)	-0.5(7)
C(24)-C(25)-C(26)-C(21)	0.3(7)
C(22)-C(21)-C(26)-C(25)	0.6(6)
C(6)-C(21)-C(26)-C(25)	177.7(4)
C(21)-C(6)-N(2)-C(7)	114.6(3)
C(2)-C(6)-N(2)-C(7)	-120.6(3)
C(6)-N(2)-C(7)-C(31)	179.7(3)
N(2)-C(7)-C(31)-C(32)	-3.1(5)
N(2)-C(7)-C(31)-C(36)	177.4(4)
C(36)-C(31)-C(32)-C(33)	-1.1(6)
C(7)-C(31)-C(32)-C(33)	179.4(4)
C(31)-C(32)-C(33)-C(34)	-0.4(6)
C(32)-C(33)-C(34)-C(35)	1.1(6)
C(32)-C(33)-C(34)-Br(1)	-177.6(3)
C(33)-C(34)-C(35)-C(36)	-0.4(6)
Br(1)-C(34)-C(35)-C(36)	178.3(3)
C(34)-C(35)-C(36)-C(31)	-1.0(6)
C(32)-C(31)-C(36)-C(35)	1.8(6)
C(7)-C(31)-C(36)-C(35)	-178.7(4)
C(5)-C(2)-C(3)-C(4)	-142.7(3)
C(1)-C(2)-C(3)-C(4)	-23.0(4)
C(6)-C(2)-C(3)-C(4)	89.6(4)
C(1)-N(1)-C(4)-C(8)	-131.4(3)
C(11)-N(1)-C(4)-C(8)	62.2(4)
C(1)-N(1)-C(4)-C(3)	-10.2(4)
C(11)-N(1)-C(4)-C(3)	-176.5(3)
C(2)-C(3)-C(4)-N(1)	20.5(4)
C(2)-C(3)-C(4)-C(8)	140.1(3)

**Table A3.2.7 Cont.**

C(201)-N(201)-C(211)-C(216)	-58.4(5)
C(204)-N(201)-C(211)-C(216)	135.8(4)
C(201)-N(201)-C(211)-C(212)	120.8(4)
C(204)-N(201)-C(211)-C(212)	-44.9(5)
C(216)-C(211)-C(212)-C(213)	0.4(6)
N(201)-C(211)-C(212)-C(213)	-178.8(4)
C(211)-C(212)-C(213)-C(214)	-0.5(6)
C(212)-C(213)-C(214)-O(202)	-178.6(4)
C(212)-C(213)-C(214)-C(215)	0.9(6)
C(215)-C(214)-O(202)-C(217)	-3.7(6)
C(213)-C(214)-O(202)-C(217)	175.8(4)
O(202)-C(214)-C(215)-C(216)	178.1(4)
C(213)-C(214)-C(215)-C(216)	-1.4(6)
C(212)-C(211)-C(216)-C(215)	-0.8(6)
N(201)-C(211)-C(216)-C(215)	178.4(4)
C(214)-C(215)-C(216)-C(211)	1.3(6)
C(211)-N(201)-C(201)-O(201)	15.6(6)
C(204)-N(201)-C(201)-O(201)	-177.6(4)
C(211)-N(201)-C(201)-C(202)	-161.7(3)
C(204)-N(201)-C(201)-C(202)	5.1(4)
O(201)-C(201)-C(202)-C(205)	43.5(5)
N(201)-C(201)-C(202)-C(205)	-139.1(3)
O(201)-C(201)-C(202)-C(203)	165.4(4)
N(201)-C(201)-C(202)-C(203)	-17.3(4)
O(201)-C(201)-C(202)-C(206)	-74.8(4)
N(201)-C(201)-C(202)-C(206)	102.6(3)
C(205)-C(202)-C(206)-N(202)	173.8(3)
C(201)-C(202)-C(206)-N(202)	-67.5(3)
C(203)-C(202)-C(206)-N(202)	44.1(4)
C(205)-C(202)-C(206)-C(221)	51.8(4)
C(201)-C(202)-C(206)-C(221)	170.5(3)
C(203)-C(202)-C(206)-C(221)	-77.8(4)
N(202)-C(206)-C(221)-C(222)	-45.7(5)
C(202)-C(206)-C(221)-C(222)	76.5(5)
N(202)-C(206)-C(221)-C(226)	131.4(4)

**Table A3.2.7 Cont.**

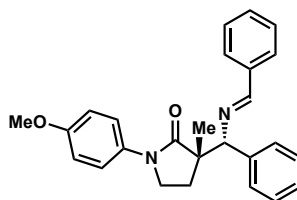
C(202)-C(206)-C(221)-C(226)	-106.4(4)
C(226)-C(221)-C(222)-C(223)	1.0(6)
C(206)-C(221)-C(222)-C(223)	178.1(4)
C(221)-C(222)-C(223)-C(224)	-0.2(7)
C(222)-C(223)-C(224)-C(225)	-0.9(7)
C(223)-C(224)-C(225)-C(226)	1.1(7)
C(222)-C(221)-C(226)-C(225)	-0.8(6)
C(206)-C(221)-C(226)-C(225)	-178.0(4)
C(224)-C(225)-C(226)-C(221)	-0.2(7)
C(221)-C(206)-N(202)-C(207)	-114.9(4)
C(202)-C(206)-N(202)-C(207)	119.7(3)
C(206)-N(202)-C(207)-C(231)	-179.4(3)
N(202)-C(207)-C(231)-C(236)	-0.3(6)
N(202)-C(207)-C(231)-C(232)	178.4(4)
C(236)-C(231)-C(232)-C(233)	-2.7(6)
C(207)-C(231)-C(232)-C(233)	178.6(4)
C(231)-C(232)-C(233)-C(234)	2.1(7)
C(232)-C(233)-C(234)-C(235)	-0.6(7)
C(232)-C(233)-C(234)-Br(2)	-178.1(3)
C(233)-C(234)-C(235)-C(236)	-0.3(7)
Br(2)-C(234)-C(235)-C(236)	177.3(3)
C(232)-C(231)-C(236)-C(235)	1.8(6)
C(207)-C(231)-C(236)-C(235)	-179.5(4)
C(234)-C(235)-C(236)-C(231)	-0.3(6)
C(205)-C(202)-C(203)-C(204)	142.4(3)
C(201)-C(202)-C(203)-C(204)	22.7(4)
C(206)-C(202)-C(203)-C(204)	-89.9(4)
C(201)-N(201)-C(204)-C(208)	131.3(4)
C(211)-N(201)-C(204)-C(208)	-61.8(5)
C(201)-N(201)-C(204)-C(203)	9.5(4)
C(211)-N(201)-C(204)-C(203)	176.4(3)
C(202)-C(203)-C(204)-N(201)	-20.0(4)
C(202)-C(203)-C(204)-C(208)	-140.1(3)

---

Symmetry transformations used to generate equivalent atoms:



**A3.3 X-RAY CRYSTAL STRUCTURE ANALYSIS OF IMINE 70**



**70**

Contents

*Table A3.3.1. Experimental Details*

*Table A3.3.2. Crystal Data*

*Table A3.3.3. Atomic Coordinates*

*Table A3.3.4. Full Bond Distances and Angles*

*Table A3.3.5. Anisotropic Displacement Parameters*

*Table A3.3.6. Hydrogen Atomic Coordinates*

*Table A3.3.7. Torsion Angles*

**Figure A3.3.1 X-Ray Crystal Structure of Imine 70.**

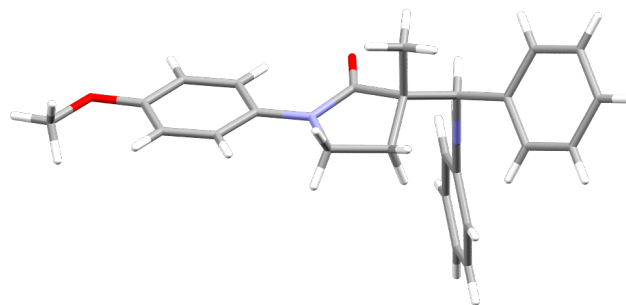


**Table A3.3.1** Experimental Details for X-Ray Structure Determination of Imine **70**.

Low-temperature diffraction data ( $\phi$ - and  $\omega$ -scans) were collected on a Bruker AXS KAPPA APEX II diffractometer coupled to an PHOTON 100 CMOS detector with graphite monochromated Mo  $K_{\alpha}$  radiation ( $\lambda = 0.71073 \text{ \AA}$ ) for the structure of compound **70**. The structure was solved by direct methods using SHELXS and refined against  $F^2$  on all data by full-matrix least squares with SHELXL-2017 using established refinement techniques. All non-hydrogen atoms were refined anisotropically. All hydrogen atoms were included into the model at geometrically calculated positions and refined using a riding model. The isotropic displacement parameters of all hydrogen atoms were fixed to 1.2 times the  $U$  value of the atoms they are linked to (1.5 times for methyl groups).

Compound **70** crystallizes in the monoclinic space group  $P2_1/c$  with one molecule in the asymmetric unit.

**Table A3.3.2** Crystal Data and Structure Refinement for Imine **70**.

Identification code	D19141	
Empirical formula	C <sub>26</sub> H <sub>26</sub> N <sub>2</sub> O <sub>2</sub>	
Formula weight	398.49	
Temperature	100(2) K	
Wavelength	0.71073 Å	
Crystal system	Monoclinic	
Space group	P2 <sub>1</sub> /c	
Unit cell dimensions	a = 19.640(5) Å	a = 90°.
	b = 6.1440(16) Å	b = 94.127(6)°.
	c = 17.135(5) Å	g = 90°.
Volume	2062.3(9) Å <sup>3</sup>	
Z	4	
Density (calculated)	1.283 Mg/m <sup>3</sup>	
Absorption coefficient	0.081 mm <sup>-1</sup>	
F(000)	848	
Crystal size	0.300 x 0.300 x 0.200 mm <sup>3</sup>	
Theta range for data collection	2.079 to 35.630°.	
Index ranges	-31 ≤ h ≤ 31, -10 ≤ k ≤ 9, -27 ≤ l ≤ 27	
Reflections collected	110686	
Independent reflections	9463 [R(int) = 0.0390]	
Completeness to theta = 25.242°	99.6 %	
Absorption correction	Semi-empirical from equivalents	
Max. and min. transmission	0.7471 and 0.7041	
Refinement method	Full-matrix least-squares on F <sup>2</sup>	
Data / restraints / parameters	9463 / 0 / 273	
Goodness-of-fit on F <sup>2</sup>	1.042	
Final R indices [I > 2σ(I)]	R1 = 0.0400, wR2 = 0.1106	
R indices (all data)	R1 = 0.0501, wR2 = 0.1175	
Extinction coefficient	n/a	
Largest diff. peak and hole	0.569 and -0.261 e.Å <sup>-3</sup>	

**Table A3.3.3** Atomic Coordinates ( $\times 10^4$ ) and Equivalent Isotropic Displacement Parameters ( $\text{\AA}^2 \times 10^3$ ) for Imine **70**.  $U(\text{eq})$  is Defined as One Third of the Trace of the Orthogonalized  $U^{ij}$  Tensor.

	x	y	z	U(eq)
N(1)	8328(1)	3132(1)	6113(1)	12(1)
C(1)	8676(1)	3351(1)	6862(1)	12(1)
C(2)	9154(1)	1784(1)	7114(1)	15(1)
C(3)	9517(1)	1929(1)	7843(1)	15(1)
C(4)	9401(1)	3674(1)	8328(1)	13(1)
O(1)	9723(1)	3979(1)	9059(1)	17(1)
C(7)	10207(1)	2372(1)	9326(1)	18(1)
C(5)	8928(1)	5261(1)	8079(1)	16(1)
C(6)	8563(1)	5110(1)	7359(1)	15(1)
C(8)	7960(1)	4706(1)	5707(1)	11(1)
O(2)	7793(1)	6481(1)	5955(1)	16(1)
C(9)	7834(1)	3953(1)	4858(1)	11(1)
C(10)	7920(1)	1487(1)	4926(1)	14(1)
C(11)	8439(1)	1213(1)	5628(1)	14(1)
C(12)	8412(1)	4983(1)	4425(1)	16(1)
C(13)	7134(1)	4755(1)	4502(1)	11(1)
C(21)	7033(1)	4224(1)	3637(1)	12(1)
C(22)	6815(1)	2168(1)	3376(1)	15(1)
C(23)	6738(1)	1711(1)	2578(1)	18(1)
C(24)	6876(1)	3300(1)	2033(1)	18(1)
C(25)	7093(1)	5351(1)	2286(1)	18(1)
C(26)	7169(1)	5804(1)	3086(1)	15(1)
N(2)	6588(1)	3781(1)	4924(1)	13(1)
C(14)	6227(1)	5086(1)	5297(1)	14(1)
C(31)	5657(1)	4350(1)	5743(1)	15(1)
C(32)	5370(1)	5814(1)	6247(1)	21(1)
C(33)	4830(1)	5180(2)	6680(1)	26(1)
C(34)	4574(1)	3086(2)	6606(1)	27(1)

**Table A3.3.3 Cont.**

C(35)	4854(1)	1613(2)	6101(1)	25(1)
C(36)	5396(1)	2241(1)	5672(1)	19(1)

---

**Table A3.3.4** Bond Lengths [ $\text{\AA}$ ] and angles [ $^\circ$ ] for Imine **70**.

---

N(1)-C(8)	1.3677(9)
N(1)-C(1)	1.4158(9)
N(1)-C(11)	1.4682(9)
C(1)-C(2)	1.3926(9)
C(1)-C(6)	1.4031(10)
C(2)-C(3)	1.3955(10)
C(2)-H(2)	0.9500
C(3)-C(4)	1.3859(10)
C(3)-H(3)	0.9500
C(4)-O(1)	1.3737(9)
C(4)-C(5)	1.3934(10)
O(1)-C(7)	1.4236(9)
C(7)-H(7A)	0.9800
C(7)-H(7B)	0.9800
C(7)-H(7C)	0.9800
C(5)-C(6)	1.3859(10)
C(5)-H(5)	0.9500
C(6)-H(6)	0.9500
C(8)-O(2)	1.2236(8)
C(8)-C(9)	1.5301(9)
C(9)-C(10)	1.5282(10)
C(9)-C(12)	1.5363(9)
C(9)-C(13)	1.5449(9)
C(10)-C(11)	1.5291(10)
C(10)-H(10A)	0.9900
C(10)-H(10B)	0.9900
C(11)-H(11A)	0.9900
C(11)-H(11B)	0.9900
C(12)-H(12A)	0.9800
C(12)-H(12B)	0.9800
C(12)-H(12C)	0.9800
C(13)-N(2)	1.4624(9)
C(13)-C(21)	1.5160(10)

**Table A3.3.4 Cont.**

C(13)-H(13)	1.0000
C(21)-C(26)	1.3939(10)
C(21)-C(22)	1.3973(10)
C(22)-C(23)	1.3930(10)
C(22)-H(22)	0.9500
C(23)-C(24)	1.3919(11)
C(23)-H(23)	0.9500
C(24)-C(25)	1.3901(11)
C(24)-H(24)	0.9500
C(25)-C(26)	1.3945(10)
C(25)-H(25)	0.9500
C(26)-H(26)	0.9500
N(2)-C(14)	1.2735(9)
C(14)-C(31)	1.4707(10)
C(14)-H(14)	0.9500
C(31)-C(32)	1.3943(10)
C(31)-C(36)	1.3955(12)
C(32)-C(33)	1.3922(12)
C(32)-H(32)	0.9500
C(33)-C(34)	1.3836(15)
C(33)-H(33)	0.9500
C(34)-C(35)	1.3917(13)
C(34)-H(34)	0.9500
C(35)-C(36)	1.3901(11)
C(35)-H(35)	0.9500
C(36)-H(36)	0.9500
C(8)-N(1)-C(1)	126.65(6)
C(8)-N(1)-C(11)	112.01(5)
C(1)-N(1)-C(11)	120.53(5)
C(2)-C(1)-C(6)	118.47(6)
C(2)-C(1)-N(1)	119.08(6)
C(6)-C(1)-N(1)	122.44(6)
C(1)-C(2)-C(3)	121.57(6)
C(1)-C(2)-H(2)	119.2

**Table A3.3.4 Cont.**

C(3)-C(2)-H(2)	119.2
C(4)-C(3)-C(2)	119.43(6)
C(4)-C(3)-H(3)	120.3
C(2)-C(3)-H(3)	120.3
O(1)-C(4)-C(3)	124.65(6)
O(1)-C(4)-C(5)	115.86(6)
C(3)-C(4)-C(5)	119.49(6)
C(4)-O(1)-C(7)	116.77(6)
O(1)-C(7)-H(7A)	109.5
O(1)-C(7)-H(7B)	109.5
H(7A)-C(7)-H(7B)	109.5
O(1)-C(7)-H(7C)	109.5
H(7A)-C(7)-H(7C)	109.5
H(7B)-C(7)-H(7C)	109.5
C(6)-C(5)-C(4)	121.14(6)
C(6)-C(5)-H(5)	119.4
C(4)-C(5)-H(5)	119.4
C(5)-C(6)-C(1)	119.89(6)
C(5)-C(6)-H(6)	120.1
C(1)-C(6)-H(6)	120.1
O(2)-C(8)-N(1)	126.75(6)
O(2)-C(8)-C(9)	124.83(6)
N(1)-C(8)-C(9)	108.26(5)
C(10)-C(9)-C(8)	102.55(5)
C(10)-C(9)-C(12)	111.35(5)
C(8)-C(9)-C(12)	105.12(5)
C(10)-C(9)-C(13)	115.92(5)
C(8)-C(9)-C(13)	110.89(5)
C(12)-C(9)-C(13)	110.24(5)
C(9)-C(10)-C(11)	103.49(5)
C(9)-C(10)-H(10A)	111.1
C(11)-C(10)-H(10A)	111.1
C(9)-C(10)-H(10B)	111.1
C(11)-C(10)-H(10B)	111.1
H(10A)-C(10)-H(10B)	109.0



**Table A3.3.4 Cont.**

N(1)-C(11)-C(10)	103.82(5)
N(1)-C(11)-H(11A)	111.0
C(10)-C(11)-H(11A)	111.0
N(1)-C(11)-H(11B)	111.0
C(10)-C(11)-H(11B)	111.0
H(11A)-C(11)-H(11B)	109.0
C(9)-C(12)-H(12A)	109.5
C(9)-C(12)-H(12B)	109.5
H(12A)-C(12)-H(12B)	109.5
C(9)-C(12)-H(12C)	109.5
H(12A)-C(12)-H(12C)	109.5
H(12B)-C(12)-H(12C)	109.5
N(2)-C(13)-C(21)	110.25(5)
N(2)-C(13)-C(9)	109.73(5)
C(21)-C(13)-C(9)	111.51(5)
N(2)-C(13)-H(13)	108.4
C(21)-C(13)-H(13)	108.4
C(9)-C(13)-H(13)	108.4
C(26)-C(21)-C(22)	118.76(6)
C(26)-C(21)-C(13)	119.69(6)
C(22)-C(21)-C(13)	121.54(6)
C(23)-C(22)-C(21)	120.38(6)
C(23)-C(22)-H(22)	119.8
C(21)-C(22)-H(22)	119.8
C(24)-C(23)-C(22)	120.35(7)
C(24)-C(23)-H(23)	119.8
C(22)-C(23)-H(23)	119.8
C(25)-C(24)-C(23)	119.72(7)
C(25)-C(24)-H(24)	120.1
C(23)-C(24)-H(24)	120.1
C(24)-C(25)-C(26)	119.77(7)
C(24)-C(25)-H(25)	120.1
C(26)-C(25)-H(25)	120.1
C(21)-C(26)-C(25)	121.01(7)
C(21)-C(26)-H(26)	119.5

**Table A3.3.4 Cont.**

C(25)-C(26)-H(26)	119.5
C(14)-N(2)-C(13)	116.44(6)
N(2)-C(14)-C(31)	122.70(7)
N(2)-C(14)-H(14)	118.6
C(31)-C(14)-H(14)	118.6
C(32)-C(31)-C(36)	119.38(7)
C(32)-C(31)-C(14)	118.70(7)
C(36)-C(31)-C(14)	121.92(6)
C(33)-C(32)-C(31)	120.41(8)
C(33)-C(32)-H(32)	119.8
C(31)-C(32)-H(32)	119.8
C(34)-C(33)-C(32)	119.82(8)
C(34)-C(33)-H(33)	120.1
C(32)-C(33)-H(33)	120.1
C(33)-C(34)-C(35)	120.28(8)
C(33)-C(34)-H(34)	119.9
C(35)-C(34)-H(34)	119.9
C(36)-C(35)-C(34)	119.98(9)
C(36)-C(35)-H(35)	120.0
C(34)-C(35)-H(35)	120.0
C(35)-C(36)-C(31)	120.13(7)
C(35)-C(36)-H(36)	119.9
C(31)-C(36)-H(36)	119.9

---

Symmetry transformations used to generate equivalent atoms:

**Table A3.3.5** Anisotropic Displacement Parameters ( $\text{\AA}^2 \times 10^3$ ) for Imine **70**. The

Anisotropic Displacement Factor Exponent Takes the Form:  $-2p^2[h^2a^{*2}U^{11} + \dots + 2hka^*b^*U^{12}]$ .

	U <sup>11</sup>	U <sup>22</sup>	U <sup>33</sup>	U <sup>23</sup>	U <sup>13</sup>	U <sup>12</sup>
N(1)	14(1)	10(1)	11(1)	-1(1)	0(1)	2(1)
C(1)	12(1)	12(1)	11(1)	0(1)	1(1)	1(1)
C(2)	18(1)	14(1)	14(1)	-2(1)	-1(1)	4(1)
C(3)	17(1)	16(1)	14(1)	0(1)	-1(1)	4(1)
C(4)	14(1)	16(1)	10(1)	1(1)	1(1)	0(1)
O(1)	20(1)	21(1)	11(1)	0(1)	-2(1)	4(1)
C(7)	18(1)	19(1)	15(1)	5(1)	-2(1)	-1(1)
C(5)	18(1)	18(1)	11(1)	-2(1)	1(1)	5(1)
C(6)	16(1)	16(1)	12(1)	-2(1)	1(1)	5(1)
C(8)	12(1)	10(1)	11(1)	0(1)	1(1)	0(1)
O(2)	22(1)	11(1)	14(1)	-2(1)	-1(1)	4(1)
C(9)	12(1)	11(1)	10(1)	-1(1)	1(1)	0(1)
C(10)	16(1)	11(1)	14(1)	-3(1)	-2(1)	2(1)
C(11)	16(1)	10(1)	15(1)	-2(1)	-1(1)	3(1)
C(12)	14(1)	19(1)	15(1)	1(1)	3(1)	-2(1)
C(13)	13(1)	11(1)	11(1)	0(1)	1(1)	0(1)
C(21)	12(1)	13(1)	11(1)	0(1)	1(1)	0(1)
C(22)	16(1)	14(1)	14(1)	-1(1)	0(1)	-1(1)
C(23)	19(1)	19(1)	16(1)	-4(1)	-1(1)	-2(1)
C(24)	16(1)	26(1)	12(1)	-3(1)	0(1)	-1(1)
C(25)	18(1)	24(1)	12(1)	3(1)	1(1)	-3(1)
C(26)	17(1)	16(1)	13(1)	2(1)	1(1)	-2(1)
N(2)	12(1)	15(1)	12(1)	1(1)	2(1)	1(1)
C(14)	14(1)	16(1)	13(1)	1(1)	1(1)	3(1)
C(31)	13(1)	21(1)	12(1)	2(1)	1(1)	5(1)
C(32)	18(1)	28(1)	18(1)	-2(1)	3(1)	8(1)
C(33)	18(1)	43(1)	18(1)	-1(1)	5(1)	11(1)
C(34)	16(1)	44(1)	22(1)	10(1)	6(1)	7(1)

**Table A3.3.5 Cont.**

C(35)	16(1)	30(1)	28(1)	9(1)	6(1)	2(1)
C(36)	16(1)	22(1)	20(1)	3(1)	4(1)	2(1)

---

**Table A3.3.6** Hydrogen Coordinates ( $\times 10^4$ ) and Isotropic Displacement Parameters ( $\text{\AA}^2 \times 10^3$ ) for Imine **70**.

	x	y	z	U(eq)
H(2)	9236	588	6782	19
H(3)	9841	842	8004	19
H(7A)	9986	942	9321	26
H(7B)	10386	2723	9860	26
H(7C)	10584	2344	8980	26
H(5)	8854	6468	8409	19
H(6)	8237	6196	7201	18
H(10A)	8095	869	4446	17
H(10B)	7482	773	5022	17
H(11A)	8355	-146	5916	17
H(11B)	8911	1187	5460	17
H(12A)	8854	4512	4670	24
H(12B)	8379	6573	4452	24
H(12C)	8372	4522	3876	24
H(13)	7113	6372	4565	14
H(22)	6719	1074	3745	18
H(23)	6590	307	2406	21
H(24)	6822	2984	1489	22
H(25)	7189	6441	1917	22
H(26)	7315	7209	3256	18
H(14)	6329	6596	5287	17
H(32)	5544	7254	6296	25
H(33)	4638	6181	7024	31
H(34)	4206	2651	6901	32
H(35)	4676	179	6050	29
H(36)	5589	1232	5330	23

**Table A3.3.7** Torsion Angles [°] for Imine **70**.

---

C(8)-N(1)-C(1)-C(2)	-165.03(6)
C(11)-N(1)-C(1)-C(2)	3.74(9)
C(8)-N(1)-C(1)-C(6)	14.04(10)
C(11)-N(1)-C(1)-C(6)	-177.19(6)
C(6)-C(1)-C(2)-C(3)	0.16(11)
N(1)-C(1)-C(2)-C(3)	179.27(6)
C(1)-C(2)-C(3)-C(4)	-0.12(11)
C(2)-C(3)-C(4)-O(1)	179.43(7)
C(2)-C(3)-C(4)-C(5)	-0.44(10)
C(3)-C(4)-O(1)-C(7)	-0.06(10)
C(5)-C(4)-O(1)-C(7)	179.81(6)
O(1)-C(4)-C(5)-C(6)	-178.90(6)
C(3)-C(4)-C(5)-C(6)	0.98(11)
C(4)-C(5)-C(6)-C(1)	-0.94(11)
C(2)-C(1)-C(6)-C(5)	0.37(10)
N(1)-C(1)-C(6)-C(5)	-178.71(6)
C(1)-N(1)-C(8)-O(2)	-9.85(11)
C(11)-N(1)-C(8)-O(2)	-179.43(6)
C(1)-N(1)-C(8)-C(9)	165.62(6)
C(11)-N(1)-C(8)-C(9)	-3.95(7)
O(2)-C(8)-C(9)-C(10)	-162.44(6)
N(1)-C(8)-C(9)-C(10)	21.98(7)
O(2)-C(8)-C(9)-C(12)	81.04(8)
N(1)-C(8)-C(9)-C(12)	-94.54(6)
O(2)-C(8)-C(9)-C(13)	-38.09(9)
N(1)-C(8)-C(9)-C(13)	146.33(5)
C(8)-C(9)-C(10)-C(11)	-30.46(6)
C(12)-C(9)-C(10)-C(11)	81.50(7)
C(13)-C(9)-C(10)-C(11)	-151.42(5)
C(8)-N(1)-C(11)-C(10)	-15.83(7)
C(1)-N(1)-C(11)-C(10)	173.87(6)
C(9)-C(10)-C(11)-N(1)	28.62(7)
C(10)-C(9)-C(13)-N(2)	52.92(7)

**Table A3.3.7 Cont.**

C(8)-C(9)-C(13)-N(2)	-63.45(7)
C(12)-C(9)-C(13)-N(2)	-179.44(5)
C(10)-C(9)-C(13)-C(21)	-69.53(7)
C(8)-C(9)-C(13)-C(21)	174.11(5)
C(12)-C(9)-C(13)-C(21)	58.11(7)
N(2)-C(13)-C(21)-C(26)	140.78(6)
C(9)-C(13)-C(21)-C(26)	-97.07(7)
N(2)-C(13)-C(21)-C(22)	-40.19(8)
C(9)-C(13)-C(21)-C(22)	81.96(8)
C(26)-C(21)-C(22)-C(23)	0.15(10)
C(13)-C(21)-C(22)-C(23)	-178.88(6)
C(21)-C(22)-C(23)-C(24)	-0.10(11)
C(22)-C(23)-C(24)-C(25)	0.13(11)
C(23)-C(24)-C(25)-C(26)	-0.21(11)
C(22)-C(21)-C(26)-C(25)	-0.23(10)
C(13)-C(21)-C(26)-C(25)	178.82(6)
C(24)-C(25)-C(26)-C(21)	0.26(11)
C(21)-C(13)-N(2)-C(14)	-121.09(6)
C(9)-C(13)-N(2)-C(14)	115.72(6)
C(13)-N(2)-C(14)-C(31)	179.47(6)
N(2)-C(14)-C(31)-C(32)	168.35(7)
N(2)-C(14)-C(31)-C(36)	-11.84(10)
C(36)-C(31)-C(32)-C(33)	0.23(11)
C(14)-C(31)-C(32)-C(33)	-179.96(7)
C(31)-C(32)-C(33)-C(34)	-0.27(12)
C(32)-C(33)-C(34)-C(35)	-0.03(12)
C(33)-C(34)-C(35)-C(36)	0.36(12)
C(34)-C(35)-C(36)-C(31)	-0.40(12)
C(32)-C(31)-C(36)-C(35)	0.11(11)
C(14)-C(31)-C(36)-C(35)	-179.70(7)

---

Symmetry transformations used to generate equivalent atoms:

## CHAPTER 2

### *Enantioselective Dearomative Allylic Alkylation of Pyridines*<sup>†</sup>

#### 2.1 INTRODUCTION

Aromatic compounds are stable, feedstock chemicals available with numerous substitution patterns that find application in various areas such as materials science<sup>1</sup> and pharmaceuticals.<sup>2</sup> However, there is an increasing demand to develop methods to convert these readily available, aromatic chemicals into value-added, enantioenriched saturated compounds with increased complexity.<sup>3</sup> The development of asymmetric, catalytic dearomatization methods of *N*-heterocycles has garnered significant attention over the past twenty years from the synthetic and medicinal chemistry communities since saturated and partially saturated *N*-heterocycles are high demand building blocks.<sup>4</sup> This is because these stereogenic saturated and partially saturated *N*-heterocycles, in particular six-membered *N*-heterocycles, are among the most common motifs in pharmaceuticals and natural products.<sup>5</sup>

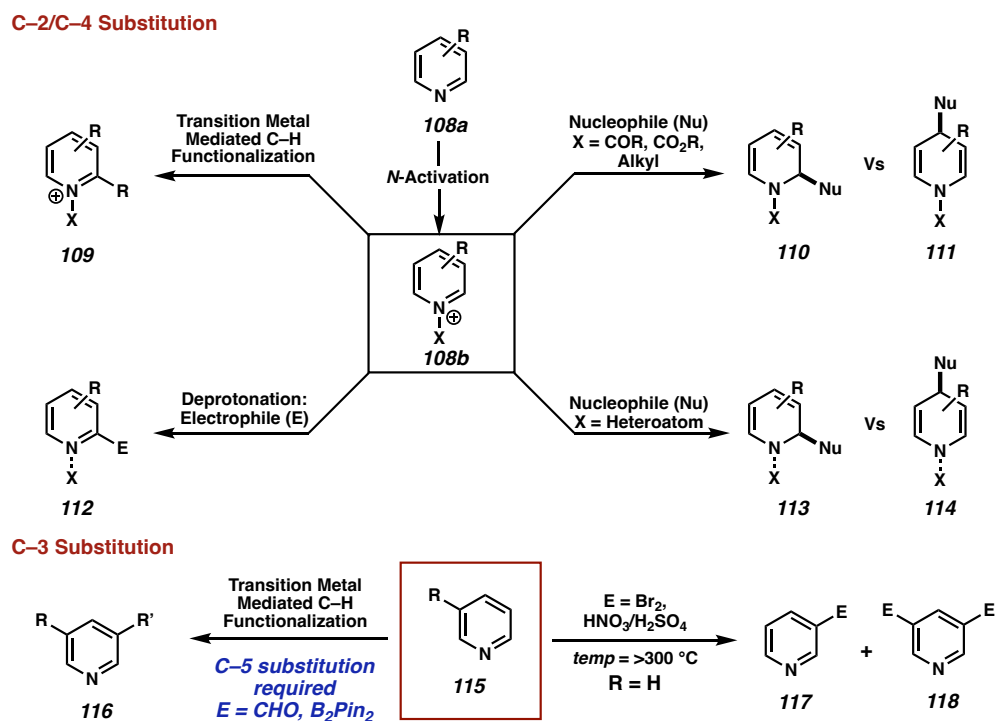
The enantioselective, dearomative functionalization of pyridines has emerged as a valuable strategy to access the corresponding saturated *N*-heterocycle building blocks due to the high commercial and synthetic availability of various substituted pyridines. These methods predominantly require a sequential protocol involving the stoichiometric *N*-acylation, *N*-alkylation or *N*-oxidation followed by nucleophilic addition into the activated

<sup>†</sup>This research was performed in collaboration with Steffen Gresßies and Lars Süße



pyridine ring **108b** (Scheme 2.1.1).<sup>6</sup> As a result, the site-selectivity of the nucleophilic addition is predominantly dictated by the stereoelectronic effects from the pyridine substituents or directed by the *N*-acyl or *N*-alkyl substituent.<sup>7</sup> Exploiting this sequential dearomative addition protocol of pyridines results in nucleophilic addition at C-2 or C-4 of the pyridine, depending on the hardness of the incoming nucleophile. Friedel-Crafts-like alkylation reactions favor C-3 substitution; however, harsh reaction conditions and pyridine substrates bearing electron donating substituents are typically required for the reaction to take place.<sup>8</sup> Consequently, enantioselective dearomative functionalization reactions at C-3 of pyridines remains underexplored in the synthetic chemistry community.

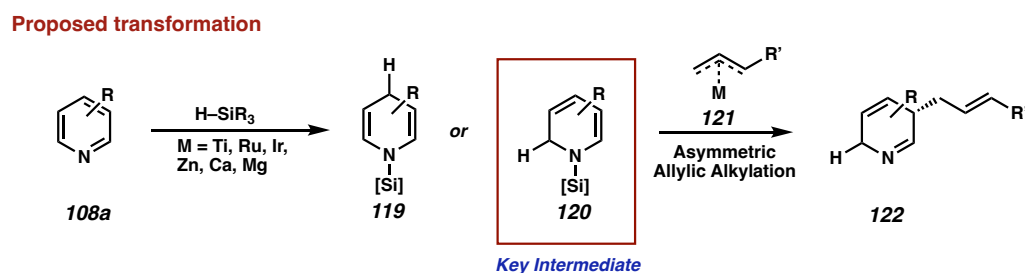
**Scheme 2.1.1** Approaches toward the dearomative functionalization of pyridines



A rising strategy toward the dearomatization of pyridines involves the catalytic hydrosilylation as many strategies have been developed with several heterogeneous catalysts,<sup>9</sup> transition metal catalysts (Ti, Ru, Ir, Zn),<sup>10</sup> as well as main group metals (Ca,

Mg)<sup>11</sup> and organic catalysts (boranes).<sup>12</sup> The resulting *N*-silylated enamines **119** or **120** are highly unstable to moisture and cannot be purified via column chromatography; however, derivatization can lead to stable saturated, or partially saturated, *N*-heterocyclic products.<sup>13</sup> We hypothesized that *N*-silyl dihydropyridines **120**, obtained via a dearomative 1,2-hydrosilylation, can act as enamine C-pronucleophiles at C-3 of the pyridine to undergo an asymmetric dearomative C-3 functionalization of readily available pyridine substrates. In particular, we envisioned that the *N*-silyl enamine **120** would be a competent nucleophile in a Pd-catalyzed asymmetric allylic alkylation reaction (Scheme 2.1.2).

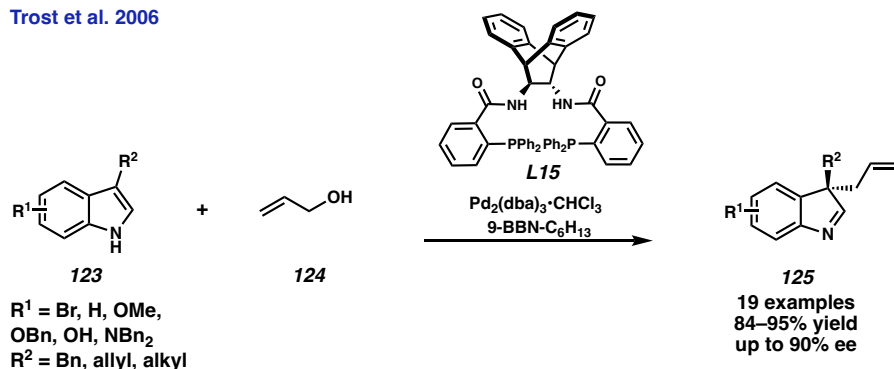
**Scheme 2.1.2** Proposed transformation featuring a telescoped dearomative hydrosilylation, asymmetric allylic alkylation of pyridines



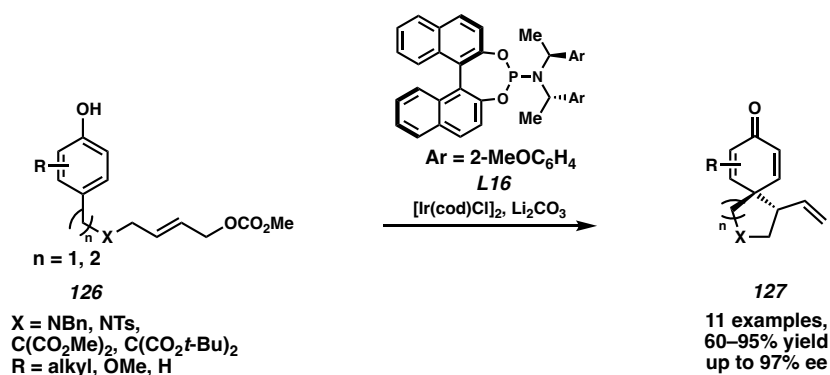
Transition metal-catalyzed asymmetric allylic alkylation (AAA) reactions are established and reliable transformations to form tertiary and quaternary centers via numerous combinations of nucleophiles and electrophiles.<sup>14,15</sup> Due to the versatility of this transformation, a vibrant area of research has emerged to convert readily available aromatic compounds into enantioenriched, saturated substrates via dearomative, transition metal-catalyzed asymmetric allylic alkylation reactions.<sup>16</sup> Trost reported the first enantioselective Pd-catalyzed dearomative allylic alkylation at the C-3 position of indoles in 2006 (Scheme 2.1.3).<sup>17</sup> Since then, the reactivity of numerous electron-rich heteroaromatics<sup>18</sup> and electron-rich benzene derivatives (phenols, anilines) have been explored (Scheme 2.1.3).<sup>19</sup>

**Scheme 2.1.3** Dearomative asymmetric allylic alkylation of electron-rich arenes

Trost et al. 2006



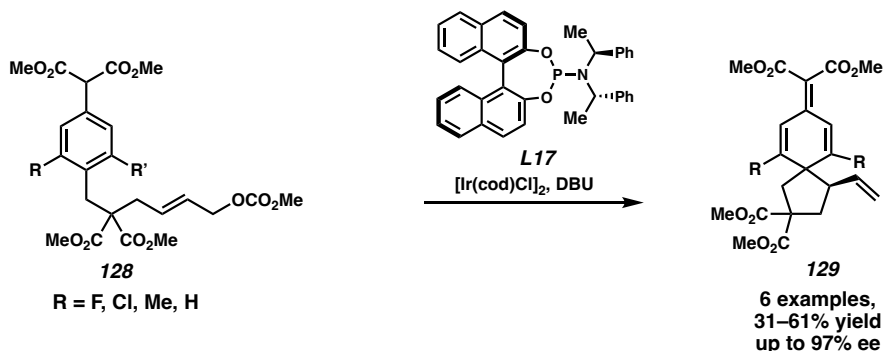
You et al. 2011



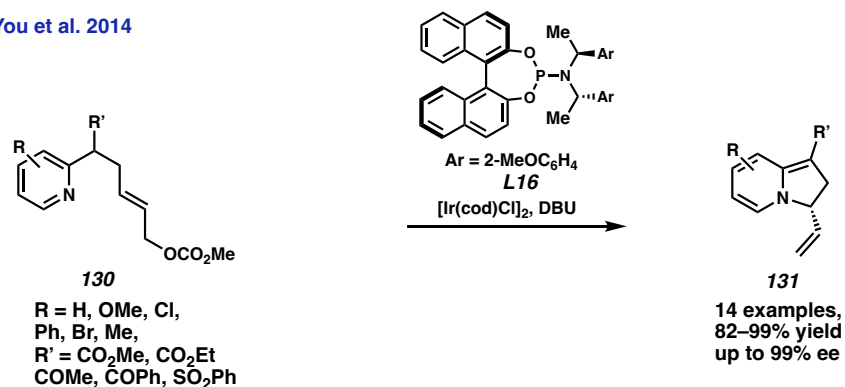
Recently in 2018, You reported the first intramolecular, Ir-catalyzed dearomative allylation of simple benzenes, further expanding this field (Scheme 2.1.4).<sup>20</sup> This strategy requires the highly acidic, benzylic malonate C–H in arene **128** to be present to promote the desired spirocyclization in high enantioselectivity. In 2014, You published the intramolecular allylic *N*-alkylation of pyridines to deliver the corresponding bicycles **131** in high enantioselectivities.<sup>21</sup> Despite these advances, the existing dearomative asymmetric allylic alkylation technology leverages the intrinsic nucleophilicity of the (hetero)aromatic substrates, even installing highly acidic benzylic positions to assist in the transformation. The expansion to C-alkylation of electron-poor heterocycles such as pyridines remains elusive, primarily due to their poor nucleophilicity at carbon.

**Scheme 2.1.4** Dearomative asymmetric allylic alkylation using inherent nucleophilicity of arenes

You et al. 2018



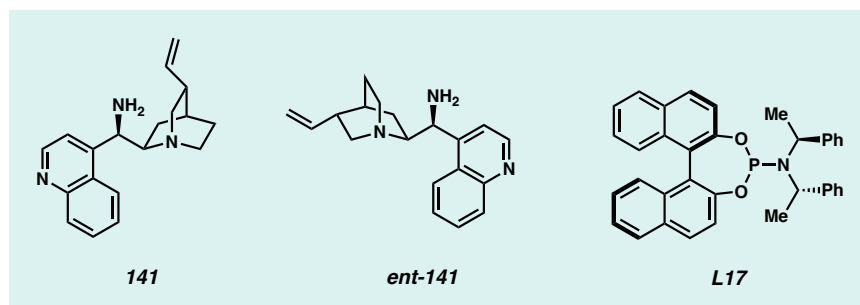
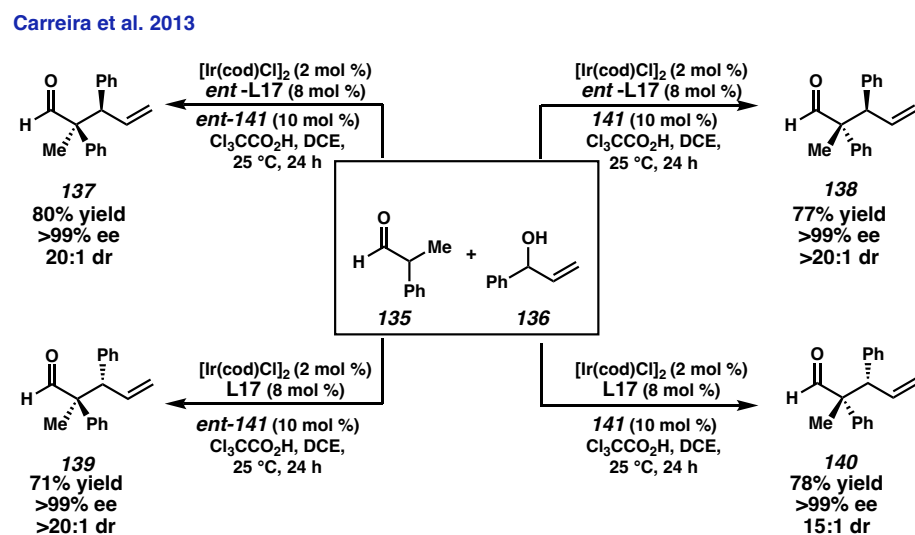
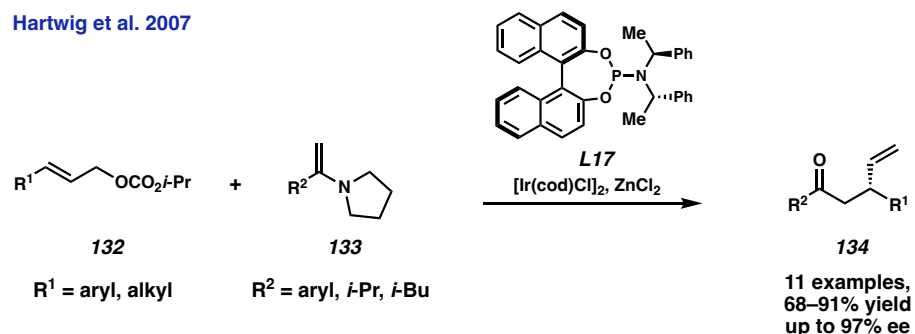
You et al. 2014



We hypothesized that 1,2-hydrosilylation of pyridines would result in an *N*-silyl enamine intermediate with sufficient nucleophilicity at the C-3 position to facilitate an asymmetric allylic alkylation reaction. Although underexplored relative to their enolate congeners, the catalytic asymmetric allylic alkylation reactions of enamines are known in the literature.<sup>22</sup> In 2007, Hartwig reported the allylic alkylation of terminal enamines **133** under iridium catalysis leading to enantioenriched β-allyl ketones **134** after hydrolysis of the imine intermediate formed after the allylic alkylation (Scheme 2.1.5).<sup>23</sup> The expansion of enamine allylic alkylation was reported by Carreira and coworkers in 2013. They report a method in which a chiral amine catalyst, **141** or *ent*-**141**, combines with the aldehyde to *in situ* generate the enamine nucleophile. This enamine nucleophile then undergoes an

iridium catalyzed allylic alkylation to deliver the desired  $\beta$ -allyl substituted aldehyde product in high diastereo- and enantioselectivity (Scheme 2.1.5).<sup>24</sup>

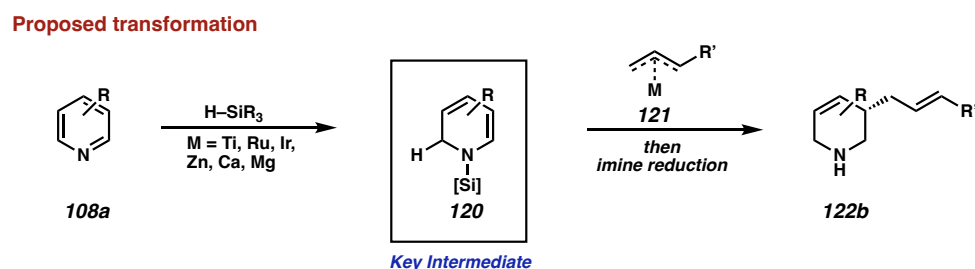
**Scheme 2.1.5** Asymmetric allylic alkylation reaction of enamine nucleophiles



Utilizing a similar enamine intermediate derived from the dearomative hydrosilylation of pyridines should allow for the asymmetric allylic alkylation of pyridines at the C-3 position, which inverts the inherent selectivity of the heteroaromatic substrate

(Scheme 2.1.6). Furthermore, we propose the corresponding *N*-silyl iminium intermediate after the C–3 alkylation could be reduced via a second hydrosilylation, resulting in the formation of chiral tetrahydropyridine products possessing a stereocenter  $\beta$ -relative to nitrogen. This would serve as the first dearomative, asymmetric allylic alkylation protocol of pyridines to deliver chiral tetrahydropyridine products bearing a stereocenter at the former C–3 position the pyridine.

**Scheme 2.1.6** Proposed transformation to deliver chiral tetrahydropyridine products

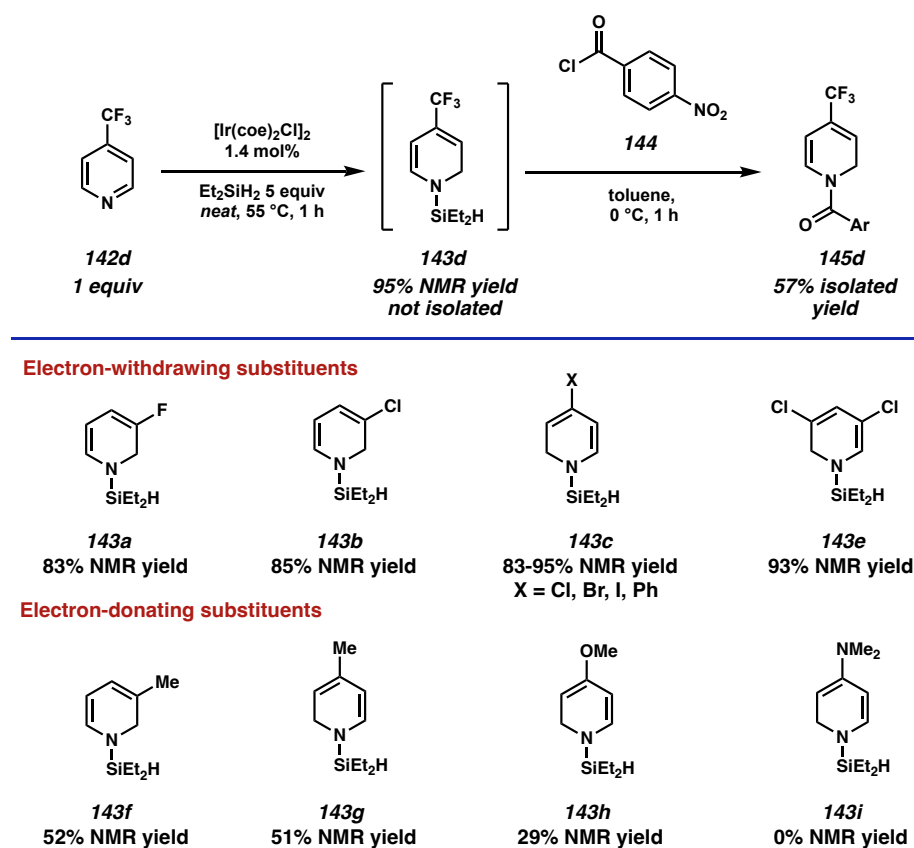


## 2.2 INITIAL INVESTIGATION INTO THE DEAROMATIVE ASYMMETRIC ALLYLIC ALKYLATION OF PYRIDINES

For the dearomative hydrosilylation, we selected the iridium(I)-catalyzed hydrosilylation of pyridines (and other *N*-heterocycles) reported by Chang and coworkers in 2016 (Scheme 2.2.1).<sup>13</sup> Due to its low loading of the commercially available  $[\text{Ir}(\text{coe})\text{Cl}]_2$  catalyst and neat reaction conditions, we envisioned that this hydrosilylation protocol would be ideal for the telescoped reaction conditions. The instability of the *N*-silyl enamine intermediate **143** formed after the dearomative 1,2-hydrosilylation primed us to investigate telescoped reaction conditions to avoid the unfeasible isolation of the air- and moisture-sensitive enamine intermediate. They showed that electron-withdrawing substituents at C–3 or C–4 of the pyridine substrates was well tolerated, delivering the corresponding *N*-silyl enamines **143a–e** in exquisite regioselectivity and good yield. Unfortunately, neither

substitution at C–2 nor the substitution of electron-releasing groups were shown to be well tolerated on the pyridine substrates. Consequently, the scope of our pyridine substrates was limited to C–3 and C–4 substituted pyridines due to the limitations of the dearomative hydrosilylation technology.

**Scheme 2.2.1** Chang et al. Ir-catalyzed 1,2- hydrosilylation of pyridines **142**



We began our initial investigation into the enantioselective, dearomative allylic alkylation of pyridines using 3-fluoropyridine **142a** as our pro-nucleophile (Table 2.2.1). To test the hydrosilylation, we treated 3-fluoropyridine **142a** with 1 mol% of  $[\text{Ir}(\text{coe})\text{Cl}]_2$  and 5 equivalents of diethyl silane at 50 °C for 3 hours. In accordance with Chang’s results, we found almost quantitative conversion to the *N*-silyl dihydropyridine **143a** confirmed via

LC/MS. This mixture was added to a solution of Pd<sub>2</sub>(dba)<sub>3</sub> (2.5 mol%), PPh<sub>3</sub> (15 mol %) and cinnamyl methyl carbonate **146** (1.5 equiv) in DCM at 40 °C for 16 hours.

**Table 2.2.1** Ligand optimization screen of the dearomatization/asymmetric allylic alkylation of 3-fluoropyridine **142a**

Entry	Ligand	147a	148a	149a
1	PPh <sub>3</sub>	2% yield n.d.	11% yield	<5% yield
2	L17	<5% yield 48% ee	n.d.	<5% yield
3	L18	<5% yield 42% ee	n.d.	<5% yield
4	L19	<5% yield 28% ee	17% yield	<5% yield
5	L20	<5% yield 0% ee	n.d.	<5% yield
6	L21	n.d. n.d.	n.d.	n.d.
7	L15	5% yield 30% ee	12% yield	7% yield
8	L22	34% yield 96% ee	12% yield	7% yield
9	L23	n.d. n.d.	n.d.	n.d.
10	L24	n.d. n.d.	n.d.	n.d.

**L17**

**L18**  
Ar = 3,5-*t*Bu-4-OMeC<sub>6</sub>H<sub>2</sub>

**L19**

**L20**

**L21**

**L15**

**L22**

**L23: Ar = *o*-Tolyl**  
**L24: Ar = 4-OMeC<sub>6</sub>H<sub>4</sub>**



To our delight, we observed the desired dearomative allylic alkylation product **147a** in trace quantities via LC/MS. However, two side products were also detected. Namely, the rearomatized 3-alkylated pyridine **148a** was observed as the major product (11%) alongside a bisalkylated side product **149a** determined to be the double alkylation at C-3 (Table 2.2.1, entry 1). After this promising hit, we screened a variety of phosphine ligands to increase the yield of the desired allylic alkylation product. Initial screening of monodentate phosphines revealed that more electron-rich, electron-deficient, or more sterically demanding phosphine ligands relative to PPh<sub>3</sub> could improve the outcome of this reaction. Having established a proof of concept for this reaction pathway, we turned our attention toward developing an asymmetric variant of the dearomative allylic alkylation. To control the stereochemistry at the C-3-position, several privileged chiral monodentate and bidentate phosphine ligands, such as PHOX **L21**, phosphoramidite **L17**, BINAP **L19**, DTBM-SegPhos **L18**, and DIOP **L20** were investigated (Table 2.2.1, entries 2–6). Unfortunately, less than 5% of the desired product was observed in all reaction. However, enantioinduction was observed using the Trost scaffold **L15** (Table 2.2.1, entry 7) and Feringa's phosphoramidite **L17** (Table 2.2.1, entry 2) in up to 30% ee and 48% ee respectively. Employing Trost-DACH ligand **L22** (7 mol%) resulted in significantly increased conversion of the *N*-silyl enamine delivering the desired allylic alkylation product **147a** in an improved 34% yield and an excellent enantioselectivity of 96% (Table 2.2.1, entry 8). With this promising result using the Trost-DACH ligand **L22**, we focused our efforts toward the derivatization of the scaffold to improve the performance in the transformation. Various ligands bearing different phosphine aryl group substitution and backbone modifications were synthesized. Unfortunately, modifications on the ligand did

not result in an improved performance in the transformation, ultimately leading us to use Trost-DACH ligand **L22** moving forward (Table 2.2.1, entries 9–10).

**Table 2.2.2** Solvent optimization screen of the dearomatization/asymmetric allylic alkylation of 3-fluoropyridine **142a**

Entry	Solvent	147a	148a	149a
1	CH <sub>2</sub> Cl <sub>2</sub>	34% yield 96% ee	12% yield	7% yield
2	PhH	18% yield 98% ee	11% yield	<5% yield
3	THF	15% yield 98% ee	24% yield	<5% yield
4	Dioxane	20% yield 98% ee	15% yield	<5% yield
5	MeCN	n.d.	n.d.	n.d.
6	HFIP	n.d.	n.d.	n.d.
7	DCE	22% yield n.d.	15% yield	n.d.
8	DMF	n.d.	n.d.	n.d.

We performed a solvent screen and determined that CH<sub>2</sub>Cl<sub>2</sub> to be the ideal solvent, delivering the desired allylic alkylation product **147a** in a modest yield (34% yield), but excellent enantioselectivity (96% ee). Other solvents such as benzene, THF and 1,4-dioxane delivered the mono alkylated product **147a** in higher enantioselectivity (98% ee), albeit in much lower yields (Table 2.2.2, entries 2–4). Solvents such as MeCN, HFIP and DMF completely inhibited the allylic alkylation (Table 2.2.2, entries 5–7). DCE delivered the desired alkylation product **147a**; however, the yield of the product was lower compared to the reaction performed in DCM (Table 2.2.2, entry 8).

$\text{Pd}(\text{OAc})_2$  was found to be the optimal Pd source during our optimization campaign, while other precursors such as  $\text{Pd}_2\text{dba}_3 \cdot \text{CHCl}_3$  gave similar results (Table 2.2.3, entries 1–2). Other Pd sources investigated such as  $\text{Pd}_2\text{dmba}_3$  or  $[\text{Pd}(\text{cinnamyl})\text{Cl}]_2$  resulted in a decreased yield of the desired allylic alkylation product **147a** (Table 2.2.3, entries 3–4).

**Table 2.2.3** Pd-catalyst screen of the dearomatization/asymmetric allylic alkylation of 3-fluoropyridine **142a**

Entry	Pd Source	147a	148a	149a
1	$\text{Pd}(\text{OAc})_2$ (5 mol%)	38% yield 96% ee	8% yield	5% yield
2	$\text{Pd}_2\text{dba}_3 \cdot \text{CHCl}_3$	38% yield 96% ee	9% yield	10% yield
3	$\text{Pd}_2\text{dmba}_3$	23% yield n.d.	5% yield	<5% yield
4	$[\text{Pd}(\text{cinnamyl})\text{Cl}]_2$	28% yield n.d.	12% yield	<5% yield

We focused our efforts toward the investigation of various additives to improve the conversion of silyl enamine **143a** toward the desired allylic alkylation product **147a** (Table 2.2.4). Generally, the addition of stoichiometric base additives led toward a decrease in the desired allylic alkylation product with an increase in the observed pyridine aromatized allyl product **148a** (Table 2.2.4, entries 1–4). To our delight, the addition of alkali metal fluoride sources such as CsF and NaF led to a general increase in yield of the desired allylic alkylation product **147a** (Table 2.2.4, entries 5–8). We observed that introduction of catalytic amounts of sodium fluoride resulted in an increase conversion to the desired allylic alkylation product **147a** (49% yield) with no reduction in the

enantioselectivity (96% ee). Further exploration of additives for the allylic alkylation step had no beneficial effect relative to the results obtained utilizing catalytic amounts of sodium fluoride and cinnamyl methyl carbonate **146a** as the electrophile.

**Table 2.2.4** Additive screen of the dearomatization/asymmetric allylic alkylation of 3-fluoropyridine **142a**

Entry	Additive	147a	148a	149a
1	LiOt-Bu (1.0 equiv)	n.d.	n.d.	n.d.
2	LiOAc (1.0 equiv)	32% yield	n.d.	<5% yield
3	DBU (1.0 equiv)	5% yield	n.d.	<5% yield
4	Et <sub>3</sub> N (1.0 equiv)	38% yield	n.d.	<5% yield
5	CsF (1.0 equiv)	44% yield	96% ee	<5% yield
6	CsF (0.2 equiv)	48% yield	n.d.	<5% yield
7	NaF (0.2 equiv)	49% yield	96% ee	8% yield
8	NaF (0.1 equiv)	49% yield	96% ee	8% yield
9	AcOH (0.5 equiv)	35% yield	n.d.	n.d.
10	ZnOTf <sub>2</sub> (0.2 equiv)	n.d.	n.d.	n.d.
11	PhB (0.2 equiv)	n.d.	n.d.	n.d.
12	NaBH(OAc) <sub>3</sub>	11% yield	n.d.	<5% yield

Our final efforts toward optimization was investigating the effects of Ir: Pd-catalyst ratio on the desired telescoped transformation (Table 2.2.5). Using 3-chloropyridine **142b** as the pronucleophile and altering the amount of the iridium dimer to 0.5 or 2.5 mol% resulted in significantly decreased amount of the monoalkylated product **147b** (Table 2.2.5, entries 2 and 3). In the case of 0.5 mol% iridium, the desired product **147b** was obtained in a diminished 5% yield while both the 3-alkylated pyridine **148b** and double alkylation

product **149b** were obtained in an increased 34% yield and 45% yield respectively (Table 2.2.5, entry 2). With high iridium catalyst loadings, the *N*-silyl enamine **143b** undergoes a second hydrosilylation event prior to the asymmetric allylic alkylation, resulting in trace products observed resulting from enamine alkylation. This suggests that the iridium catalyst is critical for the initial generation of the *N*-silyl enamine nucleophile **143** as well as controlling the fate of the imine intermediate formed after the first Pd-catalyzed allylic alkylation event. Both catalysts are required for the reaction as no desired product was obtained without the presence of either the Ir- or Pd-catalyst.

**Table 2.2.5** Catalyst loading screen of the dearomatization/asymmetric allylic alkylation of 3-chloropyridine **142b**

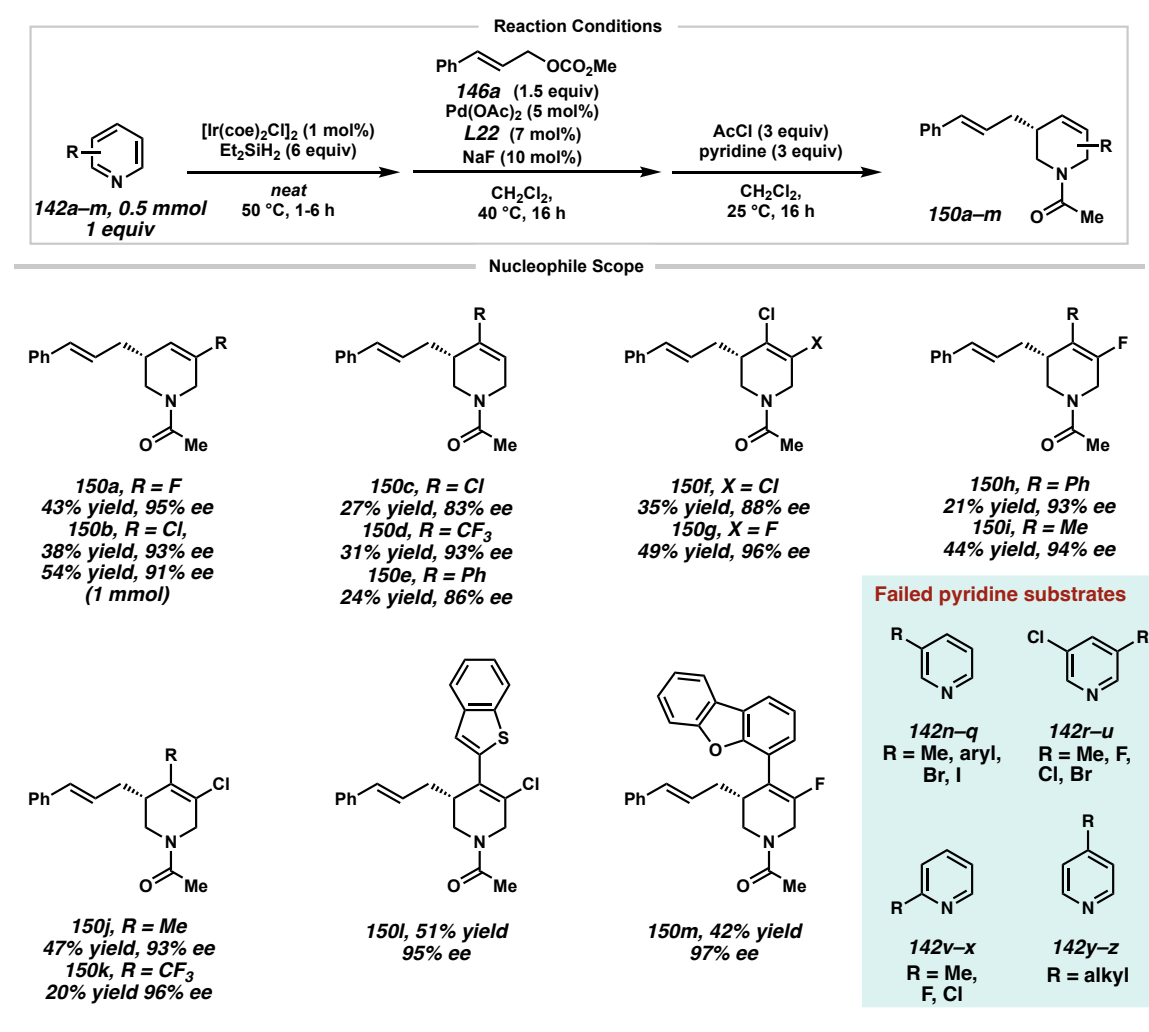
Entry	X	Y	147b	148b	149b	
1	1 mol%	5 mol%	37% yield	93% ee	16% yield	24% yield
2	0.5 mol%	5 mol%	14% yield	n.d.	34% yield	45% yield
3	2.5 mol%	5 mol%	5% yield	n.d.	<5% yield	<5% yield
4	1 mol%	10 mol%	28% yield	n.d.	12% yield	<5% yield

## 2.3 SCOPE OF THE DEAROMATIVE ASYMMETRIC ALLYLIC ALKYLATION OF PYRIDINES

In the reaction setting, the iridium-catalyzed hydrosilylation was performed under argon. After the indicated time, this reaction mixture was added to a pre-stirred mixture of palladium catalyst, **L22** and carbonate **146** in  $\text{CH}_2\text{Cl}_2$  under argon and heated to 40 °C for

the indicated time. With the optimized conditions in hand, we investigated the substrate scope of the telescoped pyridine hydrosilylation/enantioselective allylic alkylation (Scheme 2.3.1). For simplified handling during the purification, the product amines **147** were protected by *N*-acylation in an additional step in the same pot to deliver *N*-Acylated product **150**.

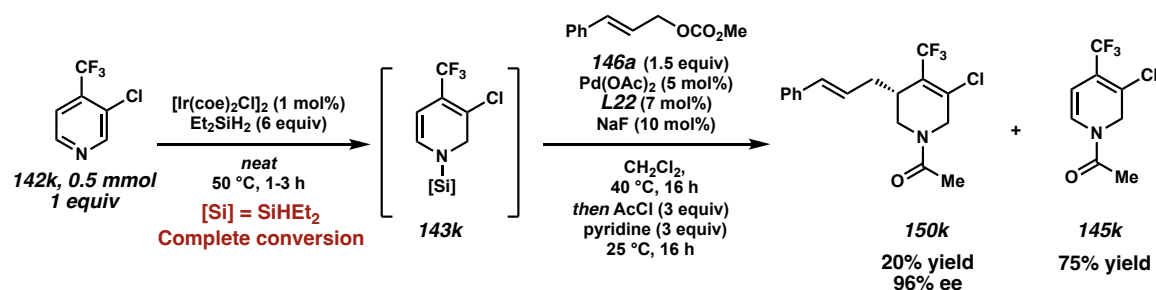
**Scheme 2.3.1** Pyridine pronucleophile scope of the enantioselective allylic alkylation



Various electron-poor pyridines reacted smoothly to the desired products **150a-d** and **150f-k** in moderate yields (between 21–51%), but in most cases with excellent

enantioselectivity (above 90% ee). Substituents are generally tolerated in the 3 and 4 position of the pyridine (Scheme 2.3.1). Substituents on the 2 or 6 position of the pyridine did not yield any desired product. This was expected since no C–2/C–6 substitution was shown to be tolerated in the original hydrosilylation report, most likely due to the steric hinderance for the first hydrosilylation step. Motifs such as 4-aryl or 4-heteroaryl pyridines (**150e**, **150h** and **150l–m**) also gave the desired products in moderate yields and excellent enantioselectivity. Unfortunately, pyridines pronucleophiles with substitution at C–3 with groups such as Br, I, Me or aryl were not tolerated in the reaction. 3,5-disubstitution was also not tolerated, even though these substrates were shown to undergo the Ir-catalyzed hydrosilylation. Alternative pro-nucleophiles such as pyrimidines, pyrazines, isoquinolines and quinolines were also not tolerated in the sequence, presumably due to the inability to engage with the optimized Pd-catalyst for the asymmetric allylic alkylation. Additionally C–2 substitution or alkyl substitution at C–4 of the pyridine pro-nucleophile was not tolerated.

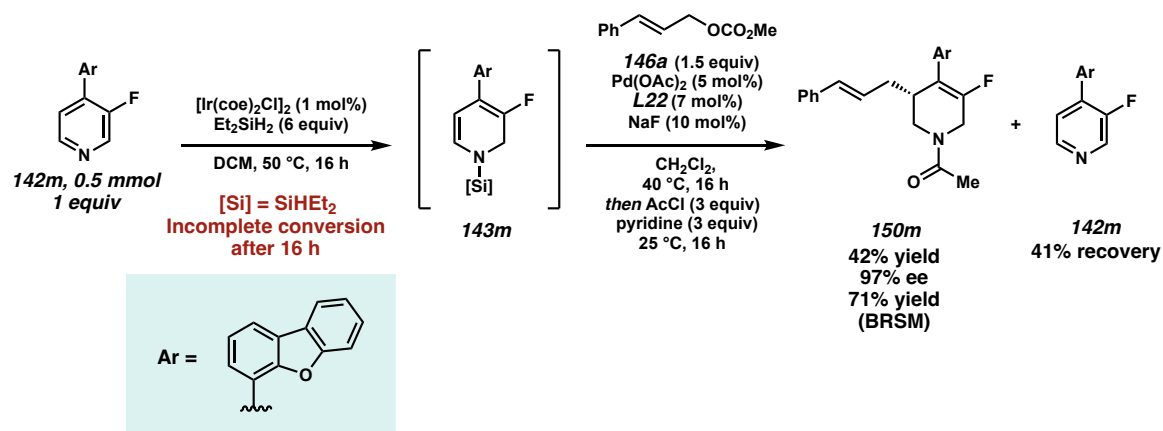
**Scheme 2.3.2** Outcome of the pyridine asymmetric allylic alkylation using electron-poor pyridine substrates



For highly electron deficient pyridines such as 3-chloro,4-trifluoromethylpyridine **142k**, the lower isolated yield of the desired allylic alkylation product **150k** was due to the significantly slower Pd-catalyzed allylic alkylation. This was suggested by the isolation of

the acetylated dihydropyridine product **145k** in 75% yield while the desired allylic alkylation product **150k** was obtained in a 20% yield (Scheme 2.3.2). More electron-rich pyridines were challenging in this reaction mainly due to the significantly slower iridium catalyzed hydrosilylation reaction previously reported. Residual pyridine in the reaction mixture was not completely inhibiting to the palladium catalyzed allylic alkylation; however, it decreased the overall yield of the desired allylic alkylation product. Contrary to the results observed using 3-fluoropyridine **142a** and 3-chloropyridine **142b** during the optimization of the reaction conditions, there was minimal formation of the undesired rearomatization product **148** or double alkylation product **148** for the more electron-rich pyridines (**150e**, **150h–i** and **150l–m**).

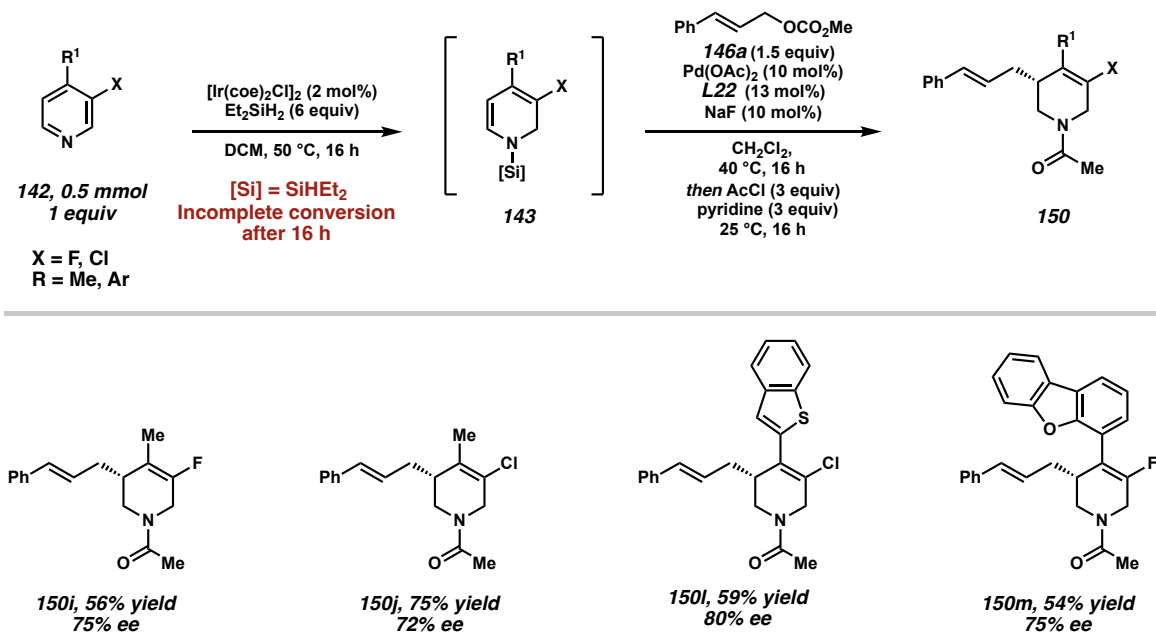
**Scheme 2.3.3** Outcome of the pyridine asymmetric allylic alkylation using electron-rich pyridine substrates



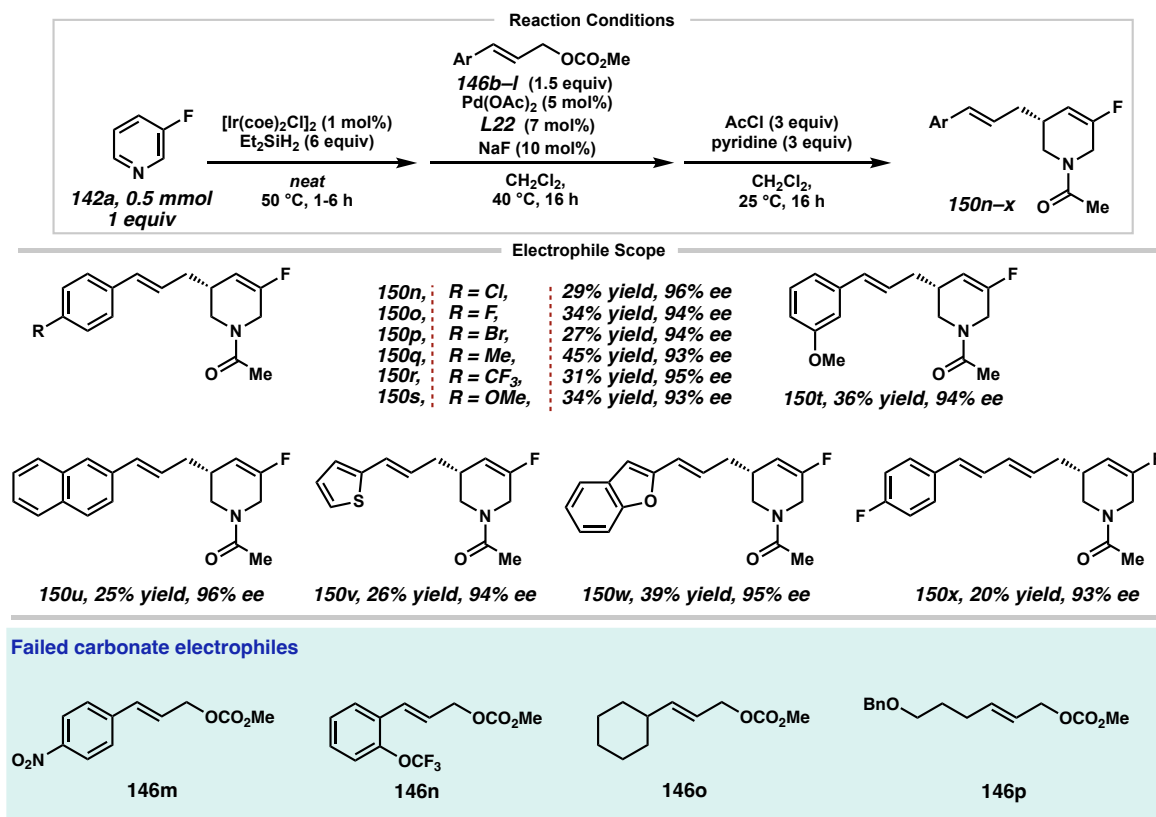
The lower isolated yield was predominantly due to unreacted starting material pyridine in the iridium-catalyzed hydrosilylation. For example, 3-fluoro-4-dibenzofuran substituted product **150m** was obtained in a 42% yield over three steps, but a 71% yield based on recovered starting material pyridine **142m** (Scheme 2.3.3).



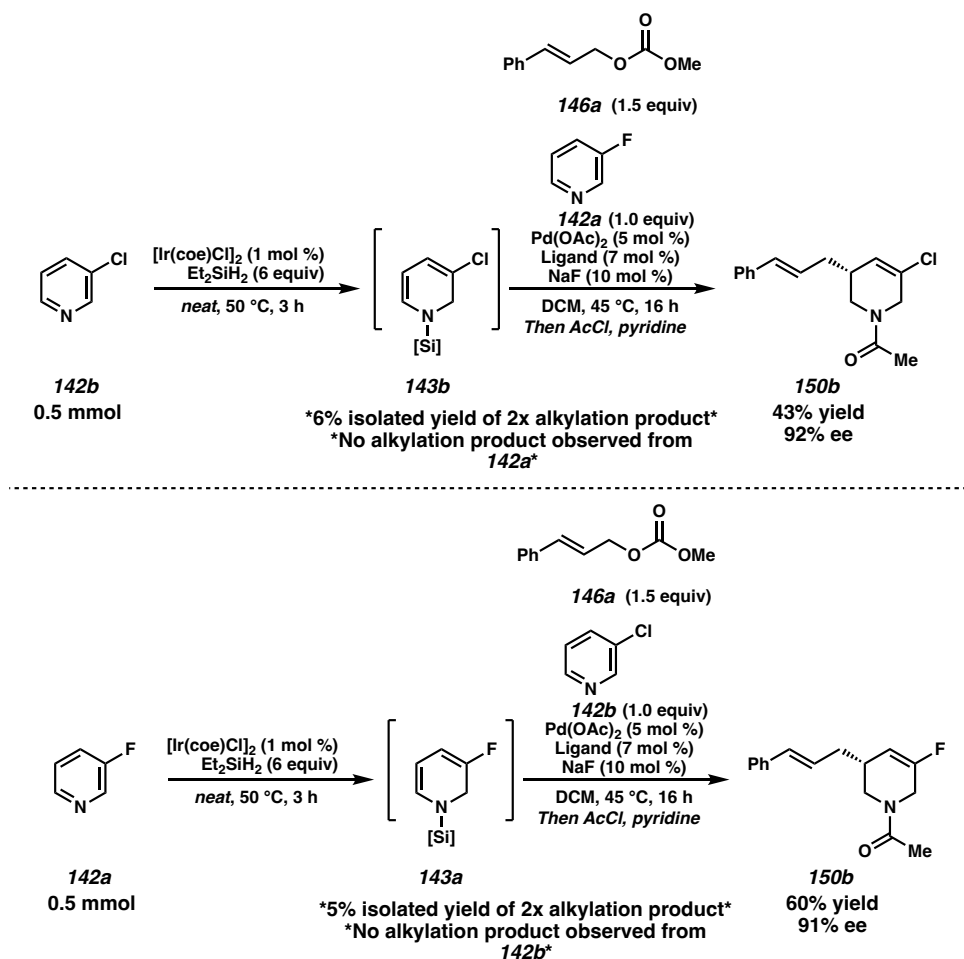
**Scheme 2.3.4** Outcome of the pyridine asymmetric allylic alkylation using electron-rich pyridine substrates using higher catalyst loadings



Increasing the iridium catalyst loading increased the overall yield for the more electron-rich pyridines **150i–j**, **150l–m**; however, the desired allylic alkylation products were obtained in a decrease in enantioselectivity for each of the four substrates investigated (Scheme 2.3.4). We hypothesize that the increased Ir-catalyst loading results in greater conversion of the more electron rich pyridine **142** to the corresponding *N*-silyl enamine **143**. Unfortunately, this increased Ir- and Pd-catalyst loading promotes an undesired racemization of the newly formed stereogenic center (potentially via a metal catalyzed imine-enamine tautomerization after allylic alkylation) resulting in a decreased observed enantioselectivity of the allylic alkylation product **150**.

**Scheme 2.3.5** Carbonate electrophile scope of the enantioselective allylic alkylation

The electrophile scope on the other hand tolerates electron donating as well as withdrawing substituents on the arene (Scheme 2.3.5), giving the corresponding products in moderate yields and excellent enantioselectivity (**150n–150s**). *Meta*-substitution on the arene also delivered the desired product (**150t**), while *ortho*-substituted cinnamyl carbonates showed no conversion in this transformation (**146n**). The use of *para*-NO<sub>2</sub> substituted arene electrophile **146m** did not deliver any desired product, potentially due to the reduction of the nitro group under the hydrosilylation conditions. Fortunately, heteroaromatic carbonates could be applied in this reaction as shown by products **150v** and **150w**. While simple alkyl substituted allylic carbonates did not afford any product (**146o–p**), we found that a conjugated diene precursor delivered the diene product **150x** in low yield but excellent enantioselectivity.

**Scheme 2.3.6** Mixed pyridine control experiment

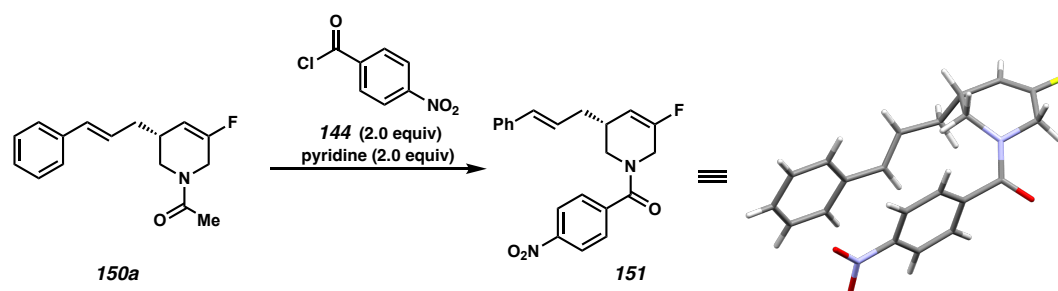
In control experiments, doping the reaction with an additional equivalent of a 3-halopyridine during the Pd-catalyzed allylic alkylation step resulted in an increase in yield and selectivity of the desired monoalkylation product for both pyridines investigated (Scheme 2.3.6). Our hypothesis is that the 3-halopyridine additive buffers the reaction mixture during the Pd-catalyzed allylic alkylation to limit the undesired enamine tautomerization that leads to the double alkylation product. Since the undesired tautomerization is minimized, the yield of the desired alkylation product **150** increases with the addition of an excess equivalent of pyridine. Additionally, no allylic alkylation product

of the doped pyridine was observed, suggesting the Ir-catalyzed dearomative hydrosilylation is not occurring during the Pd-catalyzed allylic alkylation step.

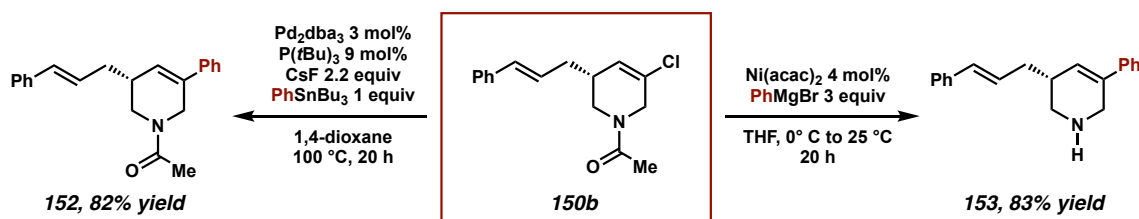
## 2.4 PRODUCT DERIVITIZATIONS FROM THE ASYMMETRIC ALLYLIC ALKYLATION

To unambiguously confirm the structure of the newly formed products (i.e. **150**) and to identify the absolute stereochemistry of these products, **150a** was derivatized with 4-nitrobenzoyl chloride **144** (Scheme 2.4.1). Slow evaporation of a solution of the corresponding amide **151** in methanol delivered crystals suitable for X-ray analysis. By analogy, the absolute configuration was adopted for the remaining scope entries.

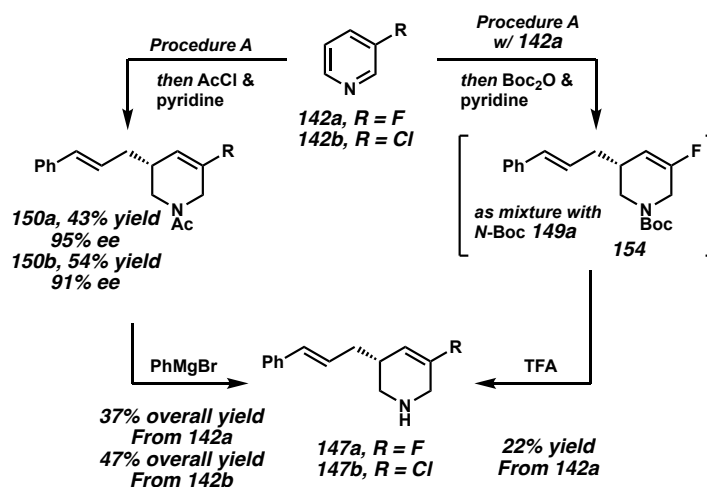
**Scheme 2.4.1** X-ray crystallization of derivatized tetrahydropyridine product **151**



The products **150** bearing a vinyl chloride handle also allowed further derivatization via cross-coupling chemistry, as demonstrated for **150b** (Scheme 2.4.2). Typical Stille conditions with  $\text{PhSnBu}_3$  delivered the C–C cross coupled products **152** in 82% yield, while a Ni-catalyzed Kumada reaction provided the *N*-deprotected C–C cross coupled product **153** with similar yield. (Scheme 2.4.2), showing the synthetic utility of these motifs.

**Scheme 2.4.2** Divergent cross coupling methods of vinyl halide product

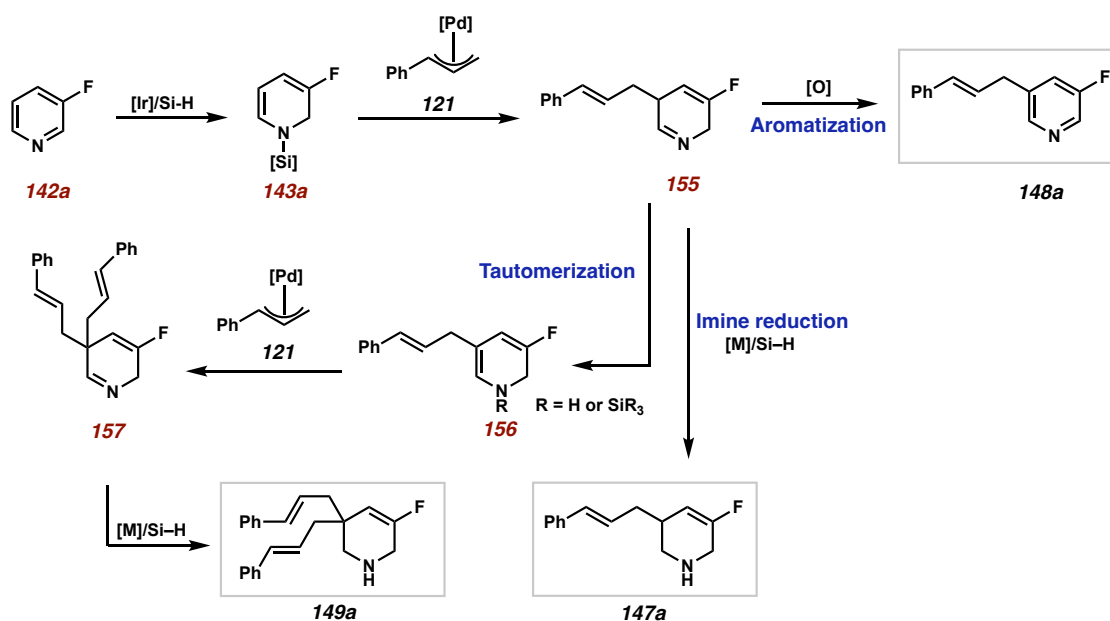
From a synthetic perspective, the free N–H-products such as **147** and **153** are also of high interest. However, the direct purification by column chromatography after the second step, the Pd-catalyzed allylic alkylation, proved to be challenging due to the polarity of amine product **147** as well as the complex reaction mixture of rearomatized product **148** and bisalkylated product **140**. *N*-Boc protection of the reaction mixture after allylic alkylation and a subsequent purification delivers an inseparable mixture of the *N*-Boc protected desired product **154** as well as bisalkylated *N*-Boc side product **149**. An acidic deprotection with TFA allowed the isolation of the pure N–H-product **147a** in 22% yield over all 4 steps (Scheme 2.4.3). Alternatively, the *N*-acetylated compounds **150** can be treated with PhMgBr to give the free N–H-product **147** in a 85–88% yield (37% yield over 4 steps for amine **147a**, 47% yield over 4 steps for amine **147b**).

**Scheme 2.4.3** Synthesis of chiral N–H tetrahydropyridine products

## 2.5 PROPOSED MECHANISM OF THE DEAROMATIVE, ASYMMETRIC ALLYLIC ALKYLATION

Based on these results and our understanding, the proposed reaction sequence begins with the iridium-catalyzed 1,2-hydrosilylation of the pyridine substrate **142** leading to the *N*-silyl enamine intermediate **143** (Scheme 2.5.1). The palladium-catalyzed allylic alkylation leads to cyclic imine (or *N*-silyl iminium ion) intermediate **155**. There are several plausible pathways from this key intermediate **155** to result in the three products obtained after the telescoped reaction. The excess of silane in the reaction mixture and the resulting overall reductive conditions in the presence of the two transition metals can lead to a reduction of the imine, delivering the desired chiral allylic alkylation product **147**.

**Scheme 2.5.1** Proposed mechanism for the formation of the observed products



Another pathway, which could explain the formation of the bisalkylated product **149**, is the tautomerization of the imine **155** to the enamine **156**, resulting in a nucleophile that can participate in an additional alkylation event. Reduction of the product imine **157**

leads to the bisalkylated side product **149**. Additionally, the proposed tautomerization results in the ablation of the set stereocenter, thus conditions that promote this undesired tautomerization result in lower yield as well as lower enantioselectivity of the desired allylic alkylation product **147**. The observed rearomatized product **148** can potentially form at different stages during the proposed sequence, but would require an oxidant (i.e., air).

## 2.6 SYNTHESIS OF BISALKYLATED TETRAHYDROPYRIDINE PRODUCT

During the investigation of the reaction scope, we observed the bisalkylated side products **149** occur in different ratios based on the substrate. Since the motifs can be of synthetic interest as well, the transformation was optimized toward these scaffolds using 3-chloropyridine **142b** as the standard substrate. After screening alkylating reagents with leaving groups of various basicity and various additives (**LG1–12**), it was discovered that catalytic loading of benzoic acid (20 mol%) significantly shifts the selectivity toward the bisalkylated product **149b** (Table 2.6.1).

**Table 2.6.1** Alkylating reagents screen of the dearomative allylic alkylation

Entry	LG =	147b	148b	149b
1	LG1	37% yield	16% yield	24% yield
2	LG2	20% yield	18% yield	38% yield
3	LG3	31% yield	10% yield	32% yield
4	LG4	22% yield	21% yield	24% yield
5	LG5	28% yield	7% yield	38% yield
6	LG6	4% yield	17% yield	<5% yield
7	LG7	14% yield	18% yield	38% yield
8	LG8	20% yield	21% yield	13% yield
9	LG9	n.d.	n.d.	n.d.
10	LG10	13% yield	5% yield	5% yield
11	LG11	n.d.	n.d.	n.d.
12	LG12	n.d.	n.d.	n.d.
13*	LG1*	17% yield	7% yield	61% yield

\*20 mol% PhCO<sub>2</sub>H\*

LG1

LG2

LG3

LG4

LG5

LG6

LG7

LG8

LG9

LG10

LG11

LG12

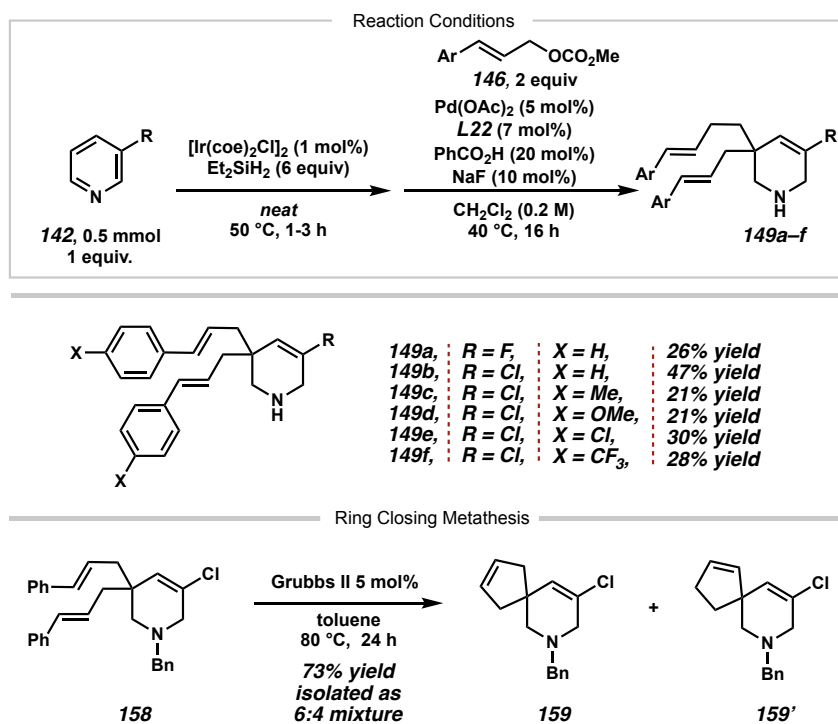
<sup>1</sup> ee of product **147b** not determined.

The electronic properties of the alkylating reagent seem to have less of an influence on the outcome of the reaction toward the bisalkylated product. The bisalkylated products **149** enable a potential ring closing metathesis (RCM) to yield spirocyclic compounds. Therefore, the *N*-benzyl product **158** was treated with typical RCM conditions under ruthenium catalysis. The spirocyclic compound **159** was successfully formed in good yield



of 73%, although as a 6:4 mixture of isomers (**159**:**159'**) that is formed by the isomerization of the disubstituted olefin (Scheme 2.6.1).

**Scheme 2.6.1** Scope of bisalkylated products and RCM derivatization



## 2.7 CONCLUSION

In conclusion, we have developed the first intermolecular asymmetric allylic alkylation (AAA) using electron poor arenes, namely pyridines, as C-pro-nucleophiles. A step wise one-pot sequence allows rapid access to interesting molecular scaffolds in excellent enantioselectivities, although in moderate yields. The products are valuable building blocks for further exploration. In particular, the chlorine-substituted tetrahydropyridines are shown to be of particular use for the synthetic community as complex building blocks.

## 2.8 EXPERIMENTAL SECTION

### 2.8.1 MATERIALS AND METHODS

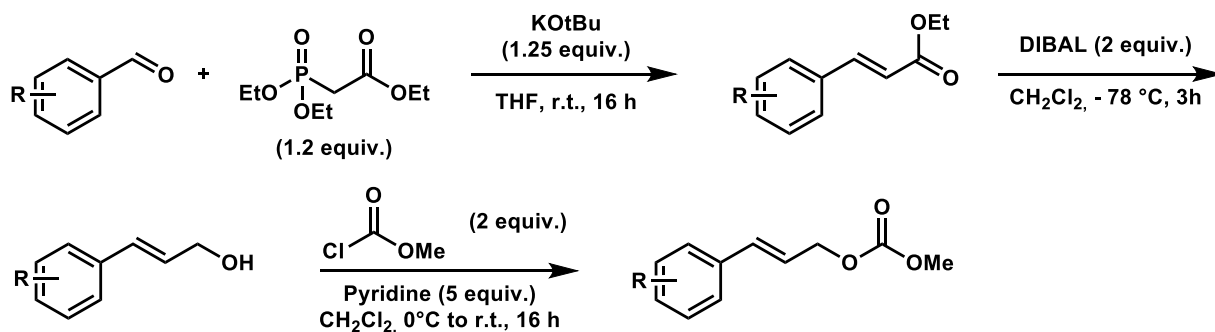
Unless otherwise stated, reactions were performed in oven-dried glassware under an argon or nitrogen atmosphere using dry, deoxygenated solvents. Solvents were dried by passage through an activated alumina column under argon. Reaction temperatures stated in the manuscript, or this document are reported as temperature of the surrounding metal heating blocks. TLC was performed using E. Merck silica gel 60 F254 precoated glass plates (0.25 mm) and visualized by UV fluorescence quenching or KMnO<sub>4</sub> staining. Silicycle SiliaFlash® P60 Academic Silica gel (particle size 40–63 μm) was used for flash chromatography. <sup>1</sup>H NMR spectra were recorded on Varian Inova 500 MHz and Bruker 400 MHz spectrometers and are reported relative to residual CHCl<sub>3</sub> (δ 7.26 ppm) or MeOH (δ 4.87 ppm). <sup>13</sup>C NMR spectra were recorded on a Varian Inova 500 MHz spectrometer (125 MHz) and Bruker 400 MHz spectrometers (101 MHz) and are reported relative to CHCl<sub>3</sub> (δ 77.16 ppm) or MeOH (δ 49.00 ppm). <sup>19</sup>F NMR and <sup>31</sup>P NMR Spectra are reported without reference. Data for <sup>1</sup>H NMR are reported as follows: chemical shift (δ ppm) (multiplicity, coupling constant (Hz), integration). Multiplicities are reported as follows: s = singlet, d = doublet, t = triplet, q = quartet, p = pentet, sept = septuplet, m = multiplet, and br s = broad singlet. Data for <sup>13</sup>C NMR are reported in terms of chemical shifts (δ ppm) plus (multiplicity, coupling constant (Hz)) in appropriate cases. IR spectra were obtained by use of a Perkin Elmer Spectrum BXII spectrometer or Nicolet 6700 FTIR spectrometer using thin films deposited on NaCl plates and reported in frequency of absorption (cm<sup>-1</sup>). Optical rotations were measured with a Jasco P-2000 polarimeter operating on the sodium D-line (589 nm), using a 100 mm path-length cell. Analytical

SFC was performed with a Mettler SFC supercritical CO<sub>2</sub> analytical chromatography system utilizing Chiralpak (AD-H, AS-H or IC) or Chiralcel (OD-H, OJ-H, or OB-H) columns (4.6 mm x 25 cm) obtained from Daicel Chemical Industries, Ltd. High resolution mass spectra (HRMS) were obtained from Agilent 6200 Series TOF with an Agilent G1978A Multimode source in electrospray ionization (ESI+), atmospheric pressure chemical ionization (APCI+), or mixed ionization mode (MM: ESI-APCI+). Absolute configuration of **151** was determined by X-ray diffraction, and all other products are assigned by analogy. Reagents were purchased from commercial sources and used as received unless otherwise stated. 3-Fluoropyridine, 3-chloropyridine, 4-chloropyridine and 4-(trifluoromethyl)-pyridine were distilled over CaH<sub>2</sub> under nitrogen atmosphere prior to use. Diethylsilane was used as received. No significant differences in reactivity and yield were observed from different commercial sources (SigmaAldrich, Gelest or Alfa Aesar). The used Iridium ([Ir(coe)<sub>2</sub>Cl]<sub>2</sub>) catalyst was purchased from Strem Chemicals, Inc, transferred to the glovebox and used as received. The used Palladium catalyst (Pd(OAc)<sub>2</sub>) was purchased from SigmaAldrich, transferred to the glovebox and used as received.

## 2.8.2 EXPERIMENTAL PROCEDURES

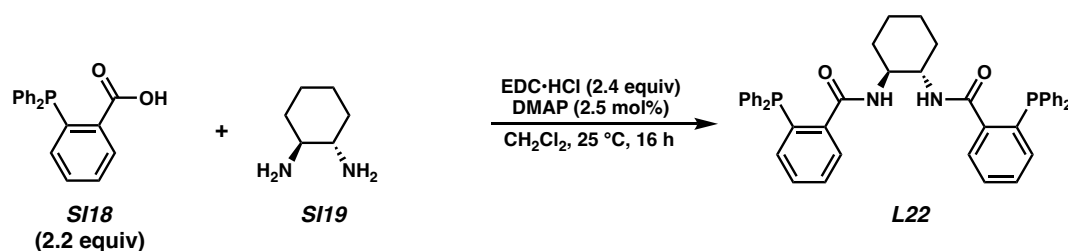
### General Procedure 1: Synthesis of carbonate reagents (**146**)

All carbonate reagents **146** used in this study have previously been described in the literature and were prepared accordingly. The general synthetic route can be seen in General Procedure 1. The analytical data agrees with the literature.



### General Procedure 2: Ligand preparation (L)

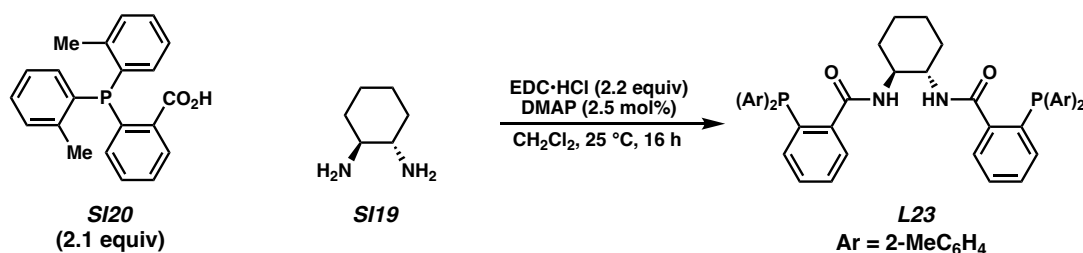
Ligands **L22–24** were prepared either according to literature procedure, are commercially available or as described below. The detailed procedure for the optimized ligand **L22** that is used in this study can be seen below in Scheme 2.



### *N,N'*-((1*S*,2*S*)-cyclohexane-1,2-diyl)bis(2-(diphenylphosphanyl)benzamide) (**L22**):

DACH-Trost-Ligand **L22** was prepared following the reaction in Scheme 2 according to a literature procedure (*European Journal of Organic Chemistry* **2007**, 7, 1145). Therefore, commercial 2-(diphenylphosphanyl)benzoic acid **SI18** (15.48 g, 50.6 mmol, 2.2 equiv) was dissolved in CH<sub>2</sub>Cl<sub>2</sub> (120 mL). DMAP (70 mg, 0.575 mmol, 2.5 mol%) was added, followed by EDC·HCl (10.58 g, 55.2 mmol, 2.4 equiv). The mixture was stirred at room temperature for 5 min. (1*S*,2*S*)-Cyclohexane-1,2-diamine **SI19** (2.63 g, 23 mmol, 1.0 equiv) in CH<sub>2</sub>Cl<sub>2</sub> (30 mL) was added and the resulting mixture was stirred at room temperature for 16 hours. The reaction was quenched with saturated NH<sub>4</sub>Cl solution (~100 mL). The phases were separated, and the organic phase was dried over magnesium sulfate

and filtered. The crude reaction mixture was submitted to flash column chromatography over silica gel using hexane/EtOAc = 7/3 as the eluent to yield a white solid **L22** (11.5 g). The white solids were redissolved in boiling MeCN (~350 mL) and slowly cooled to room temperature overnight to yield white crystals (9.5 g, 13.75 mmol, 69% yield);  $^1\text{H}$  NMR (300 MHz,  $\text{CDCl}_3$ )  $\delta$  7.60 – 7.55 (m, 2H), 7.34 – 7.16 (m, 24H), 6.94 – 6.87 (m, 2H), 6.32 (d,  $J$  = 7.2 Hz, 2H), 3.85 – 3.71 (m, 2H), 1.90 – 1.80 (m, 2H), 1.70 – 1.59 (m, 2H), 1.28 – 1.15 (m, 2H), 1.05 – 0.90 (m, 2H);  $^{31}\text{P}$  NMR (121 MHz,  $\text{CDCl}_3$ ):  $\delta$  -9.75. All characterization data match those reported.

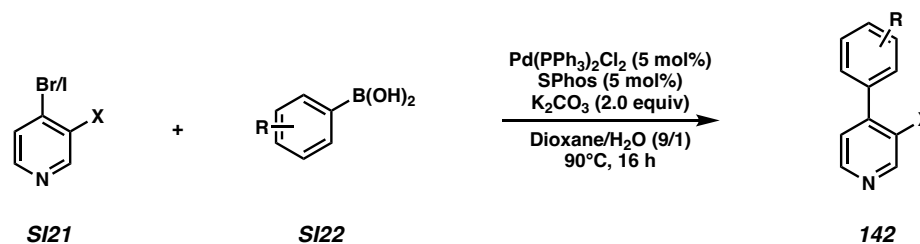


***N,N'*-((1*S*,2*S*)-cyclohexane-1,2-diyl)bis(2-(di-*o*-tolylphosphanyl)benzamide) (L23):** 2-(di-*o*-tolylphosphanyl)benzoic acid **SI20** (0.97 g, 2.9 mmol, 2.1 equiv) was dissolved in  $\text{CH}_2\text{Cl}_2$  (10 mL). DMAP (4.3 mg, 0.035 mmol, 2.5 mol%) was added, followed by EDC·HCl (0.59 g, 3.08 mmol, 2.2 equiv). The mixture was stirred at room temperature for 5 min. (1*S*,2*S*)-Cyclohexane-1,2-diamine **SI19** (160 mg, 1.4 mmol, 1.0 equiv) in  $\text{CH}_2\text{Cl}_2$  (5 mL) was added and the resulting mixture was stirred at room temperature for 16 hours. The reaction was quenched with saturated  $\text{NH}_4\text{Cl}$  solution (~20 mL). The phases were separated, and the organic phase was dried over magnesium sulfate and filtered. The crude reaction mixture was submitted to flash column chromatography over silica gel using hexane/EtOAc = 7/3 as the eluent to yield a white solid **L23** (0.81 g, 1.1 mmol, 79% yield);

$^1\text{H}$  NMR (400 MHz,  $\text{CDCl}_3$ )  $\delta$  7.60 – 7.55 (m, 2H), 7.30 – 7.15 (m, 12H), 7.08 (t,  $J = 7.2$  Hz, 2H), 7.02 – 6.96 (m, 2H), 6.87 (ddd,  $J = 7.5, 3.8, 1.5$  Hz, 2H), 6.77 – 6.69 (m, 4H), 6.44 – 6.32 (bs, 2H), 3.77 – 3.66 (m, 2H), 2.33 (dd,  $J = 6.8, 1.6$  Hz, 12H), 1.84 – 1.76 (m, 2H), 1.63 – 1.55 (m, 2H), 1.20 – 1.11 (m, 2H), 0.90 – 0.78 (m, 2H);  $^{13}\text{C}$  NMR (101 MHz,  $\text{CDCl}_3$ ) (several signals overlap, see spectra)  $\delta$  169.22, 169.21, 142.40, 142.14, 141.96, 141.68, 135.72, 135.60, 135.38, 135.26, 134.54, 134.42, 134.35, 132.95, 132.90, 130.20, 130.18, 130.14, 130.10, 128.90, 128.75, 128.63, 127.80, 127.75, 126.42, 126.06, 53.71, 31.53, 24.56, 21.33, 21.25, 21.12, 21.04;  $^{31}\text{P}$  NMR (121 MHz,  $\text{CDCl}_3$ ):  $\delta$  -24.79; IR (Neat Film, NaCl) 3750, 3352, 3287, 3055, 3005, 2936, 2856, 2358, 2242, 1922, 1732, 1696, 1636, 1586, 1522, 1464, 1453, 1434, 1378, 1328, 1306, 1269, 1202, 1161, 1130, 1033, 910, 872, 829, 799, 751, 733  $\text{cm}^{-1}$ ; (MM:ESI $^+$ )  $m/z$  calc'd for  $\text{C}_{48}\text{H}_{49}\text{N}_2\text{O}_2\text{P}_2$   $[\text{M}+\text{H}]^+$ : 747.3269, found 747.3271.

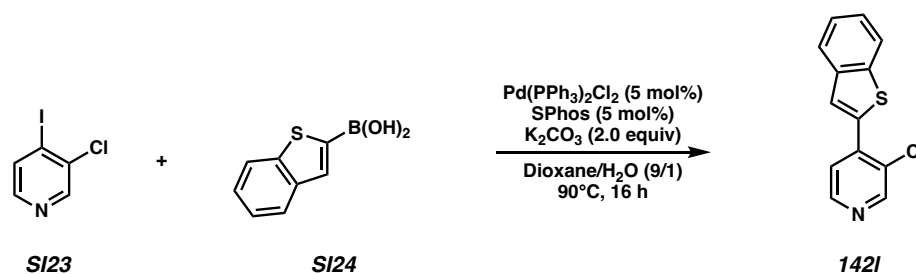
### General Procedure 3: Synthesis of Pyridine substrates

The pyridines (**142**) that were used in this study were either prepared according to literature procedure, were commercially available or were prepared as described below.

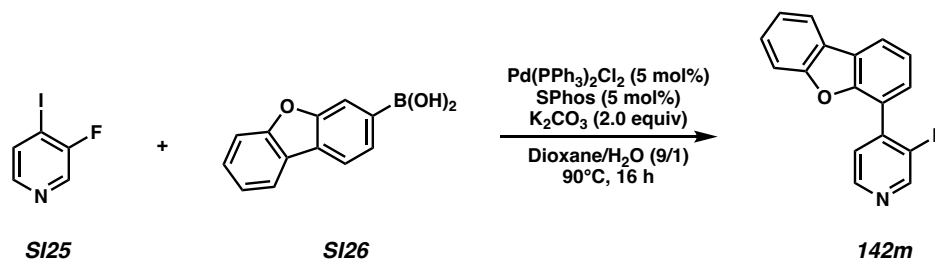


$\text{Pd(PPh}_3)_2\text{Cl}_2$  (5 mol%), SPhos (5 mol%) and  $\text{K}_2\text{CO}_3$  (2.0 equiv) were added to a 25 mL screw vial under air. The solid aryl boronic acid **SI22** (1.2 equiv) was added, followed by the pyridine **SI21** (1.0 equiv), if solid. The vial was sealed with a septum screw cap and evacuated using standard Schlenk line technology. The atmosphere was refilled with

nitrogen. Dioxane and water (9/1) were added subsequently (~0.2 M) and the mixture was stirred at room temperature. Pyridine **SI21** (1.0 equiv) was added, if liquid. The reaction mixture was then heated to 90 °C for 16 hours. The mixture was cooled to room temperature and diluted with EtOAc (~100 mL) and brine (~100 mL). The phases were separated and the organic phase was dried over magnesium sulfate and filtered. The pure aryl pyridines **142** were separated by flash column chromatography over silica gel using hexane/EtOAc (typically 9/1 to 8/2) as eluent.

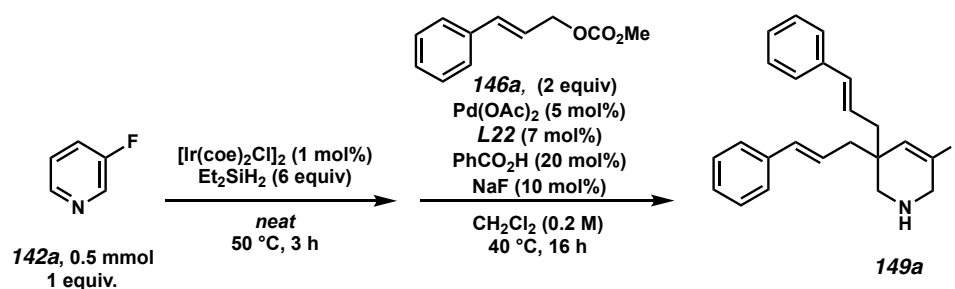


**4-(benzo[b]thiophen-2-yl)-3-chloropyridine (142I)** was synthesized following the general procedure using 4-iodo-3-chloropyridine **SI23** (1.0 g, 4.2 mmol, 1.0 equiv) and benzo[b]thiophen-2-ylboronic acid **SI24** (0.90 g, 5.04 mmol, 1.2 equiv). The desired product **142I** was obtained as white solids (0.72 g, 2.93 mmol, 70% yield); <sup>1</sup>H NMR (400 MHz, CDCl<sub>3</sub>) δ 8.71 (s, 1H), 8.51 (d, *J* = 5.1 Hz, 1H), 7.90 – 7.84 (m, 3H), 7.52 (dd, *J* = 5.1, 0.6 Hz, 1H), 7.43 – 7.38 (m, 2H); <sup>13</sup>C NMR (101 MHz, CDCl<sub>3</sub>) δ 151.05, 148.00, 140.45, 140.13, 139.67, 137.18, 129.50, 126.42, 125.71, 124.97, 124.79, 124.58, 122.25; IR (Neat Film, NaCl) 3054, 1578, 1473, 1435, 1396, 1239, 1103, 1040, 955, 864, 830, 761, 744, 722 cm<sup>-1</sup>; (MM:ESI<sup>+</sup>) *m/z* calc'd for C<sub>13</sub>H<sub>9</sub>ClNS: 246.0144, found 246.0140.



**4-(dibenzo[b,d]furan-4-yl)-3-fluoropyridine (142m)**: was synthesized following the general procedure using 4-iodo-3-fluoropyridine **SI25** (1.0 g, 4.5 mmol, 1.0 equiv) and dibenzo[b,d]furan-4-ylboronic acid **SI26** (1.14 g, 5.4 mmol, 1.2 equiv). The desired product **142m** was obtained as white solids (0.5 g, 1.9 mmol, 42% yield) after column chromatography (Hexane/EtOAc = 9/1):  $R_f = 0.38$ ;  $^1\text{H NMR}$  (400 MHz,  $\text{CDCl}_3$ )  $\delta$  8.65 (d,  $J = 2.1$  Hz, 1H), 8.58 (dd,  $J = 4.9, 1.0$  Hz, 1H), 8.06 (dd,  $J = 7.7, 1.3$  Hz, 1H), 8.01 (ddd,  $J = 7.7, 1.3, 0.7$  Hz, 1H), 7.73 (dd,  $J = 6.3, 4.9$  Hz, 1H), 7.63 – 7.57 (m, 2H), 7.52 – 7.44 (m, 2H), 7.39 (td,  $J = 7.5, 1.0$  Hz, 1H);  $^{13}\text{C NMR}$  (101 MHz,  $\text{CDCl}_3$ )  $\delta$  156.85 (d,  $J = 258.9$  Hz), 156.30, 153.41, 145.93 (d,  $J = 5.2$  Hz), 139.22 (d,  $J = 25.3$  Hz), 131.78 (d,  $J = 12.0$  Hz), 128.22 (d,  $J = 3.7$  Hz), 127.81, 125.62, 125.26, 123.95, 123.27, 123.13, 121.92, 120.95, 117.58, 112.02;  $^{19}\text{F NMR}$  (282 MHz,  $\text{CDCl}_3$ )  $\delta$  -128.92 (d,  $J = 6.4$  Hz); IR (Neat Film, NaCl) 3055, 1601, 1470, 1450, 1421, 1406, 1264, 1206, 1188, 1153, 1050, 842, 831, 793, 743, 620  $\text{cm}^{-1}$ ; (MM:ESI $^+$ )  $m/z$  calc'd for  $\text{C}_{17}\text{H}_{13}\text{FNO}$ : 264.0825, found 264.0818.

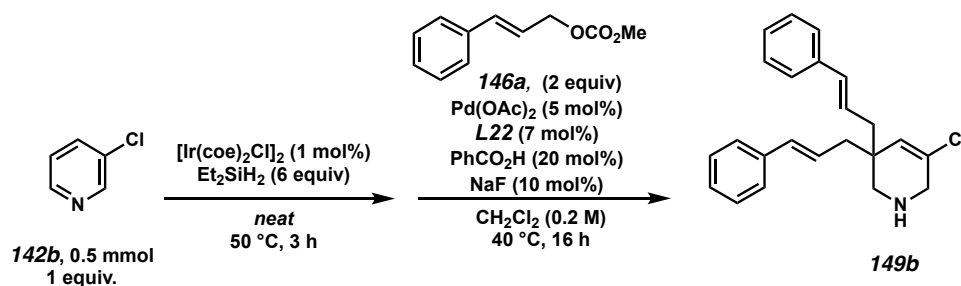
#### General Procedure 4: Synthesis of bisalkylated products



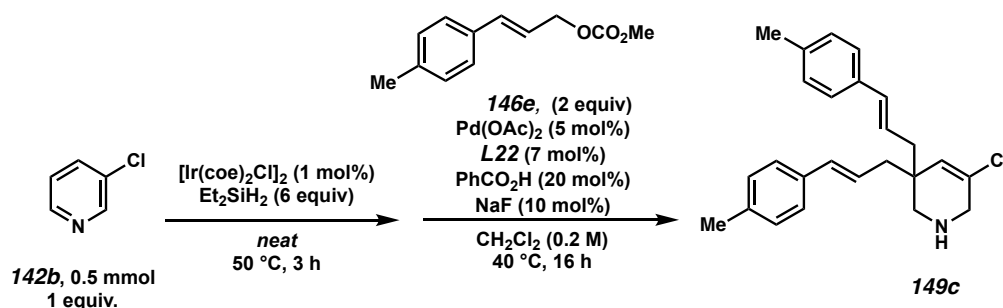


**3,3-dicinnamyl-5-fluoro-1,2,3,6-tetrahydropyridine (149a):** In a 2 mL screw vial, equipped with a magnetic stir bar, pyridine **142a** (0.5 mmol, 1.0 equiv) was added and the resulting reaction mixture was stirred at 50 °C for 3 hours. A separate 10 mL screw vial equipped with a magnetic stir bar was transferred to the glovebox. Ligand **L22** (24.2 mg, 0.035 mmol, 7 mol%), NaF (2.1 mg, 0.05 mmol, 10 mol%), PhCOOH (12.2 mg, 0.1 mmol, 20 mol%) and palladium(II) acetate (Pd(OAc)<sub>2</sub>, 5.6 mg, 0.025 mmol, 5 mol%) were added. The vial was closed with a septum screw cap and transferred out of the glovebox. Dichloromethane (CH<sub>2</sub>Cl<sub>2</sub>, 2.5 mL) was added at room temperature under nitrogen. The mixture was stirred for 5 minutes. Cinnamyl methyl carbonate **146a** (192.2 mg, 1.0 mmol, 2.0 equiv) was added, followed by the reaction mixture from the 2 mL vial. The resulting mixture was then stirred at 40 °C for 24 h. Afterwards, the reaction mixture was cooled to room temperature and acetic acid (1 mL) was added and the mixture was stirred at room temperature for 2 hours. The mixture was diluted with dichloromethane and an aqueous work up with 4 M NaOH solution was performed to neutralize the acetic acid. The aqueous phase was extracted with dichloromethane once and ethyl acetate once. The combined organic fractions were dried over magnesium sulfate. The solvent was evaporated and the residue was submitted to flash column chromatography over silica gel using a solvent mixture of hexane/acetone = 7/3 as the eluent. The desired compound **149a** was obtained as colorless oil (43.7 mg, 0.131 mmol, 26% yield over two steps); <sup>1</sup>H NMR (400 MHz, CDCl<sub>3</sub>) δ 7.29 – 7.20 (m, 8H), 7.16 – 7.11 (m, 2H), 6.36 (d, *J* = 15.7 Hz, 2H), 6.13 (dt, *J* = 15.5, 7.5 Hz, 2H), 5.15 (d, *J* = 18.3 Hz, 1H), 3.48 (bs, 1H), 3.25 (d, *J* = 1.5 Hz, 2H), 2.68 (s, 2H), 2.28 – 2.17 (m, 4H); <sup>13</sup>C NMR (101 MHz, CDCl<sub>3</sub>) δ 158.98 (d, *J* = 264.0 Hz), 137.39, 133.55, 128.72, 127.44, 126.25, 125.71, 108.17 (d, *J* = 10.2 Hz), 51.98 (d, *J* = 2.0

Hz), 43.70 (d,  $J = 30.2$  Hz), 42.32 (d,  $J = 2.3$  Hz), 39.76 (d,  $J = 4.7$  Hz)  $^{19}\text{F}$  NMR (282 MHz,  $\text{CDCl}_3$ ):  $\delta -110.42$  (d,  $J = 18.3$  Hz); ; IR (Neat Film, NaCl) 3335, 3058, 3025, 2919, 2850, 2358, 1698, 1652, 1598, 1576, 1558, 1495, 1448, 1372, 1270, 1159, 1092, 1027, 967, 922, 853, 745, 694  $\text{cm}^{-1}$ ; (MM:ESI $^+$ )  $m/z$  calc'd for  $\text{C}_{23}\text{H}_{25}\text{FN}$   $[\text{M}+\text{H}]^+$ : 334.1971, found 334.1958.

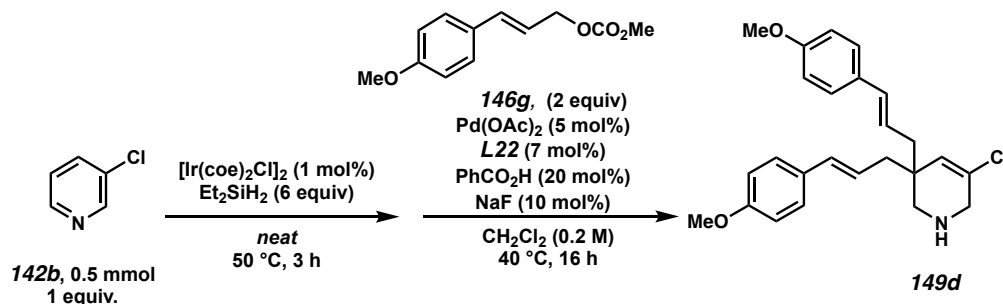


**5-chloro-3,3-dicinnamyl-1,2,3,6-tetrahydropyridine (149b)** was synthesized following the above general procedure A using 3-chloropyridine **142b** (47  $\mu\text{L}$ , 0.5 mmol, 1.0 equiv) as substrate. The desired compound **149b** was obtained as colorless oil (82.2 mg, 0.235 mmol, 47% yield over two steps);  $^1\text{H}$  NMR (400 MHz,  $\text{CDCl}_3$ )  $\delta$  7.28 – 7.20 (m, 8H), 7.16 – 7.11 (m, 2H), 6.36 (d,  $J = 15.8$  Hz, 2H), 6.11 (dt,  $J = 15.5, 7.5$  Hz, 2H), 5.76 – 5.72 (m, 1H), 3.28 (d,  $J = 1.7$  Hz, 2H), 2.71 (s, 2H), 2.42 (bs, 1H), 2.28 – 2.16 (m, 4H);  $^{13}\text{C}$  NMR (101 MHz,  $\text{CDCl}_3$ )  $\delta$  137.32, 133.68, 132.23, 130.07, 128.71, 127.47, 126.25, 125.41, 51.48, 50.00, 41.90, 41.58; IR (Neat Film, NaCl) 3336, 3054, 3025, 2916, 2358, 1651, 1599, 1494, 1448, 1072, 1004, 966, 856, 744, 692  $\text{cm}^{-1}$ ; (MM:ESI $^+$ )  $m/z$  calc'd for  $\text{C}_{23}\text{H}_{25}\text{ClN}$   $[\text{M}+\text{H}]^+$ : 350.1676, found: 350.1671;



**5-chloro-3,3-bis((*E*)-3-(*p*-tolyl)allyl)-1,2,3,6-tetrahydropyridine (149c):** was

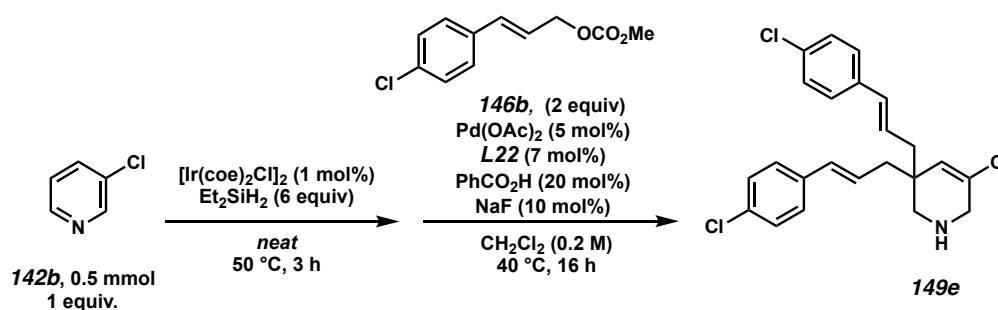
synthesized following the above general procedure 4 using 3-chloropyridine **142b** (47.5  $\mu L$ , 0.5 mmol, 1.0 equiv) as substrate and (*E*)-methyl 3-(*p*-tolyl)allyl carbonate **146e** (206 mg, 1.0 mmol, 2.0 equiv). The desired compound was obtained as colorless oil **149c** (40 mg, 0.106 mmol, 21% yield over two steps);  $^1H$  NMR (400 MHz,  $CDCl_3$ ):  $\delta$  7.26 (d,  $J = 8.1$  Hz, 4H), 7.13 (d,  $J = 7.8$  Hz, 4H), 6.42 (d,  $J = 15.8$  Hz, 2H), 6.14 (dt,  $J = 15.5, 7.5$  Hz, 2H), 5.82 (s, 1H), 3.36 (d,  $J = 1.7$  Hz, 2H), 2.79 (s, 2H), 2.34 (s, 6H), 2.29 (ddd,  $J = 8.0, 4.9, 1.3$  Hz, 4H), 2.03 (s, 1H);  $^{13}C$  NMR (101 MHz,  $CDCl_3$ ):  $\delta$  137.3, 134.6, 133.5, 132.2, 130.2, 129.4, 126.2, 124.4, 51.5, 49.2, 41.9, 41.6, 21.3; IR (Neat Film, NaCl) 3023, 2920, 2359, 1747, 1699, 1651, 1512, 1435, 1264, 1108, 968, 795  $cm^{-1}$ ; (MM:ESI $^+$ )  $m/z$  calc'd for  $C_{23}H_{25}ClN$  [ $M+H$ ] $^+$ : 378.1989, found: 378.2011.



**5-chloro-3,3-bis((*E*)-3-(4-methoxyphenyl)allyl)-1,2,3,6-tetrahydropyridine (149d):**

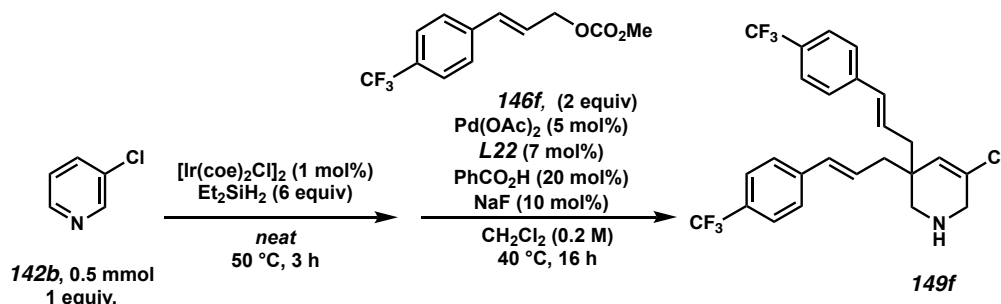
was synthesized following the above general procedure 4 using 3-chloropyridine **142b**

(47.5  $\mu$ L, 0.5 mmol, 1.0 equiv) as the pyridine substrate and (*E*)-3-(4-methoxyphenyl)allyl methyl carbonate **146g** (222 mg, 1.0 mmol, 2.0 equiv). The desired compound was obtained as colorless oil **149d** (57 mg, 0.139 mmol, 28% yield over two steps);  $^1\text{H}$  NMR (400 MHz,  $\text{CDCl}_3$ )  $\delta$  7.21 (d,  $J = 8$  Hz, 4H), 6.78 (d,  $J = 8$  Hz, 4H), 6.31 (d,  $J = 15.8$  Hz, 2H), 5.98 (ddd,  $J = 15.4, 8.0, 7.1$  Hz, 2H), 5.75 (s, 1H), 3.73 (s, 6H), 3.29 (s, 2H), 2.87 (br s, 1H), 2.72 (s, 2H), 2.26 – 2.14 (m, 4H);  $^{13}\text{C}$  NMR (101 MHz,  $\text{CDCl}_3$ )  $\delta$  159.1, 133.0, 130.3, 130.2, 128.3, 127.4, 123.2, 114.1, 55.4, 51.5, 50.0, 41.9, 41.6; IR (Neat Film, NaCl) 3029, 3002, 2931, 2834, 1653, 1606, 1576, 1510, 1461, 1441, 1298, 1248, 1174, 1107, 1034, 1034, 967, 905, 839, 753, 644  $\text{cm}^{-1}$ ; (MM:ESI $^+$ )  $m/z$  calc'd for  $\text{C}_{25}\text{H}_{29}\text{ClNO}_2$  [M+H] $^+$ : 410.1887, found: 410.1861.



**5-chloro-3,3-bis((*E*)-3-(4-chlorophenyl)allyl)-1,2,3,6-tetrahydropyridine (149e)**: was synthesized following the above general procedure 4 using 3-chloropyridine **142b** (47.5  $\mu$ L, 0.5 mmol, 1.0 equiv) as substrate and (*E*)-3-(4-chlorophenyl)allyl methyl carbonate **146b** (226 mg, 1.0 mmol, 2.0 equiv). The desired compound was obtained as yellowish oil **149e** (63 mg, 0.150 mmol, 30% yield over two steps);  $^1\text{H}$  NMR (400 MHz,  $\text{CDCl}_3$ ):  $\delta$  7.27 (s, 8H), 6.40 (d,  $J = 15.8$  Hz, 2H), 6.25 – 6.03 (m, 2H), 5.81 (s, 1H), 3.37 (d,  $J = 1.7$  Hz, 2H), 2.79 (s, 2H), 2.35 – 2.27 (m, 4H), 2.21 (br s, 1H);  $^{13}\text{C}$  NMR (101 MHz,  $\text{CDCl}_3$ ):  $\delta$  135.7, 133.1, 132.5, 132.5, 129.8, 128.9, 127.5, 126.1, 51.5, 49.6, 41.9, 41.6; IR (Neat

Film, NaCl) 3027, 2917, 2839, 2359, 1651, 1489, 1434, 1404, 1264, 1093, 1012, 969, 896, 846, 736  $\text{cm}^{-1}$ ; (MM:ESI<sup>+</sup>)  $m/z$  calc'd for  $\text{C}_{23}\text{H}_{22}\text{Cl}_3\text{N}$   $[\text{M}+\text{H}]^+$ : 418.0896, found: 418.0882.



### 5-chloro-3,3-bis((*E*)-3-(4-(trifluoromethyl)phenyl)allyl)-1,2,3,6-tetrahydropyridine

**(149f)**: was synthesized following the above general procedure 4 using 3-chloropyridine **142b** (47.5  $\mu\text{L}$ , 0.5 mmol, 1.0 equiv) as substrate and (*E*)-methyl (3-(4-(trifluoromethyl)phenyl)allyl) carbonate **146f** (260 mg, 1.0 mmol, 2.0 equiv). The desired compound was obtained as colorless oil **149f** (52 mg, 0.107 mmol, 21% yield over two steps);  $^1\text{H}$  NMR (400 MHz,  $\text{CDCl}_3$ )  $\delta$  7.57 (d,  $J = 8.2$  Hz, 4H), 7.44 (d,  $J = 8.3$  Hz, 4H), 6.50 (d,  $J = 15.8$  Hz, 2H), 6.30 (dt,  $J = 15.6, 7.5$  Hz, 2H), 5.83 (s, 1H), 3.40 (s, 2H) 2.82 (s, 2H), 2.53–2.28 (m, 5H);  $^{13}\text{C}$  NMR (101 MHz,  $\text{CDCl}_3$ )  $\delta$  140.1, 132.7, 132.4, 129.6, 129.4 (q,  $J = 32.3$  Hz), 128.1, 126.4, 125.7 (q,  $J = 3.9$  Hz), 124.3 (q,  $J = 272$  Hz), 51.3, 49.9, 42.0, 41.6;  $^{19}\text{F}$  NMR (282 MHz,  $\text{CDCl}_3$ )  $\delta$  -62.5; IR (Neat Film, NaCl) 2921, 1652, 1615, 1415, 1326, 1170, 1160, 1123, 1068, 1016, 971, 953, 861  $\text{cm}^{-1}$ ; (MM:ESI<sup>+</sup>)  $m/z$  calc'd for  $\text{C}_{25}\text{H}_{23}\text{ClF}_6\text{N}$   $[\text{M}+\text{H}]^+$ : 486.1423, found: 486.1413.

### General Procedure 5: Synthesis of monoalkylated products (electron poor pyridine substrates)

Some compounds **150** were synthesized as followed (as mentioned in the product characterization): In a 2 mL screw vial, equipped with a magnetic stir bar, the corresponding pyridine **142** (0.5 mmol, 1.0 equiv) if solid was added to the vial. The vial

was then transferred to an argon filled glovebox. Chlor-bis-(cycloocten)-iridium(I) dimer ( $[\text{Ir}(\text{coe})_2\text{Cl}]_2$ , 4.5 mg, 0.005 mmol, 1 mol%) was added to the vial. The vial was closed with a septum screw cap. The vial was transferred out of the glovebox. Diethyl silane ( $\text{Et}_2\text{SiH}_2$ , 389  $\mu\text{L}$ , 3.0 mmol, 6.0 equiv) was added and the resulting mixture was stirred at room temperature for 4 minutes. Pyridine **142** (0.5 mmol, 1.0 equiv) if liquid was added and the resulting reaction mixture was stirred at 50 °C for the appropriate time (0.5 – 3 hours). A separate 10 mL screw vial equipped with a magnetic stir bar was transferred to the glovebox. Ligand **L22** (24.2 mg, 0.035 mmol, 7 mol%), NaF (2.1 mg, 0.05 mmol, 10 mol%) and palladium(II) acetate ( $\text{Pd}(\text{OAc})_2$ , 5.6 mg, 0.025 mmol, 5 mol%) were added. The vial was closed with a septum screw cap and transferred out of the glovebox. Dichloromethane ( $\text{CH}_2\text{Cl}_2$ , 2.5 mL) was added at room temperature under nitrogen. The mixture was stirred for 5 minutes. Cinnamyl methyl carbonate **146** (144.2 mg, 0.75 mmol, 1.5 equiv) was added, followed by the reaction mixture from the 2 mL vial. The resulting mixture was then stirred at 40 °C for 24 h. The mixture was then cooled to room temperature and diluted with additional dichloromethane (2.5 mL). Pyridine (121  $\mu\text{L}$ , 1.5 mmol, 3.0 equiv) was added as a base, followed by acetyl chloride (107  $\mu\text{L}$ , 1.5 mmol, 3.0 equiv). The mixture was stirred at room temperature for 16 h. Afterwards, acetic acid (0.5 mL) was added and the mixture was stirred at room temperature for 2 hours. The mixture was diluted with dichloromethane and an aqueous work up with 4 M NaOH solution was performed to neutralize the acetic acid. The aqueous phase was extracted with dichloromethane once and ethyl acetate once. The combined organic fractions were dried over magnesium sulfate. The solvent was evaporated and the residue was submitted to flash

column chromatography over silica gel using a solvent mixture of hexane/ethyl acetate (typically 7/3 to 1/1) as the eluent.

**General Procedure 6: Synthesis of monoalkylated products (electron neutral or electron rich pyridine substrates)**

Some compounds **150** were synthesized as followed (as mentioned in the product characterization): In a 2 mL screw vial, equipped with a magnetic stir bar, the corresponding pyridine **142** (0.5 mmol, 1.0 equiv) if solid was added to the vial. The vial was then transferred to an argon filled glovebox. Chlor-bis-(cycloocten)-iridium(I) dimer ( $[\text{Ir}(\text{coe})_2\text{Cl}]_2$ , 2.3 mg, 0.0025 mmol, 0.5 mol%) was added to the vial. Diethyl silane ( $\text{Et}_2\text{SiH}_2$ , 389  $\mu\text{L}$ , 3.0 mmol, 6.0 equiv) was added and the resulting mixture was stirred at room temperature for 4 minutes. Pyridine **142** (0.5 mmol, 1.0 equiv) if liquid was added and the vial was closed with a screw cap and the resulting reaction mixture was stirred at 45 °C for 6 h. The mixture was cooled to room temperature and additional  $[\text{Ir}(\text{coe})_2\text{Cl}]_2$  catalyst (2.3 mg, 0.0025 mmol, 0.5 mol%) and  $\text{Et}_2\text{SiH}_2$  (195  $\mu\text{L}$ , 1.5 mmol, 3 equiv) were added and the mixture was again stirred at 45 °C for 12 hours. The mixture was again cooled to room temperature and additional  $[\text{Ir}(\text{coe})_2\text{Cl}]_2$  catalyst (2.3 mg, 0.0025 mmol, 0.5 mol%) and  $\text{Et}_2\text{SiH}_2$  (195  $\mu\text{L}$ , 1.5 mmol, 3 equiv) were added for the third time and the mixture again stirred at 45 °C for 2 hours. Afterwards, the mixture was transferred out of the glovebox. A separate 10 mL screw vial equipped with a magnetic stir bar was transferred to the glovebox. Ligand **L22** (24.2 mg, 0.035 mmol, 7 mol%), NaF (2.1 mg, 0.05 mmol, 10 mol%) and palladium(II) acetate ( $\text{Pd}(\text{OAc})_2$ , 5.6 mg, 0.025 mmol, 5 mol%) were added. The vial was closed with a septum screw cap and transferred out of the glovebox. Dichloromethane ( $\text{CH}_2\text{Cl}_2$ , 2.5 mL) was added at room temperature under

nitrogen. The mixture was stirred for 5 minutes. Cinnamyl methyl carbonate **146** (144.2 mg, 0.75 mmol, 1.5 equiv) was added, followed by the reaction mixture from the 2 mL vial. The resulting mixture was then stirred at 40 °C for 24 h. The mixture was then cooled to room temperature and diluted with additional dichloromethane (2.5 mL). Pyridine (121  $\mu$ L, 1.5 mmol, 3.0 equiv) was added as a base, followed by acetyl chloride (107  $\mu$ L, 1.5 mmol, 3.0 equiv). The mixture was stirred at room temperature for 16 h. Afterwards, acetic acid (0.5 mL) was added and the mixture stirred at room temperature for 2 hours. The mixture was diluted with dichloromethane and an aqueous work up with 4 M NaOH solution was performed to neutralize the acetic acid. The aqueous phase was extracted with dichloromethane once and ethyl acetate once. The combined organic fractions were dried over magnesium sulfate. The solvent was evaporated and the residue was submitted to flash column chromatography over silica gel using a solvent mixture of hexane/ethyl acetate as the eluent.

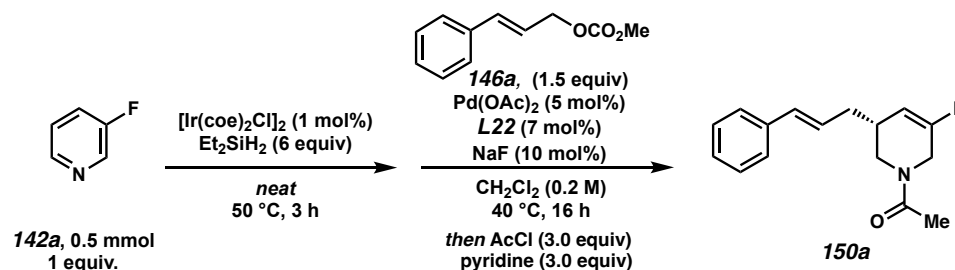
**General Procedure 7: Synthesis of monoalkylated products (electron neutral or electron rich pyridine substrates)**

Some compounds **150** were synthesized as followed (as mentioned in the product characterization): In a 4 mL screw vial, equipped with a magnetic stir bar, the corresponding pyridine **142** (0.5 mmol, 1.0 equiv) if solid was added to the vial. The vial was then transferred to an argon filled glovebox. Chlor-bis-(cycloocten)-iridium(I) dimer ( $[\text{Ir}(\text{coe})_2\text{Cl}]_2$ , 6.9 mg, 0.0075 mmol, 1.5 mol%) was added to the vial. Diethyl silane ( $\text{Et}_2\text{SiH}_2$ , 518  $\mu$ L, 4.0 mmol, 8.0 equiv) was added followed by dichloromethane ( $\text{CH}_2\text{Cl}_2$ , 1.0 mL), and the resulting mixture was stirred at room temperature for 20 minutes. Pyridine **142** (0.5 mmol, 1.0 equiv) if liquid was added neat to the reaction mixture and the vial was



closed with a screw cap. The resulting reaction mixture was stirred at 45 °C for 6–16 h (depending on the pyridine). Afterwards, the mixture was transferred out of the glovebox. A separate 10 mL screw vial equipped with a magnetic stir bar was transferred to the glovebox. Ligand **L22** (24.2 mg, 0.035 mmol, 7 mol%), NaF (2.1 mg, 0.05 mmol, 10 mol%) and palladium(II) acetate (Pd(OAc)<sub>2</sub>, 5.6 mg, 0.025 mmol, 5 mol%) were added. The vial was closed with a septum screw cap and transferred out of the glovebox. Dichloromethane (CH<sub>2</sub>Cl<sub>2</sub>, 2.5 mL) was added at room temperature under nitrogen. The mixture was stirred for 5 minutes. Cinnamyl methyl carbonate **146** (144.2 mg, 0.75 mmol, 1.5 equiv) was added, followed by the reaction mixture from the 2 mL vial. The resulting mixture was then stirred at 40 °C for 24 h. The mixture was then cooled to room temperature and diluted with additional dichloromethane (2.5 mL). Pyridine (121 μL, 1.5 mmol, 3.0 equiv) was added as a base, followed by acetyl chloride (107 μL, 1.5 mmol, 3.0 equiv). The mixture was stirred at room temperature for 16 h. Afterwards, acetic acid (0.5 mL) was added and the mixture stirred at room temperature for 2 hours. The mixture was diluted with dichloromethane and an aqueous work up with 4 M NaOH solution was performed to neutralize the acetic acid. The aqueous phase was extracted with dichloromethane once and ethyl acetate once. The combined organic fractions were dried over magnesium sulfate. The solvent was evaporated and the residue was submitted to flash column chromatography over silica gel using a solvent mixture of hexane/ethyl acetate (typically 7/3 to 2/8) as the eluent.

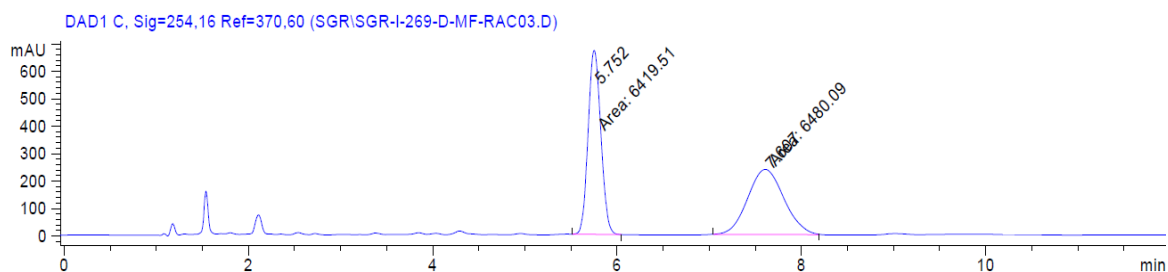
## Product characterization for monoalkylated amine products 150



**(R)-1-(3-cinnamyl-5-fluoro-3,6-dihydropyridin-1(2H)-yl)ethan-1-one (150a):** was synthesized following the general procedure 5. Therefore, 3-fluoropyridine **142a** (43  $\mu\text{L}$ , 0.5 mmol, 1.0 equiv) was used. The desired product **150a** was isolated as colorless oil (55.3 mg, 0.213 mmol, 43% yield over three steps);  $^1\text{H}$  NMR (400 MHz,  $\text{CDCl}_3$ ) (as a mixture of E/Z amide bond isomers)  $\delta$  7.37 – 7.27 (m, 4H), 7.25 – 7.18 (m, 1H), 6.48 – 6.40 (m, 1H), 6.20 – 6.10 (m, 1H), 5.47 – 5.40 (m, 0.4H), 5.36 (ddt,  $J = 16.1, 3.5, 1.5$  Hz, 0.6H), 4.18 – 4.05 (m, 1.4H), 3.97 (dt,  $J = 4.0, 2.0$  Hz, 0.6H), 3.90 (dd,  $J = 13.1, 4.6$  Hz, 0.4H), 3.53 (dd,  $J = 13.4, 4.5$  Hz, 0.6H), 3.26 (dt,  $J = 13.4, 6.8$  Hz, 1H), 2.56 – 2.44 (m, 1H), 2.34 – 2.17 (m, 2H), 2.13 – 2.11 (m, 3H);  $^{13}\text{C}$  NMR (101 MHz,  $\text{CDCl}_3$ ) (as a mixture of E/Z amide bond isomers, signals of minor isomer are indicated with an asterisk \*):  $\delta$  169.81, 169.64\*, 156.33 (d,  $J = 255.5$  Hz), 154.84 (d  $J = 255.2$  Hz)\*, 137.34\*, 137.04, 133.01, 132.75\*, 128.75, 128.63\*, 127.62, 127.35\*, 126.68, 126.24\*, 126.19, 106.12 (d,  $J = 11.0$  Hz)\*, 104.49 (d,  $J = 12.3$  Hz), 47.65, 44.84 (d,  $J = 39.2$  Hz)\*, 42.99\*, 41.16 (d,  $J = 39.9$  Hz), 36.86 (d  $J = 2.0$  Hz)\*, 36.77 (d,  $J = 2.3$  Hz), 34.29 (d,  $J = 6.3$  Hz), 33.37 (d,  $J = 5.9$  Hz)\*, 22.02\*, 21.55;  $^{19}\text{F}$  NMR (282 MHz,  $\text{CD}_3\text{OD}$ ) (as a mixture of E/Z amide bond isomers, signals of minor isomer are indicated with an asterisk \*):  $\delta$  –114.85 (dd,  $J = 16.4, 5.0$  Hz), –116.04 (dd,  $J = 16.4, 5.1$  Hz)\*; IR (Neat Film, NaCl) 3853, 3745, 3675, 3648, 3026, 2914, 2362, 2334, 1707, 1652, 1491, 1436, 1380, 1361, 1274, 1230, 1162, 1106,

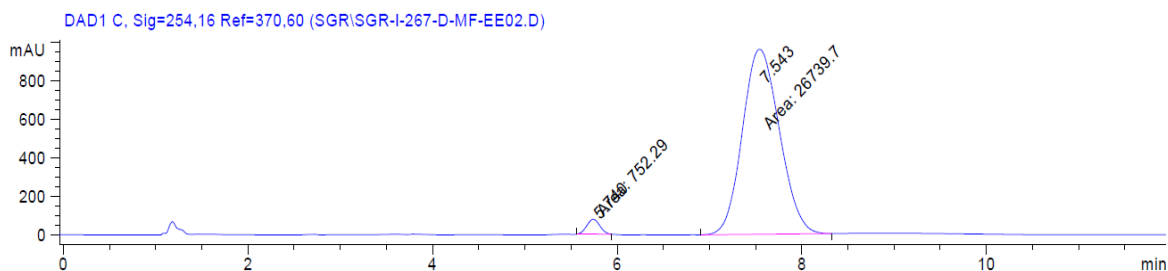
1070, 1032, 969, 831, 745, 695, 682, 618  $\text{cm}^{-1}$ ; (MM:ESI<sup>+</sup>)  $m/z$  calc'd for  $\text{C}_{16}\text{H}_{19}\text{FNO}$   
 $[\text{M}+\text{H}]^+$ : 260.1451, found: 260.1438;  $[\alpha]_{\text{D}}^{25}$ :  $-42.82$  (c 1.0,  $\text{CHCl}_3$ ).

Chiral SFC Separation: 20% MeOH, 2.5 mL/min, AD-H column,  $\lambda = 254$  nm,  $t_{\text{R}}$  (min):  
 minor = 5.75 (area: 2.74%), major = 7.61 (area: 97.26%), 94.5% enantiomeric excess.



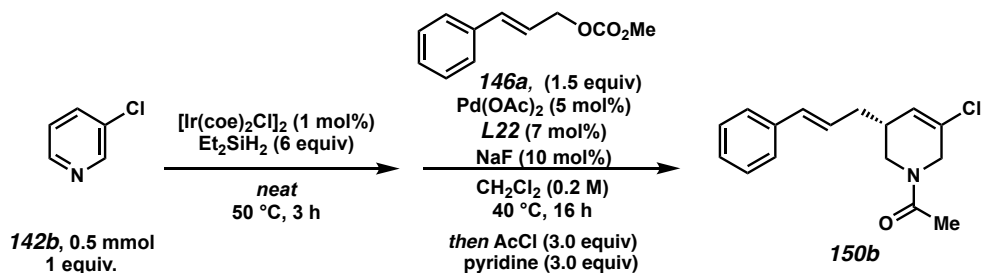
Signal 2: DAD1 C, Sig=254,16 Ref=370,60

Peak #	RetTime [min]	Type	Width [min]	Area [mAU*s]	Height [mAU]	Area %
1	5.752	MM	0.1593	6419.50684	671.81226	49.7652
2	7.607	MM	0.4550	6480.09131	237.34406	50.2348

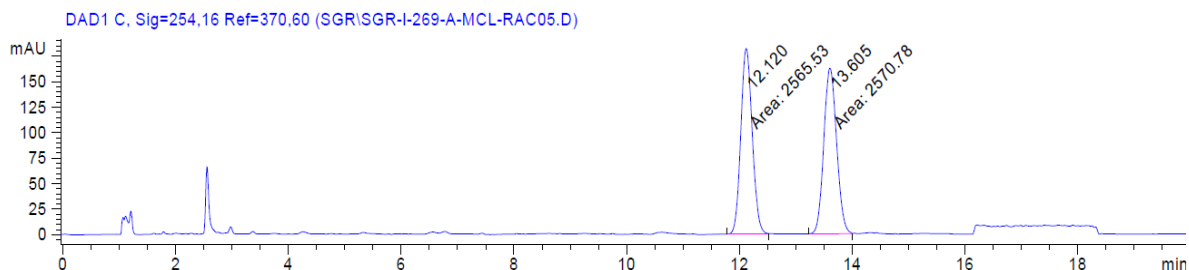


Signal 2: DAD1 C, Sig=254,16 Ref=370,60

Peak #	RetTime [min]	Type	Width [min]	Area [mAU*s]	Height [mAU]	Area %
1	5.740	MM	0.1632	752.29022	76.81909	2.7364
2	7.543	MM	0.4648	2.67397e4	958.75690	97.2636

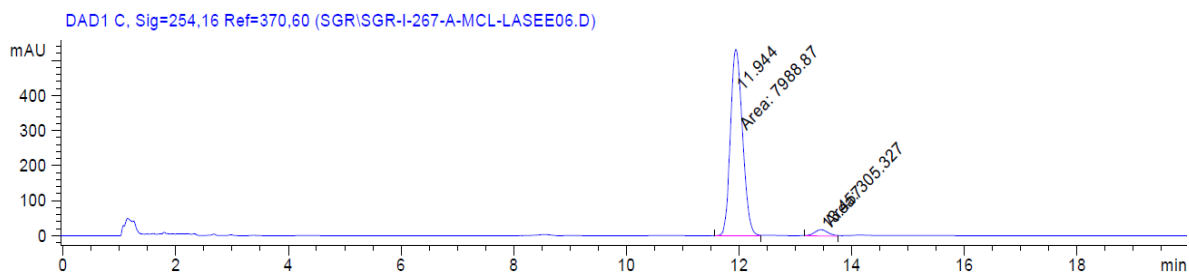


**(R)-1-(5-chloro-3-cinnamyl-3,6-dihydropyridin-1(2H)-yl)ethan-1-one (150b):** was synthesized following the general procedure 5. Therefore, 3-chloropyridine **142b** (48  $\mu\text{L}$ , 0.5 mmol, 1.0 equiv) was used. The desired product **150b** was isolated as colorless oil (38.0 mg, 0.138 mmol, 38% yield over three steps);  $^1\text{H}$  NMR (400 MHz,  $\text{CD}_3\text{OD}$ ) (as a mixture of E/Z amide bond isomers):  $\delta$  7.40 – 7.35 (m, 2H), 7.32 – 7.25 (m, 2H), 7.23 – 7.16 (m, 1H), 6.53 – 6.43 (m, 1H), 6.29 – 6.19 (m, 1H), 6.03 (dt,  $J = 3.8, 1.9$  Hz, 0.4H), 5.99 (dt,  $J = 3.7, 1.8$  Hz, 0.6H), 4.23 – 4.02 (m, 2H), 3.75 (dd,  $J = 13.1, 4.7$  Hz, 0.4H), 3.69 (dd,  $J = 13.7, 4.7$  Hz, 0.6 H), 3.45 (dd,  $J = 13.1, 6.3$  Hz, 0.4H), 3.37 – 3.32 (m, 0.6H), 2.65 – 2.57 (m, 0.6H), 2.52 – 2.45 (m, 0.4H), 2.34 – 2.18 (m, 2H), 2.13 – 2.11 (m, 3H);  $^{13}\text{C}$  NMR (101 MHz,  $\text{CD}_3\text{OD}$ ) (as a mixture of E/Z amide bond isomers, signals of minor isomer are indicated with an asterisk \*):  $\delta$  172.01, 172.00\*, 138.77\*, 138.58, 134.01, 133.86\*, 129.59, 129.52\*, 129.22\*, 129.07, 128.44\*, 128.36, 128.21\*, 128.11, 127.72, 127.15, 51.06\*, 48.16, 47.26, 43.15\*, 38.22, 37.74\*, 37.30\*, 37.11, 21.69\*, 21.23; IR (Neat Film, NaCl) 3853, 3745, 3675, 3648, 3026, 2914, 2362, 2334, 1707, 1652, 1491, 1436, 1380, 1361, 1274, 1230, 1162, 1106, 1070, 1032, 969, 831, 745, 695, 682, 618  $\text{cm}^{-1}$ ; (MM:ESI $^+$ )  $m/z$  calc'd for  $\text{C}_{16}\text{H}_{19}\text{ClNO}$  [M+H] $^+$ : 276.1155, found: 276.1174;  $[\alpha]_{\text{D}}^{25}$ : –22.17 (c 1.0,  $\text{CHCl}_3$ ); Chiral SFC Separation: 10% *i*PrOH, 2.5 mL/min, AD-H column,  $\lambda = 254$  nm,  $t_{\text{R}}$  (min): major = 11.94 (area: 96.32%), minor = 13.46 (area: 3.68%), 92.6% enantiomeric excess.



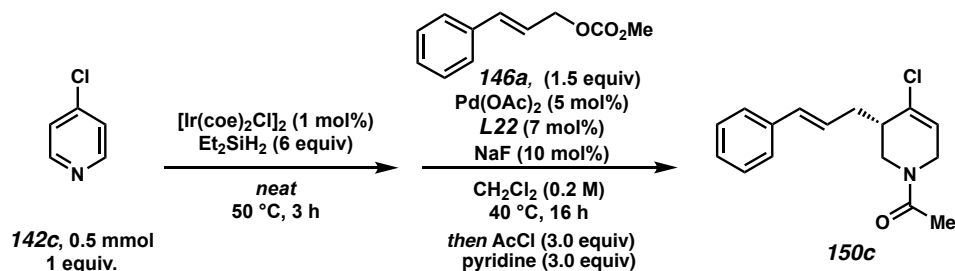
Signal 2: DAD1 C, Sig=254,16 Ref=370,60

Peak #	RetTime [min]	Type	Width [min]	Area [mAU*s]	Height [mAU]	Area %
1	12.120	MM	0.2348	2565.52881	182.12392	49.9488
2	13.605	MM	0.2635	2570.78491	162.62581	50.0512



Signal 2: DAD1 C, Sig=254,16 Ref=370,60

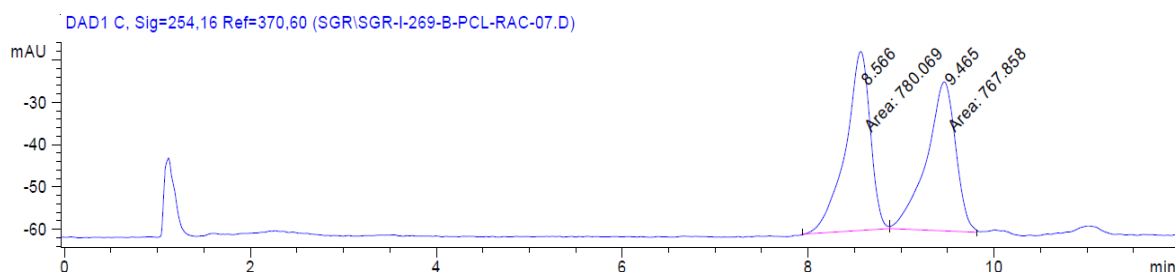
Peak #	RetTime [min]	Type	Width [min]	Area [mAU*s]	Height [mAU]	Area %
1	11.944	MM	0.2497	7988.87451	533.30609	96.3188
2	13.457	MM	0.2841	305.32715	17.91254	3.6812



**(S)-1-(4-chloro-3-cinnamyl-3,6-dihydropyridin-1(2H)-yl)ethan-1-one (150c):** was synthesized following the general procedure 5. Therefore, 4-chloropyridine **142c** (57 mg,

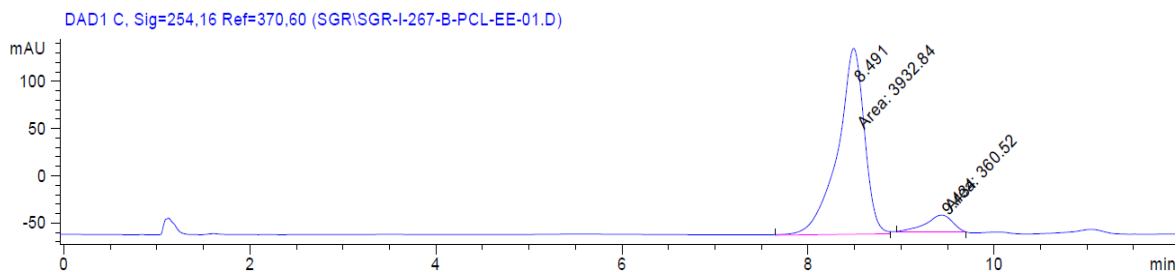
0.5 mmol, 1.0 equiv) was used. The desired product **150c** was isolated as colorless oil (37.5 mg, 0.136 mmol, 27% yield over three steps);  $^1\text{H}$  NMR (400 MHz,  $\text{CD}_3\text{OD}$ ) (as a mixture of E/Z amide bond isomers):  $\delta$  7.39 – 7.34 (m, 2H), 7.31 – 7.24 (m, 2H), 7.22 – 7.15 (m, 1H), 6.57 – 6.45 (m, 1H), 6.29 – 6.19 (m, 1H), 5.94 – 5.89 (m, 1H), 4.41 – 4.34 (m, 1H), 4.16 (dd,  $J = 17.7, 3.9$  Hz, 0.5H), 3.96 (dt,  $J = 17.7, 2.6$  Hz, 0.5H), 3.81 (dd,  $J = 13.7, 3.3$  Hz, 0.5H), 3.73 (dt,  $J = 18.8, 2.6$  Hz, 0.5H), 3.54 (dd,  $J = 13.7, 4.2$  Hz, 0.5H), 3.19 (dd,  $J = 13.2, 4.3$  Hz, 0.5H), 2.74 – 2.47 (m, 2H), 2.42 – 2.21 (m, 1H), 2.11 (s, 1.5H), 2.06 (s, 1.5H);  $^{13}\text{C}$  NMR (101 MHz,  $\text{CD}_3\text{OD}$ ) (as a mixture of E/Z amide bond isomers, approx. 1/1 mixture):  $\delta$  172.49, 172.33, 138.88, 138.56, 135.14, 134.17, 134.10, 134.05, 129.60, 129.50, 128.40, 128.18, 127.81, 127.39, 127.17, 127.16, 123.17, 122.71, 48.03, 47.05, 43.74, 43.72, 43.48, 43.14, 35.18, 35.13, 21.61, 21.26; IR (Neat Film, NaCl) 3866, 3733, 3648, 2922, 2358, 1646, 1425, 1360, 1237, 1032, 1010, 969, 822, 770, 746, 718, 699  $\text{cm}^{-1}$ ; (MM:ESI $^+$ )  $m/z$  calc'd for  $\text{C}_{16}\text{H}_{19}\text{ClNO}$   $[\text{M}+\text{H}]^+$ : 276.1155, found: 276.1131;  $[\alpha]_{\text{D}}^{25}$ : –31.97 (c 0.33,  $\text{CHCl}_3$ );

Chiral SFC Separation: 7% MeOH, 2.5 mL/min, AS-H column,  $\lambda = 254$  nm,  $t_{\text{R}}$  (min): major = 8.49 (area: 91.60%), minor = 9.43 (area: 8.40%), 83.2% enantiomeric excess.



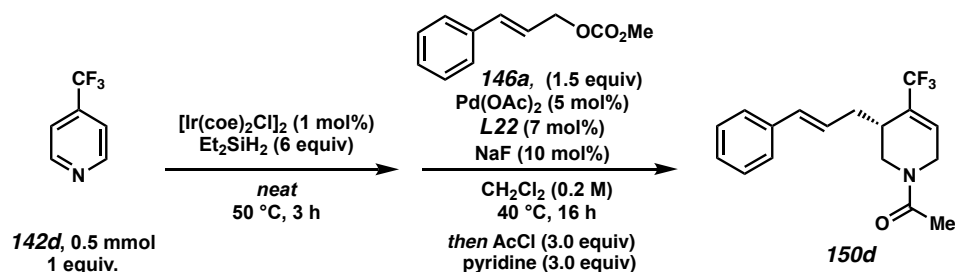
Signal 2: DAD1 C, Sig=254,16 Ref=370,60

Peak #	RetTime [min]	Type	Width [min]	Area [mAU*s]	Height [mAU]	Area %
1	8.566	MM	0.3074	780.06921	42.29282	50.3944
2	9.465	MM	0.3637	767.85803	35.18404	49.6056



Signal 2: DAD1 C, Sig=254,16 Ref=370,60

Peak #	RetTime [min]	Type	Width [min]	Area [mAU*s]	Height [mAU]	Area %
1	8.491	MM	0.3327	3932.83862	197.04034	91.6028
2	9.434	MM	0.3316	360.51987	18.12246	8.3972

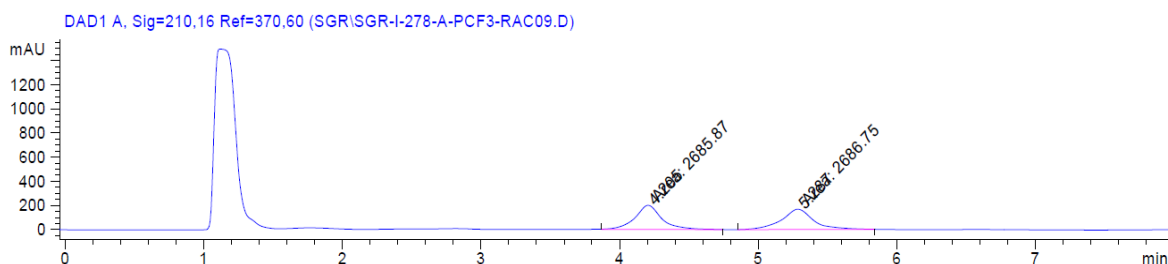


**(R)-1-(3-cinnamyl-4-(trifluoromethyl)-3,6-dihydropyridin-1(2H)-yl)ethan-1-one**

**(150d)**: was synthesized following the general procedure 5. Therefore, 4-(trifluoromethyl)pyridine **142d** (58  $\mu\text{L}$ , 0.5 mmol, 1.0 equiv) was used. The desired product **150d** was isolated as colorless oil (47.3 mg, 0.153 mmol, 31% yield over three steps);  $^1\text{H}$  NMR (400 MHz,  $\text{CD}_3\text{OD}$ ) (as a mixture of E/Z amide bond isomers):  $\delta$  7.39 – 7.35 (m, 2H), 7.32 – 7.25 (m, 2H), 7.23 – 7.16 (m, 1H), 6.55 – 6.42 (m, 2H), 6.28 – 6.19 (m, 1H), 4.67 (dd,  $J = 13.2, 1.8$  Hz, 0.5H), 4.59 (dt,  $J = 20.7, 3.2$  Hz, 0.5H), 4.34 (dt,  $J = 19.4, 3.3$

Hz, 0.5H), 4.08 – 4.00 (m, 0.5H), 3.95 (dd,  $J = 13.5, 2.2$  Hz, 0.5H), 3.75 – 3.66 (m, 0.5H), 3.30 – 3.18 (m, 0.5H), 2.83 – 2.73 (m, 1H), 2.66 – 2.58 (m, 1H), 2.49 (ddd,  $J = 13.8, 7.2, 2.5$  Hz, 0.5H), 2.33 – 2.15 (m, 1H), 2.10 (s, 1.5H), 2.08 (s, 1.5H);  $^{13}\text{C}$  NMR (101 MHz,  $\text{CD}_3\text{OD}$ ) (as a mixture of E/Z amide bond isomers, approx. 1/1 mixture,  $^{\S} = \text{E/Z}$  signal overlapping):  $\delta$  172.95, 172.71, 138.84, 138.45, 134.25, 134.16, 131.50 (q,  $J = 30.1$  Hz), 130.76 (q,  $J = 30.1$  Hz), 130.33 (q,  $J = 6.1$  Hz), 129.99 (q,  $J = 6.2$  Hz), 129.63, 129.51, 128.48, 128.21, 127.96, 127.41, 127.20, 127.17, 125.03 (q,  $J = 271.8$  Hz), 124.97 (q,  $J = 271.6$  Hz), 46.89, 45.92, 42.67, 41.88, 36.04 $^{\S}$ , 35.27 $^{\S}$ , 21.73, 21.34;  $^{19}\text{F}$  NMR (282 MHz,  $\text{CD}_3\text{OD}$ ) (as a mixture of E/Z amide bond isomers, roughly 1/1 mixture):  $\delta$  -67.86 (q,  $J = 2.7$  Hz), -67.98 (q,  $J = 3.0$  Hz); IR (Neat Film, NaCl) 3674, 3310, 3026, 2922, 1734, 1652, 1490, 1423, 1373, 1337, 1296, 1261, 1241, 1206, 1162, 1115, 1072, 1019, 986, 836, 825, 742, 695, 676, 658  $\text{cm}^{-1}$ ; (MM:ESI $^+$ )  $m/z$  calc'd for  $\text{C}_{17}\text{H}_{19}\text{F}_3\text{NO}$  [M+H] $^+$ : 310.1419, found: 310.1417;  $[\alpha]_{\text{D}}^{25}$ : -47.62 (c 1.0,  $\text{CHCl}_3$ );

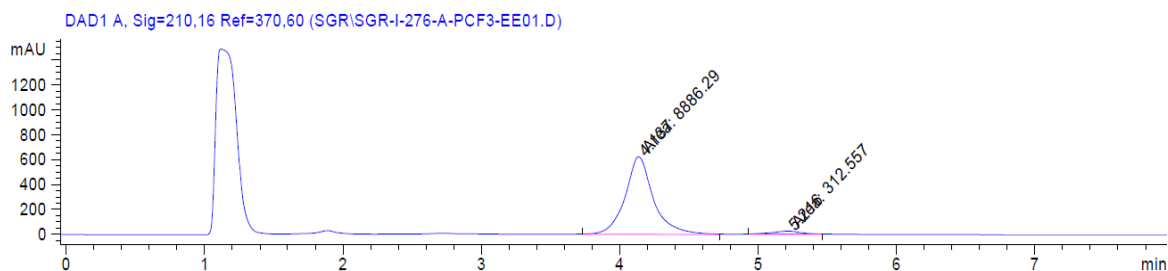
Chiral SFC Separation: 5% MeOH, 2.5 mL/min, AS-H column,  $\lambda = 210$  nm,  $t_{\text{R}}$  (min): major = 4.14 (area: 96.60%), minor = 5.22 (area: 3.40%), 93.2% enantiomeric excess.



Signal 1: DAD1 A, Sig=210,16 Ref=370,60

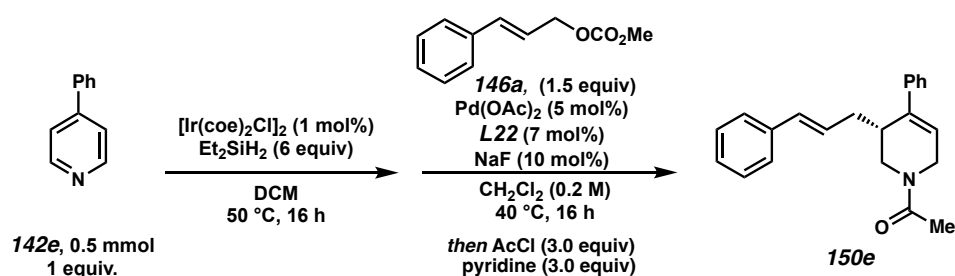
Peak #	RetTime [min]	Type	Width [min]	Area [mAU*s]	Height [mAU]	Area %
1	4.205	MM	0.2237	2685.87476	200.10240	49.9918
2	5.287	MM	0.2657	2686.75220	168.53705	50.0082





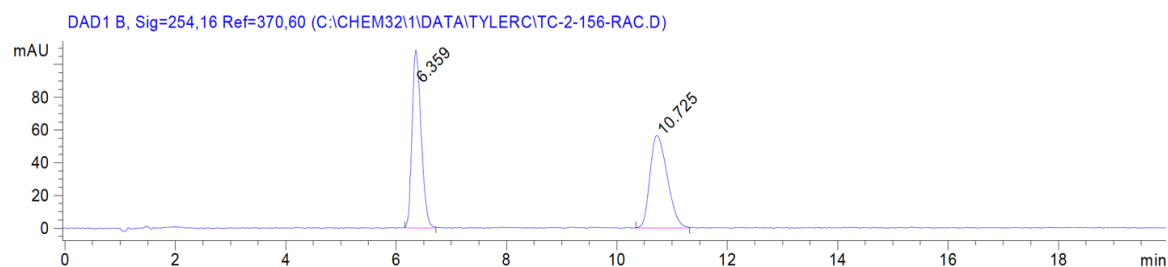
Signal 1: DAD1 A, Sig=210,16 Ref=370,60

Peak #	RetTime [min]	Type	Width [min]	Area [mAU*s]	Height [mAU]	Area %
1	4.137	MM	0.2372	8886.29492	624.26160	96.6022
2	5.216	MM	0.2225	312.55685	23.41279	3.3978



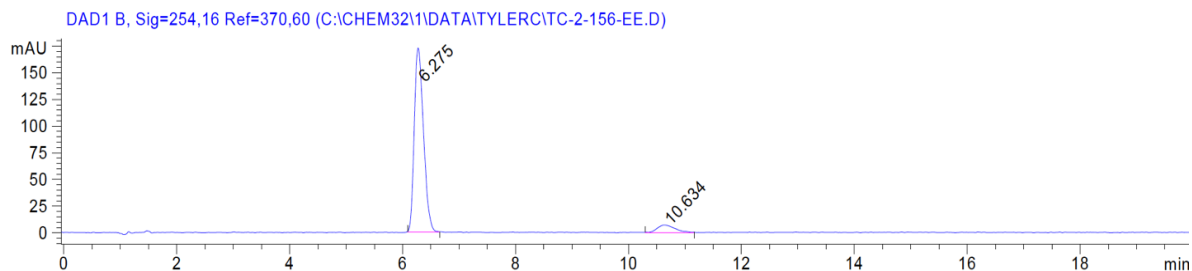
**(R)-1-(3-cinnamyl-4-phenyl-3,6-dihydropyridin-1(2H)-yl)ethan-1-one (150e):** was synthesized following the general procedure 6 or 7. Therefore, 4-phenylpyridine **142e** (78.1 mg, 0.5 mmol, 1.0 equiv) was used. The desired product **150e** was isolated as pale-yellow oil (38.3 mg, 0.120 mmol, 24% yield over three steps);  $^1\text{H}$  NMR (400 MHz,  $\text{CD}_3\text{OD}$ ) (as a mixture of E/Z amide bond isomers):  $\delta$  7.45 – 7.40 (m, 2H), 7.38 – 7.32 (m, 2H), 7.30 – 7.20 (m, 5H), 7.18 – 7.11 (m, 1H), 6.37 (d,  $J = 15.8$  Hz, 0.5H), 6.32 (d,  $J = 15.8$  Hz, 0.5H), 6.21 – 6.12 (m, 1H), 6.02 (t,  $J = 3.4$  Hz, 0.5H), 5.98 (t,  $J = 3.3$  Hz, 0.5H), 4.62 (d,  $J = 12.6$  Hz, 0.5H), 4.56 (dd,  $J = 19.7, 3.6$  Hz, 0.5H), 4.27 (dd,  $J = 18.4, 3.9$  Hz, 0.5H), 4.13 – 4.02 (m, 0.5H), 3.99 – 3.93 (m, 0.5H), 3.80 – 3.72 (m, 0.5H), 3.46 (dd,  $J = 13.3, 3.4$  Hz, 0.5H), 3.14 – 3.08 (m, 0.5H), 3.06 – 2.95 (m, 1H), 2.40 – 2.14 (m, 2H), 2.12 (s, 1.5H), 2.10 (s,

1.5H);  $^{13}\text{C}$  NMR (101 MHz,  $\text{CD}_3\text{OD}$ ) (as a mixture of E/Z amide bond isomers, roughly 1/1 mixture,  $\delta$  = E/Z signal overlapping):  $\delta$  172.64, 172.48, 141.71, 141.14, 141.04, 140.93, 139.03, 138.66, 133.43, 133.24, 129.67 $\delta$ , 129.53, 129.41, 129.12, 128.67, 128.61, 128.57, 128.23, 127.97, 127.09 $\delta$ , 127.07, 127.01, 121.92, 121.64, 47.82, 47.13, 43.69, 42.94, 38.72, 38.59, 36.34, 36.28, 21.74, 21.34; IR (Neat Film, NaCl) 3216, 3056, 3027, 2929, 1633, 1494, 1435, 1370, 1331, 1265, 1075, 1035, 971, 882, 766, 740, 698  $\text{cm}^{-1}$ ; (MM:ESI $^+$ )  $m/z$  calc'd for  $\text{C}_{22}\text{H}_{23}\text{NO}$   $[\text{M}+\text{H}]^+$ : 318.1858, found: 318.1854;  $[\alpha]_{\text{D}}^{25}$ :  $-4.93$  (c 0.85,  $\text{CHCl}_3$ ); Chiral SFC Separation: 20% iPrOH, 2.5 mL/min, AD-H column,  $\lambda = 254$  nm,  $t_{\text{R}}$  (min): major = 6.680 (area: 93.0%), minor = 11.213 (area: 7.0%), 86.0% enantiomeric excess.



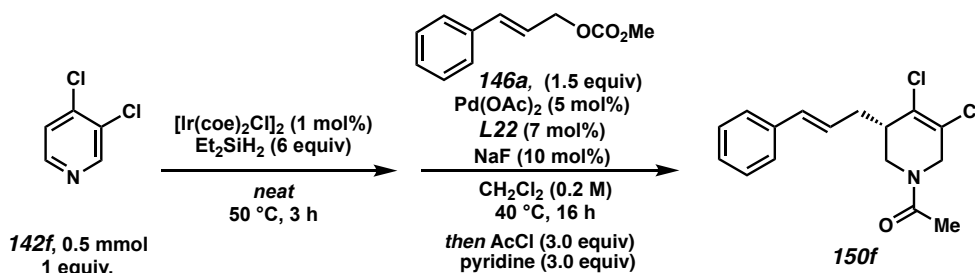
Signal 2: DAD1 B, Sig=254,16 Ref=370,60

Peak #	RetTime [min]	Type	Width [min]	Area [mAU*s]	Height [mAU]	Area %
1	6.359	BB	0.1777	1244.61230	108.63536	50.4051
2	10.725	BB	0.3412	1224.60437	56.42291	49.5949



Signal 2: DAD1 B, Sig=254,16 Ref=370,60

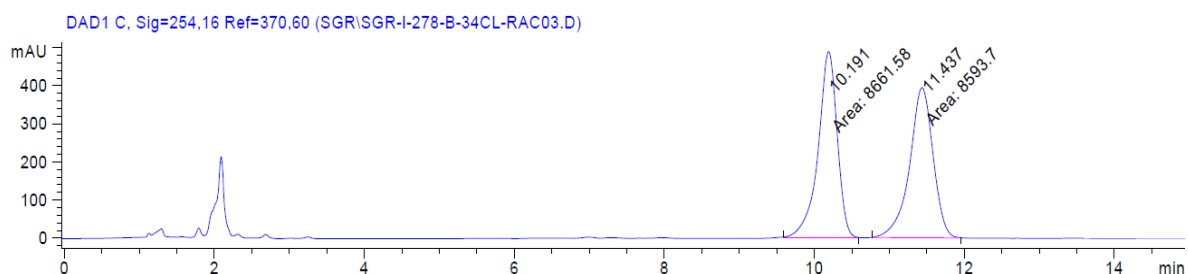
Peak #	RetTime [min]	Type	Width [min]	Area [mAU*s]	Height [mAU]	Area %
1	6.275	BB	0.1763	1960.29517	172.92909	93.0373
2	10.634	BB	0.3147	146.70486	6.93692	6.9627



**(S)-1-(4,5-dichloro-3-cinnamyl-3,6-dihydropyridin-1(2H)-yl)ethan-1-one (150f)**: was synthesized following the general procedure 5. Therefore, 3,4-dichloropyridine **142f** (74.0 mg, 0.5 mmol, 1.0 equiv) was used. The desired product **150f** was isolated as colorless oil (55.0 mg, 0.177 mmol, 35% yield over three steps);  $^1\text{H}$  NMR (400 MHz,  $\text{CD}_3\text{OD}$ ) (as a mixture of E/Z amide bond isomers):  $\delta$  7.39 – 7.35 (m, 2H), 7.32 – 7.26 (m, 2H), 7.24 – 7.17 (m, 1H), 6.57 – 6.46 (m, 1H), 6.26 – 6.17 (m, 1H), 4.57 – 4.51 (m, 0.5H), 4.42 (dd,  $J$  = 13.3, 2.0 Hz, 0.5H), 4.32 (dt,  $J$  = 17.0, 1.2 Hz, 0.5H), 4.16 (dd,  $J$  = 17.0, 1.9 Hz, 0.5H), 3.92 (dd,  $J$  = 17.9, 1.5 Hz, 0.5H), 3.82 (dd,  $J$  = 13.9, 3.2 Hz, 0.5H), 3.58 (dd,  $J$  = 13.9, 4.1 Hz, 0.5H), 3.18 (dd,  $J$  = 13.3, 4.2 Hz, 0.5H), 2.81 – 2.68 (m, 1H), 2.66 – 2.56 (m, 1H), 2.39 (dddd,  $J$  = 14.6, 9.3, 8.0, 1.1 Hz, 0.5H), 2.31 – 2.21 (m, 0.5H), 2.11 (s, 1.5H), 2.10 (s, 1.5H);  $^{13}\text{C}$  NMR (101 MHz,  $\text{CD}_3\text{OD}$ ) (as a mixture of E/Z amide bond isomers, roughly 1/1 mixture,  $^{\S}$  = E/Z signal overlapping):  $\delta$  172.09, 171.97, 138.73, 138.40, 134.47, 134.46, 132.13, 131.04, 129.62, 129.52, 128.50, 128.27, 127.32, 127.19 $^{\S}$ , 127.01, 126.21, 125.45, 51.77, 48.17, 47.77, 44.88, 44.82, 42.82, 35.22 $^{\S}$ , 21.61, 21.16; IR (Neat Film, NaCl) 3853,

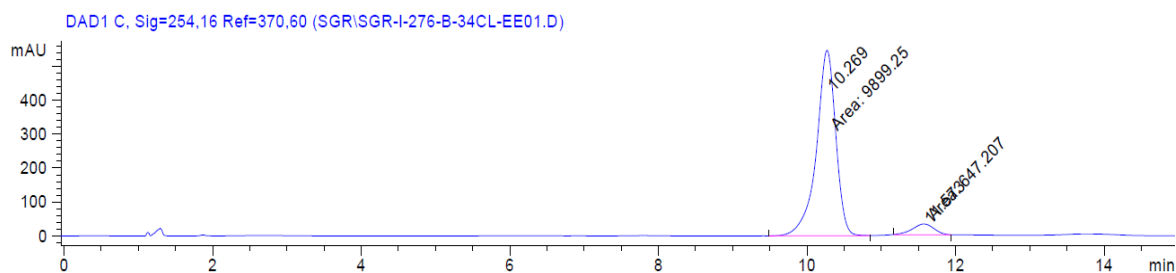
3734, 3648, 3025, 2919, 2339, 2358, 1716, 1654, 1492, 1420, 1363, 1330, 1276, 1234, 1143, 1032, 985, 884, 825, 749, 695, 682  $\text{cm}^{-1}$ ; (MM:ESI<sup>+</sup>)  $m/z$  calc'd for  $\text{C}_{16}\text{H}_{18}\text{Cl}_2\text{NO}$  [M+H]<sup>+</sup>: 310.0765, found: 310.0756;  $[\alpha]_{\text{D}}^{25}$ :  $-18.23$  (c 1.0,  $\text{CHCl}_3$ );

Chiral SFC Separation: 10% MeOH, 2.5 mL/min, OD-H column,  $\lambda = 254$  nm,  $t_{\text{R}}$  (min): major = 10.27 (area: 93.86%), minor = 11.57 (area: 6.14%), 87.7% enantiomeric excess.



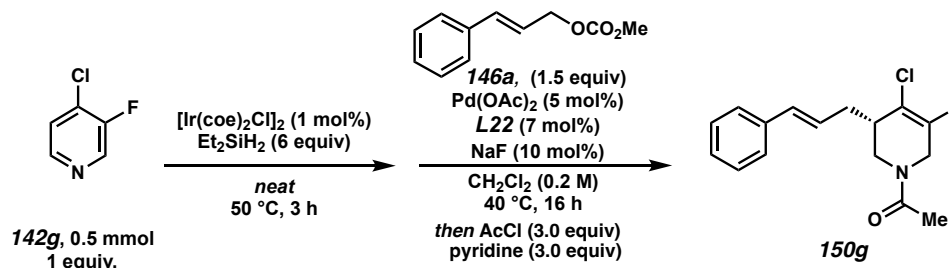
Signal 2: DAD1 C, Sig=254,16 Ref=370,60

Peak #	RetTime [min]	Type	Width [min]	Area [mAU*s]	Height [mAU]	Area %
1	10.191	MM	0.2949	8661.58203	489.44498	50.1967
2	11.437	MM	0.3629	8593.69727	394.65631	49.8033



Signal 2: DAD1 C, Sig=254,16 Ref=370,60

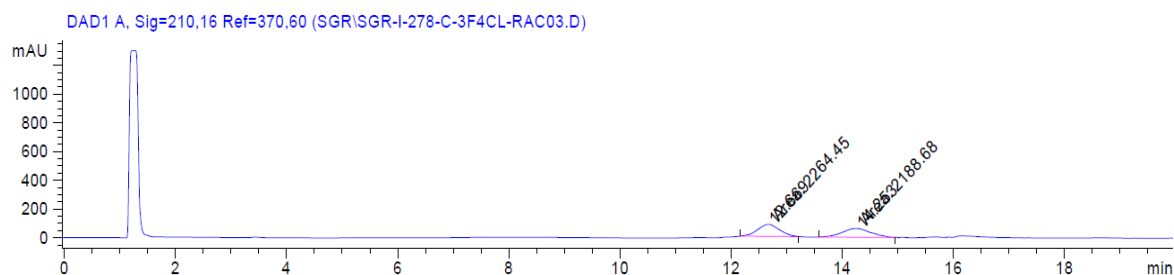
Peak #	RetTime [min]	Type	Width [min]	Area [mAU*s]	Height [mAU]	Area %
1	10.269	MM	0.3012	9899.25098	547.71069	93.8633
2	11.573	MM	0.3375	647.20721	31.95667	6.1367



**(S)-1-(4-chloro-3-cinnamyl-5-fluoro-3,6-dihydropyridin-1(2H)-yl)ethan-1-one**

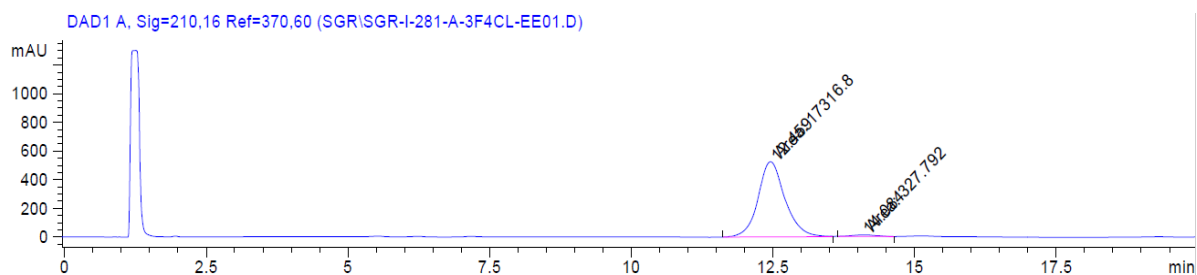
**(150g)**: was synthesized following the general procedure 5. Therefore, 4-chloro-3-fluoropyridine **142g** (65.8 mg, 0.5 mmol, 1.0 equiv) was used. The desired product **150g** was isolated as colorless oil (72.2 mg, 0.246 mmol, 49% yield over three steps);  $^1\text{H}$  NMR (400 MHz,  $\text{CD}_3\text{OD}$ ) (as a mixture of E/Z amide bond isomers):  $\delta$  7.39 – 7.33 (m, 2H), 7.32 – 7.24 (m, 2H), 7.23 – 7.15 (m, 1H), 6.57 – 6.44 (m, 1H), 6.27 – 6.16 (m, 1H), 4.49 – 4.41 (m, 0.6H), 4.34 – 4.24 (m, 0.8H), 4.15 – 4.07 (m, 0.4H), 3.93 – 3.85 (m, 0.6H), 3.74 (dd,  $J = 13.9, 3.3$  Hz, 0.6H), 3.54 (dd,  $J = 13.8, 4.1$  Hz, 0.6H), 3.19 (dd,  $J = 13.4, 4.1, 0.4$ H), 2.74 – 2.49 (m, 2H), 2.40 – 2.29 (m, 0.6H), 2.27 – 2.17 (m, 0.4H), 2.13 – 2.06 (m, 3H);  $^{13}\text{C}$  NMR (101 MHz,  $\text{CD}_3\text{OD}$ ) (as a mixture of E/Z amide bond isomers, signals of minor isomer are indicated with an asterisk \*):  $\delta$  172.39, 172.35\*, 152.61 (d,  $J = 257.2$  Hz), 152.00 (d,  $J = 258.0$  Hz)\*, 138.73\*, 138.42, 134.40\*, 134.38, 129.62, 129.52\*, 128.47, 128.25\*, 127.40, 127.18 $^{\S}$ , 127.08\*, 113.29 (d,  $J = 11.2$  Hz)\*, 112.32 (d,  $J = 11.8$  Hz), 48.03, 46.24 (d,  $J = 37.0$  Hz)\*, 43.11\*, 42.67 (d,  $J = 37.5$  Hz), 42.04, 41.91\*, 34.91, 34.89\*, 21.62\*, 21.16;  $^{19}\text{F}$  NMR (282 MHz,  $\text{CD}_3\text{OD}$ ) (as a mixture of E/Z amide bond isomers, signals of minor isomer are indicated with an asterisk \*):  $\delta$  –116.04 (d,  $J = 5.9$  Hz), –116.99 (d,  $J = 5.8$  Hz)\*; IR (Neat Film, NaCl) 3363, 2931, 1716, 1652, 1435, 1372, 1236, 1036, 992, 734, 699  $\text{cm}^{-1}$ ; (MM:ESI $^+$ )  $m/z$  calc'd for  $\text{C}_{16}\text{H}_{18}\text{ClFNO}$   $[\text{M}+\text{H}]^+$ : 294.1061, found: 294.1045;  $[\alpha]_{\text{D}}^{25}$ : –25.73 (c 1.0,  $\text{CHCl}_3$ );

Chiral SFC Separation: 10% iPrOH, 2.5 mL/min, OD-H column,  $\lambda = 210$  nm,  $t_R$  (min):  
major = 12.46 (area: 98.14%), minor = 14.08 (area: 1.86%), 96.3% enantiomeric excess.



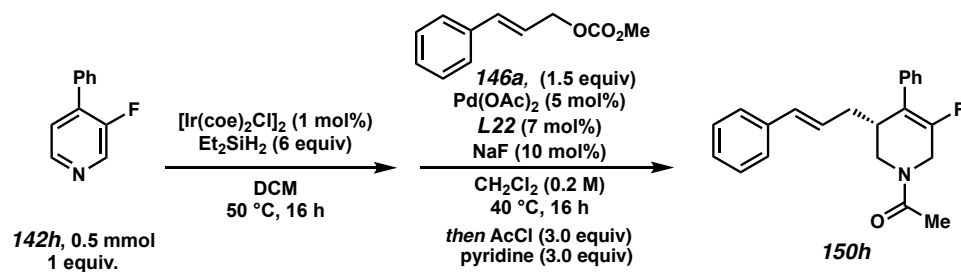
Signal 1: DAD1 A, Sig=210,16 Ref=370,60

Peak #	RetTime [min]	Type	Width [min]	Area [mAU*s]	Height [mAU]	Area %
1	12.669	MM	0.4542	2264.45215	83.09532	50.8508
2	14.253	MM	0.5970	2188.67920	61.09854	49.1492



Signal 1: DAD1 A, Sig=210,16 Ref=370,60

Peak #	RetTime [min]	Type	Width [min]	Area [mAU*s]	Height [mAU]	Area %
1	12.459	MM	0.5493	1.73168e4	525.40576	98.1423
2	14.084	MM	0.4721	327.79208	11.57163	1.8577

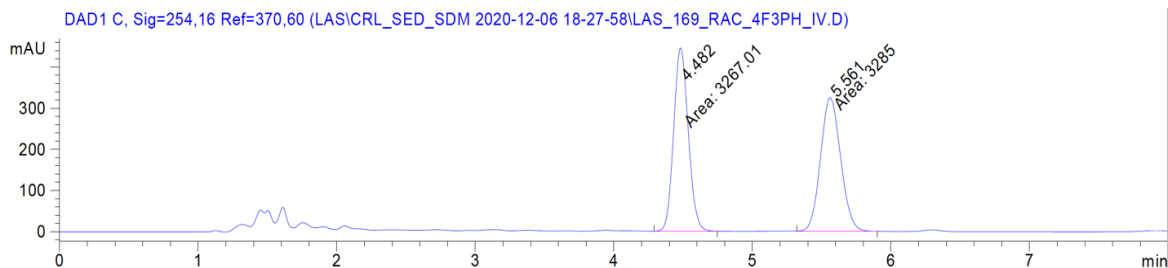


**(R)-1-(3-cinnamyl-5-fluoro-4-phenyl-3,6-dihydropyridin-1(2H)-yl)ethan-1-one**

**(150h)**: was synthesized following the general procedure 6 or 7. Therefore, 3-fluoro-4-phenylpyridine **142h** (86.6 mg, 0.5 mmol, 1.0 equiv) was used. The desired product **150h** was isolated as colorless oil (34.7 mg, 0.103 mmol, 21% yield over three steps); <sup>1</sup>H NMR (400 MHz, CD<sub>3</sub>OD) (as a mixture of E/Z amide bond isomers): δ 7.43 – 7.35 (m, 4H), 7.32 – 7.21 (m, 5H), 7.19 – 7.12 (m, 1H), 6.42 – 6.29 (m, 1H), 6.16 – 6.07 (m, 1H), 4.62 (d, *J* = 18.1 Hz, 0.6H), 4.51 (dd, *J* = 13.2, 2.4 Hz, 0.4H), 4.39 (d, *J* = 17.0 Hz, 0.4H), 4.10 (dt, *J* = 16.9, 1.6 Hz, 0.4H), 3.90 (dd, *J* = 13.7, 2.8 Hz, 0.6H), 3.80 (d, *J* = 18.0 Hz, 0.6H), 3.55 (dd, *J* = 13.6, 3.8 Hz, 0.6H), 3.14 (dd, *J* = 13.2, 3.9 Hz, 0.4H), 3.10 – 3.02 (m, 0.6H), 2.97 – 2.89 (m, 0.4H), 2.37 – 2.29 (m, 0.6H), 2.25 – 2.18 (m, 1H), 2.17 – 2.13 (m, 3H), 2.11 – 2.05 (m, 0.4H); <sup>13</sup>C NMR (101 MHz, CD<sub>3</sub>OD) (as a mixture of E/Z amide bond isomers, signals of minor isomer are indicated with an asterisk \*, § = E/Z signal overlapping): δ 171.23, 171.16\*, 150.92 (d, *J* = 254.8 Hz), 150.40 (d, *J* = 255.3 Hz)\*, 137.52\*, 137.18, 134.41\*, 134.30, 132.32, 132.21\*, 128.20\*, 128.17, 128.13, 128.10§, 128.03\*, 127.25\*, 127.23, 126.89, 126.82\*, 126.66§, 125.71\*, 125.69, 117.69 (d, *J* = 5.4 Hz)\*, 117.05 (d, *J* = 6.0 Hz), 46.55, 44.44 (d, *J* = 41.8 Hz)\*, 41.62\*, 41.00 (d, *J* = 42.1 Hz), 38.11 (d, *J* = 3.7 Hz), 37.78 (d, *J* = 3.4 Hz)\*, 34.80 (d, *J* = 3.0 Hz)§, 20.36\*, 19.92; <sup>19</sup>F NMR (282 MHz, CD<sub>3</sub>OD) (as a mixture of E/Z amide bond isomers, signals of minor isomer are indicated with an asterisk \*): δ –119.33 (d, *J* = 5.6 Hz), –120.31 (d, *J* = 5.7 Hz)\*; IR (Neat Film, NaCl) 3024, 2930, 1734, 1652, 1496, 1426, 1373, 1242, 1205, 1180, 1051, 1009, 970, 820, 749, 698 cm<sup>-1</sup>; (MM:ESI<sup>+</sup>) *m/z* calc'd for C<sub>22</sub>H<sub>23</sub>FNO [M+H]<sup>+</sup>: 336.1764, found: 336.1774; [α]<sub>D</sub><sup>25</sup>: –67.87 (c 1.0, CHCl<sub>3</sub>);

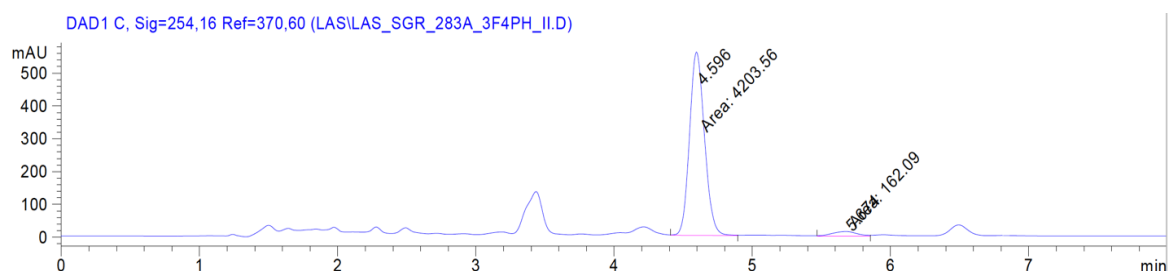
Chiral SFC Separation: 30% MeOH, 2.5 mL/min, OJ-H column,  $\lambda = 254$  nm,  $t_R$  (min):

major = 4.596 (area: 96.3%), minor = 5.677 (area: 3.7%), 92.6.% enantiomeric excess.



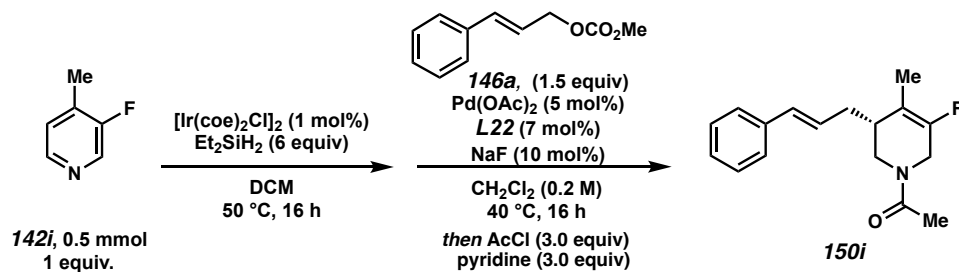
Signal 2: DAD1 C, Sig=254,16 Ref=370,60

Peak #	RetTime [min]	Type	Width [min]	Area [mAU*s]	Height [mAU]	Area %
1	4.482	MM	0.1217	3267.01074	447.36011	49.8627
2	5.561	MM	0.1682	3285.00098	325.46252	50.1373



Signal 2: DAD1 C, Sig=254,16 Ref=370,60

Peak #	RetTime [min]	Type	Width [min]	Area [mAU*s]	Height [mAU]	Area %
1	4.596	MM	0.1251	4203.55566	559.99762	96.2872
2	5.674	MM	0.1996	162.08955	13.53266	3.7128

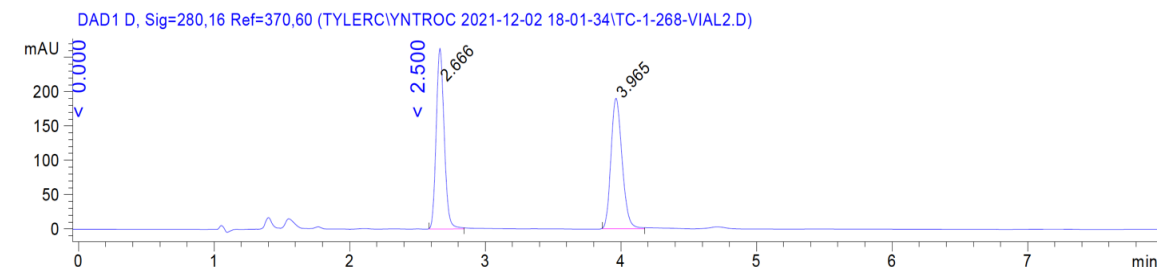




**(R)-1-(3-cinnamyl-5-fluoro-4-methyl-3,6-dihydropyridin-1(2H)-yl)ethan-1-one**

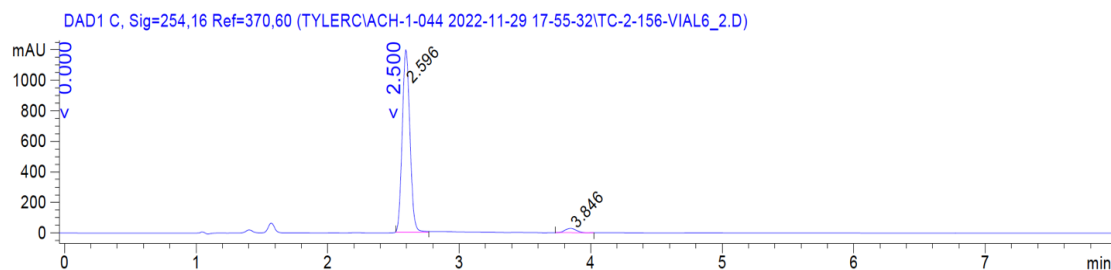
**(150i)**: was synthesized following the general procedure 7. Therefore, 3-fluoro-4-methylpyridine **142i** (52  $\mu$ L, 0.5 mmol, 1.0 equiv) was used. The desired product **150i** was isolated as pale-yellow oil (60.2 mg, 0.22 mmol, 44% yield over three steps);  $^1\text{H}$  NMR (400 MHz,  $\text{CDCl}_3$ ) (as a mixture of E/Z amide bond isomers):  $\delta$  7.39 – 7.29 (m, 4H), 7.26 – 7.17 (m, 1H), 6.46 (ddd,  $J = 15.8, 3.8, 2.3$  Hz, 1H), 6.28 – 6.07 (m, 1H), 4.54 – 4.38 (m, 0.65H), 4.20 (dd,  $J = 13.2, 3.3$  Hz, 0.35H), 4.00 (dt,  $J = 15.9, 2.0$  Hz, 0.35H), 3.90 (dtd,  $J = 16.1, 2.0, 1.1$  Hz, 0.35H), 3.77 – 3.66 (m, 0.65H), 3.62 (dd,  $J = 13.4, 3.0$  Hz, 0.65H), 3.30 (ddd,  $J = 13.3, 3.9, 1.0$  Hz, 0.65H), 3.11 (dd,  $J = 13.2, 4.0$  Hz, 0.35H), 2.45 – 2.29 (m, 0.7H), 2.23 – 2.14 (overlap, 2.3H), 2.10 (s, 2H), 2.08 (s, 1H), 1.75 (dd,  $J = 4.5, 2.3$  Hz, 3H);  $^{13}\text{C}$  NMR (101 MHz,  $\text{CDCl}_3$ ) (as a mixture of E/Z amide bond isomers, signals of minor isomer are indicated with an asterisk \*)  $\delta$  170.2, 169.8\*, 150.5 (d,  $J = 248.7$  Hz), 149.3 (d,  $J = 248.7$  Hz)\*, 137.6\*, 137.0, 132.9, 132.6\*, 128.8, 128.6\*, 127.8, 127.6, 127.7\*, 127.2\*, 126.3\*, 126.2, 112.7 (d,  $J = 8.4$  Hz)\*, 111.1 (d,  $J = 9.5$  Hz), 46.4, 44.8 (d,  $J = 41.0$  Hz)\*, 41.9\*, 41.8 (d,  $J = 41.8$  Hz), 39.5 (d,  $J = 4.8$  Hz), 38.8 (d,  $J = 4.4$  Hz)\*, 34.5 (d,  $J = 2.7$  Hz)\*, 34.4 (d,  $J = 3.1$  Hz), 22.0\*, 21.5, 12.4 (dd,  $J = 6.2, 1.8$  Hz);  $^{19}\text{F}$  NMR (282 MHz,  $\text{CDCl}_3$ ) (as a mixture of E/Z amide bond isomers, signals of minor isomer are indicated with an asterisk \*):  $\delta$  -120.71 – -120.73 (m), -122.01 – -122.04 (m)\*; IR (Neat Film, NaCl) 3022, 2918, 1728, 1648, 1438, 1387, 1369, 1234, 1158, 1070, 969, 918, 750, 724, 693  $\text{cm}^{-1}$ ; (MM:ESI $^+$ )  $m/z$  calc'd for  $\text{C}_{17}\text{H}_{21}\text{FNO}$   $[\text{M}+\text{H}]^+$ : 274.1602, found 274.1605;  $[\alpha]_{\text{D}}^{25}$ : -8.75 (c 1.0,  $\text{CHCl}_3$ );

Chiral SFC Separation: 25% iPrOH, 2.5 mL/min, AD-H column,  $\lambda = 254$  nm or 280 nm,  $t_R$  (min): major = 2.596 (area: 96.8%), minor = 3.846 (area: 3.2%), 93.5% enantiomeric excess.



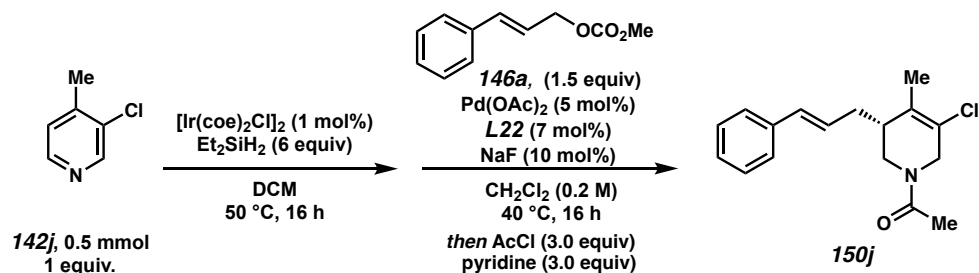
Signal 3: DAD1 D, Sig=280,16 Ref=370,60

Peak #	RetTime [min]	Type	Width [min]	Area [mAU*s]	Height [mAU]	Area %
1	2.666	BB	0.0644	1081.70117	260.62692	49.7744
2	3.965	BB	0.0910	1091.50793	190.15250	50.2256



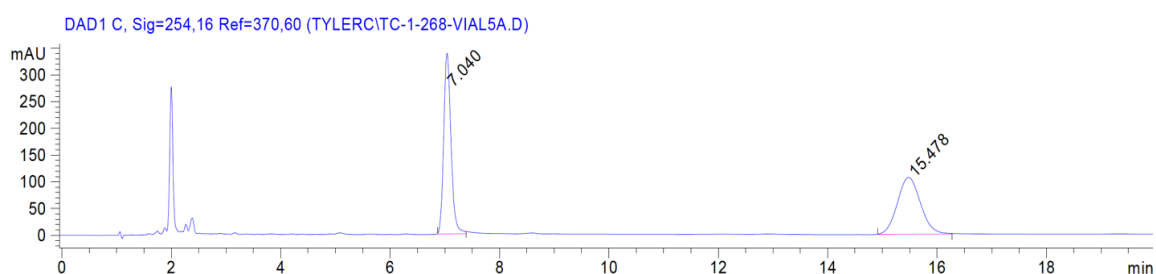
Signal 2: DAD1 C, Sig=254,16 Ref=370,60

Peak #	RetTime [min]	Type	Width [min]	Area [mAU*s]	Height [mAU]	Area %
1	2.596	BB	0.0678	4862.83008	1186.93994	96.7838
2	3.846	BB	0.0895	161.59549	28.79920	3.2162



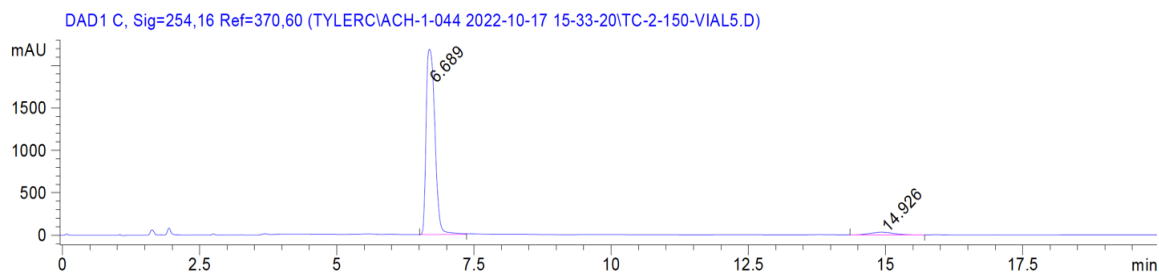
**(R)-1-(5-chloro-3-cinnamyl-4-methyl-3,6-dihydropyridin-1(2H)-yl)ethan-1-one**

**(150j)**: was synthesized following the general procedure 7. Therefore, 3-chloro-4-methylpyridine **142j** (55  $\mu$ L, 0.5 mmol, 1.0 equiv) was used. The desired product was isolated as pale-yellow oil **150j** (68.2 mg, 0.235 mmol, 47% yield over three steps);  $^1\text{H}$  NMR (400 MHz,  $\text{CDCl}_3$ ) (as a mixture of E/Z amide bond isomers):  $\delta$  7.41 – 7.27 (m, 4H), 7.27 – 7.13 (m, 1H), 6.46 (dt,  $J = 15.7, 1.5$  Hz, 1H), 6.28 – 6.08 (m, 1H), 4.57 (dt,  $J = 18.0, 1.9$  Hz, 0.65H), 4.35 (dd,  $J = 13.2, 2.9$  Hz, 0.35H), 4.07 (dt,  $J = 16.6, 1.9$  Hz, 0.35H), 3.96 (dt,  $J = 16.6, 2.0$  Hz, 0.35H), 3.81 – 3.64 (m, 1.3H), 3.40 – 3.26 (m, 0.65H), 3.04 (dd,  $J = 13.2, 4.0$  Hz, 0.35H), 2.56 – 2.47 (m, 0.75H), 2.41 – 2.24 (m, 1.35H), 2.23 – 2.15 (m, 1H), 2.10 (s, 3H), 1.97 – 1.87 (m, 3H);  $^{13}\text{C}$  NMR (101 MHz,  $\text{CDCl}_3$ ) (as a mixture of E/Z amide bond isomers, signals of minor isomer are indicated with an asterisk \*)  $\delta$  169.89, 169.43\*, 137.51\*, 136.96, 133.05, 132.80\*, 132.69\*, 130.79, 128.79, 128.59\*, 127.67, 127.61, 127.24\*, 127.16\*, 126.26\*, 126.13, 123.49, 121.87\*, 50.54\*, 46.89, 46.01, 42.22, 41.94\*, 41.52\*, 34.60\*, 34.33, 21.94\*, 21.43, 18.38\*, 18.33; IR (Neat Film, NaCl) 3236, 3027, 2924, 1644, 1434, 1369, 1241, 1014, 972, 894, 749, 694, 655  $\text{cm}^{-1}$ ; (MM:ESI $^+$ )  $m/z$  calc'd for  $\text{C}_{17}\text{H}_{21}\text{ClNO}$   $[\text{M}+\text{H}]^+$ : 290.1306, found 290.1317;  $[\alpha]_{\text{D}}^{25}$ :  $-9.97$  (c 1.0,  $\text{CHCl}_3$ ); Chiral SFC Separation: 15% iPrOH, 2.5 mL/min, AD-H column,  $\lambda = 254$  nm,  $t_{\text{R}}$  (min): major = 6.689 (area: 96.5%), minor = 14.926 (area: 3.5%), 93.0% enantiomeric excess.



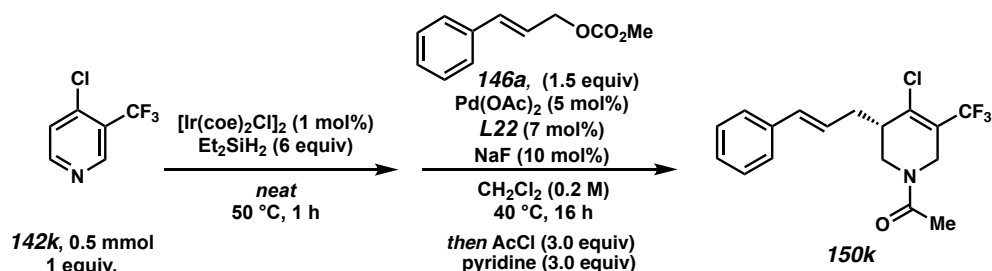
Signal 2: DAD1 C, Sig=254,16 Ref=370,60

Peak #	RetTime [min]	Type	Width [min]	Area [mAU*s]	Height [mAU]	Area %
1	7.040	BB	0.1443	3134.57324	337.63516	49.9836
2	15.478	BB	0.4555	3136.62598	106.54130	50.0164



Signal 2: DAD1 C, Sig=254,16 Ref=370,60

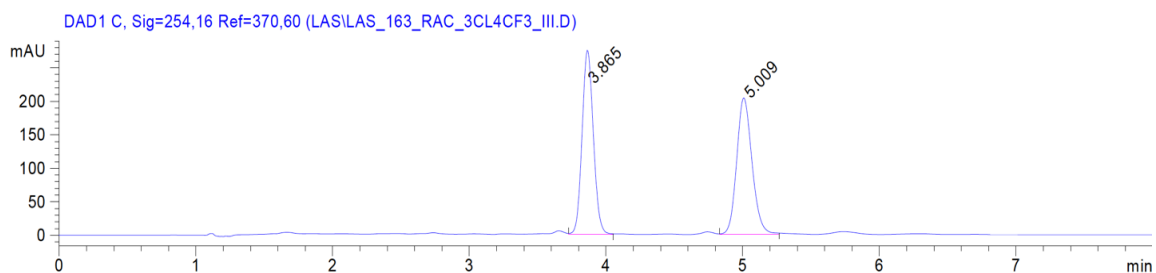
Peak #	RetTime [min]	Type	Width [min]	Area [mAU*s]	Height [mAU]	Area %
1	6.689	BB	0.1781	2.43808e4	2186.42725	96.5063
2	14.926	BB	0.4392	882.61859	31.47048	3.4937



**(R)-1-(5-chloro-3-cinnamyl-4-(trifluoromethyl)-3,6-dihydropyridin-1(2H)-yl)ethan-1-one (150k)**: was synthesized following the general procedure B. Therefore, 3-chloro-4-(trifluoromethyl)pyridine **142k** (90.8 mg, 0.5 mmol, 1.0 equiv) was used. The desired product **150k** was isolated as colorless oil (33.9 mg, 0.099 mmol, 20% yield over three steps);  $^1\text{H}$  NMR (400 MHz,  $\text{CD}_3\text{OD}$ ) (as a mixture of E/Z amide bond isomers):  $\delta$  7.40 – 7.35 (m, 2H), 7.32 – 7.26 (m, 2H), 7.24 – 7.16 (m, 1H), 6.55 – 6.43 (m, 1H), 6.27 – 6.18 (m, 1H), 4.80 – 4.69 (m, 1H), 4.51 – 4.43 (m, 0.5H), 4.25 – 4.16 (m, 0.5H), 4.01 – 3.95 (m,

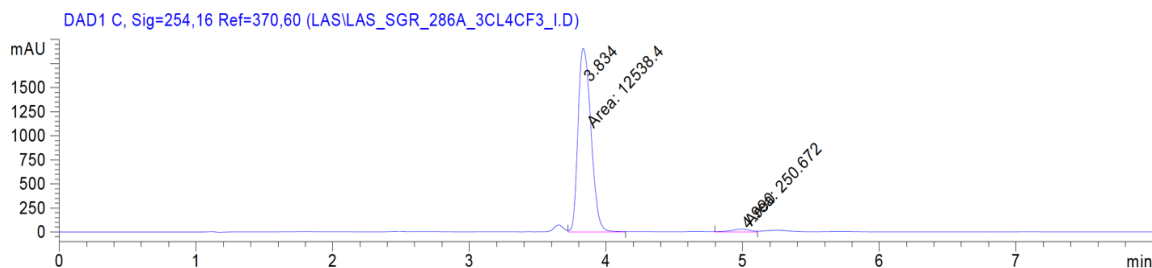
0.5H), 3.84 – 3.75 (m, 0.5H), 3.37 – 3.32 (m, 0.5H), 2.95 – 2.89 (m, 0.5H), 2.83 – 2.72 (m, 1H), 2.57 – 2.49 (m, 0.5H), 2.44 – 2.36 (m, 0.5H), 2.35 – 2.25 (m, 0.5H), 2.21 – 2.15 (m, 0.5H), 2.13 (s, 1.5H), 2.11 (s, 1.5H);  $^{13}\text{C}$  NMR (101 MHz,  $\text{CD}_3\text{OD}$ ) (as a mixture of E/Z amide bond isomers, roughly 1/1 mixture. § denotes overlap of isomers):  $\delta$  172.45, 172.23, 138.71, 138.32, 135.74, (q,  $J = 3.9$  Hz), 135.13 (q,  $J = 4.0$  Hz), 134.64<sup>§</sup>, 129.65, 129.53, 129.39, 129.09, 128.58, 128.33, 127.29, 127.22, 127.21, 126.91, 124.04 (q,  $J = 274.1$  Hz), 123.97 (q,  $J = 274.0$  Hz), 51.72, 48.51, 46.36, 41.26, 38.18, 38.16, 36.19, 36.14, 21.68, 21.24;  $^{19}\text{F}$  NMR (282 MHz,  $\text{CD}_3\text{OD}$ ) (as a mixture of E/Z amide bond isomers, roughly 1/1 mixture):  $\delta$  -62.48, -62.63; IR (Neat Film, NaCl) 3026, 2927, 1735, 1653, 1493, 1423, 1364, 1287, 1262, 1242, 1210, 1185, 1132, 1052, 985, 887, 772, 744, 694, 649, 610  $\text{cm}^{-1}$ ; (MM:ESI<sup>+</sup>)  $m/z$  calc'd for  $\text{C}_{17}\text{H}_{18}\text{ClF}_3\text{NO}$   $[\text{M}+\text{H}]^+$ : 344.1029, found: 344.1021;  $[\alpha]_{\text{D}}^{25}$ : -7.31 (c 1.0,  $\text{CHCl}_3$ );

Chiral SFC Separation: 10% MeOH, 2.5 mL/min, OJ-H column,  $\lambda = 254$  nm,  $t_{\text{R}}$  (min): major = 3.834 (area: 98.0%), minor = 4.990 (area: 2.0%), 96.0.% enantiomeric excess.



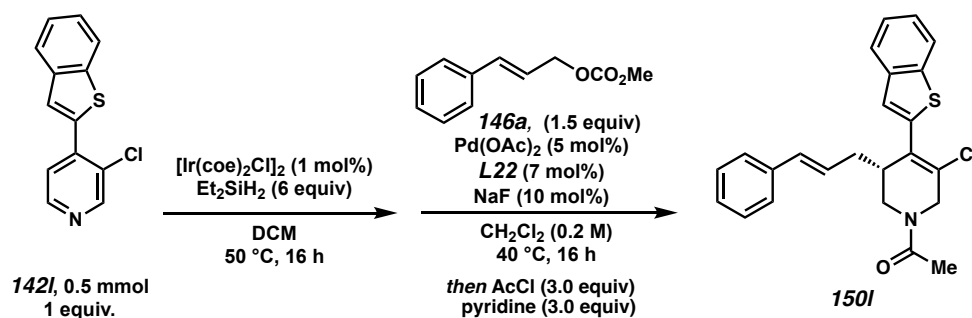
Signal 2: DAD1 C, Sig=254,16 Ref=370,60

Peak #	RetTime [min]	Type	Width [min]	Area [mAU*s]	Height [mAU]	Area %
1	3.865	VB	0.0869	1570.85596	273.97107	49.6514
2	5.009	VB	0.1194	1592.91370	203.42432	50.3486



Signal 2: DAD1 C, Sig=254,16 Ref=370,60

Peak #	RetTime [min]	Type	Width [min]	Area [mAU*s]	Height [mAU]	Area %
1	3.834	MM	0.1089	1.25384e4	1919.23767	98.0400
2	4.990	MM	0.1466	250.67191	28.49819	1.9600



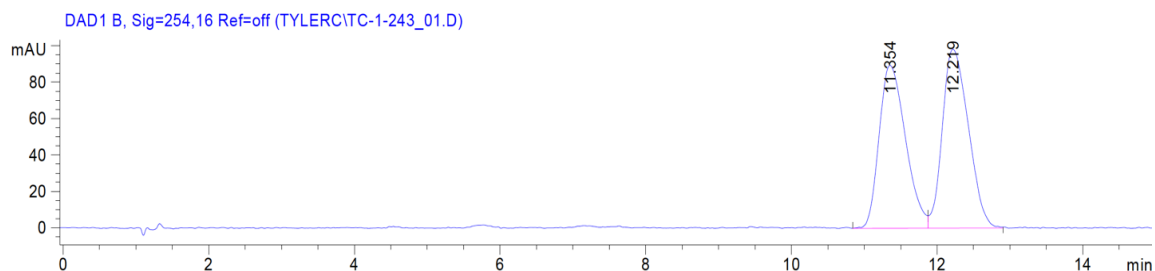
**(R)-1-(4-(benzo[b]thiophen-2-yl)-5-chloro-3-cinnamyl-3,6-dihydropyridin-1(2H)-**

**yl)ethan-1-one (150I):** was synthesized following the general procedure 6 or 7. Therefore, 4-(benzo[b]thiophen-2-yl)-3-chloropyridine **142I** (122.9 mg, 0.5 mmol, 1.0 equiv) was used. The desired product **150I** was isolated as yellow oil (103.8 mg, 0.255 mmol, 51% yield over three steps);  $^1\text{H}$  NMR (400 MHz,  $\text{CD}_3\text{OD}$ ) (as a mixture of E/Z amide bond isomers signals of minor isomer are indicated with an asterisk \*, § = two signals overlapping):  $\delta$  7.81 – 7.73 (m, 2H), 7.51 (s, 0.4H)\*, 7.50 (s, 0.6H), 7.35 – 7.27 (m, 2H), 7.24 – 7.09 (m, 5H), 6.33 (d,  $J = 7.6$  Hz, 0.4H)\*, 6.29 (d,  $J = 7.6$  Hz, 0.6H), 6.16 – 6.04 (m, 1H), 4.74 (d,  $J = 19.0$  Hz, 0.6H), 4.59 (d,  $J = 11.8$  Hz, 0.4H)\*, 4.40 (d,  $J = 17.9$  Hz,

0.4H)\*, 4.11 (dd,  $J = 17.9, 1.2$  Hz, 0.4H)\*, 3.86 – 3.75 (m, 1.2H)<sup>§</sup>, 3.38 (dd,  $J = 13.5, 3.4, 0.6$ H), 3.05 – 2.98 (m, 0.6H), 2.96 – 2.86 (m, 0.8H)\*<sup>§</sup>, 2.40 – 2.12 (m, 2H), 2.08 (s, 1.2H)\*, 2.05 (s, 1.8H); <sup>13</sup>C NMR (101 MHz, CD<sub>3</sub>OD) (as a mixture of E/Z amide bond isomers, signals of minor isomer are indicated with an asterisk \*, § = E/Z signal overlapping):  $\delta$  172.13, 171.95\*, 141.10<sup>§</sup>, 140.57<sup>§</sup>, 140.53, 140.49<sup>§</sup>, 140.34\*, 138.76\*, 138.37, 133.93, 133.91\*, 132.12\*, 131.29, 129.54, 129.43\*, 128.36, 128.21, 128.11\*, 127.84\*, 127.15\*, 127.12, 126.50<sup>§</sup>, 126.05<sup>§</sup>, 125.72\*, 125.63, 124.94\*, 124.92, 122.95<sup>§</sup>, 52.00\*, 48.71, 46.94, 43.48\*, 43.45, 42.06\*, 36.32\*, 36.27, 21.68\*, 21.26; IR (Neat Film, NaCl) 3055, 3025, 2926, 1652, 1495, 1435, 1359, 1305, 1238, 1157, 1129, 1068, 1030, 968, 922, 860, 832, 745, 728, 695, 613 cm<sup>-1</sup>; (MM:ESI<sup>+</sup>)  $m/z$  calc'd for C<sub>24</sub>H<sub>23</sub>ClNOS [M+H]<sup>+</sup>: 408.1189, found: 408.1208;

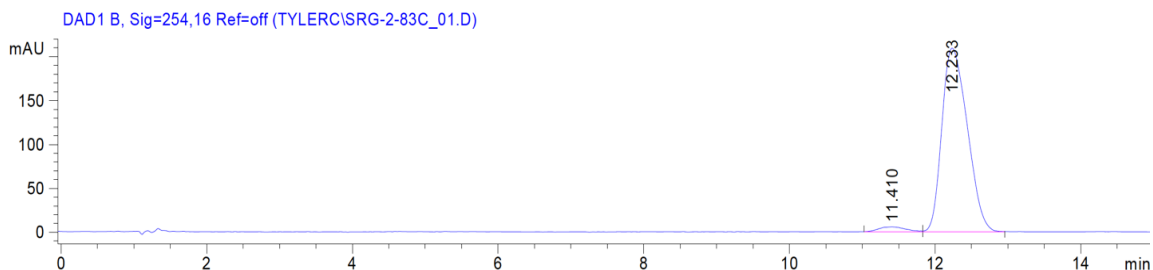
$[\alpha]_D^{25}$ : – 81.02 (c 1.0, CHCl<sub>3</sub>);

Chiral SFC Separation: 30% MeOH, 2.5 mL/min, IC column,  $\lambda = 254$  nm,  $t_R$  (min): major = 12.233 (area: 97.3%), minor = 11.410 (area: 2.7%), 94.6.% enantiomeric excess.



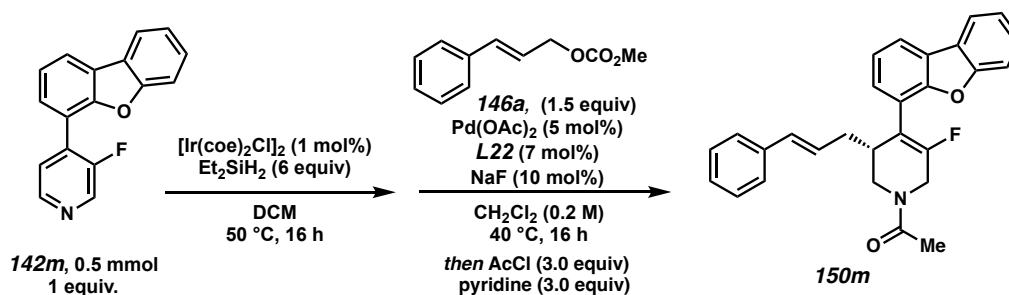
Signal 2: DAD1 B, Sig=254,16 Ref=off

Peak #	RetTime [min]	Type	Width [min]	Area [mAU*s]	Height [mAU]	Area %
1	11.354	VV	0.3963	2260.10962	89.58550	48.0283
2	12.219	VB	0.3680	2445.68018	98.39331	51.9717



Signal 2: DAD1 B, Sig=254,16 Ref=off

Peak #	RetTime [min]	Type	Width [min]	Area [mAU*s]	Height [mAU]	Area %
1	11.410	BV	0.3061	138.32794	5.48661	2.6563
2	12.233	VB	0.3909	5069.24756	209.07002	97.3437



**(R)-1-(3-cinnamyl-4-(dibenzo[*b,d*]furan-4-yl)-5-fluoro-3,6-dihydropyridin-1(2H)-**

**yl)ethan-1-one (150m):** was synthesized following the general procedure 6 or 7.

Therefore, 4-(dibenzo[*b,d*]furan-4-yl)-3-fluoropyridine **142m** (131.6 mg, 0.5 mmol, 1.0

equiv) was used. The desired product **150m** was isolated as yellow amorphous solid (89.2

mg, 0.21 mmol, 42% yield over three steps);  $^1\text{H}$  NMR (400 MHz,  $\text{CDCl}_3$ ) (as a mixture of

*E/Z* amide bond isomers):  $\delta$  8.01 – 7.96 (m, 1H), 7.93 (td,  $J = 5.2, 3.7$  Hz, 1H), 7.61 (dt,  $J$

$= 8.2, 0.9$  Hz, 1H), 7.49 (ddd,  $J = 8.4, 7.3, 1.4$  Hz, 1H), 7.43 – 7.32 (m, 3H), 7.28 – 7.12

(m, 5H), 6.33 (d,  $J = 15.9$  Hz, 0.65H), 6.27 (d,  $J = 15.8$  Hz, 0.35H), 6.10 (t,  $J = 7.6$  Hz,

0.35H), 6.01 (ddd,  $J = 15.8, 8.5, 5.8$  Hz, 0.65H), 4.80 (dd,  $J = 18.3, 1.6$  Hz, 0.65H), 4.37 –

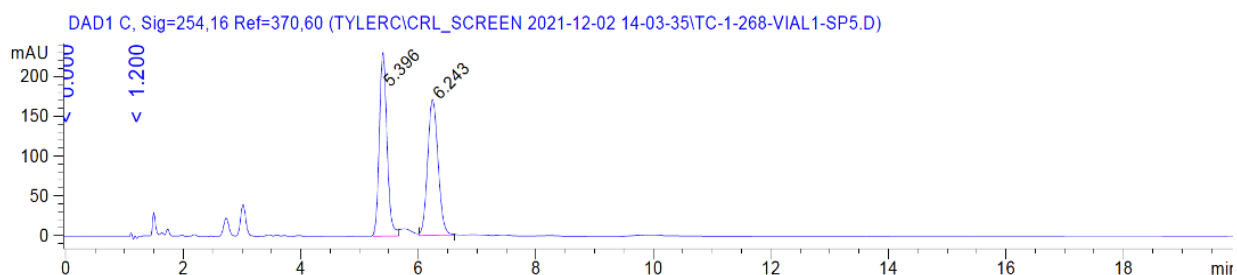
4.26 (m, 0.70H), 4.14 (dd,  $J = 16.8, 2.0$  Hz, 0.35H), 3.99 (dd,  $J = 18.3, 1.8$  Hz, 0.65H),

3.84 (dd,  $J = 13.4, 3.4$  Hz, 0.65H), 3.69 (dd,  $J = 13.4, 4.0$  Hz, 0.65H), 3.58 (dd,  $J = 13.3,$



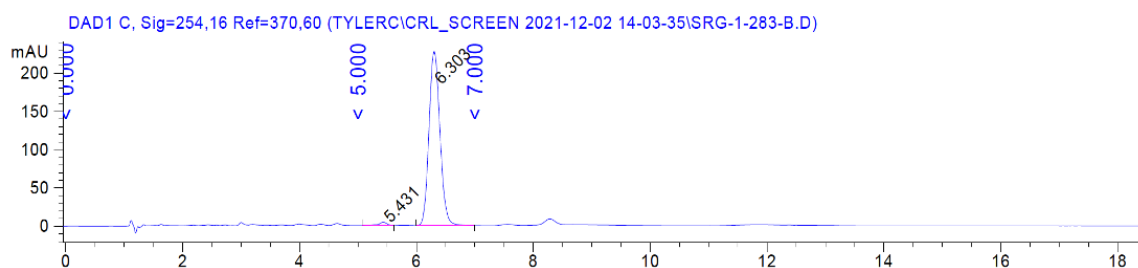
4.3 Hz, 0.35H), 3.32 – 3.20 (m, 1H), 2.42 – 2.32 (m, 0.70H), 2.32 – 2.23 (m, 1.3H), 2.21 (d,  $J = 4.9$  Hz, 3H);  $^{13}\text{C}$  NMR (101 MHz,  $\text{CDCl}_3$ ) (as a mixture of E/Z amide bond isomers, signals of minor isomer are indicated with an asterisk \*)  $\delta$  170.18, 169.74 (d,  $J = 1.7$  Hz)\*, 156.14\*, 156.11, 153.62 (overlap)\*, 152.52 (d,  $J = 258.3$  Hz), 151.19 (d,  $J = 258.2$  Hz)\*, 137.41\*, 136.91, 132.77, 132.51\*, 128.59, 128.41\*, 128.03, 128.00, 127.72\*, 127.69\*, 127.52\*, 127.43, 127.03\*, 126.87\*, 126.10\*, 126.01, 124.76, 124.19, 122.97 (overlap)\*, 122.88 (overlap)\*, 120.82, 120.38\*, 120.35\*, 118.85 (d,  $J = 1.9$  Hz), 114.34 (d,  $J = 6.7$  Hz)\*, 113.02 (d,  $J = 7.7$  Hz), 111.85 (overlap)\*, 46.76, 45.24 (d,  $J = 39.7$  Hz)\*, 42.33\*, 41.70 (d,  $J = 40.5$  Hz), 38.35 (d,  $J = 3.0$  Hz), 37.54 (d,  $J = 2.8$  Hz)\*, 35.26 (d,  $J = 2.8$  Hz)\*, 35.16 (d,  $J = 3.0$  Hz), 22.08\*, 21.53;  $^{19}\text{F}$  NMR (282 MHz,  $\text{CDCl}_3$ ) (as a mixture of E/Z amide bond isomers, signals of minor isomer are indicated with an asterisk \*):  $\delta$  -112.15 – -112.26 (m), -113.31 (d,  $J = 4.7$  Hz)\*; IR (Neat Film, NaCl) 3439, 3027, 2930, 1648, 1450, 1414, 1378, 1352, 1257, 1233, 1180, 1046, 1012, 983, 922, 843, 798, 752, 737  $\text{cm}^{-1}$ ; (MM:ESI<sup>+</sup>)  $m/z$  calc'd for  $\text{C}_{24}\text{H}_{23}\text{ClNOS}$   $[\text{M}+\text{H}]^+$ : 426.1864, found 426.1872;  $[\alpha]_{\text{D}}^{25}$ : -17.72 (c 0.304,  $\text{CHCl}_3$ );

Chiral SFC Separation: 30% MeOH, 2.5 mL/min, AD-H column,  $\lambda = 254$  nm,  $t_{\text{R}}$  (min): major = 6.303 (area: 98.5%), minor = 5.431 (area: 1.5%), 97.0% enantiomeric excess.



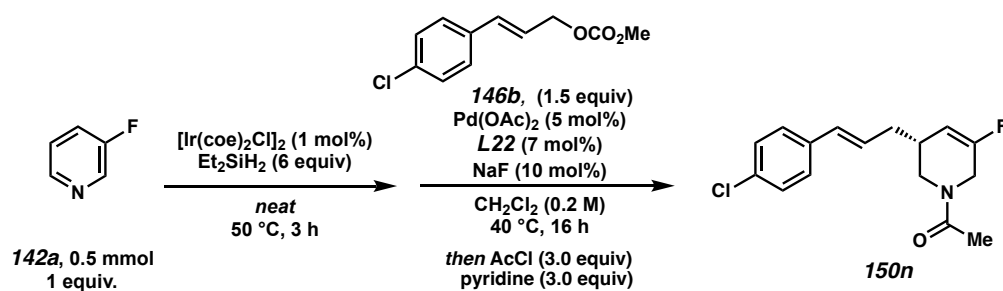
Signal 2: DAD1 C, Sig=254,16 Ref=370,60

Peak #	RetTime [min]	Type	Width [min]	Area [mAU*s]	Height [mAU]	Area %
1	5.396	BB	0.1392	2114.76562	230.07974	50.1048
2	6.243	BB	0.1920	2105.91846	170.63986	49.8952



Signal 2: DAD1 C, Sig=254,16 Ref=370,60

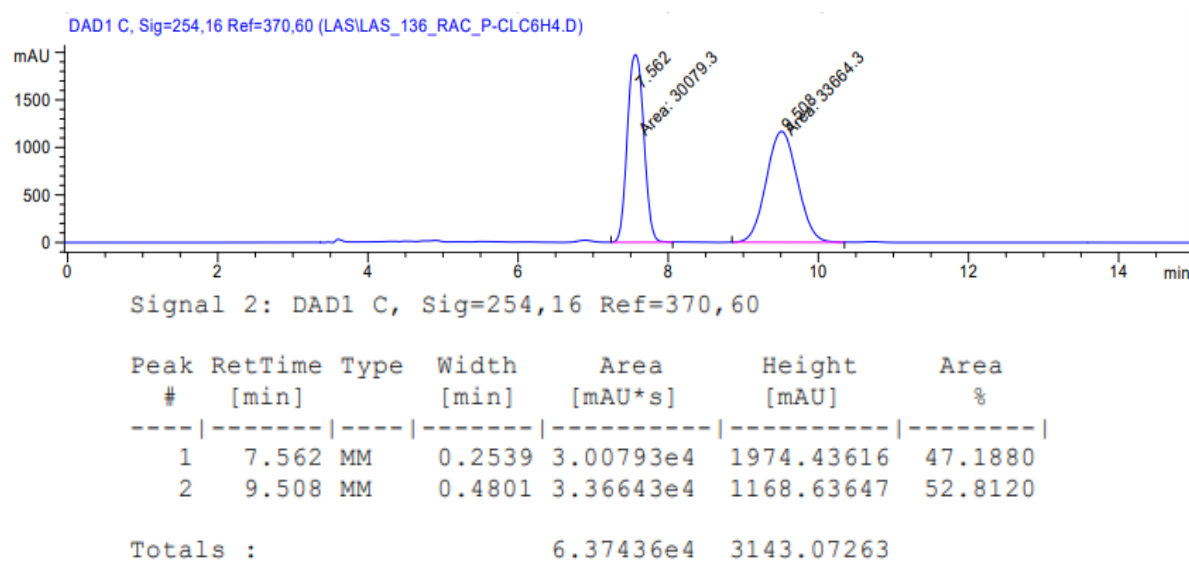
Peak #	RetTime [min]	Type	Width [min]	Area [mAU*s]	Height [mAU]	Area %
1	5.431	BV	0.1582	44.71070	4.19887	1.4915
2	6.303	VB	0.2013	2953.04980	227.77563	98.5085

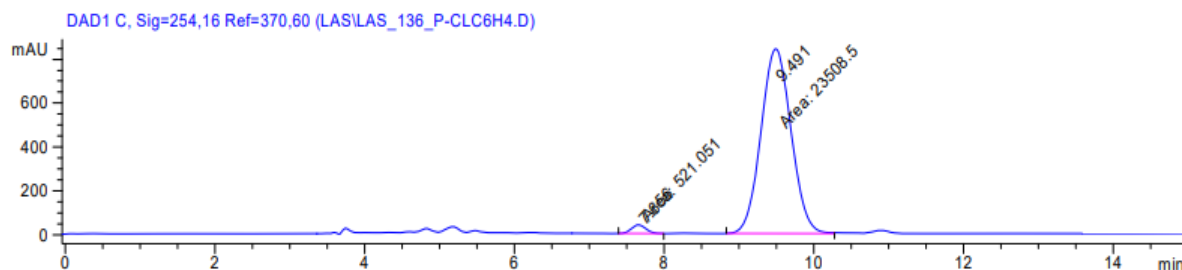


**(*R,E*)-1-(3-(3-(4-chlorophenyl)allyl)-5-fluoro-3,6-dihydropyridin-1(2H)-yl)ethan-1-one (150n)**: was synthesized following the general procedure 6 using 3-fluoropyridine **142a** (43  $\mu$ L, 0.5 mmol, 1.0 equiv) as substrate and (*E*)-3-(4-chlorophenyl)allyl methyl carbonate **146b** (170 mg, 0.75 mmol, 1.5 equiv). The desired compound **150n** was obtained as yellowish oil (42 mg, 0.143 mmol, 29% yield over three steps);  $^1\text{H}$  NMR (400 MHz,  $\text{CDCl}_3$ ) (as a mixture of *E/Z* amide bond isomers):  $\delta$  7.30–7.23 (m, 4H), 6.44–6.34 (m, 1H), 6.18–6.06 (m, 1H), 5.46–5.30 (m, 1H), 4.18–4.04 (m, 1H), 4.02–3.91 (m, 1H), 3.84

(dd,  $J = 13.1, 4.7$  Hz, 0.4H), 3.53 (dd,  $J = 13.4, 4.5$  Hz, 0.6H), 3.36–3.21 (m, 1H), 2.57–2.42 (m, 1H), 2.32–2.15 (m, 2H), 2.11 (s, 3H);  $^{13}\text{C}$  NMR (101 MHz,  $\text{CDCl}_3$ ) (as a mixture of E/Z amide bond isomers, signals of minor isomer are indicated with an asterisk \*):  $\delta$  169.8, 169.7\*, 156.4 (d,  $J = 257$  Hz), 154.9 (d,  $J = 256$  Hz)\*, 135.8\*, 135.5, 133.2, 132.9\*, 131.8, 131.6\*, 128.9, 128.7\*, 127.4\*, 127.4, 127.4, 106.0 (d,  $J = 11.0$  Hz)\*, 104.3 (d,  $J = 12.5$  Hz), 47.7, 44.8 (d,  $J = 39$  Hz)\*, 42.9\*, 41.1 (d,  $J = 40$  Hz), 36.8 (d,  $J = 2.2$  Hz)\*, 36.7 (d,  $J = 2.6$  Hz), 34.2 (d,  $J = 6.2$  Hz), 33.3 (d,  $J = 5.9$  Hz)\*, 22.0\*, 21.5;  $^{19}\text{F}$  NMR (282 MHz,  $\text{CDCl}_3$ ) (as a mixture of E/Z amide bond isomers, signals of minor isomer are indicated with an asterisk \*):  $\delta$  -112.2 (dd,  $J = 15.9, 5.0$  Hz), -114.2 (dd,  $J = 16.1, 5.2$  Hz)\*; IR (Neat Film, NaCl) 2913, 2356, 1705, 1645, 1490, 1428, 1231, 1091, 1012, 973, 828, 729  $\text{cm}^{-1}$ ; (MM:ESI<sup>+</sup>)  $m/z$  calc'd for  $\text{C}_{16}\text{H}_{18}\text{ClFNO}$   $[\text{M}+\text{H}]^+$ : 294.1061, found: 294.1080;  $[\alpha]_{\text{D}}^{25}$ : -33.26 (c 1.0,  $\text{CHCl}_3$ );

Chiral SFC Separation: 30% MeOH, 2.5 mL/min, AD-H column,  $\lambda = 254$  nm,  $t_{\text{R}}$  (min): minor = 7.65 (area: 2.17%), major = 9.41 (area: 97.83%), 95.7% enantiomeric excess.

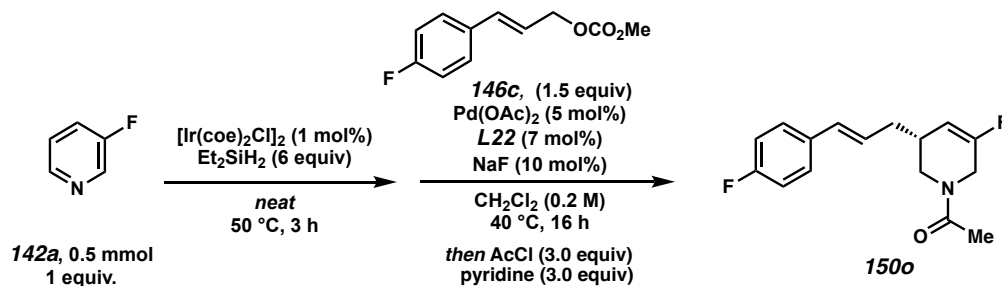




Signal 2: DAD1 C, Sig=254,16 Ref=370,60

Peak #	RetTime [min]	Type	Width [min]	Area [mAU*s]	Height [mAU]	Area %
1	7.656	MM	0.2214	521.05127	39.22103	2.1684
2	9.491	MM	0.4650	2.35085e4	842.62915	97.8316

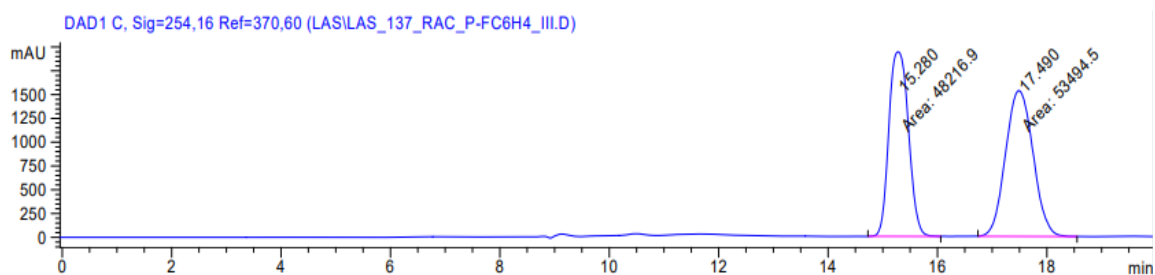
Totals : 2.40295e4 881.85018



**(R,E)-1-(5-fluoro-3-(3-(4-fluorophenyl)allyl)-3,6-dihydropyridin-1(2H)-yl)ethan-1-one (150o)**: was synthesized following the general procedure 5 using 3-fluoropyridine **142a** (43  $\mu\text{L}$ , 0.5 mmol, 1.0 equiv) as substrate and (*E*)-3-(4-fluorophenyl)allyl methyl carbonate **146c** (158 mg, 0.75 mmol, 1.5 equiv). The desired compound **150o** was obtained as yellowish oil (47 mg, 0.169 mmol, 34% yield over three steps);  $^1\text{H}$  NMR (400 MHz,  $\text{CDCl}_3$ ) (as a mixture of *E/Z* amide bond isomers):  $\delta$  7.33–7.27 (m, 2H), 7.03–6.94 (m, 2H), 6.40 (dd,  $J = 15.8, 7.2$  Hz, 1H), 6.12–6.00 (m, 1H), 5.46–5.30 (m, 1H), 4.18–4.05 (m, 1H), 4.03–3.91 (m, 1H), 3.86 (dd,  $J = 13.1, 4.7$  Hz, 0.4H), 3.53 (dd,  $J = 13.6, 4.5$  Hz, 0.6H), 3.33–3.22 (m, 1H), 2.50 (br s, 1H), 2.30–2.15 (m, 2H), 2.12 (s, 3H);  $^{13}\text{C}$  NMR (101 MHz,

CDCl<sub>3</sub>) (as a mixture of E/Z amide bond isomers, signals of minor isomer are indicated with an asterisk \*):  $\delta$  169.8, 169.7\*, 162.3 (d,  $J = 248$  Hz), 162.2 (d,  $J = 246$  Hz)\*, 156.4 (d,  $J = 257$  Hz), 154.9 (d,  $J = 257$  Hz)\*, 133.52 (d,  $J = 3.3$  Hz)\*, 133.20 (d,  $J = 3.3$  Hz), 131.8, 131.6\*, 127.7 (d,  $J = 8.1$  Hz)\*, 127.7 (d,  $J = 8.1$  Hz), 126.4 (d,  $J = 2.6$  Hz)\*, 126.4 (d,  $J = 2.2$  Hz), 115.6 (d,  $J = 22.2$  Hz), 115.5 (d,  $J = 21.2$  Hz)\*, 106.1 (d,  $J = 11$  Hz)\*, 104.4 (d,  $J = 12.5$  Hz), 47.7, 44.8 (d,  $J = 39.2$  Hz)\*, 42.9\*, 41.2 (d,  $J = 40$  Hz), 36.8 (d,  $J = 2.2$  Hz)\*, 36.7 (d,  $J = 2.6$  Hz), 34.3 (d,  $J = 6.2$  Hz), 33.4 (d,  $J = 5.9$  Hz)\*, 22.0\*, 21.5; <sup>19</sup>F NMR (282 MHz, CDCl<sub>3</sub>) (as a mixture of E/Z amide bond isomers, signals of minor isomer are indicated with an asterisk \*):  $\delta$  -112.35 (dd,  $J = 16.3, 5.0$  Hz), -114.30 (dd,  $J = 16.1, 5.7$  Hz)\*, -114.55 – (-114.70)(m), -115.05 – (-115.20)(m)\*; IR (Neat Film, NaCl) 2922, 2360, 1646, 1508, 1428, 1228, 837, 728 cm<sup>-1</sup>; (MM:ESI<sup>+</sup>)  $m/z$  calc'd for C<sub>16</sub>H<sub>18</sub>F<sub>2</sub>-NO [M+H]<sup>+</sup>: 278.1356, found: 278.1364; [ $\alpha$ ]<sub>D</sub><sup>25</sup>: -43.08 (c 1.0, CHCl<sub>3</sub>);

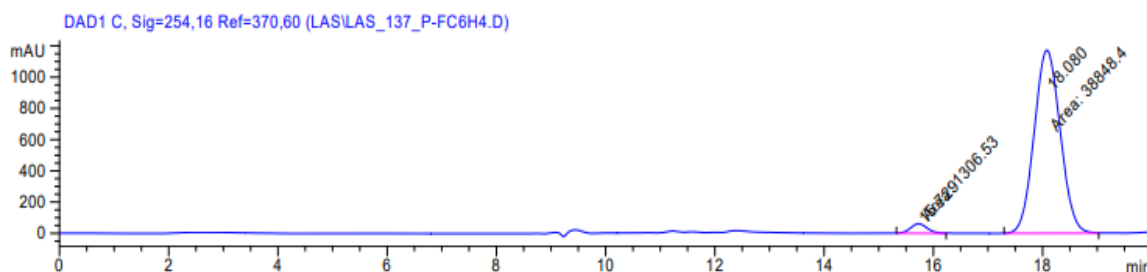
Chiral SFC Separation: 10% MeOH, 2.5 mL/min, AD-H column,  $\lambda = 254$  nm,  $t_R$  (min): minor = 15.73 (area: 3.25%), major = 18.08 (area: 96.75%), 93.5% enantiomeric excess;



Signal 2: DAD1 C, Sig=254,16 Ref=370,60

Peak #	RetTime [min]	Type	Width [min]	Area [mAU*s]	Height [mAU]	Area %
1	15.280	MM	0.4145	4.82169e4	1938.92371	47.4056
2	17.490	MM	0.5819	5.34945e4	1532.15027	52.5944

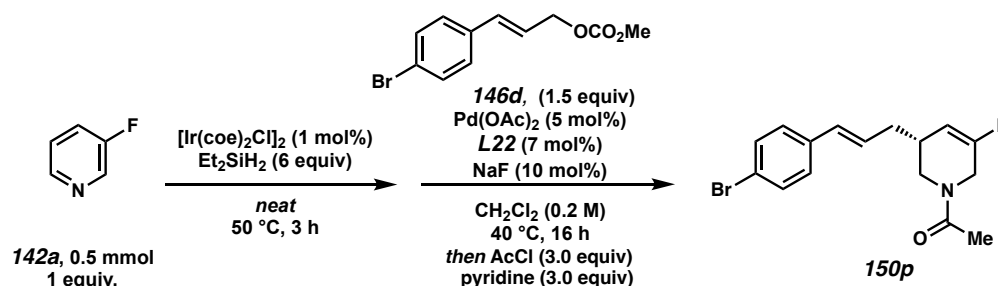
Totals : 1.01711e5 3471.07397



Signal 2: DAD1 C, Sig=254,16 Ref=370,60

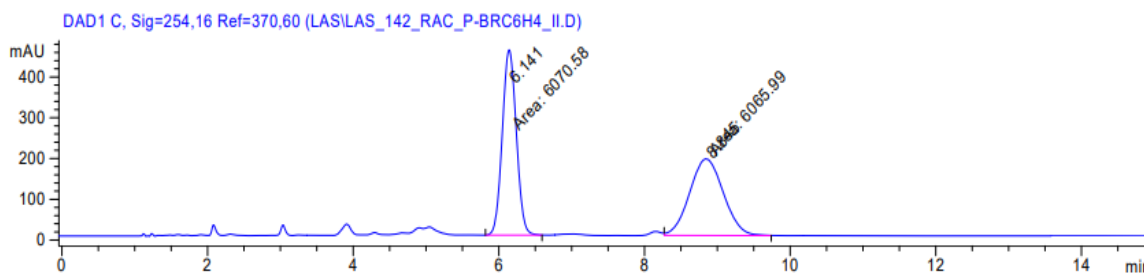
Peak #	RetTime [min]	Type	Width [min]	Area [mAU*s]	Height [mAU]	Area %
1	15.729	MM	0.3570	1306.52649	60.98846	3.2537
2	18.080	MM	0.5522	3.88484e4	1172.47803	96.7463

Totals : 4.01549e4 1233.46649



**(*R,E*)-1-(3-(3-(4-bromophenyl)allyl)-5-fluoro-3,6-dihydropyridin-1(2H)-yl)ethan-1-one (150p)**: was synthesized following the general procedure 5 using 3-fluoropyridine **142a** (43  $\mu$ L, 0.5 mmol, 1.0 equiv) as substrate and (*E*)-3-(4-bromophenyl)allyl methyl carbonate **146d** (203 mg, 0.75 mmol, 1.5 equiv). The desired compound **150p** was obtained as yellowish oil (45 mg, 0.133 mmol, 27% yield over three steps);  $^1\text{H}$  NMR (400 MHz,  $\text{CDCl}_3$ ) (as a mixture of *E/Z* amide bond isomers):  $\delta$  7.45–7.38 (m, 2H), 7.20 (d,  $J = 7.6$  Hz, 2H), 6.37 (dd,  $J = 15.9, 6.7$  Hz, 1H), 6.20–6.08 (m, 1H), 5.45–5.30 (m, 1H), 4.18–4.04 (m, 1H), 4.03–3.90 (m, 1H), 3.83 (dd,  $J = 13.1, 4.7$  Hz, 0.4H), 3.53 (dd,  $J = 13.4, 4.5$  Hz,

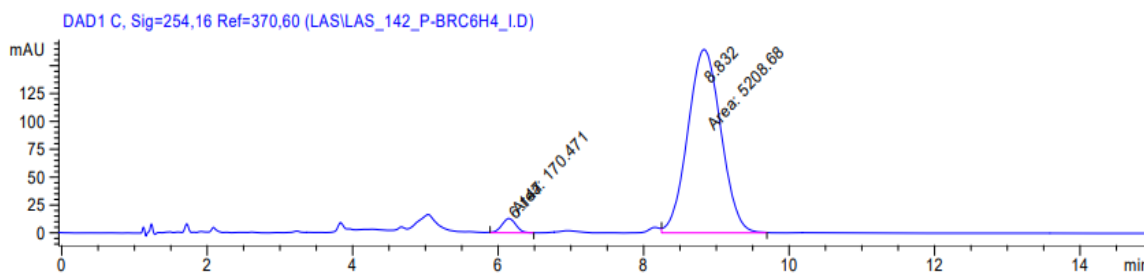
0.6H), 3.34–3.20 (m, 1H), 2.48 (br s, 1H), 2.32–2.16 (m, 2H), 2.11 (s, 3H);  $^{13}\text{C}$  NMR (101 MHz,  $\text{CDCl}_3$ ) (as a mixture of E/Z amide bond isomers, signals of minor isomer are indicated with an asterisk \*):  $\delta$  169.8\*, 169.7, 156.4 (d,  $J = 257$  Hz), 154.9 (d,  $J = 257$  Hz)\*, 136.3\*, 135.9, 131.9\*, 131.8, 131.7, 131.6\*, 127.8\*, 127.7, 127.6\*, 127.5, 121.3, 121.0\*, 106.1 (d,  $J = 11.4$  Hz)\*, 104.3 (d,  $J = 12.5$  Hz), 47.7, 44.8 (d,  $J = 39.2$  Hz)\*, 42.9\*, 41.1 (d,  $J = 39.6$  Hz), 36.8 (d,  $J = 2.2$  Hz)\*, 36.8 (d,  $J = 2.6$  Hz), 34.2 (d,  $J = 6.6$  Hz), 33.3 (d,  $J = 5.9$  Hz)\*, 22.0\*, 21.5;  $^{19}\text{F}$  NMR (282 MHz,  $\text{CDCl}_3$ ) (as a mixture of E/Z amide bond isomers, signals of minor isomer are indicated with an asterisk \*):  $\delta$  -112.22 (dd,  $J = 16.1$ , 4.7 Hz), -114.16 (dd,  $J = 16.3$ , 5.4 Hz); IR (Neat Film, NaCl) 2917, 2358, 1706, 1648, 1486, 1426, 1379, 1229, 1164, 1071, 1007, 969, 838  $\text{cm}^{-1}$ ; (MM:ESI $^+$ )  $m/z$  calc'd for  $\text{C}_{16}\text{H}_{18}\text{BrFNO}$  [M+H] $^+$ : 338.0556, found: 338.0554;  $[\alpha]_{\text{D}}^{25}$ : -36.48 (c 1.0,  $\text{CHCl}_3$ ); Chiral SFC Separation: 30% MeOH, 2.5 mL/min, AD-H column,  $\lambda = 254$  nm,  $t_{\text{R}}$  (min): minor = 6.15 (area: 3.17%), major = 8.83 (area: 96.83%), 93.6% enantiomeric excess.



Signal 2: DAD1 C, Sig=254,16 Ref=370,60

Peak #	RetTime [min]	Type	Width [min]	Area [mAU*s]	Height [mAU]	Area %
1	6.141	MM	0.2225	6070.58252	454.82550	50.0189
2	8.845	MM	0.5376	6065.99072	188.07510	49.9811

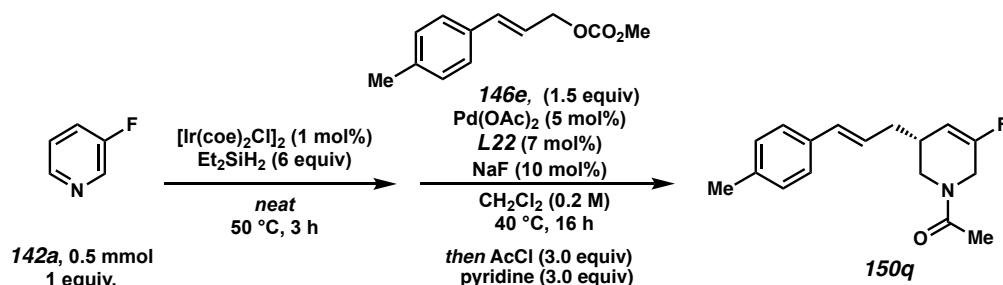
Totals : 1.21366e4 642.90060



Signal 2: DAD1 C, Sig=254,16 Ref=370,60

Peak #	RetTime [min]	Type	Width [min]	Area [mAU*s]	Height [mAU]	Area %
1	6.147	MM	0.2215	170.47104	12.82446	3.1691
2	8.832	FM	0.5278	5208.68311	164.49005	96.8309

Totals : 5379.15414 177.31451



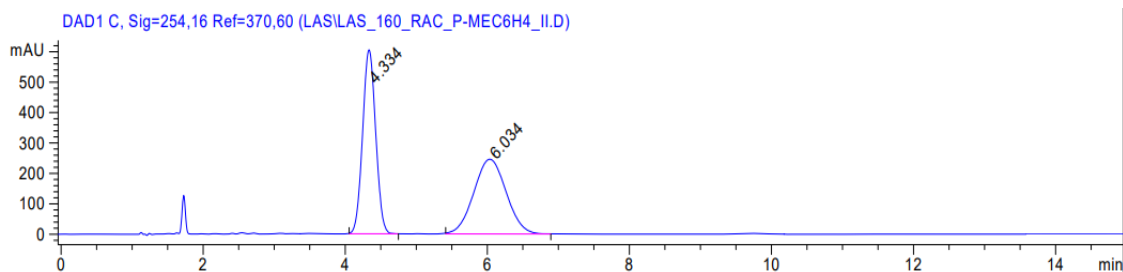
**(*R,E*)-1-(5-fluoro-3-(*p*-tolyl)allyl)-3,6-dihydropyridin-1(2H)-yl)ethan-1-one**

**(150q)**: was synthesized following the general procedure 5 using 3-fluoropyridine **142a** (43  $\mu\text{L}$ , 0.5 mmol, 1.0 equiv) as substrate and (*E*)-methyl 3-(*p*-tolyl)allyl carbonate **146e** (174 mg, 0.75 mmol, 1.5 equiv). The desired compound **150q** was obtained as colorless oil (61 mg, 0.223 mmol, 45% yield over three steps);  $^1\text{H}$  NMR (400 MHz,  $\text{CDCl}_3$ ) (as a mixture of *E/Z* amide bond isomers):  $\delta$  7.27–7.21 (m, 2H), 7.16–7.08 (m, 2H), 6.40 (dd,  $J = 15.8, 7.6$  Hz, 1H), 6.15–6.03 (m, 1H), 5.48–5.30 (m, 1H), 4.19–4.03 (m, 1H), 4.01–3.94 (m, 1H), 3.91 (dd,  $J = 13.1, 4.7$  Hz, 0.4H), 3.52 (dd,  $J = 13.5, 4.5$  Hz, 0.6H), 3.24 (td,  $J = 13.4, 6.5$  Hz, 1H), 2.49 (br s, 1H), 2.35–2.30 (m, 3H), 2.30–2.16 (m, 2H), 2.11 (s, 3H);  $^{13}\text{C}$



NMR (101 MHz, CDCl<sub>3</sub>) (as a mixture of E/Z amide bond isomers, signals of minor isomer are indicated with an asterisk \*):  $\delta$  169.8, 169.6\*, 156.24 (d,  $J$  = 255 Hz), 154.7 (d,  $J$  = 256 Hz)\*, 137.4, 137.1\*, 134.5\*, 134.2, 132.8, 132.5\*, 129.4, 129.3\*, 126.1\*, 126.0, 125.6, 125.6\*, 106.1 (d,  $J$  = 11.0 Hz)\*, 104.5 (d,  $J$  = 12.1 Hz), 47.0, 44.8 (d,  $J$  = 39 Hz)\*, 43.0\*, 41.1 (d,  $J$  = 39 Hz), 36.8 (d,  $J$  = 2.2 Hz)\*, 36.7 (d,  $J$  = 2.6 Hz), 34.3 (d,  $J$  = 6.2 Hz), 33.4 (d,  $J$  = 5.9 Hz)\*, 22.0\*, 21.5, 21.5\*, 21.2; <sup>19</sup>F NMR (282 MHz, CDCl<sub>3</sub>):  $\delta$  -112.55 (dd,  $J$  = 15.9, 5.0 Hz), -114.44 (dd,  $J$  = 16.3, 5.4 Hz); IR (Neat Film, NaCl) 3022, 2919, 2357, 1708, 1652, 1512, 1427, 1380, 1274, 1230, 1161, 1109, 1035, 970, 825, 788 cm<sup>-1</sup>; (MM:ESI<sup>+</sup>)  $m/z$  calc'd for C<sub>16</sub>H<sub>18</sub>BrFNO [M+H]<sup>+</sup>: 274.1607, found: 274.1610; [ $\alpha$ ]<sub>D</sub><sup>25</sup>: -41.25 (c 1.0, CHCl<sub>3</sub>);

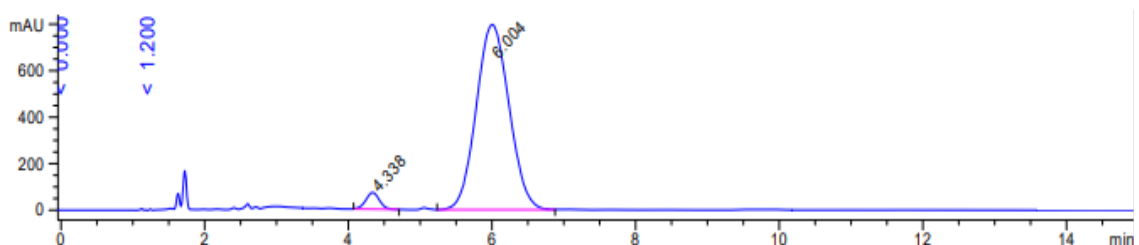
Chiral SFC Separation: 30% MeOH, 2.5 mL/min, AD-H column,  $\lambda$  = 254 nm,  $t_R$  (min): minor = 4.34 (area: 3.57%), major = 6.00 (area: 96.43%), 92.86% enantiomeric excess.



Signal 2: DAD1 C, Sig=254,16 Ref=370,60

Peak #	RetTime [min]	Type	Width [min]	Area [mAU*s]	Height [mAU]	Area %
1	4.334	BB	0.2012	7725.56982	604.15234	49.8360
2	6.034	BB	0.4972	7776.40967	245.71536	50.1640

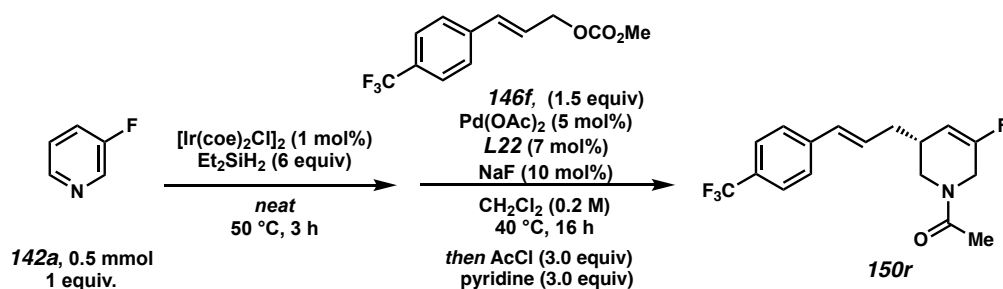
Totals : 1.55020e4 849.86771



Signal 2: DAD1 C, Sig=254,16 Ref=370,60

Peak #	RetTime [min]	Type	Width [min]	Area [mAU*s]	Height [mAU]	Area %
1	4.338	BB	0.2011	939.37775	71.56826	3.5722
2	6.004	VB	0.4994	2.53577e4	796.44708	96.4278

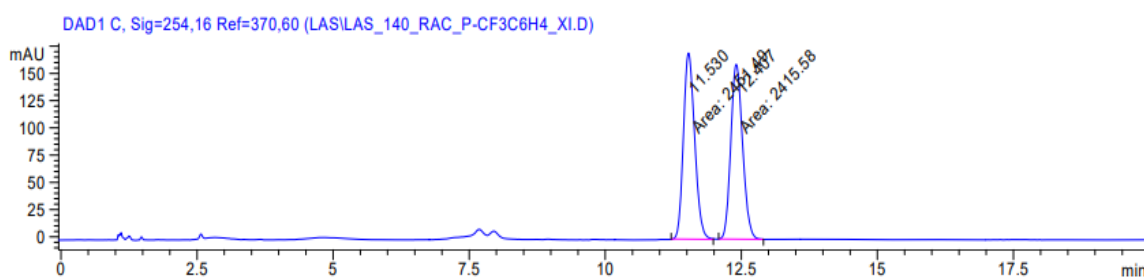
Totals : 2.62971e4 868.01534



**(*R,E*)-1-(5-fluoro-3-(3-(4-(trifluoromethyl)phenyl)allyl)-3,6-dihydropyridin-1(2H)-yl)ethan-1-one (150r)**: was synthesized following the general procedure 5 using 3-fluoropyridine **142a** (43  $\mu$ L, 0.5 mmol, 1.0 equiv) as substrate and (*E*)-methyl (3-(4-(trifluoromethyl)phenyl)allyl) carbonate **146f** (195 mg, 0.75 mmol, 1.5 equiv). The desired compound **150r** was obtained as colorless oil (50 mg, 0.153 mmol, 31% yield over three steps);  $^1\text{H}$  NMR (400 MHz,  $\text{CDCl}_3$ ) (as a mixture of *E/Z* amide bond isomers):  $\delta$  7.59–7.51 (m, 2H), 7.47–7.40 (m, 2H), 6.56–6.43 (m, 1H), 6.33–6.20 (m, 1H), 5.48–5.30 (m, 1H), 4.19–4.06 (m, 1H), 4.04–3.93 (m, 1H), 3.85–3.78 (m, 0.4H), 3.59–3.50 (m, 0.6H), 3.40–3.22 (m, 1H), 2.60–2.45 (br s, 1H), 2.38–2.19 (m, 2H), 2.12 (s, 3H);  $^{13}\text{C}$  NMR (101 MHz,  $\text{CDCl}_3$ ) (as a mixture of *E/Z* amide bond isomers, signals of minor isomer are indicated with an asterisk \*):  $\delta$  169.8, 169.7\*, 156.5 (d,  $J = 256$  Hz), 155.0 (d,  $J = 256$  Hz)\*, 140.8\*,

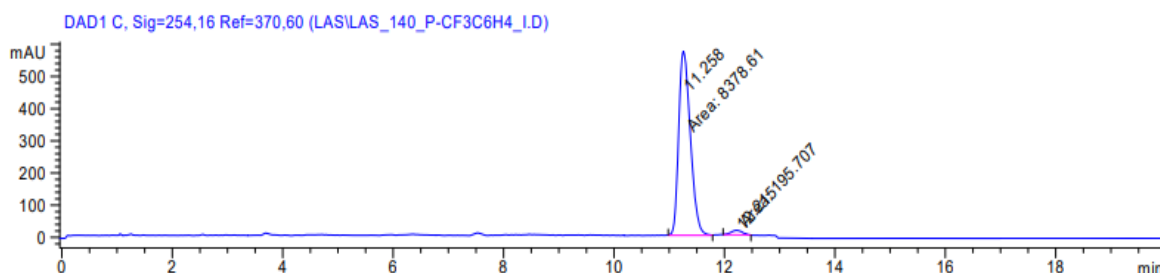
140.5, 131.8, 131.6\*, 129.6\*, 129.5, 129.3, 129.0\*, 126.4\*, 126.4, 125.8 (q,  $J = 3.7$  Hz), 125.6 (q,  $J = 4.0$  Hz)\*, 106.0 (d,  $J = 11.4$  Hz)\*, 104.3 (d,  $J = 12.5$  Hz), 47.8, 44.9 (d,  $J = 39$  Hz), 42.8\*, 41.2 (d,  $J = 40$  Hz), 36.9, 36.8\*, 34.2 (d,  $J = 6.2$  Hz), 33.3 (d,  $J = 6.2$  Hz)\*, 22.0\*, 21.6; The carbon atom for the CF<sub>3</sub>-group was not detected; <sup>19</sup>F NMR (282 MHz, CDCl<sub>3</sub>) (as a mixture of E/Z amide bond isomers, signals of minor isomer are indicated with an asterisk \*):  $\delta$  -62.44\* (s), -62.50 (s), -112.06 (dd,  $J = 15.9, 5.0$  Hz), -114.02 (dd,  $J = 16.3, 5.0$  Hz)\*; IR (Neat Film, NaCl) 2921, 2357, 1651, 1434, 1326, 1233, 1163, 1121, 1067, 1016, 839 cm<sup>-1</sup>; (MM:ESI<sup>+</sup>)  $m/z$  calc'd for C<sub>17</sub>H<sub>18</sub>F<sub>4</sub>NO [M+H]<sup>+</sup>: 328.1325, found: 328.1338;  $[\alpha]_D^{25}$ : -26.31 (c 1.0, CHCl<sub>3</sub>);

Chiral SFC Separation: 7% *i*PrOH, 2.5 mL/min, AD-H column,  $\lambda = 254$  nm,  $t_R$  (min): major = 11.26 (area: 97.72%), minor = 12.22 (area: 2.28%), 95.4% enantiomeric excess.



Signal 2: DAD1 C, Sig=254,16 Ref=370,60

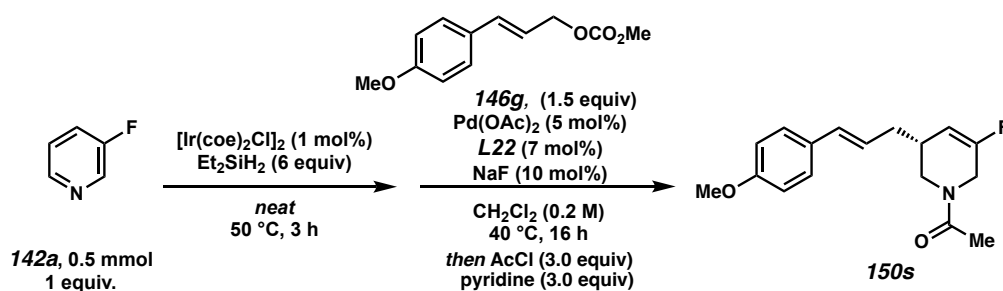
Peak #	RetTime [min]	Type	Width [min]	Area [mAU*s]	Height [mAU]	Area %
1	11.530	MM	0.2391	2451.48804	170.85316	50.3689
2	12.407	MM	0.2509	2415.58301	160.48860	49.6311
Totals :				4867.07104	331.34177	



Signal 2: DAD1 C, Sig=254,16 Ref=370,60

Peak #	RetTime [min]	Type	Width [min]	Area [mAU*s]	Height [mAU]	Area %
1	11.258	MM	0.2440	8378.60938	572.39178	97.7175
2	12.215	MM	0.2372	195.70685	13.75326	2.2825

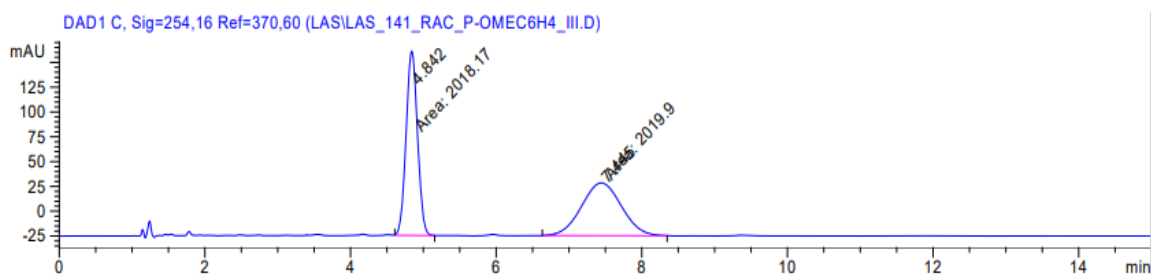
Totals : 8574.31622 586.14504



**(*R,E*)-1-(5-fluoro-3-(3-(4-methoxyphenyl)allyl)-3,6-dihydropyridin-1(2H)-yl)ethan-1-one (150s)**: was synthesized following the general procedure 5 using 3-fluoropyridine **142a** (43  $\mu$ L, 0.5 mmol, 1.0 equiv) as substrate and (*E*)-3-(4-methoxyphenyl)allyl methyl carbonate **146g** (168 mg, 0.75 mmol, 1.5 equiv). The desired compound **150s** was obtained as colorless oil (49 mg, 0.169 mmol, 34% yield over three steps);  $^1\text{H}$  NMR (400 MHz,  $\text{CDCl}_3$ ) (as a mixture of *E/Z* amide bond isomers):  $\delta$  7.31–7.23 (m, 2H), 6.88–6.80 (m, 2H), 6.44–6.32 (m, 1H), 6.07–5.93 (m, 1H), 5.48–5.30 (m, 1H), 4.18–4.05 (m, 1H), 4.02–3.93 (s, 1H), 3.93–3.87 (m, 0.4H), 3.81–3.79 (m, 3H), 3.52 (dd,  $J = 13.6, 4.6$  Hz, 0.6H), 3.33–3.17 (m, 1H), 2.49 (br s, 1H), 2.39–2.13 (m, 2H), 2.11 (s, 3H);  $^{13}\text{C}$  NMR (101 MHz,  $\text{CDCl}_3$ ) (as a mixture of *E/Z* amide bond isomers, signals of minor isomer are indicated

with an asterisk \*):  $\delta$  169.8, 169.6\*, 159.2, 159.0\*, 156.3 (d,  $J = 256$  Hz), 154.8 (d,  $J = 256$  Hz)\*, 132.4, 132.1\*, 130.2\*, 129.9, 127.4\*, 127.3, 124.4\*, 124.4, 114.1, 114.0\*, 106.2 (d,  $J = 11.0$  Hz)\*, 104.6 (d,  $J = 12.5$  Hz), 55.4, 55.4\*, 47.6, 44.8 (d,  $J = 39$  Hz)\*, 43.0\*, 41.2 (d,  $J = 40$  Hz), 36.8 (d,  $J = 2.2$  Hz)\*, 36.8 (d,  $J = 2.6$  Hz), 34.4 (d,  $J = 6.2$  Hz), 33.5 (d,  $J = 5.9$  Hz)\*, 22.0\*, 21.5;  $^{19}\text{F}$  NMR (282 MHz,  $\text{CDCl}_3$ ) (as a mixture of E/Z amide bond isomers, signals of minor isomer are indicated with an asterisk \*):  $\delta$  -112.61 (dd,  $J = 15.9$ , 5.0 Hz), -114.52 (dd,  $J = 16.8$ , 5.4 Hz)\*; IR (Neat Film, NaCl) 2915, 2365, 1647, 1511, 1456, 1248, 1173, 1159, 1032  $\text{cm}^{-1}$ ; (MM:ESI $^+$ )  $m/z$  calc'd for  $\text{C}_{17}\text{H}_{21}\text{FNO}_2$  [M+H] $^+$ : 290.1556, found: 290.1563;  $[\alpha]_{\text{D}}^{25}$ : -35.38 (c 1.0,  $\text{CHCl}_3$ );

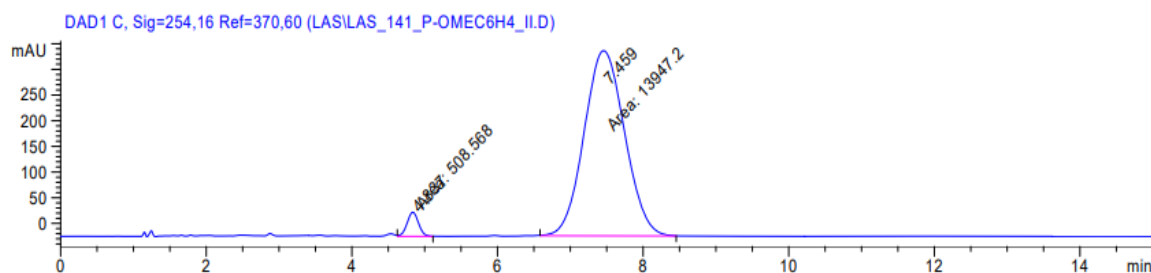
Chiral SFC Separation: 35% MeOH, 2.5 mL/min, AD-H column,  $\lambda = 254$  nm,  $t_{\text{R}}$  (min): minor = 4.84 (area: 3.52%), major = 7.46 (area: 96.48%), 93.0% enantiomeric excess.



Signal 2: DAD1 C, Sig=254,16 Ref=370,60

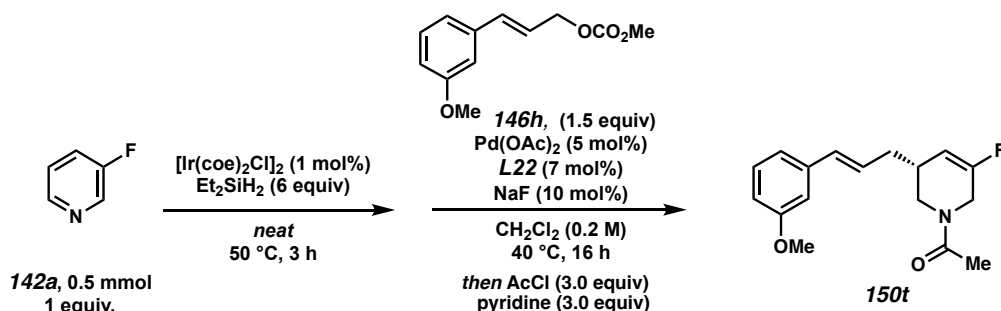
Peak #	RetTime [min]	Type	Width [min]	Area [mAU*s]	Height [mAU]	Area %
1	4.842	MM	0.1808	2018.17383	186.01950	49.9786
2	7.445	MM	0.6333	2019.90381	53.15785	50.0214

Totals : 4038.07764 239.17735



Signal 2: DAD1 C, Sig=254,16 Ref=370,60

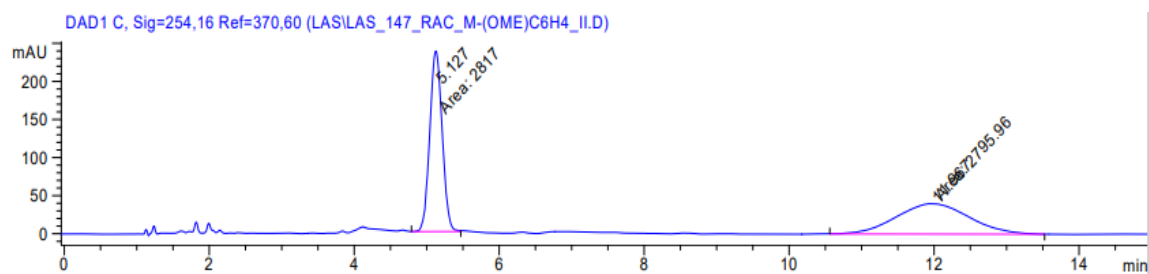
Peak #	RetTime [min]	Type	Width [min]	Area [mAU*s]	Height [mAU]	Area %
1	4.837	MM	0.1804	508.56772	46.98798	3.5181
2	7.459	MM	0.6439	1.39472e4	360.99673	96.4819
Totals :				1.44558e4	407.98472	



**(*R,E*)-1-(5-fluoro-3-(3-methoxyphenyl)allyl)-3,6-dihydropyridin-1(2H)-yl)ethan-1-one (**150t**):** was synthesized following the general procedure 5 using 3-fluoropyridine **142a** (43  $\mu\text{L}$ , 0.5 mmol, 1.0 equiv) as substrate and (*E*)-3-(3-methoxyphenyl)allyl methyl carbonate **146h** (167 mg, 0.75 mmol, 1.5 equiv). The desired compound **150t** was obtained as colorless oil (52 mg, 0.180 mmol, 36% yield over three steps);  $^1\text{H}$  NMR (400 MHz,  $\text{CD}_2\text{Cl}_2$ ) (as a mixture of *E/Z* amide bond isomers):  $\delta$  7.26–7.18 (m, 1H), 6.98–6.93 (m, 1H), 6.91–6.87 (m, 1H), 6.81–6.74 (m, 1H), 6.42 (dd,  $J = 15.8, 9.7$  Hz, 1H), 6.25–6.14 (m, 1H), 5.48–5.34 (m, 1H), 4.15–3.92 (m, 2H), 3.86–3.77 (m, 3.4H), 3.54 (dd,  $J = 13.2, 4.9$  Hz, 0.6H), 3.30–3.20 (m, 1H), 2.58–2.42 (m, 1H), 2.32–2.15 (m, 2H), 2.10–2.06 (m, 3H);  $^{13}\text{C}$  NMR (101 MHz,  $\text{CD}_2\text{Cl}_2$ ) (as a mixture of *E/Z* amide bond isomers, signals of minor isomer are indicated with an asterisk \*):  $\delta$  169.7, 169.6\*, 160.3, 160.3\*, 156.8 (d,  $J = 256$  Hz), 155.5 (d,  $J = 256$  Hz)\*, 139.2\*, 139.0, 132.8, 132.6\*, 129.9, 129.8\*, 127.7\*, 127.7, 119.0, 119.0\*, 113.2, 113.1\*, 111.8, 111.7\*, 106.2 (d,  $J = 11.0$  Hz)\*, 104.9 (d,  $J = 12.1$  Hz), 55.5, 55.5\*, 47.9, 45.0 (d,  $J = 39$  Hz)\*, 43.0\*, 41.2 (d,  $J = 40$  Hz), 37.1\*, 36.9, 34.6

(d,  $J = 6.2$  Hz), 33.7 (d,  $J = 5.9$  Hz)\*, 22.1\*, 21.6;  $^{19}\text{F}$  NMR (282 MHz,  $\text{CD}_2\text{Cl}_2$ ) (as a mixture of E/Z amide bond isomers, signals of minor isomer are indicated with an asterisk \*):  $\delta$ -113.52 (dd,  $J = 16.6, 4.7$  Hz), -115.27 (dd,  $J = 16.8, 4.5$  Hz); IR (Neat Film, NaCl) 2922, 2359, 1706, 1651, 1598, 1578, 1431, 1380, 1264, 1233, 1158, 1041, 972, 834, 776, 689  $\text{cm}^{-1}$ ; (MM:ESI $^+$ )  $m/z$  calc'd for  $\text{C}_{17}\text{H}_{21}\text{FNO}_2$   $[\text{M}+\text{H}]^+$ : 290.1556, found: 290.1560;  $[\alpha]_{\text{D}}^{25}$ : -40.94 (c 1.0,  $\text{CHCl}_3$ );

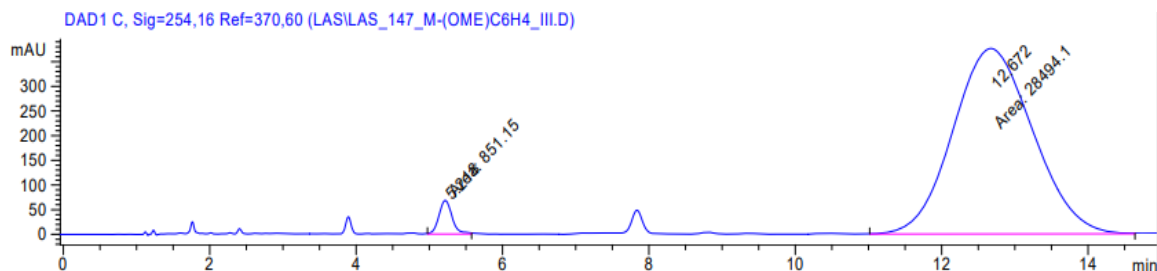
Chiral SFC Separation: 30% MeOH, 2.5 mL/min, AD-H column,  $\lambda = 254$  nm,  $t_{\text{R}}$  (min): minor = 5.22 (area: 2.90%), major = 12.67 (area: 97.10%), 94.2% enantiomeric excess.



Signal 2: DAD1 C, Sig=254,16 Ref=370,60

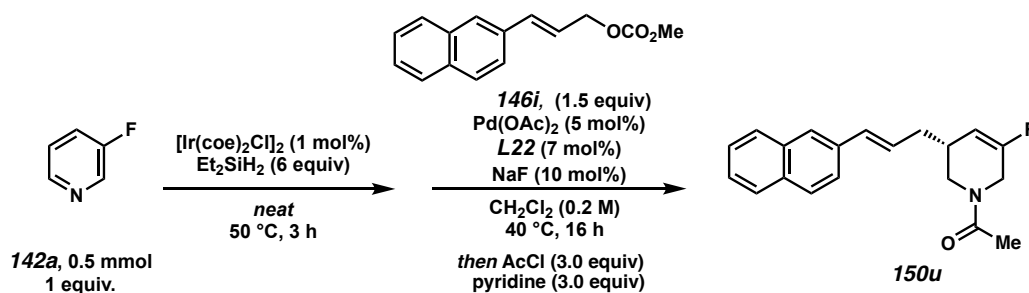
Peak #	RetTime [min]	Type	Width [min]	Area [mAU*s]	Height [mAU]	Area %
1	5.127	MM	0.1978	2816.99536	237.34180	50.1874
2	11.967	MM	1.1664	2795.95776	39.95090	49.8126

Totals : 5612.95313 277.29269



Signal 2: DAD1 C, Sig=254,16 Ref=370,60

Peak #	RetTime [min]	Type	Width [min]	Area [mAU*s]	Height [mAU]	Area %
1	5.218	MM	0.2081	851.15015	68.15288	2.9005
2	12.672	MM	1.2638	2.84941e4	375.75864	97.0995
Totals :				2.93453e4	443.91151	

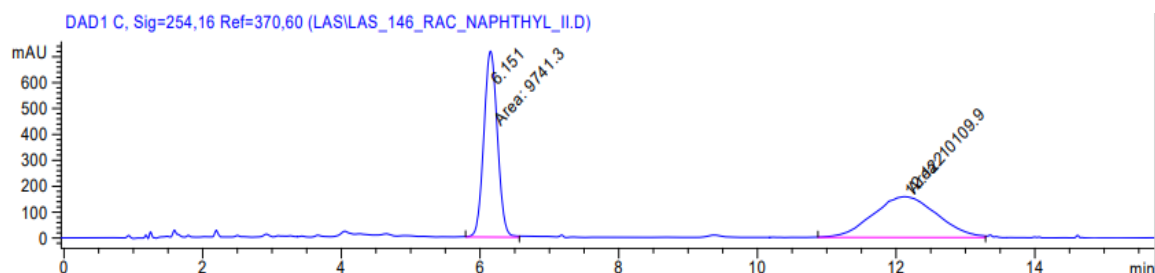


**(*R,E*)-1-(5-fluoro-3-(3-(naphthalen-2-yl)allyl)-3,6-dihydropyridin-1(2H)-yl)ethan-1-one (**150u**):** was synthesized following the general procedure 5 using 3-fluoropyridine **142a** (43  $\mu\text{L}$ , 0.5 mmol, 1.0 equiv) as substrate and (*E*)-methyl 3-(naphthalen-2-yl)allyl carbonate **146i** (181 mg, 0.75 mmol, 1.5 equiv). The desired compound **150u** was obtained as colorless oil (39 mg, 0.126 mmol, 25% yield over three steps);  $^1\text{H}$  NMR (400 MHz,  $\text{CD}_2\text{Cl}_2$ ) (as a mixture of *E/Z* amide bond isomers):  $\delta$  7.85–7.77 (m, 3H), 7.72 (s, 1H), 7.64–7.58 (m, 1H), 7.52–7.40 (m, 2H), 6.67–6.58 (m, 1H), 6.39–6.28 (m, 1H), 5.53–5.37 (m, 1H), 4.18–3.95 (m, 2H), 3.84 (dd,  $J = 13.0, 4.7$  Hz, 0.4H), 3.56 (dd,  $J = 13.6, 4.5$  Hz, 0.6H), 3.37–3.23 (m, 1H), 2.60–2.46 (m, 1H), 2.40–2.22 (m, 2H), 2.11–2.07 (m, 3H);  $^{13}\text{C}$  NMR (101 MHz,  $\text{CD}_2\text{Cl}_2$ ) (as a mixture of *E/Z* amide bond isomers, signals of minor isomer are indicated with an asterisk \*, one signal is overlapping):  $\delta$  169.7, 169.6\*, 156.8 (d,  $J = 256$  Hz), 155.5 (d,  $J = 256$  Hz)\*, 135.3\*, 135.0, 134.1\*, 134.0, 133.3, 133.2\*, 133.0, 132.8\*, 128.5, 128.4\*, 128.2, 128.0, 128.0\*, 127.9\*, 126.7, 126.6\*, 126.2, 126.1, 126.0\*,



126.0\*, 123.9\*, 123.8, 106.3 (d,  $J = 11.0$  Hz)\*, 104.9 (d,  $J = 12.1$  Hz), 47.9, 45.0 (d,  $J = 39$  Hz)\*, 43.6\*, 41.2 (d,  $J = 39$  Hz), 37.2 (d,  $J = 2.2$  Hz)\*, 37.1 (d,  $J = 2.6$  Hz), 34.6 (d,  $J = 6.2$  Hz), 33.8 (d,  $J = 5.9$  Hz)\*, 22.1\*, 21.6;  $^{19}\text{F}$  NMR (282 MHz,  $\text{CD}_2\text{Cl}_2$ ) (as a mixture of E/Z amide bond isomers, signals of minor isomer are indicated with an asterisk \*):  $\delta$ -113.47 (dd,  $J = 16.8, 5.0$  Hz), -115.23 (dd,  $J = 16.6, 5.2$  Hz); IR (Neat Film, NaCl) 2918, 2359, 2339, 1737, 1712, 1651, 1506, 1428, 1383, 1271, 1229, 1165, 967, 897, 860, 825, 748, 617  $\text{cm}^{-1}$ ; (MM:ESI $^+$ )  $m/z$  calc'd for  $\text{C}_{20}\text{H}_{21}\text{FNO}$   $[\text{M}+\text{H}]^+$ : 310.1602, found: 310.1289;  $[\alpha]_{\text{D}}^{25}$ : -47.73 (c 1.0,  $\text{CHCl}_3$ );

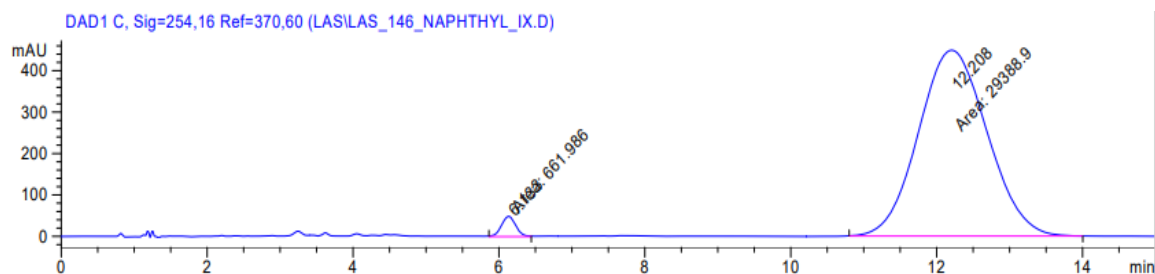
Chiral SFC Separation: 45% MeOH, 2.5 mL/min, AD-H column,  $\lambda = 254$  nm,  $t_{\text{R}}$  (min): minor = 6.13 (area: 2.20%), major = 12.21 (area: 97.80%), 95.6% enantiomeric excess.



Signal 2: DAD1 C, Sig=254,16 Ref=370,60

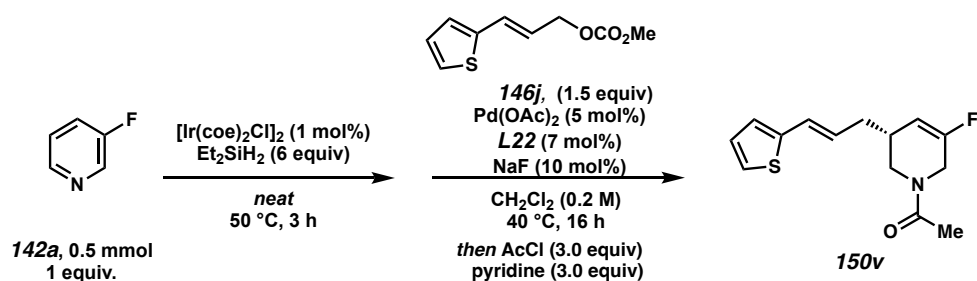
Peak #	RetTime [min]	Type	Width [min]	Area [mAU*s]	Height [mAU]	Area %
1	6.151	MM	0.2260	9741.30273	718.51941	49.0717
2	12.122	MM	1.0702	1.01099e4	157.44484	50.9283

Totals : 1.98512e4 875.96425



Signal 2: DAD1 C, Sig=254,16 Ref=370,60

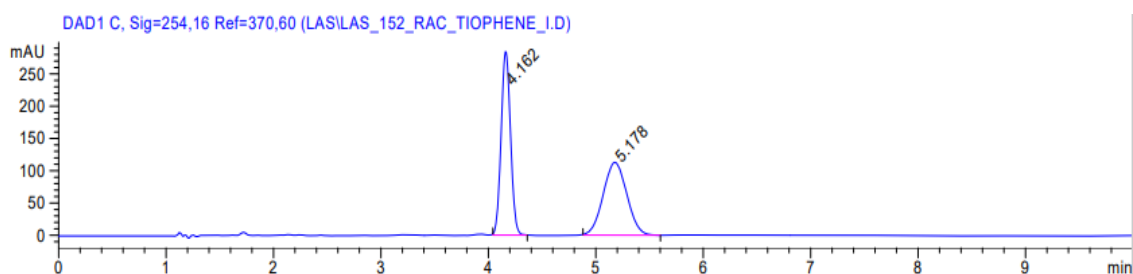
Peak #	RetTime [min]	Type	Width [min]	Area [mAU*s]	Height [mAU]	Area %
1	6.133	MM	0.2259	661.98602	48.84750	2.2029
2	12.208	MM	1.0918	2.93889e4	448.63095	97.7971
Totals :				3.00509e4	497.47845	



**(R,E)-1-(5-fluoro-3-(3-(thiophen-2-yl)allyl)-3,6-dihydropyridin-1(2H)-yl)ethan-1-one (150v)**: was synthesized following the general procedure 5 using 3-fluoropyridine **142a** (43  $\mu\text{L}$ , 0.5 mmol, 1.0 equiv) as substrate and (*E*)-methyl (3-(thiophen-2-yl)allyl) carbonate **146j** (149 mg, 0.75 mmol, 1.5 equiv). The desired compound **150v** was obtained as colorless oil (34 mg, 0.128 mmol, 26% yield over three steps);  $^1\text{H}$  NMR (400 MHz,  $\text{CDCl}_3$ ) (as a mixture of *E/Z* amide bond isomers):  $\delta$  7.12 (dd,  $J = 11.0, 5.1$  Hz, 1H), 6.98–6.92 (m, 1H), 6.92–6.88 (m, 1H), 6.61–6.52 (m, 1H), 6.04–5.92 (m, 1H), 5.47–5.30 (m, 1H), 4.18–3.92 (m, 2H), 3.84 (dd,  $J = 13.1, 4.6$  Hz, 0.4H), 3.53 (dd,  $J = 13.4, 4.5$  Hz, 0.6H), 3.33–3.22 (m, 1H), 2.55–2.40 (s, 1H), 2.30–2.14 (m, 2H), 2.12 (s, 3H);  $^{13}\text{C}$  NMR (101 MHz,  $\text{CDCl}_3$ ) (as a mixture of *E/Z* amide bond isomers, signals of minor isomer are indicated with an asterisk \*):  $\delta$  169.8, 169.7\*, 156.4 (d,  $J = 256$  Hz), 154.9 (d,  $J = 256$  Hz)\*, 142.5\*, 142.1, 127.5, 127.4\*, 126.5\*, 126.4, 126.2, 125.9\*, 125.3, 125.1\*, 124.0, 123.7\*, 106.0 (d,  $J = 11.0$  Hz)\*, 104.4 (d,  $J = 12.5$  Hz), 47.7, 44.9 (d,  $J = 39$  Hz)\*, 42.9\*, 41.2 (d,  $J = 40$

Hz), 36.7 (d,  $J = 2.2$  Hz)\*, 36.63 (d,  $J = 2.6$  Hz), 34.3 (d,  $J = 6.2$  Hz), 33.3 (d,  $J = 5.9$  Hz)\*, 22.0\*, 21.6;  $^{19}\text{F}$  NMR (282 MHz,  $\text{CDCl}_3$ ) (as a mixture of E/Z amide bond isomers, signals of minor isomer are indicated with an asterisk \*):  $\delta$  -112.35 (dd,  $J = 16.3, 5.0$  Hz), -114.23 (dd,  $J = 16.3, 5.0$  Hz)\*; IR (Neat Film, NaCl) 2921, 2358, 1732, 1651, 1427, 1378, 1236, 1159, 1039, 697  $\text{cm}^{-1}$ ; (MM:ESI $^+$ )  $m/z$  calc'd for  $\text{C}_{20}\text{H}_{21}\text{FNO}$   $[\text{M}+\text{H}]^+$ : 266.1009, found: 266.1006;  $[\alpha]_{\text{D}}^{25}$ : -35.56 (c 1.0,  $\text{CHCl}_3$ );

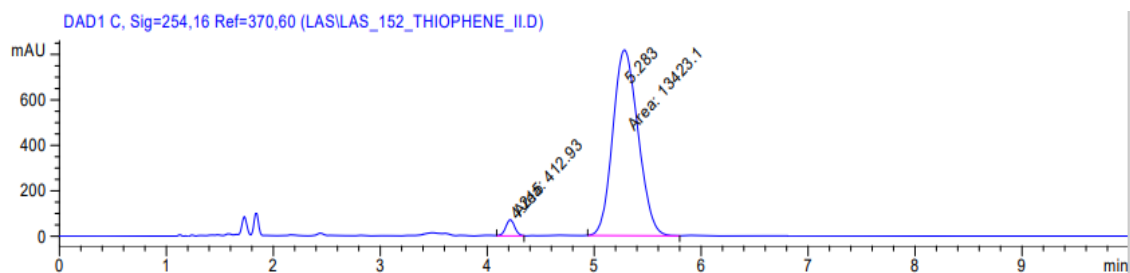
Chiral SFC Separation: 30% MeOH, 2.5 mL/min, AD-H column,  $\lambda = 254$  nm,  $t_{\text{R}}$  (min): minor = 4.22 (area: 2.98%), major = 5.28 (area: 97.02%), 94.0% enantiomeric excess.



Signal 2: DAD1 C, Sig=254,16 Ref=370,60

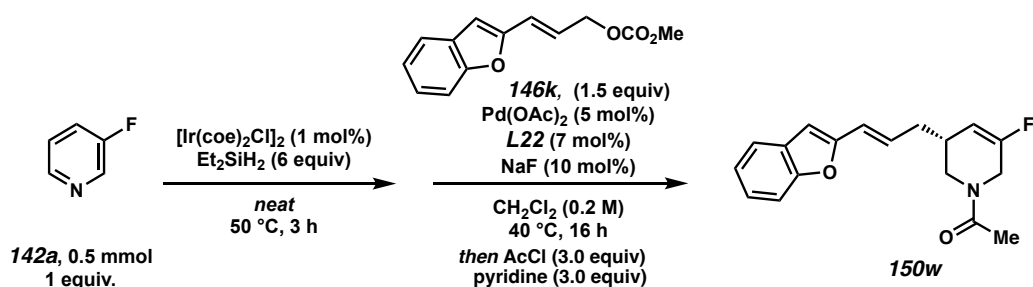
Peak #	RetTime [min]	Type	Width [min]	Area [mAU*s]	Height [mAU]	Area %
1	4.162	BB	0.0991	1731.62109	283.99393	50.0738
2	5.178	BB	0.2385	1726.51636	112.82227	49.9262

Totals : 3458.13745 396.81620



Signal 2: DAD1 C, Sig=254,16 Ref=370,60

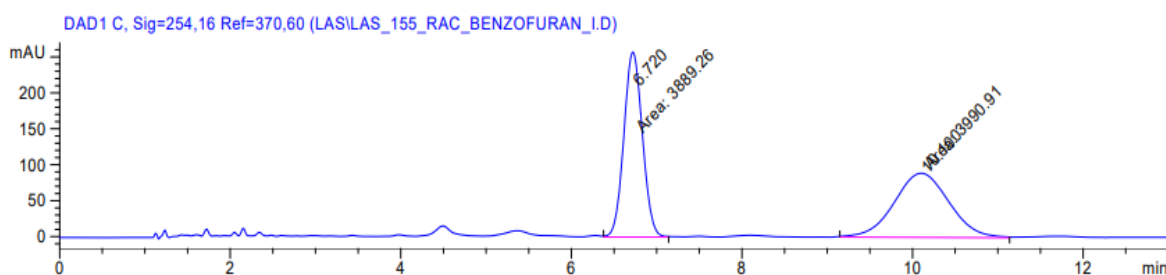
Peak #	RetTime [min]	Type	Width [min]	Area [mAU*s]	Height [mAU]	Area %
1	4.215	MM	0.0971	412.92996	70.84860	2.9845
2	5.283	MM	0.2736	1.34231e4	817.65662	97.0155
Totals :				1.38360e4	888.50522	



**(R,E)-1-(3-(3-(benzofuran-2-yl)allyl)-5-fluoro-3,6-dihydropyridin-1(2H)-yl)ethan-1-one (150w)**: was synthesized following the general procedure 5 using 3-fluoropyridine **142a** (43  $\mu\text{L}$ , 0.5 mmol, 1.0 equiv) as substrate and (*E*)-3-(benzofuran-2-yl)allyl methyl carbonate **146k** (174 mg, 0.75 mmol, 1.5 equiv). The desired compound **150w** was obtained as colorless oil (58 mg, 0.194 mmol, 39% yield over three steps);  $^1\text{H}$  NMR (400 MHz,  $\text{CDCl}_3$ ) (as a mixture of *E/Z* amide bond isomers):  $\delta$  7.47–7.38 (m, 1H), 7.38–7.32 (m, 1H), 7.22–7.06 (m, 2H), 6.46–6.40 (m, 1H), 6.35–6.27 (m, 2H), 5.42–5.24 (m, 1H), 4.12–3.84 (m, 2H), 3.75 (dd,  $J = 12.7, 4.6$  Hz, 0.4H), 3.47 (dd,  $J = 12.5, 4.5$  Hz, 0.6H), 3.28 (dd,  $J = 13.1, 6.5$  Hz, 0.4H), 3.19 (dd,  $J = 13.6, 6.1$  Hz, 0.6H), 2.52–2.37 (s, 1H), 2.30–2.11 (m, 2H), 2.07–2.00 (m, 3H);  $^{13}\text{C}$  NMR (101 MHz,  $\text{CDCl}_3$ ) (as a mixture of *E/Z* amide bond isomers, signals of minor isomer are indicated with an asterisk \*):  $\delta$  169.8, 169.7\*, 156.4 (d,  $J = 257$  Hz), 155.0 (d,  $J = 257$  Hz)\*, 154.8, 154.7\*, 154.5\*, 154.2, 129.2, 129.1\*, 129.0, 128.9\*, 124.6, 124.4\*, 123.0, 122.8\*, 121.5, 121.3\*, 121.0, 120.9\*, 110.9,

110.9\*, 105.9 (d,  $J = 11.0$  Hz)\*, 104.4 (d,  $J = 12.5$  Hz), 104.1, 103.8\*, 47.6, 44.8 (d,  $J = 39$  Hz)\*, 42.8\*, 41.1 (d,  $J = 40$  Hz), 36.8 (d,  $J = 2.6$  Hz)\*, 36.7 (d,  $J = 2.6$  Hz), 34.2 (d,  $J = 6.2$  Hz), 33.2 (d,  $J = 5.9$  Hz)\*, 22.0\*, 21.5;  $^{19}\text{F}$  NMR (282 MHz,  $\text{CDCl}_3$ ) (as a mixture of E/Z amide bond isomers, signals of minor isomer are indicated with an asterisk \*):  $\delta$ -112.16 (dd,  $J = 16.1, 4.7$  Hz), -114.03 (dd,  $J = 16.1, 5.2$  Hz)\*; IR (Neat Film, NaCl) 2917, 2357, 1711, 1650, 1452, 1380, 1254, 1230, 1163, 1105, 965, 882, 826, 751  $\text{cm}^{-1}$ ; (MM:ESI $^+$ )  $m/z$  calc'd for  $\text{C}_{18}\text{H}_{19}\text{FNO}_2$   $[\text{M}+\text{H}]^+$ : 300.1400, found: 300.1385;  $[\alpha]_{\text{D}}^{25}$ : -34.73 (c 1.0,  $\text{CHCl}_3$ );

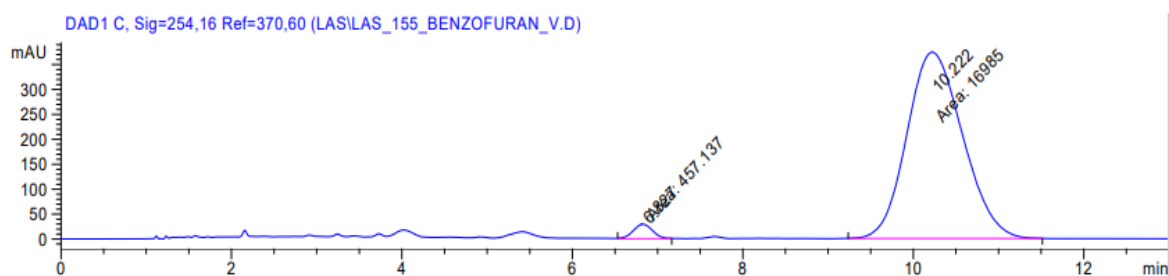
Chiral SFC Separation: 30% MeOH, 2.5 mL/min, AD-H column,  $\lambda = 254$  nm,  $t_{\text{R}}$  (min): minor = 6.83 (area: 2.62%), major = 10.22 (area: 97.38%), 94.8% enantiomeric excess.



Signal 2: DAD1 C, Sig=254,16 Ref=370,60

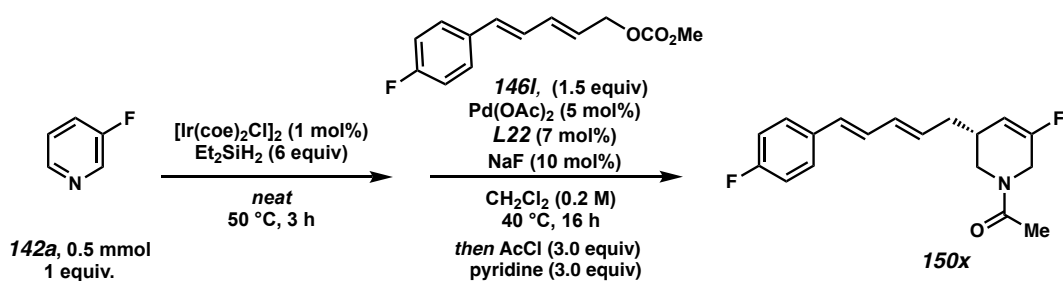
Peak #	RetTime [min]	Type	Width [min]	Area [mAU*s]	Height [mAU]	Area %
1	6.720	MM	0.2516	3889.25513	257.60300	49.3550
2	10.100	MM	0.7447	3990.90601	89.32148	50.6450

Totals : 7880.16113 346.92448



Signal 2: DAD1 C, Sig=254,16 Ref=370,60

Peak #	RetTime [min]	Type	Width [min]	Area [mAU*s]	Height [mAU]	Area %
1	6.827	MM	0.2607	457.13745	29.22491	2.6209
2	10.222	MM	0.7577	1.69850e4	373.63022	97.3791
Totals :				1.74421e4	402.85512	

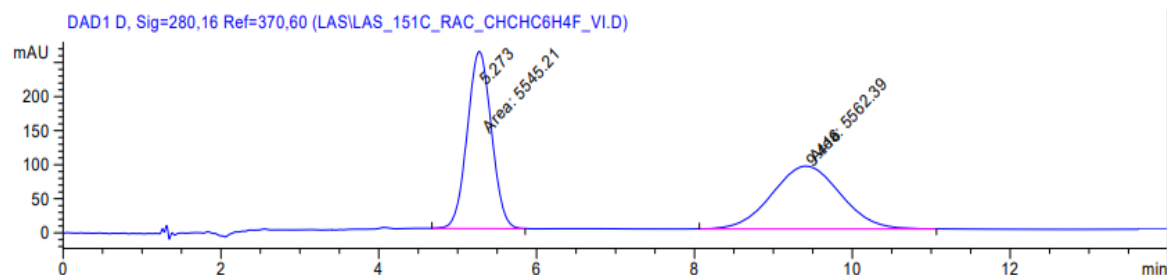


### 1-((*R*)-5-fluoro-3-((*2E,4E*)-5-(4-fluorophenyl)penta-2,4-dien-1-yl)-3,6-

**dihydropyridin-1(2H)-yl)ethan-1-one (150x):** was synthesized following the general procedure 5 using 3-fluoropyridine **142a** (43  $\mu\text{L}$ , 0.5 mmol, 1.0 equiv) as substrate and (*2E,4E*)-5-(4-fluorophenyl)penta-2,4-dien-1-yl methyl carbonate **146I** (236 mg, 0.75 mmol, 1.5 equiv). The desired compound **150x** was obtained as colorless oil (31 mg, 0.102 mmol, 20% yield over three steps);  $^1\text{H}$  NMR (400 MHz,  $\text{CD}_2\text{Cl}_2$ ) (as a mixture of *E/Z* amide bond isomers):  $\delta$  7.34–7.21 (m, 2H), 6.99–6.85 (m, 2H), 6.69–6.56 (m, 1H), 6.44–6.30 (m, 1H), 6.24–6.09 (m, 1H), 5.71 (ddd,  $J = 14.9, 7.5, 7.5$  Hz, 1H), 5.37–5.24 (m, 1H), 4.08–3.83 (m, 2H), 3.72 (dd,  $J = 13.1, 4.7$  Hz, 0.4H), 3.44 (dd,  $J = 13.5, 4.6$  Hz, 0.6H), 3.20–3.07 (m, 1H), 2.47–2.29 (m, 1H), 2.19–2.05 (m, 2H), 2.04–1.96 (s, 3H);  $^{13}\text{C}$  NMR (101 MHz,  $\text{CD}_2\text{Cl}_2$ ) (as a mixture of *E/Z* amide bond isomers, signals of minor isomer are indicated with an asterisk \*):  $\delta$  169.8, 169.7\*, 162.6 (d,  $J = 247$  Hz), 162.5 (d,  $J = 246$  Hz)\*, 156.8 (d,  $J = 255$  Hz), 155 (d,  $J = 256$  Hz)\*, 134.2 (d,  $J = 2.9$  Hz)\*, 134.0 (d,  $J = 3.3$

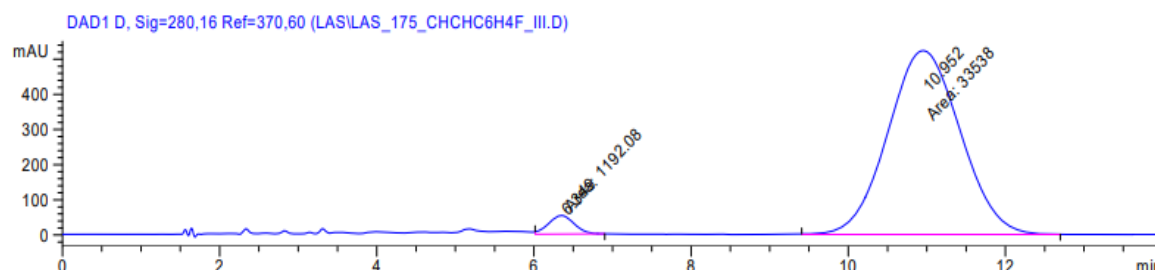
Hz), 133.4, 133.2\*, 132.1\*, 131.8, 130.3, 130.0\*, 129.1 (d,  $J = 2.6$  Hz)\*, 128.9 (d,  $J = 2.2$  Hz), 128.1 (d,  $J = 7.7$  Hz), 128.1 (d,  $J = 8.1$  Hz)\*, 115.9 (d,  $J = 21.6$  Hz), 115.8 (d,  $J = 22.0$  Hz)\*, 106.3 (d,  $J = 11$  Hz)\*, 104.9 (d,  $J = 12.1$  Hz), 47.9, 45.0 (d,  $J = 39$  Hz)\*, 42.9\*, 41.2 (d,  $J = 40$  Hz), 36.9 (d,  $J = 2.2$  Hz)\*, 36.8 (d,  $J = 2.2$  Hz), 34.6 (d,  $J = 6.2$  Hz), 33.7 (d,  $J = 5.9$  Hz)\*, 22.1\*, 21.7;  $^{19}\text{F}$  NMR (282 MHz,  $\text{CD}_2\text{Cl}_2$ ) (as a mixture of E/Z amide bond isomers, signals of minor isomer are indicated with an asterisk \*):  $\delta$  -113.6 (dd,  $J = 16.1$ , 4.7 Hz,  $\text{C}_{\text{AlkylF}}$ ), -115.24 – (-115.43 (m,  $\text{C}_{\text{AlkylF}}$ \*,  $\text{C}_{\text{ArylF}}$ ), -115.48 – (-115.60 (m,  $\text{C}_{\text{ArylF}}$ \*)); IR (Neat Film, NaCl) 2916, 1707, 1650, 1599, 1507, 1428, 1379, 1275, 1228, 1159, 1095, 1060, 1034, 989, 833  $\text{cm}^{-1}$ ; (MM:ESI $^+$ )  $m/z$  calc'd for  $\text{C}_{18}\text{H}_{20}\text{F}_2\text{NO}$  [M+H] $^+$ : 304.1513, found: 304.1500;  $[\alpha]_{\text{D}}^{25}$ : -33.48 (c 1.0,  $\text{CHCl}_3$ );

Chiral SFC Separation: 40% MeOH, 2.5 mL/min, AD-H column,  $\lambda = 280$  nm,  $t_{\text{R}}$  (min): minor = 6.35 (area: 3.43%), major = 10.95 (area: 96.57%), 93.1% enantiomeric excess.

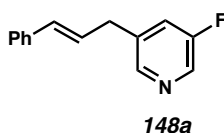


Signal 3: DAD1 D, Sig=280,16 Ref=370,60

Peak #	RetTime [min]	Type	Width [min]	Area [mAU*s]	Height [mAU]	Area %
1	5.273	MM	0.3555	5545.20654	259.98407	49.9226
2	9.416	MM	1.0051	5562.39063	92.23834	50.0774
Totals :				1.11076e4	352.22241	



### Product Characterization: Rearomatized alkylation product **148a**

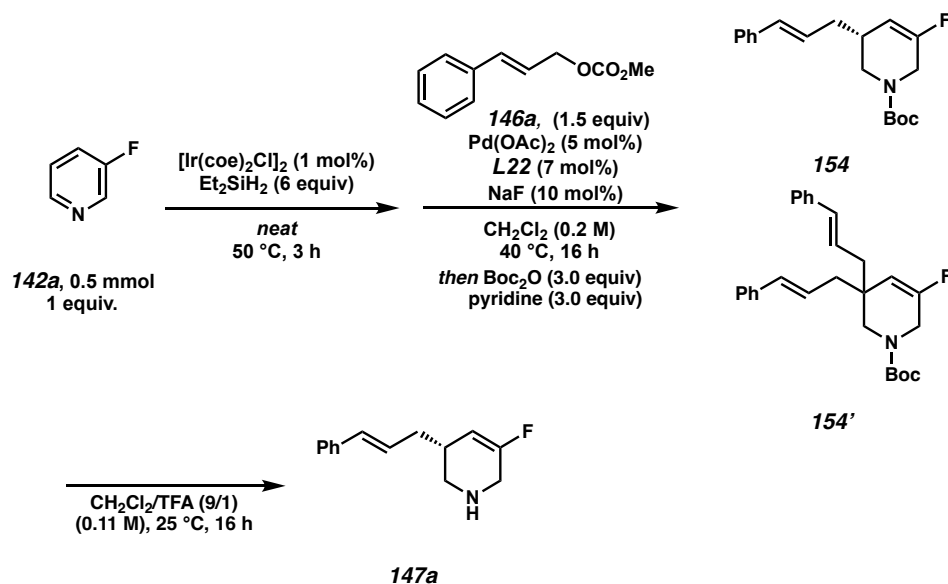


**3-cinnamyl-5-fluoropyridine (148a)**: was synthesized as followed. In a 2 mL screw vial equipped with a magnetic stir bar was then transferred to an argon filled glovebox. Chlor-bis-(cycloocten)-iridium(I) dimer ( $[\text{Ir}(\text{coe})_2\text{Cl}]_2$ , 2.3 mg, 0.0025 mmol, 0.5 mol%) was added to the vial, closed with a septum screw cap and transferred out of the glovebox. Diethyl silane ( $\text{Et}_2\text{SiH}_2$ , 97  $\mu\text{L}$ , 0.75 mmol, 1.5 equiv) was added and the resulting mixture was stirred at room temperature for 4 minutes. 3-fluoropyridine **142a** (43  $\mu\text{L}$ , 0.5 mmol, 1.0 equiv) was added and the resulting reaction mixture was stirred at 50 °C for 5 h. A separate 10 mL screw vial equipped with a magnetic stir bar was transferred to the glovebox. Ligand **L22** (24.2 mg, 0.035 mmol, 7 mol%) and palladium(II) acetate ( $\text{Pd}(\text{OAc})_2$ , 5.6 mg, 0.025 mmol, 5 mol%) were added. The vial was closed with a septum screw cap and transferred out of the glovebox. Dichloromethane ( $\text{CH}_2\text{Cl}_2$ , 2.5 mL) was added at room temperature under nitrogen. The mixture was stirred for 5 minutes Cinnamyl methyl carbonate **146a** (192.2 mg, 1.0 mmol, 2.0 equiv) was added, followed by the reaction mixture from the 2 mL vial. The resulting mixture was then stirred at 40 °C for 16 h. Afterwards, the reaction mixture was cooled to room temperature and the solvent was



evaporated. The residue was submitted to flash column chromatography over silica gel using a solvent mixture of hexane/ethyl acetate = 8/2 as the eluent. The desired product **148a** was obtained as colorless oil (30.1 mg, 0.14 mmol, 28% yield);  $^1\text{H}$  NMR (400 MHz,  $\text{CDCl}_3$ ):  $\delta$  8.36 – 8.33 (m, 2H), 7.38 – 7.34 (m, 2H), 7.34 – 7.27 (m, 3H), 7.26 – 7.21 (m, 1H), 6.49 (d,  $J = 15.8$  Hz, 1H), 6.29 (dt,  $J = 15.8, 6.9$  Hz, 1H), 3.58 (d, 6.7 Hz, 2H);  $^{13}\text{C}$  NMR (101 MHz,  $\text{CDCl}_3$ ):  $\delta$  159.72 (d,  $J = 256.8$  Hz), 146.00 (d,  $J = 3.7$  Hz), 137.54 (d,  $J = 3.2$  Hz), 136.91, 136.22 (d,  $J = 23.1$  Hz), 132.78, 128.76, 127.74, 126.86, 126.34, 123.01 (d,  $J = 17.8$  Hz), 36.00 (d,  $J = 1.4$  Hz);  $^{19}\text{F}$  NMR (282 MHz,  $\text{CDCl}_3$ ):  $\delta$  -127.24 (dd,  $J = 9.3, 1.7$  Hz); IR (Neat Film, NaCl) 3734, 3029, 2922, 2358, 1599, 1576, 1496, 1448, 1431, 1259, 1144, 1026, 965, 879, 808, 780, 754, 697, 676  $\text{cm}^{-1}$ ; (MM:ESI $^+$ )  $m/z$  calc'd for  $\text{C}_{14}\text{H}_{13}\text{FN}$   $[\text{M}+\text{H}]^+$ : 214.1032, found: 214.1005;

### General Procedure 8: Isolation of Free NH Amine Product 147

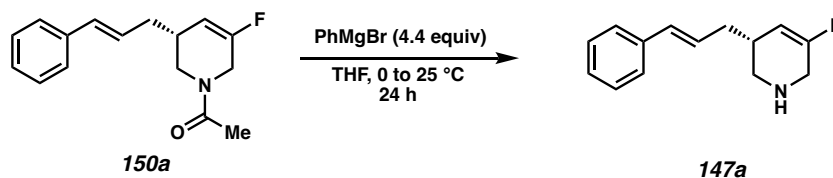


**(R)-3-cinnamyl-5-fluoro-1,2,3,6-tetrahydropyridine (147a)**: was synthesized in a following the synthetic sequence described as general procedure 8. A 10 mL screw vial

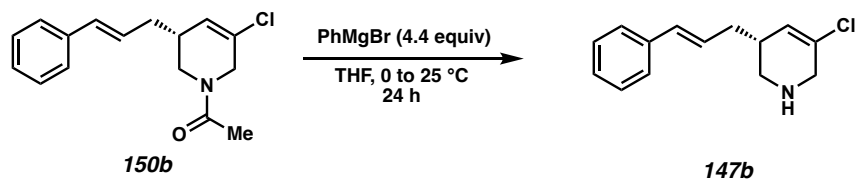
was transferred to an argon filled glovebox. Chlor-bis-(cycloocten)-iridium(I) dimer ( $[\text{Ir}(\text{coe})_2\text{Cl}]_2$ , 22.4 mg, 0.025 mmol, 1 mol%) was added to the vial. The vial was closed with a septum screw cap. The vial was transferred out of the glovebox. Diethyl silane ( $\text{Et}_2\text{SiH}_2$ , 1.94 mL, 15.0 mmol, 6.0 equiv) was added and the resulting mixture was stirred at room temperature for 4 minutes. 3-fluoropyridine **142a** (215  $\mu\text{L}$ , 2.5 mmol, 1.0 equiv) was added and the resulting reaction mixture was stirred at 50 °C for 3 hours. A separate 25 mL screw vial equipped with a magnetic stir bar was transferred to the glovebox. Ligand **L22** (120.8 mg, 0.175 mmol, 7 mol%), NaF (10.5 mg, 0.25 mmol, 10 mol%) and palladium(II) acetate ( $\text{Pd}(\text{OAc})_2$ , 28.1 mg, 0.125 mmol, 5 mol%) were added. The vial was closed with a septum screw cap and transferred out of the glovebox. Dichloromethane ( $\text{CH}_2\text{Cl}_2$ , 12.5 mL) was added at room temperature under nitrogen. The mixture was stirred for 5 minutes. Cinnamyl methyl carbonate **146a** (720.8 mg, 3.75 mmol, 1.5 equiv) was added, followed by the reaction mixture from the 10 mL vial. The resulting mixture was then stirred at 40 °C for 24 h. The mixture was then cooled to room temperature and diluted with additional dichloromethane (10 mL). Pyridine (604  $\mu\text{L}$ , 7.5 mmol, 3.0 equiv) was added as a base, followed by di-tert-butyl dicarbonate ( $\text{Boc}_2\text{O}$ , 1.72 mL, 7.5 mmol, 3.0 equiv). The mixture was stirred at room temperature for 16 h and then transferred to a 50 mL flask and diluted with MeOH (20 mL). Imidazole (510 mg, 7.5 mmol, 3.0 equiv) were added and the mixture was stirred for 2 hours to decompose residual  $\text{Boc}_2\text{O}$ . The solvent was evaporated and the crude subjected to flash column chromatography over silica gel using a solvent mixture of hexane/ethyl acetate (20/1) as the eluent. An inseparable mixture of the mono-alkylated **154** and bisalkylated **154'** N-Boc compounds were isolated as colorless oil and directly used for the deprotection step. The mixture was redissolved in

CH<sub>2</sub>Cl<sub>2</sub> (20 mL) at room temperature. TFA (2mL) was added dropwise and the resulting solution was stirred at room temperature for 16 hours. An aqueous workup with 4M NaOH was performed to neutralize the TFA. The aqueous phase was extracted with EtOAc three times and the combined organic phases were dried over magnesium sulfate and filtered. The mono-alkylated NH tetrahydropyridine **147a** was purified by flash column chromatography over silica gel using a solvent mixture of hexane/acetone (7/3 to 1/1) as the eluent. The desired compound was isolated as colorless oil (122 mg, 0.56 mmol, 22% yield over 4 steps). The absolute configuration was adopted from product **150a**. The enantioselectivity was not again measured for the free N-H product **147a**; <sup>1</sup>H NMR (400 MHz, CDCl<sub>3</sub>): δ 7.37 – 7.28 (m, 4H), 7.24 – 7.19 (m, 1H), 6.46 – 6.40 (m, 1H), 6.17 (dt, *J* = 15.8, 7.3 Hz, 1H), 5.29 (ddt, *J* = 17.7, 3.1, 1.5 Hz, 1H), 3.42 – 3.30 (m, 2H), 3.03 (ddd, *J* = 12.9, 4.9, 2.1 Hz, 1H), 2.56 (ddd, *J* = 12.9, 7.1, 1.0 Hz, 1H), 2.43 (tqt, *J* = 7.4, 5.1, 2.5 Hz, 1H), 2.32 – 2.19 (m, 2H), 2.11 (bs, 1H); <sup>13</sup>C NMR (101 MHz, CDCl<sub>3</sub>): δ 159.12 (d, *J* = 261.9 Hz), 137.45, 132.20, 128.67, 127.63, 127.30, 126.16, 104.91 (d, *J* = 11.0 Hz), 48.13 (d, *J* = 1.7 Hz), 44.20 (d, *J* = 30.1 Hz), 37.54 (d, *J* = 2.2 Hz), 35.10 (d, *J* = 4.8 Hz); <sup>19</sup>F NMR (282 MHz, CDCl<sub>3</sub>): δ -110.91 (dd, *J* = 17.5, 5.3 Hz); IR (Neat Film, NaCl) 3280, 3056, 3025, 2914, 2844, 1700, 1598, 1494, 1448, 1367, 1279, 1156, 1108, 1070, 1047, 1029, 966, 910, 841, 744, 694 cm<sup>-1</sup>; (MM:ESI<sup>+</sup>) *m/z* calc'd for C<sub>14</sub>H<sub>17</sub>FN [M+H]<sup>+</sup>: 218.1345, found: 218.1343; [α]<sub>D</sub><sup>25</sup>: - 8.24 (c 0.9, CHCl<sub>3</sub>).

**General Procedure 9: Alternative route to free NH product 147**



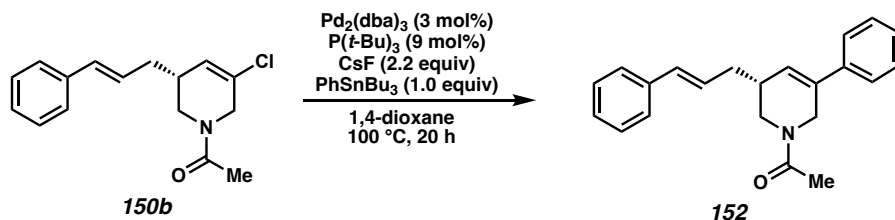
**(R)-3-cinnamyl-5-fluoro-1,2,3,6-tetrahydropyridine (147a)**: was synthesized following the synthetic sequence described as general procedure 9. (*R*)-1-(3-cinnamyl-5-fluoro-3,6-dihydropyridin-1(2H)-yl)ethan-1-one **150a** (26 mg, 0.1 mmol, 1.0 equiv) was dissolved in tetrahydrofuran (THF, 180  $\mu$ L) in a 4 mL screw cap vial equipped with a septum screw cap. The reaction mixture was cooled to 0 °C and a solution of phenyl magnesium bromide (PhMgBr 1 M in THF, 440  $\mu$ L, 0.44 mmol, 4.4 equiv) was added slowly at 0 °C. The reaction was allowed to warm to ambient temperature and stirred for 24 hours. The reaction mixture was then cooled to 0 °C and an aqueous workup with 2 M HCl (2.0 mL) was added dropwise. The acidic aqueous layer was extracted with EtOAc (3 x 5 mL) to remove any organic impurities. The acidic aqueous phase was then basified with NaHCO<sub>3</sub> and the resulting aqueous phase was then extracted with EtOAc (3 x 5 mL). The resulting organic layer was dried with Na<sub>2</sub>SO<sub>4</sub> and filtered and the solvent was evaporated and the mono-alkylated N–H tetrahydropyridine **147a** was purified by flash column chromatography over silica gel using a solvent mixture of hexane/acetone (7/3 to 1/1) as the eluent. The desired compound was isolated as colorless oil (17.4 mg, 0.08 mmol, 80% yield). The enantioselectivity was not again measured for the free N-H product **147a**. The spectra match the spectra of free amine **147a** using the method described in General procedure 8. Note: some product was observed in the organic layer prior to basification, product can be obtained by flash column chromatography over silica gel using a solvent mixture of hexane/acetone (7/3 to 1/1) as the eluent.\*



**(R)-5-chloro-3-cinnamyl-1,2,3,6-tetrahydropyridine (147b):** was synthesized following the general procedure 9. (R)-1-(3-cinnamyl-5-chloro-3,6-dihydro-2H-pyridin-1-yl)ethan-1-one **150b** (27.5 mg, 0.1 mmol, 1.0 equiv). The desired compound **147b** was obtained as colourless oil (20.5 mg, 0.088 mmol, 88% yield). The absolute configuration was adopted from product **150b**. The enantioselectivity was not again measured for the free N-H product **147b**;  $^1\text{H NMR}$  (400 MHz,  $\text{CDCl}_3$ ):  $\delta$  7.38 – 7.28 (m, 4H), 7.25 – 7.20 (m, 1H), 6.44 (d,  $J = 16.0$  Hz, 1H), 6.22 – 6.10 (m, 1H), 5.90 (dt,  $J = 3.5, 1.7$  Hz, 1H), 3.50 – 3.34 (m, 2H), 3.09 (dd,  $J = 13.1, 5.1$  Hz, 1H), 2.61 (dd,  $J = 13.1, 7.4$  Hz, 1H), 2.43 (ddq,  $J = 10.1, 5.0, 2.7$  Hz, 1H), 2.26 (tdd,  $J = 7.4, 4.0, 1.3$  Hz, 1H);  $^{13}\text{C NMR}$  (101 MHz,  $\text{CDCl}_3$ ) 137.36, 132.48, 131.88, 128.71, 127.41, 127.22, 127.05, 126.21, 50.14, 47.43, 37.54, 37.08; IR (Neat Film, NaCl) 3332, 3026, 2919, 2851, 1654, 1449, 969, 749, 697  $\text{cm}^{-1}$ ; (MM:ESI $^+$ )  $m/z$  calc'd for  $\text{C}_{14}\text{H}_{17}\text{ClN}$   $[\text{M}+\text{H}]^+$ : 234.1044, found 234.1048;  $[\alpha]_{\text{D}}^{25}$ :  $-13.39$  (c 0.93,  $\text{CHCl}_3$ );

### Product Derivatizations

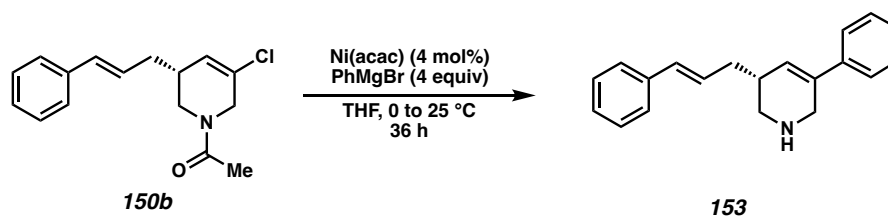
#### General Procedure 10: Stille Cross Coupling of vinyl chloride 150b



**(R)-1-(3-cinnamyl-5-phenyl-3,6-dihydropyridin-1(2H)-yl)ethan-1-one (152):** was synthesized following the synthetic sequence described as general procedure 10. A 4 mL screw cap vial was transferred to an argon filled glovebox. Bis(dibenzylideneacetone)palladium(0) (Pd<sub>2</sub>dba<sub>3</sub>, 3 mg, 0.003 mmol, 3 mol%) was added to a vial with tri-*tert*-butylphosphine (P(*t*-Bu)<sub>3</sub>, 2 mg, 0.009 mmol, 9 mol%) and cesium fluoride (CsF, 33 mg, 0.22 mmol, 2.2 equiv). Dioxane (200 μL) was added to mixture and stirred at ambient temperature for 5 minutes. (*R*)-1-(3-cinnamyl-5-chloro-3,6-dihydropyridin-1(2H)-yl)ethan-1-one **150b** (27.5 mg, 0.1 mmol, 1.0 equiv) was dissolved in dioxane (200 μL) and added to the reaction mixture followed by tributylphenylstannane (PhSnBu<sub>3</sub>, 34 μL, 0.1 mmol, 1.0 equiv). The reaction mixture was sealed with a septum screw cap and heated to 100 °C for 20 hours. The reaction mixture was cooled to room temperature, filtered through a plug of silica and washed with copious amounts of ethyl acetate. The solvent was evaporated and the crude reaction mixture was purified by flash chromatography over silica gel using a solvent mixture of hexane/EtOAc (7/3 to 2/8) as the eluent. The desired compound was isolated as a pale-yellow oil **152** (26.1 mg, 0.082 mmol, 82% yield). The absolute configuration was adopted from product **150b**. The enantioselectivity was not again measured for the cross-coupled product **152**; <sup>1</sup>H NMR (400 MHz, CDCl<sub>3</sub>) (as a mixture of E/Z amide bond isomers): δ 7.48 – 7.28 (m, 9H), 7.26 – 7.19 (m, 1H), 6.55 – 6.44 (m, 1H), 6.32 – 6.23 (m, 1H), 6.23 – 6.14 (m, 1H), 4.54 (dt, *J* = 18.0, 2.2 Hz, 0.65H), 4.39 (dt, *J* = 18.1, 2.3 Hz, 0.65H), 4.30 (dt, *J* = 4.8, 2.4 Hz, 0.7H), 4.14 (dd, *J* = 12.8, 5.0 Hz, 0.35H), 3.67 (dd, *J* = 13.2, 4.7 Hz, 0.65H), 3.40 – 3.30 (m, 0.65H), 3.22 (dd, *J* = 12.8, 7.5 Hz, 0.35H), 2.68 – 2.55 (m, 1H), 2.46 – 2.29 (m, 2H), 2.18 (s, 1H), 2.18 (s, 1.1H), 2.17 (s, 1.9H); <sup>13</sup>C NMR (101 MHz, CDCl<sub>3</sub>) (as a mixture of E/Z

amide bond isomers, signals of minor isomer are indicated with an asterisk \*):  $\delta$  169.9, 169.7\*, 138.82\*, 138.7, 137.5, 137.2\*, 135.2, 133.8\*, 132.8, 132.5\*, 128.8\*, 128.8, 128.7 (overlap)\*, 128.1\*, 128.0\*, 127.9, 127.6, 127.3\*, 127.3 (overlap)\*, 127.3, 126.3\*, 126.2, 125.8\*, 125.5 (overlap)\*, 125.2, 47.6, 47.6\*, 43.5, 43.0\*, 37.0\*, 36.8, 36.4\*, 35.5, **29.8**, 22.2\*, 21.8; IR (Neat Film, NaCl) 3236, 3027, 2924, 2853, 1625, 1447, 1317, 1269, 1033, 970, 751, 696, 689, 665  $\text{cm}^{-1}$ ; (MM:ESI<sup>+</sup>)  $m/z$  calc'd for  $\text{C}_{22}\text{H}_{24}\text{N}[\text{M}+\text{H}]^+$ : 318.1852, found 318.1867;  $[\alpha]_{\text{D}}^{25}$ :  $-5.14$  (c 1.0,  $\text{CHCl}_3$ ).

### General Procedure 11: Kumada Cross Coupling of vinyl chloride **150b**



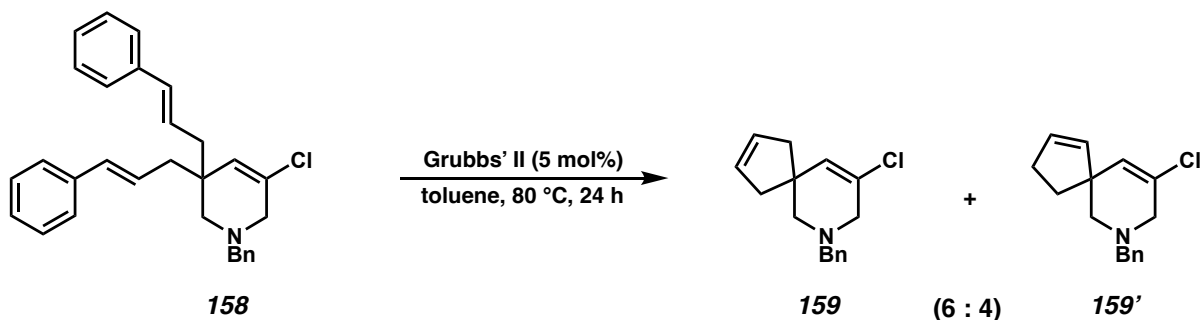
**(R)-3-cinnamyl-5-phenyl-1,2,3,6-tetrahydropyridine (153)**: was synthesized following the synthetic sequence described as general procedure 11. A 4 mL screw cap vial was charged with nickel(II) acetylacetonate ( $\text{Ni}(\text{acac})_2$ , 1.0 mg, 0.004 mmol, 4 mol%) and dissolved in tetrahydrofuran (THF, 100  $\mu\text{L}$ ). The reaction mixture was cooled to 0 °C, and phenyl magnesium bromide (PhMgBr 1 M in THF, 400  $\mu\text{L}$ , 0.4 mmol, 4.0 equiv) was added to the reaction mixture dropwise. (R)-1-(3-cinnamyl-5-chloro-3,6-dihydropyridin-1(2H)-yl)ethan-1-one **150b** (27.5 mg, 0.1 mmol, 1.0 equiv) was dissolved in tetrahydrofuran (THF, 200  $\mu\text{L}$ ) and added to the reaction mixture at 0 °C and allowed to warm to ambient temperature overnight. After 36 hours, the reaction was cooled to 0 °C and an aqueous workup was performed with saturated  $\text{NH}_4\text{Cl}$  (1 mL). The aqueous phase

was extracted with EtOAc (3 x 10 mL) and the organic layer was dried over Na<sub>2</sub>SO<sub>4</sub> and filtered. The solvent was evaporated and the crude reaction mixture was purified by flash chromatography over silica gel using a solvent mixture of methanol/ethyl acetate (1/9) with 1% triethyl amine as the eluent. The desired compound was isolated as a pale-yellow amorphous solid **153** (22.8 mg, 0.083 mmol, 83% yield). The absolute configuration was adopted from product **150b**. The enantioselectivity was not again measured for the cross-coupled product **153**; <sup>1</sup>H NMR (400 MHz, CDCl<sub>3</sub>) δ 7.39 – 7.27 (m, 8H), 7.22 (d, *J* = 7.0 Hz, 2H), 6.51 (d, *J* = 15.7 Hz, 1H), 6.21 (s, 1H), 6.15 (dd, *J* = 15.5, 7.5 Hz, 1H), 4.07 (d, *J* = 16.4 Hz, 1H), 3.98 (d, *J* = 16.5 Hz, 1H), 3.56 (dd, *J* = 12.3, 5.4 Hz, 1H), 3.06 (s, 1H), 2.88 (t, *J* = 10.9 Hz, 1H), 2.44 (t, *J* = 6.9 Hz, 2H). Et<sub>3</sub>N•HCl present <sup>1</sup>H NMR (400 MHz, CDCl<sub>3</sub>) δ 3.13 (q, *J* = 7.3 Hz, 2H) 1.44 – 1.34 (m, 3H). \*Note: Titration of amine **153** with Et<sub>3</sub>N resulted in better resolution in peaks due to solubility issues of **153** in CDCl<sub>3</sub>\* <sup>1</sup>H NMR (400 MHz, CDCl<sub>3</sub>) δ 7.39 – 7.28 (m, 8H), 7.25 – 7.19 (m, 2H), 6.48 (d, *J* = 15.8 Hz, 1H), 6.22 (dt, *J* = 15.8, 7.2 Hz, 1H), 6.16 (s, 1H), 3.92 – 3.75 (m, 2H), 3.36 – 3.26 (m, 1H), 2.79 – 2.63 (m, 2H), 2.41 – 2.31 (m, 2H) (without Et<sub>3</sub>N titration); <sup>13</sup>C NMR (101 MHz, CDCl<sub>3</sub>) δ 137.11, 136.92, 133.75, 130.70, 128.93, 128.75, 128.60, 127.69, 126.48, 126.36, 125.44, 125.30, 44.90, 43.25, 36.66, 32.63, Et<sub>3</sub>N•HCl present <sup>13</sup>C NMR (101 MHz, CDCl<sub>3</sub>) δ 46.07, 8.78 \*Note: Titration of amine **9** with Et<sub>3</sub>N resulted in better resolution in peaks due to solubility issues of **9** in CDCl<sub>3</sub>\* <sup>13</sup>C NMR (101 MHz, CDCl<sub>3</sub>) δ 138.93, 137.36, 134.68, 132.64, 128.70, 128.69, 127.83, 127.41, 127.16, 126.84, 126.25, 125.17, 46.98, 45.58, 37.32, 34.65; (without Et<sub>3</sub>N titration); IR (Neat Film, NaCl) 3335, 2924, 1634, 1447, 969, 738, 751, 694 cm<sup>-1</sup>; (MM:ESI<sup>+</sup>) *m/z* calc'd for C<sub>20</sub>H<sub>22</sub>N [M+H]<sup>+</sup>: 276.1747, found 276.1755; [α]<sub>D</sub><sup>25</sup>: – 6.80 (c 0.833, CHCl<sub>3</sub>);



**General Procedure 12: N-Bn formation of bisalkylated NH product**

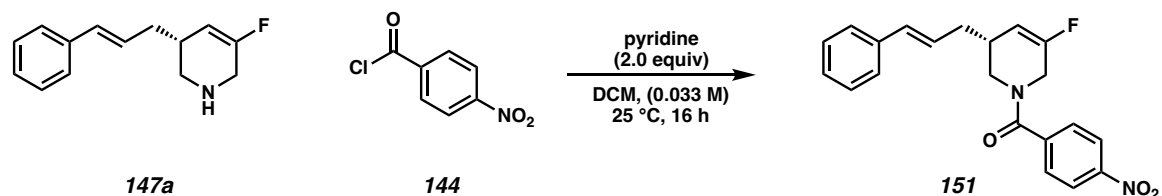
**1-Benzyl-5-chloro-3,3-dicinnamyl-1,2,3,6-tetrahydropyridine (158):** Benzyl bromide (247  $\mu$ L, 2.07 mmol, 3.0 equiv) and triethyl amine (96  $\mu$ L, 0.69 mmol, 1.0 equiv) were added to 5-chloro-3,3-bis((*E*)-3-(phenyl)allyl)-1,2,3,6-tetrahydropyridine **149b** (242 mg, 0.69 mmol, 1.0 equiv) in dichloromethane (4 mL). The resulting reaction mixture was stirred at room temperature for 19 h. The reaction was quenched with a saturated aqueous ammonium chloride solution (2 mL). The phases were separated and the aqueous phase was extracted with dichloromethane (3 x 2 mL). The combined organic phases were washed with brine (1 x 2 mL), dried over sodium sulphate, and concentrated under reduced pressure. Purification of the residue by flash chromatography on silica gel using *n*-hexane/ethyl acetate gave the title compound **158** (260 mg, 0.59 mmol, 86%) as colorless oil; <sup>1</sup>H NMR (400 MHz, CDCl<sub>3</sub>):  $\delta$  7.38–7.27 (m, 13H), 7.25–7.19 (m, 2H), 6.36 (d, *J* = 15.8 Hz, 2H), 6.13 (dt, *J* = 15.4, 7.4 Hz, 2H), 5.79 (s, 1H), 3.57 (s, 2H), 3.10 (s, 2H), 2.43–2.25 (m, 6H); <sup>13</sup>C NMR (101 MHz, CDCl<sub>3</sub>) (*one carbon signal is overlapping*):  $\delta$  138.3, 137.6, 133.2, 130.2, 129.2, 129.1, 128.6, 128.5, 127.4, 127.3, 126.2, 126.0, 62.6, 58.8, 58.0, 42.8, 41.2; IR (Neat Film, NaCl) 3028, 2922, 2853, 2358, 1681, 1495, 1452, 1265, 1073, 1028, 970, 826, 738, 699, 676 cm<sup>-1</sup>; (MM:ESI<sup>+</sup>) *m/z* calc'd for C<sub>30</sub>H<sub>31</sub>ClN [M+H]<sup>+</sup>: 440.2145, found: 440.2150;

**General Procedure 13: Ring Closing metathesis of bisalkylated products**

**1-Benzyl-5-chloro-3,3-dicinnamyl-1,2,3,6-tetrahydropyridine (159):** A solution of 1-benzyl-5-chloro-3,3-dicinnamyl-1,2,3,6-tetrahydropyridine **158** (50 mg, 0.11 mmol, 1.0 equiv) in toluene (1 mL) was added to a 10-mL screw vial charged with dichloro[1,3-bis(2,4,6-trimethylphenyl)-2-imidazolinydene](benzylidene)-(tricyclohexylphosphine)ruthenium(II) (Grubbs' II, 4.8 mg, 5.7  $\mu$ mol, 5 mol%) under a nitrogen atmosphere. The resulting mixture was stirred at 80°C for 24 hours. The reaction mixture was cooled to room temperature and filtered through a small plug silica gel. The volatiles were removed under reduced pressure. Purification of the residue by flash chromatography on silica gel using *n*-hexane/ethyl acetate (100:0 to 20:1) gave the title compound **159** in mixture with the isomer **159'** (21 mg, 0.081 mmol, 73%, ratio 6:4 for **159:159'**) as colorless oil;  $^1\text{H}$  NMR (400 MHz,  $\text{CDCl}_3$ ):  $\delta$  7.31 (dd,  $J = 13.6, 6.6$  Hz, 4H), 7.27 – 7.21 (m, 1H), 5.81 (s, 0.4H), 5.74 (d,  $J = 5.9$  Hz, 0.4H), 5.65 (s, 0.4H), 5.59 – 5.54 (m, 1.2H), 5.31 – 5.30 (m, 1H), 3.57 (s, 2H), 3.04 (s, 2H), 2.34 (d,  $J = 45.6$  Hz, 5H), 1.85 – 1.68 (m, 1H);  $^{13}\text{C}$  NMR (101 MHz,  $\text{CDCl}_3$ ):  $\delta$  138.7, 136.5, 132.6, 131.8, 130.6, 129.3, 129.2, 128.6, 128.1, 128.0, 127.5, 127.5, 62.3, 62.2, 61.3, 59.4, 58.2, 57.9, 53.1, 45.9, 45.0, 35.5, 31.3; IR (Neat Film, NaCl) 3028, 2917, 2840, 2798, 2358, 1654, 1494, 1457, 1312,

1148, 1064, 967, 848, 741, 698, 680  $\text{cm}^{-1}$ ; (MM:ESI<sup>+</sup>)  $m/z$  calc'd for  $\text{C}_{16}\text{H}_{19}\text{ClN}$   $[\text{M}+\text{H}]^+$ : 260.1206, found: 260.1226.

### General Procedure 13: Synthesis of *N*-acyl compounds from free *N*-H product 147



#### (*R*)-(3-cinnamyl-5-fluoro-3,6-dihydropyridin-1(2H)-yl)(4-nitrophenyl)methanone

(**151**): was synthesized following the reaction in described as general procedure 13. Therefore, (*R*)-3-cinnamyl-5-fluoro-1,2,3,6-tetrahydropyridine **147a** (35.9 mg, 0.165 mmol, 1.0 equiv) was dissolved in  $\text{CH}_2\text{Cl}_2$  (5 mL) under air at room temperature. Pyridine (26.6  $\mu\text{L}$ , 0.33 mmol, 2.0 equiv) was added, followed by 4-nitrobenzoyl chloride **144** (61.2 mg, 0.33 mmol, 2.0 equiv). The resulting mixture was stirred at room temperature for 16 hours and then quenched with brine. The aqueous phase was extracted with EtOAc. The combined organic phases were dried over magnesium sulfate and filtered. The crude was subjected to flash column chromatography over silica gel using a solvent mixture of hexane/EtOAc (7/3) as the eluent. The desired compound **151** was obtained as white solids (60.0 mg, 0.164 mmol, 99%). <sup>1</sup>H NMR (400 MHz,  $\text{CD}_3\text{OD}$ ): (as a mixture of E/Z amide bond isomers)  $\delta$  8.33 – 8.19 (m, 2H), 7.71 – 7.60 (m, 2H), 7.42 – 7.12 (m, 5H), 6.53 (d,  $J$  = 15.8 Hz, 0.3H), 6.36 – 6.25 (m, 0.3H), 6.20 (d,  $J$  = 15.9 Hz, 0.7H), 6.01 – 5.90 (dt,  $J$  = 15.2 Hz, 0.7H), 5.48 (d,  $J$  = 16.2 Hz, 1H), 4.38 – 4.24 (m, 1.4H), 4.00 – 3.92 (m, 0.6H), 3.90 – 3.68 (m, 0.7H), 3.52 (dd,  $J$  = 13.6, 4.6 Hz, 0.7H), 3.27 (dd,  $J$  = 13.7, 6.1 Hz, 0.6H), 2.68 – 2.48 (m, 1H), 2.39 – 2.21 (m, 1.3H), 2.13 – 2.03 (m, 0.7H); <sup>13</sup>C NMR (101 MHz,  $\text{CD}_3\text{OD}$ ): (as a mixture of E/Z amide bond isomers, signals of minor isomer are indicated

with an asterisk \*)  $\delta$  170.77, 170.49\*, 156.51 (d,  $J = 253.8$  Hz), 156.07 (d,  $J = 252.8$  Hz)\*, 150.05\*, 149.83, 142.70, 142.61\*, 138.80\*, 138.29, 133.89\*, 133.67, 129.55\*, 129.47, 129.46, 129.31\*, 128.32, 127.77\*, 127.61, 127.21\*, 126.91, 124.91, 106.76 (d,  $J = 10.1$  Hz)\*, 106.16 (d,  $J = 12.1$  Hz), 47.15 (d,  $J = 40.3$  Hz)\*, 44.67, 42.16 (d,  $J = 40.8$  Hz), 37.98\*, 36.95, 35.34 (d,  $J = 6.3$  Hz), 34.65\*;  $^{19}\text{F}$  NMR (282 MHz,  $\text{CD}_3\text{OD}$ ): (as a mixture of E/Z amide bond isomers, signal of minor isomer is indicated with an asterisk \*)  $\delta$  -114.94 (dd,  $J = 16.2, 4.9$  Hz), -115.88 – -116.01 (m)\*; IR (Neat Film, NaCl) 3027, 2913, 2856, 1709, 1643, 1601, 1521, 1495, 1434, 1380, 1347, 1380, 1347, 1314, 1286, 1263, 1179, 1132, 1107, 1030, 1012, 969, 863, 853, 772, 742, 696  $\text{cm}^{-1}$ ; (MM:ESI<sup>+</sup>)  $m/z$  calc'd for  $\text{C}_{16}\text{H}_{19}\text{ClN}$  [M+H]<sup>+</sup>: 367.1458, found: 367.1483.

## 2.9 NOTES AND REFERENCES

<sup>1</sup> (a) Aumaitre, C.; Morin, J.-F. Polycyclic Aromatic Hydrocarbons as Potential Building Blocks for Organic Solar Cells. *The Chemical Record* **2019**, *19* (6), 1142–1154. (b) Zhang, L.; Cao, Y.; Colella, N. S.; Liang, Y.; Brédas, J.-L.; Houk, K. N.; Briseno, A. L. Unconventional, Chemically Stable, and Soluble Two-Dimensional Angular Polycyclic Aromatic Hydrocarbons: From Molecular Design to Device Applications. *Acc. Chem. Res.* **2015**, *48* (3), 500–509.

<sup>2</sup> (a) Ali, Y.; Hamid, S. A.; Rashid, U. Biomedical Applications of Aromatic Azo Compounds. *Mini reviews in medicinal chemistry* **2018**, *18* (18), 1548–1558. (b) Al-Mulla, A. A Review: Biological Importance of Heterocyclic Compounds. *Der Pharma Chemica* **2017**, *9* (13), 141–147. (c) Saini, M. S.; Kumar, A.; Dwivedi, J.; Singh, R. A Review:

Biological Significances of Heterocyclic Compounds. *Int. J. Pharm. Sci. Res* **2013**, *4* (3), 66–77.

<sup>3</sup> (a) Lovering, F.; Bikker, J.; Humblet, C. Escape from Flatland: Increasing Saturation as an Approach to Improving Clinical Success. *Journal of medicinal chemistry* **2009**, *52* (21), 6752–6756. (b) Cox, B.; Booker-Milburn, K. I.; Elliott, L. D.; Robertson-Ralph, M.; Zdorichenko, V. Escaping from Flatland:[2+ 2] Photocycloaddition; Conformationally Constrained Sp<sup>3</sup>-Rich Scaffolds for Lead Generation. *ACS Medicinal Chemistry Letters* **2019**, *10* (11), 1512–1517. (c) Lovering, F. Escape from Flatland 2: Complexity and Promiscuity. *MedChemComm* **2013**, *4* (3), 515–519.

<sup>4</sup> (a) Yang, Z.-P.; Wu, Q.-F.; Shao, W.; You, S.-L. Iridium-Catalyzed Intramolecular Asymmetric Allylic Dearomatization Reaction of Pyridines, Pyrazines, Quinolines, and Isoquinolines. *J. Am. Chem. Soc.* **2015**, *137* (50), 15899–15906. (b) Dudnik, A. S.; Weidner, V. L.; Motta, A.; Delferro, M.; Marks, T. J. Atom-Efficient Regioselective 1,2- Dearomatization of Functionalized Pyridines by an Earth-Abundant Organolanthanide Catalyst. *Nature Chemistry* **2014**, *6* (12), 1100–1107. (c) Yang, Z.-P.; Wu, Q.-F.; You, S.-L. Direct Asymmetric Dearomatization of Pyridines and Pyrazines by Iridium-Catalyzed Allylic Amination Reactions. *Angewandte Chemie International Edition* **2014**, *53* (27), 6986–6989. (d) Park, S.; Chang, S. Catalytic Dearomatization of N-Heteroarenes with Silicon and Boron Compounds. *Angewandte Chemie International Edition* **2017**, *56* (27), 7720–7738.

<sup>5</sup> (a) Vitaku, E.; Smith, D. T.; Njardarson, J. T. Analysis of the Structural Diversity, Substitution Patterns, and Frequency of Nitrogen Heterocycles among U.S. FDA Approved Pharmaceuticals. *J. Med. Chem.* **2014**, *57*, 10257–10274. (b) Heravi, M. M.; Zadsirjan, V.

Prescribed Drugs Containing Nitrogen Heterocycles: An Overview. *RSC Adv.* **2020**, *10*, 44247–44311.

<sup>6</sup> (a) Barbe, G.; Pelletier, G.; Charette, A. B. Intramolecular Pyridine Activation–Dearomatization Reaction: Highly Stereoselective Synthesis of Polysubstituted Indolizidines and Quinolizidines. *Org. Lett.* **2009**, *11* (15), 3398–3401. (b) Arnott, G.; Brice, H.; Clayden, J.; Blaney, E. Electrophile-Induced Dearomatizing Spirocyclization of N-Arylisonicotinamides: A Route to Spirocyclic Piperidines. *Org. Lett.* **2008**, *10* (14), 3089–3092. (c) Comins, D. L.; Kuethe, J. T.; Hong, H.; Lakner, F. J.; Concolino, T. E.; Rheingold, A. L. Diastereoselective Addition of Prochiral Metallo Enolates to Chiral 1-Acylpyridinium Salts. *J. Am. Chem. Soc.* **1999**, *121* (11), 2651–2652. (d) Bull, J. A.; Mousseau, J. J.; Pelletier, G.; Charette, A. B. Synthesis of Pyridine and Dihydropyridine Derivatives by Regio- and Stereoselective Addition to N-Activated Pyridines. *Chem. Rev.* **2012**, *112*, 2642–2713.

<sup>7</sup> (a) Roche, S. P.; Porco Jr., J. A. Dearomatization Strategies in the Synthesis of Complex Natural Products. *Angewandte Chemie International Edition* **2011**, *50* (18), 4068–4093. (b) Charette, A. B.; Grenon, M.; Lemire, A.; Pourashraf, M.; Martel, J. Practical and Highly Regio- and Stereoselective Synthesis of 2-Substituted Dihydropyridines and Piperidines: Application to the Synthesis of (–)-Coniine. *J. Am. Chem. Soc.* **2001**, *123* (47), 11829–11830. (c) Lemire, A.; Grenon, M.; Pourashraf, M.; Charette, A. B. Nucleophilic Addition to 3-Substituted Pyridinium Salts: Expedient Syntheses of (–)-L-733,061 and (–)-CP-99,994. *Org. Lett.* **2004**, *6* (20), 3517–3520. (d) Focken, T.; Charette, A. B. Stereoselective Synthesis of Pyridinones: Application to the Synthesis of (–)-Barrenazines. *Org. Lett.* **2006**, *8* (14), 2985–2988.

<sup>8</sup> For a review on C–H functionalization of pyridines at C–3, see: Murakami, K.; Yamada, S.; Kaneda, T.; Itami, K. C–H Functionalization of Azines. *Chem. Rev.* **2017**, *117* (13), 9302–9332.

<sup>9</sup> For selected hydrosilylation reviews using heterogeneous catalysis, see: (a) Ríos, P.; Rodríguez, A.; Conejero, S. Activation of Si–H and B–H Bonds by Lewis Acidic Transition Metals and p-Block Elements: Same, but Different. *Chem. Sci.* **2022**, *13*, 7392–7418. (b) Lipke, M. C.; Liberman-Martin, A. L.; Tilley, T. D. Electrophilic Activation of Silicon–Hydrogen Bonds in Catalytic Hydrosilations. *Angew. Chem. Int. Ed.* **2017**, *56*, 2260–2294.

<sup>10</sup> For examples with Ti, see: (a) Hao, L.; Harrod, J. F.; Lebus, A.-M.; Mu, Y.; Shu, R.; Samuel, E.; Woo, H.-G. Homogeneous Catalytic Hydrosilylation of Pyridines. *Angew. Chem. Int. Ed.* **1998**, *37*, 3126–3129. (b) Gutsulyak, D. V.; van der Est, A.; Nikonov, G. I. Facile Catalytic Hydrosilylation of Pyridines. *Angew. Chem. Int. Ed.* **2011**, *50*, 1384–1387. For examples with Ru, see: (c) Lee, S.-H.; Gutsulyak, D. V.; Nikonov, G. I. Chemo- and Regioselective Catalytic Reduction of N-Heterocycles by Silane. *Organometallics* **2013**, *32*, 4457–4464. (d) Königs, C. D. F.; Klare, H. F. T.; Oestreich, M. Catalytic 1,4-Selective Hydrosilylation of Pyridines and Benzannulated Congeners. *Angew. Chem. Int. Ed.* **2013**, *52*, 10076–10079. (e) Bähr, S.; Oestreich, M. A Neutral Ru<sup>II</sup> Hydride Complex for the Regio- and Chemoselective Reduction of N-Silylpyridinium Ions. *Chem. Eur. J.* **2018**, *24*, 5613–5622. (f) Behera, D.; Thiyagarajan, S.; Anjalikrishna, P. K.; Suresh, C. H.; Gunanathan, C. Ruthenium(II)-Catalyzed Regioselective 1,2-Hydrosilylation of N-Heteroarenes and Tetrel Bonding Mechanism. *ACS Catal.* **2021**, *11*, 5885–5893. For examples with Ir, see: (g) Lortie, J. L.; Dudding, T.; Gabidullin, B. M.; Nikonov, G. I.

Zinc-Catalyzed Hydrosilylation and Hydroboration of N-Heterocycles. *ACS Catal.* **2017**, *7*, 8454–8459. For examples with Zn, see: (h) Wang, X.; Zhang, Y.; Yuan, D.; Yao, Y. Regioselective Hydroboration and Hydrosilylation of N-Heteroarenes Catalyzed by a Zinc Alkyl Complex. *Org. Lett.* **2020**, *22*, 5695–5700. (i) Prybil, J. W.; Wallace, R.; Warren, A.; Klingman, J.; Vaillant, R.; Hall, M. B.; Yang, X.; Brennessel, W. W.; Chin, R. M. Silylation of Pyridine, Picolines, and Quinoline with a Zinc Catalyst. *ACS Omega* **2020**, *5*, 1528–1539. For the theoretical prediction of Ni(I)-catalyst for the hydrosilylation of pyridine, see: (j) Singh, V.; Sakaki, S.; Deshmukh, M. M. Theoretical Prediction of Ni(I)-Catalyst for Hydrosilylation of Pyridine and Quinoline. *J. Comput. Chem.* **2019**, *40*, 2119–2130.

<sup>11</sup> Intemann, J.; Bauer, H.; Pahl, J.; Maron, L.; Harder, S. Calcium Hydride Catalyzed Highly 1,2-Selective Pyridine Hydrosilylation. *Chem. Eur. J.* **2015**, *21*, 11452–11461.

<sup>12</sup> For a review, see: (a) Oestreich, M.; Hermeke, J.; Mohr, J. A Unified Survey of Si–H and H–H Bond Activation Catalysed by Electron-Deficient Boranes. *Chem. Soc. Rev.* **2015**, *44*, 2202–2220. For selective examples, see (b) Gandhamsetty, N.; Park, S.; Chang, S. Selective Silylative Reduction of Pyridines Leading to Structurally Diverse Azacyclic Compounds with the Formation of Sp<sup>3</sup> C–Si Bonds. *J. Am. Chem. Soc.* **2015**, *137*, 15176–15184. (c) Petrushko, W. D.; Nikonov, G. I. Mono(Hydrosilylation) of N-Heterocycles Catalyzed by B(C<sub>6</sub>F<sub>5</sub>)<sub>3</sub> and Silylium Ion. *Organometallics* **2020**, *39*, 4717–4722.

<sup>13</sup> Jeong, J.; Park, S.; Chang, S. Iridium-Catalyzed Selective 1,2-Hydrosilylation of N-Heterocycles. *Chem. Sci.* **2016**, *7*, 5362–5370.

<sup>14</sup> For selected reviews, see: (a) Trost, B. M.; Van Vranken, D. L. Asymmetric Transition Metal-Catalyzed Allylic Alkylations. *Chem. Rev.* **1996**, *96*, 395–422. (b) Trost, B. M.;



Crawley, M. L. Asymmetric Transition-Metal-Catalyzed Allylic Alkylations: Applications in Total Synthesis. *Chem. Rev.* **2003**, *103*, 2921–2944. (c) Lu, Z.; Ma, S. Metal-Catalyzed Enantioselective Allylation in Asymmetric Synthesis. *Angew. Chem. Int. Ed.* **2008**, *47*, 258–297. (d) Cheng, Q.; Tu, H.-F.; Zheng, C.; Qu, J.-P.; Helmchen, G.; You, S.-L. Iridium-Catalyzed Asymmetric Allylic Substitution Reactions. *Chem. Rev.* **2019**, *119*, 1855–1969. (e) Liu, Y.; Han, S.-J.; Liu, W.-B.; Stoltz, B. M. Catalytic Enantioselective Construction of Quaternary Stereocenters: Assembly of Key Building Blocks for the Synthesis of Biologically Active Molecules. *Acc. Chem. Res.* **2015**, *48*, 740–751.

<sup>15</sup> For selected reviews and examples for Pd catalysis, see: (a) Trost, B. M.; Schultz, J. E. Palladium-Catalyzed Asymmetric Allylic Alkylation Strategies for the Synthesis of Acyclic Tetrasubstituted Stereocenters. *Synthesis* **2019**, *51*, 1–30. (b) Hong, A. Y.; Stoltz, B. M. The Construction of All-Carbon Quaternary Stereocenters by Use of Pd-Catalyzed Asymmetric Allylic Alkylation Reactions in Total Synthesis. *Eur. J. Org. Chem.* **2013**, *2013*, 2745–2759. (c) Guerrero Rios, I.; Rosas-Hernandez, A.; Martin, E. Recent Advances in the Application of Chiral Phosphine Ligands in Pd-Catalysed Asymmetric Allylic Alkylation. *Molecules* **2011**, *16*, 970–1010. (d) Trost, B. M.; Machacek, M. R.; Aponick, A. Predicting the Stereochemistry of Diphenylphosphino Benzoic Acid (DPPBA)-Based Palladium-Catalyzed Asymmetric Allylic Alkylation Reactions: A Working Model. *Acc. Chem. Res.* **2006**, *39*, 747–760. For selected examples, see: (e) Trost, B. M.; Dietsch, T. J. New Synthetic Reactions. Asymmetric Induction in Allylic Alkylations. *J. Am. Chem. Soc.* **1973**, *95*, 8200–8201. (f) Trost, B. M.; Xu, J.; Schmidt, T. Palladium-Catalyzed Decarboxylative Asymmetric Allylic Alkylation of Enol Carbonates. *J. Am. Chem. Soc.*

**2009**, *131*, 18343–18357. (g) Alexy, E. J.; Zhang, H.; Stoltz, B. M. Catalytic Enantioselective Synthesis of Acyclic Quaternary Centers: Palladium-Catalyzed Decarboxylative Allylic Alkylation of Fully Substituted Acyclic Enol Carbonates. *J. Am. Chem. Soc.* **2018**, *140*, 10109–10112. (h) Behenna, D. C.; Stoltz, B. M. The Enantioselective Tsuji Allylation. *J. Am. Chem. Soc.* **2004**, *126*, 15044–15045. (i) Mohr, J. T.; Behenna, D. C.; Harned, A. M.; Stoltz, B. M. Deracemization of Quaternary Stereocenters by Pd-Catalyzed Enantioconvergent Decarboxylative Allylation of Racemic  $\beta$ -Ketoesters. *Angew. Chem. Int. Ed.* **2005**, *44*, 6924–6927. (j) Keith, J. A.; Behenna, D. C.; Sherden, N.; Mohr, J. T.; Ma, S.; Marinescu, S. C.; Nielsen, R. J.; Oxgaard, J.; Stoltz, B. M.; Goddard, W. A. I. The Reaction Mechanism of the Enantioselective Tsuji Allylation: Inner-Sphere and Outer-Sphere Pathways, Internal Rearrangements, and Asymmetric C–C Bond Formation. *J. Am. Chem. Soc.* **2012**, *134*, 19050–19060. (k) Chen, J.-P.; Ding, C.-H.; Liu, W.; Hou, X.-L.; Dai, L.-X. Palladium-Catalyzed Regio-, Diastereo-, and Enantioselective Allylic Alkylation of Acylsilanes with Monosubstituted Allyl Substrates. *J. Am. Chem. Soc.* **2010**, *132*, 15493–15495. (l) Behenna, D. C.; Mohr, J. T.; Sherden, N. H.; Marinescu, S. C.; Harned, A. M.; Tani, K.; Seto, M.; Ma, S.; Novák, Z.; Krout, M. R.; McFadden, R. M.; Roizen, J. L.; Enquist Jr., J. A.; White, D. E.; Levine, S. R.; Petrova, K. V.; Iwashita, A.; Virgil, S. C.; Stoltz, B. M. Enantioselective Decarboxylative Alkylation Reactions: Catalyst Development, Substrate Scope, and Mechanistic Studies. *Chem. Eur. J.* **2011**, *17*, 14199–14223. (m) Bai, D.-C.; Yu, F.-L.; Wang, W.-Y.; Chen, D.; Li, H.; Liu, Q.-R.; Ding, C.-H.; Chen, B.; Hou, X.-L. Palladium/N-Heterocyclic Carbene Catalysed Regio and Diastereoselective Reaction of Ketones with Allyl Reagents via Inner-Sphere Mechanism. *Nat. Commun.* **2016**, *7*, 11806.

(n) Behenna, D. C.; Liu, Y.; Yurino, T.; Kim, J.; White, D. E.; Virgil, S. C.; Stoltz, B. M. Enantioselective Construction of Quaternary N-Heterocycles by Palladium-Catalyzed Decarboxylative Allylic Alkylation of Lactams. *Nature Chem.* **2012**, *4*, 130–133.

<sup>16</sup> For a review, see: (a) Zhuo, C.-X.; Zheng, C.; You, S.-L. Transition-Metal-Catalyzed Asymmetric Allylic Dearomatization Reactions. *Acc. Chem. Res.* **2014**, *47*, 2558–2573. For selected examples, see: (b) Trost, B. M.; Bai, W.-J.; Hohn, C.; Bai, Y.; Cregg, J. J. Palladium-Catalyzed Asymmetric Allylic Alkylation of 3-Substituted 1H-Indoles and Tryptophan Derivatives with Vinylcyclopropanes. *J. Am. Chem. Soc.* **2018**, *140*, 6710–6717. (c) Liu, Y.; Du, H. Pd-Catalyzed Asymmetric Allylic Alkylations of 3-Substituted Indoles Using Chiral P/Olefin Ligands. *Org. Lett.* **2013**, *15*, 740–743. (d) Kaiser, T. M.; Yang, J. Catalytic Enantioconvergent Decarboxylative Allylic Alkylation of Allyl Indolenin-3-Carboxylates. *Eur. J. Org. Chem.* **2013**, *2013*, 3983–3987. (e) Gao, R.-D.; Xu, Q.-L.; Zhang, B.; Gu, Y.; Dai, L.-X.; You, S.-L. Palladium(0)-Catalyzed Intermolecular Allylic Dearomatization of Indoles by a Formal [4+2] Cycloaddition Reaction. *Chem. Eur. J.* **2016**, *22*, 11601–11604.

<sup>17</sup> Trost, B. M.; Quancard, J. Palladium-Catalyzed Enantioselective C-3 Allylation of 3-Substituted-1H-Indoles Using Trialkylboranes. *J. Am. Chem. Soc.* **2006**, *128*, 6314–6315.

<sup>18</sup> For a review, see: Wu, W.-T.; Zhang, L.; You, S.-L. Catalytic Asymmetric Dearomatization (CADA) Reactions of Phenol and Aniline Derivatives. *Chem. Soc. Rev.* **2016**, *45*, 1570–1580. Selected examples for phenols as nucleophile:

<sup>19</sup> Wu, Q.-F.; Liu, W.-B.; Zhuo, C.-X.; Rong, Z.-Q.; Ye, K.-Y.; You, S.-L. Iridium-Catalyzed Intramolecular Asymmetric Allylic Dearomatization of Phenols. *Angew. Chem. Int. Ed.* **2011**, *50*, 4455–4458. (c) Yang, Z.-P.; Wu, Q.-F.; Shao, W.; You, S.-L. Iridium-

Catalyzed Intramolecular Asymmetric Allylic Dearomatization Reaction of Pyridines, Pyrazines, Quinolines, and Isoquinolines. *J. Am. Chem. Soc.* **2015**, *137*, 15899–15906. (d) Yang, Z.-P.; Jiang, R.; Zheng, C.; You, S.-L. Iridium-Catalyzed Intramolecular Asymmetric Allylic Alkylation of Hydroxyquinolines: Simultaneous Weakening of the Aromaticity of Two Consecutive Aromatic Rings. *J. Am. Chem. Soc.* **2018**, *140*, 3114–3119. (e) Nemoto, T.; Ishige, Y.; Yoshida, M.; Kohno, Y.; Kanematsu, M.; Hamada, Y. Novel Method for Synthesizing Spiro[4.5]Cyclohexadienones through a Pd-Catalyzed Intramolecular Ipso-Friedel–Crafts Allylic Alkylation of Phenols. *Org. Lett.* **2010**, *12*, 5020–5023. (f) Xu, Q.-L.; Dai, L.-X.; You, S.-L. Enantioselective Synthesis of Tetrahydroisoquinolines via Iridium-Catalyzed Intramolecular Friedel–Crafts-Type Allylic Alkylation of Phenols. *Org. Lett.* **2012**, *14*, 2579–2581. (g) Suzuki, Y.; Nemoto, T.; Kakugawa, K.; Hamajima, A.; Hamada, Y. Asymmetric Synthesis of Chiral 9,10-Dihydrophenanthrenes Using Pd-Catalyzed Asymmetric Intramolecular Friedel–Crafts Allylic Alkylation of Phenols. *Org. Lett.* **2012**, *14*, 2350–2353. (h) Zhuo, C.-X.; You, S.-L. Palladium-Catalyzed Intermolecular Asymmetric Allylic Dearomatization Reaction of Naphthol Derivatives. *Angew. Chem. Int. Ed.* **2013**, *52*, 10056–10059. (i) Zhuo, C.-X.; You, S.-L. Palladium-Catalyzed Intermolecular Allylic Dearomatization Reaction of  $\alpha$ -Substituted  $\beta$ -Naphthol Derivatives: Scope and Mechanistic Investigation. *Adv. Synth. Catal.* **2014**, *356*, 2020–2028. (j) Zhao, Z.-L.; Xu, Q.-L.; Gu, Q.; Wu, X.-Y.; You, S.-L. Enantioselective Synthesis of 4-Substituted Tetrahydroisoquinolines via Palladium-Catalyzed Intramolecular Friedel–Crafts Type Allylic Alkylation of Phenols. *Org. Biomol. Chem.* **2015**, *13*, 3086–3092.

- <sup>20</sup> Yang, Z.-P.; Jiang, R.; Wu, Q.-F.; Huang, L.; Zheng, C.; You, S.-L. Iridium-Catalyzed Intramolecular Asymmetric Allylic Dearomatization of Benzene Derivatives. *Angew. Chem. Int. Ed.* **2018**, *57*, 16190–16193.
- <sup>21</sup> Yang, Z.-P.; Wu, Q.-F.; You, S.-L. Direct Asymmetric Dearomatization of Pyridines and Pyrazines by Iridium-Catalyzed Allylic Amination Reactions. *Angew. Chem. Int. Ed.* **2014**, *53*, 6986–6989.
- <sup>22</sup> Afewerki, S.; Córdova, A. Enamine/Transition Metal Combined Catalysis: Catalytic Transformations Involving Organometallic Electrophilic Intermediates. *Topics in Current Chemistry* **2019**, *377* (6), 38.
- <sup>23</sup> Weix, D. J.; Hartwig, J. F. Regioselective and Enantioselective Iridium-Catalyzed Allylation of Enamines. *J. Am. Chem. Soc.* **2007**, *129*, 7720–7721.
- <sup>24</sup> Krautwald, S.; Sarlah, D.; Schafroth, M. A.; Carreira, E. M. Enantio- and Diastereodivergent Dual Catalysis:  $\alpha$ -Allylation of Branched Aldehydes. *Science* **2013**, *340* (6136), 1065–1068.

## **APPENDIX 4**

*Spectra Relevant to Chapter 2:*

*Enantioselective Dearomative Allylic Alkylation of Pyridines*

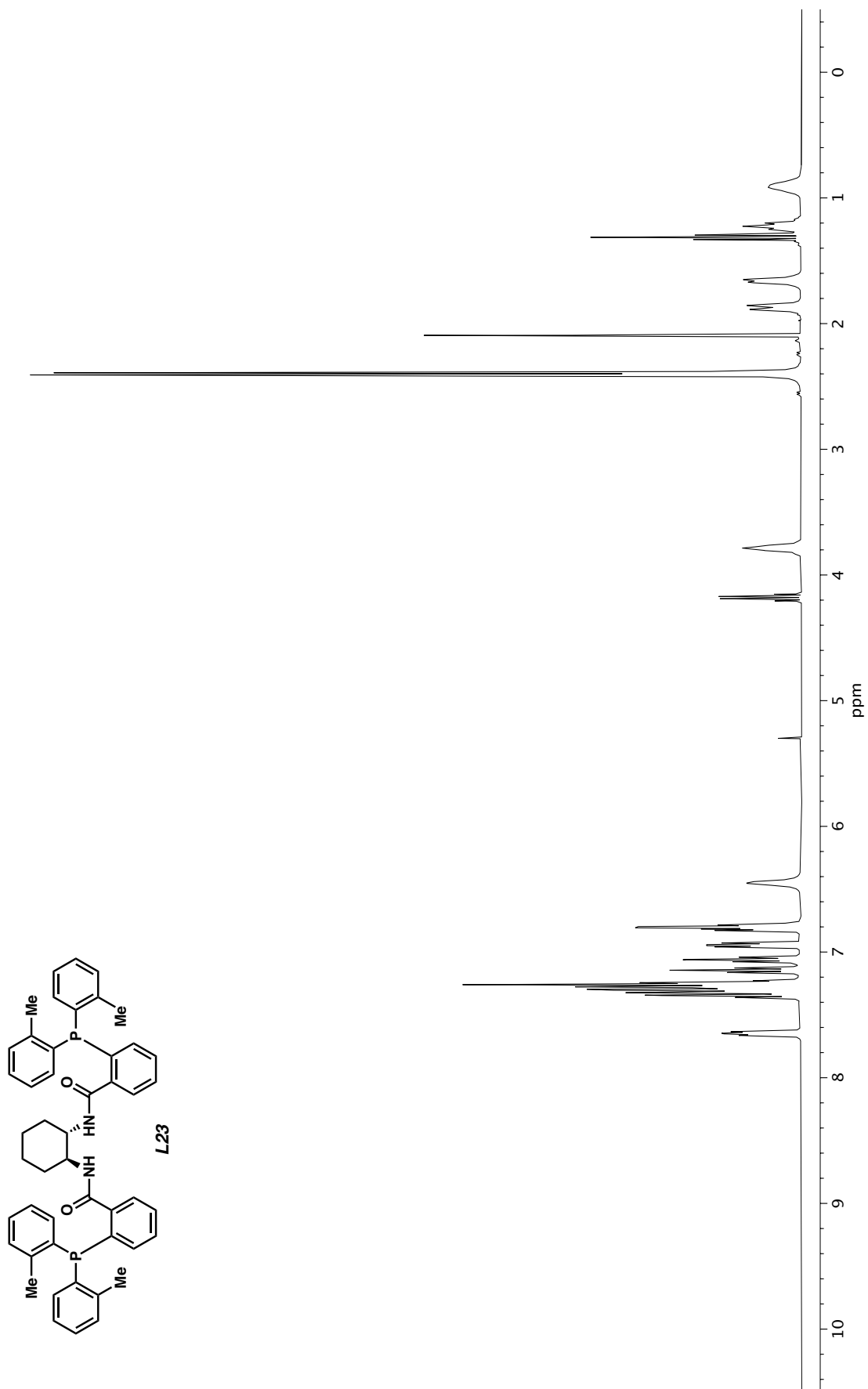
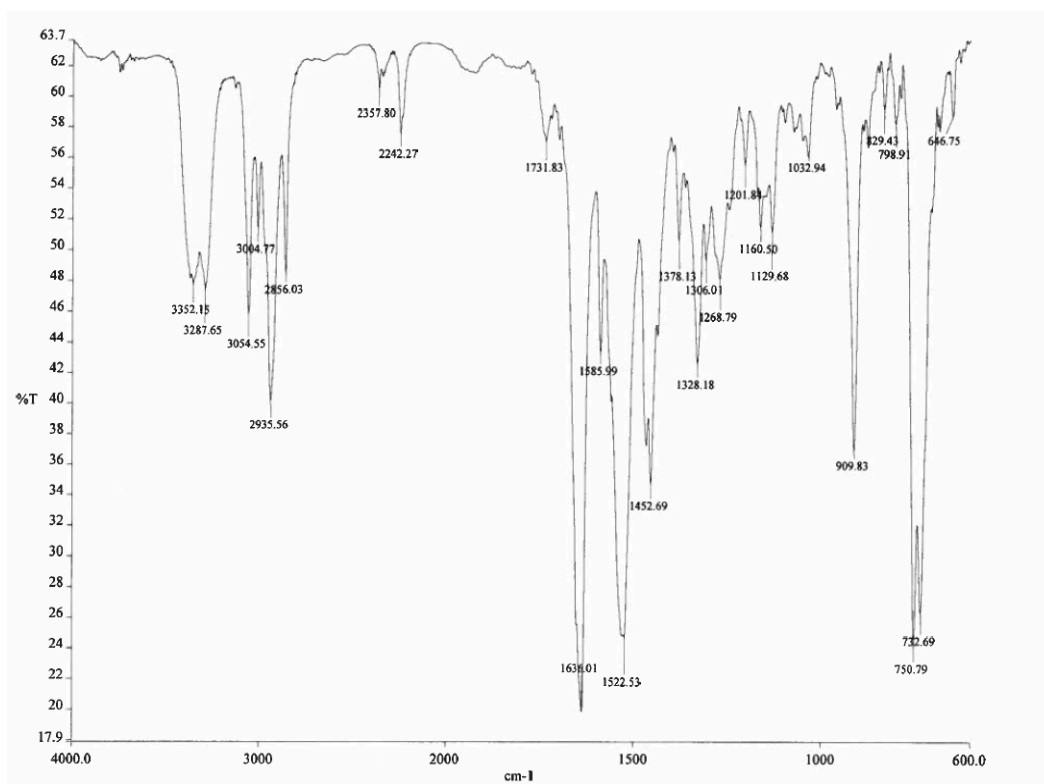
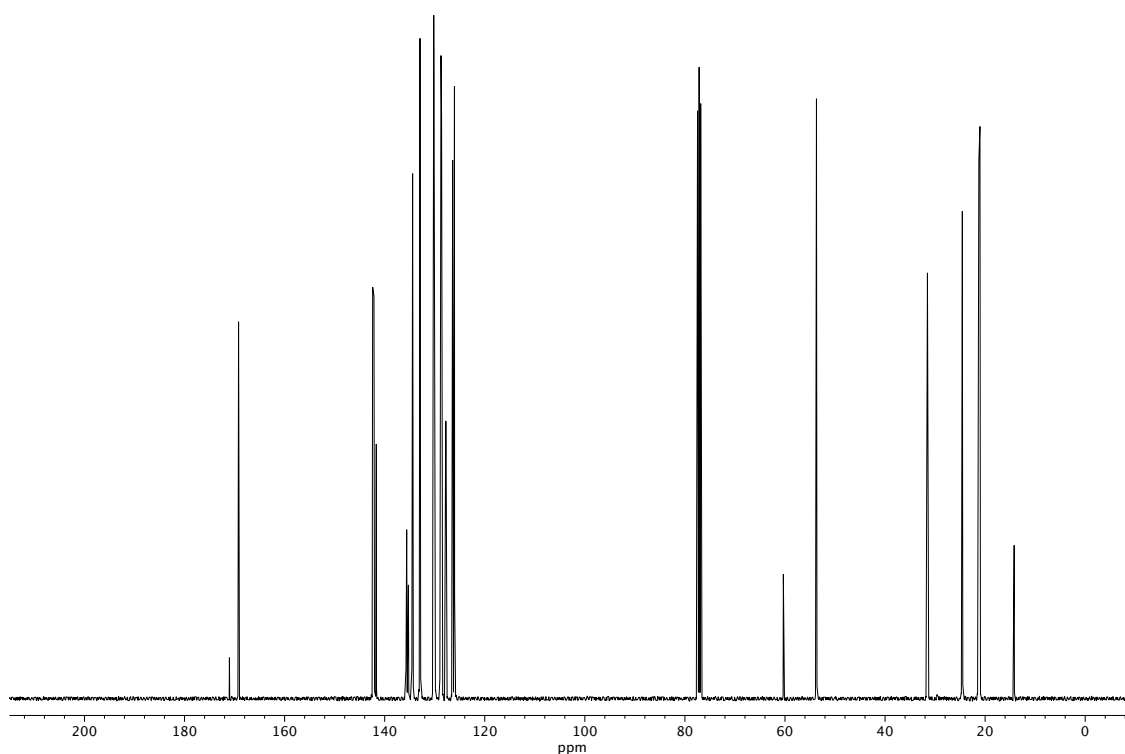


Figure A4.1  $^1\text{H}$  NMR (400 MHz,  $\text{CDCl}_3$ ) of compound L23.



**Figure A4.2** Infrared spectrum (Thin Film, NaCl) of compound **L23**.



**Figure A4.3** <sup>13</sup>C NMR (100 MHz, CDCl<sub>3</sub>) of compound **L23**.



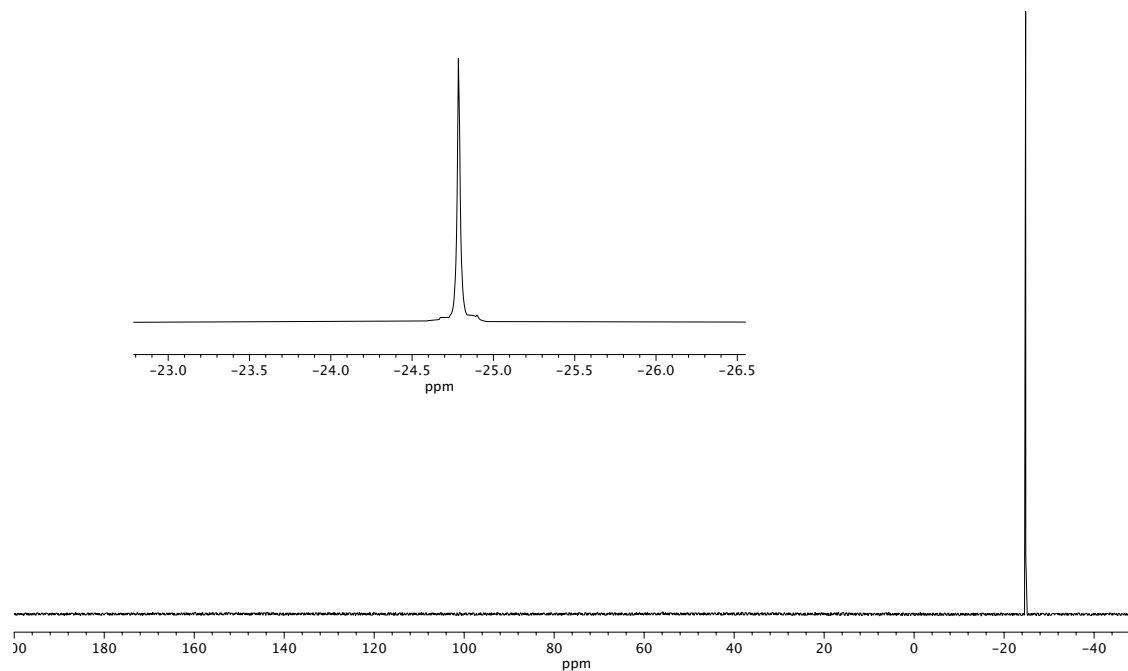


**Figure A4.4.**  $^{31}\text{P}$  NMR (121 MHz,  $\text{CDCl}_3$ ) of compound **L23**.

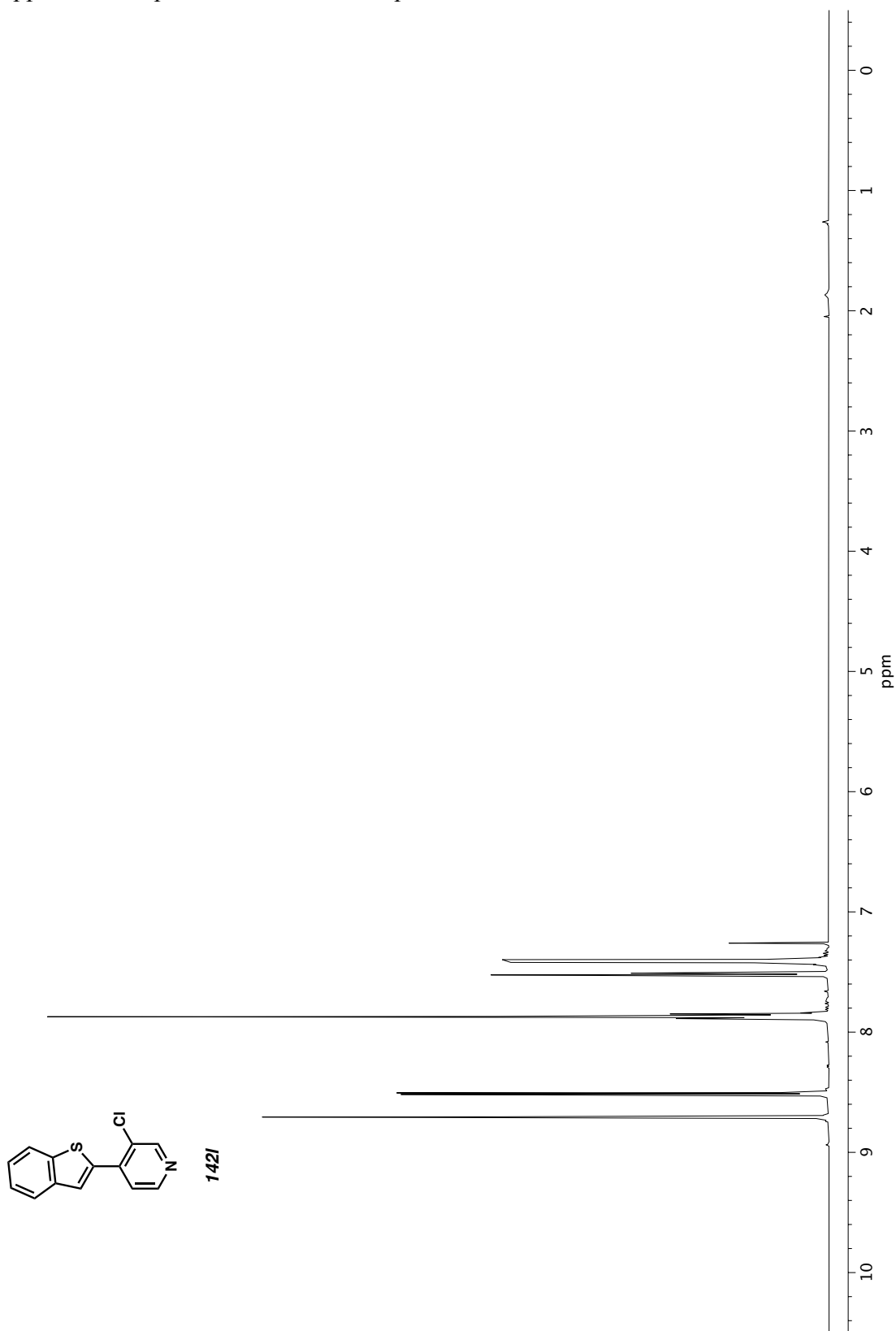


Figure A4.5. <sup>1</sup>H NMR (400 MHz, CDCl<sub>3</sub>) of compound **142I**.

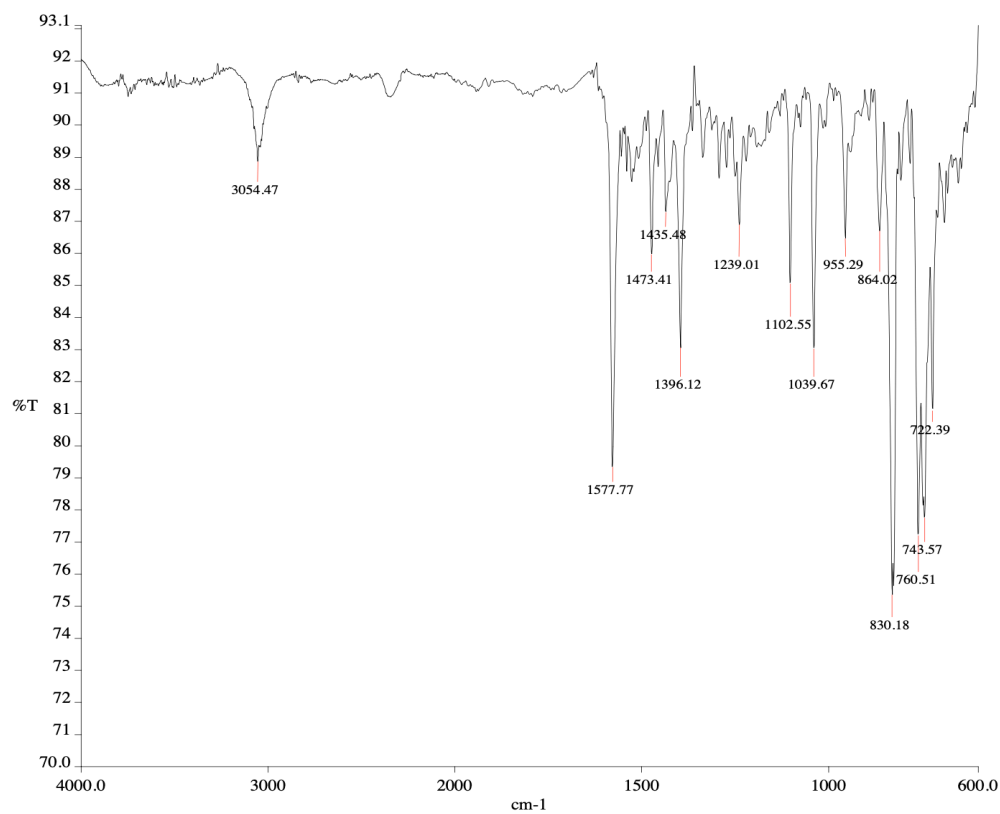


Figure A4.6 Infrared spectrum (Thin Film, NaCl) of compound **142I**.

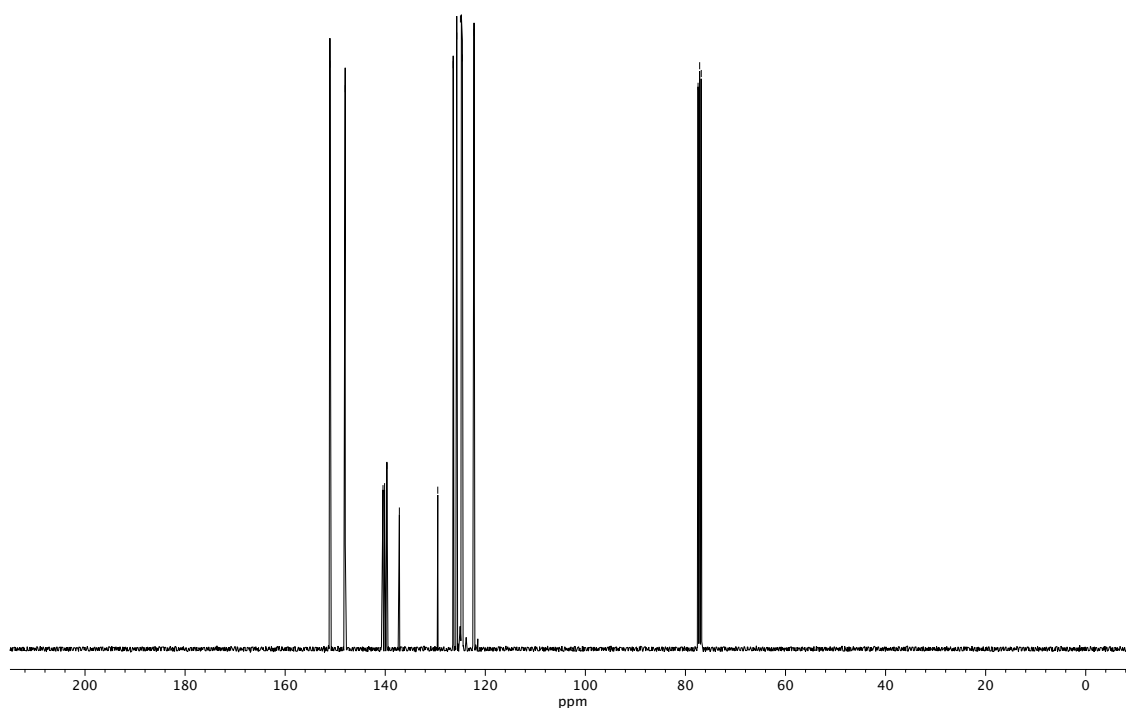
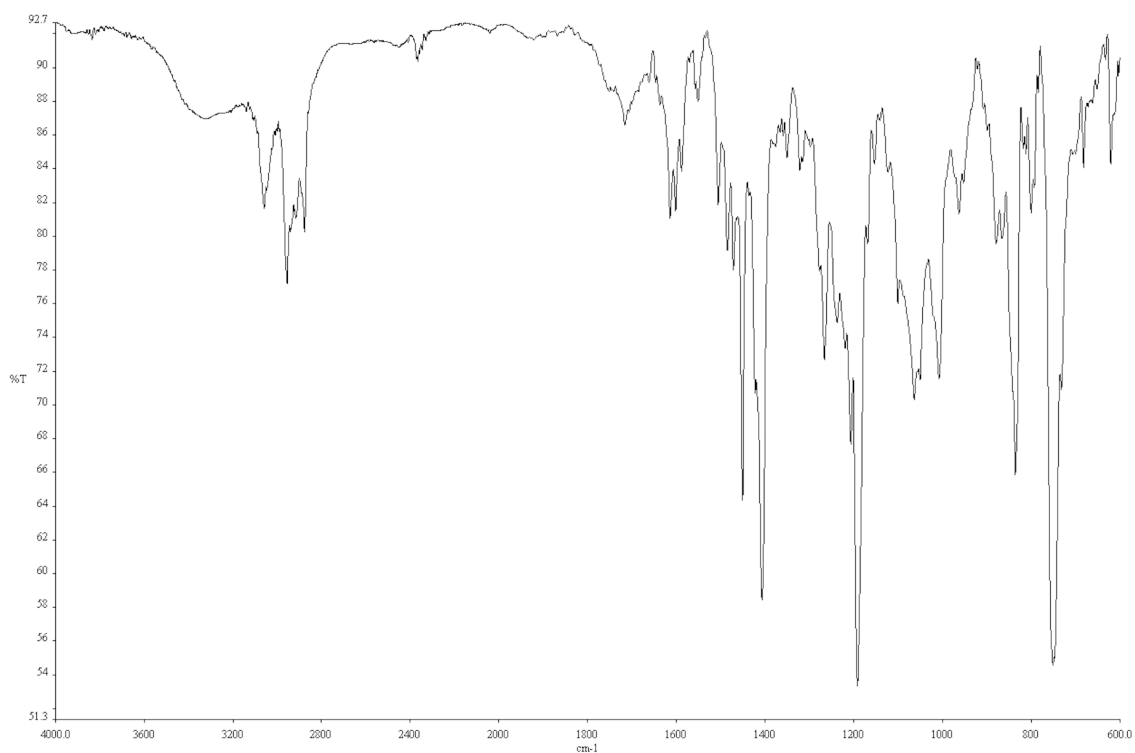
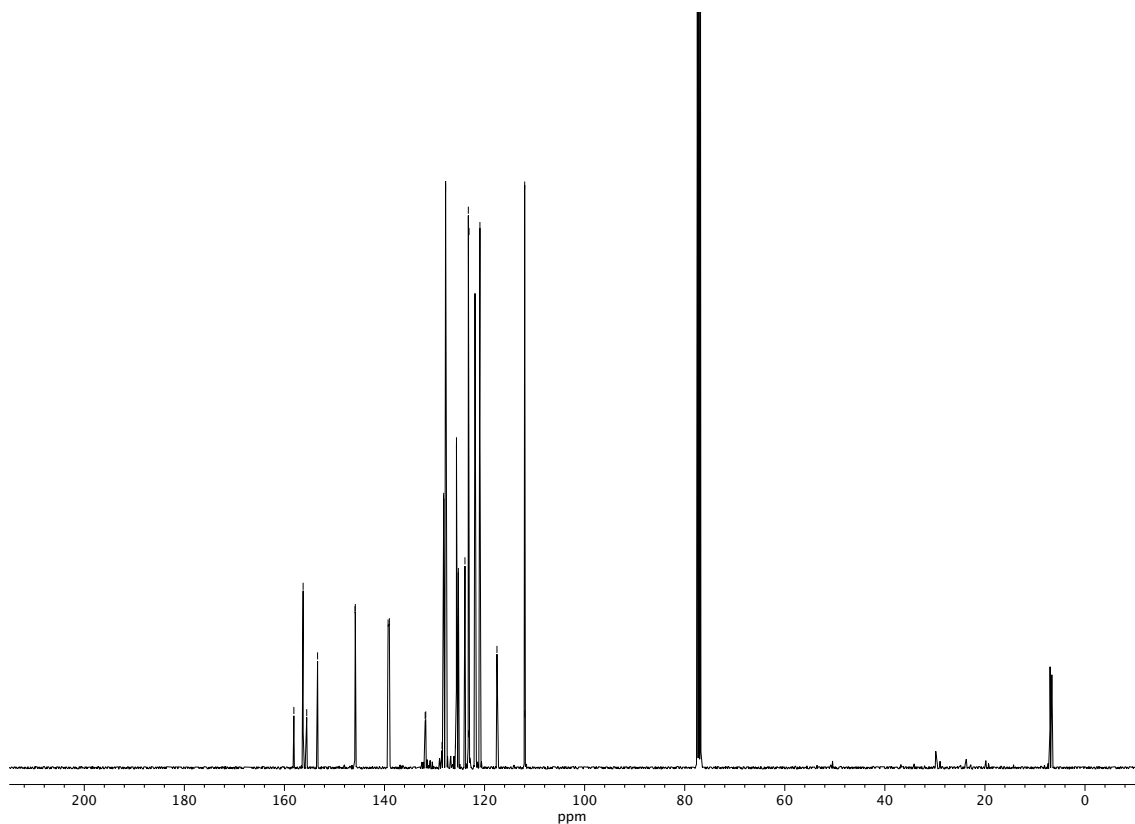


Figure A4.7 <sup>13</sup>C NMR (100 MHz, CDCl<sub>3</sub>) of compound **142I**.

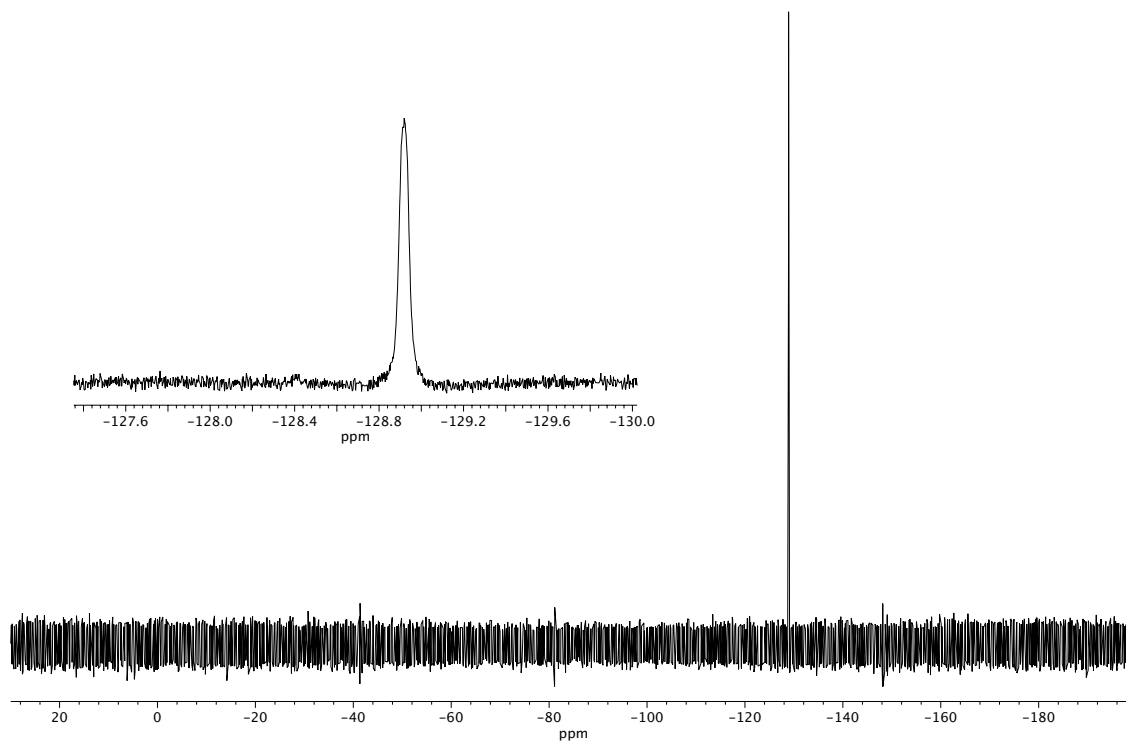




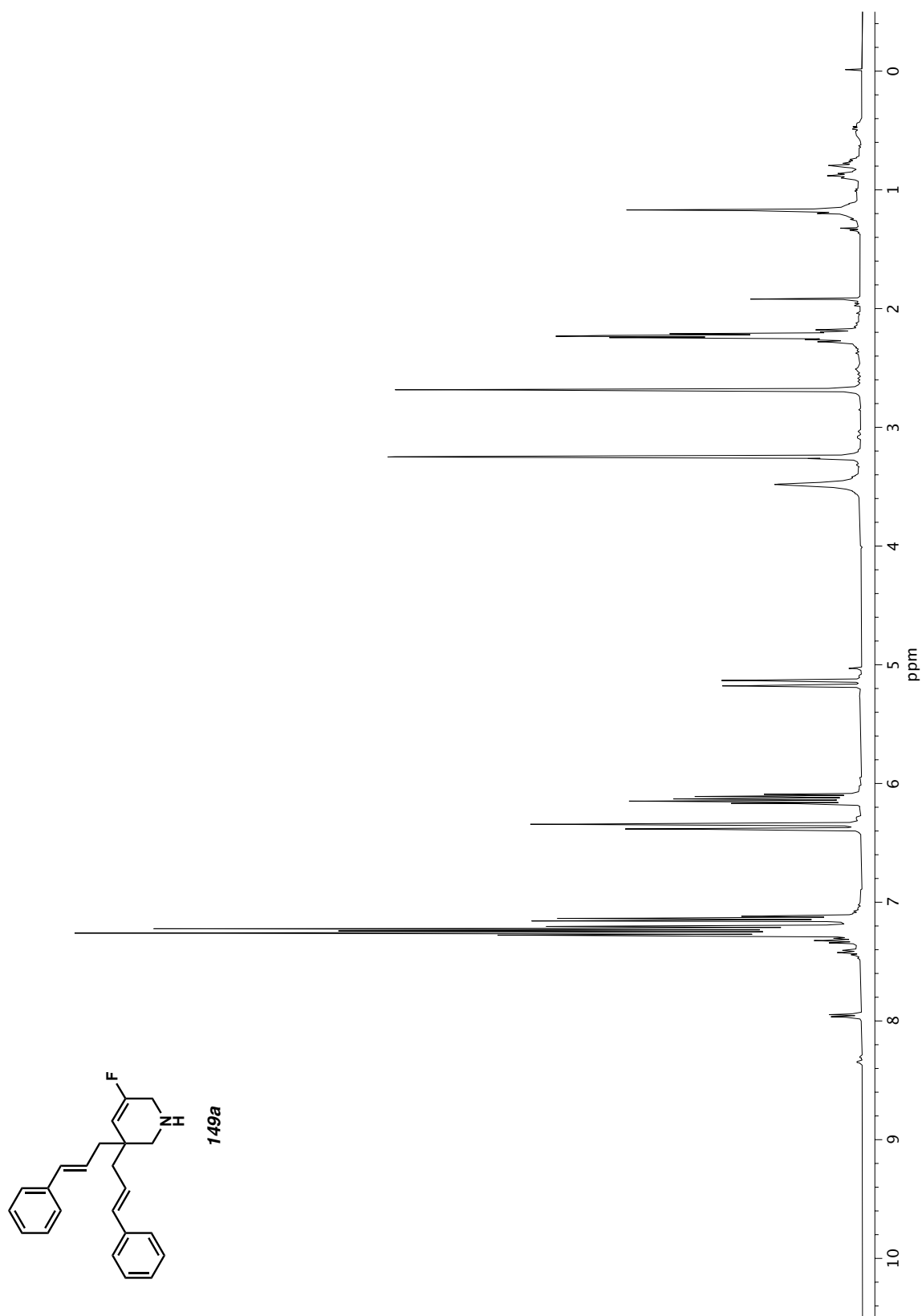
**Figure A4.9** Infrared spectrum (Thin Film, NaCl) of compound **142m**.

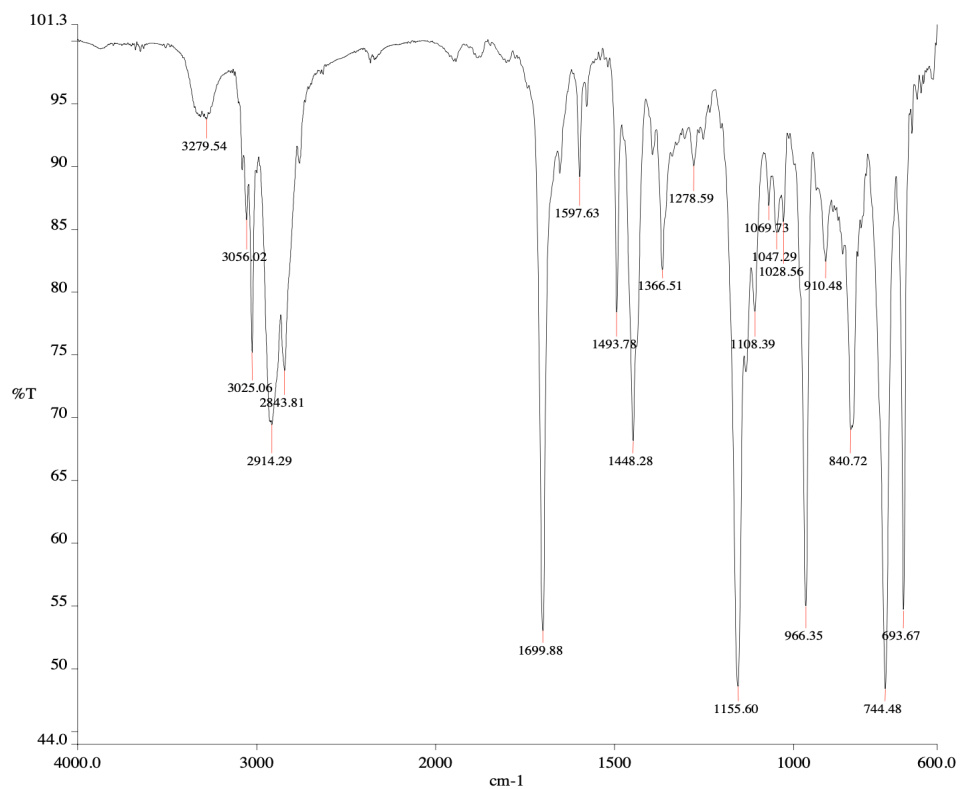


**Figure A4.10** <sup>13</sup>C NMR (100 MHz, CDCl<sub>3</sub>) of compound **142m**.

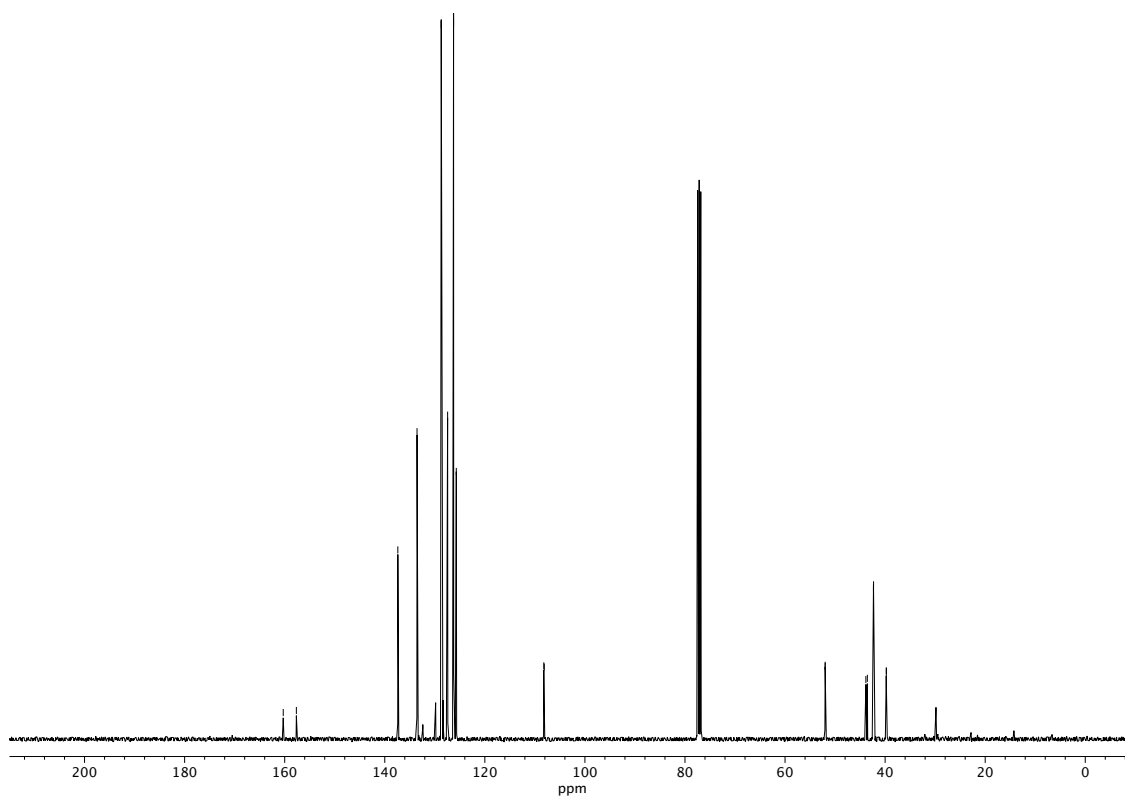


**Figure A4.11**  $^{19}\text{F}$  NMR (282 MHz,  $\text{CDCl}_3$ ) of compound **142m**.

Figure A4.12 <sup>1</sup>H NMR (400 MHz, CDCl<sub>3</sub>) of compound **149a**.

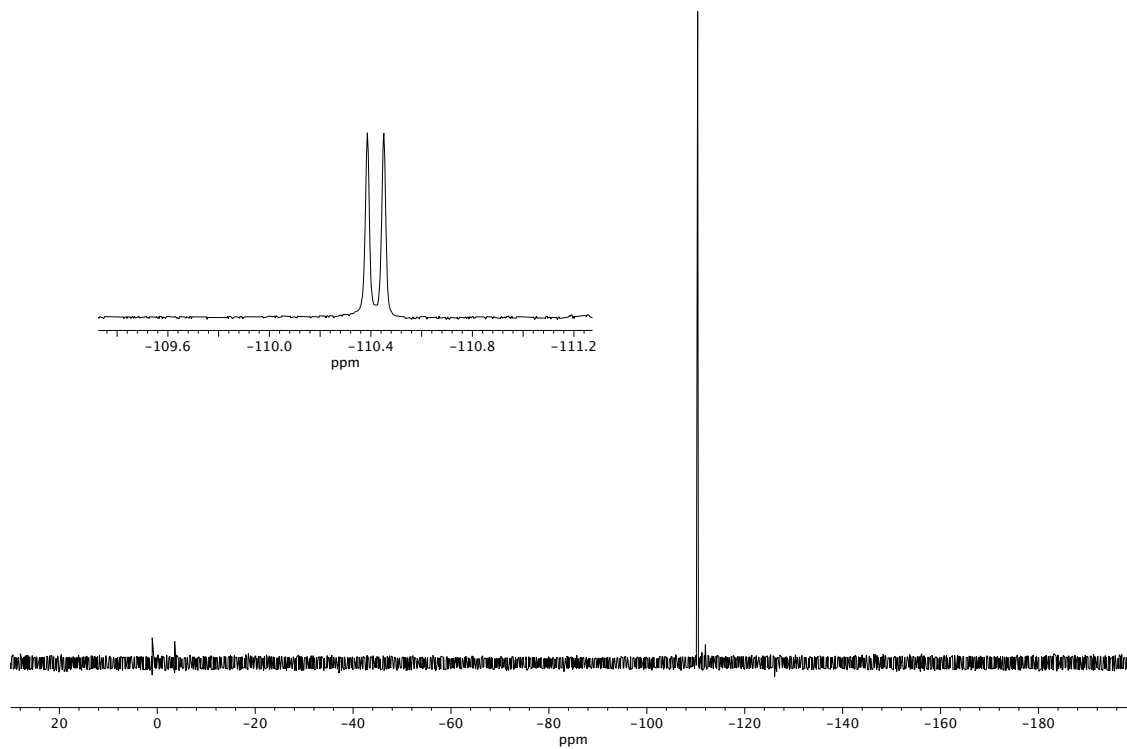


**Figure A4.13** Infrared spectrum (Thin Film, NaCl) of compound **149a**.

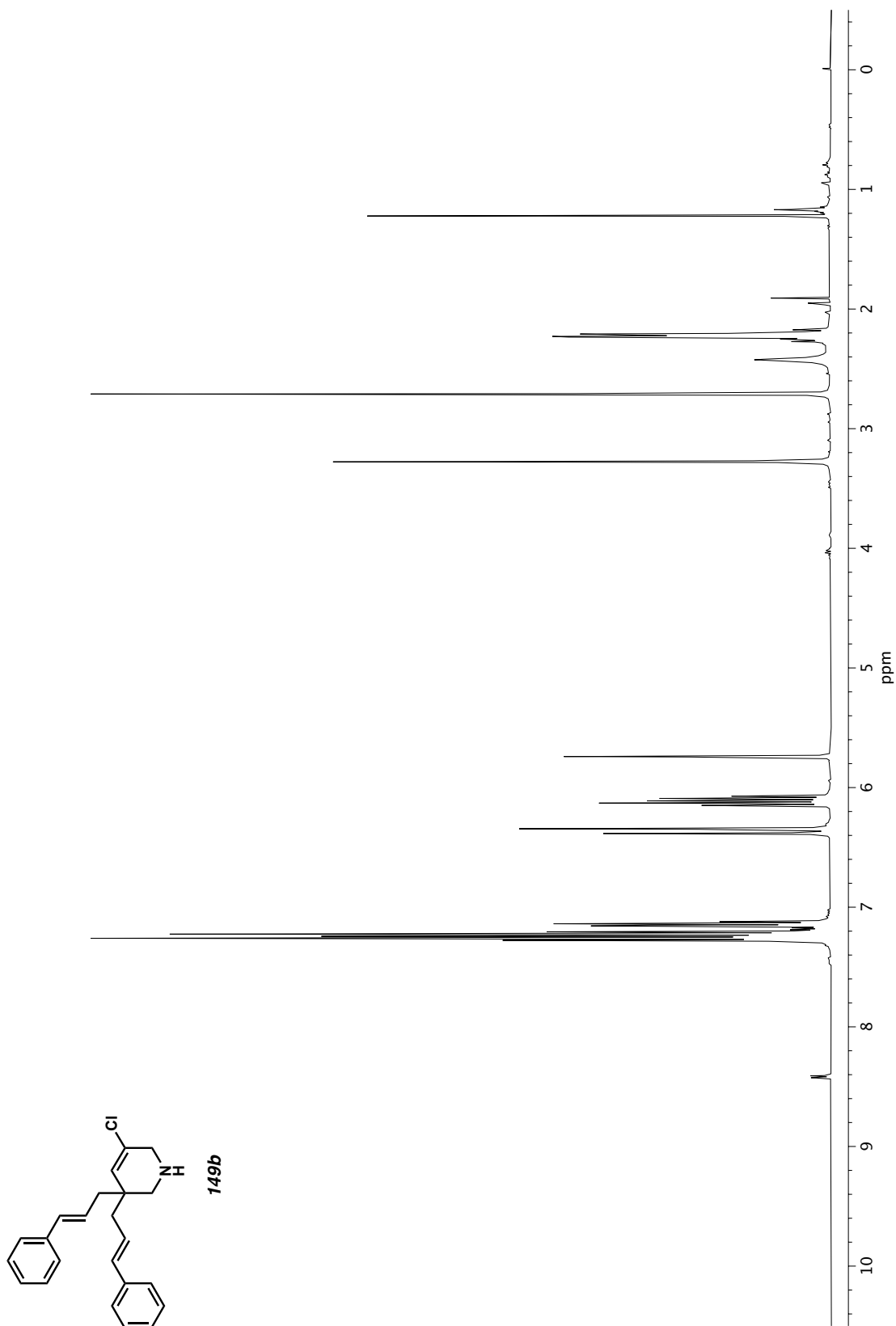


**Figure A4.14** <sup>13</sup>C NMR (100 MHz, CDCl<sub>3</sub>) of compound **149a**.

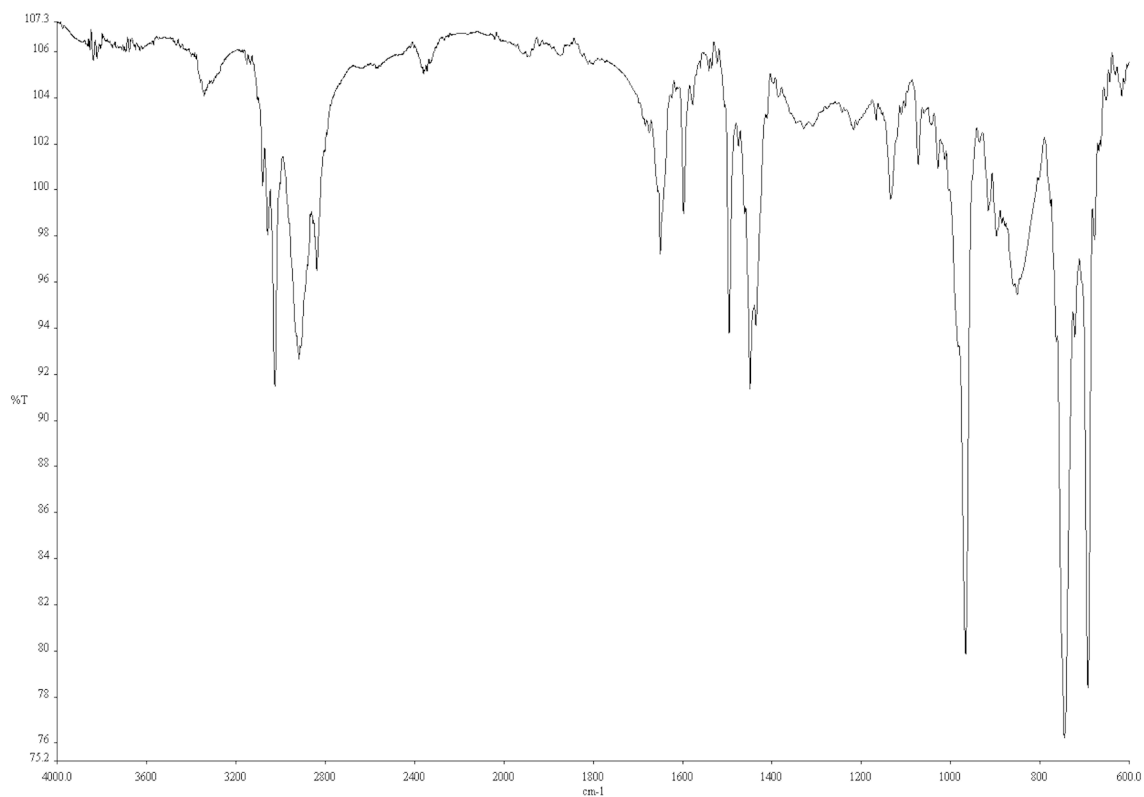




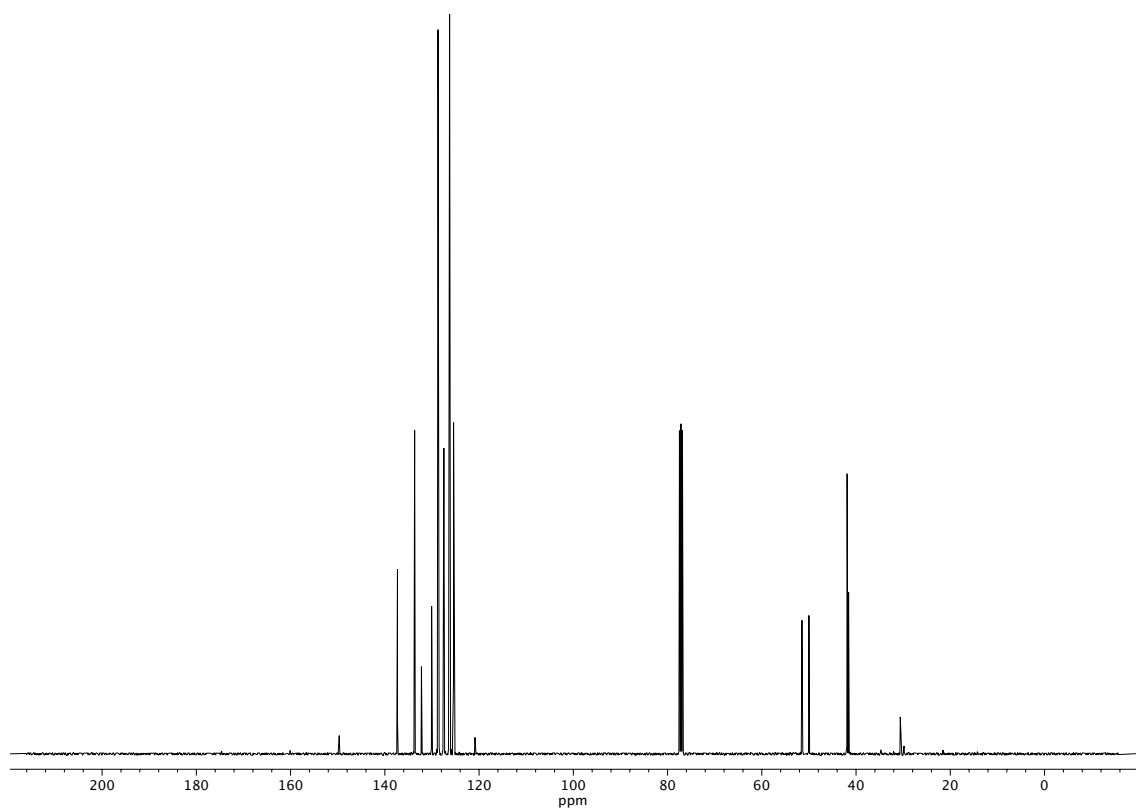
**Figure A4.15**  $^{19}\text{F}$  NMR (282 MHz,  $\text{CDCl}_3$ ) of compound **149a**.



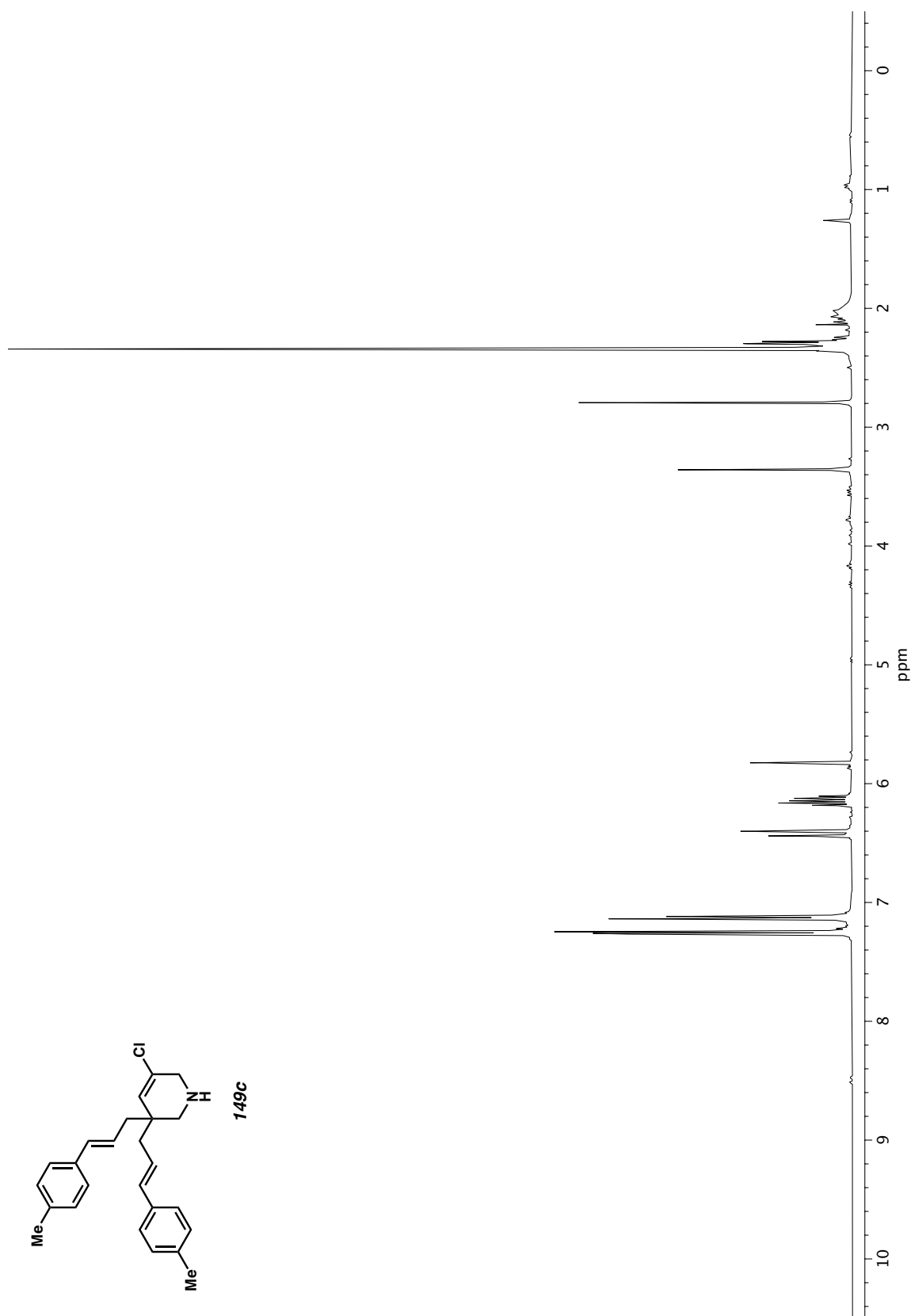
**Figure A4.16**  $^1\text{H}$  NMR (400 MHz,  $\text{CDCl}_3$ ) of compound **149b**.

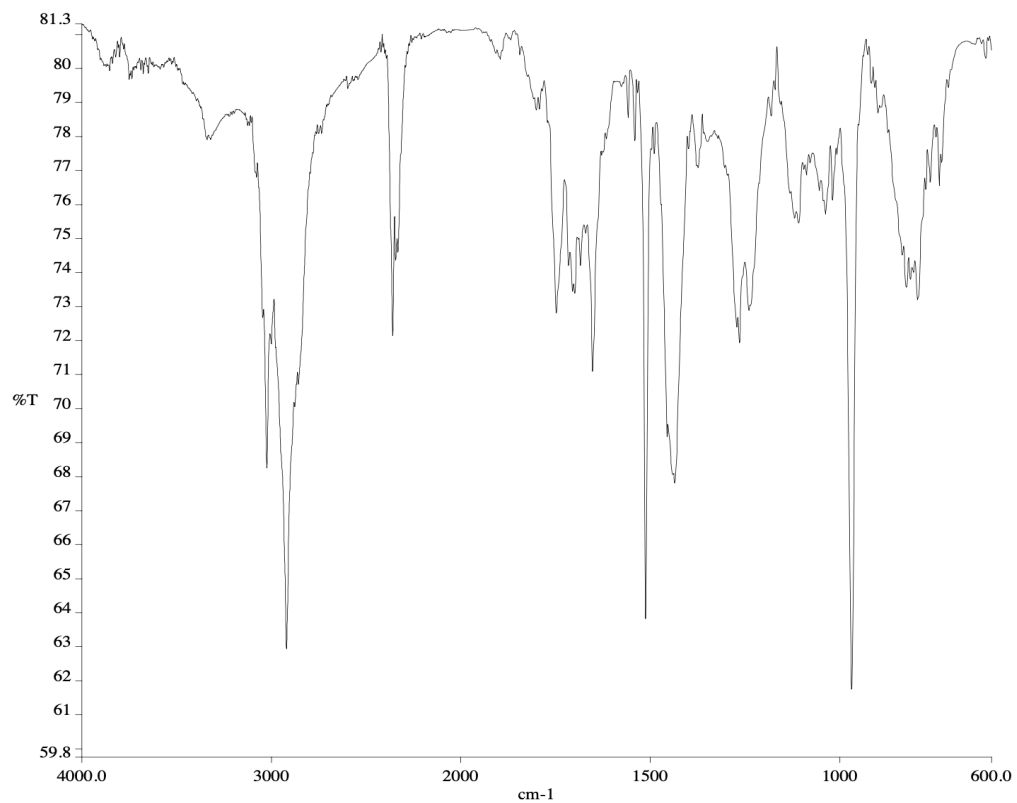


**Figure A4.17** Infrared spectrum (Thin Film, NaCl) of compound **149b**.

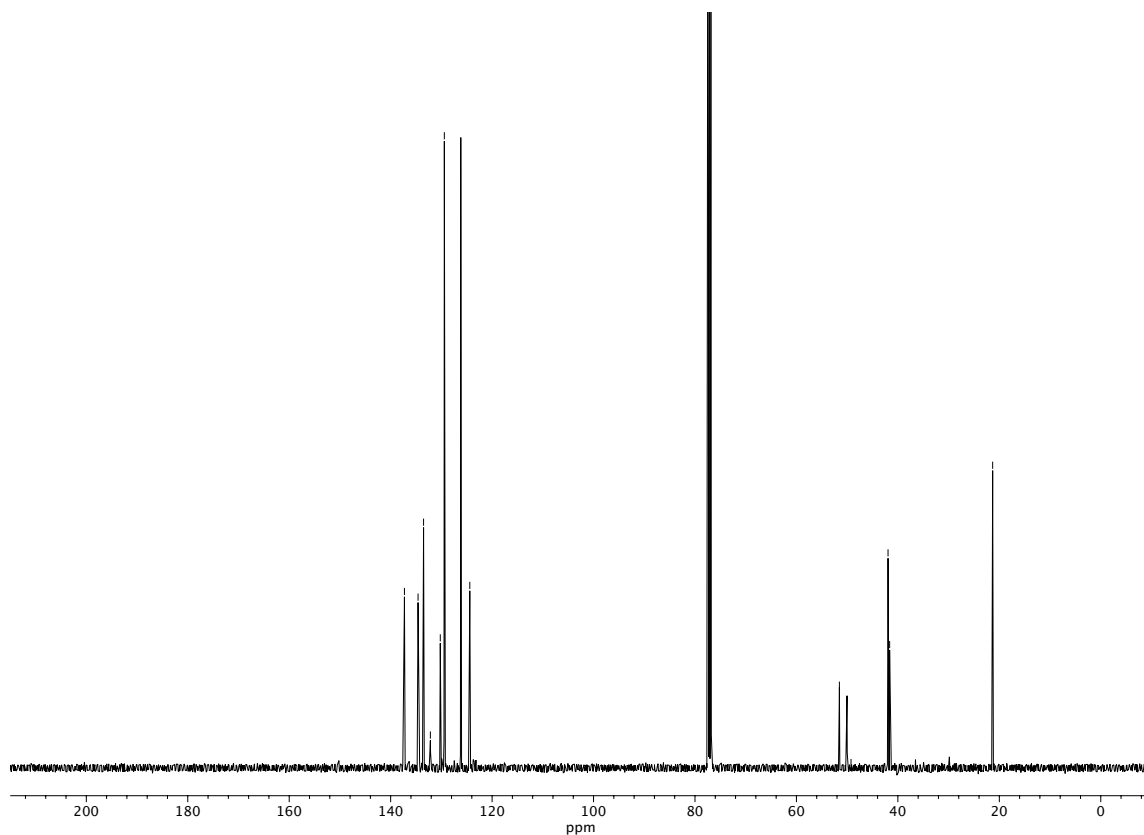


**Figure A4.18**  $^{13}\text{C}$  NMR (100 MHz,  $\text{CDCl}_3$ ) of compound **149b**.

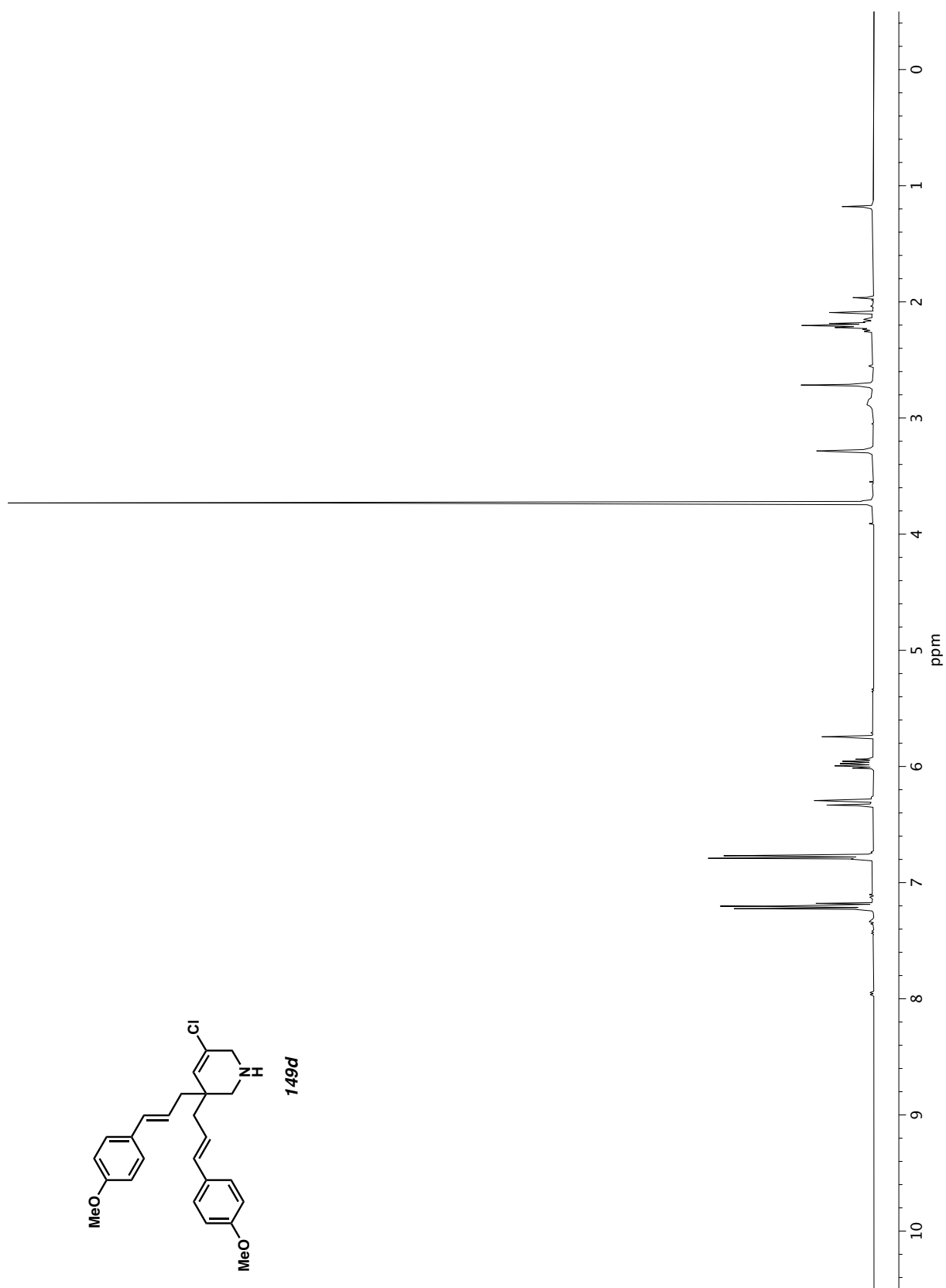
Figure A4.19  $^1\text{H}$  NMR (400 MHz,  $\text{CDCl}_3$ ) of compound **149c**.

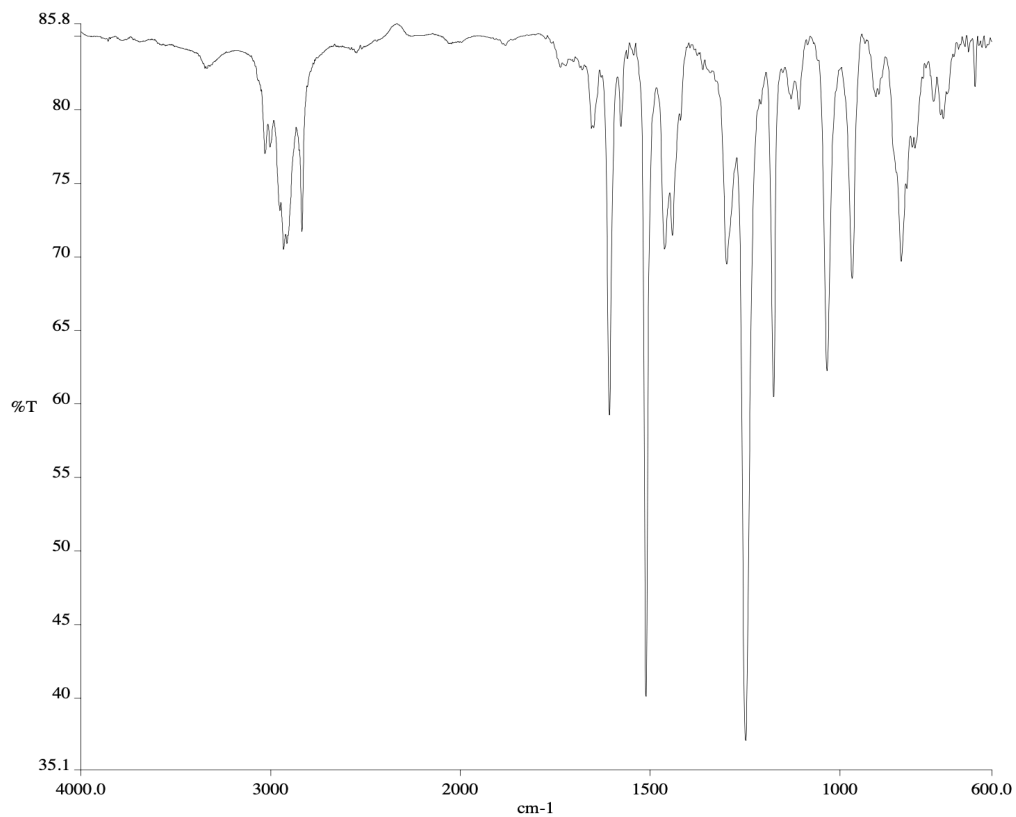


**Figure A4.20** Infrared spectrum (Thin Film, NaCl) of compound **149c**.

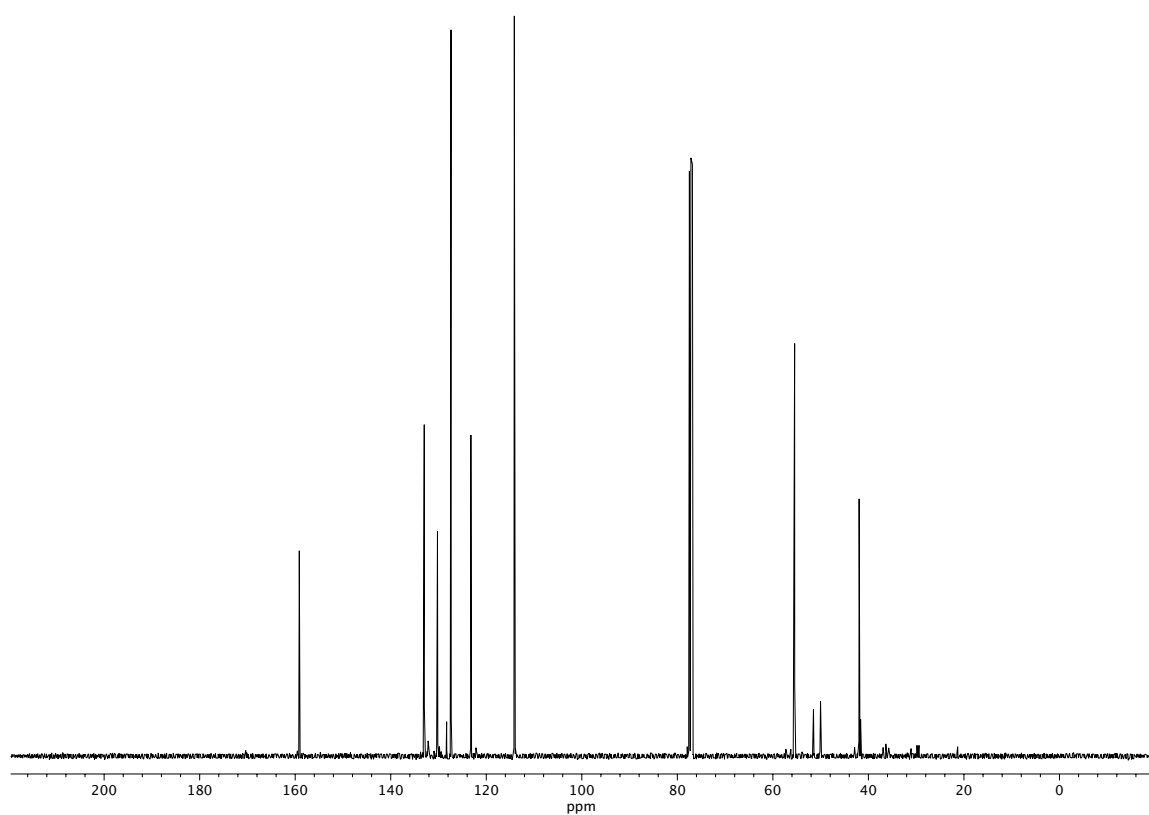


**Figure A4.21** <sup>13</sup>C NMR (100 MHz, CDCl<sub>3</sub>) of compound **149c**.

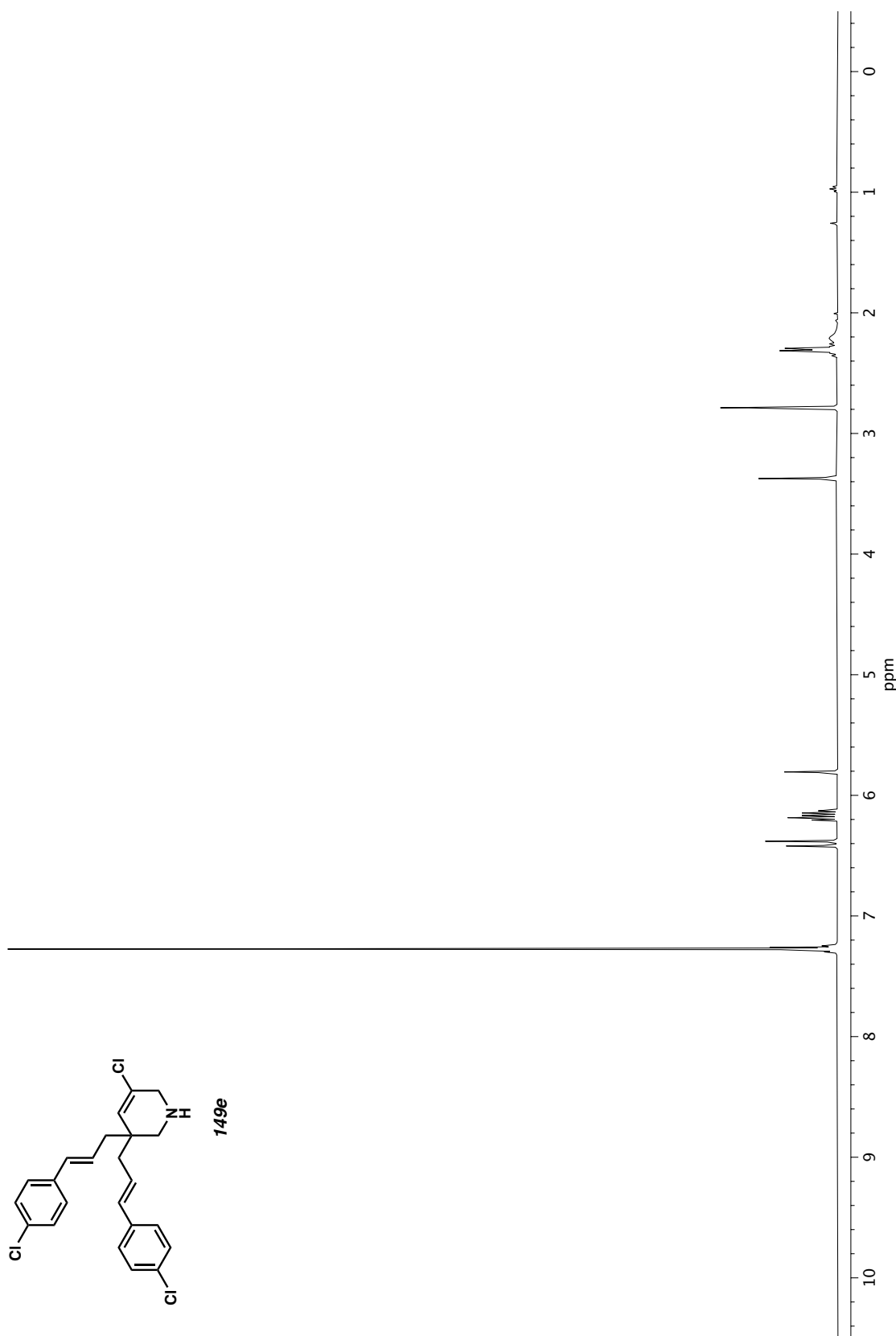




**Figure A4.23** Infrared spectrum (Thin Film, NaCl) of compound **149d**.

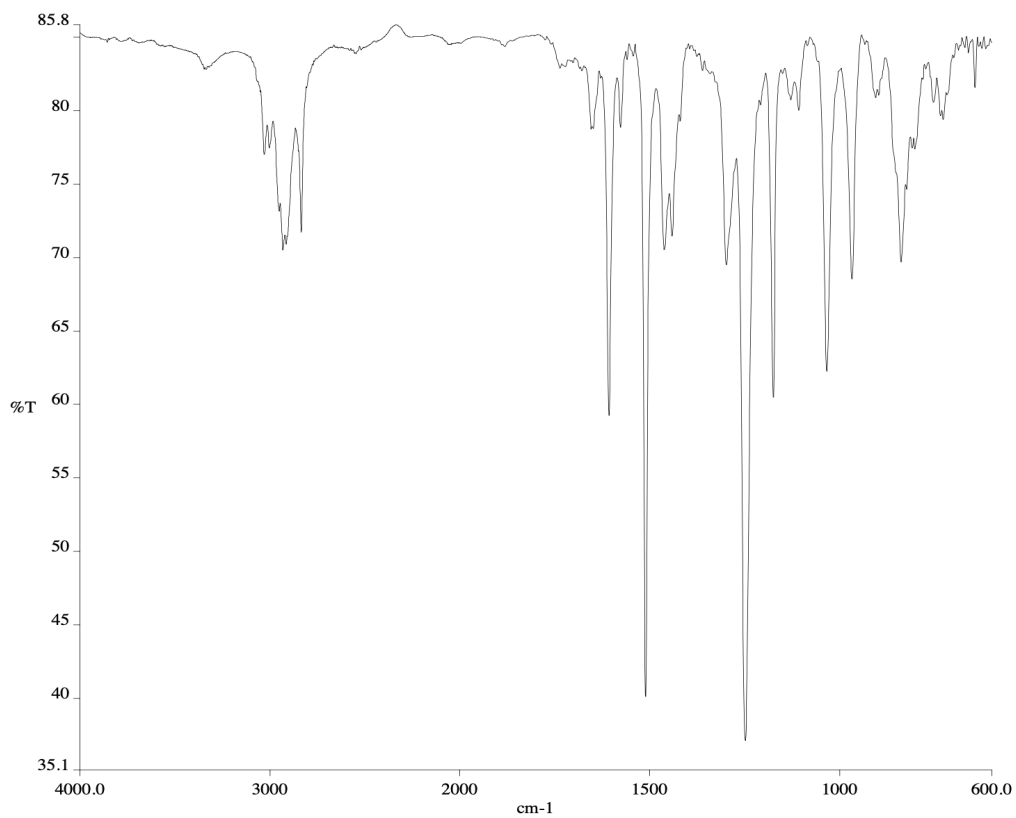


**Figure A4.24** <sup>13</sup>C NMR (100 MHz, CDCl<sub>3</sub>) of compound **149d**.

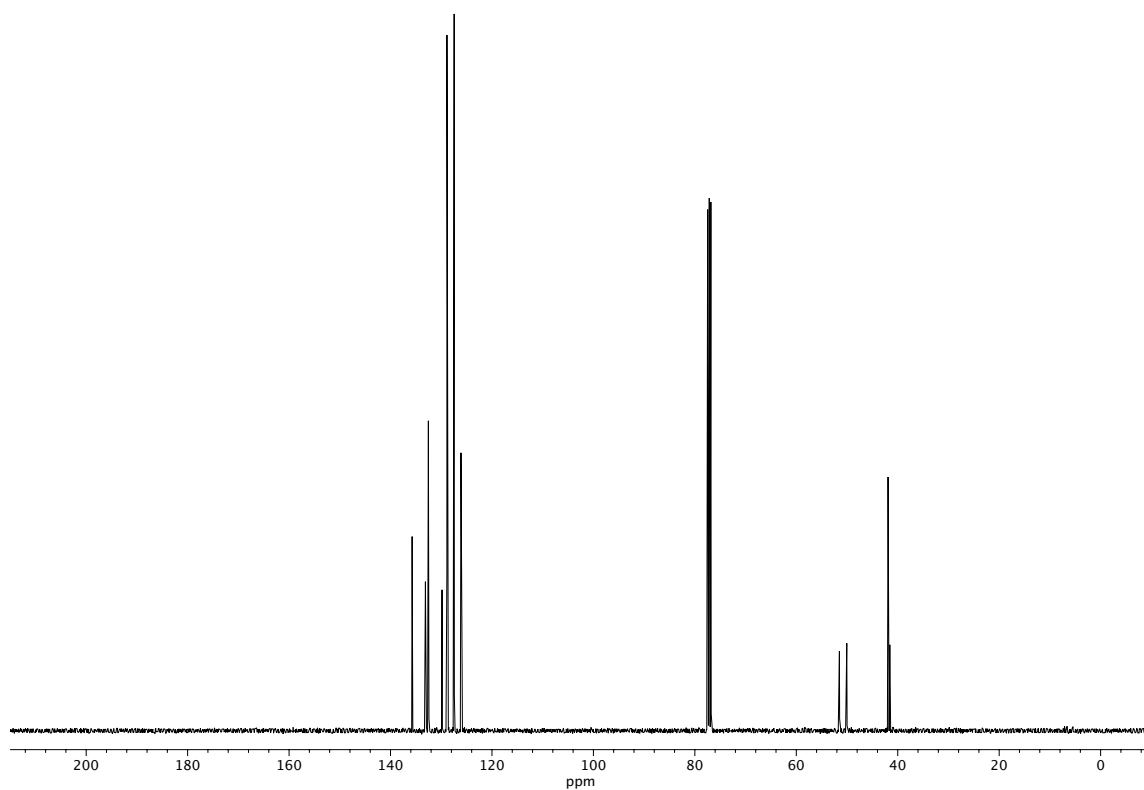


**Figure A4.25** <sup>1</sup>H NMR (400 MHz, CDCl<sub>3</sub>) of compound **149e**.

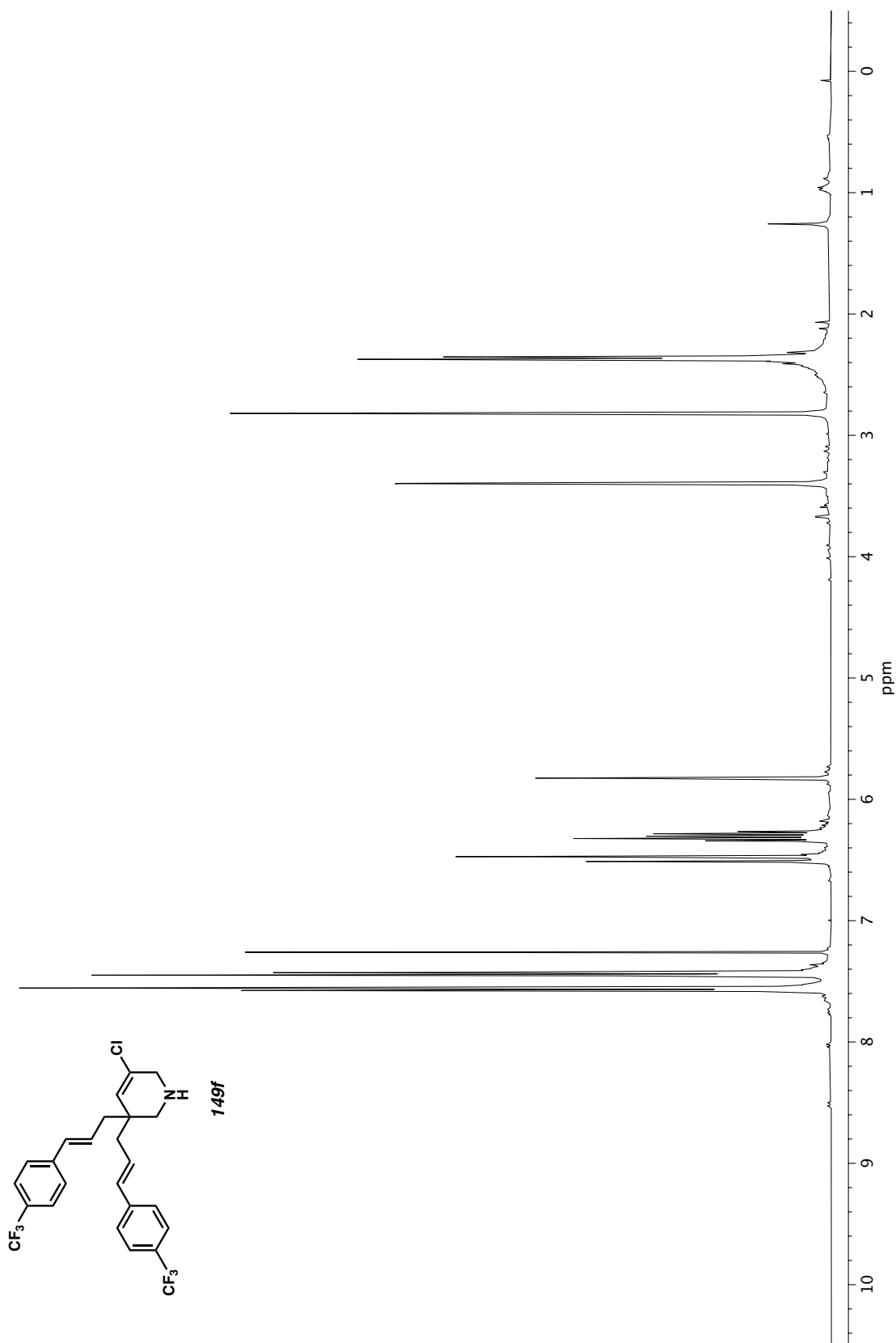




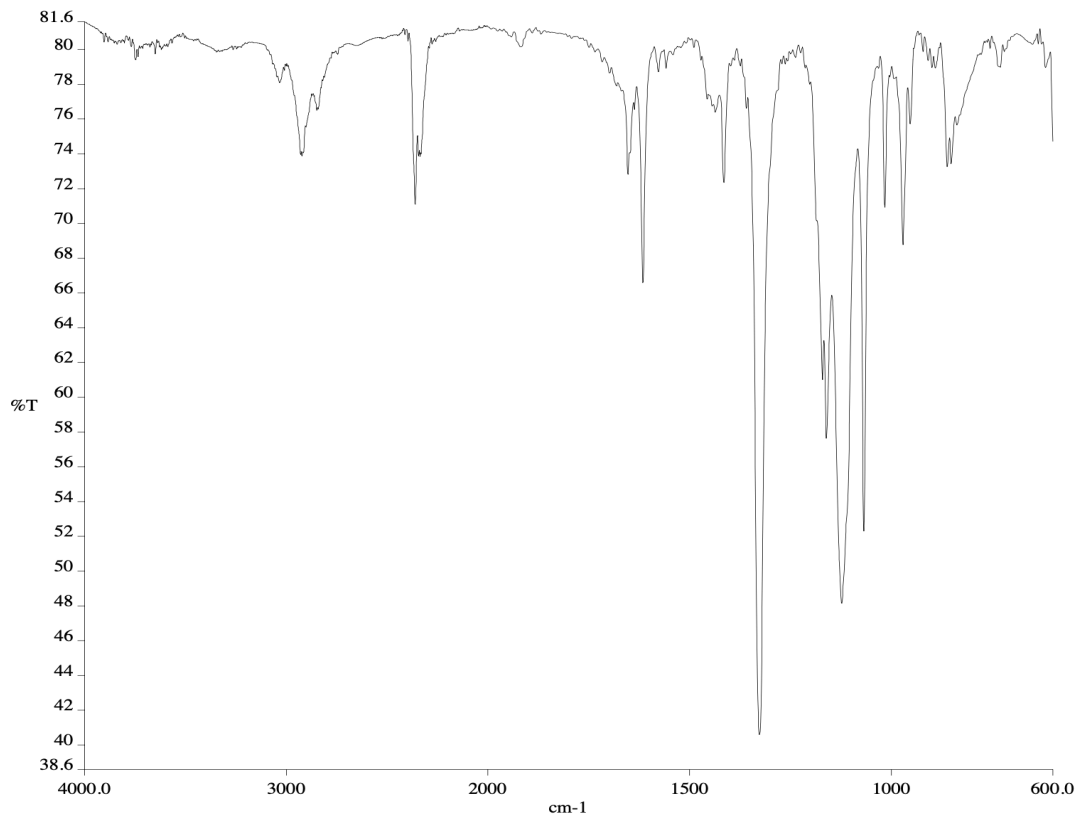
**Figure A4.26** Infrared spectrum (Thin Film, NaCl) of compound **149e**.



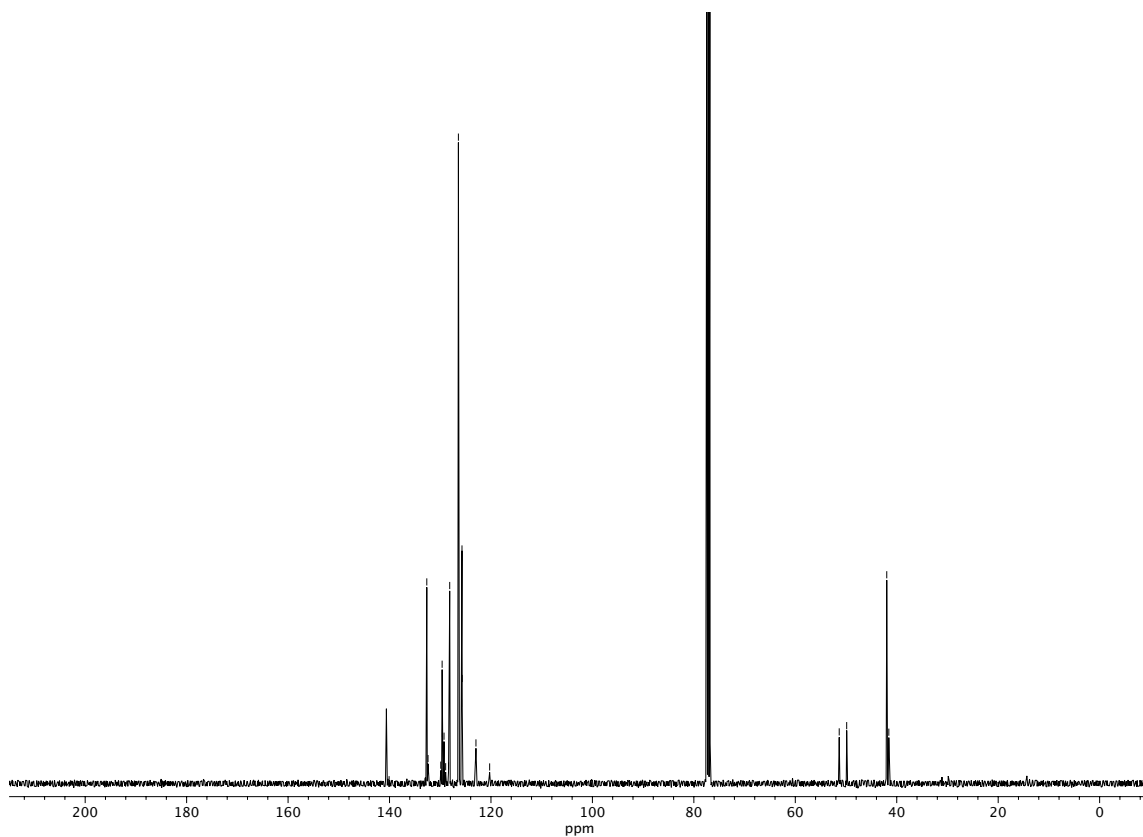
**Figure A4.27** <sup>13</sup>C NMR (100 MHz, CDCl<sub>3</sub>) of compound **149e**.



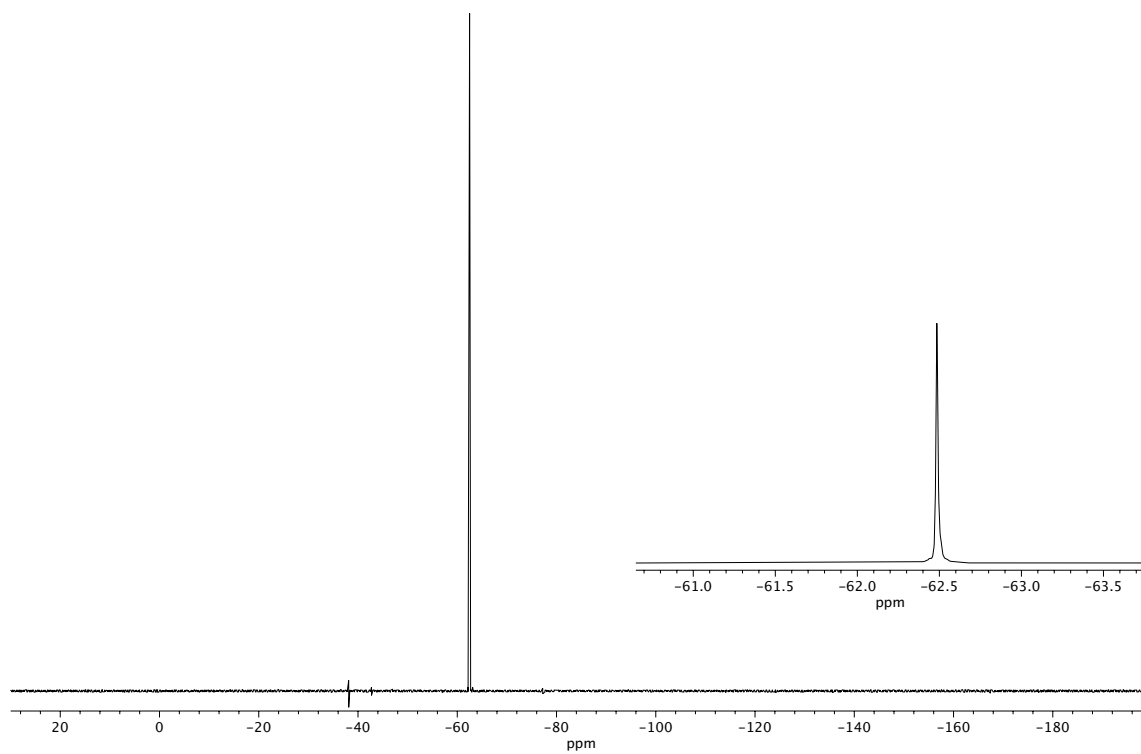
**Figure A4.28**  $^1\text{H}$  NMR (400 MHz,  $\text{CDCl}_3$ ) of compound **149f**.



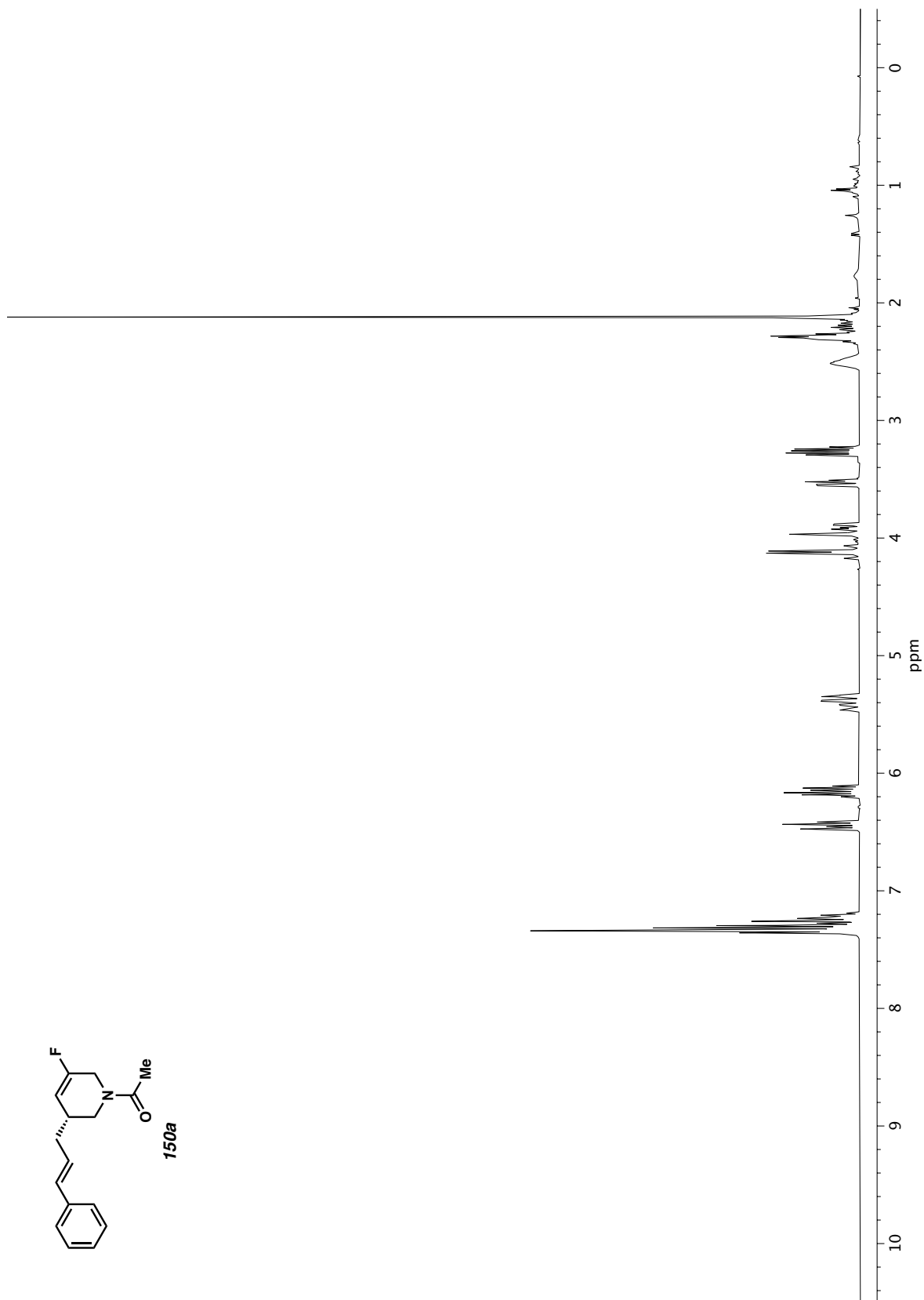
**Figure A4.29** Infrared spectrum (Thin Film, NaCl) of compound **149f**.

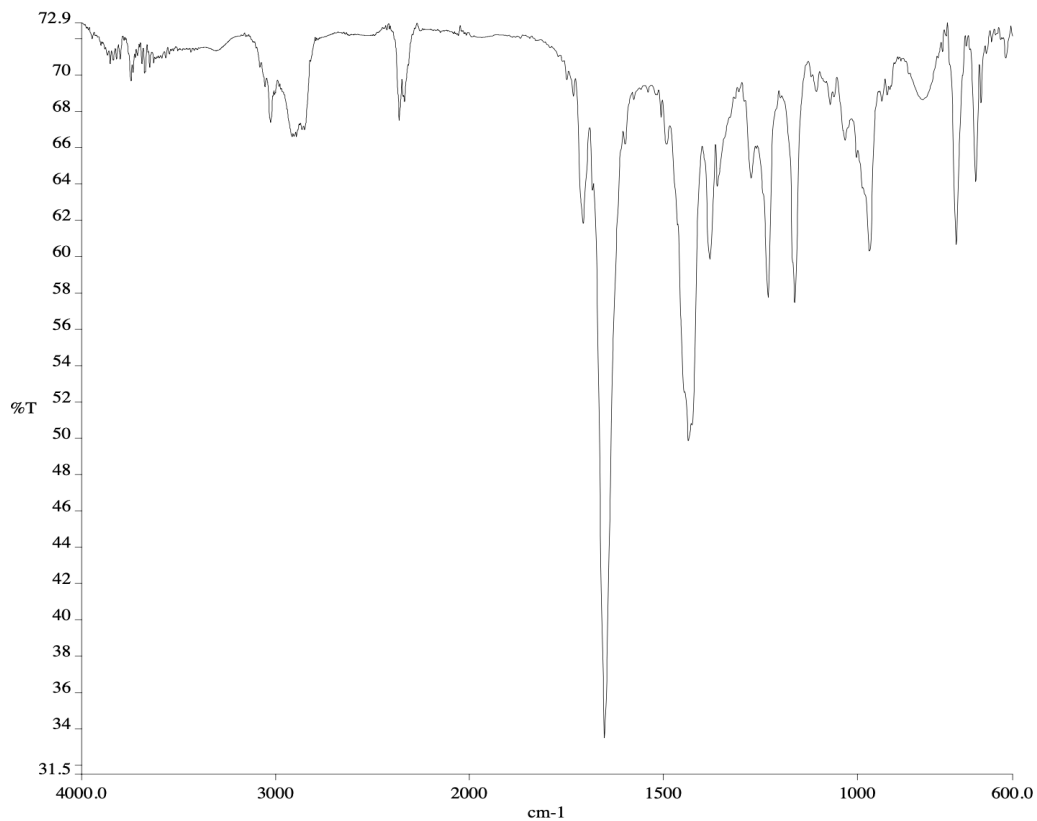


**Figure A4.30** <sup>13</sup>C NMR (100 MHz, CDCl<sub>3</sub>) of compound **149f**.

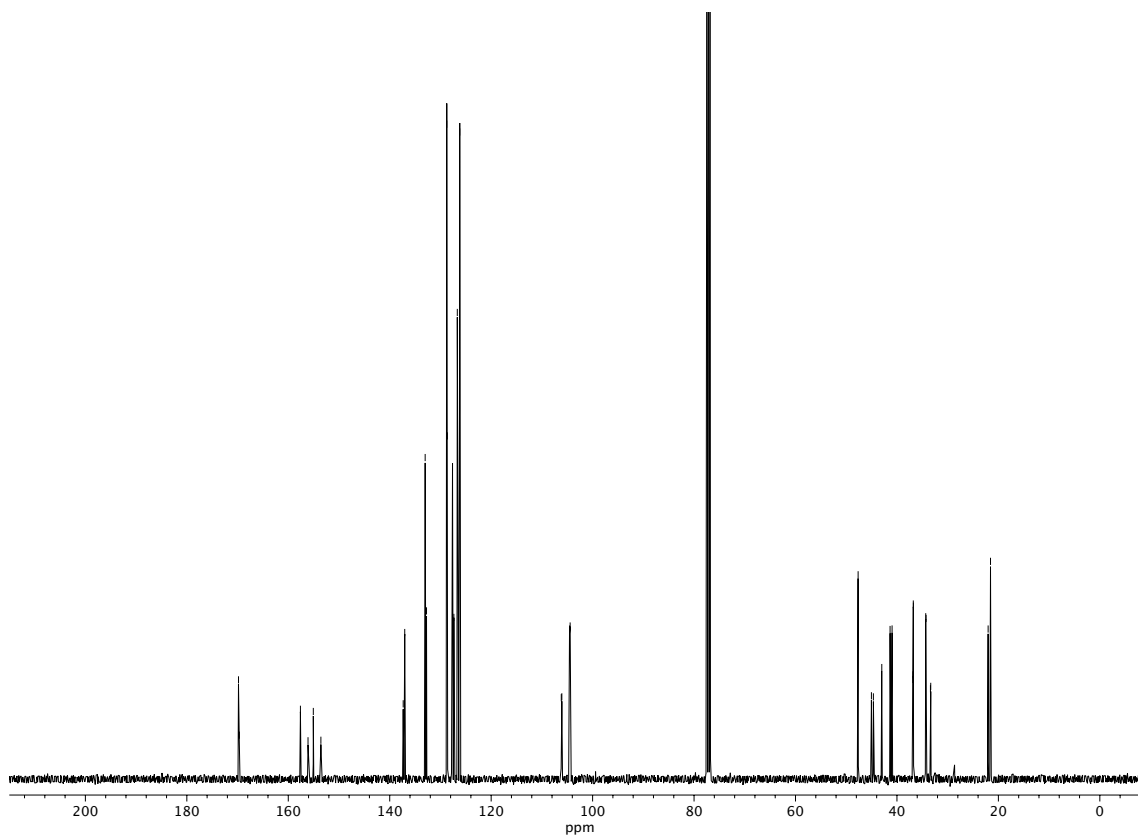


**Figure A4.31**  $^{19}\text{F}$  NMR (282 MHz,  $\text{CDCl}_3$ ) of compound **149f**.

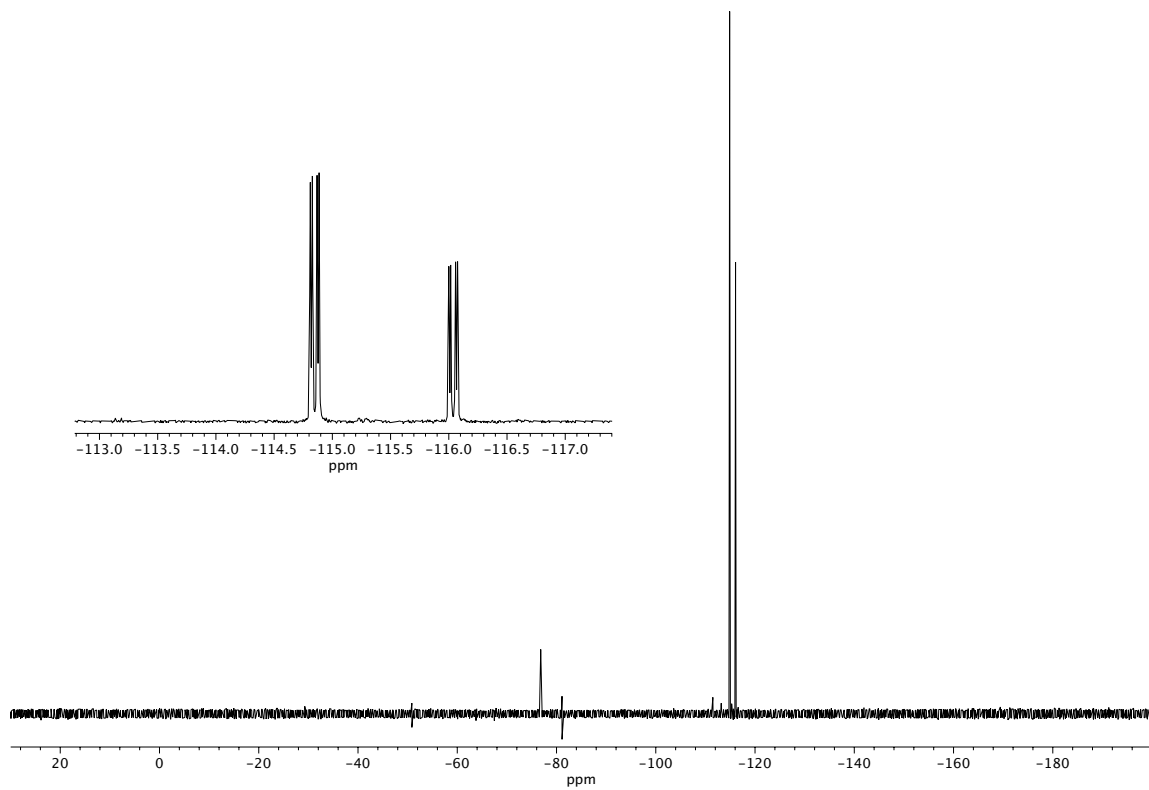




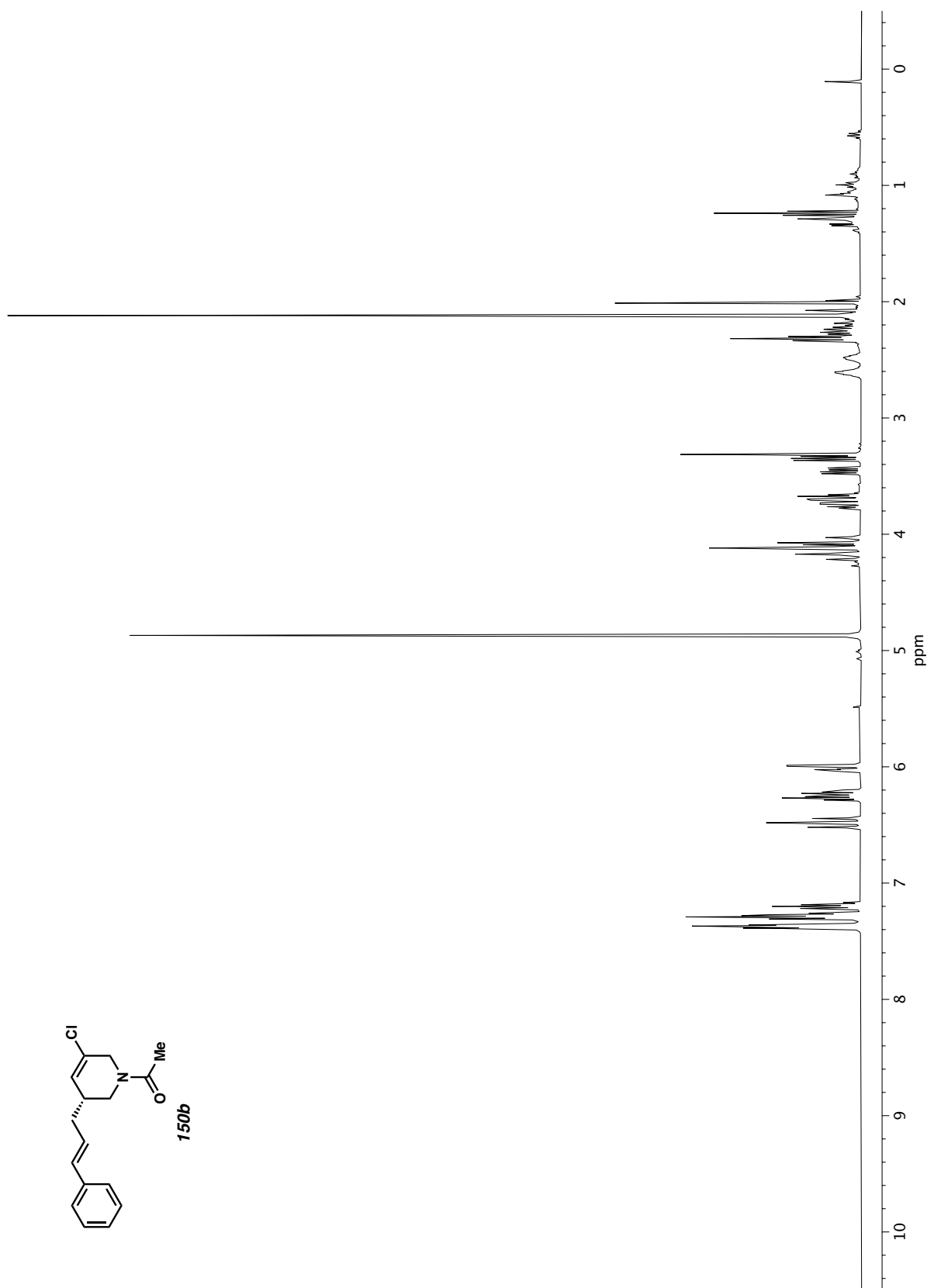
**Figure A4.33** Infrared spectrum (Thin Film, NaCl) of compound **150a**.



**Figure A4.34** <sup>13</sup>C NMR (100 MHz, CDCl<sub>3</sub>) of compound **150a**.

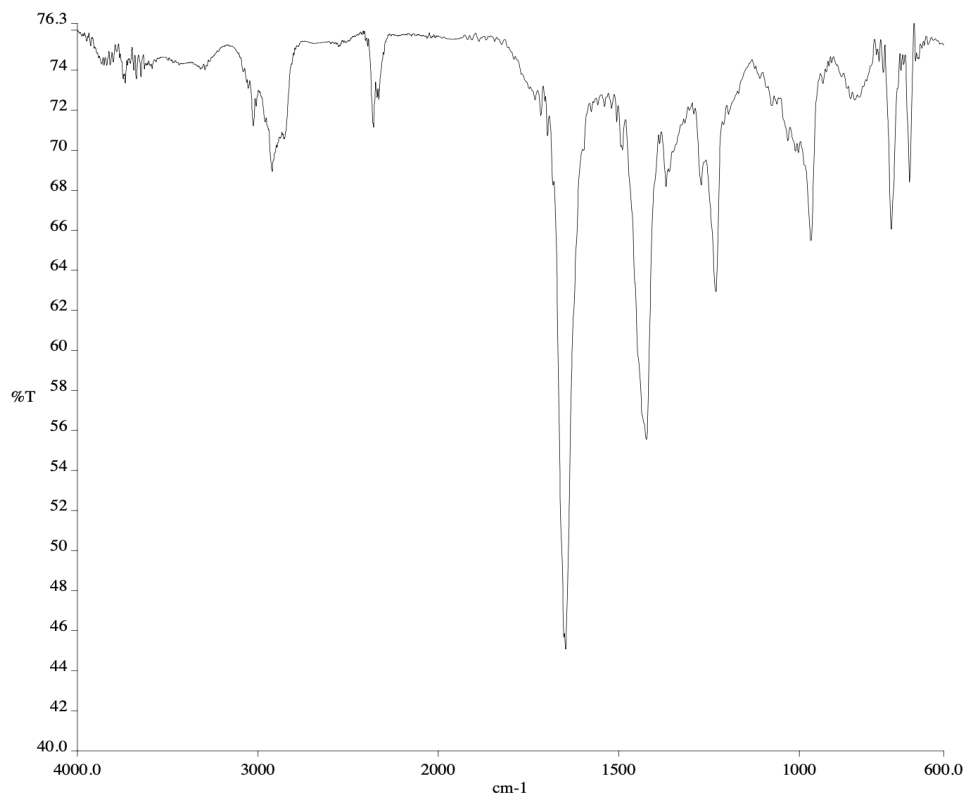


**Figure A4.35**  $^{19}\text{F}$  NMR (282 MHz,  $\text{CDCl}_3$ ) of compound **150a**.

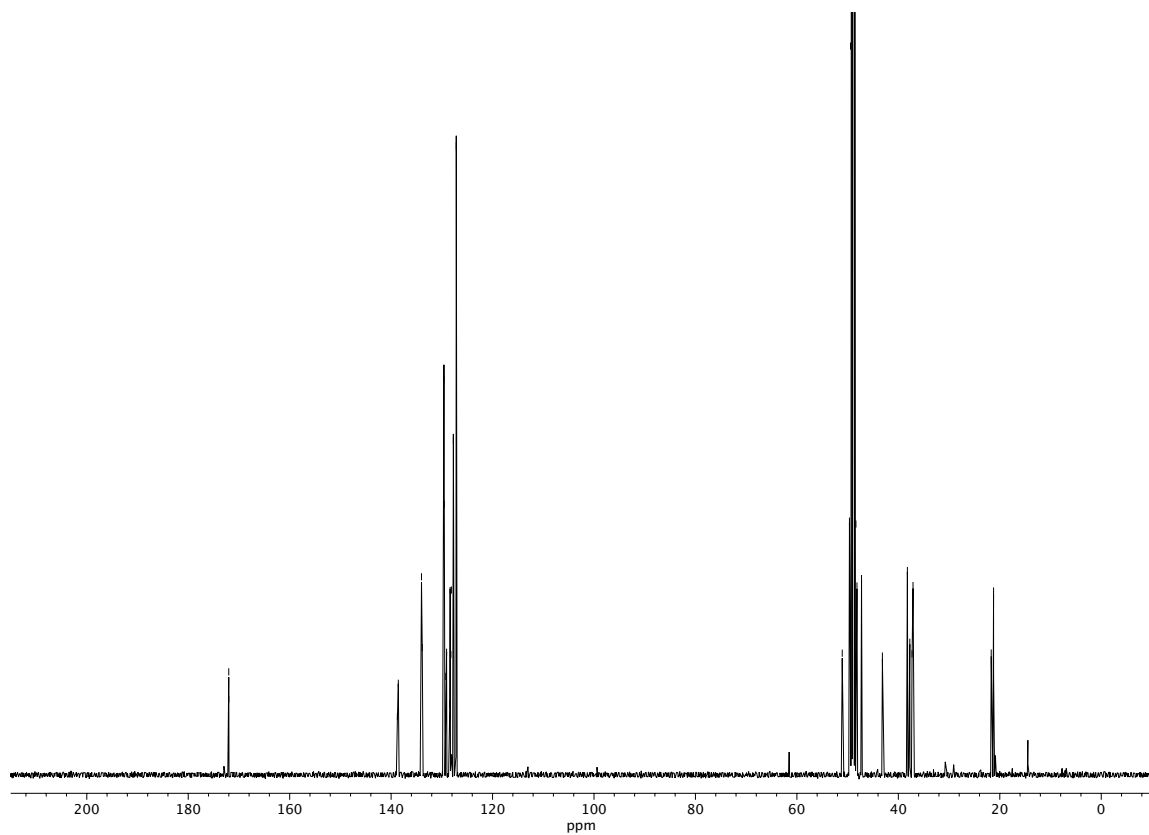


**Figure A4.36**  $^1\text{H}$  NMR (400 MHz,  $\text{CD}_3\text{OD}$ ) of compound **150b**.

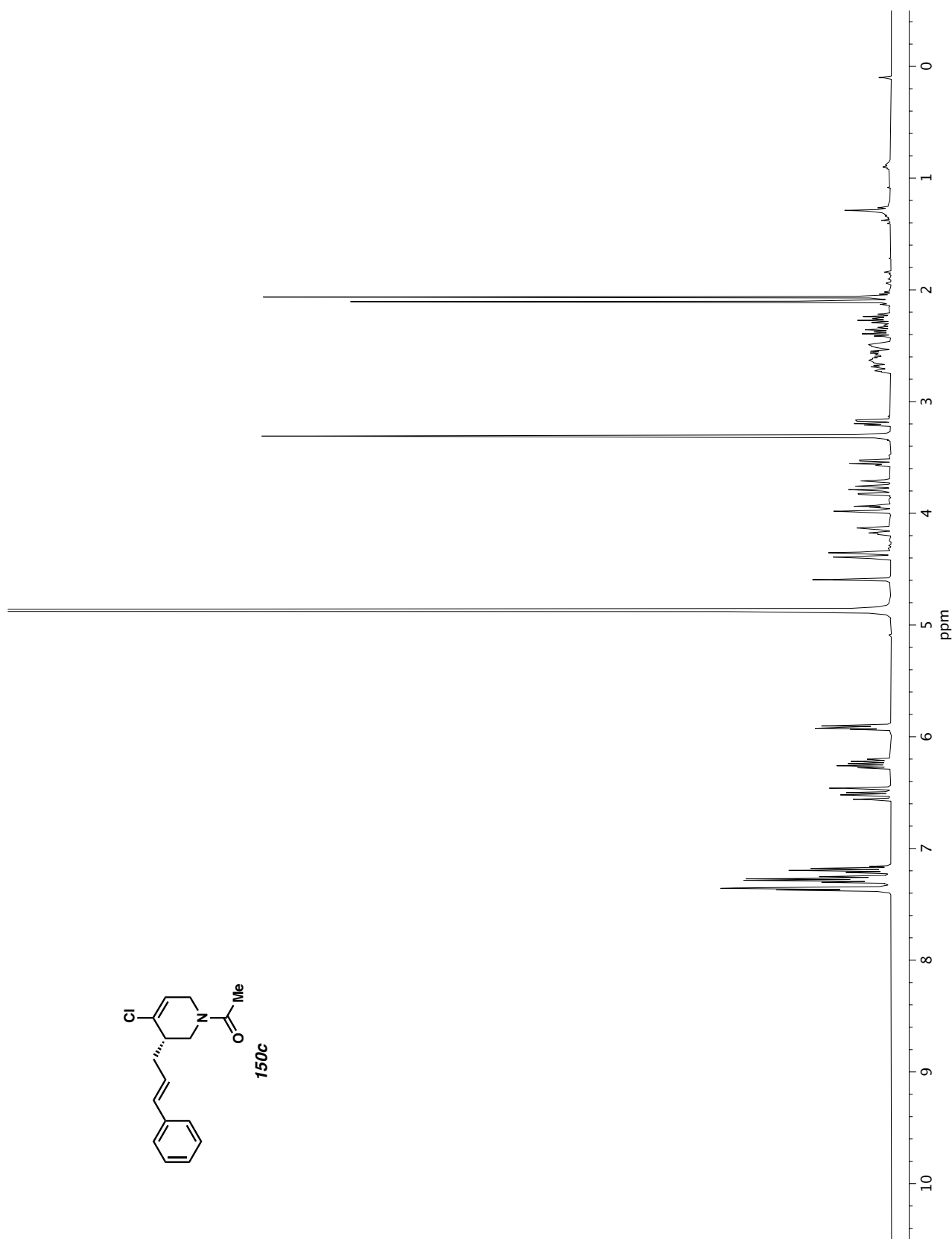




**Figure A4.37** Infrared spectrum (Thin Film, NaCl) of compound **150b**.



**Figure A4.38** <sup>13</sup>C NMR (100 MHz, CD<sub>3</sub>OD) of compound **150b**.



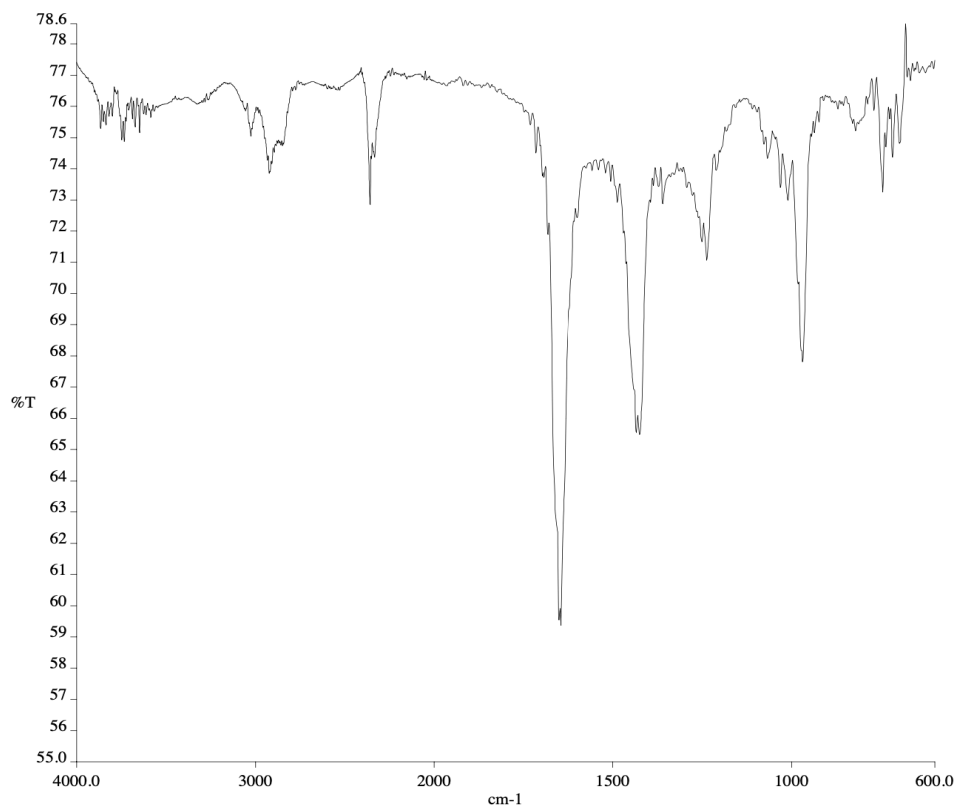


**Figure A4.40** Infrared spectrum (Thin Film, NaCl) of compound **150c**.

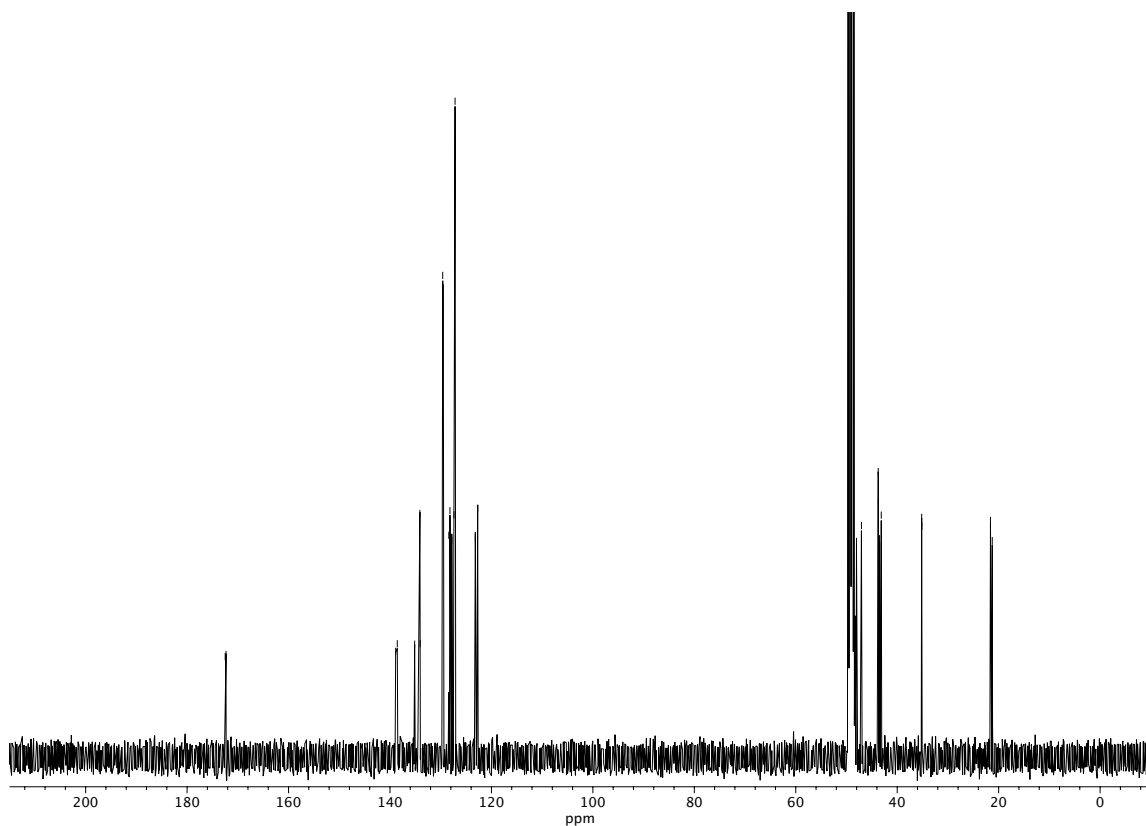


**Figure A4.41** <sup>13</sup>C NMR (100 MHz, CD<sub>3</sub>OD) of compound **150c**.

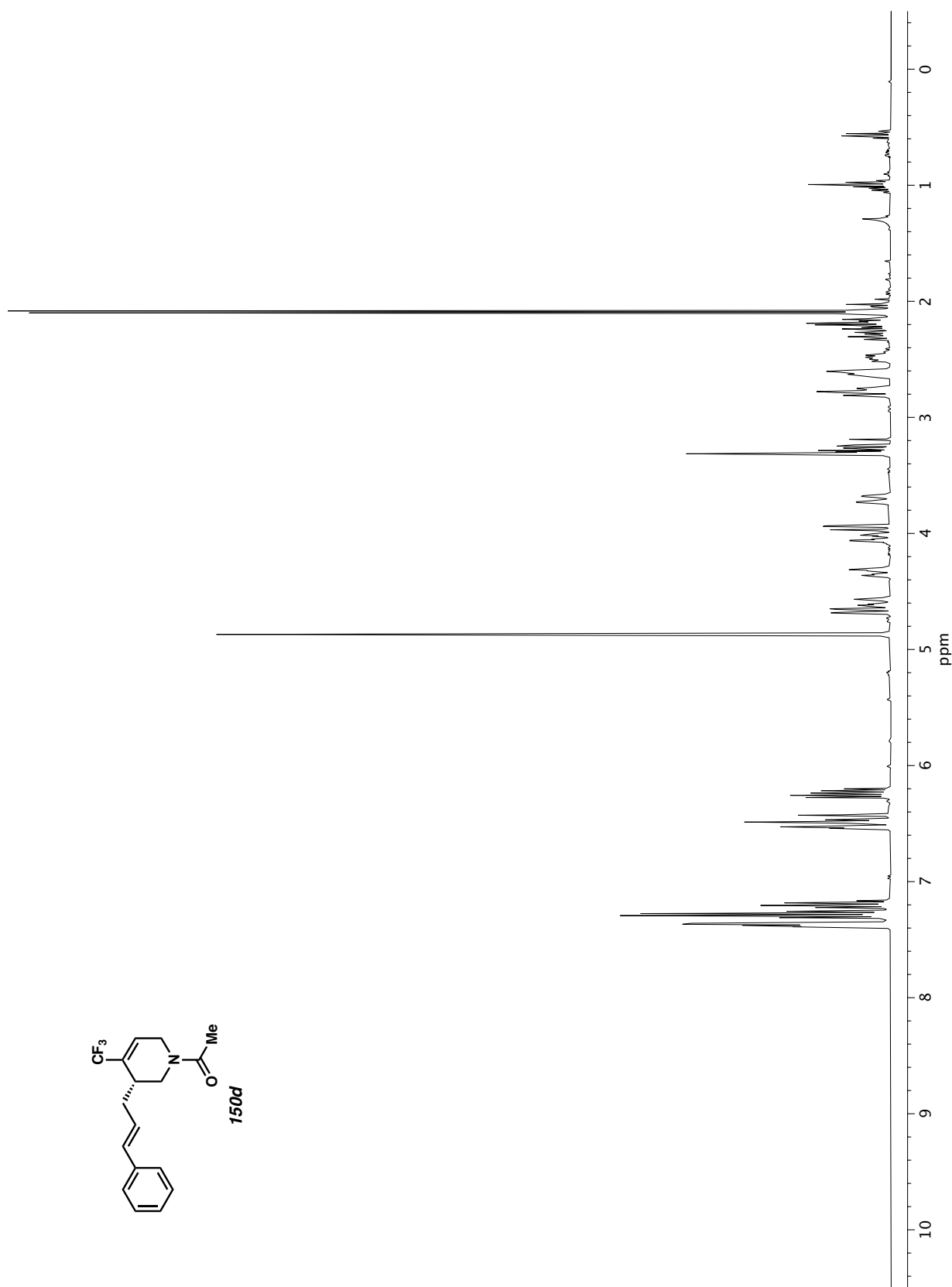


**Figure A4.42**  $^1\text{H}$  NMR (400 MHz,  $\text{CD}_3\text{OD}$ ) of compound **150d**.

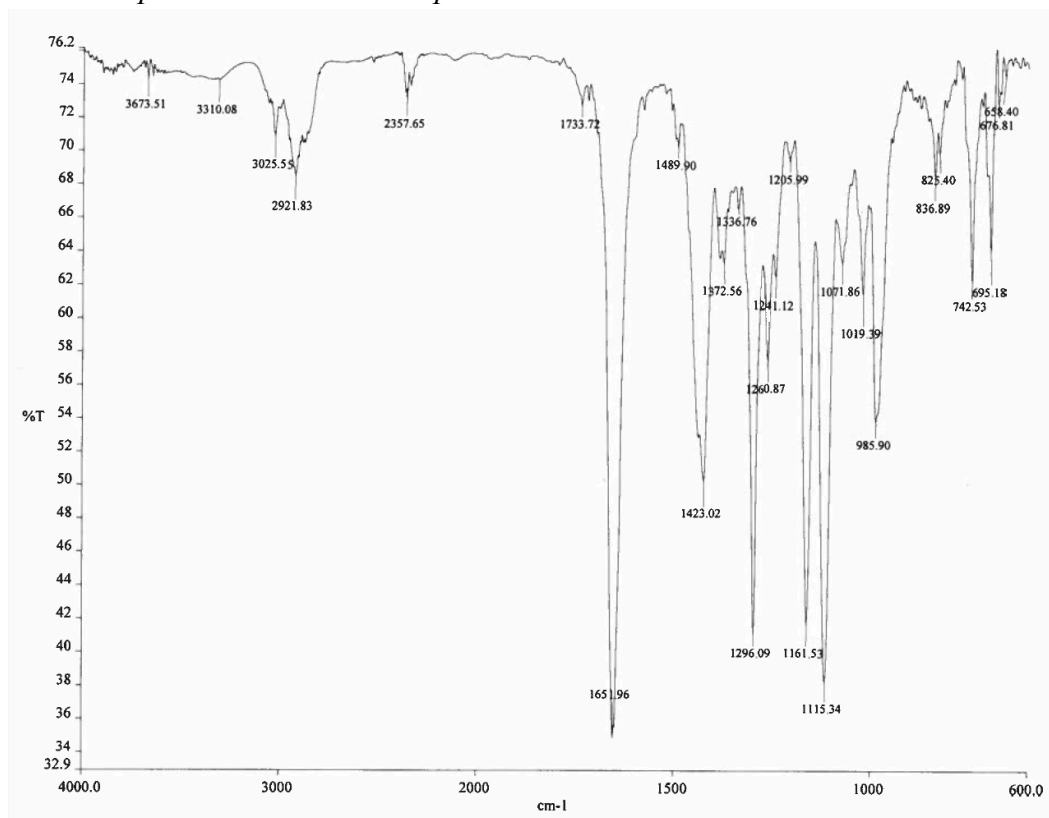


Figure A4.43 Infrared spectrum (Thin Film, NaCl) of compound **150d**.

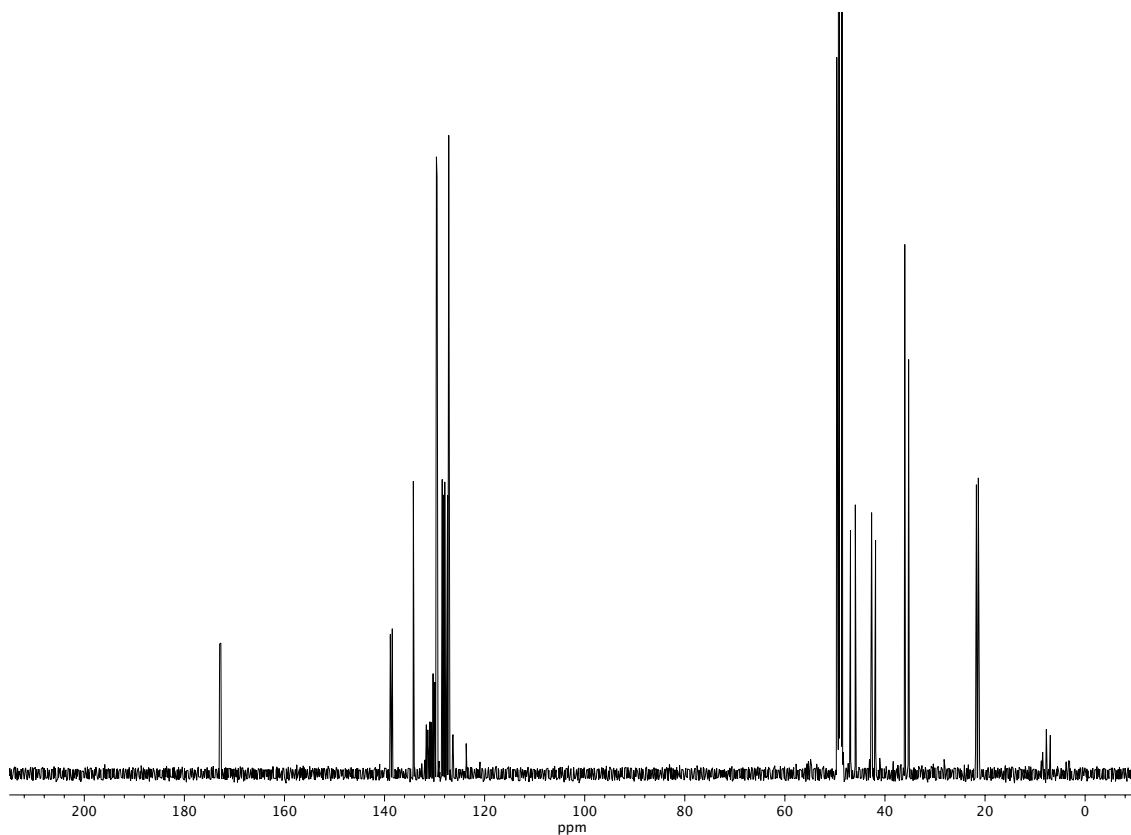


Figure A4.44 <sup>13</sup>C NMR (100 MHz, CD<sub>3</sub>OD) of compound **150d**.

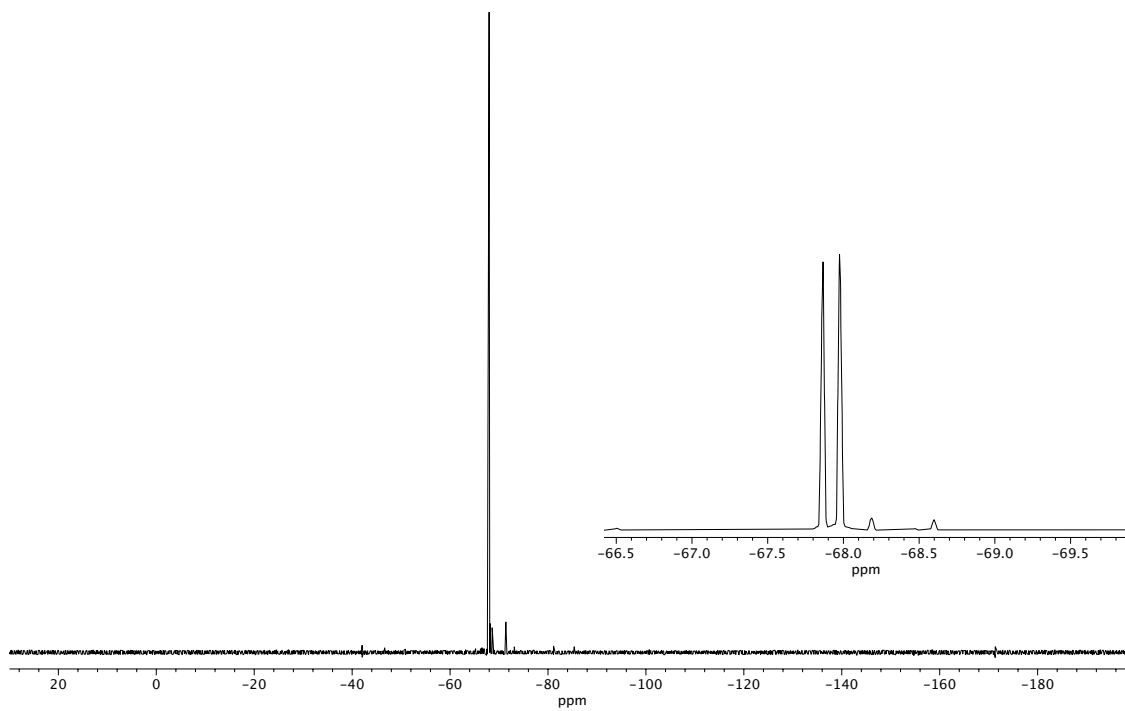
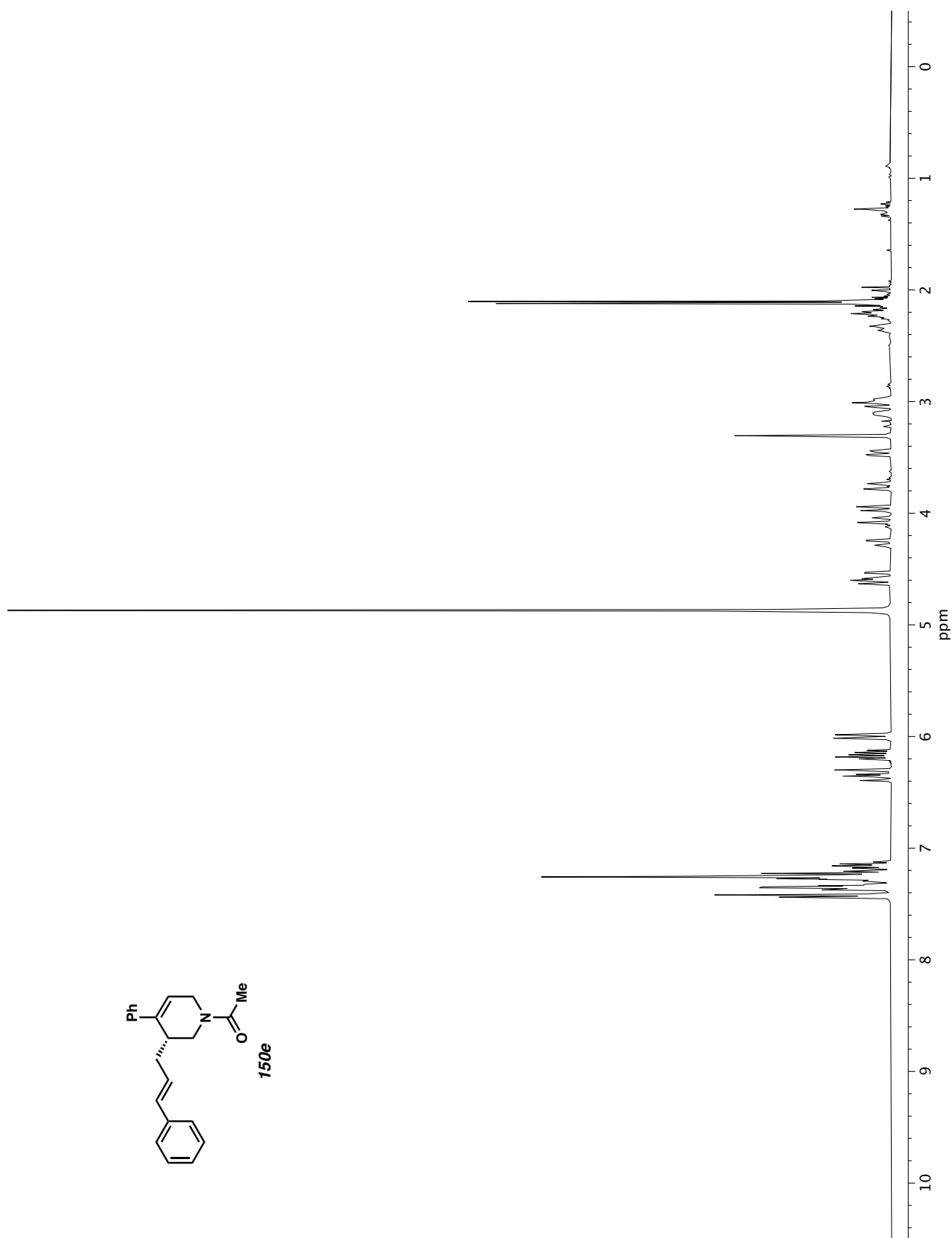


Figure A4.45  $^{19}\text{F}$  NMR (282 MHz,  $\text{CD}_3\text{OD}$ ) of compound 150d.



**Figure A4.46**  $^1\text{H}$  NMR (400 MHz,  $\text{CD}_3\text{OD}$ ) of compound **150e**.

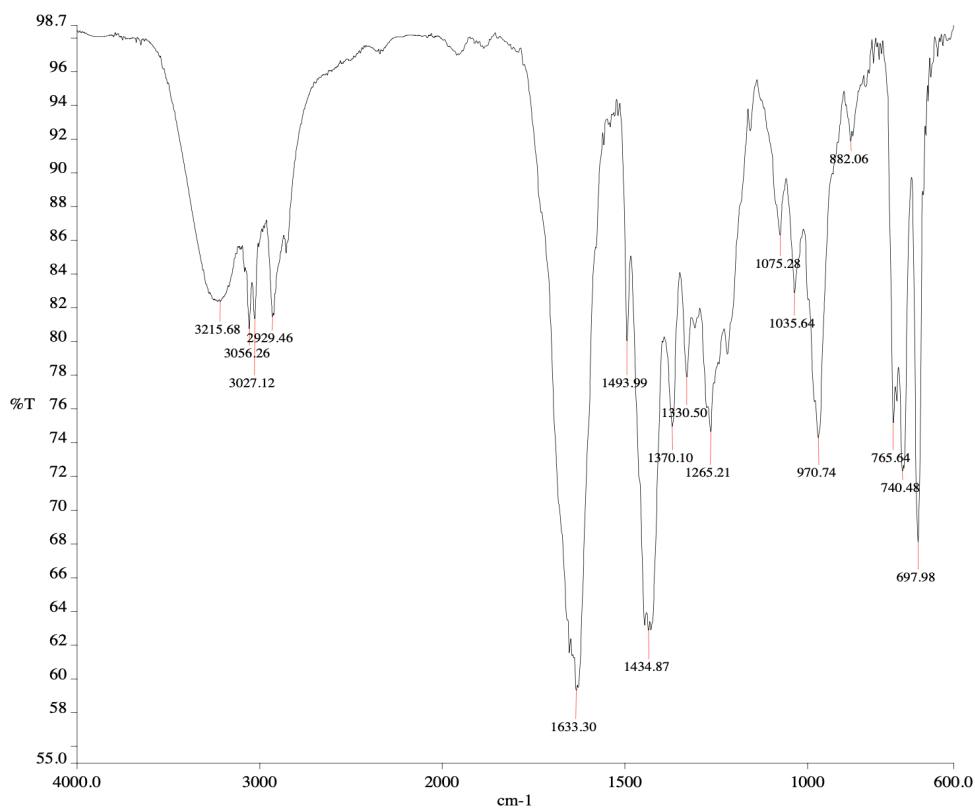


Figure A4.47 Infrared spectrum (Thin Film, NaCl) of compound **150e**.

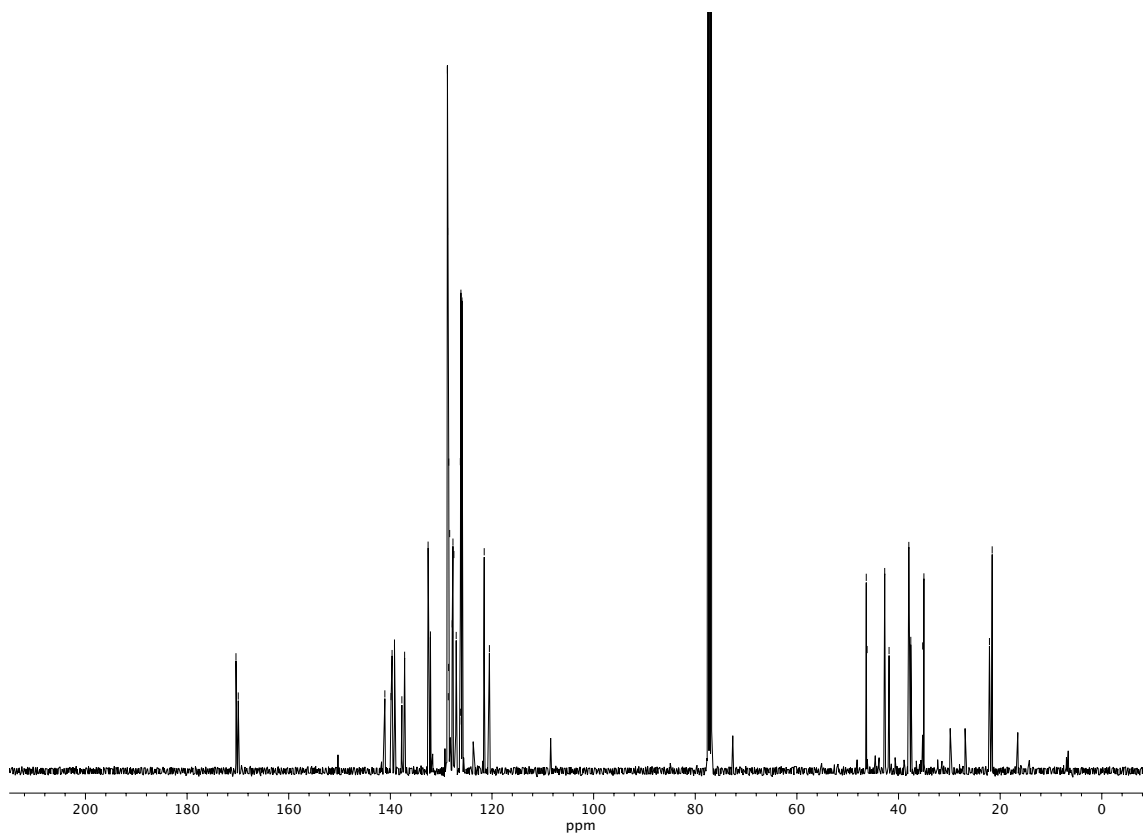
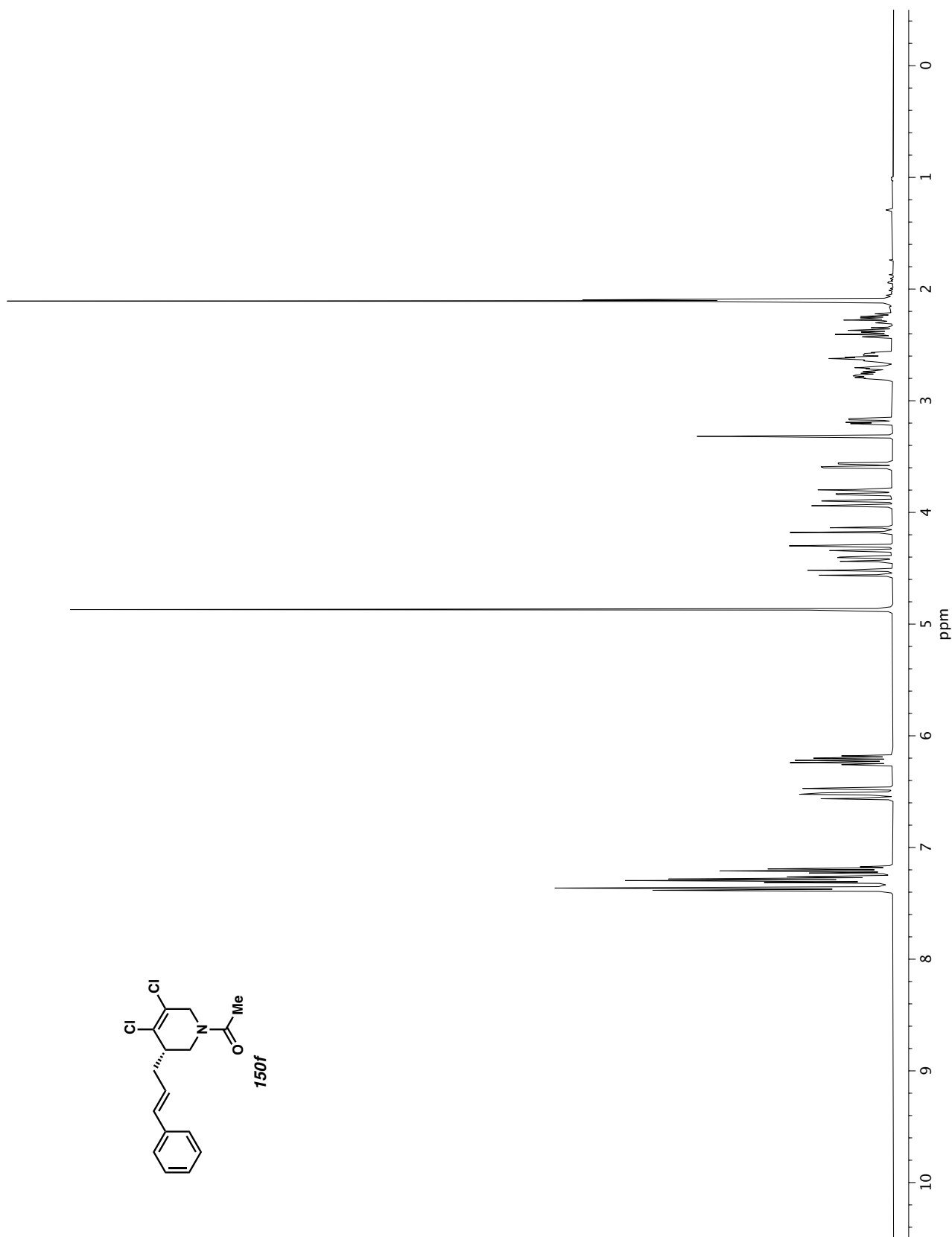


Figure A4.48 <sup>13</sup>C NMR (100 MHz, CDCl<sub>3</sub>) of compound **150e**.





**Figure A4.49**  $^1\text{H}$  NMR (400 MHz,  $\text{CD}_3\text{OD}$ ) of compound **150f**.

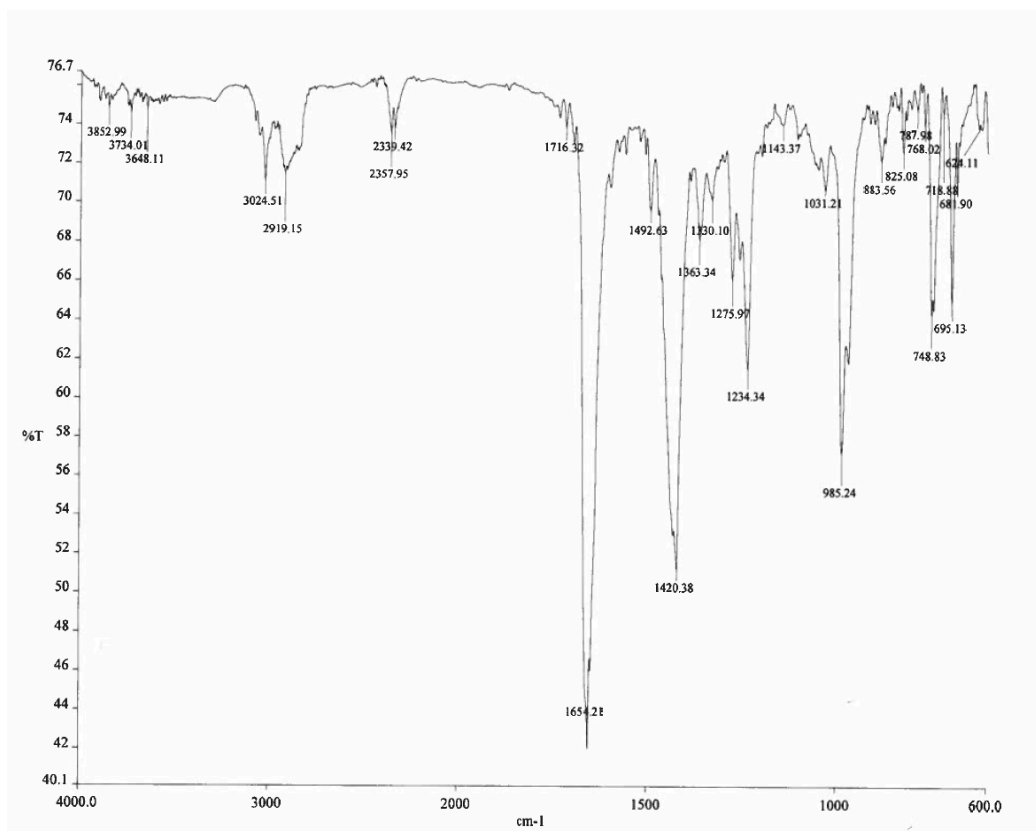


Figure A4.50 Infrared spectrum (Thin Film, NaCl) of compound **150f**.

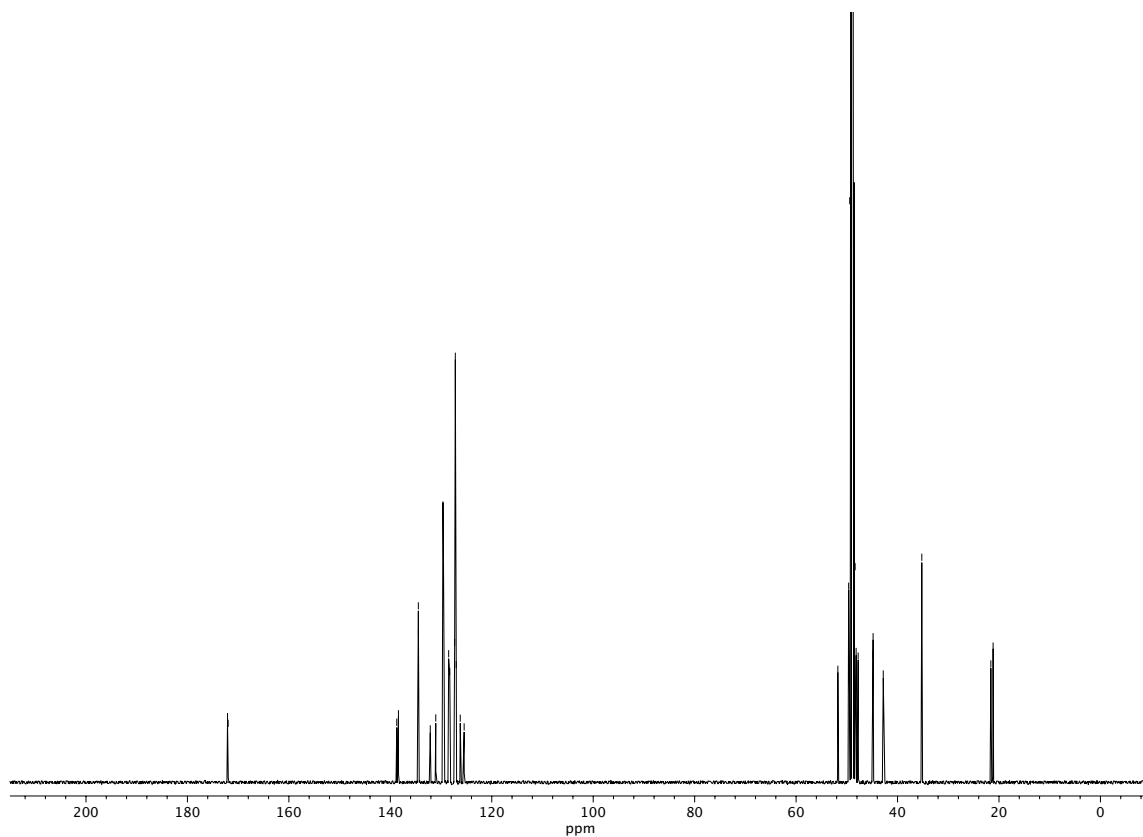
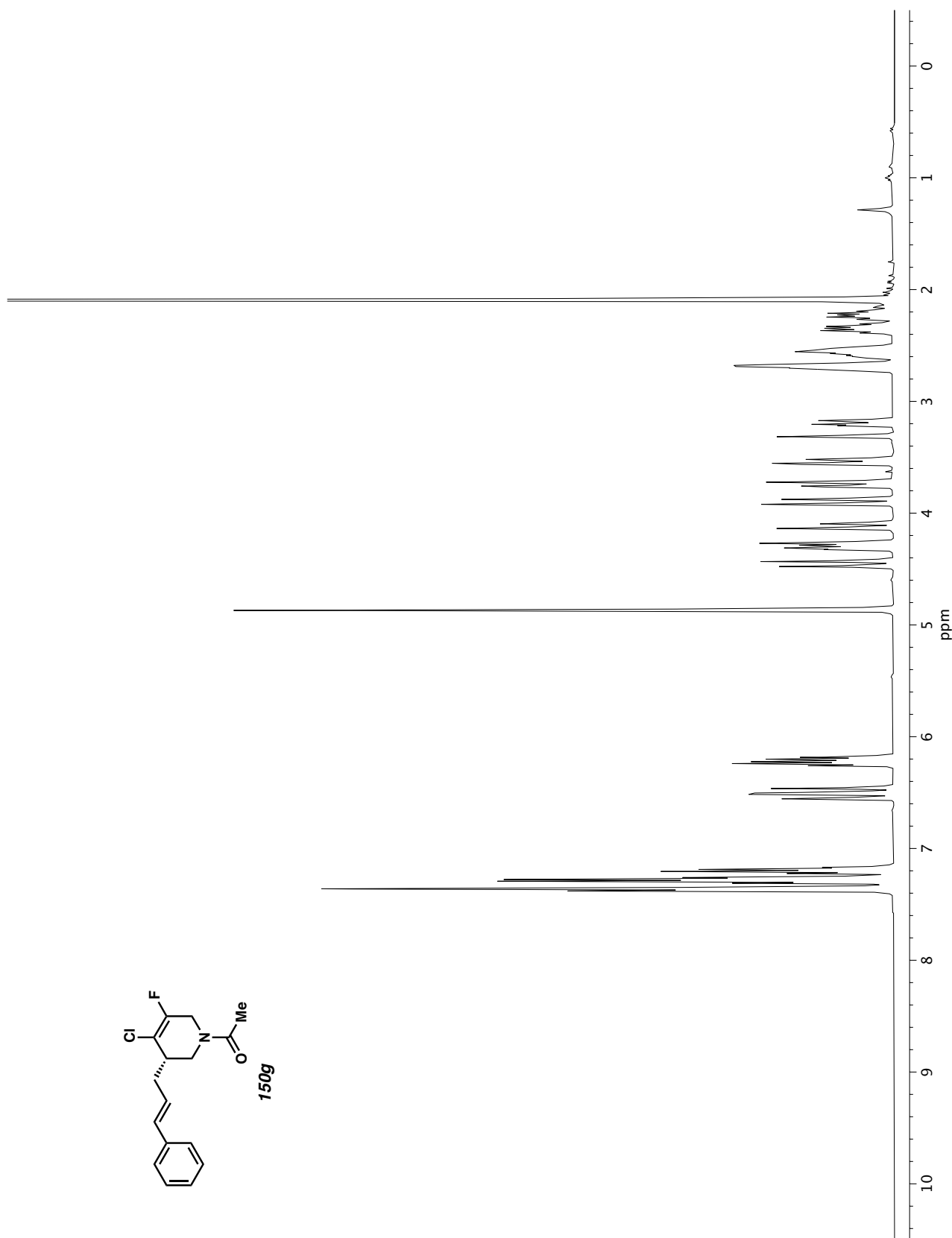
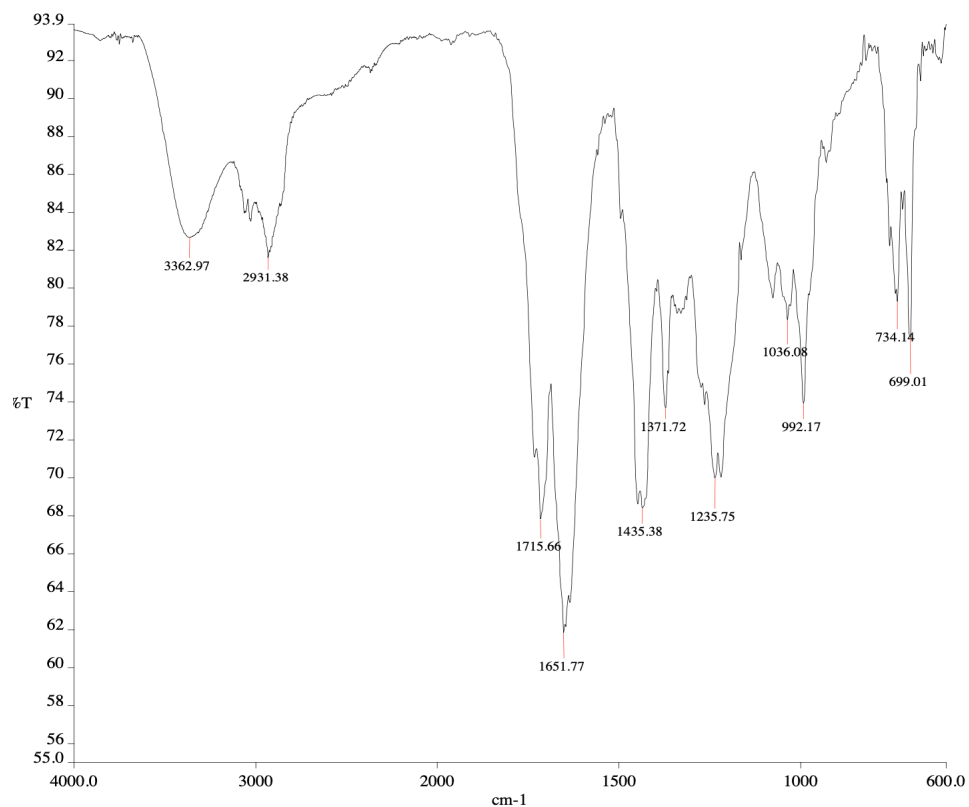


Figure A4.51 <sup>13</sup>C NMR (100 MHz, CD<sub>3</sub>OD) of compound **150f**.



**Figure A4.52**  $^1\text{H}$  NMR (400 MHz,  $\text{CD}_3\text{OD}$ ) of compound **150g**.



**Figure A4.53** Infrared spectrum (Thin Film, NaCl) of compound **150g**.

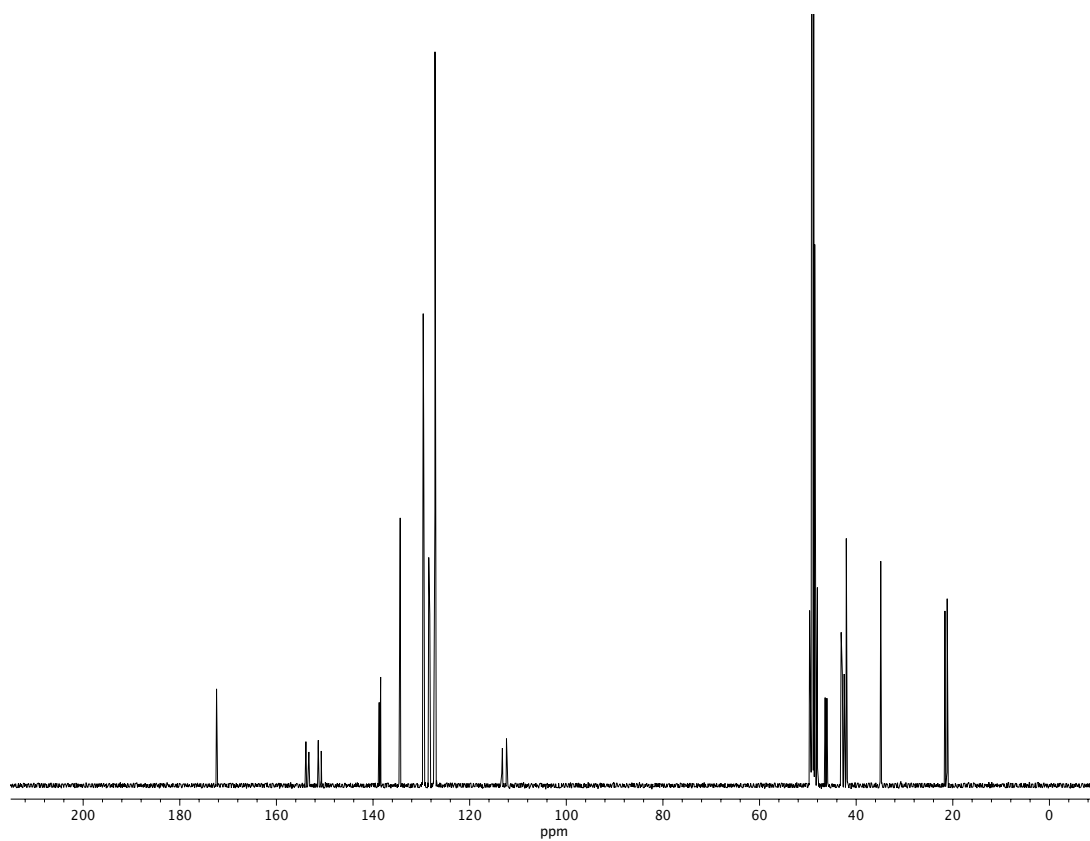


**Figure A4.54** <sup>13</sup>C NMR (100 MHz, CD<sub>3</sub>OD) of compound **150g**.

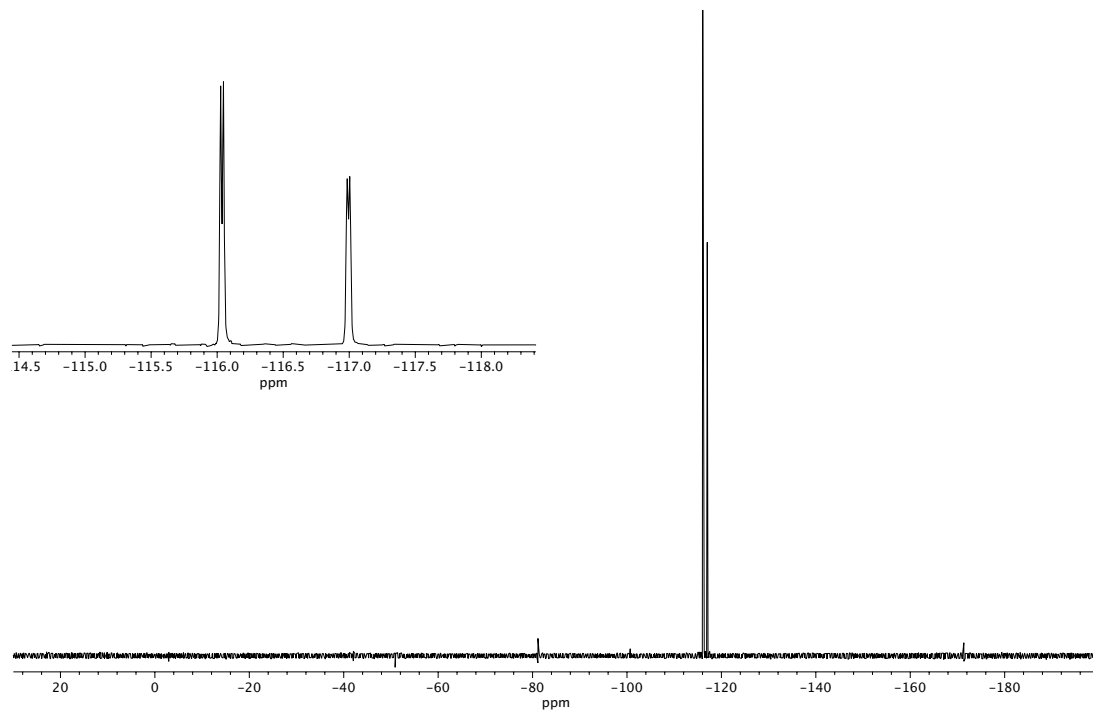


**Figure A4.55**  $^{19}\text{F}$  NMR (282 MHz,  $\text{CD}_3\text{OD}$ ) of compound **150g**.

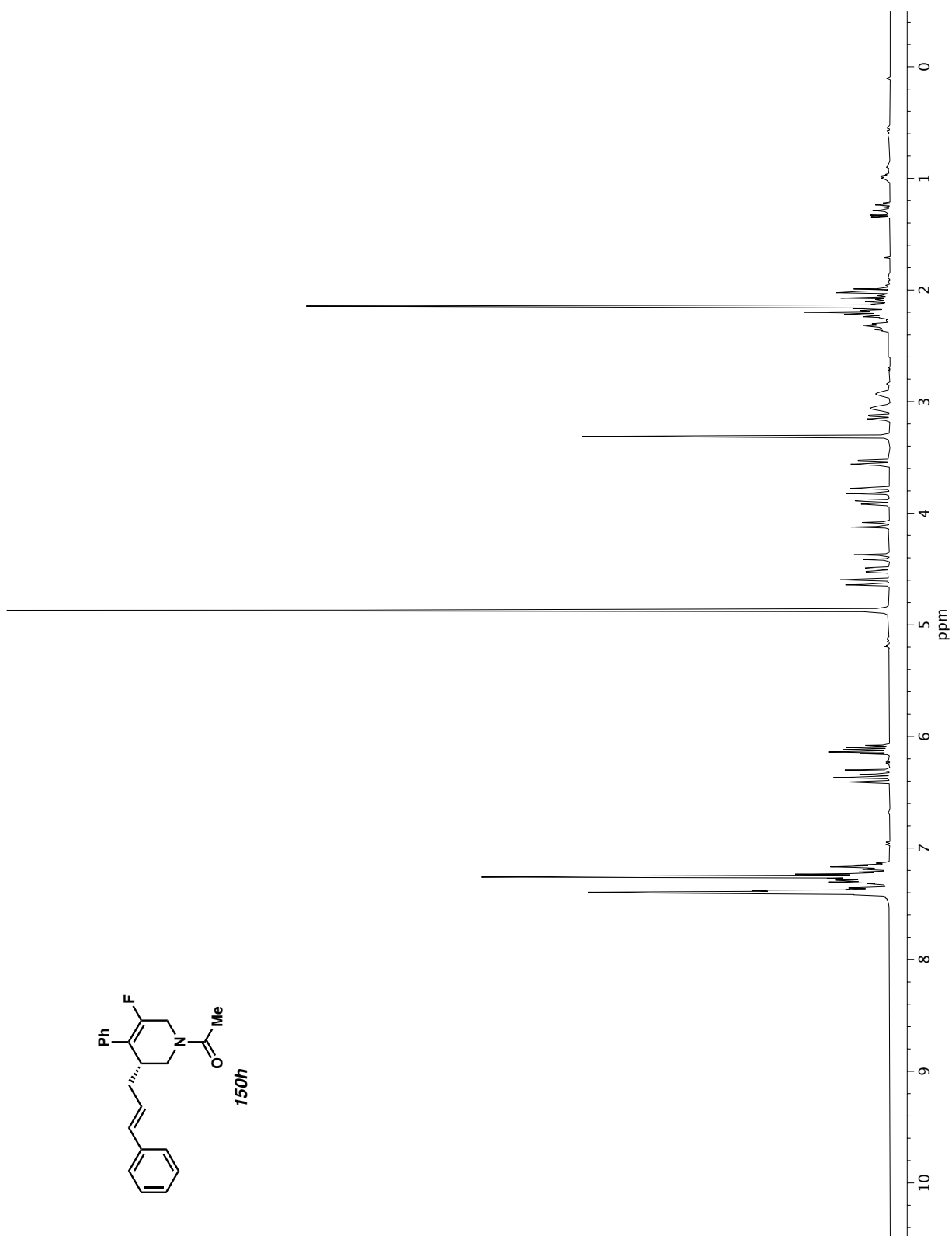


**Figure A4.56**  $^1\text{H NMR}$  (400 MHz,  $\text{CD}_3\text{OD}$ ) of compound **150h**.

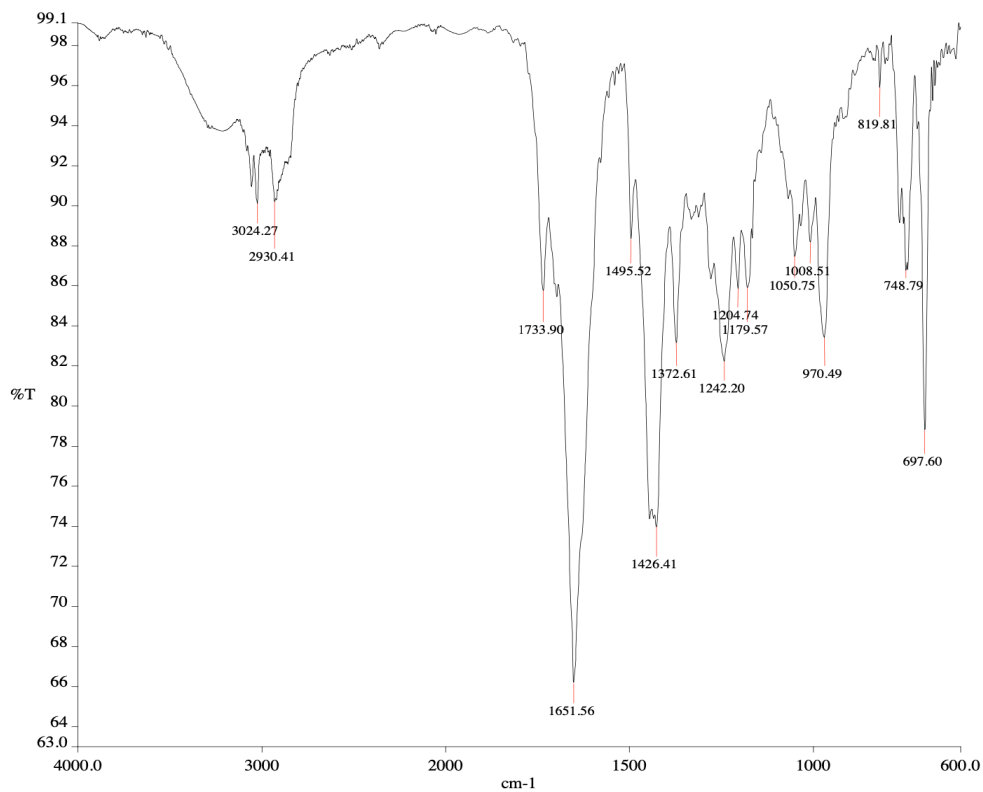


Figure A4.57 Infrared spectrum (Thin Film, NaCl) of compound **150h**.

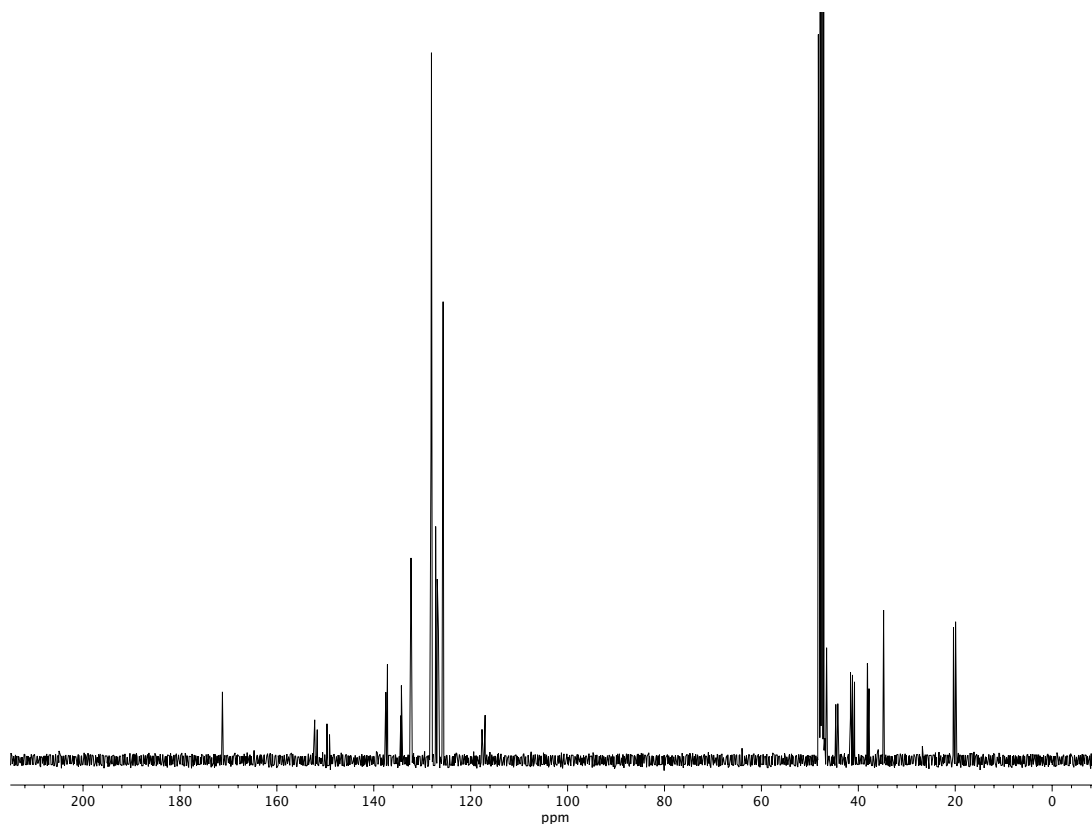
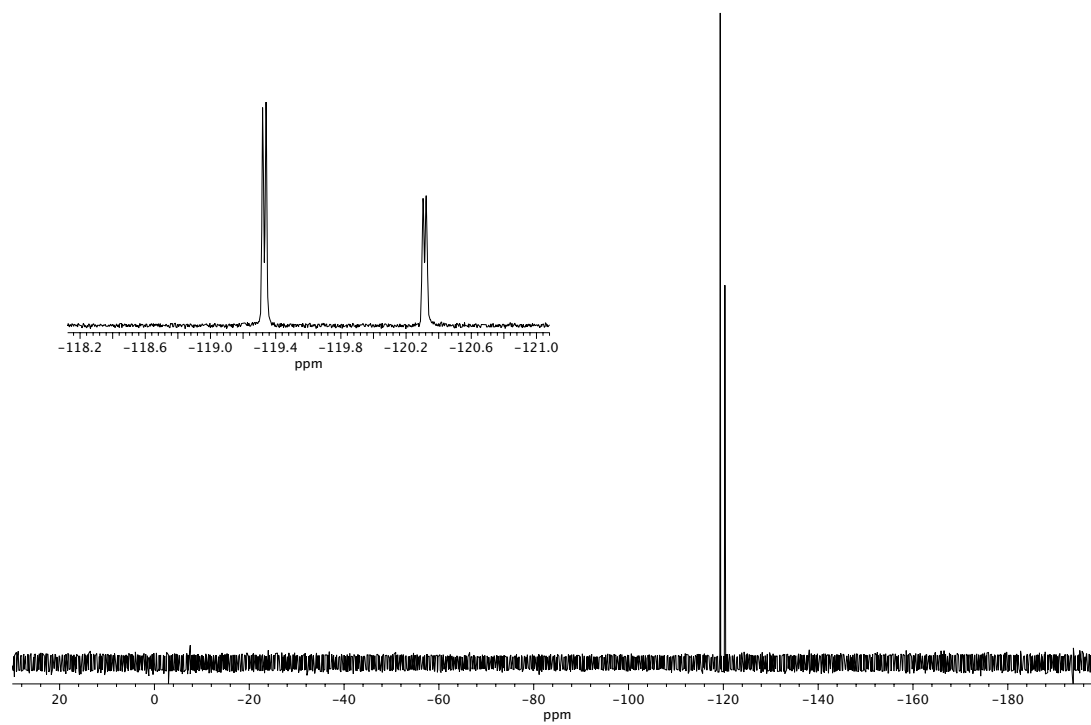
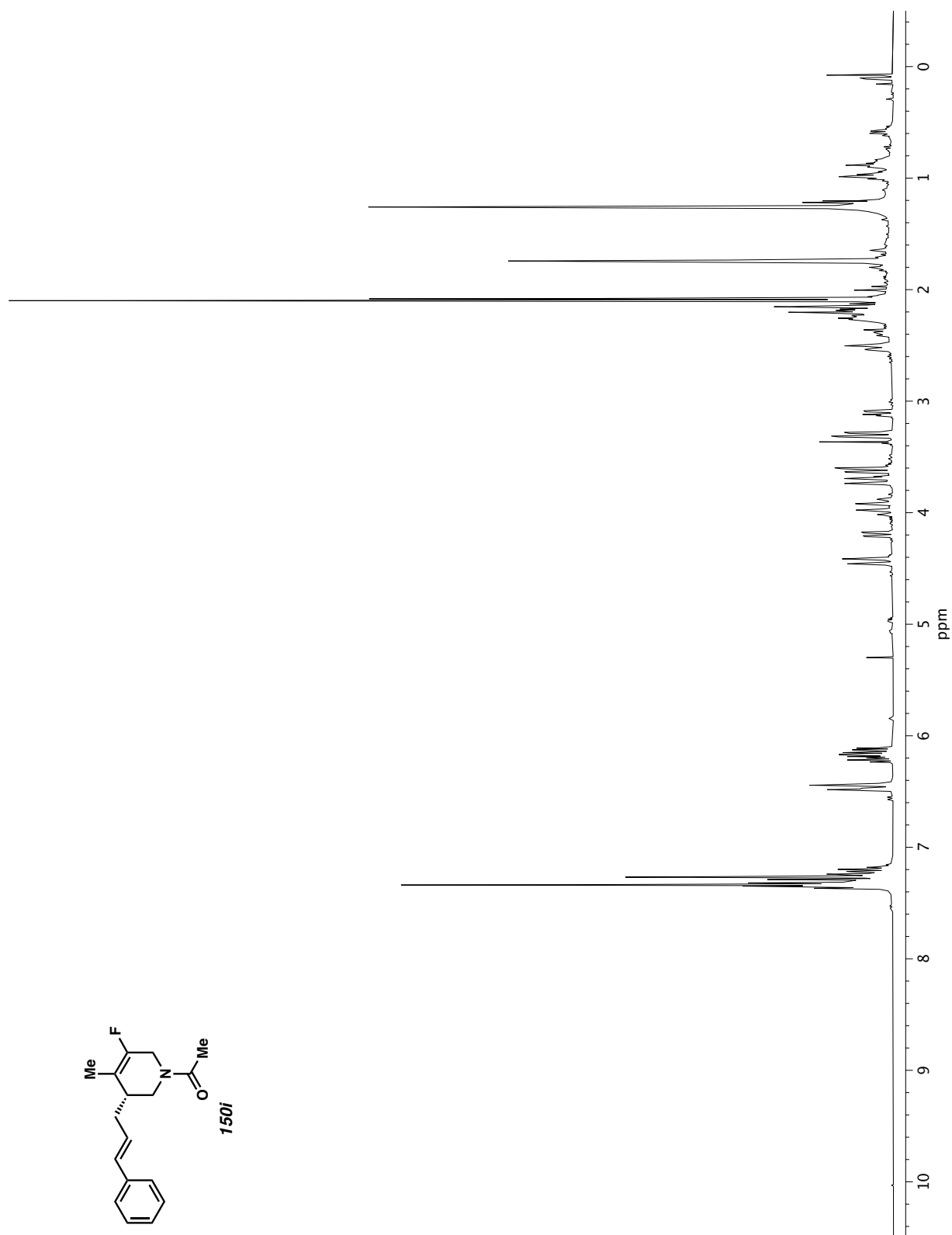


Figure A4.58 <sup>13</sup>C NMR (100 MHz, CD<sub>3</sub>OD) of compound **150h**.



**Figure A4.59**  $^{19}\text{F}$  NMR (282 MHz,  $\text{CD}_3\text{OD}$ ) of compound **150h**.





**Figure A4.60**  $^1\text{H}$  NMR (400 MHz,  $\text{CDCl}_3$ ) of compound **150i**.

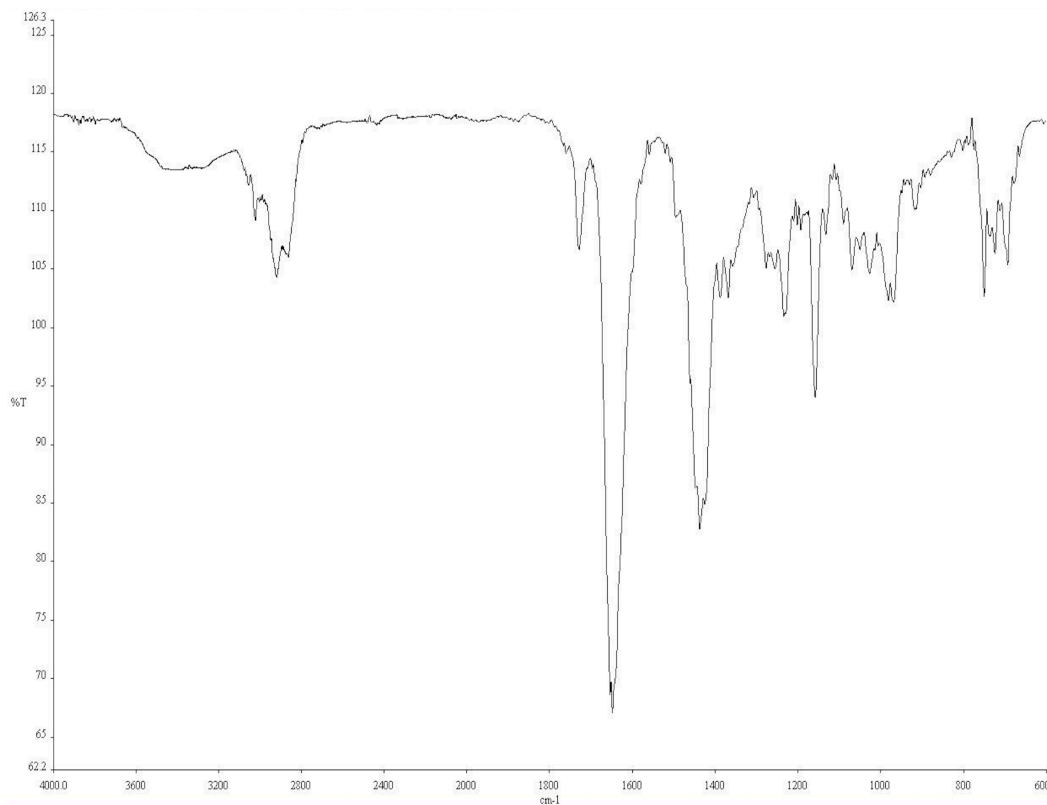


**Figure A4.61** Infrared spectrum (Thin Film, NaCl) of compound **150i**.

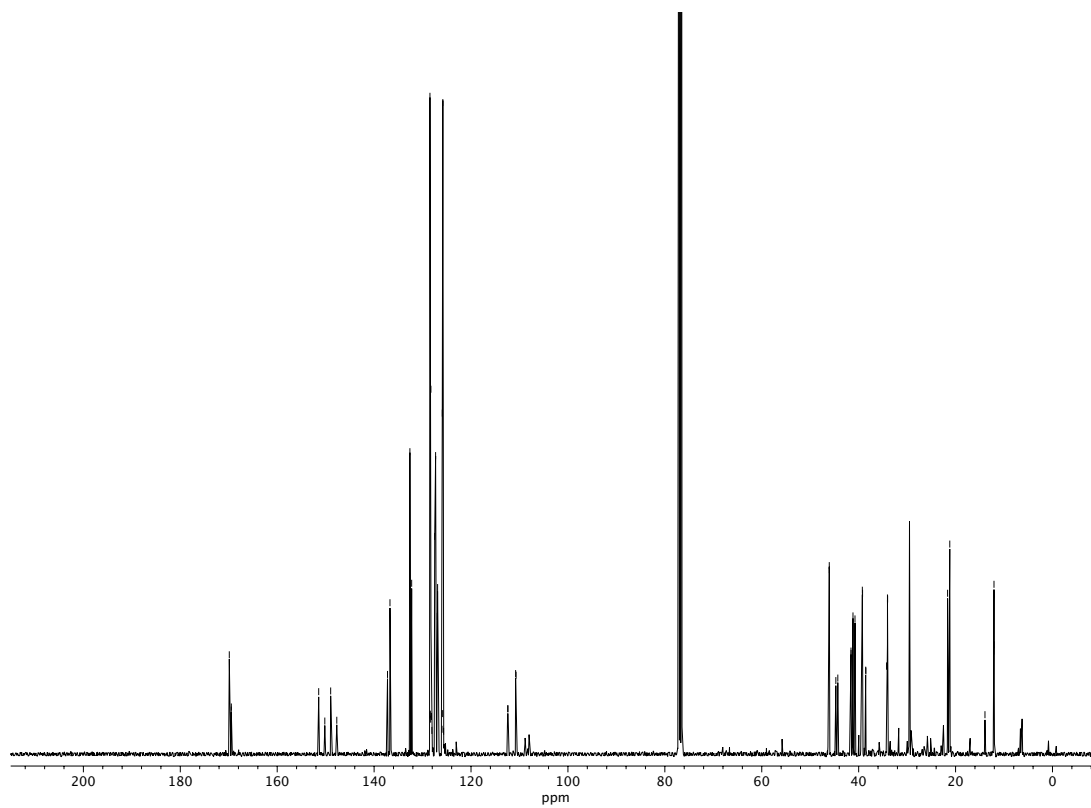


**Figure A4.62** <sup>13</sup>C NMR (100 MHz, CDCl<sub>3</sub>) of compound **150i**.

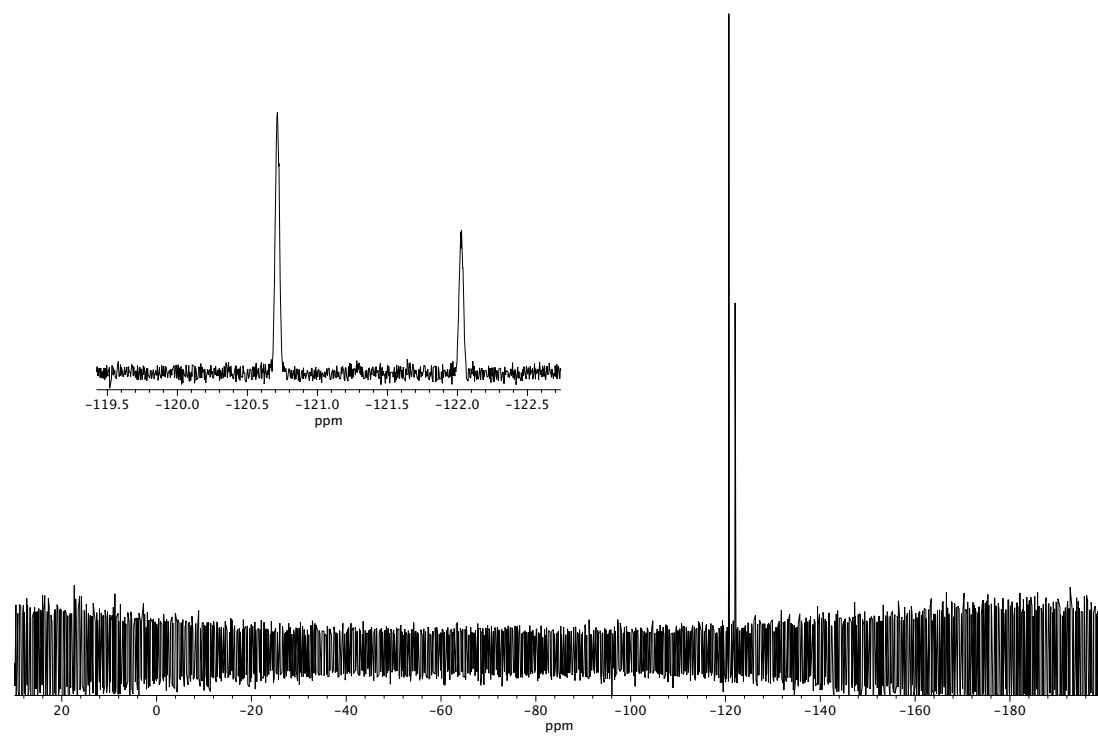


**Figure A4.63**  $^{19}\text{F}$  NMR (282 MHz,  $\text{CDCl}_3$ ) of compound **150i**.

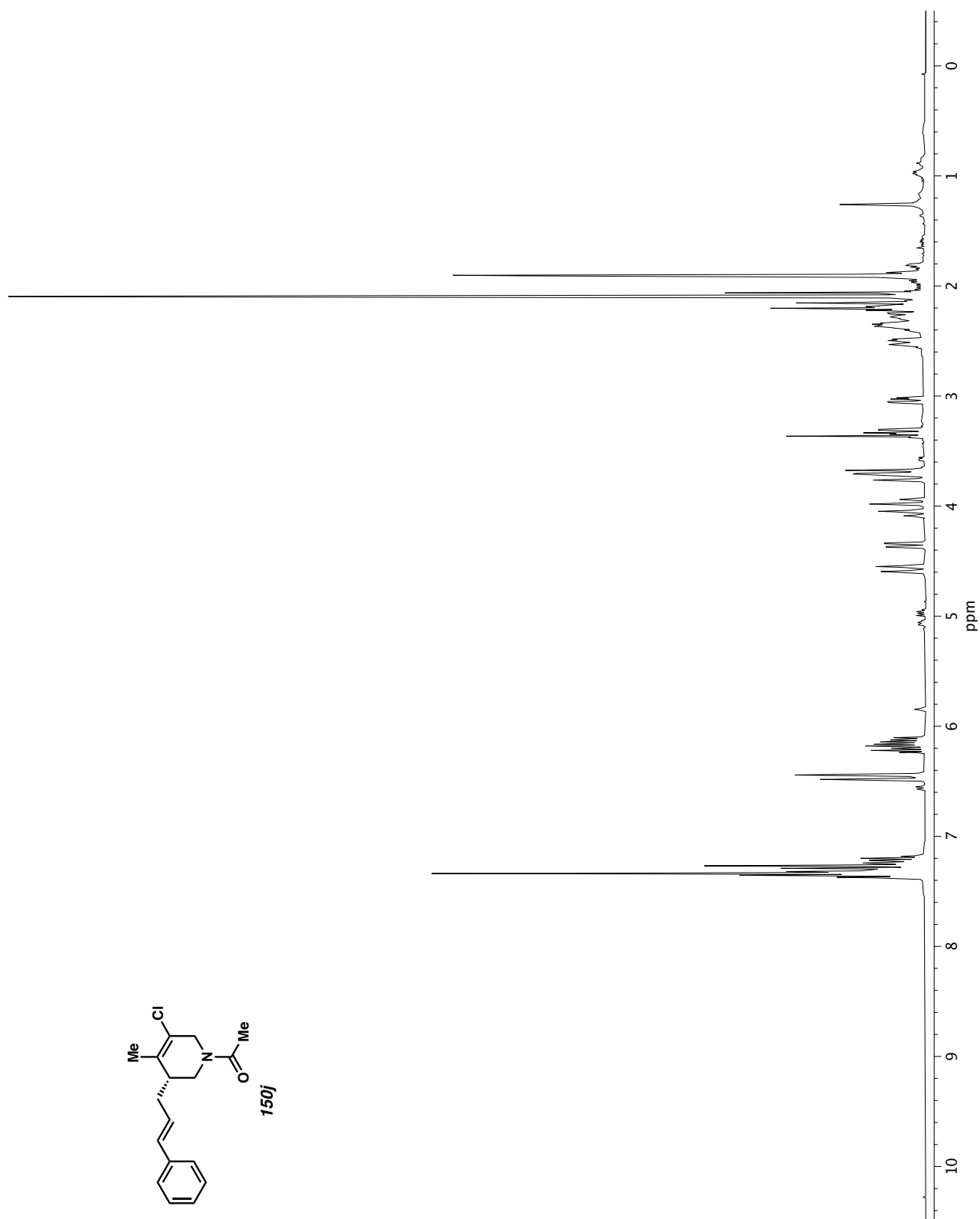


**Figure A4.64**  $^1\text{H NMR}$  (400 MHz,  $\text{CDCl}_3$ ) of compound **150j**.

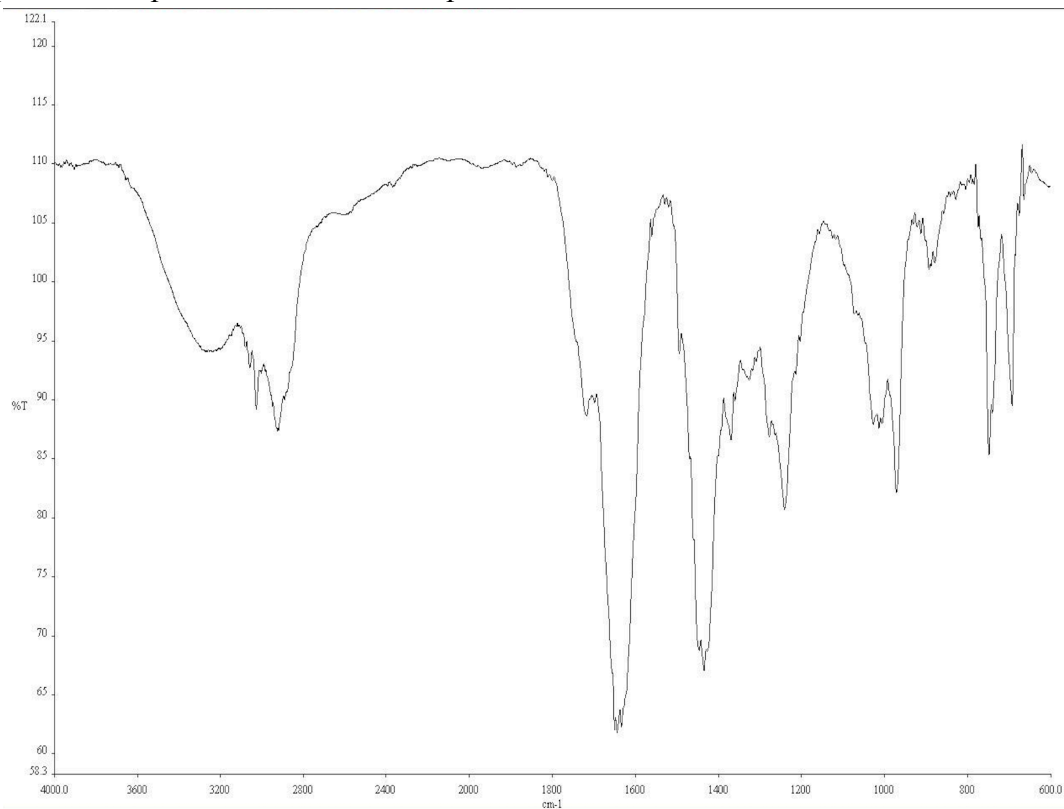


**Figure A4.65** Infrared spectrum (Thin Film, NaCl) of compound **150j**.

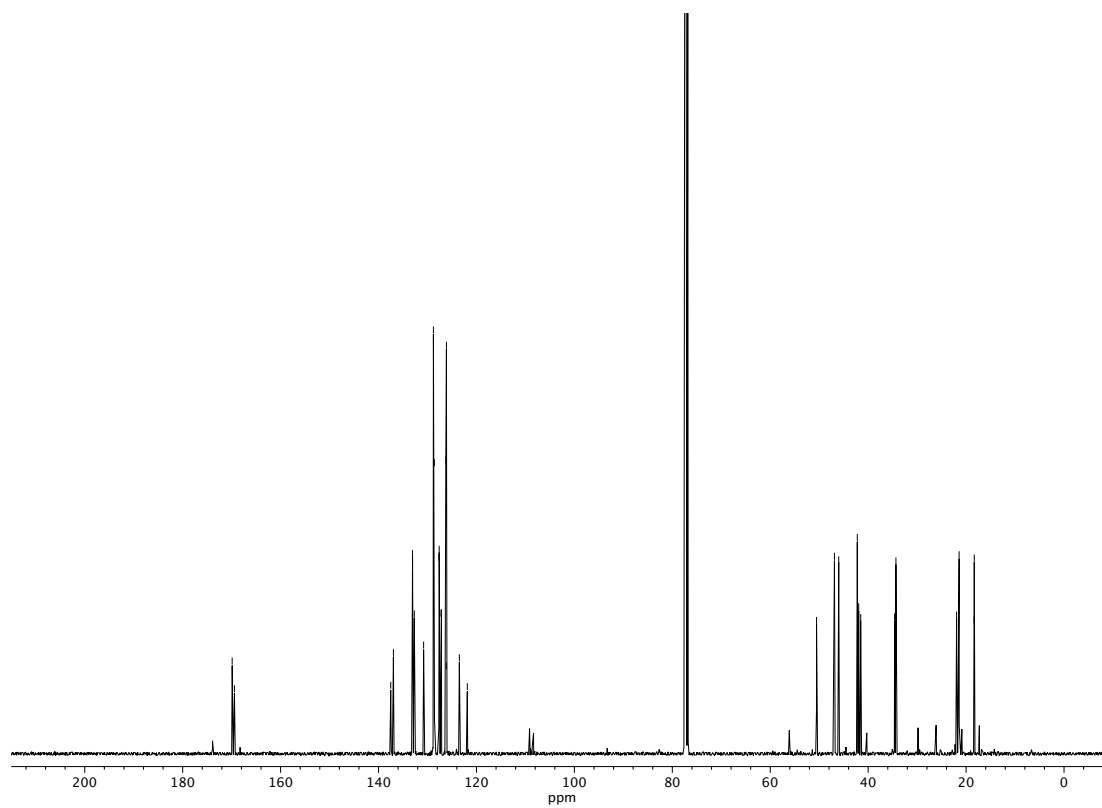


**Figure A4.66**  $^{13}\text{C}$  NMR (100 MHz,  $\text{CDCl}_3$ ) of compound **150j**.

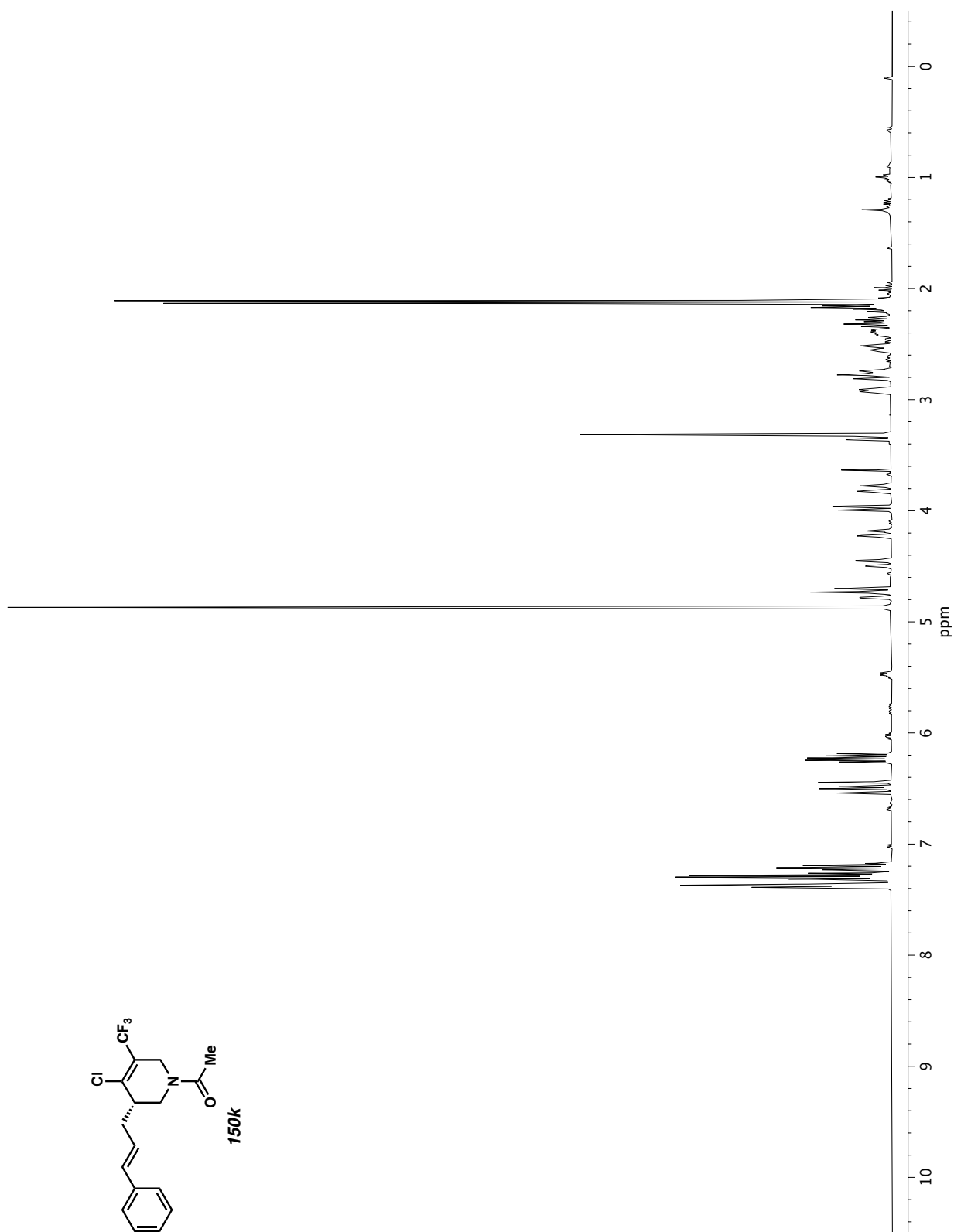


**Figure A4.67**  $^1\text{H}$  NMR (400 MHz,  $\text{CD}_3\text{OD}$ ) of compound **150k**.

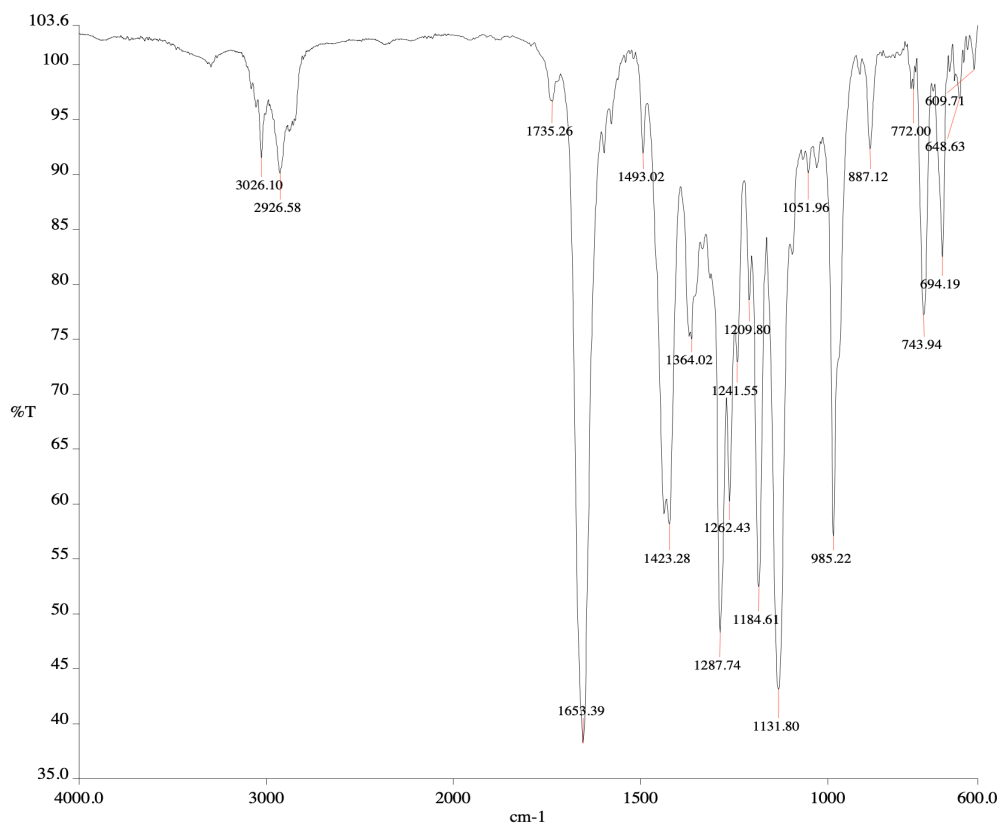


**Figure A4.68** Infrared spectrum (Thin Film, NaCl) of compound **150k**.

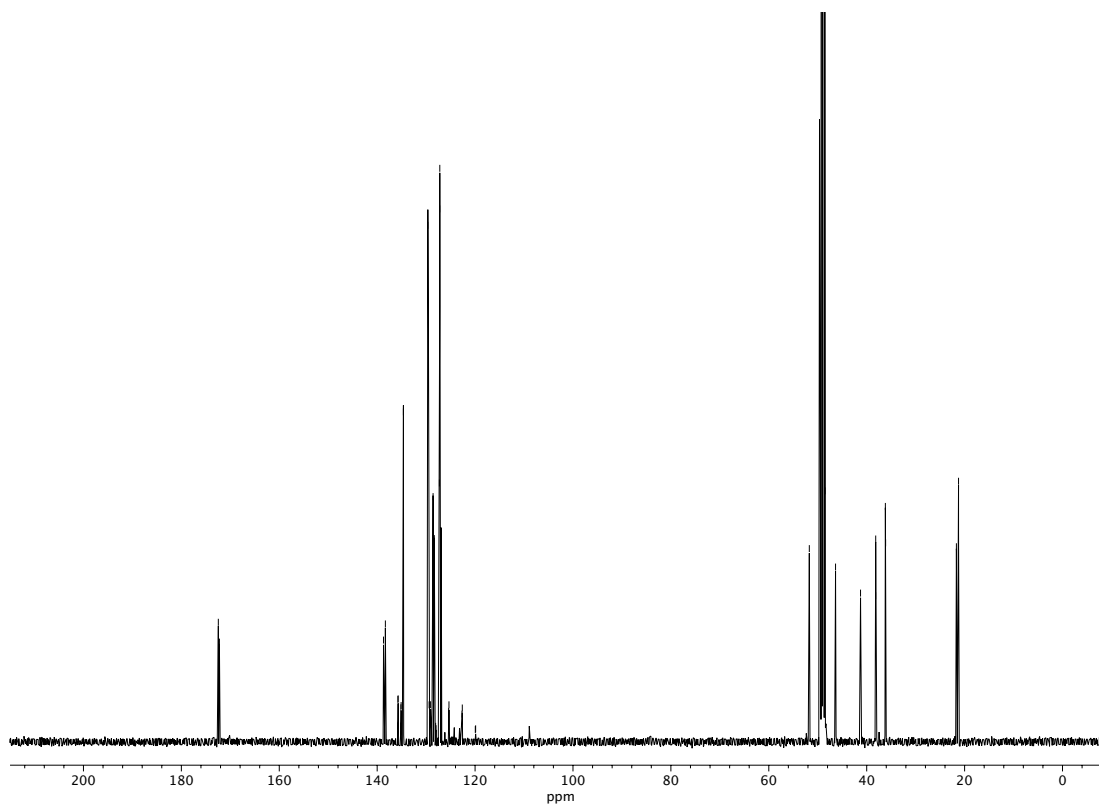


**Figure A4.69** <sup>13</sup>C NMR (100 MHz, CD<sub>3</sub>OD) of compound **150k**.

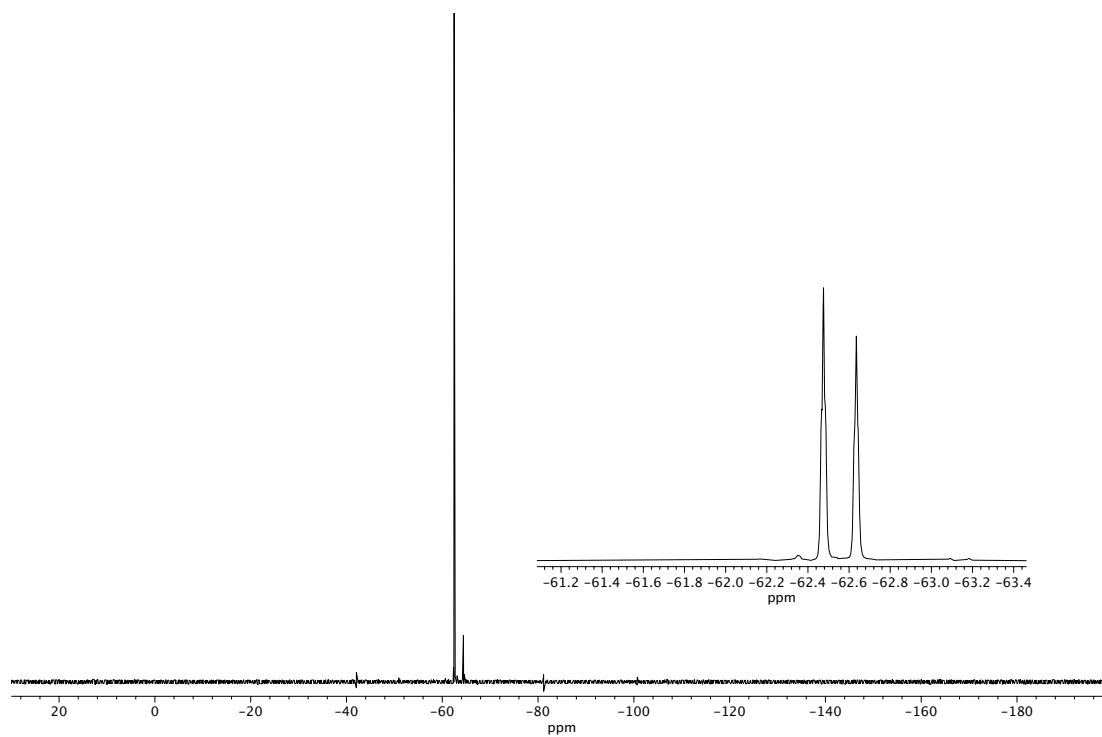


**Figure A4.70**  $^{19}\text{F}$  NMR (282 MHz,  $\text{CD}_3\text{OD}$ ) of compound **150k**.



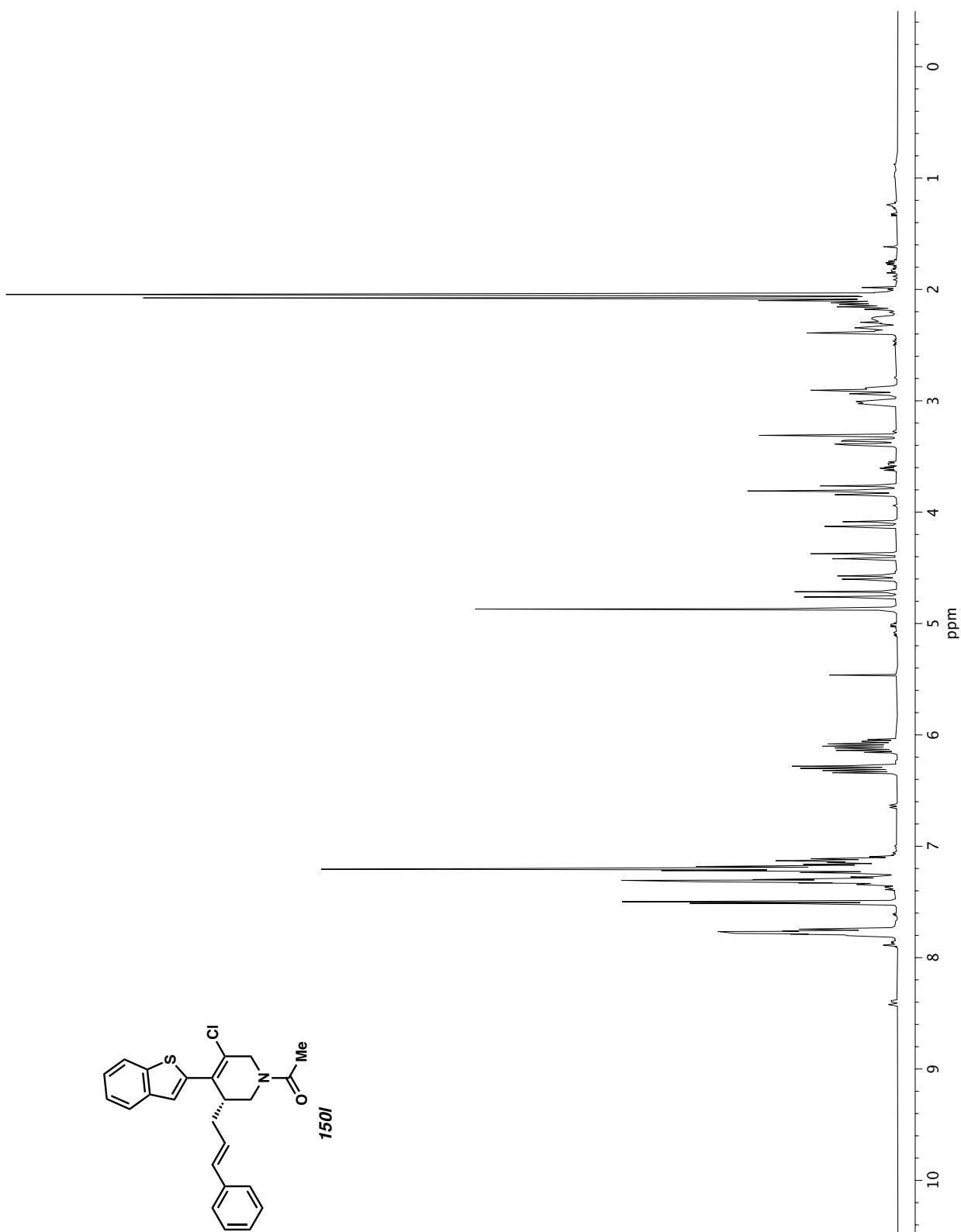


Figure A4.71  $^1\text{H NMR}$  (400 MHz,  $\text{CD}_3\text{OD}$ ) of compound **150I**.

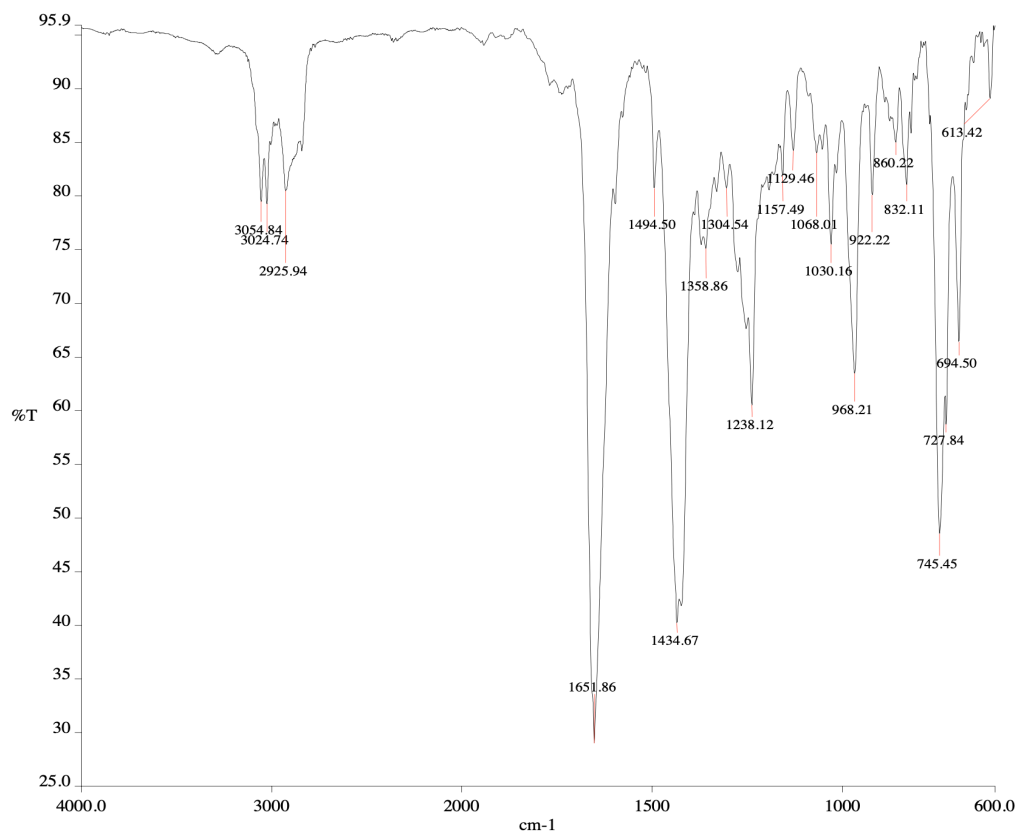


Figure A4.72 Infrared spectrum (Thin Film, NaCl) of compound **150I**.

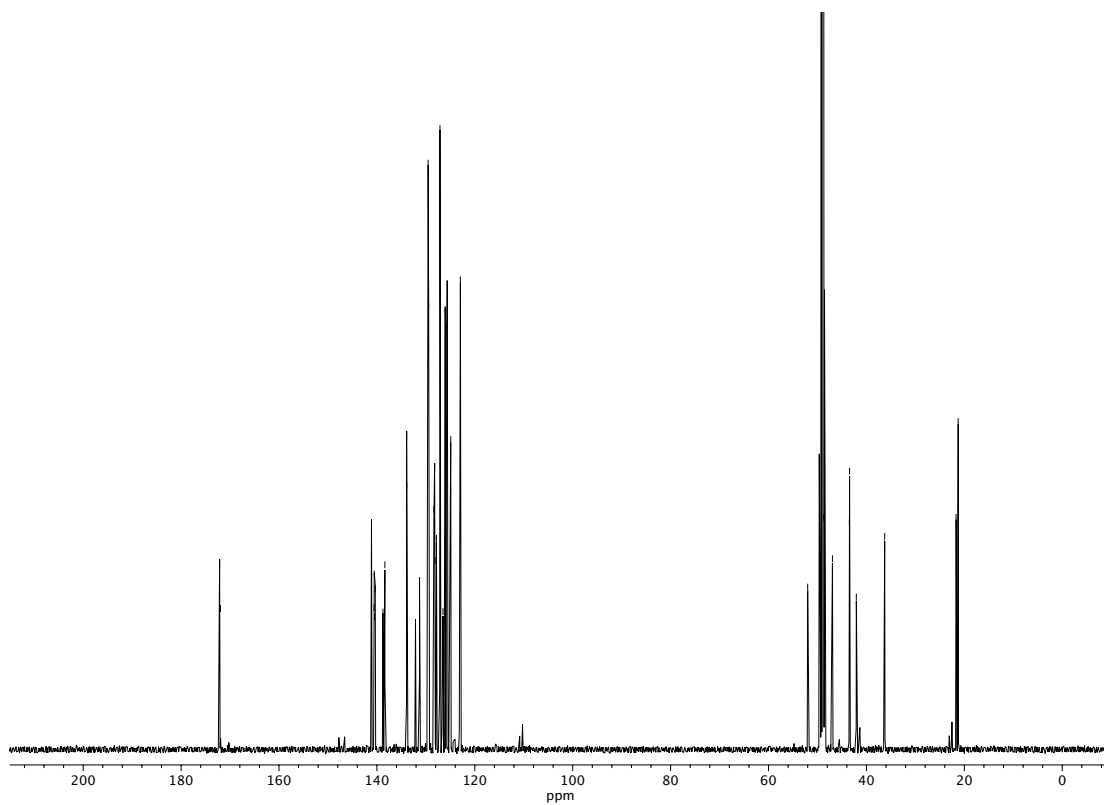
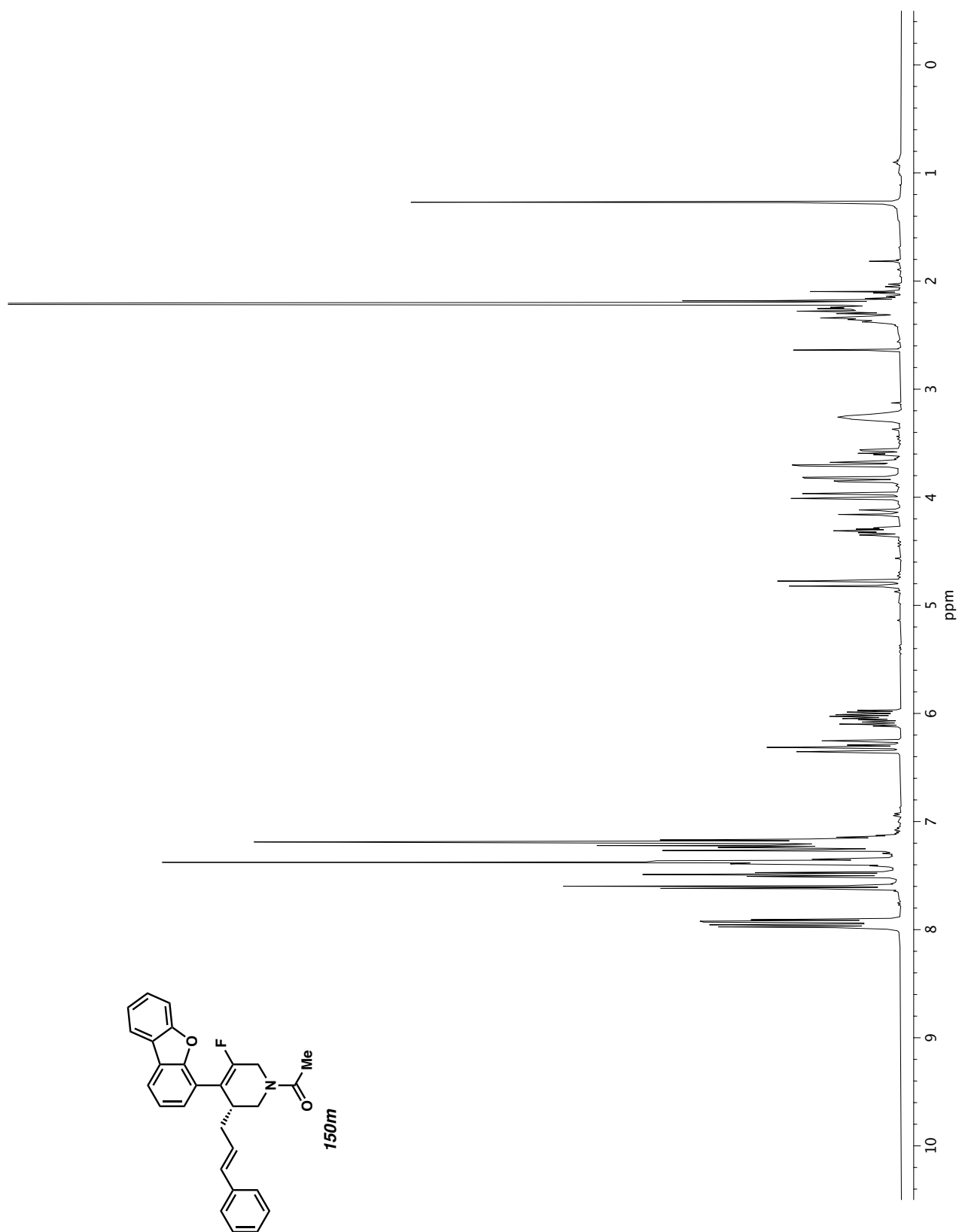
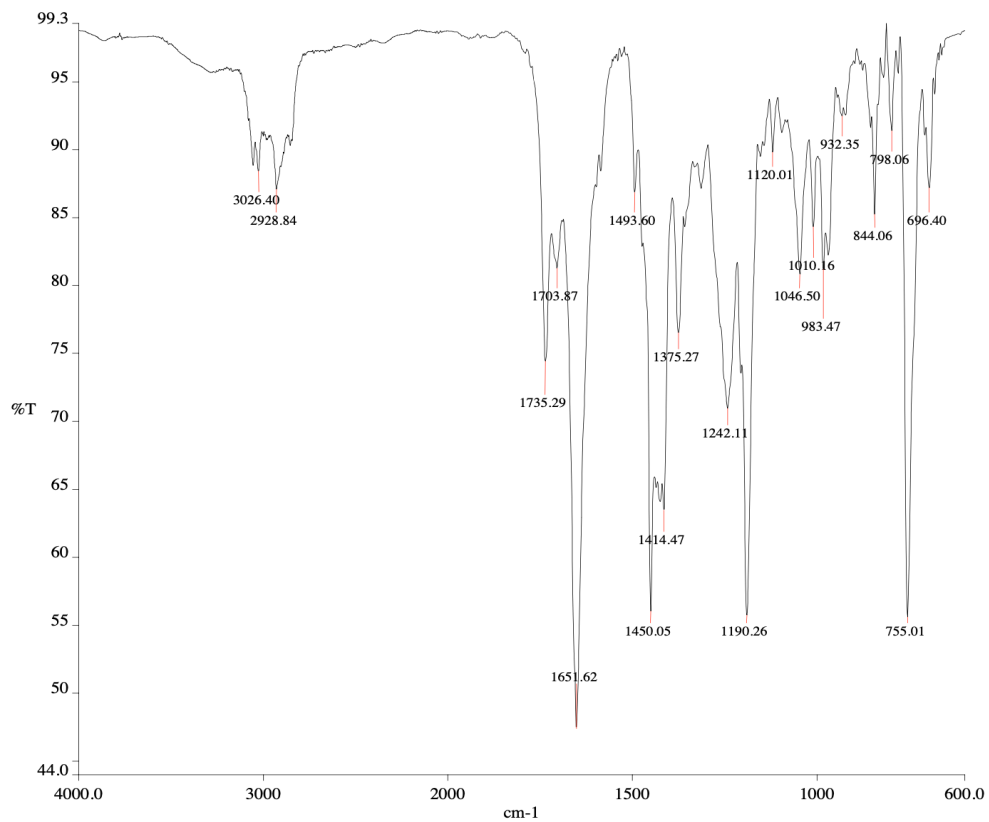


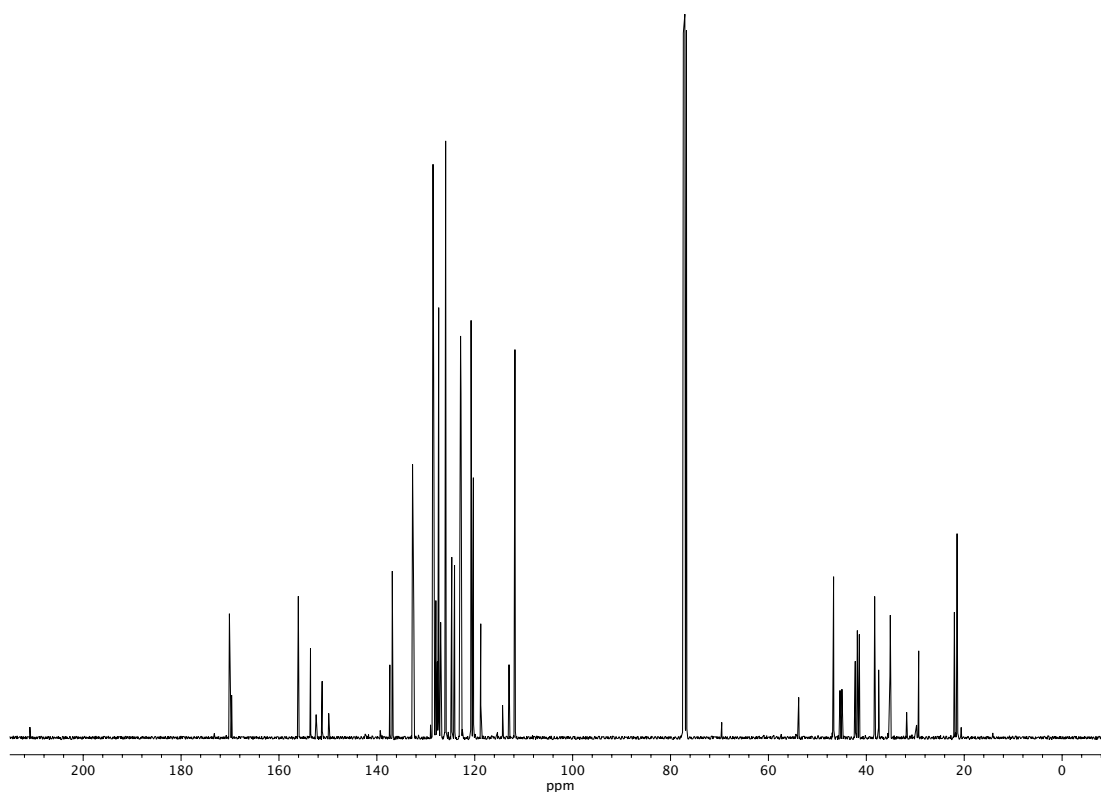
Figure A4.73 <sup>13</sup>C NMR (100 MHz, CD<sub>3</sub>OD) of compound **150I**.



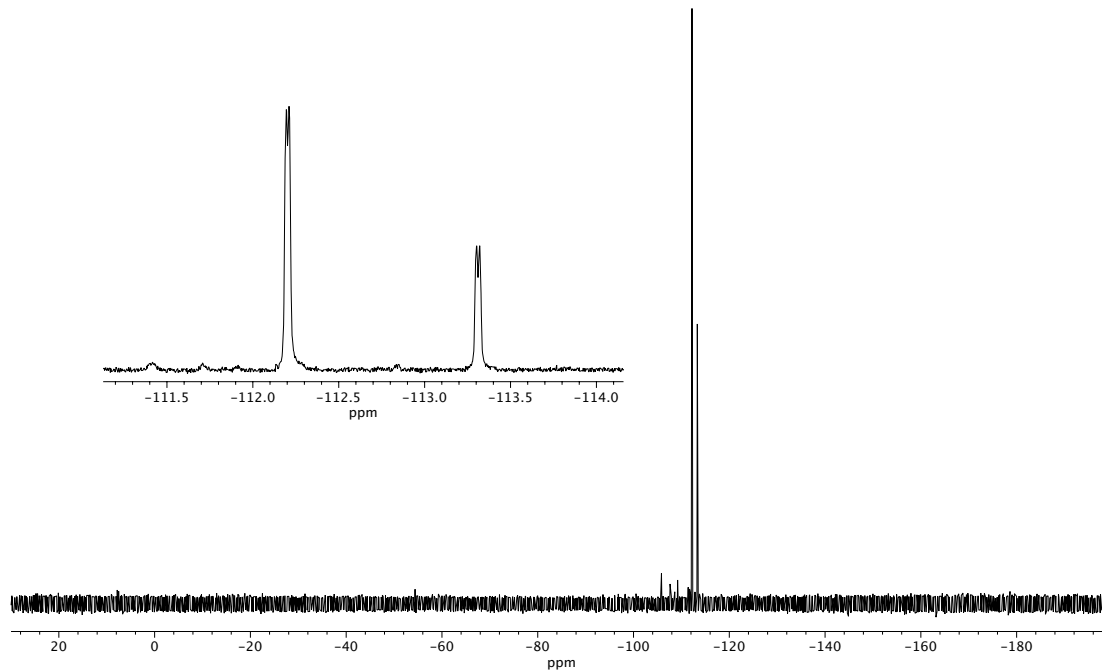
**Figure A4.74**  $^1\text{H NMR}$  (400 MHz,  $\text{CDCl}_3$ ) of compound **150m**.



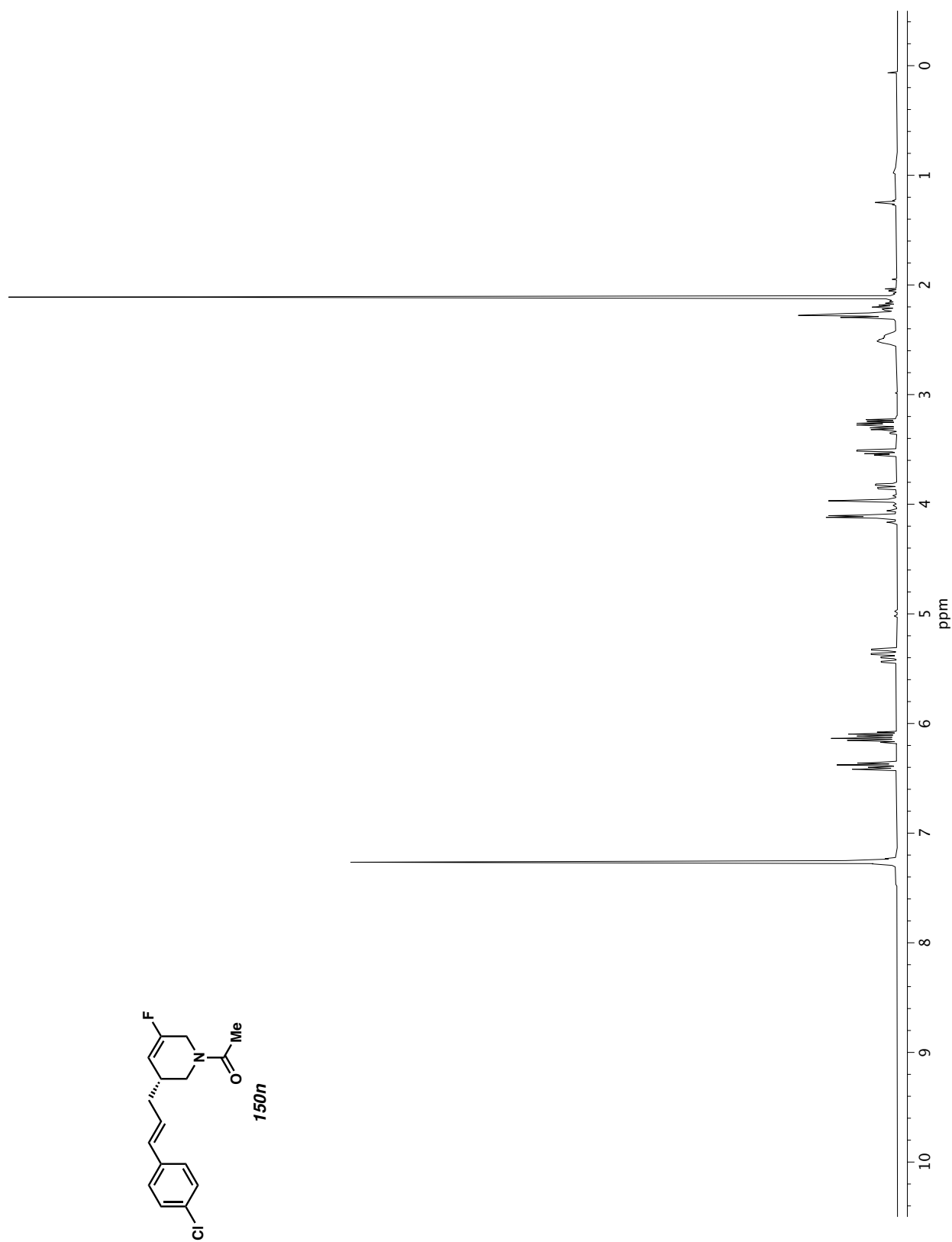
**Figure A4.75** Infrared spectrum (Thin Film, NaCl) of compound **150m**.



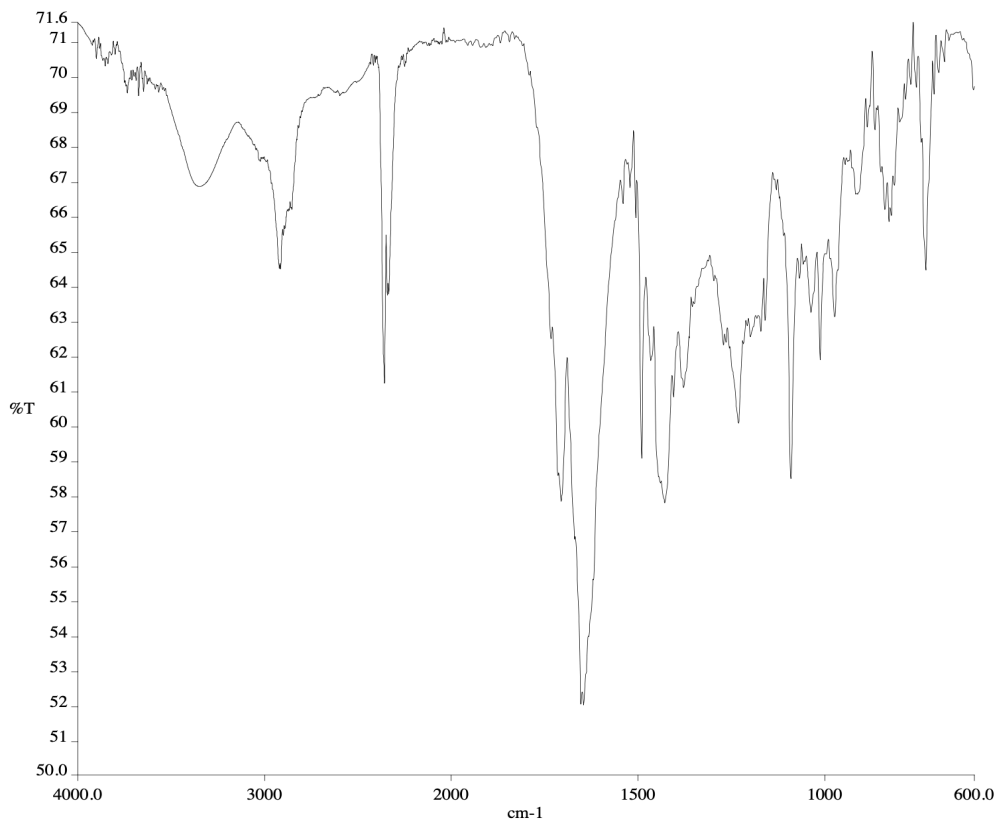
**Figure A4.76** <sup>13</sup>C NMR (100 MHz, CDCl<sub>3</sub>) of compound **150m**.



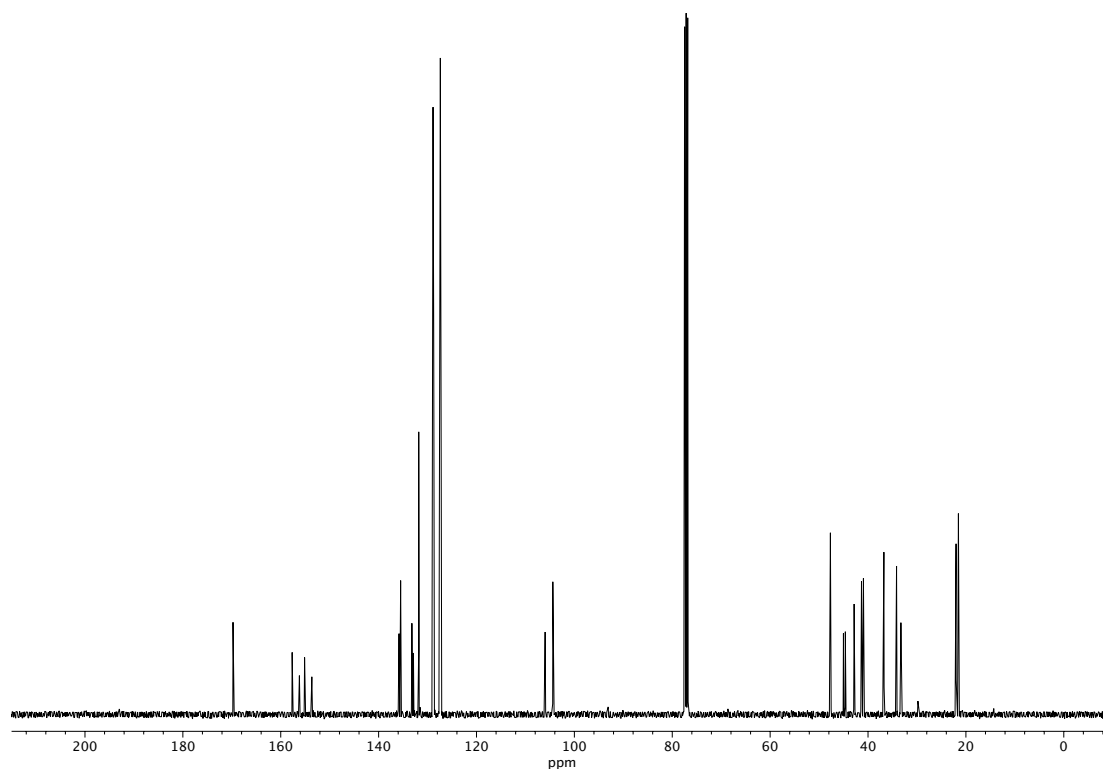
**Figure A4.77**  $^{19}\text{F}$  NMR (282 MHz,  $\text{CDCl}_3$ ) of compound **150m**.



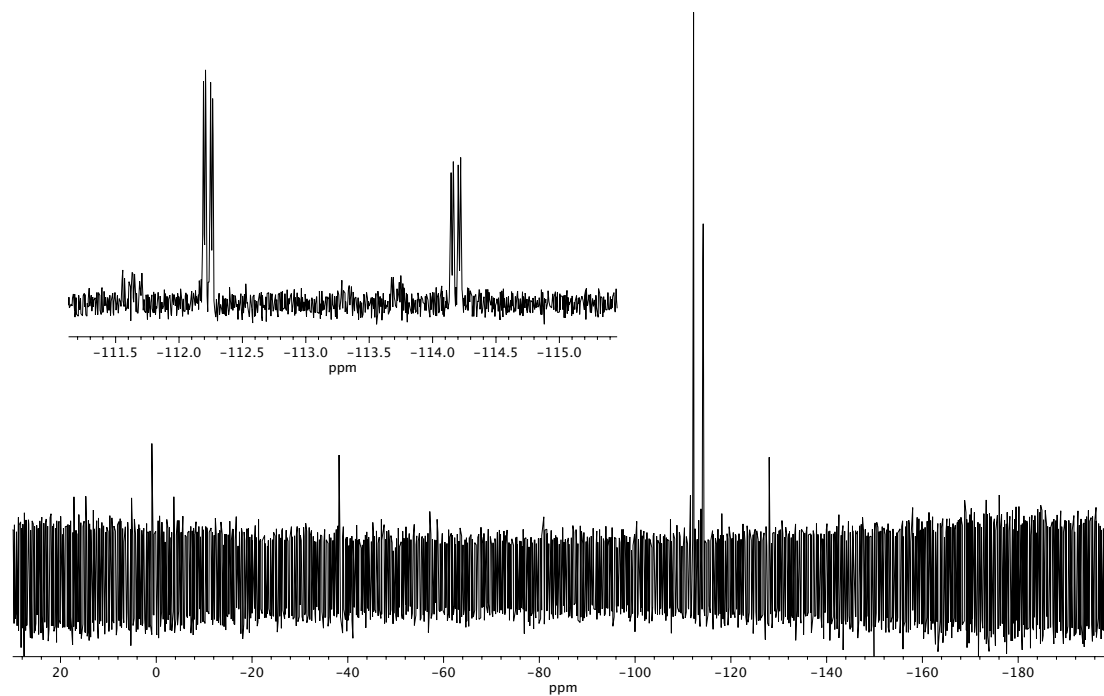
**Figure A4.78**  $^1\text{H}$  NMR (400 MHz,  $\text{CDCl}_3$ ) of compound **150n**.



**Figure A4.79** Infrared spectrum (Thin Film, NaCl) of compound **150n**.

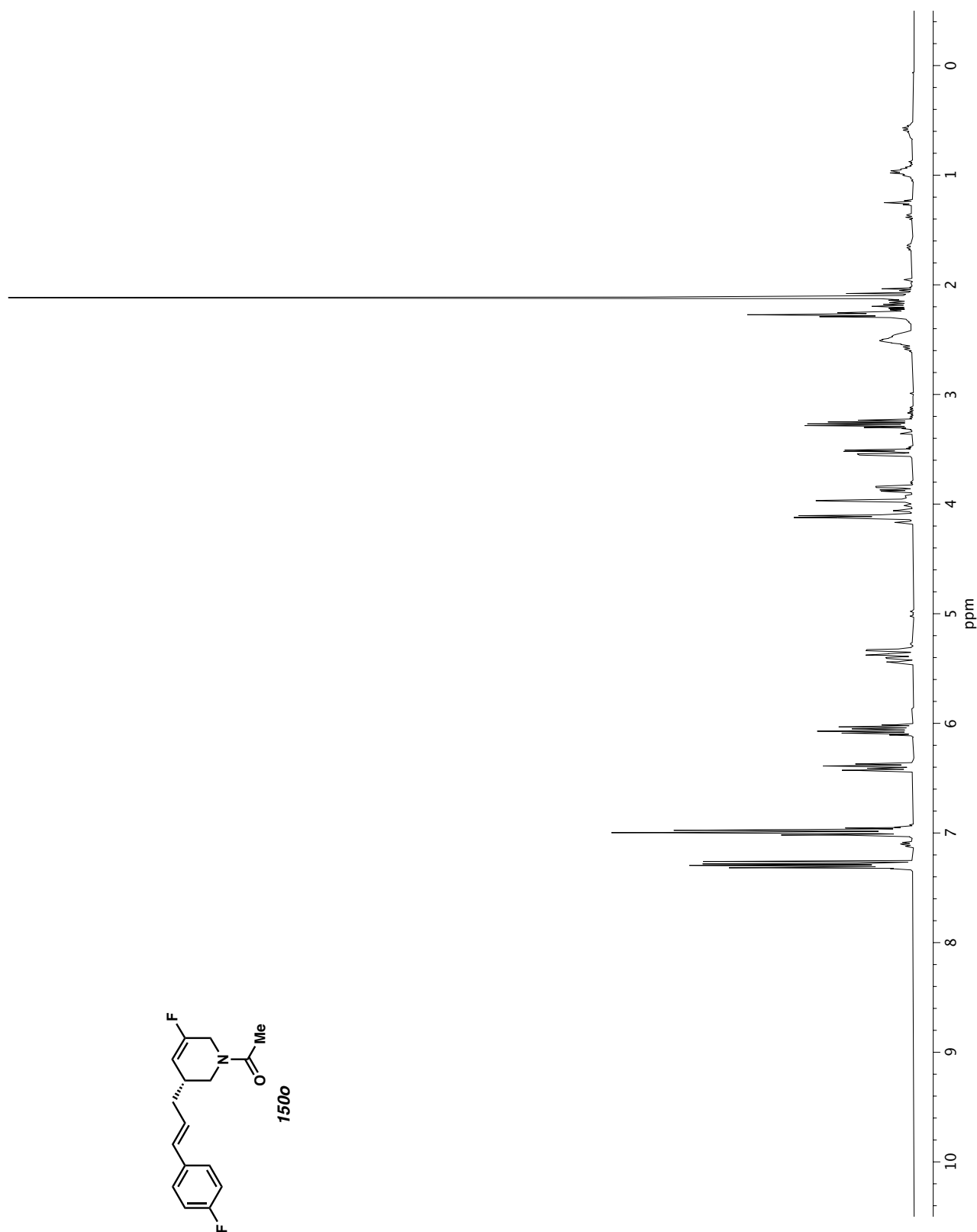


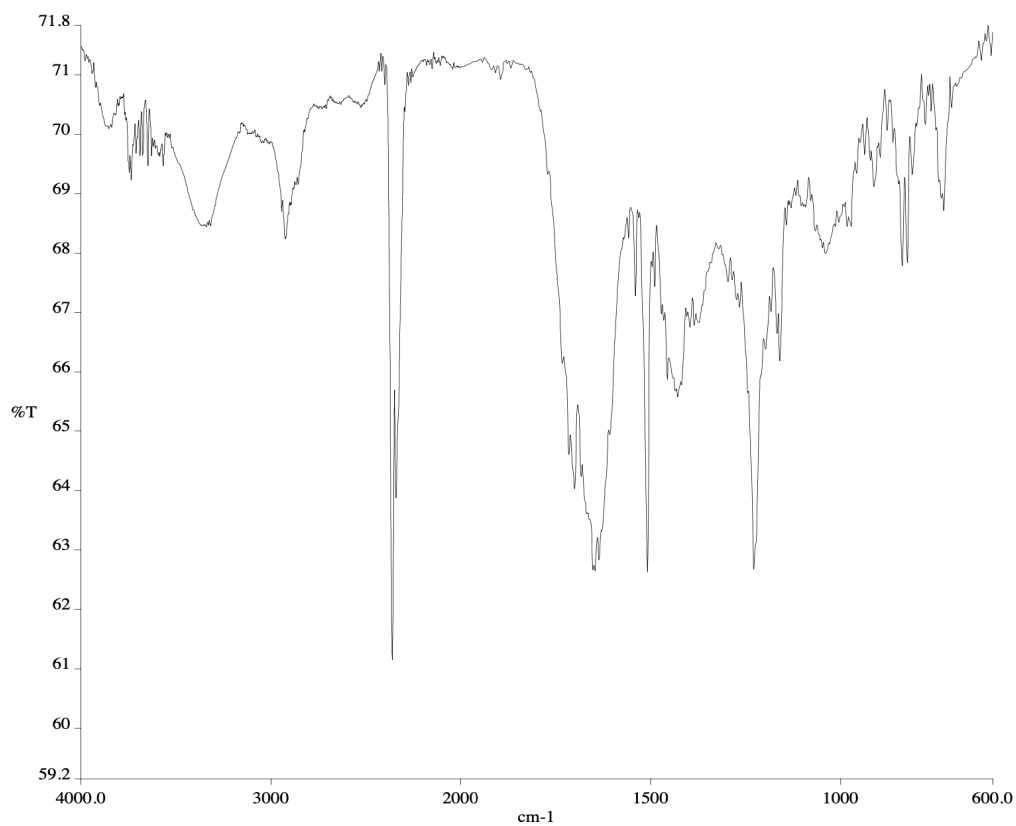
**Figure A4.80** <sup>13</sup>C NMR (100 MHz, CDCl<sub>3</sub>) of compound **150n**.



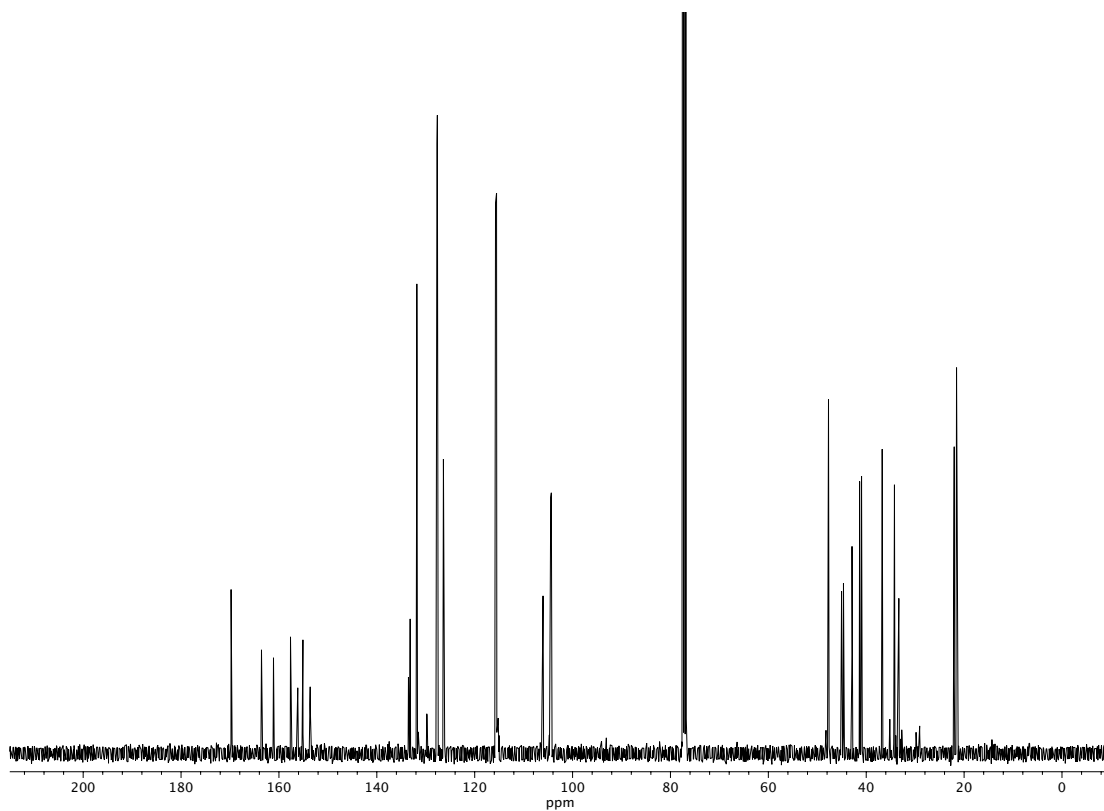
**Figure A4.81**  $^{19}\text{F}$  NMR (282 MHz,  $\text{CDCl}_3$ ) of compound **150n**.



Figure A4.82  $^1\text{H}$  NMR (400 MHz,  $\text{CDCl}_3$ ) of compound **150o**.



**Figure A4.83** Infrared spectrum (Thin Film, NaCl) of compound **150o**.



**Figure A4.84** <sup>13</sup>C NMR (100 MHz, CDCl<sub>3</sub>) of compound **150o**.

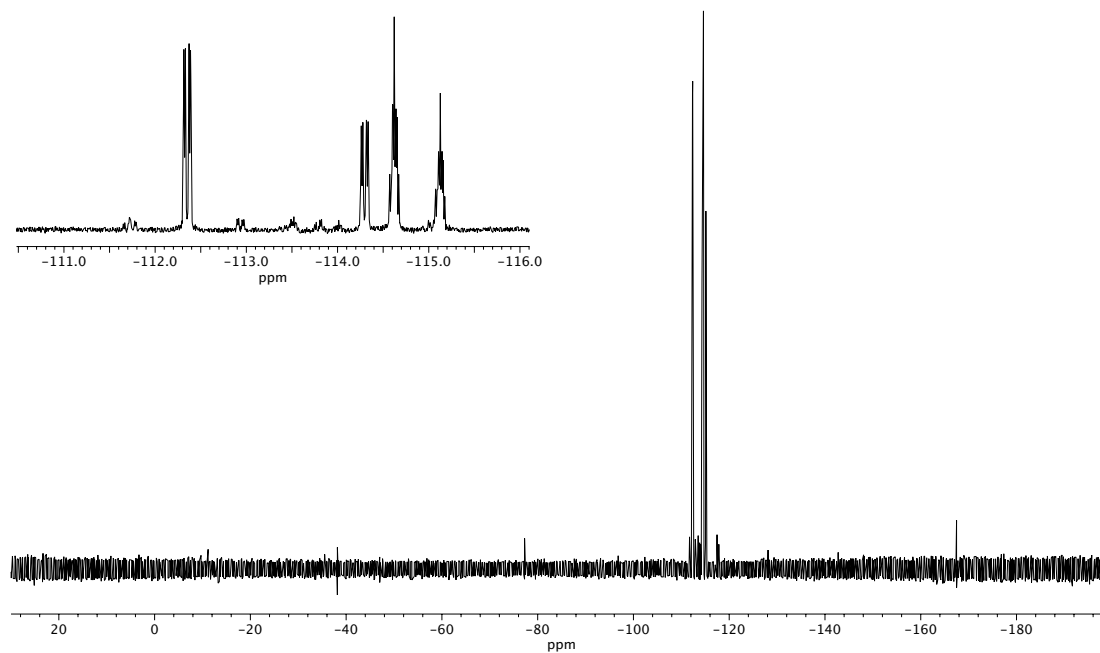


**Figure A4.85**  $^{19}\text{F}$  NMR (282 MHz,  $\text{CDCl}_3$ ) of compound **150o**.

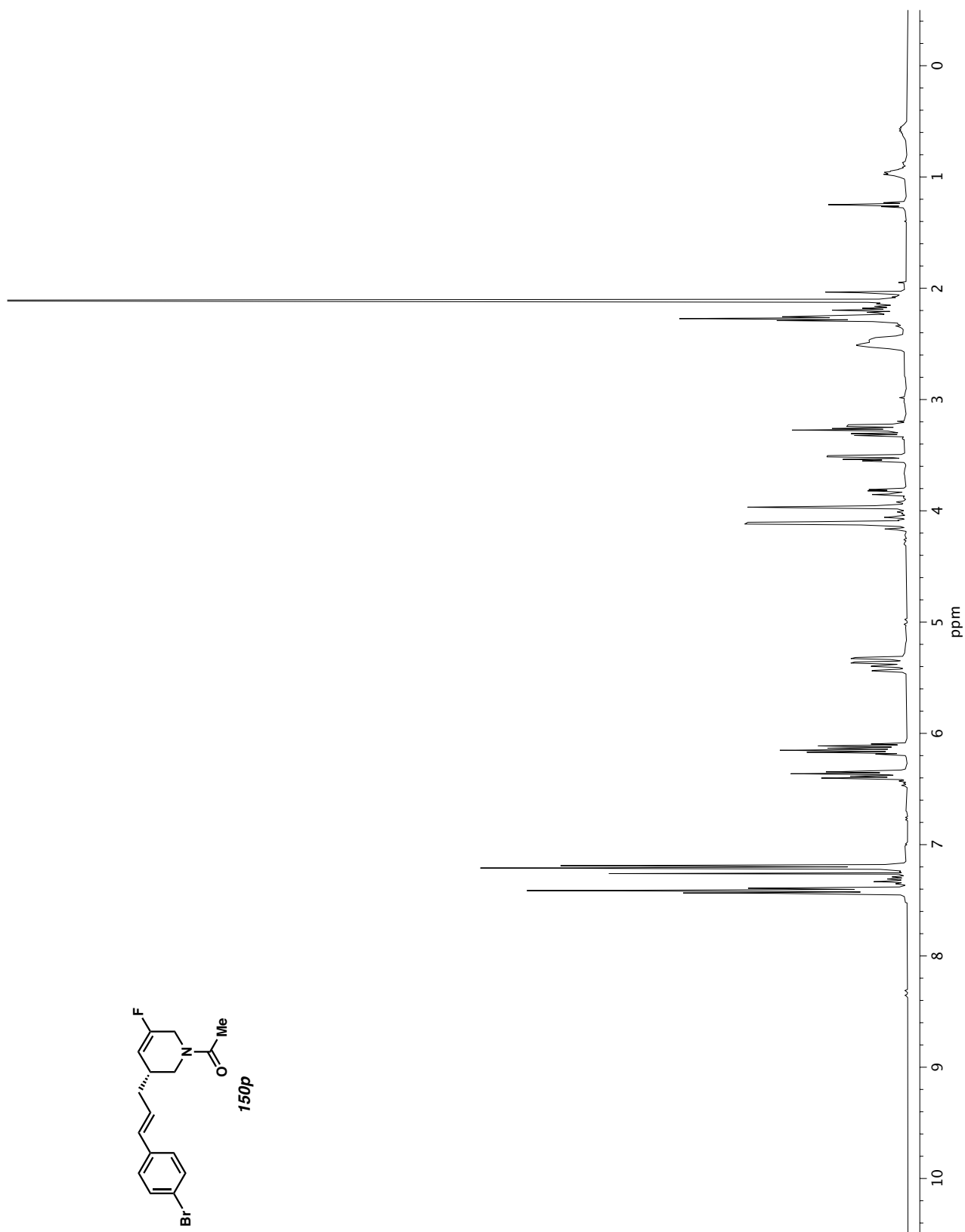
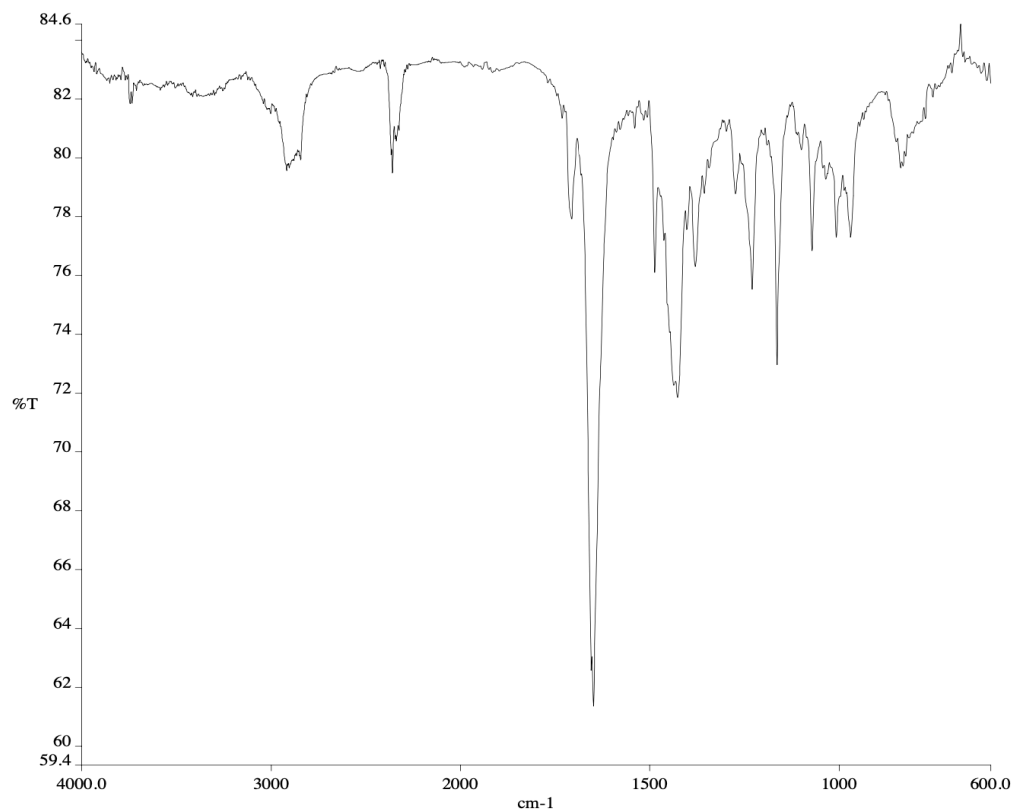
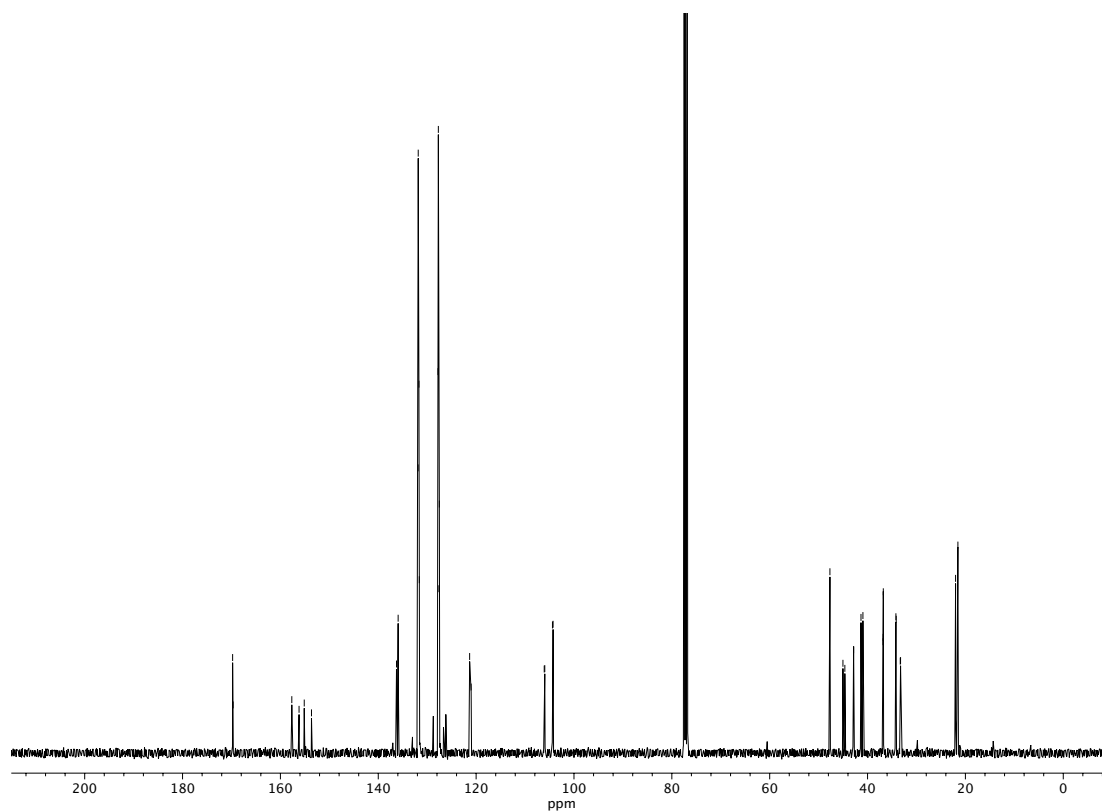


Figure A4.86  $^1\text{H}$  NMR (400 MHz,  $\text{CDCl}_3$ ) of compound **150p**.



**Figure A4.87** Infrared spectrum (Thin Film, NaCl) of compound **150p**.



**Figure A4.88** <sup>13</sup>C NMR (100 MHz, CDCl<sub>3</sub>) of compound **150p**.

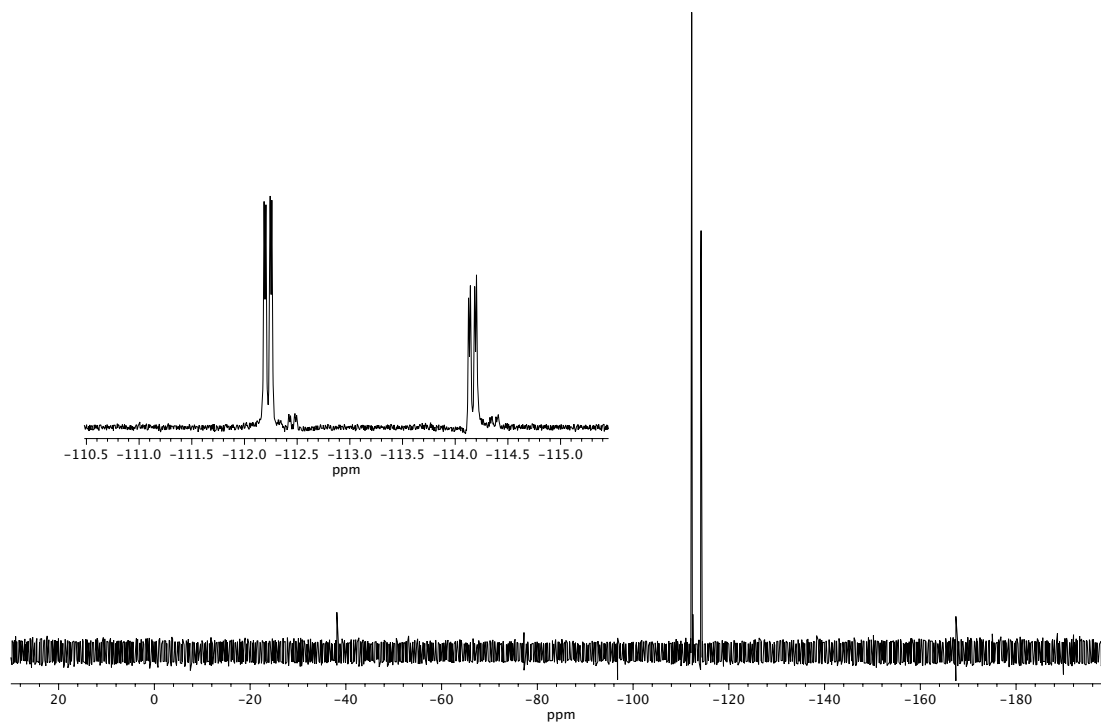


**Figure A4.89**  $^{13}\text{C}$  NMR (100 MHz,  $\text{CDCl}_3$ ) of compound **150p**.

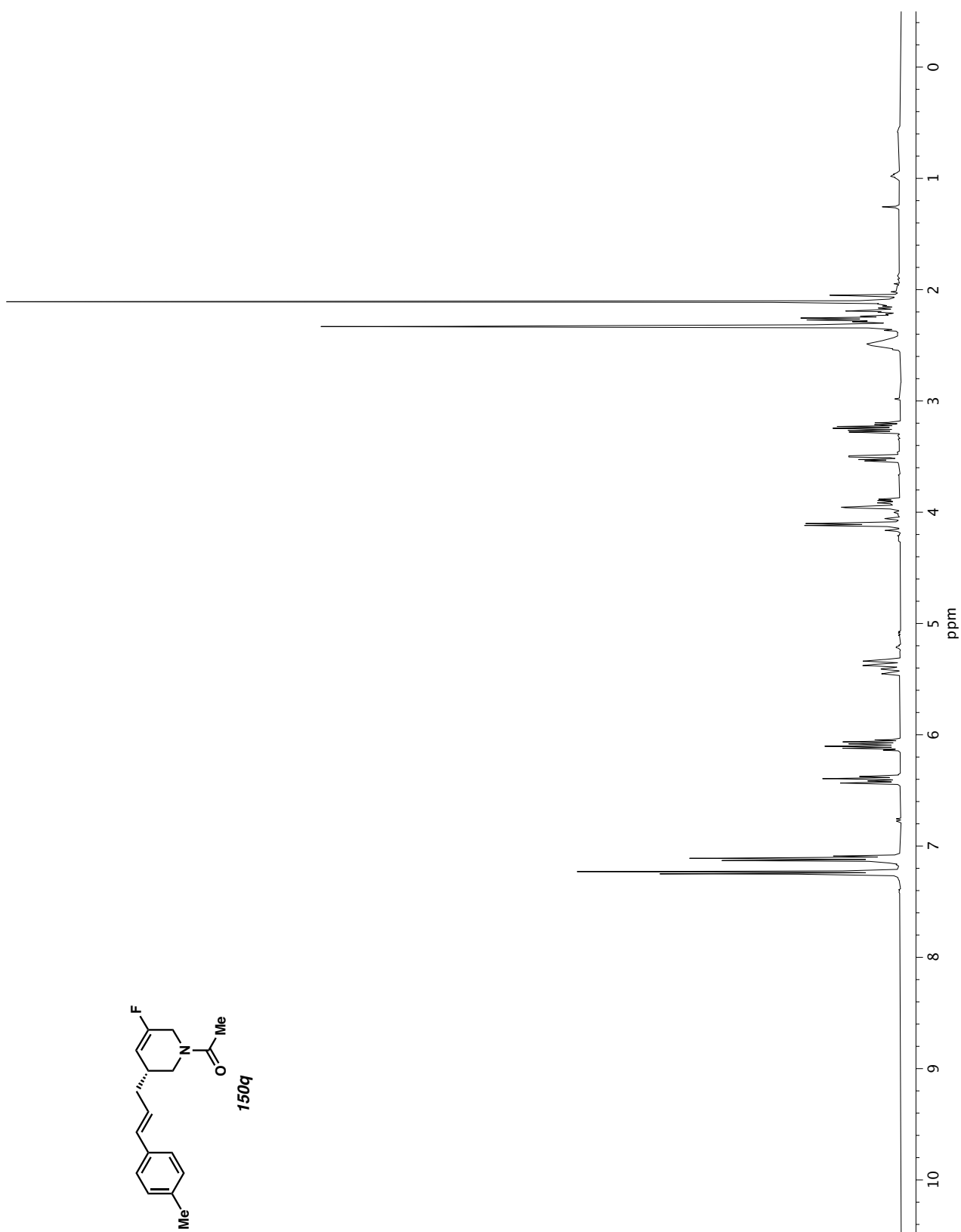


**Figure A4.90** <sup>1</sup>H NMR (400 MHz, CDCl<sub>3</sub>) of compound **150q**.

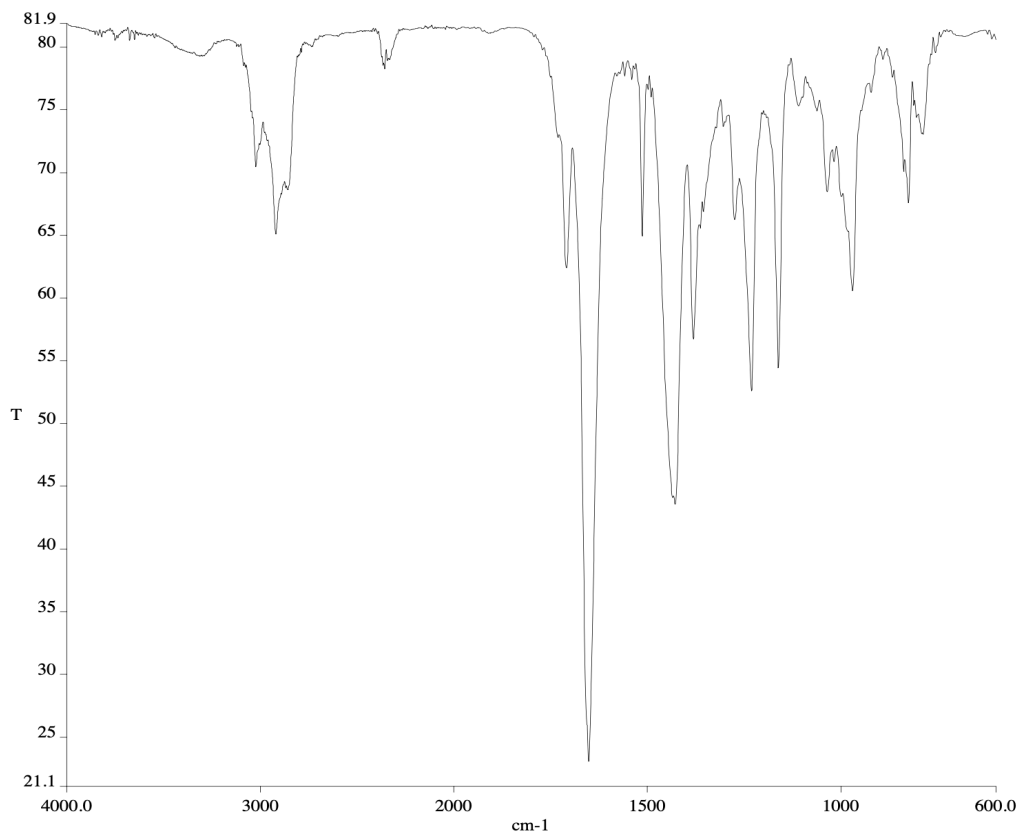


**Figure A4.91** Infrared spectrum (Thin Film, NaCl) of compound **150q**.

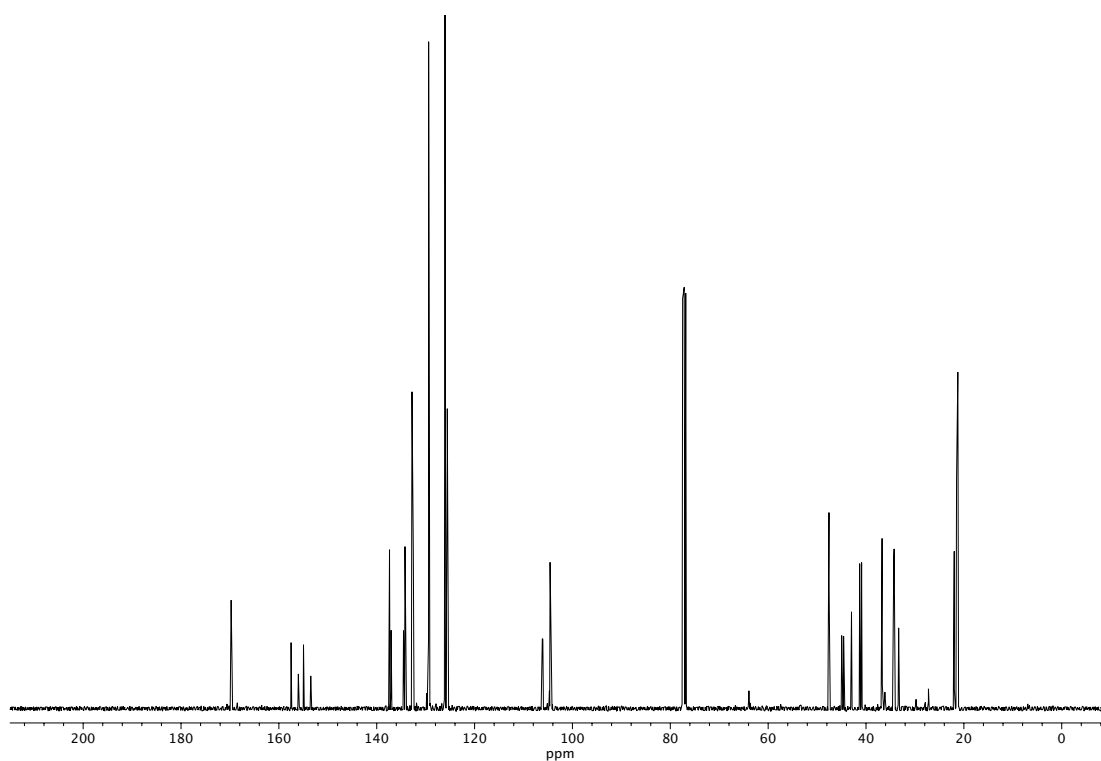


**Figure A4.92** <sup>13</sup>C NMR (100 MHz, CDCl<sub>3</sub>) of compound **150q**.



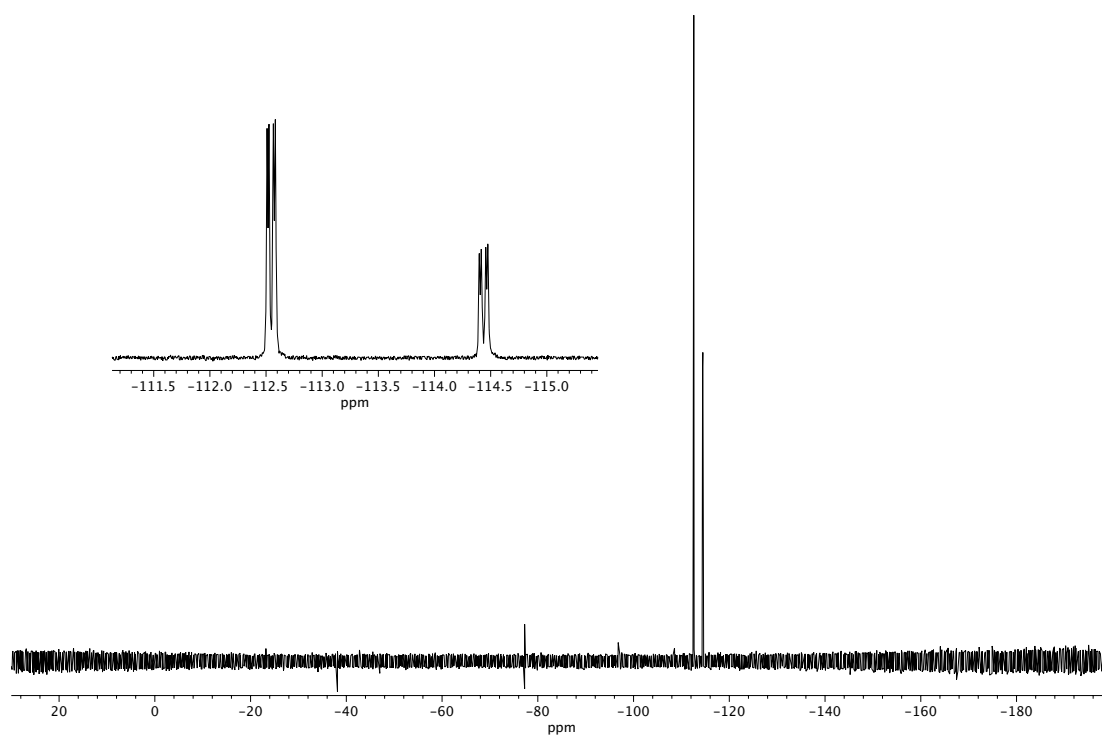


**Figure A4.93**  $^{19}\text{F}$  NMR (282 MHz,  $\text{CDCl}_3$ ) of compound **150q**.

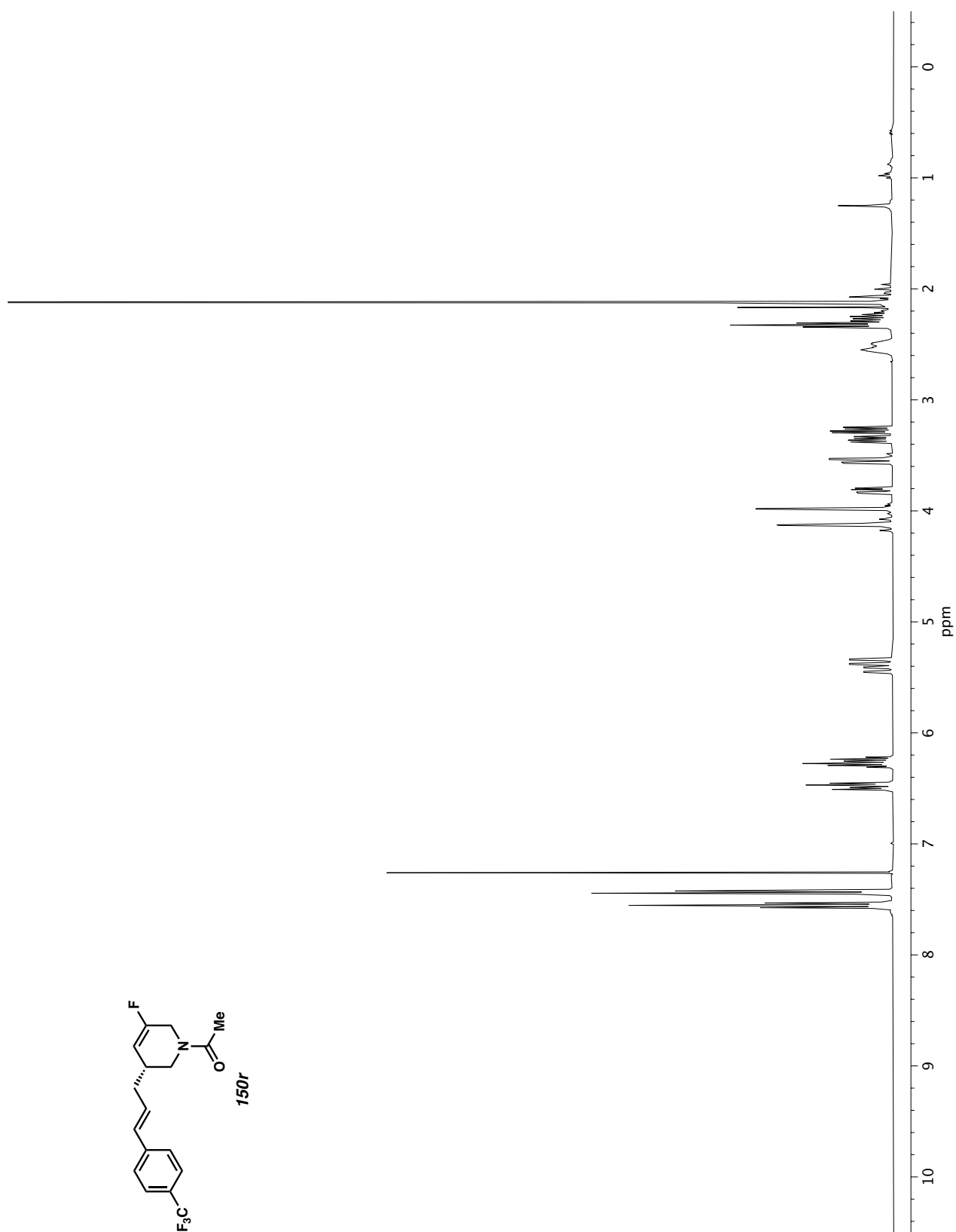


**Figure A4.94**  $^1\text{H}$  NMR (400 MHz,  $\text{CDCl}_3$ ) of compound **150r**.

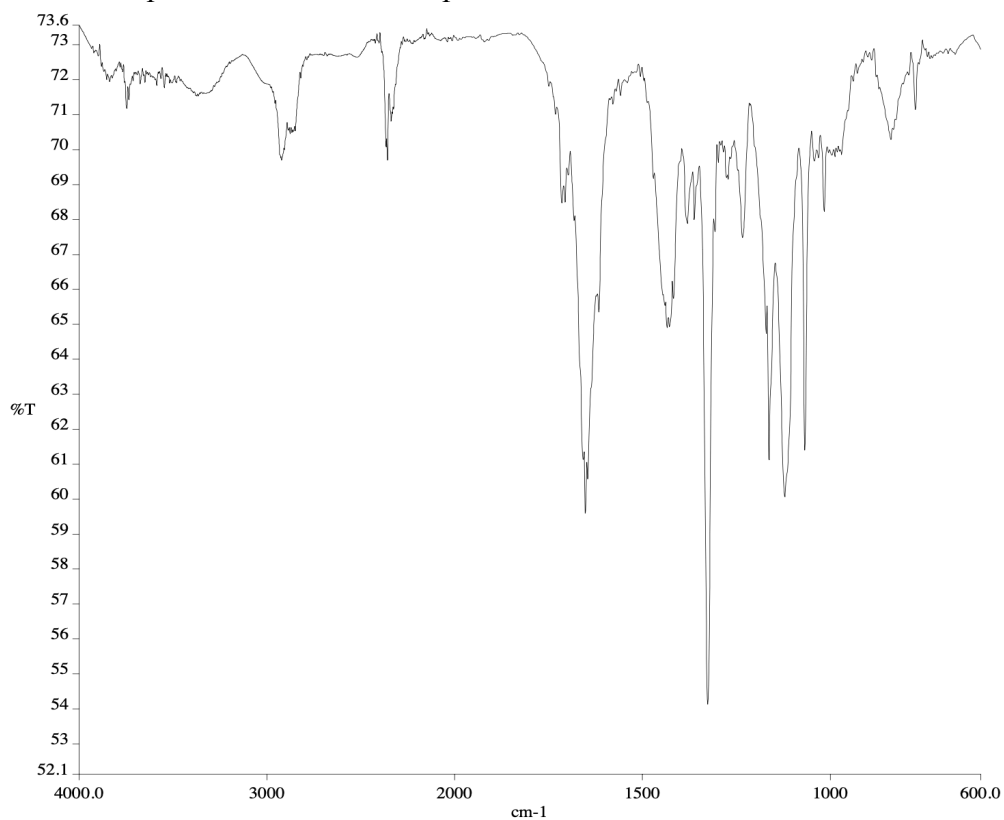


**Figure A4.95** Infrared spectrum (Thin Film, NaCl) of compound **150r**.

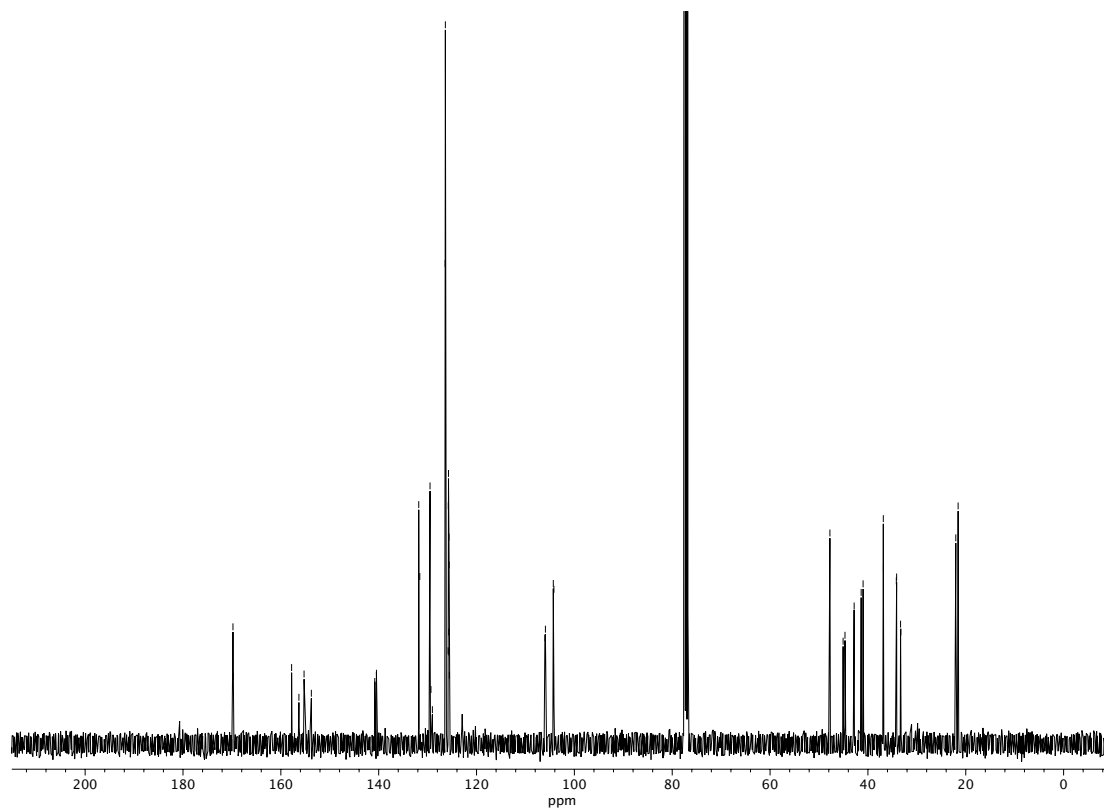


**Figure A4.96** <sup>13</sup>C NMR (100 MHz, CDCl<sub>3</sub>) of compound **150r**.

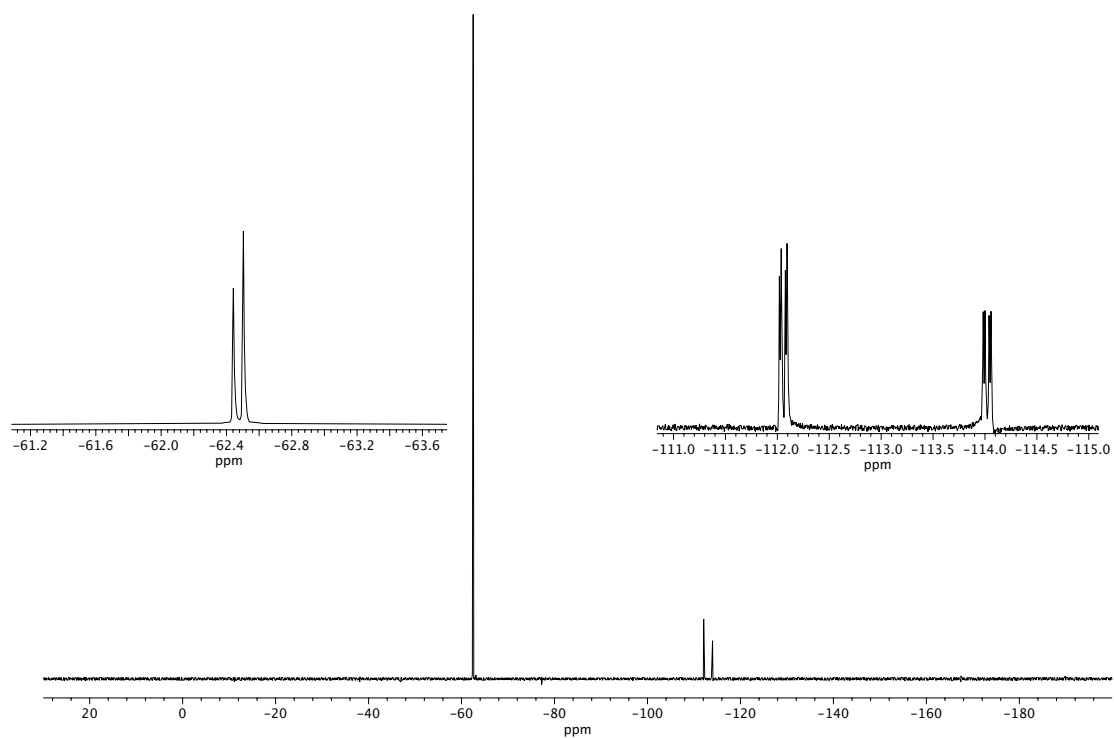


**Figure A4.97**  $^{19}\text{F}$  NMR (282 MHz,  $\text{CDCl}_3$ ) of compound **150r**.

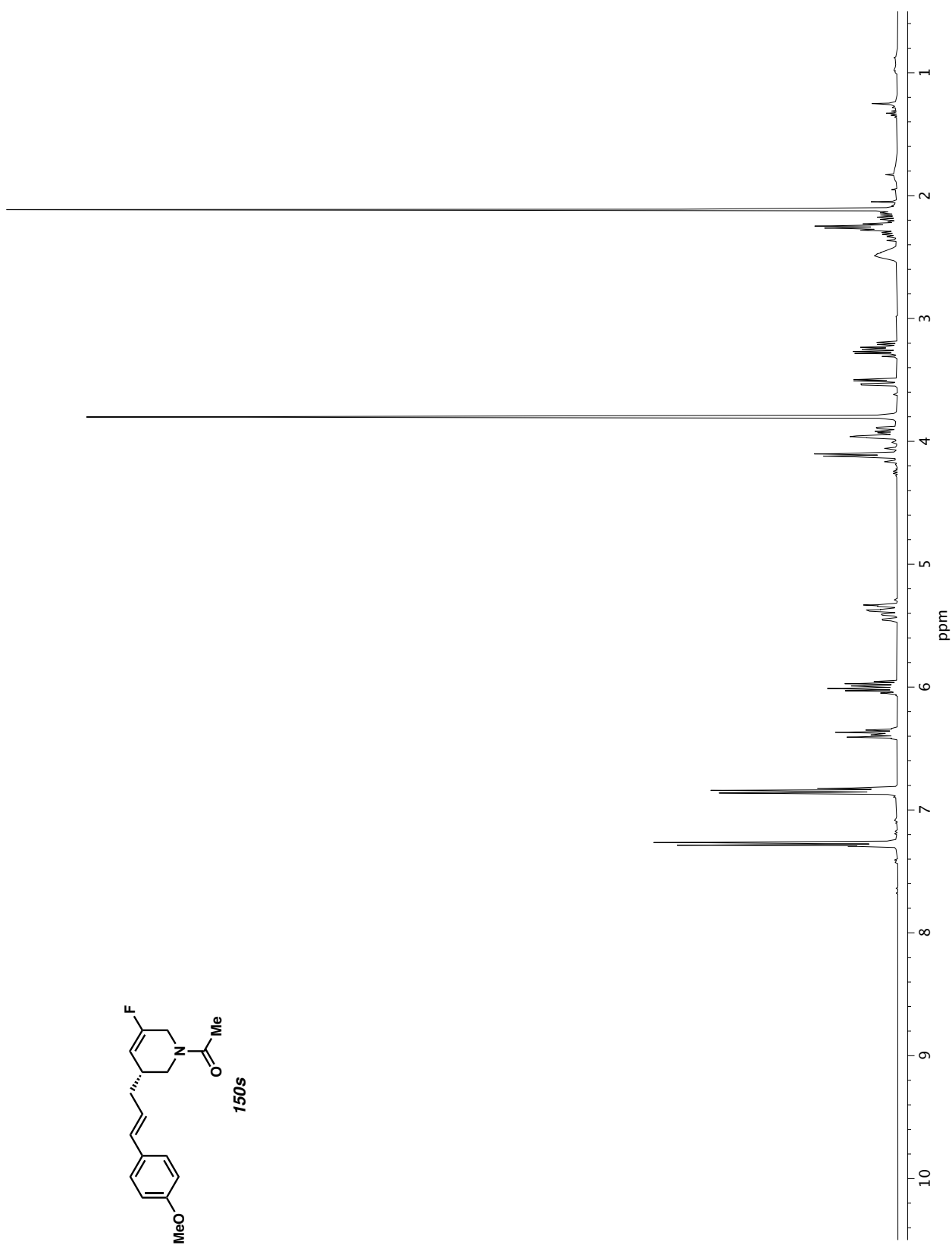


**Figure A4.98**  $^1\text{H}$  NMR (400 MHz,  $\text{CDCl}_3$ ) of compound **150s**.

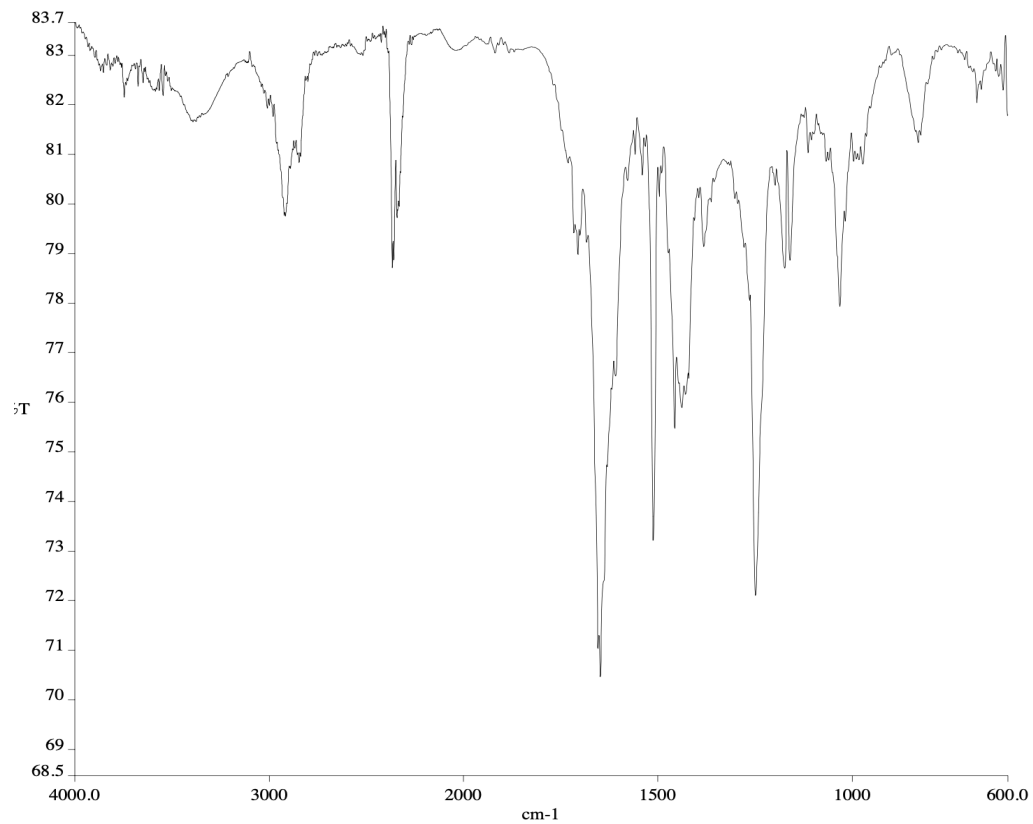


**Figure A4.99** Infrared spectrum (Thin Film, NaCl) of compound **150s**.

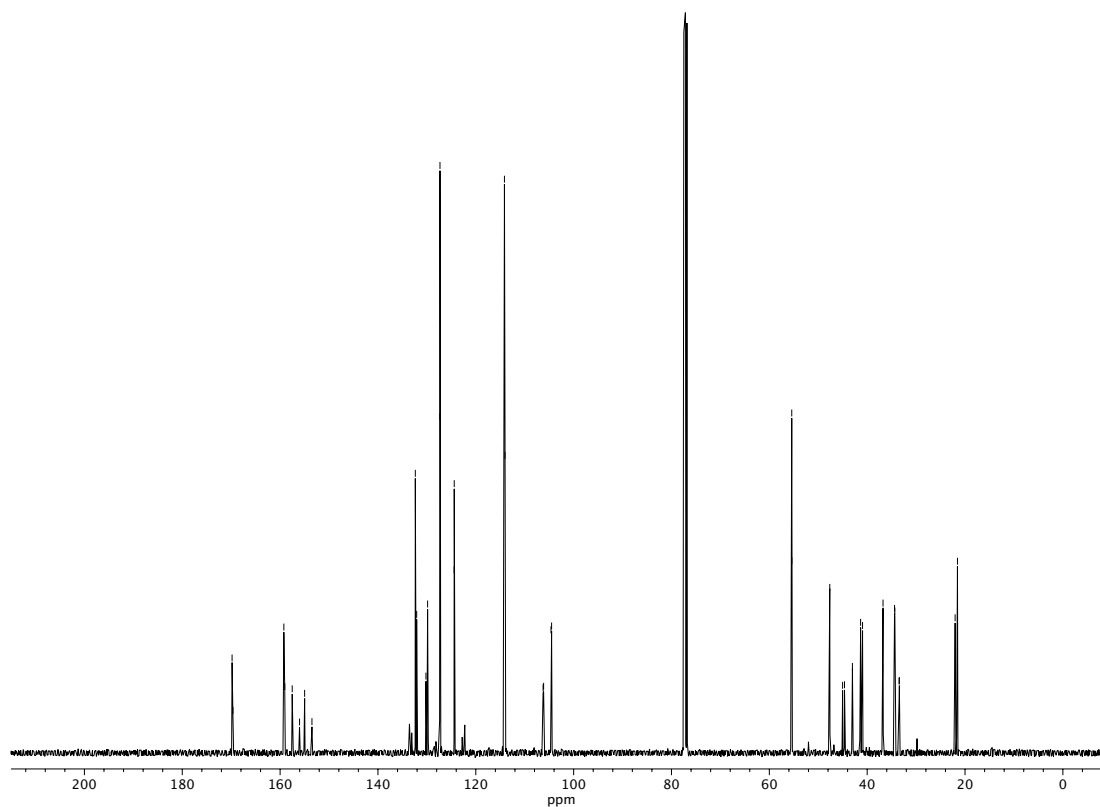


**Figure A4.100** <sup>13</sup>C NMR (100 MHz, CDCl<sub>3</sub>) of compound **150s**.

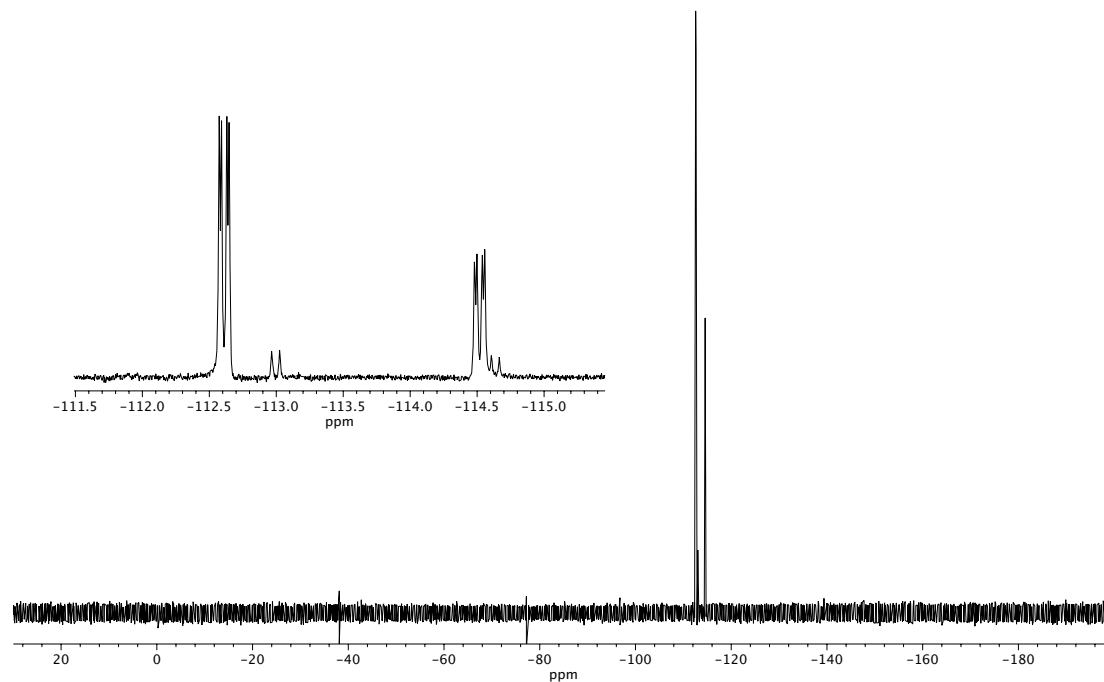


**Figure A4.101**  $^{19}\text{F}$  NMR (282 MHz,  $\text{CDCl}_3$ ) of compound 150s.

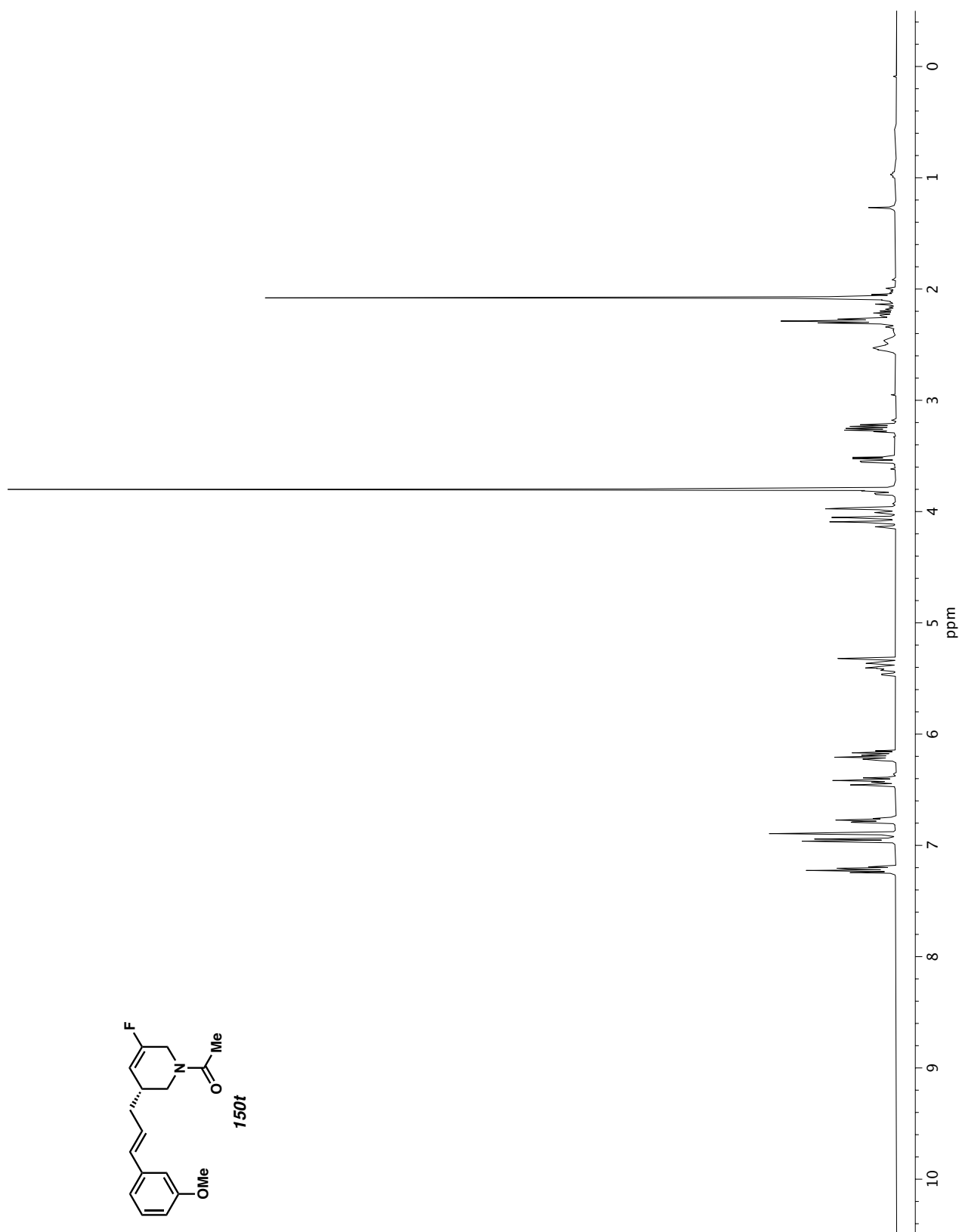


**Figure A4.102**  $^1\text{H}$  NMR (400 MHz,  $\text{CD}_2\text{Cl}_2$ ) of compound **150t**.



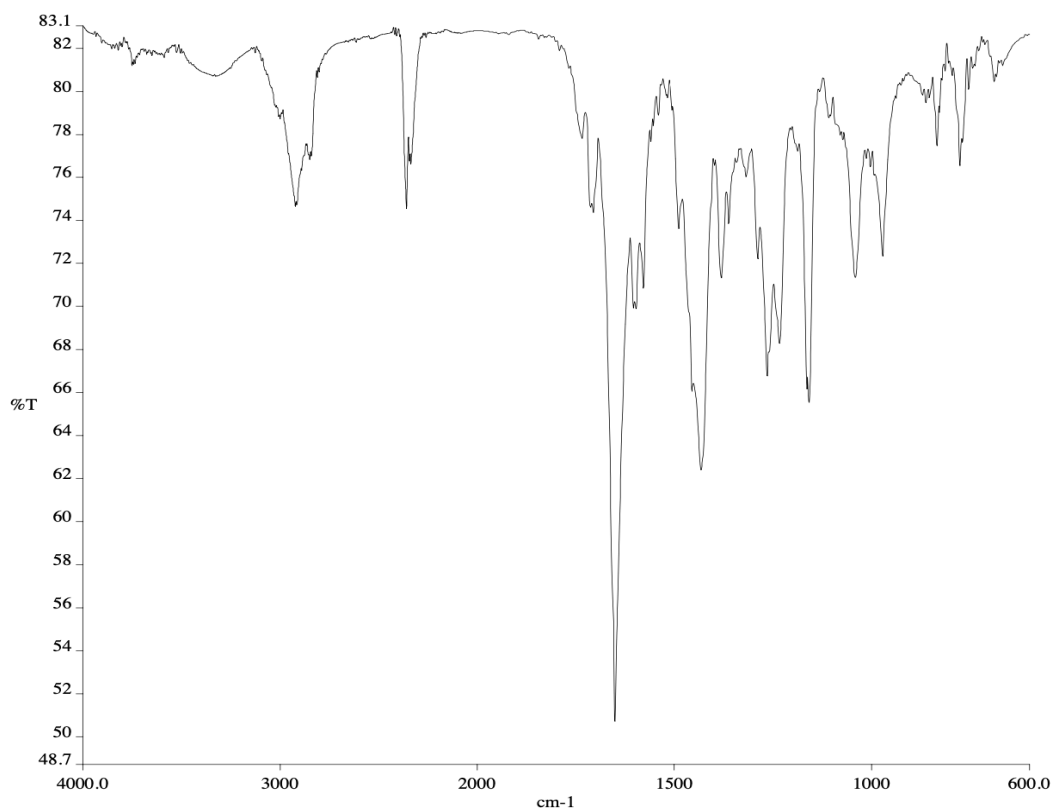


**Figure A4.103** Infrared spectrum (Thin Film, NaCl) of compound **150t**.

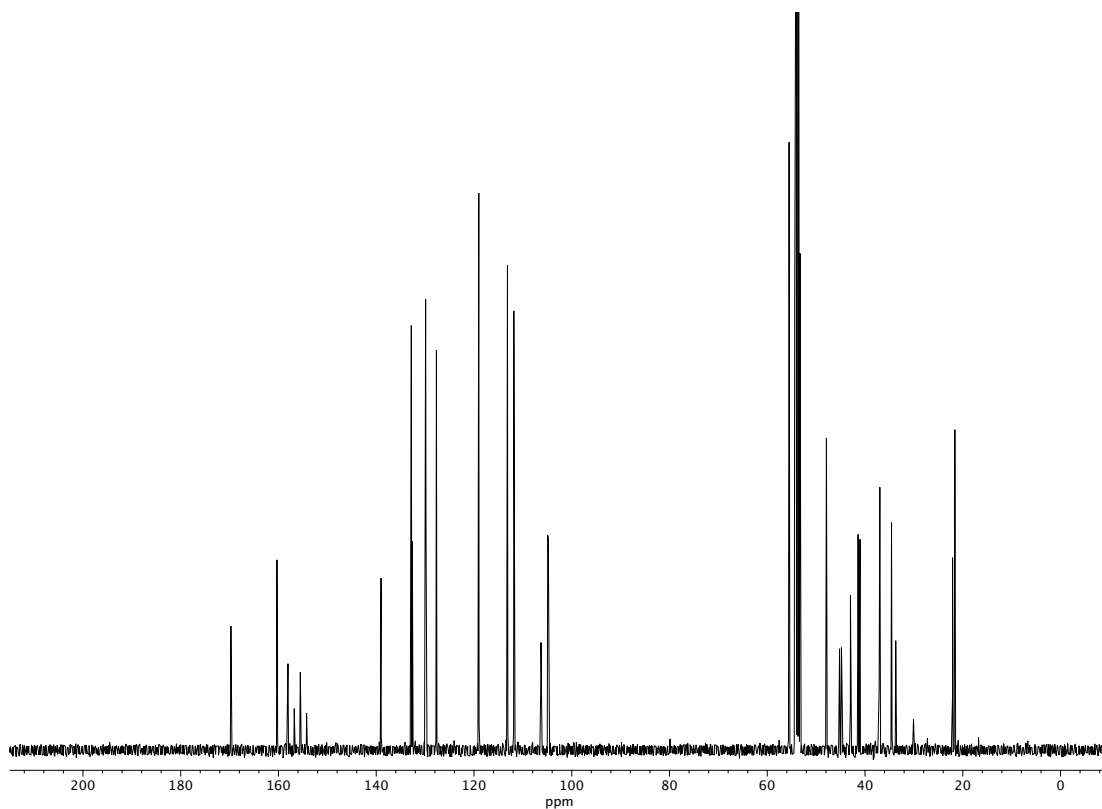


**Figure A4.104** <sup>13</sup>C NMR (100 MHz, CD<sub>2</sub>Cl<sub>2</sub>) of compound **150t**.

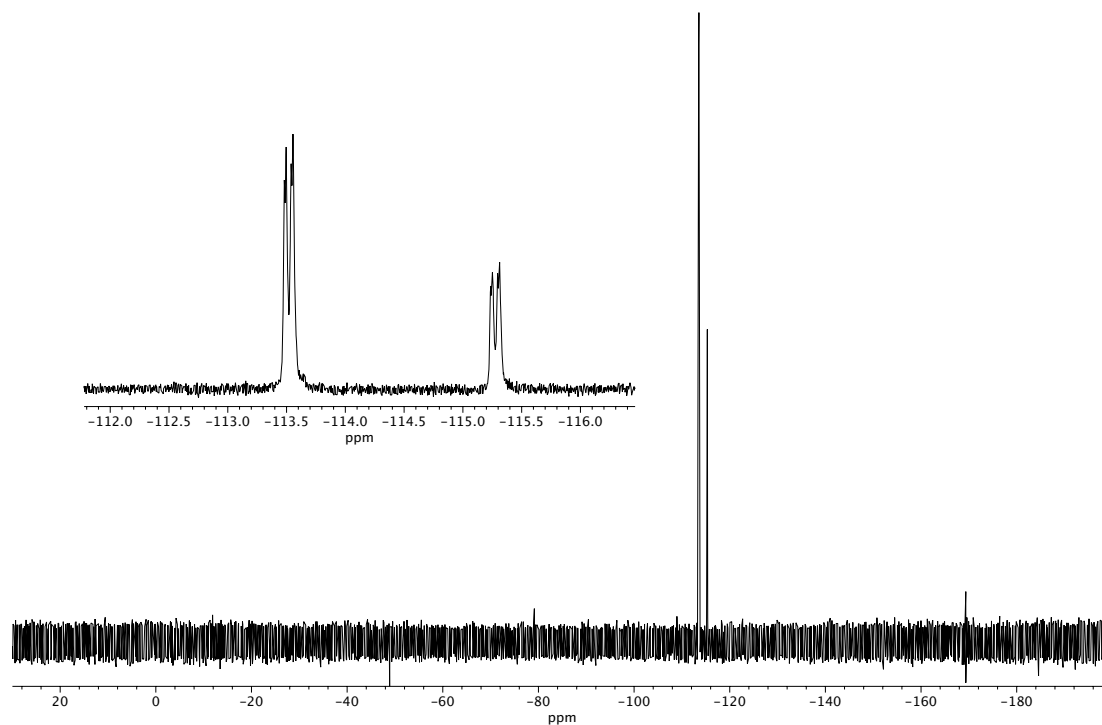


**Figure A4.105**  $^{19}\text{F}$  NMR (282 MHz,  $\text{CD}_2\text{Cl}_2$ ) of compound **150t**.

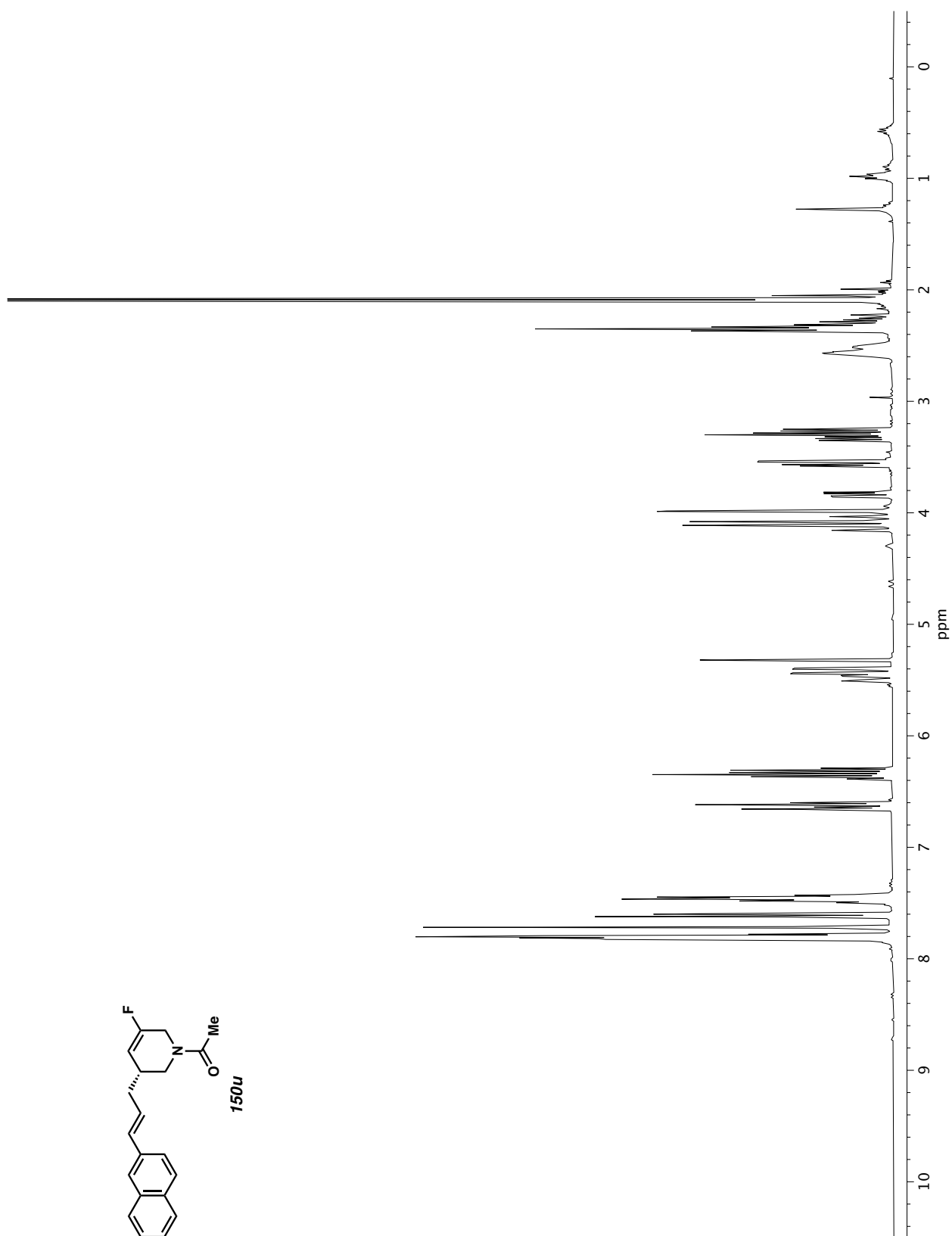


**Figure A4.106**  $^1\text{H}$  NMR (400 MHz,  $\text{CD}_2\text{Cl}_2$ ) of compound **150u**.

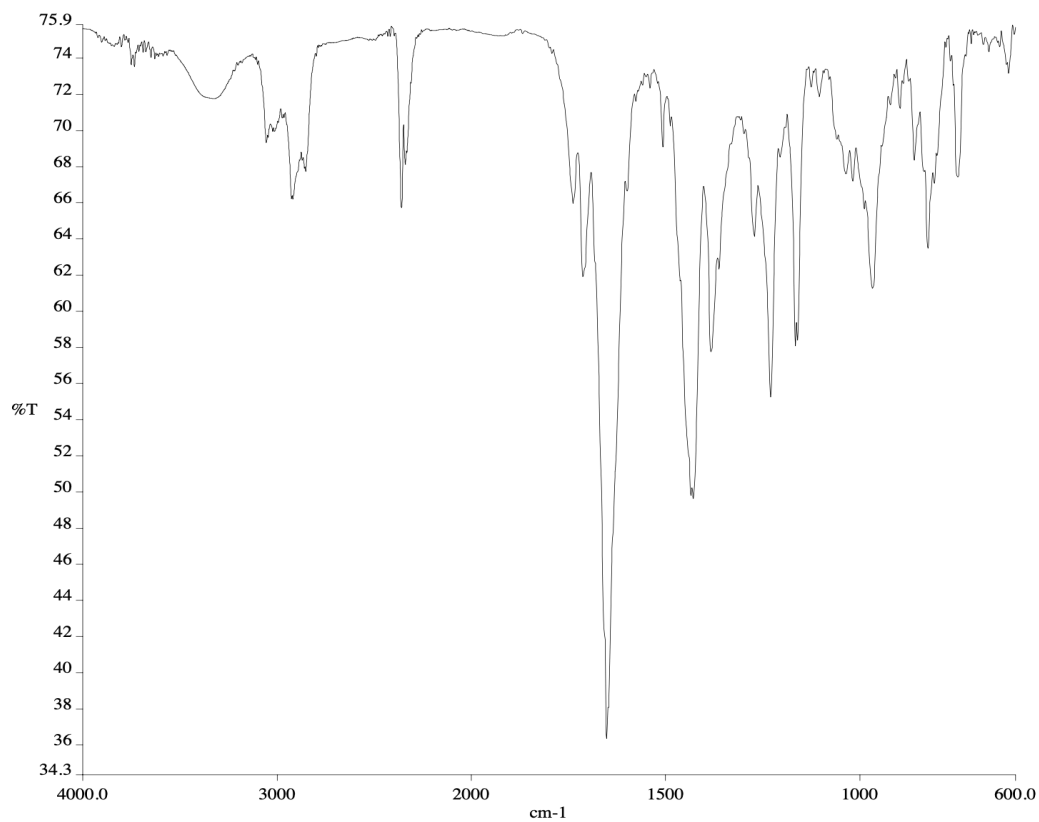


**Figure A4.107** Infrared spectrum (Thin Film, NaCl) of compound **150u**.

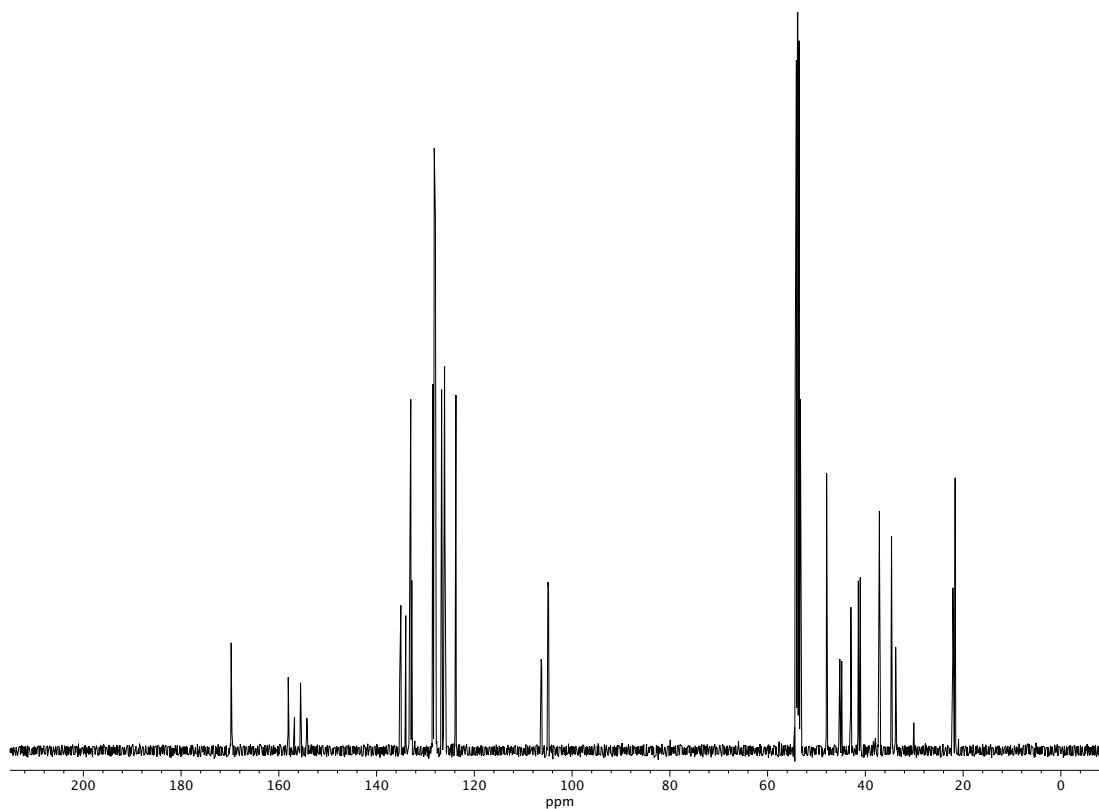


**Figure A4.108** <sup>13</sup>C NMR (100 MHz, CD<sub>2</sub>Cl<sub>2</sub>) of compound **150u**.

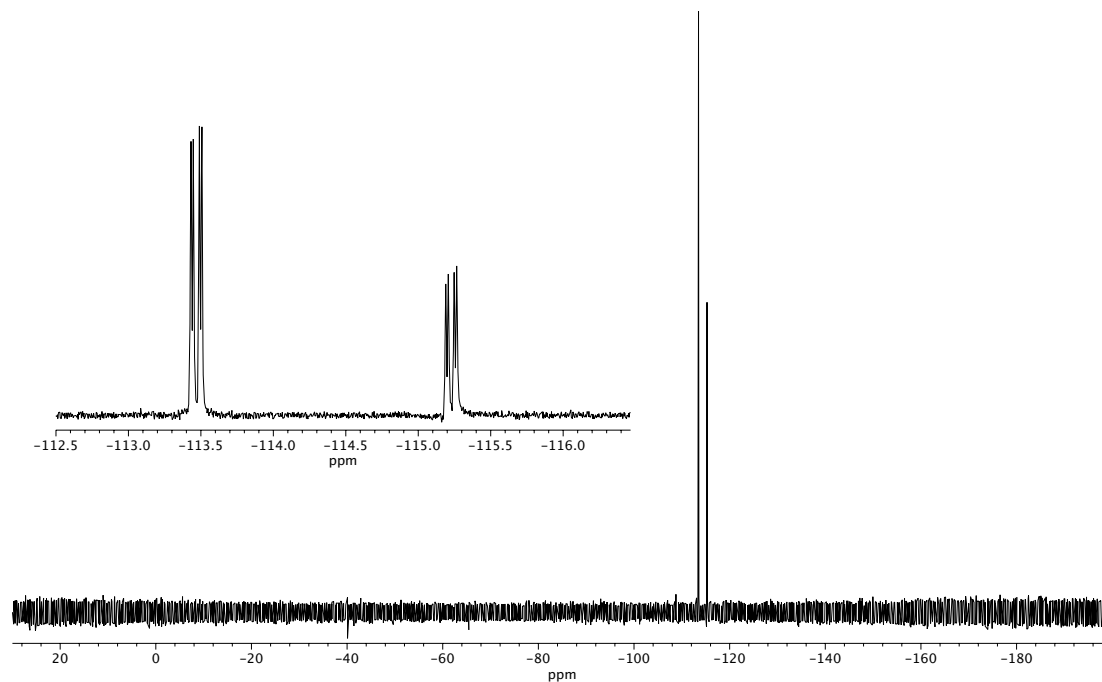


**Figure A4.109**  $^{19}\text{F}$  NMR (282 MHz,  $\text{CD}_2\text{Cl}_2$ ) of compound **150u**.

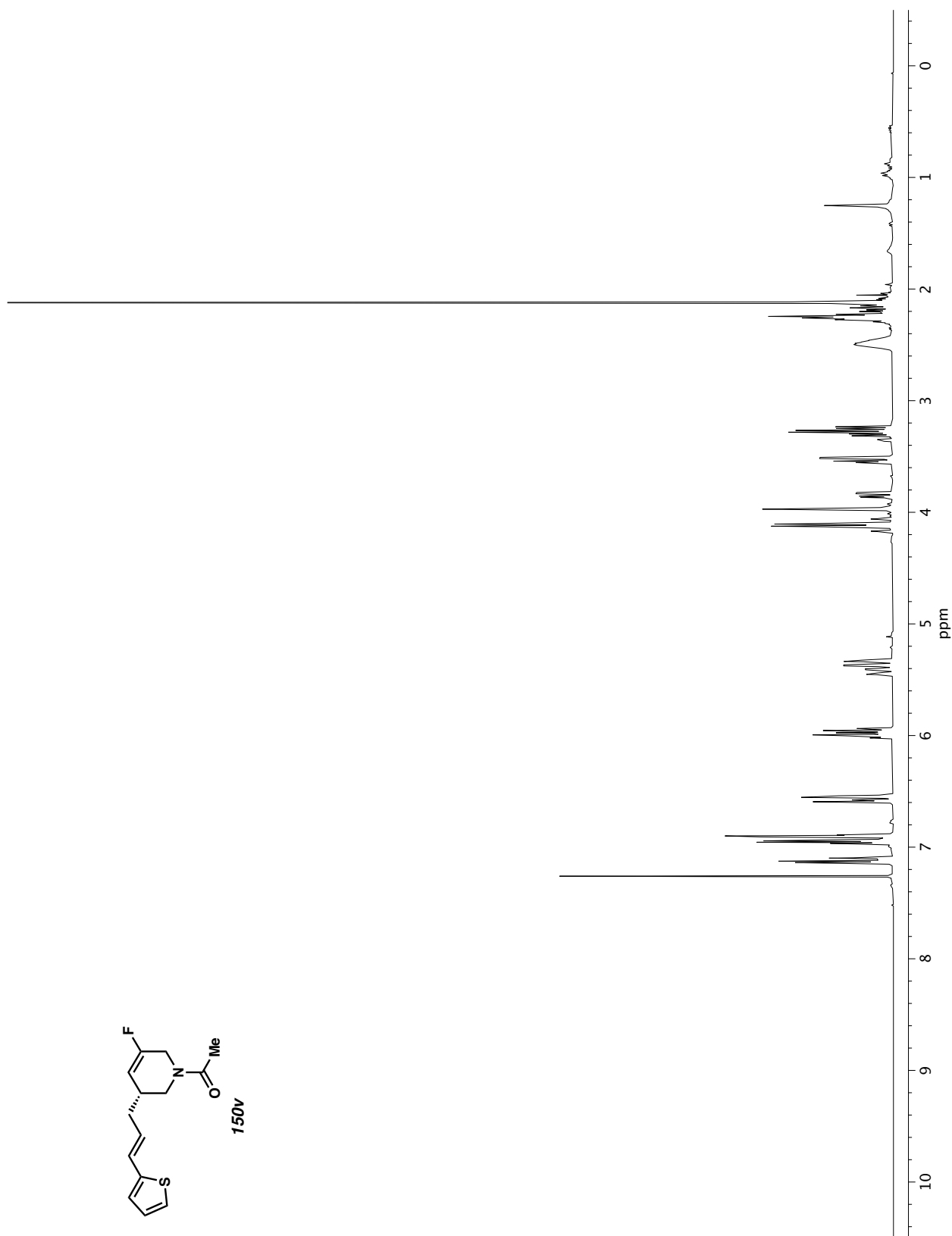
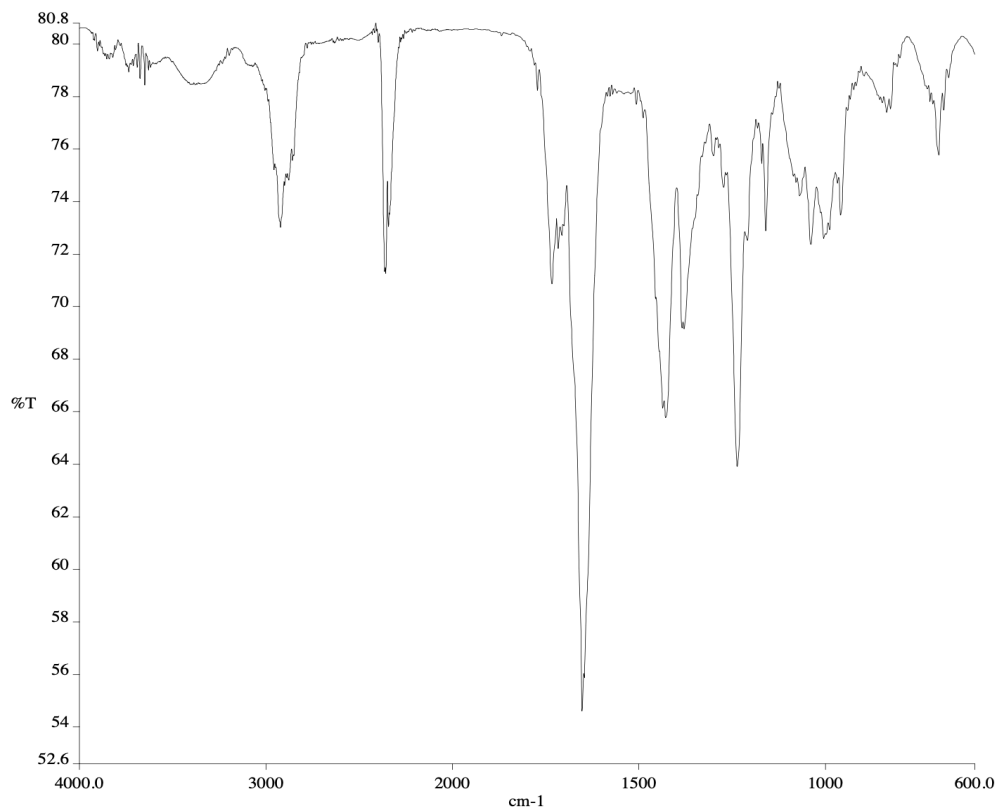
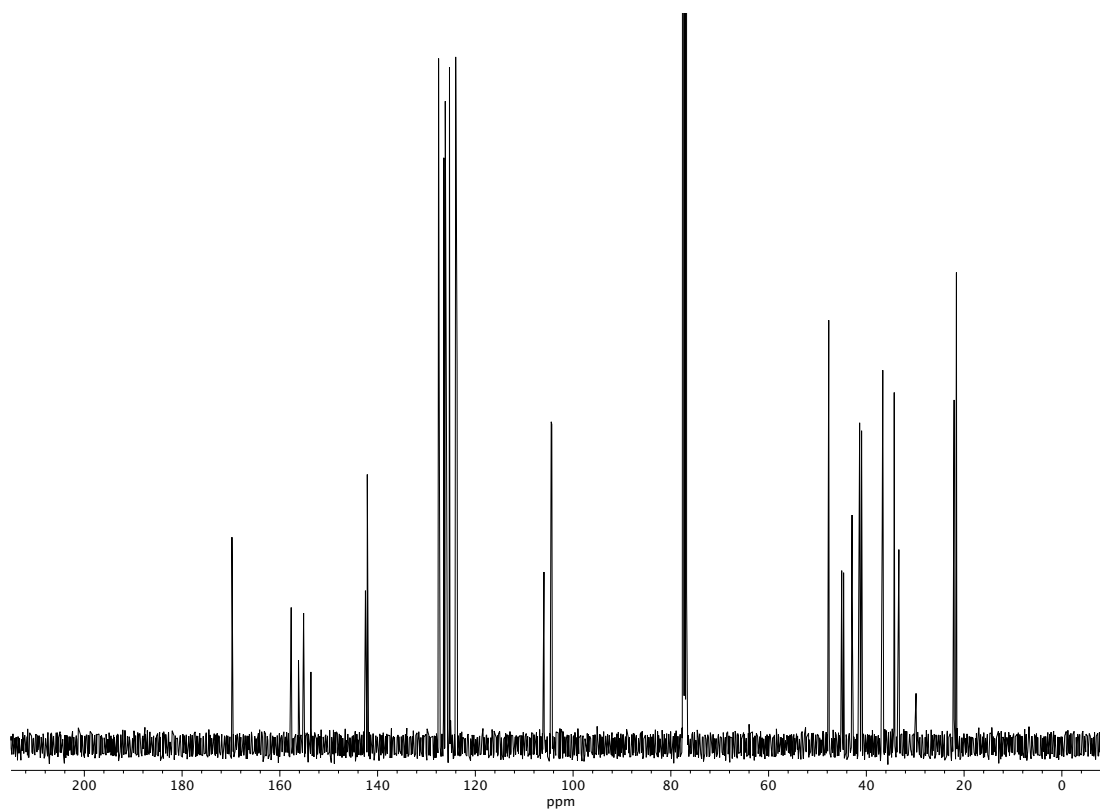


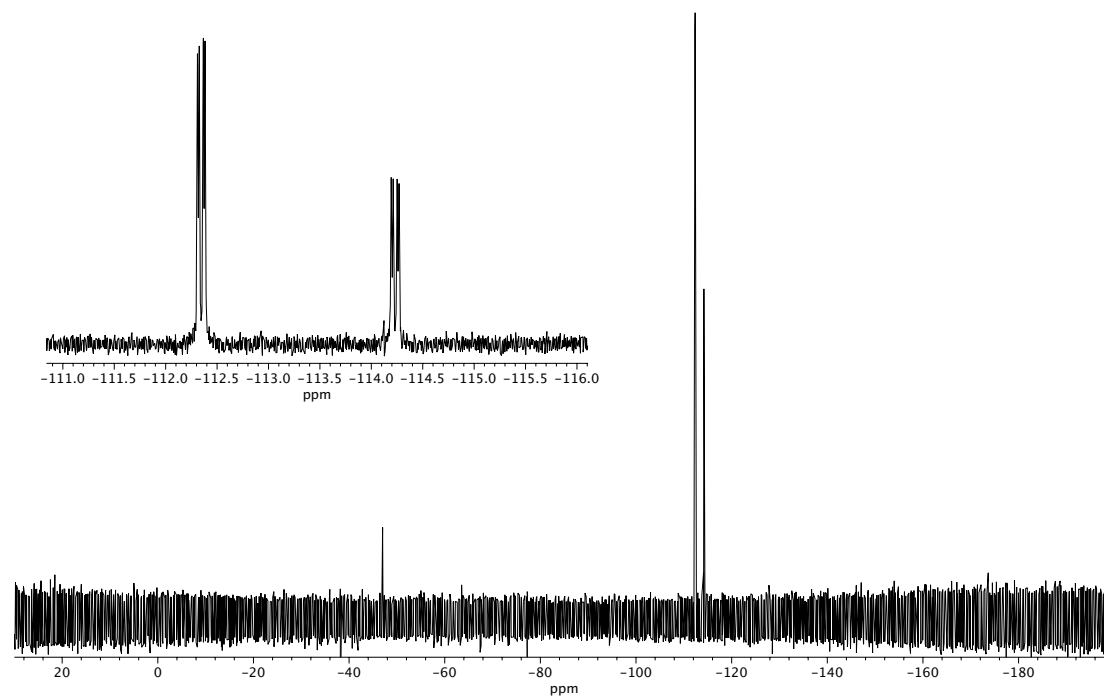
Figure A4.110 <sup>1</sup>H NMR (400 MHz, CDCl<sub>3</sub>) of compound 150v.



**Figure A4.111** Infrared spectrum (Thin Film, NaCl) of compound **150v**.

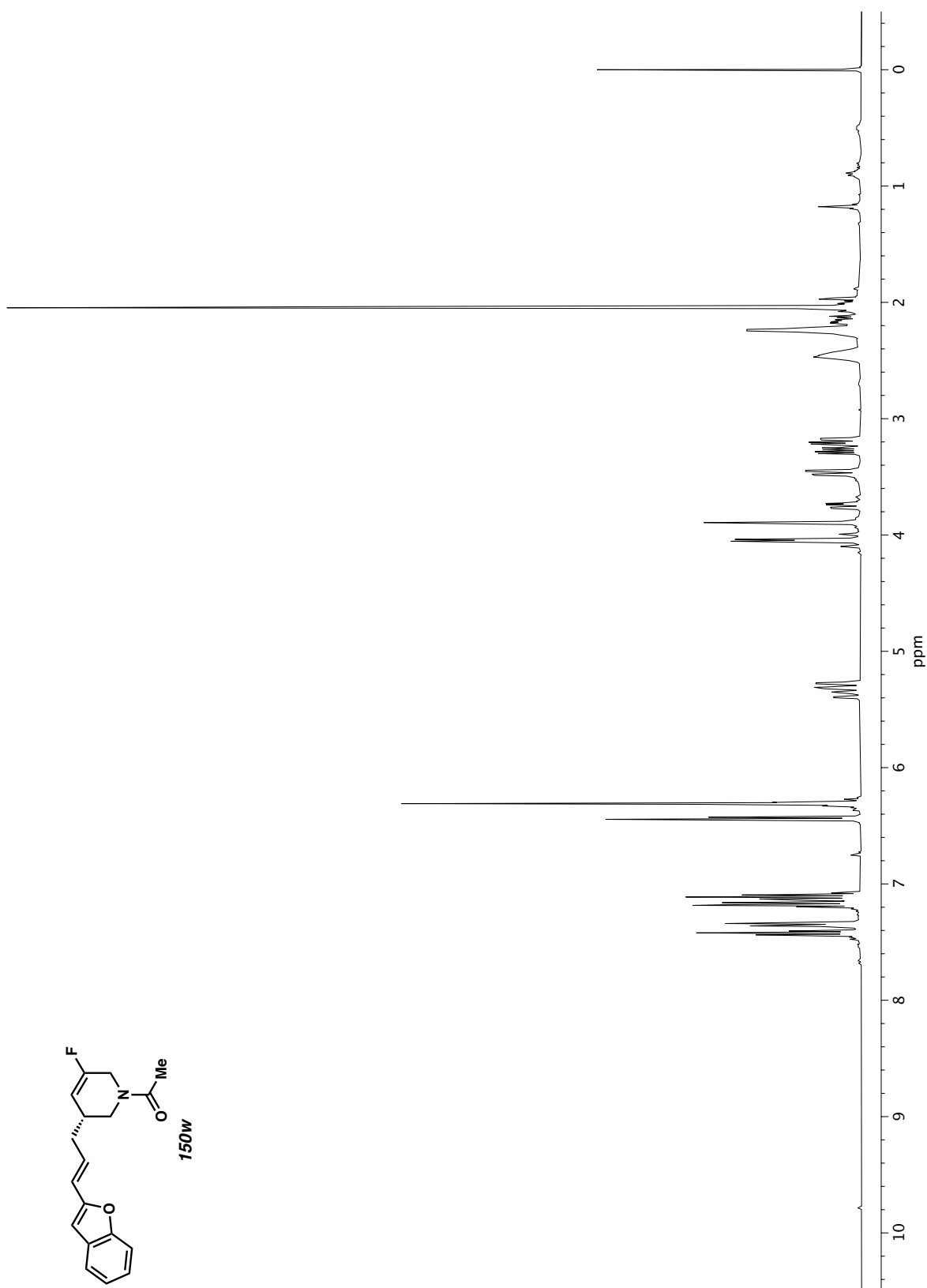


**Figure A4.112** <sup>13</sup>C NMR (100 MHz, CDCl<sub>3</sub>) of compound **150v**.

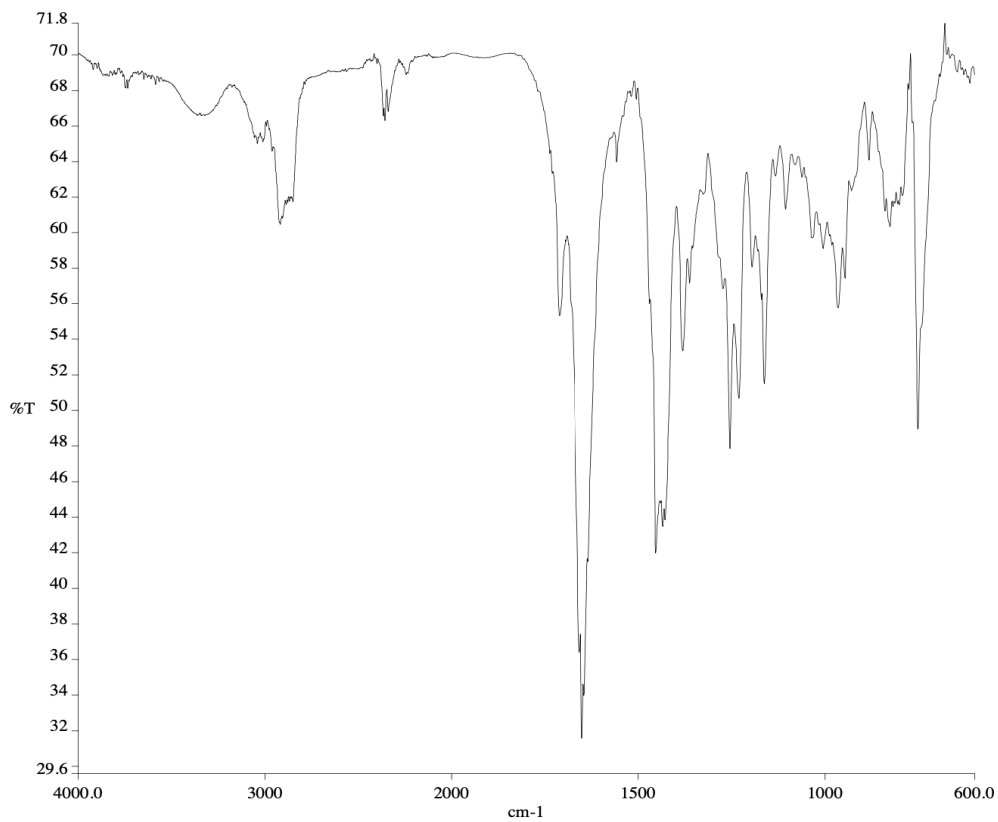


**Figure A4.113**  $^{19}\text{F}$  NMR (282 MHz,  $\text{CDCl}_3$ ) of compound **150v**.

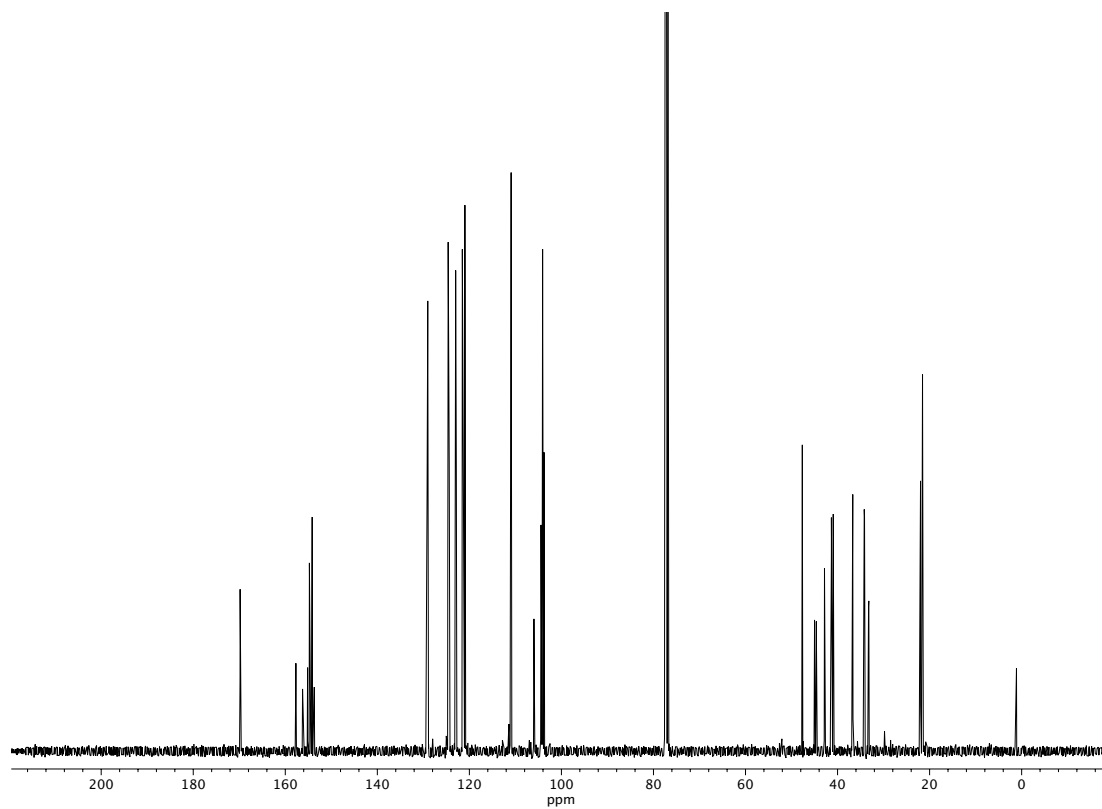




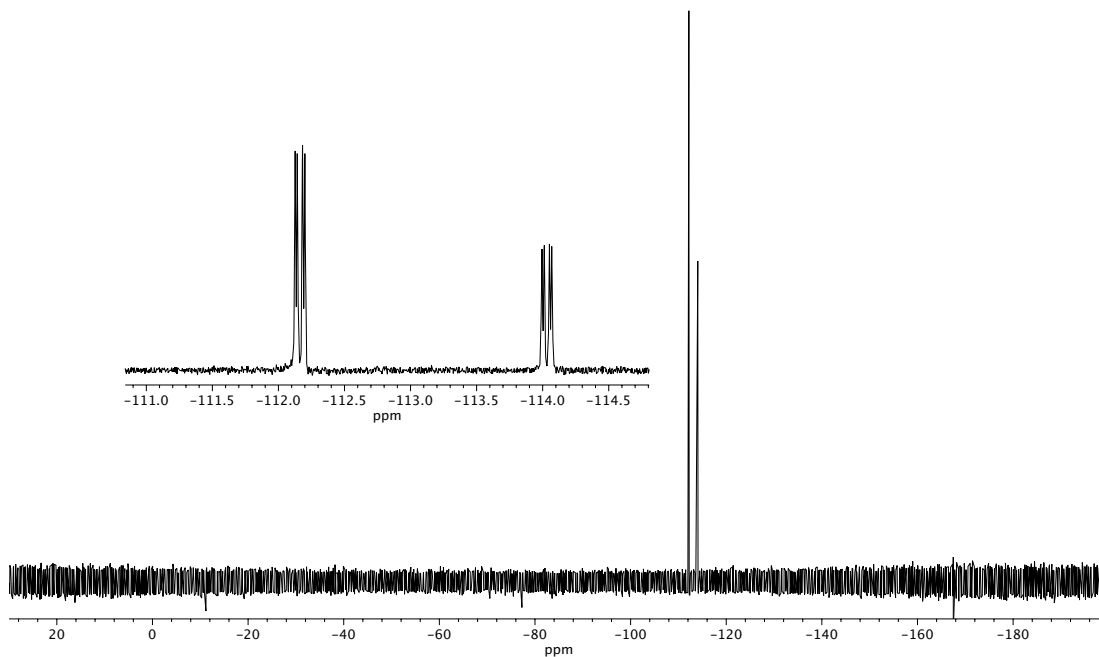
**Figure A4.114**  $^1\text{H}$  NMR (400 MHz,  $\text{CDCl}_3$ ) of compound **150w**.



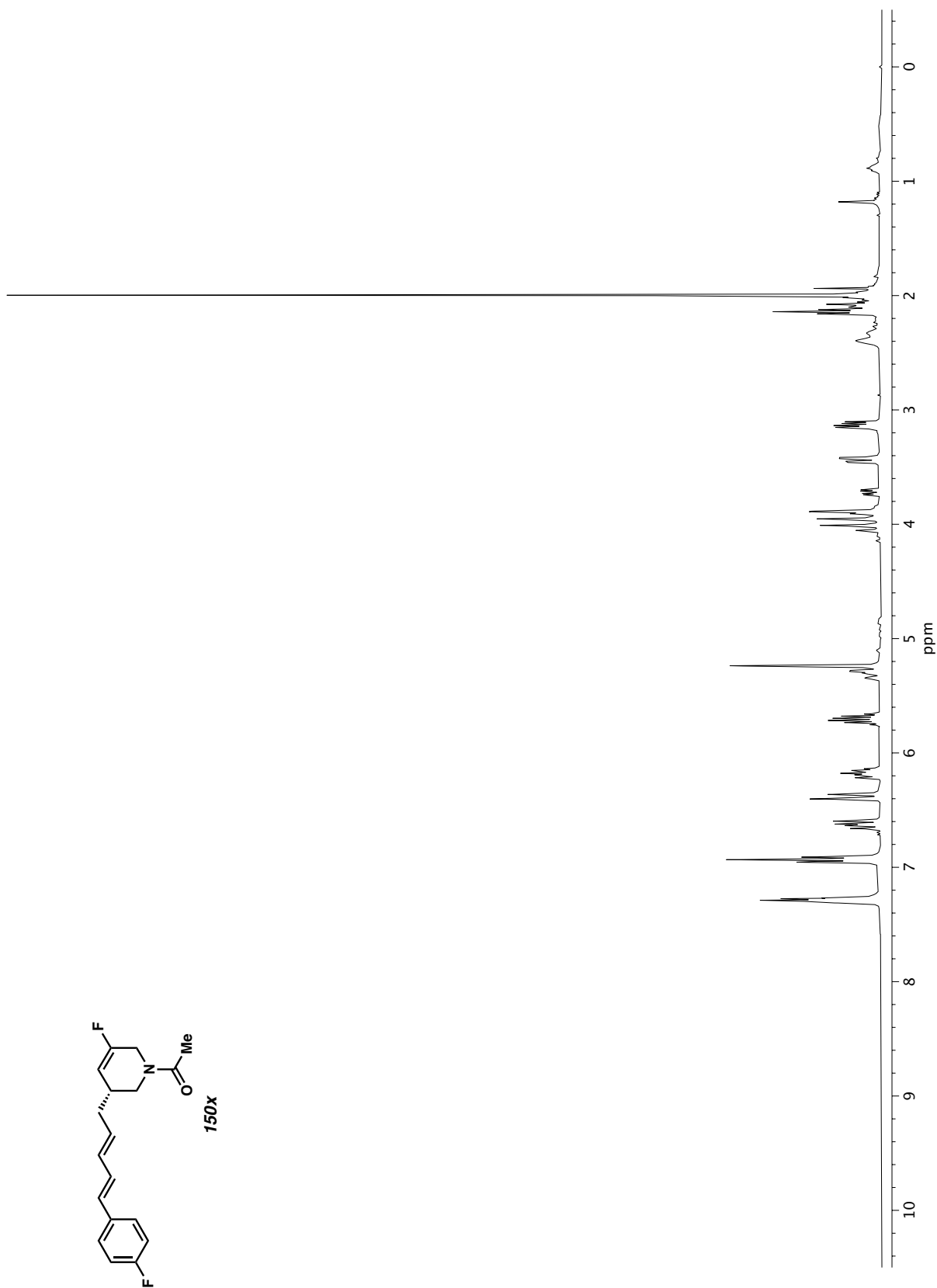
**Figure A4.115** Infrared spectrum (Thin Film, NaCl) of compound **150w**.



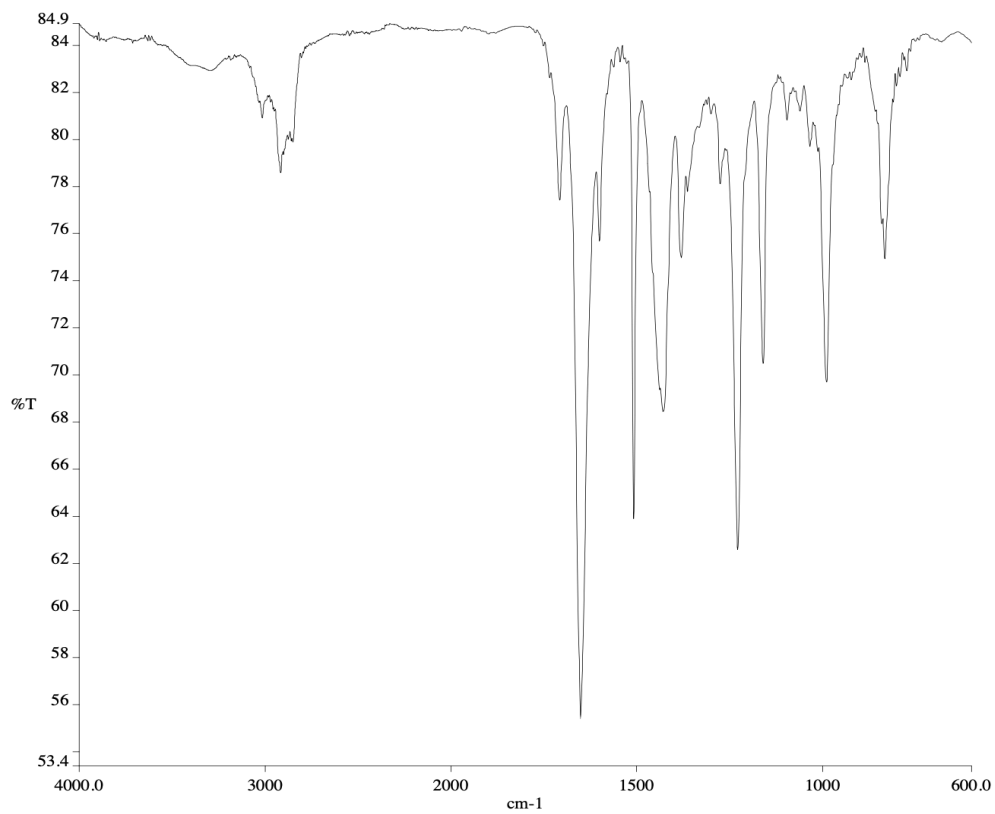
**Figure A4.116** <sup>13</sup>C NMR (100 MHz, CDCl<sub>3</sub>) of compound **150w**.



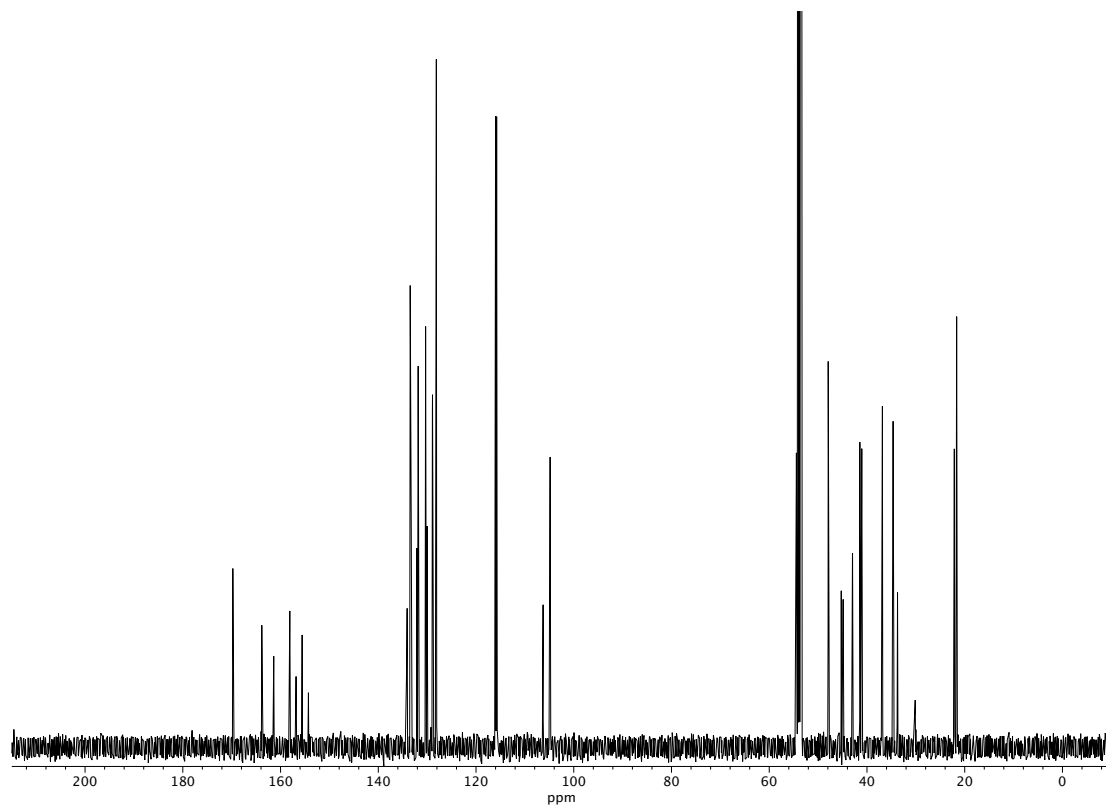
**Figure A4.117**  $^{19}\text{F}$  NMR (282 MHz,  $\text{CDCl}_3$ ) of compound **150w**.



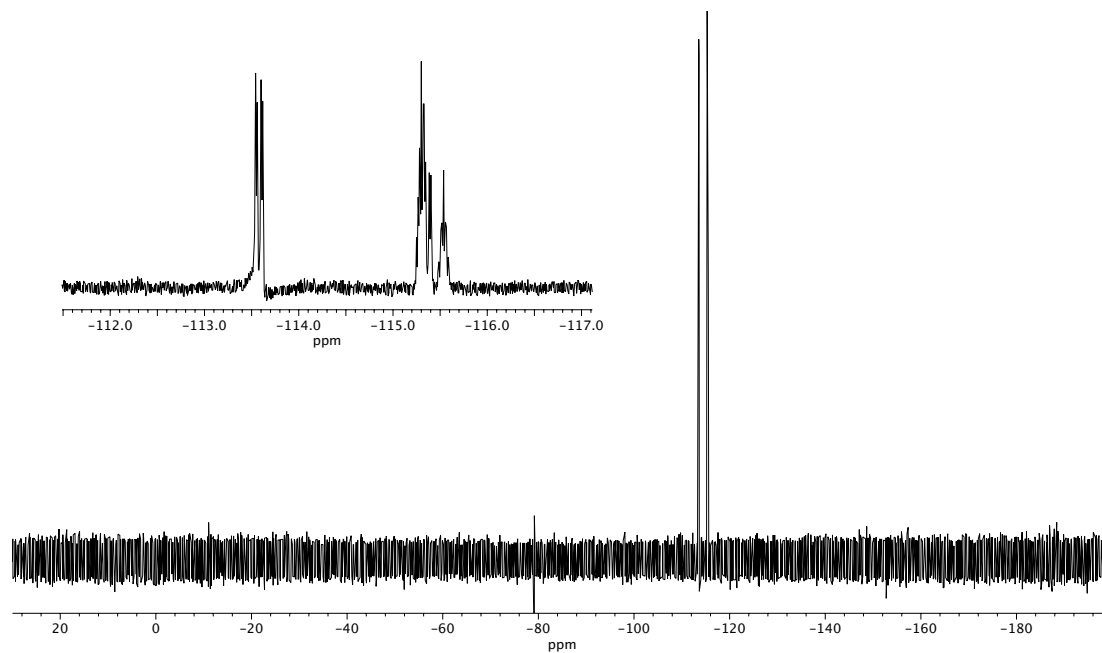
**Figure A4.118** <sup>1</sup>H NMR (400 MHz, CD<sub>2</sub>Cl<sub>2</sub>) of compound **150x**.



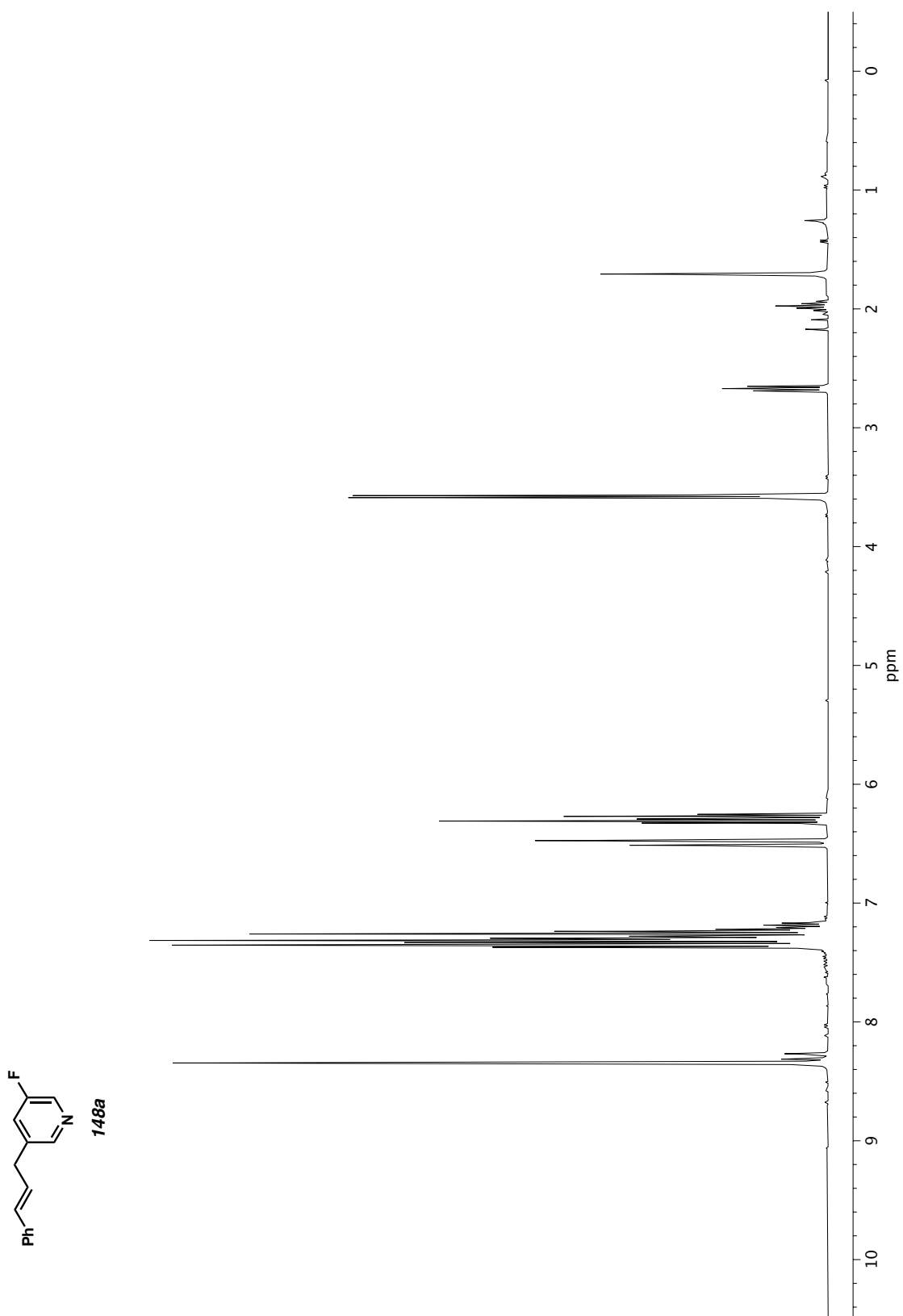
**Figure A4.119** Infrared spectrum (Thin Film, NaCl) of compound **150x**.



**Figure A4.120** <sup>13</sup>C NMR (100 MHz, CD<sub>2</sub>Cl<sub>2</sub>) of compound **150x**.



**Figure A4.121**  $^{19}\text{F}$  NMR (282 MHz,  $\text{CD}_2\text{Cl}_2$ ) of compound **150x**.

Figure A4.122  $^1\text{H}$  NMR (400 MHz,  $\text{CDCl}_3$ ) of compound **148a**.

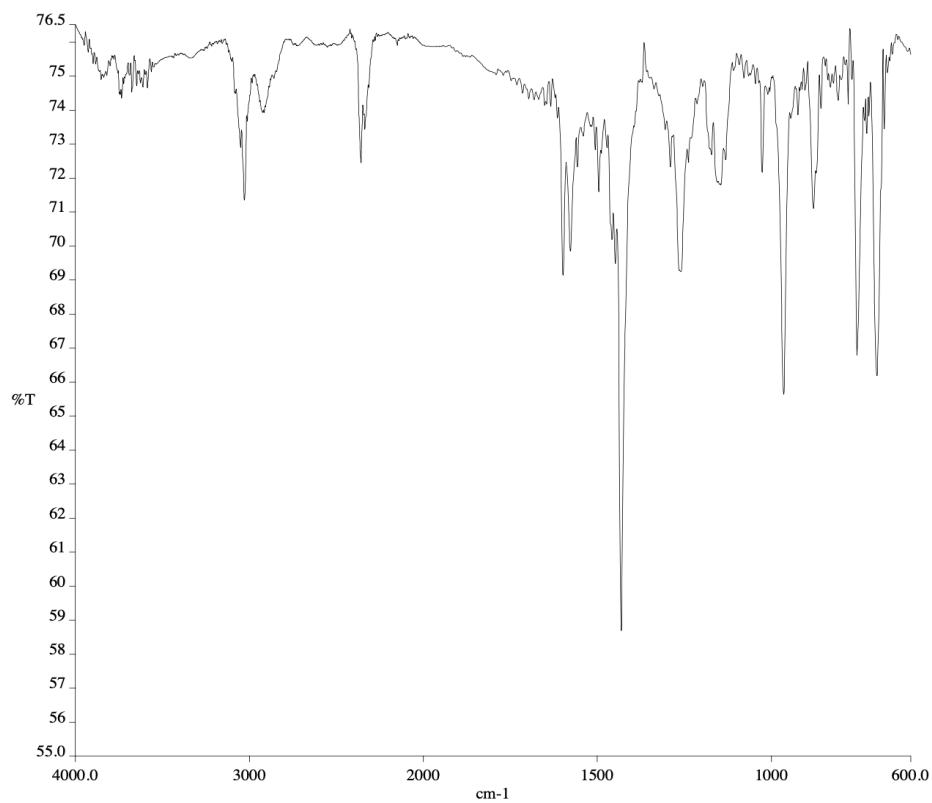


**Figure A4.123** Infrared spectrum (Thin Film, NaCl) of compound **148a**.

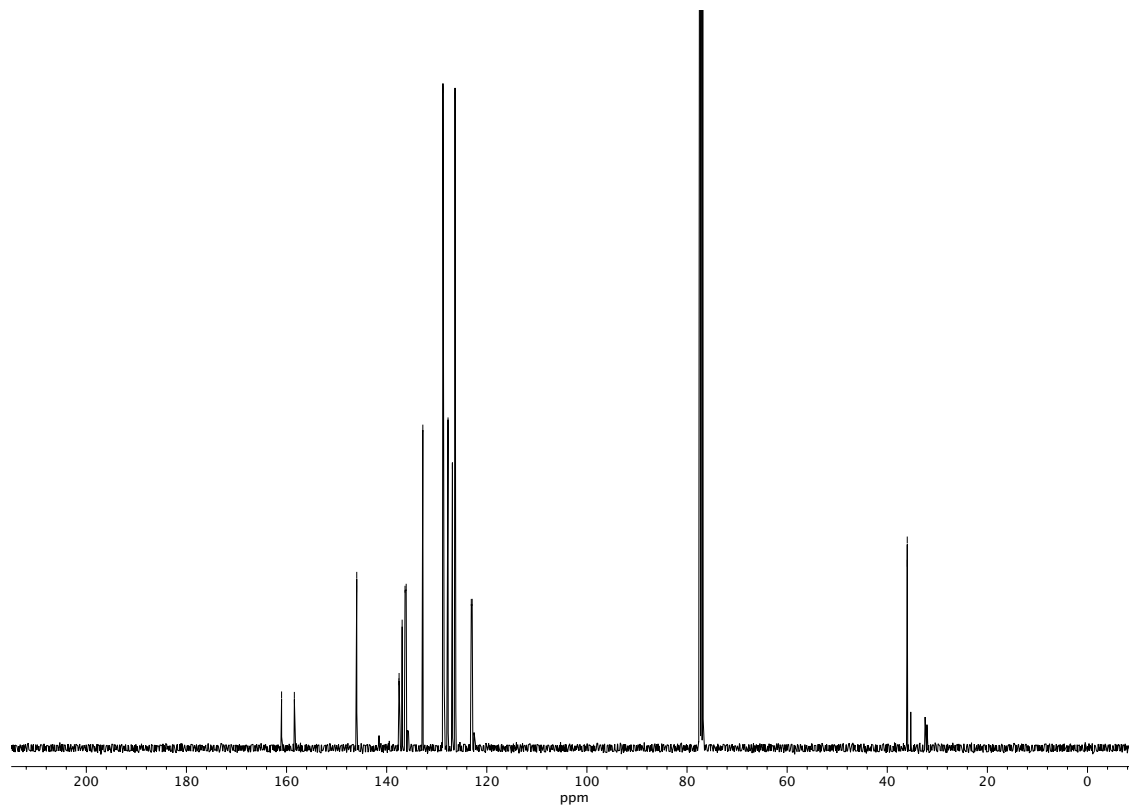


**Figure A4.124** <sup>13</sup>C NMR (100 MHz, CDCl<sub>3</sub>) of compound **148a**.



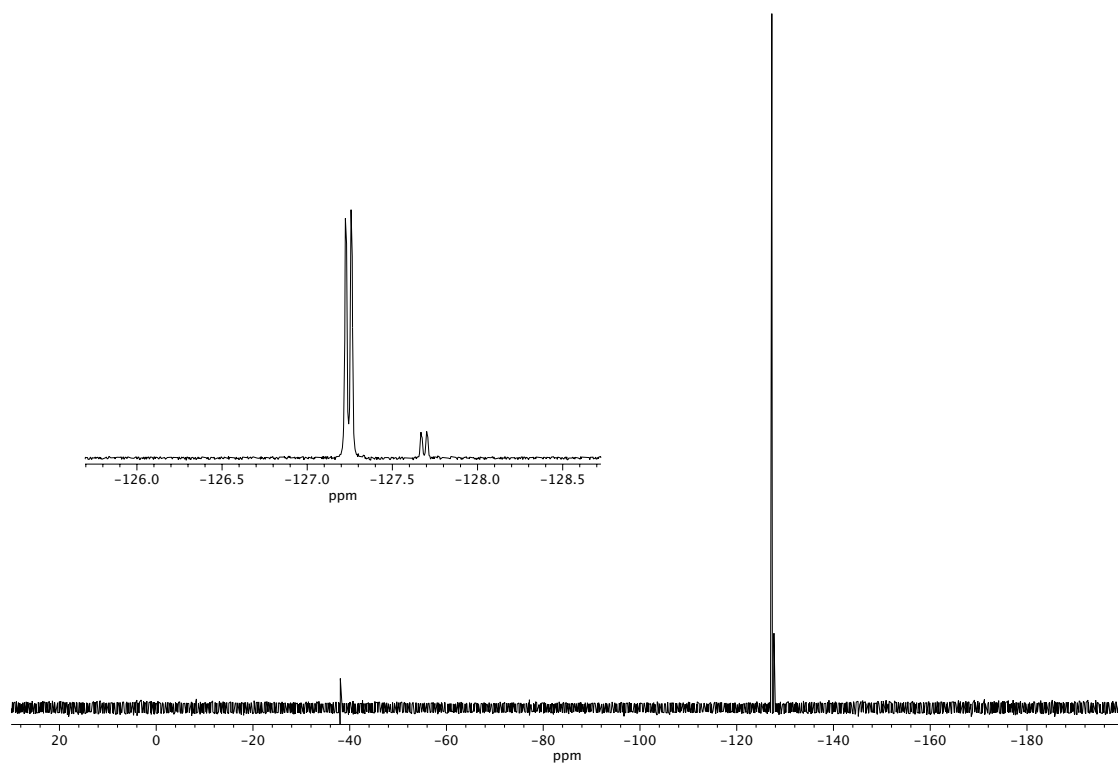


**Figure A4.125**  $^{19}\text{F}$  NMR (282 MHz,  $\text{CDCl}_3$ ) of compound **148a**.

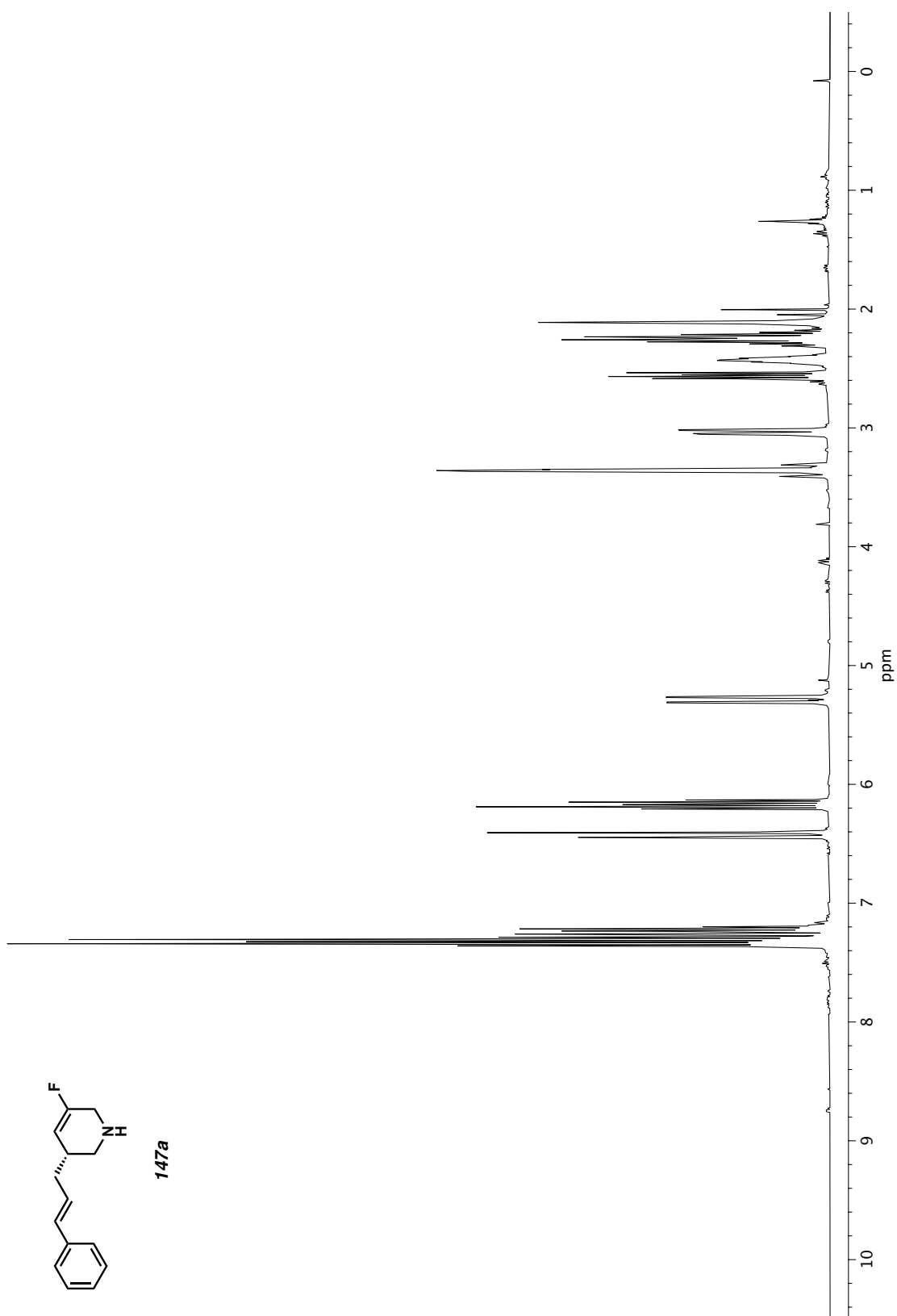
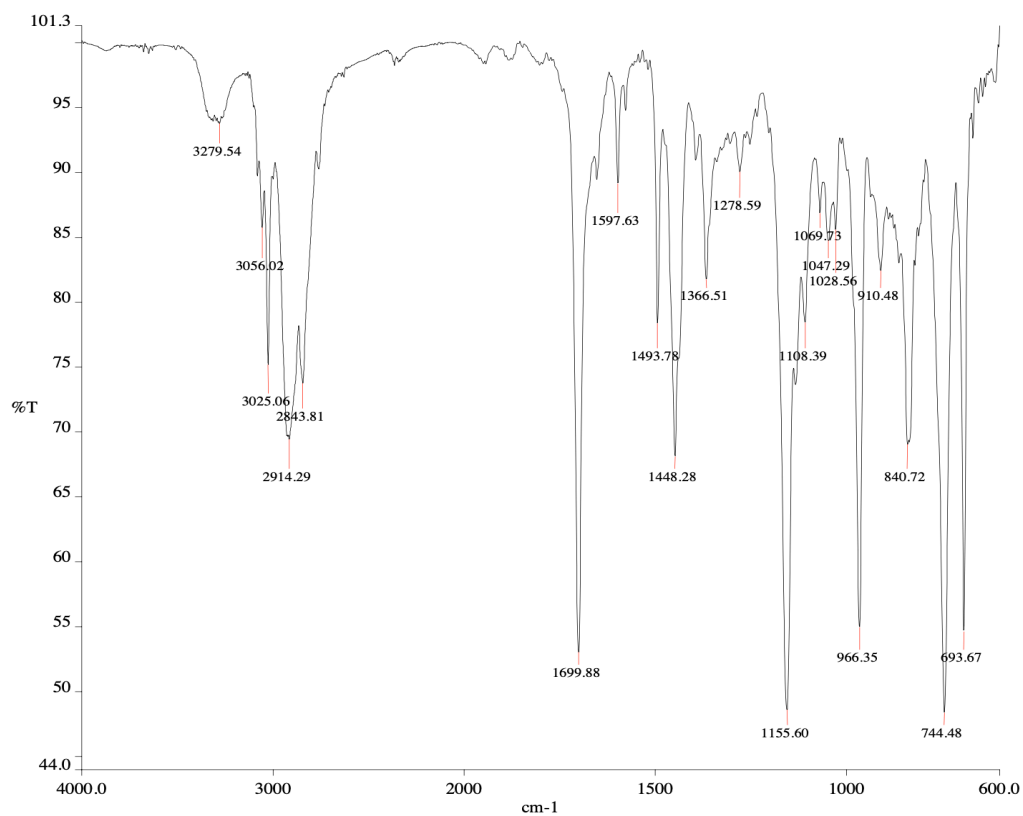
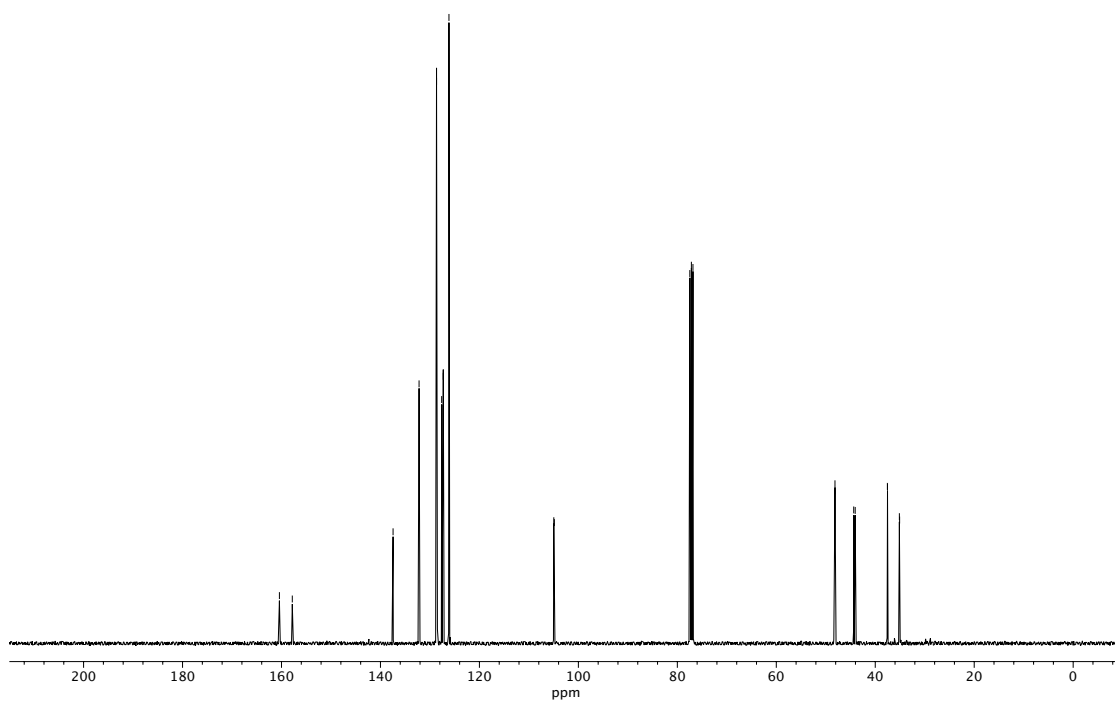


Figure A4.126  $^1\text{H}$  NMR (400 MHz,  $\text{CDCl}_3$ ) of compound **147a**.



**Figure A4.127** Infrared spectrum (Thin Film, NaCl) of compound **147a**.



**Figure A4.128** <sup>13</sup>C NMR (100 MHz, CDCl<sub>3</sub>) of compound **147a**.

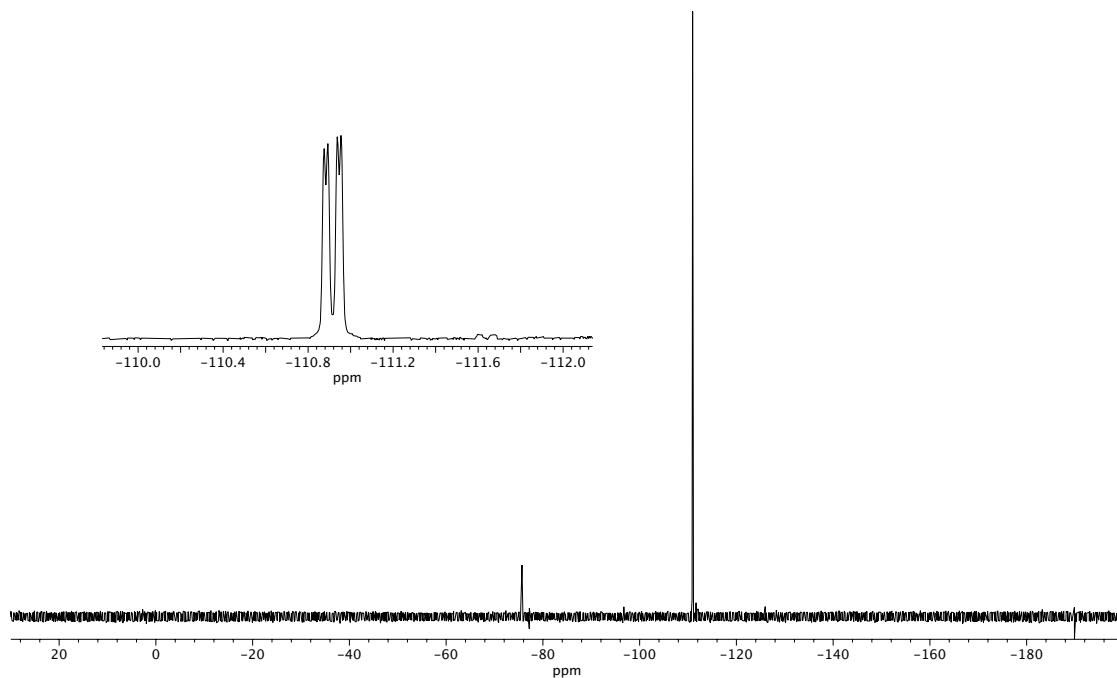


Figure A4.129  $^{19}\text{F}$  NMR (282 MHz,  $\text{CDCl}_3$ ) of compound **147a**.

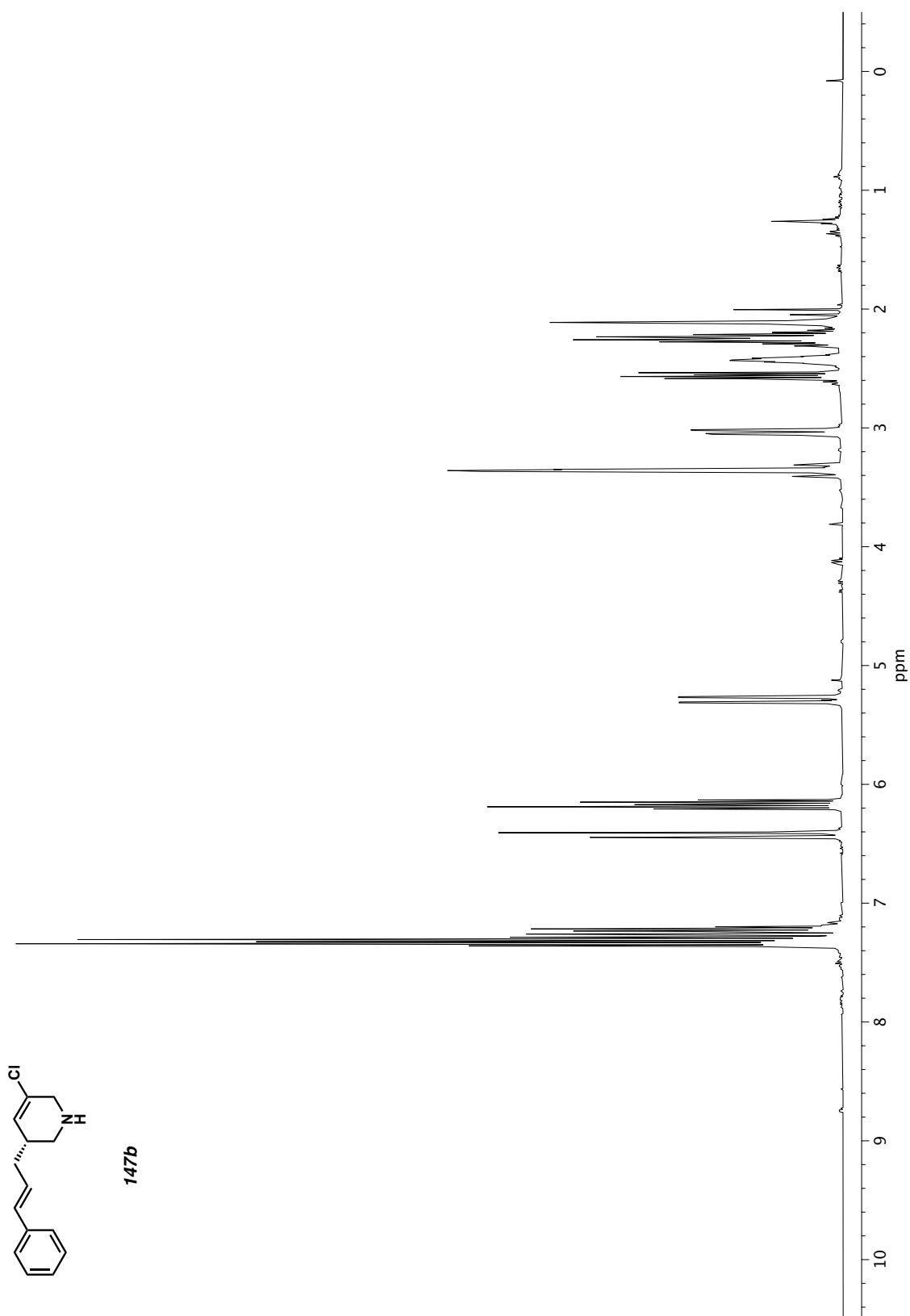
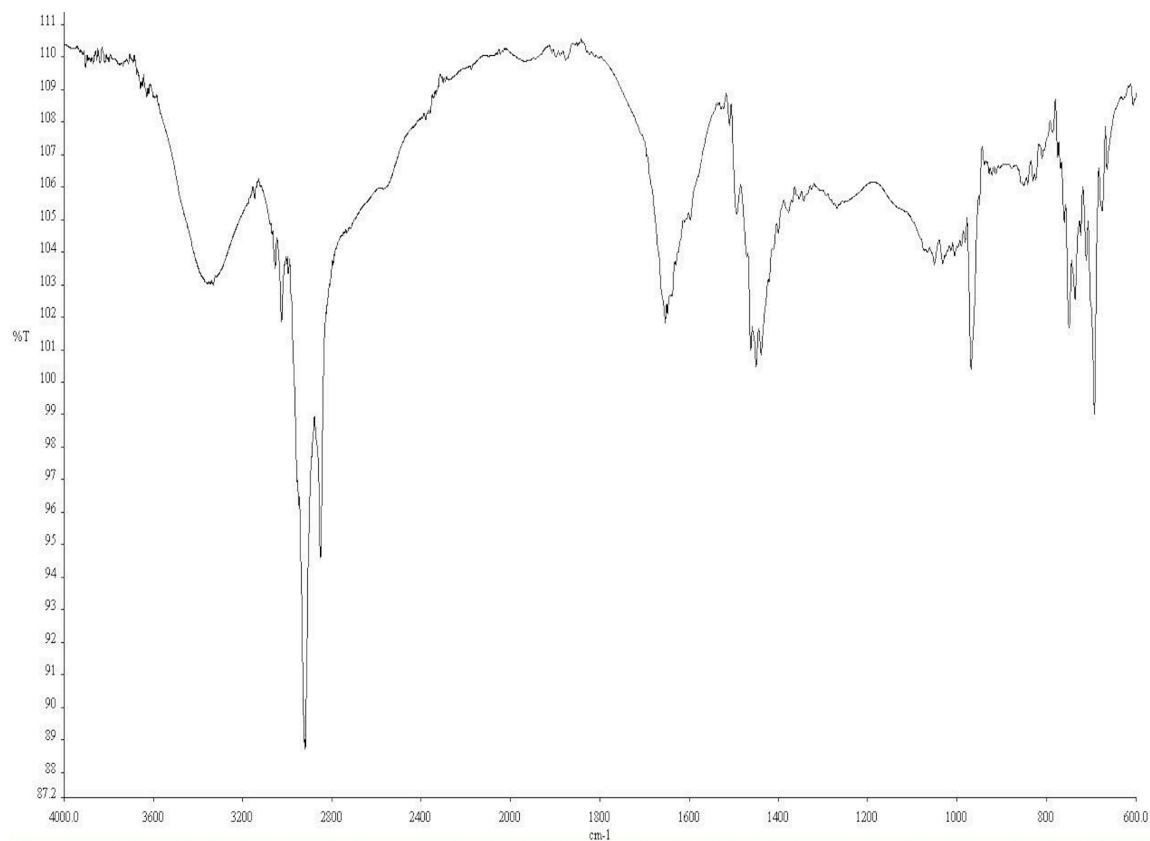
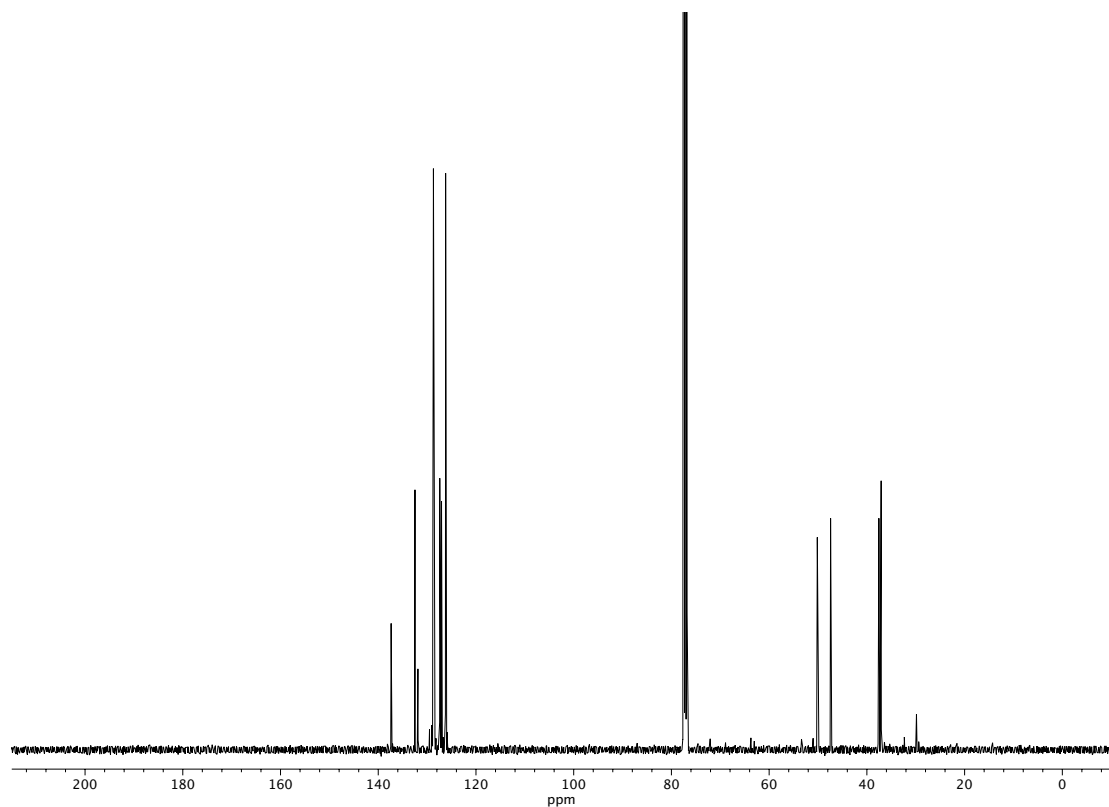


Figure A4.130 <sup>1</sup>H NMR (400 MHz, CDCl<sub>3</sub>) of compound **147b**.



**Figure A4.131** Infrared spectrum (Thin Film, NaCl) of compound **147b**.



**Figure A4.132** <sup>13</sup>C NMR (100 MHz, CDCl<sub>3</sub>) of compound **147b**.

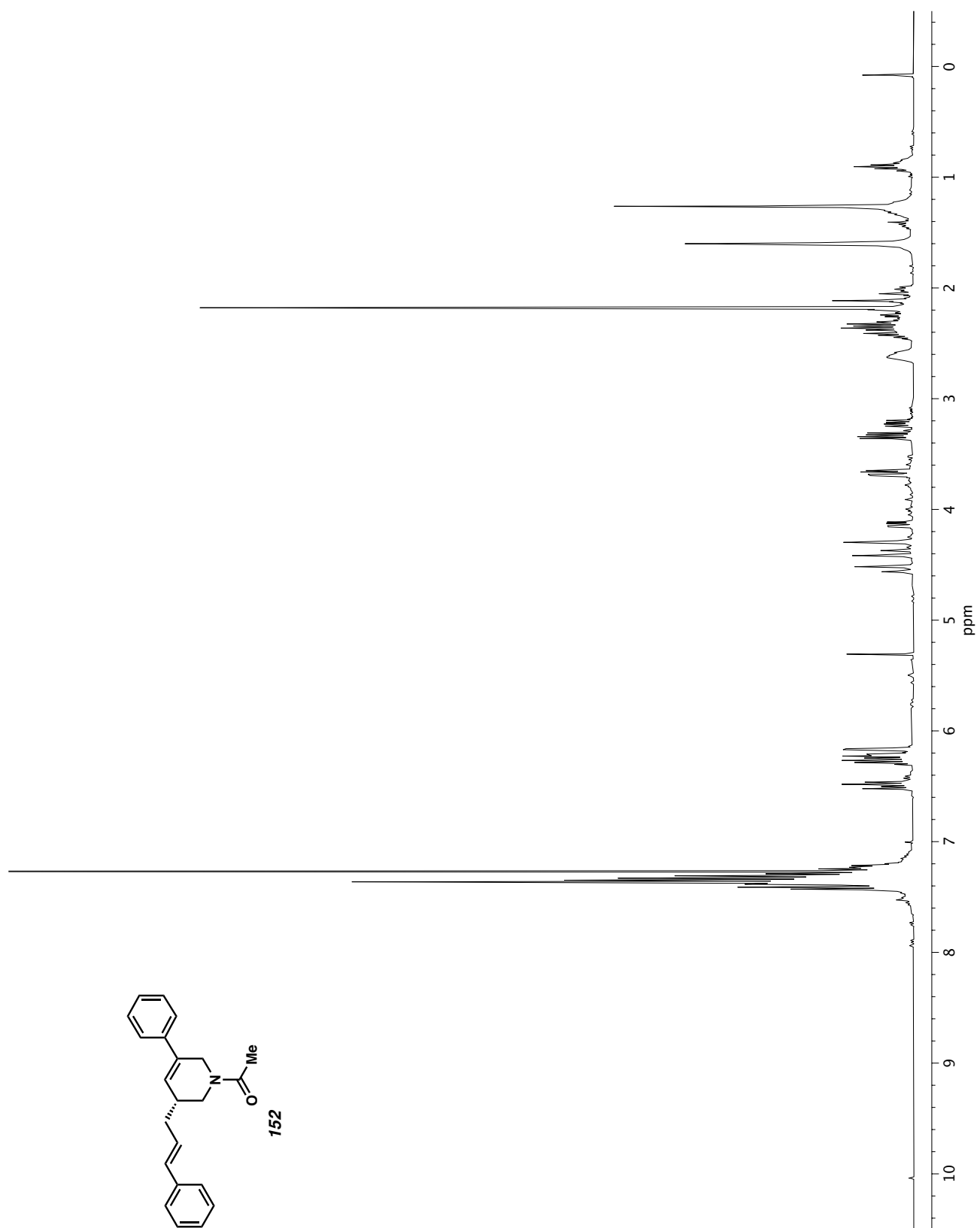
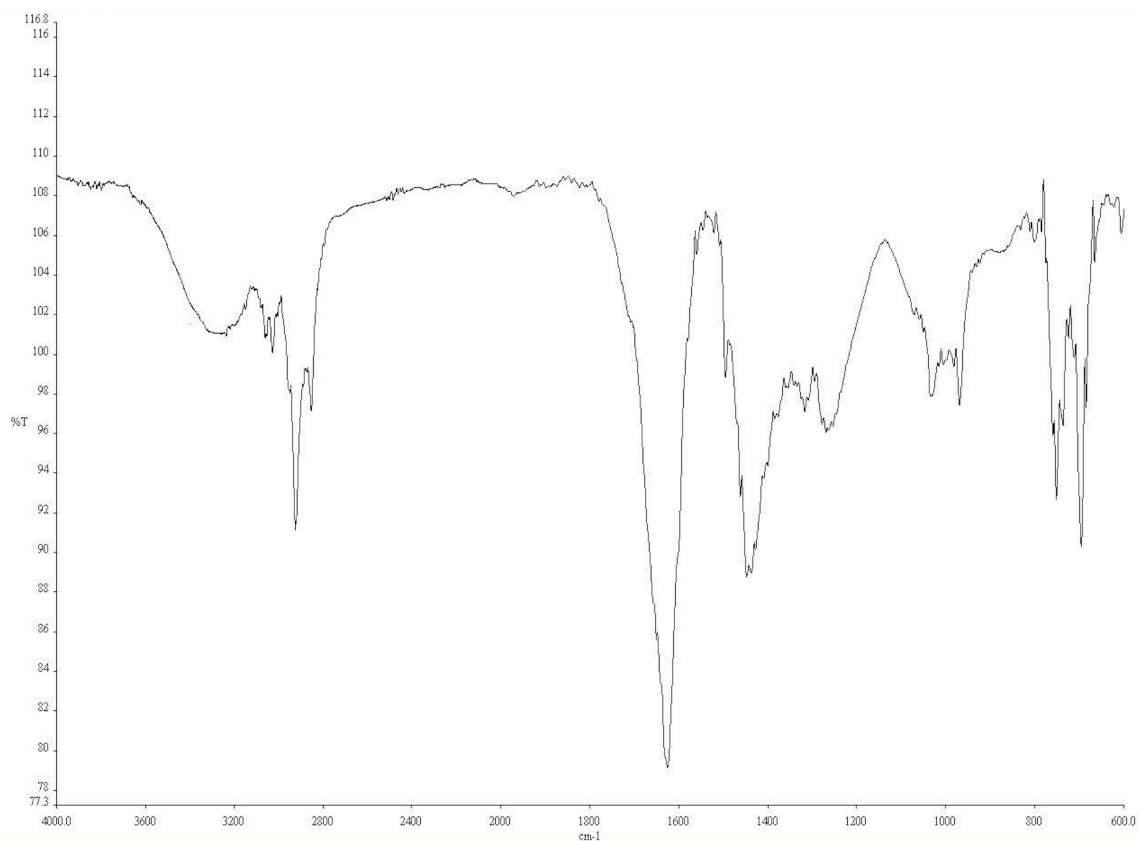
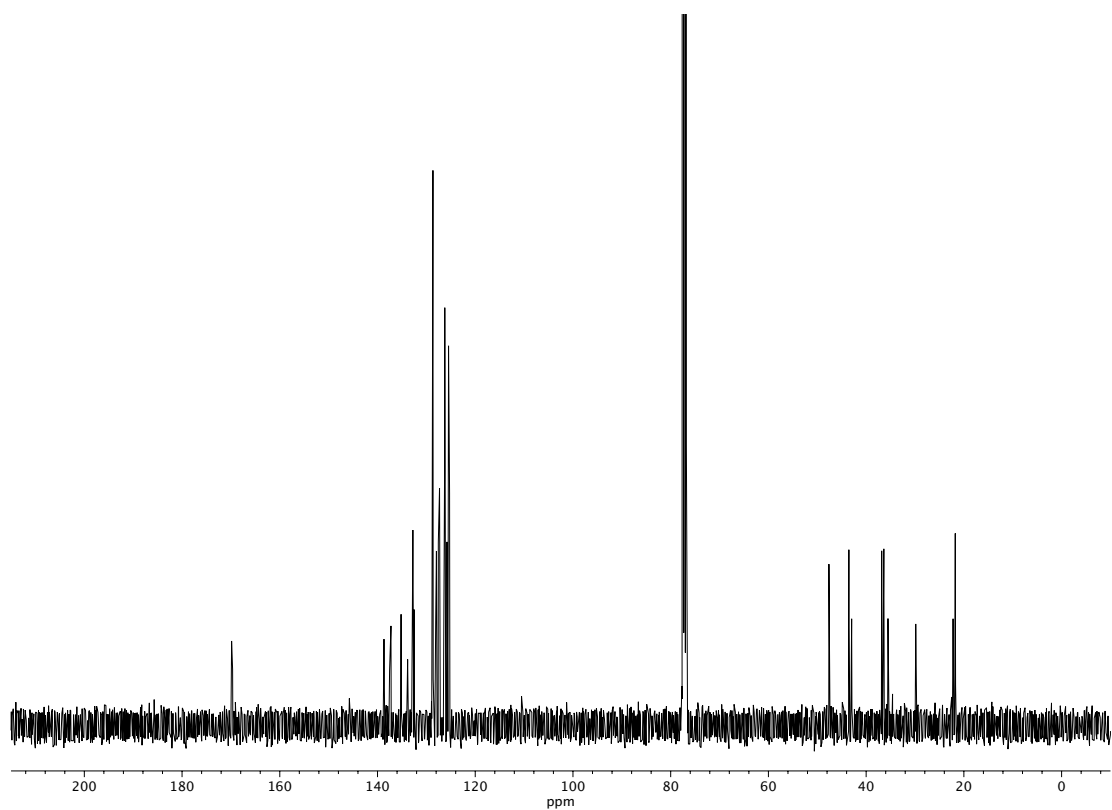


Figure A4.133  $^1\text{H}$  NMR (400 MHz,  $\text{CDCl}_3$ ) of compound **152**.



**Figure A4.134** Infrared spectrum (Thin Film, NaCl) of compound **152**.



**Figure A4.135** <sup>13</sup>C NMR (100 MHz, CDCl<sub>3</sub>) of compound **152**.



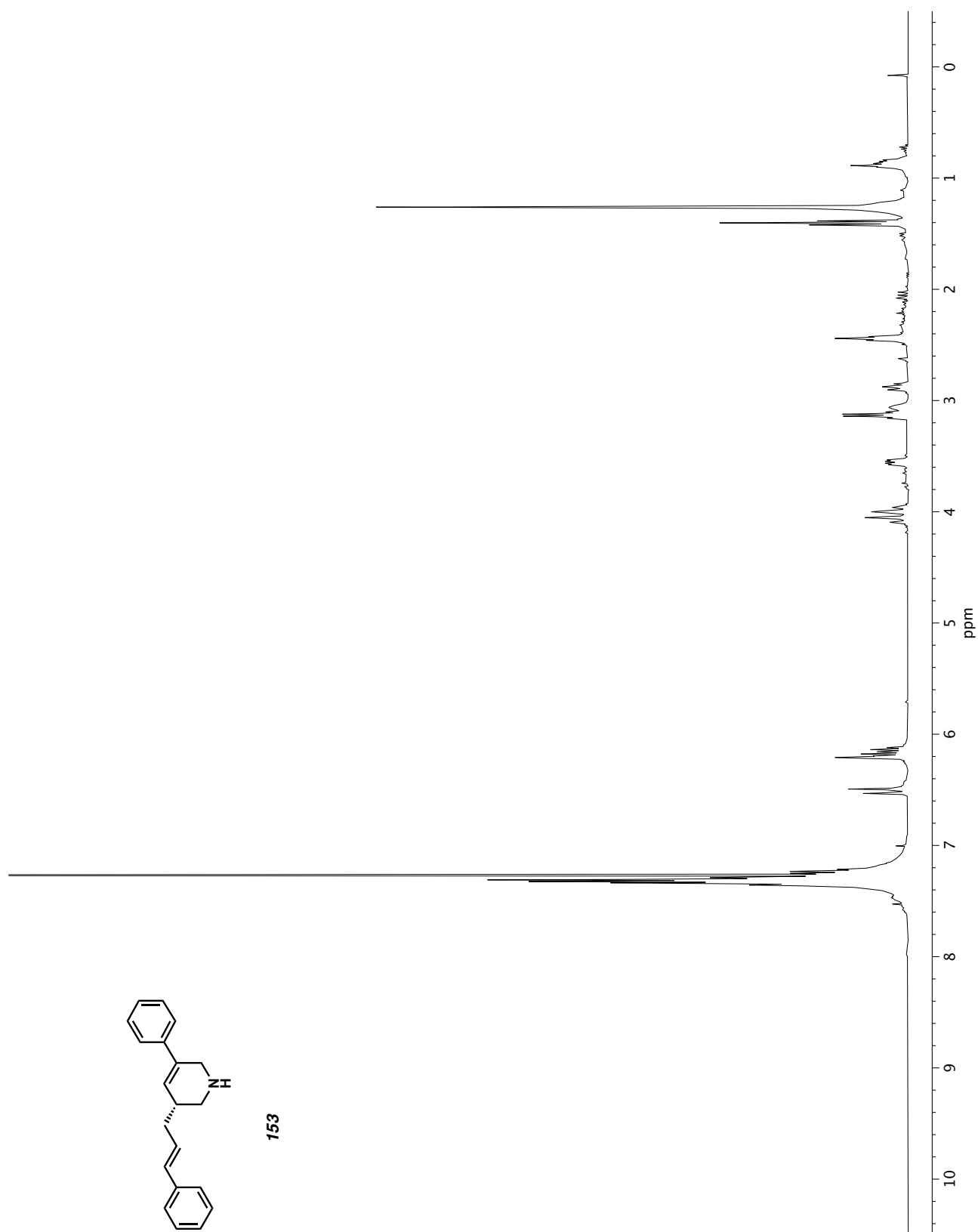
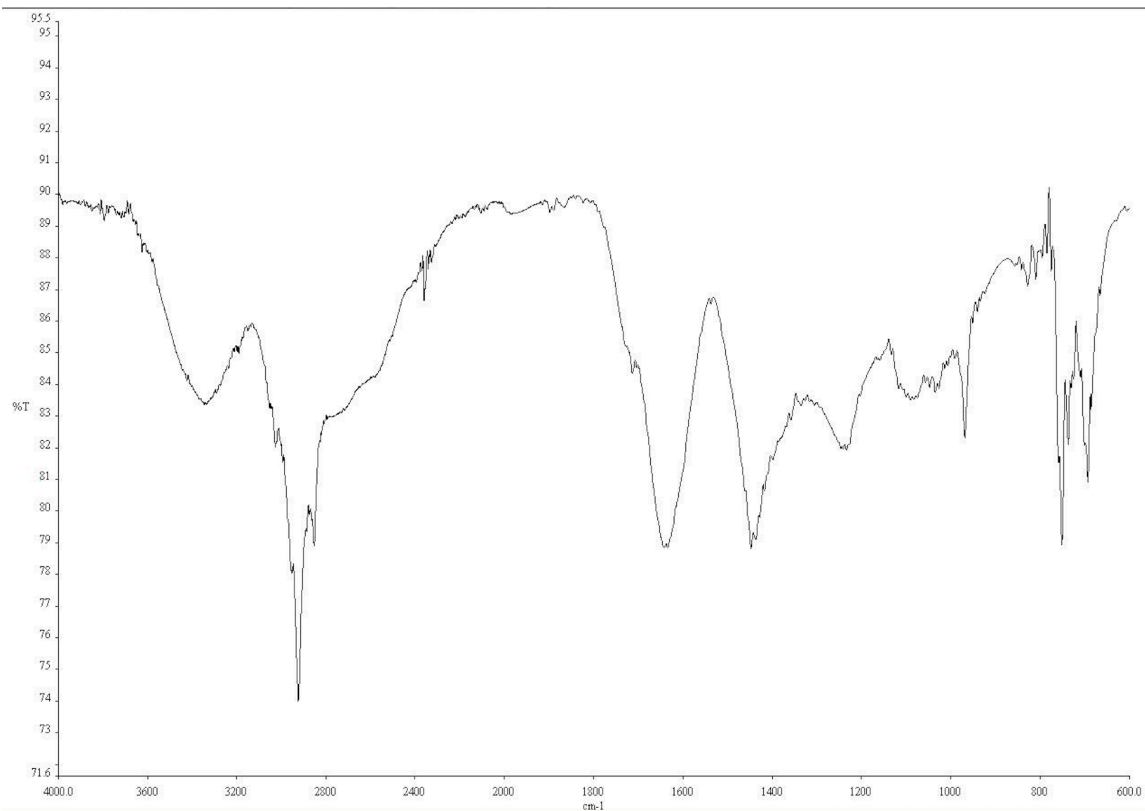
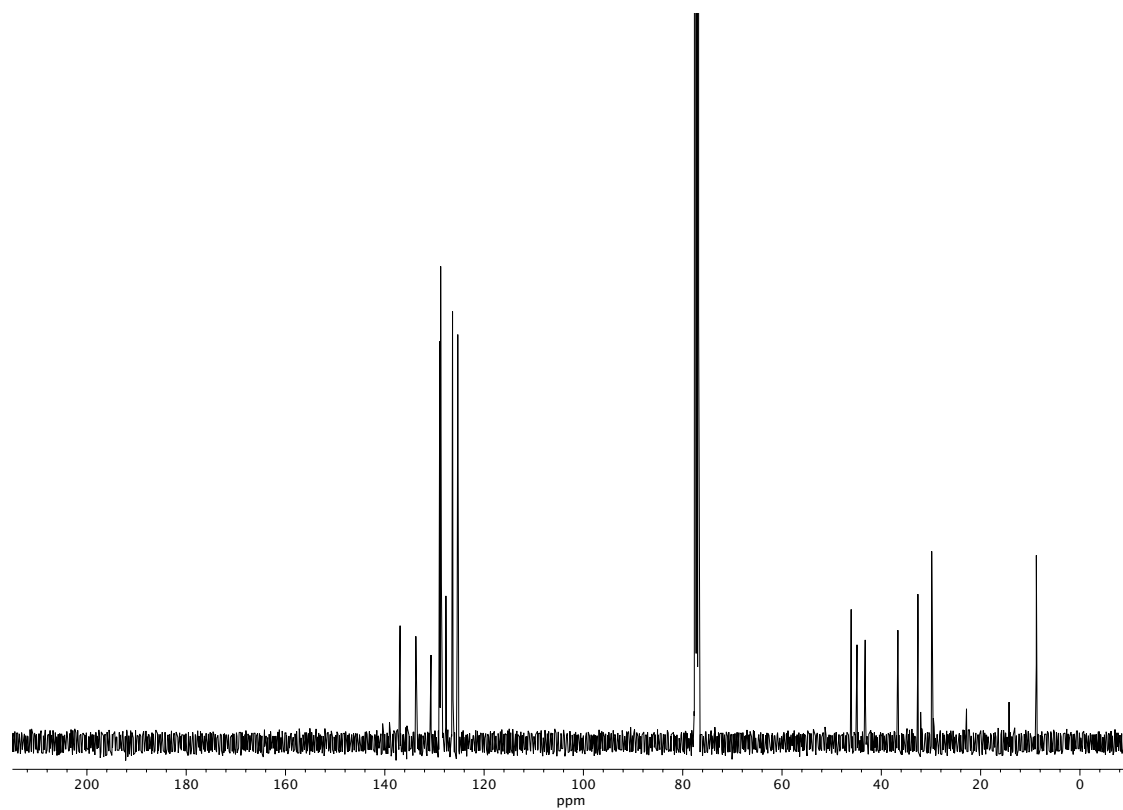


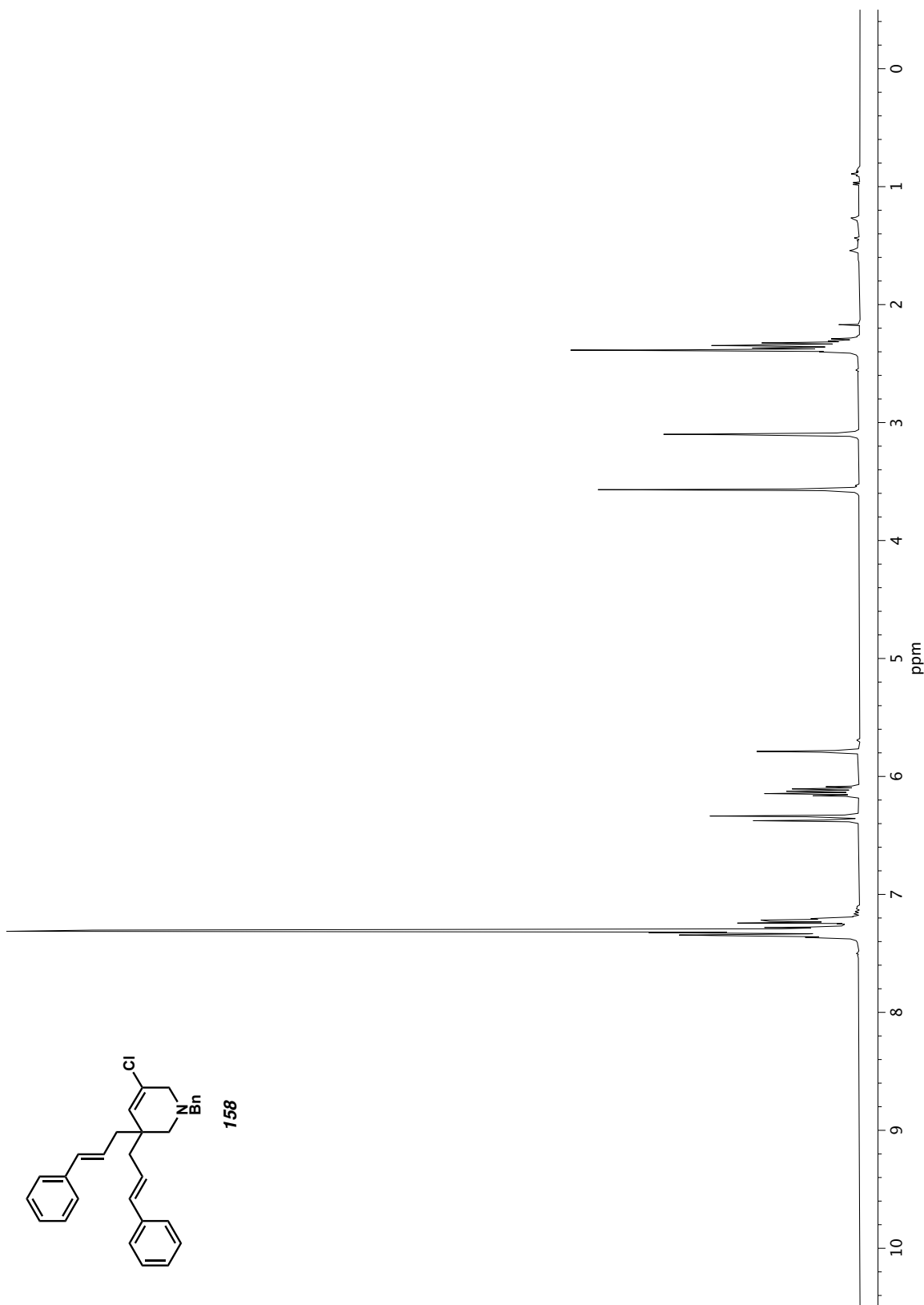
Figure A4.136  $^1\text{H}$  NMR (400 MHz,  $\text{CDCl}_3$ ) of compound **153**.

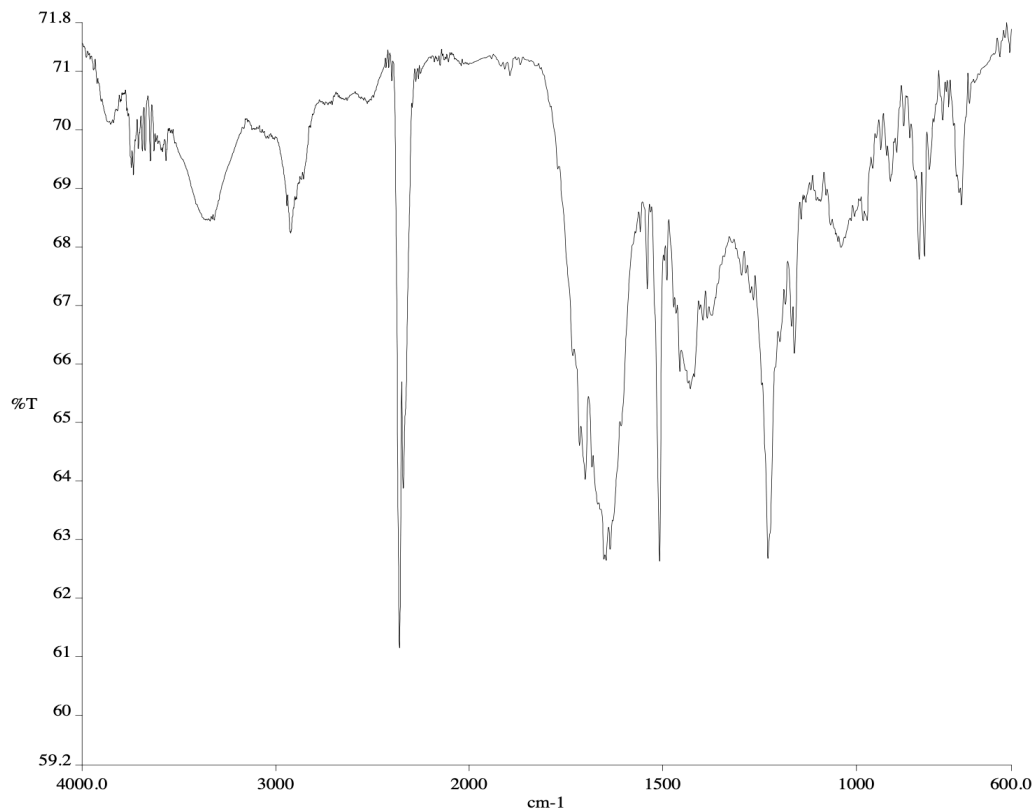


**Figure A4.137** Infrared spectrum (Thin Film, NaCl) of compound **153**.

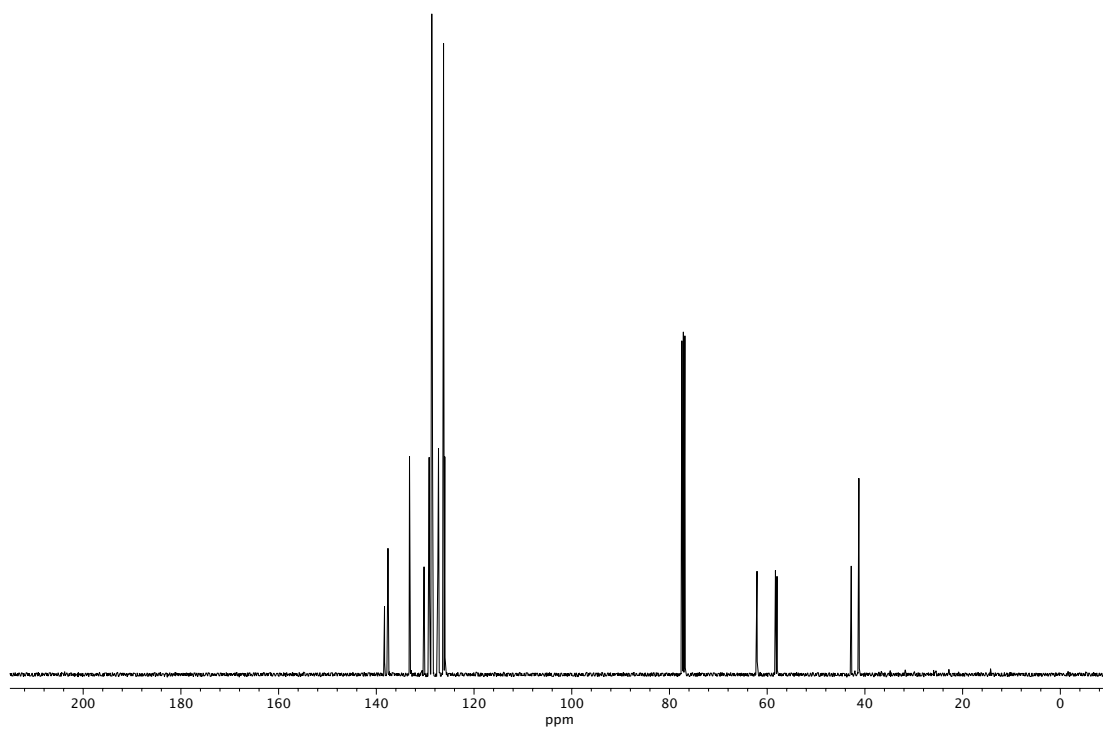


**Figure A4.138** <sup>13</sup>C NMR (100 MHz, CDCl<sub>3</sub>) of compound **153**.

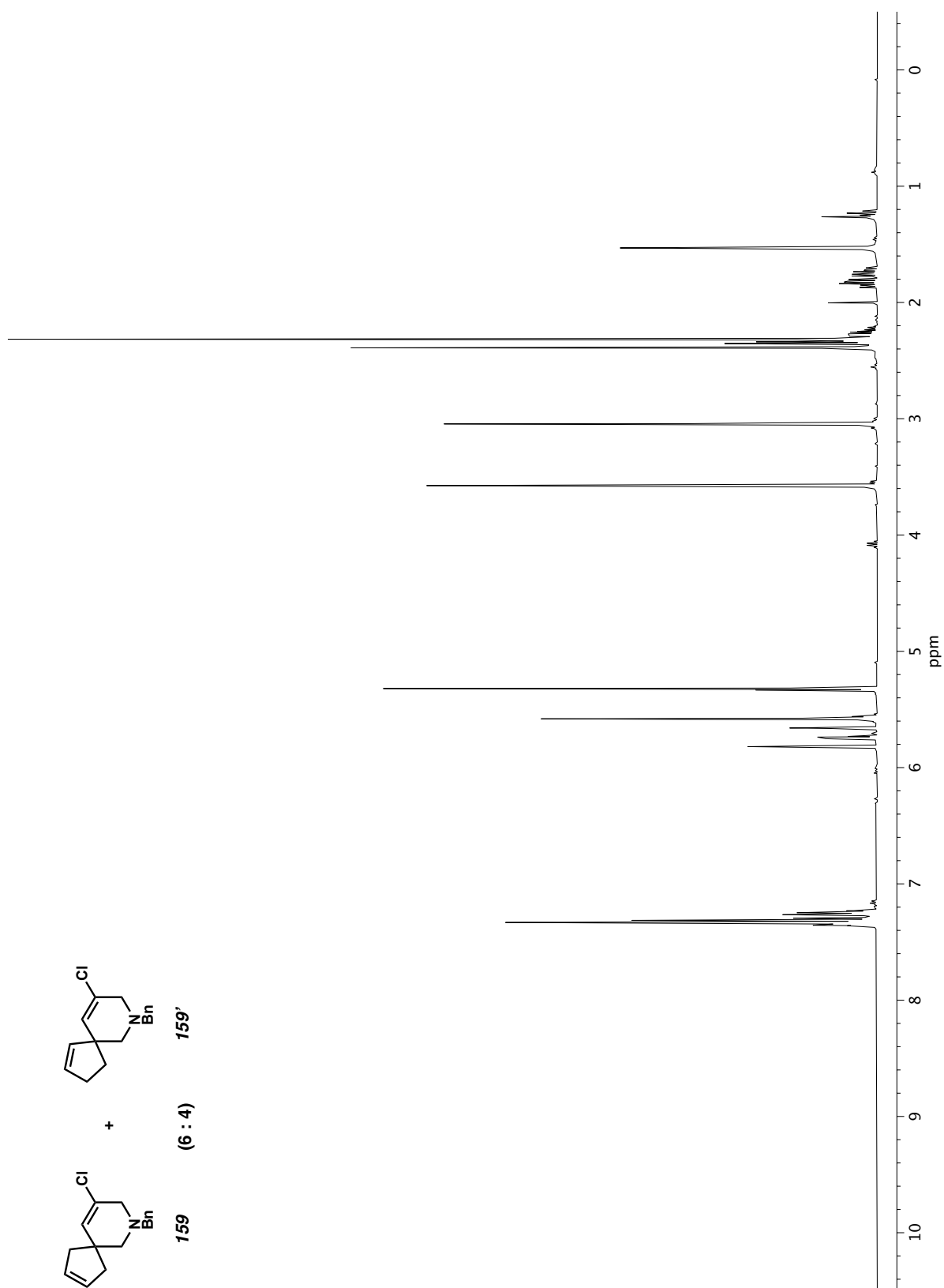
Figure A4.139  $^1\text{H}$  NMR (400 MHz,  $\text{CDCl}_3$ ) of compound **158**.

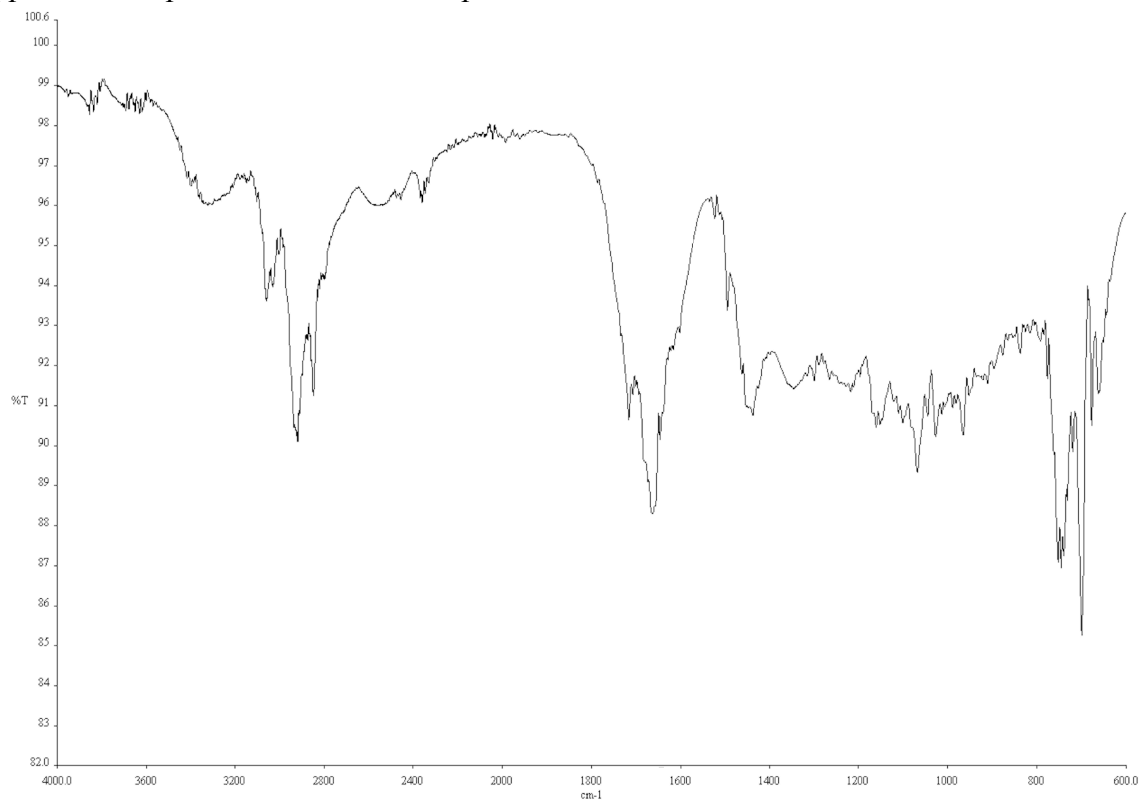


**Figure A4.140** Infrared spectrum (Thin Film, NaCl) of compound **158**.

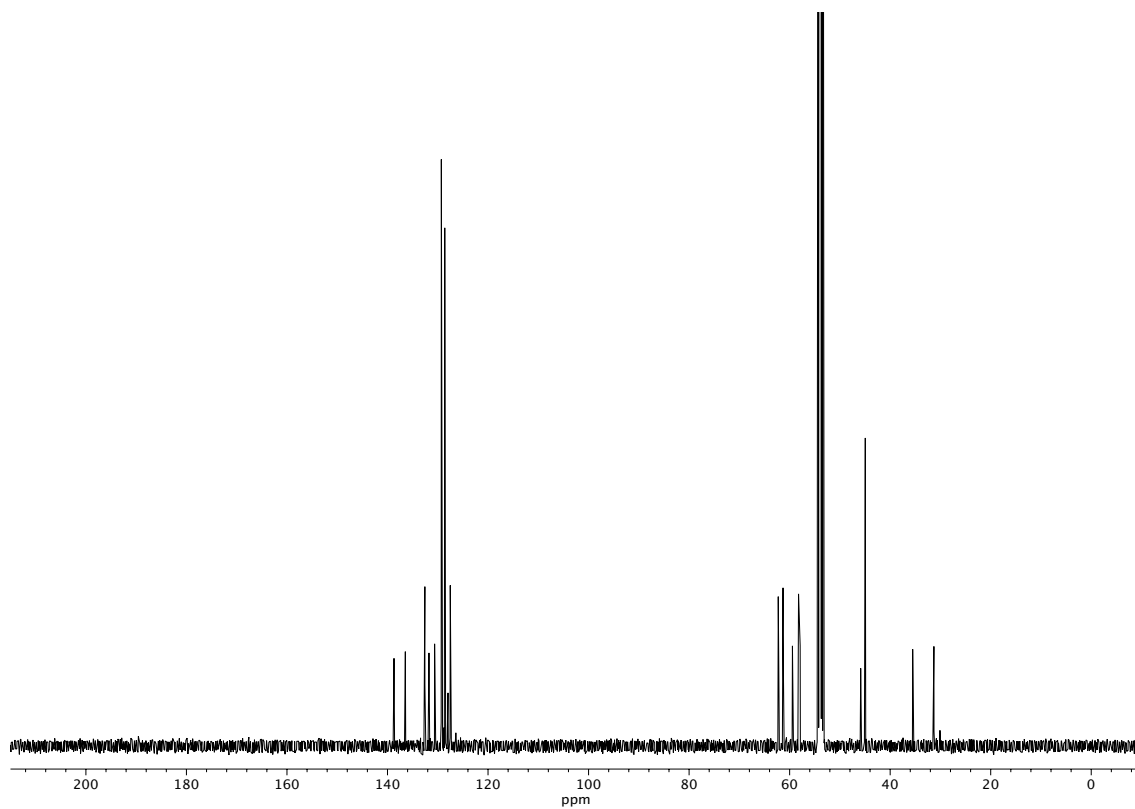


**Figure A4.141** <sup>13</sup>C NMR (100 MHz, CDCl<sub>3</sub>) of compound **158**.

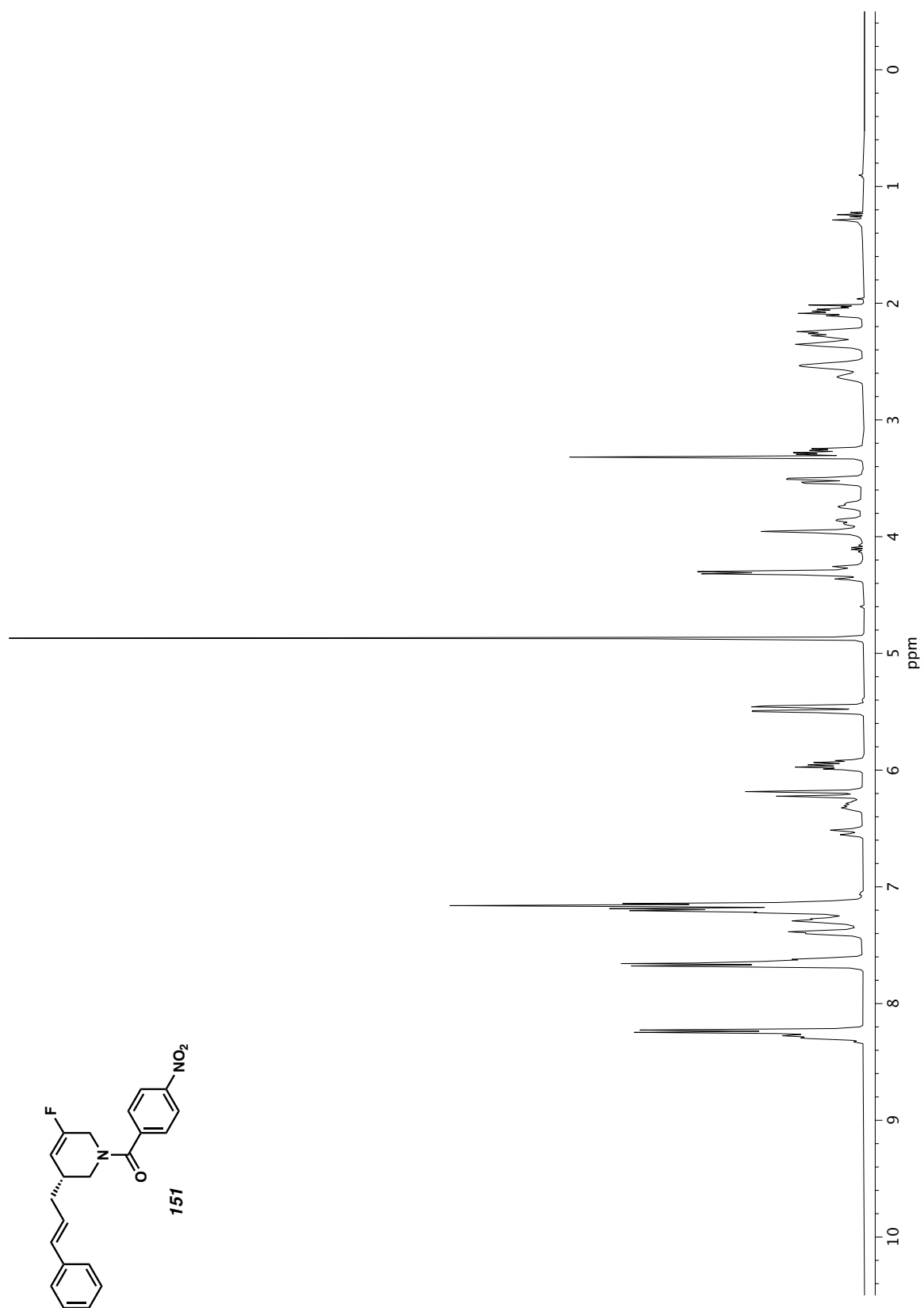




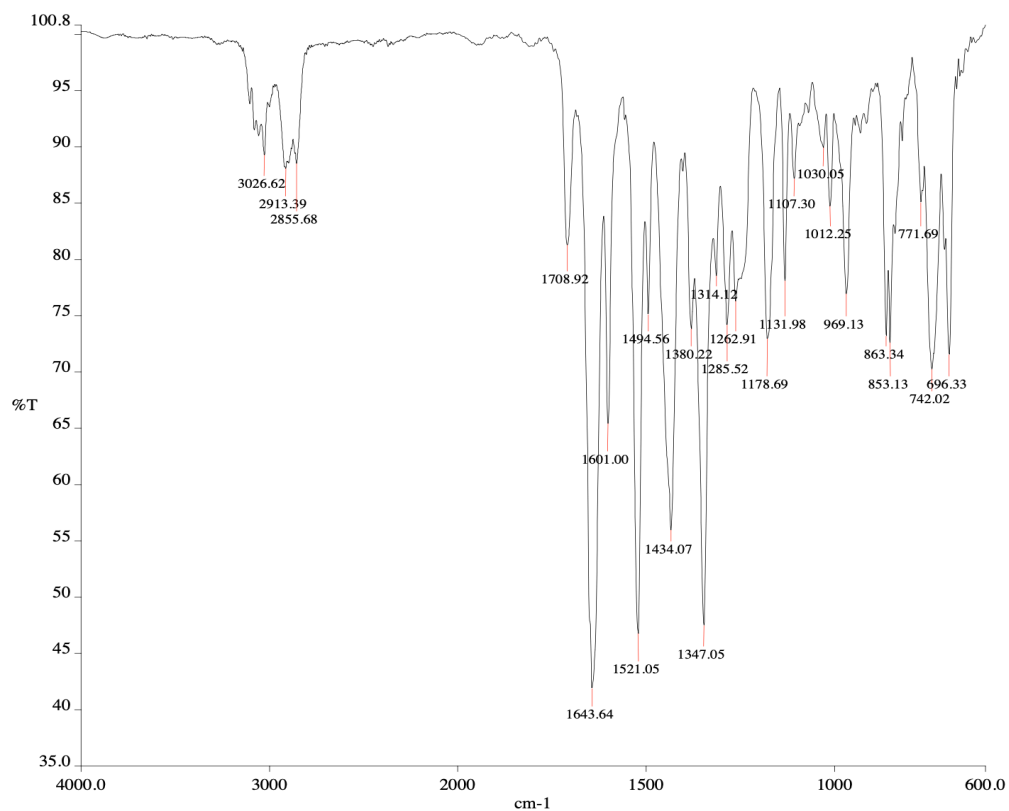
**Figure A4.143** Infrared spectrum (Thin Film, NaCl) of compound **159/159'**



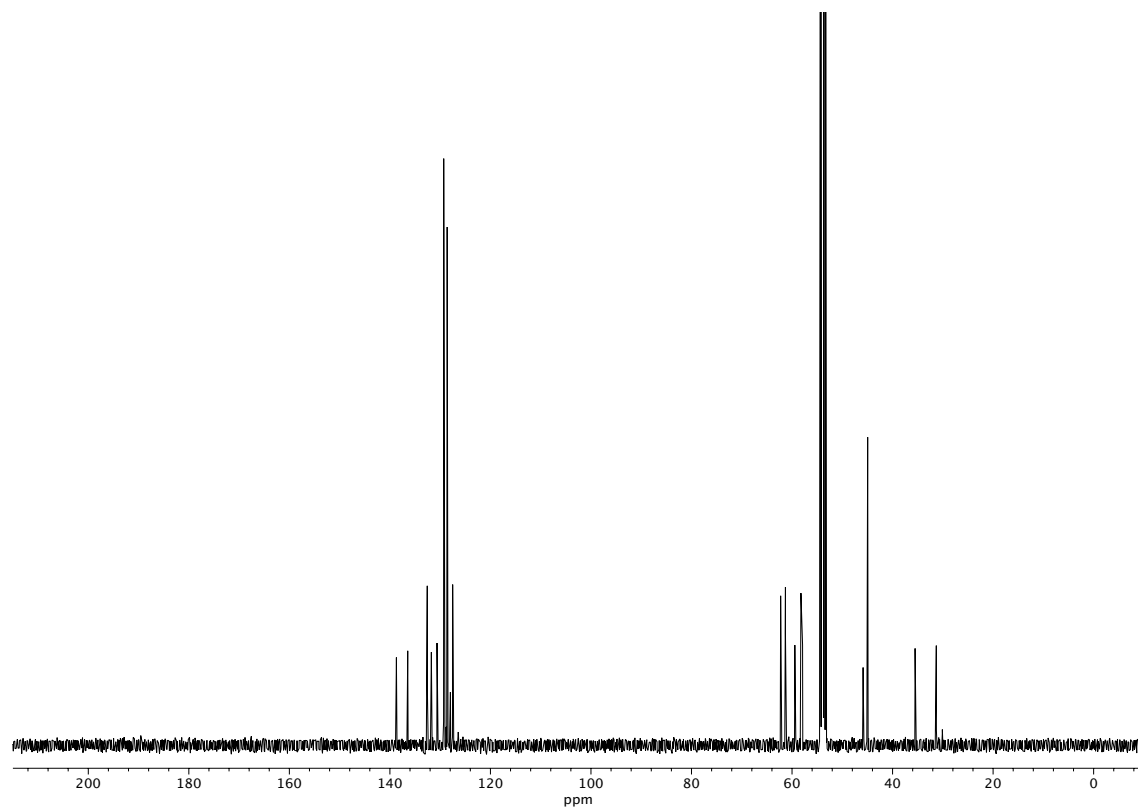
**Figure A4.144** <sup>13</sup>C NMR (100 MHz, CDCl<sub>3</sub>) of compound **159/159'**



**Figure A4.145**  $^1\text{H}$  NMR (400 MHz,  $\text{CD}_3\text{OD}$ ) of compound **151**.

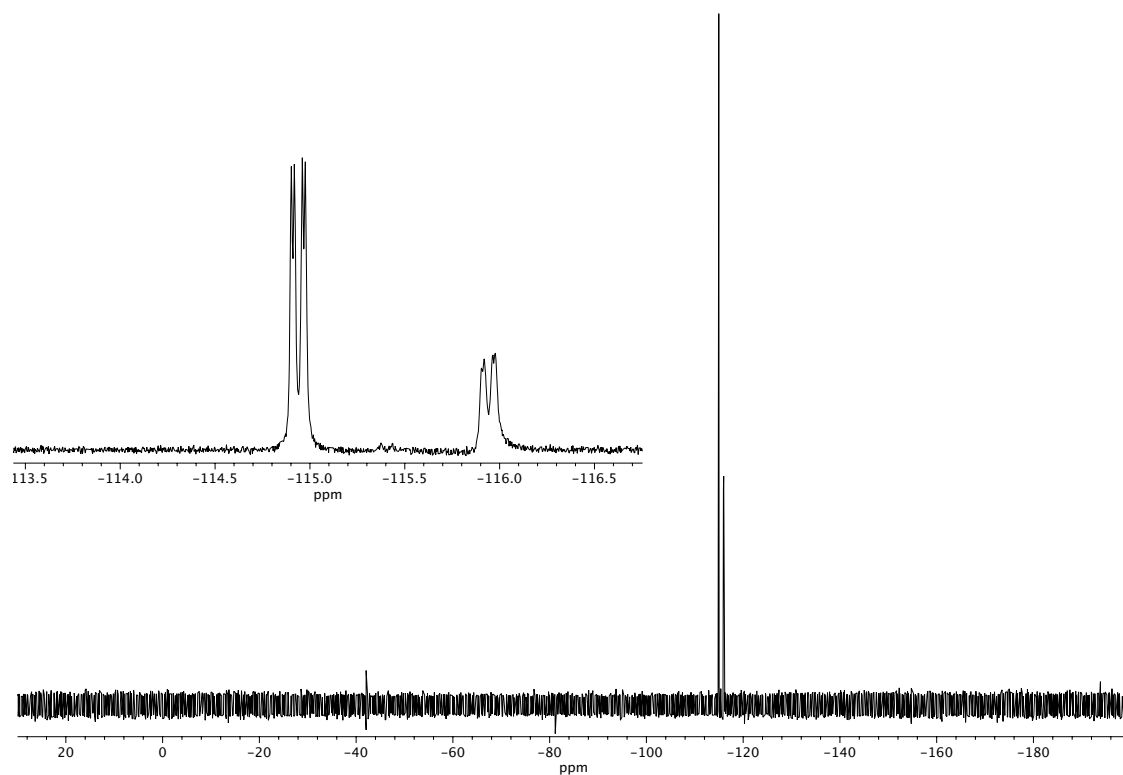


**Figure A4.146** Infrared spectrum (Thin Film, NaCl) of compound **151**.



**Figure A4.147** <sup>13</sup>C NMR (100 MHz, CD<sub>3</sub>OD) of compound **151**.

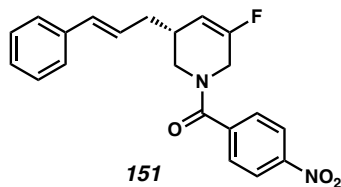




**Figure A4.148**  $^{19}\text{F}$  NMR (282 MHz,  $\text{CD}_3\text{OD}$ ) of compound **151**.

## **APPENDIX 5**

*X-Ray Crystallography Reports Relevant to Chapter 2:  
Enantioselective Dearomative Allylic Alkylation of Pyridines*

**A5.1 X-RAY CRYSTAL STRUCTURE ANALYSIS OF AMIDE 151**Contents

*Table A5.1.1. Experimental Details*

*Table A5.1.2. Crystal Data*

*Table A5.1.3. Atomic Coordinates*

*Table A5.1.4. Full Bond Distances and Angles*

*Table A5.1.5. Anisotropic Displacement Parameters*

*Table A5.1.6. Hydrogen Atomic Coordinates*

*Table A5.1.7. Torsion Angles*

*Table A5.1.8. Hydrogen Bond Distances and Angles*

**Figure A5.1.1** X-Ray Coordinate of compound **151**.

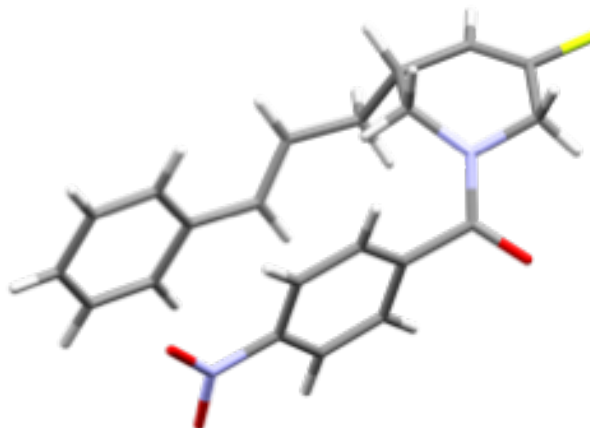


**Table A5.1.1** Experimental Details for X-Ray Structure Determination of Amide **151**.

Low-temperature diffraction data ( $\phi$ - and  $\omega$ -scans) were collected on a Bruker AXS D8 VENTURE KAPPA diffractometer coupled to a PHOTON II CPAD detector with Cu  $K_{\alpha}$  radiation ( $\lambda = 1.54178 \text{ \AA}$ ) from an I $\mu$ S micro-source for the structure of compound **151**. The structure was solved by direct methods using SHELXS (Sheldrick, G. M. *Acta Cryst.* **1990**, A46, 467-473.) and refined against  $F^2$  on all data by full-matrix least squares with SHELXL-2017 (Sheldrick, G. M. *Acta Cryst.* **2015**, C71, 3-8.) using established refinement techniques (Müller, P. *Crystallography Reviews* **2009**, 15, 57-83). All non-hydrogen atoms were refined anisotropically. All hydrogen atoms were included into the model at geometrically calculated positions and refined using a riding model. The isotropic displacement parameters of all hydrogen atoms were fixed to 1.2 times the  $U$  value of the atoms they are linked to (1.5 times for methyl groups).

Compound **151** crystallizes in the triclinic space group  $P1$  with two molecules in the asymmetric unit.

**Table A5.1.2** Crystal data and structure refinement for compound **151**.

Identification code	Compound <b>151</b>	
Empirical formula	C <sub>42</sub> H <sub>38</sub> F <sub>2</sub> N <sub>4</sub> O <sub>6</sub>	
Formula weight	732.76	
Temperature	106(2) K	
Wavelength	1.54178 Å	
Crystal system	Triclinic	
Space group	P1	
Unit cell dimensions	a = 7.5776(5) Å	α = 71.507(6)°.
	b = 9.8771(9) Å	β = 76.607(4)°.
	c = 13.5619(9) Å	γ = 70.196(8)°.
Volume	896.88(13) Å <sup>3</sup>	
Z	1	
Density (calculated)	1.357 Mg/m <sup>3</sup>	
Absorption coefficient	0.815 mm <sup>-1</sup>	
F(000)	384	
Crystal size	0.250 x 0.150 x 0.100 mm <sup>3</sup>	
Theta range for data collection	3.470 to 74.499°.	
Index ranges	-9 ≤ h ≤ 9, -12 ≤ k ≤ 12, -16 ≤ l ≤ 16	
Reflections collected	29009	
Independent reflections	7038 [R(int) = 0.0265]	
Completeness to theta = 67.679°	99.7 %	
Absorption correction	Semi-empirical from equivalents	
Max. and min. transmission	0.7538 and 0.6794	
Refinement method	Full-matrix least-squares on F <sup>2</sup>	
Data / restraints / parameters	7038 / 3 / 487	
Goodness-of-fit on F <sup>2</sup>	1.039	
Final R indices [I > 2σ(I)]	R1 = 0.0251, wR2 = 0.0666	
R indices (all data)	R1 = 0.0252, wR2 = 0.0666	
Absolute structure parameter	0.05(2)	
Extinction coefficient	n/a	
Largest diff. peak and hole	0.162 and -0.158 e.Å <sup>-3</sup>	

**Table A5.1.3** Atomic coordinates ( $\times 10^4$ ) and equivalent isotropic displacement parameters ( $\text{\AA}^2 \times 10^3$ ) for compound **151**.  $U(\text{eq})$  is defined as one third of the trace of the orthogonalized  $U^{ij}$  tensor.

	x	y	z	U(eq)
N(1)	3744(2)	7545(2)	8229(1)	20(1)
C(6)	2563(2)	6705(2)	8395(1)	21(1)
C(11)	3068(2)	5579(2)	7770(1)	20(1)
C(12)	3195(2)	4099(2)	8322(1)	23(1)
C(13)	3628(3)	3023(2)	7785(1)	25(1)
C(14)	3923(2)	3451(2)	6699(1)	23(1)
N(2)	4425(2)	2302(2)	6126(1)	28(1)
O(2)	4342(3)	1053(2)	6619(1)	44(1)
O(3)	4889(2)	2662(2)	5171(1)	39(1)
C(15)	3771(2)	4915(2)	6128(1)	23(1)
C(16)	3314(2)	5986(2)	6673(1)	23(1)
O(1)	1111(2)	6825(2)	9034(1)	29(1)
C(1)	3228(2)	8677(2)	8808(1)	22(1)
C(2)	4929(3)	8576(2)	9236(1)	23(1)
F(1)	4465(2)	9437(1)	9925(1)	31(1)
C(3)	6683(3)	7789(2)	9022(1)	25(1)
C(4)	7208(2)	6925(2)	8205(1)	22(1)
C(7)	7881(3)	5229(2)	8673(1)	25(1)
C(8)	8587(2)	4410(2)	7829(1)	24(1)
C(9)	8227(3)	3169(2)	7871(1)	25(1)
C(21)	8824(2)	2377(2)	7039(1)	25(1)
C(22)	8998(3)	857(2)	7296(2)	36(1)
C(23)	9488(3)	111(2)	6514(2)	44(1)
C(24)	9787(3)	851(3)	5475(2)	39(1)
C(25)	9631(3)	2360(3)	5206(2)	39(1)
C(26)	9158(3)	3116(2)	5983(2)	31(1)
C(5)	5584(2)	7403(2)	7559(1)	20(1)

**Table A5.1.3 Cont.**

N(101)	6170(2)	2464(2)	1720(1)	21(1)
C(106)	4459(2)	3365(2)	1472(1)	20(1)
C(111)	3397(2)	4513(2)	2074(1)	19(1)
C(112)	2685(2)	5983(2)	1504(1)	23(1)
C(113)	1732(2)	7092(2)	2015(1)	25(1)
C(114)	1482(2)	6691(2)	3104(1)	22(1)
N(102)	589(2)	7862(2)	3668(1)	27(1)
O(102)	-41(2)	9137(2)	3153(1)	37(1)
O(103)	538(2)	7498(2)	4625(1)	36(1)
C(115)	2064(2)	5231(2)	3691(1)	21(1)
C(116)	3030(2)	4138(2)	3167(1)	19(1)
O(101)	3728(2)	3288(2)	776(1)	31(1)
C(101)	7173(3)	1327(2)	1147(2)	26(1)
C(102)	9157(2)	1389(2)	772(1)	24(1)
F(101)	10032(2)	555(1)	69(1)	31(1)
C(103)	10047(2)	2107(2)	1049(1)	25(1)
C(104)	9074(2)	2969(2)	1864(1)	22(1)
C(107)	8688(2)	4663(2)	1375(1)	23(1)
C(108)	8056(2)	5529(2)	2185(1)	24(1)
C(109)	6543(2)	6705(2)	2183(1)	23(1)
C(121)	5883(2)	7606(2)	2952(1)	23(1)
C(122)	4483(3)	8971(2)	2726(2)	27(1)
C(123)	3865(3)	9880(2)	3413(2)	33(1)
C(124)	4645(3)	9453(2)	4329(2)	35(1)
C(125)	6019(3)	8099(3)	4568(2)	34(1)
C(126)	6613(3)	7175(2)	3896(1)	28(1)
C(105)	7264(2)	2550(2)	2451(1)	21(1)

---

**Table A5.1.4** Bond lengths [ $\text{\AA}$ ] and angles [ $^\circ$ ] for compound **151**.

---

N(1)-C(6)	1.353(2)
N(1)-C(1)	1.4621(19)
N(1)-C(5)	1.467(2)
C(6)-O(1)	1.229(2)
C(6)-C(11)	1.505(2)
C(11)-C(12)	1.396(2)
C(11)-C(16)	1.397(2)
C(12)-C(13)	1.382(2)
C(12)-H(12)	0.9500
C(13)-C(14)	1.383(2)
C(13)-H(13)	0.9500
C(14)-C(15)	1.386(2)
C(14)-N(2)	1.472(2)
N(2)-O(2)	1.218(2)
N(2)-O(3)	1.228(2)
C(15)-C(16)	1.384(2)
C(15)-H(15)	0.9500
C(16)-H(16)	0.9500
C(1)-C(2)	1.494(2)
C(1)-H(1A)	0.9900
C(1)-H(1B)	0.9900
C(2)-C(3)	1.311(3)
C(2)-F(1)	1.3670(19)
C(3)-C(4)	1.510(2)
C(3)-H(3)	0.9500
C(4)-C(5)	1.532(2)
C(4)-C(7)	1.538(2)
C(4)-H(4)	1.0000
C(7)-C(8)	1.503(2)
C(7)-H(7A)	0.9900
C(7)-H(7B)	0.9900
C(8)-C(9)	1.325(3)
C(8)-H(8)	0.9500
C(9)-C(21)	1.475(2)



**Table A5.1.4 Cont.**

C(9)-H(9)	0.9500
C(21)-C(26)	1.394(3)
C(21)-C(22)	1.395(3)
C(22)-C(23)	1.391(3)
C(22)-H(22)	0.9500
C(23)-C(24)	1.372(3)
C(23)-H(23)	0.9500
C(24)-C(25)	1.387(3)
C(24)-H(24)	0.9500
C(25)-C(26)	1.392(3)
C(25)-H(25)	0.9500
C(26)-H(26)	0.9500
C(5)-H(5A)	0.9900
C(5)-H(5B)	0.9900
N(101)-C(106)	1.348(2)
N(101)-C(101)	1.464(2)
N(101)-C(105)	1.470(2)
C(106)-O(101)	1.232(2)
C(106)-C(111)	1.505(2)
C(111)-C(116)	1.394(2)
C(111)-C(112)	1.395(2)
C(112)-C(113)	1.385(3)
C(112)-H(112)	0.9500
C(113)-C(114)	1.387(3)
C(113)-H(113)	0.9500
C(114)-C(115)	1.383(2)
C(114)-N(102)	1.474(2)
N(102)-O(102)	1.221(2)
N(102)-O(103)	1.227(2)
C(115)-C(116)	1.385(2)
C(115)-H(115)	0.9500
C(116)-H(116)	0.9500
C(101)-C(102)	1.487(2)
C(101)-H(10A)	0.9900
C(101)-H(10B)	0.9900

**Table A5.1.4 Cont.**

C(102)-C(103)	1.307(3)
C(102)-F(101)	1.3653(18)
C(103)-C(104)	1.512(2)
C(103)-H(103)	0.9500
C(104)-C(105)	1.535(2)
C(104)-C(107)	1.542(2)
C(104)-H(104)	1.0000
C(107)-C(108)	1.497(2)
C(107)-H(10C)	0.9900
C(107)-H(10D)	0.9900
C(108)-C(109)	1.327(3)
C(108)-H(108)	0.9500
C(109)-C(121)	1.476(2)
C(109)-H(109)	0.9500
C(121)-C(126)	1.395(3)
C(121)-C(122)	1.399(3)
C(122)-C(123)	1.392(2)
C(122)-H(122)	0.9500
C(123)-C(124)	1.382(3)
C(123)-H(123)	0.9500
C(124)-C(125)	1.384(3)
C(124)-H(124)	0.9500
C(125)-C(126)	1.387(3)
C(125)-H(125)	0.9500
C(126)-H(126)	0.9500
C(105)-H(10E)	0.9900
C(105)-H(10F)	0.9900
C(6)-N(1)-C(1)	118.35(13)
C(6)-N(1)-C(5)	127.02(13)
C(1)-N(1)-C(5)	114.55(13)
O(1)-C(6)-N(1)	122.72(15)
O(1)-C(6)-C(11)	119.18(15)
N(1)-C(6)-C(11)	118.10(14)
C(12)-C(11)-C(16)	120.15(15)

**Table A5.1.4 Cont.**

C(12)-C(11)-C(6)	117.74(14)
C(16)-C(11)-C(6)	122.03(14)
C(13)-C(12)-C(11)	120.09(15)
C(13)-C(12)-H(12)	120.0
C(11)-C(12)-H(12)	120.0
C(12)-C(13)-C(14)	118.47(16)
C(12)-C(13)-H(13)	120.8
C(14)-C(13)-H(13)	120.8
C(13)-C(14)-C(15)	122.82(16)
C(13)-C(14)-N(2)	118.58(15)
C(15)-C(14)-N(2)	118.60(15)
O(2)-N(2)-O(3)	123.48(16)
O(2)-N(2)-C(14)	118.51(15)
O(3)-N(2)-C(14)	118.01(15)
C(16)-C(15)-C(14)	118.25(16)
C(16)-C(15)-H(15)	120.9
C(14)-C(15)-H(15)	120.9
C(15)-C(16)-C(11)	120.16(15)
C(15)-C(16)-H(16)	119.9
C(11)-C(16)-H(16)	119.9
N(1)-C(1)-C(2)	108.81(13)
N(1)-C(1)-H(1A)	109.9
C(2)-C(1)-H(1A)	109.9
N(1)-C(1)-H(1B)	109.9
C(2)-C(1)-H(1B)	109.9
H(1A)-C(1)-H(1B)	108.3
C(3)-C(2)-F(1)	120.93(16)
C(3)-C(2)-C(1)	127.66(16)
F(1)-C(2)-C(1)	111.40(14)
C(2)-C(3)-C(4)	120.60(16)
C(2)-C(3)-H(3)	119.7
C(4)-C(3)-H(3)	119.7
C(3)-C(4)-C(5)	110.36(14)
C(3)-C(4)-C(7)	112.79(14)
C(5)-C(4)-C(7)	112.91(13)

**Table A5.1.4 Cont.**

C(3)-C(4)-H(4)	106.8
C(5)-C(4)-H(4)	106.8
C(7)-C(4)-H(4)	106.8
C(8)-C(7)-C(4)	111.51(14)
C(8)-C(7)-H(7A)	109.3
C(4)-C(7)-H(7A)	109.3
C(8)-C(7)-H(7B)	109.3
C(4)-C(7)-H(7B)	109.3
H(7A)-C(7)-H(7B)	108.0
C(9)-C(8)-C(7)	125.00(16)
C(9)-C(8)-H(8)	117.5
C(7)-C(8)-H(8)	117.5
C(8)-C(9)-C(21)	126.33(16)
C(8)-C(9)-H(9)	116.8
C(21)-C(9)-H(9)	116.8
C(26)-C(21)-C(22)	118.15(17)
C(26)-C(21)-C(9)	121.81(16)
C(22)-C(21)-C(9)	119.99(17)
C(23)-C(22)-C(21)	120.51(19)
C(23)-C(22)-H(22)	119.7
C(21)-C(22)-H(22)	119.7
C(24)-C(23)-C(22)	120.96(19)
C(24)-C(23)-H(23)	119.5
C(22)-C(23)-H(23)	119.5
C(23)-C(24)-C(25)	119.29(19)
C(23)-C(24)-H(24)	120.4
C(25)-C(24)-H(24)	120.4
C(24)-C(25)-C(26)	120.3(2)
C(24)-C(25)-H(25)	119.9
C(26)-C(25)-H(25)	119.9
C(25)-C(26)-C(21)	120.82(18)
C(25)-C(26)-H(26)	119.6
C(21)-C(26)-H(26)	119.6
N(1)-C(5)-C(4)	111.53(13)
N(1)-C(5)-H(5A)	109.3

**Table A5.1.4 Cont.**

C(4)-C(5)-H(5A)	109.3
N(1)-C(5)-H(5B)	109.3
C(4)-C(5)-H(5B)	109.3
H(5A)-C(5)-H(5B)	108.0
C(106)-N(101)-C(101)	118.01(14)
C(106)-N(101)-C(105)	127.73(13)
C(101)-N(101)-C(105)	114.06(13)
O(101)-C(106)-N(101)	122.89(15)
O(101)-C(106)-C(111)	118.73(15)
N(101)-C(106)-C(111)	118.38(14)
C(116)-C(111)-C(112)	119.72(15)
C(116)-C(111)-C(106)	122.18(14)
C(112)-C(111)-C(106)	118.02(14)
C(113)-C(112)-C(111)	120.59(15)
C(113)-C(112)-H(112)	119.7
C(111)-C(112)-H(112)	119.7
C(112)-C(113)-C(114)	118.00(15)
C(112)-C(113)-H(113)	121.0
C(114)-C(113)-H(113)	121.0
C(115)-C(114)-C(113)	122.74(15)
C(115)-C(114)-N(102)	118.05(15)
C(113)-C(114)-N(102)	119.20(15)
O(102)-N(102)-O(103)	124.06(16)
O(102)-N(102)-C(114)	117.96(15)
O(103)-N(102)-C(114)	117.98(14)
C(114)-C(115)-C(116)	118.36(15)
C(114)-C(115)-H(115)	120.8
C(116)-C(115)-H(115)	120.8
C(115)-C(116)-C(111)	120.36(15)
C(115)-C(116)-H(116)	119.8
C(111)-C(116)-H(116)	119.8
N(101)-C(101)-C(102)	109.27(14)
N(101)-C(101)-H(10A)	109.8
C(102)-C(101)-H(10A)	109.8
N(101)-C(101)-H(10B)	109.8

**Table A5.1.4 Cont.**

C(102)-C(101)-H(10B)	109.8
H(10A)-C(101)-H(10B)	108.3
C(103)-C(102)-F(101)	121.33(15)
C(103)-C(102)-C(101)	127.62(15)
F(101)-C(102)-C(101)	111.05(14)
C(102)-C(103)-C(104)	120.31(16)
C(102)-C(103)-H(103)	119.8
C(104)-C(103)-H(103)	119.8
C(103)-C(104)-C(105)	110.90(14)
C(103)-C(104)-C(107)	111.40(14)
C(105)-C(104)-C(107)	112.08(13)
C(103)-C(104)-H(104)	107.4
C(105)-C(104)-H(104)	107.4
C(107)-C(104)-H(104)	107.4
C(108)-C(107)-C(104)	112.63(14)
C(108)-C(107)-H(10C)	109.1
C(104)-C(107)-H(10C)	109.1
C(108)-C(107)-H(10D)	109.1
C(104)-C(107)-H(10D)	109.1
H(10C)-C(107)-H(10D)	107.8
C(109)-C(108)-C(107)	124.73(16)
C(109)-C(108)-H(108)	117.6
C(107)-C(108)-H(108)	117.6
C(108)-C(109)-C(121)	126.67(16)
C(108)-C(109)-H(109)	116.7
C(121)-C(109)-H(109)	116.7
C(126)-C(121)-C(122)	117.92(16)
C(126)-C(121)-C(109)	123.09(16)
C(122)-C(121)-C(109)	118.98(16)
C(123)-C(122)-C(121)	120.86(17)
C(123)-C(122)-H(122)	119.6
C(121)-C(122)-H(122)	119.6
C(124)-C(123)-C(122)	120.34(19)
C(124)-C(123)-H(123)	119.8
C(122)-C(123)-H(123)	119.8

**Table A5.1.4 Cont.**

C(123)-C(124)-C(125)	119.35(18)
C(123)-C(124)-H(124)	120.3
C(125)-C(124)-H(124)	120.3
C(124)-C(125)-C(126)	120.56(18)
C(124)-C(125)-H(125)	119.7
C(126)-C(125)-H(125)	119.7
C(125)-C(126)-C(121)	120.91(18)
C(125)-C(126)-H(126)	119.5
C(121)-C(126)-H(126)	119.5
N(101)-C(105)-C(104)	111.07(13)
N(101)-C(105)-H(10E)	109.4
C(104)-C(105)-H(10E)	109.4
N(101)-C(105)-H(10F)	109.4
C(104)-C(105)-H(10F)	109.4
H(10E)-C(105)-H(10F)	108.0

---

Symmetry transformations used to generate equivalent atoms:

**Table A5.1.5** Anisotropic displacement parameters ( $\text{\AA}^2 \times 10^3$ ) for compound **151**. The anisotropic displacement factor exponent takes the form:  $-2p^2[h^2 a^*{}^2 U^{11} + \dots + 2 h k a^* b^* U^{12}]$

	U <sup>11</sup>	U <sup>22</sup>	U <sup>33</sup>	U <sup>23</sup>	U <sup>13</sup>	U <sup>12</sup>
N(1)	19(1)	20(1)	21(1)	-10(1)	-1(1)	-4(1)
C(6)	20(1)	22(1)	21(1)	-7(1)	-5(1)	-3(1)
C(11)	17(1)	22(1)	23(1)	-9(1)	-4(1)	-4(1)
C(12)	26(1)	26(1)	19(1)	-5(1)	-4(1)	-9(1)
C(13)	31(1)	18(1)	26(1)	-4(1)	-8(1)	-7(1)
C(14)	24(1)	21(1)	25(1)	-9(1)	-8(1)	-2(1)
N(2)	35(1)	21(1)	28(1)	-10(1)	-11(1)	-1(1)
O(2)	72(1)	20(1)	40(1)	-11(1)	-5(1)	-11(1)
O(3)	62(1)	29(1)	24(1)	-12(1)	-13(1)	-3(1)
C(15)	28(1)	24(1)	20(1)	-6(1)	-7(1)	-6(1)
C(16)	26(1)	19(1)	24(1)	-5(1)	-7(1)	-5(1)
O(1)	22(1)	35(1)	34(1)	-19(1)	4(1)	-10(1)
C(1)	23(1)	20(1)	24(1)	-10(1)	-1(1)	-4(1)
C(2)	29(1)	21(1)	22(1)	-10(1)	-2(1)	-9(1)
F(1)	34(1)	30(1)	34(1)	-21(1)	-5(1)	-5(1)
C(3)	25(1)	26(1)	28(1)	-11(1)	-4(1)	-10(1)
C(4)	19(1)	26(1)	24(1)	-11(1)	2(1)	-8(1)
C(7)	23(1)	25(1)	24(1)	-10(1)	-3(1)	-3(1)
C(8)	20(1)	25(1)	25(1)	-8(1)	-1(1)	-2(1)
C(9)	24(1)	24(1)	24(1)	-5(1)	-3(1)	-4(1)
C(21)	21(1)	22(1)	31(1)	-9(1)	0(1)	-4(1)
C(22)	41(1)	24(1)	40(1)	-6(1)	3(1)	-11(1)
C(23)	46(1)	25(1)	60(1)	-19(1)	9(1)	-14(1)
C(24)	37(1)	40(1)	48(1)	-29(1)	13(1)	-16(1)
C(25)	50(1)	39(1)	32(1)	-16(1)	8(1)	-18(1)
C(26)	38(1)	23(1)	31(1)	-10(1)	3(1)	-10(1)
C(5)	21(1)	22(1)	19(1)	-8(1)	1(1)	-6(1)
N(101)	20(1)	20(1)	23(1)	-11(1)	-2(1)	-2(1)
C(106)	20(1)	22(1)	18(1)	-6(1)	-1(1)	-6(1)
C(111)	16(1)	21(1)	23(1)	-8(1)	-4(1)	-4(1)



**Table A5.1.5 Cont.**

C(112)	22(1)	24(1)	21(1)	-3(1)	-5(1)	-4(1)
C(113)	23(1)	18(1)	30(1)	-2(1)	-7(1)	-3(1)
C(114)	18(1)	19(1)	30(1)	-11(1)	-4(1)	-2(1)
N(102)	22(1)	21(1)	38(1)	-14(1)	-4(1)	-1(1)
O(102)	37(1)	18(1)	48(1)	-9(1)	-2(1)	0(1)
O(103)	43(1)	30(1)	36(1)	-20(1)	-12(1)	3(1)
C(115)	19(1)	22(1)	22(1)	-7(1)	-3(1)	-5(1)
C(116)	19(1)	16(1)	22(1)	-4(1)	-5(1)	-3(1)
O(101)	28(1)	38(1)	29(1)	-17(1)	-9(1)	-3(1)
C(101)	27(1)	25(1)	31(1)	-17(1)	0(1)	-5(1)
C(102)	25(1)	18(1)	24(1)	-9(1)	-1(1)	2(1)
F(101)	30(1)	28(1)	34(1)	-20(1)	4(1)	-1(1)
C(103)	18(1)	25(1)	28(1)	-8(1)	-1(1)	0(1)
C(104)	18(1)	23(1)	25(1)	-11(1)	-6(1)	0(1)
C(107)	21(1)	26(1)	25(1)	-10(1)	-3(1)	-5(1)
C(108)	22(1)	26(1)	26(1)	-11(1)	-5(1)	-7(1)
C(109)	23(1)	25(1)	24(1)	-9(1)	-3(1)	-8(1)
C(121)	21(1)	24(1)	26(1)	-9(1)	2(1)	-11(1)
C(122)	29(1)	24(1)	30(1)	-9(1)	-2(1)	-9(1)
C(123)	33(1)	24(1)	42(1)	-15(1)	4(1)	-10(1)
C(124)	36(1)	39(1)	37(1)	-24(1)	11(1)	-18(1)
C(125)	35(1)	50(1)	23(1)	-16(1)	4(1)	-18(1)
C(126)	26(1)	32(1)	25(1)	-10(1)	2(1)	-9(1)
C(105)	19(1)	22(1)	21(1)	-8(1)	-5(1)	-1(1)

---

**Table A5.1.6** Hydrogen coordinates ( $\times 10^4$ ) and isotropic displacement parameters ( $\text{\AA}^2 \times 10^3$ ) for compound **151**.

	x	y	z	U(eq)
H(12)	2983	3831	9068	28
H(13)	3721	2013	8153	30
H(15)	3976	5175	5383	28
H(16)	3167	7002	6300	27
H(1A)	2196	8511	9390	26
H(1B)	2774	9681	8336	26
H(3)	7633	7761	9385	30
H(4)	8303	7213	7710	27
H(7A)	8909	4989	9091	29
H(7B)	6818	4893	9149	29
H(8)	9351	4812	7219	29
H(9)	7514	2749	8499	31
H(22)	8781	328	8011	43
H(23)	9617	-927	6702	52
H(24)	10097	336	4946	47
H(25)	9849	2879	4489	47
H(26)	9062	4148	5790	37
H(5A)	5579	8371	7041	25
H(5B)	5790	6657	7167	25
H(112)	2856	6224	759	28
H(113)	1264	8098	1631	30
H(115)	1806	4984	4436	25
H(116)	3445	3128	3554	23
H(10A)	6528	1507	541	32
H(10B)	7167	328	1613	32
H(103)	11311	2087	736	30
H(104)	9959	2673	2390	27
H(10C)	9858	4866	936	28
H(10D)	7700	5008	912	28
H(108)	8792	5214	2740	28

**Table A5.1.6 Cont.**

H(109)	5810	6996	1630	27
H(122)	3946	9282	2095	33
H(123)	2904	10799	3251	39
H(124)	4241	10083	4791	42
H(125)	6560	7800	5196	41
H(126)	7530	6236	4081	33
H(10E)	7606	1574	2973	25
H(10F)	6476	3304	2832	25

---

**Table A5.1.7** Torsion angles [°] for compound **151**.

---

C(1)-N(1)-C(6)-O(1)	-2.3(2)
C(5)-N(1)-C(6)-O(1)	174.18(16)
C(1)-N(1)-C(6)-C(11)	177.95(14)
C(5)-N(1)-C(6)-C(11)	-5.6(2)
O(1)-C(6)-C(11)-C(12)	-54.8(2)
N(1)-C(6)-C(11)-C(12)	124.94(17)
O(1)-C(6)-C(11)-C(16)	122.02(18)
N(1)-C(6)-C(11)-C(16)	-58.2(2)
C(16)-C(11)-C(12)-C(13)	2.2(3)
C(6)-C(11)-C(12)-C(13)	179.10(15)
C(11)-C(12)-C(13)-C(14)	-0.2(3)
C(12)-C(13)-C(14)-C(15)	-1.1(3)
C(12)-C(13)-C(14)-N(2)	178.69(16)
C(13)-C(14)-N(2)-O(2)	8.7(2)
C(15)-C(14)-N(2)-O(2)	-171.54(18)
C(13)-C(14)-N(2)-O(3)	-172.07(17)
C(15)-C(14)-N(2)-O(3)	7.7(2)
C(13)-C(14)-C(15)-C(16)	0.3(3)
N(2)-C(14)-C(15)-C(16)	-179.48(15)
C(14)-C(15)-C(16)-C(11)	1.7(2)
C(12)-C(11)-C(16)-C(15)	-3.0(2)
C(6)-C(11)-C(16)-C(15)	-179.77(15)
C(6)-N(1)-C(1)-C(2)	134.31(15)
C(5)-N(1)-C(1)-C(2)	-42.60(17)
N(1)-C(1)-C(2)-C(3)	9.7(2)
N(1)-C(1)-C(2)-F(1)	-170.11(13)
F(1)-C(2)-C(3)-C(4)	-175.73(14)
C(1)-C(2)-C(3)-C(4)	4.5(3)
C(2)-C(3)-C(4)-C(5)	12.6(2)
C(2)-C(3)-C(4)-C(7)	-114.69(19)
C(3)-C(4)-C(7)-C(8)	-173.93(14)
C(5)-C(4)-C(7)-C(8)	60.10(18)
C(4)-C(7)-C(8)-C(9)	-138.02(18)
C(7)-C(8)-C(9)-C(21)	177.01(16)

**Table A5.1.7 Cont.**

C(8)-C(9)-C(21)-C(26)	-26.6(3)
C(8)-C(9)-C(21)-C(22)	155.9(2)
C(26)-C(21)-C(22)-C(23)	-0.2(3)
C(9)-C(21)-C(22)-C(23)	177.45(19)
C(21)-C(22)-C(23)-C(24)	-0.8(3)
C(22)-C(23)-C(24)-C(25)	1.2(4)
C(23)-C(24)-C(25)-C(26)	-0.6(4)
C(24)-C(25)-C(26)-C(21)	-0.3(3)
C(22)-C(21)-C(26)-C(25)	0.7(3)
C(9)-C(21)-C(26)-C(25)	-176.85(19)
C(6)-N(1)-C(5)-C(4)	-114.51(17)
C(1)-N(1)-C(5)-C(4)	62.08(17)
C(3)-C(4)-C(5)-N(1)	-43.69(18)
C(7)-C(4)-C(5)-N(1)	83.57(16)
C(101)-N(101)-C(106)-O(101)	-1.3(2)
C(105)-N(101)-C(106)-O(101)	173.15(16)
C(101)-N(101)-C(106)-C(111)	178.58(14)
C(105)-N(101)-C(106)-C(111)	-6.9(2)
O(101)-C(106)-C(111)-C(116)	126.28(18)
N(101)-C(106)-C(111)-C(116)	-53.6(2)
O(101)-C(106)-C(111)-C(112)	-50.4(2)
N(101)-C(106)-C(111)-C(112)	129.66(16)
C(116)-C(111)-C(112)-C(113)	4.6(2)
C(106)-C(111)-C(112)-C(113)	-178.61(15)
C(111)-C(112)-C(113)-C(114)	-1.1(2)
C(112)-C(113)-C(114)-C(115)	-3.1(3)
C(112)-C(113)-C(114)-N(102)	175.88(15)
C(115)-C(114)-N(102)-O(102)	-175.07(16)
C(113)-C(114)-N(102)-O(102)	5.9(2)
C(115)-C(114)-N(102)-O(103)	5.5(2)
C(113)-C(114)-N(102)-O(103)	-173.51(16)
C(113)-C(114)-C(115)-C(116)	3.7(2)
N(102)-C(114)-C(115)-C(116)	-175.26(14)
C(114)-C(115)-C(116)-C(111)	-0.1(2)
C(112)-C(111)-C(116)-C(115)	-4.0(2)

**Table A5.1.7 Cont.**

C(106)-C(111)-C(116)-C(115)	179.39(15)
C(106)-N(101)-C(101)-C(102)	131.28(16)
C(105)-N(101)-C(101)-C(102)	-43.96(19)
N(101)-C(101)-C(102)-C(103)	12.3(3)
N(101)-C(101)-C(102)-F(101)	-168.29(13)
F(101)-C(102)-C(103)-C(104)	-177.36(14)
C(101)-C(102)-C(103)-C(104)	2.0(3)
C(102)-C(103)-C(104)-C(105)	13.8(2)
C(102)-C(103)-C(104)-C(107)	-111.81(19)
C(103)-C(104)-C(107)-C(108)	-169.49(14)
C(105)-C(104)-C(107)-C(108)	65.58(18)
C(104)-C(107)-C(108)-C(109)	-129.96(18)
C(107)-C(108)-C(109)-C(121)	-178.94(16)
C(108)-C(109)-C(121)-C(126)	-11.1(3)
C(108)-C(109)-C(121)-C(122)	167.76(18)
C(126)-C(121)-C(122)-C(123)	1.2(2)
C(109)-C(121)-C(122)-C(123)	-177.79(16)
C(121)-C(122)-C(123)-C(124)	0.7(3)
C(122)-C(123)-C(124)-C(125)	-1.3(3)
C(123)-C(124)-C(125)-C(126)	0.0(3)
C(124)-C(125)-C(126)-C(121)	1.9(3)
C(122)-C(121)-C(126)-C(125)	-2.4(3)
C(109)-C(121)-C(126)-C(125)	176.48(16)
C(106)-N(101)-C(105)-C(104)	-112.83(18)
C(101)-N(101)-C(105)-C(104)	61.85(18)
C(103)-C(104)-C(105)-N(101)	-43.68(18)
C(107)-C(104)-C(105)-N(101)	81.51(17)

---

Symmetry transformations used to generate equivalent atoms:

## **APPENDIX 6**

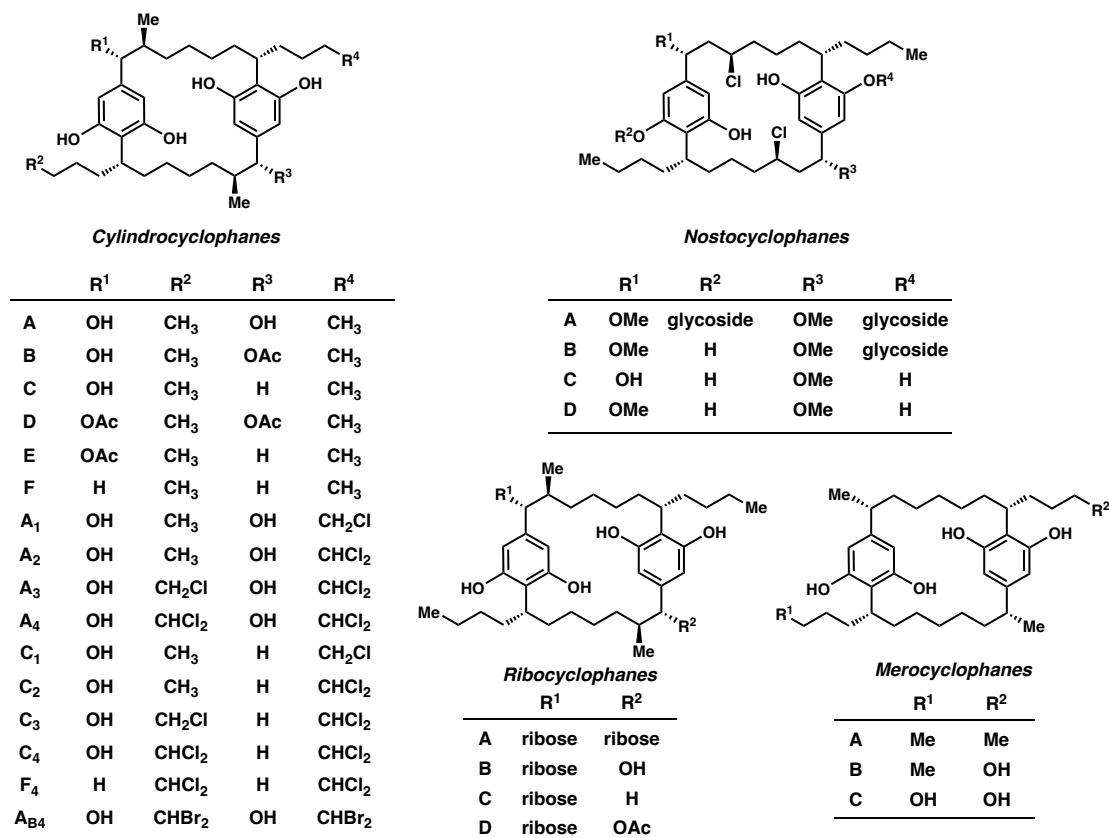
### *Progress Toward the Total Synthesis of (-)-Cylindrocyclophane A<sup>†</sup>*

#### **A6.1 INTRODUCTION**

The selective functionalization of unactivated carbon-hydrogen (C–H) bonds has been described as the “holy grail” of chemical reactivity and represents one of the biggest challenges in the organic chemistry community.<sup>1</sup> C–H activation enables access to novel chemical space and re-shapes how chemists think about constructing molecules, demonstrating the potential to broadly impact scientific research. While significant advances have been made in the past three decades, the field of C–H functionalization has seen its biggest resurgence from the NSF Center for Selective C–H Functionalization (CCHF).<sup>2</sup> The ultimate goal of the CCHF was to fundamentally change how chemists think about breaking and building molecules. With the collective effort of scientists within the framework of the CCHF, the result has been the ability to tackle interdisciplinary challenges in the realm of C–H functionalization.<sup>3</sup> One such “grand challenge” has been to apply new C–H functionalization methods to synthesize a natural product via novel disconnections.<sup>4</sup> In this chapter, we will describe the development of a route to the complex natural product class known as the [7.7]-paracyclophanes, that heavily relies on C–H functionalization logic.

<sup>†</sup>This research was performed in collaboration with Aaron T. Bosse, Camila Suarez, Liam R. Hunt, Elizabeth Goldstein, Hojoon Park, Jin-Quan Yu and Huw M.L. Davies

**Figure A6.1.1** Representative examples of the [7.7]paracyclophane natural products

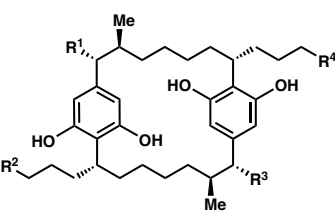


Since their first introduction by Cram and Steinberg in 1951, [m.n]paracyclophanes have inspired chemists with their macrocyclic structure (Figure A6.1.1).<sup>5</sup> It wasn't until 1990 that the first [7.7]paracyclophane natural products were isolated by Moore and coworkers from two species of terrestrial blue-green algae, *Cylindrospermum licheniforme* Kutzing and *Nostoclickia* (Roth) Bornet.<sup>6</sup> Since this initial report, teams led by Orjala and Mundt have isolated dozens of other [7.7]paracyclophane natural products.<sup>7</sup> These new natural products isolated from this campaign are the ribocyclophanes,<sup>7a</sup> carbamidocyclophanes<sup>7b,7c</sup> and merocyclophanes.<sup>7d,7e</sup> These three join the cylindrocyclophanes<sup>7f</sup> and nostocyclophanes<sup>7g</sup> as the five subclasses of [m.n]paracyclophane natural products. Additionally, some of them display antimicrobial



activity against Gram-positive pathogens with minimum inhibitory concentrations (MIC's) in the range of 0.1–0.2  $\mu\text{M}$  toward resistant Gram-positive bacteria, methicillin-resistant staphylococcus *aureus* (MRSA), along with activity against *S. pneumoniae* with MIC's between 0.2–3  $\mu\text{M}$  (Figure A6.1.2).<sup>8</sup> The most promising of the natural products reveal antimicrobial activity with MIC's at around 50-fold lower than their corresponding  $\text{IC}_{50}$  value against non-tumorigenic cell line HaCaT, which demonstrates the possibility for selective antimicrobial activity over general cytotoxicity.<sup>8</sup>

**Figure A6.1.2** Biological activity of select cylindrocyclophanes

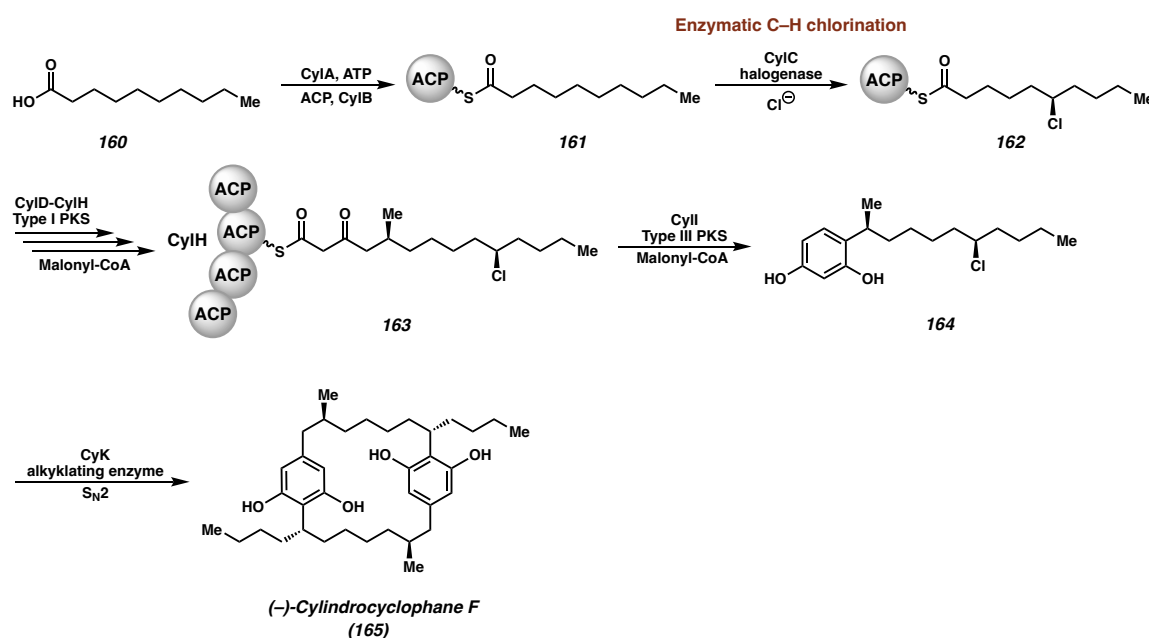


Cylindrocyclophanes	Cylindrocyclophanes				Antimicrobial testing Gram-positive bacteria		Cytotoxic testing
	R <sup>1</sup>	R <sup>2</sup>	R <sup>3</sup>	R <sup>4</sup>	MRSA MIC ( $\mu\text{M}$ )	<i>S. pneumoniae</i> MIC ( $\mu\text{M}$ )	HaCaT $\text{IC}_{50}$ ( $\mu\text{M}$ )
A	OH	CH <sub>3</sub>	OH	CH <sub>3</sub>	0.1–1.1 $\mu\text{M}$	0.3–2.2 $\mu\text{M}$	5.0 $\pm$ 1.9 $\mu\text{M}$
D	OAc	CH <sub>3</sub>	OAc	CH <sub>3</sub>	0.9 $\mu\text{M}$	2.4 $\mu\text{M}$	11 $\pm$ 1.0 $\mu\text{M}$
A <sub>1</sub>	OH	CH <sub>3</sub>	OH	CH <sub>2</sub> Cl	1.02 $\mu\text{M}$	2.1 $\mu\text{M}$	11.3 $\mu\text{M}$
A <sub>2</sub>	OH	CH <sub>3</sub>	OH	CHCl <sub>2</sub>	0.96 $\mu\text{M}$	1.99 $\mu\text{M}$	11.5 $\mu\text{M}$
A <sub>3</sub>	OH	CH <sub>2</sub> Cl	OH	CHCl <sub>2</sub>	0.45 $\mu\text{M}$	0.92 $\mu\text{M}$	8.6 $\mu\text{M}$
A <sub>4</sub>	OH	CHCl <sub>2</sub>	OH	CHCl <sub>2</sub>	0.43 $\mu\text{M}$	0.87 $\mu\text{M}$	9.3 $\mu\text{M}$

Led by the team that first isolated (-)-cylindrocyclophane A, Moore and coworkers tried to elucidate the biosynthetic pathway by introducing <sup>2</sup>H, <sup>13</sup>C, and <sup>18</sup>O-labeled sodium acetates to *C. lichenforme* cultures.<sup>9</sup> While NMR analysis of isolated metabolites resulted in a proposed pathway, the team was unable to unravel the key dimerization event to form the macrocyclic structure. It would not be until 2012 when Balskus and coworkers identified the cylindrocyclophane biosynthetic gene cluster in *C. lichenforme*.<sup>10</sup> Furthermore, they were able to characterize several components of the polyketide synthase (PKS) machinery, and in 2017 proposed the biosynthetic pathway to (-)-

cylindrocyclophane F.<sup>11</sup> While this work focuses on (-)-cylindrocyclophane A, the biosynthetic approach to access (-)-cylindrocyclophane F is similar to the approach to (-)-cylindrocyclophane A and therefore is relevant to the discussion.

**Scheme A6.1.1** Proposed biosynthesis toward (-)-cylindrocyclophane F (**165**)



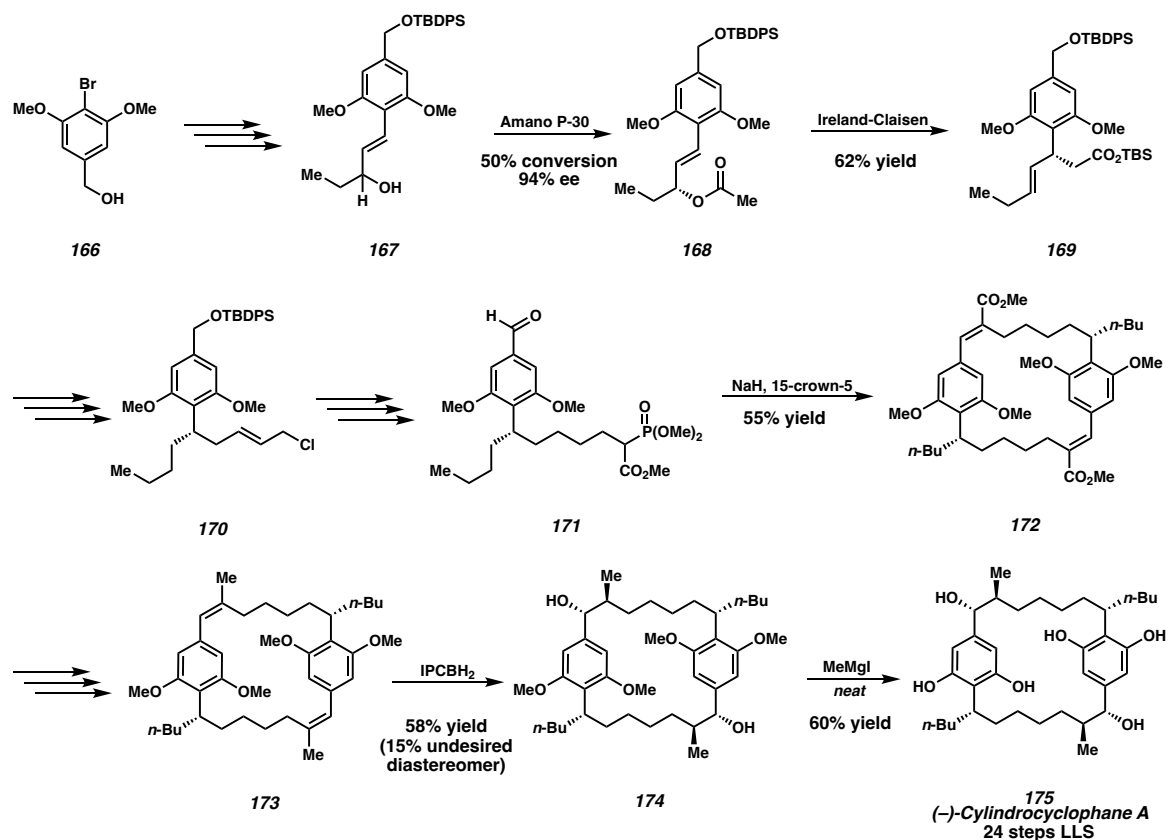
The biosynthesis starts with decanoic acid **160** converting the decanoyl-acyl carrier protein (ACP) thioester **161** (Scheme A6.1.1).<sup>11c</sup> From there, the next transformation is the key step uncovered by Balskus and coworkers. Decanoyl-CylB thioester **161** undergoes a regio- and enantioselective chlorination by halogenase CylC to deliver chlorodecanoyl thioester **162**. With the chlorinated product **162**, CylD-CylH catalyzes enzymatic reactions through a type I PKS assembly in the presence of malonyl-CoA to convert **162** into intermediate **163**. This intermediate is then converted to resorcinol **164** to deliver malonyl-CoA under type III PKS CylII enzymatic catalysis. Lastly, CylK functions as an alkylating enzyme promoting the double S<sub>N</sub>2 dimerization of resorcinol **164** to form (-)-cylindrocyclophane F (**165**).

The unique molecule architecture combined with promising biological activity has generated considerable synthetic interest in these compounds. To date, (-)-cylindrocyclophane A (**175**) has been the target of three total syntheses.<sup>12</sup> Historically, the approach has been the same, involving the exploitation of the inherent C<sub>2</sub> symmetry of the natural product via a convergent dimerization approach. The three approaches that will be outlined leverage different dimerization techniques to furnish the desired [7.7]paracyclophane natural product core. Despite being an elegant way to synthesize (-)-cylindrocyclophane A (**175**), this strategy cannot be applied to the numerous known unsymmetrical paracyclophanes. Furthermore, none of the strategies are ideally suited for the synthesis of analogs since the diversification required for analog synthesis would have to occur early in the synthetic sequence of the monomer precursors.

The first total synthesis was accomplished by Hoye and coworkers in 2000 utilizing a key Horner-Wadsworth-Emmons (HWE) coupling of monomer **171** to provide the macrocyclic dimer **172** that was further elaborated to (-)-cylindrocyclophane A (**175**) (Scheme A6.1.2).<sup>12a</sup> The synthesis of the monomer **171** utilizes a commercially available lipase enzyme (Amano P-30) to perform a kinetic resolution of alcohol **167**. An Ireland-Claisen rearrangement of alcohol **167** delivered the first benzylic stereocenter in 62% yield and 94% ee from the enzymatic resolution. After several functional group manipulations, the HWE reaction of monomer **171** provided the macrocycle **172** in 55% yield. The necessary benzylic alcohols and adjacent methyl groups were installed via a late-stage asymmetric hydroboration of styrene **172** utilizing (+)-ipc-borane. Tetrademethylation of the tetramethyl phenyl ether **174** delivered (-)-cylindrocyclophane A (**175**) in 24 steps longest linear sequence (LLS). This strategy of unmasking the resorcinol motif of the

natural product as the last step has been exploited by the other two reported total syntheses of (-)-cylindrocyclophane A (**175**).

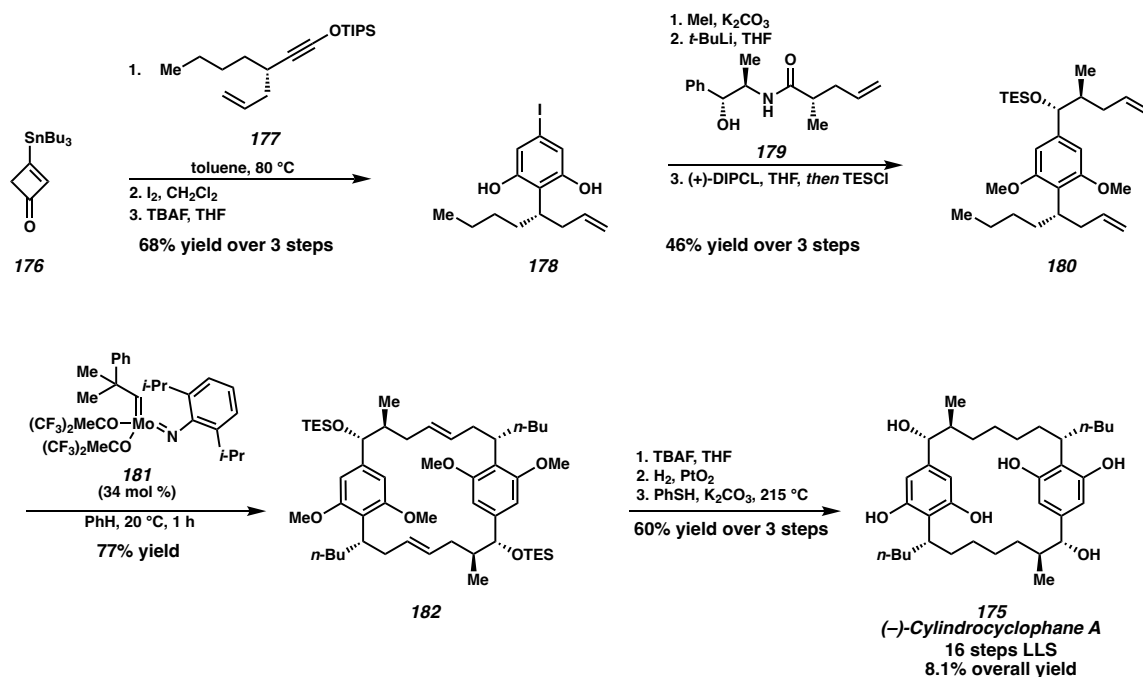
**Scheme A6.1.2** Hoye's total synthesis of (-)-cylindrocyclophane A (**175**)



In back-to-back publications, Smith and coworkers disclosed a route that leverages a dimeric ring-closing olefin metathesis (RCM) to form the 22-membered macrocycle (Scheme A6.1.3).<sup>12b,12c</sup> Building the monomer subunit needed for the RCM, Smith and coworker synthesizes the resorcinol ring **178** through a Danheiser benzannulation of **176** using alkyne **177**. The key RCM macrocyclization of the monomer **180** was achieved using a Schrock molybdenum-based catalyst **181** to deliver the desired macrocycle **182** in 77% yield. The endgame involved double deprotection and alkene hydrogenation to afford (-)-cylindrocyclophane A (**175**). The phenols in **178** were protected as the phenyl methyl

ethers due to facile oxidation of the resorcinol to the corresponding quinone and subsequent decomposition. Through this strategy, Smith and coworkers were able to access (-)-cylindrocyclophane A (**175**) in 16 steps LLS with an 8.1% overall yield, which is the shortest synthesis to date.

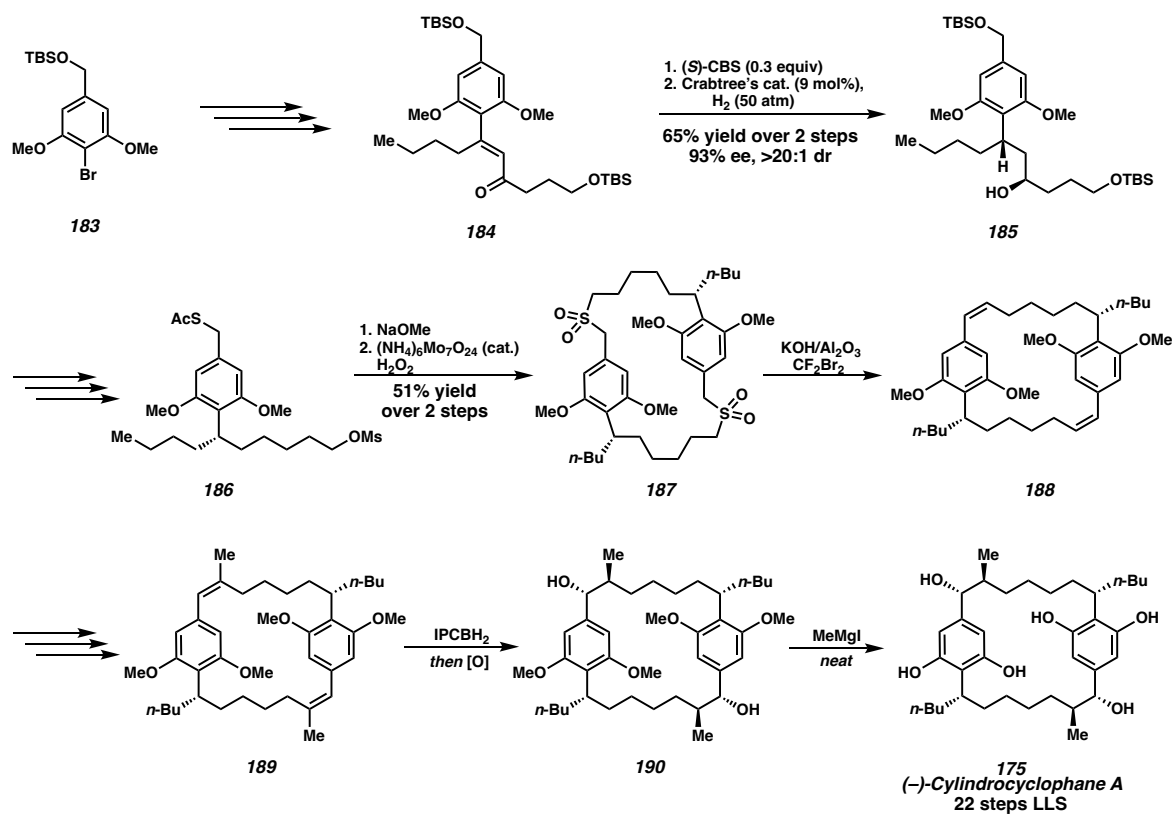
**Scheme A6.1.3** Smith's total synthesis of (-)-cylindrocyclophane A (**175**)



The final and most recent total synthesis of (-)-cylindrocyclophane A (**175**) was reported by Nicolaou and coworkers in 2010 (Scheme A6.1.4).<sup>12d</sup> This approach involved a key dimerization via a Ramberg-Bäcklund olefination of monomer **186** that forms the desired macrocycle **187** in a 51% yield over two steps. To synthesize the monomer subunit, a CBS reduction of enone **184** followed by a directed, diastereoselective olefin hydrogenation to set the necessary benzylic stereocenter in compound **185**. After the dimerization to deliver macrocycle **187**, the asymmetric hydroboration strategy developed in the Hoyer synthesis<sup>12a</sup> of (-)-cylindrocyclophane A was applied to styrene **189** to set the

final stereocenters and oxygenation present in the natural product. A global demethylation of the phenyl methyl ethers in macrocycle **190** was performed to complete their total synthesis of (-)-cylindrocyclophane A (**175**) in a 22 step LLS.

**Scheme A6.1.4** Nicolaou's total synthesis of (-)-cylindrocyclophane A (**175**)

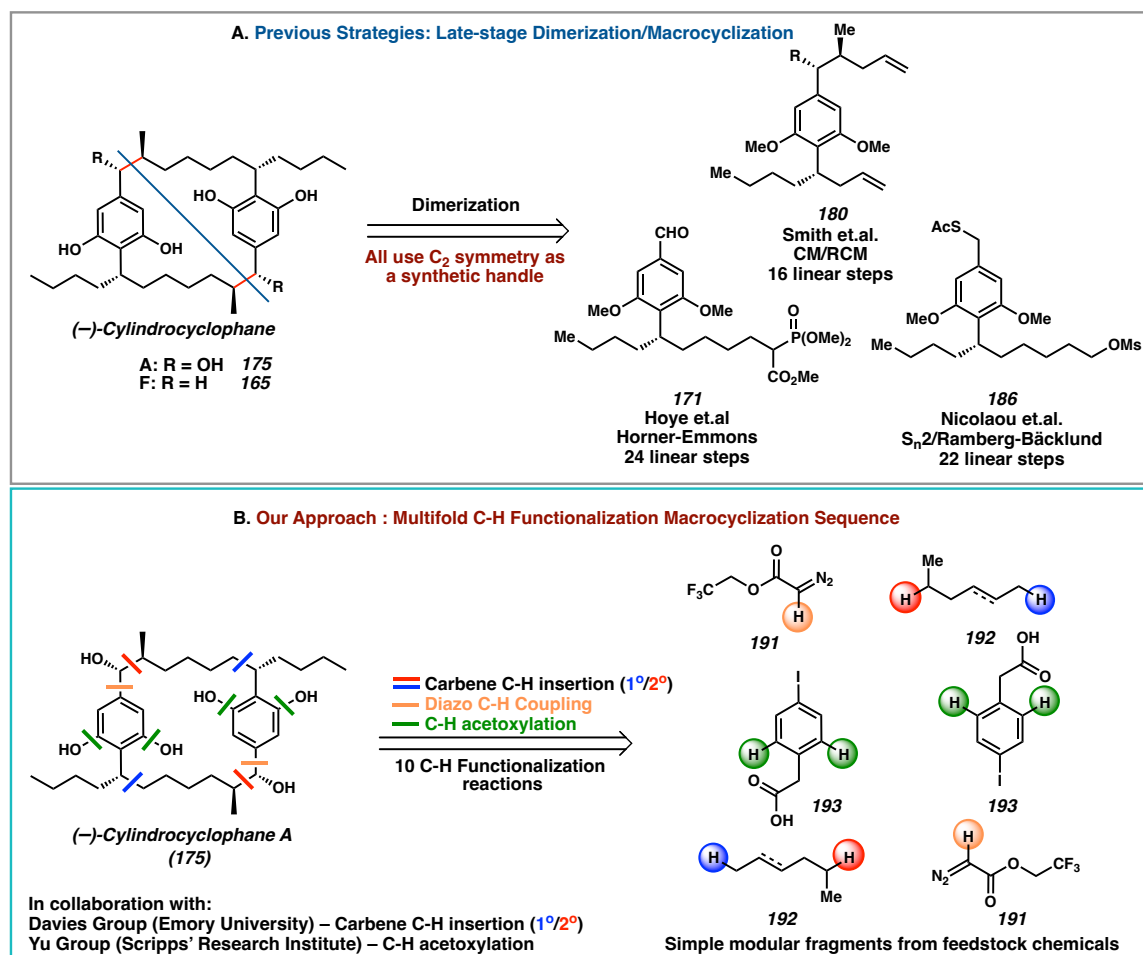


The importance of the inherent symmetry in (-)-cylindrocyclophane A (**175**) and other C<sub>2</sub> symmetric paracyclophane natural products can be seen since all the past total syntheses utilize a key dimerization approach to access the macrocyclic natural product core. Previous strategies toward (-)-cylindrocyclophane A (**175**) involved the linear synthesis of functionalized monomeric subunits possessing at least one benzylic stereocenter and a protected resorcinol motif that could be unmasked to finish the total synthesis. We proposed that a late-stage, C–H functionalization strategy would enable a more flexible and modular strategy that can rapidly access the [m,n]paracyclophane core

that is shared among many members and analogs of the natural product family. Seminal research in both the Davies lab<sup>13</sup> at Emory University and the Yu lab<sup>14</sup> at the Scripps' Research Institute developed during the lifetime of the CCHF inspired a C–H functionalization approach toward the total synthesis of (-)-cylindrocyclophane A (175).

## A6.2 PRIOR COLLABORATIVE WORK WITHIN THE CCHF

**Scheme A6.2.1** Summary of strategies and our generalized C–H functionalization macrocyclization sequence



In 2016, the Davies group developed a chiral dirhodium catalyst, Rh<sub>2</sub>(3,5-di(*p*-*t*-BuC<sub>6</sub>H<sub>4</sub>)TPCP)<sub>4</sub> (or Rh<sub>2</sub>(*R*-DiBic)<sub>4</sub>), that is selective to undergo C–H insertion between a

donor-acceptor carbene and the most accessible methylene C(sp<sup>3</sup>)-H bond in a molecule.<sup>13a</sup>

This work inspired a collaboration between the Stoltz group and the Davies group as we proposed this methodology could allow for novel retrosynthetic disconnections of the cylindrocyclophane core that would provide an efficient, modular and flexible synthesis of (-)-cylindrocyclophane A (**175**). In addition, the use of C-H activation technology to generate macrocycles is underexplored in the literature. The White group has reported a strategy to oxidatively activate an allylic C-H bond to form a macrocycle.<sup>15</sup> Another recent example was reported by Baran and coworkers where two aromatic C-H bonds are coupled together through a copper mediated oxidative process to furnish the desired macrocycle.<sup>16</sup> Thus, the success of this research would advance C-H insertion technology as a viable strategy for the synthetic community to access macrocyclic cores.

Further catalyst development studies in the Davies group identified an *ortho*-chlorotriarylcyclopropanecarboxylate (TPCP) ligand for the asymmetric methylene C(sp<sup>3</sup>)-H selective C-H insertion chemistry.<sup>13c</sup> Encouraged by the promising new catalyst, Rh<sub>2</sub>(*R*-2-Cl-5-BrTPCP)<sub>4</sub>, an ambitious retrosynthetic analysis of (-)-cylindrocyclophane A (**175**) was proposed that incorporated a 10 total C-H functionalization reactions in the forward sense (Scheme A6.2.1). This strategy proposed four stereoselective carbene-induced C-H functionalization reactions to generate six stereocenters,<sup>13a,c</sup> two palladium-catalyzed C-H functionalization reactions of diazocarbonyl compounds<sup>13d</sup> and four directed C-H acetoxylation reactions to arrive back at the simple feedstock trifluoroethyl diazoacetate **191**, *n*-hexane **192** and *p*-iodo phenylacetic acid **193** (Scheme A6.2.1).<sup>14</sup> Not only would this synthesis provide a more efficient route to the chiral, highly oxygenated macrocycle, but this modular strategy could also be applied to access various natural

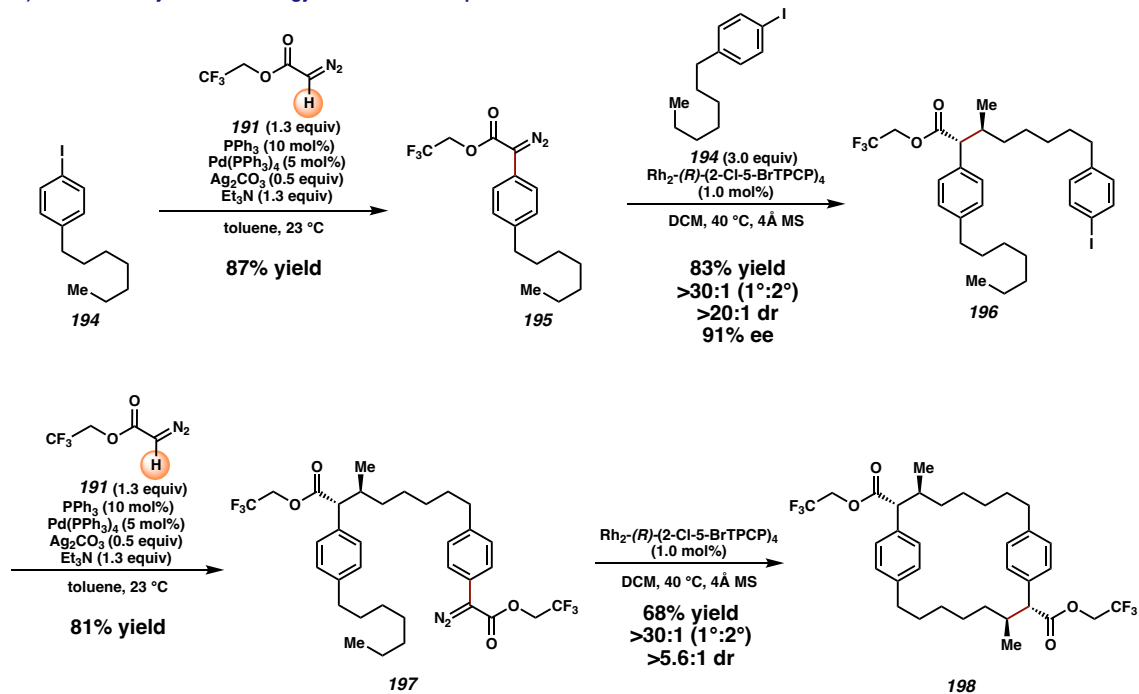


products and analogues to the [m.n]paracyclophane family to probe their structure activity relationships (SAR).

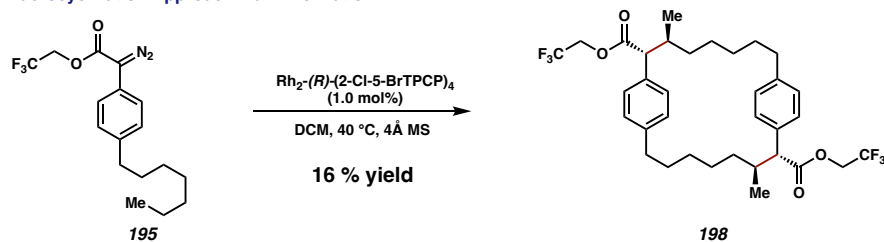
The collaboration began by investigating the validity of the macrocyclization strategy utilizing the catalysts developed by the Davies group (Scheme A6.2.2, A).<sup>17</sup> The aryl iodide **194** was coupled<sup>13d</sup> with diazocarboxylate **191** to yield the donor-acceptor carbene precursor **195** in an 87% yield. This aryl diazocarboxylate **195** was primed to undergo a methylene C(sp<sup>3</sup>)-H selective C-H insertion reaction with aryl iodide **194** to yield the insertion product **196** in excellent yield, regio-, diastereo- and enantioselectivity.<sup>13a</sup> An additional Pd-catalyzed C-H cross coupling reaction with diazocarboxylate **191** delivered donor-acceptor carbene precursor **197** in 81% yield. The macrocyclization with Rh<sub>2</sub>(*R*-2-Cl-5-BrTPCP)<sub>4</sub> delivered the macrocycle **198** in 68% yield and a 5.6:1 dr. Notably, direct dimerization of donor-acceptor carbene precursor **195** could be achieved at a significantly reduced 16% yield due to extensive polymerization of the substrate under the reaction conditions (Scheme A6.2.2, B). Additionally, the presence of 2,6-disubstitution on the arene **199** resulted in significantly reduced yield and diastereoselectivity of the key methylene C(sp<sup>3</sup>)-H selective C-H insertion reaction (Scheme A6.2.2, C). Thus, we chose to investigate strategies to introduce the 2,6-bis-oxygenation after the key macrocyclization step in our total synthesis. ‘

**Scheme A6.2.2** Validation of Rh-catalyzed selective C–H insertion as a  
macrocyclization strategy using a model system

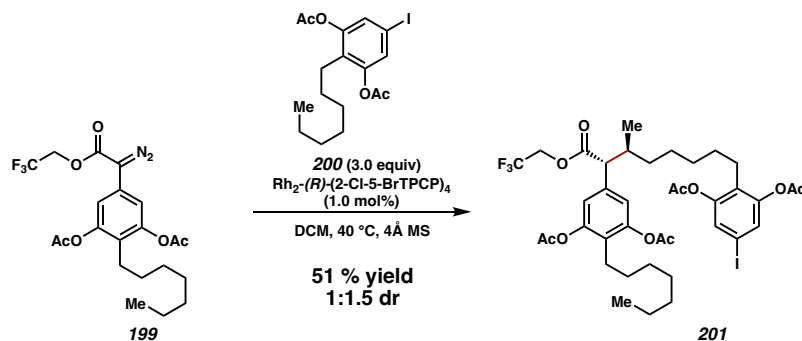
**A) Model Macrocyclization Strategy from Davies Group**



**B) Inferior Macrocyclization Approach via Dimerization**

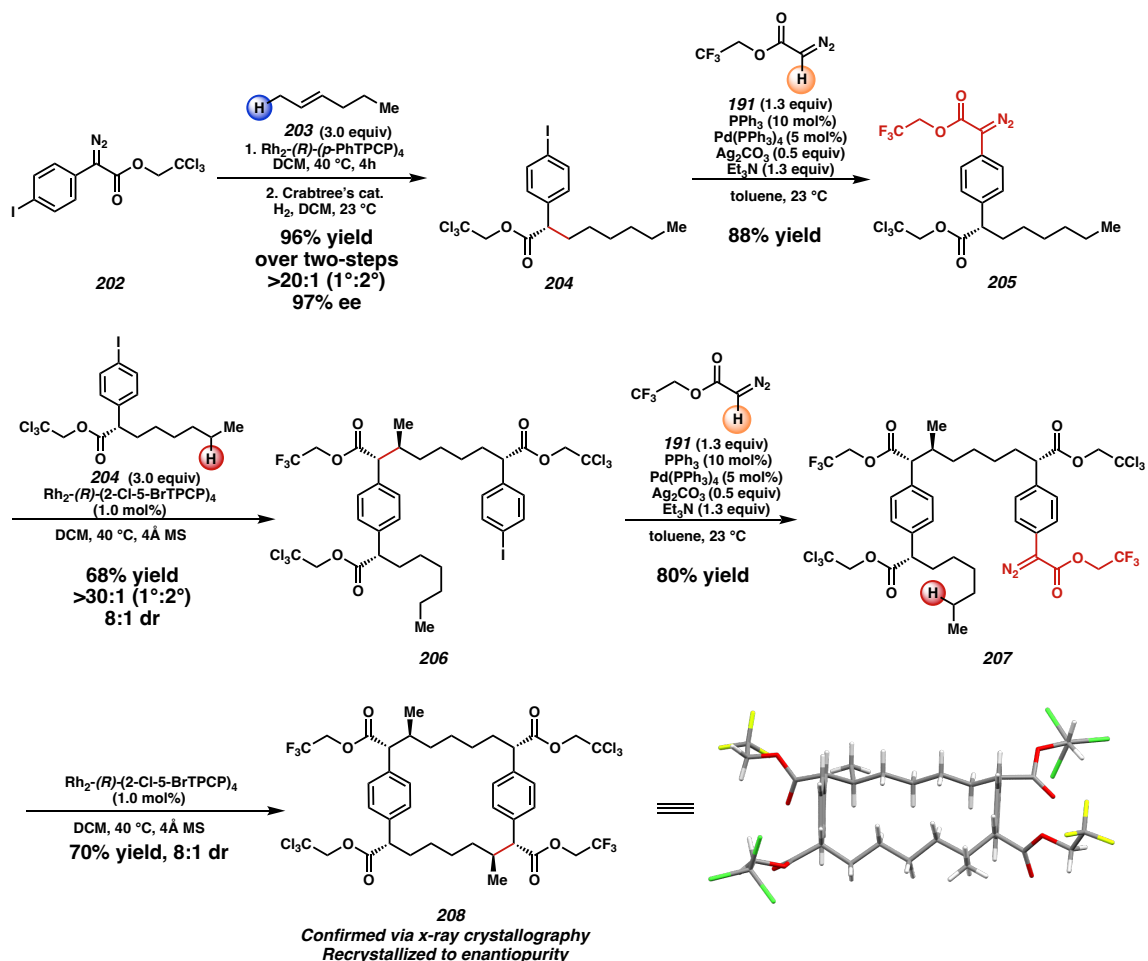


**C) Challenging C–H Insertion with 2,6-bisacetoxy Substitution**



During the course of the CCHF consortium, the Yu group disclosed a Weinreb amide directed *ortho*-C–H acetoxylation of arenes that would be well suited to introduce the necessary oxidation after the macrocycle is formed.<sup>14</sup> Unfortunately, the presence of the Weinreb amide during the C–H insertion chemistry was not amenable since the additional activated  $\alpha$ -nitrogen and  $\alpha$ -oxygen protons interfered with the Rh-catalyzed carbene chemistry. Thus, amidation from the trifluoroethyl carboxylate to the Weinreb amide must be explored post macrocycle formation.

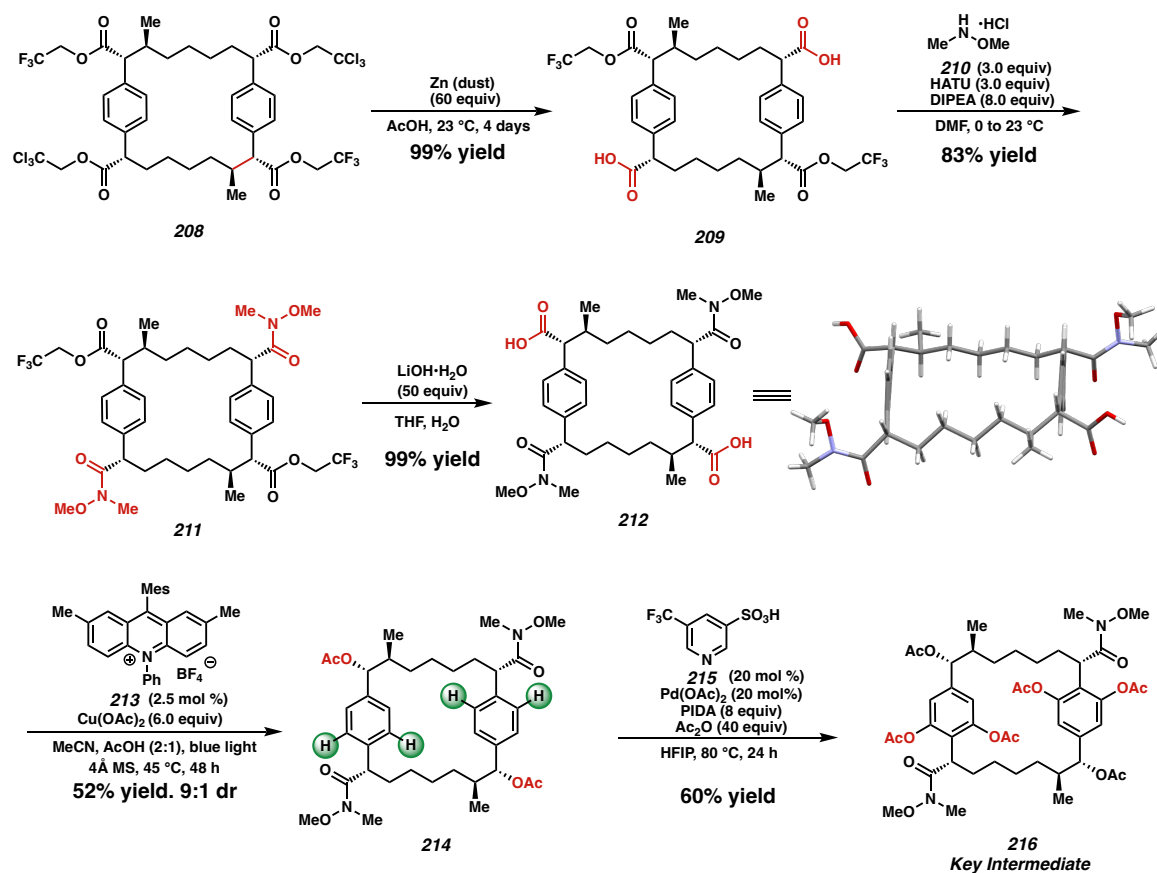
**Scheme A6.2.3** Forward synthesis to elaborate phenyl acetic acid derivative **202** to chiral macrocycle **208** using various C–H functionalization reactions



With our collaborators as Emory, the synthesis began with the primary C–H insertion of *trans*-2-hexene **203** with known aryldiazoacetate **202** (available in 93% yield over two steps from 4-iodophenylacetic acid **193**).<sup>18,19</sup> The optimal dirhodium catalyst was shown to be Rh<sub>2</sub>(*R-p*-PhTPCP)<sub>4</sub>, which was developed by the Davies group and shown to be selective for primary C(sp<sup>3</sup>)–H functionalization of activated C–H bonds.<sup>19</sup> The use of *n*-hexane afforded the desired C–H insertion product **204** in approximately 20% yield due to an unfavorable mixture between the primary C–H and secondary C–H insertion products.<sup>19</sup> Thus, *trans*-2-hexene **203** was chosen as the C–H insertion substrate as the desired product is afforded in excellent yield (96% yield) and excellent enantioselectivity (97% ee) (Scheme A6.2.3). Notably, this reaction could be scaled up to >25 g scale with no loss of efficiency. The desired alkane insertion product **204** could be gained after facile olefin hydrogenation with Crabtree's catalyst with no detected cleavage of the aryl iodide.<sup>20</sup> The aryl iodide can then undergo a Pd-catalyzed cross coupling with diazoacetate **191** to deliver the donor/acceptor carbene precursor **205** in 88% yield.<sup>13d</sup> Treating the aryldiazoacetate **205** with aryl iodide **204** as the C–H insertion substrate using Rh<sub>2</sub>(*R*-2-Cl-5-BrTPCP)<sub>4</sub> as the catalyst delivered the desired C–H insertion product **206** in good yield (68% yield) and excellent stereo- and regiocontrol (>20:1 (1° C–H :2° C–H), 95:5 dr (major:all others)). Subjected the corresponding aryl iodide to the Pd-catalyzed C–H cross coupling conditions with diazoacetate **191** afforded macrocyclization precursor **207** in a 77% yield. With the donor/acceptor carbene precursor in hand, we then subjected the diazo compound **207** to the key macrocyclization using Rh<sub>2</sub>(*R*-2-Cl-5-BrTPCP)<sub>4</sub> to generate the desired macrocycle **208** in 70% yield and an 8:1 dr. To achieve a successful macrocyclization, the reaction must be performed on >2 mmol scale to minimize the

background reaction of carbene insertion into advantageous water. Additionally, the diazo compound **207** must be freshly prepared and used directly in the subsequent step or it will decompose due to trace metals present from the previous transition metal catalyzed transformations. We obtained the macrocyclic product **208** in high enantioselectivity due to the Horeau principle,<sup>21</sup> and the macrocycle **208** can be recrystallized to diastereo- and enantiopurity. The absolute stereochemistry was confirmed via X-ray crystallography that matches the stereocenters present in (-)-cylindrocyclophane A (**175**).

**Scheme A6.2.4** Elaboration of macrocycle to key hexa-acetylated intermediate **216**



With macrocycle in hand, we moved our efforts toward investigation the necessary functional group manipulations to make the Weinreb amide **212** (Scheme A6.2.4). The Troc esters in macrocycle **208** were chemoselectively cleaved using Zn and AcOH to

deliver the dicarboxylic acid compound **209** in quantitative yield.<sup>22</sup> Amide coupling of the diacid **209** using HATU and the hydroxylamine **210** delivered the Weinreb amide **211** in an 85% yield.<sup>23</sup> Hydrolysis of the trifluoroethyl esters delivered the desired dicarboxylic acid compound **212** in a 97% yield. With the carboxylic acid in hand, we subjected the macrocycle **212** to a Cu-catalyzed oxidative decarboxylation reaction using photocatalyst **213**, which delivered the desired bisacetoxy compound **214** in a 52% yield and a 9:1 dr.<sup>24</sup> To our delight, the radical intermediates involved in the oxidative decarboxylation to yield bisacetoxy macrocycle **214** did not entirely ablate the desired stereocenters present in the starting diacid **212**. The moderate 9:1 dr in **214** could be rationalized by the facial selectivity imparted by the adjacent methyl group, or the steric profile of the overall macrocycle preferring the desired diastereomer.<sup>25</sup>

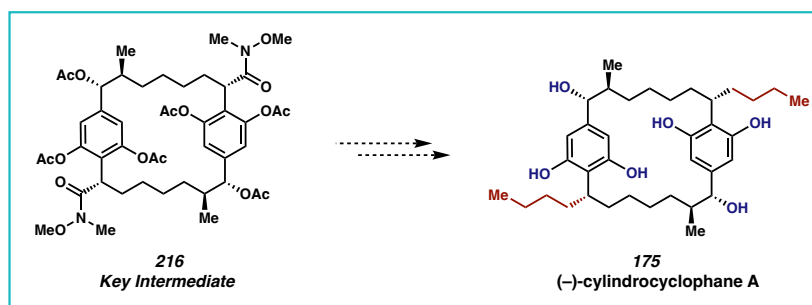
With the desired benzylic oxygenation installed, we moved our efforts toward conducting the final C–H functionalization reaction we proposed in our synthesis (Scheme A6.2.4). Key to the success of the directed *ortho* C–H oxidation was the use of the pyridine sulfonic acid ligand **215** developed by Yu and coworkers.<sup>14b</sup> This pyridine ligand **215** was proposed to greatly accelerate the rate-determining step of the transformation by lowering the energy barrier for the CMD transition state put forward by the Yu group. This was necessary as sequential acetoxylation without the ligand was shown to be slow and produce an undesirable mixture of mono:bis:tri:tetra-acetoxylation products. Upon applying the acetoxylation conditions with the pyridine ligand **215**, we obtained the tetra-acetoxylation product **216** in a 60% yield. The tetra C–H acetoxylation of Weinreb amide **214** signified the successful application of 12 C–H functionalization reactions to rapidly achieve a

functionalized macrocycle **216** that can be elaborated toward (-)-cylindrocyclophane A (**175**).

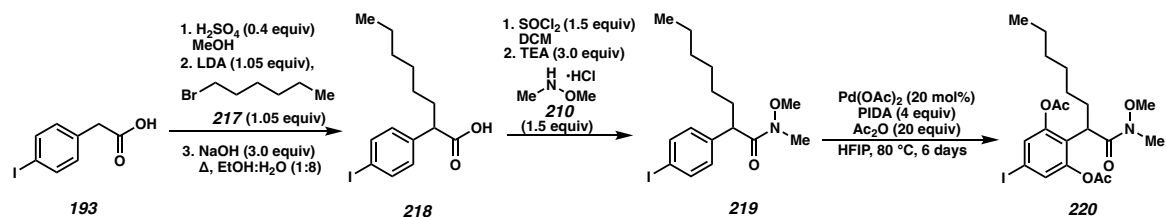
### A6.3 DEVELOPMENT OF MODEL TO ELABORATE KEY MACROCYCLIC INTERMEDIATE TO (-)-CYLINDROCYCLOPHANE A

With the desired hexa-acetate compound **216** in hand, we then focused our efforts toward installing the butyl side chain present in the natural product. To achieve this, the Weinreb amide in the key intermediate **216** must be converted to the butyl side chain as well as a global deprotection of the six acetates with no ablation of the stereocenters. We designed a model Weinreb amide substrate **220** possessing the key 2,6-bisacetoxymethyl arene to investigate the conversion of the Weinreb amide moiety to the butyl side chain necessary to complete our total synthesis (Scheme A6.3.1).

**Scheme A6.3.1** Elaboration of key intermediate **216** toward (-)-cylindrocyclophane A (**175**) and synthesis of truncated model Weinreb amide **220**

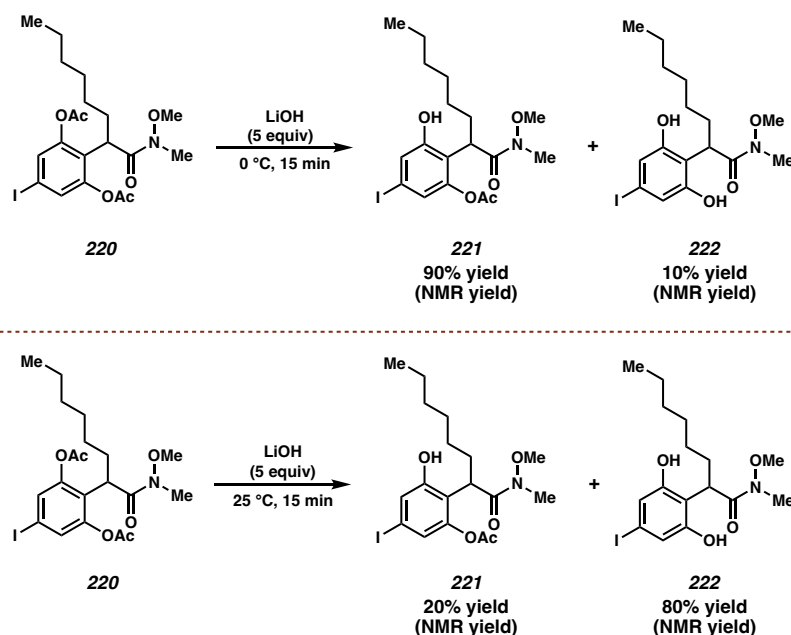


#### Truncated Model



Previous total syntheses of (-)-cylindrocyclophane A (**175**) unmasked the resorcinol motif as the final transformation,<sup>11</sup> leading us to believe that carrying through the unprotected tetraphenol through multiple synthetic steps would be challenging. Thus, we initially explored methods to chemoselectively modify the Weinreb amide in the presence of the moderately labile and sterically congesting 2,6-bisacetoxy functional groups. Treatment of the model compound **220** with LiOH at 0 °C for 15 minutes led to a 9:1 mixture of mono:bis phenol compounds **221** and **222** with no evidence of hydrolysis of the Weinreb amide (Scheme A6.3.2). Allowing the hydrolysis to continue for 15 minutes at 25 °C resulted in a 1:4 mixture of mono:bis phenol compounds **221** and **222** with no Weinreb amide hydrolysis. Hydrolysis of model compound **220** performed at elevated temperatures or prolonged reaction times led to non-specified decomposition, presumably due to the oxidation of the resorcinol promoted by the aqueous basic conditions.

**Scheme A6.3.2** Outcome of hydrolysis of model Weinreb amide **220**

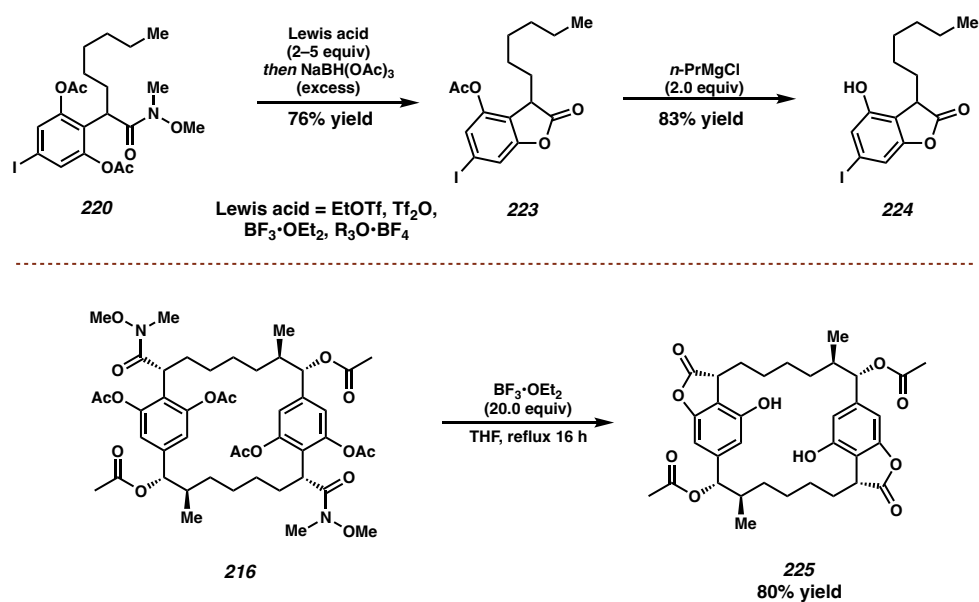


After the failure of selective hydrolysis, we then focused our efforts toward using the higher Lewis basicity of the Weinreb amide to activate the amide **220** and form the



imide, which we would then reduce to the aldehyde in the presence of the phenolic acetates (Scheme A6.3.3).<sup>26</sup> Unfortunately, treatment of the model Weinreb amide **220** with a variety of activating agents such as EtOTf, Tf<sub>2</sub>O, Me<sub>3</sub>O•BF<sub>4</sub>, Et<sub>3</sub>O•BF<sub>4</sub> or BF<sub>3</sub>•OEt<sub>2</sub> led to an unexpected lactone formation to afford the monoacetoxy lactone compound **223**. Treatment of the Weinreb amide macrocyclic intermediate **216** with BF<sub>3</sub>•OEt<sub>2</sub> led to clean formation of the bis lactone compound **225** in an 83% yield. However, in the model system, reduction of this lactone with *n*-PrMgCl led to deacetylated product **224**. More forcing conditions led nonspecific decomposition, presumably due to the formation of benzofuran that can occur after the reduction of the lactone carbonyl.

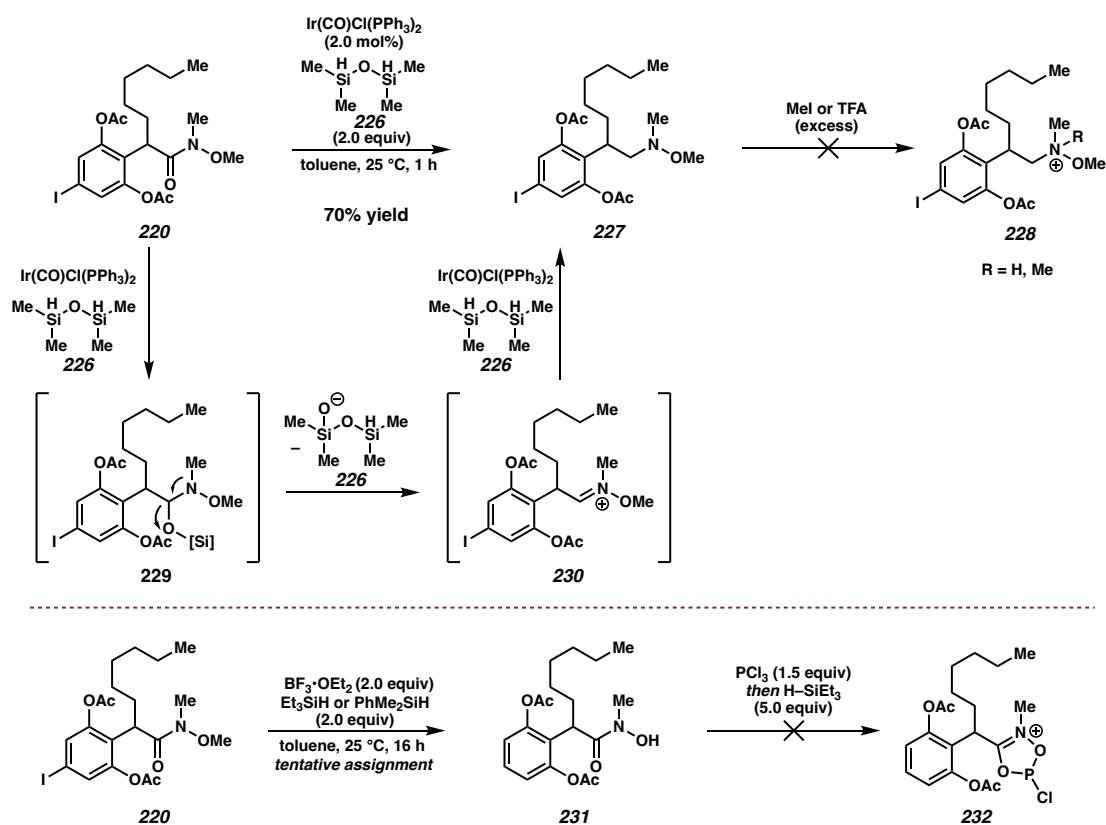
**Scheme A6.3.3** Unexpected Lewis acid promoted deacetylation/lactone formation of model Weinreb amide **220** and macrocycle **216**



Inspired by the recent research from the Dixon group, we believed that the Weinreb amide **220** could undergo an Ir-catalyzed hydrosilylation in the presence of the less Lewis basic acetates (Scheme A6.3.4).<sup>27</sup> Unfortunately, treatment of the model compound with Vaska's catalyst and TMDS **226** led to the overreduction of the amide **220** to the

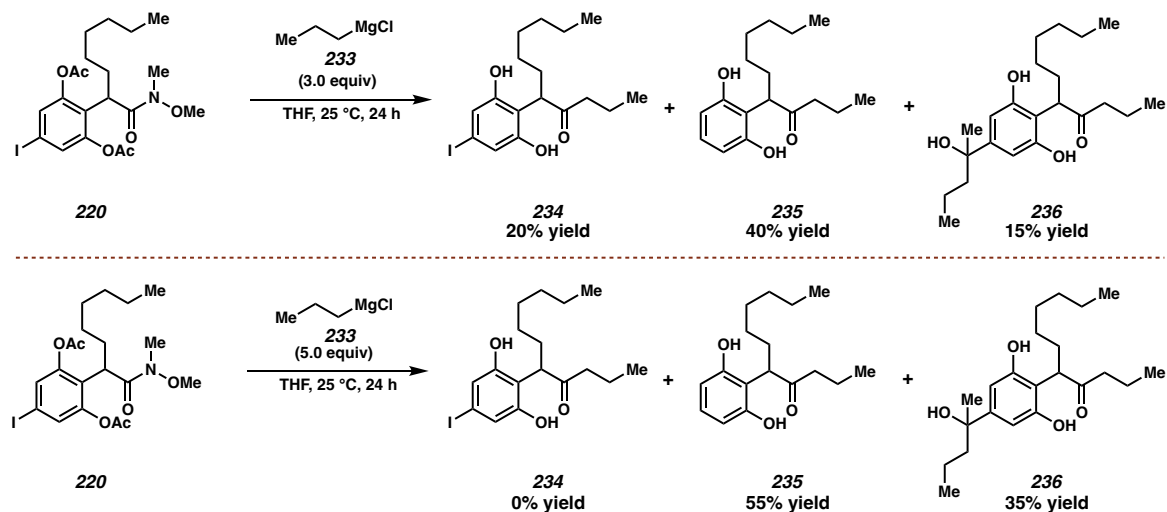
corresponding amine **227**. Typically, monoreduction of the amide to the silyl hemiaminal is observed which is persistent until aqueous workup to reveal the aldehyde. However, we propose the silylated hemiaminal **229** in our model system collapses to form the OMe,Me iminium **230** which undergoes a second hydrosilylation to deliver the undesired OMe-hydroxylamine **227**. Modifying the silane source or the iridium catalyst did not result in the formation of the desired aldehyde. Using  $\text{BF}_3 \cdot \text{OEt}_2$  as a Lewis acid in the presence of a silane resulted in demethylation and protodeiodination of the Weinreb amide **220**, which we could not further functionalize to the desired aldehyde.

**Scheme A6.3.4** Undesired transformations of Weinreb amide **220** utilizing Ir-catalyzed or  $\text{BF}_3 \cdot \text{OEt}_2$  promoted hydrosilylation strategies



Failure to productively functionalize the Weinreb amide in arene **220** selectively in the presence of the 2,6-bisacetoxy arene moiety moved us to investigate non-selective functionalization methods. Treatment of the model Weinreb amide **220** with 3 equivalents of *n*-PrMgCl **233** led to the formation of the desired ketone product **234** in a 20% yield with along with the unexpected protodeiodinated product **235** in a 40% yield (Scheme A6.3.5). Surprisingly, a small amount of ketone product **236** containing a tertiary benzylic alcohol was observed in a 15% yield. We believe the *n*-PrMgCl transmetallates onto the aryl iodide to form the corresponding aryl magnesium species, which can undergo protodemetalation to deliver the observed protodehalogenated major product.<sup>28</sup> Additionally, the Grignard addition into the phenolic acetate liberates an equivalent of 2-pentanone, which combines with the *in situ* generated aryl magnesium species to result in the benzylic tertiary alcohol observed in ketone product **236**. Increasing the amount of *n*-PrMgCl **233** to 5 equivalents results in a 55% yield of the protodehalogenated ketone product **235** and a 35% yield of the tertiary benzylic alcohol product **236**.

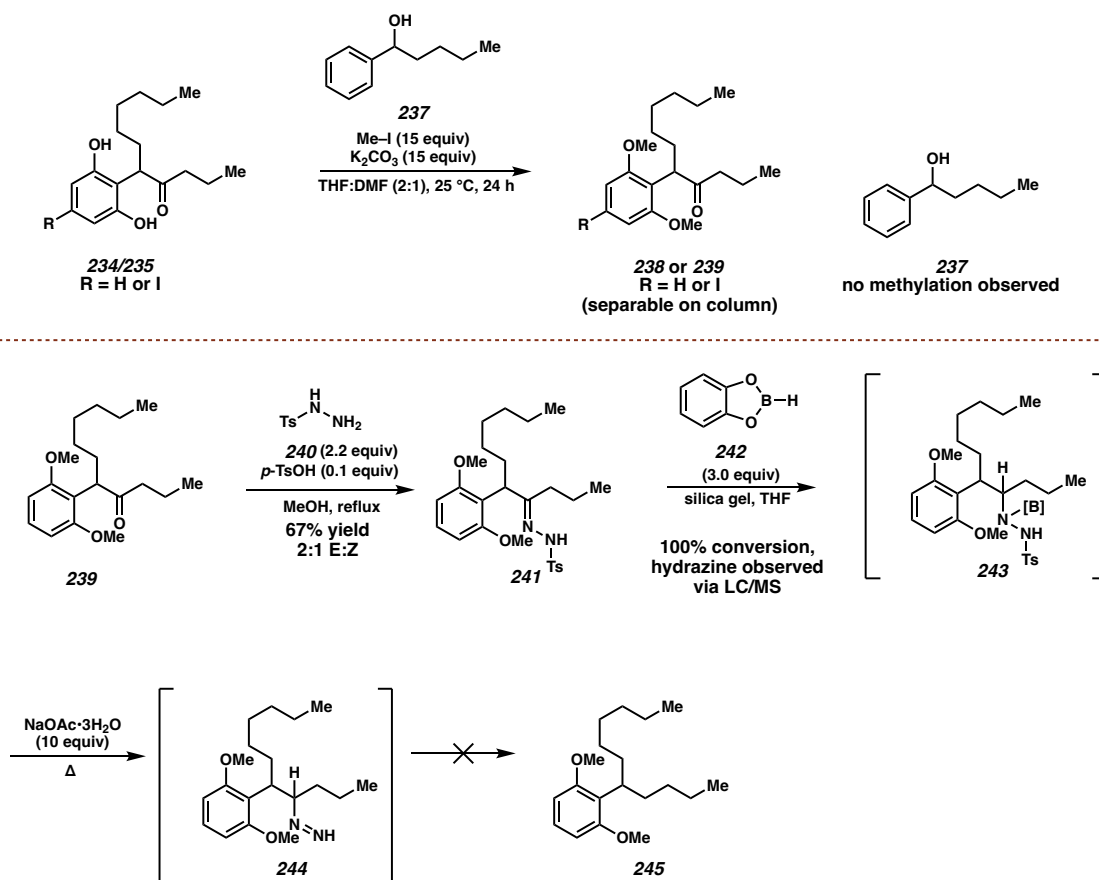
**Scheme A6.3.5** Treatment of model Weinreb amide **220** with *n*-PrMgCl **233**



**A6.4 MODELING THE DEOXYGENATION NECESSARY TO COMPLETE  
THE TOTAL SYNTHESIS OF (-)-CYLINDROCYCLOPHANE A**

With the necessary C–C bond formed in the model system, we focused our efforts toward modeling the final ketone deoxygenation necessary to finish the total synthesis in the natural product system. Our first proposed sequence involved a Wolff-Kishner type diazo decomposition strategy.<sup>29</sup> Predicting the proximal phenols in the ketone products **234** or **235** would negatively impact the transformation, we investigated the methyl protection of the phenols to the corresponding aryl methyl ethers in ketone **238** or **239**.<sup>30</sup>

**Scheme A6.4.1** Phenol selective methylation followed by attempted diazo decomposition strategy from model ketone **234/235**

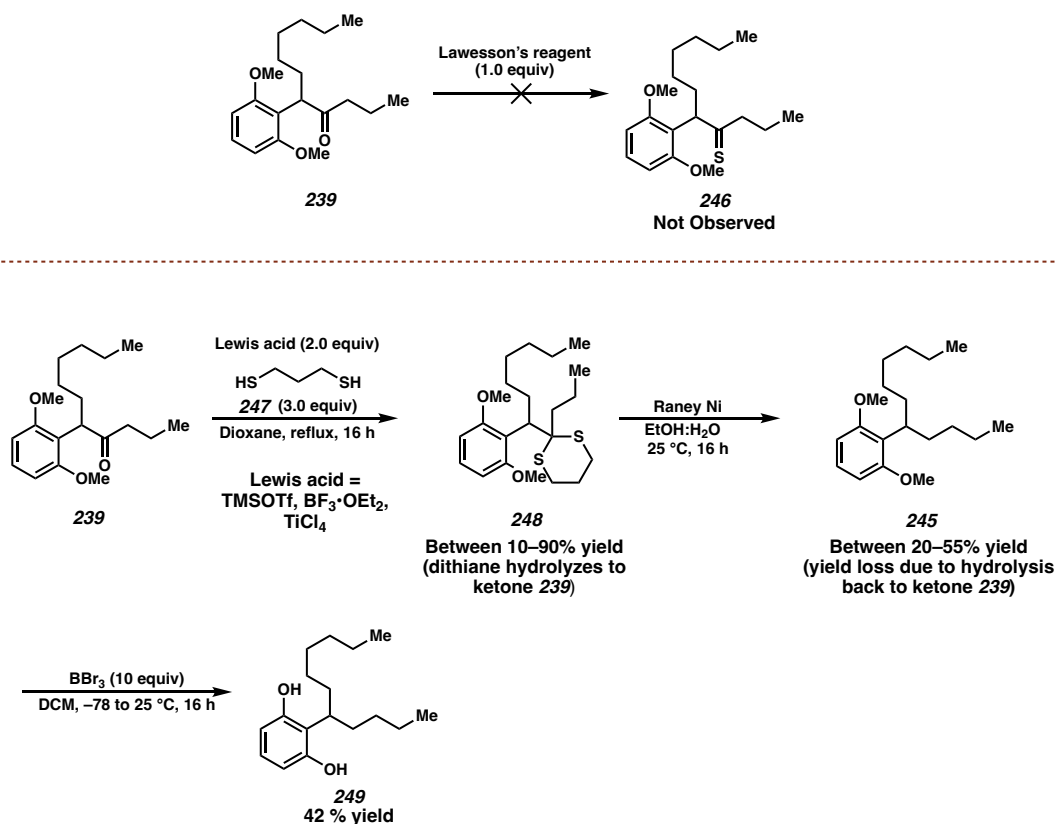


To our delight, the methylation of the mixture of phenols **234** and **235** in the presence of an exogenous benzylic alcohol **237** led to the isolation of the desired bismethyl ether **238** and **239** in 95% combined yield with no benzylic alcohol methylation observed (Scheme A6.4.1). At this stage, the aryl iodide **238** can be separated *via* column chromatography. Treatment of the bismethyl ether ketone **239** with TsNHNH<sub>2</sub> **240** and catalytic amount of *p*-TsOH led to the formation of the desired hydrazone **241** in 67% yield and a 2:1 ratio of E:Z isomers. Reduction of the hydrazone **241** with catechol borane **242** in the presence of silica led to complete conversion to the desired hydrazine **243** (observed *via* LC/MS). Unfortunately, diazo formation from hydrazine **243** followed by alkyl diazo decomposition of diazo **244** did not lead to the desired alkane product **245**. Due to the inability to convert the borylated hydrazine **243** to the desired alkane **245**, we believed any deoxygenation conditions invoking an alkyl diazo such as the Wolff-Kishner reduction would not be amenable for our system.

We focused our efforts toward ketone deoxygenation through a metal promoted desulfurization strategy (Scheme A6.4.2).<sup>31</sup> We proposed converting the ketone to a thiocarbonyl or dithiane would prime use for a metal promoted desulfurization to yield the desired alkane. Unfortunately, treatment of the bismethyl aryl ether compound **239** with Lawesson's reagent did not yield the desired thiocarbonyl compound **240**. To our delight, the Lewis acid catalyzed dithiane formation of the model ketone **239** led to the desired dithiane **248**. However, the isolated yield of the dithiane **248** was found to be highly inconsistent due to observed hydrolysis of the crude dithiane to the starting material ketone **239** during both aqueous workup and column chromatography. Additionally, the Raney Ni promoted Mozingo reduction requires aqueous conditions,<sup>31b</sup> resulting in additional

hydrolysis of the dithiane **248** back to the starting material ketone **239** before desulfurization can occur. Nevertheless, the two-step sequence can be performed to yield the desired alkane **245** in up to 40% yield over the two steps. In our hands, optimization of the desulfurization sequence using alternative dithiols or alternative Lewis acids did not lead to an increase in the yield of the desired alkane **245** of our model system.

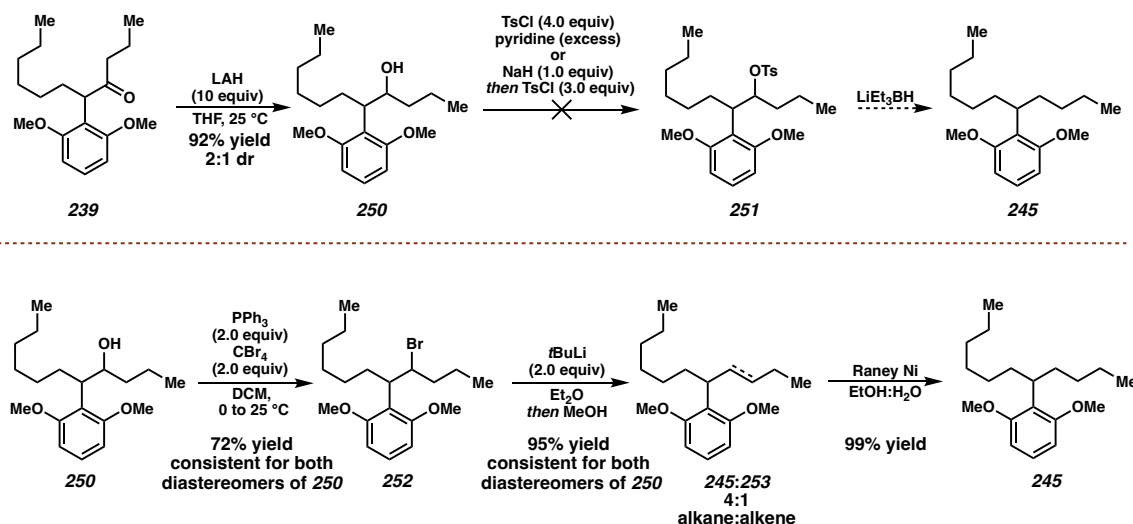
**Scheme A6.4.2** Summary of desulfurization strategies to convert ketone **239** to desired alkane **245**



Dissatisfied with the efficiency of the desulfurization sequence, we focused our efforts toward an alcohol deoxygenation strategy. Treatment of the ketone **239** with NaBH<sub>4</sub> did not lead to any desired alcohol product. Gratifyingly, reduction of the ketone **239** with LAH at ambient temperatures led to quantitative conversion to the corresponding alcohol

**250** in a 2:1 ratio of separable diastereomers (Scheme A6.4.4). We believed that converting the alcohol **250** to the tosylate **251** followed by reduction with  $\text{LiEt}_3\text{BH}$  would deliver the desired alkane product **245**.<sup>32</sup> Unfortunately, the desired tosylate formation was never observed, presumably due to the large steric hinderance from the 2,6-bismethoxy substitution. We then investigated conversion of the alcohol **250** to the corresponding alkyl halide, which could undergo a metal promoted protodehalogenation reaction to deliver the desired alkane.<sup>33</sup>

**Scheme A6.4.3** Summary of alcohol deoxygenation strategies to elaborate model ketone **239** to desired alkane **245**



To our delight, the standard Appel reaction conditions cleanly delivered the corresponding alkyl bromide **252** in good yield for both alcohol diastereomers (ran independently). Treatment of the alkyl bromide **252** with *t*-BuLi cleanly underwent a lithium-halogen exchange reaction, which could be protonated with methanol to deliver the desired alkane **245** in 80% yield.<sup>34</sup> The remaining 20% was isolated as a disubstituted alkene **253**, presumably from the *t*-BuLi mediated  $\text{E}_2$  elimination of the alkyl halide **252**.

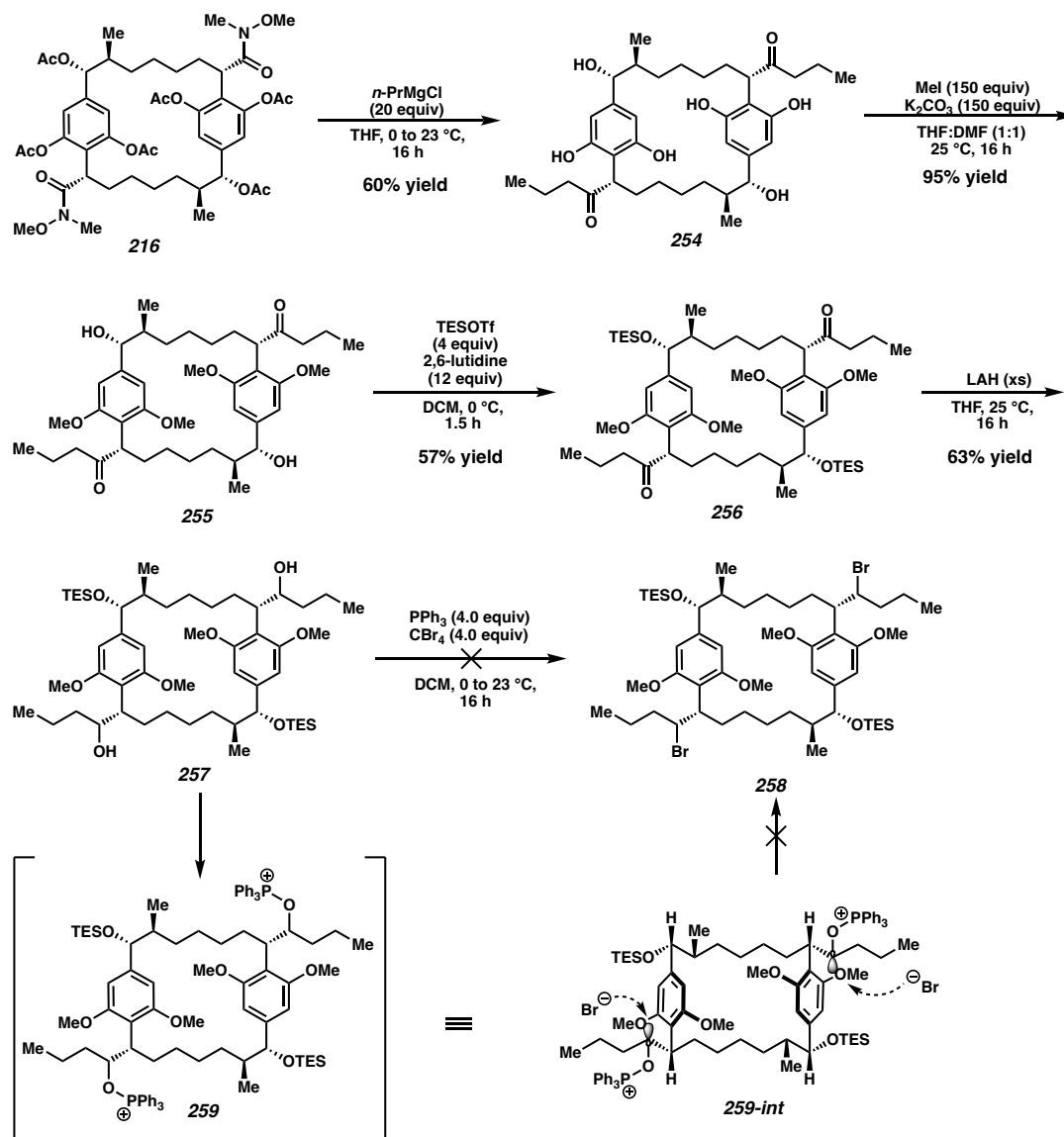
Treatment of the alkene:alkane mixture with Raney Ni led to complete convergence to the desired alkane product **245**. This model substrate could then be demethylated with BBr<sub>3</sub> to deliver the resorcinol **249** in a 42% yield (Scheme A6.4.2).

#### A6.5 FAILED ATTEMPT TO CARRY KEY MACROCYCLIC INTERMEDIATE 216 TO (-)-CYLINDROCYCLOPHANE A USING APPEL STRATEGY

Satisfied with the route established in the model system, we focused our efforts toward completing the total synthesis of (-)-cylindrocyclophane A (**175**) (Scheme A6.5.1). Treatment of the bis-Weinreb amide intermediate **216** with *n*-PrMgCl (20 equiv) resulted in the isolation of the desired hexahydroxyl product **254** in a 60% yield. Methylation of the phenols with Me-I and K<sub>2</sub>CO<sub>3</sub> led to the formation of the desired tetramethylated product **255** in 87% yield with no evidence of undesired benzylic alcohol methylation. At this stage, we protected with benzylic alcohols with TESOTf and 2,6-lutidine to deliver the bis silyl ether **256** in 57% yield. Reduction of the ketones in macrocycle **256** with LAH led to the corresponding diol **257** in a 63% yield as a complex mixture of inconsequential diastereomers. Devastatingly, multiple attempts at the Appel reaction on the macrocycle led to no product formation or any recovery of any discernable macrocyclic products. We propose that the C-O σ\* orbital in macrocycle **259** is shielded by the proximal 2,6-bismethoxy substitution, and the macrocycle **259** is locked in a conformation in which the bromide cannot perform the S<sub>N</sub>2 displacement reaction. Thus, the activated oxyphosphonium intermediate **259** is never displaced by the bromide ion during the reaction and decomposes when subjected to column chromatography.



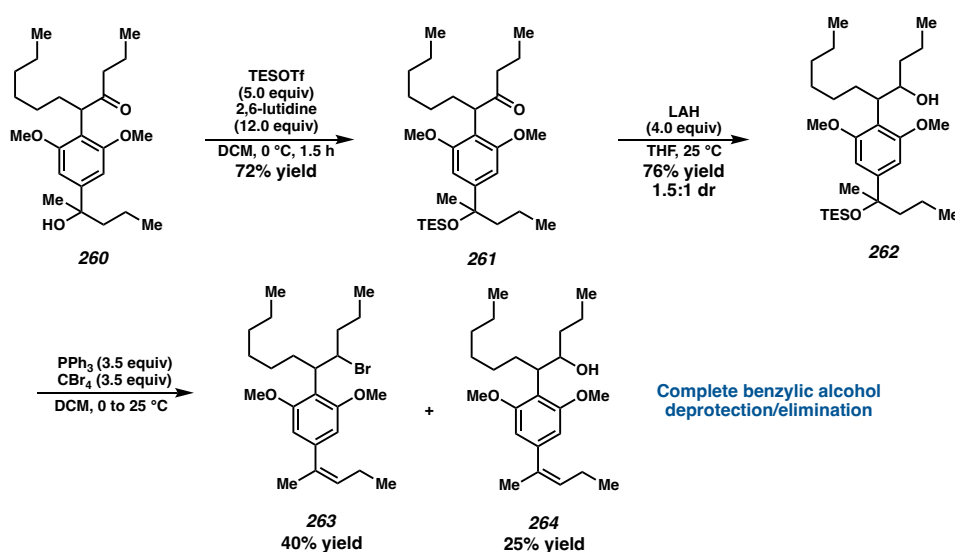
**Scheme A6.5.1** Failed Appel reaction of diol **257** synthesized from key macrocyclic  
intermediate **216**



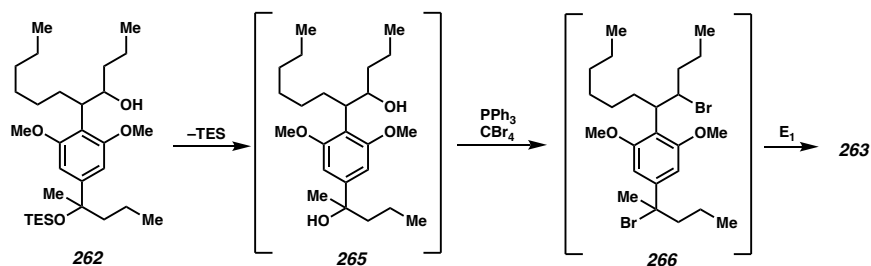
To further support this hypothesis, we subjected the model compound **260** possessing a benzylic tertiary alcohol to the developed deoxygenation sequence (Scheme A6.5.2). To our surprise, subjecting the alcohol **262** to the Appel reaction conditions resulted in the formation of styrene **263** in a 40% yield, with the major side product being

the incomplete Appel reaction product **264**. We believe the styrene formation occurs due to an unexpected TES deprotection of silyl ether **263** to the corresponding diol **265**, which can undergo two Appel reactions to yield dibromide **266**. The tertiary benzylic bromide in **266** then spontaneously undergoes an E<sub>1</sub> elimination to yield the styrene **263**.

**Scheme A6.5.2** Detrimental benzylic silyl ether elimination of **262** promoted via Appel reaction conditions



via

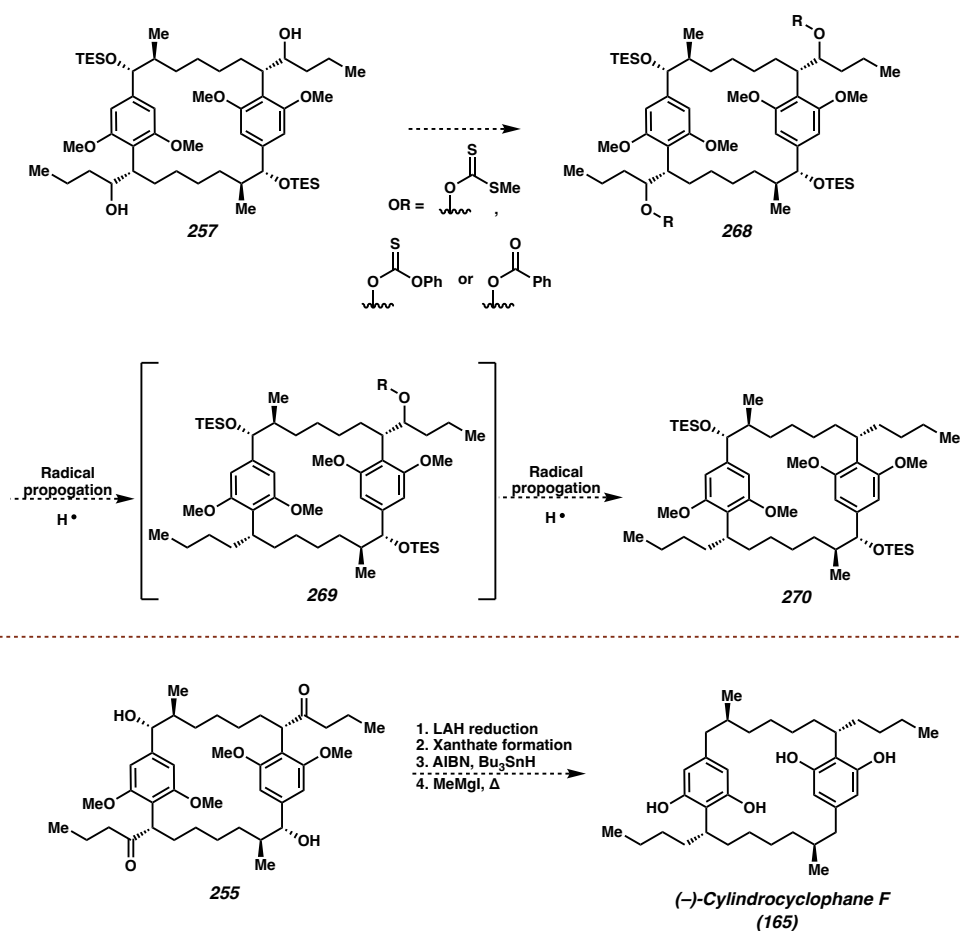


Notably, reducing ketone **261** with LAH and subjecting the corresponding diol **265** to the reaction conditions results in the formation of alkyl bromide **264** in 75% yield (Scheme A6.5.3). This alkyl bromide **264** can be exhaustively reduced to the corresponding alkane **267** using Raney Ni; however, the formal elimination of the benzylic silyl ether **262**



substitution. Furthermore, this alcohol deoxygenation strategy could be used to elaborate macrocycle tetramethyl ether **255** to (-)-cylindrocyclophane F (**165**) in four steps.

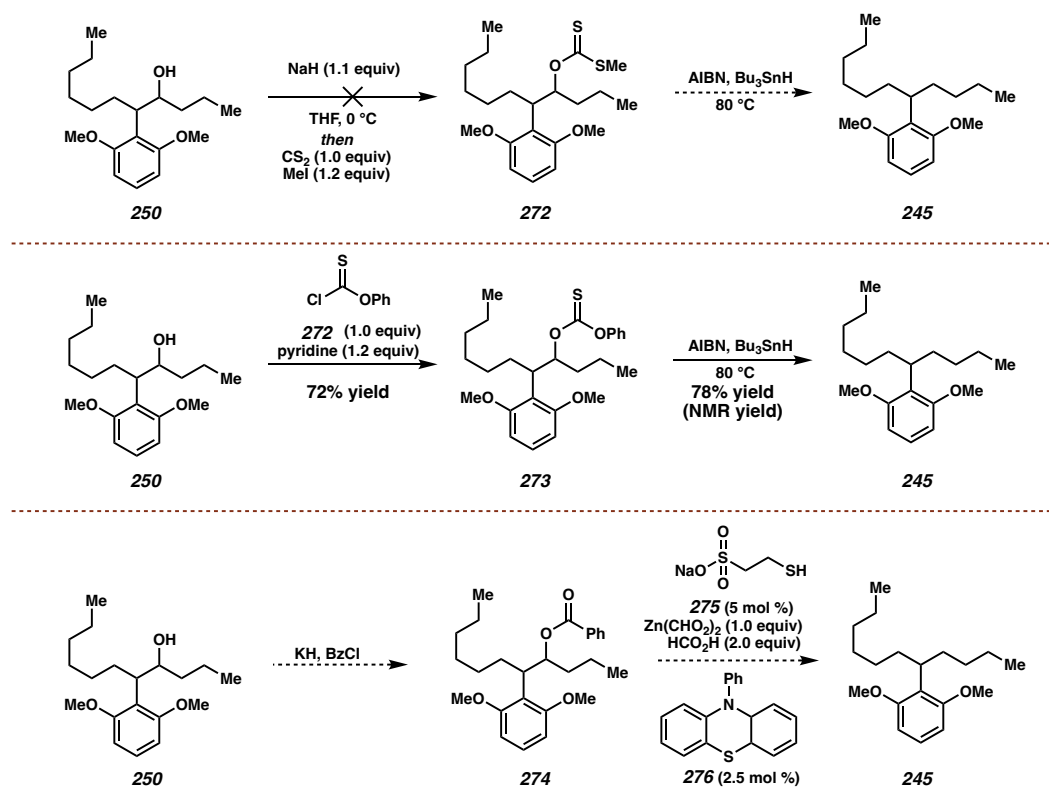
**Scheme A6.6.1** Proposed radical deoxygenation sequence to deliver alkane **270** or (-)-cylindrocyclophane F (**165**) from synthesized macrocyclic intermediates



Formation of the xanthate ester by deprotonating alcohol **250** with NaH followed by addition of CS<sub>2</sub> and MeI was not successful in our hands (Scheme A6.6.2). Subjecting the model alcohol to *O*-phenyl chlorothionoformate **271** with pyridine yielded *O*-phenyl thiocarbonate **272**, which has been shown to be an active substrate in a Barton-McCombie type radical deoxygenation.<sup>37</sup> Treatment of thiocarbonate **272** with AIBN and Bu<sub>3</sub>SnH delivered the desired alkane in 78% yield along with inseparable butyl tin byproducts.

Additionally, a recent report by Wickens and coworkers disclosed a benzoyl ester photoredox deoxygenation sequence that we wish to explore to provide an alternative, ambient temperature radical deoxygenation protocol that does not generate stoichiometric tin byproducts.<sup>38</sup> Due to limited access to the key Weinreb amide macrocycle **216**, we were inspired to thoroughly model the endgame strategy and determine a handful of viable deoxygenation conditions prior to moving back toward finishing the total synthesis.

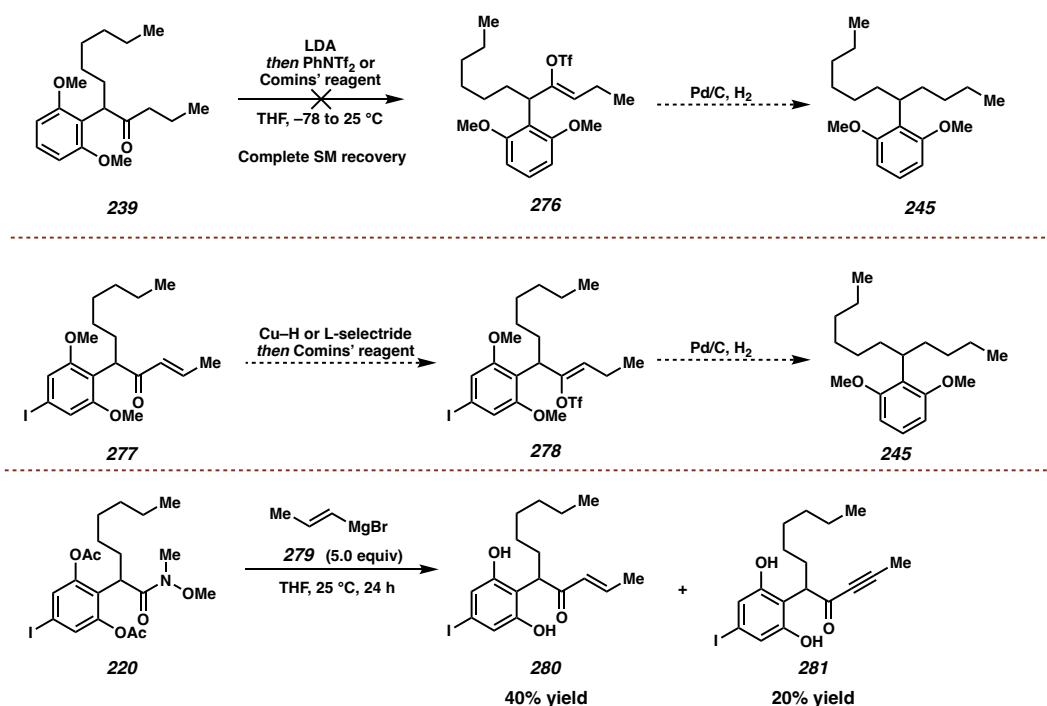
**Scheme A6.6.2** Barton-McCombie type deoxygenation of model alcohol **250** to alkane **245**



In addition to the Barton-McCombie type radical deoxygenation, we wished to investigate the validity of enol triflate formation from the ketone, followed by a metal catalyzed, two-step protodetriflation/olefin hydrogenation to deliver the corresponding

alkane product **245** (Scheme A6.6.3).<sup>39</sup> Direct deprotonation of ketone **239** with LDA followed by triflation with Comins' reagent or PhNTf<sub>2</sub> did not deliver the desired enol triflate product **276**. We hypothesize that the 2,6-bismethoxy substitution prevented the enol formation of ketone **239** with the bulky LDA base. However, using smaller bases such as KH could potentially deprotonate the benzylic proton  $\alpha$ - to the ketone in **239**, which would ablate the stereocenter present in the natural product system.

**Scheme A6.6.3** Proposed strategy to synthesize alkane **245** through an exhaustive reduction of enol triflate **276** or **278**



To overcome the regioselectivity issue of enol formation, we proposed that a conjugate reduction of enone **277** with L-selectride<sup>40</sup> or a bulky Cu-H reducing agent<sup>41</sup> would deliver the desired disubstituted enolate, which could then be trapped with Comins' reagent to yield our proposed enol triflate intermediate **278**.<sup>42</sup> Generation of the desired propenyl Grignard reagent **279** and addition into the model Weinreb amide **220** led to a

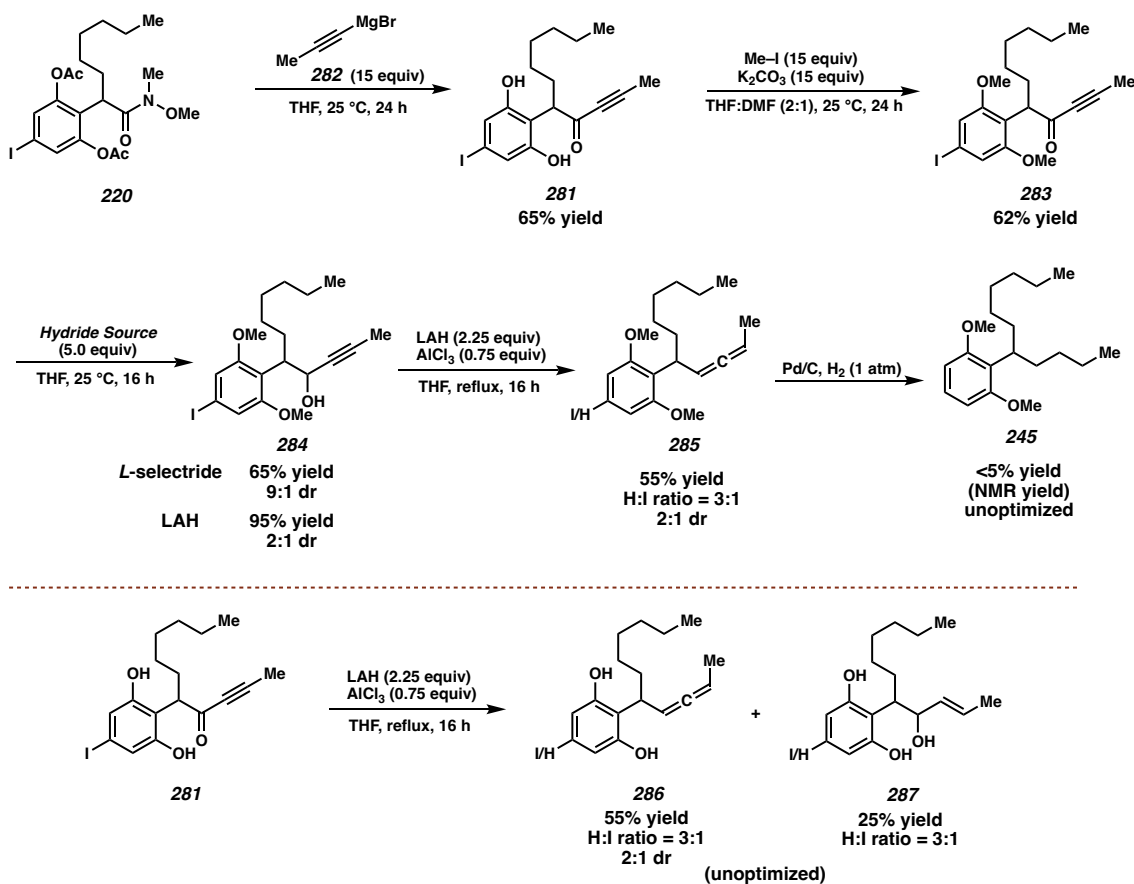
40% yield of the desired enone **280** as well as an unexpected 20% yield of ynone product **281**. This most likely occurred due to formation of 1-propynyl-Grignard during the magnesium-halogen exchange reaction of 1-bromo-propene to generate 1-propenyl-Grignard **279**. Interestingly, the  $sp^2$  or  $sp$  Grignard reagents did not show extensive transmetallation onto the aryl iodide as observed using the  $sp^3$  *n*-propyl-Grignard reagent. However, the mixture of enone **280** and ynone **281** products caused us to reevaluate our approach (Scheme A6.6.3).

To circumvent this undesired mixture, we chose to investigate the addition of propynyl magnesium bromide **282** into the model Weinreb amide **220** (Scheme A6.6.4). The corresponding ynone **281**. From the ynone, we propose that 1,2-reduction of the ynone to the propargylic alcohol followed by an  $AlH_3$  promoted reductive deoxygenation would yield the corresponding allene,<sup>43</sup> which could be hydrogenated to deliver the desired alkane side chain.<sup>44</sup> Treatment of the model Weinreb amide **220** with excess 1-propynyl-MgBr **282** delivered the desired ynone product **281** in a 65% yield. Bismethylation of the resorcinol **281** led to the bismethyl aryl ether **283** in 65% yield, which was poised to undergo the reductive deoxygenation strategy.

To our surprise, *L*-selectride led to predominant 1,2-addition of the ynone to deliver the propargylic alcohol **284** in 62% yield and a 9:1 dr of inconsequential diastereomers. Treatment of the ynone with LAH led to a 2:1 mixture of diastereomers of the corresponding propargylic alcohol **284** in 95% yield. Subjecting the mixture of diastereomers with  $AlH_3$  delivered the desired allene **285** as an inconsequential mixture of allene diastereomers. However, the  $AlH_3$  reduction also resulted in protodeiodination which led to a complicated mixture of allene diastereomers and proto:iodo isomers. In our

hands, reduction of allene **285** with Pd/C and H<sub>2</sub> led to trace yield of product and potential olefin isomerization. The poor reactivity of Pd/C could be attributed to the H-I generated from Pd-mediated oxidative addition of the aryl iodide, which could poison the catalyst or cause undesired side reactions. Thus, we wished to explore conditions to reduce the allene to the corresponding alkane with a model substrate without any aryl iodide substitution to omit any possible Pd-mediated oxidative insertion.

**Scheme A6.6.4** Synthesis of alkane **245** through an AlH<sub>3</sub> promoted propargylic alcohol deoxygenation/allene reduction sequence



However, to maximize the knowledge gained from this established model system, we wanted to investigate the transformation of the model ynone **281** to the corresponding allene without the need for methyl protection of the resorcinol. Gratifyingly, treatment of



the ynone **281** with  $\text{AlH}_3$  directly led to good conversion to the corresponding allene **286**.

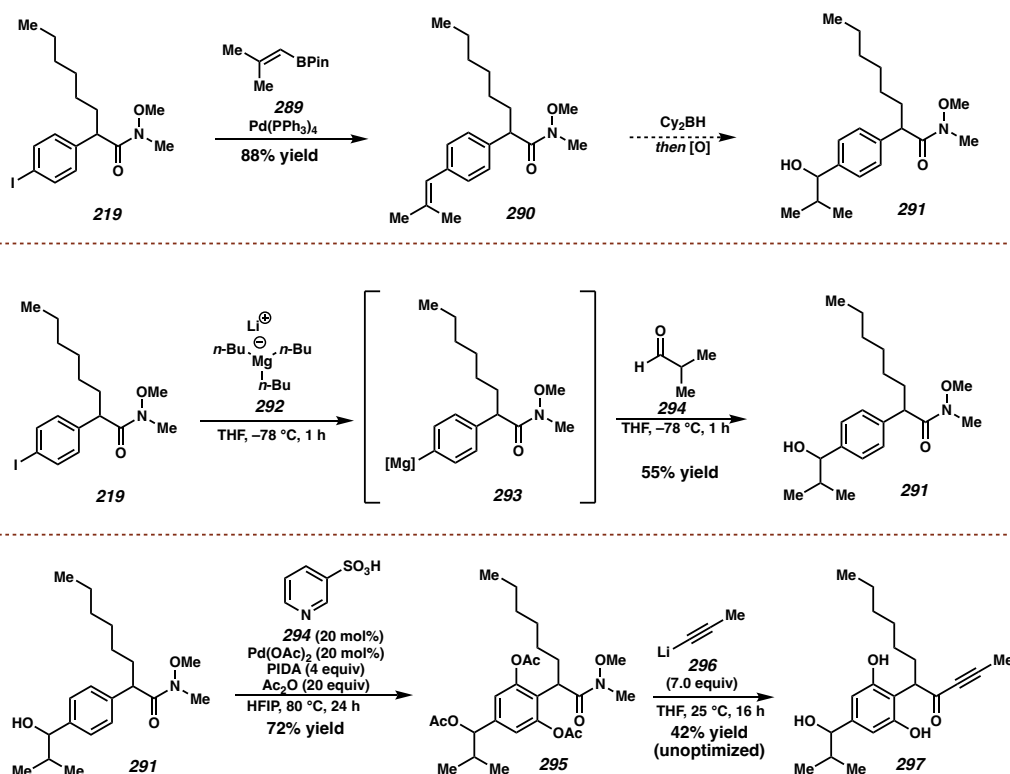
However, we obtained a 25% yield of the allylic alcohol **287** resulting from 1,4-reduction of the propargylic alcohol with no aluminum mediate deoxygenation. We are currently investigating a more efficient, direct reduction of ynone **281** to allene **286** without the protection of the proximal 2,6-hydroxyls.

#### A6.7 SECOND GENERATION MODEL DESIGN: EVALUATION OF FUNCTIONAL GROUP TOLERANCE OF 2°-BENZYLIC ALCOHOL

Due to the unexpected benzylic alcohol silyl deprotection/elimination observed during the Appel reaction, we wish to exhaustively validate the tolerance of a secondary benzylic alcohol throughout our two developing model deoxygenation approaches. To achieve this, we subjected aryl iodide **219** under Pd-catalyzed Suzuki cross coupling conditions with isopropenyl-Bpin **289** to afford trisubstituted styrene **290** in 88% yield (Scheme A6.7.1). With the trisubstituted styrene **290** in hand, we could perform the hydroboration strategy developed by Hoyer and coworkers to deliver the corresponding benzylic alcohol **291**. However, we discovered a more efficient route through the treatment of aryl iodide with *n*- $\text{Bu}_3\text{MgLi}$  magnesate complex **292** to promote the magnesium-iodide exchange reaction. The newly formed aryl Grignard reagent **293** is unable to react with the Weinreb amide at  $-78\text{ }^\circ\text{C}$ , thus addition of aldehyde **294** to the Grignard **293** at  $-78\text{ }^\circ\text{C}$  delivered the desired benzylic alcohol **291** in a 55% yield. The moderate yield is due to incomplete magnesium-iodide exchange of the starting aryl iodide **219**; however, the conversion was acceptable to move forward with the model studies. To our delight, performing the C–H acetoxylation reaction with commercially available pyridine ligand **294** led to the isolation of the triacetate model Weinreb amide **295** in 72% yield. Treatment

of the triacetate **295** with 1-propynyl-MgBr led to very poor conversion to the desired ynone **297**. However, using alkynyl lithium **296** converted the model triacetate **295** to the desired ynone **297** in a 42% yield under unoptimized reaction conditions.

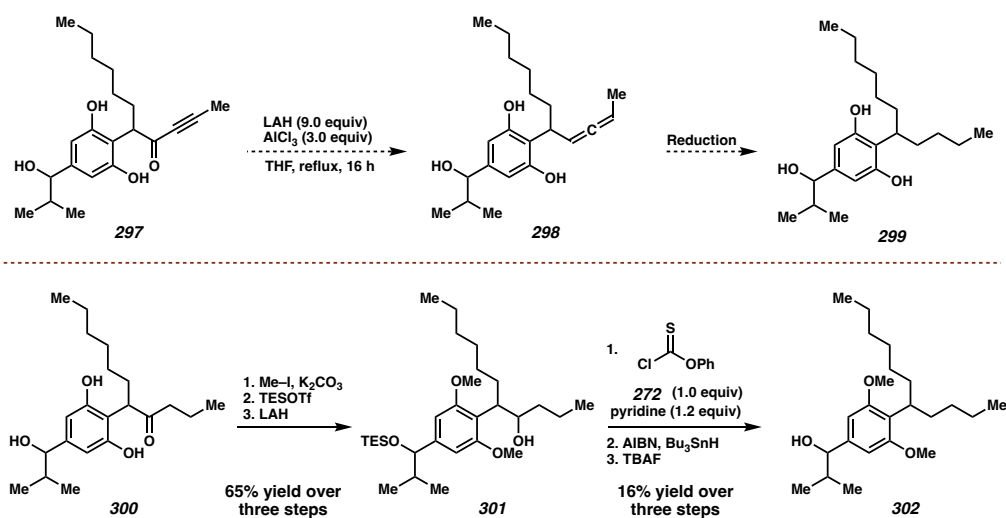
**Scheme A6.7.1** Proposed model substrate for endgame deoxygenation



With model triacetate **295**, we can thoroughly investigate the two promising deoxygenation routes to probe the tolerance of the secondary benzylic alcohol. The ynone **297** will be treated with excess  $\text{AlH}_3$  under reflux in THF to promote the deoxygenative allylic reduction to deliver allene **298**. If necessary, methyl protection of the resorcinol motif can be performed to investigate the allene reduction pathway. Additionally, treatment of Weinreb amide **295** with  $n\text{-PrLi}$  or  $n\text{-PrMgCl}$  could deliver model ketone **300**, which we will subject to the Barton-McCombie type radical deoxygenation to rule out benzylic alcohol elimination observed during the Appel-mediated alcohol deoxygenation pathway.

To our delight, we have shown that we can perform our model deoxygenation sequence to elaborate model ketone **300** to the desired alkane **302** with retention of the benzylic alcohol. The establishment of deoxygenation conditions in this model will then be used to elaborate the key macrocycle **216** to (-)-cylindrocyclophane A (**175**).

**Scheme A6.7.2** Modeling the endgame deoxygenation from both allene reduction and Barton-McCombie type deoxygenation



## A6.8 CONCLUSION

In conclusion a novel synthesis to (-)-cylindrocyclophane A was developed using C–H functionalization logic. Completion of this work would represent a major milestone in total synthesis, encompassing 6 C–H functionalization steps and primarily constructing the carbon skeleton through these steps. The proposed synthetic approach described herein is versatile and can access a wide variety of [7.7]paracyclophane derivatives and their analogs, previously inaccessible with traditional synthetic methods. In the future, the

modular route disclosed here will allow for SAR and MOA analysis to probe the promising biological activity and determine if this class of compounds warrants further development as potential drug candidates. At the beginning of the project, a model study of the [7.7]paracyclophane core was completed where the model [7.7]paracyclophane was formed in >99% enantiopurity with an overall yield of 46% from the starting aryldiazoacetate. Notably, this macrocyclization is the first example of an enantioselective macrocyclization by means of functionalization of an unactivated C(sp<sup>3</sup>)-H bond, pushing the boundaries of not only the C-H functionalization field, but representing a novel entry to macrocyclic rings. With the proof of principle validated we conducted several additional model studies to determine the best route to the natural product, resulting in the work discussed here. With the optimal route unraveled, 14 out of the 15 total steps have been achieved, including the four-fold acetoxylation, indicating successful use of all the desired C-H functionalization steps. We anticipate that this project will serve as a pinnacle for what C-H functionalization can achieve in total synthesis, acting as a model for future total syntheses utilizing C-H functionalization logic.

## **A6.9            EXPERIMENTAL**

### **A6.9.1        MATERIALS AND METHODS**

Reactions were carried out under nitrogen in flame-dried unless otherwise specified. Dichloromethane, diethyl ether, tetrahydrofuran, and toluene were purified using a *Glass Contour Solvent System*. Dichloromethane used for C-H functionalization reactions was distilled under nitrogen from calcium hydride onto 4Å molecular sieves and stored under nitrogen for 24 h prior to use. Flash column chromatography was performed

on Silicycle SiliaFlash P60 silica gel (60 Å pore size, 40–63 µm particle size, 230–400 mesh) and ACS reagent grade solvents. Reactions were monitored by thin layer chromatography (TLC) carried out on with aluminum-sheet or glass-backed silica gel plates, visualizing with UV light, and staining with aqueous KMnO<sub>4</sub>.

All <sup>1</sup>H NMR spectra were recorded at either 400 MHz, 500 MHz, or 600 MHz on Varian-400, Varian-500, or Bruker-600 spectrometers. <sup>13</sup>C NMR spectra were recorded at either 101 MHz, 126 MHz, or 151 MHz on Varian-400, Varian-500, or Bruker-600 spectrometers. <sup>19</sup>F NMR spectra were recorded at 282, 376 or 565 MHz on Varian-300, Varian-400 or Bruker-600 spectrometer. NMR spectra were obtained from solutions of CDCl<sub>3</sub> 0.03% TMS, C<sub>6</sub>D<sub>6</sub>, MeOD, and AcOD-d<sub>4</sub> with residual solvent serving as internal standard (7.26 ppm for <sup>1</sup>H or 0.00ppm and 77.16 ppm for <sup>13</sup>C in CDCl<sub>3</sub>, 7.16 ppm for <sup>1</sup>H and 128.06 for <sup>13</sup>C in C<sub>6</sub>D<sub>6</sub>, 3.31 ppm for <sup>1</sup>H and 49.00 for <sup>13</sup>C in MeOD, and 2.04 ppm for <sup>1</sup>H and 20.0 for <sup>13</sup>C in AcOD-d<sub>4</sub>). NMR shifts were reported in parts per million (δ ppm). Abbreviations for signal multiplicity are as follow: s = singlet, d = doublet, t = triplet, q = quartet, m = multiplet, brs = broad singlet, dd = doublet of doublet, etc. Coupling constants (J values) were calculated directly from the spectra.

All reagents were purchased from commercial sources (Sigma Aldrich, Thermo Fisher, TCI Chemicals, AK Scientific, Oakwood Chemical, Acros Organics, Combi-Blocks, Strem, Enamine, and Santa Cruz Biotechnology) and used as received without purification. IR spectra were collected on a Nicolet iS10 FT-IR spectrometer (cm<sup>-1</sup>). Optical rotations were measured on Jasco P-2000 polarimeters. Mass spectra were taken on a Thermo Finnigan LTQ-FTMS spectrometer with APCI, ESI or NSI by the Department of Chemistry at Emory University. Racemic standards were generated by performing

reactions with the appropriate racemic dirhodium catalyst for the reaction by dissolving an equimolar mixture of the R and S catalyst in a minimal amount of dichloromethane and concentrating under vacuum. The enantiomeric excess (ee) was determined by High performance liquid chromatography analysis was performed on either Varian Prostar chiral HPL instrument, Agilent 1100 Technologies HPLC instruments, or Agilent Technologies 1290 Infinity UHPLC instrument, and the data outlined below varies in presentation based on the software used for each system. Chiral HPLC conditions were determined by obtaining separation of the racemic products generated using a mixture of the appropriate catalysts. The HPLC instruments used isopropanol/hexane gradient and commercial ChiralPak/ChiralCel columns from Daicel Chemical Industries, notably ChiralPak AD-H (5  $\mu\text{m}$  particle size, 4.6 mm vs. 250 mm), ChiralCel OZ-H (5  $\mu\text{m}$  particle size, 4.6 mm vs. 250 mm), and ChiralCel OD-H (5  $\mu\text{m}$  particle size, 4.6 mm vs. 250 mm), ChiralCel AS-H (5  $\mu\text{m}$  particle size, 4.6 mm vs. 250 mm), and ChiralCel OJ-H (5  $\mu\text{m}$  particle size, 4.6 mm vs. 250 mm).

### Substrates and reagents

The following compounds were prepared according to published procedures:

2,2,2-trifluoroethyl 2-diazoacetate<sup>13d</sup>

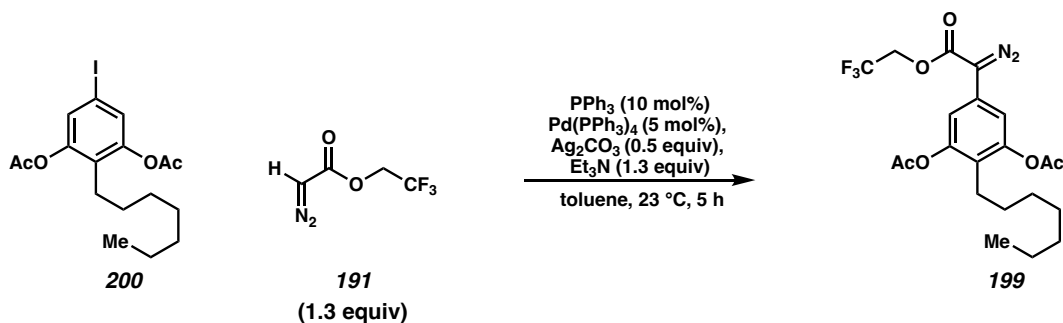
$\text{Rh}_2(\text{R-2-Cl-5-BrTPCP})_4$ <sup>13b</sup>

$\text{Rh}_2[\text{R-tris}(p\text{-}^t\text{BuC}_6\text{H}_4)\text{TPCP}]_4$ <sup>19</sup>

$\text{Rh}_2(\text{R-p-ph-TPCP})_4$ <sup>13c</sup>

5-(trifluoromethyl)-3-pyridinesulfonic acid<sup>14c</sup> (*synthesized by Hojoon Park*)

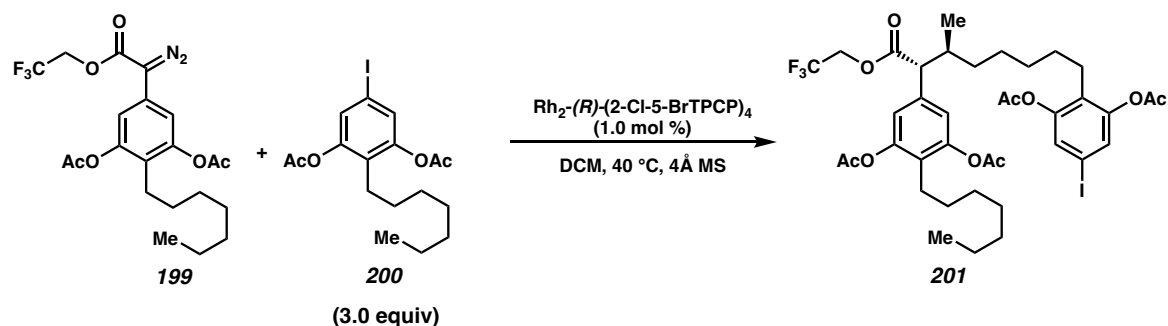
**A6.9.2 SYNTHETIC PROCEDURES**



**5-(1-diazo-2-oxo-2-(2,2,2-trifluoroethoxy)ethyl)-2-heptyl-1,3-phenylene diacetate**

**(199):** The procedure is adapted from the literature<sup>13d</sup>: A 10-ml round-bottom flask with stir bar was flame dried under vacuum. Once cool enough all solids were added first:  $\text{PPh}_3$  (6.3 mg, 23.9  $\mu\text{mol}$ , 0.1 equiv),  $\text{Pd}(\text{PPh}_3)_4$  (13.8 mg, 12.0  $\mu\text{mol}$ , 0.05 equiv) and  $\text{Ag}_2\text{CO}_3$  (33.0 mg, 0.12 mmol, 0.5 equiv). After solids added, the reaction vessel was purged with argon three times. Next the liquids were added: toluene (1.0 ml),  $\text{Et}_3\text{N}$  (0.04 m, 0.311 mmol, 1.3 equiv), 2-heptyl-5-iodo-1,3-phenylene diacetate **200** (100 mg, 0.239 mmol, 1 equiv), and finally the 2,2,2-trifluoroethyl 2-diazoacetate **191** (52.2 mg, 0.311 mmol, 1.3 equiv) was added last. The resulted mixture was stirred at 23 °C for 5 h and then, filtered through a short silica plug (3.5 cm diameter, 5 cm height), eluting with ethyl acetate until elutes clear. The crude product was concentrated and purified by column chromatography (10% ether in pentane) to afford the product **199** as a red oil (77 mg, 0.167 mmol, 70% yield);  $^1\text{H}$  NMR (600 MHz,  $\text{CDCl}_3$ )  $\delta$  7.08 (s, 2H), 4.63 (q,  $J = 8.3$  Hz, 2H), 2.40 (t,  $J = 7.78$  Hz, 2H), 2.32 (s, 6H), 1.46 – 1.41 (m, 2H), 1.32 – 1.23 (m, 8H), 0.88 (t,  $J = 7.23$  Hz, 3H);  $^{13}\text{C}$  NMR (151 MHz,  $\text{CDCl}_3$ )  $\delta$  168.9, 162.6, 150.3, 125.8, 123.5, 122.7 (q,  $J = 277.5$  Hz) 115.5, 60.3 (q,  $J = 37.0$  Hz), 31.6, 29.5, 28.9, 28.9, 24.6, 22.6, 20.8, 14.1; IR (Neat Film) 2827, 2858, 2099, 1766, 1624, 1577, 1416, 1369, 1283, 1160, 1108, 1041, 1020,

975, 893, 840  $\text{cm}^{-1}$ ; (MM:ESI<sup>+</sup>)  $m/z$  calcd for  $\text{C}_{21}\text{H}_{29}\text{F}_3\text{N}_3\text{O}_6$  ( $\text{M}+\text{NH}_4$ )<sup>+</sup> 476.2003 found  
476.2003



**2-((6*S*,7*R*)-7-(3,5-diacetoxy-4-heptylphenyl)-6-methyl-8-oxo-8-(2,2,2-**

**trifluoroethoxy)octyl)-5-iodo-1,3-phenylene diacetate (201):** A 10-ml flame-dried

round-bottom flask with condenser was charged with 4 Å MS and  $\text{Rh}_2(\text{R}-2\text{-Cl-5-BrTPCP})_4$

(3.92 mg, 2.05  $\mu\text{mol}$ , 1.0 mol %) and then, purged three times with argon. 2-heptyl-5-iodo-

1,3-phenylene diacetate **200** (257 mg, 0.614 mmol, 3.0 equiv) and distilled  $\text{CH}_2\text{Cl}_2$  (0.8

ml) were added next, then the mixture was heated to 40 °C and refluxed for at least 10 min

before addition of the diazo compounds. Next, 5-(1-diazo-2-oxo-2-(2,2,2-

trifluoroethoxy)ethyl)-2-heptyl-1,3-phenylene diacetate **199** (94 mg, 0.205 mmol, 1.0

equiv) was purged under argon in a 20-mL scintillation vial, then diluted with distilled

$\text{CH}_2\text{Cl}_2$  (0.8 ml). Then, under reflux conditions and argon atmosphere, the diazo solution

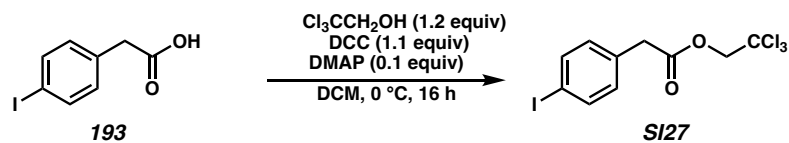
was added to the reaction vessel dropwise via syringe pump over 3 h. The reaction mixture

was stirred at 40 °C for another 30 min and concentrated under vacuum for crude  $^1\text{H}$  NMR.

The crude product was purified by flash column chromatography (5% ether in pentane) to

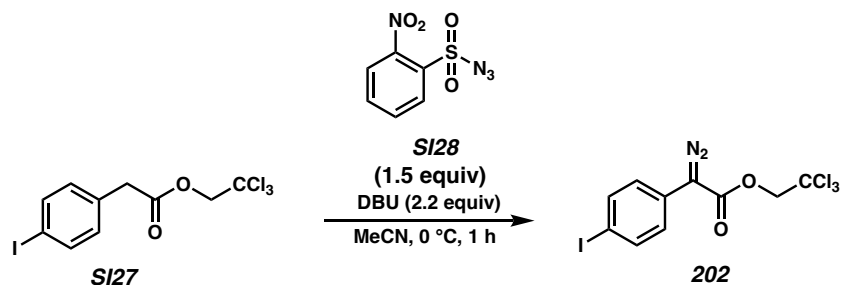


afford the product **201** as an opaque oil (87mg, 0.103 mmol, 51% yield, 1:1.5 dr); <sup>1</sup>H NMR (400 MHz, CDCl<sub>3</sub>) δ 7.29 (s, 2H), 6.93 (s, 2H), 4.61 (dq, *J* = 12.7, 8.5 Hz, 1H), 4.28 (dq, *J* = 12.7, 8.4 Hz, 1H), 3.32 (d, *J* = 10.1 Hz, 1H), 2.38 (dd, *J* = 9.1, 6.7 Hz, 2H), 2.30 (s, 6H), 2.28 (s, 6H), 2.15 – 2.07 (m, 1H), 1.48 – 1.38 (m, 3H), 1.36 – 1.17 (m, 16H), 1.17 – 1.09 (m, 1H), 0.97 (d, *J* = 6.5 Hz, 3H), 0.88 (t, *J* = 7.0 Hz, 3H); <sup>13</sup>C NMR (151 MHz, CDCl<sub>3</sub>) δ 171.6, 168.8, 168.7, 149.9, 149.6, 135.5, 129.2, 127.8, 127.0, 122.8 (q, *J* = 277.3 Hz), 120.3, 88.4, 60.3 (q, *J* = 36.6 Hz), 57.2, 36.7, 33.2, 31.6, 29.6, 29.5, 28.9, 28.8 (d, *J* = 2.2 Hz), 26.0, 24.7 (d, *J* = 7.1 Hz), 22.6, 20.8, 20.7, 17.3, 14.0; <sup>19</sup>F NMR (376 MHz, CDCl<sub>3</sub>) δ -73.6 (dt, *J* = 12.9, 8.4 Hz); IR (Neat Film) 2928, 2858, 1768, 1595, 1572, 1464, 1431, 1402, 1369, 1278, 1190, 1131, 1109, 1041, 1021, 979, 909 cm<sup>-1</sup>; (MM:ESI<sup>+</sup>) *m/z* calcd for C<sub>38</sub>H<sub>49</sub>F<sub>31</sub>O<sub>10</sub> (M+H)<sup>+</sup> 849.2324 found 849.2342; [α]<sup>20</sup><sub>D</sub>: +1.9° (c = 0.8, CHCl<sub>3</sub>)

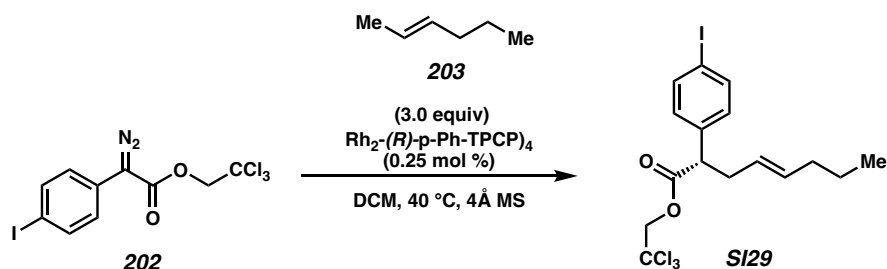


**2,2,2-trichloroethyl 2-(4-iodophenyl)acetate (SI27):** To a 250-ml round bottom flask purged with argon was added the 2-(4-iodophenyl)acetic acid **193** (10.0 g, 38.2 mmol, 1 equiv), DMAP (467 mg, 3.8 mmol, 0.1 equiv), trichloroethanol (4.4 ml, 45.8 mmol, 1.2 equiv) and 84 ml of DCM. Then the reaction mixture was cooled to 0 °C via ice bath. At 0 °C, DCC (8.67 g, 42 mmol, 1.1 equiv) was dissolved in 42 ml of DCM and added slowly to the reaction over a few minutes. The reaction mixture was then stirred overnight. Then the reaction was filtered over celite, washing the solid with ether. The filtrate was concentrated and purified by flash column chromatography (hexane/ethyl acetate = 9/1) to provide a white solid (14.9, 38.1 mmol, >99% yield). The physical and spectral data were

identical to those previously reported for this compound;<sup>18</sup> <sup>1</sup>H NMR (400 MHz, CDCl<sub>3</sub>) δ 7.69 – 7.65 (m, 2H), 7.10 – 7.05 (m, 2H), 4.75 (s, 2H), 3.71 (s, 2H).

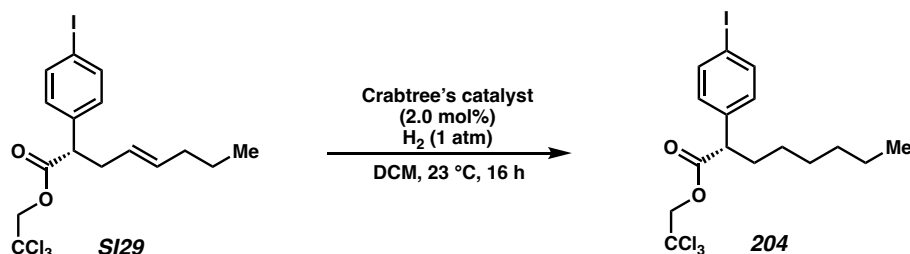


**2,2,2-trichloroethyl 2-diazo-2-(4-iodophenyl)acetate (202):** To a flame-dried 100-ml round-bottom flask purged under argon was added 2,2,2-trichloroethyl 2-(4-iodophenyl)acetate **SI27** (5.0 g, 12.7 mmol, 1.0 equiv), 43 ml of acetonitrile and *o*-NBSA **SI28** (4.35 g, 19.1 mmol, 1.5 equiv). Then the reaction was cooled to 0 °C via ice bath and DBU (4.21 ml, 28 mmol, 2.2 equiv) was added dropwise at 0 °C. The reaction was stirred for 1 hr at 0 °C. Then the mixture was quenched with sat. NH<sub>4</sub>Cl. The layers were separated and then extracted with ether (x3). The organic layer was washed with sat. brine, dried with MgSO<sub>4</sub> and concentrated under reduced pressure. The crude residue was purified by flash column chromatography (hexane/diethyl ether = 9/1) to provide an orange solid **202** (93% yield). The physical and spectral data were identical to those previously reported for this compound;<sup>18</sup> <sup>1</sup>H NMR (600 MHz, CDCl<sub>3</sub>) δ 7.73 – 7.70 (m, 2H), 7.28 – 7.23 (m, 2H), 4.91 (s, 2H).

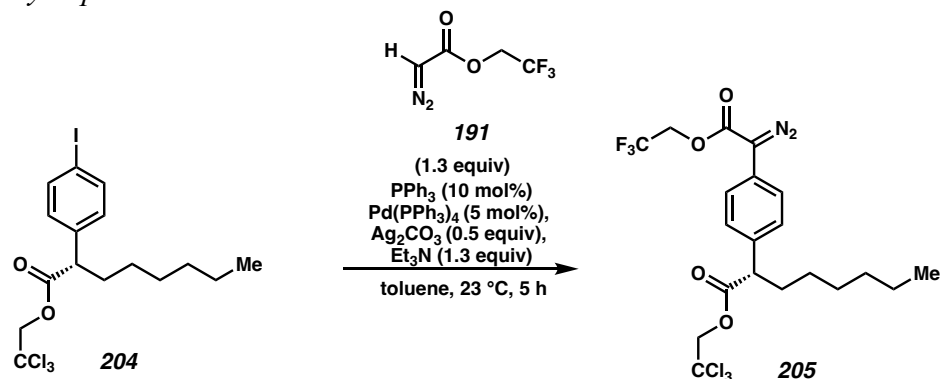


**2,2,2-trichloroethyl (S,E)-2-(4-iodophenyl)oct-4-enoate (SI29):** A 250-ml flame-dried round-bottom flask with condenser was charged with 4 Å MS and  $\text{Rh}_2(\text{R-p-ph-TPCP})_4$  (52 mg, 0.03 mmol, 0.25 mol%) and then, purged three times with nitrogen. *Trans*-2-hexene **203** (4.5 ml, 35.8 mmol, 3.0 equiv) and distilled  $\text{CH}_2\text{Cl}_2$  (48 ml) were added next, then the mixture was heated to 40 °C and refluxed for at least 10 min before addition of the diazo compounds. Next, 2,2,2-trichloroethyl 2-diazo-2-(4-iodophenyl)acetate **202** (5.0 g, 11.9 mmol, 1.0 equiv) was purged under nitrogen in a 100-mL round-bottom flask, then diluted with distilled  $\text{CH}_2\text{Cl}_2$  (48 ml). Then, under reflux conditions and nitrogen atmosphere, the diazo solution was added to the reaction vessel dropwise via syringe pump, or addition funnel with larger scales, over 3 h. The reaction mixture was stirred at 40 °C for another 30 min and concentrated under vacuum for crude  $^1\text{H}$  NMR. The crude product was purified by flash column chromatography (3% ether in petroleum ether) to afford the product as an opaque oil **SI29** (96% yield, >20:1 rr, 96% ee). This compound is disclosed in a publication;<sup>4c</sup>  $^1\text{H}$  NMR (600 MHz,  $\text{CDCl}_3$ )  $\delta$  7.65 (d,  $J = 8.3$  Hz, 2H), 7.10 (d,  $J = 8.3$  Hz, 2H), 5.50 (ddd,  $J = 15.1, 7.5, 6.0$  Hz, 1H), 5.31 (ddd,  $J = 15.3, 7.7, 6.1$  Hz, 1H), 4.73 (d,  $J = 12.0$  Hz, 1H), 4.67 (d,  $J = 12$  Hz, 1H), 3.69 (dd,  $J = 8.4, 7.0$  Hz, 1H), 2.80 (dt,  $J = 15.0, 7.8$  Hz, 1H), 2.50 (dt,  $J = 13.7, 7.0$  Hz, 1H), 1.91 (q,  $J = 7.2$  Hz, 2H), 1.31 (h,  $J = 7.3$  Hz, 2H), 0.83 (t,  $J = 7.4$  Hz, 3H);  $^{13}\text{C}$  NMR (151 MHz,  $\text{CDCl}_3$ )  $\delta$  171.4, 137.7, 137.3, 134.0, 130.1, 125.6, 94.7, 93.1, 74.1, 51.5, 36.1, 34.5, 30.3, 29.6, 22.4, 13.5; IR (Neat Film) 2955, 2923, 2854, 2257, 1751, 1586, 1484, 1436, 1403, 1372, 1336, 1258, 1204, 1138, 1062, 1006, 968, 819, 801, 751, 718, 517, 498, 438  $\text{cm}^{-1}$ ; (MM:ESI<sup>+</sup>)  $m/z$  calcd for  $\text{C}_{16}\text{H}_{19}\text{Cl}_3\text{IO}_2$  (M+H)<sup>+</sup> 474.9495 found 474.9489;  $[\alpha]_D^{20}$ : +23.5° (c = 0.67,  $\text{CHCl}_3$ ); HPLC (ADH, 0.5 %

*i*-propanol in hexane, 1 mL min<sup>-1</sup>, 1 mg mL<sup>-1</sup>, 30 min, UV 210 nm) retention times of 6.4 min (major) and 7.2 min (minor) 96% *e.e.* with Rh<sub>2</sub>(*R*-p-PhTPCP)<sub>4</sub>.



**2,2,2-trichloroethyl (S)-2-(4-iodophenyl)octanoate (204):** To a 500-ml round-bottom flask flame-dried and purged under nitrogen was added 2,2,2-trichloroethyl (*S,E*)-2-(4-iodophenyl)oct-4-enoate **SI29** (5.37 g, 11.3 mmol, 1.0 equiv), crabtree's catalyst (90.9 mg, 113 μmol, 1.0 mol %) then DCM (113 mL). Then the atmosphere was exchanged with hydrogen and the reaction was run for 2 h. After 2 h crabtree's catalyst (90.9 mg, 113 μmol, 1.0 mol %) was added again and the atmosphere was exchanged with hydrogen then let stir overnight. The reaction mixture was then concentrated under vacuum and purified by flash column chromatography (10% ether in hexane) to afford the product **204** as an opaque oil. (>99% yield). <sup>1</sup>H NMR (600 MHz, CDCl<sub>3</sub>) δ 7.65 (d, *J* = 8.2 Hz, 2H), 7.10 (d, *J* = 8.2 Hz, 2H), 4.74 (d, *J* = 12 Hz, 1H), 4.67 (d, *J* = 12.0 Hz, 1H), 3.62 (t, *J* = 7.7 Hz, 1H), 2.11 (dtt, *J* = 12.8, 8.3, 4.8 Hz, 1H), 1.81 (dtt, *J* = 12.8, 8.3, 4.8 Hz, 1H), 1.27 (dtt, *J* = 31.4, 14.0, 11.5, 5.0 Hz, 8H), 0.86 (t, *J* = 6.9 Hz, 3H); <sup>13</sup>C NMR (151 MHz, CDCl<sub>3</sub>) δ 171.9, 137.8, 137.7, 130.1, 94.8, 93.0, 74.0, 51.1, 33.0, 31.5, 28.9, 27.3, 22.5, 14.0; IR (neat) 2953, 2926, 2856, 1751, 1484, 1465, 1403, 1372, 1263, 1200, 1140, 1062, 1007, 821, 793, 758, 719, 572, 500 cm<sup>-1</sup>; (MM:ESI<sup>+</sup>) *m/z* calcd for C<sub>16</sub>H<sub>21</sub>Cl<sub>3</sub>IO<sub>2</sub> (M+H)<sup>+</sup> 476.9652 found 476.9646. [α]<sub>D</sub><sup>20</sup>: +12.8° (c = 1.0, CHCl<sub>3</sub>)

**2,2,2-trichloroethyl****(S)-2-(4-(1-diazo-2-oxo-2-(2,2,2-**

**trifluoroethoxy)ethyl)phenyl)octanoate (205):** The procedure is adapted from the

literature<sup>13b</sup>: A 250-ml round-bottom flask with stir bar was flame dried under vacuum.

Once cool enough all solids were added first: PPh<sub>3</sub> (297 mg, 1.13 mmol, 0.1 equiv),

Pd(PPh<sub>3</sub>)<sub>4</sub> (653 mg, 0.565 mmol, 0.05 equiv) and Ag<sub>2</sub>CO<sub>3</sub> (1.56 g, 5.65 mmol, 0.5 equiv).

After solids added, the reaction vessel was purged with nitrogen three times. Next the

liquids were added: toluene (45 ml), Et<sub>3</sub>N (2.05 ml, 14.7 mmol, 1.3 equiv), 2,2,2-

trichloroethyl (S)-2-(4-iodophenyl)octanoate **204** (5.40 g, 11.3 mmol, 1.0 equiv), and

finally the 2,2,2-trifluoroethyl 2-diazoacetate **191** (2.47 g, 14.7 mmol, 1.3 equiv) was added

last. The resulted mixture was stirred at room temperature (23 °C) for 5 h and then, filtered

through a short silica plug (3.5 cm *diameter*, 5 cm *height*), eluting with ethyl acetate until

elutes clear. The crude product was concentrated and purified by flash column

chromatography (3% ether in hexane) to afford the product **205** as a red oil (88% yield).

<sup>1</sup>H NMR (600 MHz, CDCl<sub>3</sub>) δ 7.45 – 7.37 (m, 4H), 4.75 – 4.67 (m, 2H), 4.65 (q, *J* = 8.3

Hz, 2H), 3.68 (t, *J* = 7.7 Hz, 1H), 2.14 (dt, *J* = 13.3, 8.5 Hz, 1H), 1.82 (dt, *J* = 13.3, 8.5 Hz,

1H), 1.35 – 1.19 (m, 8H), 0.86 (t, *J* = 6.9 Hz, 3H); <sup>13</sup>C NMR (151 MHz, CDCl<sub>3</sub>) δ 172.1,

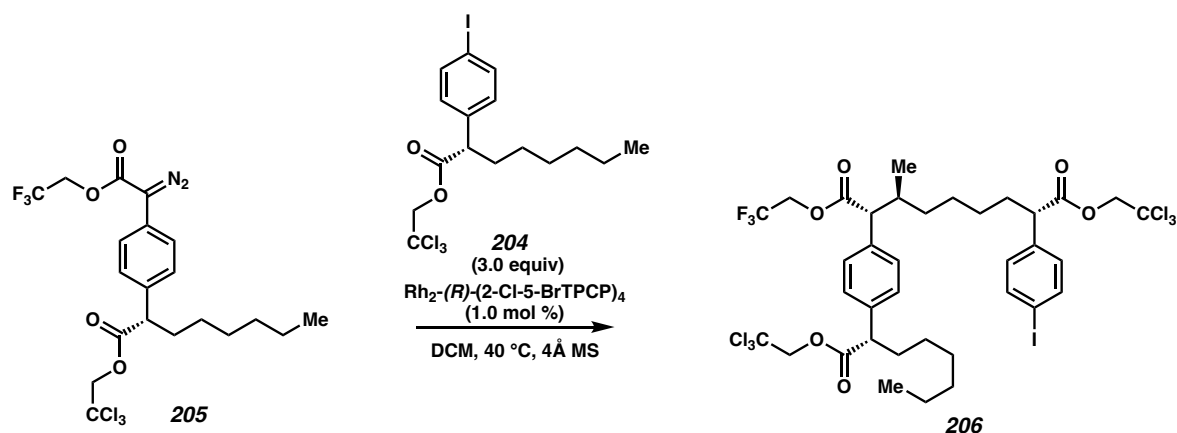
163.1, 136.4, 128.9, 124.2, 123.6, 122.0 (q, *J* = 277.2 Hz), 94.8, 74.0, 60.2 (q, *J* = 36.6 Hz),

51.0, 33.0, 31.5, 28.9, 27.3, 22.5, 14.0;  $^{19}\text{F}$  NMR (565 MHz,  $\text{CDCl}_3$ )  $\delta$  -73.9 (t,  $J = 8.3$  Hz);

IR (Neat Film) 2929, 2858, 2092, 1751, 1716, 1514, 1452, 1411, 1353, 1281, 1241, 1169,

1139, 1074, 974, 924, 838, 761, 720, 652, 572, 513, 427  $\text{cm}^{-1}$ ; (MM:ESI $^+$ )  $m/z$  calcd for

$\text{C}_{20}\text{H}_{22}\text{Cl}_3\text{F}_3\text{N}_2\text{O}_4\text{Na}$  ( $\text{M}+\text{Na}$ ) $^+$  539.0495 found 539.0493.  $[\alpha]_D^{20}$ : +6.4 $^\circ$  ( $c = 1.0$ ,  $\text{CHCl}_3$ ).



**9-(2,2,2-trichloroethyl) 1-(2,2,2-trifluoroethyl) (2R,3S,8S)-8-(4-iodophenyl)-3-methyl-**

**2-(4-((S)-1-oxo-1-(2,2,2-trichloroethoxy)octan-2-yl)phenyl)nonanedioate (206):** A

100-ml flame-dried round-bottom flask with condenser was charged with 4 Å MS and

$\text{Rh}_2$ -(R-2-Cl-5-BrTPCP) $_4$  (53.6 mg, 0.028 mmol, 1.0 mol %) and then, purged three times

with nitrogen. 2,2,2-trichloroethyl (S)-2-(4-iodophenyl)octanoate **204** (4.01 g, 8.40 mmol,

3.0 equiv) and distilled  $\text{CH}_2\text{Cl}_2$  (11 ml) were added next, then the mixture was heated to

40 °C and refluxed for at least 10 min before addition of the diazo compounds. Next, 2,2,2-

trichloroethyl (S)-2-(4-(1-diazo-2-oxo-2-(2,2,2-trifluoroethoxy)ethyl)phenyl)octanoate

**205** (1.45 g, 2.80 mmol, 1.0 equiv) was purged under argon in a 20-mL scintillation vial,

then diluted with distilled  $\text{CH}_2\text{Cl}_2$  (11 ml). Then, under reflux conditions and nitrogen

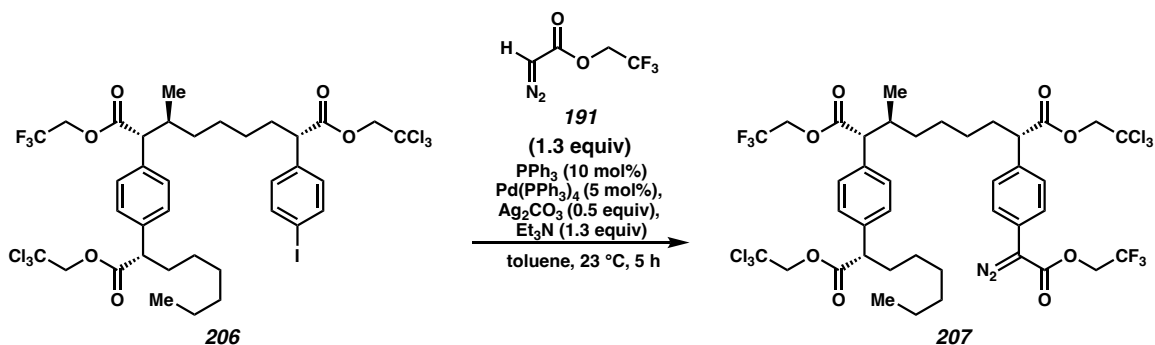
atmosphere, the diazo **205** solution was added to the reaction vessel dropwise via syringe

pump over 3 h. The reaction mixture was stirred at 40 °C for another 30 min and

concentrated under vacuum for crude  $^1\text{H}$  NMR. The crude product was purified by flash column chromatography (3% ether in hexane) to afford the product **206** as an opaque oil. (68% yield, >20:1 rr, 95:5:< 5:< 5 dr); Note 1: Solvent must be carefully dried (distilled over  $\text{CaH}_2$  and stored on activated 4 Å MS). Note 2: The drawn absolute and relative major stereochemistry is drawn based on analogy to the model system. Further confirmation of this assignment is achieved for x-ray structure of a later intermediate. Since chiral centers are already present in the substrates the asymmetric induction for the two new chiral centers formed by the catalyst is reported as diastereoselectivity. The diastereomeric ratio of the relative stereochemistry for the two new stereogenic centers was determined by the methyl shielding in the crude  $^1\text{H}$  NMR. The diastereomeric ratio caused by the catalyst was determined by chiral HPLC. The product from the racemic catalyst was not cleanly separable by HPLC, however both *S* and *R* catalyzed reactions were conducted to distinguish between the two peaks. The resolution was not great; thus, the racemic and *R*-chiral reactions were reduced by DIBAL-H to confirm the absolute diastereoselectivity.

$^1\text{H}$  NMR (600 MHz,  $\text{CDCl}_3$ )  $\delta$  7.64 (d,  $J = 8.1$  Hz, 2H), 7.29 (d,  $J = 8.1$  Hz, 2H), 7.24 (d,  $J = 8.1$  Hz, 2H), 7.04 (d,  $J = 8.2$  Hz, 2H), 4.77 – 4.62 (m, 4H), 4.53 (dq,  $J = 12.8, 8.4$  Hz, 1H), 4.31 (dq,  $J = 12.8, 8.3$  Hz, 1H), 3.66 (t,  $J = 7.7$  Hz, 1H), 3.55 (t,  $J = 7.7$  Hz, 1H), 3.33 (d,  $J = 10.5$  Hz, 1H), 2.16 (dtq,  $J = 18.2, 8.9, 4.7, 3.9$  Hz, 2H), 2.03 (dtd,  $J = 14.0, 8.9, 5.5$  Hz, 1H), 1.86 – 1.77 (m, 1H), 1.69 (ddt,  $J = 19.3, 13.3, 6.1$  Hz, 1H), 1.36 – 1.19 (m, 10H), 1.13 (dtt,  $J = 25.2, 15.4, 7.1$  Hz, 4H), 0.98 (d,  $J = 6.6$  Hz, 3H), 0.87 (h,  $J = 6.9$  Hz, 3H);  $^{13}\text{C}$  NMR (151 MHz,  $\text{CDCl}_3$ )  $\delta$  172.3, 172.1, 171.8, 137.7, 137.7, 137.6, 136.1, 130.0, 128.7, 128.4, 122.8 (q,  $J = 277.3$  Hz), 94.9, 94.7, 93.0, 74.0, 73.9, 60.2 (q,  $J = 36.6$  Hz), 57.7, 51.2, 50.9, 36.1, 33.0, 32.9, 32.9, 31.5, 28.9, 27.4, 27.3, 25.9, 22.5, 17.5, 14.1;  $^{19}\text{F}$

NMR (376 MHz, CDCl<sub>3</sub>)  $\delta$  -73.7 (t,  $J$  = 8.3 Hz); IR (Neat Film) 2930, 2858, 2361, 1751, 1510, 1485, 1456, 1404, 1372, 1276, 1166, 1134, 1061, 1006, 979, 821, 753, 718, 572, 504, 493, 450, 430 cm<sup>-1</sup>; (MM:ESI<sup>+</sup>)  $m/z$  calcd for C<sub>36</sub>H<sub>46</sub>Cl<sub>6</sub>F<sub>3</sub>NIO<sub>6</sub> (M+NH<sub>4</sub>)<sup>+</sup> 982.0453 found 982.0482;  $[\alpha]_D^{20}$ : +3.8° ( $c$  = 1.05, CHCl<sub>3</sub>); HPLC [for better separation, the ester product was reduced with DIBAL-H to (2*R*,3*S*,8*S*)-2-(4-((*S*)-1-hydroxyoctan-2-yl)phenyl)-8-(4-iodophenyl)-3-methylnonane-1,9-diol **SI30**] (ODH, 5.0 % *i*-propanol in hexane, 1.0 mL min<sup>-1</sup>, 1.0 mg mL<sup>-1</sup>, 90 min, UV 210 nm) retention times of 63.6 min (major) and 72.8 min (minor) 91% dr with Rh<sub>2</sub>(*R*-2-Cl-5-BrTPCP)<sub>4</sub>.



**9-(2,2,2-trichloroethyl) 1-(2,2,2-trifluoroethyl) (2*R*,3*S*,8*S*)-8-(4-(1-diazo-2-oxo-2-(2,2,2-trifluoroethoxy)ethyl)phenyl)-3-methyl-2-(4-((*S*)-1-oxo-1-(2,2,2-**

**trichloroethoxy)octan-2-yl)phenyl)nonanedioate (207):** The procedure is adapted from

the literature<sup>13b</sup>: A 25-ml round-bottom flask with stir bar was flame dried under vacuum.

Once cool enough all solids were added first: PPh<sub>3</sub> (34.8 mg, 0.133 mmol, 0.1 equiv),

Pd(PPh<sub>3</sub>)<sub>4</sub> (76.6 mg, 0.066 mmol, 0.05 equiv) and Ag<sub>2</sub>CO<sub>3</sub> (183 mg, 0.663 mmol, 0.5

equiv). After solids added, the reaction vessel was purged with nitrogen three times. Next

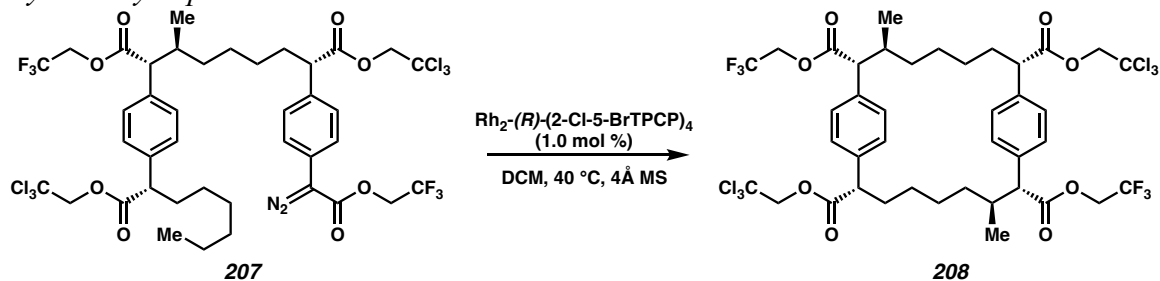
the liquids were added: toluene (5.3 ml), Et<sub>3</sub>N (0.240 ml, 1.72 mmol, 1.3 equiv), 9-(2,2,2-

trichloroethyl) 1-(2,2,2-trifluoroethyl) (2*R*,3*S*,8*S*)-8-(4-iodophenyl)-3-methyl-2-(4-((*S*)-1-

oxo-1-(2,2,2-trichloroethoxy)octan-2-yl)phenyl)nonanedioate **206** (1.283 g, 1.33 mmol,



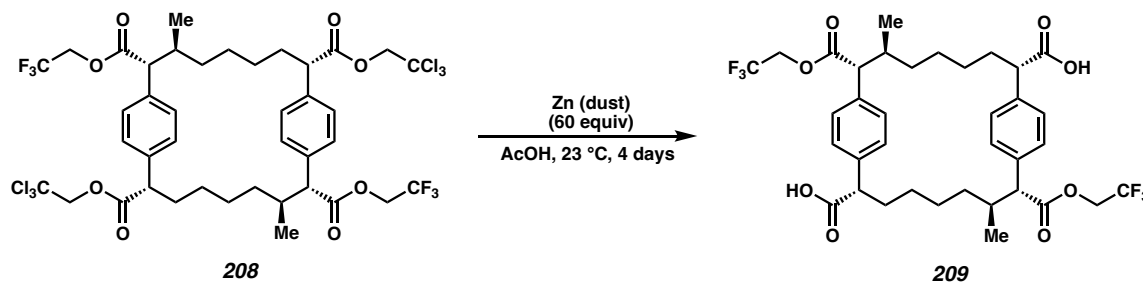
1.0 equiv), and finally the 2,2,2-trifluoroethyl 2-diazoacetate **191** (289.8 mg, 1.72 mmol, 1.3 equiv) was added last. The resulted mixture was stirred at room temperature (23 °C) for 5 h and then, filtered through a short silica plug (3.5 cm *diameter*, 5 cm *height*), eluting with ethyl acetate until elutes clear. The crude product was concentrated and purified by flash column chromatography (3% ether in hexane) to afford the product **207** as a red oil (77% yield). <sup>1</sup>H NMR (600 MHz, CDCl<sub>3</sub>) δ 7.41 (d, *J* = 8.1 Hz, 2H), 7.34 (d, *J* = 8.2 Hz, 2H), 7.29 (d, *J* = 8.0 Hz, 2H), 7.25 (d, *J* = 8.0 Hz, 2H), 4.75 – 4.61 (m, 6H), 4.53 (dq, *J* = 12.7, 8.3 Hz, 1H), 4.31 (dq, *J* = 12.7, 8.3 Hz, 1H), 3.66 (t, *J* = 7.7 Hz, 1H), 3.61 (t, *J* = 7.7 Hz, 1H), 3.33 (d, *J* = 10.5 Hz, 1H), 2.15 (dddd, *J* = 22.7, 13.3, 9.9, 3.9 Hz, 2H), 2.09 – 2.01 (m, 1H), 1.86 – 1.77 (m, 1H), 1.77 – 1.66 (m, 1H), 1.36 – 1.20 (m, 10H), 1.19 – 1.07 (m, 4H), 0.98 (d, *J* = 6.5 Hz, 3H), 0.86 (t, *J* = 6.9 Hz, 3H); <sup>13</sup>C NMR (151 MHz, CDCl<sub>3</sub>) δ 172.3, 172.1, 172.0, 163.1, 137.7, 136.2, 136.1, 128.8, 128.7, 128.4, 126.8, 122.9 (qd, *J* = 277.3, 3.9 Hz), 94.9, 94.8, 74.0, 73.9, 60.2 (qd, *J* = 36.7, 10.9 Hz), 57.7, 51.2, 50.9, 36.1, 33.0, 33.0, 32.9, 31.5, 28.9, 27.4, 27.4, 26.0, 22.5, 17.5, 14.0; <sup>19</sup>F NMR (376 MHz, CDCl<sub>3</sub>) δ -73.7 (t, *J* = 8.4 Hz), -73.9 (t, *J* = 8.4 Hz); IR (Neat Film) 2930, 2858, 2361, 2093, 1750, 1718, 1514, 1410, 1353, 1280, 1242, 1166, 1137, 1074, 976, 838, 756, 719, 652, 571, 513, 484, 450, 435 cm<sup>-1</sup>; (MM:ESI<sup>+</sup>) *m/z* calcd for C<sub>40</sub>H<sub>48</sub>Cl<sub>6</sub>F<sub>6</sub>N<sub>3</sub>O<sub>8</sub> (M+NH<sub>4</sub>)<sup>+</sup> 1022.1477 found 1022.1523; [α]<sub>D</sub><sup>20</sup>: +4.3° (c = 0.8, CHCl<sub>3</sub>)



**Macrocycle X (208):** A 100-ml flame-dried round-bottom flask with condenser were charged with 4 Å MS and  $\text{Rh}_2(\text{R})\text{-}(2\text{-Cl-5-BrTPCP})_4$  (34.7 mg, 0.01 mmol, 1.0 mol%), then purged three times under nitrogen. Distilled  $\text{CH}_2\text{Cl}_2$  (18 ml) was added using oven dried syringes, then the mixture was heated to 40 °C and refluxed for at least 10 min before addition of the diazo compounds. Next, 9-(2,2,2-trichloroethyl) 1-(2,2,2-trifluoroethyl) ((*2R,3S,8S*))-8-(4-(1-diazo-2-oxo-2-(2,2,2-trifluoroethoxy)ethyl)phenyl)-3-methyl-2-(4-((*S*)-1-oxo-1-(2,2,2-trichloroethoxy)octan-2-yl)phenyl)nonanedioate **207** (1.83 g, 1.82 mmol, 1.0 equiv) was used immediately after its synthesis and purged under nitrogen in a 50-mL round-bottom flask, then diluted with distilled  $\text{CH}_2\text{Cl}_2$  (18 ml). Then, under reflux conditions and nitrogen atmosphere, the diazo solution was added to the reaction vessel dropwise via syringe pump over 3 h. The reaction mixture was stirred at 40 °C for another 30 min and concentrated under vacuum for crude  $^1\text{H}$  NMR, showing the product was formed in 8:1 dr. The crude product was purified by flash column chromatography (10% ether in hexane) to afford the product **208** as a white solid and single diastereomer (70% yield). Alternatively, the crude mixture can be recrystallized in 20% ether in hexane to yield the diastereopure product **208** as a white solid (62% yield). The absolute configuration and relative configuration are determined by x-ray crystallography.

Note 1: Solvent must be carefully dried (distilled over  $\text{CaH}_2$  and stored on activated 4 Å MS). Note 2: The crude material obtained shows two diastereomeric signals in 8:1. The

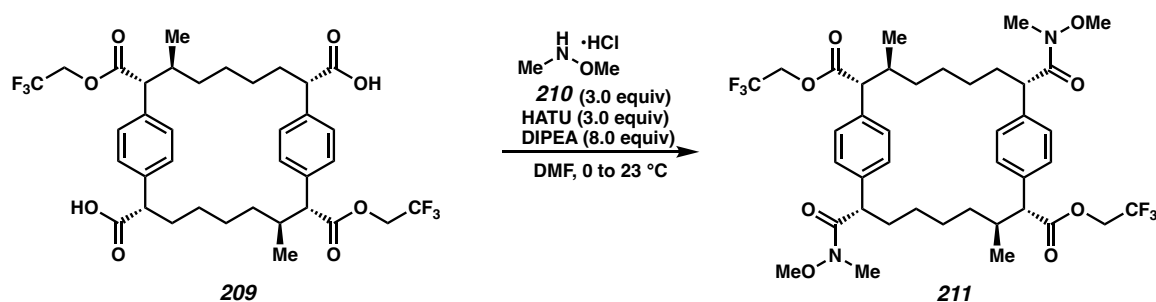
change in dr from the starting material is due to the Horeau principle. Recrystallization gave the desired diastereomer in 62% yield and the NMR appears as a signal diastereomer.  $^1\text{H}$  NMR (600 MHz,  $\text{CDCl}_3$ )  $\delta$  7.21 (s, 8H), 4.73 (dd,  $J = 12.0, 1.0$  Hz, 2H), 4.62 (dd,  $J = 12.0, 1.1$  Hz, 2H), 4.53 (dq,  $J = 12.8, 8.4$  Hz, 2H), 4.27 (dq,  $J = 12.7, 8.3$  Hz, 2H), 3.52 (dd,  $J = 11.4, 4.4$  Hz, 2H), 3.19 (d,  $J = 11.4$  Hz, 2H), 2.14 – 2.07 (m, 2H), 1.97 – 1.82 (m, 4H), 1.49 – 1.39 (m, 2H), 1.00 (d,  $J = 6.4$  Hz, 6H), 0.94 (qt,  $J = 12.5, 6.3$  Hz, 4H), 0.76 (t,  $J = 12.8$  Hz, 2H), 0.70 – 0.61 (m, 4H);  $^{13}\text{C}$  NMR (151 MHz,  $\text{CDCl}_3$ )  $\delta$  172.1, 172.1, 136.8, 136.4, 128.6, 122.8 (q,  $J = 277.2$  Hz), 94.8, 73.9, 60.2 (q,  $J = 36.7$  Hz), 58.7, 51.4, 37.0, 33.8, 33.1, 27.9, 27.3, 17.8;  $^{19}\text{F}$  NMR (376 MHz,  $\text{CDCl}_3$ )  $\delta$  -73.7 (t,  $J = 8.5$  Hz); IR (Neat Film) 2935, 2860, 1749, 1511, 1466, 1407, 1374, 1276, 1222, 1164, 1128, 1062, 979, 909, 835, 809, 762, 726, 645, 572, 539, 462, 450, 440, 431  $\text{cm}^{-1}$ ; (MM:ESI $^+$ )  $m/z$  calcd for  $\text{C}_{40}\text{H}_{44}\text{Cl}_6\text{F}_6\text{O}_8$  (M+H) $^+$  977.1150 found 977.1177;  $[\alpha]_D^{20}$ : -7.6 $^\circ$  ( $c = 0.34$ ,  $\text{CHCl}_3$ ).



**(2*S*,7*S*,8*R*,10*S*,15*S*,16*R*)-7,15-dimethyl-8,16-bis((2,2,2-trifluoroethoxy)carbonyl)-**

**1,9(1,4)-dibenzenacyclohexadecaphane-2,10-dicarboxylic acid (209):** To a 250-ml round-bottom flask was added macrocycle **208** (893 mg, 0.912 mmol, 1.0 equiv) then zinc (3.58 g, 54.7 mmol, 60 equiv) and acetic acid (46ml). Stir for 4 days at room temperature. The crude mixture was diluted with water then filtered washing with EtOAc. The eluent was then further diluted with EtOAc, then washed with water (x2), brine (x8), then dried

with MgSO<sub>4</sub> and concentrated under reduced pressure. The crude product was clean by <sup>1</sup>H NMR and carried forward as a white solid **209** (>99% yield); <sup>1</sup>H NMR (600 MHz, CDCl<sub>3</sub>) δ 7.20 (d, *J* = 7.5 Hz, 4H), 7.15 (d, *J* = 7.8 Hz, 4H), 4.55 (dq, *J* = 12.7, 8.4 Hz, 2H), 4.23 (dq, *J* = 12.8, 8.4 Hz, 2H), 3.39 (dd, *J* = 11.6, 4.2 Hz, 2H), 3.18 (d, *J* = 11.3 Hz, 2H), 2.11 – 2.03 (m, 2H), 1.87 (t, *J* = 13.0 Hz, 2H), 1.80 (dd, *J* = 12.3, 7.9 Hz, 2H), 1.46 – 1.37 (m, 2H), 0.99 (d, *J* = 6.3 Hz, 6H), 0.89 (q, *J* = 10.5, 9.7 Hz, 4H), 0.73 (t, *J* = 12.7 Hz, 2H), 0.68 – 0.52 (m, 4H); <sup>13</sup>C NMR (151 MHz, CDCl<sub>3</sub>) δ 179.0, 176.5, 172.2, 171.2, 137.1, 136.3, 128.6, 122.9 (q, *J* = 277.2 Hz), 60.3 (q, *J* = 36.5 Hz), 58.7, 51.3, 37.2, 33.9, 33.0, 27.9, 27.3, 21.0, 20.6, 17.7, 14.2; <sup>19</sup>F NMR (376 MHz, CDCl<sub>3</sub>) δ -73.7 (td, *J* = 8.5, 5.6 Hz); IR (Neat Film) 2933, 2858, 1749, 1705, 1511, 1468, 1407, 1385, 1275, 1225, 1167, 1128, 1058, 1021, 979, 910, 840, 731, 697, 660 cm<sup>-1</sup>; (MM:ESI<sup>-</sup>) *m/z* calcd for C<sub>36</sub>H<sub>41</sub>F<sub>6</sub>O<sub>8</sub> (M-H)<sup>-</sup> 715.2706 found 715.2703; [α]<sub>D</sub><sup>20</sup>: +13.9° (c = 0.8, EtOAc).



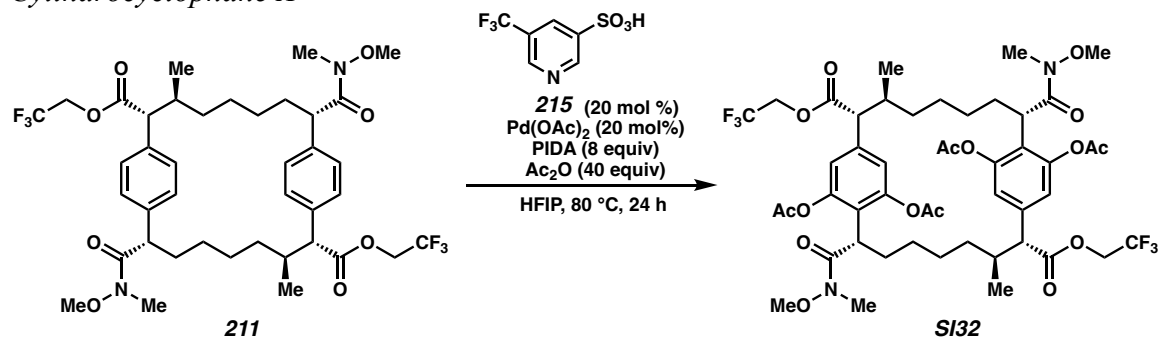
bis(2,2,2-trifluoroethyl)

(2*R*,3*S*,8*S*,10*R*,11*S*,16*S*)-8,16-

bis(methoxy(methyl)carbamoyl)-3,11-dimethyl-1,9(1,4)-

**dibenzocyclohexadecaphane-2,10-dicarboxylate (211):** To a 50-ml flame-dried round-bottom flask was added (2*S*,7*S*,8*R*,10*S*,15*S*,16*R*)-7,15-dimethyl-8,16-bis((2,2,2-trifluoroethoxy)carbonyl)-1,9(1,4)-dibenzocyclohexadecaphane-2,10-dicarboxylic acid **209** (988 mg, 1.38 mmol, 1.0 equiv) in N,N-dimethylformamide (7 ml). The mixture was

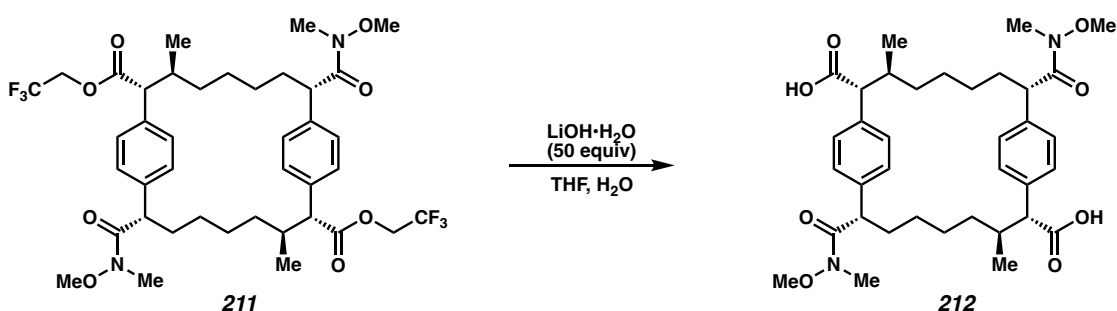
then cooled to 0 °C. HATU (1.57 g, 4.14 mmol, 3.0 equiv) and then N-ethyl-N-isopropylpropan-2-amine (1.92 mL, 11.0 mmol, 8.0 equiv) was added at 0 °C. The reaction was then stirred for 20 min at 0 °C. Then N,O-dimethylhydroxylamine hydrochloride **210** (403 mg, 4.14 mmol, 3.0 equiv) was added 0 °C, then the reaction was stirred overnight and let warm to room temperature. The reaction was dilute with EtOAc and water, then separated and washed with brine (x8), dried with MgSO<sub>4</sub> and concentrated under reduced pressure. The crude product was purified by flash column chromatography (25% EtOAc in hexane) to afford the product **211** as a white solid (85% yield); <sup>1</sup>H NMR (600 MHz, CDCl<sub>3</sub>) δ 7.17 (s, 8H), 4.46 (dq, *J* = 12.7, 8.5 Hz, 2H), 4.33 (dq, *J* = 12.7, 8.4 Hz, 2H), 3.79 (s, 2H), 3.36 (s, 6H), 3.16 (d, *J* = 11.4 Hz, 2H), 3.10 (s, 6H), 2.09 – 2.03 (m, 2H), 1.89 – 1.80 (m, 2H), 1.74 – 1.66 (m, 2H), 1.41 (t, *J* = 12.1 Hz, 2H), 0.99 (d, *J* = 6.4 Hz, 6H), 0.92 (qt, *J* = 11.5, 5.7 Hz, 4H), 0.80 (t, *J* = 12.9 Hz, 2H), 0.67 – 0.51 (m, 4H); <sup>13</sup>C NMR (151 MHz, CDCl<sub>3</sub>) δ 172.2, 138.9, 135.7, 128.7, 128.5, 122.9 (q, *J* = 277.2 Hz), 61.1, 60.1 (q, *J* = 36.5 Hz), 58.8, 47.8, 37.1, 34.0, 33.6, 33.3, 32.2, 28.1, 27.5, 17.8; <sup>19</sup>F NMR (376 MHz, CDCl<sub>3</sub>) δ -73.8 (t, *J* = 8.4 Hz); IR (Neat Film) 2934, 2857, 1751, 1656, 1510, 1409, 1382, 1274, 1164, 1126, 1056, 1022, 979, 909, 841, 803, 730, 646, 623, 566, 532, 452, 433, 424 cm<sup>-1</sup>; (MM:ESI<sup>+</sup>) *m/z* calcd for C<sub>40</sub>H<sub>53</sub>F<sub>6</sub>N<sub>2</sub>O<sub>8</sub> (M+H)<sup>+</sup> 803.3706 found 803.3702; [α]<sub>D</sub><sup>20</sup>: -2° (c = 0.3, CHCl<sub>3</sub>)



bis(2,2,2-trifluoroethyl) (2*R*,3*S*,8*S*,10*R*,11*S*,16*S*)-1<sup>3</sup>,1<sup>5</sup>,9<sup>2</sup>,9<sup>6</sup>-tetraacetoxy-8,16-bis(methoxy(methyl)carbamoyl)-3,11-dimethyl-1,9(1,4)-dibenzenacyclohexadecaphane-2,10-dicarboxylate (**SI32**):

The procedure is adapted from the literature<sup>4c</sup>: To a flame-dried 8-ml vial was added Pd(OAc)<sub>2</sub> (11.7 mg, 51.8 μmol, 20 mol %), PhI(OAc)<sub>2</sub> (669 mg, 2.07 mmol, 8.0 equiv), 5-(trifluoromethyl)-3-pyridinesulfonic acid **215** (11.7 mg, 51.8 μmol, 20 mol %), and bis(2,2,2-trifluoroethyl) (2*R*,3*S*,8*S*,10*R*,11*S*,16*S*)-8,16-bis(methoxy(methyl)carbamoyl)-3,11-dimethyl-1,9(1,4)-dibenzenacyclohexadecaphane-2,10-dicarboxylate **211** (208.0 mg, 269.1 μmol, 1.0 equiv). Then HFIP (2.6 ml) and Ac<sub>2</sub>O (0.98 ml, 10.4 mmol, 40 equiv) were added and the septum cap was exchanged with a Teflon septum-lined screw cap and heated to 80 °C for 24 h. The reaction was cooled to room temperature, diluted with EtOAc and filtered over celite. The eluent was concentrated under reduced pressure and purified by flash column chromatography (30% to 50% EtOAc in hexanes) to deliver the product **SI32** as a tan solid (77% yield); <sup>1</sup>H NMR (400 MHz, CDCl<sub>3</sub>) δ 7.00 (d, *J* = 1.7 Hz, 2H), 6.89 (d, *J* = 1.7 Hz, 2H), 4.50 – 4.33 (m, 4H), 3.98 (dd, *J* = 12.0, 4.3 Hz, 2H), 3.16 (d, *J* = 11.4 Hz, 2H), 3.00 (s, 6H), 2.91 (s, 6H), 2.32 (s, 6H), 2.21 (s, 6H), 1.94 (qd, *J* = 12.8, 11.8, 3.6 Hz, 4H), 1.79 (ddd, *J* = 13.5, 9.5, 4.1 Hz, 2H), 1.51 – 1.37 (m, 3H), 0.99 (d, *J* = 6.4 Hz, 6H), 0.95 – 0.78 (m, 5H), 0.73 – 0.61 (m, 2H), 0.52 (q, *J* = 12.3 Hz, 2H); <sup>13</sup>C NMR

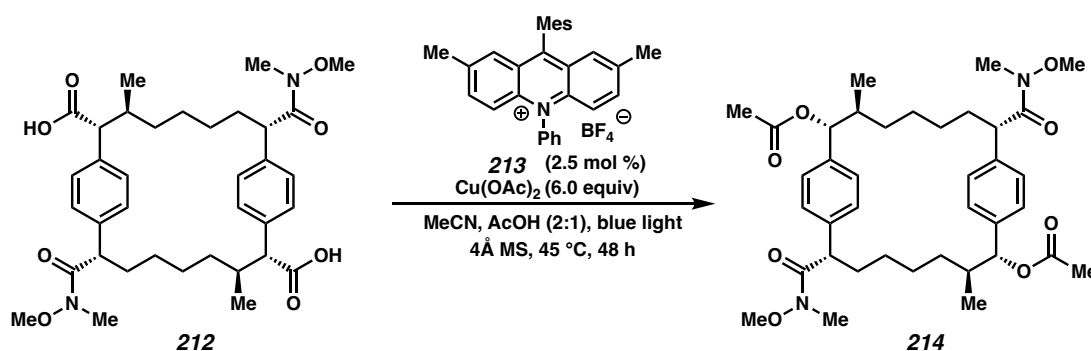
(101 MHz, CDCl<sub>3</sub>)  $\delta$  172.9, 171.5, 168.7, 167.7, 149.3, 148.7, 136.3, 124.3, 122.7 (q,  $J$  = 277.5 Hz) 122.0, 119.1, 60.4, 60.0, 59.7, 58.3, 39.9, 37.7, 34.1, 31.9, 30.2, 28.0, 27.4, 21.2, 20.6, 17.8; <sup>19</sup>F NMR (376 MHz, CDCl<sub>3</sub>)  $\delta$  -73.8 (t,  $J$  = 8.4 Hz); IR (Neat Film) 2934, 2858, 1769, 1757, 1659, 1619, 1577, 1431, 1412, 1368, 1285, 1275, 1180, 1131, 1087, 1032, 979, 906, 842, 804, 730 cm<sup>-1</sup>; (MM:ESI<sup>+</sup>)  $m/z$  calcd for C<sub>48</sub>H<sub>58</sub>F<sub>6</sub>N<sub>2</sub>O<sub>16</sub>Na<sub>2</sub> [M+2Na-2H]<sup>+</sup> 1078.3847 found 1078.5087; [ $\alpha$ ]<sub>D</sub><sup>20</sup>: +38.5° (c = 0.85, CHCl<sub>3</sub>)



**(2R,3S,8S,10R,11S,16S)-8,16-bis(methoxy(methyl)carbamoyl)-3,11-dimethyl-**

**1,9(1,4)-dibenzenacyclohexadecaphane-2,10-dicarboxylic acid (212):** To a 10-ml round-bottom was added bis(2,2,2-trifluoroethyl) (2R,3S,8S,10R,11S,16S)-8,16-bis(methoxy(methyl)carbamoyl)-3,11-dimethyl-1,9(1,4)-dibenzenacyclohexadecaphane-2,10-dicarboxylate **211** (60.0 mg, 74.7  $\mu$ mol, 1.0 equiv) then THF (1.5 ml) and water (1.5 ml) was added. Then lithium hydroxide hydrate (157 mg, 3.74 mmol, 50 equiv) was added to the reaction and then let stir at room temperature overnight. The reaction was diluted with water and acidify with 2M HCl. The product was extracted with EtOAc (x2), dried with MgSO<sub>4</sub> and concentrated under reduced pressure. The crude product **212** was clean by <sup>1</sup>H NMR and carried forward as a white solid (97% yield); <sup>1</sup>H NMR (600 MHz, AcOD)  $\delta$  7.25 (d,  $J$  = 7.7 Hz, 4H), 7.18 (d,  $J$  = 8.0 Hz, 4H), 3.90 (s, 2H), 3.50 (s, 6H), 3.11 (s, 6H), 3.04 (d,  $J$  = 11.3 Hz, 2H), 2.10 – 2.03 (m, 2H), 1.70 (ddt,  $J$  = 18.3, 13.2, 8.5 Hz, 4H), 1.50

- 1.41 (m, 2H), 1.03 (d,  $J = 6.3$  Hz, 6H), 0.98 – 0.88 (m, 3H), 0.88 – 0.81 (m, 2H), 0.67 (dtd,  $J = 22.7, 11.9, 5.5$  Hz, 4H);  $^{13}\text{C}$  NMR (151 MHz, AcOD)  $\delta$  180.1, 176.1, 139.7, 138.8, 138.2, 137.9, 129.7, 61.8, 60.2, 52.3, 48.6, 37.4, 34.8, 34.1, 33.7, 32.7, 28.9, 28.0, 18.2, 14.3; IR (Neat Film) 2918, 2950, 2360, 2106, 1693, 1650, 1383, 1777, 989, 799, 668, 592  $\text{cm}^{-1}$ ; (MM:ESI $^{+}$ )  $m/z$  calcd for  $\text{C}_{36}\text{H}_{50}\text{N}_2\text{O}_8\text{Na}$  ( $\text{M}+\text{Na}$ ) $^{+}$  661.3465 found 661.3452;  $[\alpha]_{\text{D}}^{20}$ : +9.5 $^{\circ}$  ( $c = 0.5$ , AcOH)

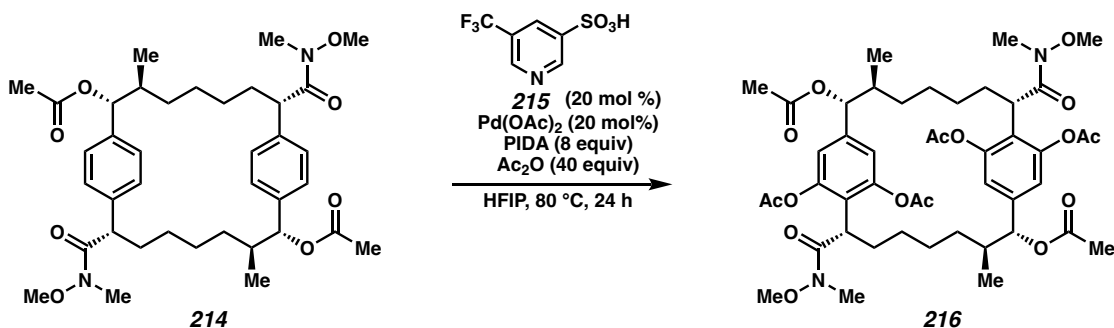


**(2R,3S,8S,10R,11S,16S)-8,16-bis(methoxy(methyl)carbamoyl)-3,11-dimethyl-**

**1,9(1,4)-dibenzenacyclohexadecaphane-2,10-diyl diacetate (214):** The procedure is adapted from the literature<sup>24</sup>: To a flame-dried 8-ml vial purged under nitrogen (x3) was added 4 Å MS,  $\text{Cu}(\text{OAc})_2$  (42.6 mg, 235  $\mu\text{mol}$ , 6.0 equiv), 9-mesityl-2,7-dimethyl-10-phenyl-acridinium tetrafluoroborate **213** (0.5 mg, 1.0  $\mu\text{mol}$ , 2.5 mol %), and (2R,3S,8S,10R,11S,16S)-8,16-bis(methoxy(methyl)carbamoyl)-3,11-dimethyl-1,9(1,4)-dibenzenacyclohexadecaphane-2,10-dicarboxylic acid **212** (25.0 mg, 39.1  $\mu\text{mol}$ , 1.0 equiv). Then acetonitrile (1.7 ml) and acetic acid (0.85 ml) was added to the reaction mixture. The reaction was then degassed via nitrogen bubbling for 10 min using an 18-gauge needle and another exit needle. The reaction was then sealed placed and two blue lights placed against the vial and wrapped in tin foil. The mixture was stirred under blue light for 48 h. The crude mixture was cooled to room temperature and filtered over celite



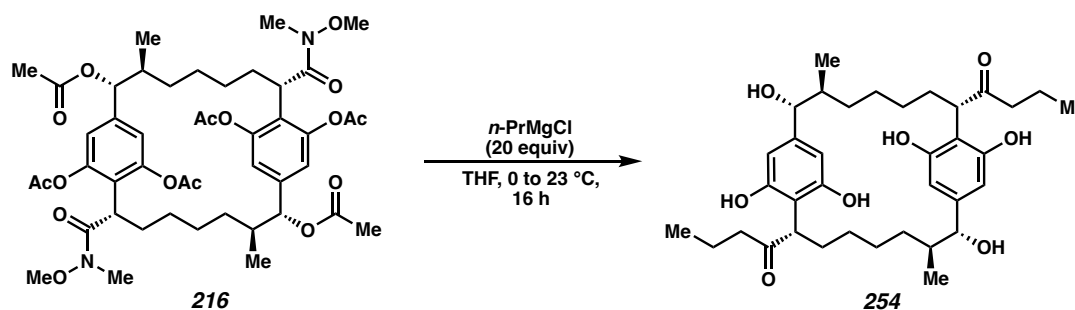
eluting with EtOAc. The eluent was concentrated under vacuum, diluted with EtOAc and washed with water, then brine (x4), dried with MgSO<sub>4</sub> and concentrated under reduced pressure for crude <sup>1</sup>H NMR analysis, showing the product was formed in 9:1 dr. The crude product was purified by flash column chromatography (30% EtOAc in hexane) to afford the product **214** as a white solid and single diastereomer by <sup>1</sup>H NMR (52% yield); <sup>1</sup>H NMR (600 MHz, CDCl<sub>3</sub>) δ 7.22 – 7.14 (m, 8H), 5.17 (d, *J* = 10.5 Hz, 2H), 3.83 (s, 2H), 3.40 (s, 6H), 3.11 (s, 6H), 1.99 (s, 6H), 1.84 – 1.74 (m, 4H), 1.74 – 1.67 (m, 2H), 1.47 – 1.37 (m, 2H), 0.99 (d, *J* = 6.4 Hz, 6H), 0.95 – 0.85 (m, 4H), 0.65 (dddd, *J* = 49.4, 24.7, 12.2, 5.2 Hz, 6H); <sup>13</sup>C NMR (151 MHz, CDCl<sub>3</sub>) δ 170.4, 138.6, 128.2, 127.6, 81.3, 61.2, 47.6, 38.9, 33.8, 32.7, 29.7, 28.0, 27.6, 21.2, 16.1; IR (Neat Film) 2934, 2857, 1736, 1660, 1510, 1465, 1373, 1240, 1019, 991, 970, 916, 801, 730, 600, 565 cm<sup>-1</sup>; (MM:ESI<sup>+</sup>) *m/z* calcd for C<sub>38</sub>H<sub>55</sub>N<sub>2</sub>O<sub>8</sub> (M+H)<sup>+</sup> 667.3958 found 667.3959; [α]<sub>D</sub><sup>20</sup>: +79.8° (c = 0.85, CHCl<sub>3</sub>)



**(2*S*,7*S*,8*R*,10*S*,15*S*,16*R*)-2,10-bis(methoxy(methyl)carbamoyl)-7,15-dimethyl-1,9(1,4)-dibenzenacyclohexadecaphane-1<sup>2</sup>,1<sup>6</sup>,9<sup>3</sup>,9<sup>5</sup>,8,16-hexayl hexaacetate (**216**):**

The procedure is adapted from the literature<sup>4c</sup>: To a flame-dried 8-ml vial was added Pd(OAc)<sub>2</sub> (2.0mg, 9.0 μmol, 20 mol %), PhI(OAc)<sub>2</sub> (116 mg, 360 μmol, 8.0 equiv), 5-(trifluoromethyl)-3-pyridinesulfonic acid **215** (2.0mg, 9.0 μmol, 20 mol %), and

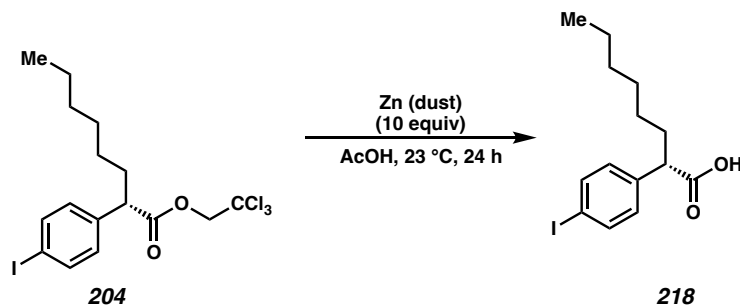
(2*R*,3*S*,8*S*,10*R*,11*S*,16*S*)-8,16-bis(methoxy(methyl)carbamoyl)-3,11-dimethyl-1,9(1,4)-dibenzencyclohexadecaphane-2,10-diyl diacetate **214** (30.0 mg, 45.0  $\mu\text{mol}$ , 1.0 equiv). Then HFIP (1.0ml) and  $\text{Ac}_2\text{O}$  (0.17 ml, 1.8 mmol, 40 equiv) were added and the septum cap was exchanged with a Teflon septum-lined screw cap and heated to 80 °C for 48 h. The reaction was cooled to room temperature, diluted with EtOAc and filtered over celite. The eluent was concentrated under reduced pressure and purified by flash column chromatography (50% EtOAc in hexanes) to deliver the product **216** as a white solid (60% yield);  $^1\text{H}$  NMR (600 MHz,  $\text{CDCl}_3$ )  $\delta$  6.97 (s, 2H), 6.86 (s, 2H), 5.20 (d,  $J = 10.0$  Hz, 2H), 4.01 – 3.96 (m, 2H), 3.02 (s, 6H), 2.95 (s, 6H), 2.31 (s, 6H), 2.22 (s, 6H), 2.00 (s, 6H), 1.83 (p,  $J = 8.1$  Hz, 5H), 1.73 – 1.65 (m, 3H), 1.45 (tt,  $J = 10.1, 5.7$  Hz, 2H), 1.04 – 0.96 (m, 3H), 0.95 (d,  $J = 6.5$  Hz, 6H), 0.82 – 0.77 (m, 3H), 0.66 – 0.57 (m, 2H);  $^{13}\text{C}$  NMR (151 MHz,  $\text{CDCl}_3$ )  $\delta$  170.1, 169.0, 167.5, 149.1, 148.4, 139.4, 120.8, 117.8, 80.0, 59.9, 40.0, 39.2, 32.6, 30.3, 27.9, 27.3, 21.1, 21.1, 20.7, 15.7; IR (neat) 2931, 2360, 1771, 1744, 1663, 1431, 1370, 1232, 1182, 1035, 900, 516  $\text{cm}^{-1}$ ; (MM:ESI $^+$ )  $m/z$  calcd for  $\text{C}_{46}\text{H}_{63}\text{N}_2\text{O}_{16}$  ( $\text{M}+\text{H}$ ) $^+$  899.4178 found 899.4181;  $[\alpha]^{20}_{\text{D}}$ : +64° ( $c = 0.1, \text{CHCl}_3$ )



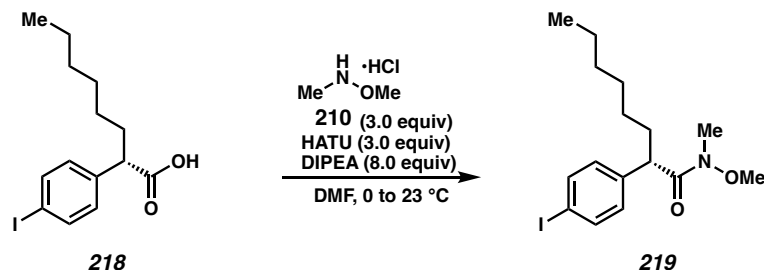
**1,1'-((2*S*,7*S*,8*R*,10*S*,15*S*,16*R*)-1 $^2$ ,1 $^6$ ,9 $^3$ ,9 $^5$ ,8,16-hexahydroxy-7,15-dimethyl-1,9(1,4)-dibenzencyclohexadecaphane-2,10-diyl)bis(butan-1-one) (**254**):** To a flame-dried 4-ml vial purged under nitrogen (x3) was added (2*S*,7*S*,8*R*,10*S*,15*S*,16*R*)-2,10-

bis(methoxy(methyl)carbamoyl)-7,15-dimethyl-1,9(1,4)-dibenzenacyclohexadecaphane-1<sup>2</sup>,1<sup>6</sup>,9<sup>3</sup>,9<sup>5</sup>,8,16-hexayl hexaacetate **216** (45.0mg, 0.05 mmol, 1 equiv) then THF (3 mL). The mixture was then cooled to 0 °C in an ice bath for 10 min. At 0 °C *n*-propylmagnesium chloride (1.0 M in 2-Me-THF, 1.0 ml, 20 equiv, 1 mmol) was added dropwise and the reaction was let warmed to room temperature overnight. The mixture was then cooled to 0 °C and quenched with water, acidified with sat. NH<sub>4</sub>Cl, then extracted with EtOAc, washed with brine, dried with MgSO<sub>4</sub> and concentrated under reduced pressure. The crude product was purified by prepLC (Agilent 1100 HPLC, 9.4x250 C8 column, 20% ACN/H<sub>2</sub>O 0.5min at 2.5ml/min, 20-70% ACN for 6.5min at 5ml/min, 100% ACN for 1min) to deliver the product as a white solid. The product can also be purified via column chromatography (80% EtOAc in hexanes with 1% MeOH) to deliver the desired hexa-hydroxy macrocycle **254** as a white solid (18.5 mg, 0.03 mmol, 60% yield)

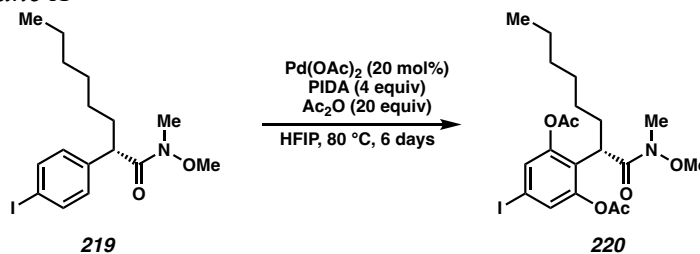
<sup>1</sup>H NMR (400 MHz, MeOD) δ 6.30 (s, 2H), 6.18 (s, 2H), 3.90 (dd, *J* = 10.4, 4.8 Hz, 2H), 3.79 (d, *J* = 9.7 Hz, 2H), 2.21 (td, *J* = 7.3, 1.9 Hz, 4H), 1.93 – 1.76 (m, 4H), 1.47 (h, *J* = 7.5, 5.2 Hz, 9H), 1.09 (d, *J* = 6.4 Hz, 6H), 1.04 – 0.96 (m, 2H), 0.77 (t, *J* = 7.4 Hz, 6H), 0.66 (dd, *J* = 11.7, 6.9 Hz, 2H); (MM:ESI<sup>-</sup>) *m/z* calcd for C<sub>36</sub>H<sub>52</sub>O<sub>8</sub> (M-H)<sup>-</sup> 611.3662 found 611.3604.



**(S)-2-(4-iodophenyl)octanoic acid (218):** To a 100-ml round-bottom flask was added 2,2,2-trichloroethyl (S)-2-(4-iodophenyl)octanoate **204** (527 mg, 1.1 mmol, 1.0 equiv) then zinc (721 mg, 11.0 mmol, 10 equiv) and acetic acid (14ml). Stir for 24 h at room temperature. The crude mixture was diluted with water then filtered washing with EtOAc. The eluent was then further diluted with EtOAc, then washed with water (x2), brine (x8), then dried with MgSO<sub>4</sub> and concentrated under reduced pressure. The crude product **218** was clean by <sup>1</sup>H NMR and carried forward as a yellow oil (99% yield); <sup>1</sup>H NMR (600 MHz, CDCl<sub>3</sub>) δ 7.65 (d, *J* = 8.1 Hz, 2H), 7.06 (d, *J* = 8.1 Hz, 2H), 3.48 (t, *J* = 7.7 Hz, 1H), 2.04 (tdd, *J* = 12.3, 8.4, 4.6 Hz, 1H), 1.74 (pd, *J* = 8.9, 8.3, 5.0 Hz, 1H), 1.34 – 1.16 (m, 8H), 0.86 (t, *J* = 7.0 Hz, 3H); <sup>13</sup>C NMR (151 MHz, CDCl<sub>3</sub>) δ 178.9, 138.1, 137.7, 130.0, 92.9, 50.9, 32.9, 31.5, 28.9, 27.3, 22.5, 14.0; IR (Neat Film) 3023, 2953, 2924, 2855, 1710, 1586, 1484, 1416, 1401, 1378, 1275, 1227, 1204, 1182, 1122, 1063, 1006, 936, 815, 745, 724, 698 cm<sup>-1</sup>; (MM:ESI<sup>-</sup>) *m/z* calcd for C<sub>14</sub>H<sub>18</sub>IO<sub>2</sub> (M-H)<sup>-</sup> 345.0351 found 345.0346.

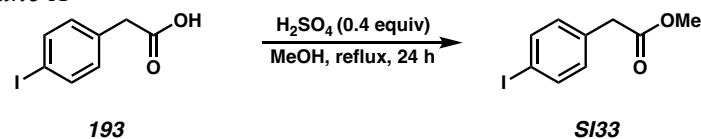


**(S)-2-(4-iodophenyl)-N-methoxy-N-methyloctanamide (219):** To a 50-ml flame-dried round-bottom flask was added (S)-2-(4-iodophenyl)octanoic acid **218** (382 mg, 1.1 mmol, 1.0 equiv) in N,N-dimethylformamide (2.8 ml). The mixture was then cooled to 0 °C. HATU (503 mg, 1.32 mmol, 1.2 equiv) and then N-ethyl-N-isopropylpropan-2-amine (0.58 mL, 3.31 mmol, 3.0 equiv) was added at 0 °C. The reaction was then stirred for 20min at 0 °C. Then N,O-dimethylhydroxylamine hydrochloride **210** (161 mg, 1.66 mmol, 1.5 equiv) was added 0 °C, then the reaction was stirred overnight and let warm to room temperature. The reaction was diluted with EtOAc and water, then separated and washed with brine (x8), dried with MgSO<sub>4</sub> and concentrated under reduced pressure. The crude product was purified by flash column chromatography (20% ether in hexane) to afford the product **219** as an opaque oil (78% yield); <sup>1</sup>H NMR (600 MHz, CDCl<sub>3</sub>) δ 7.62 (d, *J* = 8.3 Hz, 2H), 7.08 (d, *J* = 8.2 Hz, 2H), 3.92 (s, 1H), 3.51 (s, 3H), 3.15 (s, 3H), 2.07 – 1.97 (m, 1H), 1.72 – 1.63 (m, 1H), 1.31 – 1.19 (m, 8H), 0.85 (t, *J* = 6.8 Hz, 3H); <sup>13</sup>C NMR (151 MHz, CDCl<sub>3</sub>) δ 174.2, 140.0, 137.5, 130.2, 92.1, 61.3, 47.0, 33.9, 32.2, 31.6, 29.1, 27.6, 22.5, 14.0; IR (Neat Film) 2930, 2853, 1742, 1659, 1483, 1459, 1380, 1177, 1115, 1060, 1006, 806, 627, 610 cm<sup>-1</sup>; (MM:ESI<sup>+</sup>) *m/z* calcd for C<sub>16</sub>H<sub>25</sub>INO<sub>2</sub> (M+H)<sup>+</sup> 390.0852 found 390.0859.

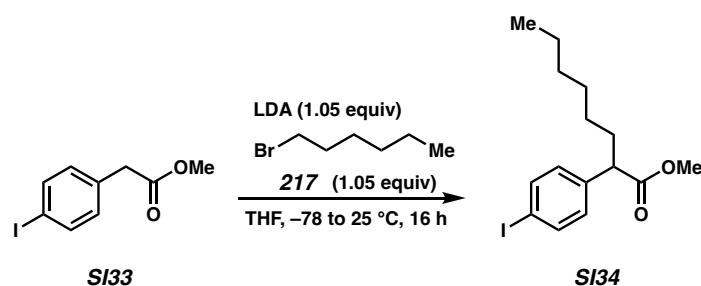


**(S)-5-iodo-2-(1-(methoxy(methyl)amino)-1-oxooctan-2-yl)-1,3-phenylene diacetate**

**(220):** The procedure is adapted from the literature<sup>9</sup>: To a flame-dried 20-ml vial was added Pd(OAc)<sub>2</sub> (38.6 mg, 172 μmol, 20 mol %), PhI(OAc)<sub>2</sub> (1.11 g, 3.44 mmol, 4.0 equiv), and (S)-2-(4-iodophenyl)-N-methoxy-N-methyloctanamide **219** (335 mg, 861 μmol, 1.0 equiv). Then HFIP (8.6 ml) and Ac<sub>2</sub>O (1.63 ml, 117.2 mmol, 20 equiv) were added and the septum cap was exchanged with a Teflon septum-lined screw cap and heated to 80 °C for 6 days. The reaction was cooled to room temperature, diluted with EtOAc and filtered over celite. The eluent was concentrated under reduced pressure and purified by flash column chromatography (30% ether in hexanes) to deliver the product **220** as a yellow oil (58% yield); <sup>1</sup>H NMR (600 MHz, CDCl<sub>3</sub>) δ 7.33 (s, 2H), 3.93 – 3.88 (m, 1H), 3.13 (s, 3H), 3.06 (s, 3H), 2.29 (s, 6H), 2.11 (dddd, *J* = 13.8, 10.5, 7.2, 4.6 Hz, 1H), 1.31 – 1.19 (m, 8H), 1.14 – 1.07 (m, 1H), 0.86 (t, *J* = 7.0 Hz, 3H); <sup>13</sup>C NMR (151 MHz, CDCl<sub>3</sub>) δ 172.6, 168.5, 149.2, 129.8, 126.6, 89.1, 60.3, 39.9, 32.1, 31.7, 30.0, 29.2, 27.6, 22.6, 20.7, 14.1; IR (Neat Film) 2930, 1770, 1665, 1589, 1459, 1368, 1189, 1036, 907 cm<sup>-1</sup>; (MM:ESI<sup>+</sup>) *m/z* calcd for C<sub>20</sub>H<sub>28</sub>INO<sub>6</sub> (M+H)<sup>+</sup> 506.1040 found 506.1031.

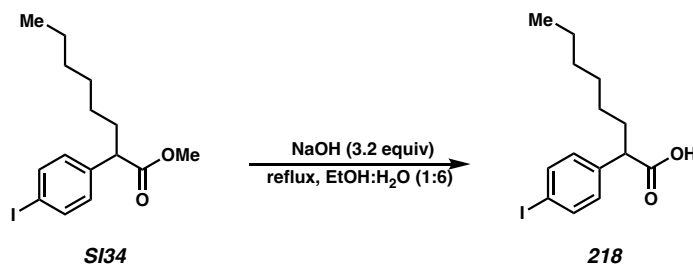


**Methyl 2-(4-iodophenyl)acetate (SI33):** To a 250 mL round bottom flask was added MeOH (100 mL) and 2-(4-iodophenyl)acetic acid **193** (20.2 g, 77.4 mmol, 1.0 equiv). Concentrated sulfuric acid (1.65 mL, 30.9 mmol, 0.4 equiv) was added slowly and the reaction mixture was heated to reflux for 24 hours. The volatiles were removed via rotary evaporation and the crude residue was taken up in EtOAc (100 mL). The organic layer was washed with Sat'd NaCl (75 mL), Sat'd NaHCO<sub>3</sub> (75 mL) and then the organic layer was dried over Na<sub>2</sub>SO<sub>4</sub>. The organic layer was then dried via rotary evaporator to afford methyl ester **SI33** as a brown oil (21.3 g, 77.3 mmol, 99% yield). The crude reaction mixture was pure enough to be used directly in the next step. The physical and spectral data were identical to those previously reported for this compound; <sup>1</sup>H NMR (400 MHz, CDCl<sub>3</sub>) δ 7.66 (d, *J* = 8.3 Hz, 2H), 7.12 – 6.86 (m, 2H), 3.70 (s, 3H), 3.57 (s, 2H); <sup>13</sup>C NMR (101 MHz, CDCl<sub>3</sub>) δ 171.48, 137.68, 133.58, 131.32, 92.69, 52.20, 40.66.



**Methyl 2-(4-iodophenyl)octanoate (SI34):** To a flame dried 500 mL round bottom was added *i*-PrNH<sub>2</sub> (9.6 mL, 68.5 mmol, 1.05 equiv) and THF (100 mL). The mixture was cooled to -78 °C, then a solution of *n*-BuLi (2.5M in hexanes, 27.4 mL, 68.5 mmol, 1.05 equiv) was added slowly and the reaction mixture was stirred at -78 °C for 15 minutes.

After 15 minutes, a solution of methyl 2-(4-iodophenyl)acetate **SI33** (18.0 g, 65 mmol, 1.0 equiv) was added as a solution in THF slowly at  $-78\text{ }^{\circ}\text{C}$ . After the addition, the reaction mixture was stirred at  $-78\text{ }^{\circ}\text{C}$  for 15 minutes. After stirring for 15 minutes, 1-bromo-hexane **217** (9.5 mL, 68.5 mmol, 1.05 equiv) was added slowly. The reaction was stirred at  $-78\text{ }^{\circ}\text{C}$  then slowly allowed to warm to ambient temperature overnight. After 16 hours, the reaction was quenched with 1N  $\text{NH}_4\text{Cl}$  and allowed to stir for 30 minutes. The aqueous layer was extracted with EtOAc (3 x 100 mL) and the combined organic layers were dried over  $\text{Na}_2\text{SO}_4$ . The organic layer was dried via rotary evaporator to deliver the alkylated product **SI34** as a brown oil (23.1 g total, 63 mmol, 97% yield).  $^1\text{H NMR}$  (400 MHz,  $\text{CDCl}_3$ )  $\delta$  7.68 – 7.61 (m, 2H), 7.10 – 7.02 (m, 2H), 3.66 (s, 3H), 3.42 (t,  $J = 6.9\text{ Hz}$ , 1H), 2.07 – 1.99 (m, 1H), 1.86 (dq,  $J = 8.8, 7.0\text{ Hz}$ , 1H), 1.73 (ddd,  $J = 11.3, 6.7, 3.8\text{ Hz}$ , 1H), 1.53 – 1.38 (m, 1H), 1.35 – 1.17 (m, 14H), 0.94 – 0.82 (m, 5H). Note: on larger scale, O-alkylation product can occur. The mixture of C-alkylation and O-alkylation can be carried forward to the next step without further purification.

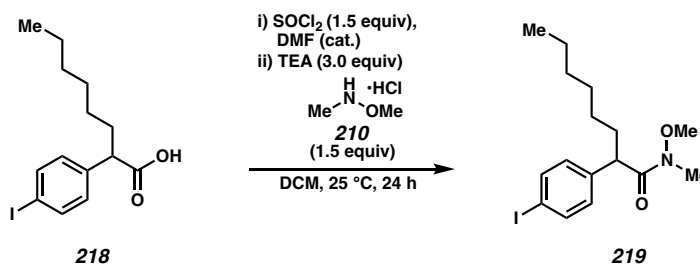


**2-(4-iodophenyl)octanoic acid (218):** To a 500 mL round bottom flask was added methyl 2-(4-iodophenyl)octanoate **SI34** (23.1 g, 63 mmol, 1.0 equiv) and dissolved in EtOH (40 mL). Deionized water (240 mL) was then added followed by NaOH (8.0 g, 200 mmol, 3.2 equiv). The reaction mixture was heated to reflux and stirred overnight. After 16 hours, the reaction was allowed to cool, diluted with EtOAc and then acidified with 1N HCl. The



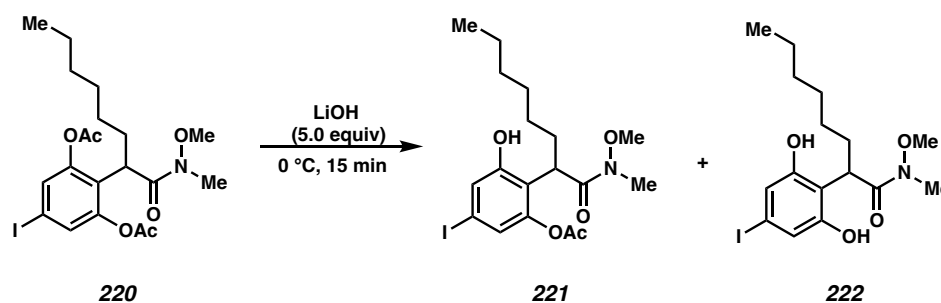
layers were separated and the aqueous layer was extracted with EtOAc (3 x 150 mL). The combined organic layers were washed with Sat'd NaCl (150 mL) and then dried over Na<sub>2</sub>SO<sub>4</sub>. The organic layer was then concentrated via rotary evaporator and columned via flash chromatography to afford alkylated carboxylic acid **218** as a black oil (20.3 g, 58.6 mmol, 93% yield). The physical and spectral data were identical to those previously reported for this compound using the enantioselective model approach above.

Note: starting material acid **193** could be recovered from the O-alkylated isomer present from the previous step

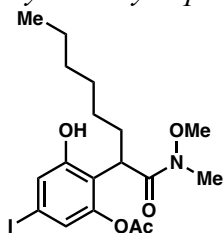


**2-(4-iodophenyl)-N-methoxy-N-methyloctanamide (219):** To a flame dried 250 mL round bottom flask was added 2-(4-iodophenyl)octanoic acid **218** (11 g, 31.7 mmol, 1.0 equiv) in DCM (150 mL). The reaction mixture was cooled to 0 °C followed by addition of oxalyl chloride (4.1 mL, 47.6 mmol, 1.5 equiv). Bubbles may form. After the addition of oxalyl chloride, DMF (2 drops) was added to the reaction mixture and allowed to warm to ambient temperature. Once warmed to 25 °C, bubbles were observed. The reaction was stirred for three hours, or until the observation of gas evolution ceased. After the specified time, the volatiles were carefully removed via rotary evaporation. Note: the corresponding acyl chloride is very pungent and should be concentrated in a hood if possible. Meanwhile, N,O-dimethylhydroxylamine hydrochloride **210** (4.6 g, 47.6 mmol, 1.5 equiv) was free based in DCM (150 mL) and Et<sub>3</sub>N (13.3 mL, 95.1 mmol, 3.0 equiv) and stirred until the

amine was fully dissolved. After the solution is prepared, it was added slowly to the crude acyl chloride obtained from rotary evaporation. The reaction was allowed to stir at ambient temperature overnight. After 16 hours, the reaction was quenched with 1N NaOH. The layers were separated, and the aqueous layer was extracted with EtOAc (3 x 150 mL). The combined organic layers were dried over Na<sub>2</sub>SO<sub>4</sub> and concentrated via rotary evaporator to deliver Weinrab amide **219** as an orange-brown oil (11.6 g, 29.8 mmol, 94% yield) without need for further purification. The physical and spectral data were identical to those previously reported for this compound using the enantioselective model approach above. Note: CDI under reflux in DCM can be used instead of the conditions provided to deliver the amide product **219** in good yield.



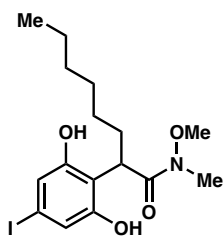
The hydrolysis of model Weinreb amide was performed as follows. The amide **220** (30.4 mg, 0.06 mmol, 1.0 equiv) was dissolved in THF (0.25 mL) and DI H<sub>2</sub>O (0.25 mL). The reaction mixture was cooled to 0 °C and LiOH (7 mg, 0.3 mmol, 5.0 equiv) was added in one portion. The reaction was stirred at 0 °C for the allotted time (15 minutes), and then quenched with Sat'd NH<sub>4</sub>Cl. The layers were separated, and the aqueous layer was extracted with EtOAc (3 x 10 mL) to deliver hydrolyzed model products. Products were sufficiently pure for analysis via crude NMR, but not separated via column chromatography.



221

**3-hydroxy-5-iodo-2-(1-(methoxy(methyl)amino)-1-oxooctan-2-yl)phenyl acetate**

**(221):** Monophenol **221** was prepared from the procedure reported above. LiOH (7 mg, 0.3 mmol, 5.0 equiv) was used and the reaction was stirred at 0 °C for 15 minutes. Product **221** was obtained as a 9:1 mixture of mono:bis phenol products (22 mg, 0.048 mmol, 80% yield). <sup>1</sup>H NMR (400 MHz, CDCl<sub>3</sub>) δ 10.71 (s, 1H), 7.20 (d, *J* = 1.7 Hz, 1H), 6.93 (d, *J* = 1.8 Hz, 1H), 4.49 (t, *J* = 7.9 Hz, 1H), 3.74 (s, 3H), 3.25 (s, 3H), 2.32 (d, *J* = 1.3 Hz, 3H), 2.10 – 2.00 (m, 1H), 1.90 – 1.80 (m, 1H), 1.25 – 1.10 (m, 8H), 0.93 – 0.81 (m, 3H); <sup>13</sup>C NMR (101 MHz, CDCl<sub>3</sub>) δ 176.03, 168.74, 158.81, 149.18, 126.08, 123.06, 117.31, 92.07, 61.98, 37.38, 32.41, 31.67, 30.42, 29.00, 27.79, 22.73, 20.90, 14.17.

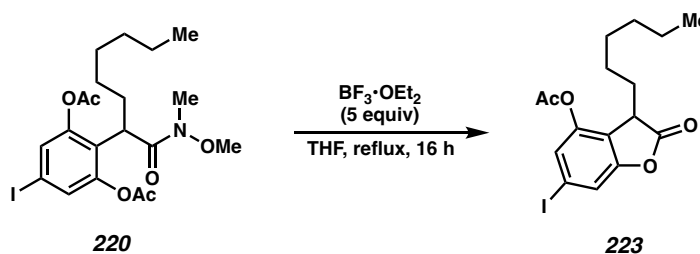


222

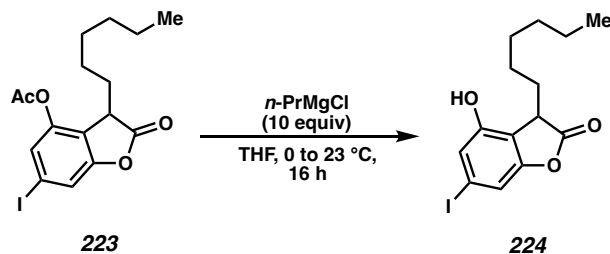
**2-(2,6-dihydroxy-4-iodophenyl)-N-methoxy-N-methyloctanamide (222):**

Bisphenol **222** can be prepared from the procedure reported above. LiOH (7 mg, 0.03 mmol, 5.0 equiv) was used and the reaction was stirred at 25 °C for 15 minutes. Product **222** was obtained as a 4:1 mixture of bis:mono phenol products (21 mg, 0.05 mmol, 83% yield). <sup>1</sup>H NMR (400 MHz, CDCl<sub>3</sub>) δ 7.36 (dd, *J* = 1.3, 0.6 Hz, 1H), 7.29 (d, *J* = 1.3 Hz, 1H), 4.92 (t,

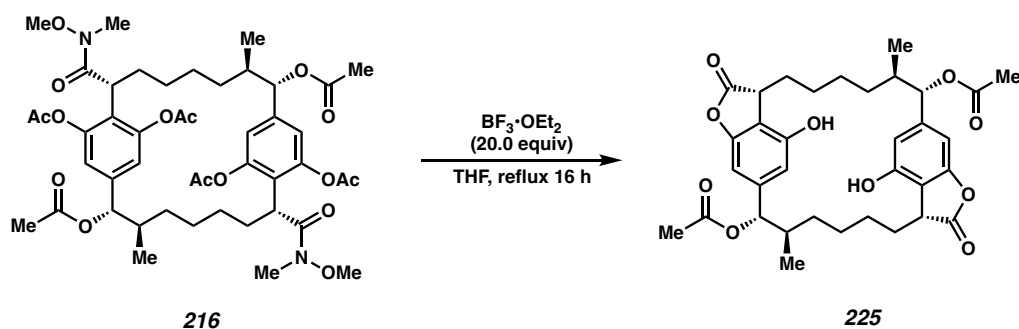
$J = 7.9$  Hz, 1H), 3.76 (s, 3H), 3.25 (s, 3H), 2.11 – 1.99 (m, 1H), 1.91 – 1.80 (m, 1H), 1.22 – 1.13 (m, 8H), 0.94 – 0.80 (m, 3H);  $^{13}\text{C}$  NMR (101 MHz,  $\text{CDCl}_3$ )  $\delta$  175.65, 167.84, 154.87, 147.04, 127.00, 119.57, 117.90, 91.85, 62.18, 43.32, 32.41, 31.75, 31.47, 30.55, 29.07, 27.62, 25.43, 22.58, 20.84, 14.12.



**3-hexyl-6-iodo-2-oxo-2,3-dihydrobenzofuran-4-yl acetate (223):** A solution of Weinreb amide **220** (30 mg, 0.06 mmol, 1.0 equiv) was dissolved in THF (1 mL) followed by addition of  $\text{BF}_3 \cdot \text{OEt}_2$  (37  $\mu\text{L}$ , 0.3 mmol, 5.0 equiv) at 25 °C. The reaction was heated to reflux for 16 hours, then cooled to 25 °C. Once cool, sat'd  $\text{NH}_4\text{Cl}$  (2 mL) was added to the reaction mixture. The layers were separated, and the aqueous layer was extracted with EtOAc (3 x 5 mL). The combined organic layers were dried over  $\text{Na}_2\text{SO}_4$  then concentrated via rotary evaporator. The crude oil was purified via column chromatography (35% EtOAc in hexanes) to deliver lactone product **223** (18.8 mg, 0.047 mmol, 78% yield);  $^1\text{H}$  NMR (400 MHz,  $\text{CDCl}_3$ )  $\delta$  7.37 (dd,  $J = 1.3, 0.6$  Hz, 1H), 7.29 (d,  $J = 1.3$  Hz, 1H), 3.75 (dd,  $J = 6.3, 4.4$  Hz, 1H), 2.32 (s, 3H), 2.04 (ddt,  $J = 16.1, 14.1, 5.0$  Hz, 1H), 1.93 – 1.81 (m, 1H), 1.32 – 1.14 (m, 8H), 0.95 – 0.76 (m, 3H);  $^{13}\text{C}$  NMR (101 MHz,  $\text{CDCl}_3$ )  $\delta$  175.64, 167.83, 154.89, 147.06, 127.00, 119.58, 117.91, 91.85, 43.33, 31.49, 29.86, 29.09, 25.45, 22.60, 20.85, 14.13.



**3-hexyl-4-hydroxy-6-iodobenzofuran-2(3H)-one (224):** To a 1-dram vial was added lactone **223** (8 mg, 0.02 mmol, 1.0 equiv) dissolved in THF (1.0 mL) and cooled to 0 °C. A solution of *n*-PrMgCl (1M in 2-Me-THF, 200  $\mu$ L, 0.2 mmol, 10 equiv) was added in one portion to the reaction mixture followed. The reaction was allowed to warm to 25 °C and stirred 16 hours. After the stir period, the reaction was quenched with MeOH (1.0 mL) and stirred for 30 minutes at ambient temperature. Then, 1N NH<sub>4</sub>Cl (2.0 mL) was added. The layers were separated, and the aqueous layer was extracted with EtOAc (3 x 5 mL). The combined organic layers were dried over Na<sub>2</sub>SO<sub>4</sub> and concentrated via rotary evaporator to afford a crude oil, which was purified via column chromatography (45% acetone in hexanes) to deliver phenol **224** as a yellow oil (6.5 mg, 0.018 mmol, 90% yield). <sup>1</sup>H NMR (400 MHz, CDCl<sub>3</sub>)  $\delta$  7.08 (d, *J* = 1.3 Hz, 1H), 6.96 (d, *J* = 1.3 Hz, 1H), 5.48 (s, 1H), 4.12 – 3.99 (m, 1H), 3.79 (t, *J* = 5.3 Hz, 1H), 2.12 – 2.01 (m, 4H), 1.33 – 1.19 (m, 16H), 0.94 – 0.76 (m, 7H).

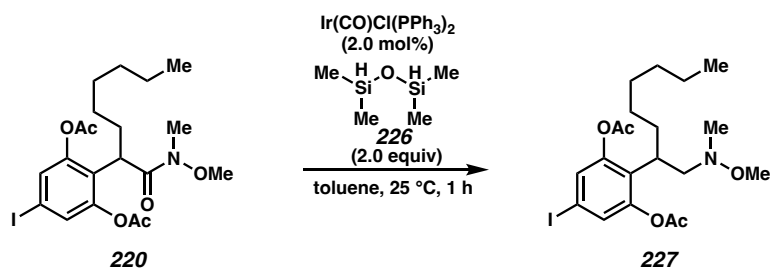


**(3aR,8R,9S,15aR,20R,21S)-8,20-dimethyl-3,15-dioxo-**

**3,3a,4,5,6,7,8,9,15,15a,16,17,18,19,20,21-hexadecahydro-1,22:10,13-**

**di(metheno)cyclodocosa[1,2-c:12,13-c']difuran-9,12,21,24-tetrayl tetraacetate (225):**

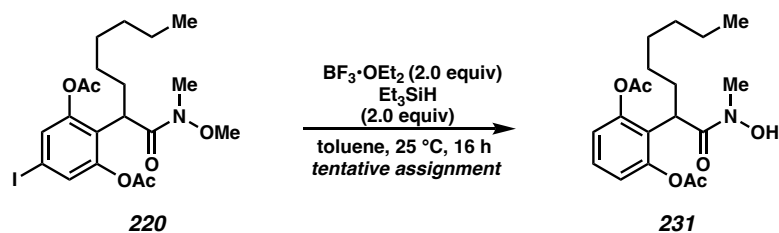
Macrocycle **216** (2 mg, 2.2  $\mu\text{mol}$ , 1.0 equiv) was dissolved in THF (1 mL). Freshly distilled  $\text{BF}_3 \cdot \text{OEt}_2$  (5.4  $\mu\text{L}$ , 0.044 mmol, 20 equiv) was added in one portion and the reaction mixture was heated to reflux. The resulting reaction mixture was stirred for 16 hours. After 16 hours, the reaction was cooled to ambient temperature and quenched with sat'd  $\text{NH}_4\text{Cl}$  (1 mL). The layers were separated and the aqueous layer was extracted with EtOAc (3 x 5 mL). The combined organic layers were dried over  $\text{Na}_2\text{SO}_4$  and concentrated via rotary evaporator. The crude oil was purified via flash chromatography (45% EtOAc in hexanes) to yield macrocycle **225** (1.1 mg, 1.76  $\mu\text{mol}$ , 80% yield) as a white solid.  $^1\text{H}$  NMR (400 MHz,  $\text{CDCl}_3$ )  $\delta$  6.85 (d,  $J = 1.2$  Hz, 2H), 6.71 (d,  $J = 1.2$  Hz, 2H), 5.26 – 5.15 (m, 2H), 3.77 (t,  $J = 4.4$  Hz, 2H), 2.26 (s, 6H), 1.96 (overlap, 8H), 1.77 (dd,  $J = 16.3, 10.7$  Hz, 2H), 1.25 – 1.09 (m, 8H), 0.92 (d,  $J = 6.6$  Hz, 6H), 0.86 – 0.73 (m, 6H).



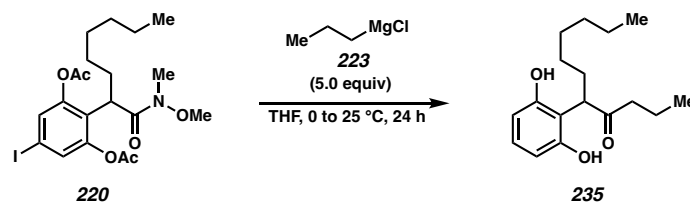
**5-iodo-2-(1-(methoxy(methyl)amino)octan-2-yl)-1,3-phenylene diacetate (227):** Model

Weinreb amide **220** (18 mg, 0.036 mmol, 1.0 equiv) and Vaska's catalyst (1.4 mg, 1.78  $\mu\text{mol}$ , 2 mol%) was dissolved in toluene (0.5 mL) followed by the addition of 1,1,3,3-

tetramethyldisiloxane **226** (16  $\mu$ L, 0.08 mmol, 2.0 equiv). The reaction was stirred at 25  $^{\circ}$ C for 1 hour. The reaction was quenched with sat'd NaHCO<sub>3</sub> (1 mL). The layers were separated, and the aqueous layer was extracted with EtOAc (3 x 5 mL). The combined organic layers were dried over Na<sub>2</sub>SO<sub>4</sub> and concentrated via rotary evaporator. The crude oil was purified via column chromatography (45% EtOAc in hexanes) to deliver amine **227** as a pale-yellow oil (12.4 mg, 0.025 mmol, 70 % yield). <sup>1</sup>H NMR (400 MHz, CDCl<sub>3</sub>)  $\delta$  7.30 (s, 2H), 3.43 (s, 3H), 3.27 – 3.17 (m, 1H), 2.81 (q,  $J$  = 7.5 Hz, 2H), 2.51 (s, 3H), 2.30 (s, 6H), 1.31 – 1.17 (m, 4H), 1.15 – 1.06 (m, 4H), 0.85 (t,  $J$  = 6.9 Hz, 4H).



**2-(1-(hydroxy(methyl)amino)-1-oxooctan-2-yl)-1,3-phenylene diacetate (231):** Model Weinreb amide **220** (10 mg, 0.02 mmol, 1.0 equiv) and triethylsilane (3.5  $\mu$ L, 0.04 mmol, 2.0 equiv) was dissolved in toluene (0.5 mL) followed by the addition of BF<sub>3</sub>•OEt<sub>2</sub> (5  $\mu$ L, 0.04 mmol, 2.0 equiv). The reaction was stirred at 25  $^{\circ}$ C overnight. The reaction was quenched with sat'd NaHCO<sub>3</sub> (2 mL). The layers were separated, and the aqueous layer was extracted with EtOAc (3 x 5 mL). The combined organic layers were dried over Na<sub>2</sub>SO<sub>4</sub> and concentrated via rotary evaporator. The crude oil **231** was sufficient for NMR analysis (6.8 mg, 0.0186 mmol, 92 % yield); <sup>1</sup>H NMR (400 MHz, CDCl<sub>3</sub>)  $\delta$  7.41 (t,  $J$  = 8.3 Hz, 1H), 7.07 (d,  $J$  = 8.3 Hz, 1H), 3.93 (t,  $J$  = 7.2 Hz, 0H), 3.13 (s, 2H), 2.39 (s, 3H), 2.26 – 2.15 (m, 0H), 1.79 – 1.66 (m, 0H), 1.32 – 1.17 (m, 8H), 0.92 – 0.82 (m, 2H).

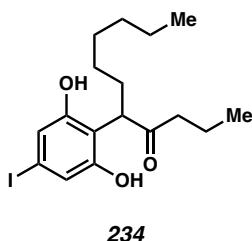


The general procedure for the Grignard addition into model Weinreb amide is as follows.

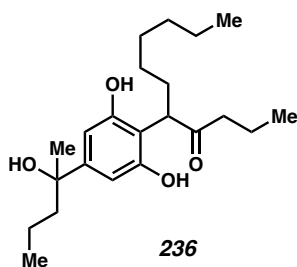
**5-(2,6-dihydroxyphenyl)undecan-4-one (235):** To a 20 mL scintillation vial was added Weinreb amide (102 mg, 0.2 mmol, 1.0 equiv) in THF (10 mL), and the reaction mixture was cooled to 0 °C. Then, a solution of Grignard reagent **223** (1.0 M in 2-Me-THF, 1 mL, 1 mmol, 5.0 equiv) was slowly added to the reaction mixture and stir at 0 °C for 1 hour. After 1 hour, the reaction was allowed to warm to ambient temperature and stirred for 24 hours. After the stir period, MeOH (1 mL) was added to the reaction mixture. The reaction mixture was then diluted with EtOAc (10 mL) and quenched with 1N HCl (4 mL). The layers were separated and the aqueous layer was extracted with EtOAc (3 x 15 mL). The organic layers were combined, dried over Na<sub>2</sub>SO<sub>4</sub> and concentrated via rotary evaporator. The crude oil was purified via column chromatography (50% EtOAc in hexanes) to deliver resorcinol product **235** as a pale-yellow oil (31 mg, 0.11 mmol, 55% yield); <sup>1</sup>H NMR (400 MHz, CDCl<sub>3</sub>) δ 6.97 (t, *J* = 8.1 Hz, 1H), 6.41 (d, *J* = 8.1 Hz, 2H), 4.55 (dd, *J* = 8.4, 7.1 Hz, 1H), 2.62 (ddd, *J* = 7.7, 6.7, 5.4 Hz, 2H), 1.99 (ddt, *J* = 13.5, 9.1, 6.8 Hz, 1H), 1.92 – 1.83 (m, 1H), 1.67 – 1.57 (m, 2H), 1.47 – 1.18 (m, 8H), 1.00 – 0.74 (m, 6H); <sup>13</sup>C NMR (101 MHz, CDCl<sub>3</sub>) δ 218.20, 155.89, 128.67, 123.44, 110.84, 109.10, 107.63, 103.92, 72.98, 47.19, 46.07, 44.28, 31.62, 29.36, 29.09, 27.79, 26.93, 22.58, 17.17, 16.83, 14.71, 14.06, 13.56. (Can scale up to 1 mmol without dramatic reduction in yield)



The Grignard products **234** and **236** could also be based on equivalents of Grignard reagent **223** used.

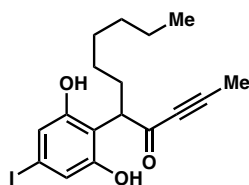


**5-(2,6-dihydroxy-4-iodophenyl)undecan-4-one (234):** was observed when using 3.0 equivalents of *n*-PrMgCl. The product **234** was obtained as a pale-yellow oil (16 mg, 0.04 mmol, 20% yield) after purification via column chromatography (40% EtOAc in hexanes); <sup>1</sup>H NMR (400 MHz, CDCl<sub>3</sub>) δ 6.79 (s, 2H), 4.49 (dd, *J* = 8.6, 6.9 Hz, 1H), 2.59 (dtd, *J* = 17.6, 7.2, 2.5 Hz, 3H), 1.67 – 1.54 (m, 4H), 1.34 – 1.18 (m, 8H), 0.98 – 0.82 (m, 6H); <sup>13</sup>C NMR (101 MHz, CDCl<sub>3</sub>) δ 218.31, 156.34, 118.46, 110.95, 92.01, 60.51, 47.01, 46.15, 44.25, 31.59, 29.72, 29.32, 29.05, 27.70, 22.58, 17.17, 16.81, 14.71, 14.05, 13.55.



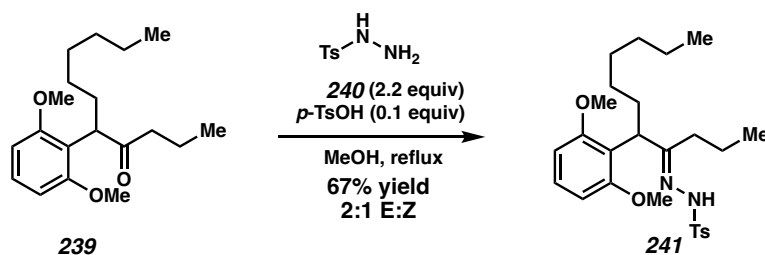
**5-(2,6-dihydroxy-4-(2-hydroxypentan-2-yl)phenyl)undecan-4-one (236):** was observed when using 5.0 equivalents of *n*-PrMgCl. The product **236** was obtained as a pale-yellow oil (25 mg, 0.07 mmol, 35% yield) after column chromatography (75% EtOAc in hexanes). This product was challenging to purify as the resorcinol **236** and was taken as an

approximately 65% pure mixture through the methylation phase.  $^1\text{H}$  NMR (400 MHz,  $\text{CDCl}_3$ )  $\delta$  6.50 (d,  $J = 1.2$  Hz, 2H), 4.52 (t,  $J = 7.7$  Hz, 1H), 2.68 – 2.54 (m, 3H), 1.78 – 1.69 (m, 1H), 1.67 – 1.56 (m, 2H), 1.48 (s, 3H), 1.28 – 1.13 (m, 12H), 0.99 – 0.76 (m, 9H).



**281**

**5-(2,6-dihydroxy-4-iodophenyl)undec-2-yn-4-one (281):** was observed when using prop-1-yn-1-ylmagnesium bromide **282** (0.5M sol'n in THF, 6 mL, 3 mmol, 15 equiv). The product **281** was obtained as a pale-yellow oil (52 mg, 0.13 mmol, 65% yield) after column chromatography (55% EtOAc in hexanes). No protodeiodination observed.  $^1\text{H}$  NMR (400 MHz,  $\text{CDCl}_3$ )  $\delta$  6.80 (s, 2H), 4.51 (dd,  $J = 9.1, 6.2$  Hz, 1H), 2.04 (s, 3H), 1.33 – 1.16 (m, 8H), 0.97 – 0.76 (m, 3H).

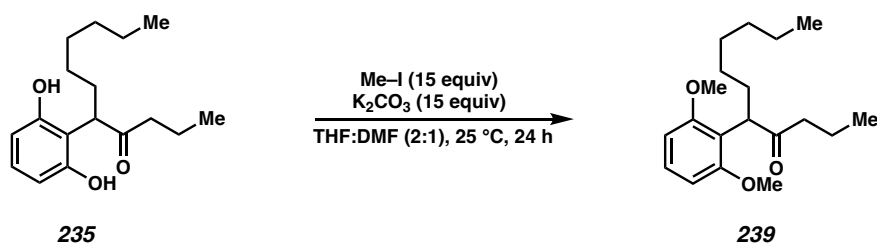


The general procedure for the hydrazone formation from the model ketone is as follows.

**(E)-N'-(5-(2,6-dimethoxyphenyl)undecan-4-ylidene)-4-**

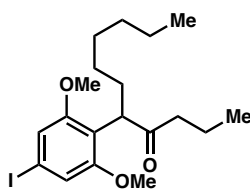
**methylbenzenesulfonylhydrazide (241):** To a 1 dram scintillation vial was added model ketone **239** (25 mg, 0.082 mmol, 1.0 equiv) and dissolved in MeOH (2.5 mL). *P*-TsOH (1.4 mg, 0.008 mmol, 0.1 equiv) was added to the reaction mixture followed by 4-methylbenzenesulfonylhydrazide **240** (33 mg, 0.18 mmol, 2.2 equiv). The reaction mixture

was heated to reflux and stirred overnight. After 16 hours, the reaction was cooled to ambient temperatures and quenched with Sat'd NaHCO<sub>3</sub> (5 mL). The layers were separated, and the aqueous layer was extracted with EtOAc (3 x 15 mL). The organic layers were combined and dried over Na<sub>2</sub>SO<sub>4</sub>, then concentrated via rotary evaporator. The corresponding white solid **241** was obtained (26 mg, 0.055 mmol, 67% yield, 2:1 E:Z ratio) after column chromatography (35% EtOAc in hexanes) <sup>1</sup>H NMR (400 MHz, CD<sub>3</sub>OD) δ 7.93 – 7.77 (m, 1.4H), 7.38 – 7.33 (m, 1.4H), 7.30 – 7.23 (m, 1H), 7.19 – 7.13 (m, 0.6H), 7.12 (t, *J* = 8.3 Hz, 0.6H), 6.63 (d, *J* = 8.4 Hz, 0.6H), 6.51 (d, *J* = 8.4 Hz, 1.4H), 4.04 (dd, *J* = 8.2, 5.8 Hz, 0.7H), 3.99 (dd, *J* = 10.0, 5.2 Hz, 0.3H), 3.75 (s, 1.8H), 3.51 (s, 4.2H), 2.43 (s, 2.1H), 2.35 (s, 0.9H), 2.15 (ddd, *J* = 13.5, 9.8, 6.2 Hz, 0.7H), 2.11 – 1.99 (m, 0.7H), 1.98 – 1.87 (m, 0.3H), 1.75 (ddt, *J* = 12.8, 9.7, 5.6 Hz, 0.3H), 1.68 – 1.45 (m, 3H), 1.41 – 1.06 (m, 8H), 0.95 – 0.68 (m, 6H); <sup>13</sup>C NMR (101 MHz, CD<sub>3</sub>OD) (2:1 mixture of isomers) δ 163.25, 162.30,\* 158.79, 157.78,\* 143.43, 143.33,\* 136.37, 135.38,\* 128.92, 128.75, 128.11, 127.72, 127.07, 117.77, 114.68, 104.27, 103.78, 54.78, 54.49, 40.85, 36.25, 35.06, 31.67, 31.46, 30.41, 29.30, 29.15, 28.78, 27.22, 26.94, 22.36, 22.20, 20.13, 20.05, 19.55, 18.18, 13.14, 13.04, 12.99, 12.88.



The general procedure for the methylation of the resorcinol in the model ketone is as follows.

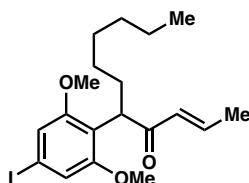
**5-(2,6-dimethoxyphenyl)undecan-4-one (239):** To a 20 mL scintillation vial was added resorcinol product **235** (278 mg, 1 mmol, 1.0 equiv) and dissolved in THF (10 mL) and DMF (5 mL). Then,  $K_2CO_3$  (2.07 g, 15 mmol, 15.0 equiv) was added in one portion followed by the addition of methyl iodide (0.96 mL, 15 mmol, 15.0 equiv). The reaction was stirred at ambient temperature for 24 hours. After the stir period, the reaction was quenched with 1N  $NH_4Cl$  and stirred for 30 minutes at ambient temperature. The layers were separated, and the aqueous layer was extracted with EtOAc (3 x 25 mL). The combined organic layers were then washed with Sat'd  $Na_2S_2O_3$  until no precipitate was observed in the aqueous layer of the wash. Then, the organic layer was washed with 1N LiCl (2 x 25 mL) and then dried over  $Na_2SO_4$ . The organic layer was concentrated via rotary evaporator to afford a crude oil, which was purified via column chromatography (10% EtOAc in hexanes) to deliver methylated product **239** as a pale-yellow oil (265 mg, 0.87 mmol, 87% yield);  $^1H$  NMR (400 MHz,  $CDCl_3$ )  $\delta$  7.21 (t,  $J = 8.3$  Hz, 1H), 6.56 (d,  $J = 8.3$  Hz, 2H), 3.94 (dd,  $J = 8.9, 5.0$  Hz, 1H), 3.78 (s, 6H), 2.21 – 2.06 (m, 3H), 1.69 – 1.55 (m, 1H), 1.54 – 1.40 (m, 2H), 1.34 – 1.12 (m, 9H), 1.03 (tt,  $J = 10.4, 6.3$  Hz, 1H), 0.95 – 0.89 (m, 2H), 0.89 – 0.75 (m, 6H);  $^{13}C$  NMR (101 MHz,  $CDCl_3$ )  $\delta$  211.58, 158.37, 128.18, 117.82, 104.04, 55.70, 48.19, 42.00, 31.98, 29.53, 28.44, 27.47, 22.83, 17.65, 14.26, 13.95.



**238**

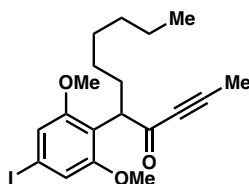
**5-(4-iodo-2,6-dimethoxyphenyl)undecan-4-one (238):** was prepared from the procedure disclosed above using model ketone **234** (25 mg, 0.06 mmol, 1.0 equiv). The bismethyl

ether product **238** was obtained as a pale-yellow oil (23.8 mg, 0.055 mmol, 89% yield) after column chromatography (10% EtOAc in hexanes);  $^1\text{H}$  NMR (400 MHz,  $\text{CDCl}_3$ )  $\delta$  6.88 (s, 2H), 3.89 – 3.84 (m, 1H), 3.76 (s, 3H), 2.11 (t,  $J = 7.3$  Hz, 3H), 1.50 (qd,  $J = 7.6$ , 3.6 Hz, 2H), 1.32 – 1.14 (m, 11H), 0.91 – 0.78 (m, 7H).



**SI35**

**(E)-5-(4-iodo-2,6-dimethoxyphenyl)undec-2-en-4-one (SI35)**: was prepared from the procedure disclosed above using model ketone **280**. The bismethyl ether product **SI35** was obtained as a pale-yellow oil (32 mg, 0.074 mmol, 64% yield) after column chromatography (10% EtOAc in hexanes). The NMR sample possessed impurities from alkylated plasticizer post column chromatography.  $^1\text{H}$  NMR (400 MHz,  $\text{CDCl}_3$ )  $\delta$  6.87 (s, 2H), 5.91 (dq,  $J = 15.5$ , 1.7 Hz, 1H), 5.75 – 5.67 (m, 1H), 4.01 (dd,  $J = 8.7$ , 5.1 Hz, 1H), 3.75 (s, 6H), 2.14 (pd,  $J = 7.5$ , 3.4 Hz, 2H), 1.72 (dd,  $J = 6.9$ , 1.7 Hz, 3H), 1.31 – 1.17 (m, 8H), 0.92 – 0.82 (m, 3H).

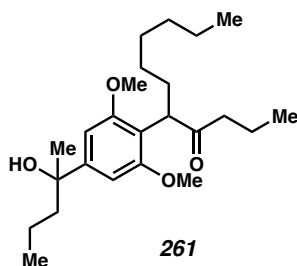


**283**

**5-(4-iodo-2,6-dimethoxyphenyl)undec-2-yn-4-one (283)**: was prepared from the procedure disclosed above using model ketone **281** (80 mg, 0.2 mmol, 1.0 equiv). The bismethyl ether product **283** was obtained as a pale-yellow oil (75.2 mg, 0.175 mmol, 87%

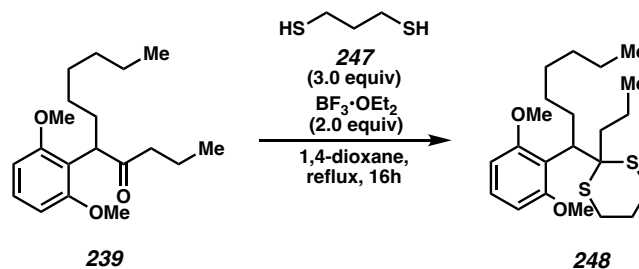
yield) after column chromatography (10% EtOAc in hexanes);  $^1\text{H NMR}$  (400 MHz,  $\text{CDCl}_3$ )

$\delta$  6.88 (s, 2H), 3.99 (dd,  $J = 9.1, 4.9$  Hz, 1H), 3.77 (s, 6H), 2.21 – 2.09 (m, 1H), 1.85 (s, 3H), 1.36 – 1.14 (m, 8H), 0.93 – 0.79 (m, 3H).



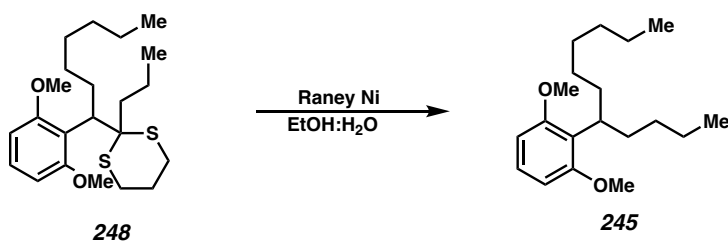
**5-(4-(2-hydroxypentan-2-yl)-2,6-dimethoxyphenyl)undecan-4-one (261):** was prepared from the procedure disclosed above using model ketone **236** (35 mg, 0.1 mmol, 1.0 equiv).

The bismethyl ether product **261** was obtained as a pale-yellow oil (27 mg, 0.07 mmol, 70% yield) after column chromatography (30% EtOAc in hexanes);  $^1\text{H NMR}$  (400 MHz,  $\text{CDCl}_3$ )  $\delta$  6.62 (s, 2H), 3.90 (dd,  $J = 8.7, 5.0$  Hz, 1H), 3.78 (s, 6H), 2.13 (t,  $J = 7.3$  Hz, 4H), 1.90 – 1.72 (m, 4H), 1.60 – 1.47 (m, 3H), 1.37 – 1.13 (m, 8H), 1.03 (ddt,  $J = 12.3, 7.2, 3.5$  Hz, 2H), 0.95 – 0.77 (m, 6H);  $^{13}\text{C NMR}$  (101 MHz,  $\text{CDCl}_3$ )  $\delta$  211.62, 157.86, 148.81, 148.78, 115.70, 100.73, 74.98, 55.55, 47.97, 46.59, 46.56, 41.87, 31.82, 29.93, 29.87, 29.36, 28.34, 27.34, 22.67, 17.53, 17.32, 17.30, 14.43, 14.11, 13.81.



**2-(4-(2,6-dimethoxyphenyl)decan-3-yl)-1,3-dithiane (248):** To a 1-dram vial was added model ketone **239** (30 mg, 0.1 mmol, 1.0 equiv) dissolved in dioxane (2 mL).  $\text{BF}_3 \cdot \text{OEt}_2$

(24  $\mu$ L, 0.2 mmol, 2.0 equiv) was added in one portion and the reaction mixture was heated to reflux overnight. After 16 hours, the reaction was quenched with DI H<sub>2</sub>O (2 mL) and diluted with EtOAc (5 mL) the layers were separated. The aqueous layer was extracted with EtOAc (3 x 10 mL). The organic phase was dried over Na<sub>2</sub>SO<sub>4</sub> and concentrated via rotary evaporator and the crude solid was triturated with DCM (3 x 5 mL) and filtrate concentrated to deliver crude oil (37 mg, 9:1 ratio **248:239**). Subjecting dithiane to column chromatography resulted in hydrolysis to the ketone starting material, so the triturated crude was carried through the next step with no purification. <sup>1</sup>H NMR (500 MHz, CDCl<sub>3</sub>)  $\delta$  7.18 (t, *J* = 8.4 Hz, 1H), 6.54 (d, *J* = 8.9 Hz, 2H), 4.02 (dd, *J* = 11.8, 3.9 Hz, 1H), 3.77 (s, 6H), 2.77 – 2.71 (m, 2H), 2.57 – 2.48 (m, 2H), 2.35 (dt, *J* = 13.7, 7.4 Hz, 2H), 1.75 (p, *J* = 7.0 Hz, 2H), 1.30 – 1.17 (m, 6H), 0.90 – 0.81 (m, 8H). (tentative assignment)



**1,3-dimethoxy-2-(undecan-5-yl)benzene (245):** To a 1 dram vial was added dithiane **248** (20 mg, 0.05 mmol, 1.0 equiv) dissolved in EtOH (1 mL). A slurry of Raney Ni (2 mL of suspension) was added to the reaction mixture and was stirred at ambient temperature for 24 hours. After 24 hours, the reaction was cooled to 0 °C and 1N HCl was slowly added to quench the remaining Raney Ni. Once the gray suspension turns blue, the aqueous layer was extracted with EtOAc (3 x 5 mL) and the combined organic layer was dried over Na<sub>2</sub>SO<sub>4</sub>. The organic layer was then concentrated via rotary evaporator and purified via

column chromatography (5% EtOAc in hexanes) to deliver the desired alkane product **245** (6 mg, 0.02 mmol, 40% yield) as a pale-yellow oil.  $^1\text{H}$  NMR (400 MHz,  $\text{CDCl}_3$ )  $\delta$  7.10 (dd,  $J = 9.2, 7.3$  Hz, 1H), 6.53 (dd,  $J = 8.2, 1.5$  Hz, 2H), 3.78 (d,  $J = 1.4$  Hz, 6H), 3.31 (ddq,  $J = 15.5, 9.7, 5.2$  Hz, 1H), 1.80 (dtd,  $J = 13.2, 9.5, 5.3$  Hz, 1H), 1.35 – 1.12 (m, 24H), 0.98 – 0.74 (m, 9H).

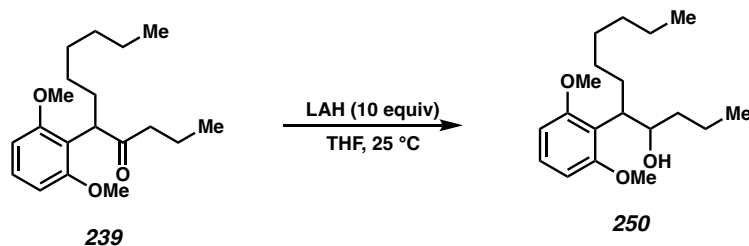
The alkane product was not separable from the hydrolyzed side product ketone **239** and was carried through the next step as a mixture of products (2:1).



**2-(undecan-5-yl)benzene-1,3-diol (249):** To a 1 dram vial was added bismethyl ether **245** (6 mg, 0.02 mmol, 1.0 equiv) in DCM (0.5 mL). The reaction mixture was cooled to  $-78$   $^\circ\text{C}$ . Then,  $\text{BBr}_3$  (19  $\mu\text{L}$ , 0.2 mmol, 10 equiv) was slowly added to the reaction mixture and the resultant solution was stirred at  $-78$   $^\circ\text{C}$  for 1 hour. After the 1 hour stir period, the reaction was allowed to slowly warm up to  $25$   $^\circ\text{C}$  and stirred overnight. Then, the reaction was quenched with sat'd  $\text{NaHCO}_3$  (2 mL) and the layers were separated. The aqueous layer was extracted with DCM (3 x 5 mL) and the combined organic layers were dried over  $\text{Na}_2\text{SO}_4$ . The organic layer was then concentrated via rotary evaporator and the crude oil was purified via column chromatography (25% EtOAc in hexanes) to deliver resorcinol **249** as a yellow oil.  $^1\text{H}$  NMR (400 MHz,  $\text{CDCl}_3$ )  $\delta$  6.90 (t,  $J = 8.0$  Hz, 1H), 6.33 (d,  $J = 7.9$  Hz, 2H), 3.11 (tt,  $J = 9.6, 5.8$  Hz, 1H), 1.85 (ddt,  $J = 14.4, 9.4, 4.4$  Hz, 2H), 1.76 – 1.58 (m,



22H), 1.39 – 1.18 (m, 48H), 0.94 – 0.81 (m, 11H); (tentative assignment, extraordinarily messy from the decomposition of ketone **239** under BBr<sub>3</sub> conditions).

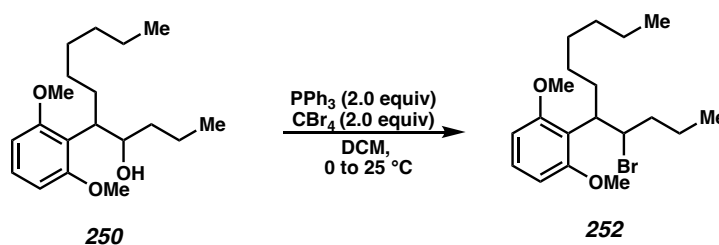


**5-(2,6-dimethoxyphenyl)undecan-4-ol (250):** To a 20 mL scintillation vial was added LAH (56 mg, 1.5 mmol, 10 equiv). The vial was cooled to 0 °C and suspended in THF (5 mL). In a separate vial, bismethoxy model ketone **239** (45 mg, 0.15 mmol, 1.0 equiv) was dissolved in THF (5 mL) and the solution was added to the LAH suspension at 0 °C. The reaction was allowed to warm to 25 °C and stirred for 4 hours. The reaction mixture was diluted with EtOAc (10 mL) and 3N NaOH (3 mL) was slowly added to quench the remaining LAH. The biphasic solution was stirred for 1 hour, the layers were separated and the aqueous layer was extracted with EtOAc (3 x 10 mL). The combined organic layers were dried over Na<sub>2</sub>SO<sub>4</sub> and then concentrated via rotary evaporator to deliver the crude oil. The crude mixture was purified via column chromatography (25% EtOAc in hexanes) to deliver alcohol **250** (41 mg, 0.134 mmol, 89% yield, 1.5:1 dr) as a pale-yellow oil. The diastereomers can be separated at this stage.

Major diastereomer: <sup>1</sup>H NMR (400 MHz, CDCl<sub>3</sub>) δ 7.09 (td, *J* = 8.3, 0.8 Hz, 1H), 6.51 (dd, *J* = 8.4, 4.7 Hz, 2H), 3.81 (ddd, *J* = 9.1, 5.9, 3.5 Hz, 1H), 3.75 (d, *J* = 3.8 Hz, 3H), 3.71 (s, 4H), 3.45 (dt, *J* = 9.6, 5.9 Hz, 1H), 1.79 (dtd, *J* = 14.1, 9.3, 5.0 Hz, 1H), 1.67 – 1.56 (m,

1H), 1.42 (tdd,  $J = 10.8, 8.5, 6.2$  Hz, 1H), 1.28 (dddd,  $J = 13.9, 6.7, 5.5, 3.8$  Hz, 2H), 1.18 – 1.06 (m, 21H), 0.98 (td,  $J = 9.4, 5.4$  Hz, 1H), 0.86 – 0.72 (m, 9H).

Minor diastereomer:  $^1\text{H}$  NMR (400 MHz,  $\text{CDCl}_3$ )  $\delta$  7.07 (t,  $J = 8.3$  Hz, 1H), 6.58 – 6.43 (m, 2H), 3.90 (ddd,  $J = 7.5, 5.8, 4.1$  Hz, 1H), 3.72 (s, 7H), 3.31 (ddd,  $J = 10.7, 5.9, 4.2$  Hz, 1H), 1.89 – 1.62 (m, 8H), 1.44 – 1.32 (m, 1H), 1.32 – 1.07 (m, 18H), 1.05 – 0.88 (m, 1H), 0.85 – 0.62 (m, 8H).

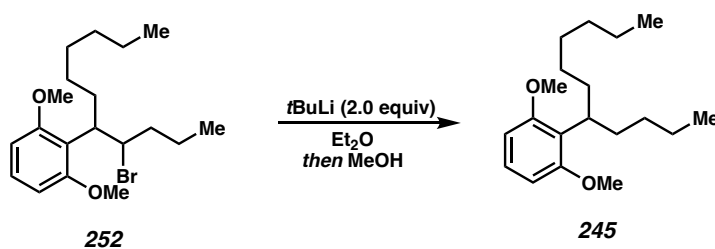


**2-(4-bromoundecan-5-yl)-1,3-dimethoxybenzene (252):** To a 1-dram vial was added model alcohol **250** (9 mg, 0.03 mmol, 1.0 equiv) and  $\text{PPh}_3$  (16 mg, 0.06 mmol, 2.0 equiv) dissolved in DCM (1 mL). The reaction was cooled to 0 °C. Once cooled,  $\text{CBr}_4$  (20 mg, 0.06 mmol, 2.0 equiv) was added in one portion and the reaction mixture was allowed to warm to 25 °C overnight. After 16 hours, the reaction was quenched with Sat'd  $\text{NaHCO}_3$  (5 mL) and the layers were separated. The aqueous layer was extracted with DCM (3 x 5 mL) and the combined organic layer was washed with sat'd  $\text{Na}_2\text{S}_2\text{O}_3$  (10 mL). The combined organic layer was dried over  $\text{Na}_2\text{SO}_4$  and concentrated via rotary evaporator. The crude oil was purified via column chromatography (10% EtOAc in hexanes) to deliver alkyl bromide **252** as a pale-yellow oil (8.5 mg, 0.22 mmol, 77% yield). Similar yield of alkyl bromide was obtained using both alcohol diastereomers.

From major diastereomer **250**:  $^1\text{H}$  NMR (400 MHz,  $\text{CDCl}_3$ )  $\delta$  7.22 – 7.08 (m, 1H), 6.55 (d,  $J = 8.3$  Hz, 2H), 4.81 (ddt,  $J = 10.2, 9.3, 2.5$  Hz, 1H), 3.81 (dd,  $J = 2.2, 0.9$  Hz, 6H), 3.80

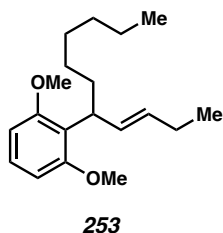
– 3.69 (m, 3H), 2.04 (dddt,  $J = 20.4, 14.9, 8.3, 2.6$  Hz, 1H), 1.93 – 1.78 (m, 2H), 1.76 – 1.42 (m, 6H), 1.23 – 1.00 (m, 2H), 0.97 (t,  $J = 7.3$  Hz, 1H), 0.93 – 0.77 (m, 5H).

From minor diastereomer **250**:  $^1\text{H NMR}$  (400 MHz,  $\text{CDCl}_3$ )  $\delta$  7.15 (td,  $J = 8.3, 1.3$  Hz, 1H), 6.52 (q,  $J = 8.1$  Hz, 2H), 4.76 (ddd,  $J = 10.6, 6.3, 1.8$  Hz, 1H), 3.80 – 3.76 (m, 8H), 3.70 (ddd,  $J = 14.3, 7.2, 3.4$  Hz, 1H), 2.15 – 2.01 (m, 1H), 1.91 – 1.78 (m, 1H), 1.53 – 1.39 (m, 2H), 1.33 – 0.94 (m, 8H), 0.92 – 0.72 (m, 9H).

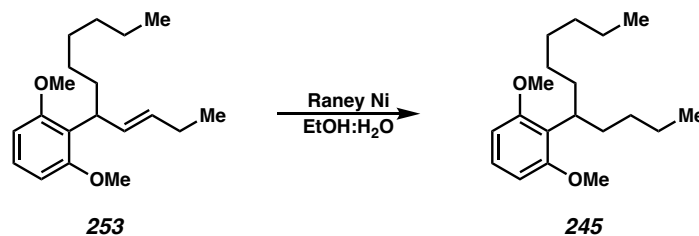


**1,3-dimethoxy-2-(undecan-5-yl)benzene (245)**: To a 1-dram vial was added model alkyl bromide **252** (8 mg, 0.022 mmol, 1.0 equiv) dissolved in  $\text{Et}_2\text{O}$  (0.5 mL). The reaction mixture was cooled to  $-78$  °C and  $t\text{-BuLi}$  (1.7M in pentane, 2.6  $\mu\text{L}$ , 0.044 mmol, 2.0 equiv) was added slowly. The reaction was warmed to 0 °C slowly and then quenched with  $\text{MeOH}$  (0.5 mL) to quench to reaction. Sat'd  $\text{NH}_4\text{Cl}$  (2 mL) was added and the layers were separated. The aqueous layer was extracted with  $\text{EtOAc}$  (3 x 5 mL) and the combined organic layers were dried over  $\text{Na}_2\text{SO}_4$  and concentrated via rotary evaporator. The crude oil purified via column chromatography (5 %  $\text{EtOAc}$  in hexanes) to deliver desired alkane product **245** (5.2 mg, 0.0176 mmol, 76% yield).  $^1\text{H NMR}$  (400 MHz,  $\text{CDCl}_3$ )  $\delta$  7.10 (dd,  $J = 9.2, 7.3$  Hz, 1H), 6.53 (dd,  $J = 8.2, 1.5$  Hz, 2H), 3.78 (d,  $J = 1.4$  Hz, 6H), 3.31 (ddq,  $J = 15.5, 9.7, 5.2$  Hz, 1H), 1.80 (dtd,  $J = 13.2, 9.5, 5.3$  Hz, 1H), 1.35 – 1.12 (m, 24H), 0.98 – 0.74 (m, 9H).

Note: A similar yield was obtained using either bromide diastereomer.

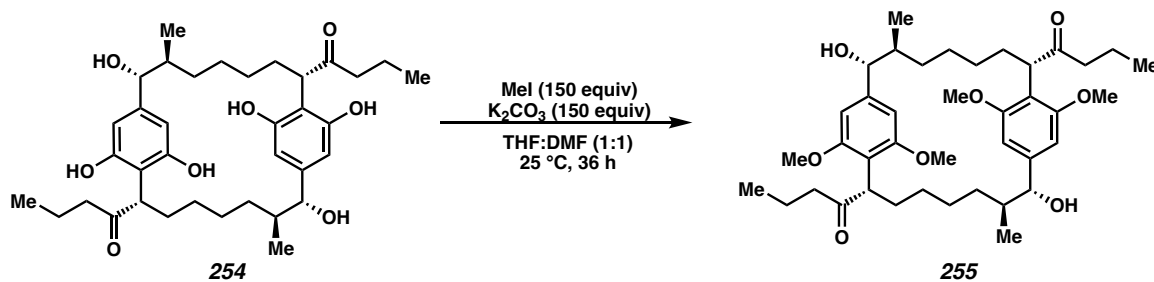


**(E)-1,3-dimethoxy-2-(undec-3-en-5-yl)benzene (253):** Note: an inseparable elimination product **253** was obtained (1.3 mg, 0.0044 mmol, 19% yield) and carried through the next reaction as a 4:1 mixture of **245:253** product. The ratio of alkane:alkene was identical for both alkyl bromide **252** diastereomers.  $^1\text{H NMR}$  (400 MHz,  $\text{CDCl}_3$ )  $\delta$  7.16 (t,  $J = 8.3$  Hz, 1H), 6.58 – 6.53 (m, 2H), 5.93 – 5.81 (m, 1H), 5.52 – 5.37 (m, 1H), 4.00 – 3.89 (m, 6H), 2.02 – 1.93 (m, 3H), 1.87 – 1.68 (m, 2H), 1.28 – 1.16 (m, 8H), 0.90 – 0.81 (m, 3H).



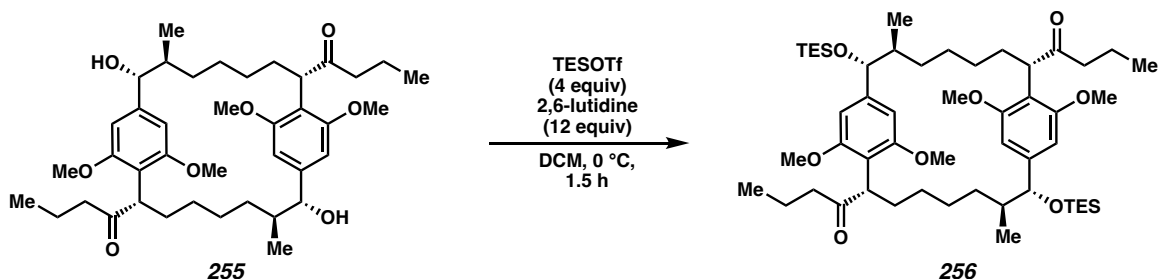
**1,3-dimethoxy-2-(undecan-5-yl)benzene (245):** To a 1-dram vial was added mixture of **245:253** (4:1, 6.5 mg, 1.0 equiv) and dissolved in ethanol. A slurry of Raney Ni (1 mL of suspension) was added to the reaction mixture and was stirred at ambient temperature for 24 hours. After 24 hours, the reaction was cooled to 0 °C and 1N HCl was slowly added to quench the remaining Raney Ni. Once the gray suspension is turned blue, the aqueous layer was extracted with EtOAc (3 x 5 mL) and the combined organic layer was dried over

Na<sub>2</sub>SO<sub>4</sub>. The organic layer was then concentrated via rotary evaporator and purified via column chromatography (5% EtOAc in hexanes) to deliver the desired alkane product **245** (6.5 mg, 0.022 mmol, 99% yield) as a pale-yellow oil.



**1,1'-((2*S*,7*S*,8*R*,10*S*,15*S*,16*R*)-8,16-dihydroxy-1<sup>2</sup>,1<sup>6</sup>,9<sup>3</sup>,9<sup>5</sup>-tetramethoxy-7,15-dimethyl-1,9(1,4)-dibenzenacyclohexadecaphane-2,10-diyl)bis(butan-1-one) (**255**):** To a 1-dram vial was added tetraphenol macrocycle **254** (18 mg, 0.03 mmol, 1.0 equiv) dissolved in THF (2 mL) and DMF (2 mL). K<sub>2</sub>CO<sub>3</sub> (600 mg, 4.4 mmol, 150 equiv) was added in one portion to the reaction mixture followed by MeI (282 μL, 4.4 mmol, 150 equiv). The reaction was stirred at ambient temperature for 36 hours. After the stir period, the reaction was quenched with 1N NH<sub>4</sub>Cl and stirred for 30 minutes at ambient temperature. The layers were separated, and the aqueous layer was extracted with EtOAc (3 x 10 mL). The combined organic layers were then washed with sat'd Na<sub>2</sub>S<sub>2</sub>O<sub>3</sub> until no precipitate was observed in the aqueous layer of the wash. Then, the organic layer was washed with 1N LiCl (2 x 10 mL) and then dried over Na<sub>2</sub>SO<sub>4</sub>. The organic layer was concentrated via rotary evaporator to afford a crude oil, which was purified via column chromatography (35% acetone in hexanes) to deliver tetramethylated macrocycle product **255** as an amorphous white solid (18 mg, 0.0285 mmol, 95% yield). <sup>1</sup>H NMR (500 MHz, CDCl<sub>3</sub>) δ 6.59 (s, 2H), 6.37 (s, 2H), 4.09 (d, *J* = 9.7 Hz, 2H), 3.93 – 3.85 (m, 4H), 3.83 (s, 6H), 3.71

(s, 6H), 2.14 (t,  $J = 7.3$  Hz, 4H), 1.31 (s, 10H), 1.17 (d,  $J = 6.4$  Hz, 8H), 0.84 (t,  $J = 7.4$  Hz, 8H).



**1,1'-((2*S*,7*S*,8*R*,10*S*,15*S*,16*R*)-1<sup>2</sup>,1<sup>6</sup>,9<sup>3</sup>,9<sup>5</sup>-tetramethoxy-7,15-dimethyl-8,16-**

**bis((triethylsilyl)oxy)-1,9(1,4)-dibenzenacyclohexadecaphane-2,10-diyl)bis(butan-1-**

**one) (256):** To a 1-dram vial was added tetramethylated macrocycle **255** (3.5 mg, 5  $\mu$ mol,

1.0 equiv) dissolved in DCM (0.5 mL) and cooled to 0 °C. 2,6-lutidine (7  $\mu$ L, 0.6 mmol,

12.0 equiv) was added to the reaction mixture followed by TESOTf (5  $\mu$ L, 0.025 mmol,

4.0 equiv). The reaction was stirred at 0 °C for 1.5 hours, then quenched with sat'd NaHCO<sub>3</sub>

(2 mL). The layers were separated, and the aqueous layer was extracted with DCM (3 x 5

mL). The combined organic layers were dried over Na<sub>2</sub>SO<sub>4</sub> and concentrated via rotary

evaporator to deliver the crude oil, which was purified via column chromatography (15%

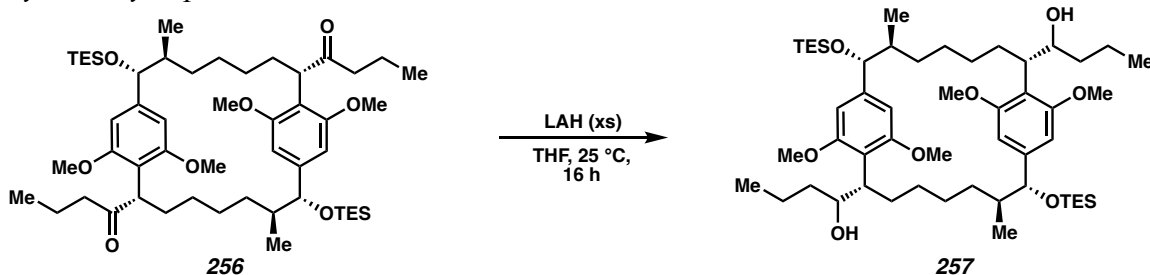
acetone in hexanes) to deliver bis silyl ether macrocycle **256** as a white amorphous solid

(2.5 mg, 2.85  $\mu$ mol, 57% yield). <sup>1</sup>H NMR (500 MHz, CDCl<sub>3</sub>)  $\delta$  6.61 – 6.46 (m, 1H), 6.26

(d,  $J = 8.0$  Hz, 1H), 3.91 (d,  $J = 9.5$  Hz, 1H), 3.87 – 3.82 (m, 1H), 3.78 (s, 2H), 3.73 – 3.62

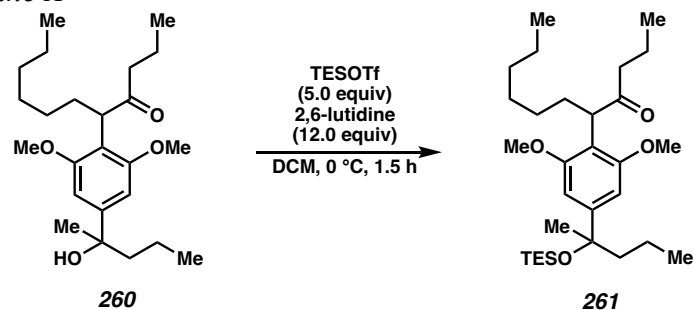
(m, 4H), 2.10 – 2.01 (m, 2H), 1.27 (s, 15H), 1.07 (q,  $J = 8.8$  Hz, 3H), 1.00 – 0.72 (m, 15H),

0.61 (t,  $J = 7.9$  Hz, 1H), 0.48 (dp,  $J = 14.8, 7.3$  Hz, 6H).



(1*S*,1'*S*)-1,1'-((2*S*,7*S*,8*R*,10*S*,15*S*,16*R*)-1<sup>2</sup>,1<sup>6</sup>,9<sup>3</sup>,9<sup>5</sup>-tetramethoxy-7,15-dimethyl-8,16-bis((triethylsilyl)oxy)-1,9(1,4)-dibenzenacyclohexadecaphane-2,10-diyl)bis(butan-1-

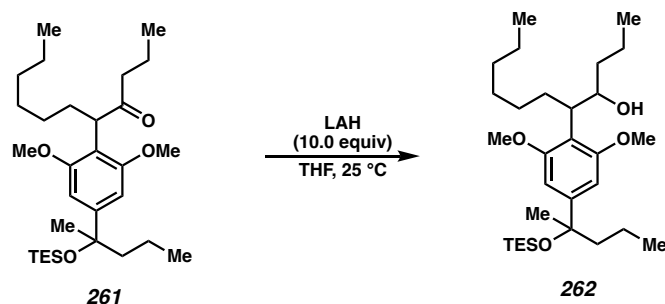
ol) (**257**): To a 1-dram vial was added LAH (8.2 mg, 0.21 mmol, 75 equiv), which was carefully suspended in THF (0.25 mL) at 0 °C. In a separate vial, bis silyl ether macrocycle **256** (2.5 mg, 2.85 μmol, 1.0 equiv) was dissolved in THF (0.25 mL) and added to the LAH suspension at 0 °C. The reaction was allowed to warm to 25 °C and stirred overnight. After 16 hours, the reaction was diluted with EtOAc (2 mL) and quenched with 30% NaOH (0.5 mL) and stirred for 30 minutes. The layers were separated, and the aqueous layer was extracted with EtOAc (3 x 5 mL). The combined organic layers were dried over Na<sub>2</sub>SO<sub>4</sub> and concentrated via rotary evaporator. The crude solid was purified via column chromatography (35% acetone in hexanes) to deliver macrocycle diol **257** as a white solid (1.6 mg, 1.8 μmol, 63% yield). <sup>1</sup>H NMR (500 MHz, CDCl<sub>3</sub>) δ 6.61 (s, 2H), 6.25 (s, 2H), 3.93 – 3.85 (m, 2H), 3.80 (s, 6H), 3.77 – 3.70 (m, 6H), 3.66 (s, 4H), 1.05 (d, *J* = 7.1 Hz, 6H), 0.94 – 0.76 (m, xxH), 0.61 (t, *J* = 8.0 Hz, 8H), 0.47 (dq, *J* = 14.7, 7.8 Hz, xxH). Grease impurities and mixture of diastereomers make analysis challenging at this stage.



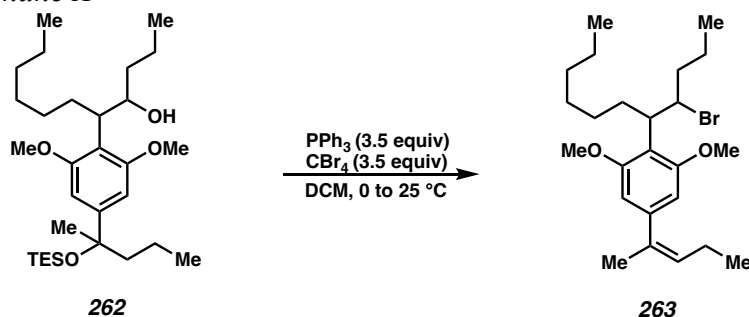
**5-(2,6-dimethoxy-4-(2-((triethylsilyl)oxy)pentan-2-yl)phenyl)undecan-4-one (261):**

To a 20 mL vial was added benzylic tertiary alcohol **260** (22 mg, 0.075 mmol, 1.0 equiv) dissolved in DCM (5 mL) and cooled to 0 °C. 2,6-lutidine (105  $\mu$ L, 0.9 mmol, 12.0 equiv) was added to the reaction mixture followed by TESOTf (85  $\mu$ L, 0.375 mmol, 5.0 equiv). The reaction was stirred at 0 °C for 1.5 hours, then quenched with sat'd NaHCO<sub>3</sub> (5 mL). The layers were separated, and the aqueous layer was extracted with DCM (3 x 5 mL). The combined organic layers were dried over Na<sub>2</sub>SO<sub>4</sub> and concentrated via rotary evaporator to deliver the crude oil, which was purified via column chromatography (20% acetone in hexanes) to deliver silyl ether **261** as a yellow oil (23 mg, 0.045 mmol, 60% yield). <sup>1</sup>H NMR (400 MHz, CDCl<sub>3</sub>)  $\delta$  6.58 (t,  $J$  = 5.9 Hz, 1H), 3.90 (dt,  $J$  = 9.4, 5.0 Hz, 1H), 3.81 – 3.73 (m, 3H), 2.48 (d,  $J$  = 8.0 Hz, 0H), 2.18 – 2.09 (m, 2H), 1.58 (d,  $J$  = 2.0 Hz, 5H), 1.54 – 1.46 (m, 2H), 1.33 – 1.16 (m, 11H), 1.01 – 0.90 (m, 6H), 0.82 (dtd,  $J$  = 13.7, 6.2, 2.0 Hz, 6H), 0.64 – 0.55 (m, 3H). Some potential styrene formation observed from TESOTf that could not be separated. 5.31 (d,  $J$  = 1.5 Hz, 0H), 5.07 (d,  $J$  = 1.6 Hz, 0H) as diagnostic peaks.

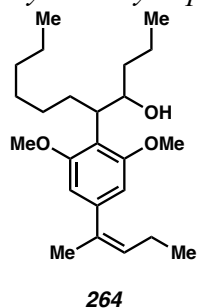




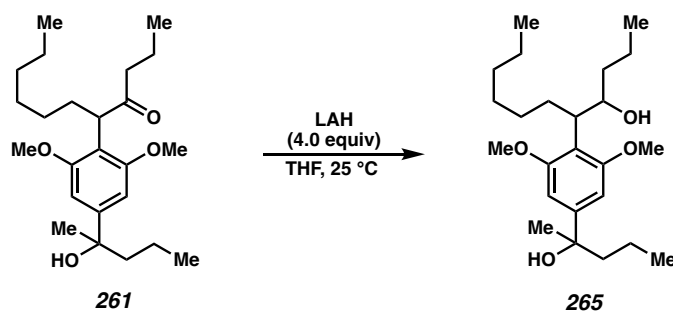
**5-(2,6-dimethoxy-4-(2-((triethylsilyl)oxy)pentan-2-yl)phenyl)undecan-4-ol (262):** To a 1-dram vial was added LAH (11.5 mg, 0.3 mmol, 10 equiv), which was carefully suspended in THF (2 mL) at 0 °C. In a separate vial, silyl ether **261** (15 mg, 0.03 mmol, 1.0 equiv) was dissolved in THF (1 mL) and added to the LAH suspension at 0 °C. The reaction was allowed to warm to 25 °C and stirred overnight. After 16 hours, the reaction was diluted with EtOAc (5 mL) and quenched with 30% NaOH (1 mL) and stirred for 30 minutes. The layers were separated, and the aqueous layer was extracted with EtOAc (3 x 5 mL). The combined organic layers were dried over Na<sub>2</sub>SO<sub>4</sub> and concentrated via rotary evaporator. The crude oil was purified via column chromatography (35% acetone in hexanes) to deliver alcohol **262** as a pale-yellow oil (11.5 mg, 0.023 mmol, 76% yield, 1.5:1 dr). <sup>1</sup>H NMR (400 MHz, CDCl<sub>3</sub>) δ 6.65 – 6.55 (m, 1H), 4.01 (d, *J* = 46.5 Hz, 0H), 3.83 – 3.74 (m, 3H), 3.67 – 3.59 (m, 0H), 3.55 – 3.30 (m, 0H), 2.52 – 2.42 (m, 0H), 1.94 – 1.80 (m, 0H), 1.78 – 1.61 (m, 0H), 1.58 (s, 1H), 1.40 – 1.12 (m, 7H), 1.00 – 0.92 (m, 3H), 0.91 – 0.80 (m, 2H), 0.65 – 0.54 (m, 2H). Mixture of diastereomers was taken to the next step.



**(E)-2-(4-bromoundecan-5-yl)-1,3-dimethoxy-5-(pent-2-en-2-yl)benzene (263):** To a 1-dram vial was added model alcohol **262** (8 mg, 0.015 mmol, 1.0 equiv) and PPh<sub>3</sub> (14.4 mg, 0.053 mmol, 3.5 equiv) dissolved in DCM (1 mL). The reaction was cooled to 0 °C. Once cooled, CBr<sub>4</sub> (17.4 mg, 0.0525 mmol, 3.5 equiv) was added in one portion and the reaction mixture was allowed to warm to 25 °C overnight. After 16 hours, the reaction was quenched with sat'd NaHCO<sub>3</sub> (2 mL) and the layers were separated. The aqueous layer was extracted with DCM (3 x 5 mL) and the combined organic layer was washed with sat'd Na<sub>2</sub>S<sub>2</sub>O<sub>3</sub> (10 mL). The combined organic layer was dried over Na<sub>2</sub>SO<sub>4</sub> and concentrated via rotary evaporator. The crude oil was purified via column chromatography (10% EtOAc in hexanes) to deliver alkyl bromide **263** as a pale-yellow oil (2.8 mg, 0.0063 mmol, 42% yield). <sup>1</sup>H NMR (400 MHz, CDCl<sub>3</sub>) δ 6.47 (d, *J* = 21.5 Hz, 1H), 5.83 – 5.70 (m, 0H), 4.78 – 4.62 (m, 0H), 4.57 – 4.47 (m, 0H), 3.78 – 3.73 (m, 2H), 3.72 (d, *J* = 2.9 Hz, 1H), 3.65 – 3.42 (m, 0H), 2.15 (td, *J* = 7.5, 3.0 Hz, 1H), 2.02 – 1.88 (m, 2H), 1.83 – 1.71 (m, 0H), 1.69 – 1.50 (m, 0H), 1.31 – 1.06 (m, 4H), 1.00 (tdd, *J* = 7.4, 3.7, 1.3 Hz, 2H), 0.91 – 0.67 (m, 3H). (1.5:1 mixture of alkyl bromide diastereomers).



**(E)-5-(2,6-dimethoxy-4-(pent-2-en-2-yl)phenyl)undecan-4-ol (264):** Was obtained as the major side product from the reaction described above.  $^1\text{H}$  NMR (400 MHz,  $\text{CDCl}_3$ )  $\delta$  6.55 – 6.47 (m, 1H), 5.83 – 5.64 (m, 2H), 3.85 – 3.78 (m, 0H), 3.76 – 3.71 (m, 19H), 3.60 (d,  $J = 10.7$  Hz, 0H), 3.47 – 3.37 (m, 1H), 2.18 – 2.05 (m, 3H), 1.98 – 1.94 (m, 2H), 1.94 – 1.88 (m, 1H), 1.30 – 1.08 (m, 49H), 0.99 (dtd,  $J = 8.7, 7.5, 4.4$  Hz, 3H), 0.90 – 0.67 (m, 8H). (mixture of alcohol diastereomers)



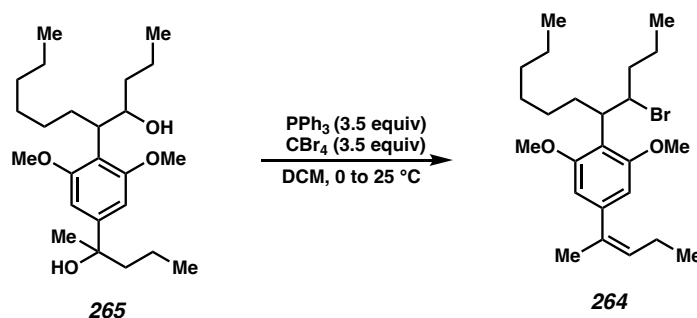
**5-(4-(2-hydroxypentan-2-yl)-2,6-dimethoxyphenyl)undecan-4-ol (265):** To a 20 mL vial was added LAH (30 mg, 0.8 mmol, 4.0 equiv), which was carefully suspended in THF (2.5 mL) at 0 °C. In a separate vial, tertiary benzylic alcohol **261** (80 mg, 0.2 mmol, 1.0 equiv) was dissolved in THF (2.5 mL) and added to the LAH suspension at 0 °C. The reaction was allowed to warm to 25 °C and stirred overnight. After 16 hours, the reaction was diluted with EtOAc (10 mL) and quenched with 30% NaOH (3 mL) and stirred for 30 minutes. The layers were separated, and the aqueous layer was extracted with EtOAc (3 x 5 mL). The combined organic layers were dried over  $\text{Na}_2\text{SO}_4$  and concentrated via rotary

evaporator. The crude oil was purified via column chromatography (45% EtOAc in hexanes) to deliver diol **265** as a pale-yellow oil (73 mg, 0.182 mmol, 91% yield, 1.5:1 dr).

The diastereomers can be separated via column chromatography at this stage.

Major diastereomer:  $^1\text{H NMR}$  (500 MHz,  $\text{CDCl}_3$ )  $\delta$  6.63 (d,  $J = 2.5$  Hz, 1H), 3.90 – 3.85 (m, 1H), 3.83 (s, 1H), 3.80 (d,  $J = 3.9$  Hz, 2H), 3.47 (dt,  $J = 9.5, 5.9$  Hz, 1H), 3.09 (d,  $J = 5.7$  Hz, 0H), 1.91 – 1.80 (m, 1H), 1.80 – 1.65 (m, 1H), 1.54 – 1.46 (m, 0H), 1.42 – 1.29 (m, 1H), 1.29 – 1.14 (m, 5H), 0.95 – 0.82 (m, 5H).

Minor diastereomer:  $^1\text{H NMR}$  (500 MHz,  $\text{CDCl}_3$ )  $\delta$  6.61 (s, 1H), 3.94 (dt,  $J = 8.2, 4.6$  Hz, 1H), 3.80 (q,  $J = 4.2$  Hz, 4H), 3.41 – 3.32 (m, 0H), 1.90 (dddd,  $J = 12.9, 11.0, 9.6, 5.0$  Hz, 0H), 1.76 (ddt,  $J = 13.6, 9.5, 4.9$  Hz, 2H), 1.72 – 1.62 (m, 0H), 1.47 (dt,  $J = 7.0, 2.0$  Hz, 0H), 1.41 – 1.16 (m, 4H), 0.93 – 0.79 (m, 4H).



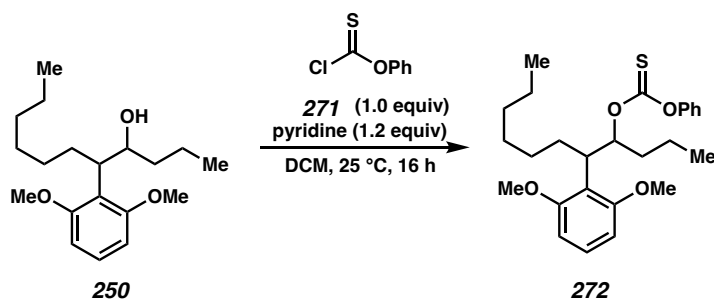
**(E)-2-(4-bromoundecan-5-yl)-1,3-dimethoxy-5-(pent-2-en-2-yl)benzene (263):** To a 1-dram vial was added model diol **265** (8 mg, 0.0152 mmol, 1.0 equiv) and  $\text{PPh}_3$  (13.7 mg, 0.0525 mmol, 3.5 equiv) dissolved in DCM (1 mL). The reaction was cooled to 0 °C. Once cooled,  $\text{CBr}_4$  (17.4 mg, 0.0525 mmol, 3.5 equiv) was added in one portion and the reaction mixture was allowed to warm to 25 °C overnight. After 16 hours, the reaction was quenched with sat'd  $\text{NaHCO}_3$  (2 mL) and the layers were separated. The aqueous layer was extracted with DCM (3 x 5 mL) and the combined organic layer was washed with sat'd  $\text{Na}_2\text{S}_2\text{O}_3$  (10

mL). The combined organic layer was dried over  $\text{Na}_2\text{SO}_4$  and concentrated via rotary evaporator. The crude oil was purified via column chromatography (10% EtOAc in hexanes) to deliver alkyl bromide **264** as a pale-yellow oil (5 mg, 0.0114 mmol, 75% yield). From minor diastereomer of alcohol:  $^1\text{H}$  NMR (500 MHz,  $\text{CDCl}_3$ )  $\delta$  6.64 – 6.55 (m, 1H), 5.86 (qd,  $J = 7.0, 1.4$  Hz, 0H), 4.71 – 4.58 (m, 1H), 3.83 (t,  $J = 8.6$  Hz, 3H), 3.57 (qd,  $J = 10.7, 3.6$  Hz, 0H), 2.27 (p,  $J = 7.5$  Hz, 1H), 2.16 – 1.99 (m, 2H), 1.95 – 1.80 (m, 1H), 1.58 – 1.41 (m, 1H), 1.35 – 1.18 (m, 1H), 1.12 (td,  $J = 7.5, 1.8$  Hz, 1H), 1.06 – 0.98 (m, 0H), 0.94 – 0.75 (m, 3H).



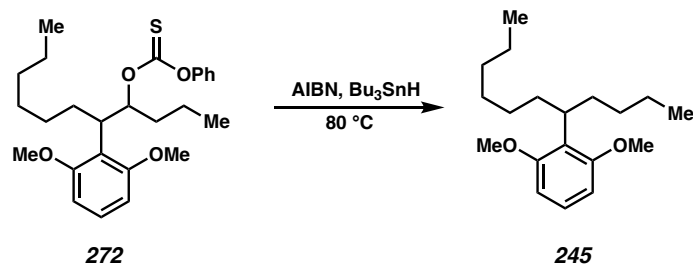
**1,3-dimethoxy-5-(pentan-2-yl)-2-(undecan-5-yl)benzene (267):** To a 1-dram vial was added alkyl bromide **264** (5 mg, 0.0114 mmol, 1.0 equiv) dissolved in ethanol (1 mL). A slurry of Raney Ni (1 mL of suspension) was added to the reaction mixture and was stirred at ambient temperature for 24 hours. After 24 hours, the reaction was cooled to 0 °C and 1N HCl was slowly added to quench the remaining Raney Ni. Once the gray suspension is turned blue, the aqueous layer was extracted with EtOAc (3 x 5 mL) and the combined organic layer was dried over  $\text{Na}_2\text{SO}_4$ . The organic layer was then concentrated via rotary evaporator and purified via column chromatography (5% EtOAc in hexanes) to deliver the desired alkane product **267** (3.4 mg, 0.0114 mmol, 99% yield) as a pale-yellow oil;  $^1\text{H}$

NMR (400 MHz, CDCl<sub>3</sub>) δ 6.34 (s, 1H), 3.76 (s, 3H), 3.22 (dtt, *J* = 11.8, 9.1, 6.0 Hz, 1H), 2.68 – 2.54 (m, 1H), 1.76 (dddd, *J* = 14.9, 9.4, 5.3, 2.5 Hz, 1H), 1.59 – 1.46 (m, 3H), 1.35 – 1.01 (m, 15H), 0.94 – 0.78 (m, 6H).

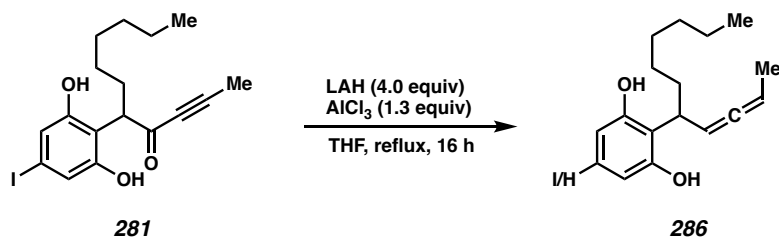


***O*-(5-(2,6-dimethoxyphenyl)undecan-4-yl) *O*-phenyl carbonothioate (272):** Alcohol **250** (33 mg, 0.107 mmol, 1.0 equiv), *O*-phenyl carbonochloridothioate (18.5 mg, 0.107 mmol, 1.0 equiv) and pyridine (34 μL, 0.13 mmol, 1.2 equiv) were dissolved in DCM (0.5 mL). The reaction was stirred at 25 °C for 16 hours, diluted with DCM (5 mL) and washed with H<sub>2</sub>O (2 x 5 mL) followed by 1M HCl (5 mL). The organic layer was then washed with NaHCO<sub>3</sub> (10 mL) and H<sub>2</sub>O (10 mL). The combined organic layer was dried over Na<sub>2</sub>SO<sub>4</sub> and concentrated via rotary evaporator. The crude oil was purified via column chromatography (5% EtOAc in hexanes) to deliver thioformate **272** (33.5 mg, 0.076 mmol, 72% yield); <sup>1</sup>H NMR (400 MHz, CDCl<sub>3</sub>) δ 7.41 – 7.33 (m, 2H), 7.29 – 7.20 (m, 2H), 7.17 – 7.03 (m, 2H), 6.65 – 6.58 (m, 2H), 6.45 (td, *J* = 10.8, 7.0 Hz, 2H), 6.13 – 6.05 (m, 0.6H), 5.93 (ddd, *J* = 9.8, 8.3, 3.1 Hz, 0.4H), 3.75 – 3.60 (m, 2H), 1.99 – 1.80 (m, 1H), 1.74 – 1.53 (m, 1H), 1.45 – 1.34 (m, 1H), 1.27 – 1.06 (m, 2H), 1.05 – 0.97 (m, 1H), 0.91 (t, *J* = 7.3 Hz, 2H), 0.81 – 0.69 (m, 3H) (mixture of 1.5:1 dr from alcohol **250**); <sup>13</sup>C NMR (101 MHz, CDCl<sub>3</sub>) δ 194.85, 194.67, 159.52, 153.58, 153.34, 129.68, 129.42, 129.16, 127.56, 126.85, 126.29, 125.96, 122.19, 121.88, 121.84, 104.10, 88.75, 87.55, 39.58, 39.19, 34.95, 34.81,

31.85, 31.73, 29.73, 29.39, 29.29, 28.67, 27.66, 27.62, 22.69, 22.66, 18.27, 17.89, 14.36, 14.18, 14.14, 14.09; (mixture of 1.5:1 dr from alcohol **250**).

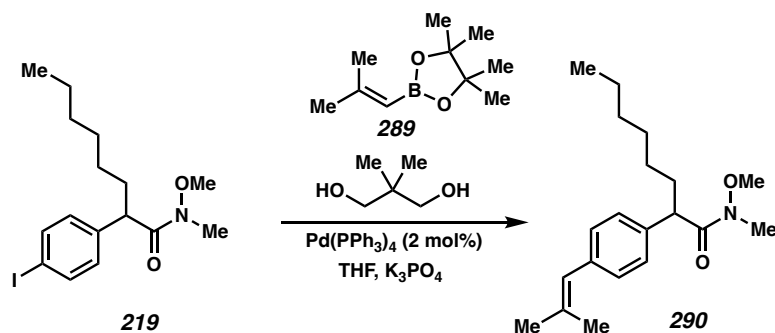
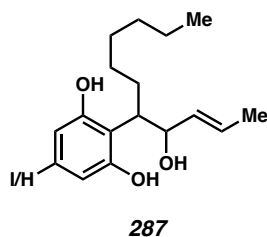


**1,3-dimethoxy-2-(undecan-5-yl)benzene (245)**: Dissolve thiocarbonate **272** (34 mg, 0.076 mmol, 1.0 equiv) in benzene (8.7 mL). Heat to reflux. Meanwhile, dissolve AIBN (2.5 mg, 0.0152 mmol, 0.2 equiv) and Bu<sub>3</sub>SnH (29 mg, 0.1 mmol, 1.3 equiv) in benzene (1.3 mL) and add to refluxing reaction mixture dropwise over 30 minutes. Reflux for 3 hours, then cool to 25 °C and add KF. Stir for an additional 3 hours at 25 °C, then filter the reaction mixture. Evaporate the volatiles via rotary evaporator and add to silica plug (5% EtOAc in hexanes) to afford the alkane **245** (17 mg, 0.06 mmol, 76% yield) yield is approximated due to the coelution of tin byproducts. The spectra of alkane **245** matches the data reported from the earlier sequences.



**2-(undeca-2,3-dien-5-yl)benzene-1,3-diol (286)**: To a stirred solution of aluminum chloride (6.1 mg, 0.036 mmol, 1.3 equiv) in THF (0.5 mL) at 0 °C was added lithium aluminum hydride (1.0M in THF, 0.11 mL, 0.11 mmol, 4.0 equiv). After 15 minutes ynone

**281** (11.2 mg, 0.028 mmol, 1.0 equiv) in THF (0.2 mL) was added and the reaction was allowed to warm to ambient temperature before being heated to reflux for 16 h and then allowed to cool to ambient temperature. To the mixture was added EtOAc (1 mL), water (1 mL), and sat. aq. Rochelle's salt (1 mL). The mixture was allowed to stir for 2 h and the phases separated. The aqueous phase was extracted with EtOAc (3 × 4 mL) and the combined organics were dried over Na<sub>2</sub>SO<sub>4</sub>, filtered, and concentrated *in vacuo*. The crude residue analyzed directly *via* <sup>1</sup>H-NMR and observed as a mixture of allene:allylic alcohol (**286**:**287**) (55% yield, 3:1 H:I ratio, 2:1 allene dr for **286**, 25% yield, 3:1 H:I dr for **287**)

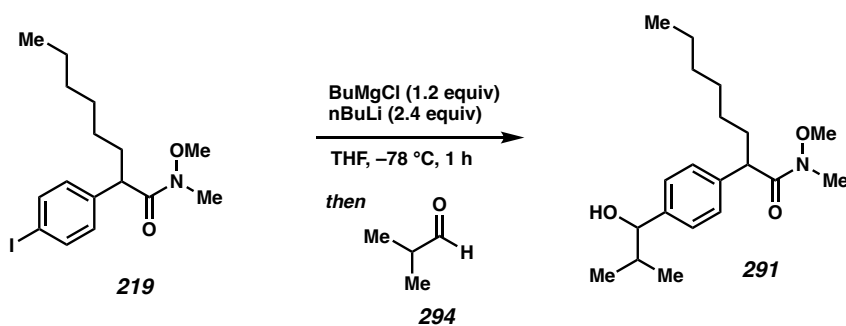


***N*-methoxy-*N*-methyl-2-(4-(2-methylprop-1-en-1-yl)phenyl)octanamide (290):**

Dissolve Weinreb amide **219** (100 mg, 0.26 mmol, 1.0 equiv) in THF (2.5 mL). Pd(PPh<sub>3</sub>)<sub>4</sub> (4.0 mg, 0.0052 mmol, 2 mol%) was added followed by borane **289** (70 mg, 0.39 mmol, 1.5 equiv) and diol (40 mg, 0.39 mmol, 1.5 equiv). The reaction mixture was sparged with N<sub>2</sub> for 15 minutes, followed by the addition of K<sub>3</sub>PO<sub>4</sub> (106 mg, 0.78 mmol, 3.0 equiv). The

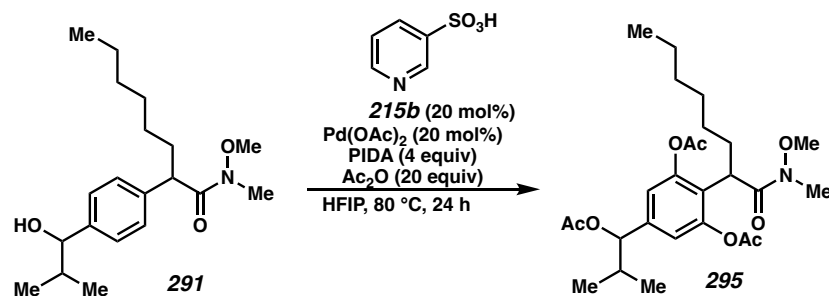


reaction was heated to 60 °C for 2 hours, the cooled to 25 °C. The reaction mixture was diluted with Et<sub>2</sub>O (10 mL) and quenched with 1N NH<sub>4</sub>Cl (10 mL). The layers were separated and the aqueous layer was extracted with Et<sub>2</sub>O (2 x 25 mL). The combined organic layers were dried over Na<sub>2</sub>SO<sub>4</sub>, concentrated via rotary evaporator and the crude oil was purified via column chromatography (10% EtOAc in hexanes) to afford styrene **290** as a yellow oil. (72 mg, 0.226, 87% yield); <sup>1</sup>H NMR (400 MHz, CDCl<sub>3</sub>) δ 7.31 – 7.26 (m, 2H), 7.18 (d, *J* = 8.0 Hz, 2H), 6.24 (t, *J* = 1.8 Hz, 1H), 3.99 (s, 1H), 3.51 (s, 3H), 3.18 (d, *J* = 1.0 Hz, 3H), 2.15 – 2.01 (m, 1H), 1.91 (d, *J* = 1.5 Hz, 3H), 1.87 (d, *J* = 1.4 Hz, 3H), 1.79 – 1.67 (m, 1H), 1.38 – 1.16 (m, 8H), 0.93 – 0.81 (m, 3H); <sup>13</sup>C NMR (101 MHz, CDCl<sub>3</sub>) δ 137.85, 137.19, 135.30, 128.82, 127.81, 124.80, 61.29, 47.24, 34.12, 32.28, 31.71, 29.23, 27.76, 26.95, 22.63, 19.47, 14.09. Note: The reaction can be performed on a 3 gram scale with no significant change in yield.



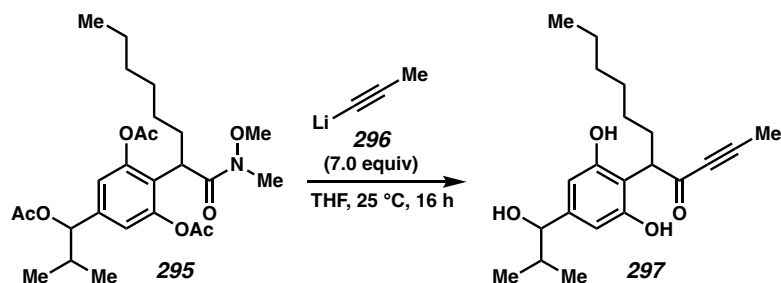
**2-(4-(1-hydroxy-2-methylpropyl)phenyl)-N-methoxy-N-methyloctanamide (291):** *n*-BuMgCl (2 M in THF, 13.2 mL, 26.4 mmol, 1.2 equiv) was cooled to 0 °C and diluted with THF (30 mL) Add *n*-BuLi (2.5 M in hexanes, 21.2 mL, 52.8 mmol, 2.4 equiv) to THF (45 mL) and slowly added to the Grignard solution at -78 °C. Stir for 10 minutes at -78 °C. Meanwhile, the Weinreb amide **219** (8.6 g, 22 mmol, 1.0 equiv) was dissolved in THF (45 mL). After the stir period, the solution of Weinreb amide **219** was added to the magnesate

reaction mixture. The resulting mixture was stirred at  $-78\text{ }^{\circ}\text{C}$  for 30 minutes. After the stir period, the aldehyde **294** (10 mL, 110 mmol, 5.0 equiv) was added to the reaction mixture and stirred at  $-78\text{ }^{\circ}\text{C}$  for 1 hour. The reaction mixture was warmed to  $25\text{ }^{\circ}\text{C}$  and add  $\text{NH}_4\text{Cl}$ . The layers were separated and the aqueous layer was extracted with EtOAc (3 x 150 mL). The organic layers were combined, dried over  $\text{Na}_2\text{SO}_4$  and concentrate via rotary evaporator. The crude oil was purified via column chromatography (75% EtOAc in hexanes) to afford benzylic alcohol **291** (4.0 g, 12.1 mmol, 55% yield). The remaining yield of product coeluted with unreacted amide **219**.  $^1\text{H}$  NMR (400 MHz,  $\text{CDCl}_3$ )  $\delta$  7.31 (d,  $J = 8.2\text{ Hz}$ , 2H), 7.25 (d,  $J = 8.2\text{ Hz}$ , 2H), 4.34 (d,  $J = 6.9\text{ Hz}$ , 1H), 4.00 (s, 1H), 3.50 (s, 3H), 3.16 (s, 3H), 2.12 – 2.00 (m, 1H), 1.95 (dq,  $J = 13.5, 7.0\text{ Hz}$ , 2H), 1.78 – 1.64 (m, 1H), 1.38 – 1.13 (m, 8H), 1.00 (dd,  $J = 6.6, 1.1\text{ Hz}$ , 3H), 0.92 – 0.83 (m, 2H), 0.79 (d,  $J = 6.8\text{ Hz}$ , 3H);  $^{13}\text{C}$  NMR (101 MHz,  $\text{CDCl}_3$ )  $\delta$  174.87, 142.17, 139.57, 127.98, 126.70, 79.83, 61.28, 47.23, 35.25, 34.13, 31.68, 29.20, 27.73, 22.61, 19.06, 18.32, 18.27, 14.08.



**5-(1-acetoxy-2-methylpropyl)-2-(1-(methoxy(methyl)amino)-1-oxooctan-2-yl)-1,3-phenylene diacetate (295):** The procedure is adapted from the literature<sup>9</sup>: To a flame-dried 250 mL flask was added  $\text{Pd}(\text{OAc})_2$  (440 mg, 2 mmol, 20 mol%),  $\text{PhI}(\text{OAc})_2$  (12.8 g, 40 mmol, 4.0 equiv), pyridine-3-sulfonic acid **215b** (315 mg, 2 mmol, 20 mol%) and Weinreb

amide **291** (3.35 mg, 10 mmol, 1.0 equiv). Then HFIP (83 ml) and Ac<sub>2</sub>O (19 ml, 200 mmol, 20 equiv) were added and the septum cap was exchanged with a Teflon septum-lined screw cap and heated to 80 °C for 24 h. The reaction was cooled to room temperature, diluted with EtOAc and filtered over celite. The eluent was concentrated under reduced pressure and purified by flash column chromatography (50% ether in hexanes) to deliver the product **295** as a yellow oil (3.5g, 7.2 mmol, 72% yield, 1.3:1 dr); <sup>1</sup>H NMR (400 MHz, CDCl<sub>3</sub>) δ 6.94 (s, 0.86H), 6.66 (d, *J* = 4.7 Hz, 1.14H), 6.24 (dd, *J* = 4.9, 2.3 Hz, 0.43H), 5.49 (t, *J* = 7.0 Hz, 0.57H), 4.02 – 3.85 (m, 0.57H), 3.47 – 3.32 (m, 0.43H), 3.23 – 2.96 (m, 6H), 2.40 – 2.23 (m, 6H), 2.15 – 2.01 (m, 8H), 1.37 – 1.20 (m, 11H), 1.04 (t, *J* = 7.2 Hz, 3H), 0.95 (dd, *J* = 6.7, 2.3 Hz, 2H), 0.91 – 0.78 (m, 5H); (1.3:1 dr) <sup>13</sup>C NMR (101 MHz, CDCl<sub>3</sub>) δ 168.81, 168.73, 149.49, 148.74, 119.25, 109.58, 109.42, 97.88, 79.47, 79.42, 60.33, 60.01, 53.44, 39.94, 39.55, 33.55, 32.55, 31.73, 30.30, 29.30, 27.69, 22.70, 21.15, 20.92, 18.39, 18.19, 16.66, 16.43, 14.10.



**5-(2,6-dihydroxy-4-(1-hydroxy-2-methylpropyl)phenyl)undec-2-yn-4-one (297):**

*Trans*-1-bromo-prop-1-ene (94 mg, 0.77 mmol, 7.0 equiv) was dissolved in THF (0.5 mL) and cooled to –78 °C followed by the addition of *n*-BuLi (2.5 M in hexanes, 0.62 mL, 1.54 mmol, 14 equiv). The reaction mixture was allowed to stir for 2 hours at –78 °C. After the stir period, Weinreb amide **295** (55 mg, 0.11 mmol, 1.0 equiv) was dissolved in THF (0.25

mL) and added slowly to the reaction mixture at  $-78\text{ }^{\circ}\text{C}$ . The reaction was warmed to  $25\text{ }^{\circ}\text{C}$  and stirred for 16 h. The reaction was quenched with MeOH (1 mL) and Sat'd  $\text{NH}_4\text{Cl}$  (3 mL). The aqueous layer was extracted with EtOAc (3 x 10 mL) and the combined organic layers were dried over  $\text{Na}_2\text{SO}_4$  and concentrated via rotary evaporator. The crude oil was purified via column chromatography (2% MeOH in EtOAc) to afford triol **297** as a red solid (16 mg, 0.046 mmol, 42% yield);  $^1\text{H}$  NMR (400 MHz,  $\text{CDCl}_3$ )  $\delta$  6.54 (br, 2H), 6.40 (s, 2H), 4.55 (dd,  $J = 8.9, 6.4$  Hz, 1H), 4.25 – 4.19 (m, 1H), 4.13 (s, 0.35H), 3.78 (t,  $J = 4.1$  Hz, 0.65H), 2.43 – 2.32 (m, 2H), 2.17 – 2.07 (m, 0H), 2.03 (d,  $J = 1.6$  Hz, 3H), 1.95 – 1.81 (m, 10H), 1.79 – 1.68 (m, 2H), 1.38 – 1.11 (m, 14H), 1.03 – 0.93 (m, 4H), 0.89 – 0.77 (m, 7H) (2:1 dr)

#### A6.10 NOTES AND REFERENCES

<sup>1</sup> B. A. Arndtsen, R. G. Bergman, T. A. Mobley, T. H. Peterson, Selective Intermolecular Carbon-Hydrogen Bond Activation by Synthetic Metal Complexes in Homogeneous Solution. *Acc. Chem. Res.* **28**, 154-162 (1995).

<sup>2</sup> H. M. L. Davies, D. Morton, Collective Approach to Advancing C–H Functionalization. *ACS Cent. Sci.* **3**, 936-943 (2017).

<sup>3</sup> For select examples of interdisciplinary challenges tackled within the CCHF, see: (a) T. A. Bedell *et al.*, Rapid Construction of a Benzo-Fused Indoxamycin Core Enabled by Site-Selective C–H Functionalizations. *Angew. Chem. Int. Ed.* **55**, 8270-8274 (2016). (b) W. Hao *et al.*, Probing Catalyst Speciation in Pd-MPAAM-Catalyzed Enantioselective C(sp<sup>3</sup>)–H Arylation: Catalyst Improvement via Destabilization of Off-Cycle Species. *ACS Catal.* **11**, 11040-11048 (2021).

<sup>4</sup> For select examples utilizing C–H functionalization in the context of total synthesis within the CCHF, see: (a) N. A. Falcone *et al.*, A C–H Functionalization Strategy Enables an Enantioselective Formal Synthesis of (-)-Aflatoxin B2. *Org. Lett.* **23**, 9393-9397 (2021). (b) R. F. Lusi, G. Sennari, R. Sarpong, Total synthesis of nine longiborneol sesquiterpenoids using a functionalized camphor strategy. *Nat. Chem.* **14**, 450-456 (2022). (c) Falcone, N. A.; Bosse, A. T.; Park, H.; Yu, J.-Q.; Davies, H. M. L.; Sorensen, E. J., A C–H Functionalization Strategy Enables an Enantioselective Formal Synthesis of (-)-Aflatoxin B2. *Org. Lett.* **2021**, *23*, 9393-9397.

<sup>5</sup> D. J. Cram, H. Steinberg, Macro Rings. I. Preparation and Spectra of the Paracyclophanes. *J. Am. Chem. Soc.* **73**, 5691-5704 (1951).

<sup>6</sup> B. S. Moore *et al.*, [7.7]Paracyclophanes from blue-green algae. *J. Am. Chem. Soc.* **112**, 4061-4063 (1990).

<sup>7</sup> For the isolation and structure elucidation of various cylindrocyclophane natural products, see: (a) D. S. May *et al.*, Ribocyclophanes A–E, Glycosylated Cyclophanes with Antiproliferative Activity from Two Cultured Terrestrial Cyanobacteria. *J. Nat. Prod.* **81**, 572-578 (2018). (b) H. T. Bui, R. Jansen, H. T. Pham, S. Mundt, Carbamidocyclophanes A-E, chlorinated paracyclophanes with cytotoxic and antibiotic activity from the Vietnamese cyanobacterium *Nostoc* sp. *J. Nat. Prod.* **70**, 499-503 (2007). (c) S. Luo *et al.*, Carbamidocyclophanes F and G with Anti-*Mycobacterium tuberculosis* Activity from the Cultured Freshwater Cyanobacterium *Nostoc* sp. *Tetrahedron letters* **55**, 686-689 (2014). (d) H. S. Kang *et al.*, Merocyclophanes A and B, antiproliferative cyclophanes from the cultured terrestrial Cyanobacterium *Nostoc* sp. *Phytochemistry* **79**, 109-115 (2012). (e) D. S. May *et al.*, Merocyclophanes C and D from the Cultured Freshwater Cyanobacterium

Nostoc sp. (UIC 10110). *J. Nat. Prod.* **80**, 1073-1080 (2017). (f) B. S. Moore, J.-L. Chen, G. M. L. Patterson, R. E. Moore, Structures of cylindrocyclophanes a–f. *Tetrahedron* **48**, 3001-3006 (1992). (g) J. L. Chen, R. E. Moore, G. M. L. Patterson, Structures of nostocyclophanes A-D. *J. Org. Chem.* **56**, 4360-4364 (1991).

<sup>8</sup> For the biological activity of paracyclophane natural products, see: (a) G. E. Chlipala *et al.*, Cylindrocyclophanes with proteasome inhibitory activity from the Cyanobacterium Nostoc sp. *J. Nat. Prod.* **73**, 1529-1537 (2010). (b) M. Preisitsch *et al.*, Anti-MRSA-acting carbamidocyclophanes H-L from the Vietnamese cyanobacterium Nostoc sp. CAVN2. *J. Antibiot* **68**, 165-177 (2015). (c) M. Preisitsch *et al.*, Effects of Halide Ions on the Carbamidocyclophane Biosynthesis in Nostoc sp. CAVN2. *Mar. Drugs* **14**, 21 (2016).

<sup>9</sup> Bobzin, S. C.; Moore, R. E., Biosynthetic origin of [7.7]paracyclophanes from cyanobacteria. *Tetrahedron* **1993**, 49 (35), 7615-7626.

<sup>10</sup> Nakamura, H.; Hamer, H. A.; Sirasani, G.; Balskus, E. P., Cylindrocyclophane Biosynthesis Involves Functionalization of an Unactivated Carbon Center. *J. Am. Chem. Soc.* **2012**, 134 (45), 18518-18521.

<sup>11</sup> For the elucidation and characterization of various relevant components of the PKS machinery toward the total synthesis of (–)-cylindrocyclophane F, see: (a) Nakamura, H.; Balskus, E. P., Using Chemical Knowledge to Uncover New Biological Function: Discovery of the Cylindrocyclophane Biosynthetic Pathway. *Synlett* **2013**, 24 (12), 1464-1470. (b) Nakamura, H.; Wang, J. X.; Balskus, E. P., Assembly line termination in cylindrocyclophane biosynthesis: discovery of an editing type II thioesterase domain in a type I polyketide synthase. *Chem. Sci.* **2015**, 6 (7), 3816-3822. (c) Nakamura, H.; Schultz, E. E.; Balskus, E. P., A new strategy for aromatic ring alkylation in cylindrocyclophane

biosynthesis. *Nat. Chem. Biol.* **2017**, *13* (8), 916-921. (d) Martins, T. P.; Rouger, C.; Glasser, N. R.; Freitas, S.; de Fraissinette, N. B.; Balskus, E. P.; Tasdemir, D.; Leão, P. N., Chemistry, bioactivity and biosynthesis of cyanobacterial alkylresorcinols. *Nat. Prod. Rep.* **2019**, *36* (10), 1437-1461.

<sup>12</sup> For the reported total syntheses of (-)-cylindrocyclophane A, see: (a) Hoye, T. R.; Humpal, P. E.; Moon, B., Total Synthesis of (-)-Cylindrocyclophane A via a Double Horner-Emmons Macrocyclic Dimerization Event. *J. Am. Chem. Soc.* **2000**, *122* (20), 4982-4983. (b) Smith, A. B.; Kozmin, S. A.; Adams, C. M.; Paone, D. V., Assembly of (-)-Cylindrocyclophanes A and F via Remarkable Olefin Metathesis Dimerizations. *J. Am. Chem. Soc.* **2000**, *122* (20), 4984-4985. (c) Smith, A. B., 3rd; Adams, C. M.; Kozmin, S. A.; Paone, D. V., Total synthesis of (-)-cylindrocyclophanes A and F exploiting the reversible nature of the olefin cross metathesis reaction. *J. Am. Chem. Soc.* **2001**, *123* (25), 5925-37. (d) Nicolaou, K. C.; Sun, Y.-P.; Korman, H.; Sarlah, D., Asymmetric Total Synthesis of Cylindrocyclophanes A and F through Cyclodimerization and a Ramberg-Bäcklund Reaction. *Angew. Chem. Int. Ed.* **2010**, *49* (34), 5875-5878.

<sup>13</sup> Davies Lab seminal work, see: (a) Liao, K.; Negretti, S.; Musaev, D. G.; Bacsá, J.; Davies, H. M. L., Site-selective and stereoselective functionalization of unactivated C-H bonds. *Nature* **2016**, *533* (7602), 230-234. (b) Liu, W.; Ren, Z.; Bosse, A. T.; Liao, K.; Goldstein, E. L.; Bacsá, J.; Musaev, D. G.; Stoltz, B. M.; Davies, H. M. L., Catalyst-Controlled Selective Functionalization of Unactivated C-H Bonds in the Presence of Electronically Activated C-H Bonds. *J. Am. Chem. Soc.* **2018**, *140* (38), 12247-12255. (c) Qin, C.; Davies, H. M. L., Role of Sterically Demanding Chiral Dirhodium Catalysts in Site-Selective C-H Functionalization of Activated Primary C-H Bonds. *J. Am. Chem. Soc.*

**2014**, *136* (27), 9792-9796. (d) Fu, L.; Mighion, J. D.; Voight, E. A.; Davies, H. M. L., Synthesis of 2,2,2,-Trichloroethyl Aryl- and Vinyl diazoacetates by Palladium-Catalyzed Cross-Coupling. *Chem. Eur. J.* **2017**, *23* (14), 3272-3275.

<sup>14</sup> (a) Li, G.; Wan, L.; Zhang, G.; Leow, D.; Spangler, J.; Yu, J.-Q., Pd(II)-Catalyzed C–H Functionalizations Directed by Distal Weakly Coordinating Functional Groups. *J. Am. Chem. Soc.* **2015**, *137* (13), 4391-4397. (b) Park, H.; Li, Y.; Yu, J.-Q., Utilizing Carbonyl Coordination of Native Amides for Palladium-Catalyzed C(sp<sup>3</sup>)–H Olefination. *Angew. Chem. Int. Ed.* **2019**, *58* (33), 11424-11428. (c) Park, H.; Chekshin, N.; Shen, P.-X.; Yu, J.-Q., Ligand-Enabled, Palladium-Catalyzed  $\beta$ -C(sp<sup>3</sup>)–H Arylation of Weinreb Amides. *ACS Catal.* **2018**, *8*, 9292-9297.

<sup>15</sup> (a) Stang, E. M.; Christina White, M., Total synthesis and study of 6-deoxyerythronolide B by late-stage C–H oxidation. *Nat. Chem.* **2009**, *1*, 547. (b) Fraunhofer, K. J.; Prabakaran, N.; Sirois, L. E.; White, M. C., Macrolactonization via Hydrocarbon Oxidation. *J. Am. Chem. Soc.* **2006**, *128* (28), 9032-9033.

<sup>16</sup> Peters, D. S.; Romesberg, F. E.; Baran, P. S., Scalable Access to Arylomycins via C–H Functionalization Logic. *J. Am. Chem. Soc.* **2018**, *140* (6), 2072-2075.

<sup>17</sup> The results of this macrocyclization strategy were further described in Liu, W.; Ren, Z.; Bosse, A. T.; Liao, K.; Goldstein, E. L.; Bacsá, J.; Musáev, D. G.; Stoltz, B. M.; Davies, H. M. L., Catalyst-Controlled Selective Functionalization of Unactivated C–H Bonds in the Presence of Electronically Activated C–H Bonds. *J. Am. Chem. Soc.* **2018**, *140* (38), 12247-12255.



<sup>18</sup> For the synthesis of starting ary diazoacetate, see: Garlets, Z. J.; Sanders, J. N.; Malik, H.; Gampe, C.; Houk, K. N.; Davies, H. M. L., Enantioselective C–H functionalization of bicyclo[1.1.1]pentanes. *Nat. Catal.* **2020**, *3* (4), 351-357.

<sup>19</sup> Liao, K.; Yang, Y.-F.; Li, Y.; Sanders, J. N.; Houk, K. N.; Musaeu, D. G.; Davies, H. M. L., Design of catalysts for site-selective and enantioselective functionalization of non-activated primary C–H bonds. *Nat. Chem.* **2018**, *10* (10), 1048-1055.

<sup>20</sup> Other metal catalyzed hydrogenations occurred with cleavage of the desired aryl iodide, for the use of Crabtree's catalyst, see: (a) Xu, Y.; Mingos, D. M. P.; Brown, J. M., Crabtree's catalyst revisited; Ligand effects on stability and durability. *Chem. Comm.* **2008**, (2), 199-201. (b) Crabtree, R. H., Deactivation in Homogeneous Transition Metal Catalysis: Causes, Avoidance, and Cure. *Chem. Rev.* **2015**, *115* (1), 127-150.

<sup>21</sup> Harned, A. M., From determination of enantiopurity to the construction of complex molecules: The Horeau principle and its application in synthesis. *Tetrahedron* **2018**, *74* (28), 3797-3841.

<sup>22</sup> Windholz, T. B.; Johnston, D. B. R., Trichloroethoxycarbonyl: a generally applicable protecting group. *Tetrahedron Lett.* **1967**, *8* (27), 2555-2557.

<sup>23</sup> Carpino, L. A., 1-Hydroxy-7-azabenzotriazole. An efficient peptide coupling additive. *J. Am. Chem. Soc.* **1993**, *115* (10), 4397-4398.

<sup>24</sup> Senaweera, S.; Cartwright, K. C.; Tunge, J. A., Decarboxylative Acetoxylation of Aliphatic Carboxylic Acids. *J. Org. Chem.* **2019**, *84* (19), 12553-12561.

<sup>25</sup> (a) Khan, S. N.; Zaman, M. K.; Li, R.; Sun, Z., A General Method for Photocatalytic Decarboxylative Hydroxylation of Carboxylic Acids. *J. Org. Chem.* **2020**, *85* (7), 5019-5026. (b) Song, H.-T.; Ding, W.; Zhou, Q.-Q.; Liu, J.; Lu, L.-Q.; Xiao, W.-J.,

Photocatalytic Decarboxylative Hydroxylation of Carboxylic Acids Driven by Visible Light and Using Molecular Oxygen. *J. Org. Chem.* **2016**, *81* (16), 7250-7255.

<sup>26</sup> Xiao, P.; Tang, Z.; Wang, K.; Chen, H.; Guo, Q.; Chu, Y.; Gao, L.; Song, Z., Chemoselective Reduction of Sterically Demanding N,N-Diisopropylamides to Aldehydes. *J. Org. Chem.* **2018**, *83* (4), 1687-1700.

<sup>27</sup> (a) Nakajima, M.; Sato, T.; Chida, N., Iridium-Catalyzed Chemoselective Reductive Nucleophilic Addition to N-Methoxyamides. *Org. Lett.* **2015**, *17* (7), 1696-1699. (b) Dixon hydrosilylation with Vaska's

<sup>28</sup> For a review on the Halogen–Magnesium exchange reaction, see: Ziegler, D. S.; Wei, B.; Knochel, P. Improving the Halogen–Magnesium Exchange by Using New Turbo-Grignard Reagents. *Chemistry – A European Journal* **2019**, *25* (11), 2695–2703.

<sup>29</sup> (a) Xie, Z.; Song, Y.; Xu, L.; Guo, Y.; Zhang, M.; Li, L.; Chen, K.; Liu, X., Rapid Synthesis of N-Tosylhydrazones under Solvent-Free Conditions and Their Potential Application Against Human Triple-Negative Breast Cancer. *ChemistryOpen* **2018**, *7* (12), 977-983. (b) Kabalka, G. W.; Yang, D. T. C.; Baker, J. D., Deoxygenation of  $\alpha,\beta$ -unsaturated aldehydes and ketones via the catecholborane reduction of the corresponding tosylhydrazones. *J. Org. Chem.* **1976**, *41* (3), 574-575. (c) Kabalka, G. W.; Baker, J. D., New mild conversion of ketones to the corresponding methylene derivatives. *J. Org. Chem.* **1975**, *40* (12), 1834-1835. (d) Hu, Y.-J.; Gu, C.-C.; Wang, X.-F.; Min, L.; Li, C.-C., Asymmetric Total Synthesis of Taxol. *J. Am. Chem. Soc.* **2021**, *143* (42), 17862-17870.

<sup>30</sup> The selective methylation of phenols in the presence of alcohols have been disclosed for complex molecules, for a select example, see: Steele, A. D.; Ernouf, G.; Lee, Y. E.; Wuest,

W. M. Diverted Total Synthesis of the Baulamycins and Analogues Reveals an Alternate Mechanism of Action. *Org. Lett.* **2018**, *20* (4), 1126–1129.

<sup>31</sup> For examples of metal catalyzed desulfurization reactions, see: (a) Becker, S.; Fort, Y.; Vanderesse, R.; Caubere, P. Activation of Reducing Agents. Sodium Hydride Containing Complex Reducing Agents. 33. NiCRA's and NiCRAL's as New Efficient Desulfurizing Reagents. *J. Org. Chem.* **1989**, *54* (20), 4848–4853. (b) Mazingo, R.; Wolf, D. E.; Harris, S. A.; Folkers, K. Hydrogenolysis of Sulfur Compounds by Raney Nickel Catalyst. *J. Am. Chem. Soc.* **1943**, *65* (6), 1013–1016. (c) Kawasaki, I.; Sakaguchi, N.; Khadeer, A.; Yamashita, M.; Ohta, S. Homonuclear Diels–Alder Dimerization of 5-Ethenyl-2-Phenylsulfanyl-1H-Imidazoles and Its Application to Synthesis of 12,12'-Dimethylageliferin. *Tetrahedron* **2006**, *62* (43), 10182–10192.

<sup>32</sup> Krishnamurthy, S. Rapid Reduction of Alkyl Tosylates with Lithium Triethylborohydride. A Convenient and Advantageous Procedure for the Deoxygenation of Simple and Hindered Alcohols. Comparison of Various Hydride Reagents. *Journal of Organometallic Chemistry* **1978**, *156* (1), 171–181.

<sup>33</sup> Chen, J.; Lin, J.-H.; Xiao, J.-C. Halogenation through Deoxygenation of Alcohols and Aldehydes. *Org. Lett.* **2018**, *20* (10), 3061–3064.

<sup>34</sup> Zook, H. D.; Goldey, R. N. Coupling of Lithium Alkyls and Alkyl Halides. Metal—Halogen Exchange Reactions. *J. Am. Chem. Soc.* **1953**, *75* (16), 3975–3976.

<sup>35</sup> For a review on radical deoxyfunctionalization strategies invoking alkyl radical intermediates, see: Anwar, K.; Merkens, K.; Aguilar Troyano, F. J.; Gómez-Suárez, A. Radical Deoxyfunctionalisation Strategies\*\*. *European Journal of Organic Chemistry* **2022**, *2022* (26), e202200330.

<sup>36</sup> (a) Barton, D. R.; McCombie, S. WJ Chem. Soc. *Perkin Trans* **1975**, *1*, 1574. (b) McCombie, S. W.; Quiclet-Sire, B.; Zard, S. Z. Reflections on the Mechanism of the Barton-McCombie Deoxygenation and on Its Consequences. *Tetrahedron* **2018**, *74* (38), 4969–4979. (c) Lopez, R. M.; Hays, D. S.; Fu, G. C. Bu<sub>3</sub>SnH-Catalyzed Barton–McCombie Deoxygenation of Alcohols. *J. Am. Chem. Soc.* **1997**, *119* (29), 6949–6950.

<sup>37</sup> For a select example of using O-phenyl thiocarbonate deoxygenation in a recent total synthesis, see: Kravina, A. G.; Carreira, E. M. Total Synthesis of Epicolactone. *Angewandte Chemie International Edition* **2018**, *57* (40), 13159–13162.

<sup>38</sup> Williams, O. P.; Chmiel, A. F.; Mikhael, M.; Bates, D. M.; Yeung, C. S.; Wickens, Z. K. Practical and General Alcohol Deoxygenation Protocol. *Angewandte Chemie International Edition* **2023**, *62* (18), e202300178.

<sup>39</sup> For reductive transformations of enol triflates to the alkene or alkane, see: (a) Cacchi, S.; Morera, E.; Ortar, G. Palladium-Catalyzed Reduction of Enol Triflates to Alkenes. *Tetrahedron Letters* **1984**, *25* (42), 4821–4824. (b) Radivoy, G.; Alonso, F.; Yus, M. Reduction of Sulfonates and Aromatic Compounds with the NiCl<sub>2</sub>·2H<sub>2</sub>O Li-Arene (Cat.) Combination. *Tetrahedron* **1999**, *55* (50), 14479–14490.

<sup>40</sup> Chamberlin, A. R.; Reich, S. H. Stereoselective Acyclic Enolate Formation via Conjugate Reduction: Correlation with Enone Conformational Preferences. *J. Am. Chem. Soc.* **1985**, *107* (5), 1440–1441.

<sup>41</sup> For a review on using Cu–H sources in conjugate reduction chemistry, see: Deutsch, C.; Krause, N. CuH-Catalyzed Reactions. *Chem. Rev.* **2008**, *108* (8), 2916–2927.

<sup>42</sup> Devi Priya, D.; Lakshman, C.; Roopan, S. M. A Review on Various Aspects of Organic Synthesis Using Comins' Reagent. *Molecular Diversity* **2021**, 1–26.

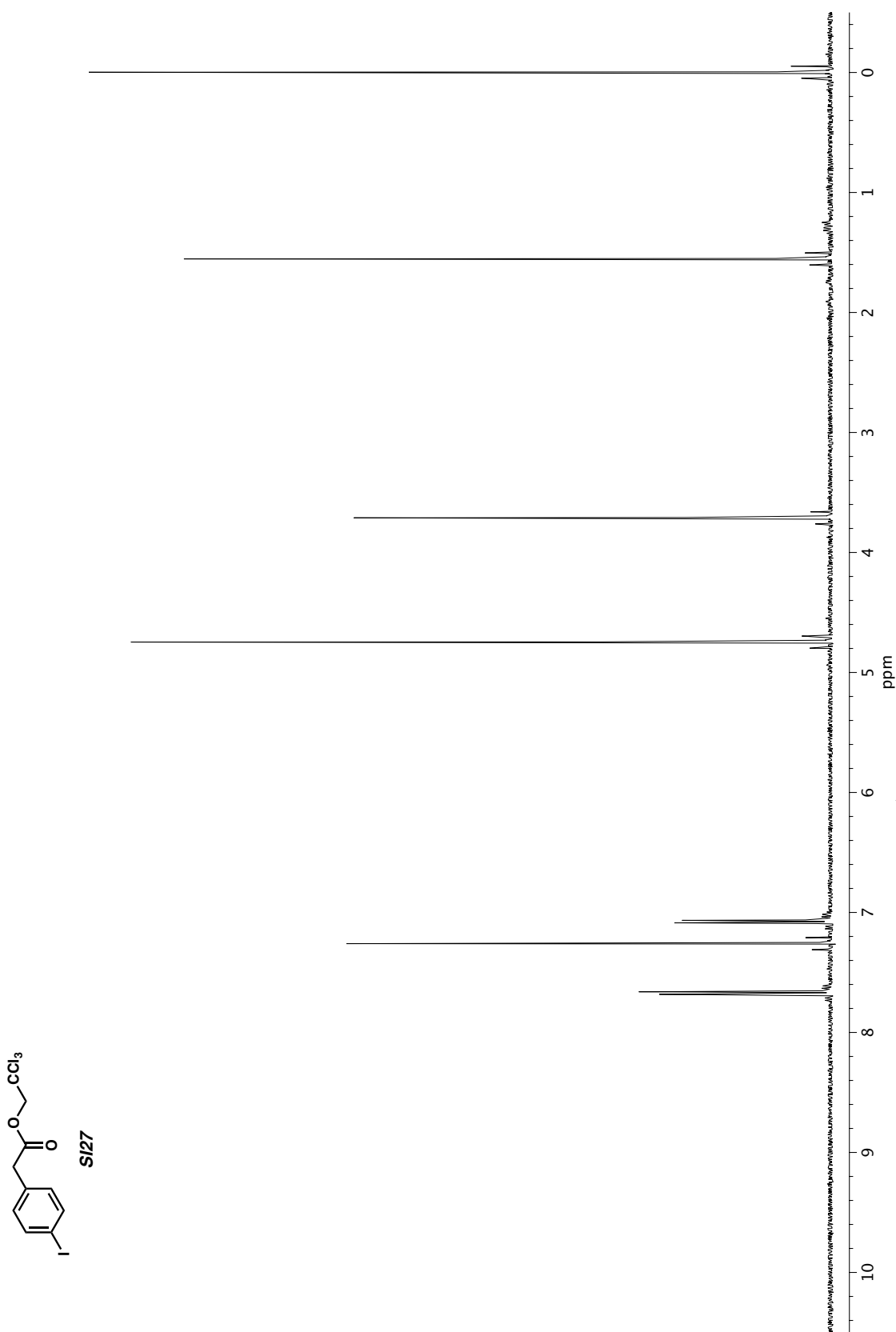
<sup>43</sup> AlH<sub>3</sub> promoted allene formation from propargylic alcohols

<sup>44</sup> (a) Crombie, L.; Jenkins, P. A.; Mitchard, D. A. Heterogeneous Catalytic Hydrogenation of Allenes over Supported Palladium: Selectivity, Stereoselectivity, and Regioselectivity. *J. Chem. Soc., Perkin Trans. 1* **1975**, No. 12, 1081–1090. (b) Okuyama, T.; Toyoshima, K.; Fueno, T. Effects of Phenyl and Alkyl Substitutions on the Hydrogenation of Allene with Diimide. *The Journal of Organic Chemistry* **1980**, 45 (9), 1604–1608.

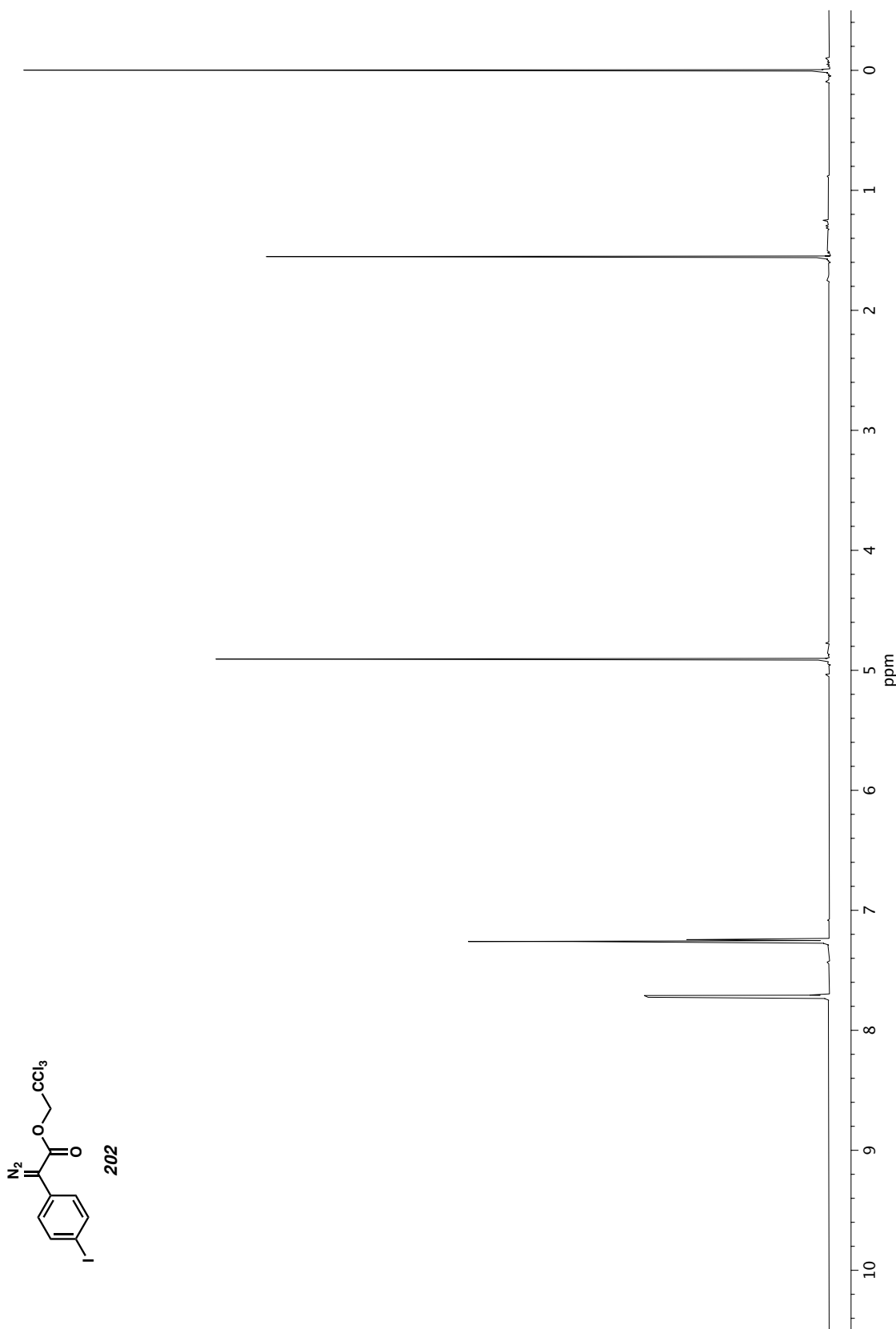
## **APPENDIX 7**

*Spectra Relevant to Appendix 6:*

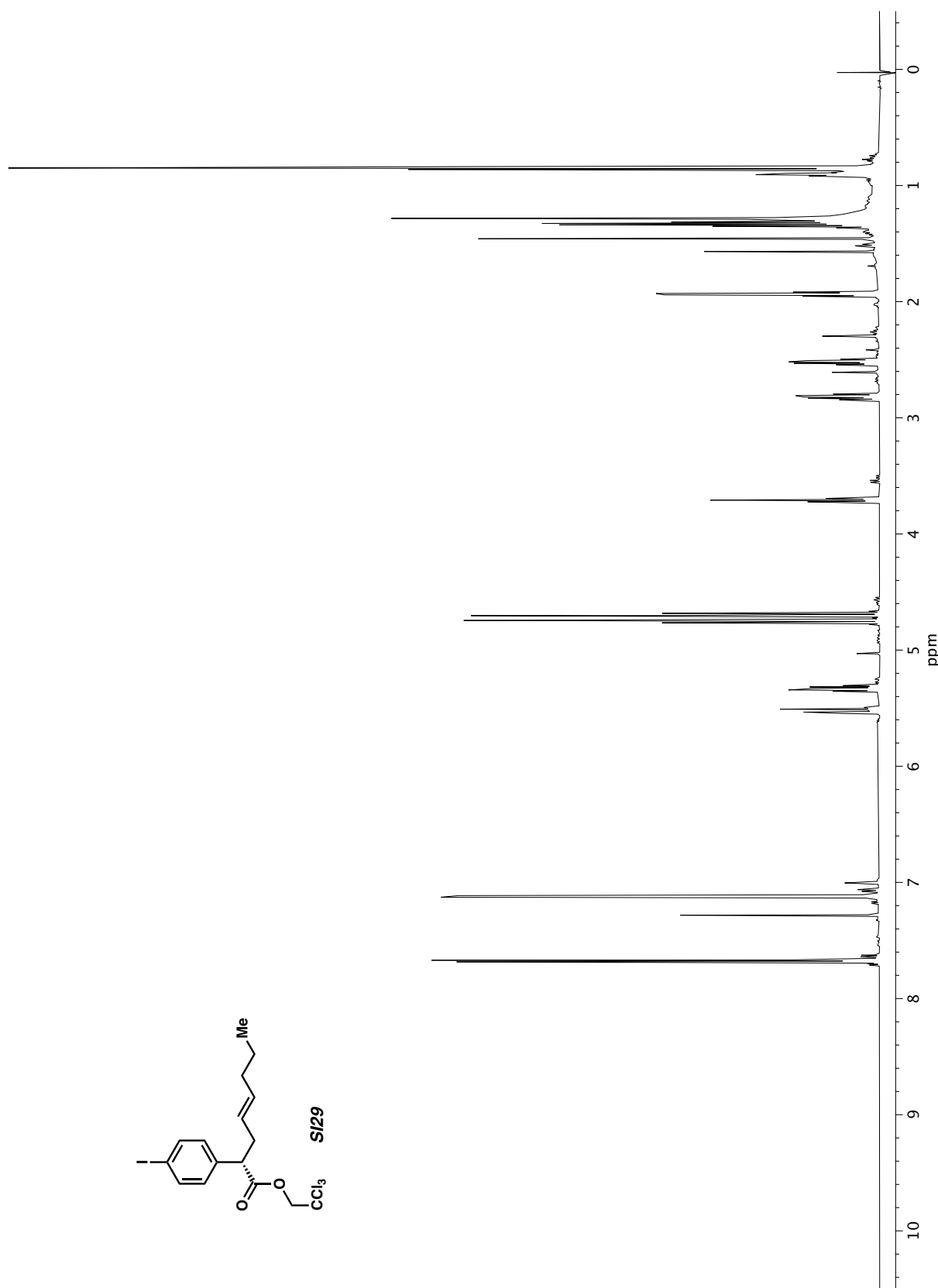
*Total Synthesis of (-)-cylindrocyclophane A*



**Figure A7.1**  $^1\text{H}$  NMR (400 MHz,  $\text{CDCl}_3$ ) of compound **SI27**.







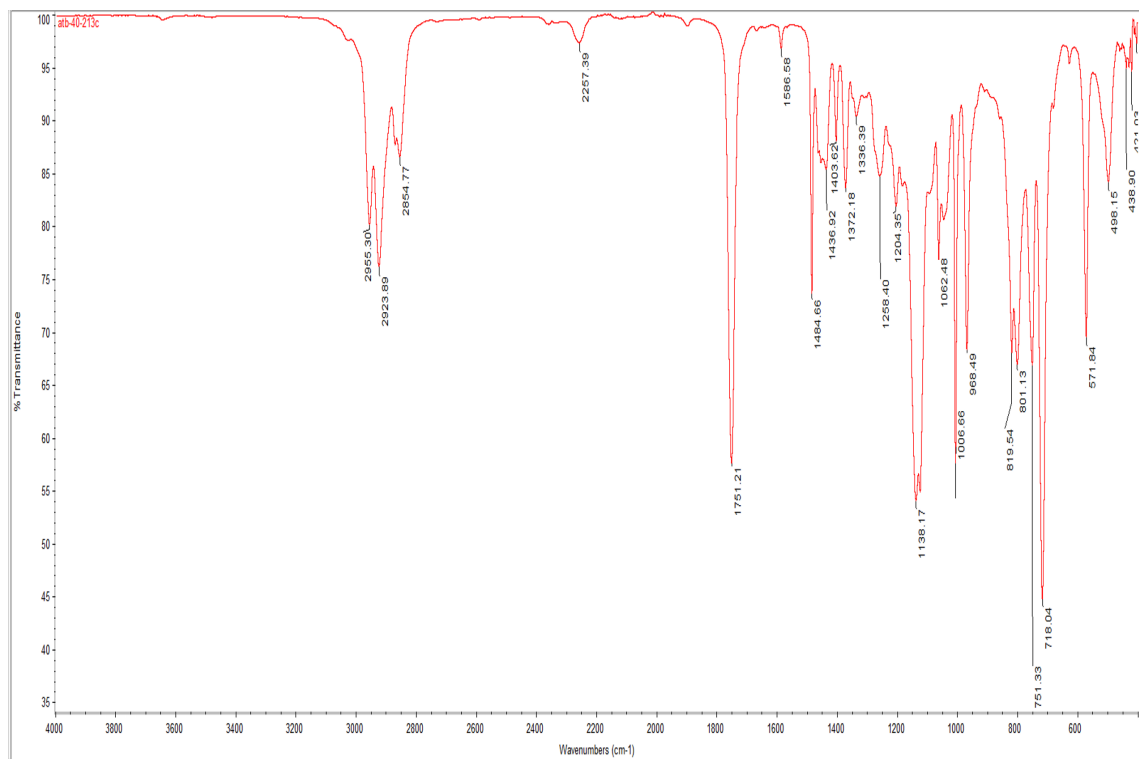


**Figure A7.4** Infrared spectrum (Thin Film, NaCl) of compound **SI29**.

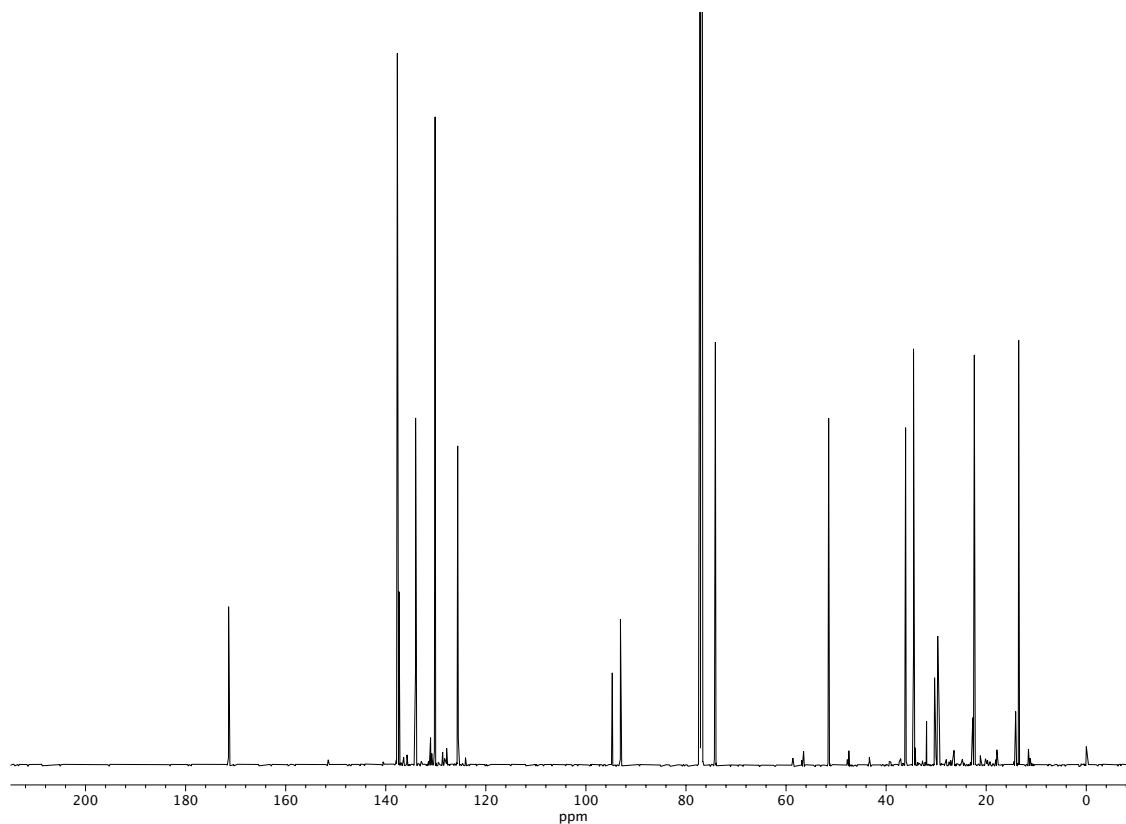


**Figure A7.5** <sup>13</sup>C NMR (151 MHz, CDCl<sub>3</sub>) of compound **SI29**.

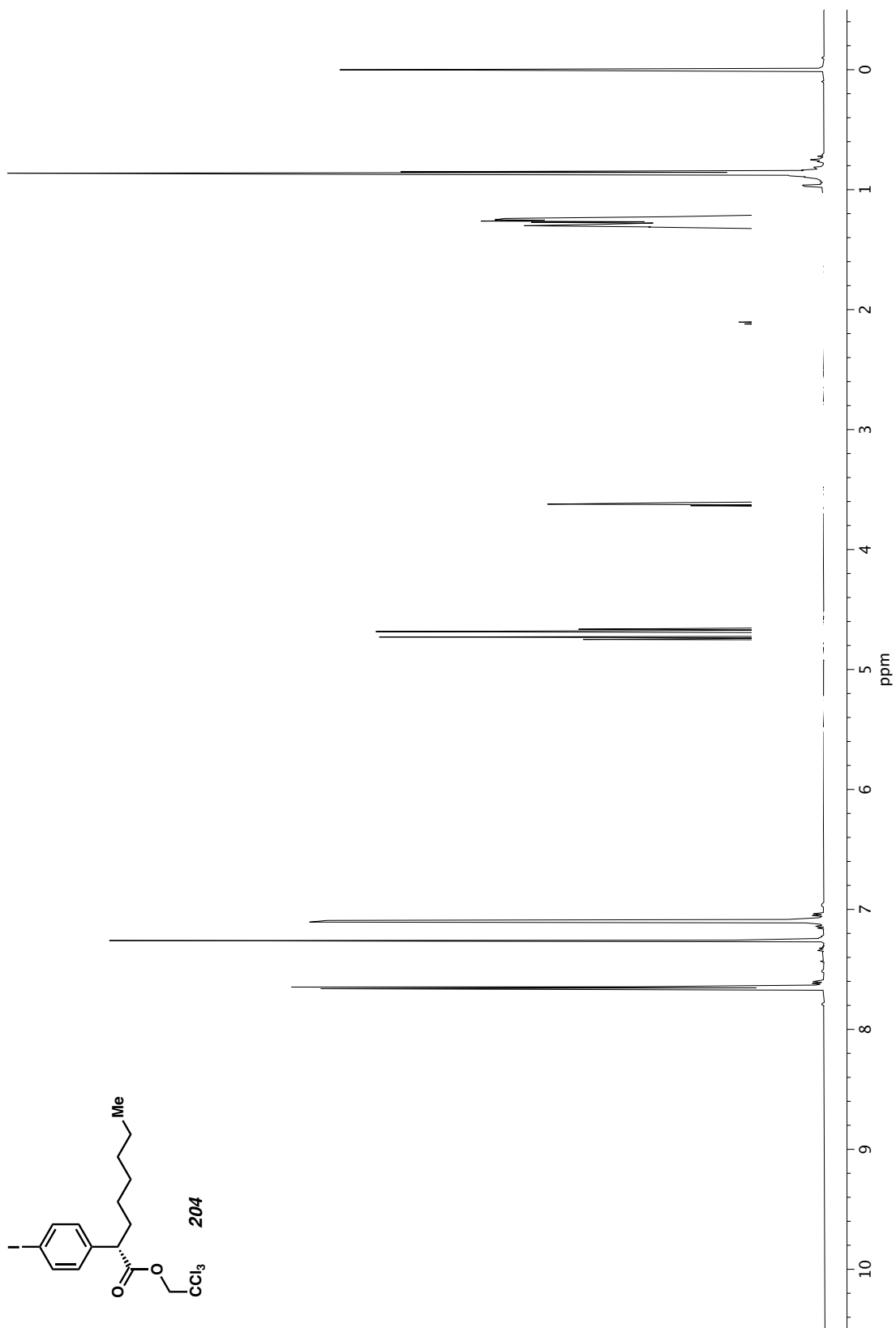


Figure A7.6  $^1\text{H}$  NMR (600 MHz,  $\text{CDCl}_3$ ) of compound **204**.

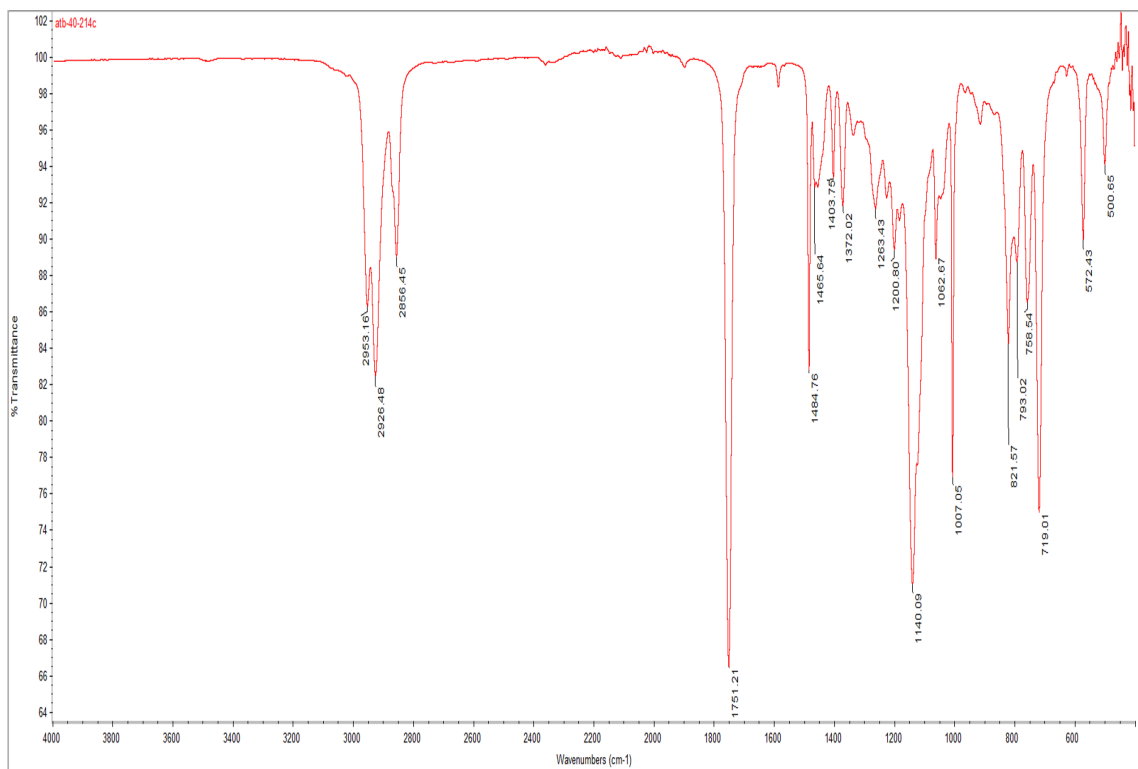


Figure A7.7 Infrared spectrum (Thin Film, NaCl) of compound 204.

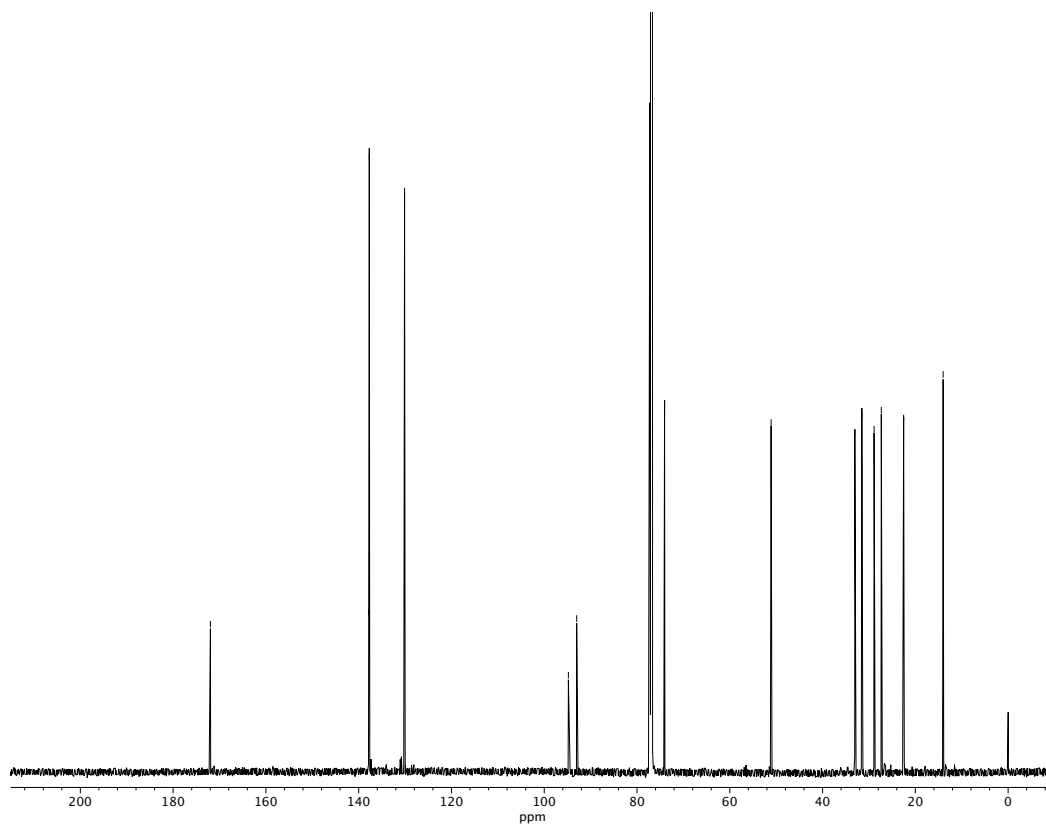


Figure A7.8 <sup>13</sup>C NMR (151 MHz, CDCl<sub>3</sub>) of compound 204.

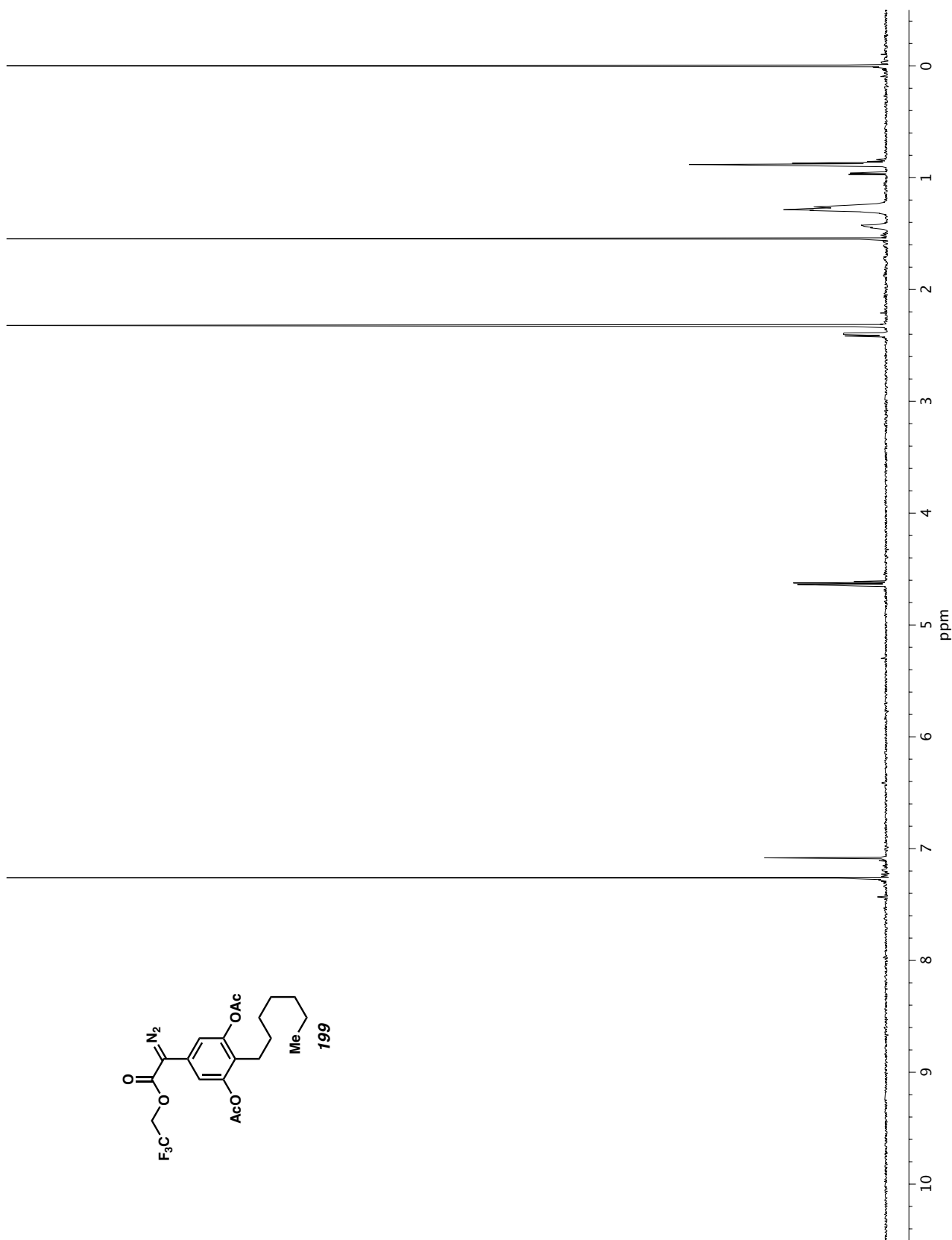


Figure A7.9 <sup>1</sup>H NMR (600 MHz, CDCl<sub>3</sub>) of compound **199**.

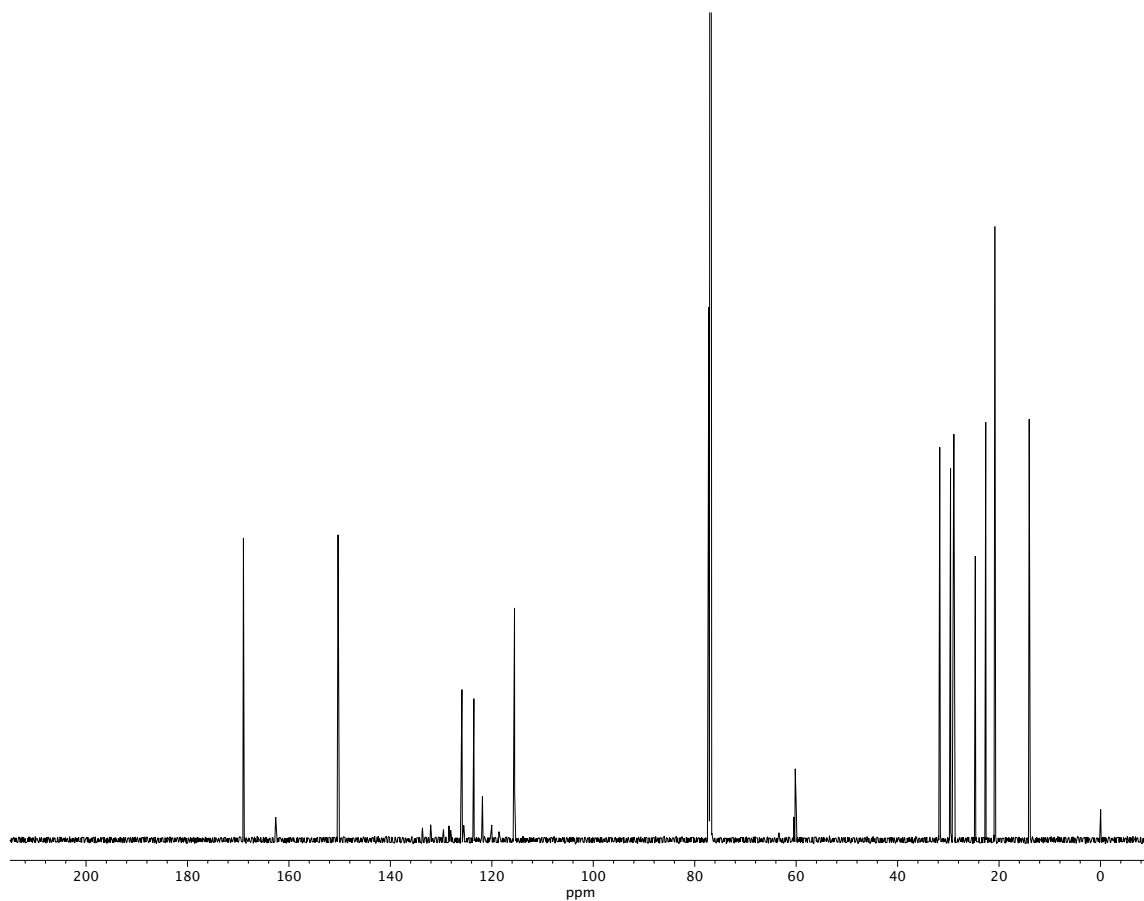
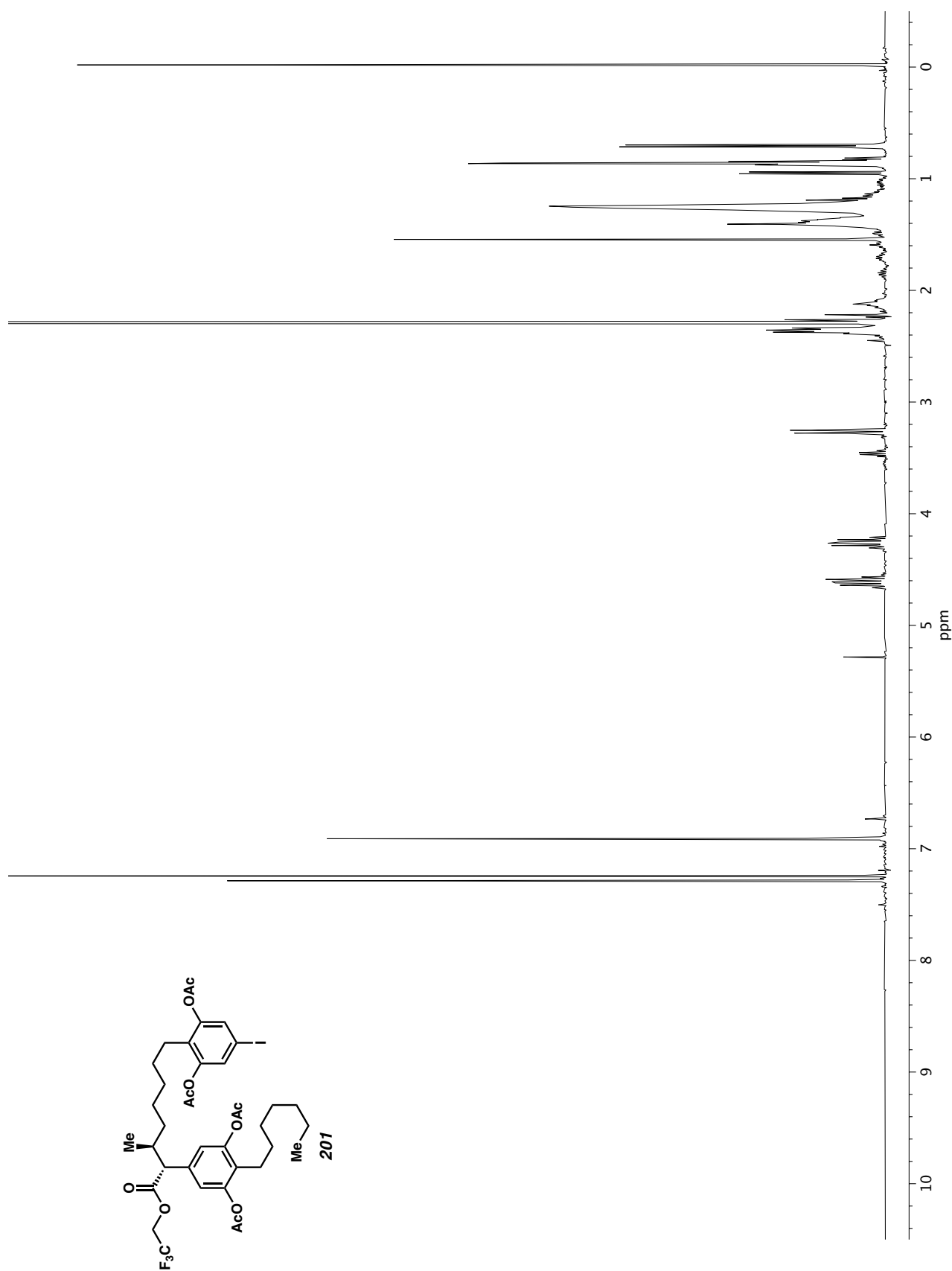


Figure A7.10  $^{13}\text{C}$  NMR (151 MHz,  $\text{CDCl}_3$ ) of compound **199**.



**Figure A7.11**  $^1\text{H}$  NMR (400 MHz, CDCl<sub>3</sub>) of compound **201**.

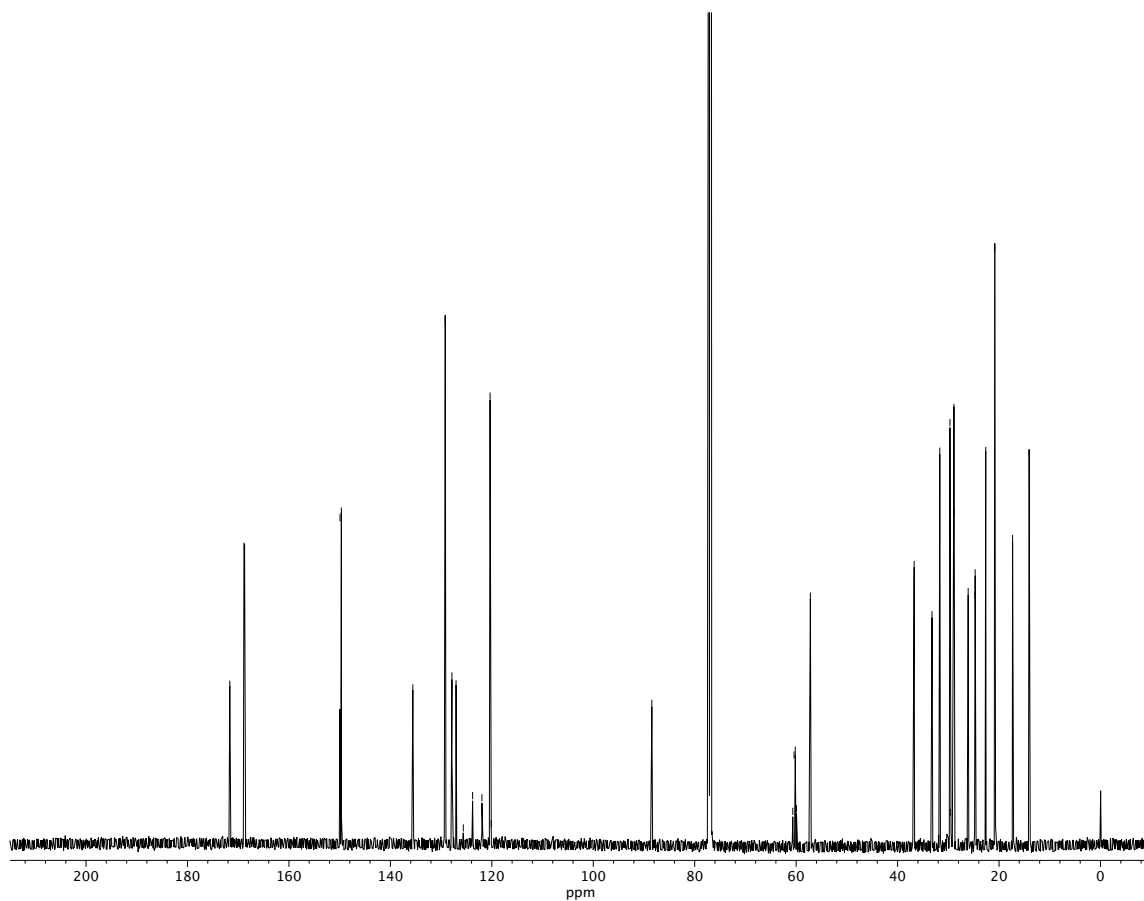
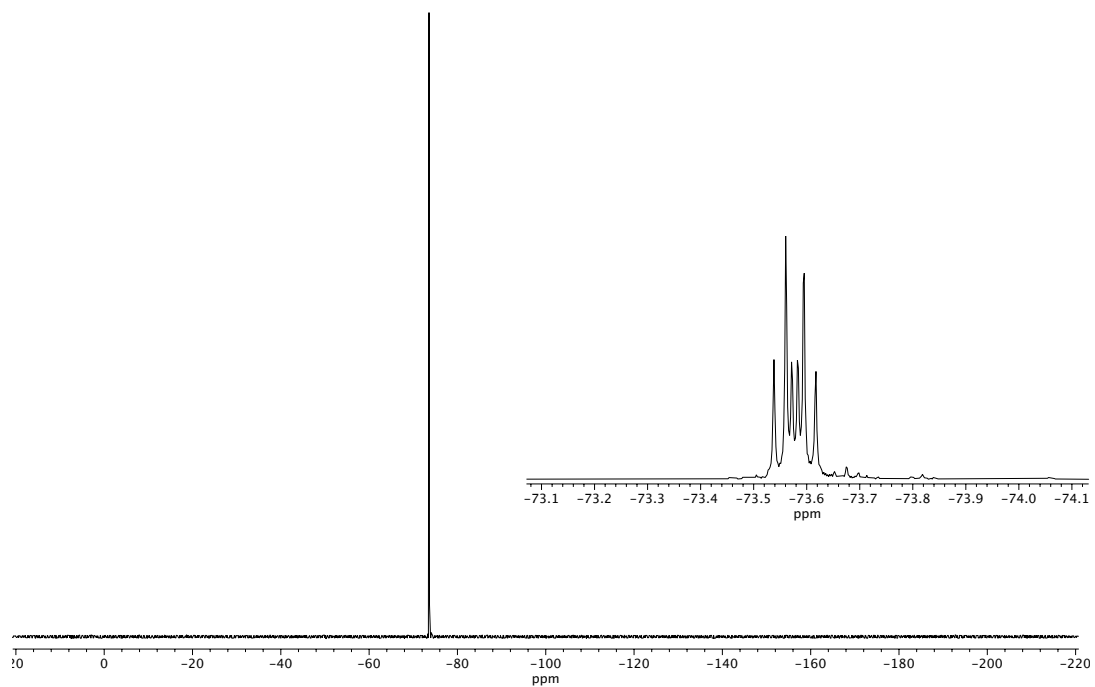
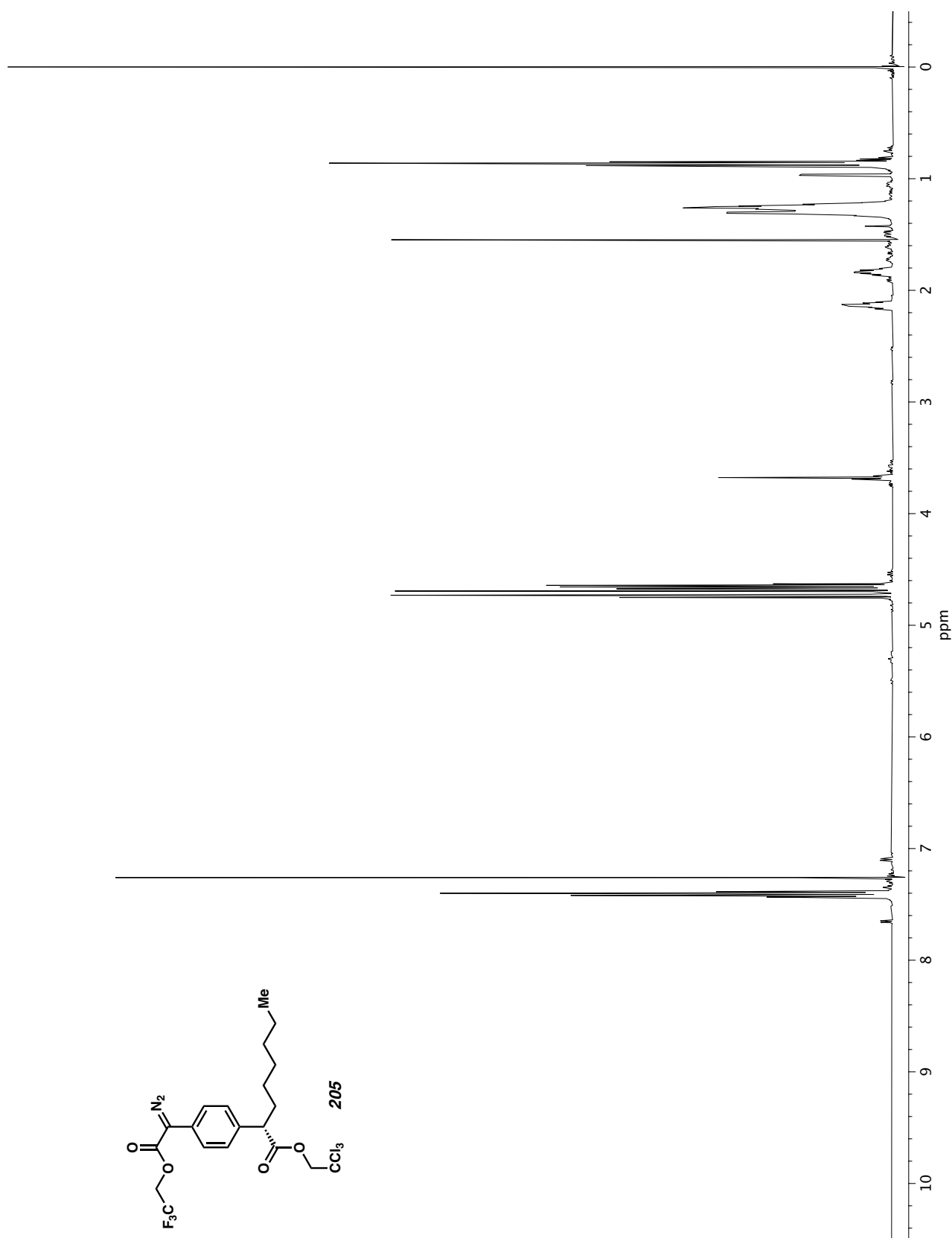


Figure A7.12  $^{13}\text{C}$  NMR (151 MHz, CDCl<sub>3</sub>) of compound 201.





**Figure A7.13**  $^{19}\text{F}$  NMR (376 MHz,  $\text{CDCl}_3$ ) of compound **201**.



**Figure A7.14** <sup>1</sup>H NMR (600 MHz, CDCl<sub>3</sub>) of compound **205**.

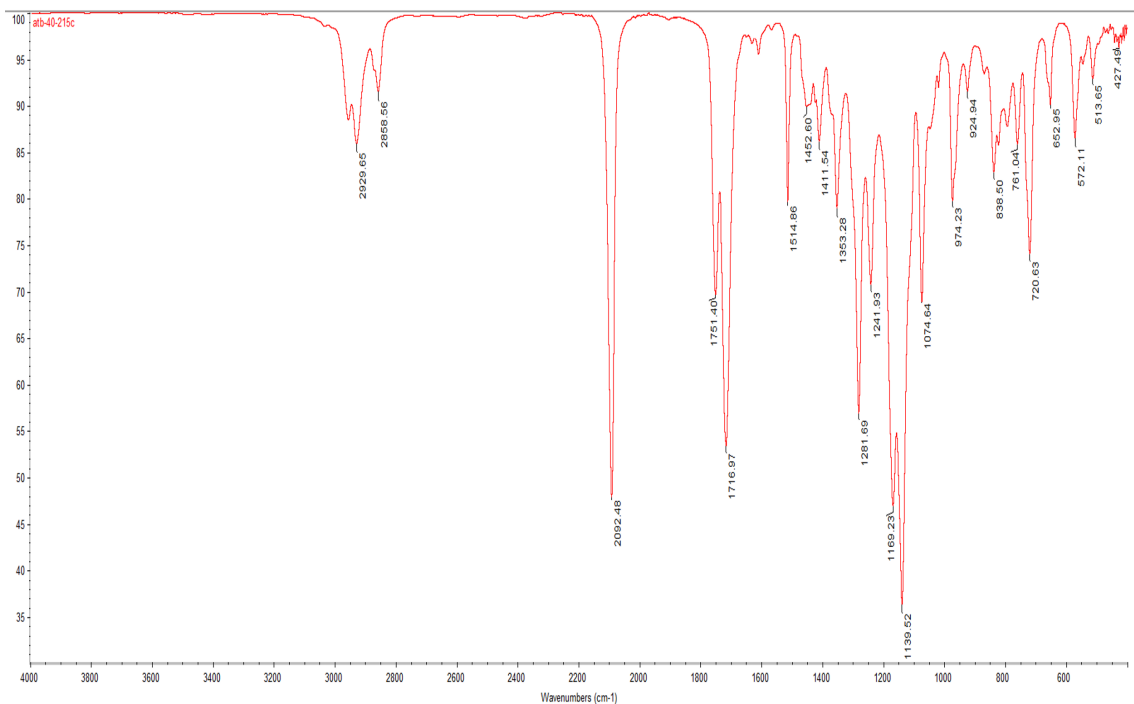


**Figure A7.15** Infrared spectrum (Thin Film, NaCl) of compound 205.

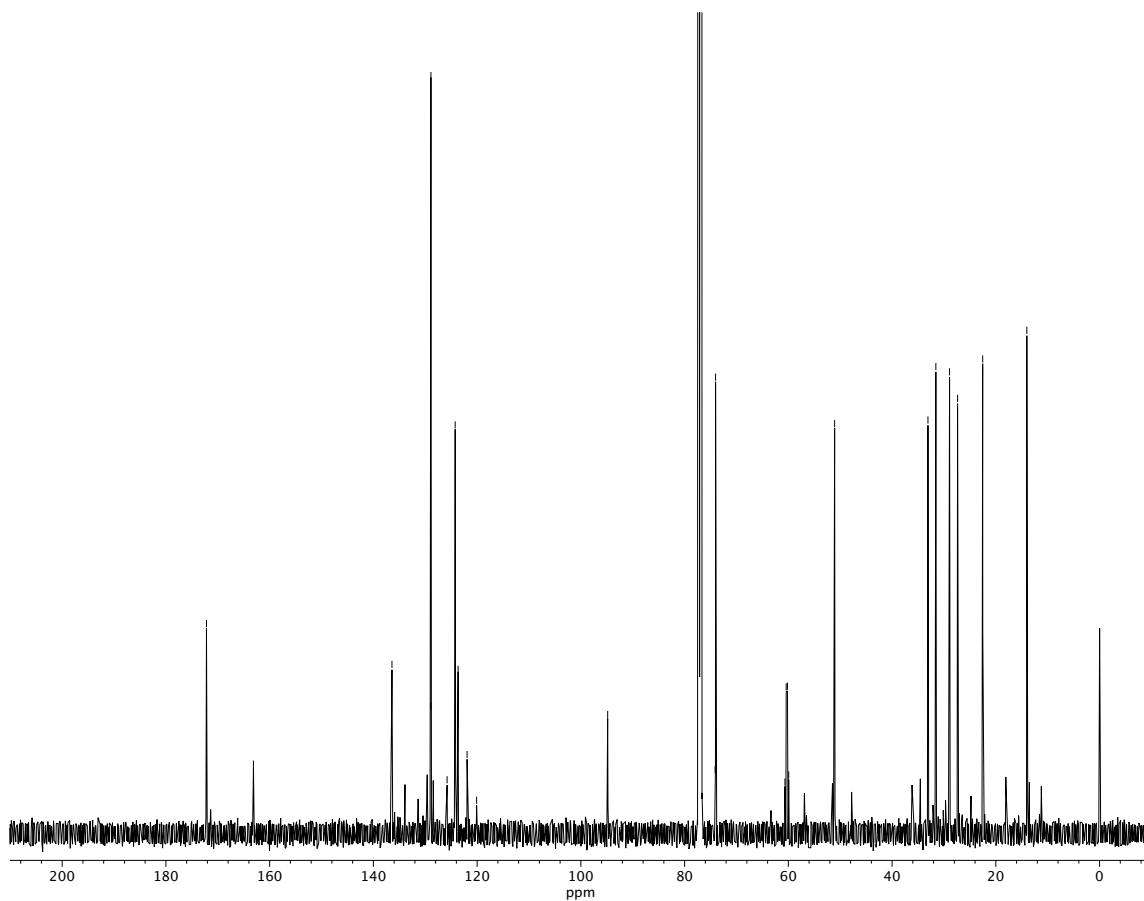


**Figure A7.16** <sup>13</sup>C NMR (151 MHz, CDCl<sub>3</sub>) of compound 205.

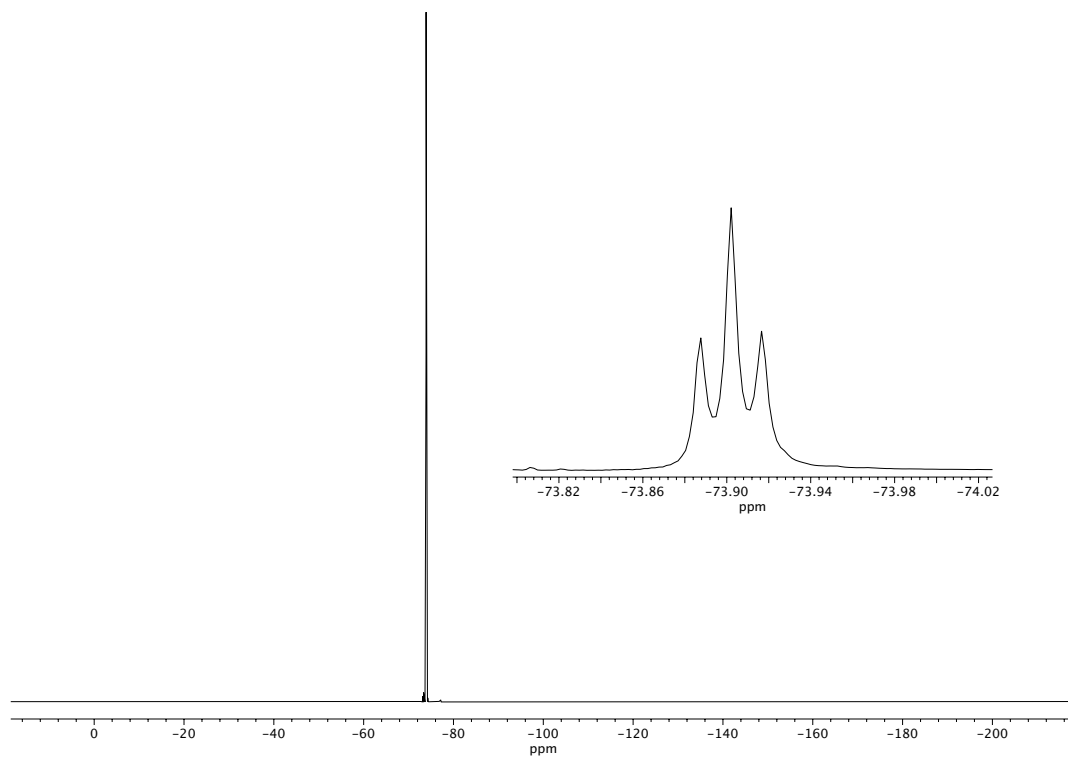


**Figure A7.17**  $^{19}\text{F}$  NMR (556 MHz,  $\text{CDCl}_3$ ) of compound **205**.

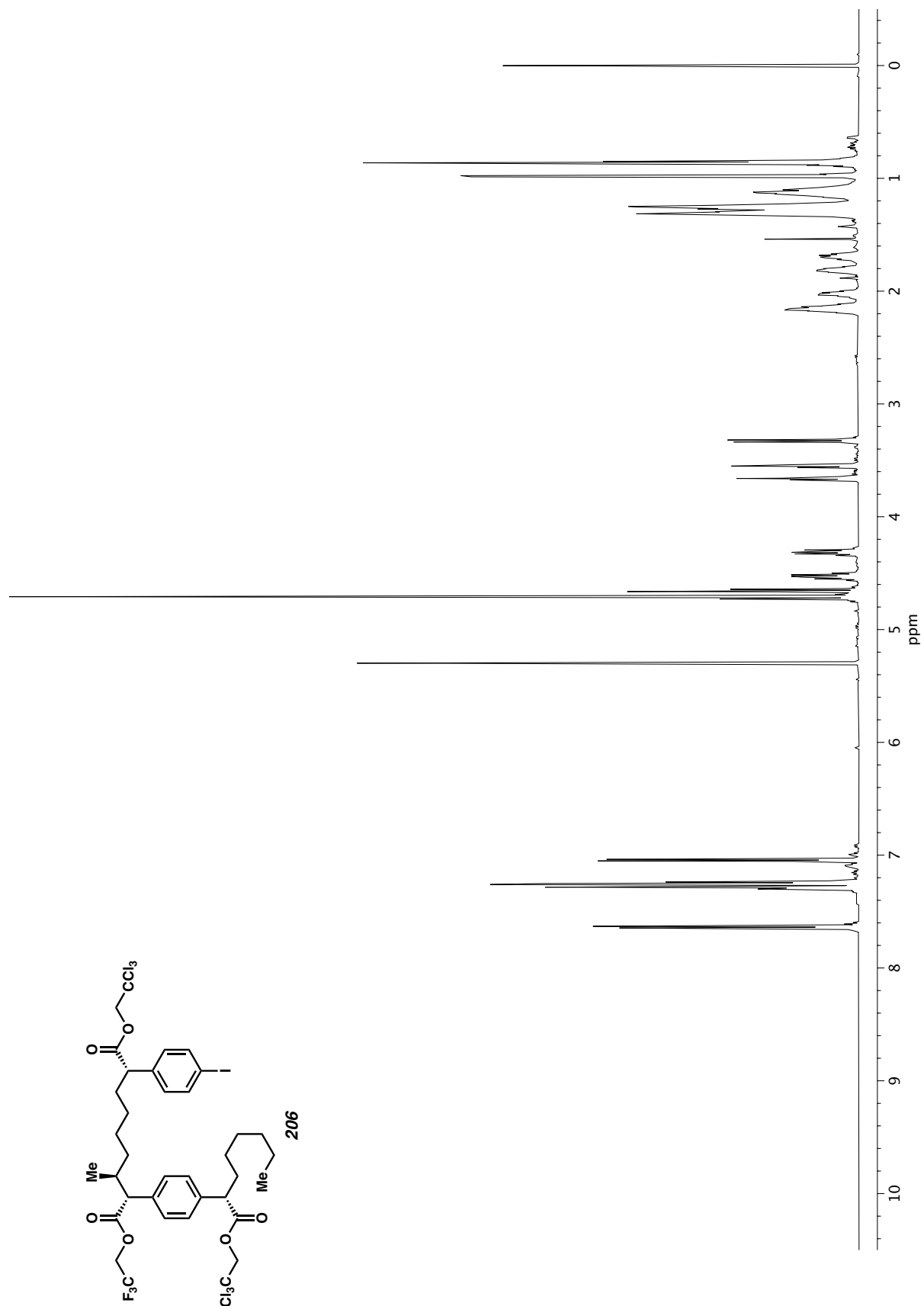


**Figure A7.18** <sup>1</sup>H NMR (600 MHz, CDCl<sub>3</sub>) of compound 206.

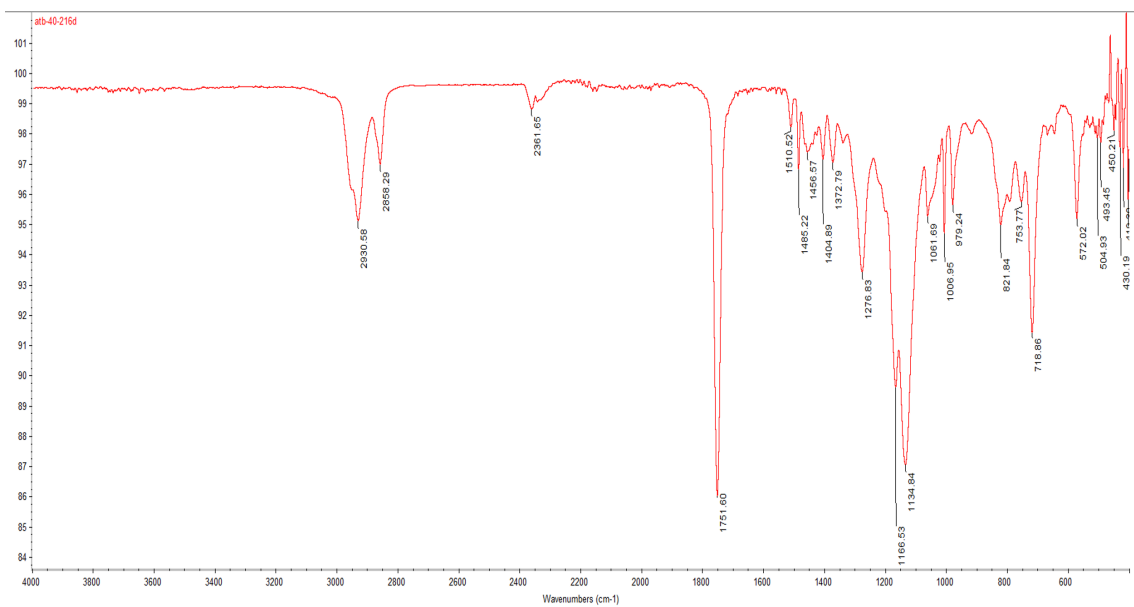


Figure A7.19 Infrared spectrum (Thin Film, NaCl) of compound 206.

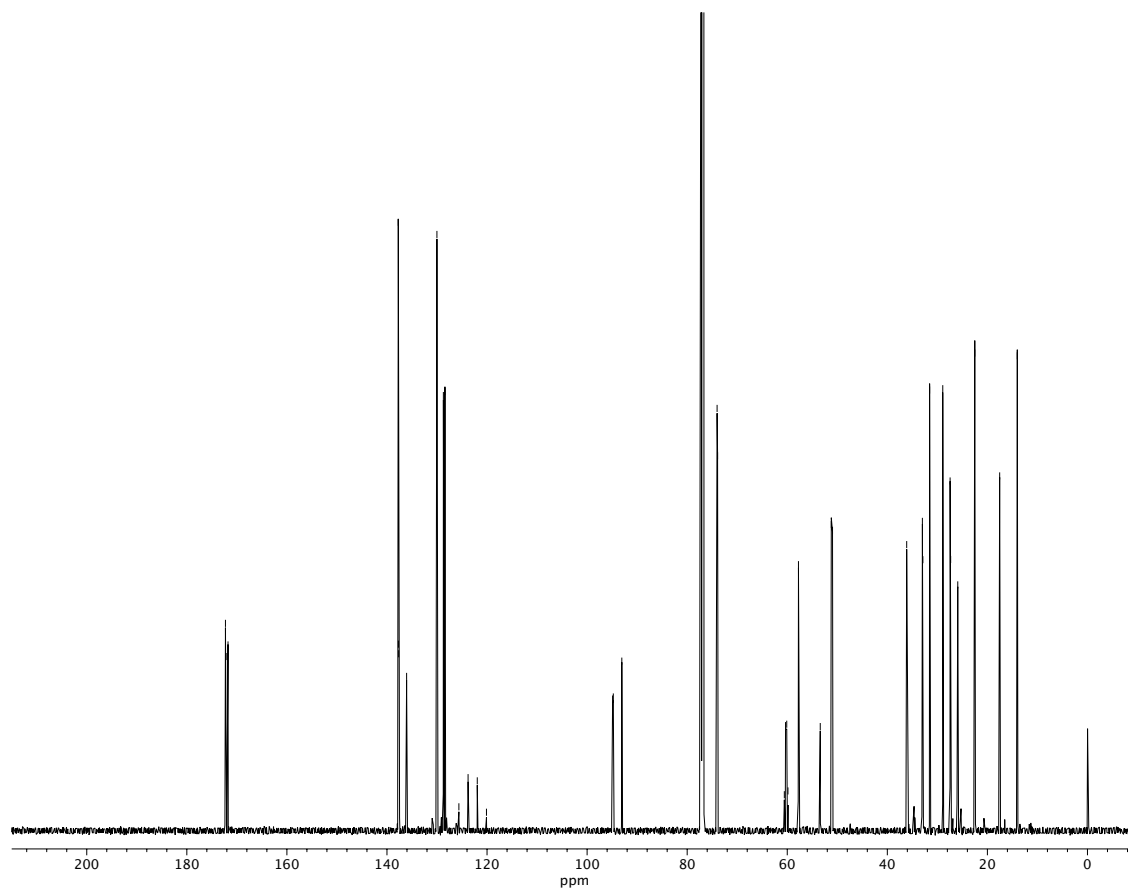
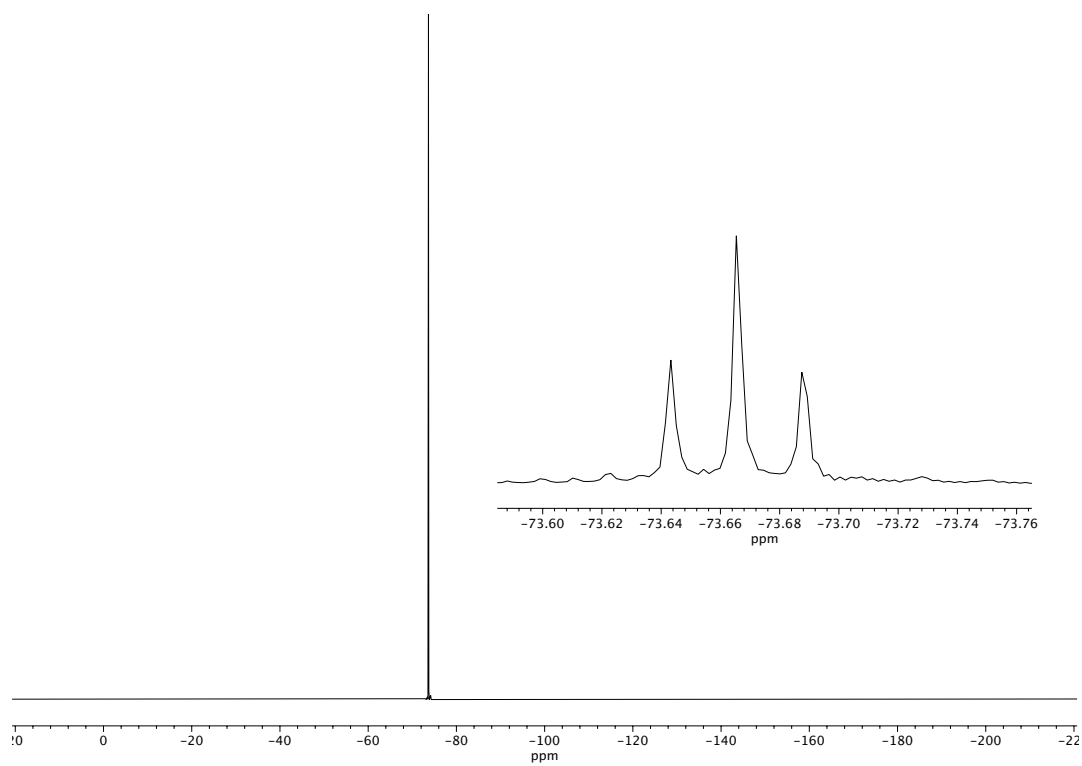


Figure A7.20 <sup>13</sup>C NMR (151 MHz, CDCl<sub>3</sub>) of compound 206.



**Figure A7.21**  $^{19}\text{F}$  NMR (376 MHz,  $\text{CDCl}_3$ ) of compound **206**.

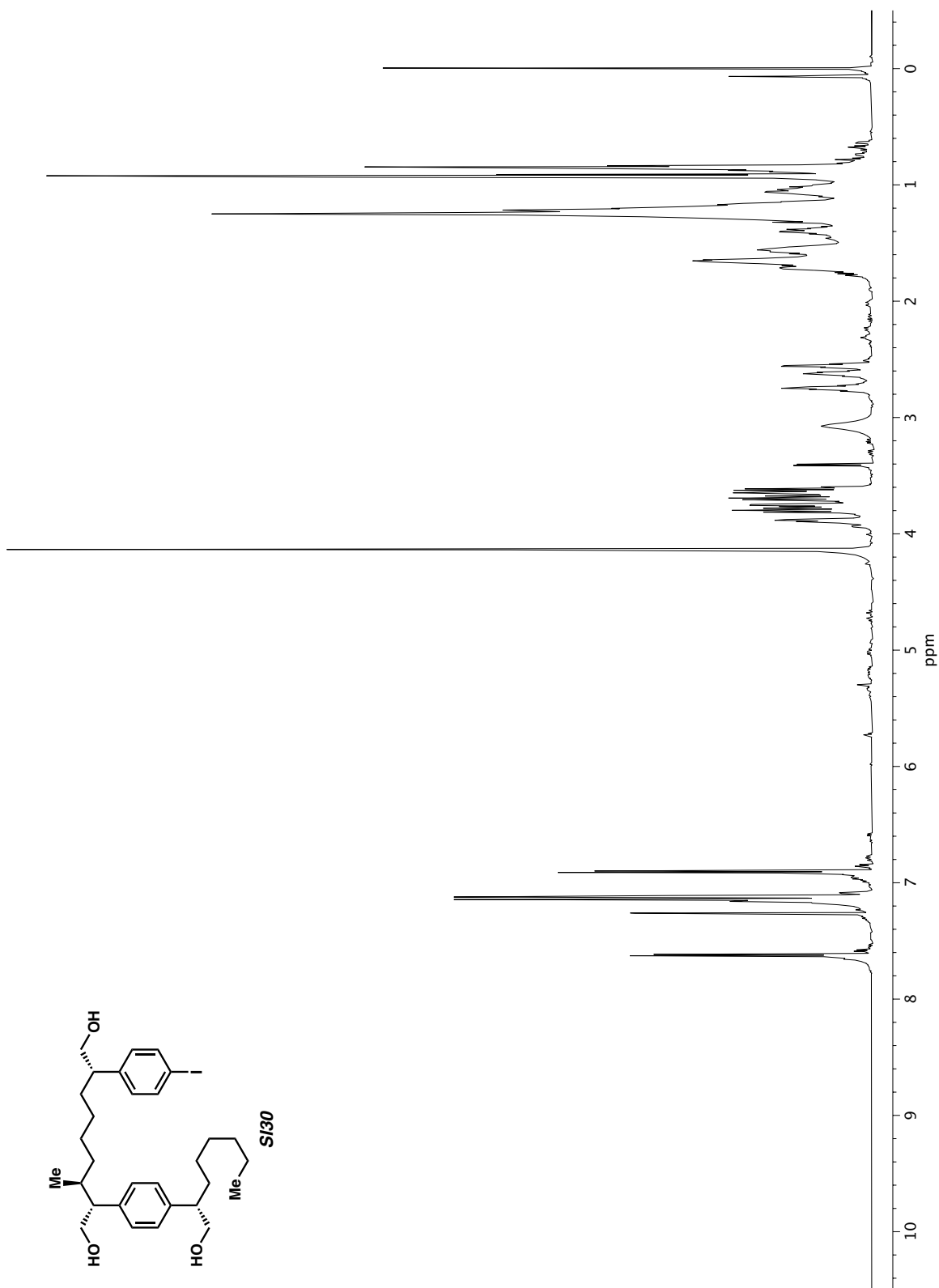
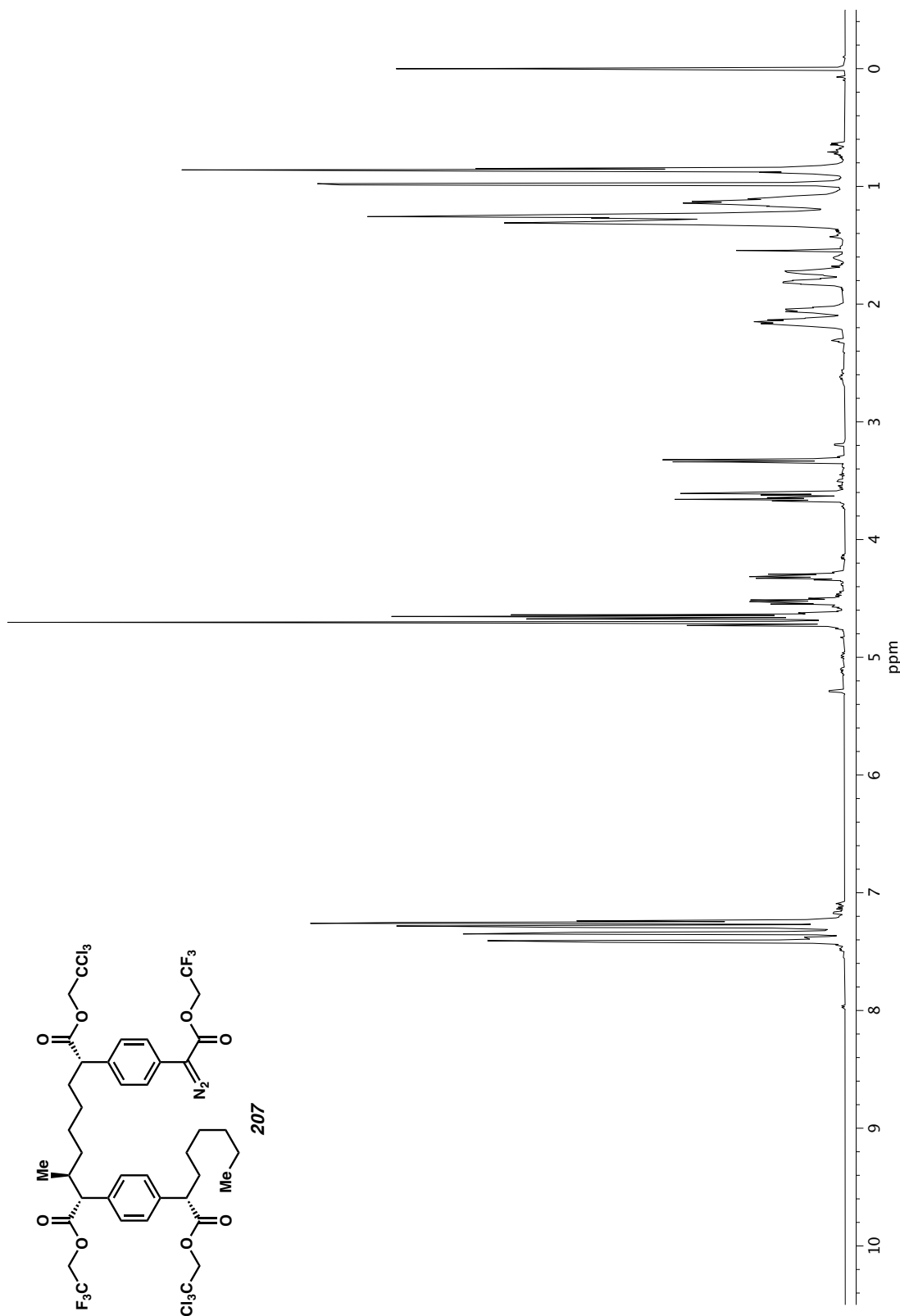
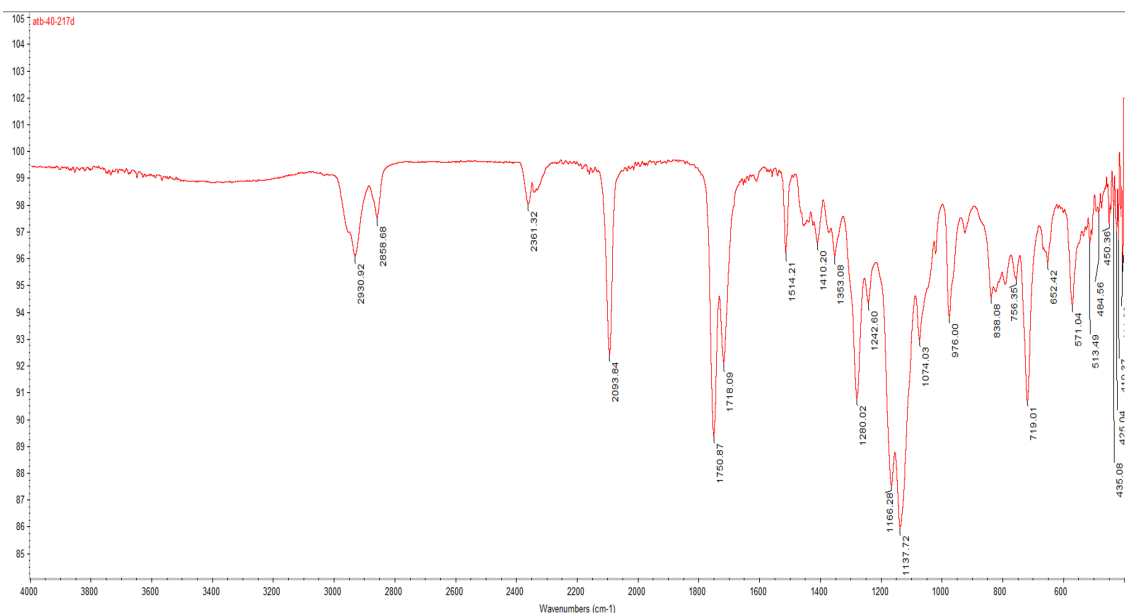


Figure A7.22  $^1\text{H}$  NMR (500 MHz,  $\text{CDCl}_3$ ) of compound **S130**.

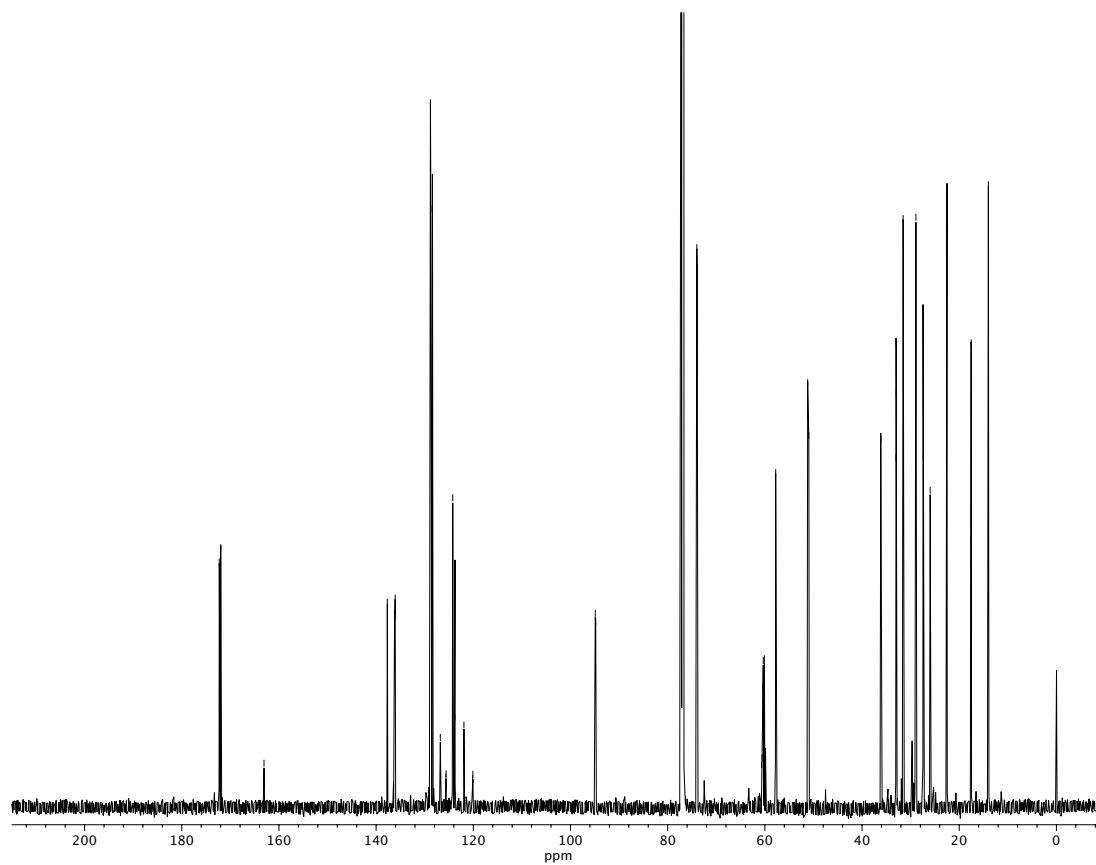




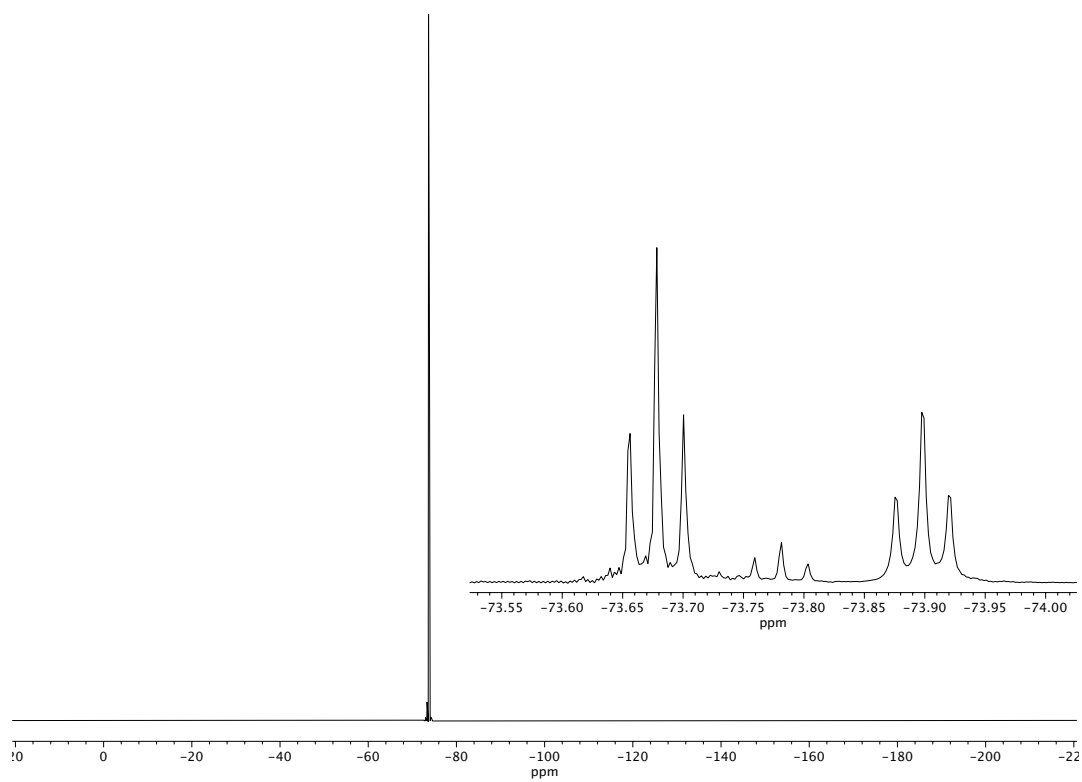
**Figure A7.23**  $^1\text{H}$  NMR (600 MHz,  $\text{CDCl}_3$ ) of compound **207**.



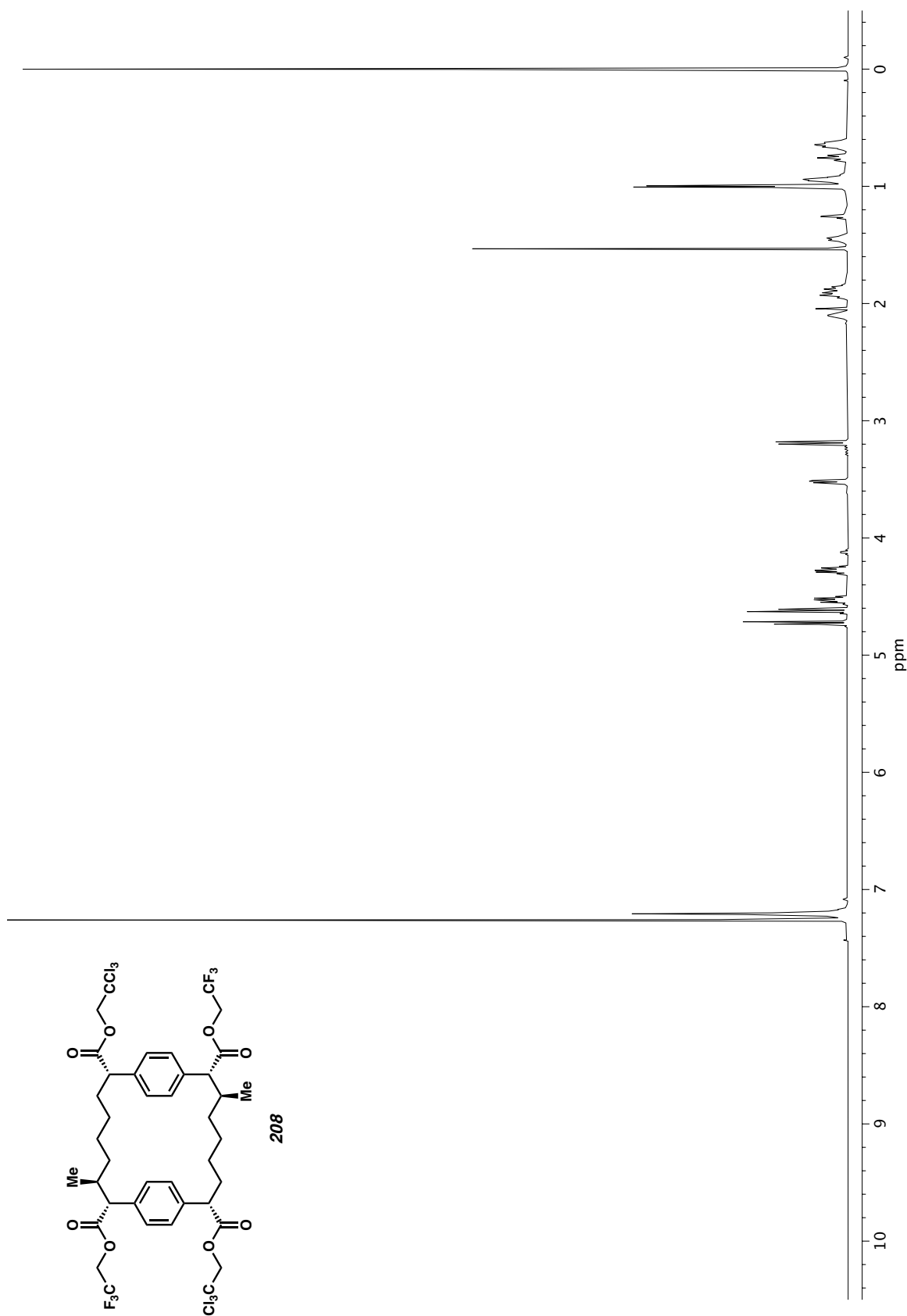
**Figure A7.24** Infrared spectrum (Thin Film, NaCl) of compound **207**.



**Figure A7.25** <sup>13</sup>C NMR (151 MHz, CDCl<sub>3</sub>) of compound **207**.



**Figure A7.26**  $^{19}\text{F}$  NMR (376 MHz,  $\text{CDCl}_3$ ) of compound 207.

Figure A7.27  $^1\text{H}$  NMR (600 MHz,  $\text{CDCl}_3$ ) of compound **208**.

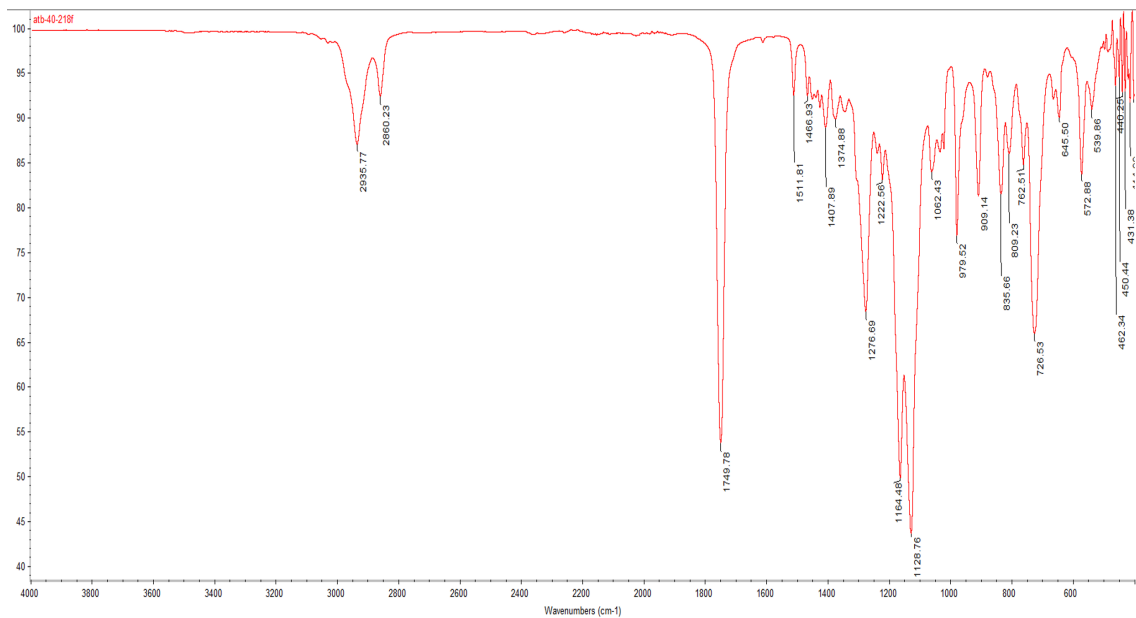


**Figure A7.28** Infrared spectrum (Thin Film, NaCl) of compound **208**.

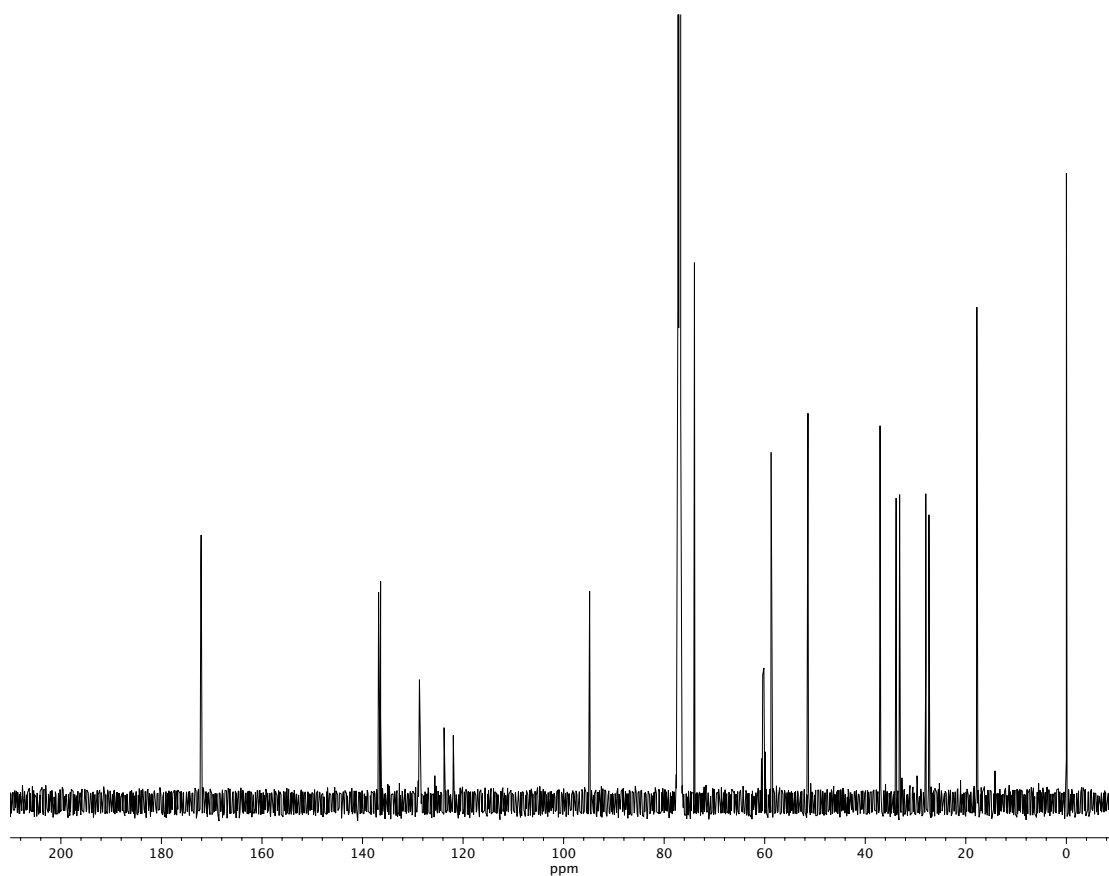


**Figure A7.29** <sup>13</sup>C NMR (151 MHz, CDCl<sub>3</sub>) of compound **208**.

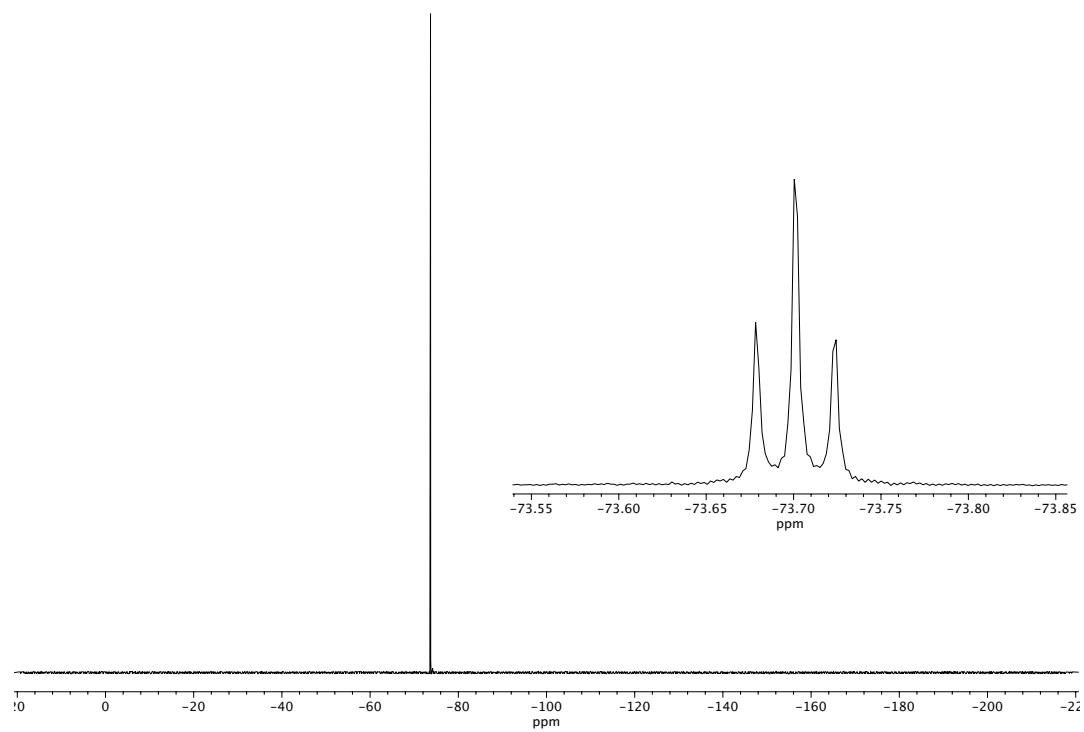


**Figure A7.30**  $^{19}\text{F}$  NMR (376 MHz,  $\text{CDCl}_3$ ) of compound **208**.

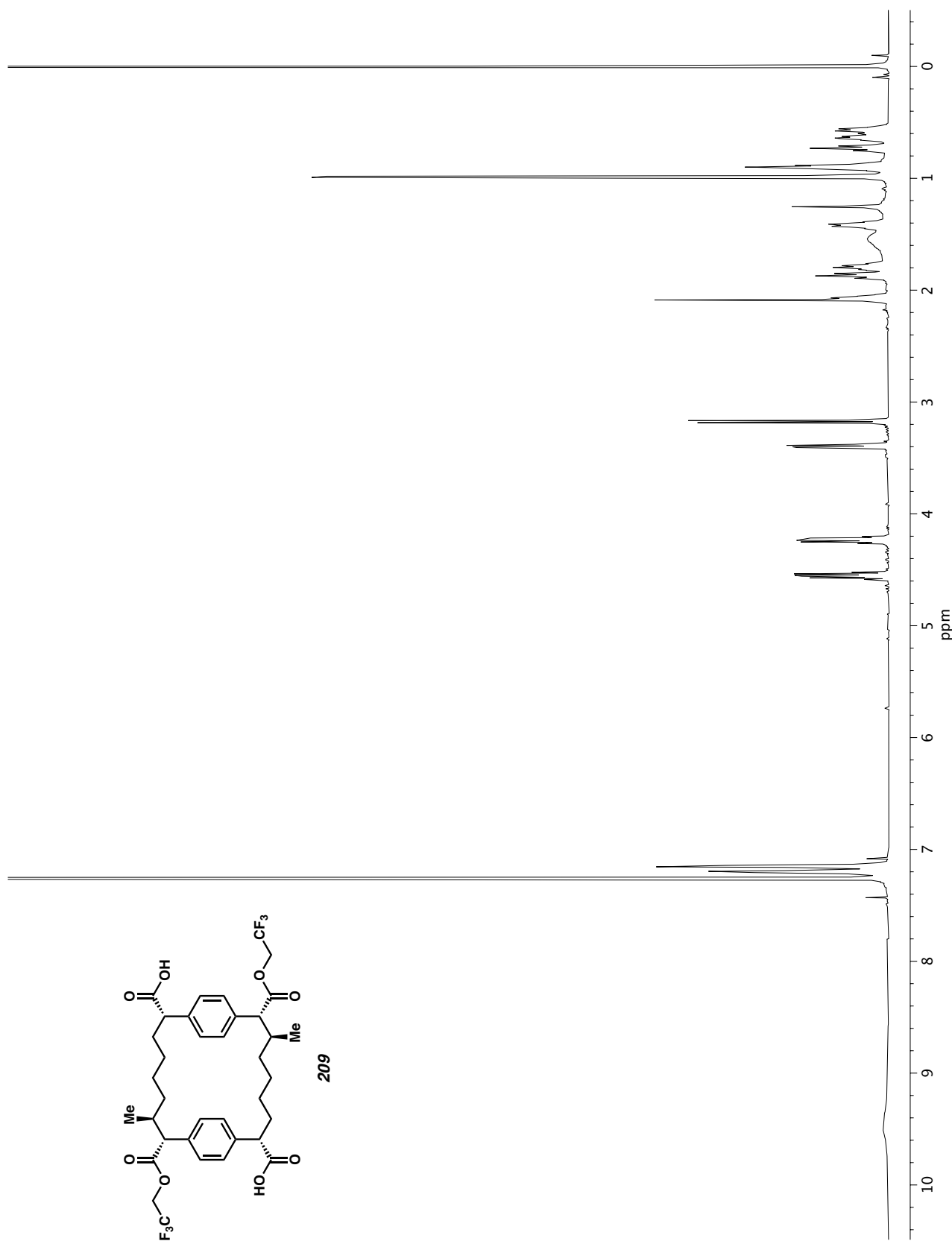


**Figure A7.31**  $^1\text{H}$  NMR (600 MHz,  $\text{CDCl}_3$ ) of compound **209**.

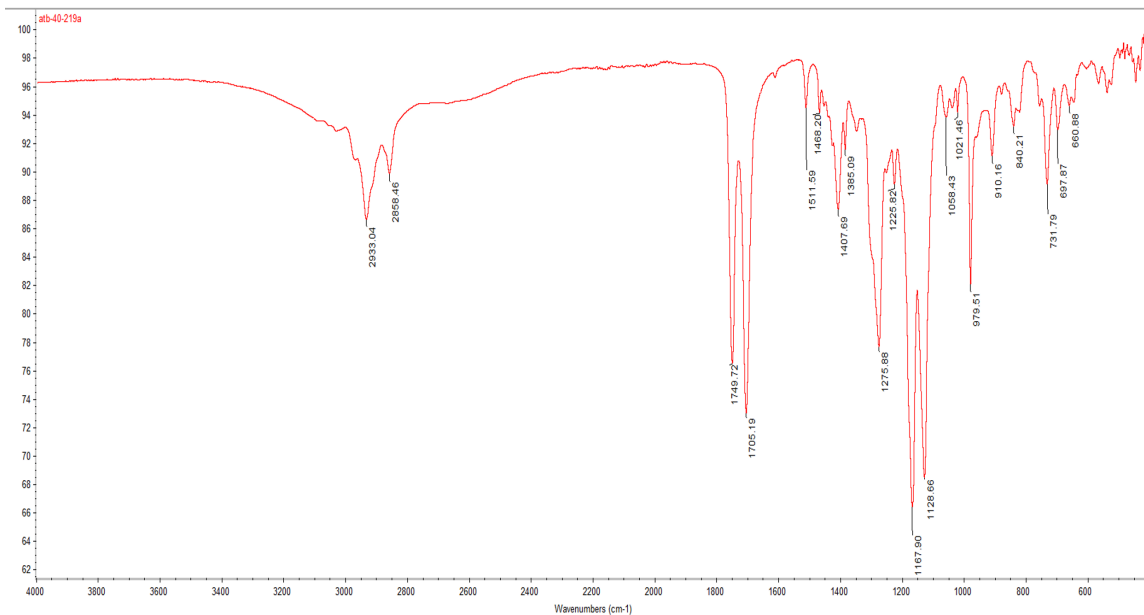


**Figure A7.32** Infrared spectrum (Thin Film, NaCl) of compound **209**.

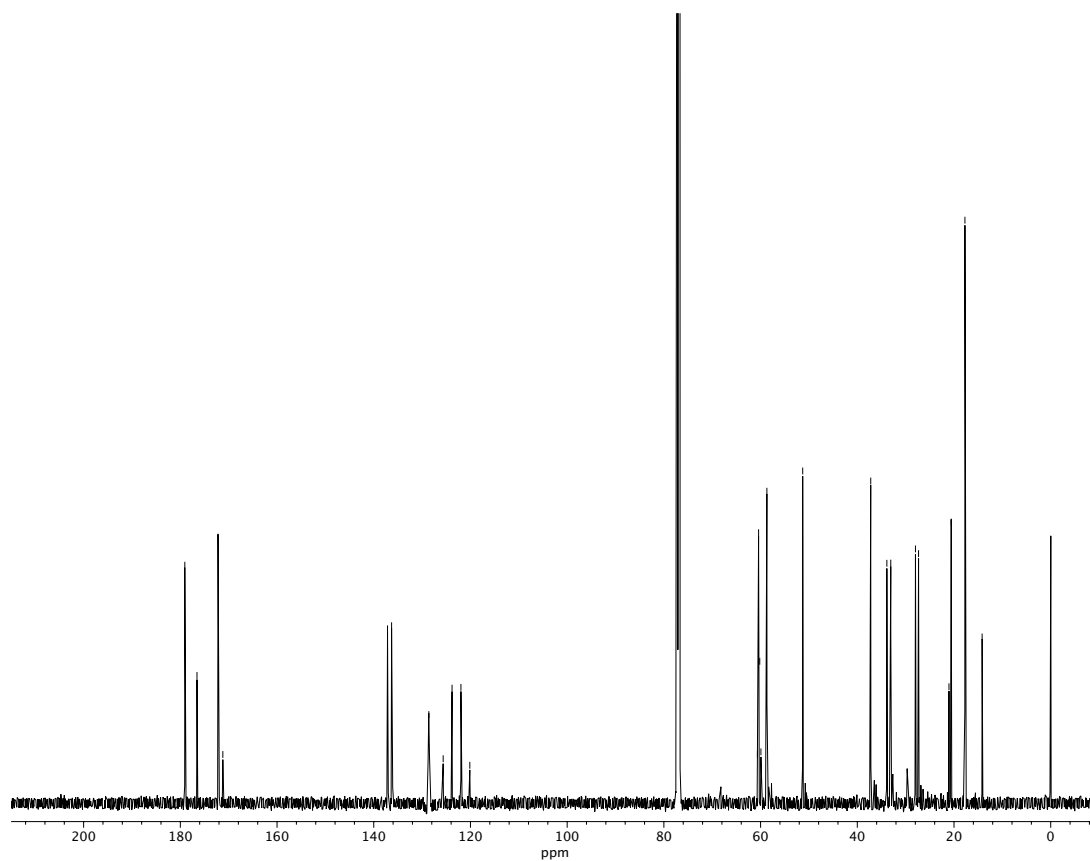


**Figure A7.33** <sup>13</sup>C NMR (151 MHz, CDCl<sub>3</sub>) of compound **209**.



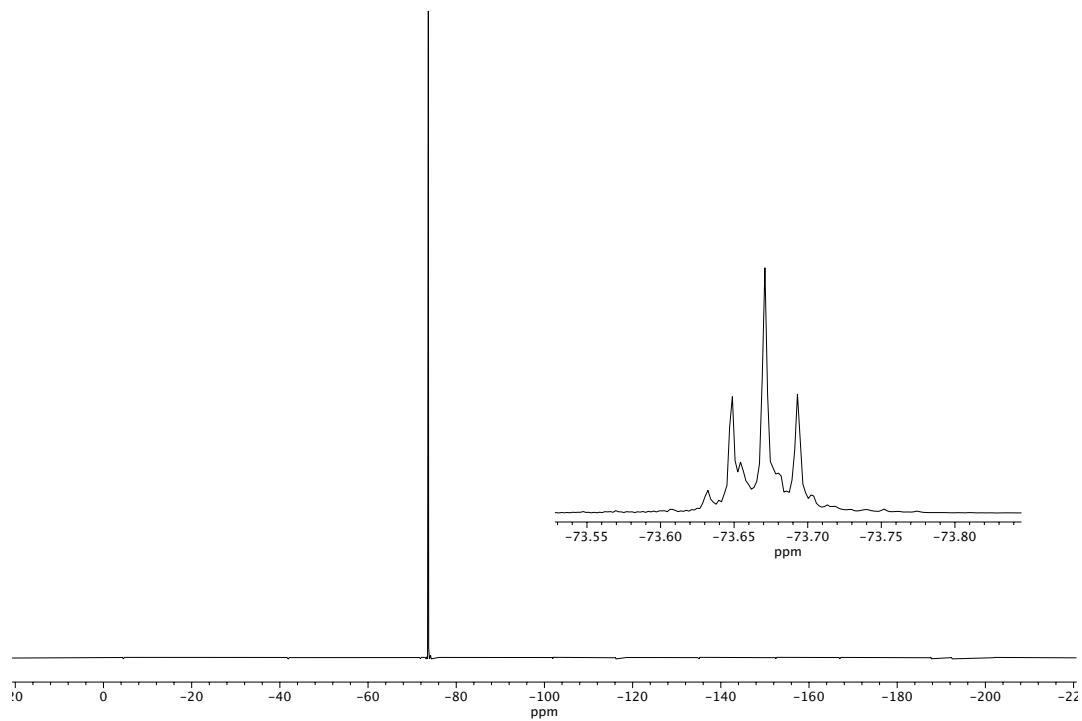


**Figure A7.34**  $^{19}\text{F}$  NMR (376 MHz,  $\text{CDCl}_3$ ) of compound **209**.

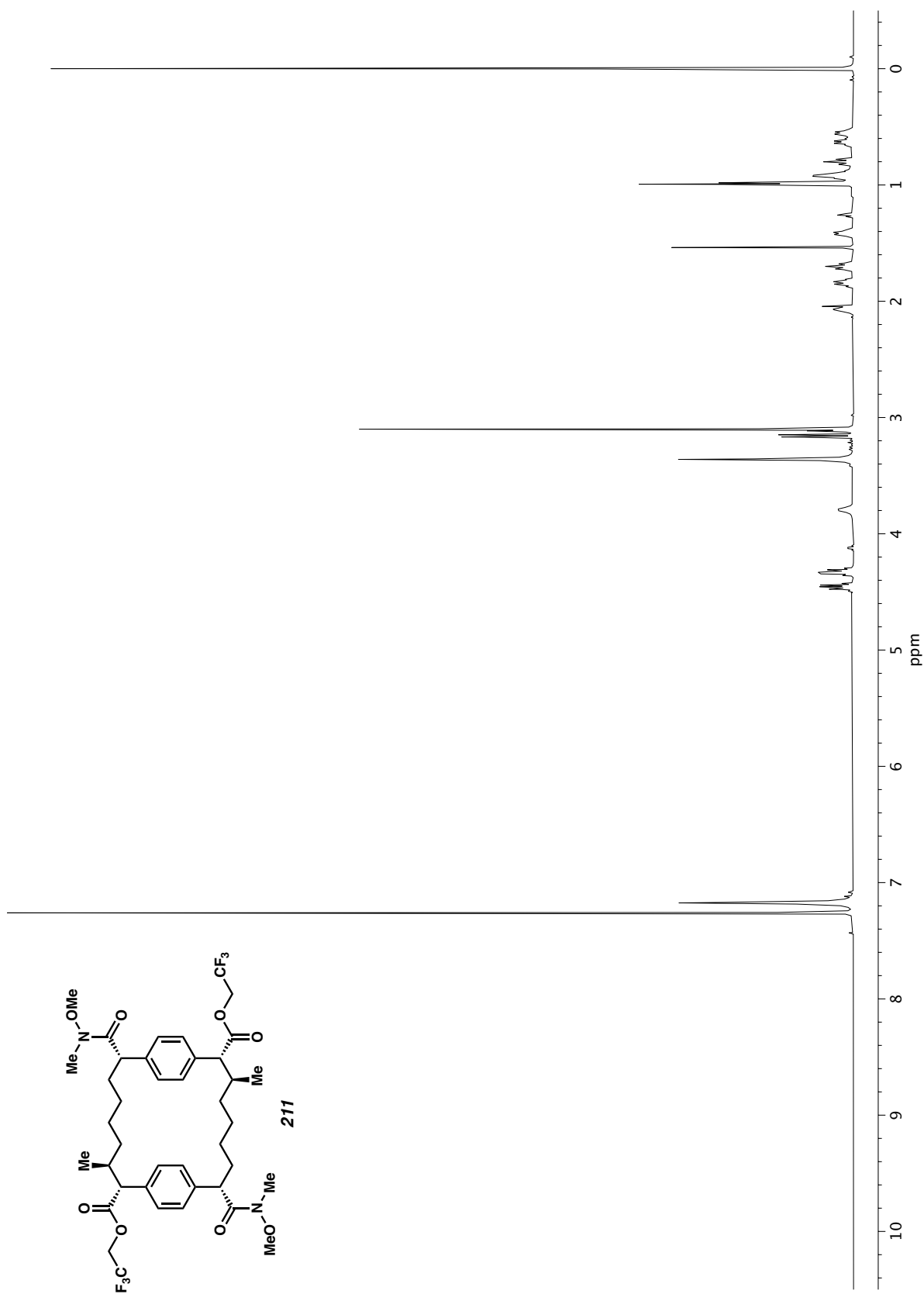


Figure A7.35  $^1\text{H}$  NMR (600 MHz,  $\text{CDCl}_3$ ) of compound **211**.

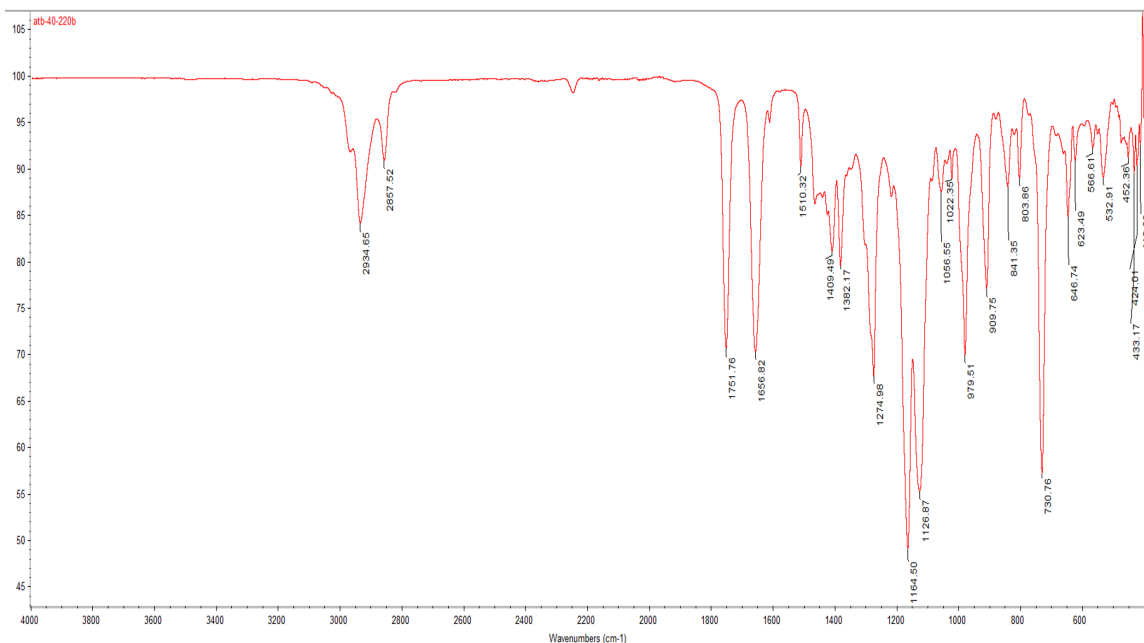


Figure A7.36 Infrared spectrum (Thin Film, NaCl) of compound 211.

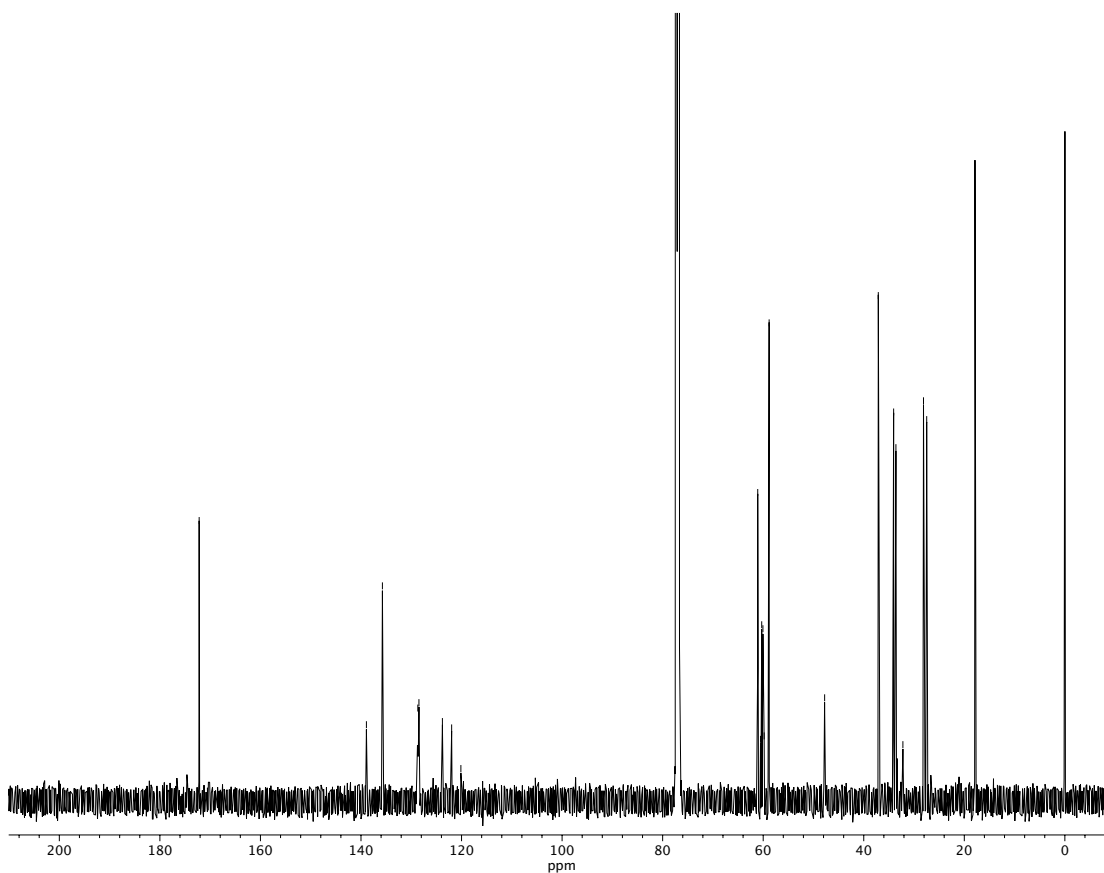
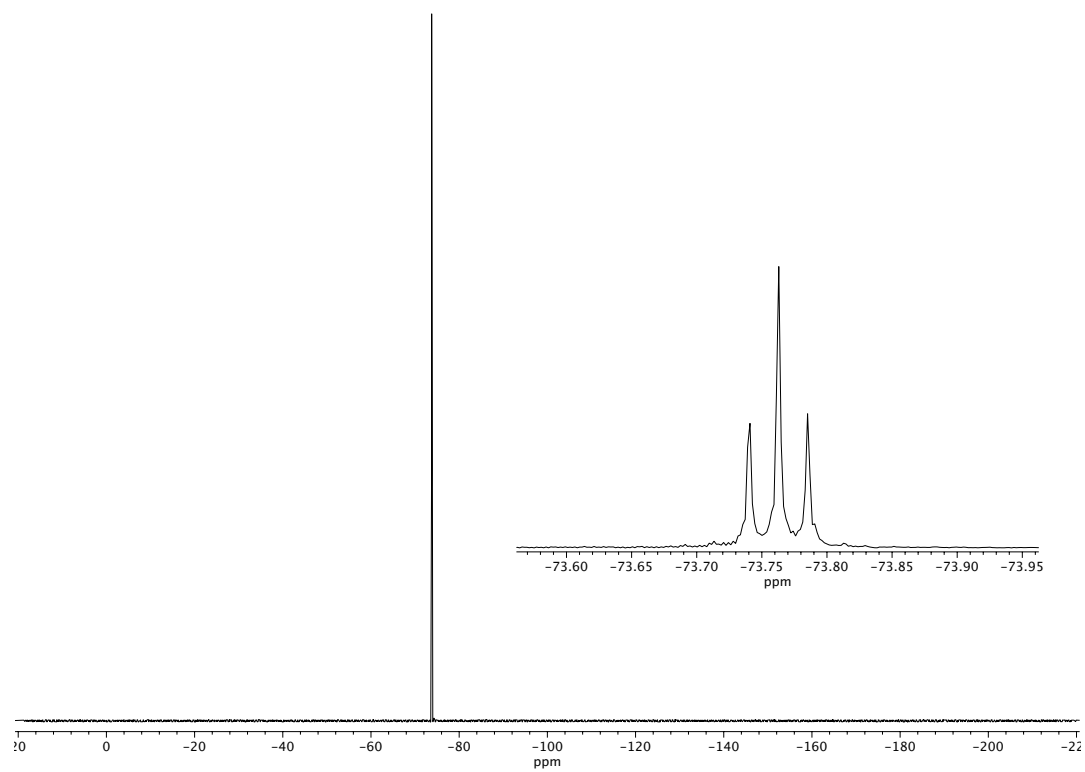


Figure A7.37 <sup>13</sup>C NMR (151 MHz, CDCl<sub>3</sub>) of compound 211.



**Figure A7.38**  $^{19}\text{F}$  NMR (376 MHz,  $\text{CDCl}_3$ ) of compound **211**.

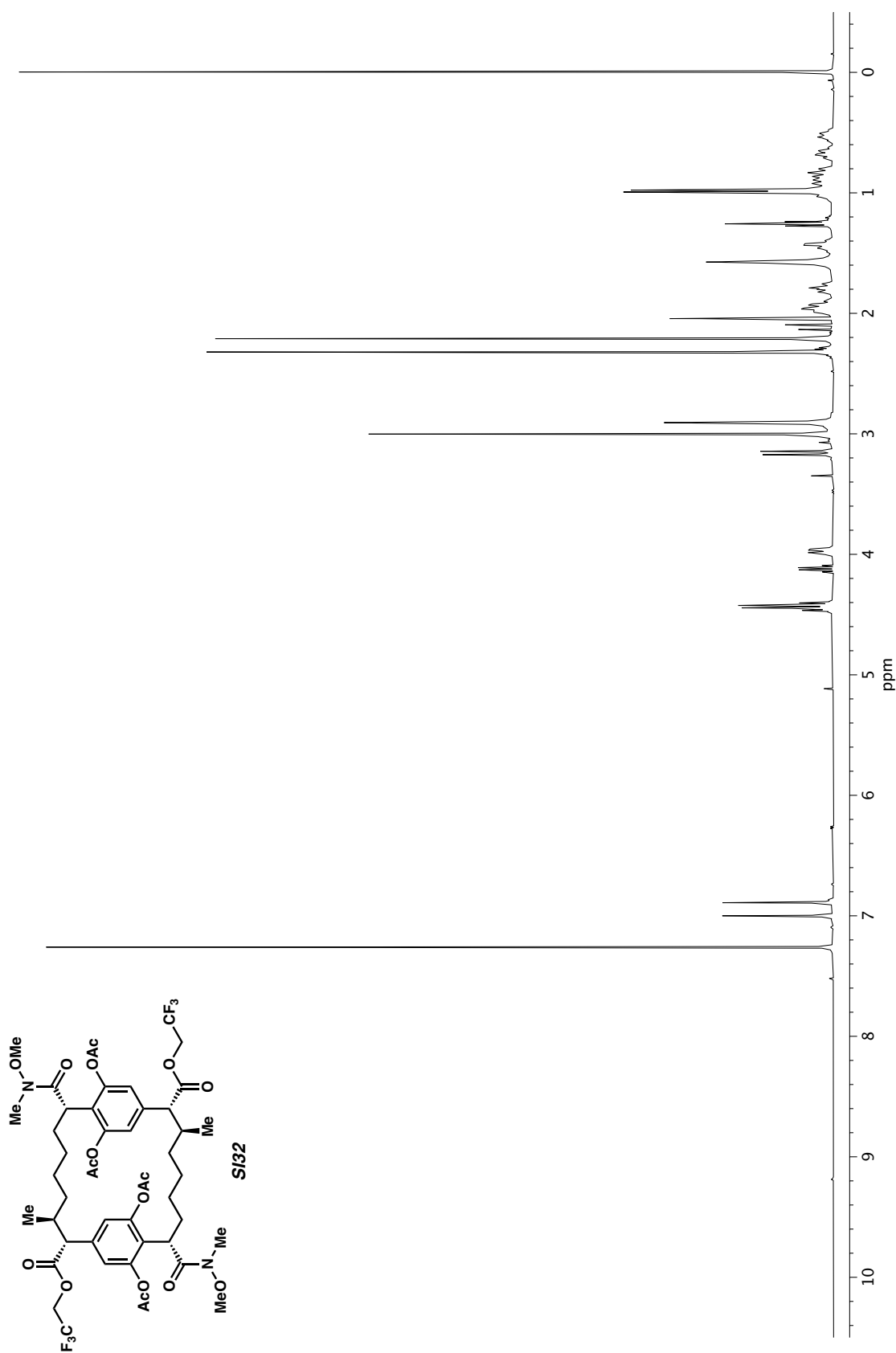


Figure A7.39  $^1\text{H}$  NMR (400 MHz, CDCl<sub>3</sub>) of compound **SI32**.

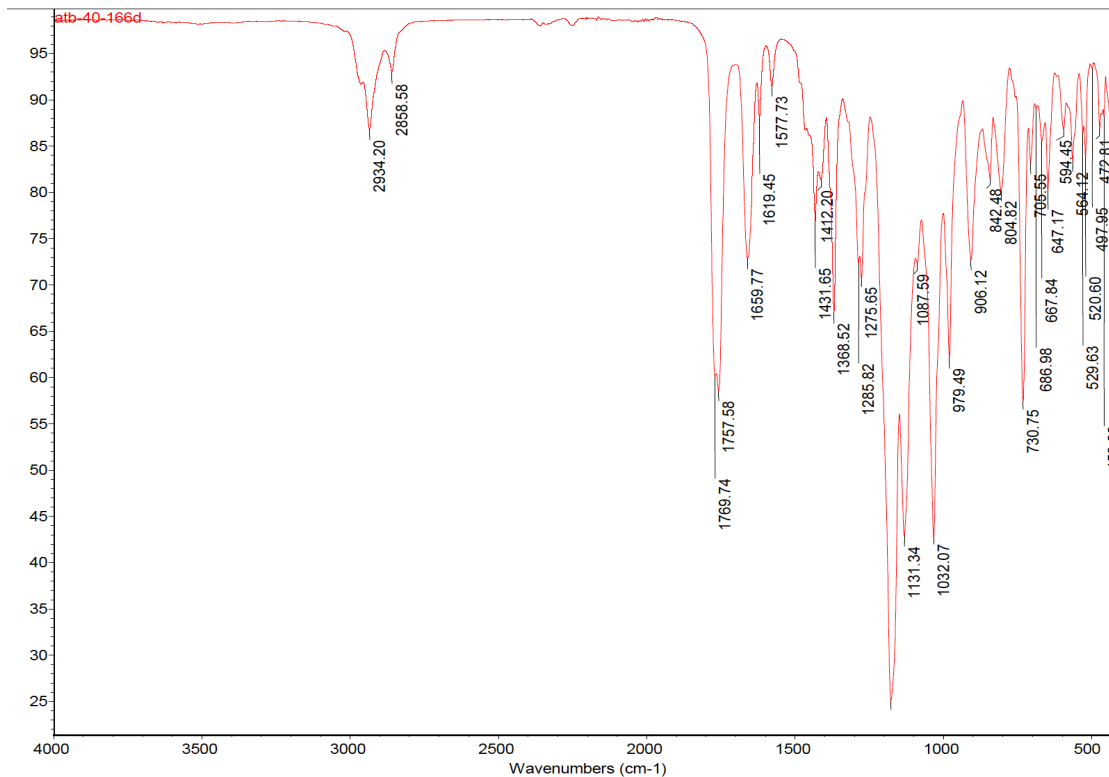


Figure A7.40 Infrared spectrum (Thin Film, NaCl) of compound SI32.

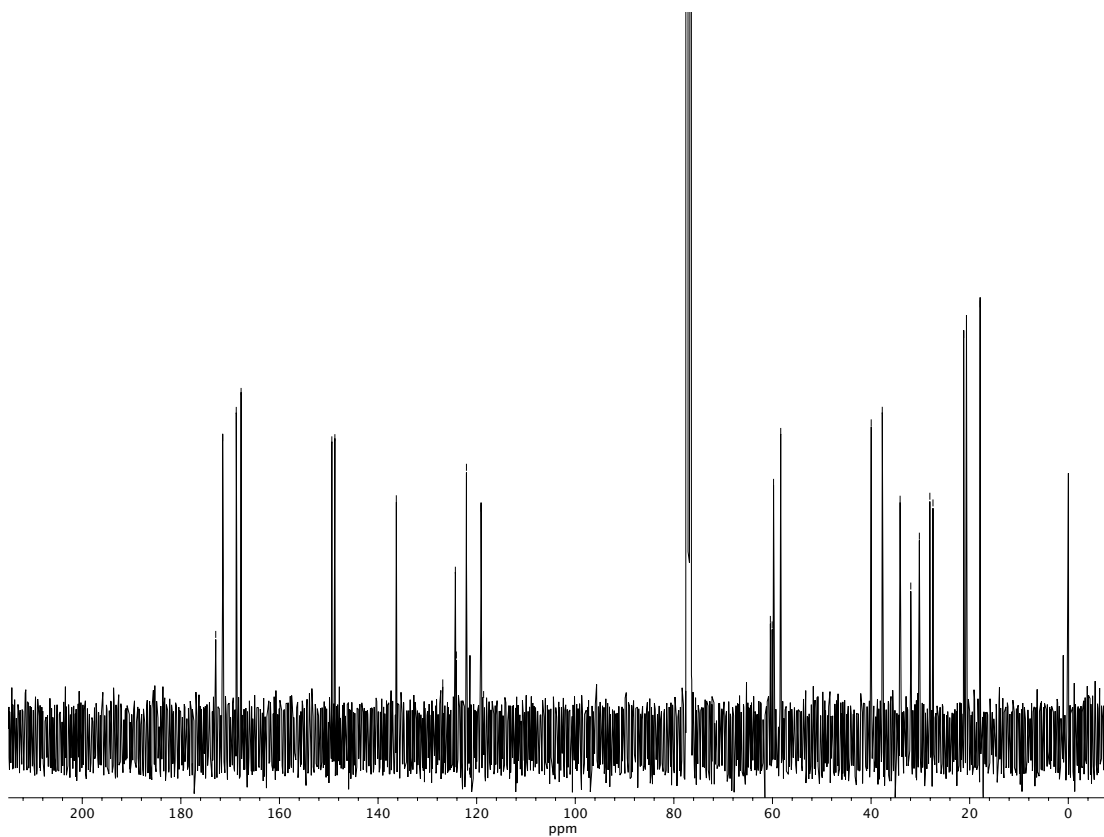
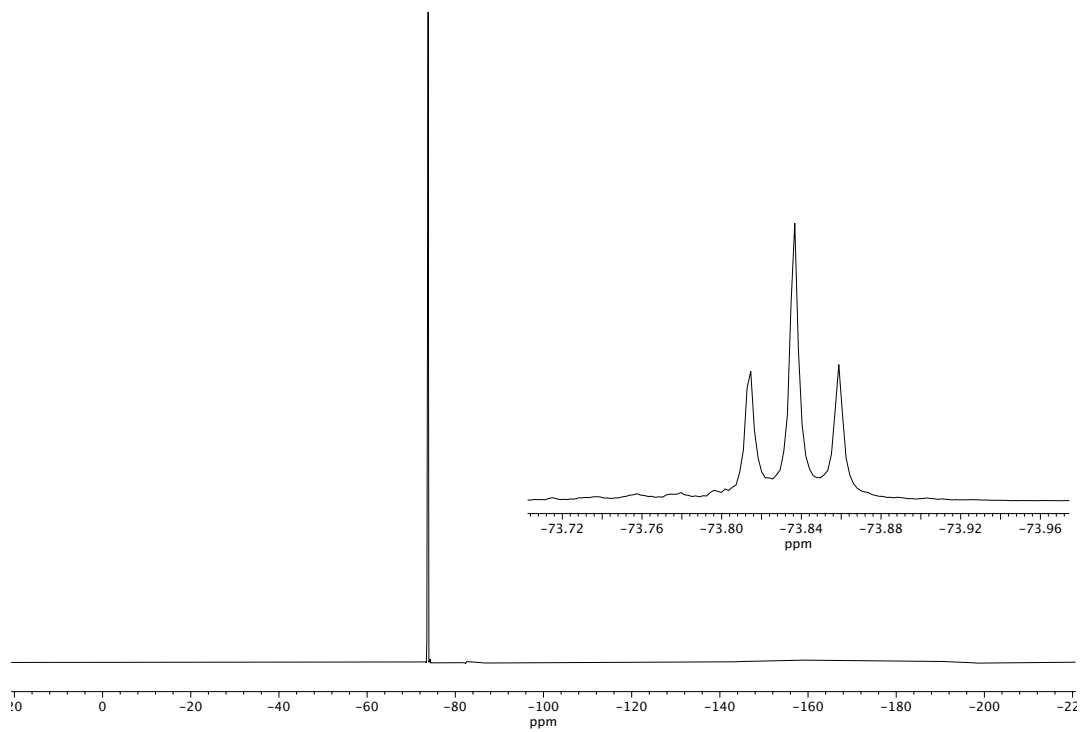


Figure A7.41 <sup>13</sup>C NMR (100 MHz, CDCl<sub>3</sub>) of compound SI32.



**Figure A7.42**  $^{19}\text{F}$  NMR (376 MHz,  $\text{CDCl}_3$ ) of compound **SI32**.

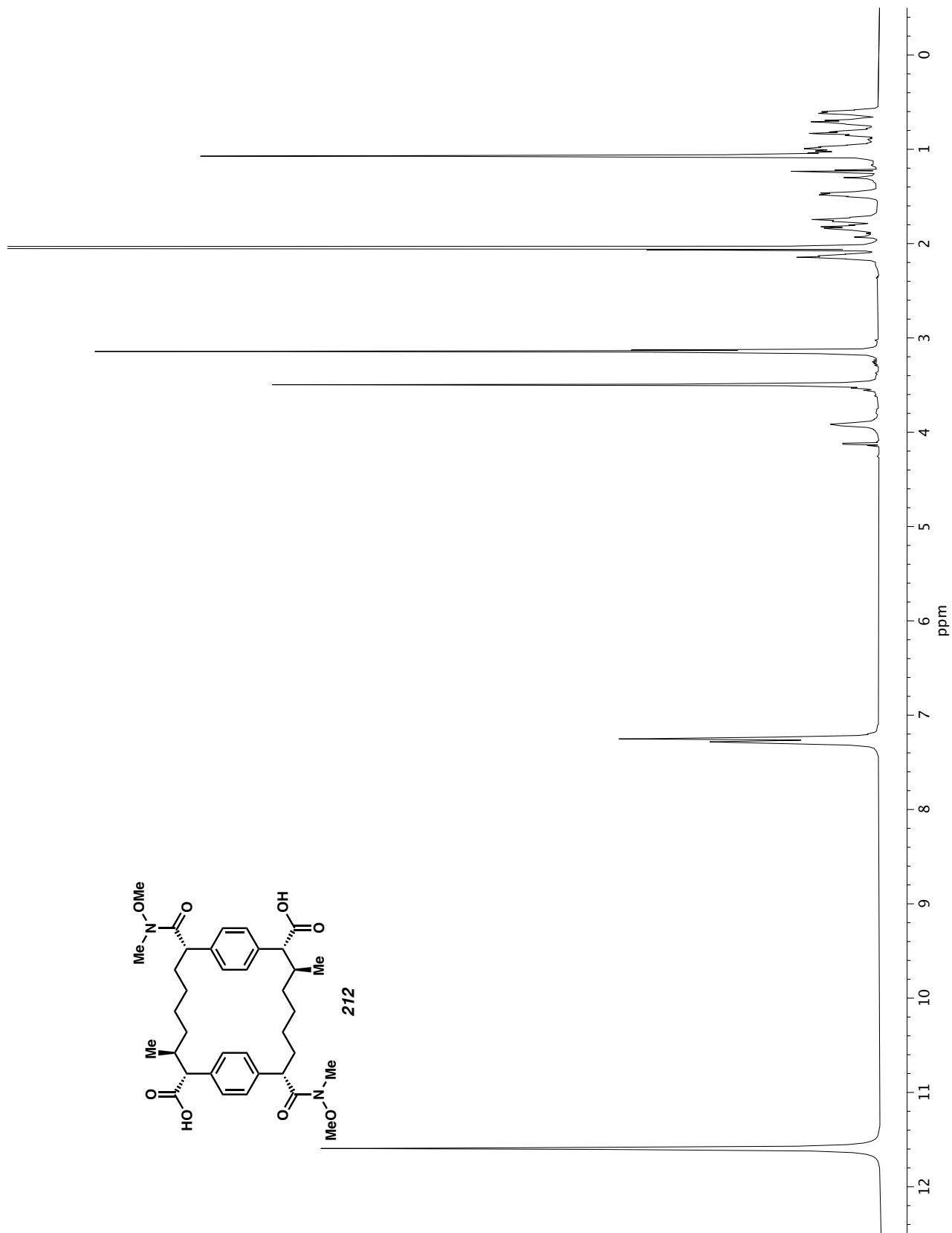


Figure A7.43  $^1\text{H}$  NMR (600 MHz,  $\text{AcOD}$ ) of compound **212**.



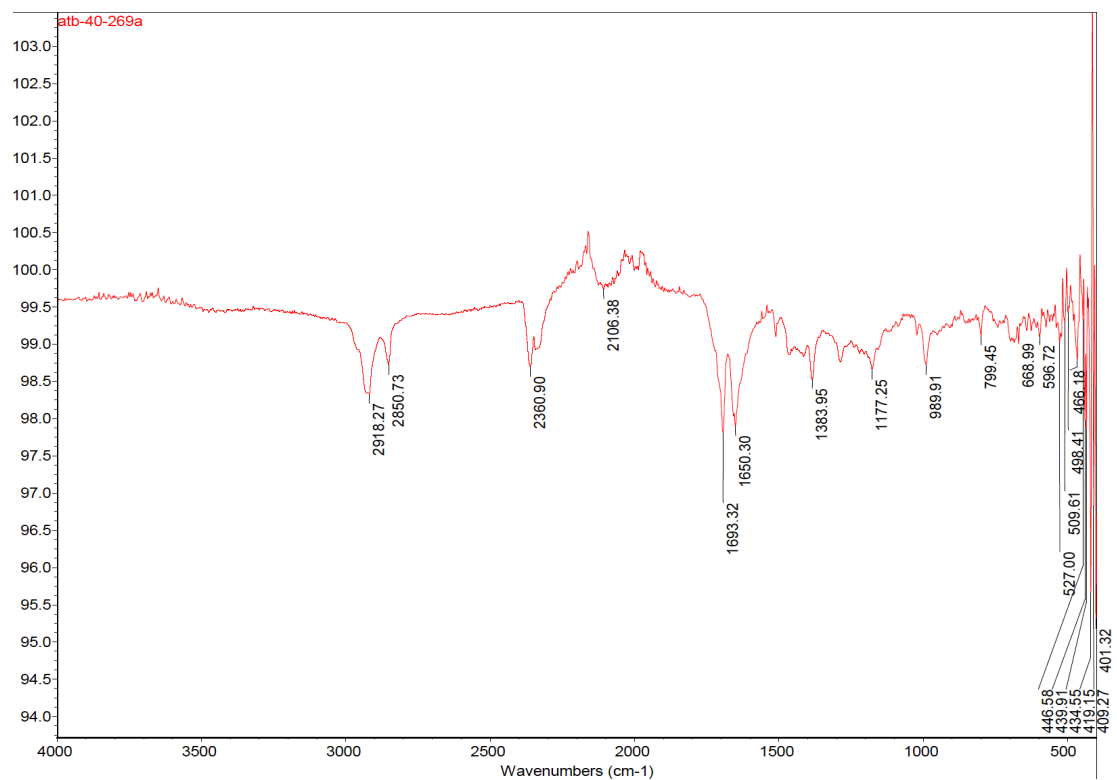


Figure A7.44 Infrared spectrum (Thin Film, NaCl) of compound **212**.

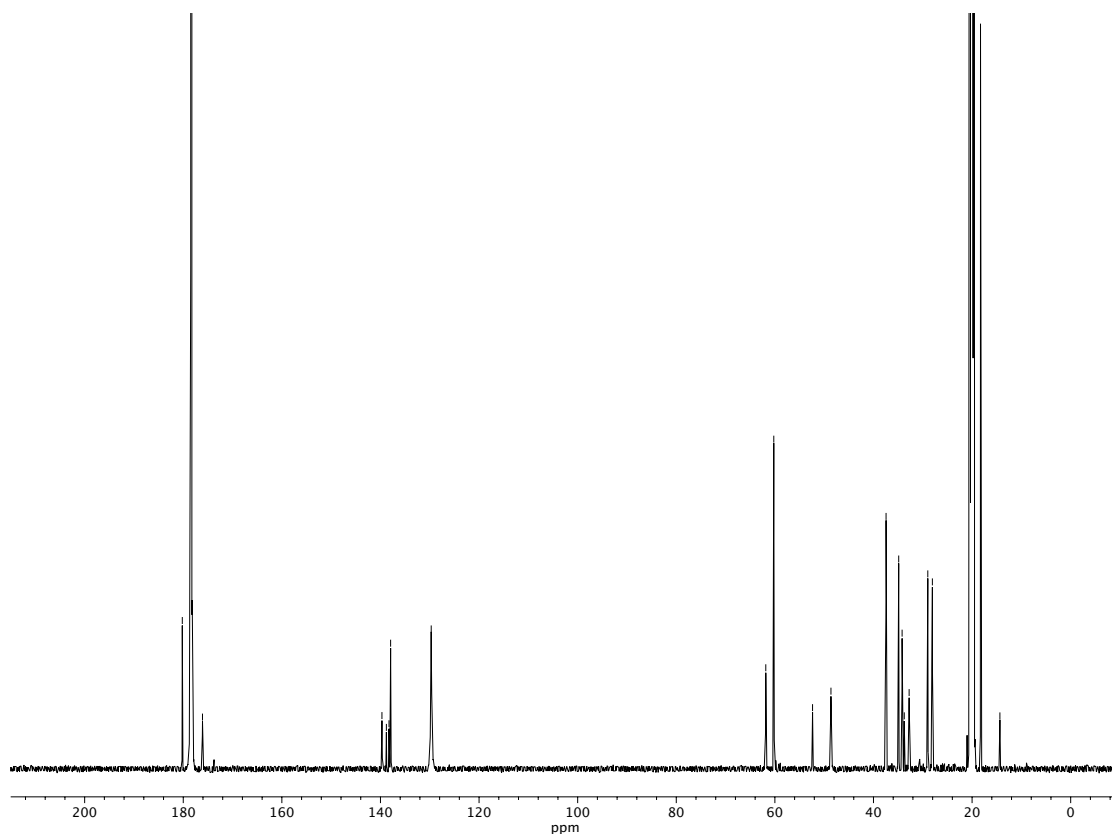


Figure A7.45 <sup>13</sup>C NMR (151 MHz, AcOD) of compound **212**.

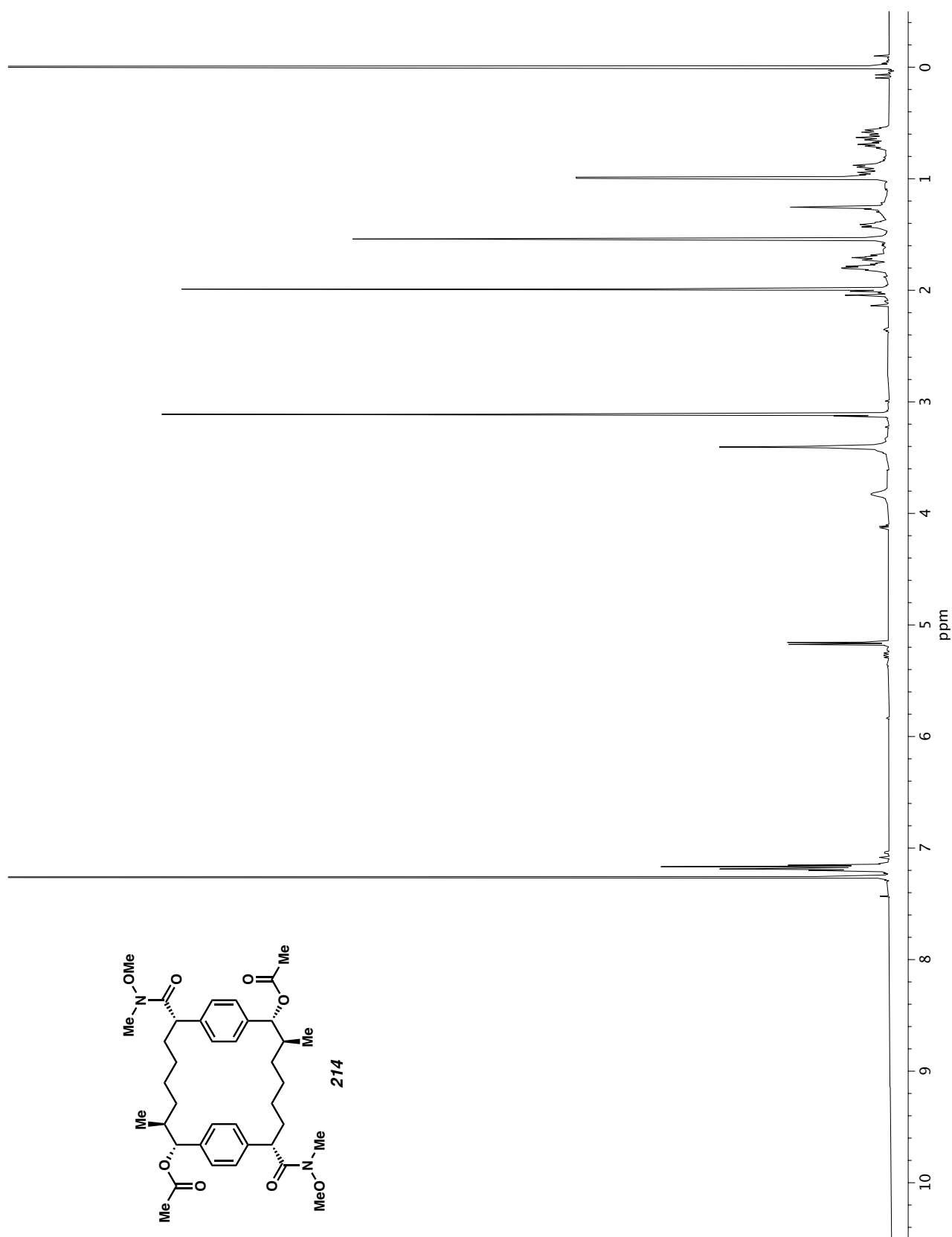
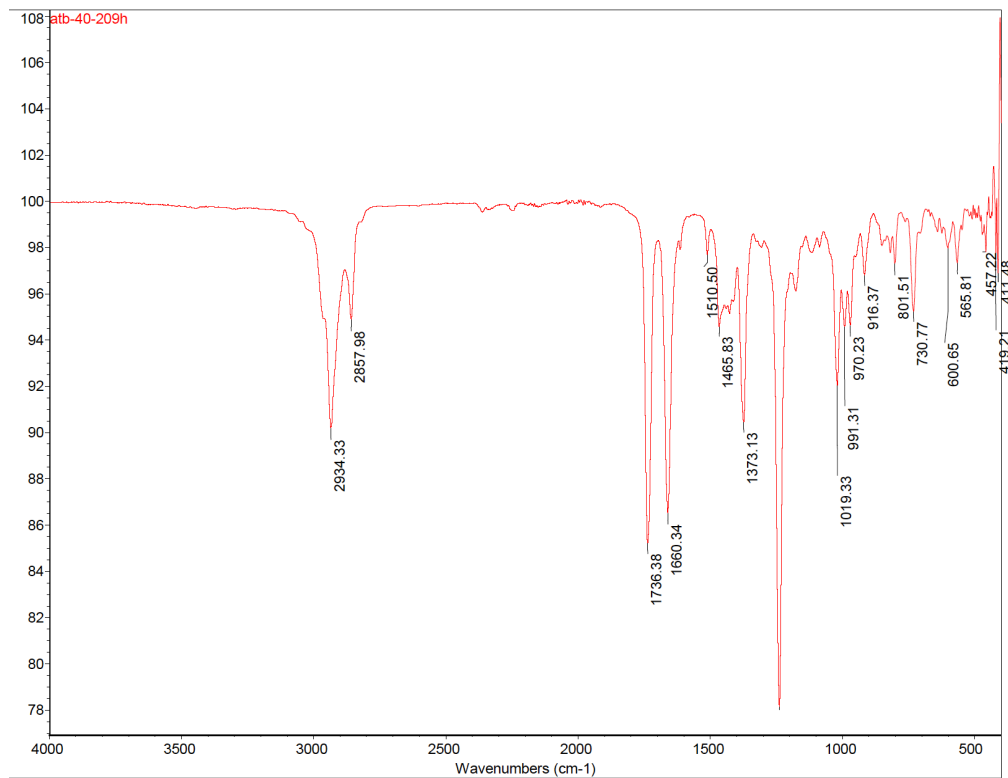
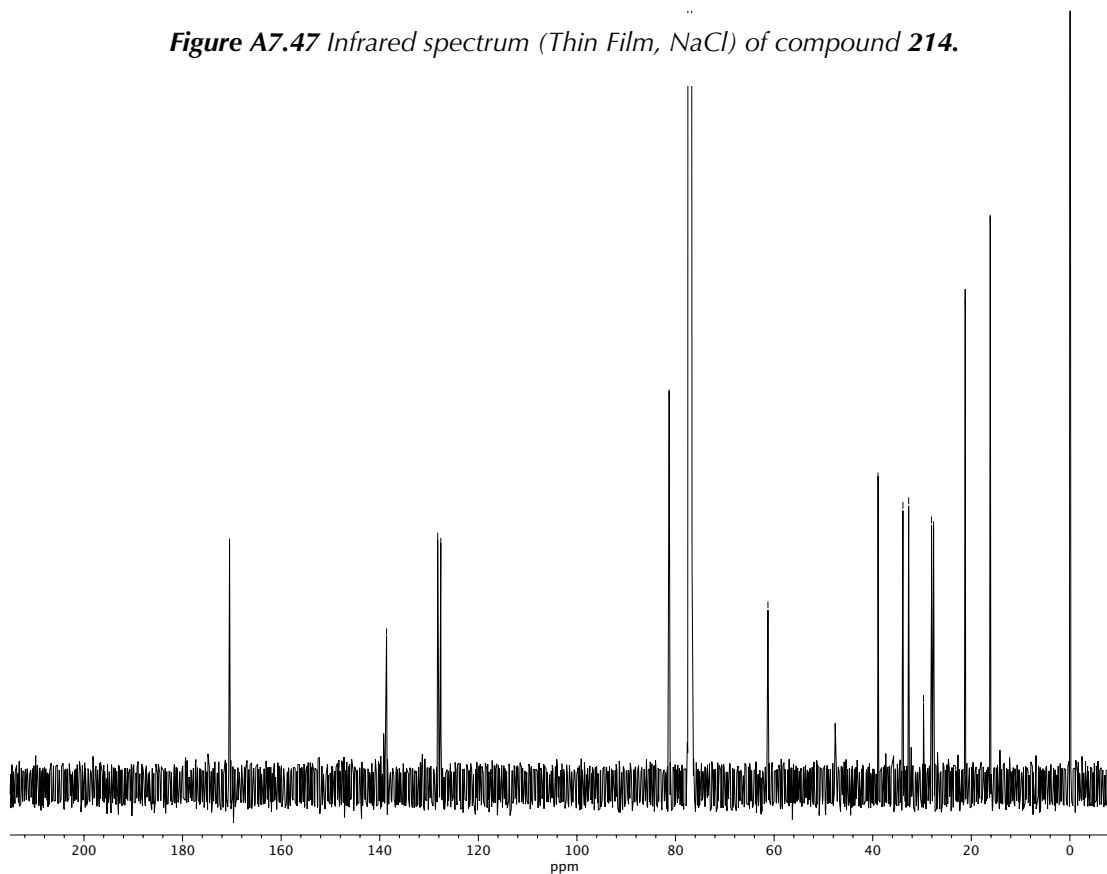


Figure A7.46  $^1\text{H}$  NMR (600 MHz,  $\text{CDCl}_3$ ) of compound 214.



**Figure A7.47** Infrared spectrum (Thin Film, NaCl) of compound **214**.



**Figure A7.48** <sup>13</sup>C NMR (151 MHz, CDCl<sub>3</sub>) of compound **214**.

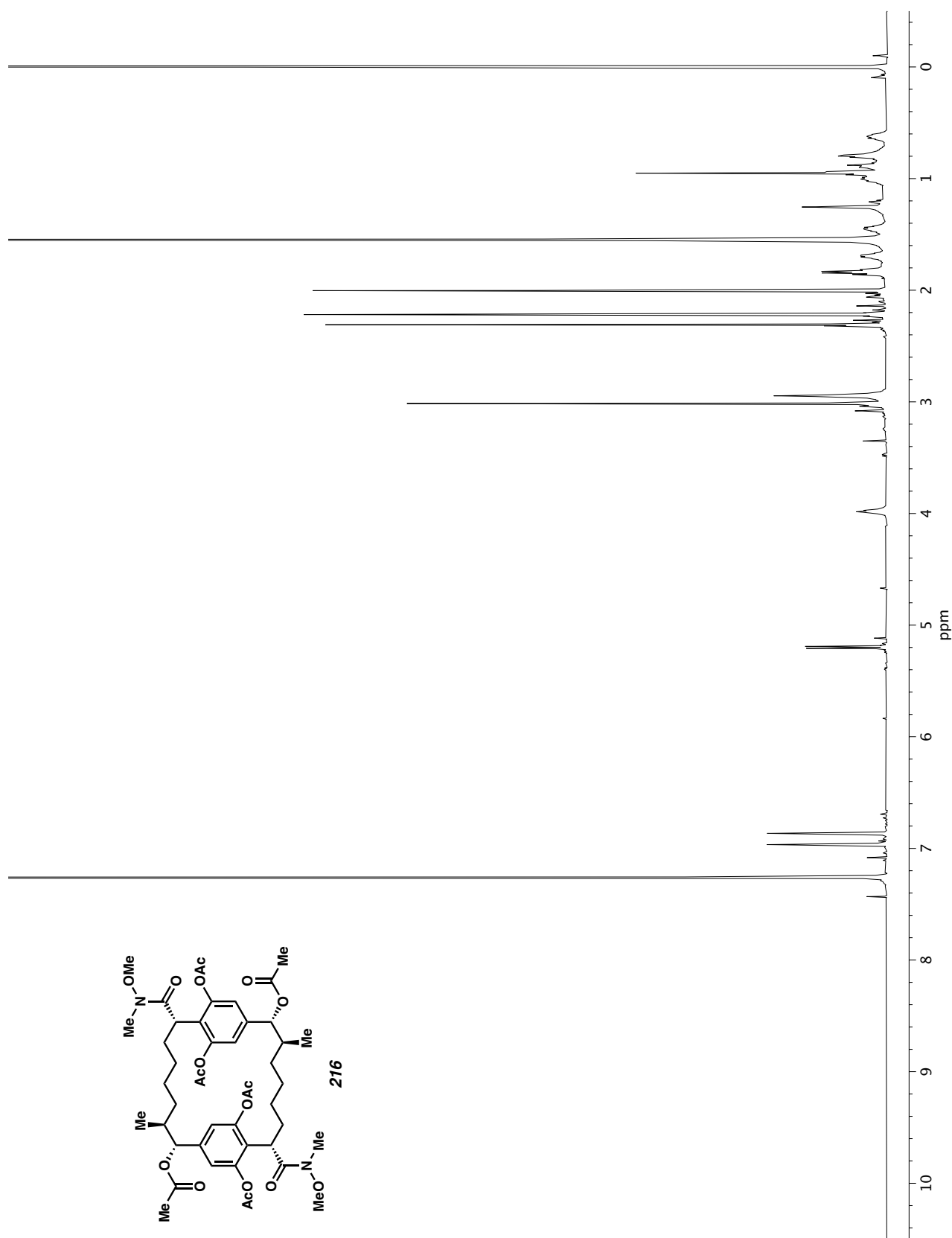


**Figure A7.49**  $^1\text{H}$  NMR (600 MHz,  $\text{CDCl}_3$ ) of compound **216**.

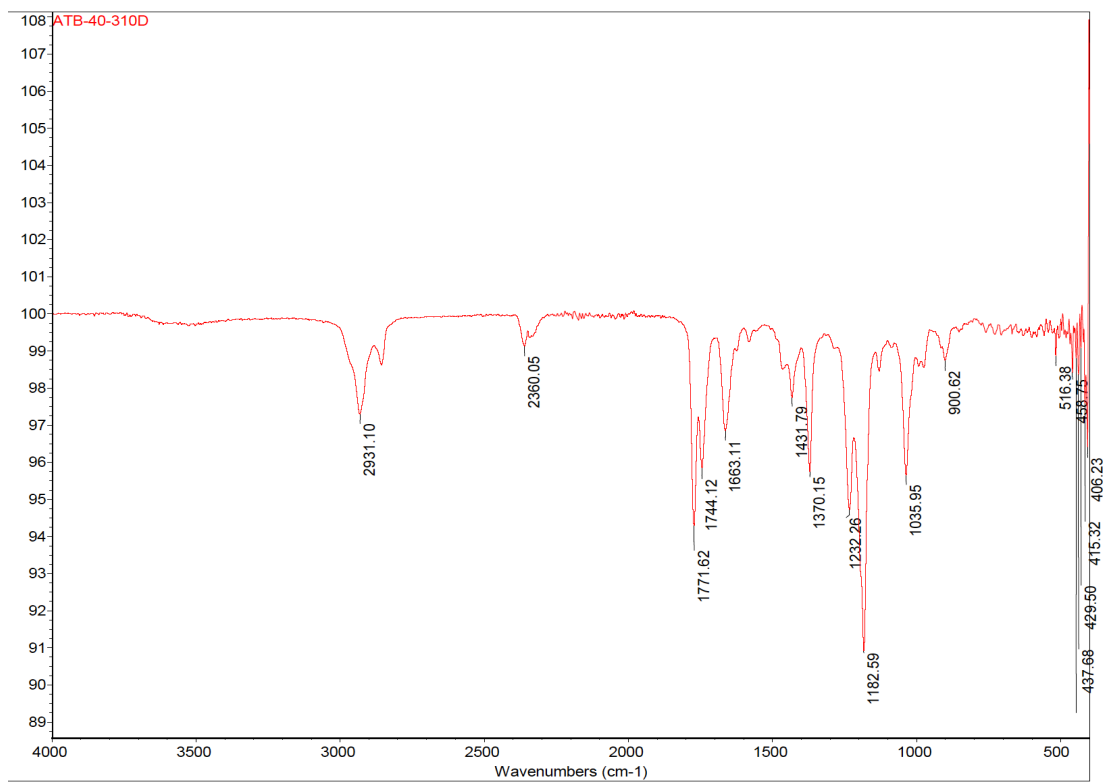


**Figure A7.50** Infrared spectrum (Thin Film, NaCl) of compound **216**.

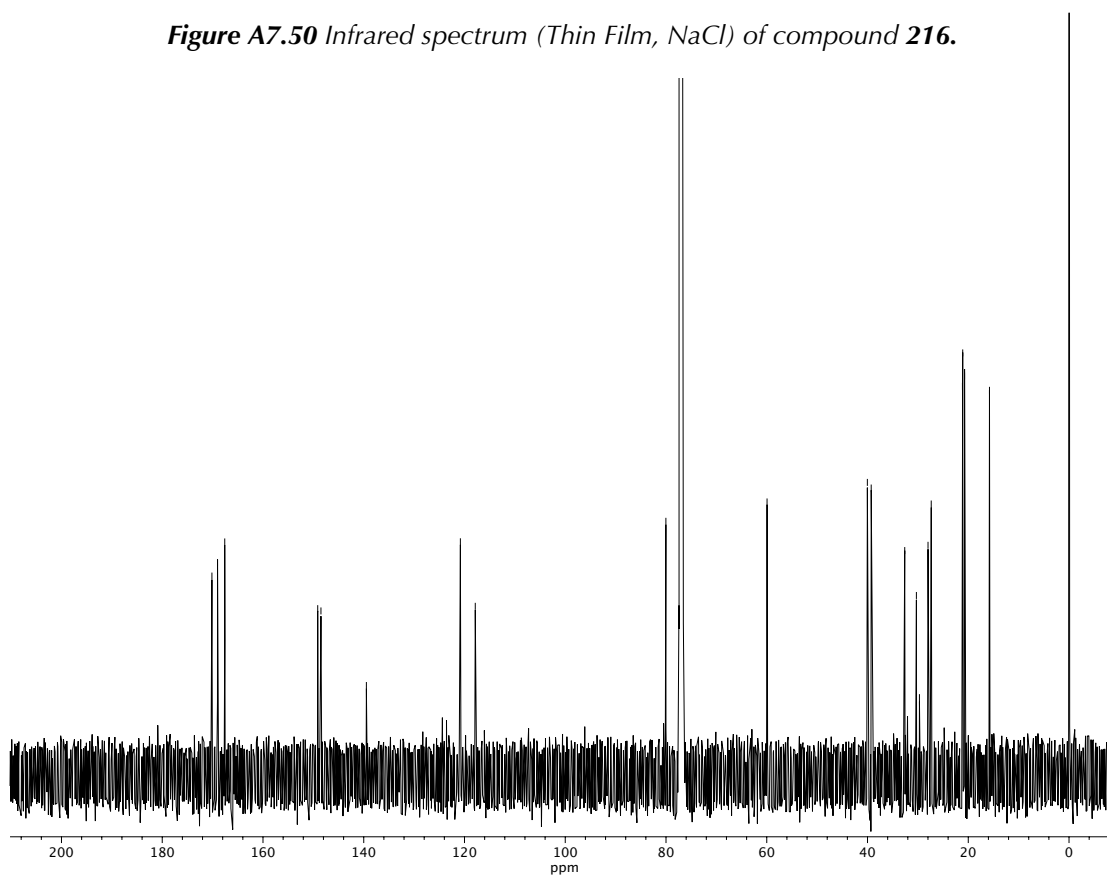


**Figure A7.51** <sup>13</sup>C NMR (151 MHz, CDCl<sub>3</sub>) of compound **216**.

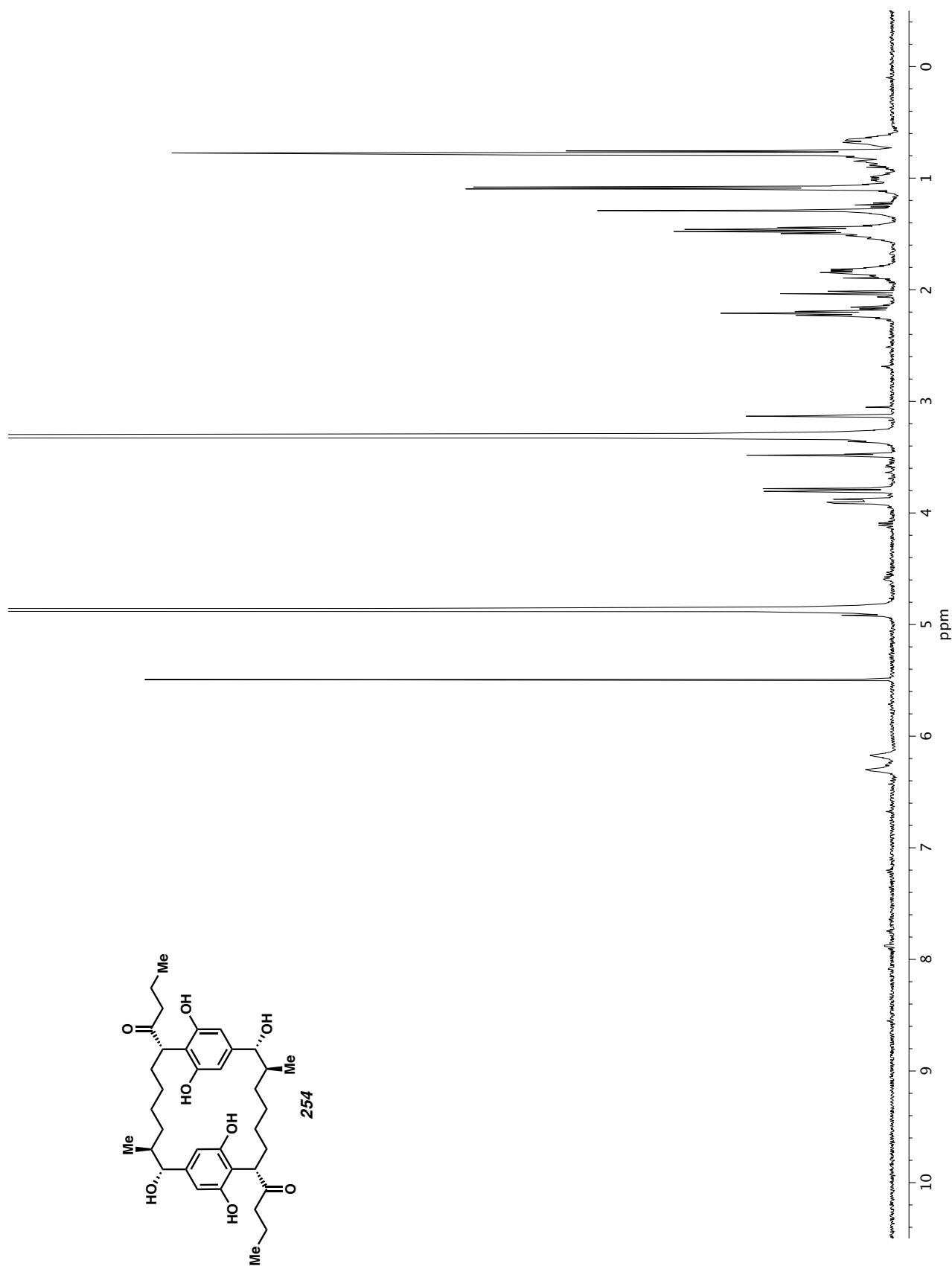


Figure A7.52  $^1\text{H}$  NMR (400 MHz,  $\text{CD}_3\text{OD}$ ) of compound 254.

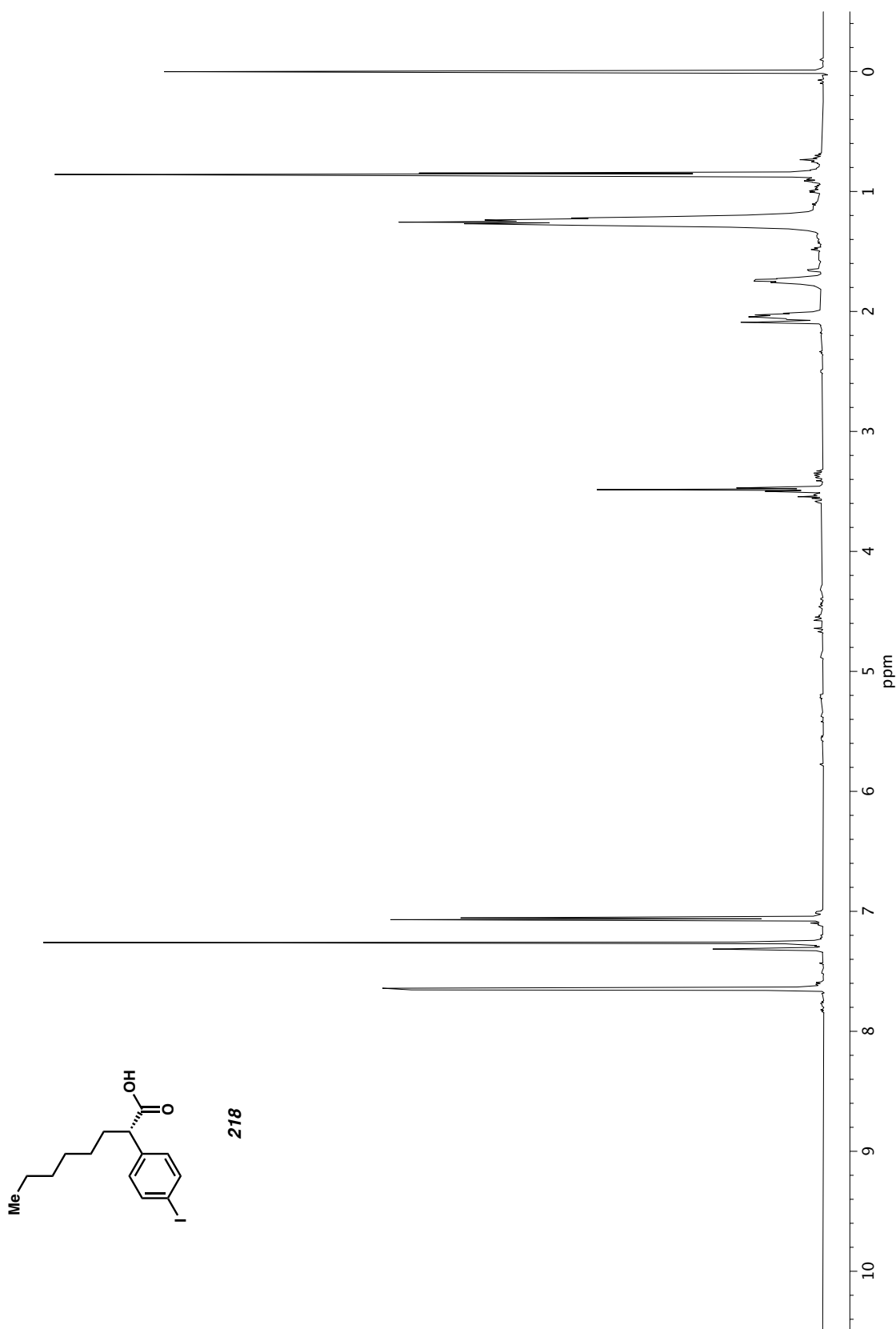


Figure A7.53 <sup>1</sup>H NMR (600 MHz, CDCl<sub>3</sub>) of compound 218.

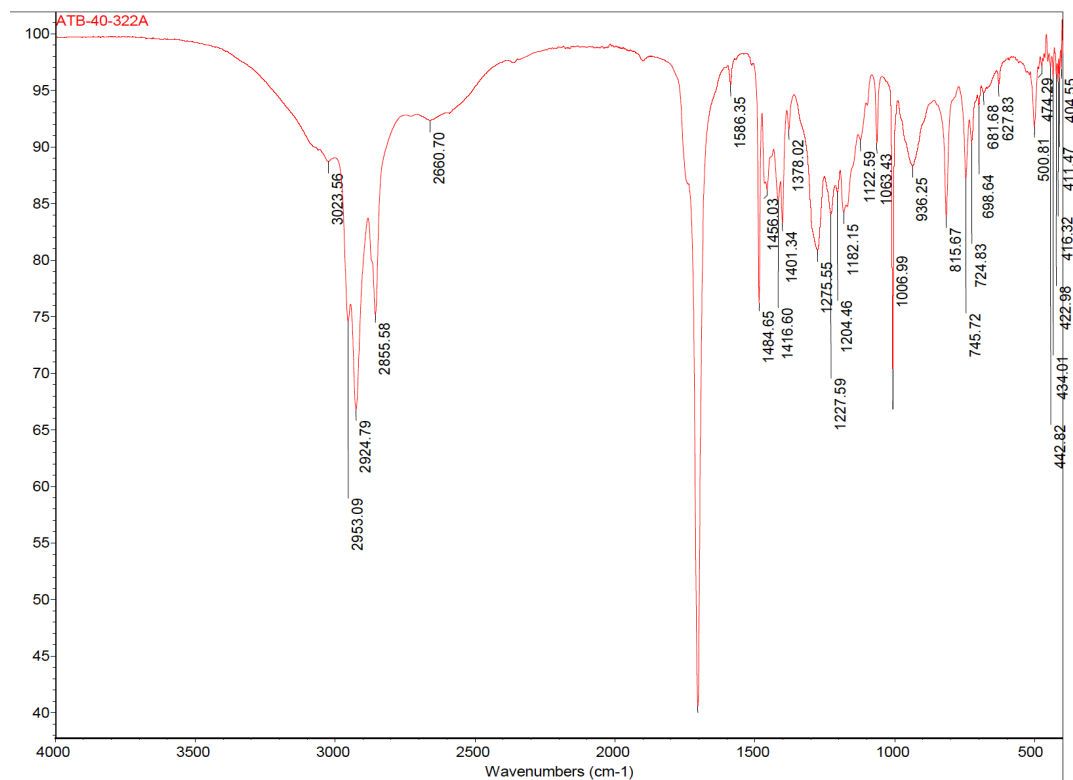


Figure A7.54 Infrared spectrum (Thin Film, NaCl) of compound **218**.

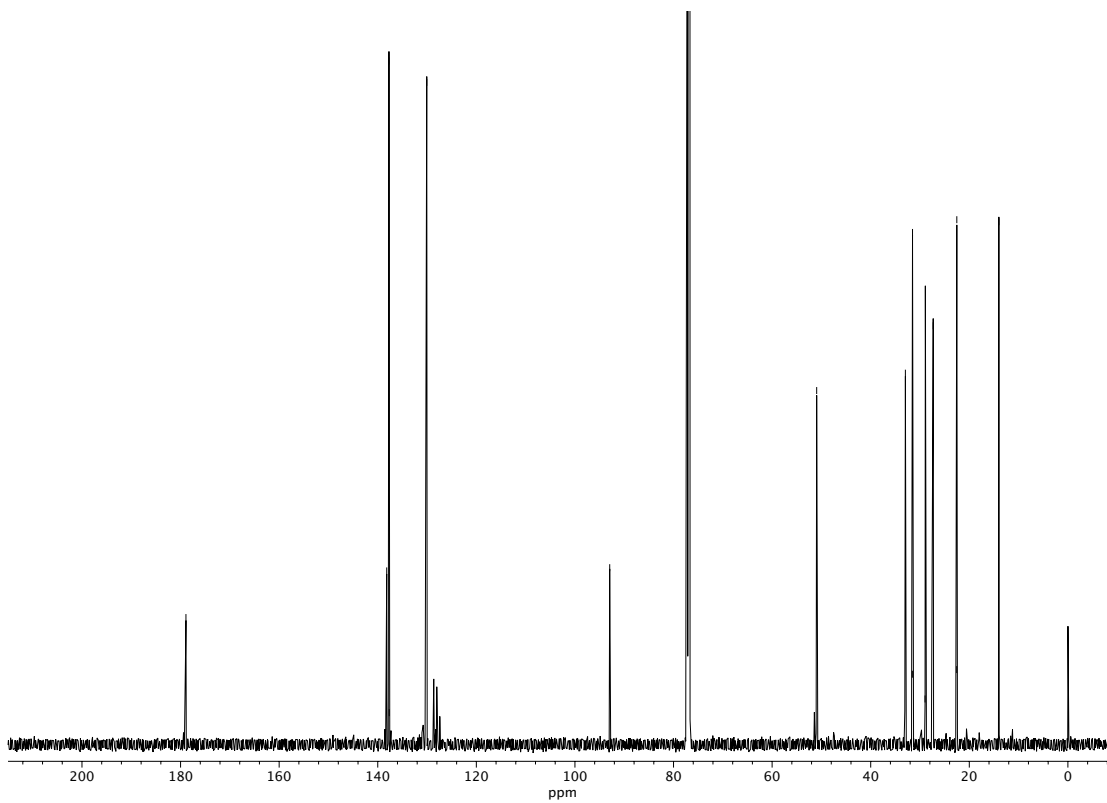
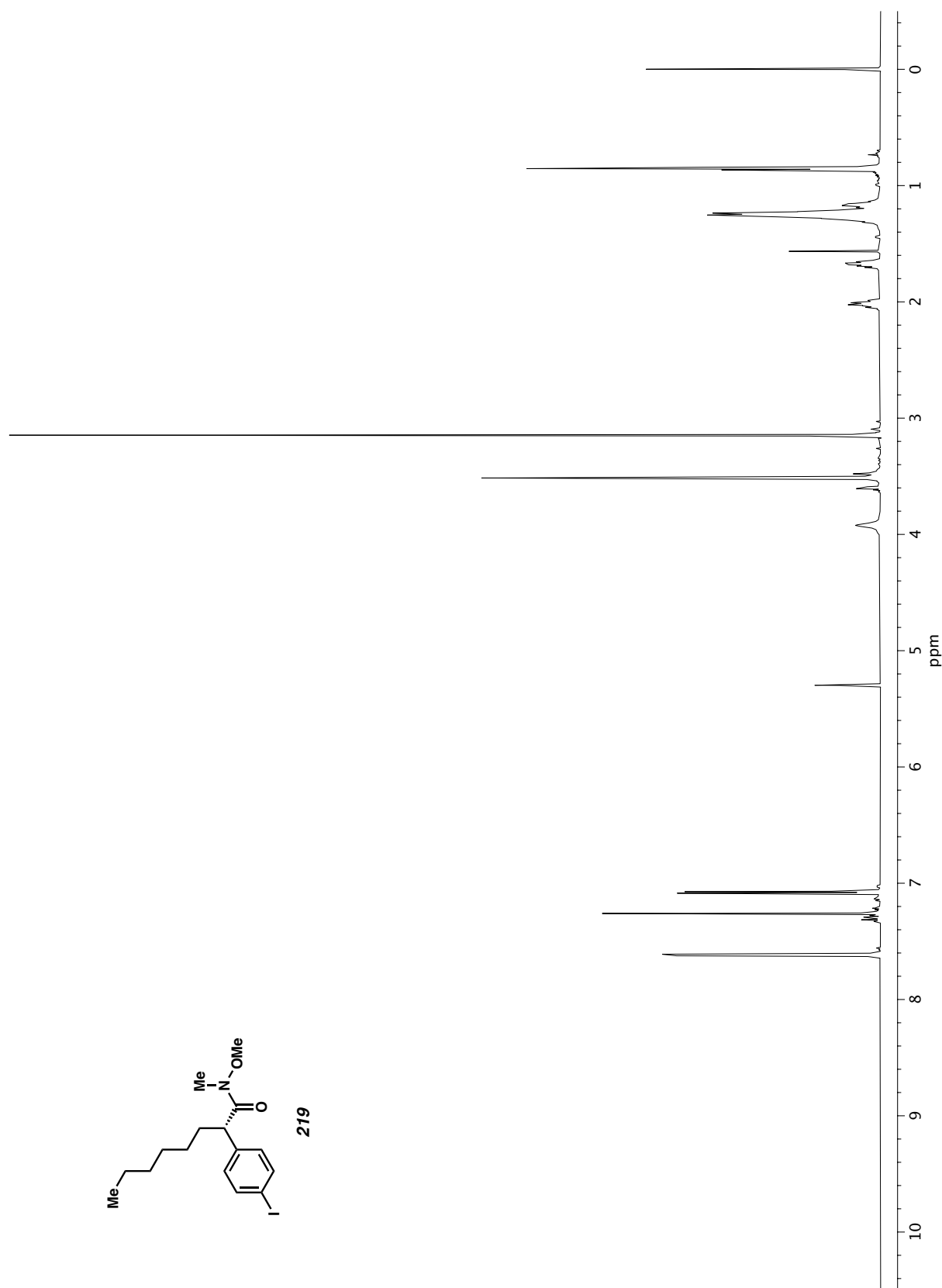
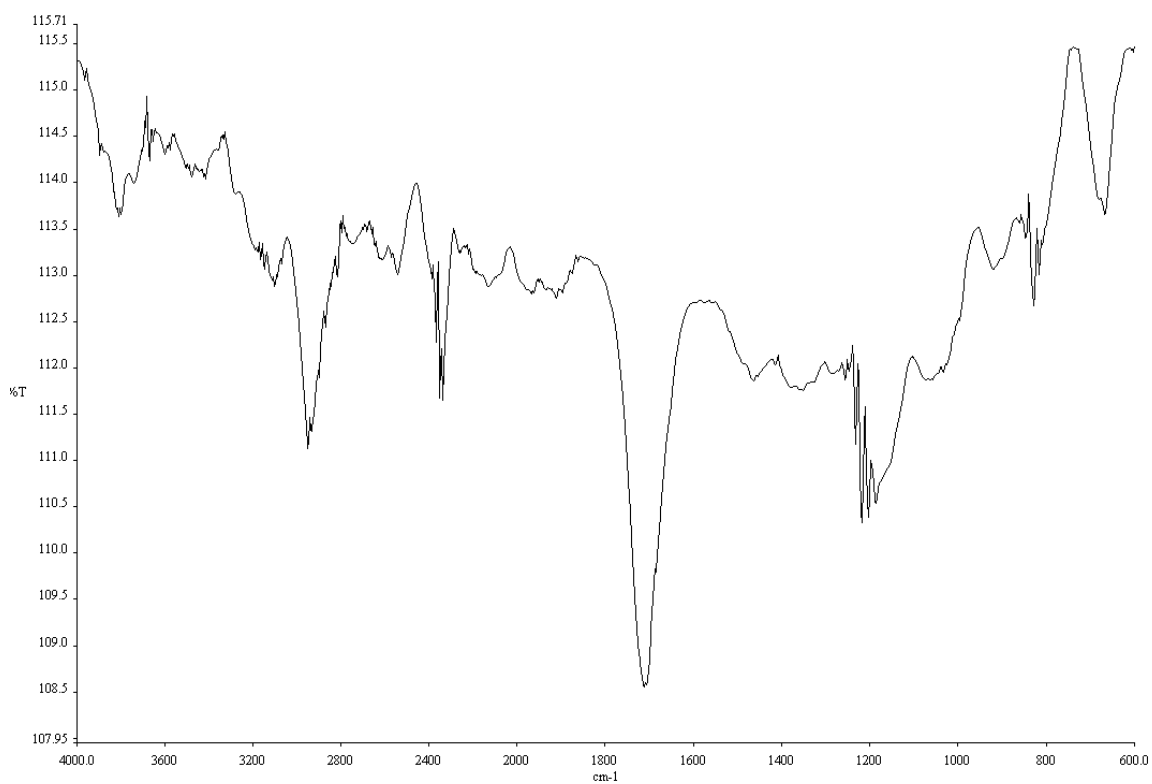


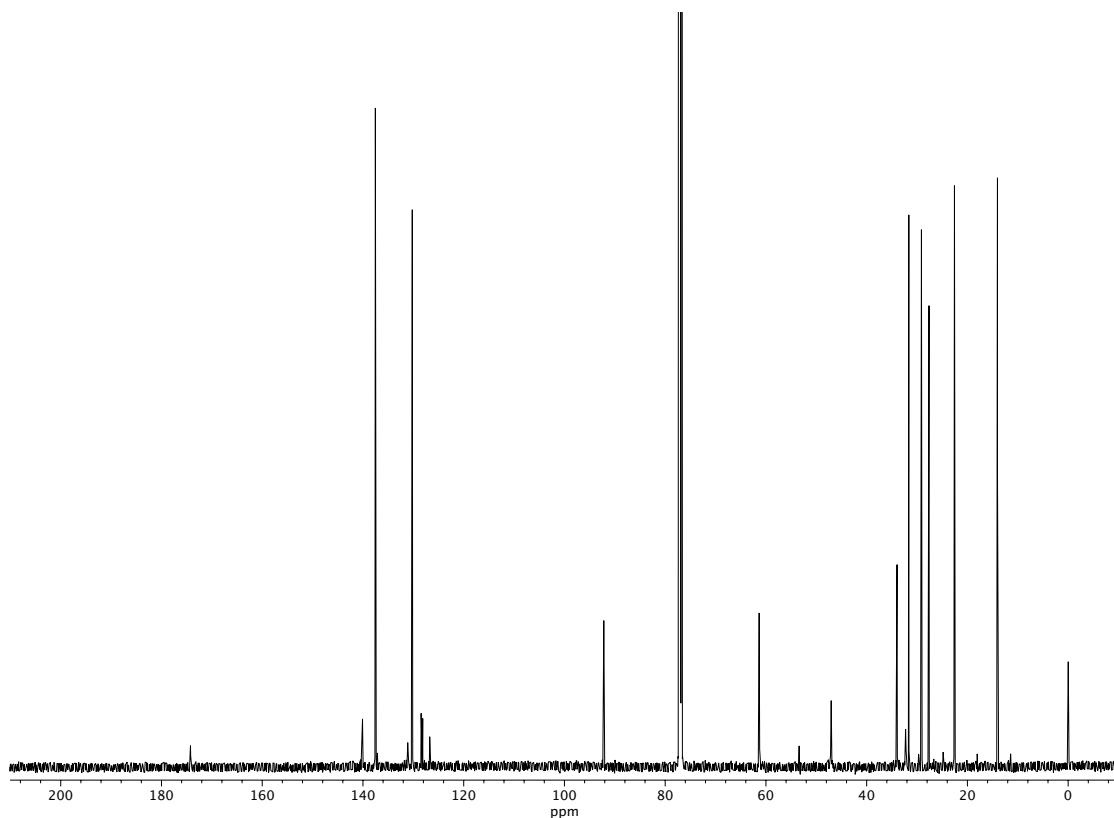
Figure A7.55 <sup>13</sup>C NMR (100 MHz, CDCl<sub>3</sub>) of compound **218**.



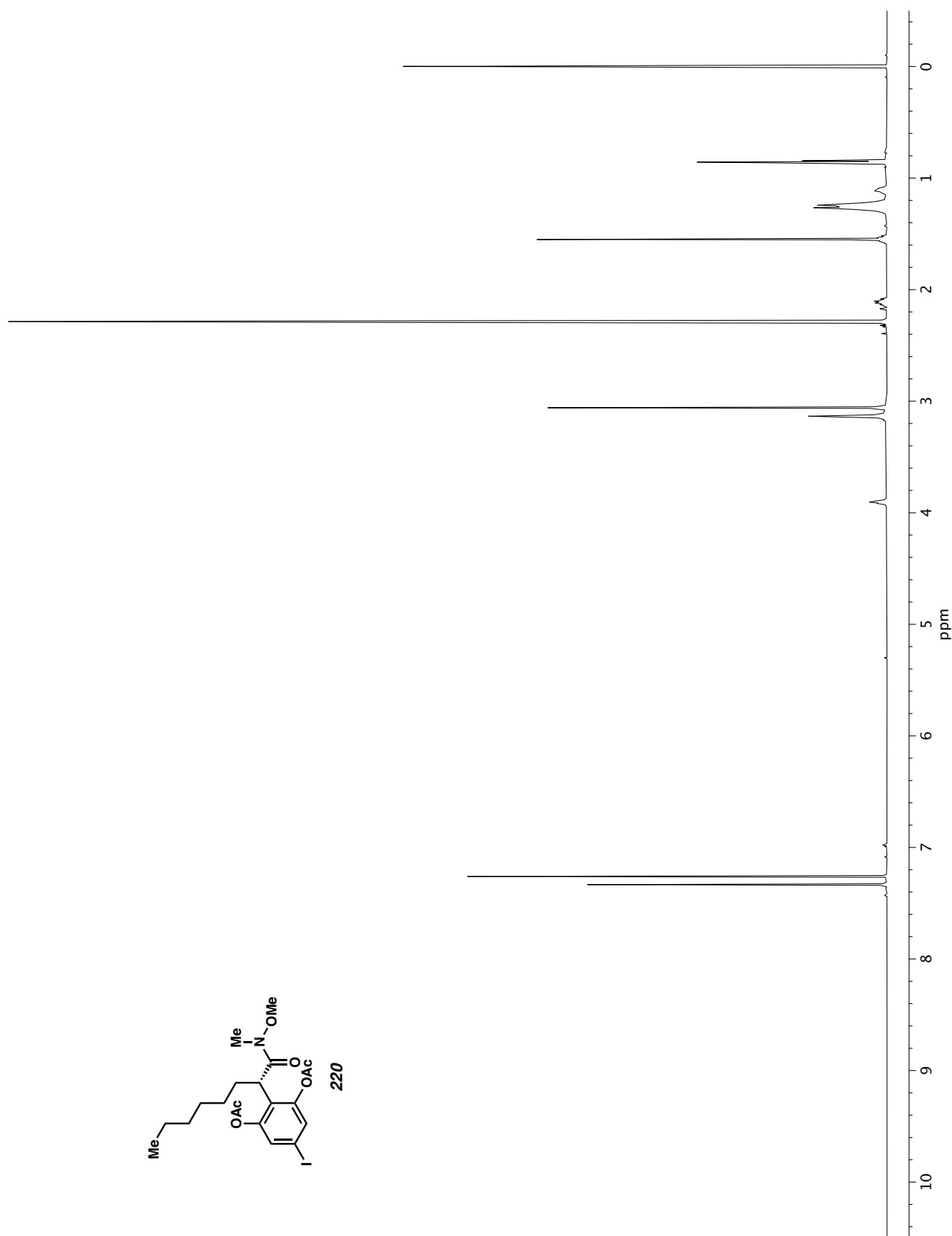
Figure A7.56  $^1\text{H}$  NMR (600 MHz,  $\text{CDCl}_3$ ) of compound 219.



**Figure A7.57** Infrared spectrum (Thin Film, NaCl) of compound **219**.



**Figure A7.58** <sup>13</sup>C NMR (151 MHz, CDCl<sub>3</sub>) of compound **219**.



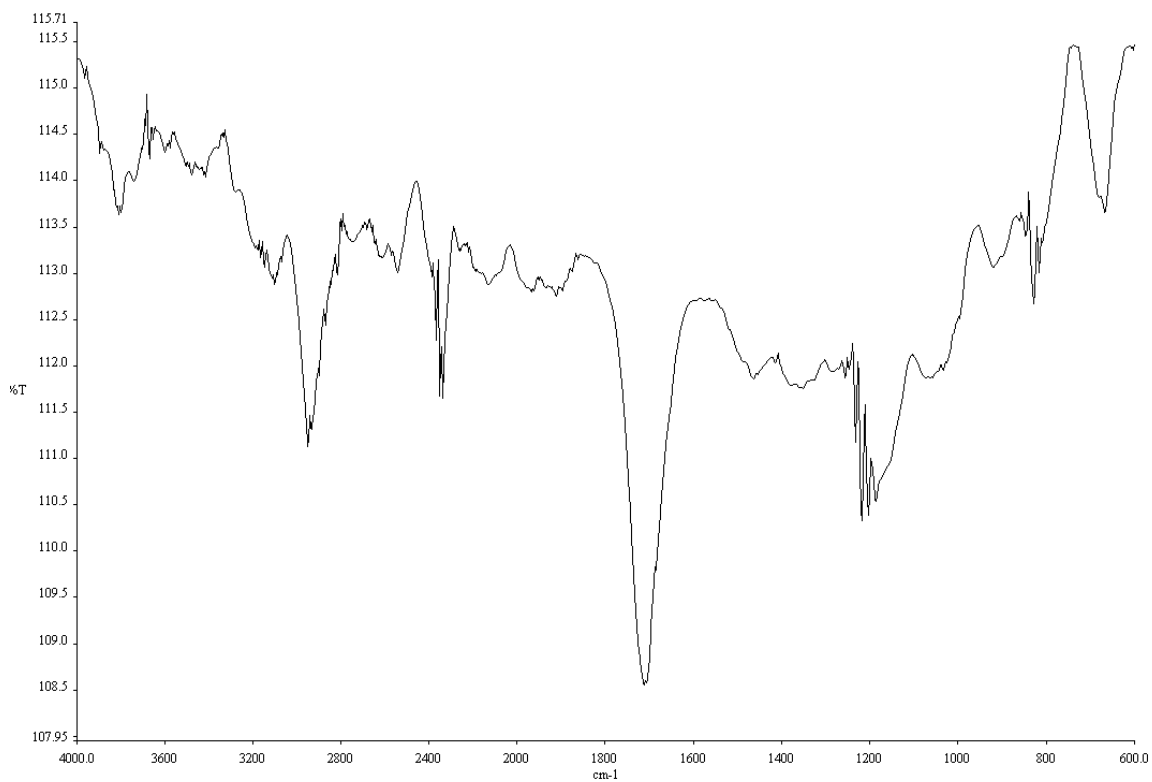


**Figure A7.60** Infrared spectrum (Thin Film, NaCl) of compound **220**.

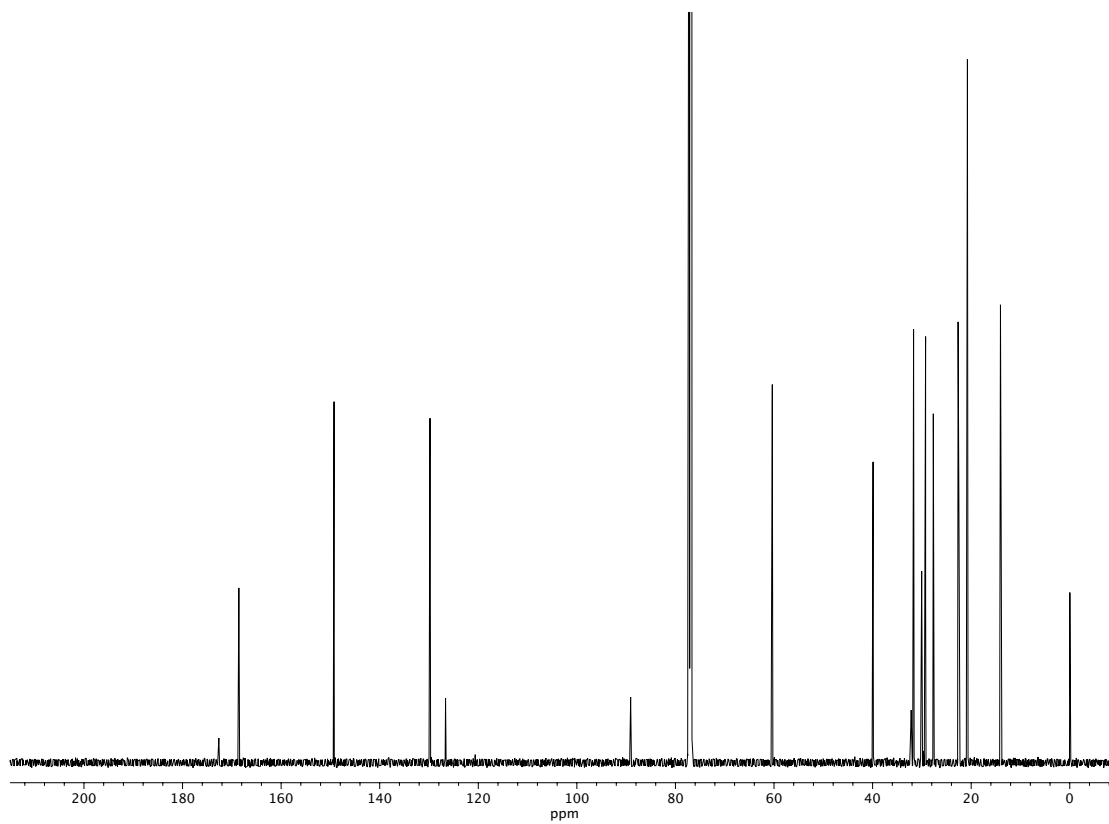


**Figure A7.61** <sup>13</sup>C NMR (151 MHz, CDCl<sub>3</sub>) of compound **220**.

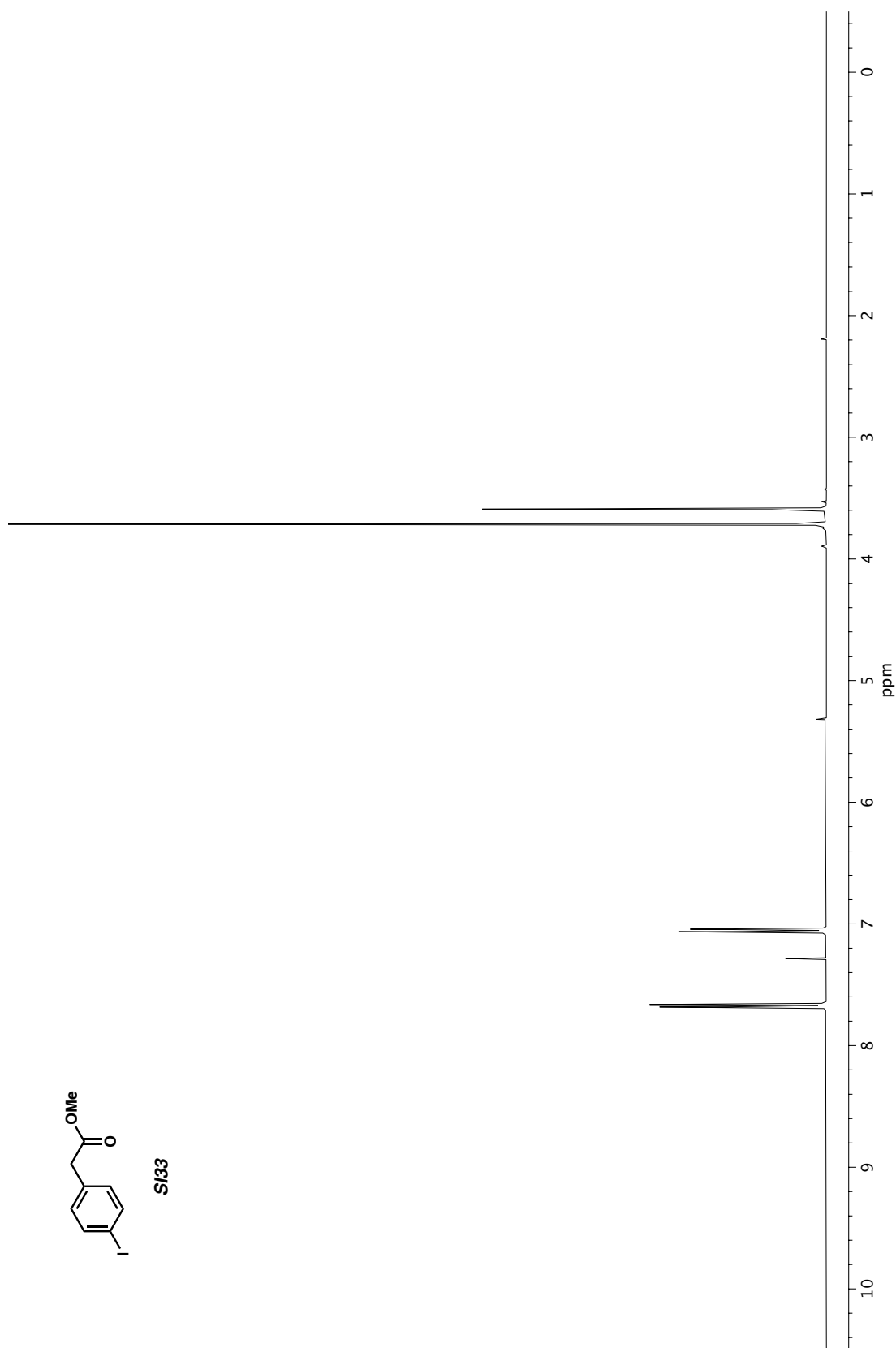


Figure A7.62 <sup>1</sup>H NMR (400 MHz, CDCl<sub>3</sub>) of compound SI33.

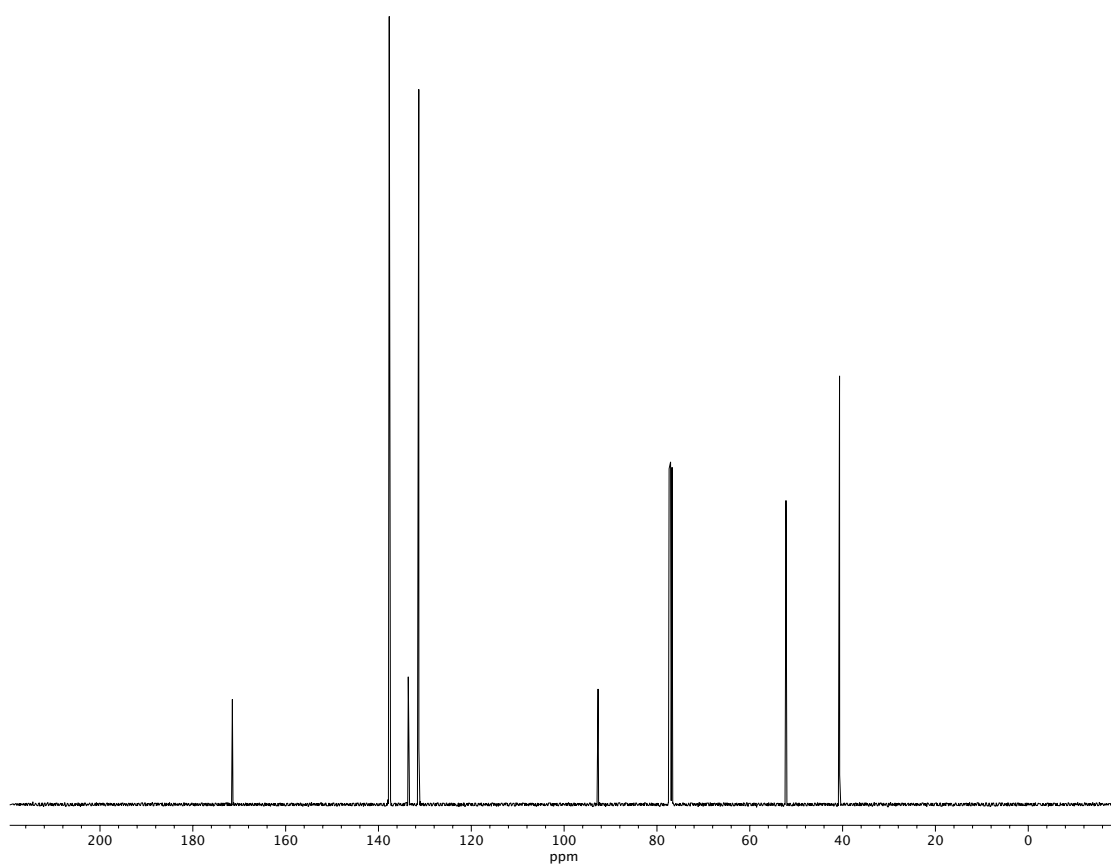


Figure A7.63  $^{13}\text{C}$  NMR (100 MHz,  $\text{CDCl}_3$ ) of compound SI33.

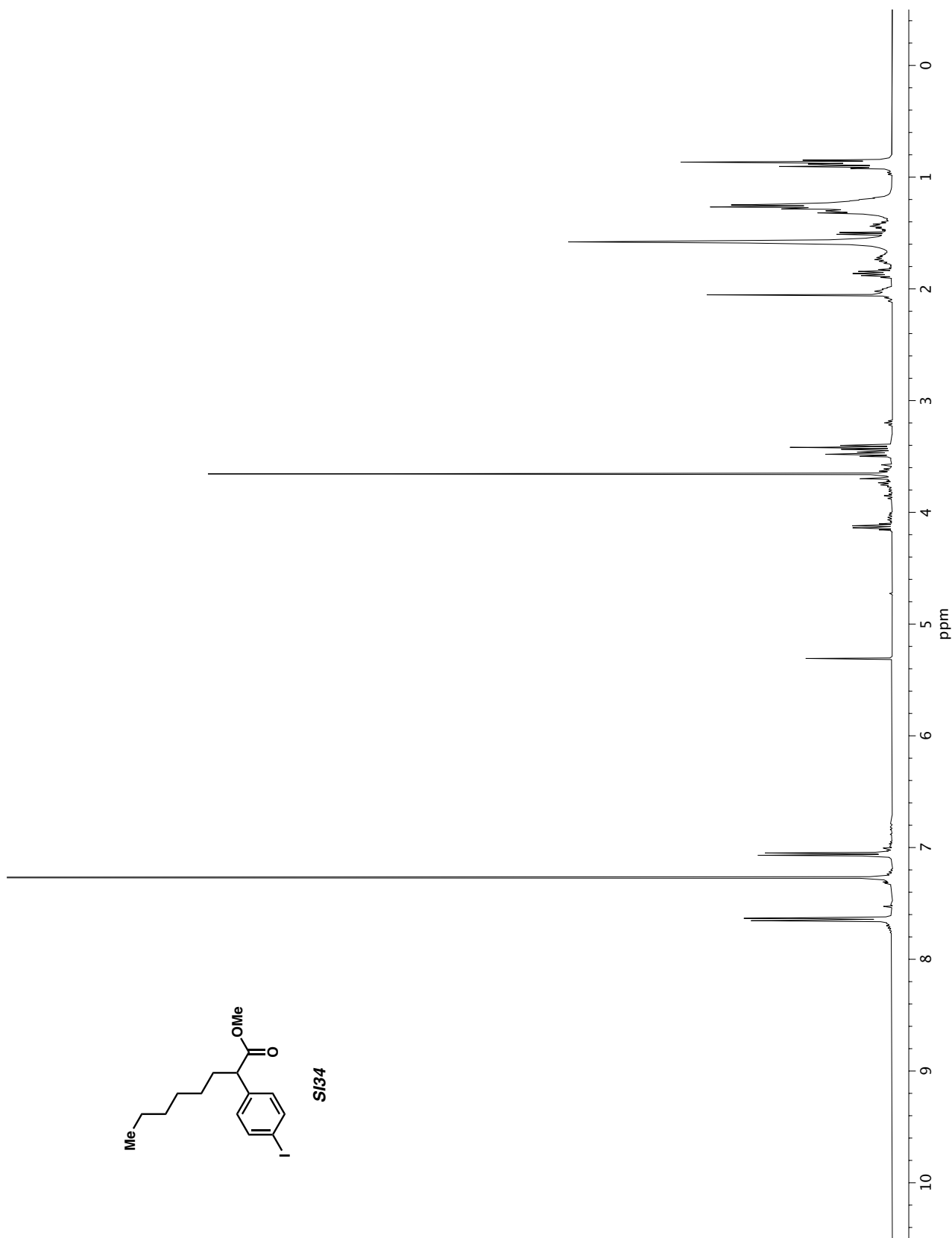
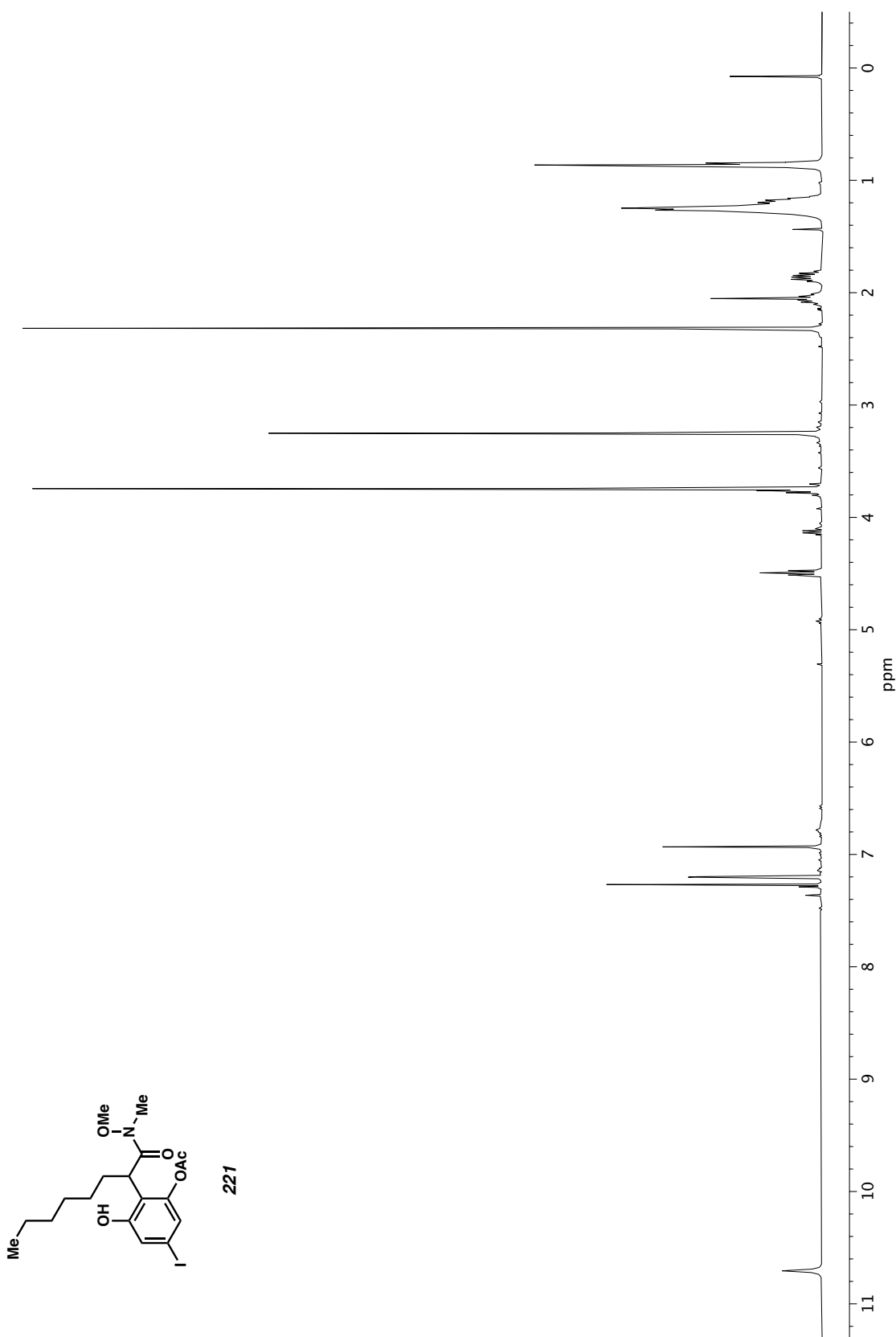


Figure A7.64 <sup>1</sup>H NMR (400 MHz, CDCl<sub>3</sub>) of compound SI34.





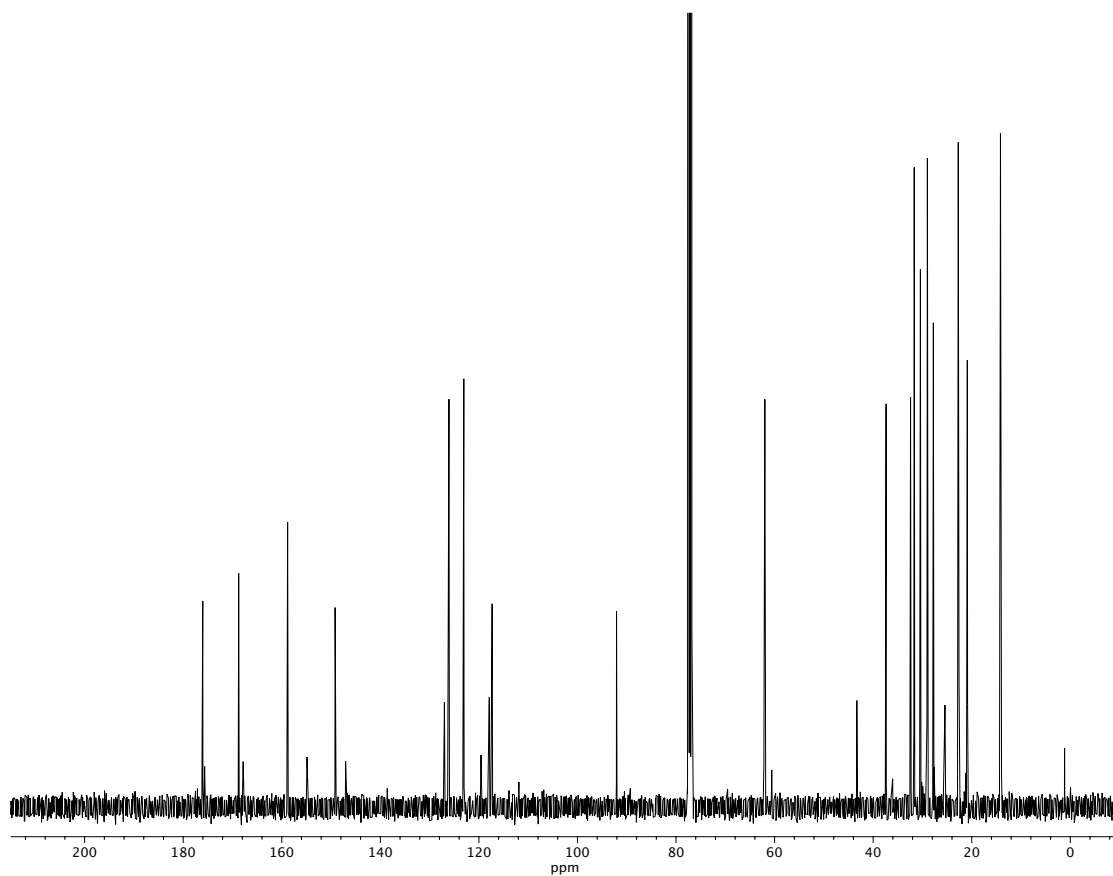
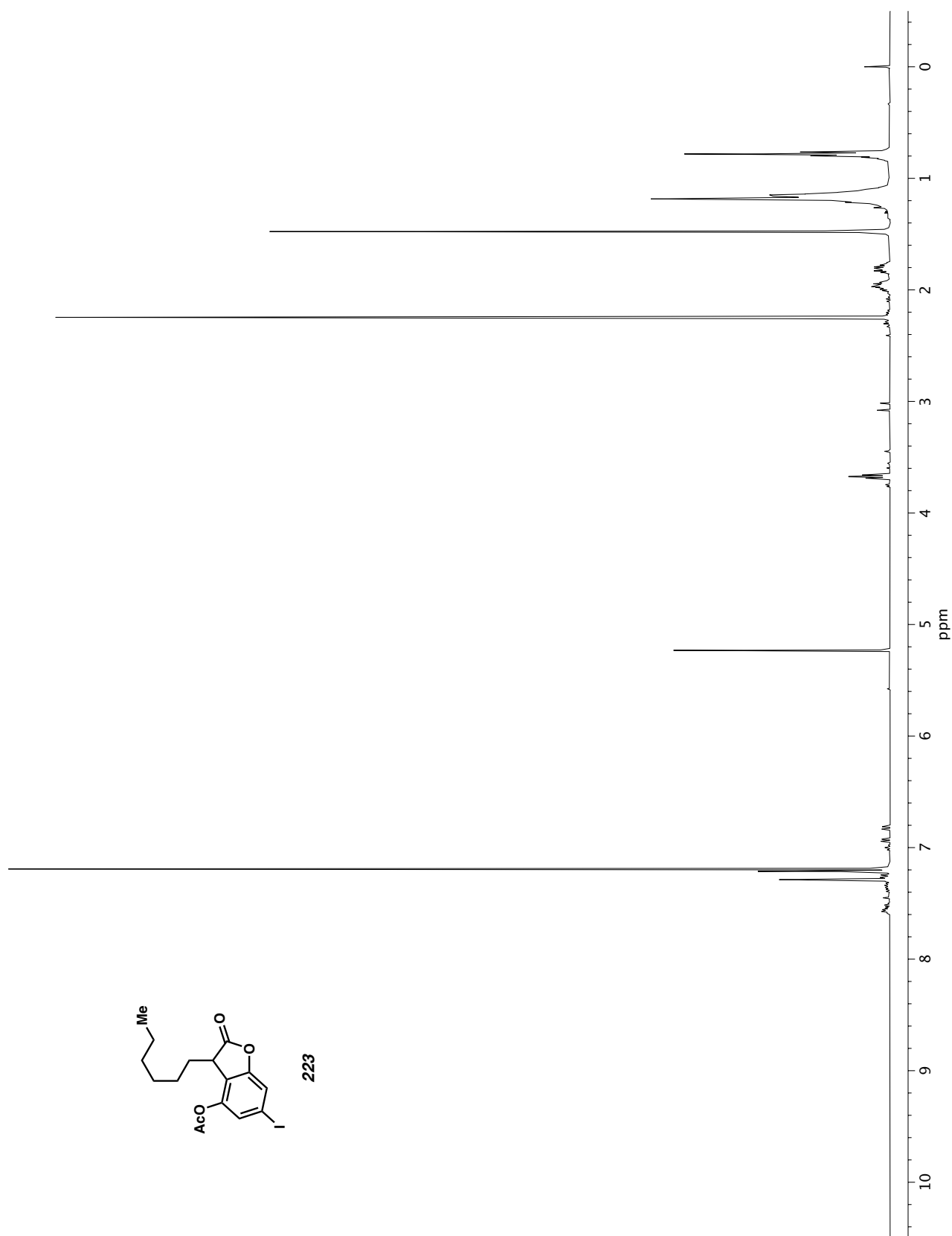
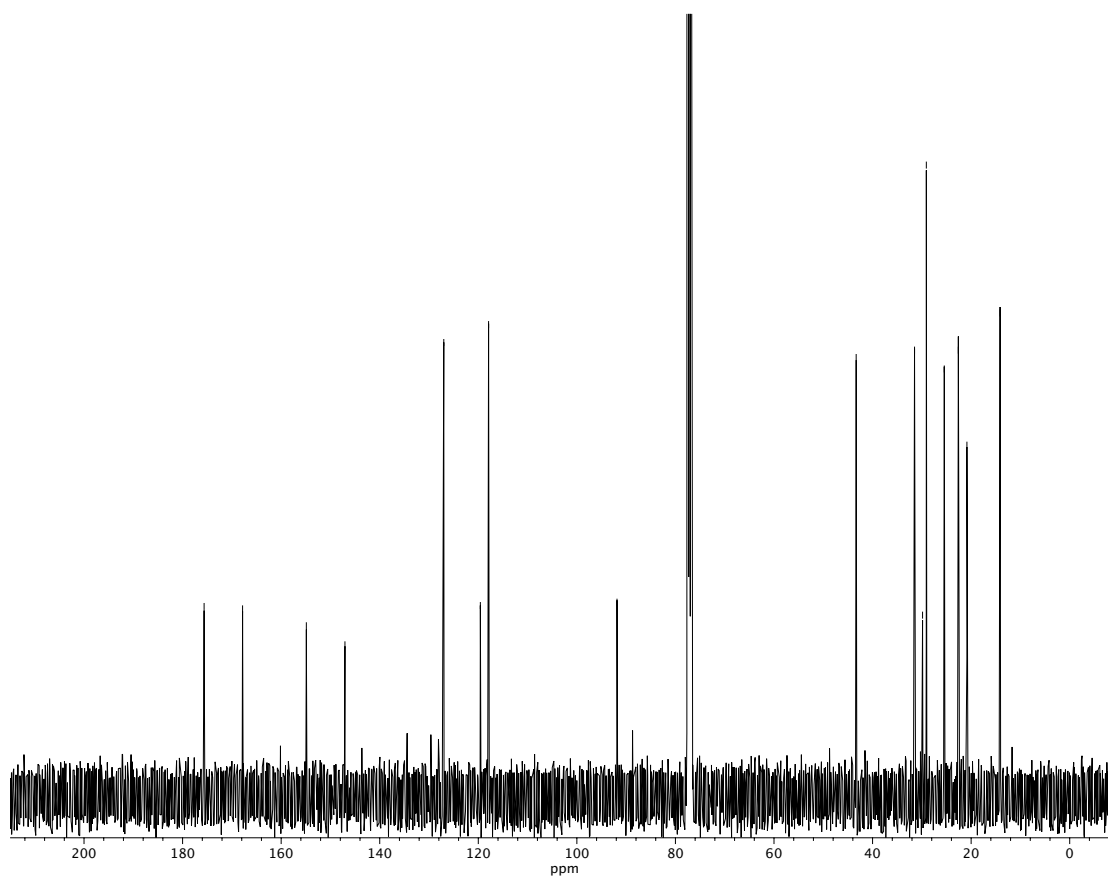


Figure A7.66  $^{13}\text{C}$  NMR (100 MHz,  $\text{CDCl}_3$ ) of compound 221.





**Figure A7.68**  $^{13}\text{C}$  NMR (100 MHz,  $\text{CDCl}_3$ ) of compound **223**.

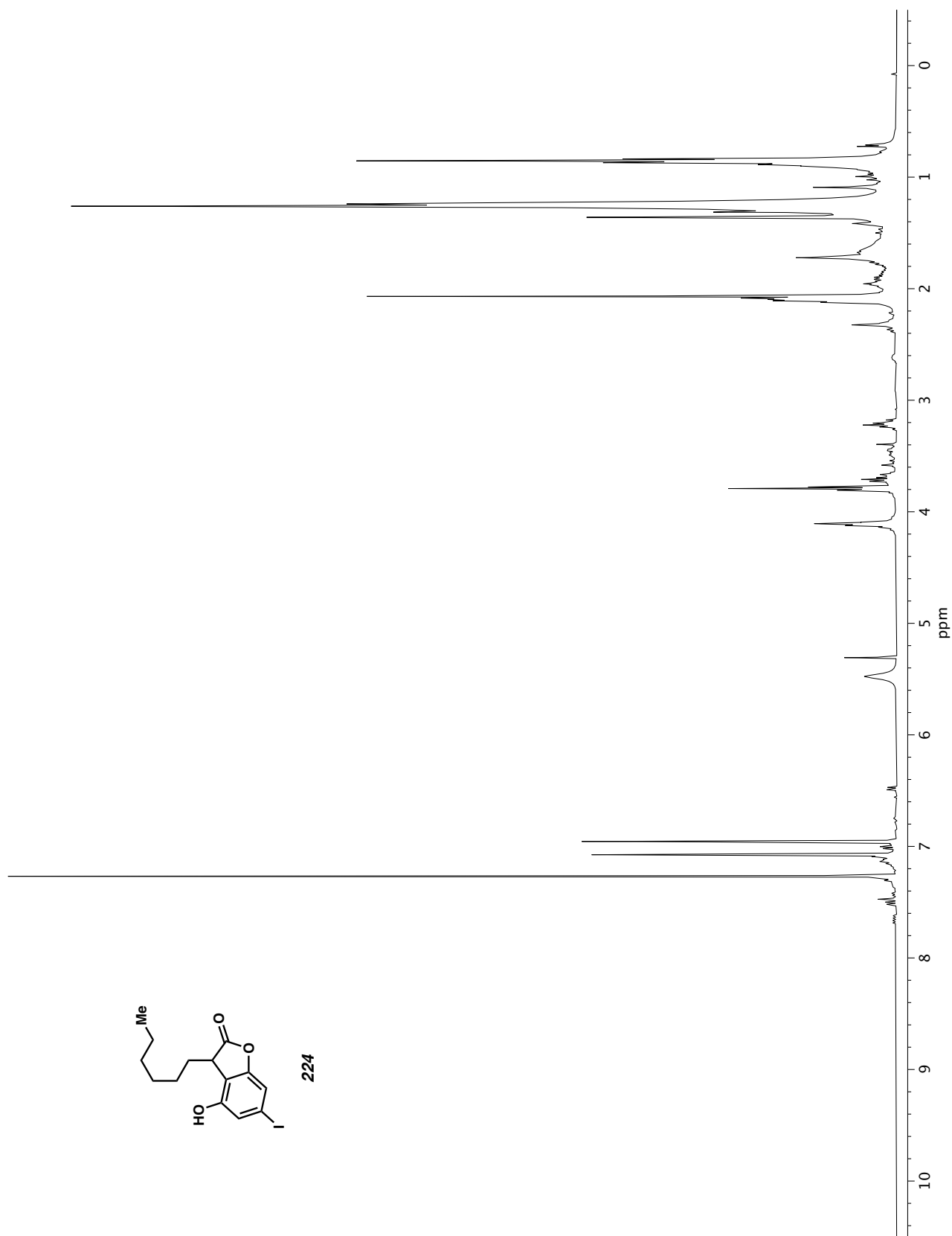
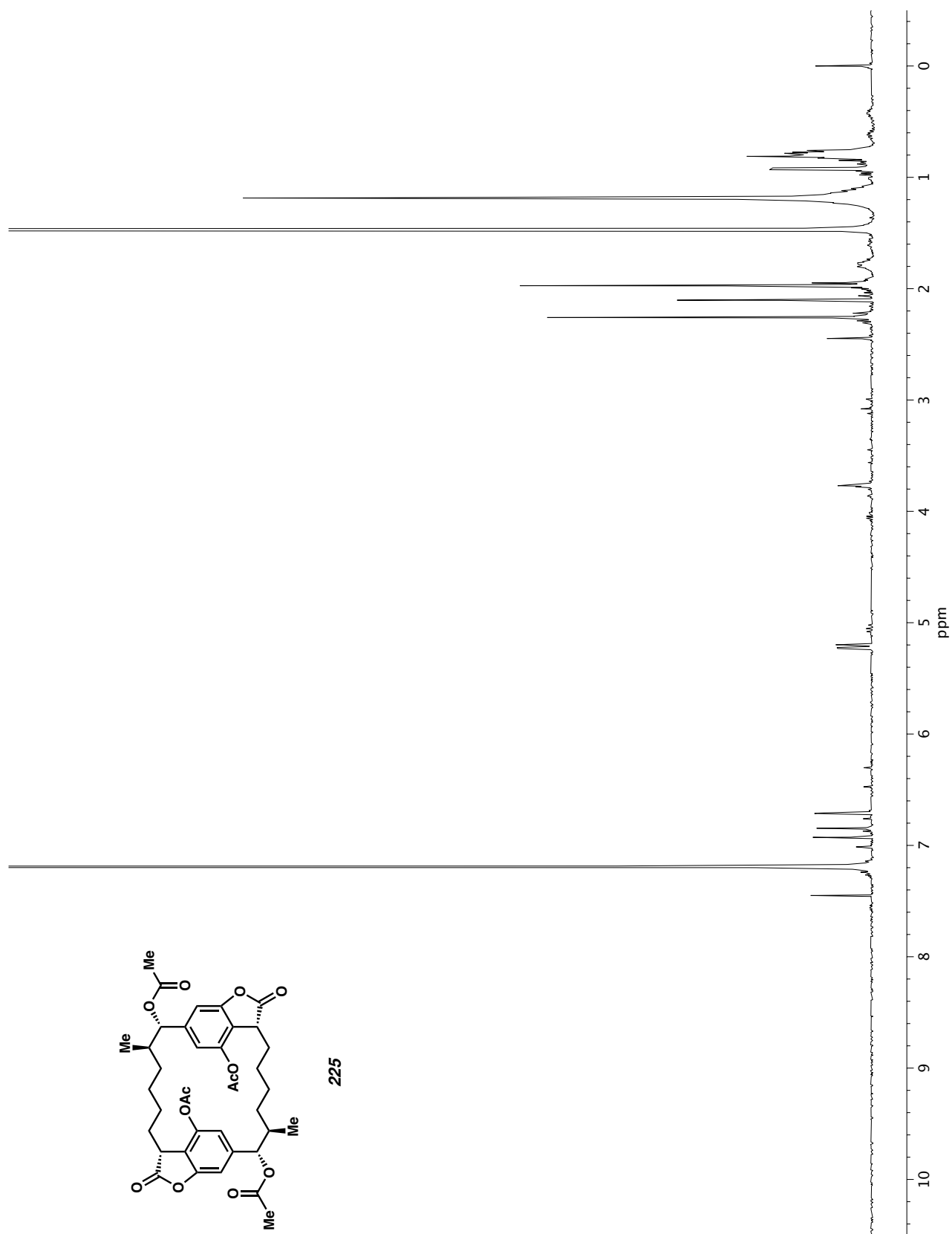


Figure A7.69  $^1\text{H}$  NMR (400 MHz,  $\text{CDCl}_3$ ) of compound 224.



**Figure A7.70**  $^1\text{H NMR}$  (400 MHz,  $\text{CDCl}_3$ ) of compound **225**.

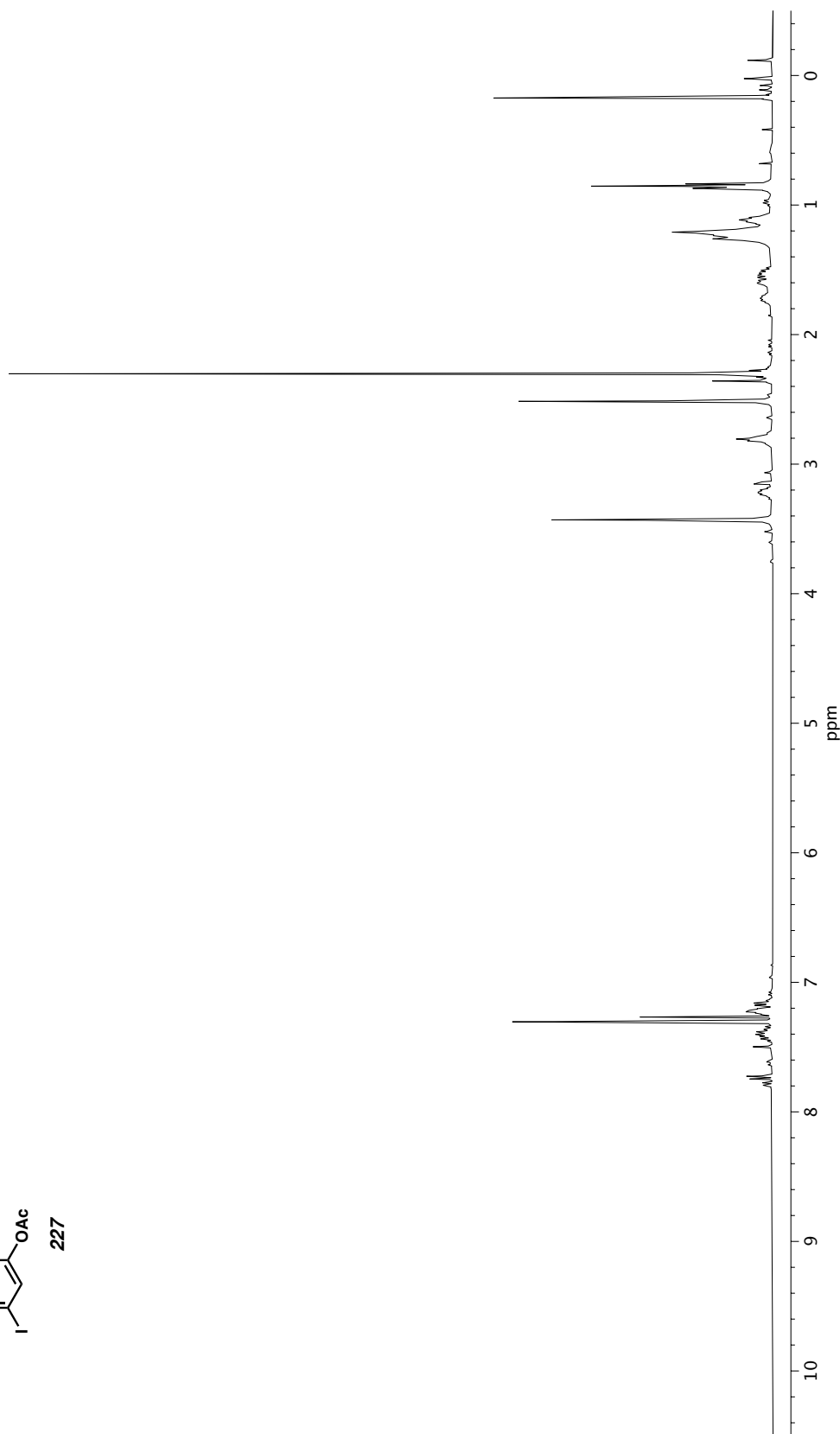
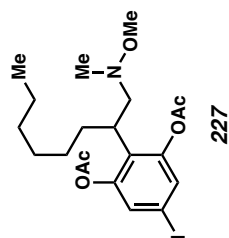


Figure A7.71 <sup>1</sup>H NMR (400 MHz, CDCl<sub>3</sub>) of compound 227.

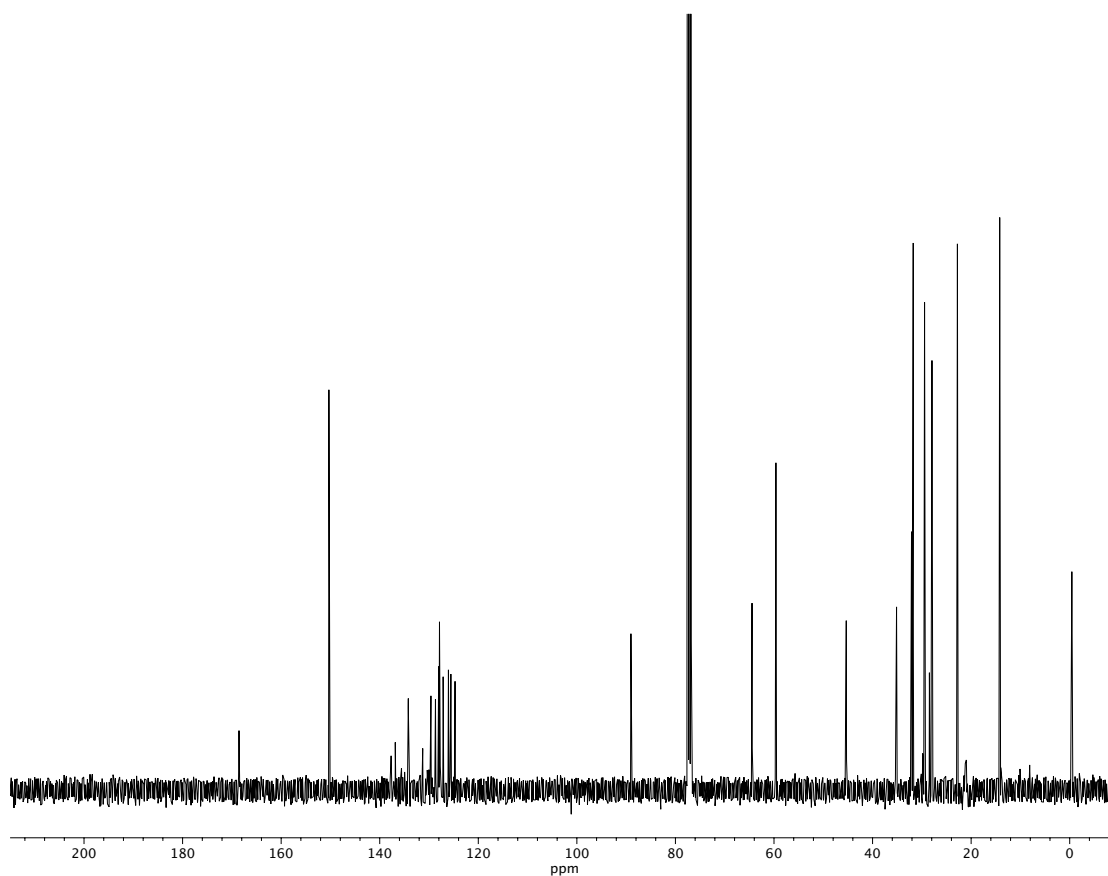


Figure A7.72  $^{13}\text{C}$  NMR (100 MHz,  $\text{CDCl}_3$ ) of compound 227.

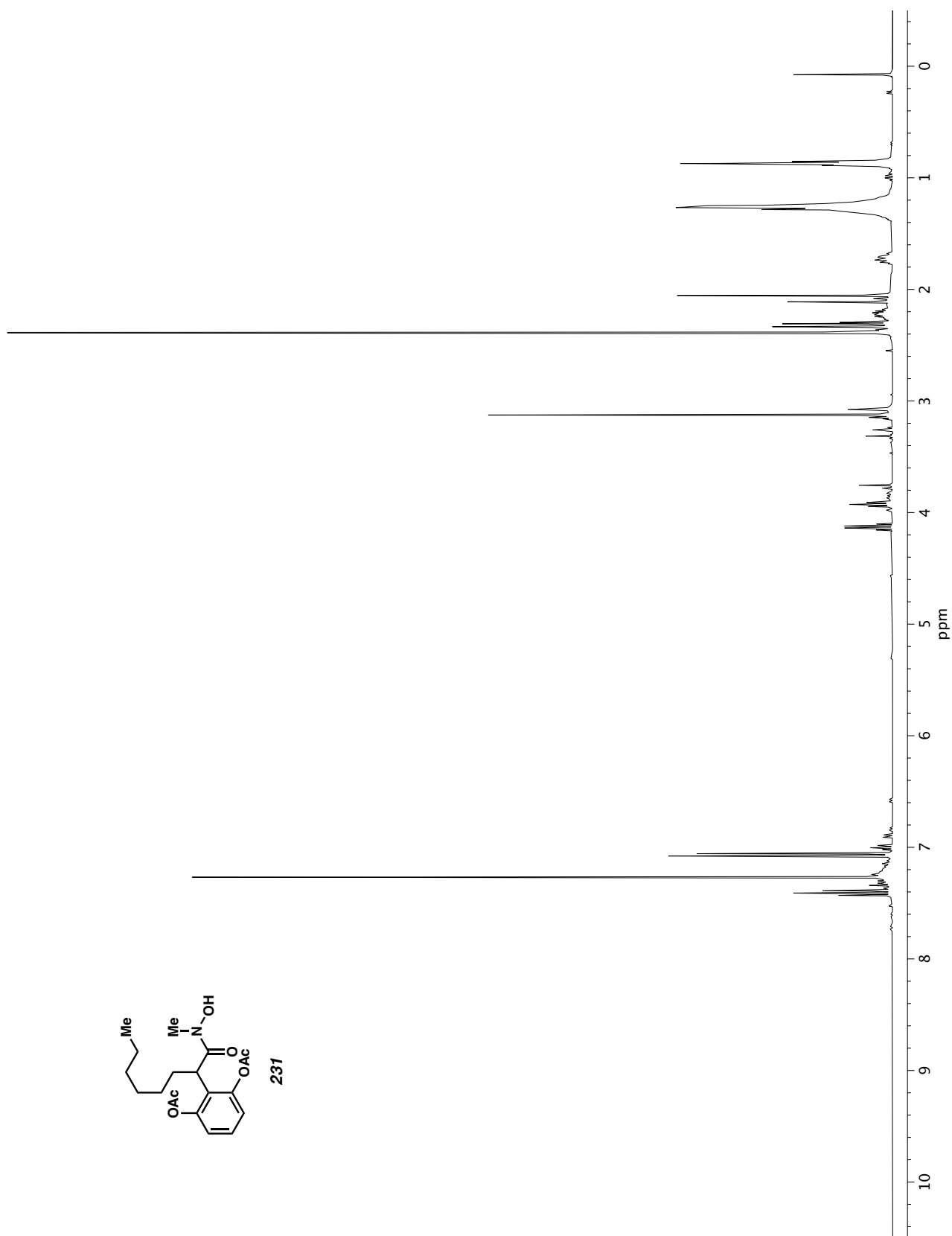


Figure A7.73  $^1\text{H}$  NMR (400 MHz,  $\text{CDCl}_3$ ) of compound 231.



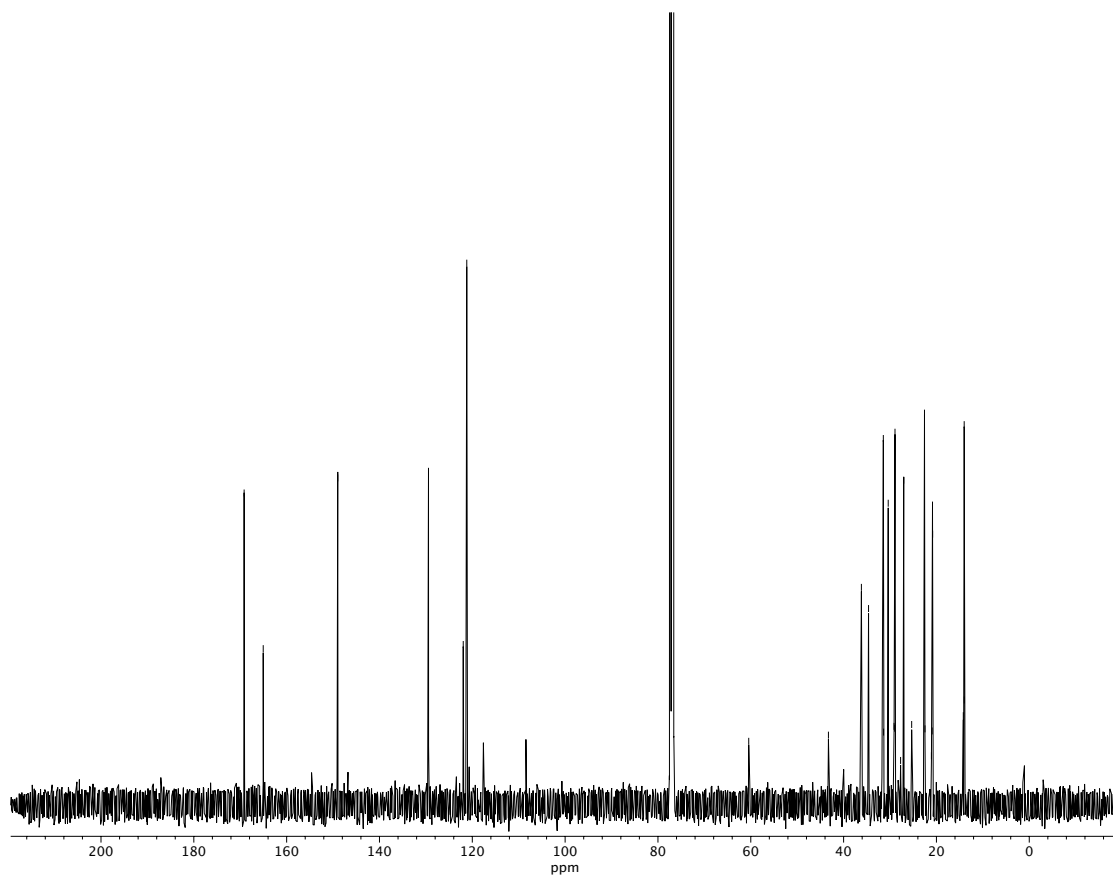


Figure A7.74  $^{13}\text{C}$  NMR (100 MHz,  $\text{CDCl}_3$ ) of compound 231.

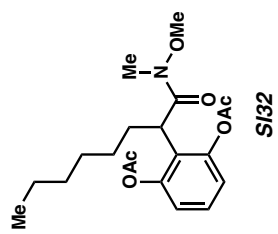
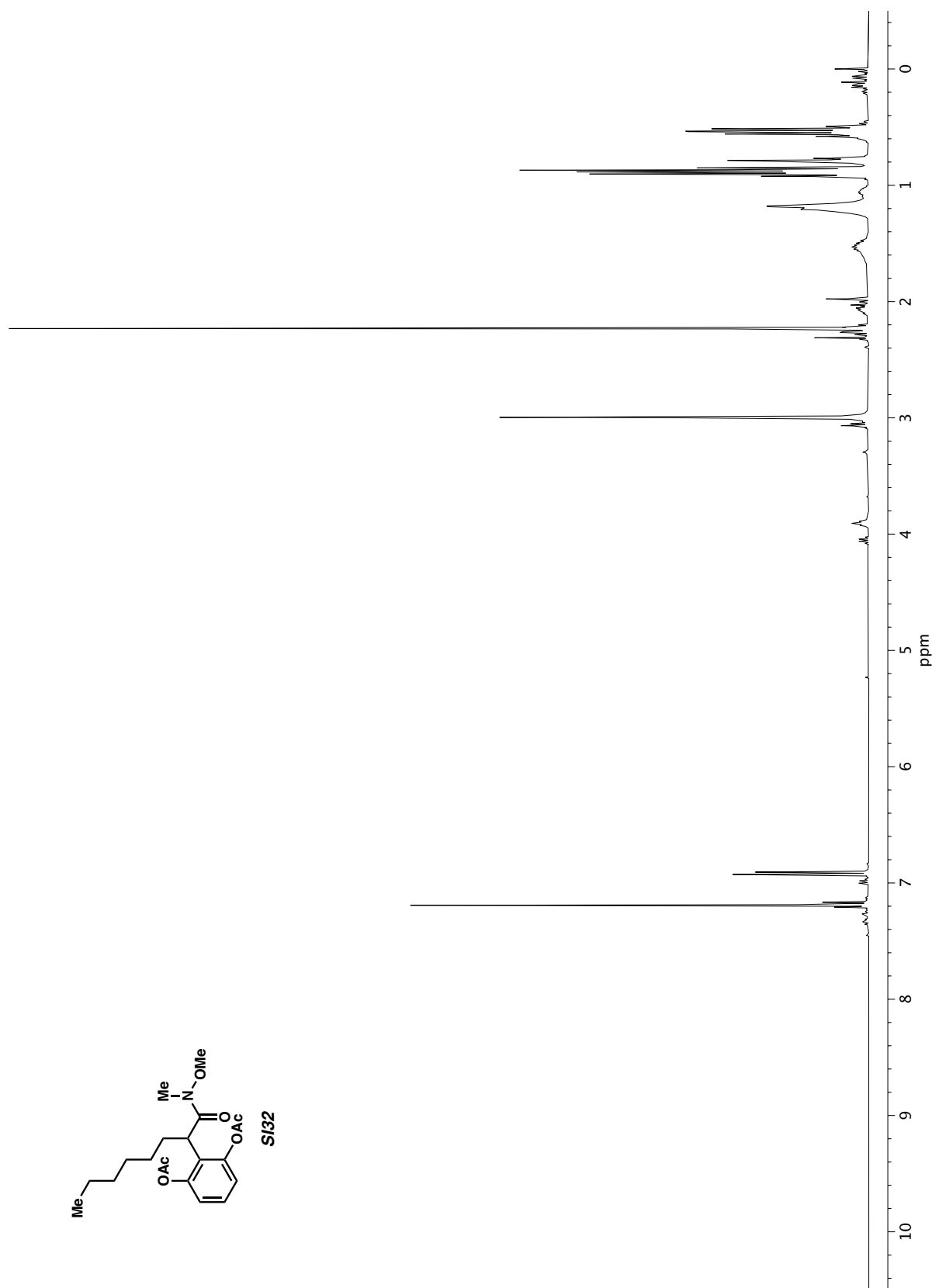
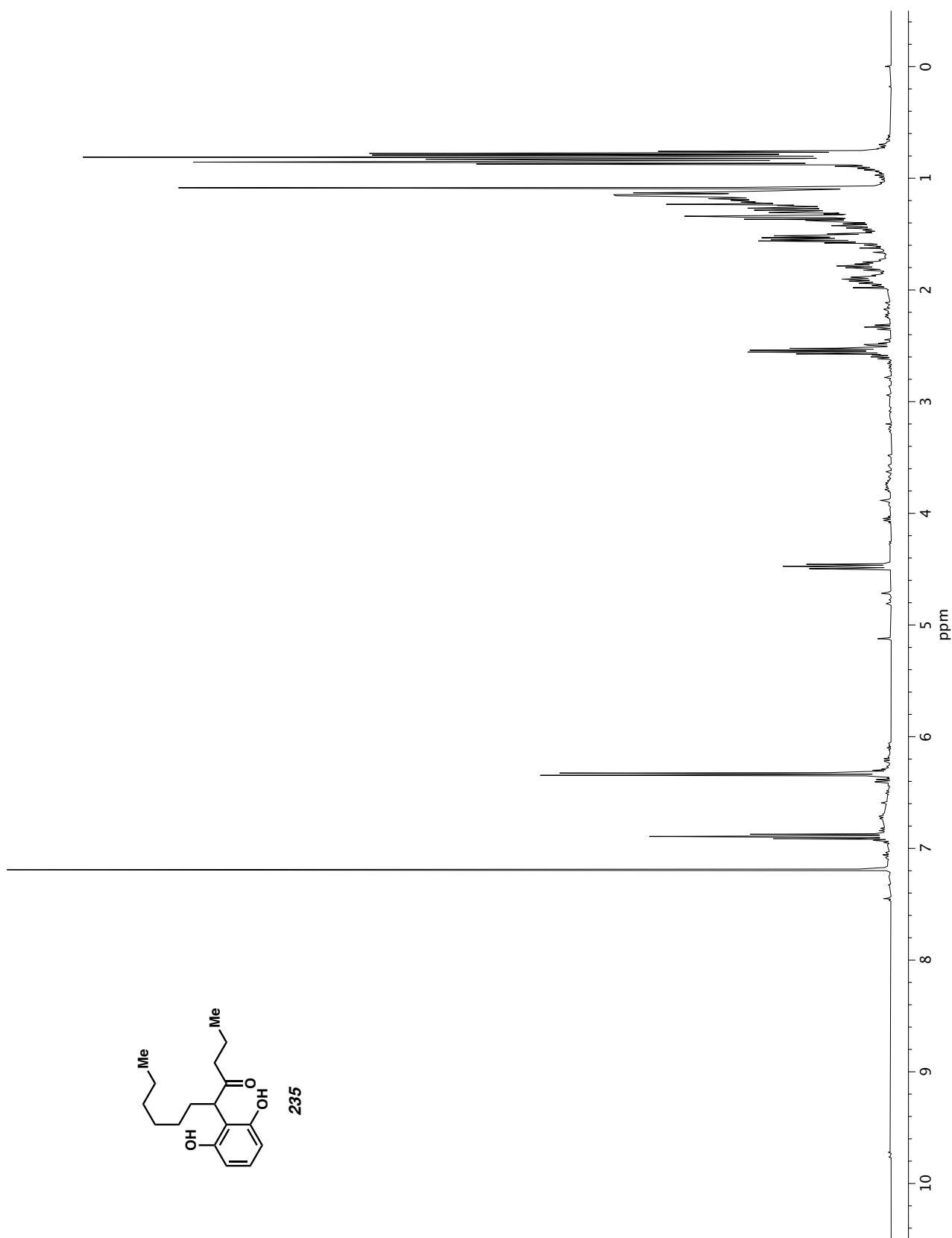


Figure A7.75 <sup>1</sup>H NMR (400 MHz, CDCl<sub>3</sub>) of compound **SI32**.

Figure A7.76  $^1\text{H}$  NMR (400 MHz,  $\text{CDCl}_3$ ) of compound 235.

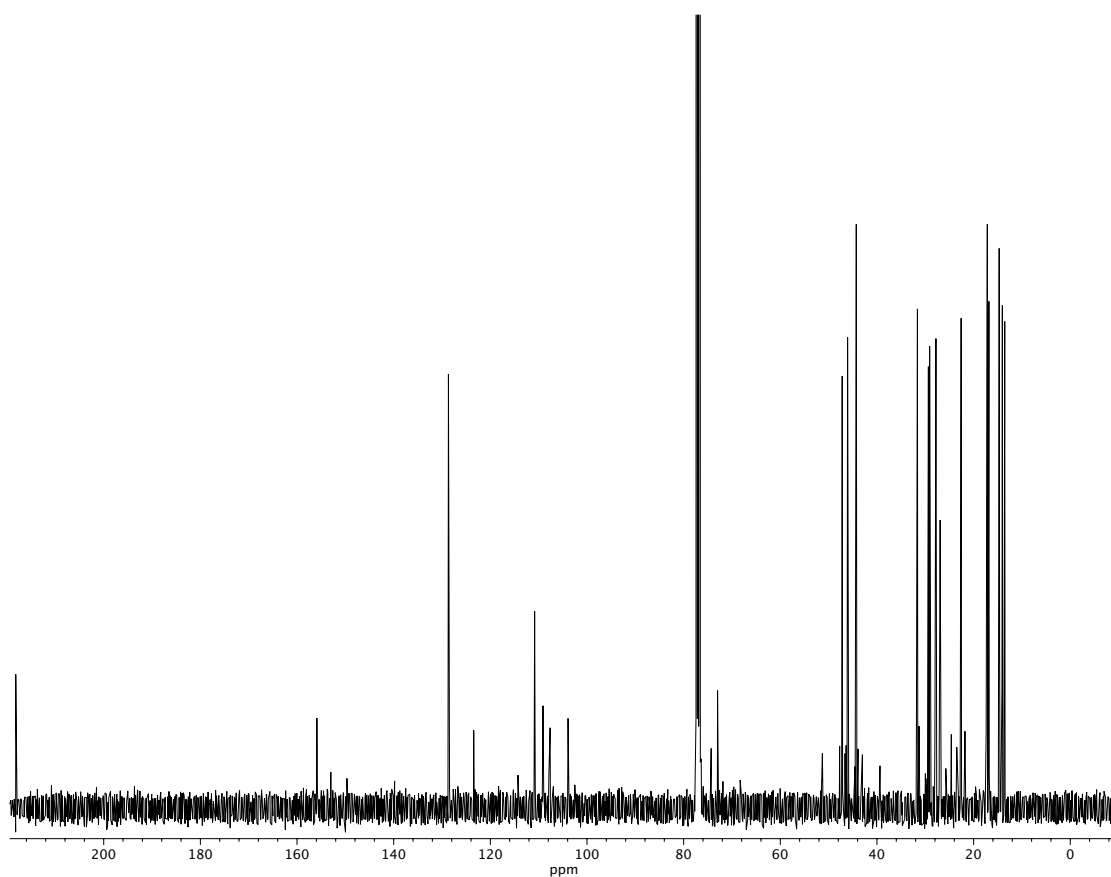


Figure A7.77  $^{13}\text{C}$  NMR (100 MHz,  $\text{CDCl}_3$ ) of compound 235.

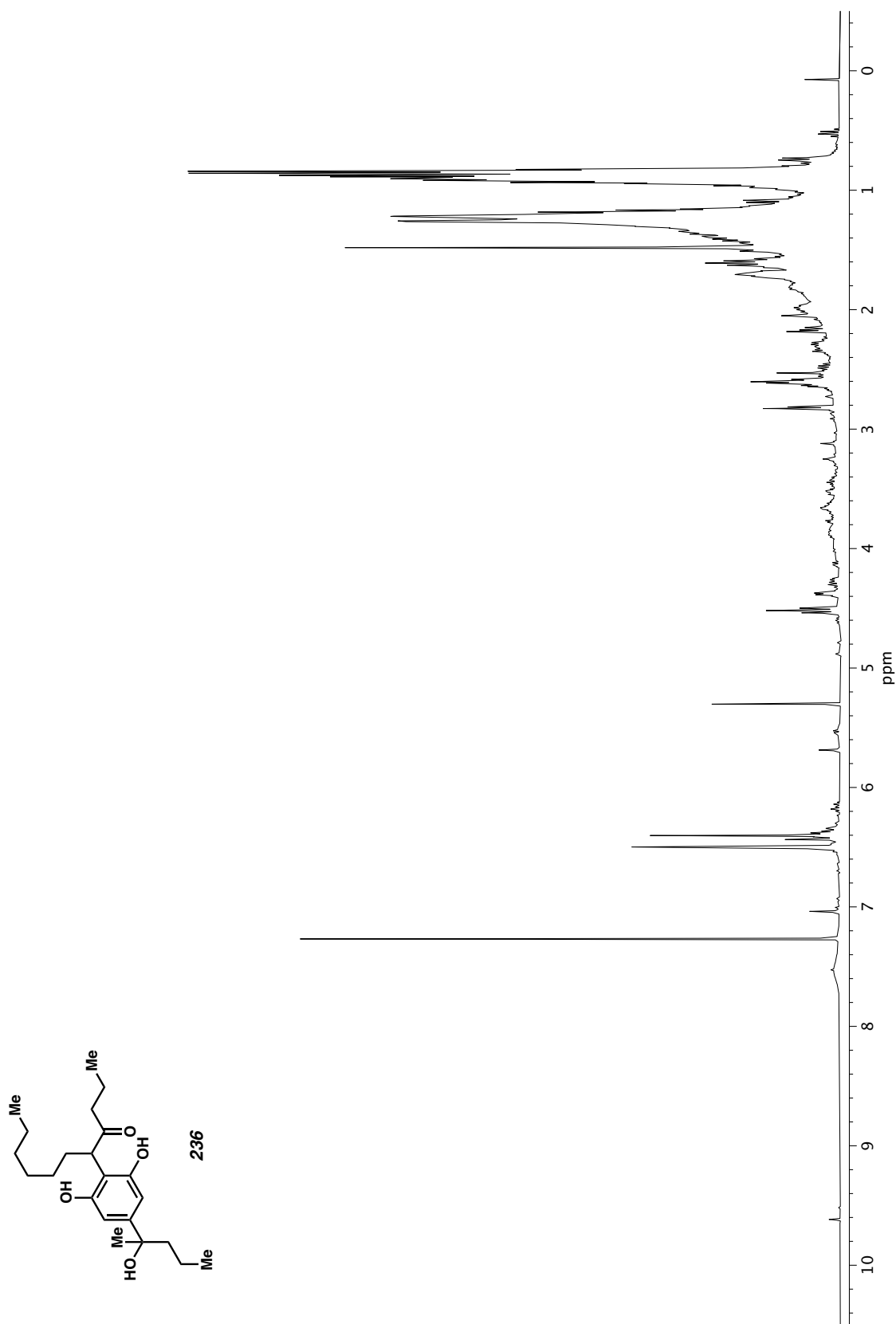
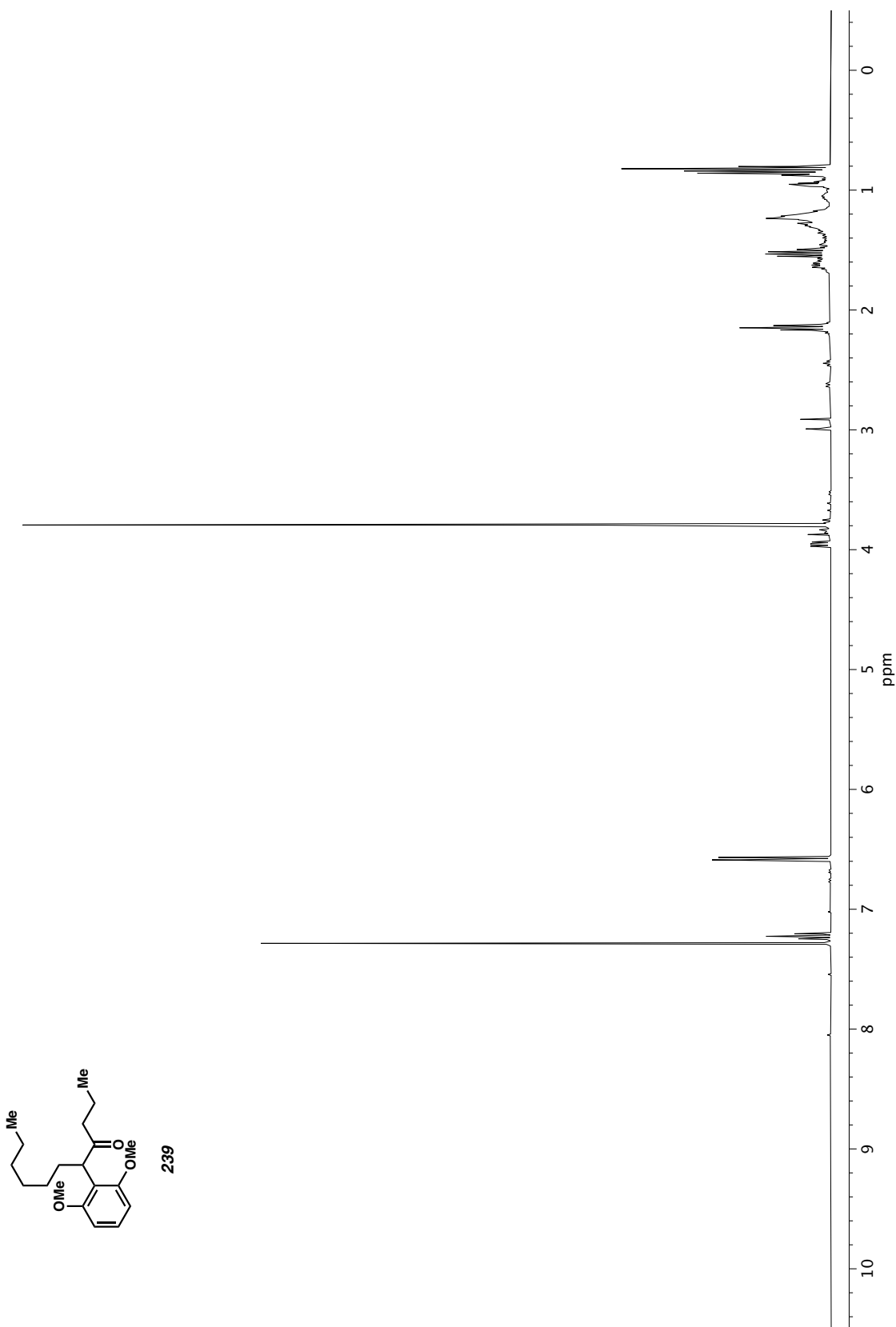


Figure A7.78 <sup>1</sup>H NMR (400 MHz, CDCl<sub>3</sub>) of compound 236.



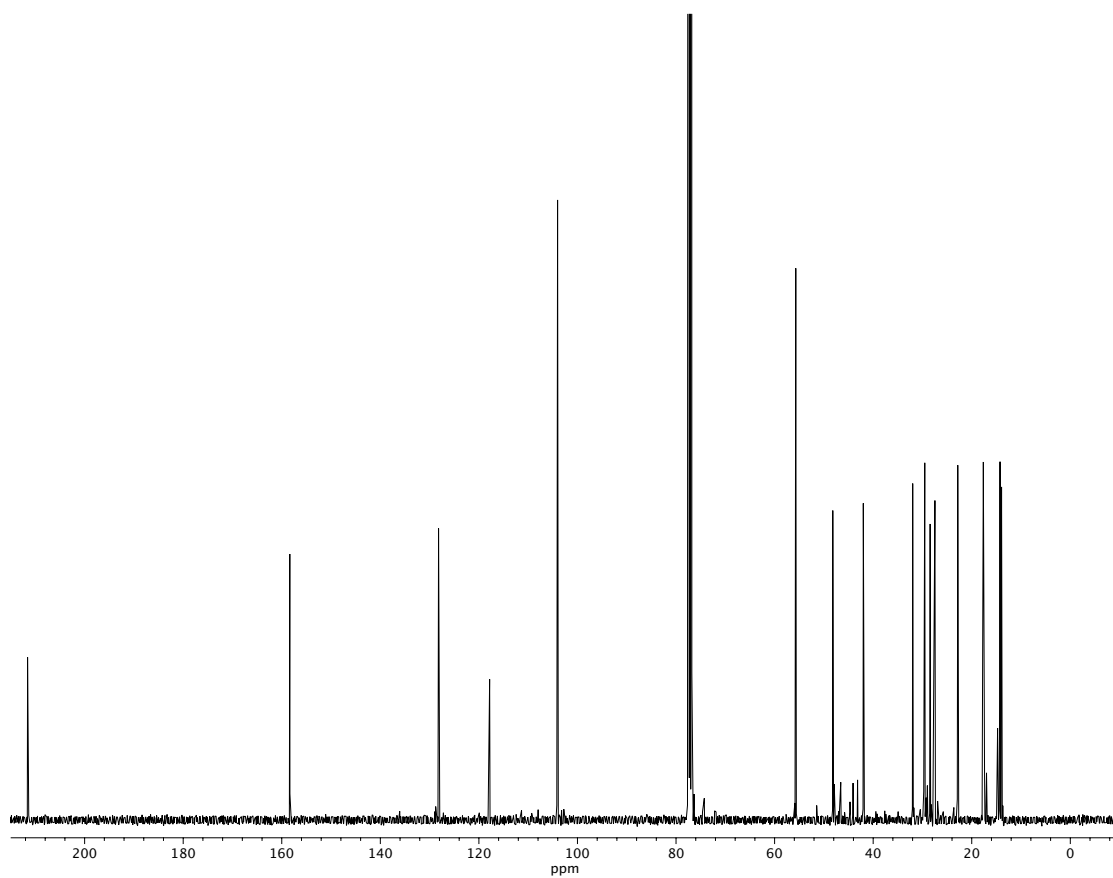


Figure A7.80  $^{13}\text{C}$  NMR (100 MHz,  $\text{CDCl}_3$ ) of compound 239.

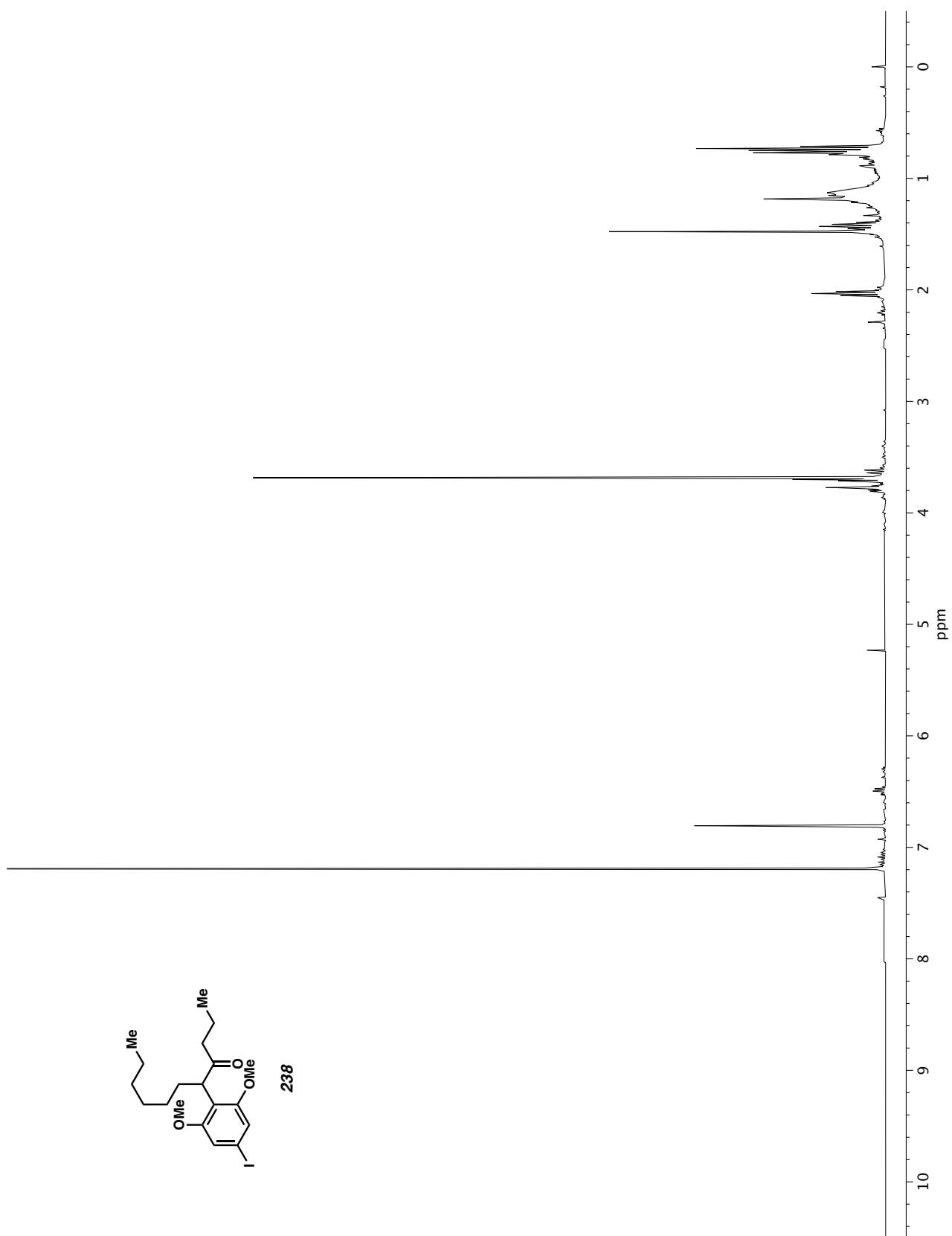


Figure A7.81  $^1\text{H}$  NMR (400 MHz,  $\text{CDCl}_3$ ) of compound 238.



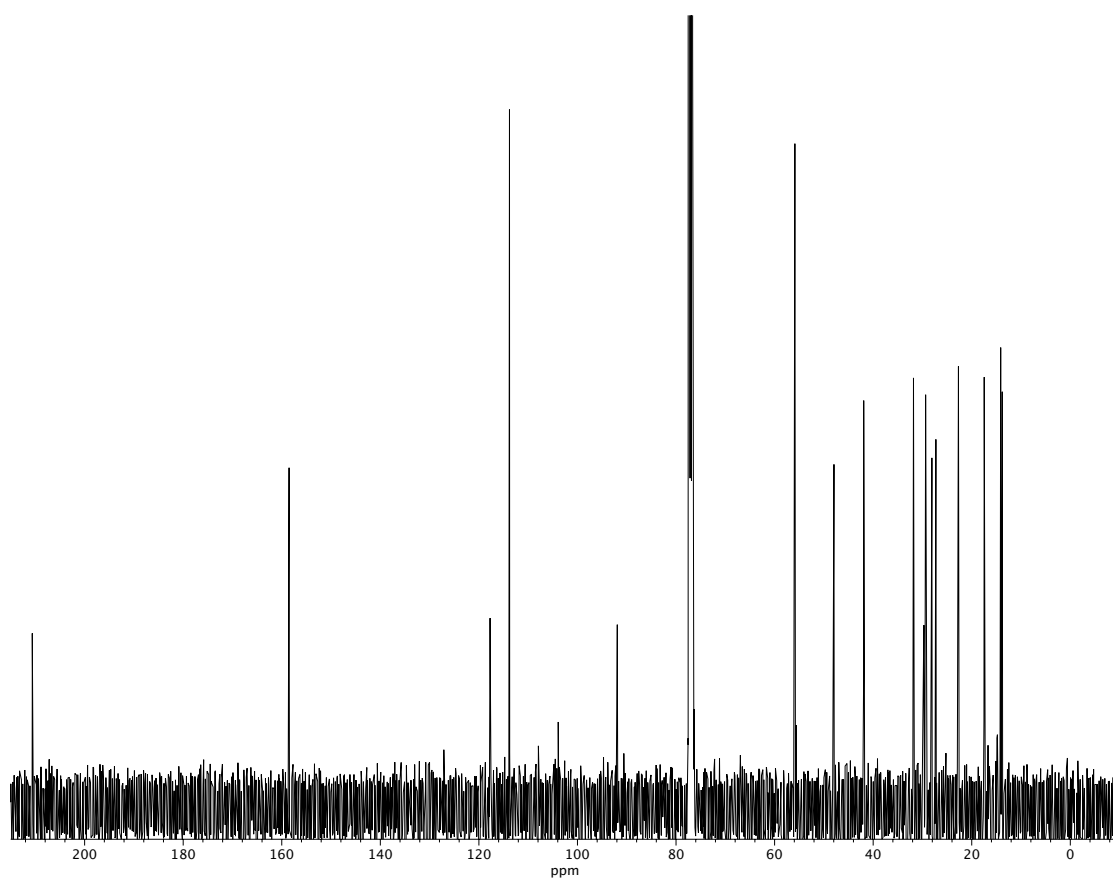


Figure A7.82  $^{13}\text{C}$  NMR (100 MHz,  $\text{CDCl}_3$ ) of compound 238.

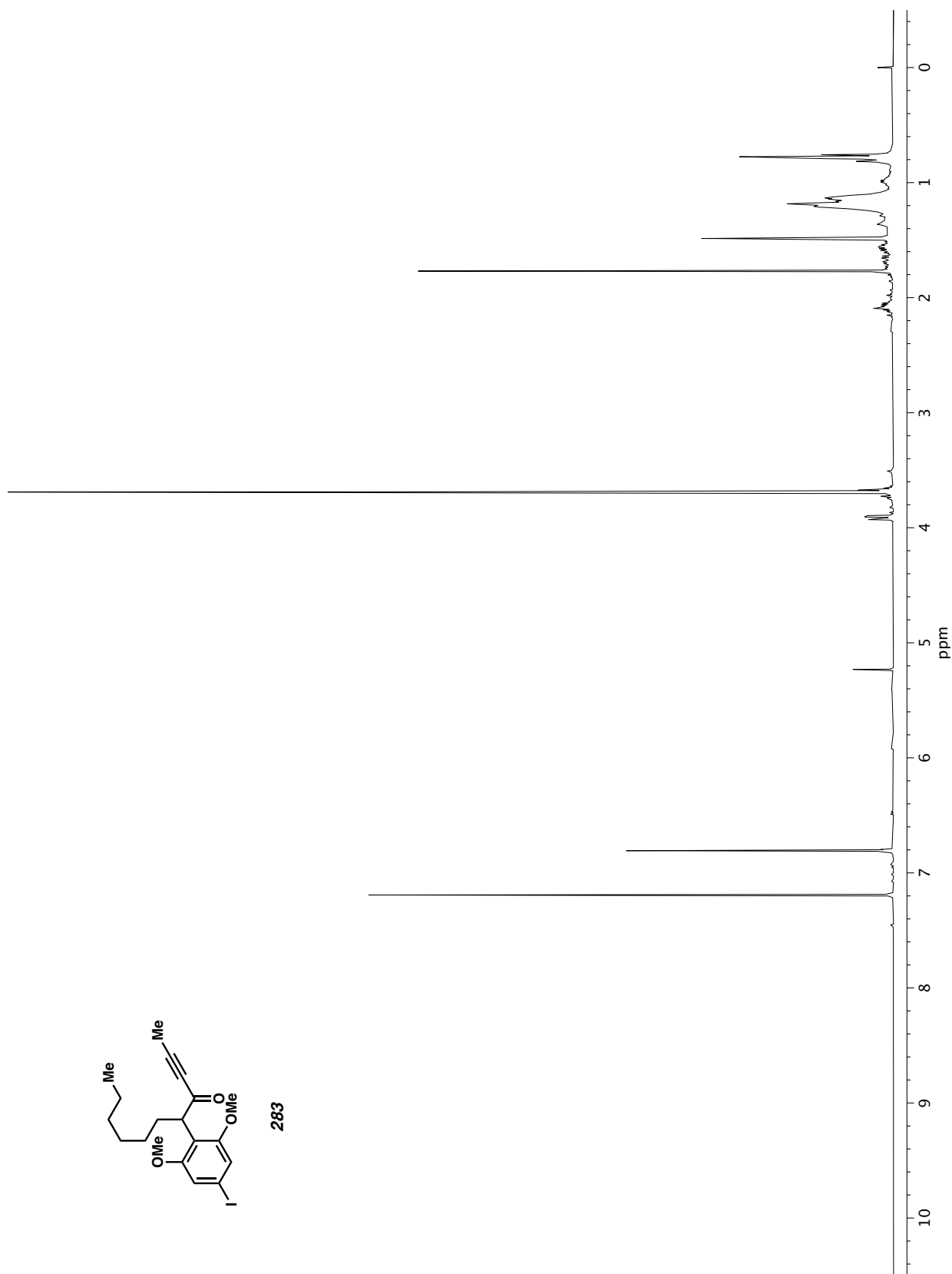
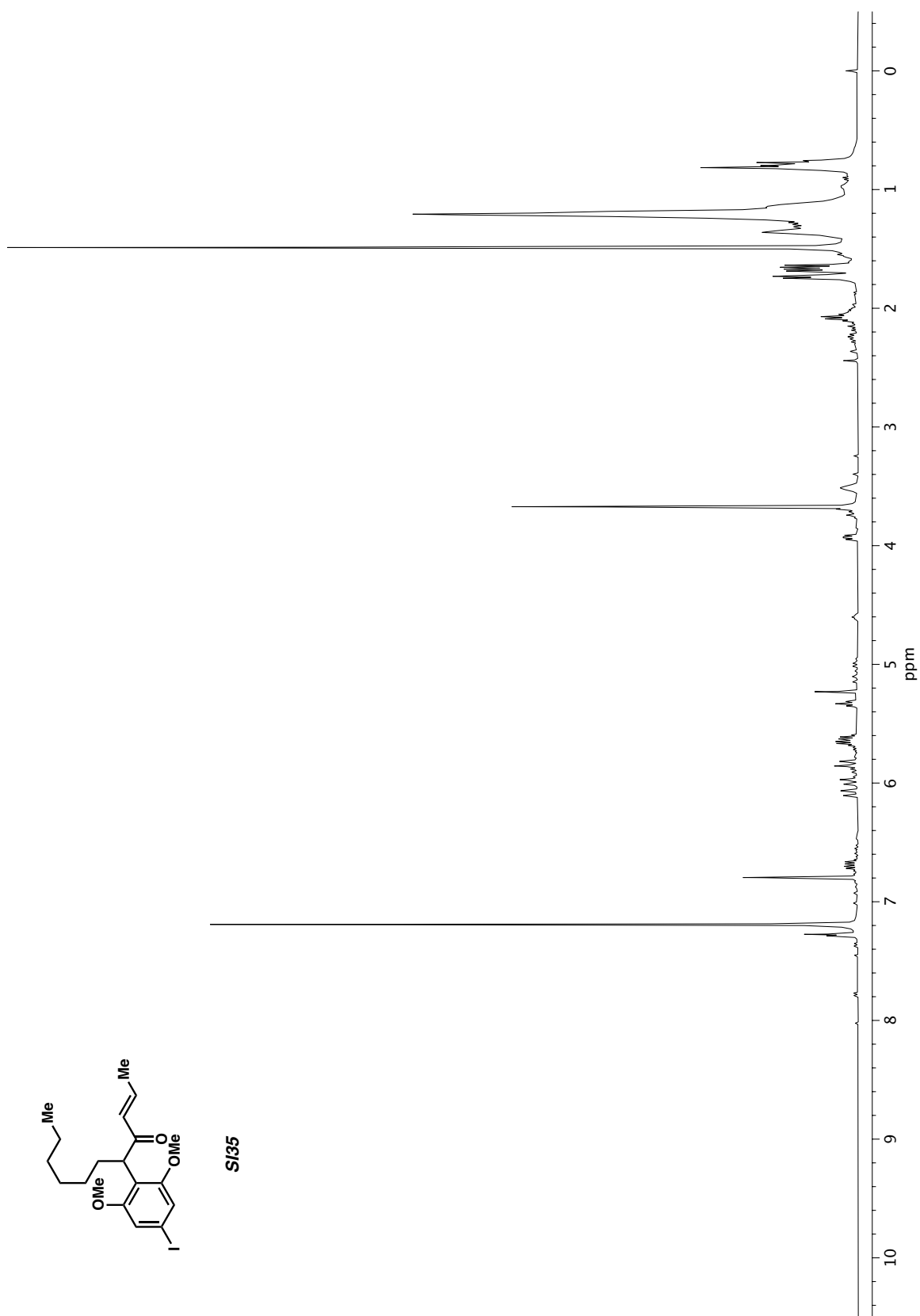
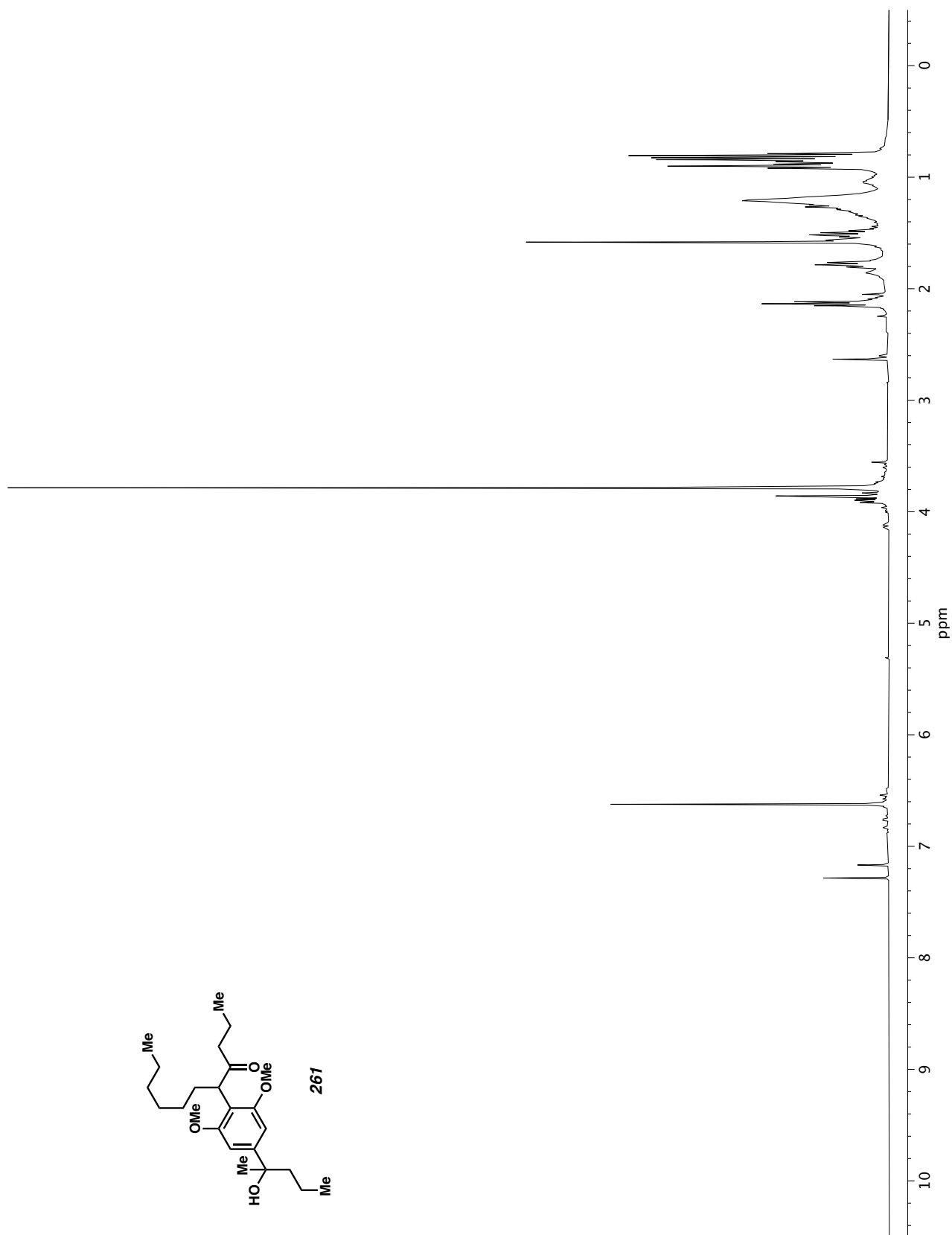


Figure A7.83  $^1\text{H}$  NMR (400 MHz,  $\text{CDCl}_3$ ) of compound 283.



**Figure A7.84** <sup>1</sup>H NMR (400 MHz, CDCl<sub>3</sub>) of compound **SI35**.



**Figure A7.85**  $^1\text{H}$  NMR (400 MHz,  $\text{CDCl}_3$ ) of compound **261**.

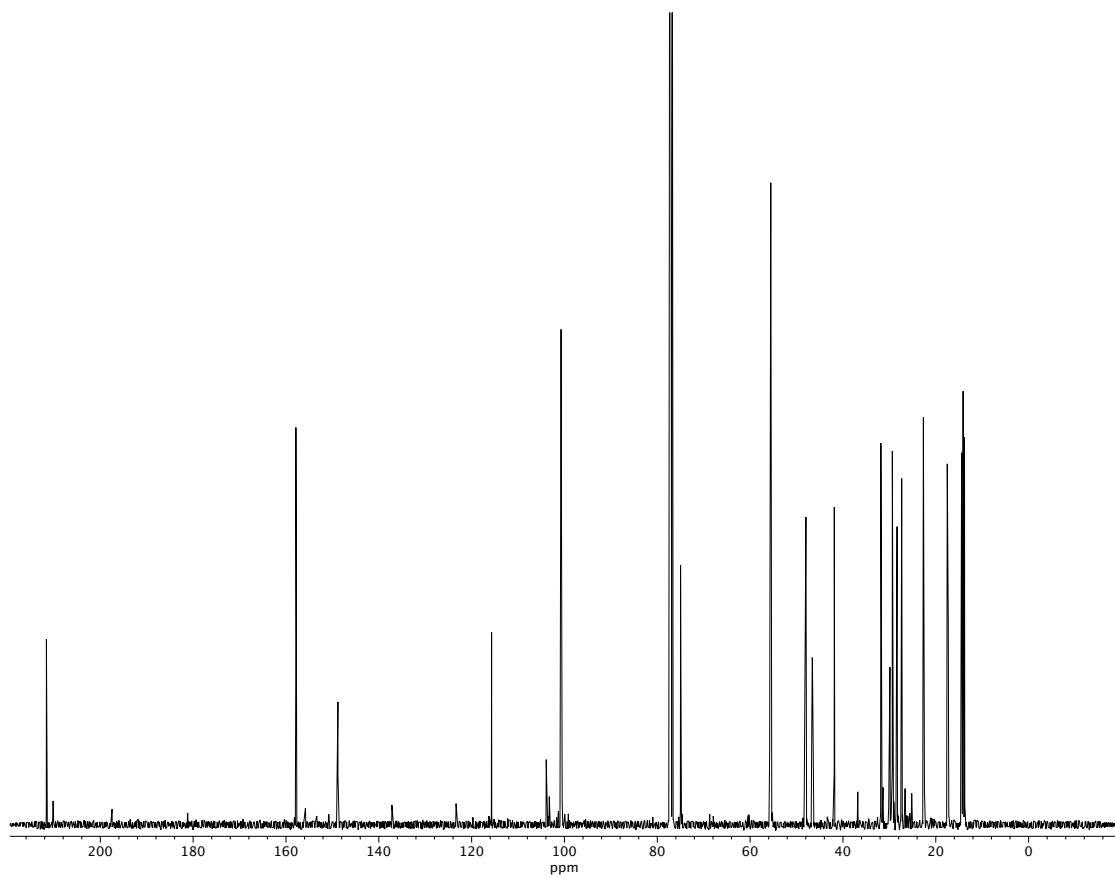


Figure A7.86  $^{13}\text{C}$  NMR (100 MHz,  $\text{CDCl}_3$ ) of compound 261.

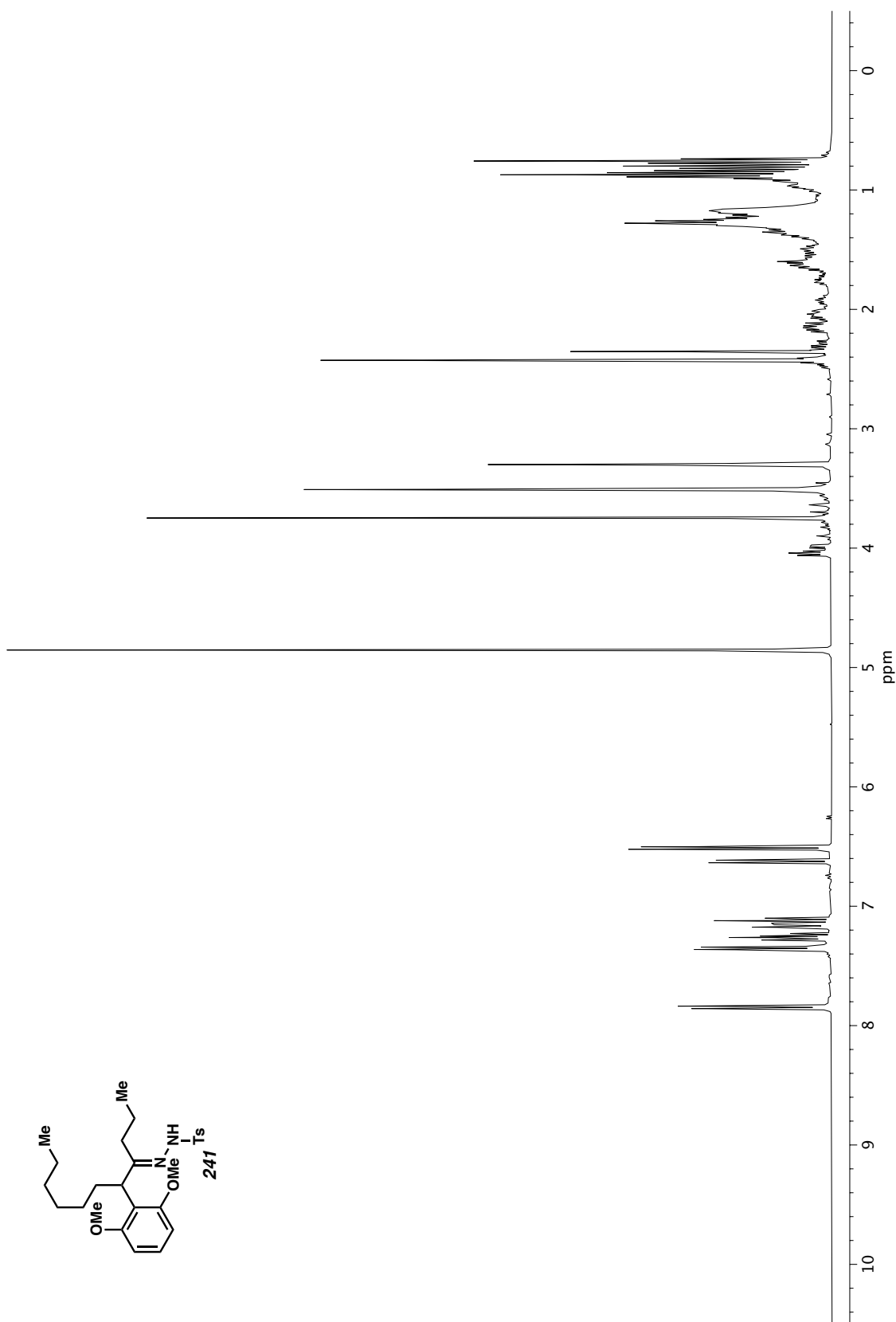


Figure A7.87  $^1\text{H}$  NMR (400 MHz,  $\text{CD}_3\text{OD}$ ) of compound **241**.

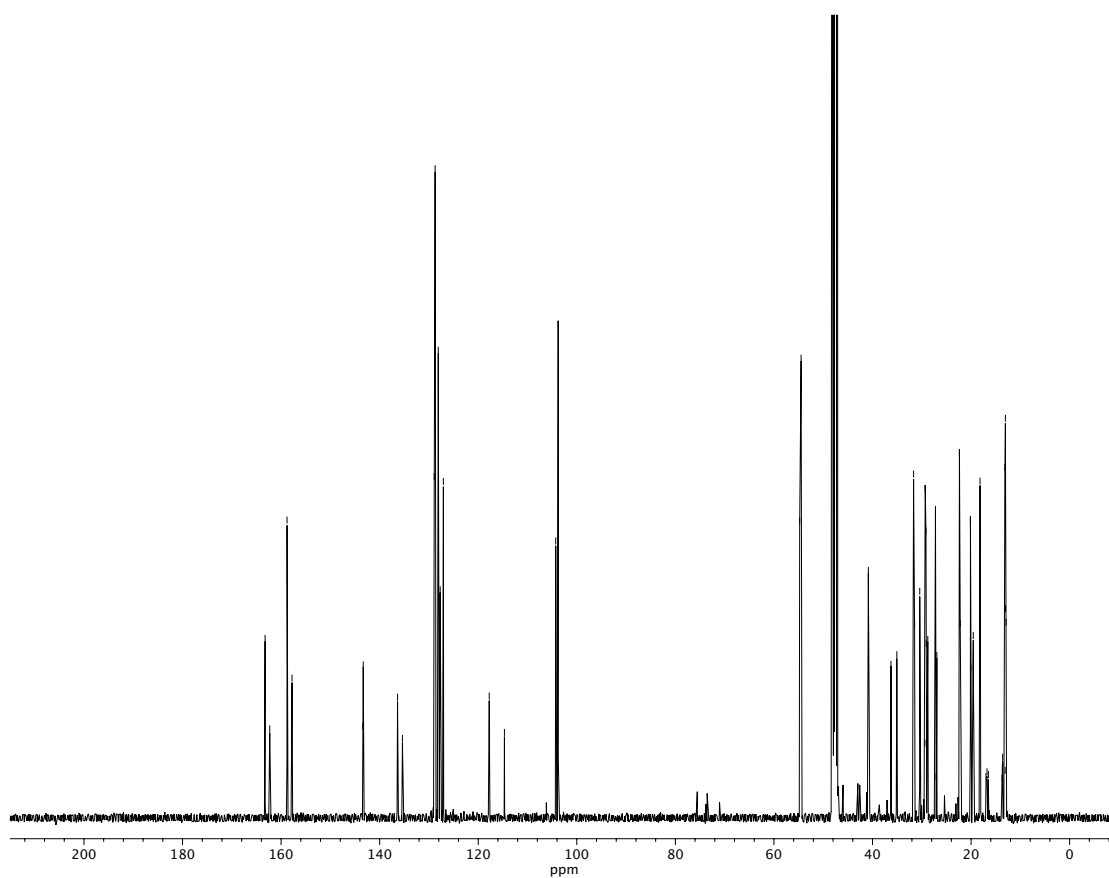


Figure A7.88  $^{13}\text{C}$  NMR (100 MHz,  $\text{CD}_3\text{OD}$ ) of compound 241.

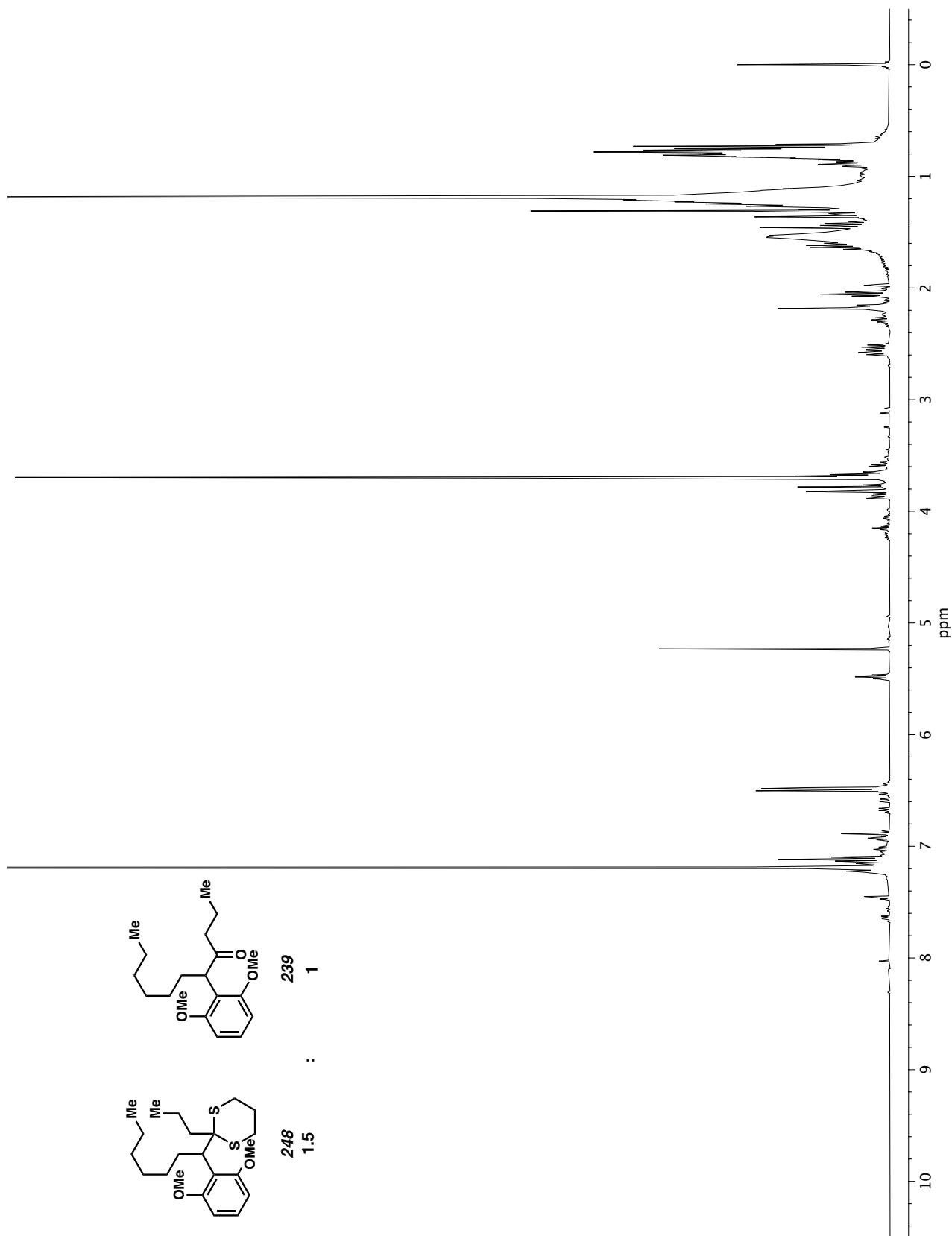
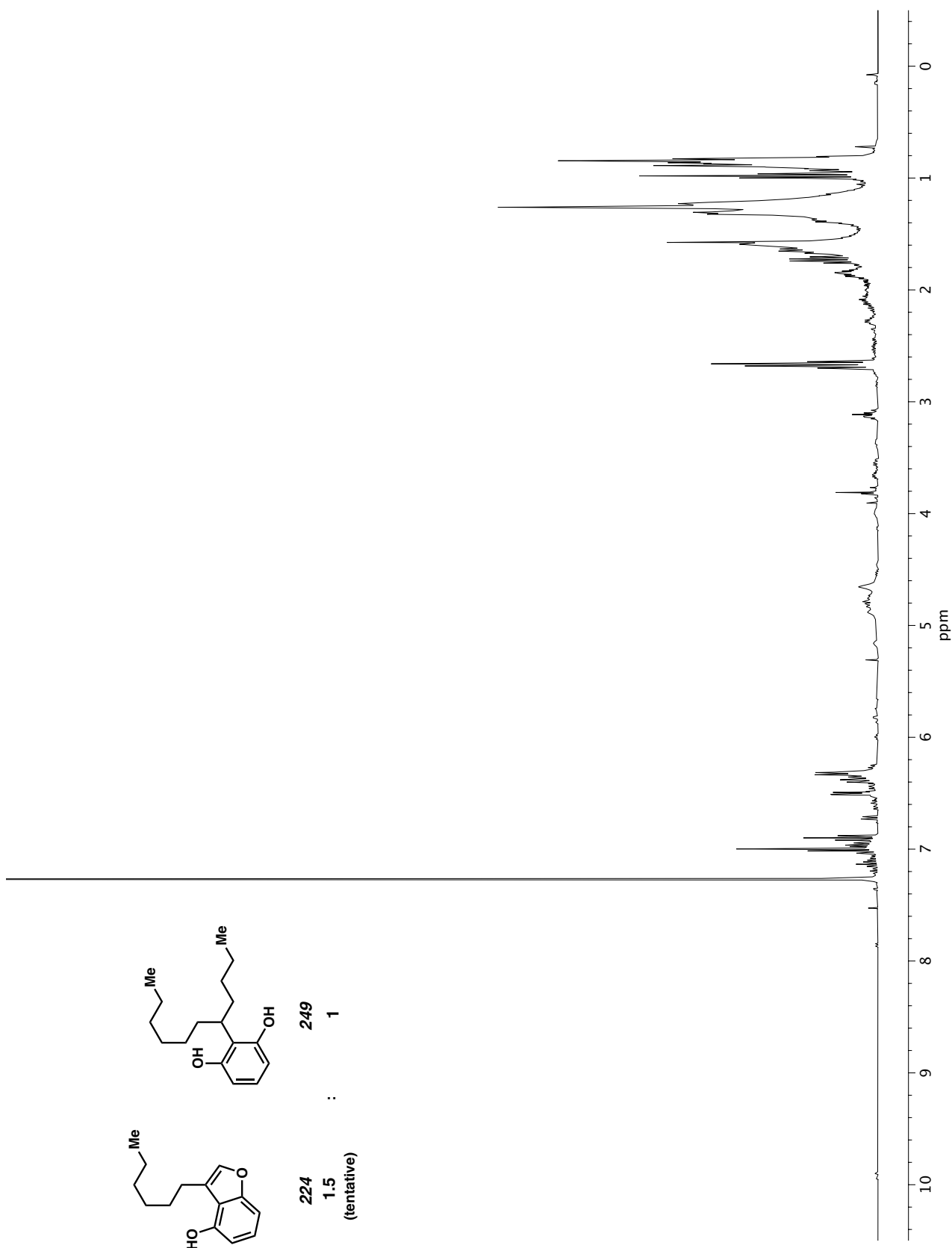
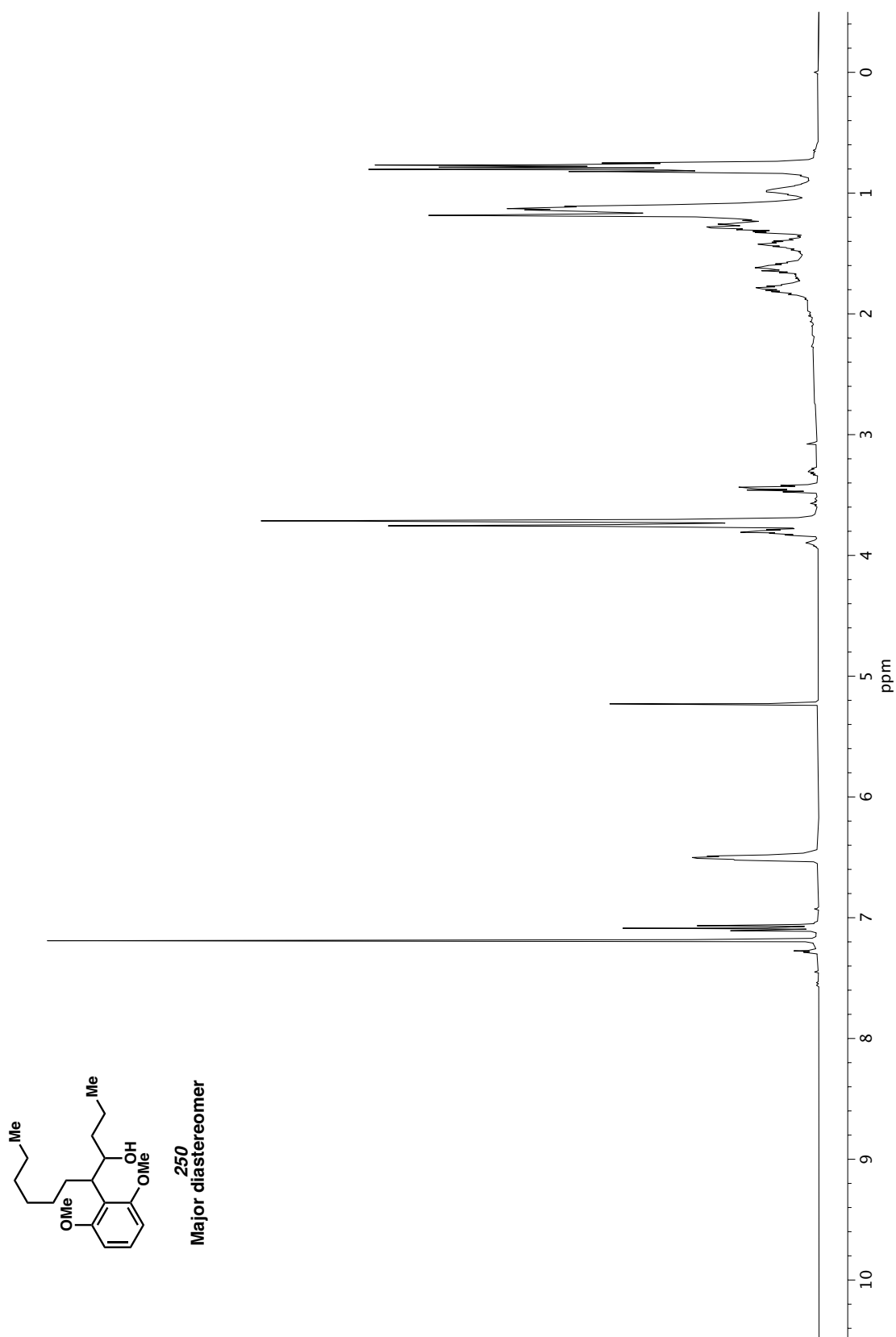


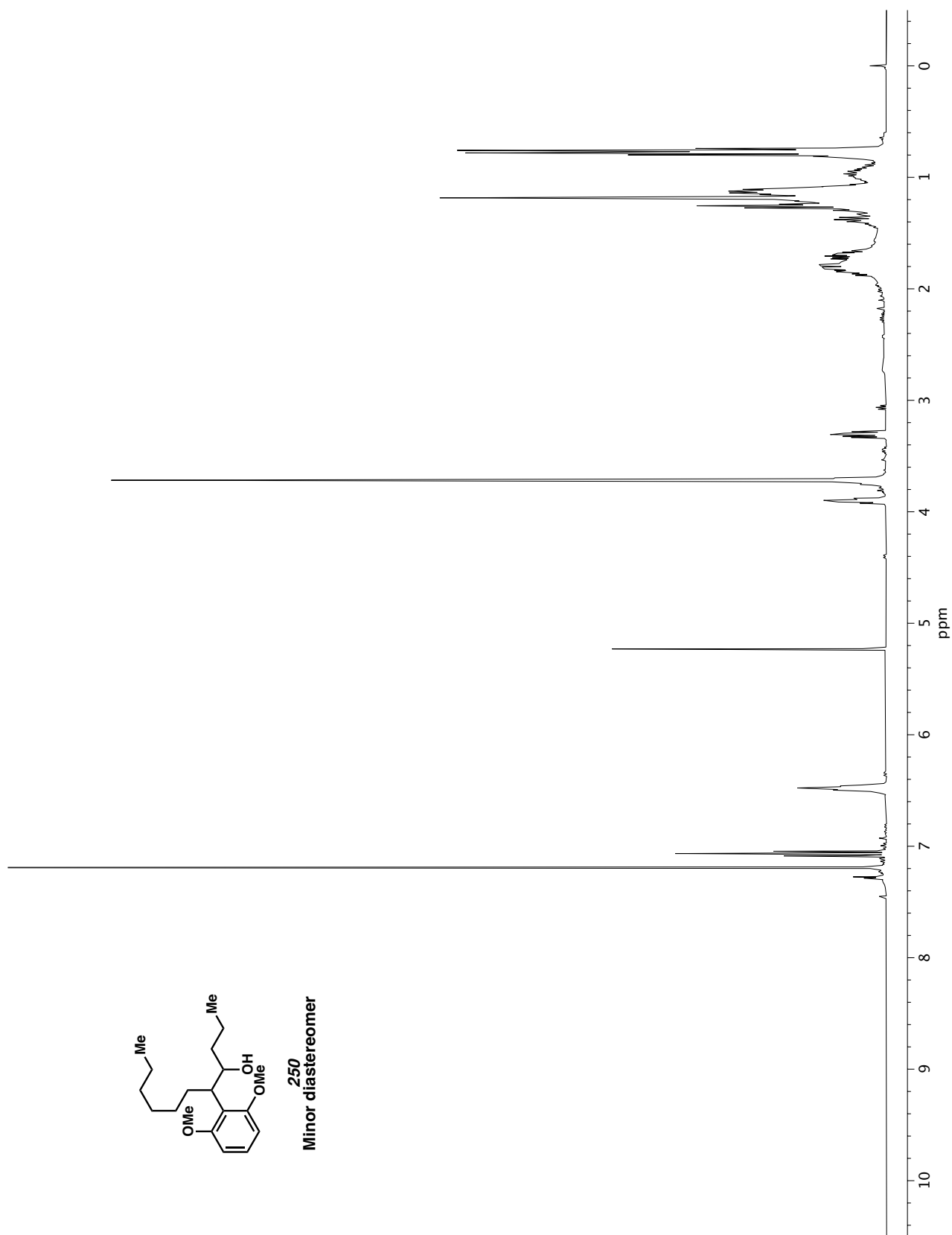
Figure A7.89 <sup>1</sup>H NMR (400 MHz, CDCl<sub>3</sub>) of compound 248.







Figure A7.92 <sup>1</sup>H NMR (400 MHz, CDCl<sub>3</sub>) of compound 250 (Major).

Figure A7.93  $^1\text{H}$  NMR (400 MHz,  $\text{CDCl}_3$ ) of compound 250 (Minor).

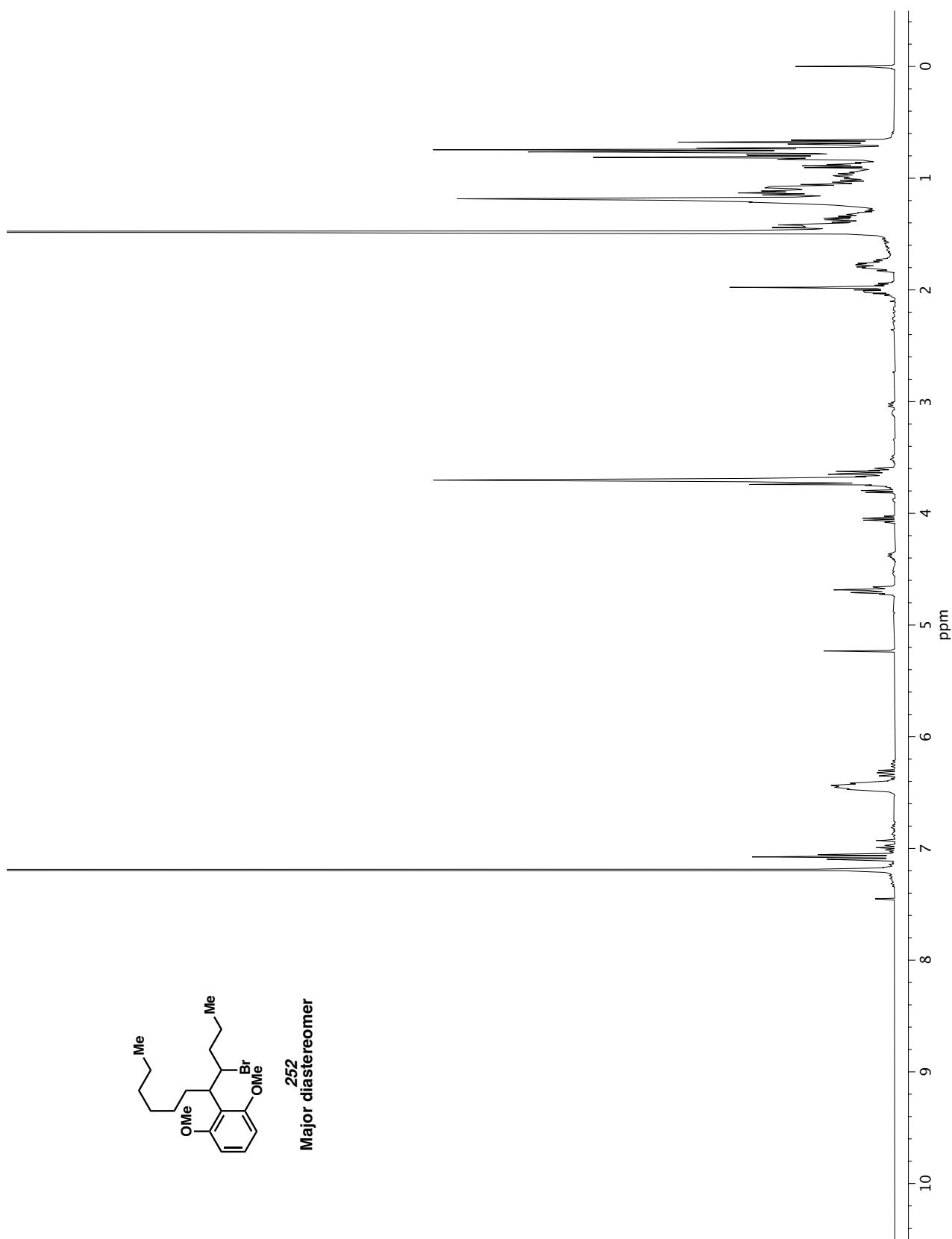
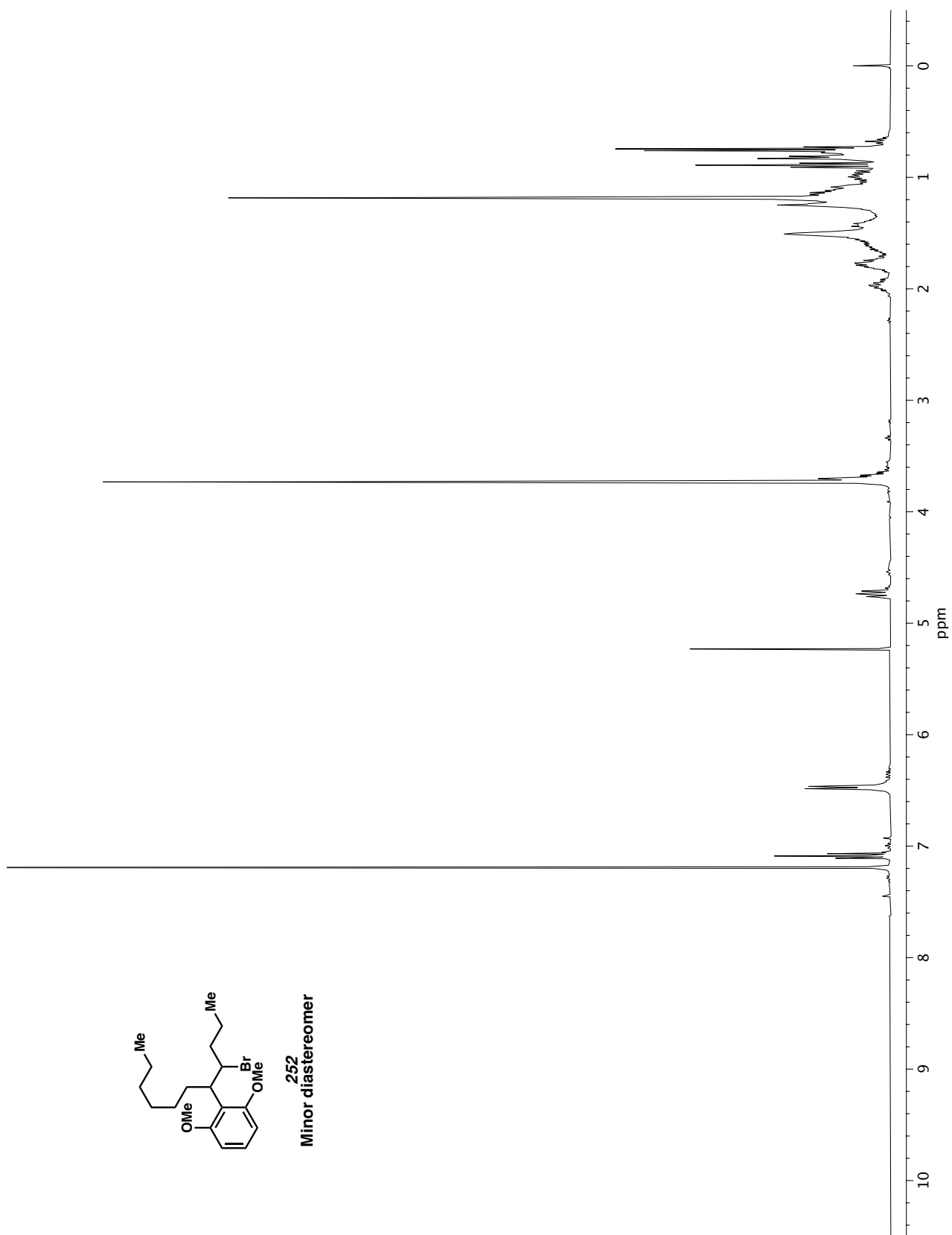
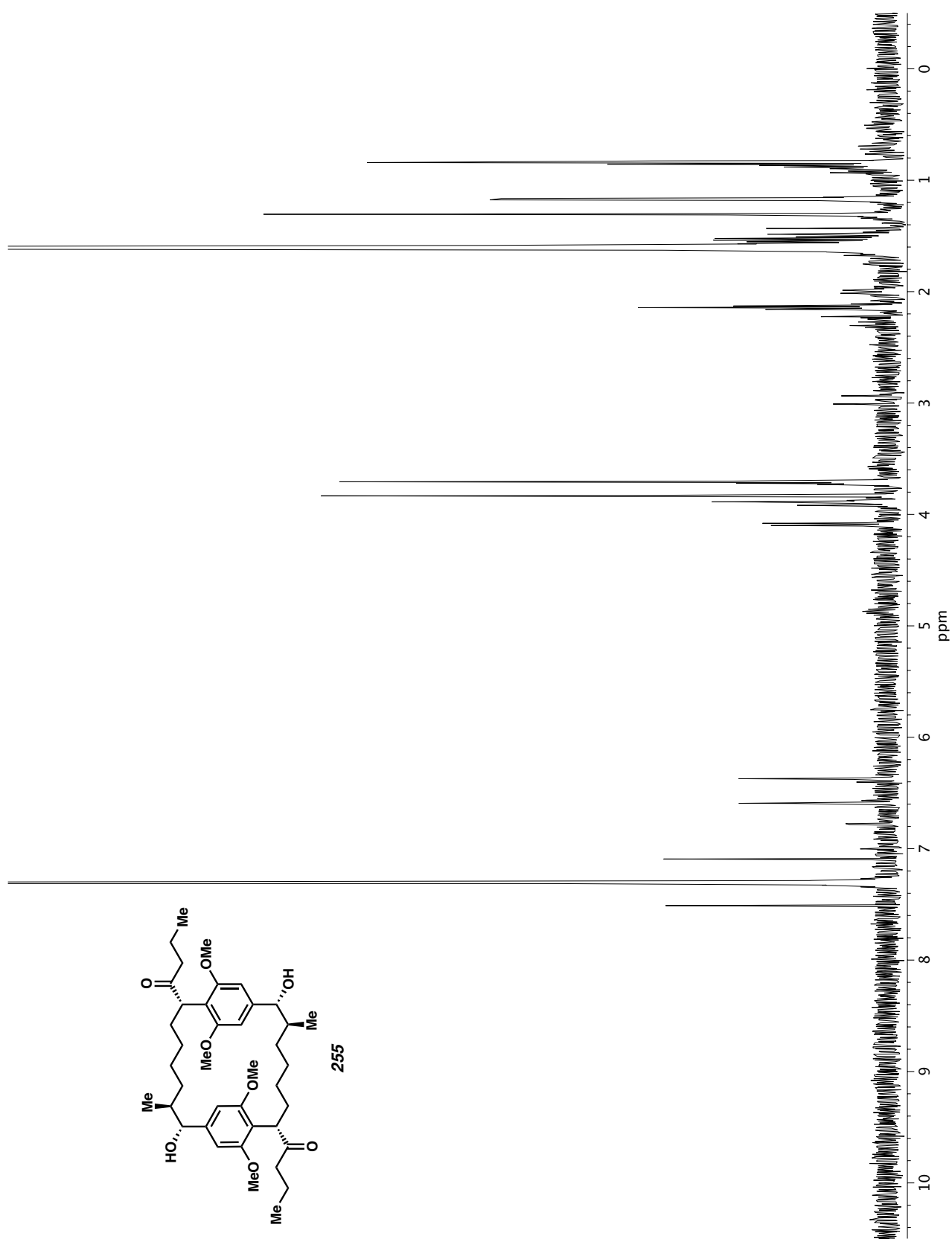


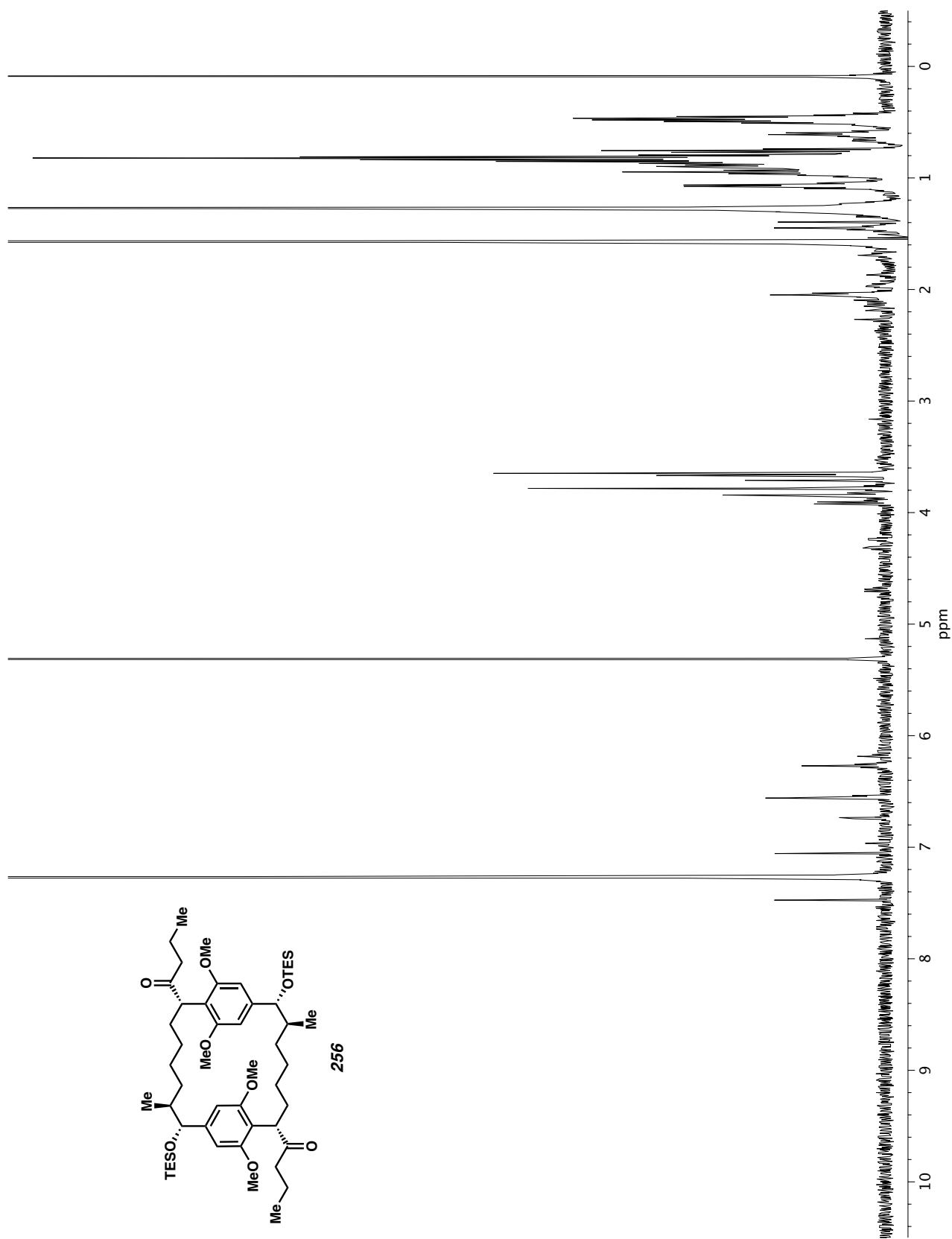
Figure A7.94 <sup>1</sup>H NMR (400 MHz, CDCl<sub>3</sub>) of compound 252 (Major).

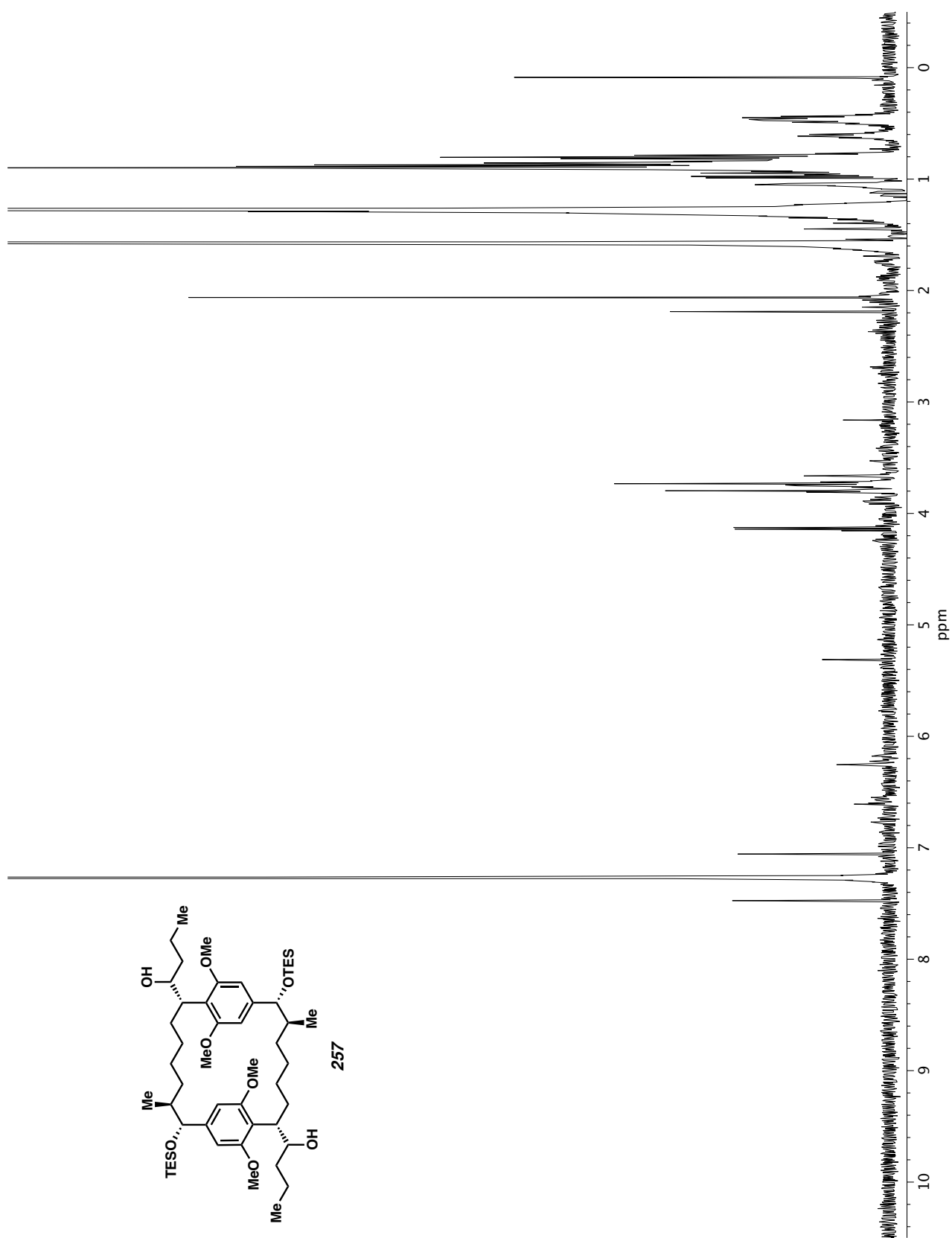
Figure A7.95  $^1\text{H}$  NMR (400 MHz,  $\text{CDCl}_3$ ) of compound 252 (Minor).

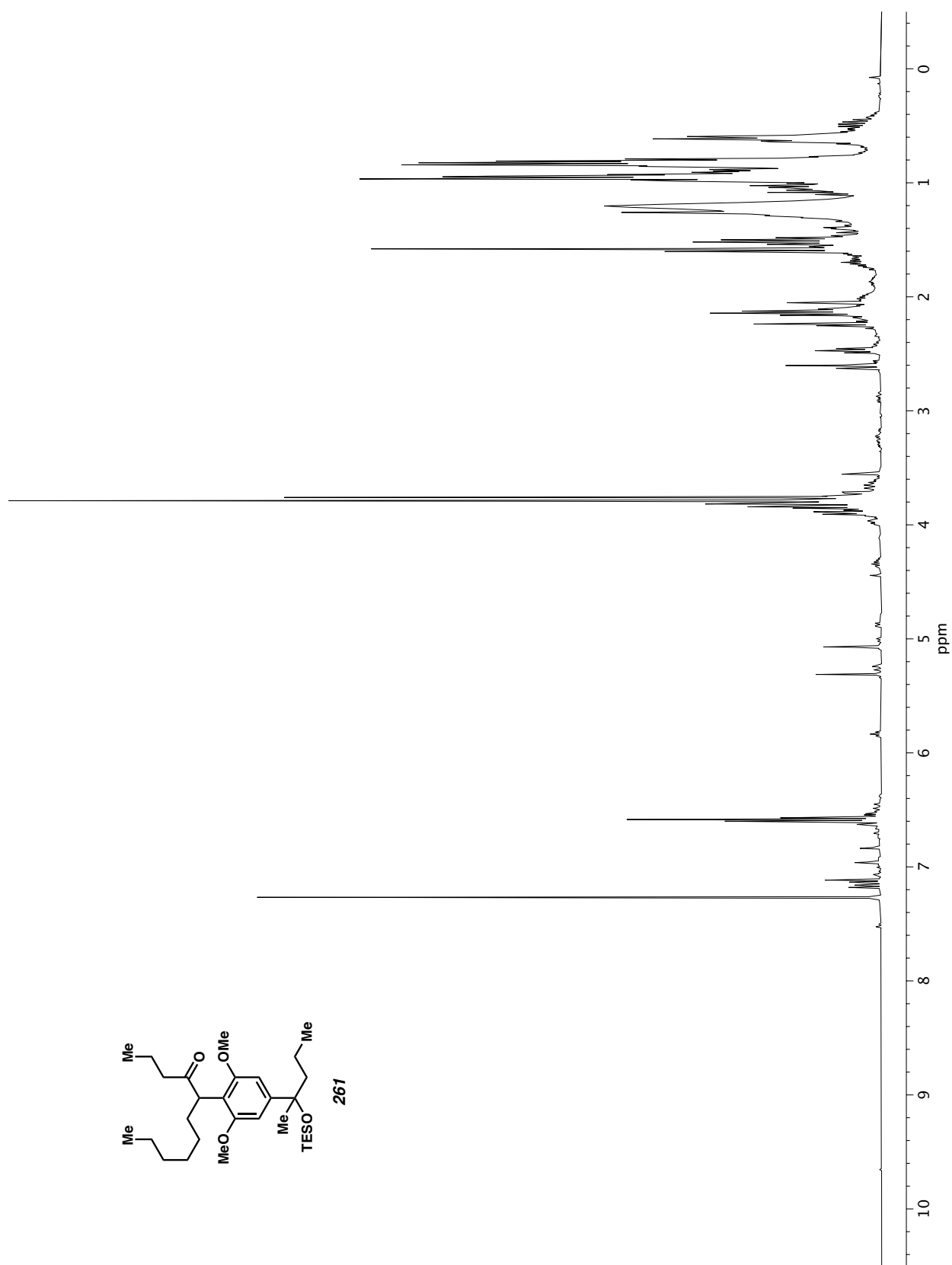


Figure A7.97  $^1\text{H}$  NMR (400 MHz,  $\text{CDCl}_3$ ) of compound 255.

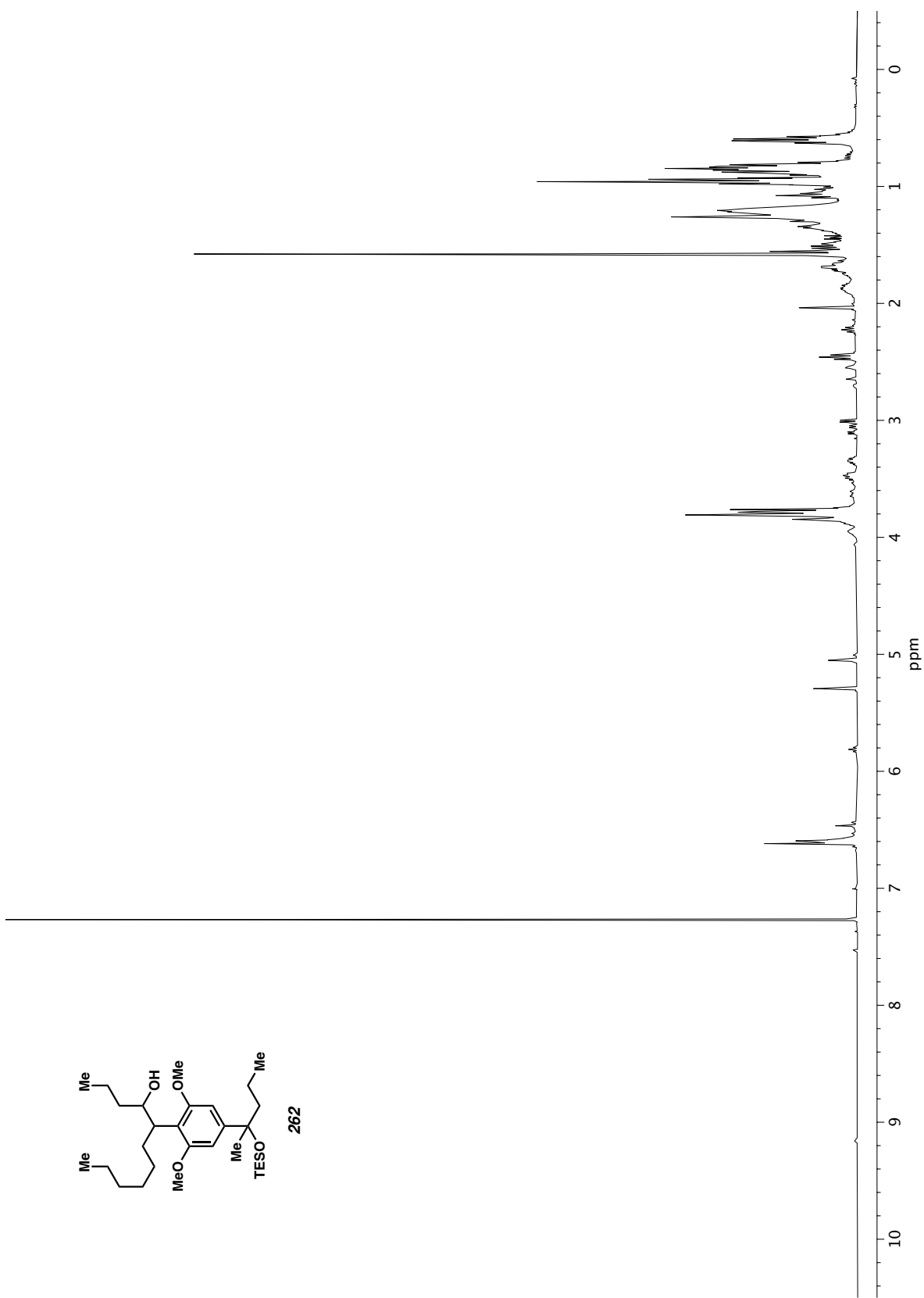


Figure A7.98  $^1\text{H}$  NMR (400 MHz,  $\text{CDCl}_3$ ) of compound 256.

Figure A7.99  $^1\text{H}$  NMR (400 MHz,  $\text{CDCl}_3$ ) of compound 257.



**Figure A7.100**  $^1\text{H}$  NMR (400 MHz,  $\text{CDCl}_3$ ) of compound **261**.



**Figure A7.101**  $^1\text{H}$  NMR (400 MHz,  $\text{CDCl}_3$ ) of compound **262**.

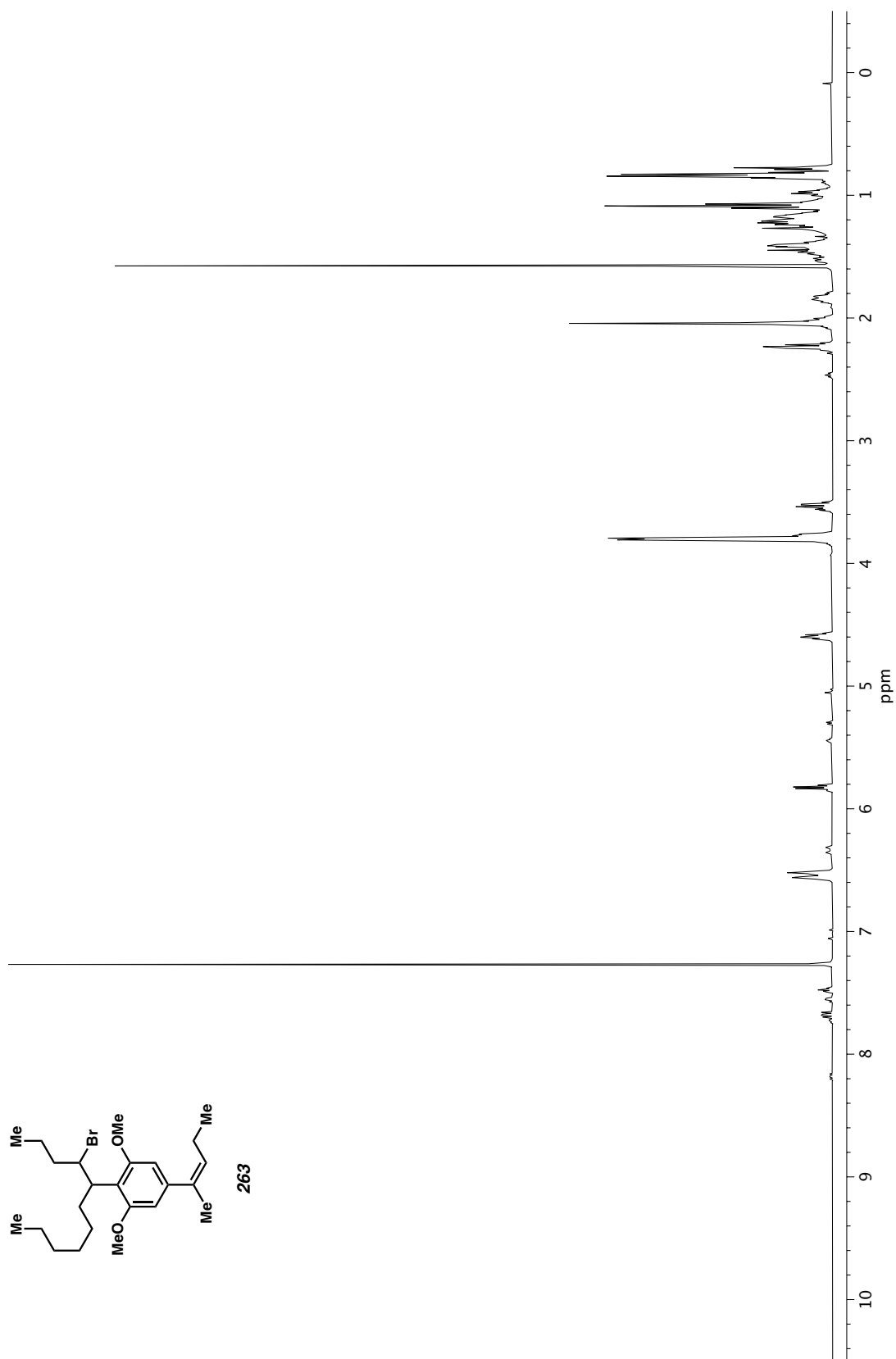
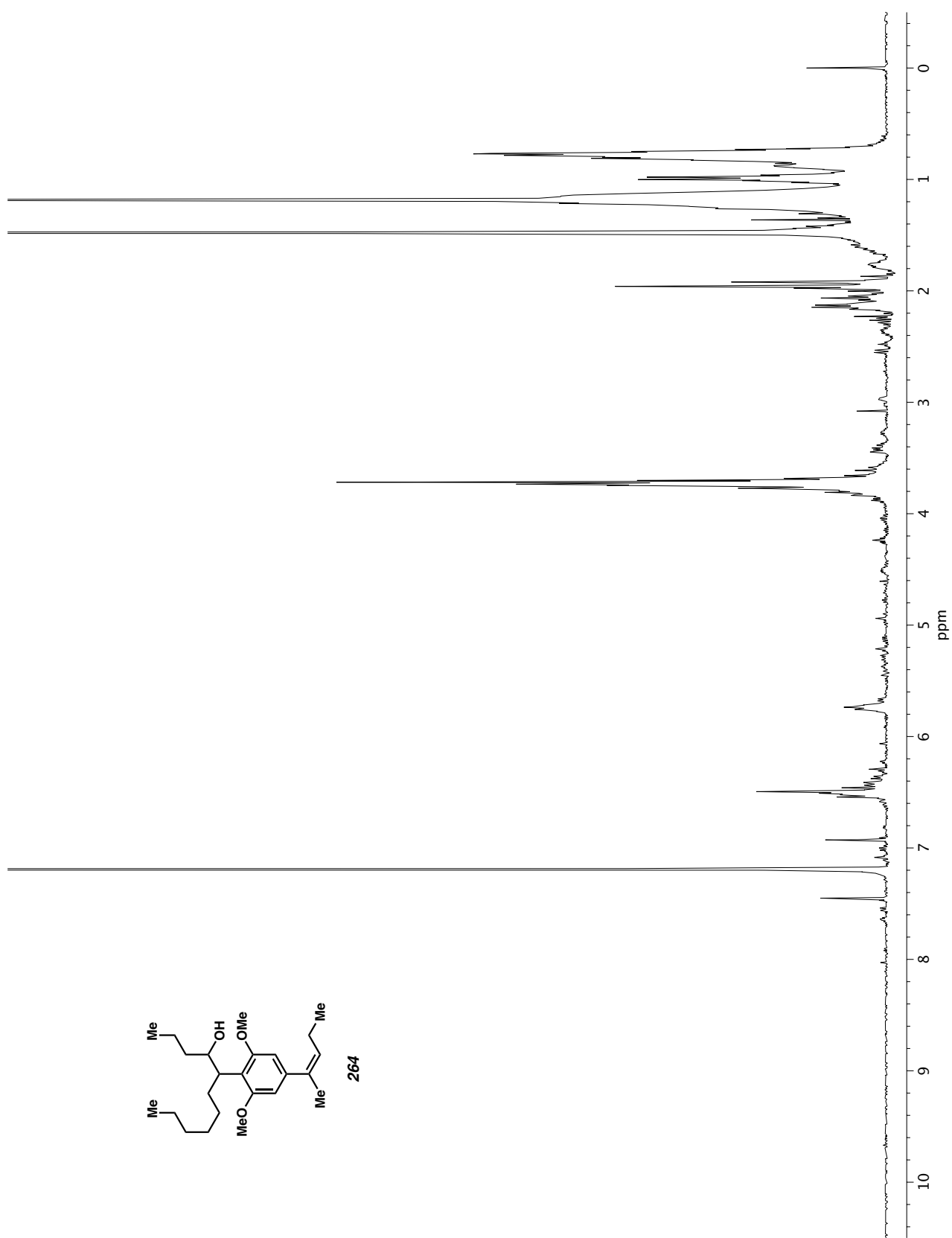


Figure A7.102  $^1\text{H}$  NMR (400 MHz,  $\text{CDCl}_3$ ) of compound **263**.



**Figure A7.103**  $^1\text{H}$  NMR (400 MHz,  $\text{CDCl}_3$ ) of compound **264**.

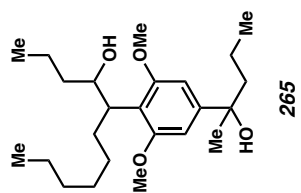
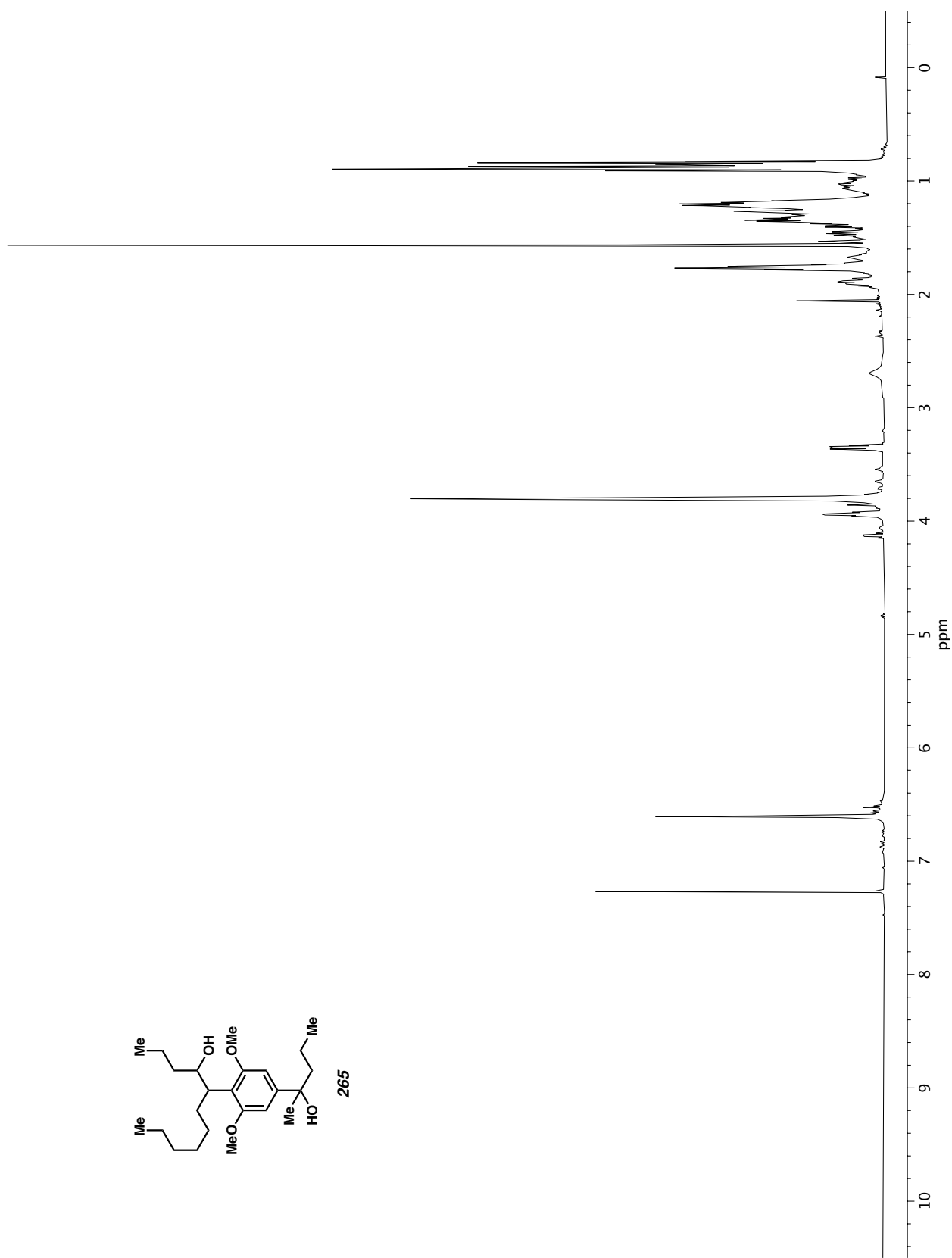
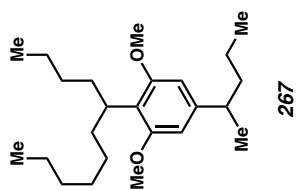
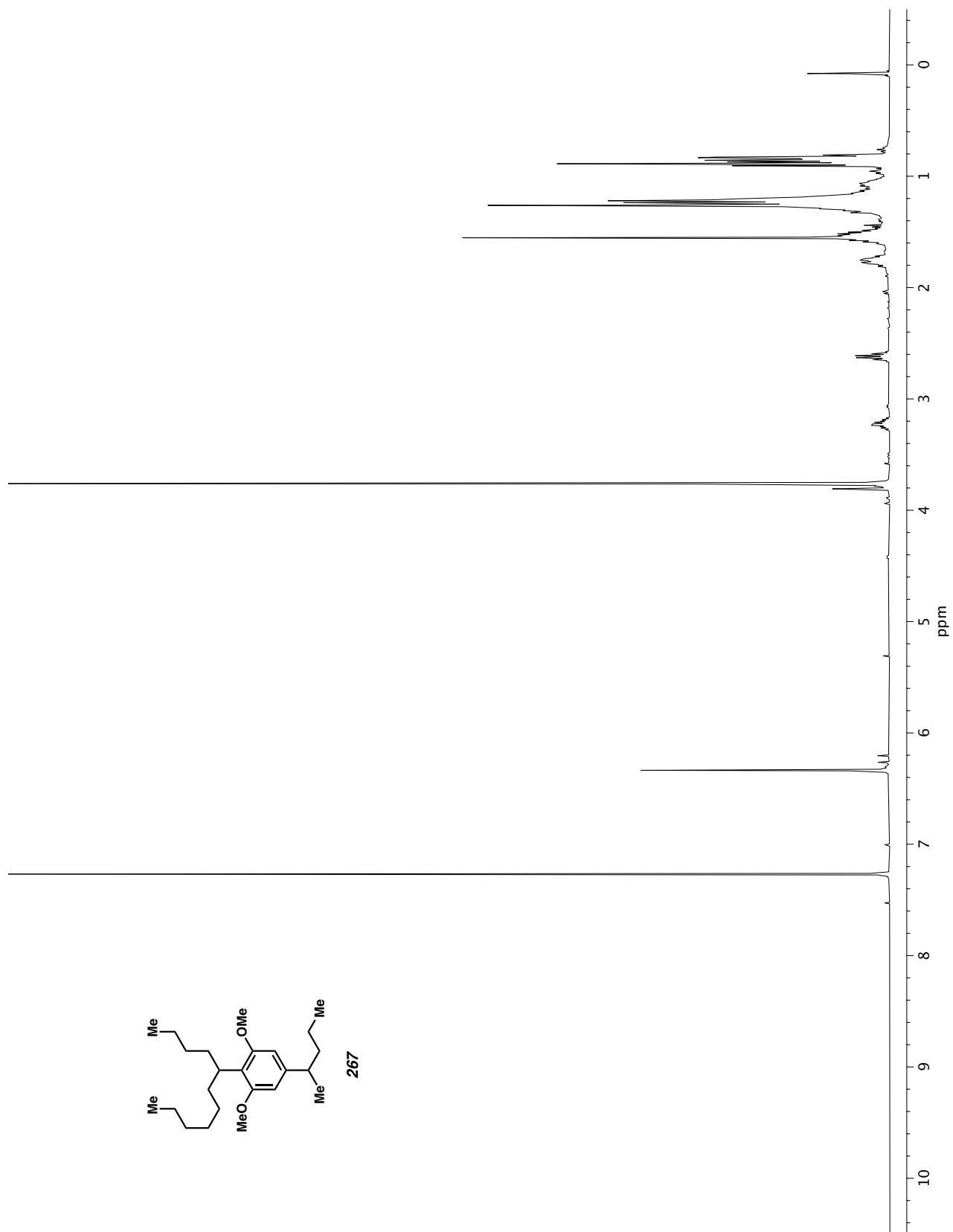


Figure A7.104 <sup>1</sup>H NMR (400 MHz, CDCl<sub>3</sub>) of compound 265.



**Figure A7.105** <sup>1</sup>H NMR (400 MHz, CDCl<sub>3</sub>) of compound **267**.



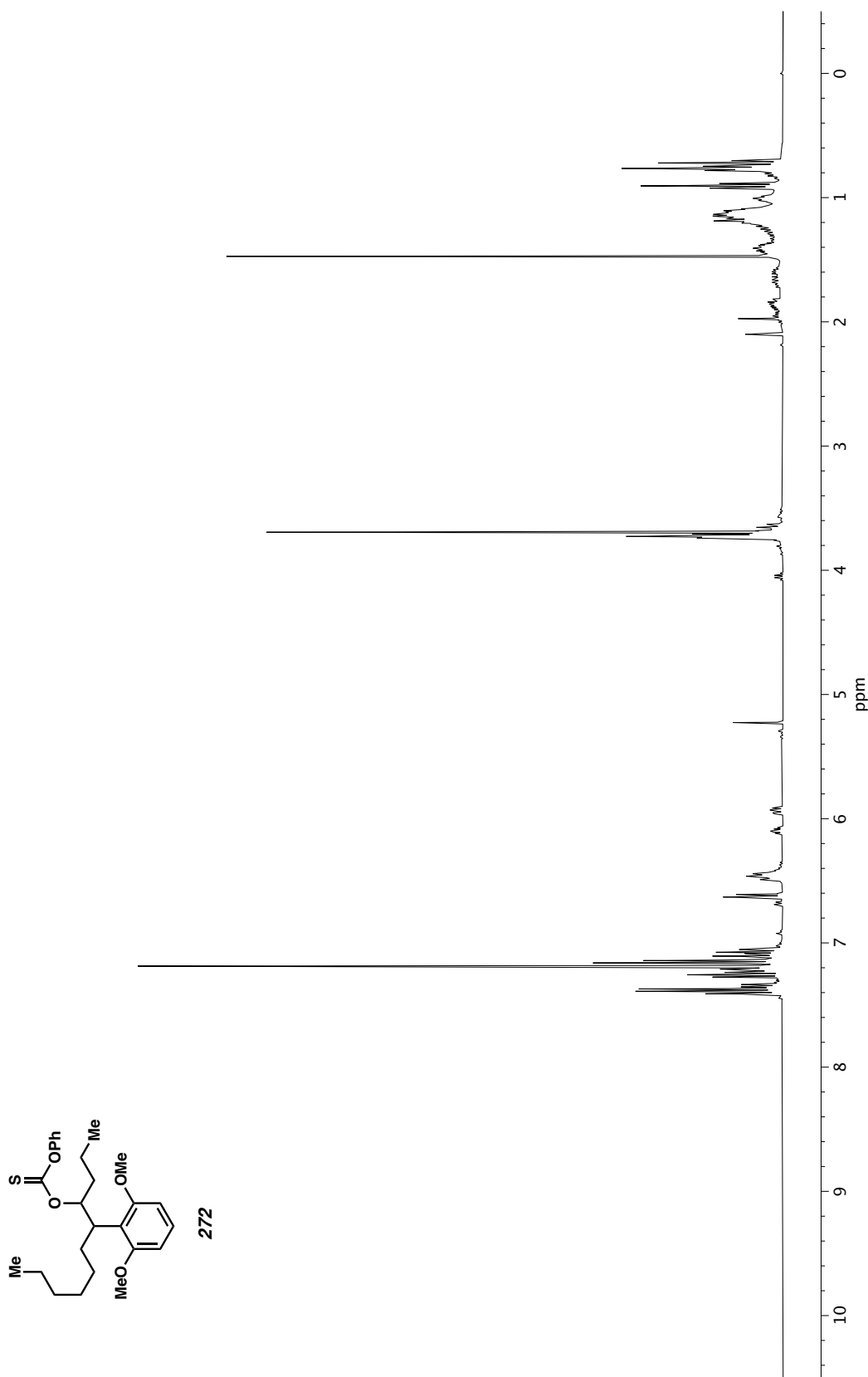


Figure A7.106 <sup>1</sup>H NMR (400 MHz, CDCl<sub>3</sub>) of compound 272.

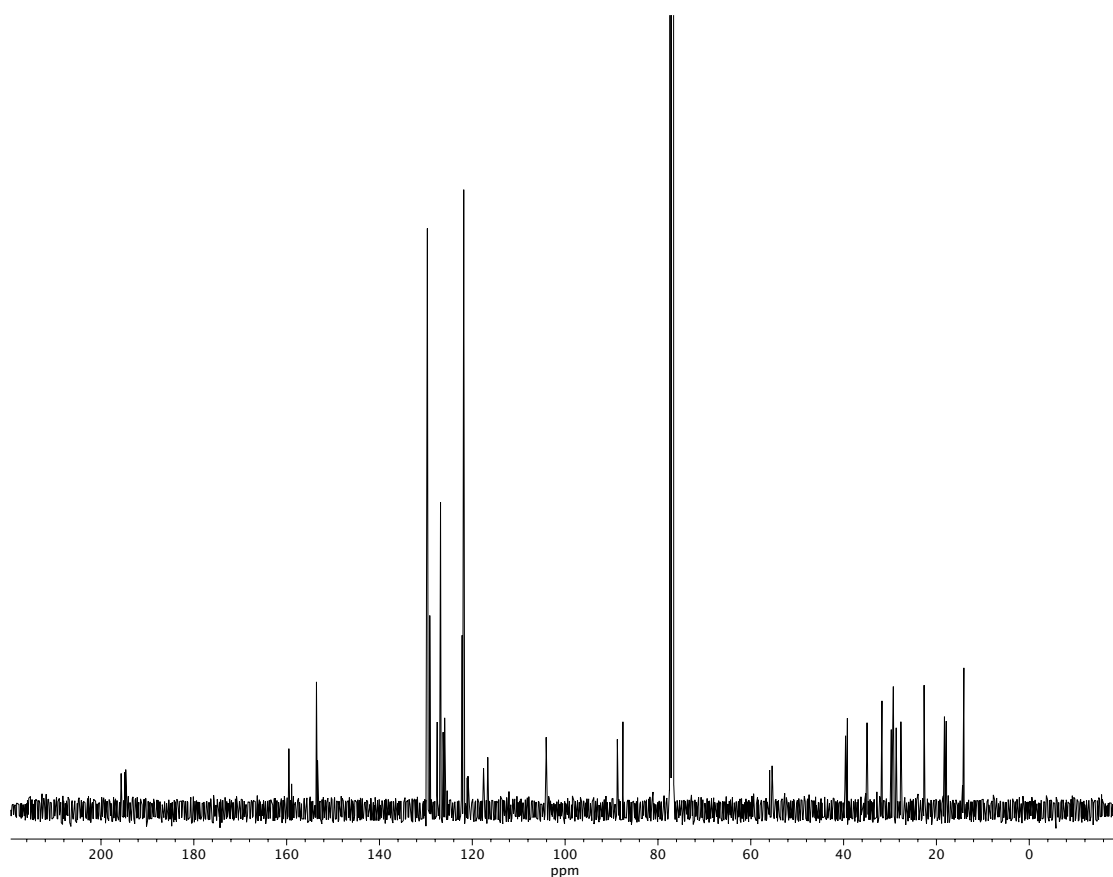


Figure A7.107  $^{13}\text{C}$  NMR (100 MHz,  $\text{CDCl}_3$ ) of compound 272.

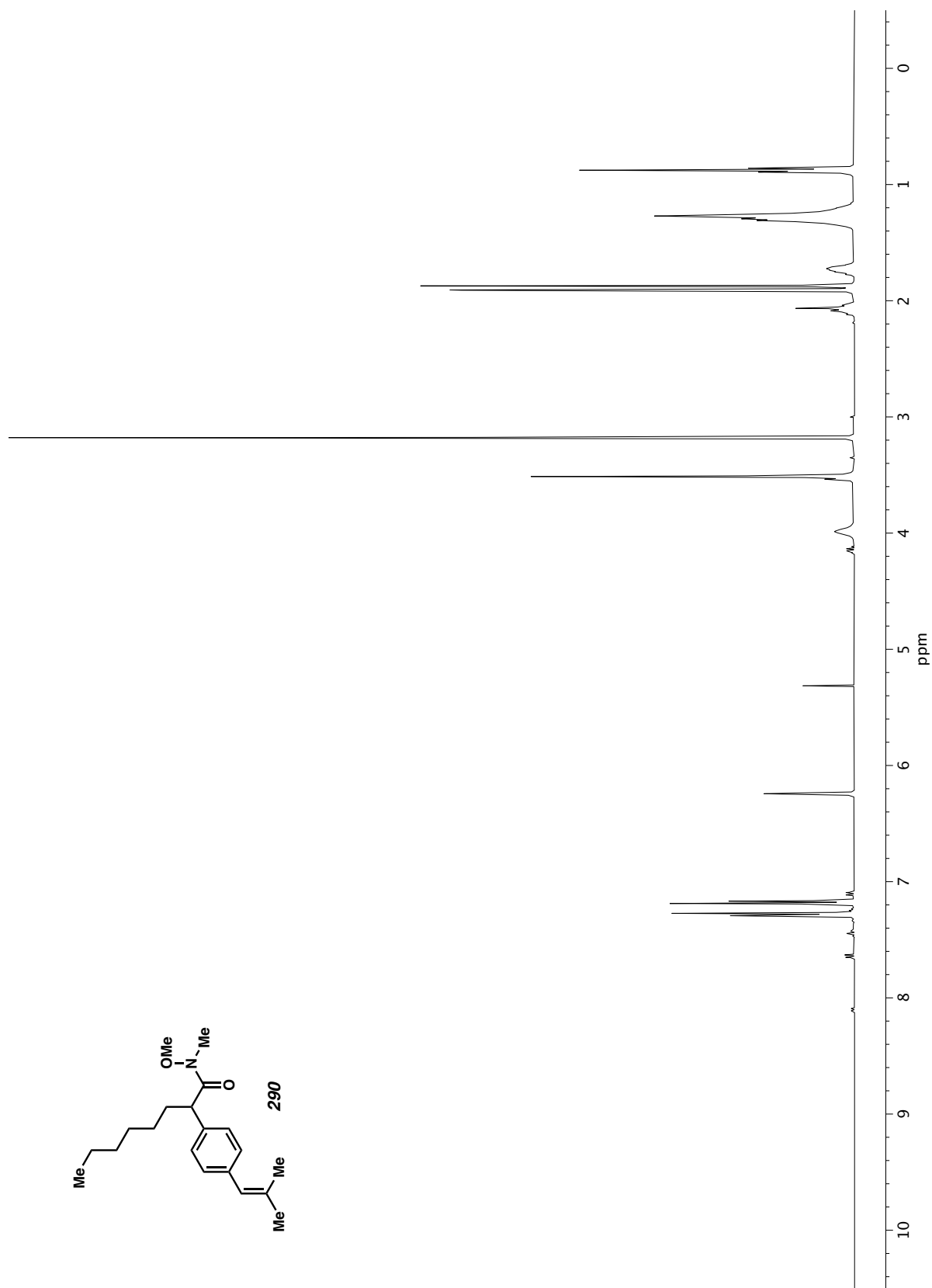


Figure A7.108  $^1\text{H}$  NMR (400 MHz,  $\text{CDCl}_3$ ) of compound 290.

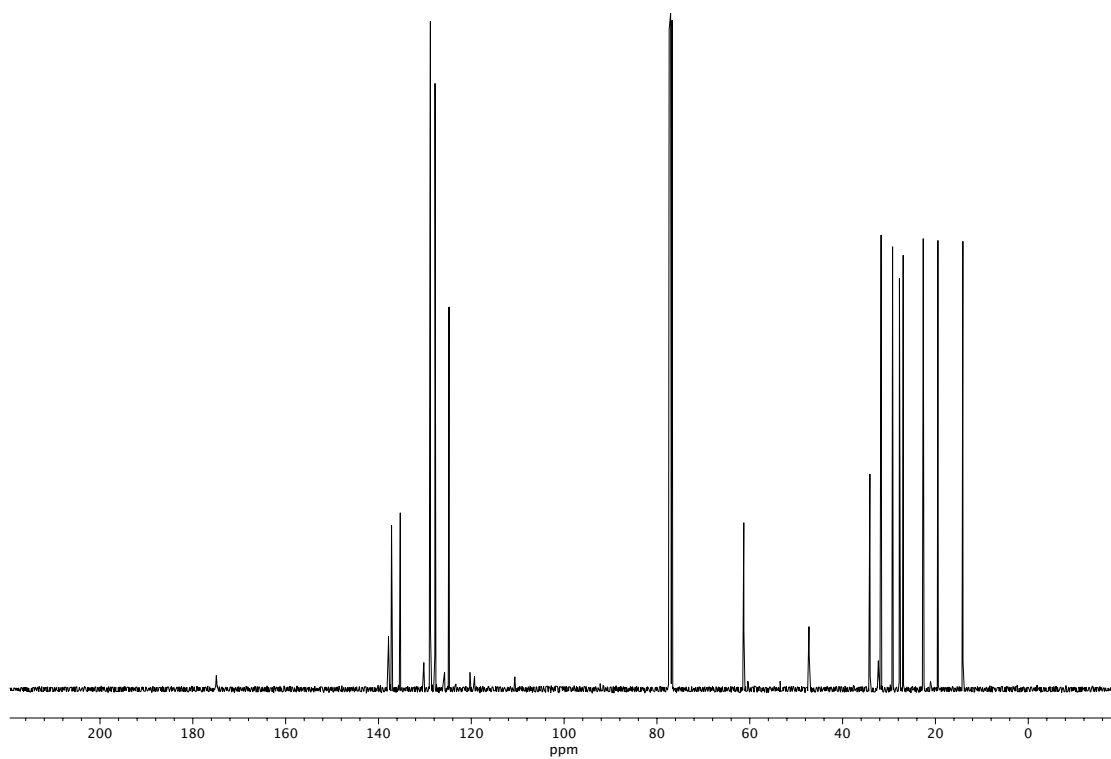


Figure A7.109  $^{13}\text{C}$  NMR (100 MHz,  $\text{CDCl}_3$ ) of compound 290.

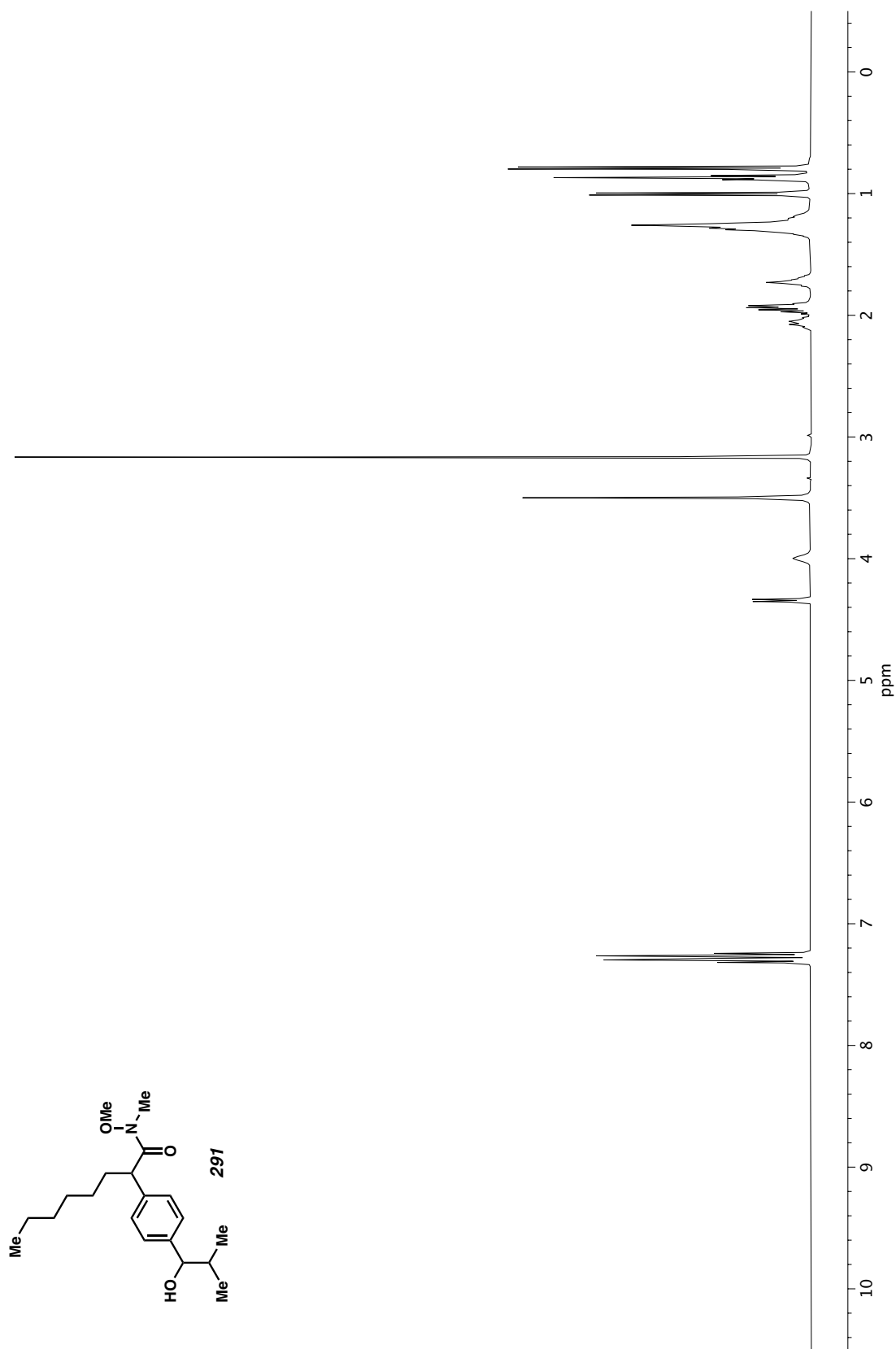


Figure A7.110 <sup>1</sup>H NMR (400 MHz, CDCl<sub>3</sub>) of compound 291.

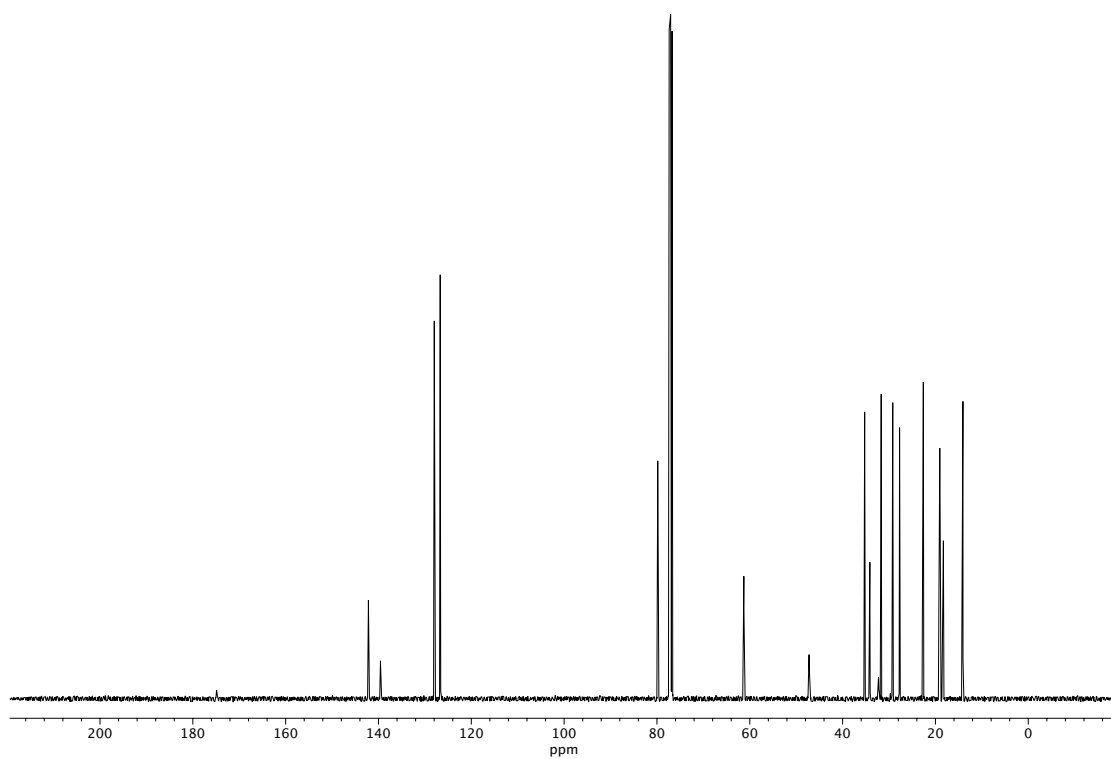


Figure A7.111  $^{13}\text{C}$  NMR (100 MHz,  $\text{CDCl}_3$ ) of compound **291**.

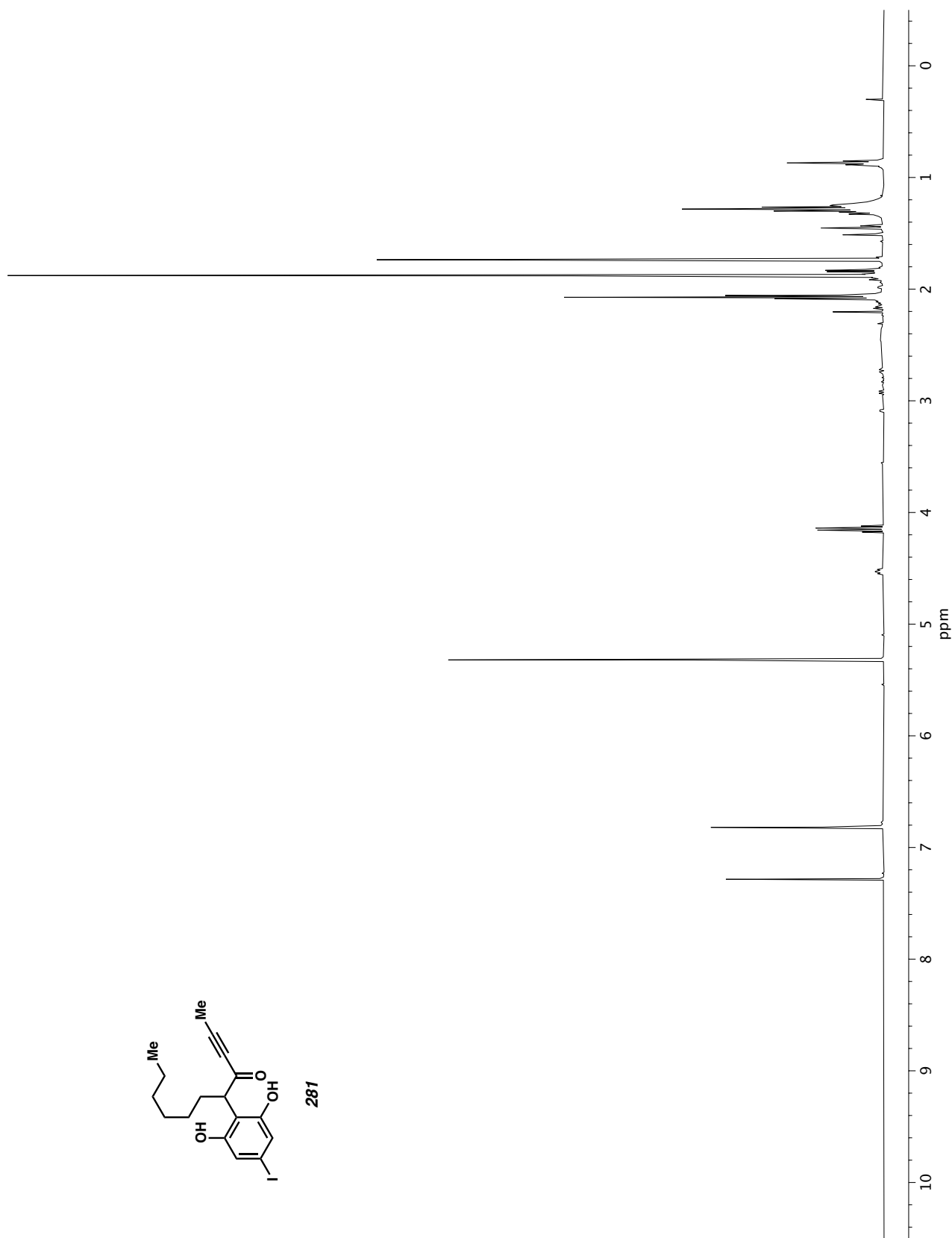


Figure A7.112 <sup>1</sup>H NMR (400 MHz, CDCl<sub>3</sub>) of compound 281.

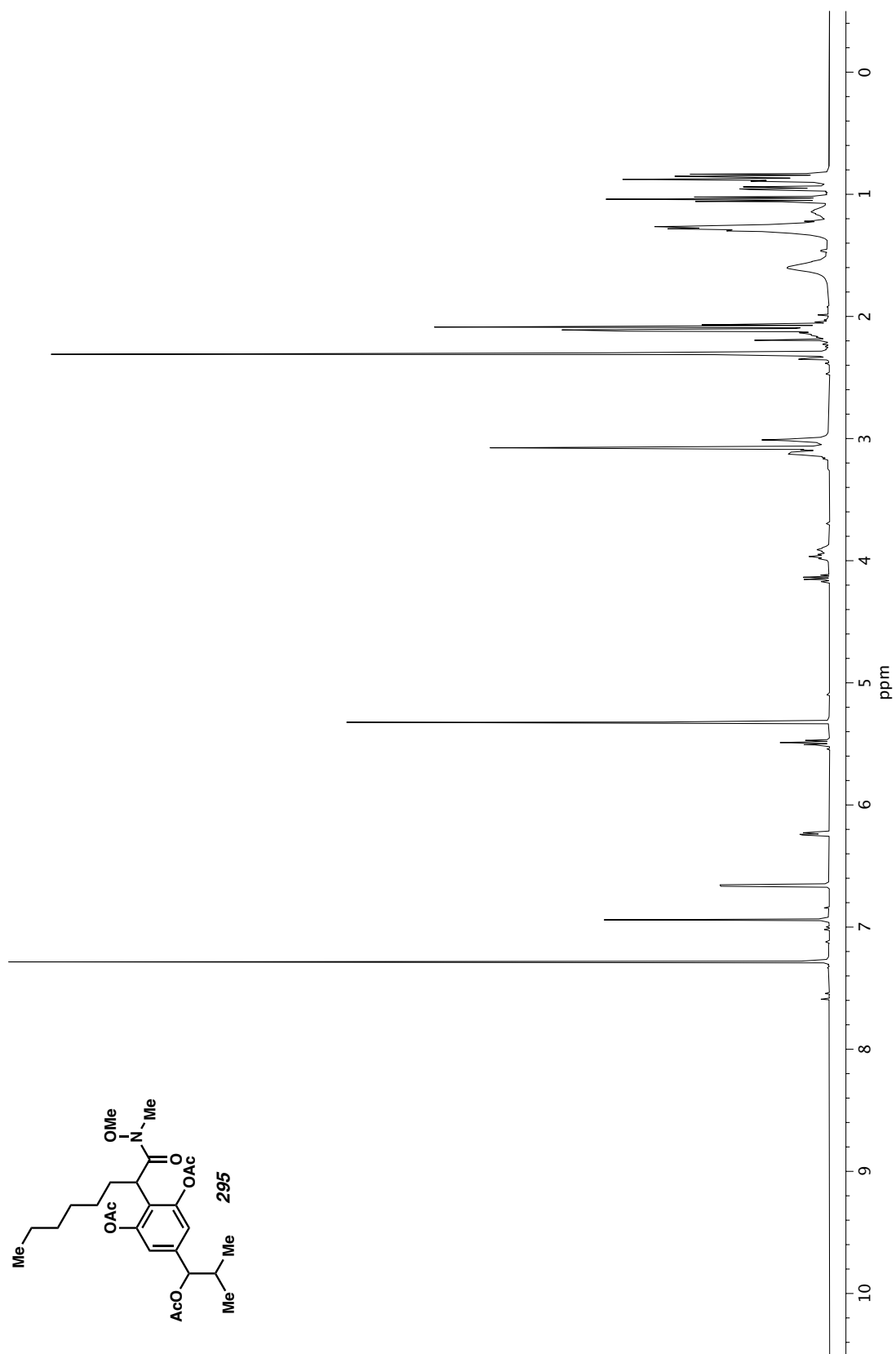
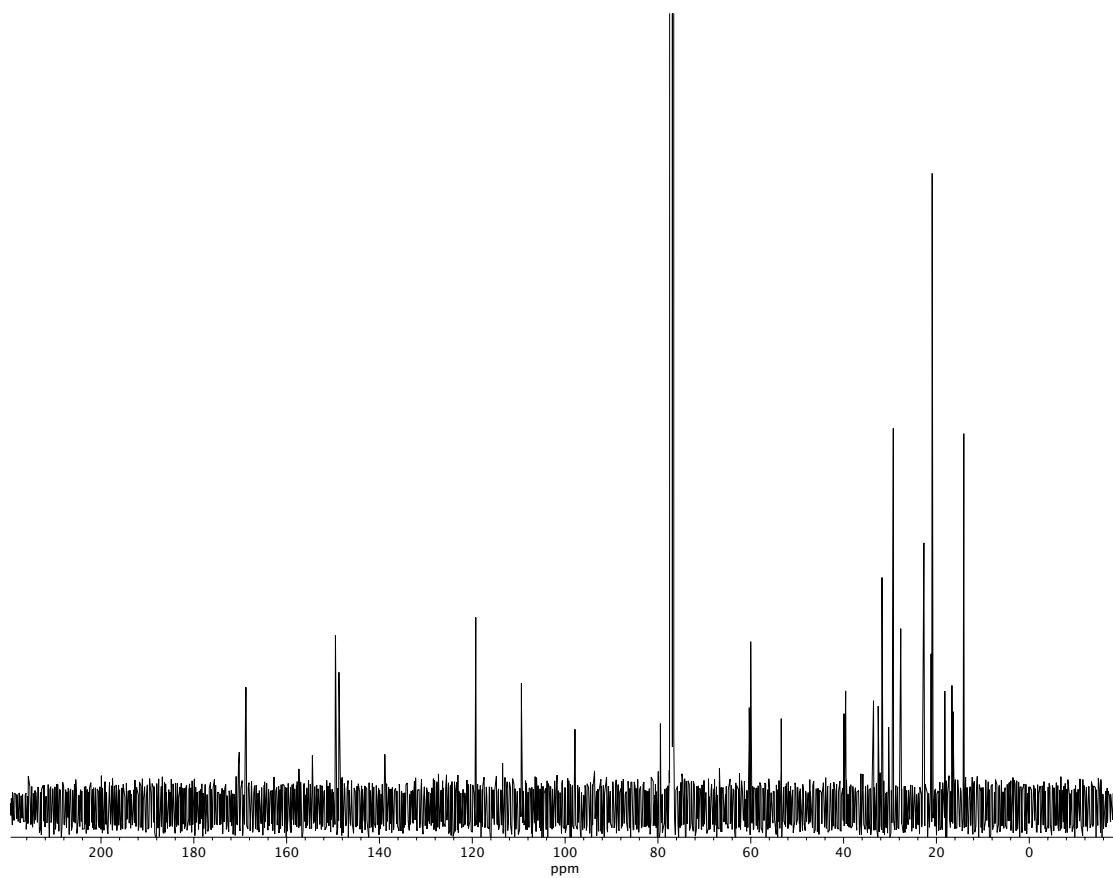


Figure A7.113  $^1\text{H}$  NMR (400 MHz,  $\text{CDCl}_3$ ) of compound 295.





**Figure A7.114**  $^{13}\text{C}$  NMR (100 MHz,  $\text{CDCl}_3$ ) of compound 295.

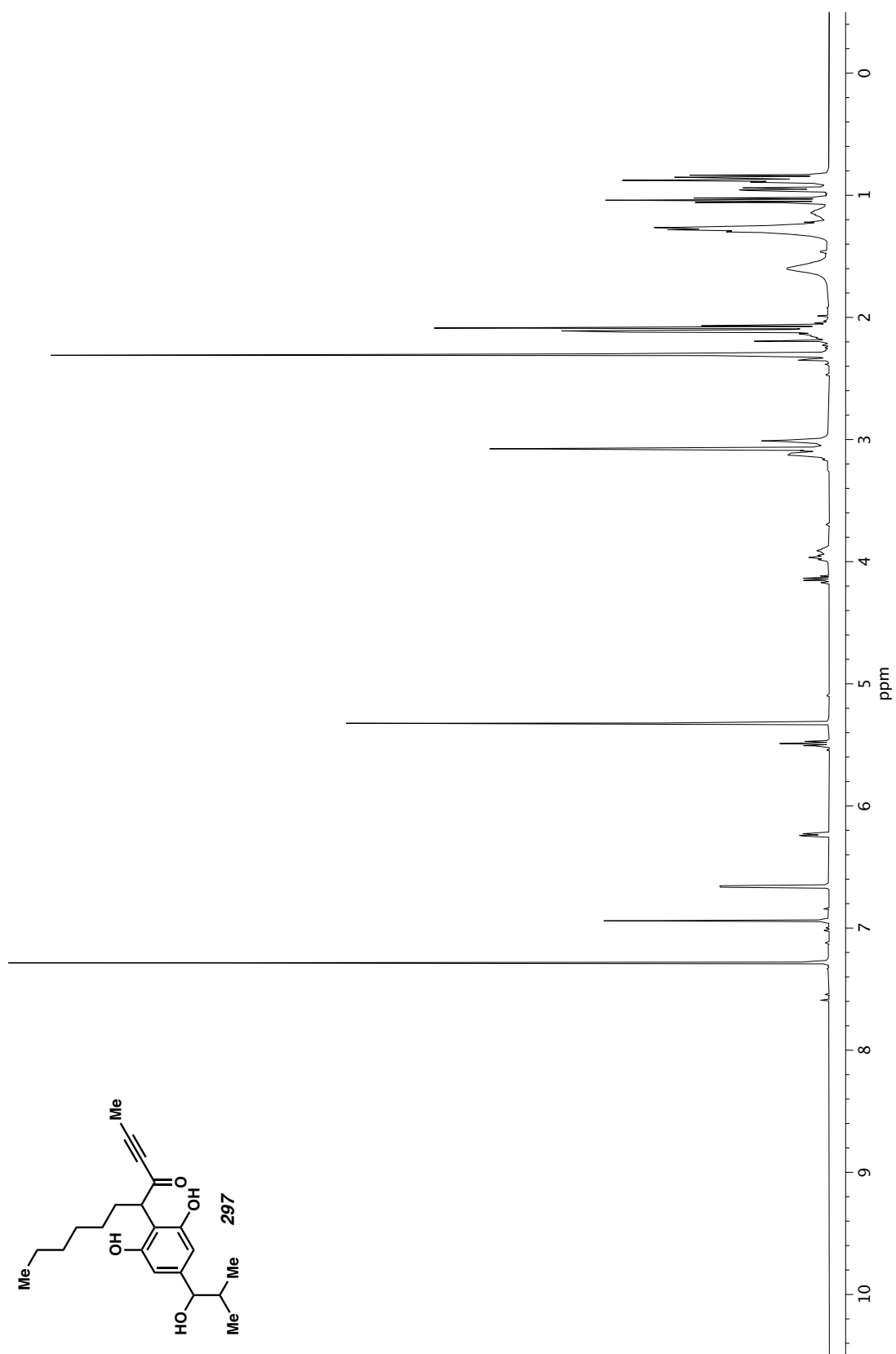


Figure A7.115  $^1\text{H}$  NMR (400 MHz,  $\text{CDCl}_3$ ) of compound 297.

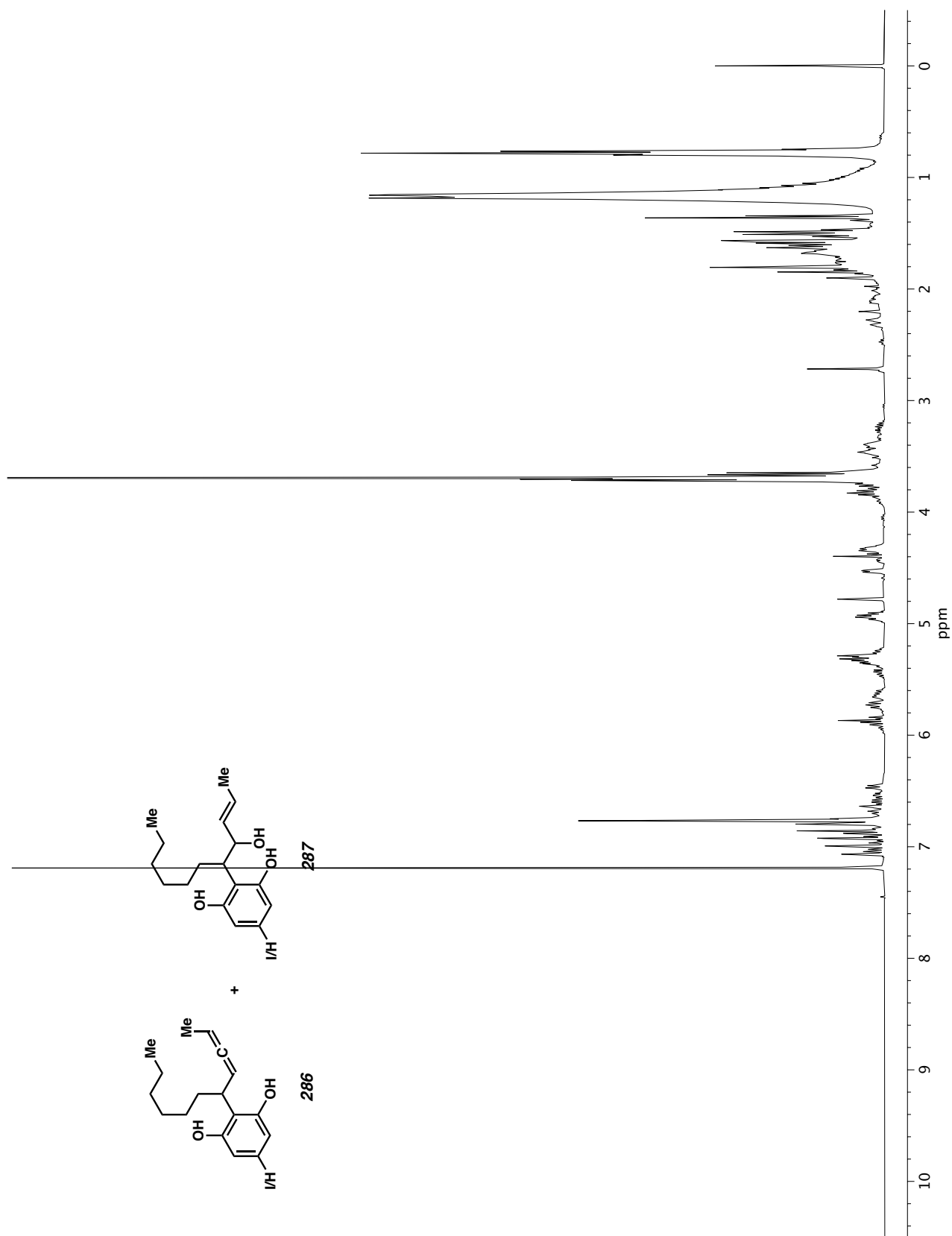
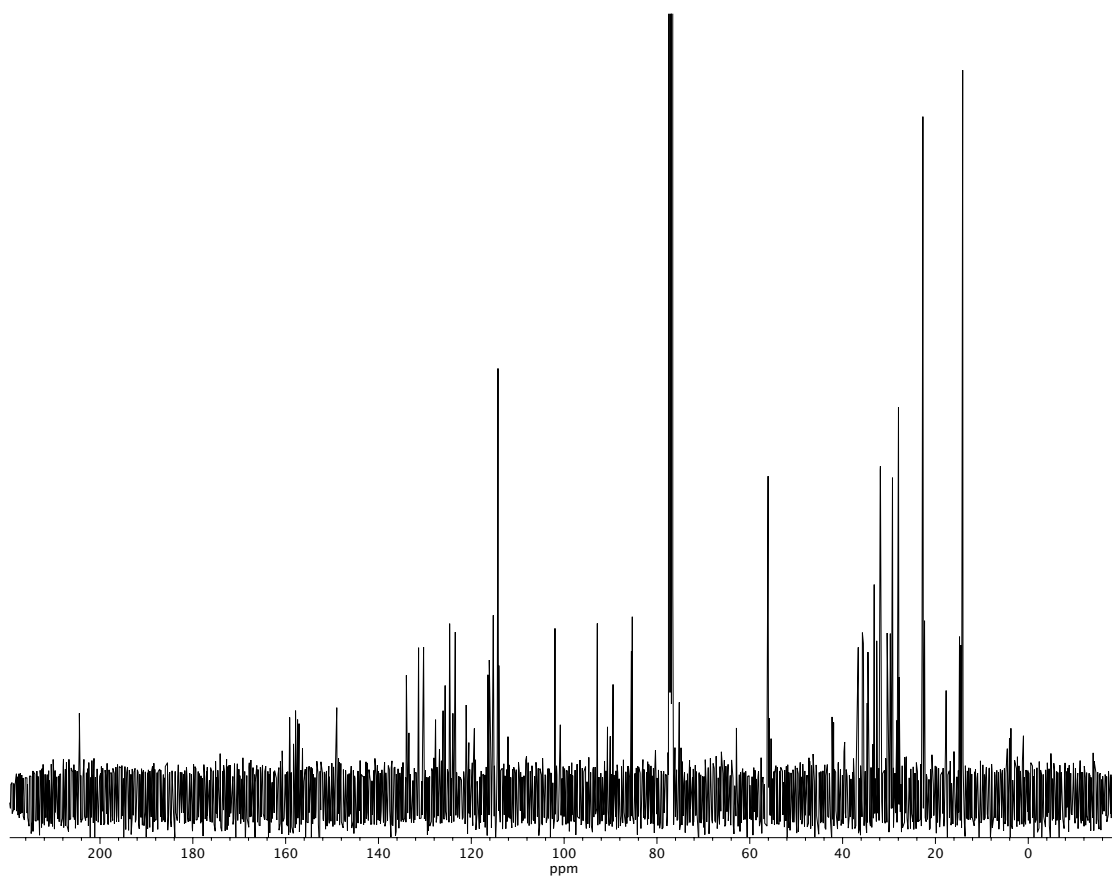


Figure A7.116 <sup>1</sup>H NMR (400 MHz, CDCl<sub>3</sub>) of compound 286/287.



**Figure A7.117**  $^{13}\text{C}$  NMR (100 MHz,  $\text{CDCl}_3$ ) of compound **286/287**.

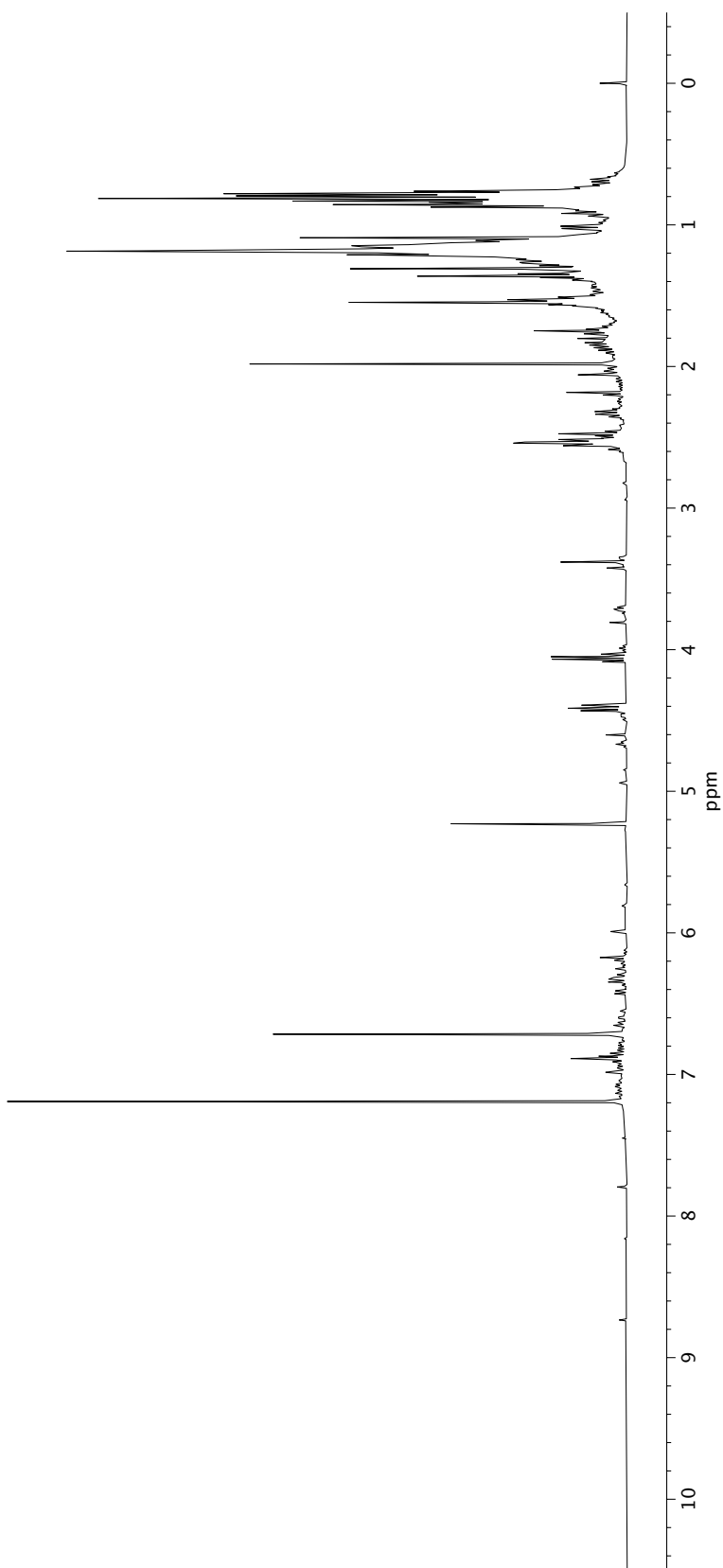
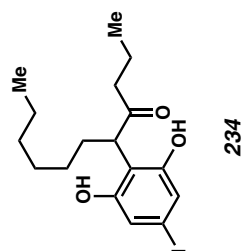
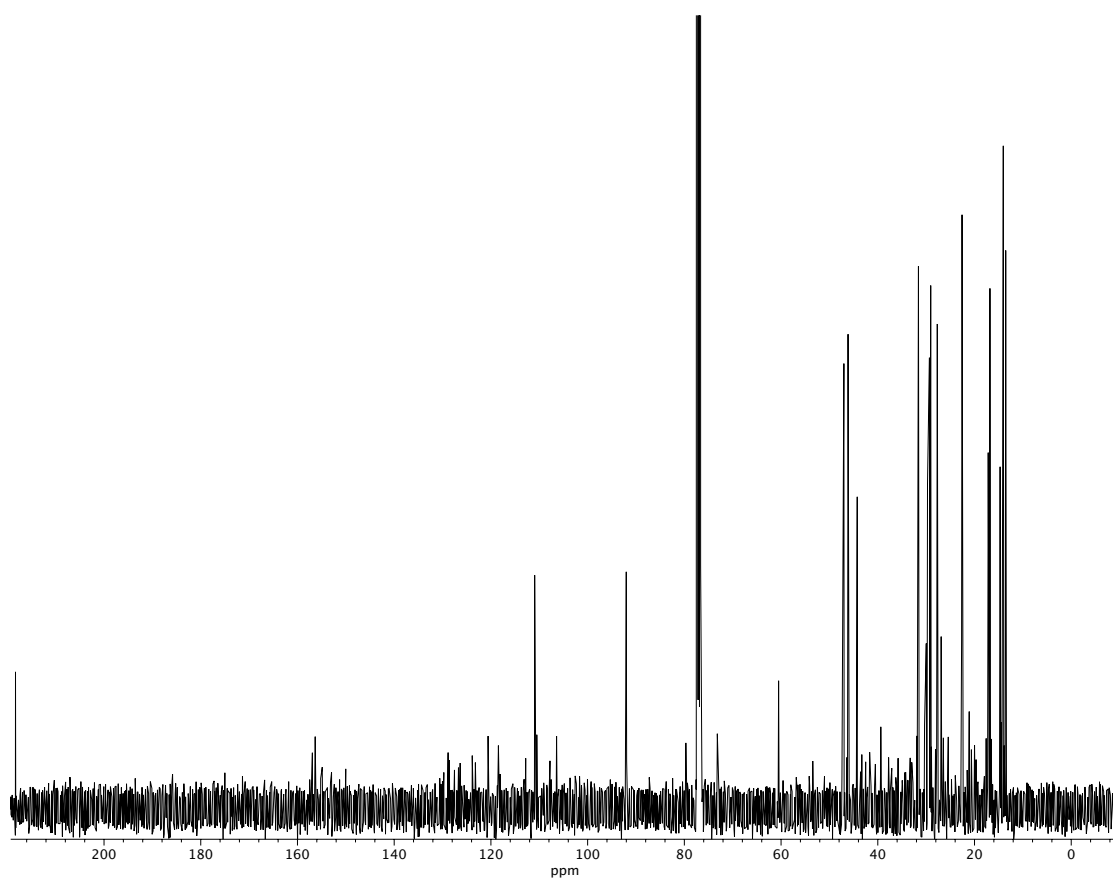


Figure A7.118 <sup>1</sup>H NMR (400 MHz, CDCl<sub>3</sub>) of compound 234.

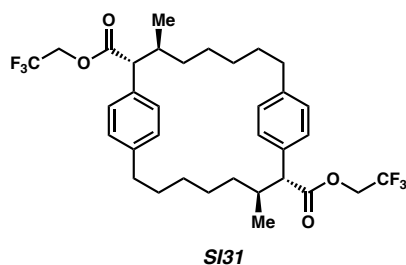


**Figure A7.119**  $^{13}\text{C}$  NMR (100 MHz,  $\text{CDCl}_3$ ) of compound **234**.

## **APPENDIX 8**

*X-Ray Crystallography Reports Relevant to Appendix 6:*

*The Total Synthesis of (–)-Cylindrocyclophane A*

**A8.1 X-RAY CRYSTAL STRUCTURE ANALYSIS OF MACROCYCLE SI31**Contents

*Table A8.1.1. Experimental Details*

*Table A8.1.2. Crystal Data*

*Table A8.1.3. Reflection Statistics*

*Table A8.1.4. Atomic Coordinates*

*Table A8.1.5. Bond Lengths and Angles*

*Table A8.1.6. Anisotropic Displacement Parameters*

*Table A8.1.7. Hydrogen Atomic Coordinates*

*Table A8.1.8. Bond Angles*

*Table A8.1.9. Torsion Angles*



**Figure A8.1.1** X-Ray Crystal Structure of Macrocycle **SI31**.

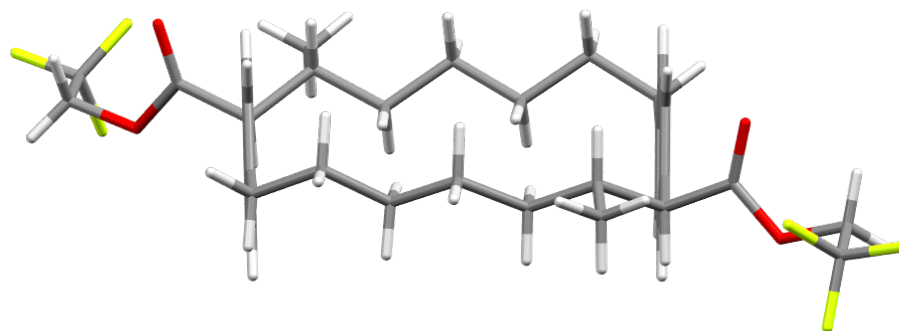


**Table A8.1.1** *Experimental Details for X-Ray Structure Determination of Macrocycle SI31.*

Single colorless needle-shaped crystals of macrocycle **SI31** were recrystallized from hexane by slow evaporation. A suitable crystal  $0.57 \times 0.06 \times 0.04 \text{ mm}^3$  was selected and mounted on a loop on a XtaLAB Synergy, Dualflex, HyPix diffractometer. The crystal was kept at a steady  $T = 100(2) \text{ K}$  during data collection. The structure was solved with the **ShelXT** (Sheldrick, 2015) structure solution program using the Intrinsic Phasing solution method and by using **Olex2** (Dolomanov et al., 2009) as the graphical interface. The model was refined with version 2018/3 of **ShelXL** (Sheldrick, 2015) using Least Squares minimisation.  $\text{C}_{34}\text{H}_{42}\text{F}_6\text{O}_4$ ,  $M_r = 628.67$ , monoclinic,  $P2$  (No. 3),  $a = 25.1525(4) \text{ \AA}$ ,  $b = 5.53398(4) \text{ \AA}$ ,  $c = 27.2474(4) \text{ \AA}$ ,  $\beta = 117.4652(19)^\circ$ ,  $\alpha = \gamma = 90^\circ$ ,  $V = 3365.19(9) \text{ \AA}^3$ ,  $T = 100(2) \text{ K}$ ,  $Z = 4$ ,  $Z' = 2$ ,  $\mu(\text{CuK}\alpha) = 0.866 \text{ mm}^{-1}$ , 42058 reflections measured, 10947 unique ( $R_{int} = 0.0510$ ) which were used in all calculations. The final  $wR_2$  was 0.0885 (all data) and  $R_I$  was 0.0363 ( $I > 2\sigma(I)$ ).

**Table A8.1.2** Crystal Data and Structure Refinement for Macrocycle **SI31**

Compound	Macrocycle SI31
Formula	C <sub>34</sub> H <sub>42</sub> F <sub>6</sub> O <sub>4</sub>
<i>D</i> <sub>calc.</sub> / g cm <sup>-3</sup>	1.241
$\mu$ /mm <sup>-1</sup>	0.866
Formula Weight	628.67
Colour	colourless
Shape	needle
Size/mm <sup>3</sup>	0.57×0.06×0.04
<i>T</i> /K	100(2)
Crystal System	monoclinic
Flack Parameter	-0.02(6)
Hooft Parameter	-0.00(5)
Space Group	<i>P</i> 2
<i>a</i> /Å	25.1525(4)
<i>b</i> /Å	5.53398(4)
<i>c</i> /Å	27.2474(4)
$\alpha$ /°	90
$\beta$ /°	117.4652(19)
$\gamma$ /°	90
<i>V</i> /Å <sup>3</sup>	3365.19(9)
<i>Z</i>	4
<i>Z</i> '	2
Wavelength/Å	1.54184
Radiation type	CuK $\alpha$
$\theta$ <sub>min</sub> /°	1.980
$\theta$ <sub>max</sub> /°	73.814
Measured Refl.	42058
Independent Refl.	10947
Reflections with <i>I</i> > 2 $\sigma$ ( <i>I</i> )	9975
<i>R</i> <sub>int</sub>	0.0510
Parameters	797
Restraints	1
Largest Peak	0.323
Deepest Hole	-0.205
Goof	0.985
<i>wR</i> <sub>2</sub> (all data)	0.0885
<i>wR</i> <sub>2</sub>	0.0853
<i>R</i> <sub>1</sub> (all data)	0.0412
<i>R</i> <sub>1</sub>	0.0363

**Structure Quality Indicators****Reflections:** d min (Cu) 0.80 |  $I/\sigma$  23.6 | Rint 5.10%**Refinement:** Shift -0.008 | Max Peak 0.3 | Min Peak -0.2 | GooF 0.985 | Flack -.02(6)

A colourless needle-shaped crystal with dimensions  $0.57 \times 0.06 \times 0.04 \text{ mm}^3$  was mounted on a loop. Data were collected using an XtaLAB Synergy, Dualflex, HyPix diffractometer equipped with an Oxford Cryosystems low-temperature device operating at  $T = 100(2) \text{ K}$ . Data were measured using  $\omega$  scans with a narrow frame width of  $0.5^\circ$  per frame for 3.5/3.7/10.0 s using  $\text{CuK}\alpha$  radiation. The total number of runs and images was based on the strategy calculation from the program CrysAlisPro (Rigaku, V1.171.39.43c, 2018). The maximum resolution that was achieved was  $\theta = 73.814^\circ$ .

The diffraction pattern was indexed using CrysAlisPro (Rigaku, V1.171.39.43c, 2018) and the unit cell was refined using CrysAlisPro (Rigaku, V1.171.39.43c, 2018) on 24772 reflections, 59% of the observed reflections.

Data reduction, scaling and absorption corrections were performed using CrysAlisPro (Rigaku, V1.171.39.43c, 2018). The final completeness is 98.70 % out to  $73.814^\circ$  in  $\theta$ . A numerical absorption correction based on Gaussian integration over a multifaceted crystal model was applied using CrysAlisPro 1.171.39.43c (Rigaku Oxford Diffraction, 2018). An empirical absorption correction using spherical harmonics as implemented by SCALE3 ABSPACK algorithm was applied. The absorption coefficient  $\mu$  of this material is  $0.866 \text{ mm}^{-1}$  at this wavelength ( $\lambda = 1.54184 \text{ \AA}$ ) and the minimum and maximum transmissions are 0.487 and 1.000.

The structure was solved and the space group  $P2$  (# 3) determined by the ShelXT (Sheldrick, 2015) structure solution program using Intrinsic Phasing and refined by Least

Squares using version 2018/3 of ShelXL-2014 (Sheldrick, 2015). All non-hydrogen atoms were refined anisotropically. Hydrogen atom positions were calculated geometrically and refined using the riding model. Hydrogen atom positions were calculated geometrically and refined using the riding model.

The value of  $Z'$  is 2. This means that there are two independent molecules in the asymmetric unit.

The Flack parameter was refined to -0.02(6). Determination of absolute structure using Bayesian statistics on Bijvoet differences using the Olex2 results in -0.00(5). Note: The Flack parameter is used to determine chirality of the crystal studied, the value should be near 0, a value of 1 means that the stereochemistry is wrong and the model should be inverted. A value of 0.5 means that the crystal consists of a racemic mixture of the two enantiomers.

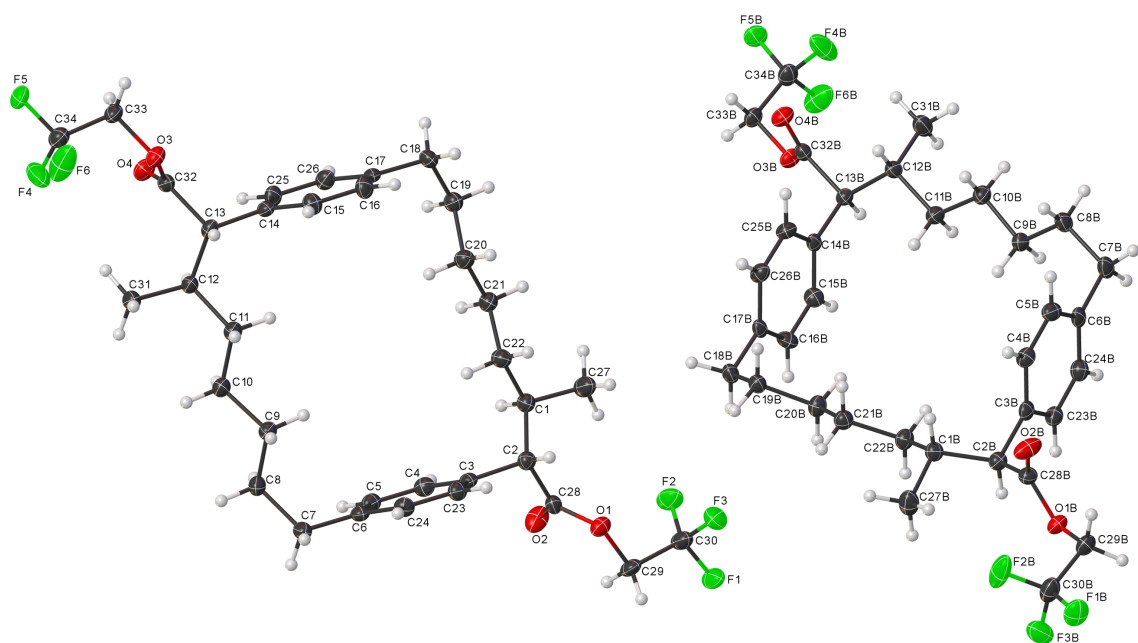


**Figure A8.1.2** The asymmetric unit contains two molecules of the compound.

**Table A8.1.3** Reflection Statistics

Total reflections (after filtering)	42062	Unique reflections	10947
Completeness	0.804	Mean $I/\sigma$	16.19
$hkl_{\max}$ collected	(30, 6, 33)	$hkl_{\min}$ collected	(-30, -6, -33)
$hkl_{\max}$ used	(27, 6, 33)	$hkl_{\min}$ used	(-30, -6, 0)
Lim $d_{\max}$ collected	100.0	Lim $d_{\min}$ collected	0.77
$d_{\max}$ used	22.32	$d_{\min}$ used	0.8
Friedel pairs	5250	Friedel pairs merged	0
Inconsistent equivalents	10	$R_{\text{int}}$	0.051
$R_{\text{sigma}}$	0.0423	Intensity transformed	0
Omitted reflections	0	Omitted by user (OMIT hkl)	4
Multiplicity	(6310, 4911, 3058, 1507, 1006, 519, 204, 88, 40, 7, 2)	Maximum multiplicity	18
Removed systematic absences	0	Filtered off (Shel/OMIT)	0

**Table A8.1.4** Fractional Atomic Coordinates ( $\times 10^4$ ) and Equivalent Isotropic Displacement Parameters ( $\text{\AA}^2 \times 10^3$ ) for Macrocycle **SI31**.  $U_{eq}$  is defined as 1/3 of the trace of the orthogonalised  $U_{ij}$ .

Atom	x	y	z	$U_{eq}$
F1	3107.8(7)	-1535(3)	3482.8(6)	40.3(4)
F2	2927.5(7)	-699(4)	4163.9(7)	43.1(5)
F3	3029.6(8)	2168(3)	3682.3(7)	44.3(5)
F4	6931.1(8)	10422(4)	11116.2(8)	54.0(5)
F5	6790.1(7)	13309(3)	11567.5(6)	34.1(4)
F6	7051.5(9)	14083(5)	10937.5(8)	63.2(7)
O1	4027.6(8)	1790(3)	4704.1(7)	24.9(4)
O2	4161.9(10)	-1186(3)	5309.5(8)	34.6(5)
O3	6006.0(8)	12270(3)	10110.3(7)	24.8(4)
O4	5755.0(8)	8401(3)	10163.3(7)	26.6(4)
C1	3780.7(11)	2906(5)	5830.5(10)	22.6(5)
C2	4251.8(11)	2953(5)	5616.8(10)	21.2(5)
C3	4891.6(11)	2815(5)	6079.4(10)	19.9(5)
C4	5096.8(12)	917(5)	6458.4(10)	23.7(6)
C5	5675.7(12)	905(5)	6887.6(10)	24.0(6)
C6	6074.6(11)	2778(5)	6953.4(10)	21.4(5)
C7	6704.0(11)	2795(5)	7419.2(10)	27.1(6)
C8	6739.8(12)	2951(5)	7994.2(10)	27.6(6)
C9	6465.4(12)	5221(5)	8095.4(10)	23.7(6)
C10	6516.9(12)	5313(5)	8675.3(10)	24.1(5)
C11	6212.8(12)	7497(5)	8772.7(10)	24.6(6)
C12	6209.5(11)	7575(5)	9334.4(9)	21.0(5)
C13	5839.4(11)	9758(5)	9353.0(10)	20.3(5)
C14	5191.4(11)	9689(5)	8912.1(10)	20.0(5)
C15	4964.7(12)	11456(5)	8505.7(11)	25.0(6)
C16	4377.1(12)	11353(5)	8087.6(11)	26.2(6)
C17	3996.1(11)	9483(5)	8059.1(10)	20.1(5)
C18	3362.9(11)	9314(5)	7599.5(10)	23.9(6)
C19	3252.2(12)	7142(5)	7217.6(11)	25.3(6)
C20	3625.5(12)	7131(5)	6911.5(11)	26.0(6)
C21	3517.0(12)	4965(5)	6538.5(11)	25.0(6)
C22	3874.2(12)	5034(5)	6215.9(11)	24.8(6)
C23	5287.2(11)	4679(5)	6142.9(10)	22.6(5)
C24	5865.8(12)	4667(5)	6573.4(10)	23.7(5)
C25	4809.6(11)	7819(5)	8889.4(10)	23.6(5)
C26	4225.4(11)	7726(5)	8470.6(10)	23.9(5)
C27	3147.2(12)	2864(6)	5349.5(11)	35.0(7)
C28	4147.1(11)	936(5)	5211.2(10)	21.4(5)
C29	3900.7(12)	18(5)	4278.4(10)	26.0(6)
C30	3240.7(12)	-13(6)	3906.9(11)	32.9(7)
C31	6844.6(11)	7687(6)	9811.7(10)	31.4(6)
C32	5860.6(11)	9970(5)	9917.2(10)	20.3(5)
C33	6063.6(11)	12761(5)	10649.8(10)	24.3(5)
C34	6708.7(12)	12639(5)	11063.1(11)	29.0(6)



Atom	x	y	z	$U_{eq}$
F1B	1848.2(8)	11712(3)	49.8(7)	39.7(4)
F2B	2053.5(8)	10844(4)	890.5(7)	53.2(6)
F3B	1882.0(8)	7990(3)	307.4(7)	43.7(4)
F4B	-2001.3(8)	-248(4)	4376.9(8)	50.5(5)
F5B	-1810.7(7)	-2763(3)	5035.6(6)	32.3(4)
F6B	-1985.5(8)	-4054(4)	4231.7(8)	51.2(5)
O1B	934.2(8)	8649(3)	534.8(7)	23.6(4)
O2B	917.9(10)	11669(3)	1080.3(8)	33.4(5)
O3B	-990.6(8)	-1732(3)	4282.2(7)	22.4(4)
O4B	-804.5(8)	2223(3)	4505.0(7)	26.6(4)
C1B	1271.4(11)	7679(5)	1922.1(10)	21.6(5)
C2B	793.8(11)	7555(5)	1304.6(10)	20.6(5)
C3B	155.1(11)	7692(5)	1223.3(9)	20.3(5)
C4B	-47.0(12)	9629(5)	1421.8(10)	22.4(5)
C5B	-630.8(12)	9684(5)	1349.5(10)	24.4(6)
C6B	-1030.0(11)	7828(5)	1080.7(9)	22.0(5)
C7B	-1664.2(11)	7860(5)	1009.2(10)	26.5(6)
C8B	-1693.1(11)	7697(5)	1557.4(10)	24.2(5)
C9B	-1433.2(11)	5398(5)	1880.1(10)	22.5(5)
C10B	-1508.1(12)	5231(5)	2401.0(10)	22.6(5)
C11B	-1201.5(12)	3046(5)	2755.0(10)	24.1(5)
C12B	-1242.2(11)	2857(5)	3298.8(10)	20.4(5)
C13B	-849.3(11)	741(5)	3648.3(9)	18.1(5)
C14B	-199.2(11)	914(4)	3765.3(9)	17.7(5)
C15B	47.6(12)	-830(5)	3567.6(10)	22.8(5)
C16B	638.0(12)	-664(5)	3658.9(11)	24.7(6)
C17B	1001.5(11)	1259(4)	3953.6(10)	19.3(5)
C18B	1643.5(11)	1494(5)	4061.0(10)	23.3(5)
C19B	1755.6(11)	3697(5)	3779.4(10)	21.7(5)
C20B	1415.4(12)	3584(5)	3151.1(10)	23.7(5)
C21B	1548.4(12)	5680(5)	2863.7(10)	23.4(5)
C22B	1177.7(12)	5569(5)	2236.1(10)	23.1(5)
C23B	-247.0(11)	5842(5)	950.0(10)	22.5(5)
C24B	-828.8(12)	5903(5)	881.9(10)	24.0(6)
C25B	163.1(11)	2841(5)	4062.7(10)	23.3(5)
C26B	749.2(11)	3003(5)	4151.5(10)	23.4(5)
C27B	1901.1(12)	7665(6)	1970.6(11)	33.0(6)
C28B	890.5(12)	9560(5)	978.9(10)	21.7(5)
C29B	1057.3(12)	10354(5)	202.4(10)	25.5(6)
C30B	1713.3(13)	10234(6)	369.5(11)	33.1(7)
C31B	-1887.4(12)	2491(6)	3189.4(11)	31.1(6)
C32B	-879.9(11)	590(4)	4189.4(10)	19.0(5)
C33B	-1060.2(11)	-2166(5)	4766.7(10)	21.9(5)
C34B	-1714.1(12)	-2286(5)	4600.9(10)	27.8(6)

**Table A8.1.5** Bond Lengths [ $\text{\AA}$ ] and angles [ $^\circ$ ] for Macrocycle **SI31**

Atom	Atom	Length/ $\text{\AA}$
F1	C30	1.342(3)
F2	C30	1.328(3)
F3	C30	1.347(4)
F4	C34	1.328(3)
F5	C34	1.345(3)
F6	C34	1.331(3)
O1	C28	1.356(3)
O1	C29	1.438(3)
O2	C28	1.201(3)
O3	C32	1.361(3)
O3	C33	1.435(3)
O4	C32	1.199(3)
C1	C2	1.543(3)
C1	C22	1.522(4)
C1	C27	1.527(4)
C2	C3	1.521(3)
C2	C28	1.506(3)
C3	C4	1.394(4)
C3	C23	1.388(4)
C4	C5	1.385(4)
C5	C6	1.395(4)
C6	C7	1.505(4)
C6	C24	1.393(4)
C7	C8	1.530(3)
C8	C9	1.518(4)
C9	C10	1.525(3)
C10	C11	1.517(4)
C11	C12	1.535(3)
C12	C13	1.540(3)
C12	C31	1.527(3)
C13	C14	1.515(3)
C13	C32	1.518(3)
C14	C15	1.388(4)
C14	C25	1.393(4)
C15	C16	1.390(4)
C16	C17	1.388(4)
C17	C18	1.508(4)
C17	C26	1.392(4)
C18	C19	1.529(4)
C19	C20	1.516(3)
C20	C21	1.513(4)
C21	C22	1.520(3)
C23	C24	1.385(4)
C25	C26	1.385(4)
C29	C30	1.494(4)
C33	C34	1.490(4)
F1B	C30B	1.347(3)
F2B	C30B	1.319(3)
F3B	C30B	1.348(4)

<b>Atom</b>	<b>Atom</b>	<b>Length/Å</b>
F4B	C34B	1.326(3)
F5B	C34B	1.341(3)
F6B	C34B	1.342(3)
O1B	C28B	1.361(3)
O1B	C29B	1.437(3)
O2B	C28B	1.194(3)
O3B	C32B	1.363(3)
O3B	C33B	1.430(3)
O4B	C32B	1.201(3)
C1B	C2B	1.554(3)
C1B	C22B	1.528(3)
C1B	C27B	1.527(3)
C2B	C3B	1.519(3)
C2B	C28B	1.509(3)
C3B	C4B	1.398(3)
C3B	C23B	1.390(4)
C4B	C5B	1.389(3)
C5B	C6B	1.386(4)
C6B	C7B	1.515(3)
C6B	C24B	1.392(4)
C7B	C8B	1.531(3)
C8B	C9B	1.513(4)
C9B	C10B	1.518(3)
C10B	C11B	1.517(4)
C11B	C12B	1.535(3)
C12B	C13B	1.545(3)
C12B	C31B	1.522(3)
C13B	C14B	1.518(3)
C13B	C32B	1.514(3)
C14B	C15B	1.384(3)
C14B	C25B	1.394(4)
C15B	C16B	1.391(3)
C16B	C17B	1.391(4)
C17B	C18B	1.508(3)
C17B	C26B	1.393(3)
C18B	C19B	1.534(3)
C19B	C20B	1.522(3)
C20B	C21B	1.520(3)
C21B	C22B	1.525(3)
C23B	C24B	1.388(4)
C25B	C26B	1.382(3)
C29B	C30B	1.497(4)
C33B	C34B	1.493(3)

**Table A8.1.6** Anisotropic Displacement Parameters ( $\text{\AA}^2 \times 10^3$ ) for Macrocycle **SI31**.

The Anisotropic Displacement Factor Exponent Takes the Form:  $-2p^2[h^2a^{*2}U^{11} + \dots + 2hka^*b^*U^{12}]$ .

Atom	$U_{11}$	$U_{22}$	$U_{33}$	$U_{23}$	$U_{13}$	$U_{12}$
F1	28.1(9)	59.4(12)	28.7(8)	-19.7(8)	9.1(7)	0.2(8)
F2	27.6(9)	68.3(13)	39.7(10)	-10.2(9)	21.0(8)	-6.9(9)
F3	40.1(11)	53.9(12)	37.5(10)	7.1(9)	16.6(8)	20.2(9)
F4	39.0(11)	61.0(13)	43.9(11)	-12.8(10)	3.6(9)	25.4(10)
F5	36.5(9)	41.8(10)	18.0(7)	-5.3(7)	7.4(7)	3.0(8)
F6	46.0(12)	105.8(19)	36.2(10)	-6.7(11)	17.7(10)	-38.8(12)
O1	32.9(11)	22.1(9)	22.0(9)	0.3(7)	14.5(8)	0.7(8)
O2	54.7(14)	16.9(10)	29.3(10)	-1.3(8)	16.8(10)	-1.8(9)
O3	33.2(11)	21.3(9)	19.2(9)	-2.1(7)	11.6(8)	-1.9(8)
O4	34.1(11)	25.2(10)	23.5(9)	0.3(8)	15.9(8)	-5.2(8)
C1	21.1(13)	24.2(13)	20.9(12)	-2.6(11)	8.2(11)	-0.1(11)
C2	21.6(13)	20.5(12)	20.7(12)	0.1(10)	9.2(11)	0.2(11)
C3	20.2(13)	22.0(12)	18.5(11)	-4.1(10)	9.9(10)	1.0(11)
C4	24.9(15)	22.7(13)	24.7(13)	-3.7(11)	12.3(12)	-3.6(11)
C5	31.0(15)	20.8(13)	21.8(12)	3.5(10)	13.6(12)	5.5(11)
C6	21.6(13)	24.1(13)	20.5(12)	-3.5(11)	11.4(11)	2.4(11)
C7	22.3(14)	34.1(15)	22.5(13)	-4.3(12)	8.3(11)	6.3(12)
C8	27.9(15)	32.6(15)	18.6(12)	1.8(11)	7.7(11)	8.8(12)
C9	25.7(14)	25.8(14)	19.4(12)	0.3(11)	10.1(11)	4.1(12)
C10	24.2(14)	29.1(14)	19.3(12)	1.2(11)	10.3(11)	1.7(11)
C11	25.9(14)	27.7(14)	19.9(12)	1.0(11)	10.4(11)	3.5(12)
C12	18.4(12)	27.5(13)	17.2(11)	0.0(10)	8.2(10)	1.2(11)
C13	20.8(13)	23.6(13)	16.1(12)	-0.3(10)	8.3(11)	-3.1(11)
C14	20.1(13)	22.8(13)	17.2(12)	-4.3(10)	8.7(11)	0.5(10)
C15	24.9(15)	21.2(13)	26.5(13)	2.5(11)	9.7(12)	0.3(11)
C16	27.6(15)	24.3(14)	22.7(13)	4.1(11)	8.1(12)	3.2(12)
C17	19.4(13)	24.8(13)	16.8(12)	-3.9(10)	9.0(11)	4.0(11)
C18	18.1(13)	28.1(14)	24.0(13)	-1.3(11)	8.4(11)	3.3(11)
C19	21.0(14)	29.5(15)	23.8(13)	-2.2(11)	9.2(11)	-0.6(11)
C20	22.9(14)	30.3(15)	25.1(13)	-3.4(11)	11.4(12)	-0.9(11)
C21	24.1(14)	27.7(14)	21.8(13)	-2.1(11)	9.4(12)	1.0(11)
C22	22.0(14)	26.5(14)	25.8(13)	-3.4(11)	11.0(12)	0.3(11)
C23	24.9(14)	21.1(12)	22.3(13)	2.5(10)	11.4(12)	2.2(11)
C24	23.1(14)	22.8(13)	26.5(13)	-0.6(11)	12.6(12)	-1.8(11)
C25	25.1(14)	24.7(13)	19.3(12)	5.2(11)	8.9(11)	2.4(11)
C26	20.0(13)	29.3(14)	22.6(12)	-2.0(11)	10.0(11)	-5.5(12)
C27	22.9(14)	52.3(19)	28.1(14)	-11.8(14)	10.4(12)	-3.4(14)
C28	18.8(13)	23.8(14)	19.3(12)	2.4(10)	7.0(11)	2.7(10)
C29	28.5(15)	32.3(15)	20.6(13)	-7.7(11)	14.2(12)	-1.8(12)
C30	24.8(15)	49.4(19)	26.5(14)	-9.8(13)	13.6(13)	-0.6(14)
C31	21.5(14)	48.2(18)	22.0(13)	-2.5(13)	7.7(12)	5.9(13)
C32	16.9(13)	23.8(13)	18.8(12)	-1.7(10)	7.0(11)	-0.3(11)
C33	28.6(14)	25.0(13)	18.5(12)	-2.4(11)	10.2(11)	2.8(12)
C34	29.8(15)	34.0(15)	23.7(13)	-3.8(12)	12.7(12)	-1.1(13)
F1B	38.2(10)	52.4(11)	34.2(9)	6.0(8)	21.7(8)	-8.8(8)

Atom	$U_{11}$	$U_{22}$	$U_{33}$	$U_{23}$	$U_{13}$	$U_{12}$
F2B	37.3(11)	92.0(16)	23.4(8)	-7.7(10)	8.3(8)	-25.9(11)
F3B	38.2(10)	50.4(11)	49.1(10)	11.1(9)	25.6(9)	12.8(9)
F4B	39.5(11)	60.0(12)	61.5(12)	34.4(10)	31.4(10)	23.2(9)
F5B	33.3(9)	40.6(10)	31.5(8)	7.2(7)	22.1(7)	1.0(7)
F6B	40.4(11)	73.9(14)	41.0(10)	-22.3(10)	20.3(9)	-26.3(10)
O1B	30.8(10)	23.9(9)	19.2(8)	-2.0(7)	14.1(8)	-1.5(8)
O2B	60.9(14)	17.3(9)	35.3(11)	-0.6(8)	33.5(11)	-0.6(9)
O3B	32.1(10)	18.1(9)	21.2(9)	1.5(7)	15.9(8)	-1.6(8)
O4B	35.2(11)	24.0(10)	24.3(9)	-5.2(8)	16.8(9)	-3.6(8)
C1B	22.4(13)	20.6(12)	21.2(12)	1.5(10)	9.5(11)	0.0(11)
C2B	23.0(13)	18.3(12)	20.8(12)	0.7(10)	10.3(11)	0.1(11)
C3B	24.2(13)	19.8(12)	15.0(11)	5.0(10)	7.4(10)	3.0(11)
C4B	27.5(15)	18.8(13)	20.4(12)	-1.6(10)	10.5(12)	-2.2(11)
C5B	30.8(15)	22.1(13)	23.1(13)	3.8(11)	14.6(12)	5.9(11)
C6B	22.8(13)	25.5(13)	15.1(11)	8.0(10)	6.7(10)	4.3(11)
C7B	22.2(13)	34.2(15)	21.2(12)	9.7(12)	8.4(11)	4.6(12)
C8B	21.1(13)	27.8(14)	22.9(12)	4.8(11)	9.5(11)	4.1(11)
C9B	22.6(14)	25.2(13)	19.1(12)	2.6(11)	9.0(11)	4.1(11)
C10B	24.5(14)	22.3(13)	19.8(12)	-0.9(10)	9.3(11)	1.4(11)
C11B	26.1(14)	26.8(14)	20.6(12)	1.0(11)	11.7(11)	4.4(11)
C12B	20.5(13)	21.6(12)	19.6(12)	2.4(10)	9.7(10)	3.7(11)
C13B	19.2(13)	18.2(12)	16.9(11)	-1.8(10)	8.5(10)	-1.4(10)
C14B	17.3(13)	19.8(12)	15.4(11)	4.7(10)	7.1(10)	1.9(10)
C15B	23.7(14)	18.3(13)	25.2(13)	-1.8(10)	10.2(12)	-0.7(10)
C16B	23.2(14)	22.7(13)	30.8(14)	1.0(11)	14.8(12)	5.8(11)
C17B	16.8(13)	23.6(13)	16.6(11)	7.1(10)	7.0(11)	3.6(10)
C18B	18.4(14)	28.9(14)	20.9(12)	4.7(11)	7.6(11)	3.6(11)
C19B	18.4(13)	24.7(13)	20.9(12)	0.6(10)	8.2(11)	0.8(11)
C20B	25.2(14)	24.0(13)	20.4(12)	1.3(11)	9.0(11)	-2.7(11)
C21B	23.8(14)	24.0(13)	22.9(13)	1.3(11)	11.3(11)	-0.4(11)
C22B	25.2(14)	21.7(13)	21.0(12)	1.2(11)	9.6(12)	-2.2(11)
C23B	26.9(15)	19.1(12)	19.3(12)	-0.2(10)	8.8(11)	2.3(11)
C24B	24.3(15)	22.2(13)	21.4(13)	0.1(11)	7.1(12)	-2.4(11)
C25B	26.9(14)	24.9(13)	22.3(12)	-3.2(11)	15.0(11)	0.0(12)
C26B	22.4(13)	26.8(13)	21.3(12)	-5.6(11)	10.4(11)	-5.9(11)
C27B	23.8(15)	45.9(18)	27.8(14)	6.3(14)	10.4(12)	-4.1(14)
C28B	24.0(14)	20.3(13)	21.7(13)	-0.2(10)	11.3(11)	3.1(11)
C29B	31.3(16)	28.1(14)	19.4(12)	1.3(11)	13.8(12)	-1.2(12)
C30B	31.0(16)	45.9(18)	22.1(14)	1.6(13)	11.9(13)	-6.7(14)
C31B	23.8(14)	42.4(17)	28.2(14)	9.0(13)	12.9(12)	6.4(13)
C32B	16.8(13)	20.0(12)	19.6(12)	2.1(10)	7.9(10)	1.2(10)
C33B	26.8(14)	23.0(13)	17.8(12)	3.4(10)	11.7(11)	-0.3(11)
C34B	27.1(14)	34.8(15)	23.0(13)	3.9(12)	12.7(12)	-1.9(13)

**Table A8.1.7** Hydrogen Coordinates ( $\times 10^4$ ) and Isotropic Displacement Parameters ( $\text{\AA}^2 \times 10^3$ ) for Macrocycle **SI31**.

Atom	x	y	z	$U_{eq}$
H1	3838.87	1417.26	6044.01	27
H2	4207.62	4485.31	5421.4	25
H4	4840.99	-360.14	6422.28	28
H5	5801.05	-375.76	7136.72	29
H7A	6916.88	4159.71	7370.2	33
H7B	6906.2	1334.9	7398.66	33
H8A	6538.59	1555.85	8047.23	33
H8B	7157.54	2870.15	8269.03	33
H9A	6045.69	5298.2	7825.73	28
H9B	6663.7	6623.82	8041.48	28
H10A	6340.63	3858.89	8736.64	29
H10B	6937.65	5329.69	8943.77	29
H11A	5801.39	7546.94	8483.22	30
H11B	6410.9	8941.41	8737.19	30
H12	6017.59	6097.78	9373.73	25
H13	6022.18	11219.04	9293.16	24
H15	5209.75	12729.35	8513.21	30
H16	4236.17	12564.47	7821	31
H18A	3269.88	10780.41	7380.3	29
H18B	3091.16	9221.46	7761.05	29
H19A	3335.86	5676.06	7435.97	30
H19B	2831.8	7113.21	6948.5	30
H20A	3539.25	8588.14	6690.01	31
H20B	4046.03	7171.75	7180.08	31
H21A	3093.65	4881.95	6279.45	30
H21B	3620.75	3509.13	6761.73	30
H22A	4296.5	5121.09	6477.84	30
H22B	3772.08	6505.72	5998.13	30
H23	5162.07	5955.91	5892.69	27
H24	6120.38	5949.12	6609.47	28
H25	4948.78	6619.38	9158.69	28
H26	3979.76	6457.4	8463.97	29
H27A	3082.42	4291.05	5128.85	52
H27B	2861.64	2813.75	5491.26	52
H27C	3099.11	1459.46	5125.95	52
H29A	4033.67	-1564.23	4443.05	31
H29B	4111.57	420.45	4067.88	31
H31A	7042.46	9106.84	9774.92	47
H31B	7063.15	6277.03	9804.09	47
H31C	6827.48	7745.84	10156.27	47
H33A	5836.99	11583.49	10740.57	29
H33B	5905.86	14354.71	10655.57	29
H1B	1216.17	9191.66	2079.88	26
H2B	842	6011.03	1153.47	25
H4B	212.4	10895.87	1604.28	27
H5B	-756.36	10992.28	1484.09	29
H7BA	-1884.57	6514.62	775.82	32

<b>Atom</b>	<b>x</b>	<b>y</b>	<b>z</b>	<b><i>U</i><sub>eq</sub></b>
H7BB	-1859.37	9339.1	821.4	32
H8BA	-1479.64	9064.2	1786.17	29
H8BB	-2108.59	7825.21	1481.74	29
H9BA	-1009.95	5319.97	1980.83	27
H9BB	-1627.82	4021.27	1645.32	27
H10C	-1346.11	6682.04	2619.1	27
H10D	-1932.21	5164.79	2297.27	27
H11C	-781.77	3079.64	2841.42	29
H11D	-1376.03	1600.41	2538.96	29
H12B	-1091.09	4361.57	3506.93	24
H13B	-1015.29	-759.67	3443.49	22
H15B	-185.46	-2136.09	3370.18	27
H16B	792.41	-1858.43	3520.68	30
H18C	1755.56	43.85	3930.99	28
H18D	1899.36	1608.16	4456.72	28
H19C	1637.8	5146.66	3904.52	26
H19D	2181.16	3813.56	3892.11	26
H20C	1515.18	2084.57	3028.49	28
H20D	989.07	3560.12	3038.74	28
H21C	1970.68	5661.14	2959.15	28
H21D	1465.5	7188.06	2996.65	28
H22C	757.11	5506.24	2145.69	28
H22D	1272.99	4079.35	2106.12	28
H23B	-124.41	4542.27	810.61	27
H24B	-1088.59	4636.94	700.23	29
H25B	8.95	4029.39	4202.81	28
H26B	981.32	4312.22	4348.7	28
H27D	1963.79	6182.78	1821.78	50
H27E	2191.46	7799.8	2352.75	50
H27F	1943.79	9005.6	1767.83	50
H29C	949.16	11971.7	260.87	31
H29D	825.95	9956.17	-186.45	31
H31D	-2039.34	1012.82	2988.64	47
H31E	-2127.92	3820.41	2975.5	47
H31F	-1901.78	2409.07	3534.97	47
H33C	-874.84	-872.72	5031.91	26
H33D	-868.03	-3675.15	4937.83	26

**Table A8.1.8** Bond Angles [°] for Macrocycle **SI31**.

Atom	Atom	Atom	Angle <sup>o</sup>
C28	O1	C29	116.5(2)
C32	O3	C33	117.09(19)
C22	C1	C2	110.3(2)
C22	C1	C27	111.9(2)
C27	C1	C2	110.8(2)
C3	C2	C1	112.92(19)
C28	C2	C1	111.1(2)
C28	C2	C3	109.3(2)
C4	C3	C2	122.7(2)
C23	C3	C2	119.3(2)
C23	C3	C4	117.9(2)
C5	C4	C3	121.0(2)
C4	C5	C6	121.2(2)
C5	C6	C7	121.8(2)
C24	C6	C5	117.4(2)
C24	C6	C7	120.8(2)
C6	C7	C8	114.0(2)
C9	C8	C7	114.6(2)
C8	C9	C10	112.8(2)
C11	C10	C9	113.5(2)
C10	C11	C12	115.6(2)
C11	C12	C13	109.6(2)
C31	C12	C11	111.5(2)
C31	C12	C13	110.5(2)
C14	C13	C12	113.5(2)
C14	C13	C32	109.11(19)
C32	C13	C12	110.7(2)
C15	C14	C13	120.7(2)
C15	C14	C25	117.8(2)
C25	C14	C13	121.4(2)
C16	C15	C14	121.0(2)
C15	C16	C17	121.5(2)
C16	C17	C18	122.0(2)
C26	C17	C16	117.2(2)
C26	C17	C18	120.8(2)
C17	C18	C19	113.9(2)
C20	C19	C18	114.4(2)
C21	C20	C19	114.0(2)
C20	C21	C22	113.4(2)
C21	C22	C1	115.8(2)
C24	C23	C3	121.0(2)
C23	C24	C6	121.5(2)
C26	C25	C14	120.8(2)
C25	C26	C17	121.7(2)
O1	C28	C2	111.8(2)
O2	C28	O1	122.5(2)
O2	C28	C2	125.7(2)
O1	C29	C30	108.6(2)
F1	C30	F3	106.4(2)



Atom	Atom	Atom	Angle <sup>o</sup>
F1	C30	C29	110.4(2)
F2	C30	F1	107.6(2)
F2	C30	F3	106.9(2)
F2	C30	C29	112.9(2)
F3	C30	C29	112.3(3)
O3	C32	C13	110.0(2)
O4	C32	O3	123.4(2)
O4	C32	C13	126.7(2)
O3	C33	C34	109.0(2)
F4	C34	F5	106.6(2)
F4	C34	F6	107.0(2)
F4	C34	C33	112.4(2)
F5	C34	C33	111.1(2)
F6	C34	F5	106.6(2)
F6	C34	C33	112.8(2)
C28B	O1B	C29B	116.5(2)
C32B	O3B	C33B	116.90(19)
C22B	C1B	C2B	109.3(2)
C27B	C1B	C2B	110.27(19)
C27B	C1B	C22B	111.7(2)
C3B	C2B	C1B	113.15(18)
C28B	C2B	C1B	110.5(2)
C28B	C2B	C3B	108.9(2)
C4B	C3B	C2B	122.1(2)
C23B	C3B	C2B	120.1(2)
C23B	C3B	C4B	117.9(2)
C5B	C4B	C3B	120.8(2)
C6B	C5B	C4B	121.3(2)
C5B	C6B	C7B	121.5(2)
C5B	C6B	C24B	117.9(2)
C24B	C6B	C7B	120.6(2)
C6B	C7B	C8B	113.2(2)
C9B	C8B	C7B	114.5(2)
C8B	C9B	C10B	112.8(2)
C11B	C10B	C9B	113.4(2)
C10B	C11B	C12B	115.3(2)
C11B	C12B	C13B	109.76(19)
C31B	C12B	C11B	111.1(2)
C31B	C12B	C13B	109.9(2)
C14B	C13B	C12B	113.73(19)
C32B	C13B	C12B	109.69(19)
C32B	C13B	C14B	109.43(19)
C15B	C14B	C13B	120.5(2)
C15B	C14B	C25B	118.0(2)
C25B	C14B	C13B	121.5(2)
C14B	C15B	C16B	121.2(2)
C15B	C16B	C17B	121.1(2)
C16B	C17B	C18B	122.5(2)
C16B	C17B	C26B	117.2(2)
C26B	C17B	C18B	120.2(2)
C17B	C18B	C19B	113.5(2)
C20B	C19B	C18B	113.1(2)

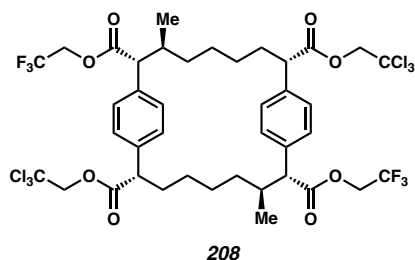
<b>Atom</b>	<b>Atom</b>	<b>Atom</b>	<b>Angle<sup>o</sup></b>
C21B	C20B	C19B	113.9(2)
C20B	C21B	C22B	112.4(2)
C21B	C22B	C1B	115.1(2)
C3B	C23B	C24B	121.0(2)
C23B	C24B	C6B	121.1(2)
C26B	C25B	C14B	120.7(2)
C25B	C26B	C17B	121.8(2)
O1B	C28B	C2B	110.6(2)
O2B	C28B	O1B	123.2(2)
O2B	C28B	C2B	126.2(2)
O1B	C29B	C30B	107.9(2)
F1B	C30B	C29B	110.3(2)
F2B	C30B	F1B	108.0(2)
F2B	C30B	F3B	106.6(3)
F2B	C30B	C29B	113.1(2)
F3B	C30B	F1B	106.9(2)
F3B	C30B	C29B	111.6(2)
O3B	C32B	C13B	109.8(2)
O4B	C32B	O3B	123.7(2)
O4B	C32B	C13B	126.4(2)
O3B	C33B	C34B	108.36(19)
F4B	C34B	F5B	107.0(2)
F4B	C34B	F6B	107.1(2)
F4B	C34B	C33B	113.1(2)
F5B	C34B	F6B	106.4(2)
F5B	C34B	C33B	111.4(2)
F6B	C34B	C33B	111.6(2)

**Table A8.1.9** Torsion Angles [°] for Macrocycle **SI31**.

Atom	Atom	Atom	Atom	Angle/°
O1	C29	C30	F1	176.0(2)
O1	C29	C30	F2	-63.5(3)
O1	C29	C30	F3	57.5(3)
O3	C33	C34	F4	-66.4(3)
O3	C33	C34	F5	174.3(2)
O3	C33	C34	F6	54.6(3)
C1	C2	C3	C4	57.5(3)
C1	C2	C3	C23	-120.4(2)
C1	C2	C28	O1	118.2(2)
C1	C2	C28	O2	-61.6(3)
C2	C1	C22	C21	-169.3(2)
C2	C3	C4	C5	-177.3(2)
C2	C3	C23	C24	177.3(2)
C3	C2	C28	O1	-116.5(2)
C3	C2	C28	O2	63.7(3)
C3	C4	C5	C6	-0.5(4)
C3	C23	C24	C6	0.8(4)
C4	C3	C23	C24	-0.7(3)
C4	C5	C6	C7	179.7(2)
C4	C5	C6	C24	0.5(3)
C5	C6	C7	C8	-63.9(3)
C5	C6	C24	C23	-0.7(3)
C6	C7	C8	C9	-61.2(3)
C7	C6	C24	C23	-179.9(2)
C7	C8	C9	C10	-179.4(2)
C8	C9	C10	C11	-176.6(2)
C9	C10	C11	C12	175.5(2)
C10	C11	C12	C13	-175.0(2)
C10	C11	C12	C31	62.3(3)
C11	C12	C13	C14	60.4(3)
C11	C12	C13	C32	-176.5(2)
C12	C13	C14	C15	-116.8(3)
C12	C13	C14	C25	61.1(3)
C12	C13	C32	O3	130.1(2)
C12	C13	C32	O4	-51.4(3)
C13	C14	C15	C16	177.5(2)
C13	C14	C25	C26	-177.3(2)
C14	C13	C32	O3	-104.2(2)
C14	C13	C32	O4	74.3(3)
C14	C15	C16	C17	-0.2(4)
C14	C25	C26	C17	-0.2(4)
C15	C14	C25	C26	0.6(4)
C15	C16	C17	C18	-178.4(2)
C15	C16	C17	C26	0.7(4)
C16	C17	C18	C19	113.9(3)
C16	C17	C26	C25	-0.5(3)
C17	C18	C19	C20	-61.7(3)
C18	C17	C26	C25	178.6(2)
C18	C19	C20	C21	179.5(2)
C19	C20	C21	C22	177.5(2)
C20	C21	C22	C1	-179.7(2)

Atom	Atom	Atom	Atom	Angle/°
C22	C1	C2	C3	59.7(3)
C22	C1	C2	C28	-177.0(2)
C23	C3	C4	C5	0.6(3)
C24	C6	C7	C8	115.2(3)
C25	C14	C15	C16	-0.4(4)
C26	C17	C18	C19	-65.1(3)
C27	C1	C2	C3	-175.9(2)
C27	C1	C2	C28	-52.6(3)
C27	C1	C22	C21	66.9(3)
C28	O1	C29	C30	103.6(3)
C28	C2	C3	C4	-66.7(3)
C28	C2	C3	C23	115.4(2)
C29	O1	C28	O2	1.7(4)
C29	O1	C28	C2	-178.0(2)
C31	C12	C13	C14	-176.4(2)
C31	C12	C13	C32	-53.2(3)
C32	O3	C33	C34	97.2(3)
C32	C13	C14	C15	119.2(2)
C32	C13	C14	C25	-62.9(3)
C33	O3	C32	O4	3.4(4)
C33	O3	C32	C13	-178.11(19)
O1B	C29B	C30B	F1B	176.8(2)
O1B	C29B	C30B	F2B	-62.1(3)
O1B	C29B	C30B	F3B	58.1(3)
O3B	C33B	C34B	F4B	-61.4(3)
O3B	C33B	C34B	F5B	178.1(2)
O3B	C33B	C34B	F6B	59.4(3)
C1B	C2B	C3B	C4B	57.0(3)
C1B	C2B	C3B	C23B	-122.2(2)
C1B	C2B	C28B	O1B	126.1(2)
C1B	C2B	C28B	O2B	-55.0(4)
C2B	C1B	C22B	C21B	-170.6(2)
C2B	C3B	C4B	C5B	-178.9(2)
C2B	C3B	C23B	C24B	178.6(2)
C3B	C2B	C28B	O1B	-109.0(2)
C3B	C2B	C28B	O2B	69.9(3)
C3B	C4B	C5B	C6B	0.1(4)
C3B	C23B	C24B	C6B	0.5(4)
C4B	C3B	C23B	C24B	-0.7(4)
C4B	C5B	C6B	C7B	179.0(2)
C4B	C5B	C6B	C24B	-0.3(3)
C5B	C6B	C7B	C8B	-65.2(3)
C5B	C6B	C24B	C23B	0.0(3)
C6B	C7B	C8B	C9B	-61.8(3)
C7B	C6B	C24B	C23B	-179.3(2)
C7B	C8B	C9B	C10B	-176.1(2)
C8B	C9B	C10B	C11B	-174.9(2)
C9B	C10B	C11B	C12B	177.5(2)
C10B	C11B	C12B	C13B	-173.2(2)
C10B	C11B	C12B	C31B	65.1(3)
C11B	C12B	C13B	C14B	55.9(3)
C11B	C12B	C13B	C32B	178.8(2)
C12B	C13B	C14B	C15B	-117.0(2)

Atom	Atom	Atom	Atom	Angle/°
C12B	C13B	C14B	C25B	61.6(3)
C12B	C13B	C32B	O3B	131.5(2)
C12B	C13B	C32B	O4B	-50.3(3)
C13B	C14B	C15B	C16B	178.3(2)
C13B	C14B	C25B	C26B	-178.1(2)
C14B	C13B	C32B	O3B	-103.0(2)
C14B	C13B	C32B	O4B	75.1(3)
C14B	C15B	C16B	C17B	0.2(4)
C14B	C25B	C26B	C17B	-0.5(4)
C15B	C14B	C25B	C26B	0.6(4)
C15B	C16B	C17B	C18B	179.9(2)
C15B	C16B	C17B	C26B	-0.1(4)
C16B	C17B	C18B	C19B	115.1(3)
C16B	C17B	C26B	C25B	0.2(4)
C17B	C18B	C19B	C20B	-63.6(3)
C18B	C17B	C26B	C25B	-179.7(2)
C18B	C19B	C20B	C21B	-176.7(2)
C19B	C20B	C21B	C22B	-177.3(2)
C20B	C21B	C22B	C1B	177.7(2)
C22B	C1B	C2B	C3B	59.8(3)
C22B	C1B	C2B	C28B	-177.7(2)
C23B	C3B	C4B	C5B	0.4(3)
C24B	C6B	C7B	C8B	114.1(3)
C25B	C14B	C15B	C16B	-0.4(4)
C26B	C17B	C18B	C19B	-64.9(3)
C27B	C1B	C2B	C3B	-177.0(2)
C27B	C1B	C2B	C28B	-54.6(3)
C27B	C1B	C22B	C21B	67.1(3)
C28B	O1B	C29B	C30B	99.4(3)
C28B	C2B	C3B	C4B	-66.3(3)
C28B	C2B	C3B	C23B	114.5(2)
C29B	O1B	C28B	O2B	4.0(4)
C29B	O1B	C28B	C2B	-177.0(2)
C31B	C12B	C13B	C14B	178.4(2)
C31B	C12B	C13B	C32B	-58.7(3)
C32B	O3B	C33B	C34B	99.1(2)
C32B	C13B	C14B	C15B	119.9(2)
C32B	C13B	C14B	C25B	-61.4(3)
C33B	O3B	C32B	O4B	4.5(3)
C33B	O3B	C32B	C13B	-177.24(19)

**A8.2 X-RAY CRYSTAL STRUCTURE ANALYSIS OF MACROCYCLE 208**Contents

*Table A8.2.1. Experimental Details*

*Table A8.2.2. Crystal Data*

*Table A8.2.3. Reflection Statistics*

*Table A8.2.4. Atomic Coordinates*

*Table A8.2.5. Bond Lengths and Angles*

*Table A8.2.6. Anisotropic Displacement Parameters*

*Table A8.2.7. Hydrogen Atomic Coordinates*

*Table A8.2.8. Bond Angles*

*Table A8.2.9. Torsion Angles*

*Table A8.2.10 Atomic Occupancies*

**Figure A8.2.1** X-Ray Crystal Structure of Macrocycle **208**.

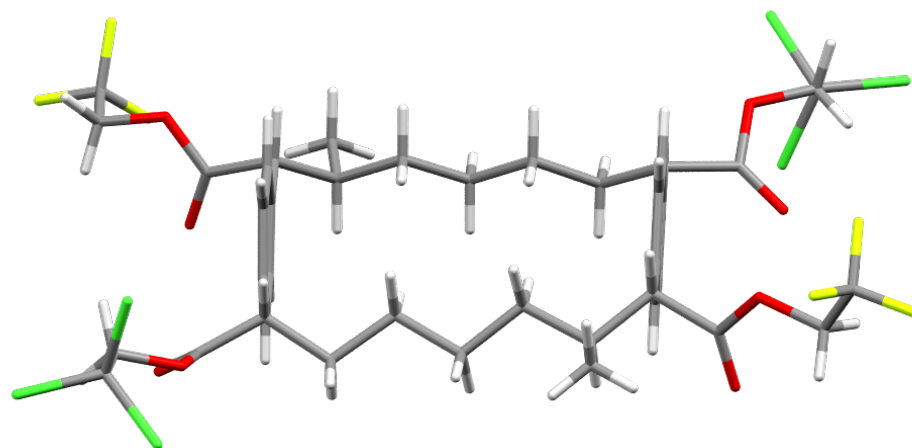


**Table A8.2.1** Experimental Details for X-Ray Structure Determination of Macrocycle **208**.

Single colorless prism-shaped crystals of macrocycle **208** were chosen from the sample as supplied. A suitable crystal with dimensions  $0.28 \times 0.21 \times 0.17 \text{ mm}^3$  was selected and mounted on a loop with paratone on a Rigaku Synergy-S diffractometer. The crystal was kept at a steady  $T = 100.0(2) \text{ K}$  during data collection. The structure was solved with the **ShelXT** 2018/2 (Sheldrick, 2018) solution program using dual methods and by using **Olex2** 1.3-alpha (Dolomanov et al., 2009) as the graphical interface. The model was refined with **ShelXL** 2018/3 (Sheldrick, 2015) using full matrix least squares minimisation on  $F^2$ .

**Crystal Data.**  $\text{C}_{40}\text{H}_{44}\text{Cl}_6\text{F}_6\text{O}_8$ ,  $M_r = 979.45$ , monoclinic,  $P2_1$  (No. 4),  $a = 11.00854(7) \text{ \AA}$ ,  $b = 27.37588(17) \text{ \AA}$ ,  $c = 15.61807(10) \text{ \AA}$ ,  $\beta = 104.1223(7)^\circ$ ,  $\alpha = \gamma = 90^\circ$ ,  $V = 4564.54(5) \text{ \AA}^3$ ,  $T = 100.0(2) \text{ K}$ ,  $Z = 4$ ,  $Z' = 2$ ,  $\mu(\text{Cu K}\alpha) = 4.074 \text{ mm}^{-1}$ , 61888 reflections measured, 17396 unique ( $R_{\text{int}} = 0.0415$ ) which were used in all calculations. The final  $wR_2$  was 0.0911 (all data) and  $R_1$  was 0.0343 ( $I \geq 2 \sigma(I)$ ).



**Table A8.2.2** Crystal Data and Structure Refinement for Macrocycle **208**

<b>Compound</b>	<b>Macrocycle 208</b>
Formula	C <sub>40</sub> H <sub>44</sub> Cl <sub>6</sub> F <sub>6</sub> O <sub>8</sub>
<i>D</i> <sub>calc.</sub> / g cm <sup>-3</sup>	1.425
$\mu$ /mm <sup>-1</sup>	4.074
Formula Weight	979.45
Color	colorless
Shape	prism-shaped
Size/mm <sup>3</sup>	0.28×0.21×0.17
<i>T</i> /K	100.0(2)
Crystal System	monoclinic
Flack Parameter	0.005(4)
Hooft Parameter	0.005(4)
Space Group	<i>P</i> 2 <sub>1</sub>
<i>a</i> /Å	11.00854(7)
<i>b</i> /Å	27.37588(17)
<i>c</i> /Å	15.61807(10)
$\alpha$ /°	90
$\beta$ /°	104.1223(7)
$\gamma$ /°	90
<i>V</i> /Å <sup>3</sup>	4564.54(5)
<i>Z</i>	4
<i>Z</i> '	2
Wavelength/Å	1.54184
Radiation type	Cu K $\alpha$
$\theta$ <sub>min</sub> /°	2.918
$\theta$ <sub>max</sub> /°	72.888
Measured Refl's.	61888
Indep't Refl's	17396
Refl's I≥2 $\sigma$ (I)	16862
<i>R</i> <sub>int</sub>	0.0415
Parameters	1177
Restraints	732
Largest Peak	0.460
Deepest Hole	-0.390
Goof	1.045
<i>wR</i> <sub>2</sub> (all data)	0.0911
<i>wR</i> <sub>2</sub>	0.0903
<i>R</i> <sub>1</sub> (all data)	0.0354
<i>R</i> <sub>1</sub>	0.0343

**Structure Quality Indicators**

<b>Reflections:</b>	d min (Cu\lambda) 2 $\theta$ =145.8°	0.81	I/ $\sigma$ (I) CIF	29.0	Rint CIF	4.15%	Full 135.4° 98% to 145.8°	99.8		
<b>Refinement:</b>	Shift CIF	0.006	Max Peak CIF	0.5	Min Peak CIF	-0.4	Goof CIF	1.045	Hoof CIF	.005(4)

A colorless prism-shaped crystal with dimensions  $0.28 \times 0.21 \times 0.17 \text{ mm}^3$  was mounted on a loop with paratone. Data were collected using a XtaLAB Synergy, Dualflex, HyPix diffractometer operating at  $T = 100.0(2) \text{ K}$ .

Data were measured using  $\omega$  scans with Cu  $K_{\alpha}$  radiation. The diffraction pattern was indexed and the total number of runs and images was based on the strategy calculation from the program CrysAlisPro 1.171.40.53 (Rigaku OD, 2019). The maximum resolution that was achieved was  $\theta = 72.888^{\circ}$  ( $0.83 \text{ \AA}$ ).

The unit cell was refined using CrysAlisPro 1.171.40.53 (Rigaku OD, 2019) on 50795 reflections, 82% of the observed reflections.

Data reduction, scaling and absorption corrections were performed using CrysAlisPro 1.171.40.53 (Rigaku OD, 2019). The final completeness is 99.80 % out to  $72.888^{\circ}$  in  $\theta$ . A numerical absorption correction based on gaussian integration over a multifaceted crystal model was performed using CrysAlisPro 1.171.41.108a (Rigaku Oxford Diffraction, 2021). An empirical absorption correction using spherical harmonics, implemented in SCALE3 ABSPACK scaling algorithm was also applied. The absorption coefficient  $\mu$  of this material is  $4.074 \text{ mm}^{-1}$  at this wavelength ( $\lambda = 1.54184 \text{ \AA}$ ) and the minimum and maximum transmissions are 0.453 and 1.000.

The structure was solved and the space group  $P2_1$  (# 4) determined by the ShelXT 2018/2 (Sheldrick, 2018) structure solution program and refined by full matrix least squares minimisation on  $F^2$  using version 2018/3 of ShelXL 2018/3 (Sheldrick, 2015). All non-

hydrogen atoms were refined anisotropically. Hydrogen atom positions were calculated geometrically and refined using the riding model.

The X-ray structure is disordered and the asymmetric unit contains two equivalent forms of the trichloro acetate with two major spatial arrangements. The group pivots about the macrocycle with the C of the CCl<sub>3</sub> group in an almost fixed position and is readily interpreted as 2 conformers. There is less than a 10% contribution from the second conformer to the overall structure.

The Flack parameter was refined to 0.005(4). Determination of absolute structure using Bayesian statistics on Bijvoet differences using the Olex2 results in 0.005(4). Note: The Flack parameter is used to determine chirality of the crystal studied, the value should be near 0, a value of 1 means that the stereochemistry is wrong and the model should be inverted. A value of 0.5 means that the crystal consists of a racemic mixture of the two enantiomers.

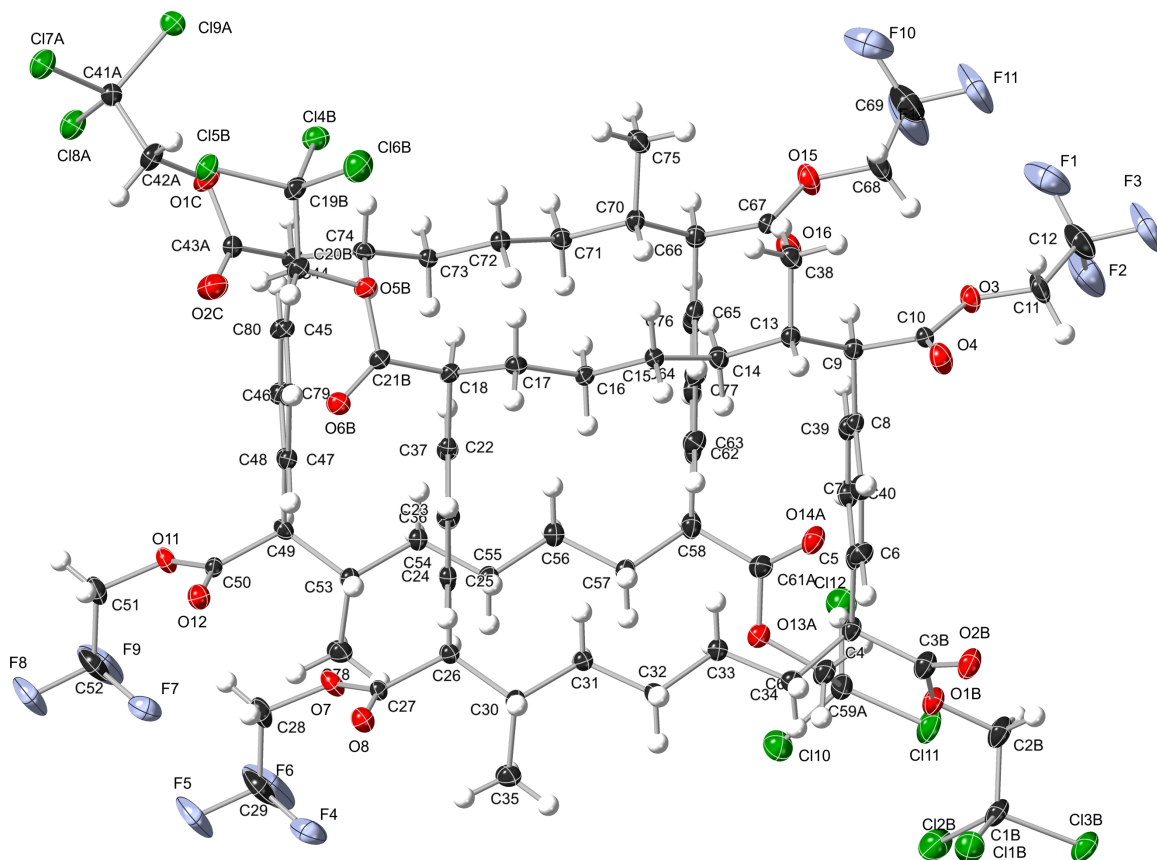


**Figure A8.2.2** A thermal ellipsoid representation of the asymmetric unit showing the orientation of the major substituents. The value of  $Z'$  is 2. This means that there are two independent molecules in the asymmetric unit.

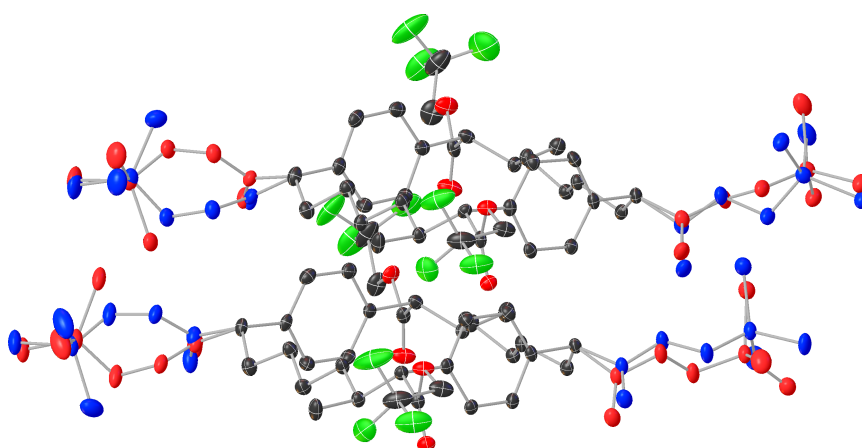


**Figure A8.2.3.** The disorder model showing the major (blue) and minor (red) substituents.

**Table A8.2.3** Reflection Statistics

Total reflections (after filtering)	61922	Unique reflections	17396
Completeness	0.954	Mean I/ $\sigma$	23.01
hkl <sub>max</sub> collected	(10, 33, 18)	hkl <sub>min</sub> collected	(-13, -32, -19)
hkl <sub>max</sub> used	(13, 33, 19)	hkl <sub>min</sub> used	(-13, -32, 0)
Lim d <sub>max</sub> collected	100.0	Lim d <sub>min</sub> collected	0.77
d <sub>max</sub> used	15.15	d <sub>min</sub> used	0.81
Friedel pairs	4597	Friedel pairs merged	0
Inconsistent equivalents	63	R <sub>int</sub>	0.0415
R <sub>sigma</sub>	0.0345	Intensity transformed	0
Omitted reflections	0	Omitted by user (OMIT hkl)	34
Multiplicity	(6157, 5992, 3763, 2350, 1471, 892, 508, 372, 225, 103, 43, 26, 1)	Maximum multiplicity	13
Removed systematic absences	0	Filtered off (Shel/OMIT)	0
Total reflections (after filtering)	42062	Unique reflections	10947
Completeness	0.804	Mean I/ $\sigma$	16.19
hkl <sub>max</sub> collected	(30, 6, 33)	hkl <sub>min</sub> collected	(-30, -6, -33)
hkl <sub>max</sub> used	(27, 6, 33)	hkl <sub>min</sub> used	(-30, -6, 0)
Lim d <sub>max</sub> collected	100.0	Lim d <sub>min</sub> collected	0.77
d <sub>max</sub> used	22.32	d <sub>min</sub> used	0.8
Friedel pairs	5250	Friedel pairs merged	0
Inconsistent equivalents	10	R <sub>int</sub>	0.051
R <sub>sigma</sub>	0.0423	Intensity transformed	0
Omitted reflections	0	Omitted by user (OMIT hkl)	4
Multiplicity	(6310, 4911, 3058, 1507, 1006, 519, 204, 88, 40, 7, 2)	Maximum multiplicity	18
Removed systematic absences	0	Filtered off (Shel/OMIT)	0

**Table A8.2.4** Fractional Atomic Coordinates ( $\times 10^4$ ) and Equivalent Isotropic Displacement Parameters ( $\text{\AA}^2 \times 10^3$ ) for Macrocycle **208**.  $U_{eq}$  is defined as 1/3 of the trace of the orthogonalised  $U_{ij}$ .

Atom	x	y	z	$U_{eq}$
F1	13332(3)	-3089.1(11)	10089(2)	58.5(7)
F2	14008(3)	-2533.0(11)	11049.7(15)	59.5(8)
F3	15263(3)	-3097.8(11)	10822.2(18)	65.6(9)
F4	8045(2)	2937.1(9)	5431.3(16)	39.6(5)
F5	6399(2)	3160.6(10)	4461(2)	52.6(7)
F6	6251(3)	2912.7(11)	5740(2)	66.3(9)
O3	13627(2)	-2210.8(10)	9351.1(14)	23.9(5)
O4	14707(2)	-1920.7(10)	8418.6(17)	28.6(5)
O7	7177(2)	1981.1(9)	5403.4(15)	22.3(5)
O8	8919(2)	1962.6(9)	4888.4(14)	21.8(4)
C4	13224(2)	315.6(12)	10022.2(17)	18.2(6)
C5	13121(3)	-185.0(12)	9581.7(18)	16.2(6)
C6	13925(3)	-339.5(13)	9056(2)	20.3(6)
C7	13773(3)	-794.1(12)	8662(2)	19.2(6)
C8	12832(3)	-1111.9(12)	8774.2(19)	16.2(6)
C9	12612(3)	-1612.7(12)	8338.9(19)	17.5(6)
C10	13766(3)	-1922.5(12)	8679.6(19)	17.9(6)
C11	14699(4)	-2497.1(14)	9736(2)	29.8(8)
C12	14318(5)	-2805.0(15)	10425(2)	41.8(10)
C13	12280(3)	-1608.5(12)	7314.7(19)	17.0(6)
C14	11219(3)	-1245.9(12)	6954.6(19)	18.2(6)
C15	10942(3)	-1159.9(11)	5961.4(19)	16.0(6)
C16	9836(3)	-815.5(11)	5660.5(19)	16.6(6)
C17	9344(3)	-768.5(11)	4660.7(19)	17.7(6)
C18	8104(3)	-477.7(12)	4454.7(15)	16.6(6)
C22	8262(3)	26.1(11)	4866.8(19)	15.3(6)
C23	9134(3)	356.1(12)	4679.9(19)	17.5(6)
C24	9287(3)	812.6(12)	5077.3(18)	16.0(6)
C25	8585(3)	947.0(11)	5677.5(18)	15.5(6)
C26	8768(3)	1445.1(11)	6124.6(19)	16.2(6)
C27	8353(3)	1822.2(11)	5405.7(19)	15.7(6)
C28	6625(3)	2324.7(14)	4728(2)	27.7(7)
C29	6843(4)	2831.3(14)	5105(3)	36.2(9)
C30	10122(3)	1534.2(12)	6670(2)	17.8(6)
C31	10404(3)	1157.2(12)	7414.7(19)	18.6(6)
C32	11736(3)	1146.8(12)	7990(2)	20.2(6)
C33	11882(3)	761.8(12)	8710(2)	20.6(6)
C34	13166(3)	742.0(12)	9349(2)	21.0(6)
C35	10265(3)	2059.9(13)	7020(2)	27.1(7)
C36	7717(3)	618.5(12)	5856(2)	18.7(6)
C37	7552(3)	160.1(12)	5448(2)	18.9(6)
C38	11899(3)	-2126.7(12)	6990(2)	23.7(7)
C39	12051(3)	-959.7(12)	9296(2)	19.9(6)
C40	12191(3)	-504.9(13)	9699(2)	20.2(6)
C11A	14844(14)	1686(3)	12243(12)	45.0(3)
C12A	16877(10)	1106(6)	13266(8)	32.7(2)
C13A	14418(9)	678(4)	12635(7)	28.6(5)

Atom	x	y	z	$U_{eq}$
O1A	14794(15)	838(5)	10884(6)	22.6(4)
O2A	15180(20)	30(5)	10930(30)	31.5(7)
C1A	15514(8)	1097(4)	12378(6)	25.0(6)
C2A	15863(11)	931(6)	11554(8)	28.6(5)
C3A	14464(12)	366(5)	10710(11)	23.7(6)
C11B	16332.9(9)	1338.0(6)	11512.5(6)	38.5(2)
C12B	14407.9(10)	1631.0(6)	12361.0(8)	45.0(3)
C13B	16697.1(9)	1198.2(6)	13397.1(6)	32.7(2)
O1B	14120.6(18)	642.3(9)	11424.9(13)	22.6(4)
O2B	15364(2)	160.9(11)	10833.2(19)	31.5(7)
C1B	15579(2)	1184.5(10)	12353.1(14)	25.0(6)
C2B	15012(2)	685.5(9)	12219.7(13)	28.6(5)
C3B	14372(2)	352.7(14)	10791.4(17)	23.7(6)
C110	9804.3(10)	1717.8(6)	12236.7(7)	37.7(3)
C111	11830.8(12)	1164.3(8)	13337.2(7)	38.7(3)
C112	9436.2(9)	703.6(6)	12609.2(6)	34.9(2)
O13A	9962(2)	914.0(9)	10886.1(13)	23.2(5)
O14A	10427(3)	118.4(15)	10802(2)	25.0(5)
C59A	10531(2)	1137.9(10)	12405.1(14)	24.1(7)
C60A	10979(2)	980.4(10)	11612.2(14)	24.4(7)
C61A	9712(2)	452.8(10)	10582.8(19)	19.5(7)
C14	11260(7)	1317(3)	11524(5)	24.4(7)
C15	11783(11)	1129(6)	13399(5)	38.7(3)
C16	9450(9)	1588(4)	12503(7)	37.7(3)
O13B	9153(8)	635(4)	11405(11)	23.2(5)
O14B	10480(30)	149(18)	10906(15)	25.0(5)
C59B	10592(8)	1146(3)	12399(4)	24.1(7)
C60B	9981(12)	653(3)	12237(7)	24.4(7)
C61B	9492(8)	360(3)	10782(6)	19.5(7)
C14B	4794.7(7)	-1581.1(5)	2684.3(5)	26.56(18)
C15B	4742.2(7)	-1286.3(5)	894.3(5)	27.51(18)
C16B	6965.1(8)	-1733.5(6)	1992.6(6)	36.2(2)
O5B	6847(2)	-847.8(8)	3172.4(12)	23.2(4)
O6B	7589(2)	-100.9(9)	2993.6(15)	24.9(5)
C19B	5687(2)	-1336.2(9)	1988.7(13)	20.7(6)
C20B	6171(2)	-836.2(9)	2290.8(13)	24.0(5)
C21B	7527(3)	-441.2(10)	3470.3(15)	19.0(5)
C14A	6940(20)	-1732(8)	1230(14)	26.56(18)
C15A	5500(20)	-1703(9)	2548(15)	26.56(18)
C16A	5350(20)	-904(7)	1313(16)	36.2(2)
O5A	6948(18)	-727(10)	3040(9)	23.2(4)
O6A	8270(50)	-95(14)	3087(11)	24.9(5)
C19A	6364(15)	-1348(5)	1947(11)	20.7(6)
C20A	7415(14)	-1092(8)	2584(17)	24.0(5)
C21A	7770(30)	-387(6)	3464(3)	19.0(5)
C17A	-7.3(8)	-1204.2(6)	723.1(5)	27.12(15)
C18A	-569.5(7)	-705.8(6)	2212.1(5)	27.12(15)
C19A	527.8(9)	-1670.4(6)	2436.4(6)	33.8(2)
O1AC	2161(2)	-815.8(11)	3013.7(15)	28.2(6)
O2AC	3584(3)	-255.1(11)	2857.4(16)	30.5(6)
C41A	491(2)	-1106.3(9)	1868.3(13)	20.6(7)
C42A	1781(2)	-881.2(10)	2099.9(13)	23.6(7)
C43A	3066(3)	-483.6(12)	3321.1(15)	19.2(6)
C17B	1940(7)	-1709(4)	1945(6)	27.12(15)

Atom	x	y	z	$U_{eq}$
Cl8B	-271(8)	-1241(4)	882(5)	27.12(15)
Cl9B	-240(8)	-1579(4)	2643(6)	33.8(2)
O1AB	2270(20)	-868(4)	2973(17)	28.2(6)
O2AB	2920(30)	-95(7)	2897(13)	30.5(6)
C41B	679(6)	-1315(3)	1971(5)	20.6(7)
C42B	1141(9)	-824(3)	2337(8)	23.6(7)
C43B	2833(14)	-451(4)	3328(3)	19.2(6)
F7	3005(2)	2918.9(9)	5342.4(16)	39.1(5)
F8	1406(2)	3152.1(9)	4338.3(18)	45.1(6)
F9	1176(3)	2907.5(10)	5600(2)	54.9(7)
F10	8134(3)	-3161.8(11)	9753(2)	69.2(9)
F11	9878(3)	-3174.1(12)	10743.5(19)	67.0(9)
F12	8399(4)	-2691.3(12)	10877.7(19)	69.9(10)
O11	2110.3(19)	1968.3(9)	5289.3(14)	20.4(4)
O12	3874.9(19)	1945.6(9)	4802.2(14)	20.3(4)
O15	8484(2)	-2190.5(10)	9410.4(16)	31.1(6)
O16	9699(2)	-1860.8(10)	8613.9(18)	32.0(6)
C44	3328(3)	-484.5(12)	4323.8(15)	17.4(6)
C45	3390(3)	22.1(11)	4715(2)	15.8(6)
C46	4282(3)	362.8(12)	4600.2(19)	17.0(6)
C47	4379(3)	814.1(12)	5011.3(19)	16.9(6)
C48	3587(3)	932.7(11)	5566.7(19)	16.5(6)
C49	3686(3)	1426.8(11)	6024.5(19)	15.5(6)
C50	3290(3)	1808.3(11)	5311.2(19)	15.7(6)
C51	1589(3)	2314.4(13)	4618(2)	25.4(7)
C52	1805(4)	2818.0(14)	4982(3)	34.4(9)
C53	5004(3)	1536.3(12)	6614.3(19)	18.1(6)
C54	5289(3)	1161.7(12)	7370(2)	20.0(6)
C55	6604(3)	1188.6(12)	7968.4(19)	18.4(6)
C56	6833(3)	798.3(13)	8685(2)	21.4(6)
C57	8172(3)	809.7(12)	9266(2)	20.0(6)
C58	8414(2)	401.8(12)	9965.3(19)	20.9(6)
C62	8212(3)	-109.3(12)	9570.9(19)	18.7(6)
C63	8902(3)	-276.7(12)	8985(2)	20.0(6)
C64	8709(3)	-740.8(12)	8621(2)	18.9(6)
C65	7810(3)	-1052.8(12)	8825(2)	18.1(6)
C66	7573(3)	-1561.9(12)	8440(2)	19.2(6)
C67	8704(3)	-1875.3(12)	8806(2)	19.8(6)
C68	9512(4)	-2494.6(15)	9826(3)	37.0(9)
C69	8961(5)	-2879.7(16)	10296(3)	45.0(11)
C70	7259(3)	-1585.0(12)	7420.1(19)	17.5(6)
C71	6171(3)	-1239.1(12)	7022.2(19)	18.3(6)
C72	5982(3)	-1150.6(12)	6040(2)	17.6(6)
C73	4879(3)	-813.3(11)	5676.9(19)	16.0(6)
C74	4557(3)	-767.8(11)	4669.7(19)	16.8(6)
C75	6933(3)	-2110.8(12)	7120(2)	21.7(6)
C76	7123(3)	-883.8(13)	9403(2)	21.3(6)
C77	7323(3)	-418.7(13)	9772(2)	21.0(6)
C78	5053(4)	2061.6(12)	6959(2)	26.5(7)
C79	2695(3)	595.1(12)	5675(2)	19.8(6)
C80	2597(3)	142.6(12)	5245(2)	19.0(6)



**Table A8.2.5** Bond Lengths [ $\text{\AA}$ ] and angles [ $^\circ$ ] for Macrocycle **208**

Atom	Atom	Length/ $\text{\AA}$
F1	C12	1.335(6)
F2	C12	1.337(5)
F3	C12	1.339(5)
F4	C29	1.329(5)
F5	C29	1.351(4)
F6	C29	1.332(5)
O3	C10	1.351(4)
O3	C11	1.422(4)
O4	C10	1.202(4)
O7	C27	1.364(4)
O7	C28	1.434(4)
O8	C27	1.198(4)
C4	C5	1.525(4)
C4	C34	1.561(4)
C4	C3A	1.524(3)
C4	C3B	1.520(3)
C5	C6	1.411(4)
C5	C40	1.393(4)
C6	C7	1.381(4)
C7	C8	1.396(4)
C8	C9	1.523(4)
C8	C39	1.386(4)
C9	C10	1.512(4)
C9	C13	1.552(4)
C11	C12	1.504(5)
C13	C14	1.532(4)
C13	C38	1.530(4)
C14	C15	1.524(4)
C15	C16	1.521(4)
C16	C17	1.528(4)
C17	C18	1.545(4)
C18	C22	1.514(4)
C18	C21B	1.517(3)
C18	C21A	1.521(3)
C22	C23	1.400(4)
C22	C37	1.384(4)
C23	C24	1.387(4)
C24	C25	1.402(4)
C25	C26	1.523(4)
C25	C36	1.389(4)
C26	C27	1.512(4)
C26	C30	1.545(4)
C28	C29	1.503(6)
C30	C31	1.529(4)
C30	C35	1.534(4)
C31	C32	1.522(4)
C32	C33	1.521(4)
C33	C34	1.520(4)
C36	C37	1.399(4)
C39	C40	1.387(5)
C11A	C1A	1.765(3)

<b>Atom</b>	<b>Atom</b>	<b>Length/Å</b>
Cl2A	C1A	1.777(3)
Cl3A	C1A	1.780(3)
O1A	C2A	1.394(3)
O1A	C3A	1.352(3)
O2A	C3A	1.202(3)
C1A	C2A	1.502(3)
Cl1B	C1B	1.767(2)
Cl2B	C1B	1.779(2)
Cl3B	C1B	1.788(2)
O1B	C2B	1.387(2)
O1B	C3B	1.348(2)
O2B	C3B	1.199(3)
C1B	C2B	1.495(3)
Cl10	C59A	1.768(2)
Cl11	C59A	1.776(2)
Cl12	C59A	1.776(2)
O13A	C60A	1.397(2)
O13A	C61A	1.353(2)
O14A	C61A	1.202(3)
C59A	C60A	1.503(3)
C61A	C58	1.523(3)
Cl4	C59B	1.765(3)
Cl5	C59B	1.777(3)
Cl6	C59B	1.780(3)
O13B	C60B	1.394(3)
O13B	C61B	1.353(3)
O14B	C61B	1.202(3)
C59B	C60B	1.502(3)
C61B	C58	1.520(3)
Cl4B	C19B	1.765(2)
Cl5B	C19B	1.7761(19)
Cl6B	C19B	1.777(2)
O5B	C20B	1.397(2)
O5B	C21B	1.358(2)
O6B	C21B	1.205(3)
C19B	C20B	1.502(3)
Cl4A	C19A	1.765(3)
Cl5A	C19A	1.777(3)
Cl6A	C19A	1.780(3)
O5A	C20A	1.395(3)
O5A	C21A	1.352(3)
O6A	C21A	1.202(3)
C19A	C20A	1.502(3)
Cl7A	C41A	1.759(2)
Cl8A	C41A	1.777(2)
Cl9A	C41A	1.777(2)
O1AC	C42A	1.397(2)
O1AC	C43A	1.348(2)
O2AC	C43A	1.201(3)
C41A	C42A	1.509(3)
C43A	C44	1.521(3)
Cl7B	C41B	1.765(3)
Cl8B	C41B	1.777(3)

<b>Atom</b>	<b>Atom</b>	<b>Length/Å</b>
Cl9B	C41B	1.780(3)
O1AB	C42B	1.394(3)
O1AB	C43B	1.353(3)
O2AB	C43B	1.202(3)
C41B	C42B	1.502(3)
C43B	C44	1.520(3)
F7	C52	1.333(5)
F8	C52	1.351(4)
F9	C52	1.341(4)
F10	C69	1.329(6)
F11	C69	1.346(5)
F12	C69	1.323(5)
O11	C50	1.363(4)
O11	C51	1.426(4)
O12	C50	1.199(4)
O15	C67	1.344(4)
O15	C68	1.427(4)
O16	C67	1.205(4)
C44	C45	1.510(4)
C44	C74	1.539(4)
C45	C46	1.397(4)
C45	C80	1.383(4)
C46	C47	1.384(4)
C47	C48	1.410(4)
C48	C49	1.521(4)
C48	C79	1.389(4)
C49	C50	1.512(4)
C49	C53	1.546(4)
C51	C52	1.488(5)
C53	C54	1.537(4)
C53	C78	1.532(4)
C54	C55	1.521(4)
C55	C56	1.523(4)
C56	C57	1.532(4)
C57	C58	1.539(4)
C58	C62	1.523(4)
C62	C63	1.401(4)
C62	C77	1.387(5)
C63	C64	1.387(4)
C64	C65	1.403(4)
C65	C66	1.515(4)
C65	C76	1.390(4)
C66	C67	1.506(4)
C66	C70	1.546(4)
C68	C69	1.495(6)
C70	C71	1.534(4)
C70	C75	1.529(4)
C71	C72	1.517(4)
C72	C73	1.520(4)
C73	C74	1.531(4)
C76	C77	1.393(5)
C79	C80	1.401(4)

**Table A8.2.6** Anisotropic Displacement Parameters ( $\text{\AA}^2 \times 10^3$ ) for Macrocycle **208**.

The Anisotropic Displacement Factor Exponent Takes the Form:  $-2p^2[h^2a^{*2}U^{11} + \dots + 2hka^*b^*U^{12}]$ .

Atom	$U_{11}$	$U_{22}$	$U_{33}$	$U_{23}$	$U_{13}$	$U_{12}$
F1	96(2)	33.2(14)	57.3(16)	11.0(12)	41.0(16)	-3.7(14)
F2	115(2)	45.0(15)	23.5(11)	11.7(10)	27.4(14)	28.4(15)
F3	108(2)	45.8(16)	42.9(15)	26.5(12)	18.5(15)	40.5(16)
F4	57.6(14)	17.7(10)	46.1(13)	-1.2(9)	17.4(11)	0.2(9)
F5	57.6(15)	33.5(13)	76.9(18)	34.4(12)	36.1(14)	26.3(11)
F6	102(2)	35.7(14)	89(2)	20.1(14)	77(2)	28.6(14)
O3	29.9(12)	26.0(12)	13.9(10)	6.4(9)	1.7(9)	2.5(9)
O4	17.9(11)	33.8(13)	34.9(13)	14.7(11)	8.0(10)	6.0(9)
O7	20.7(10)	18.9(11)	30.1(12)	9.9(9)	11.5(9)	6.1(8)
O8	22.4(11)	21.4(11)	22.2(11)	3.5(9)	6.9(9)	2.3(9)
C4	17.6(14)	20.5(15)	14.2(14)	-4.9(11)	-0.3(11)	4.3(11)
C5	18.7(13)	17.9(14)	10.0(13)	-0.7(11)	-0.6(11)	5.7(11)
C6	16.0(14)	23.5(16)	21.5(15)	-2.0(12)	5.2(12)	-1.9(11)
C7	17.7(13)	23.3(16)	17.4(14)	-2.6(11)	5.8(11)	3.2(11)
C8	15.3(13)	19.5(14)	12.2(13)	0.7(11)	0.4(11)	-0.2(11)
C9	16.5(13)	18.5(14)	16.3(14)	2.2(11)	1.9(11)	-1.7(11)
C10	20.7(15)	15.5(14)	14.9(14)	3.3(11)	-0.5(11)	-1.3(11)
C11	42(2)	21.2(16)	21.6(16)	8.1(13)	-0.5(15)	10.5(14)
C12	79(3)	27.4(19)	20.3(17)	9.0(15)	14.1(19)	13(2)
C13	17.2(13)	16.8(14)	15.7(14)	-0.2(11)	1.7(11)	1.6(11)
C14	20.7(14)	15.7(14)	16.9(14)	-1.4(11)	1.9(11)	4.3(11)
C15	15.9(13)	14.2(13)	16.7(14)	1.0(11)	1.8(11)	0.5(11)
C16	18.1(13)	14.3(14)	15.2(14)	-2.1(10)	-0.4(11)	0.1(11)
C17	20.5(14)	14.1(14)	17.7(14)	-2.4(11)	3.2(11)	-0.9(11)
C18	16.5(13)	16.6(14)	14.9(14)	-0.9(11)	0.5(11)	-2.7(11)
C22	15.4(13)	13.0(13)	14.3(14)	1.2(10)	-2.6(11)	0.4(10)
C23	19.6(14)	17.1(14)	14.4(14)	-1.0(11)	1.4(11)	-0.7(11)
C24	17.1(13)	16.5(14)	12.8(13)	2.0(11)	0.5(11)	0.9(11)
C25	16.5(13)	15.7(14)	11.6(13)	2.9(10)	-1.9(11)	1.9(10)
C26	18.7(14)	15.0(14)	14.2(13)	1.6(11)	2.9(11)	-0.6(11)
C27	15.9(13)	12.5(13)	16.7(14)	0.9(11)	0.2(11)	2.9(10)
C28	17.2(14)	28.5(18)	37.2(19)	16.8(15)	6.5(13)	8.0(12)
C29	41(2)	24.3(19)	52(2)	18.7(16)	28.0(18)	17.7(15)
C30	18.3(14)	17.6(14)	15.6(14)	0.6(11)	0.5(11)	-0.4(11)
C31	21.7(14)	16.1(14)	15.8(14)	2.0(11)	0.4(12)	-2.7(11)
C32	22.2(15)	17.5(14)	19.8(15)	3.7(12)	3.2(12)	-1.0(11)
C33	20.5(14)	19.1(15)	19.3(15)	2.7(12)	-0.7(12)	-2.0(11)
C34	21.9(14)	16.4(15)	22.5(15)	-0.6(12)	0.9(12)	0.5(11)
C35	39.0(19)	17.7(16)	20.4(16)	-3.1(12)	-0.8(14)	-3.6(13)
C36	18.0(14)	19.1(15)	19.7(14)	-2.7(11)	5.7(11)	0.6(11)
C37	15.6(13)	17.6(14)	22.3(15)	0.9(12)	2.3(11)	-0.3(11)
C38	32.0(17)	16.0(15)	20.7(15)	1.1(12)	1.7(13)	3.7(12)
C39	18.4(14)	24.2(16)	15.3(14)	2.3(12)	0.8(11)	0.2(12)
C40	18.7(14)	25.5(16)	16.6(14)	1.4(12)	5.0(11)	5.8(12)
Cl1A	30.8(5)	32.6(5)	64.4(7)	-19.5(4)	-2.3(5)	10.0(4)
Cl2A	30.5(4)	36.4(6)	25.2(5)	-13.6(4)	-4.6(3)	0.3(4)

Atom	$U_{11}$	$U_{22}$	$U_{33}$	$U_{23}$	$U_{13}$	$U_{12}$
Cl3A	24.3(8)	37.0(10)	20.2(9)	-11.0(8)	-2.9(7)	5.2(8)
O1A	21.6(8)	29.0(8)	15.0(8)	-4.9(7)	0.4(7)	2.7(7)
O2A	26.7(11)	32.1(9)	28.5(13)	-10.2(10)	-7.0(10)	8.2(9)
C1A	19.2(11)	31.3(14)	20.7(9)	-10.9(9)	-2.4(9)	1.0(11)
C2A	24.3(8)	37.0(10)	20.2(9)	-11.0(8)	-2.9(7)	5.2(8)
C3A	20.3(10)	28.7(9)	19.9(14)	-5.6(8)	0.8(9)	3.7(6)
Cl1B	32.8(5)	44.6(6)	36.7(5)	12.0(4)	6.0(4)	-9.6(4)
Cl2B	30.8(5)	32.6(5)	64.4(7)	-19.5(4)	-2.3(5)	10.0(4)
Cl3B	30.5(4)	36.4(6)	25.2(5)	-13.6(4)	-4.6(3)	0.3(4)
O1B	21.6(8)	29.0(8)	15.0(8)	-4.9(7)	0.4(7)	2.7(7)
O2B	26.7(11)	32.1(9)	28.5(13)	-10.2(10)	-7.0(10)	8.2(9)
C1B	19.2(11)	31.3(14)	20.7(9)	-10.9(9)	-2.4(9)	1.0(11)
C2B	24.3(8)	37.0(10)	20.2(9)	-11.0(8)	-2.9(7)	5.2(8)
C3B	20.3(10)	28.7(9)	19.9(14)	-5.6(8)	0.8(9)	3.7(6)
Cl10	45.3(6)	25.7(5)	38.0(6)	-5.2(4)	2.2(4)	9.5(4)
Cl11	39.1(5)	47.0(6)	21.2(4)	-7.6(4)	-9.6(4)	3.7(4)
Cl12	36.0(5)	40.2(5)	30.5(5)	6.1(4)	11.8(4)	-3.8(4)
O13A	23.3(12)	23.1(13)	20.5(12)	-1.3(10)	0.0(10)	-0.8(9)
O14A	22.8(11)	29.3(14)	19.6(13)	-7.9(11)	-1.1(10)	4.0(10)
C59A	24.9(16)	24.6(16)	19.5(15)	-0.1(12)	-0.7(13)	1.2(12)
C60A	23.7(16)	28.4(17)	17.7(15)	-0.2(13)	-1.4(12)	-3.9(13)
C61A	23.9(17)	20.7(17)	14.2(15)	-2.5(12)	5.1(13)	-1.7(13)
Cl4	23.7(16)	28.4(17)	17.7(15)	-0.2(13)	-1.4(12)	-3.9(13)
Cl5	39.1(5)	47.0(6)	21.2(4)	-7.6(4)	-9.6(4)	3.7(4)
Cl6	45.3(6)	25.7(5)	38.0(6)	-5.2(4)	2.2(4)	9.5(4)
O13B	23.3(12)	23.1(13)	20.5(12)	-1.3(10)	0.0(10)	-0.8(9)
O14B	22.8(11)	29.3(14)	19.6(13)	-7.9(11)	-1.1(10)	4.0(10)
C59B	24.9(16)	24.6(16)	19.5(15)	-0.1(12)	-0.7(13)	1.2(12)
C60B	23.7(16)	28.4(17)	17.7(15)	-0.2(13)	-1.4(12)	-3.9(13)
C61B	23.9(17)	20.7(17)	14.2(15)	-2.5(12)	5.1(13)	-1.7(13)
Cl4B	29.9(4)	25.3(4)	23.5(4)	-0.4(3)	4.7(3)	-5.9(3)
Cl5B	31.1(4)	29.7(4)	16.1(3)	-3.2(3)	-5.1(3)	-2.8(3)
Cl6B	29.5(4)	35.2(5)	41.4(5)	-6.6(4)	4.0(4)	7.7(3)
O5B	29.8(9)	19.0(8)	16.3(8)	-0.7(6)	-3.2(7)	-6.8(7)
O6B	29.5(10)	21.0(9)	21.5(10)	2.4(7)	1.2(8)	-4.5(8)
C19B	20.9(9)	21.6(9)	17.1(9)	-4.3(7)	-0.5(7)	-1.6(8)
C20B	28.7(11)	21.7(9)	16.7(9)	-1.5(7)	-3.8(7)	-5.1(8)
C21B	22.2(10)	16.2(8)	16.0(10)	-1.7(6)	-0.8(8)	-2.3(7)
Cl4A	29.9(4)	25.3(4)	23.5(4)	-0.4(3)	4.7(3)	-5.9(3)
Cl5A	29.9(4)	25.3(4)	23.5(4)	-0.4(3)	4.7(3)	-5.9(3)
Cl6A	29.5(4)	35.2(5)	41.4(5)	-6.6(4)	4.0(4)	7.7(3)
O5A	29.8(9)	19.0(8)	16.3(8)	-0.7(6)	-3.2(7)	-6.8(7)
O6A	29.5(10)	21.0(9)	21.5(10)	2.4(7)	1.2(8)	-4.5(8)
C19A	20.9(9)	21.6(9)	17.1(9)	-4.3(7)	-0.5(7)	-1.6(8)
C20A	28.7(11)	21.7(9)	16.7(9)	-1.5(7)	-3.8(7)	-5.1(8)
C21A	22.2(10)	16.2(8)	16.0(10)	-1.7(6)	-0.8(8)	-2.3(7)
Cl7A	24.1(3)	35.9(3)	20.7(3)	-4.0(2)	4.0(2)	-0.3(2)
Cl8A	24.1(3)	35.9(3)	20.7(3)	-4.0(2)	4.0(2)	-0.3(2)
Cl9A	39.4(5)	25.6(4)	29.9(5)	7.2(3)	-4.2(4)	-7.8(4)
O1AC	29.1(12)	33.6(13)	17.8(11)	-1.9(10)	-1.9(9)	-12.4(10)
O2AC	41.2(16)	33.8(14)	16.8(12)	-1.6(10)	7.4(11)	-13.3(12)
C41A	20.0(14)	20.5(16)	19.6(15)	2.5(12)	1.6(12)	-1.1(12)
C42A	18.4(15)	33.8(18)	16.9(15)	-1.9(13)	1.0(12)	-2.3(13)

Atom	$U_{11}$	$U_{22}$	$U_{33}$	$U_{23}$	$U_{13}$	$U_{12}$
C43A	18.6(14)	17.4(14)	18.8(14)	1.6(11)	-0.6(11)	0.3(11)
Cl7B	24.1(3)	35.9(3)	20.7(3)	-4.0(2)	4.0(2)	-0.3(2)
Cl8B	24.1(3)	35.9(3)	20.7(3)	-4.0(2)	4.0(2)	-0.3(2)
Cl9B	39.4(5)	25.6(4)	29.9(5)	7.2(3)	-4.2(4)	-7.8(4)
O1AB	29.1(12)	33.6(13)	17.8(11)	-1.9(10)	-1.9(9)	-12.4(10)
O2AB	41.2(16)	33.8(14)	16.8(12)	-1.6(10)	7.4(11)	-13.3(12)
C41B	20.0(14)	20.5(16)	19.6(15)	2.5(12)	1.6(12)	-1.1(12)
C42B	18.4(15)	33.8(18)	16.9(15)	-1.9(13)	1.0(12)	-2.3(13)
C43B	18.6(14)	17.4(14)	18.8(14)	1.6(11)	-0.6(11)	0.3(11)
F7	49.4(13)	18.6(10)	47.6(13)	1.1(9)	8.5(11)	-0.3(9)
F8	50.2(13)	31.1(12)	62.8(16)	28.7(11)	30.6(12)	21.3(10)
F9	83.9(19)	32.5(13)	67.2(17)	14.4(12)	54.5(16)	20.5(12)
F10	93(2)	31.1(14)	88(2)	2.2(14)	29.9(19)	-9.1(14)
F11	109(2)	45.5(16)	50.8(16)	28.5(13)	27.4(16)	41.9(16)
F12	118(3)	61.9(19)	44.4(15)	27.7(14)	47.6(17)	46.5(18)
O11	18.5(10)	19.1(11)	24.1(11)	8.2(9)	6.5(8)	5.8(8)
O12	19.5(10)	21.6(11)	20.2(11)	1.6(9)	5.8(9)	2.9(8)
O15	30.3(12)	32.2(13)	29.4(13)	16.2(11)	4.8(10)	4.0(10)
O16	20.2(11)	32.7(14)	42.6(15)	14.3(11)	6.6(10)	4.0(9)
C44	17.6(13)	17.7(14)	15.3(13)	-2.1(11)	0.9(11)	-2.0(11)
C45	17.1(13)	12.8(13)	14.6(14)	-0.6(10)	-1.7(11)	-0.5(10)
C46	15.4(13)	19.1(14)	14.9(14)	-0.7(11)	0.6(11)	1.0(11)
C47	16.4(13)	16.8(14)	14.7(13)	1.5(11)	-1.8(11)	-0.9(11)
C48	18.7(14)	13.8(14)	14.4(13)	1.8(11)	-1.0(11)	3.0(11)
C49	21.2(14)	12.9(13)	12.8(13)	2.0(10)	4.7(11)	1.2(11)
C50	16.1(13)	13.1(13)	15.2(14)	-2.1(11)	-1.6(11)	2.6(10)
C51	19.6(14)	25.8(17)	30.3(17)	14.3(14)	5.0(13)	4.0(12)
C52	35.0(19)	23.4(18)	51(2)	18.2(16)	22.6(17)	13.6(14)
C53	20.3(14)	17.3(14)	14.7(14)	1.5(11)	0.4(11)	-0.9(11)
C54	21.4(15)	19.1(15)	16.4(14)	2.6(11)	-1.2(12)	-0.7(11)
C55	20.5(14)	18.2(14)	14.8(14)	0.0(11)	1.3(11)	0.8(11)
C56	22.4(15)	21.2(15)	18.4(15)	2.4(12)	0.6(12)	0.1(12)
C57	16.6(14)	19.2(15)	21.1(15)	0.3(12)	-1.0(12)	2.1(11)
C58	22.4(15)	22.0(16)	16.0(14)	-2.2(12)	0.4(12)	6.2(12)
C62	18.0(14)	22.7(16)	12.6(14)	0.1(11)	-1.7(11)	4.0(11)
C63	14.9(14)	23.9(16)	21.6(15)	-0.7(12)	5.1(12)	-0.1(11)
C64	16.4(13)	21.5(15)	18.6(14)	-1.7(12)	3.9(11)	1.2(11)
C65	13.2(13)	24.1(16)	15.2(14)	3.0(11)	-0.1(11)	1.1(11)
C66	16.0(13)	20.9(15)	19.7(15)	4.9(12)	2.8(11)	-2.3(11)
C67	20.7(15)	15.8(14)	18.2(14)	1.1(11)	-4.1(12)	-1.5(11)
C68	47(2)	23.9(18)	37(2)	11.3(15)	3.0(17)	13.1(16)
C69	77(3)	31(2)	32(2)	9.1(16)	21(2)	16(2)
C70	17.6(13)	19.9(15)	13.3(13)	1.4(11)	0.5(11)	-0.1(11)
C71	21.6(14)	15.5(14)	16.8(14)	-1.5(11)	3.1(11)	1.9(11)
C72	17.7(13)	17.2(14)	16.6(14)	1.4(11)	1.9(11)	0.0(11)
C73	17.2(13)	13.1(14)	16.1(14)	-0.4(10)	0.8(11)	0.2(10)
C74	23.0(14)	12.7(13)	14.3(13)	-0.8(10)	3.7(11)	-1.8(11)
C75	27.2(16)	16.9(15)	20.3(15)	2.5(12)	4.7(13)	2.2(12)
C76	17.7(14)	27.4(16)	17.6(15)	4.9(12)	1.6(12)	-0.3(12)
C77	19.0(14)	28.8(17)	13.4(14)	1.8(12)	0.1(11)	6.2(12)
C78	40.2(19)	17.6(16)	18.3(16)	-2.1(12)	0.3(14)	-3.2(13)
C79	19.7(14)	18.6(15)	20.8(15)	-2.6(12)	4.3(12)	0.9(11)
C80	15.4(13)	19.0(15)	20.3(15)	-1.0(12)	-0.2(11)	-3.8(11)

**Table A8.2.7** Hydrogen Coordinates ( $\times 10^4$ ) and Isotropic Displacement Parameters ( $\text{\AA}^2 \times 10^3$ ) for Macrocycle **208**.

Atom	x	y	z	$U_{eq}$
H4	12491.1	350.96	10268.84	22
H6	14560.11	-134.02	8974.95	24
H7	14307.76	-890.4	8314.56	23
H9	11915.42	-1766.75	8525.76	21
H11A	15403.89	-2289.61	10003.42	36
H11B	14931.76	-2701.55	9294.15	36
H13	13021.08	-1511.64	7113.5	20
H14A	10462.33	-1364.57	7098.93	22
H14B	11430.92	-935.51	7253.07	22
H15A	11674.93	-1021.17	5812.44	19
H15B	10757.49	-1469.4	5654.76	19
H16A	10080.06	-493.88	5902.44	20
H16B	9156.88	-927.88	5906.69	20
H17A	9204.4	-1090.56	4395.88	21
H17B	9957.35	-601.19	4413.76	21
H18	7512.74	-657.01	4715.91	20
H23	9612.57	269.05	4288.41	21
H24	9861.03	1031.46	4944.3	19
H26	8208.1	1465.75	6524.59	19
H28A	5732.96	2263.03	4523.36	33
H28B	7000.1	2291.76	4229.78	33
H30	10698.42	1483.23	6289.47	21
H31A	9839.77	1215.7	7793.58	22
H31B	10211.2	835.92	7155.06	22
H32A	12313.19	1077.17	7625.54	24
H32B	11945.72	1465.1	8258.39	24
H33A	11261.01	822.85	9044.52	25
H33B	11701.44	444.22	8432.87	25
H34A	13335.18	1049.34	9664.88	25
H34B	13801.95	693.71	9023.3	25
H35A	11120.22	2115.97	7330.61	33
H35B	9729.92	2108.82	7414.3	33
H35C	10036.1	2283.85	6534.44	33
H36	7241.78	704.04	6250.12	22
H37	6962.61	-55.67	5568.37	23
H38A	11157.13	-2219.86	7169.5	28
H38B	12565.22	-2349.25	7239.45	28
H38C	11734.87	-2136.22	6357.78	28
H39	11418.69	-1166.88	9377.47	24
H40	11659.19	-412.6	10050.52	24
H2AA	16361.82	1180.78	11361.55	34
H2AB	16365.42	636.12	11677.45	34
H2BA	15669.86	447.32	12236.36	34
H2BB	14625.72	612.55	12700.64	34
H60A	11535.98	1226.58	11474.71	29
H60B	11443.23	677.25	11742.04	29
H60C	10618.86	404.04	12277.75	29
H60D	9530.69	586.79	12686.38	29

<b>Atom</b>	<b>x</b>	<b>y</b>	<b>z</b>	<b><math>U_{eq}</math></b>
H20A	6705.77	-719.54	1924.44	29
H20B	5472.72	-611.56	2226.93	29
H20C	7885.56	-1326.73	3000.71	29
H20D	7978.7	-948.16	2264.02	29
H42A	2367.51	-1093.2	1905.76	28
H42B	1765.98	-568.92	1803.97	28
H42C	1259.08	-614.43	1862.18	28
H42D	521.02	-672.75	2598.94	28
H44	2652.35	-663.79	4493.41	21
H46	4818.19	285.43	4242.86	20
H47	4968.22	1039.33	4921.12	20
H49	3087.6	1432.64	6397.29	19
H51A	696.72	2256.41	4402.84	30
H51B	1975.76	2277.81	4126.04	30
H53	5622.12	1499.8	6261.18	22
H54A	4691.46	1207.17	7728.41	24
H54B	5160.59	836.59	7117.19	24
H55A	6730.09	1508.42	8243.18	22
H55B	7209.18	1149.67	7614.61	22
H56A	6670.46	479.38	8410.43	26
H56B	6249.58	845.95	9053.65	26
H57A	8324.11	1123.92	9559.37	24
H57B	8757.09	774.84	8894.85	24
H58	7805.85	446.17	10324.48	25
H63	9497.43	-73.7	8838.19	24
H64	9181.38	-846.13	8236.89	23
H66	6864.42	-1701.15	8633.5	23
H68A	10141.03	-2307.71	10240.35	44
H68B	9896.54	-2639.99	9390.25	44
H70	7997.8	-1482.94	7220.54	21
H71A	5405.75	-1374.16	7126.96	22
H71B	6321.16	-927.95	7326.77	22
H72A	5839.73	-1460.62	5730.59	21
H72B	6735.89	-1007.33	5930.91	21
H73A	5070.55	-491.45	5934.17	19
H73B	4151.13	-935.24	5856.09	19
H74A	4477.42	-1091.49	4409.19	20
H74B	5232.68	-600.43	4491.9	20
H75A	6217.83	-2216.41	7319.96	26
H75B	7632.54	-2319.58	7364.1	26
H75C	6744.81	-2126.46	6487.06	26
H76	6519.32	-1084.54	9545.48	26
H77	6855.27	-314.29	10159.53	25
H78A	4839.63	2283.6	6469.83	40
H78B	5882.26	2132.22	7304.26	40
H78C	4466.49	2098	7320.34	40
H79	2160.23	669.76	6035.15	24
H80	1990.06	-79.47	5317.33	23



**Table A8.2.8** Bond Angles [°] for Macrocycle **208**.

Atom	Atom	Atom	Angle/°
C10	O3	C11	114.3(3)
C27	O7	C28	116.3(2)
C5	C4	C34	112.4(2)
C3A	C4	C5	110.7(8)
C3A	C4	C34	106.9(5)
C3B	C4	C5	111.9(2)
C3B	C4	C34	111.8(3)
C6	C5	C4	122.9(3)
C40	C5	C4	118.8(3)
C40	C5	C6	118.3(3)
C7	C6	C5	120.4(3)
C6	C7	C8	121.2(3)
C7	C8	C9	123.1(3)
C39	C8	C7	118.2(3)
C39	C8	C9	118.6(3)
C8	C9	C13	115.2(2)
C10	C9	C8	108.6(2)
C10	C9	C13	109.5(2)
O3	C10	C9	110.9(3)
O4	C10	O3	122.4(3)
O4	C10	C9	126.7(3)
O3	C11	C12	105.3(3)
F1	C12	F2	106.4(4)
F1	C12	F3	107.4(3)
F1	C12	C11	112.8(3)
F2	C12	F3	107.6(3)
F2	C12	C11	112.1(3)
F3	C12	C11	110.3(4)
C14	C13	C9	110.5(2)
C38	C13	C9	108.1(2)
C38	C13	C14	110.9(2)
C15	C14	C13	114.8(2)
C16	C15	C14	110.9(2)
C15	C16	C17	115.1(2)
C16	C17	C18	109.3(2)
C22	C18	C17	112.1(2)
C22	C18	C21B	110.3(2)
C22	C18	C21A	105.0(7)
C21B	C18	C17	112.1(2)
C21A	C18	C17	106.2(11)
C23	C22	C18	120.8(3)
C37	C22	C18	119.7(3)
C37	C22	C23	119.4(3)
C24	C23	C22	120.2(3)
C23	C24	C25	120.6(3)
C24	C25	C26	120.6(3)
C36	C25	C24	118.9(3)
C36	C25	C26	120.5(3)
C25	C26	C30	113.3(2)
C27	C26	C25	106.8(2)
C27	C26	C30	112.2(2)

Atom	Atom	Atom	Angle/°
O7	C27	C26	109.5(2)
O8	C27	O7	123.0(3)
O8	C27	C26	127.4(3)
O7	C28	C29	108.6(3)
F4	C29	F5	106.6(3)
F4	C29	F6	107.5(4)
F4	C29	C28	113.6(3)
F5	C29	C28	109.2(4)
F6	C29	F5	106.8(3)
F6	C29	C28	112.7(3)
C31	C30	C26	107.6(2)
C31	C30	C35	112.2(3)
C35	C30	C26	110.3(2)
C32	C31	C30	116.7(3)
C33	C32	C31	111.2(2)
C34	C33	C32	115.1(3)
C33	C34	C4	110.3(2)
C25	C36	C37	120.6(3)
C22	C37	C36	120.3(3)
C8	C39	C40	121.4(3)
C39	C40	C5	120.6(3)
C3A	O1A	C2A	117.4(3)
Cl1A	C1A	Cl2A	109.22(19)
Cl1A	C1A	Cl3A	109.24(18)
Cl2A	C1A	Cl3A	108.84(18)
C2A	C1A	Cl1A	111.2(2)
C2A	C1A	Cl2A	109.2(2)
C2A	C1A	Cl3A	109.1(2)
O1A	C2A	C1A	110.7(3)
O1A	C3A	C4	112.2(10)
O2A	C3A	C4	122.9(15)
O2A	C3A	O1A	123.2(4)
C3B	O1B	C2B	118.68(18)
Cl1B	C1B	Cl2B	108.33(14)
Cl1B	C1B	Cl3B	109.20(12)
Cl2B	C1B	Cl3B	108.56(12)
C2B	C1B	Cl1B	111.68(15)
C2B	C1B	Cl2B	110.51(15)
C2B	C1B	Cl3B	108.50(15)
O1B	C2B	C1B	112.50(17)
O1B	C3B	C4	109.8(2)
O2B	C3B	C4	125.7(2)
O2B	C3B	O1B	124.4(2)
C61A	O13A	C60A	117.38(19)
Cl10	C59A	Cl11	109.28(13)
Cl10	C59A	Cl12	108.98(13)
Cl11	C59A	Cl12	109.05(13)
C60A	C59A	Cl10	111.24(16)
C60A	C59A	Cl11	109.06(15)
C60A	C59A	Cl12	109.21(15)
O13A	C60A	C59A	110.34(17)
O13A	C61A	C58	112.7(2)
O14A	C61A	O13A	123.2(2)

Atom	Atom	Atom	Angle/°
O14A	C61A	C58	124.0(3)
C61B	O13B	C60B	117.2(3)
Cl4	C59B	Cl5	109.24(19)
Cl4	C59B	Cl6	109.18(18)
Cl5	C59B	Cl6	108.87(18)
C60B	C59B	Cl4	111.2(2)
C60B	C59B	Cl5	109.2(2)
C60B	C59B	Cl6	109.2(2)
O13B	C60B	C59B	110.7(3)
O13B	C61B	C58	105.4(9)
O14B	C61B	O13B	123.2(4)
O14B	C61B	C58	131.3(10)
C21B	O5B	C20B	115.82(17)
Cl4B	C19B	Cl5B	109.77(12)
Cl4B	C19B	Cl6B	108.93(12)
Cl5B	C19B	Cl6B	109.13(11)
C20B	C19B	Cl4B	111.13(15)
C20B	C19B	Cl5B	108.16(14)
C20B	C19B	Cl6B	109.70(15)
O5B	C20B	C19B	110.59(16)
O5B	C21B	C18	110.6(2)
O6B	C21B	C18	127.2(2)
O6B	C21B	O5B	122.1(2)
C21A	O5A	C20A	117.3(3)
Cl4A	C19A	Cl5A	109.27(18)
Cl4A	C19A	Cl6A	109.22(18)
Cl5A	C19A	Cl6A	108.88(18)
C20A	C19A	Cl4A	111.1(2)
C20A	C19A	Cl5A	109.2(2)
C20A	C19A	Cl6A	109.1(2)
O5A	C20A	C19A	110.6(3)
O5A	C21A	C18	110.7(4)
O6A	C21A	C18	125.4(8)
O6A	C21A	O5A	123.3(4)
C43A	O1AC	C42A	117.5(2)
Cl7A	C41A	Cl8A	109.65(12)
Cl7A	C41A	Cl9A	109.81(12)
Cl9A	C41A	Cl8A	108.78(12)
C42A	C41A	Cl7A	110.35(14)
C42A	C41A	Cl8A	108.96(15)
C42A	C41A	Cl9A	109.26(15)
O1AC	C42A	C41A	109.06(16)
O1AC	C43A	C44	107.7(2)
O2AC	C43A	O1AC	123.7(2)
O2AC	C43A	C44	128.5(2)
C43B	O1AB	C42B	117.2(3)
Cl7B	C41B	Cl8B	109.30(18)
Cl7B	C41B	Cl9B	109.21(18)
Cl8B	C41B	Cl9B	108.94(18)
C42B	C41B	Cl7B	111.1(2)
C42B	C41B	Cl8B	109.1(2)
C42B	C41B	Cl9B	109.1(2)
O1AB	C42B	C41B	110.6(3)

<b>Atom</b>	<b>Atom</b>	<b>Atom</b>	<b>Angle/°</b>
O1AB	C43B	C44	112.5(11)
O2AB	C43B	O1AB	123.1(4)
O2AB	C43B	C44	124.4(12)
C50	O11	C51	116.2(2)
C67	O15	C68	115.8(3)
C43A	C44	C74	107.0(2)
C43B	C44	C74	117.1(7)
C45	C44	C43A	113.2(2)
C45	C44	C43B	109.1(5)
C45	C44	C74	111.8(2)
C46	C45	C44	121.7(3)
C80	C45	C44	119.2(3)
C80	C45	C46	118.9(3)
C47	C46	C45	120.9(3)
C46	C47	C48	120.1(3)
C47	C48	C49	120.6(3)
C79	C48	C47	119.0(3)
C79	C48	C49	120.4(3)
C48	C49	C53	113.7(2)
C50	C49	C48	107.0(2)
C50	C49	C53	111.4(2)
O11	C50	C49	110.0(2)
O12	C50	O11	123.0(3)
O12	C50	C49	126.9(3)
O11	C51	C52	109.6(3)
F7	C52	F8	106.5(3)
F7	C52	F9	106.9(4)
F7	C52	C51	113.8(3)
F8	C52	C51	110.5(3)
F9	C52	F8	106.3(3)
F9	C52	C51	112.4(3)
C54	C53	C49	108.3(2)
C78	C53	C49	109.8(3)
C78	C53	C54	111.9(3)
C55	C54	C53	115.1(3)
C54	C55	C56	112.3(3)
C55	C56	C57	112.6(3)
C56	C57	C58	112.3(2)
C61A	C58	C57	110.8(2)
C61B	C58	C57	127.9(3)
C61B	C58	C62	106.1(4)
C62	C58	C61A	111.2(2)
C62	C58	C57	113.4(2)
C63	C62	C58	121.0(3)
C77	C62	C58	120.7(3)
C77	C62	C63	118.2(3)
C64	C63	C62	121.0(3)
C63	C64	C65	120.7(3)
C64	C65	C66	122.1(3)
C76	C65	C64	118.1(3)
C76	C65	C66	119.7(3)
C65	C66	C70	114.9(2)
C67	C66	C65	109.1(2)

<b>Atom</b>	<b>Atom</b>	<b>Atom</b>	<b>Angle/°</b>
C67	C66	C70	108.9(3)
O15	C67	C66	111.0(3)
O16	C67	O15	121.8(3)
O16	C67	C66	127.2(3)
O15	C68	C69	105.2(3)
F10	C69	F11	107.1(4)
F10	C69	C68	113.2(4)
F11	C69	C68	109.5(4)
F12	C69	F10	107.6(4)
F12	C69	F11	107.1(3)
F12	C69	C68	112.1(4)
C71	C70	C66	110.4(2)
C75	C70	C66	109.3(2)
C75	C70	C71	110.8(2)
C72	C71	C70	114.2(2)
C71	C72	C73	112.0(2)
C72	C73	C74	113.3(2)
C73	C74	C44	111.4(2)
C65	C76	C77	121.1(3)
C62	C77	C76	120.9(3)
C48	C79	C80	120.3(3)
C45	C80	C79	120.8(3)

**Table A8.2.9** Torsion Angles [°] for Macrocycle **208**.

Atom	Atom	Atom	Atom	Angle/°
O3	C11	C12	F1	58.9(4)
O3	C11	C12	F2	-61.2(4)
O3	C11	C12	F3	179.0(3)
O7	C28	C29	F4	57.2(4)
O7	C28	C29	F5	176.0(3)
O7	C28	C29	F6	-65.4(4)
C4	C5	C6	C7	-178.9(3)
C4	C5	C40	C39	178.8(3)
C5	C4	C34	C33	66.1(3)
C5	C4	C3A	O1A	157.9(15)
C5	C4	C3A	O2A	-8(3)
C5	C4	C3B	O1B	-146.4(3)
C5	C4	C3B	O2B	34.5(5)
C5	C6	C7	C8	-0.3(5)
C6	C5	C40	C39	-1.0(4)
C6	C7	C8	C9	178.8(3)
C6	C7	C8	C39	-0.1(4)
C7	C8	C9	C10	62.5(4)
C7	C8	C9	C13	-60.6(4)
C7	C8	C39	C40	0.0(4)
C8	C9	C10	O3	96.6(3)
C8	C9	C10	O4	-82.5(4)
C8	C9	C13	C14	-50.0(3)
C8	C9	C13	C38	-171.6(2)
C8	C39	C40	C5	0.6(4)
C9	C8	C39	C40	-179.0(3)
C9	C13	C14	C15	171.8(2)
C10	O3	C11	C12	-177.0(3)
C10	C9	C13	C14	-172.8(2)
C10	C9	C13	C38	65.7(3)
C11	O3	C10	O4	1.9(4)
C11	O3	C10	C9	-177.2(3)
C13	C9	C10	O3	-136.9(3)
C13	C9	C10	O4	44.1(4)
C13	C14	C15	C16	177.1(2)
C14	C15	C16	C17	-170.6(2)
C15	C16	C17	C18	170.9(2)
C16	C17	C18	C22	58.4(3)
C16	C17	C18	C21B	-176.9(2)
C16	C17	C18	C21A	172.6(7)
C17	C18	C22	C23	56.9(3)
C17	C18	C22	C37	-121.9(3)
C17	C18	C21B	O5B	83.5(3)
C17	C18	C21B	O6B	-99.3(4)
C17	C18	C21A	O5A	96.3(13)
C17	C18	C21A	O6A	-75(3)
C18	C22	C23	C24	-178.6(2)
C18	C22	C37	C36	177.9(3)
C22	C18	C21B	O5B	-150.8(3)
C22	C18	C21B	O6B	26.4(4)
C22	C18	C21A	O5A	-144.7(9)

Atom	Atom	Atom	Atom	Angle/°
C22	C18	C21A	O6A	44(3)
C22	C23	C24	C25	0.8(4)
C23	C22	C37	C36	-0.9(4)
C23	C24	C25	C26	179.1(3)
C23	C24	C25	C36	-1.1(4)
C24	C25	C26	C27	65.0(3)
C24	C25	C26	C30	-59.1(3)
C24	C25	C36	C37	0.4(4)
C25	C26	C27	O7	100.8(3)
C25	C26	C27	O8	-77.4(4)
C25	C26	C30	C31	-63.1(3)
C25	C26	C30	C35	174.2(3)
C25	C36	C37	C22	0.6(4)
C26	C25	C36	C37	-179.8(3)
C26	C30	C31	C32	174.6(3)
C27	O7	C28	C29	-96.2(3)
C27	C26	C30	C31	175.9(2)
C27	C26	C30	C35	53.2(3)
C28	O7	C27	O8	1.2(4)
C28	O7	C27	C26	-177.1(3)
C30	C26	C27	O7	-134.5(3)
C30	C26	C27	O8	47.3(4)
C30	C31	C32	C33	179.1(3)
C31	C32	C33	C34	-177.0(3)
C32	C33	C34	C4	-176.8(3)
C34	C4	C5	C6	54.9(4)
C34	C4	C5	C40	-124.9(3)
C34	C4	C3A	O1A	35(2)
C34	C4	C3A	O2A	-130(3)
C34	C4	C3B	O1B	86.5(3)
C34	C4	C3B	O2B	-92.6(4)
C35	C30	C31	C32	-63.9(4)
C36	C25	C26	C27	-114.9(3)
C36	C25	C26	C30	121.1(3)
C37	C22	C23	C24	0.2(4)
C38	C13	C14	C15	-68.3(3)
C39	C8	C9	C10	-118.6(3)
C39	C8	C9	C13	118.3(3)
C40	C5	C6	C7	0.9(4)
Cl1A	C1A	C2A	O1A	-69.7(8)
Cl2A	C1A	C2A	O1A	169.7(8)
Cl3A	C1A	C2A	O1A	50.8(8)
C2A	O1A	C3A	C4	175.1(10)
C2A	O1A	C3A	O2A	-19(3)
C3A	C4	C5	C6	-64.6(9)
C3A	C4	C5	C40	115.6(8)
C3A	C4	C34	C33	-172.2(10)
C3A	O1A	C2A	C1A	-103.0(16)
Cl1B	C1B	C2B	O1B	-60.1(2)
Cl2B	C1B	C2B	O1B	60.6(2)
Cl3B	C1B	C2B	O1B	179.49(17)
C2B	O1B	C3B	C4	173.9(2)
C2B	O1B	C3B	O2B	-7.0(5)

Atom	Atom	Atom	Atom	Angle/°
C3B	C4	C5	C6	-72.0(4)
C3B	C4	C5	C40	108.3(3)
C3B	C4	C34	C33	-167.1(2)
C3B	O1B	C2B	C1B	111.9(3)
Cl10	C59A	C60A	O13A	-64.7(2)
Cl11	C59A	C60A	O13A	174.70(17)
Cl12	C59A	C60A	O13A	55.6(2)
O13A	C61A	C58	C57	47.6(4)
O13A	C61A	C58	C62	174.7(3)
O14A	C61A	C58	C57	-134.5(4)
O14A	C61A	C58	C62	-7.5(5)
C60A	O13A	C61A	O14A	-13.1(5)
C60A	O13A	C61A	C58	164.7(2)
C61A	O13A	C60A	C59A	-112.3(3)
C61A	C58	C62	C63	-66.5(4)
C61A	C58	C62	C77	114.5(3)
Cl4	C59B	C60B	O13B	-51.9(8)
Cl5	C59B	C60B	O13B	-172.5(7)
Cl6	C59B	C60B	O13B	68.6(7)
O13B	C61B	C58	C57	83.4(5)
O13B	C61B	C58	C62	-138.2(5)
O14B	C61B	C58	C57	-95(4)
O14B	C61B	C58	C62	44(4)
C60B	O13B	C61B	O14B	-3(4)
C60B	O13B	C61B	C58	178.9(8)
C61B	O13B	C60B	C59B	108.9(6)
C61B	C58	C62	C63	-86.1(6)
C61B	C58	C62	C77	94.9(6)
Cl4B	C19B	C20B	O5B	55.1(2)
Cl5B	C19B	C20B	O5B	175.70(18)
Cl6B	C19B	C20B	O5B	-65.4(2)
C20B	O5B	C21B	C18	174.0(2)
C20B	O5B	C21B	O6B	-3.4(4)
C21B	C18	C22	C23	-68.7(3)
C21B	C18	C22	C37	112.5(3)
C21B	O5B	C20B	C19B	168.0(2)
Cl4A	C19A	C20A	O5A	170(2)
Cl5A	C19A	C20A	O5A	-70(2)
Cl6A	C19A	C20A	O5A	49(2)
C20A	O5A	C21A	C18	-105(2)
C20A	O5A	C21A	O6A	67(4)
C21A	C18	C22	C23	-57.9(12)
C21A	C18	C22	C37	123.3(12)
C21A	O5A	C20A	C19A	-163.6(13)
Cl7A	C41A	C42A	O1AC	-178.95(19)
Cl8A	C41A	C42A	O1AC	60.6(2)
Cl9A	C41A	C42A	O1AC	-58.1(2)
O1AC	C43A	C44	C45	-133.3(3)
O1AC	C43A	C44	C74	103.1(3)
O2AC	C43A	C44	C45	50.2(5)
O2AC	C43A	C44	C74	-73.4(4)
C42A	O1AC	C43A	O2AC	-2.4(5)
C42A	O1AC	C43A	C44	-179.2(3)



Atom	Atom	Atom	Atom	Angle/°
C43A	O1AC	C42A	C41A	-158.6(3)
C43A	C44	C45	C46	-61.2(4)
C43A	C44	C45	C80	122.8(3)
C43A	C44	C74	C73	-177.2(2)
Cl7B	C41B	C42B	O1AB	-32.8(19)
Cl8B	C41B	C42B	O1AB	-153.4(19)
Cl9B	C41B	C42B	O1AB	87.7(19)
O1AB	C43B	C44	C45	-154.5(12)
O1AB	C43B	C44	C74	77.3(12)
O2AB	C43B	C44	C45	25.3(13)
O2AB	C43B	C44	C74	-102.9(13)
C42B	O1AB	C43B	O2AB	-44(3)
C42B	O1AB	C43B	C44	136(3)
C43B	O1AB	C42B	C41B	176.7(19)
C43B	C44	C45	C46	-71.5(7)
C43B	C44	C45	C80	112.6(7)
C43B	C44	C74	C73	-174.7(4)
O11	C51	C52	F7	55.5(4)
O11	C51	C52	F8	175.2(3)
O11	C51	C52	F9	-66.3(4)
O15	C68	C69	F10	63.3(4)
O15	C68	C69	F11	-177.3(3)
O15	C68	C69	F12	-58.6(5)
C44	C45	C46	C47	-175.7(3)
C44	C45	C80	C79	174.9(3)
C45	C44	C74	C73	58.4(3)
C45	C46	C47	C48	1.1(4)
C46	C45	C80	C79	-1.1(4)
C46	C47	C48	C49	179.8(3)
C46	C47	C48	C79	-1.5(4)
C47	C48	C49	C50	66.1(3)
C47	C48	C49	C53	-57.4(3)
C47	C48	C79	C80	0.6(4)
C48	C49	C50	O11	103.8(3)
C48	C49	C50	O12	-73.2(4)
C48	C49	C53	C54	-64.0(3)
C48	C49	C53	C78	173.5(3)
C48	C79	C80	C45	0.7(5)
C49	C48	C79	C80	179.3(3)
C49	C53	C54	C55	174.7(3)
C50	O11	C51	C52	-95.2(3)
C50	C49	C53	C54	174.9(2)
C50	C49	C53	C78	52.5(3)
C51	O11	C50	O12	0.0(4)
C51	O11	C50	C49	-177.2(3)
C53	C49	C50	O11	-131.3(3)
C53	C49	C50	O12	51.6(4)
C53	C54	C55	C56	-178.4(3)
C54	C55	C56	C57	177.6(3)
C55	C56	C57	C58	-177.7(3)
C56	C57	C58	C61A	-174.8(2)
C56	C57	C58	C61B	-164.7(8)
C56	C57	C58	C62	59.3(3)

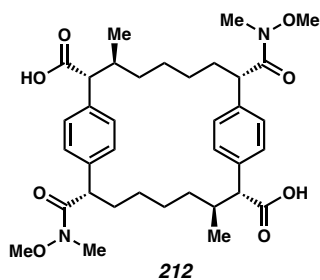
<b>Atom</b>	<b>Atom</b>	<b>Atom</b>	<b>Atom</b>	<b>Angle/°</b>
C57	C58	C62	C63	59.1(3)
C57	C58	C62	C77	-119.8(3)
C58	C62	C63	C64	-179.5(3)
C58	C62	C77	C76	179.1(3)
C62	C63	C64	C65	0.5(5)
C63	C62	C77	C76	0.1(4)
C63	C64	C65	C66	180.0(3)
C63	C64	C65	C76	-0.2(4)
C64	C65	C66	C67	67.6(4)
C64	C65	C66	C70	-55.0(4)
C64	C65	C76	C77	-0.3(4)
C65	C66	C67	O15	105.6(3)
C65	C66	C67	O16	-74.0(4)
C65	C66	C70	C71	-53.0(3)
C65	C66	C70	C75	-175.2(2)
C65	C76	C77	C62	0.3(4)
C66	C65	C76	C77	179.6(3)
C66	C70	C71	C72	167.2(2)
C67	O15	C68	C69	-167.3(3)
C67	C66	C70	C71	-175.7(2)
C67	C66	C70	C75	62.2(3)
C68	O15	C67	O16	1.8(5)
C68	O15	C67	C66	-177.8(3)
C70	C66	C67	O15	-128.3(3)
C70	C66	C67	O16	52.1(4)
C70	C71	C72	C73	178.9(2)
C71	C72	C73	C74	-172.7(2)
C72	C73	C74	C44	171.8(2)
C74	C44	C45	C46	59.7(3)
C74	C44	C45	C80	-116.3(3)
C75	C70	C71	C72	-71.6(3)
C76	C65	C66	C67	-112.3(3)
C76	C65	C66	C70	125.1(3)
C77	C62	C63	C64	-0.5(4)
C78	C53	C54	C55	-64.1(4)
C79	C48	C49	C50	-112.6(3)
C79	C48	C49	C53	124.0(3)
C80	C45	C46	C47	0.2(4)

**Table A8.2.10** Atomic Occupancies for all atoms that are not fully occupied in Macrocycle **208**.

<b>Atom</b>	<b>Occupancy</b>
Cl1A	0.0657(18)
Cl2A	0.0657(18)
Cl3A	0.0657(18)
O1A	0.0657(18)
O2A	0.0657(18)
C1A	0.0657(18)
C2A	0.0657(18)
H2AA	0.0657(18)
H2AB	0.0657(18)
C3A	0.0657(18)
Cl1B	0.9343(18)
Cl2B	0.9343(18)
Cl3B	0.9343(18)
O1B	0.9343(18)
O2B	0.9343(18)
C1B	0.9343(18)
C2B	0.9343(18)
H2BA	0.9343(18)
H2BB	0.9343(18)
C3B	0.9343(18)
Cl10	0.9093(17)
Cl11	0.9093(17)
Cl12	0.9093(17)
O13A	0.9093(17)
O14A	0.9093(17)
C59A	0.9093(17)
C60A	0.9093(17)
H60A	0.9093(17)
H60B	0.9093(17)
C61A	0.9093(17)
Cl4	0.0907(17)
Cl5	0.0907(17)
Cl6	0.0907(17)
O13B	0.0907(17)
O14B	0.0907(17)
C59B	0.0907(17)
C60B	0.0907(17)
H60C	0.0907(17)
H60D	0.0907(17)
C61B	0.0907(17)
Cl4B	0.9786(12)
Cl5B	0.9786(12)
Cl6B	0.9786(12)
O5B	0.9786(12)
O6B	0.9786(12)
C19B	0.9786(12)
C20B	0.9786(12)
H20A	0.9786(12)

<b>Atom</b>	<b>Occupancy</b>
H20B	0.9786(12)
C21B	0.9786(12)
Cl4A	0.0214(12)
Cl5A	0.0214(12)
Cl6A	0.0214(12)
O5A	0.0214(12)
O6A	0.0214(12)
C19A	0.0214(12)
C20A	0.0214(12)
H20C	0.0214(12)
H20D	0.0214(12)
C21A	0.0214(12)
Cl7A	0.9262(14)
Cl8A	0.9262(14)
Cl9A	0.9262(14)
O1AC	0.9262(14)
O2AC	0.9262(14)
C41A	0.9262(14)
C42A	0.9262(14)
H42A	0.9262(14)
H42B	0.9262(14)
C43A	0.9262(14)
Cl7B	0.0738(14)
Cl8B	0.0738(14)
Cl9B	0.0738(14)
O1AB	0.0738(14)
O2AB	0.0738(14)
C41B	0.0738(14)
C42B	0.0738(14)
H42C	0.0738(14)
H42D	0.0738(14)
C43B	0.0738(14)



**A8.3 X-RAY CRYSTAL STRUCTURE ANALYSIS OF MACROCYCLE 212**Contents

*Table A8.3.1. Experimental Details*

*Table A8.3.2. Crystal Data*

*Table A8.3.3. Reflection Statistics*

*Table A8.3.4. Atomic Coordinates*

*Table A8.3.5. Bond Lengths and Angles*

*Table A8.3.6. Anisotropic Displacement Parameters*

*Table A8.3.7. Hydrogen Atomic Coordinates*

*Table A8.3.8. Bond Angles*

*Table A8.3.9. Torsion Angles*

*Table A8.3.10. Hydrogen Bond Information*

*Table A8.3.11. Atomic Occupancies*

**Figure A8.3.1** X-Ray Crystal Structure of Macrocycle **212**.

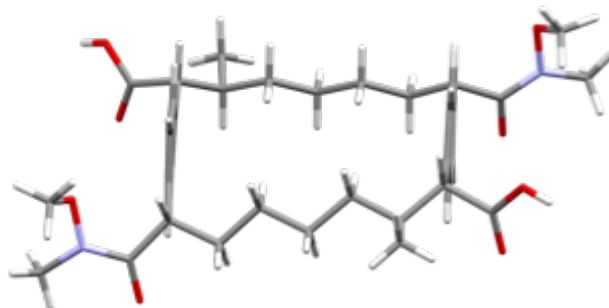


**Table A8.3.1** Experimental Details for X-Ray Structure Determination of Macrocycle **212**.

Single colorless plate crystals of macrocycle **212** from DMSO by slow evaporation. A suitable crystal with dimensions  $0.15 \times 0.08 \times 0.05 \text{ mm}^3$  was selected and mounted on a loop with paratone on a XtaLAB Synergy-S diffractometer. The crystal was kept at a steady  $T = 100(1) \text{ K}$  during data collection. The structure was solved with the ShelXT (Sheldrick, 2015) solution program using dual methods and by using Olex2 (Dolomanov et al., 2009) as the graphical interface. The model was refined with ShelXL 2018/3 (Sheldrick, 2015) using full matrix least squares minimisation on  $F^2$ .

**Crystal Data.**  $\text{C}_{40}\text{H}_{61}\text{N}_2\text{O}_{10}\text{S}_2$ ,  $M_r = 794.02$ , triclinic,  $P1$  (No. 1),  $a = 9.4562(4) \text{ \AA}$ ,  $b = 10.7610(4) \text{ \AA}$ ,  $c = 11.0648(3) \text{ \AA}$ ,  $\alpha = 102.582(3)^\circ$ ,  $\beta = 91.056(3)^\circ$ ,  $\gamma = 102.482(4)^\circ$ ,  $V = 1070.38(7) \text{ \AA}^3$ ,  $T = 100(1) \text{ K}$ ,  $Z = 1$ ,  $Z' = 1$ ,  $\mu(\text{Cu K}\alpha) = 1.585 \text{ mm}^{-1}$ , 12500 reflections measured, 5691 unique ( $R_{\text{int}} = 0.0441$ ) which were used in all calculations. The final  $wR_2$  was 0.2422 (all data) and  $R_1$  was 0.0816 ( $I \geq 2 \sigma(I)$ ).



**Table A8.3.2** Crystal Data and Structure Refinement for Macrocycle **212**

Compound	Macrocycle 212
Formula	C <sub>34</sub> H <sub>42</sub> F <sub>6</sub> O <sub>4</sub>
<i>D</i> <sub>calc.</sub> / g cm <sup>-3</sup>	1.241
<i>μ</i> /mm <sup>-1</sup>	0.866
Formula Weight	628.67
Colour	colourless
Shape	needle
Size/mm <sup>3</sup>	0.57×0.06×0.04
<i>T</i> /K	100(2)
Crystal System	monoclinic
Flack Parameter	-0.02(6)
Hooft Parameter	-0.00(5)
Space Group	<i>P</i> 2
<i>a</i> /Å	25.1525(4)
<i>b</i> /Å	5.53398(4)
<i>c</i> /Å	27.2474(4)
<i>α</i> <sup>°</sup>	90
<i>β</i> <sup>°</sup>	117.4652(19)
<i>γ</i> <sup>°</sup>	90
<i>V</i> /Å <sup>3</sup>	3365.19(9)
<i>Z</i>	4
<i>Z</i> '	2
Wavelength/Å	1.54184
Radiation type	CuK <sub>α</sub>
<i>θ</i> <sub>min</sub> <sup>°</sup>	1.980
<i>θ</i> <sub>max</sub> <sup>°</sup>	73.814
Measured Refl.	42058
Independent Refl.	10947
Reflections with <i>I</i> > 2σ( <i>I</i> )	9975
<i>R</i> <sub>int</sub>	0.0510
Parameters	797
Restraints	1
Largest Peak	0.323
Deepest Hole	-0.205
GooF	0.985
<i>wR</i> <sub>2</sub> (all data)	0.0885
<i>wR</i> <sub>2</sub>	0.0853
<i>R</i> <sub>1</sub> (all data)	0.0412
<i>R</i> <sub>1</sub>	0.0363

**Structure Quality Indicators**

<b>Reflections:</b>	d min (Cu) <b>0.81</b>	$1/\sigma(I)$ <b>19.3</b>	Rint <b>4.41%</b>	complete <b>71%</b> 99% (IUCr)
<b>Refinement:</b>	Shift <b>0.000</b>	Max Peak <b>0.6</b>	Min Peak <b>-0.5</b>	Goof <b>1.048</b>

A colorless plate-shaped crystal with dimensions  $0.15 \times 0.08 \times 0.05 \text{ mm}^3$  was mounted on a loop with paratone. Data were collected using a XtaLAB Synergy, Dualflex, HyPix diffractometer equipped with an Oxford Cryosystems low-temperature device operating at  $T = 100(1) \text{ K}$ .

Data were measured using  $\omega$  scans using Cu  $K_{\alpha}$  radiation. The diffraction pattern was indexed and the total number of runs and images was based on the strategy calculation from the program CrysAlisPro (Rigaku, V1.171.40.84a, 2020). The maximum resolution that was achieved was  $\theta = 73.009^{\circ}$  (0.81 Å).

The unit cell was refined using CrysAlisPro (Rigaku, V1.171.40.84a, 2020) on 6641 reflections, 53% of the observed reflections.

Data reduction, scaling and absorption corrections were performed using CrysAlisPro (Rigaku, V1.171.40.84a, 2020). The final completeness is 98.70 % out to  $73.009^{\circ}$  in  $\theta$ . A numerical absorption correction based on a Gaussian integration over a multifaceted crystal model absorption correction was performed using CrysAlisPro 1.171.40.79a (Rigaku Oxford Diffraction, 2020). An empirical absorption correction using spherical harmonics, implemented in SCALE3 ABSPACK scaling algorithm was also applied. The absorption coefficient  $\mu$  of this material is  $1.585 \text{ mm}^{-1}$  at this wavelength ( $\lambda = 1.54184 \text{ \AA}$ ) and the minimum and maximum transmissions are 0.764 and 1.000.

The structure was solved and the space group  $P1$  (# 1 determined by the ShelXT (Sheldrick, 2015) structure solution program using dual methods and refined by full matrix least

squares minimisation on  $F^2$  using version 2018/3 of ShelXL 2018/3 (Sheldrick, 2015). All non-hydrogen atoms were refined anisotropically. Hydrogen atom positions were calculated geometrically and refined using the riding model. Their distances were refined.

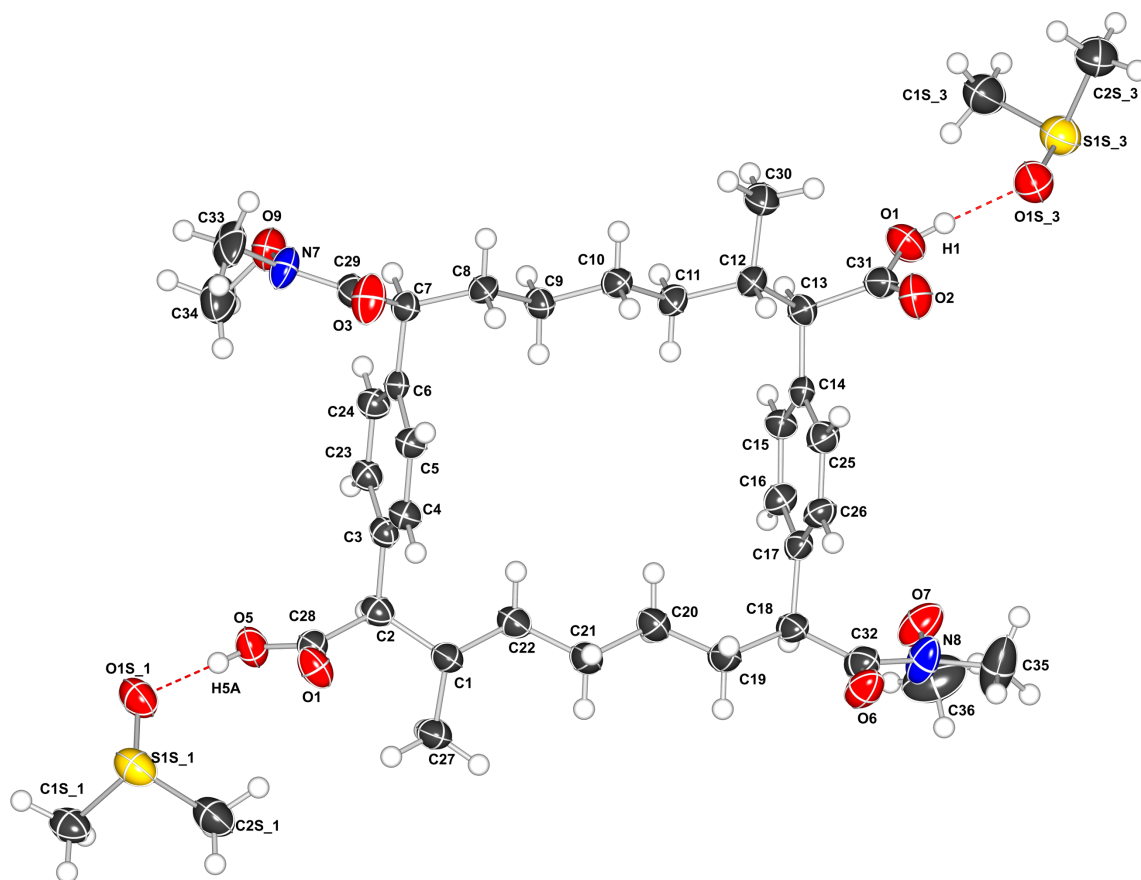


**Figure A8.3.2** Thermal ellipsoid plot of the asymmetric unit. There are two disordered solvent molecules hydrogen bonded to the main molecule. Although the structure this type is expected to have two-fold rotational symmetry, there is no rotational symmetry in the crystal and the point group of the crystal is  $C_1$ .

**Table A8.3.3** Reflection Statistics

Total reflections (after filtering)	12502	Unique reflections	5691
Completeness	0.665	Mean $I/\sigma$	12.1
$hkl_{\max}$ collected	(11, 13, 13)	$hkl_{\min}$ collected	(-11, -12, -11)
$hkl_{\max}$ used	(11, 13, 13)	$hkl_{\min}$ used	(-11, -12, -11)
Lim $d_{\max}$ collected	100.0	Lim $d_{\min}$ collected	0.77
$d_{\max}$ used	10.77	$d_{\min}$ used	0.81
Friedel pairs	1681	Friedel pairs merged	0
Inconsistent equivalents	37	$R_{\text{int}}$	0.0441
$R_{\text{sigma}}$	0.0519	Intensity transformed	0
Omitted reflections	0	Omitted by user (OMIT hkl)	2
Multiplicity	(2066, 2064, 801, 377, 166, 80, 62, 44, 22, 8, 1, 1)	Maximum multiplicity	12
Removed systematic absences	0	Filtered off (Shel/OMIT)	0

**Table A8.3.4** Fractional Atomic Coordinates ( $\times 10^4$ ) and Equivalent Isotropic Displacement Parameters ( $\text{\AA}^2 \times 10^3$ ) for Macrocycle **212**.  $U_{eq}$  is defined as 1/3 of the trace of the orthogonalised  $U_{ij}$ .

Atom	x	y	z	$U_{eq}$
C1	3051(8)	5798(7)	8750(7)	40.0(13)
C2	3899(7)	7238(7)	9191(7)	35.6(11)
C3	5300(7)	7573(6)	8564(6)	31.7(10)
C4	6369(7)	6864(7)	8553(6)	34.1(11)
C5	7645(7)	7175(7)	7979(6)	33.8(11)
C6	7878(7)	8226(6)	7371(6)	28.7(10)
C7	9234(7)	8552(7)	6700(6)	33.1(12)
C8	9393(7)	7417(7)	5656(7)	36.7(14)
C9	8142(8)	6973(7)	4688(6)	36.7(13)
C10	8325(8)	5886(7)	3617(7)	38.1(14)
C11	7010(8)	5429(7)	2675(7)	36.8(14)
C12	7121(8)	4329(7)	1570(7)	37.5(14)
C13	5643(8)	3878(7)	787(6)	35.8(13)
C14	4408(7)	3290(6)	1469(6)	32.3(12)
C15	3192(8)	3832(7)	1639(6)	35.2(13)
C16	2058(8)	3300(7)	2263(7)	37.2(14)
C17	2090(7)	2220(6)	2771(6)	34.3(13)
C18	901(8)	1694(7)	3544(7)	39.8(15)
C19	1360(9)	2100(8)	4938(7)	45.1(16)
C20	1802(9)	3567(8)	5429(7)	46.6(16)
C21	2151(9)	3961(8)	6827(7)	48.5(17)
C22	2729(8)	5420(8)	7337(7)	40.7(15)
C23	5556(7)	8634(7)	8012(6)	34.2(11)
C24	6803(8)	8947(7)	7421(6)	35.3(12)
C25	4431(8)	2177(7)	1929(7)	39.0(14)
C26	3287(8)	1673(7)	2589(7)	36.3(14)
C27	1642(8)	5610(8)	9405(7)	44.5(15)
C28	4280(8)	7559(7)	10596(7)	35.1(13)
C29	10536(8)	8946(7)	7636(7)	38.5(15)
C30	8356(9)	4768(8)	781(8)	47.8(17)
C31	5826(8)	2884(8)	-407(7)	42.2(15)
C32	473(9)	193(8)	3120(8)	46.2(16)
C33	12280(9)	10739(10)	9071(9)	66(2)
C34	9479(11)	11696(10)	8754(10)	70(3)
C35	-416(15)	-1655(9)	1284(11)	85(4)
C36	-2272(11)	332(13)	1330(14)	94(4)
N7	10972(7)	10203(6)	8237(7)	47.5(15)
N8	-336(9)	-320(7)	2040(7)	57.3(18)
O1	5517(8)	3281(7)	-1413(6)	62.3(15)
O4	4781(7)	6852(6)	11122(5)	49.7(12)
O2	6151(7)	1877(6)	-438(6)	56.6(14)
O3	11185(7)	8140(6)	7871(6)	56.7(14)
O5	4040(7)	8698(6)	11176(5)	50.5(13)
O6	914(7)	-528(6)	3682(6)	56.1(14)
O7	-706(7)	512(6)	1371(7)	63.6(16)
O9	10355(8)	11129(6)	7842(6)	60.2(15)

<b>Atom</b>	<b>x</b>	<b>y</b>	<b>z</b>	<b><i>U</i><sub>eq</sub></b>
C1S_3	6140(19)	3997(9)	-4235(14)	70(4)
C2S_3	7202(14)	2078(15)	-5555(13)	65(3)
O1S_3	6047(14)	1794(11)	-3499(8)	62.8(19)
S1S_3	5742(5)	2272(5)	-4628(4)	58.8(9)
C1S_4	4310(40)	7180(30)	14370(40)	62.2(17)
C2S_4	3130(50)	9060(30)	15600(20)	52.4(18)
O1S_4	4360(30)	9340(20)	13571(19)	57.7(15)
S1S_4	3338(14)	8315(14)	14054(12)	57.6(6)
C1S_5	5710(20)	3420(30)	-4620(30)	74(6)
C2S_5	8270(20)	4050(18)	-3360(20)	58(5)
O1S_5	6530(30)	1818(14)	-3382(15)	62.8(19)
S1S_5	7090(10)	2657(9)	-4266(8)	58.8(9)
C1S_1	3485(10)	9218(10)	15606(8)	52.4(18)
C2S_1	3082(10)	7156(10)	13719(9)	62.2(17)
O1S_1	4889(7)	9299(7)	13570(5)	57.7(15)
S1S_1	4506(4)	8446(4)	14477(3)	57.6(6)
C1S_2	7830(30)	950(20)	-5330(20)	65(3)
C2S_2	6250(30)	2700(30)	-5340(20)	60(5)
O1S_2	6320(30)	1703(19)	-3418(17)	62.8(19)
S1S_2	7343(11)	2257(9)	-4287(9)	58.8(9)

**Table A8.3.5** Bond Lengths [Å] and angles [°] for Macrocycle **212**

Atom	Atom	Length/Å
C1	C2	1.549(9)
C1	C22	1.535(9)
C1	C27	1.524(10)
C2	C3	1.517(9)
C2	C28	1.535(9)
C3	C4	1.391(8)
C3	C23	1.388(8)
C4	C5	1.384(9)
C5	C6	1.417(8)
C6	C7	1.508(8)
C6	C24	1.400(8)
C7	C8	1.523(9)
C7	C29	1.518(9)
C8	C9	1.504(9)
C9	C10	1.514(9)
C10	C11	1.529(8)
C11	C12	1.528(9)
C12	C13	1.555(9)
C12	C30	1.527(9)
C13	C14	1.501(8)
C13	C31	1.546(10)
C14	C15	1.396(9)
C14	C25	1.404(9)
C15	C16	1.375(9)
C16	C17	1.402(8)
C17	C18	1.512(9)
C17	C26	1.383(10)
C18	C19	1.536(9)
C18	C32	1.540(10)
C19	C20	1.515(10)
C20	C21	1.522(10)
C21	C22	1.522(10)
C23	C24	1.373(9)
C25	C26	1.395(9)
C28	O4	1.216(8)
C28	O5	1.323(8)
C29	N7	1.341(8)
C29	O3	1.233(8)
C31	O1	1.325(9)
C31	O2	1.182(9)
C32	N8	1.347(9)
C32	O6	1.226(9)
C33	N7	1.460(9)
C34	O9	1.435(11)
C35	N8	1.482(12)
C36	O7	1.449(12)
N7	O9	1.398(8)
N8	O7	1.374(8)
C1S_3	S1S_3	1.765(8)
C2S_3	S1S_3	1.756(9)
O1S_3	S1S_3	1.498(6)



<b>Atom</b>	<b>Atom</b>	<b>Length/Å</b>
C1S_4	S1S_4	1.766(8)
C2S_4	S1S_4	1.757(9)
O1S_4	S1S_4	1.499(6)
C1S_5	S1S_5	1.766(8)
C2S_5	S1S_5	1.756(9)
O1S_5	S1S_5	1.498(6)
C1S_1	S1S_1	1.767(8)
C2S_1	S1S_1	1.757(9)
O1S_1	S1S_1	1.501(5)
C1S_2	S1S_2	1.766(8)
C2S_2	S1S_2	1.756(9)
O1S_2	S1S_2	1.499(6)

**Table A8.3.6** Anisotropic Displacement Parameters ( $\text{\AA}^2 \times 10^3$ ) for Macrocycle **212**.

The Anisotropic Displacement Factor Exponent Takes the Form:  $-2p^2[h^2a^{*2}U^{11} + \dots + 2hka^*b^*U^{12}]$ .

Atom	$U_{11}$	$U_{22}$	$U_{33}$	$U_{23}$	$U_{13}$	$U_{12}$
C1	38(3)	47(2)	31(3)	7(2)	7(2)	4.8(19)
C2	31(2)	44(2)	33(2)	9.2(18)	3.3(16)	9.9(17)
C3	30(2)	37(2)	26(2)	4.4(18)	0.3(17)	7.7(16)
C4	33(2)	38(3)	33(3)	10(2)	4.9(18)	9.3(18)
C5	33(2)	37(2)	33(3)	9(2)	4(2)	8.0(18)
C6	28(2)	30(2)	23(2)	1.5(17)	-3.8(16)	1.2(15)
C7	30(2)	37(3)	29(3)	5(2)	0(2)	3(2)
C8	27(3)	42(3)	34(3)	3(3)	2(2)	-3(2)
C9	33(3)	44(3)	28(3)	4(3)	1(2)	3(3)
C10	35(3)	41(3)	34(3)	8(3)	1(3)	-1(3)
C11	28(3)	41(3)	36(3)	2(3)	-1(3)	1(2)
C12	35(3)	35(3)	37(3)	4(3)	2(3)	0(2)
C13	38(3)	39(3)	27(3)	7(3)	-1(3)	3(3)
C14	35(3)	29(3)	27(3)	1(2)	-2(2)	-1(2)
C15	39(3)	35(3)	32(3)	10(2)	4(3)	6(3)
C16	34(3)	36(3)	42(4)	10(3)	2(3)	7(2)
C17	34(3)	32(3)	31(3)	6(2)	-2(2)	-2(2)
C18	31(3)	49(4)	33(3)	8(3)	1(3)	-2(3)
C19	44(4)	51(4)	32(3)	10(3)	3(3)	-6(3)
C20	50(4)	52(4)	34(4)	9(3)	5(3)	5(3)
C21	49(4)	55(4)	33(4)	6(3)	7(3)	-2(3)
C22	35(3)	54(4)	32(3)	10(3)	4(3)	10(3)
C23	35(2)	39(2)	29(3)	7(2)	2(2)	9.6(18)
C24	35(2)	39(3)	33(3)	10(2)	2.8(18)	9.1(18)
C25	37(3)	39(3)	40(4)	10(3)	2(3)	5(3)
C26	37(3)	32(3)	39(3)	13(3)	2(3)	2(2)
C27	40(3)	54(4)	37(3)	9(3)	9(2)	4(3)
C28	33(3)	38(3)	33(2)	7(2)	2(2)	5(2)
C29	32(3)	44(3)	34(3)	0(3)	1(3)	5(3)
C30	39(4)	55(4)	44(4)	3(3)	11(3)	4(3)
C31	41(4)	46(4)	36(4)	11(3)	4(3)	0(3)
C32	41(4)	51(4)	41(4)	13(3)	-2(3)	-2(3)
C33	37(4)	70(5)	66(6)	-18(4)	-13(4)	-5(4)
C34	61(6)	63(5)	74(6)	-13(4)	3(5)	17(4)
C35	124(10)	44(4)	77(7)	4(4)	-46(7)	9(5)
C36	50(6)	111(9)	133(11)	58(8)	-9(6)	14(6)
N7	40(3)	37(3)	54(4)	-3(3)	-12(3)	0(2)
N8	67(4)	47(3)	49(4)	11(3)	-30(3)	-2(3)
O1	79(4)	67(3)	38(3)	13(3)	10(3)	9(3)
O4	64(3)	59(3)	31(2)	10(2)	4(2)	25(3)
O2	65(4)	51(3)	49(3)	-2(2)	1(3)	17(3)
O3	49(3)	55(3)	59(3)	-2(3)	-21(3)	16(2)
O5	68(3)	45(3)	38(3)	2(2)	6(2)	17(2)
O6	66(3)	48(3)	50(3)	21(2)	-12(3)	-6(2)
O7	53(3)	56(3)	79(4)	25(3)	-19(3)	-3(2)
O9	70(4)	45(3)	58(3)	1(2)	5(3)	7(3)

<b>Atom</b>	<b><math>U_{11}</math></b>	<b><math>U_{22}</math></b>	<b><math>U_{33}</math></b>	<b><math>U_{23}</math></b>	<b><math>U_{13}</math></b>	<b><math>U_{12}</math></b>
C1S_3	80(11)	66(6)	65(9)	14(3)	21(7)	14(3)
C2S_3	57(5)	70(4)	64(4)	11(3)	11(4)	10(4)
O1S_3	64(3)	65(3)	56(2)	7(2)	5.8(19)	13(2)
S1S_3	54.7(17)	67.3(19)	54.5(16)	14.1(15)	6.9(13)	13.6(14)
C1S_4	62(3)	82(3)	44(3)	13(2)	11(3)	19(2)
C2S_4	38(4)	74(4)	44(3)	14(2)	4(2)	11(3)
O1S_4	58(3)	76(2)	37(2)	7(2)	5(2)	17(2)
S1S_4	53.0(11)	79.7(13)	44.1(11)	16.4(9)	7.7(8)	21.0(10)
C1S_5	60(7)	82(13)	83(18)	27(11)	6(7)	17(10)
C2S_5	58(9)	74(5)	47(9)	24(8)	17(8)	18(6)
O1S_5	64(3)	65(3)	56(2)	7(2)	5.8(19)	13(2)
S1S_5	54.7(17)	67.3(19)	54.5(16)	14.1(15)	6.9(13)	13.6(14)
C1S_1	38(4)	74(4)	44(3)	14(2)	4(2)	11(3)
C2S_1	62(3)	82(3)	44(3)	13(2)	11(3)	19(2)
O1S_1	58(3)	76(2)	37(2)	7(2)	5(2)	17(2)
S1S_1	53.0(11)	79.7(13)	44.1(11)	16.4(9)	7.7(8)	21.0(10)
C1S_2	57(5)	70(4)	64(4)	11(3)	11(4)	10(4)
C2S_2	52(7)	57(13)	67(6)	16(7)	11(7)	-1(9)
O1S_2	64(3)	65(3)	56(2)	7(2)	5.8(19)	13(2)
S1S_2	54.7(17)	67.3(19)	54.5(16)	14.1(15)	6.9(13)	13.6(14)

**Table A8.3.7** Hydrogen Coordinates ( $\times 10^4$ ) and Isotropic Displacement Parameters ( $\text{\AA}^2 \times 10^3$ ) for Macrocycle **212**.

Atom	x	y	z	$U_{eq}$
H2	3227(19)	7841(17)	9011(8)	43
H4	6223(8)	6160(16)	8943(10)	41
H5	8355(16)	6690(12)	7992(6)	41
H7	9182(8)	9350(20)	6317(12)	40
H8A	10269(17)	7674(8)	5264(9)	44
H8B	9484(8)	6696(14)	6005(9)	44
H9A	8022(8)	7704(14)	4368(8)	44
H9B	7273(17)	6679(9)	5074(9)	44
H10A	8472(8)	5161(14)	3934(9)	46
H10B	9171(16)	6187(9)	3207(9)	46
H11A	6168(16)	5141(9)	3096(10)	44
H11B	6867(8)	6162(14)	2367(9)	44
H12	7322(9)	3540(20)	1905(11)	45
H13	5392(19)	4710(60)	525(19)	43
H15	3148(8)	4565(16)	1324(9)	42
H16	1243(18)	3668(10)	2352(7)	45
H18	-10(20)	2065(12)	3390(8)	48
H19A	570(16)	1751(10)	5385(10)	54
H19B	2158(16)	1726(10)	5091(7)	54
H20A	1030(16)	3950(11)	5225(8)	56
H20B	2636(17)	3910(10)	5026(10)	56
H21A	1289(17)	3682(9)	7228(10)	58
H21B	2855(15)	3509(11)	7035(8)	58
H22A	2033(14)	5876(11)	7120(8)	49
H22B	3602(17)	5699(9)	6949(10)	49
H23	4866(16)	9146(12)	8044(6)	41
H24	6939(8)	9659(16)	7042(10)	42
H25	5216(18)	1772(11)	1793(8)	47
H26	3331(8)	948(16)	2917(9)	44
H27A	1035(11)	6193(10)	9184(8)	67
H27B	1870(9)	5836(8)	10324(13)	67
H27C	1097(11)	4678(13)	9137(8)	67
H30A	8424(9)	4020(12)	83(11)	72
H30B	9292(14)	5067(9)	1306(10)	72
H30C	8163(9)	5505(12)	435(9)	72
H33A	12217(9)	10290(11)	9776(13)	99
H33B	12368(9)	11697(15)	9401(10)	99
H33C	13150(14)	10598(10)	8606(11)	99
H34A	8650(15)	11910(10)	8329(11)	105
H34B	10082(13)	12514(14)	9298(12)	105
H34C	9094(12)	11060(12)	9273(12)	105
H35A	-1427(19)	-2040(10)	902(12)	128
H35B	-151(15)	-2214(11)	1825(13)	128
H35C	276(17)	-1612(9)	613(14)	128
H36A	-2672(12)	80(14)	446(18)	141
H36B	-2529(12)	1167(16)	1754(15)	141
H36C	-2695(12)	-374(16)	1763(15)	141
H1	5753(18)	2810(30)	-2030(40)	93

<b>Atom</b>	<b>x</b>	<b>y</b>	<b>z</b>	<b><i>U</i><sub>eq</sub></b>
H5A	4320(20)	8851(12)	11910(50)	76
H1SA_3	5940(20)	4330(10)	-4982(16)	106
H1SB_3	5520(20)	4302(10)	-3562(16)	106
H1SC_3	7190(20)	4335(10)	-3937(14)	106
H2SA_3	7066(14)	2382(15)	-6332(16)	97
H2SB_3	8129(18)	2607(16)	-5087(14)	97
H2SC_3	7243(14)	1135(18)	-5773(13)	97
H1SA_4	3640(40)	6490(30)	14700(40)	93
H1SB_4	4700(40)	6770(30)	13590(50)	93
H1SC_4	5120(50)	7640(30)	15010(50)	93
H2SA_4	2450(50)	8430(30)	15980(20)	79
H2SB_4	4090(60)	9330(30)	16080(20)	79
H2SC_4	2720(50)	9850(40)	15610(20)	79
H1SA_5	6060(20)	3990(30)	-5210(30)	111
H1SB_5	4830(20)	2740(30)	-5010(30)	111
H1SC_5	5460(20)	3970(30)	-3840(30)	111
H2SA_5	8680(20)	4655(19)	-3900(20)	86
H2SB_5	7720(20)	4504(19)	-2700(20)	86
H2SC_5	9080(30)	3783(18)	-2950(20)	86
H1SA_1	3214(11)	8669(12)	16224(11)	79
H1SB_1	4079(12)	10095(14)	16039(10)	79
H1SC_1	2584(15)	9327(10)	15193(9)	79
H2SA_1	2773(11)	6546(12)	14278(11)	93
H2SB_1	2242(14)	7515(10)	13506(9)	93
H2SC_1	3420(11)	6673(11)	12941(13)	93
H1SA_2	8510(30)	1300(20)	-5920(20)	97
H1SB_2	8310(30)	440(20)	-4860(20)	97
H1SC_2	6930(30)	360(20)	-5810(20)	97
H2SA_2	6870(30)	3080(30)	-5950(20)	91
H2SB_2	5510(30)	1910(30)	-5790(20)	91
H2SC_2	5740(30)	3370(30)	-4880(20)	91

**Table A8.3.8** Bond Angles [°] for Macrocycle **212**.

Atom	Atom	Atom	Angle/°
C22	C1	C2	111.4(5)
C27	C1	C2	109.0(6)
C27	C1	C22	110.4(6)
C3	C2	C1	114.4(5)
C3	C2	C28	107.7(5)
C28	C2	C1	110.0(5)
C4	C3	C2	121.8(5)
C23	C3	C2	119.9(5)
C23	C3	C4	118.3(6)
C5	C4	C3	121.5(6)
C4	C5	C6	120.1(6)
C5	C6	C7	121.1(5)
C24	C6	C5	117.5(6)
C24	C6	C7	121.5(5)
C6	C7	C8	112.3(5)
C6	C7	C29	108.6(5)
C29	C7	C8	110.5(5)
C9	C8	C7	113.6(5)
C8	C9	C10	113.9(6)
C9	C10	C11	112.4(6)
C12	C11	C10	115.1(5)
C11	C12	C13	108.6(5)
C30	C12	C11	111.3(5)
C30	C12	C13	110.9(5)
C14	C13	C12	113.5(5)
C14	C13	C31	110.3(5)
C31	C13	C12	108.1(5)
C15	C14	C13	120.2(5)
C15	C14	C25	118.4(6)
C25	C14	C13	121.3(6)
C16	C15	C14	120.6(6)
C15	C16	C17	121.6(6)
C16	C17	C18	121.9(6)
C26	C17	C16	117.8(6)
C26	C17	C18	120.3(6)
C17	C18	C19	112.2(5)
C17	C18	C32	109.2(6)
C19	C18	C32	110.1(6)
C20	C19	C18	113.4(6)
C19	C20	C21	112.9(6)
C22	C21	C20	114.4(6)
C21	C22	C1	113.5(6)
C24	C23	C3	121.1(6)
C23	C24	C6	121.5(6)
C26	C25	C14	120.1(6)
C17	C26	C25	121.4(6)
O4	C28	C2	123.5(6)
O4	C28	O5	123.2(6)
O5	C28	C2	113.2(5)
N7	C29	C7	118.9(6)
O3	C29	C7	121.8(6)

<b>Atom</b>	<b>Atom</b>	<b>Atom</b>	<b>Angle/°</b>
O3	C29	N7	119.3(6)
O1	C31	C13	111.2(6)
O2	C31	C13	125.3(7)
O2	C31	O1	123.5(7)
N8	C32	C18	117.4(6)
O6	C32	C18	122.6(6)
O6	C32	N8	119.8(7)
C29	N7	C33	124.7(7)
C29	N7	O9	118.4(5)
O9	N7	C33	115.2(6)
C32	N8	C35	124.0(7)
C32	N8	O7	118.8(6)
O7	N8	C35	113.4(6)
N8	O7	C36	107.7(7)
N7	O9	C34	111.9(7)
C2S_3	S1S_3	C1S_3	97.8(5)
O1S_3	S1S_3	C1S_3	108.6(5)
O1S_3	S1S_3	C2S_3	105.3(5)
C2S_4	S1S_4	C1S_4	97.6(5)
O1S_4	S1S_4	C1S_4	108.3(5)
O1S_4	S1S_4	C2S_4	105.2(5)
C2S_5	S1S_5	C1S_5	97.6(5)
O1S_5	S1S_5	C1S_5	108.4(5)
O1S_5	S1S_5	C2S_5	105.4(5)
C2S_1	S1S_1	C1S_1	97.5(4)
O1S_1	S1S_1	C1S_1	107.7(4)
O1S_1	S1S_1	C2S_1	105.4(4)
C2S_2	S1S_2	C1S_2	97.6(5)
O1S_2	S1S_2	C1S_2	108.3(5)
O1S_2	S1S_2	C2S_2	105.4(5)

**Table A8.3.9** Torsion Angles [°] for Macrocycle **212**.

Atom	Atom	Atom	Atom	Angle/°
C1	C2	C3	C4	-54.3(8)
C1	C2	C3	C23	127.6(6)
C1	C2	C28	O4	45.9(8)
C1	C2	C28	O5	-135.5(6)
C2	C1	C22	C21	169.3(6)
C2	C3	C4	C5	180.0(6)
C2	C3	C23	C24	-178.9(6)
C3	C2	C28	O4	-79.4(8)
C3	C2	C28	O5	99.2(6)
C3	C4	C5	C6	-0.8(9)
C3	C23	C24	C6	-1.3(9)
C4	C3	C23	C24	2.9(9)
C4	C5	C6	C7	-177.8(5)
C4	C5	C6	C24	2.3(9)
C5	C6	C7	C8	59.8(7)
C5	C6	C7	C29	-62.7(7)
C5	C6	C24	C23	-1.3(9)
C6	C7	C8	C9	58.8(7)
C6	C7	C29	N7	-88.3(7)
C6	C7	C29	O3	90.5(8)
C7	C6	C24	C23	178.7(5)
C7	C8	C9	C10	177.3(5)
C7	C29	N7	C33	-174.0(8)
C7	C29	N7	O9	-9.7(10)
C8	C7	C29	N7	148.2(6)
C8	C7	C29	O3	-33.0(9)
C8	C9	C10	C11	178.0(5)
C9	C10	C11	C12	-179.8(6)
C10	C11	C12	C13	173.8(5)
C10	C11	C12	C30	-63.8(8)
C11	C12	C13	C14	-64.0(7)
C11	C12	C13	C31	173.4(5)
C12	C13	C14	C15	121.4(6)
C12	C13	C14	C25	-59.7(7)
C12	C13	C31	O1	-121.8(6)
C12	C13	C31	O2	60.5(9)
C13	C14	C15	C16	-179.9(5)
C13	C14	C25	C26	178.2(6)
C14	C13	C31	O1	113.6(6)
C14	C13	C31	O2	-64.1(9)
C14	C15	C16	C17	1.3(9)
C14	C25	C26	C17	2.2(10)
C15	C14	C25	C26	-2.9(9)
C15	C16	C17	C18	175.2(6)
C15	C16	C17	C26	-2.1(9)
C16	C17	C18	C19	-103.0(7)
C16	C17	C18	C32	134.7(6)
C16	C17	C26	C25	0.3(9)
C17	C18	C19	C20	58.1(8)
C17	C18	C32	N8	-75.0(9)
C17	C18	C32	O6	100.2(8)



Atom	Atom	Atom	Atom	Angle/°
C18	C17	C26	C25	-177.0(6)
C18	C19	C20	C21	175.9(6)
C18	C32	N8	C35	157.8(9)
C18	C32	N8	O7	1.3(11)
C19	C18	C32	N8	161.4(7)
C19	C18	C32	O6	-23.3(10)
C19	C20	C21	C22	174.7(6)
C20	C21	C22	C1	179.1(6)
C22	C1	C2	C3	-55.3(7)
C22	C1	C2	C28	-176.7(5)
C23	C3	C4	C5	-1.8(9)
C24	C6	C7	C8	-120.3(6)
C24	C6	C7	C29	117.3(6)
C25	C14	C15	C16	1.2(9)
C26	C17	C18	C19	74.2(8)
C26	C17	C18	C32	-48.1(8)
C27	C1	C2	C3	-177.4(6)
C27	C1	C2	C28	61.2(7)
C27	C1	C22	C21	-69.4(8)
C28	C2	C3	C4	68.4(7)
C28	C2	C3	C23	-109.7(6)
C29	C7	C8	C9	-179.9(5)
C29	N7	O9	C34	113.2(8)
C30	C12	C13	C14	173.4(5)
C30	C12	C13	C31	50.7(7)
C31	C13	C14	C15	-117.2(6)
C31	C13	C14	C25	61.7(8)
C32	C18	C19	C20	179.9(6)
C32	N8	O7	C36	-115.8(10)
C33	N7	O9	C34	-81.1(9)
C35	N8	O7	C36	85.4(11)
O3	C29	N7	C33	7.2(12)
O3	C29	N7	O9	171.4(7)
O6	C32	N8	C35	-17.6(14)
O6	C32	N8	O7	-174.1(7)

**Table A8.3.10** Hydrogen Bond information for Macrocycle **212**.

<b>D</b>	<b>H</b>	<b>A</b>	<b>d(D-H)/Å</b>	<b>d(H-A)/Å</b>	<b>d(D-A)/Å</b>	<b>D-H-A/deg</b>
01	H1	O1S_3	0.82	1.81	2.630(12)	171.8
01	H1	O1S_5	0.82	1.90	2.718(17)	173.1
01	H1	O1S_2	0.82	1.89	2.714(17)	178.6
05	H5A	O1S_4	0.82	1.79	2.58(2)	161.0
05	H5A	O1S_1	0.82	1.83	2.651(8)	175.8

**Table A8.3.11** Atomic Occupancies for all atoms that are not fully occupied inMacrocycle **212**.

<b>Atom</b>	<b>Occupancy</b>
C1S_3	0.516(3)
H1SA_3	0.516(3)
H1SB_3	0.516(3)
H1SC_3	0.516(3)
C2S_3	0.516(3)
H2SA_3	0.516(3)
H2SB_3	0.516(3)
H2SC_3	0.516(3)
O1S_3	0.516(3)
S1S_3	0.516(3)
C1S_4	0.129(4)
H1SA_4	0.129(4)
H1SB_4	0.129(4)
H1SC_4	0.129(4)
C2S_4	0.129(4)
H2SA_4	0.129(4)
H2SB_4	0.129(4)
H2SC_4	0.129(4)
O1S_4	0.129(4)
S1S_4	0.129(4)
C1S_5	0.258(3)
H1SA_5	0.258(3)
H1SB_5	0.258(3)
H1SC_5	0.258(3)
C2S_5	0.258(3)
H2SA_5	0.258(3)
H2SB_5	0.258(3)
H2SC_5	0.258(3)
O1S_5	0.258(3)
S1S_5	0.258(3)
C1S_1	0.871(4)
H1SA_1	0.871(4)
H1SB_1	0.871(4)
H1SC_1	0.871(4)
C2S_1	0.871(4)
H2SA_1	0.871(4)
H2SB_1	0.871(4)
H2SC_1	0.871(4)
O1S_1	0.871(4)
S1S_1	0.871(4)
C1S_2	0.225(3)
H1SA_2	0.225(3)
H1SB_2	0.225(3)
H1SC_2	0.225(3)
C2S_2	0.225(3)
H2SA_2	0.225(3)
H2SB_2	0.225(3)
H2SC_2	0.225(3)

<b>Atom</b>	<b>Occupancy</b>
O1S_2	0.225(3)
S1S_2	0.225(3)

## ABOUT THE AUTHOR

Tyler Casselman was born in Buffalo, New York in 1995 to James Casselman and Richelle Casselman. He was raised in the nearby suburb of East Amherst and attended Williamsville North High School, from which he graduated in 2013.

From there, he attended Boston University in Boston, Massachusetts studying chemistry as well as being part of the Kilachand Honor's College program. His original intentions to attend medical school were altered after taking organic chemistry taught by Prof. John Snyder. After completing the class, he joined the Snyder group and worked on the synthesis of 3,6-disubstituted tetrazines that could be embedded within [6,6]-nylon polymers. Mentorship from his research mentor Prof. John Snyder and his academic advisor Prof. Binyomin Abrams motivated him to continue studying synthetic organic chemistry in graduate school after completing his bachelor's degree in 2017.

In June 2017, Tyler moved to New York City to begin his graduate school career in the Leighton lab at Columbia University. In the Leighton lab, he focused on the total synthesis of nonaromatic polyketide natural products using enantioselective allylation techniques developed in the Leighton lab. In 2019, Tyler transferred from Columbia University to the California Institute of Technology to finish his graduate studies under the guidance of Prof. Brian Stoltz. In the Stoltz group, Tyler has focused on the development of reaction methodologies, particularly using catalytic hydrosilylation to activate nitrogen containing molecules for their use in enantioselective transformations. Additionally, he has participated in a collaboration dedicated toward the total synthesis of (-)-cylindrocyclophane A using C-H functionalization logic. In June 2023, Tyler will begin his professional career as a chemist at Snapdragon in Boston, Massachusetts.